U.S. Geological Survey Data Release

High-Flow Field Experiments to Inform Everglades Restoration: Experimental Data 2010 to 2016

By Jay Choi, Judson Harvey, Laurel Larsen, Katherine Skalak, Brendan Buskirk, Allison Swartz, Jennifer Lewis, Jesus Gomez-Velez, Morgan Maglio, Geoff Sinclair, Trevor Langstrom, Jai Singh and Alex Walker

U.S. Geological Survey, Reston VA

Acknowledgments

This project was funded in significant part by USGS's Greater Everglades Priority Ecosystems Science (GEPES), the U.S. Army Corps of Engineers (MIPR W32CS550357675), the USGS-National Park Service Partnership as a part of the USGS National Water Quality Program and by the USGS National Research Program. The authors are grateful for research collaboration with colleagues at the USGS Florida Water Science Center (Davie), South Florida Water Management District, Florida International University, University of Hawaii, and University of California - Berkeley. We thank S. Newman and C. Saunders for providing the Lab analysis of Total Phosphorus samples. Use of trade, product, or firm names is for descriptive purposes only and does not imply endorsement by the U.S. Government.

Contents

High-Flow Field Experiments to Inform Everglades Restoration: Experimental Data 2010 to 2016

By Jay Choi, Jud Harvey, Laurel Larsen, Katherine Skalak, Brendan Buskirk, Allison Swartz, Jennifer Lewis, Jesus Gomez-Velez, Morgan Maglio, Geoff Sinclair, Trevor Langstrom, Jai Singh, and Alex Walker

Data Background

The Everglades was once an expansive subtropical ecosystem comprised of hydrologically interconnected cypress forests, sawgrass sloughs, marl prairies, and mangrove estuaries encompassing more than 3.6 million ha (Davis et al., 1994). These primary landscape features were physically defined by oligotrophic waters, low topographic relief, large spatial extent, seasonally dynamic rainfall and surface water patterns, hydrologic gradients and sheet flow, and an estuarine system (Ogden et al., 1999). These features supported great populations of wading birds with foraging ranges were tightly coupled with the dynamic hydropatterns.

The Everglades was once a single vast and well-connected expanse of floodplain that experienced unconstrained sheet flow. Over the last century, the Everglades ecosystem has been degraded by the unintended effects of water management and by spillover effects of agricultural and urban development. A vast network of canals, levees, control structures, and conservation areas was built to drain the Everglades and control floods and later the system was adjusted to store water for domestic supply and to meet agricultural and industrial needs. The largest of these projects was the Central and Southern Florida (C&SF) project constructed during the 1950s-1970s (Light and Dineen,

1994) which sought to manage the hydrology of a wetland system in which the flow quantity, timing, and distribution had been substantially altered. Unintended side effects included a loss of more than 50% of the aerial extent of the Everglades, subsidence of peat in many areas, and the creation of a highly compartmentalized flow system with excessive drying in the northern areas and in the southern area comprised of Everglades National Park. An additional unintended side effect of water management has been an impairment of water quality that has led to habitat degradation through eutrophication.

The 7 million people that inhabit southeast Florida are directly dependent on water management for flood control, water supply, irrigation, and transportation. Furthermore, congress decided that the Everglades has national significance and deserves preservation and restoration. Management of the Everglades and its resources must therefore strike a balance between the needs of the ecosystem with all societal interests; thus, an adaptive management approach is being implemented (Ogden et al., 2005). Key to the plan is the use of "best available science" and "adaptive assessment" which ensures plan flexibility to allow for modification as new information is obtained (Ogden et al., 2003). An "applied science strategy" has also been developed to incorporate science into the planning and implementation of water management (e.g., Ogden et al., 2003; Ogden et al., 2005).

Over the last four decades, a wealth of scientific knowledge has been gained about the Everglades and the south Florida natural system. This information has been synthesized into conceptual models that identify the major anthropogenic drivers and stressors, the ecological effect of these stressors, and the best biological attributes or indicators of these ecological responses for the primary landscape features of south Florida (see Ogden et al., 2005). The primary landscapes types are the Everglades ridge and slough landscape (Ogden 2005), southern marl prairies (Davis et al., 2005a), Everglades mangrove estuaries (Davis et al., 2005b), and Florida Bay (Rudnick et al., 2005). The Everglades ridge and slough conceptual model identifies the loss of sheet flow and shortened

hydroperiods in some areas and ponding in others as having degraded large areas of the landscape. The underlying causes include the reduced water storage capacity of the Everglades and increased compartmentalization with levees and canals as key stressors the ridge and slough landscapes plant community composition and distribution and abundance of aquatic animals. The disruption of sheet flow is the least understood stressor (Science Coordination Team, 2003) because there is no modern day analog in which to evaluate how the higher levels of sheet flow, prevalent more than a century ago, influenced sediment and nutrient transport or how flow created and maintained the subtle topographic differences between the ground surface elevations of ridges and sloughs, as well effects on how the connectivity of sloughs affected primary and secondary production on the landscape, including supporting fish and other prey species in the quantities necessary to sustain large super colonies of wading birds.

The Decompartmentalization Physical Model (DPM)

Description of Decompartmentalization Physical Model Project

The DPM is a multi-year program of high-flow field experiments conducted within the Everglades in an area that has been isolated from flow for sixty years. The work was supported by the U.S. Army Corps of Engineers and the research undertaken by scientists from the South Florida Water Management District, U.S. Geological Survey, Florida International University, University of Hawaii, and University of California-Berkeley. The purpose of the DPM experiments were to provide scientific information to help guide the congressionally authorized Everglades restoration project known as the Comprehensive Everglades Restoration Plan (CERP). At a cost of ten billion dollars, CERP outlines an Everglades-wide restoration project that will protect internationally valued wildlife resources and the potable water supply for south Floridians while also increasing resilience to drought. The DPM project will inform one of CERP's centerpiece projects, the Decompartmentalization and Sheet Flow Enhancement Project (DECOMP). Specifically, the DPM experiment will identify factors that influence effectiveness of restoration, specifically how effective flow restoration is in protecting highly valued ecological resources.

Twenty-three specific physical and biological hypotheses are addressed by the experiment and are detailed in the DPM Science Plan (DPM Science Team, 2010). The central research questions addressed by the DPM are summarized as follows:

Sheet Flow Questions: How does sheet flow improve the long term stability of the disappearing and highly valued ridge and slough landscape? To what extent do entrainment, transport, and settling of suspended particulates differ in ridge and slough habitats under high and low flow conditions? Also, does high flow cause changes in water chemistry and consequently changes in

sediment and periphyton metabolism and organic matter decomposition that influence function and stability of the ridge and slough landscape and its valued support of fish and wildlife?

Canal Backfill Questions: Will canal backfill treatments act as sediment traps, reducing overland transport of sediment? Will high flows entrain nutrient-rich canal sediments and carry them into the water column downstream? To what extent are these functions altered by the various canal backfill options, including partial and full backfills?

DPM was designed to test the benefits of sheet flow by evaluating surface water flows and interactions with vegetation and bed sediment that affect suspended particle entrainment and phosphorus transport. Measurements were made along a gradient of increased sheet flow as it varies with distance from the location of breaches in the levee. Field monitoring of hydrologic and biological parameters at DPM were conducted under low-flow (baseline) and high-flow (impact) conditions in the affected flow way and in non-impacted wetland and canal "control" sites. The operational window of the S-152 culverts was subject to certain water level and phosphorus concentration triggers limiting operation to the months of November, December and January. The first high-flow event was initiated on 11/5/2013 and the second on 11/6/2014, and the third on 11/16/2015 and 11/19/2015. The third high-flow event had two high-flow pulses. The first one was between 11/16/2015 and 11/17/2015, and the second one was between 11/19/2016 and 1/28/2016. Here we summarize objectives, methods, and data collected by the USGS National Research Program, Eastern Branch, in Reston, Virginia and by the University of California, Berkeley. Many complementary studies are being conducted by collaborators, including investigations of how levee removal and canal backfilling are affecting fish movement between previously isolated areas. In addition to serving Everglades restoration, the DPM will inform similar adaptive management programs throughout the nation's network of federally managed river corridors, floodplains, and riparian ecosystems.

Site Locations, Time Period of Operation, and Overview of Data Collection

The DPM infrastructure included gated culverts and levee gaps that moved flow from one basin to another and that increased sheet flow through an area of the Everglades known as the "pocket", a 2-km wide wetland that has been hydrologically isolated between levees for approximately 60 years. The ten gated culverts (S-152) conveyed flow beneath the L-67A levee (Figure 1) and had a combined capacity to produce sheet flows that generated water velocities approximately ten times greater than current flows. At a location 2.5 kilometers downstream, the experimental wetland was modified by removal of a 3,000 foot portion of the L-67C levee that allowed water to cross a canal into a different sub-basin. Three degrees of backfilling of the L-67C canal gap were tested in terms of how backfilling affected transport of sediment and phosphorus to downstream areas.

A hydrologic modeling network was set up at DPM to measure the movement of water, solutes, and suspended materials with sheet flow. Fourteen stations were routinely visited through the wet season during which instruments were calibrated for quality assurance and data were downloaded. The hydrologic monitoring network served as a framework for measuring other physical and ecological processes such as flow field dynamics, suspended particle sources and concentrations, physical characteristics of particles such as size and organic content, particle-phosphorus content, and the role of vegetation community type and stem density in influencing flow and particle dynamics. In addition, various environmental and introduced tracers were measured during the flow releases to capture local scale and larger scale surface water and groundwater flow patterns.

The high-flow measurement network included fourteen measurement sites. From northwest to southeast the sites were Z51, Z51_USGS, Z53NE_2014, Z53NE_2015, RS1U, RS1D, RS1SE, Z53B, RS2, S1, UB1, UB2, UB3, DB1, DB2, DB3 and MB0, MB1, MB2, MB3 along the L67C canal (fig 1). There are also two control stations (C1 and C2) that were located in areas removed from the main

influence of sheet flow enhancement. Three of the measurement sites (UB1, UB2, UB3) were located on the upstream side of the L-67C canal in the vicinity of where the levee had been removed, allowing flow to cross from the pocket into Water Conservation Area 3B. There were also four sites located in the L-67C canal (MB0, MB1, MB2, and MB3) and three sites located on the downstream side of the canal (DB1, DB2, DB3) (fig 1).

The USGS-Reston measurements at DPM are categorized either as continuous/autonomous (i.e., self-collecting instruments emplaced for the wet season) or discrete/portable (e.g. measurements made over a period of hours to days). Data collection occurred from 2010 to 2016 between the onset of the wet season (usually August) through the onset of the dry season (usually March). The 2010-2011 wet season was brief and ended with a severe fire that burned vegetation (but not peat) throughout the experimental area. Measurements between 2010 and 2013 provided baseline low-flow data before the construction of the culverts and levee gaps that allowed high-flow to begin. The construction of culverts and the levee gap and canal backfill treatments were completed in summer of 2013 and the DPM experiment became operational in early November of 2013 with the first high-flow experiment lasting through December of that year. The following year the flow enhancement experiment began in early November and lasted through the end of January 2015. Between middle of November 2015 and end of January 2016, there were two high-flow experiments (11/16/2015 – 11/17/2015 and 11/19/2015 – 1/28/2016).

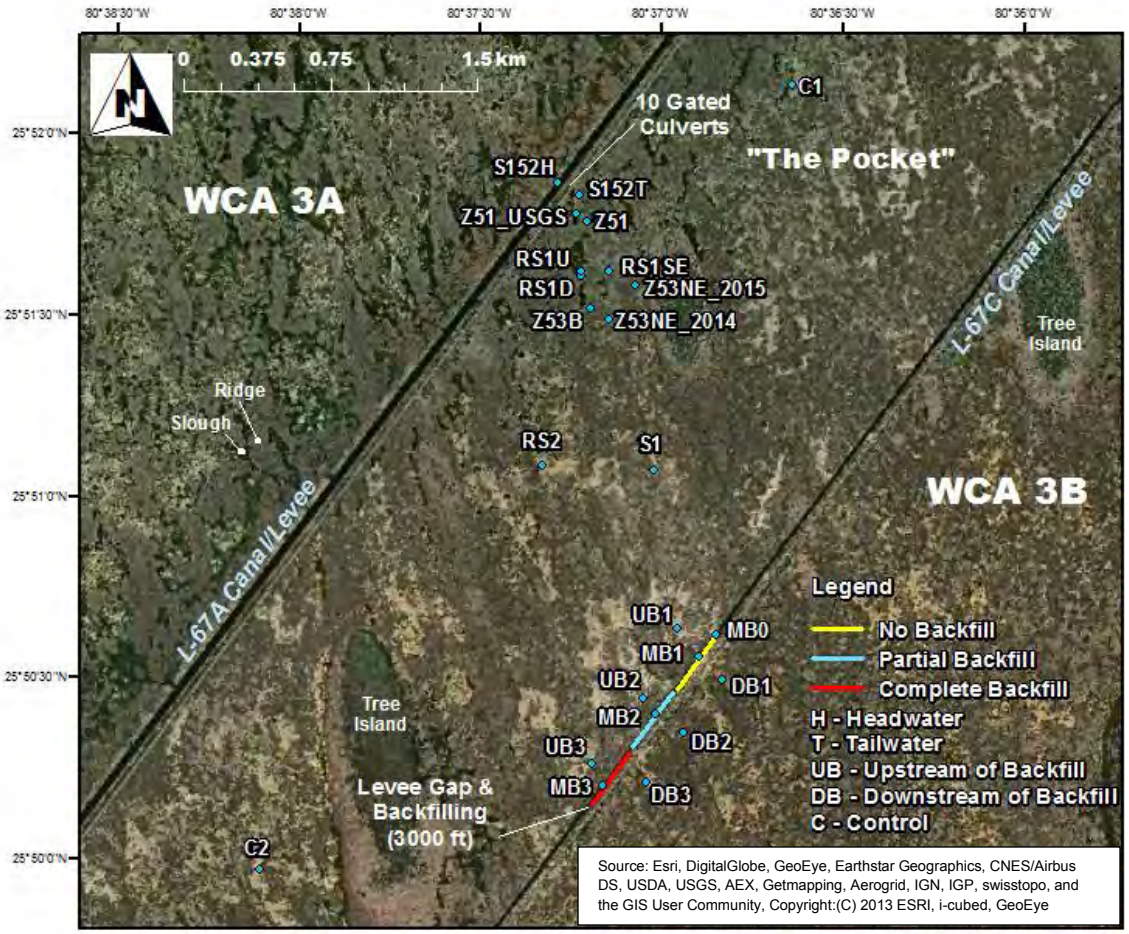

Figure 1. Map of the DECOMP Physical Model (DPM) experimental site located in "the pocket" between the L-67A and L-67C canal/levee structures. Hydrologic and biological response variables are measured at 18 marsh sites and 4 canal sites using a Before-After-Control-Impact (BACI) experimental design. Abbreviations are as follows: C = control; RS = ridge/slough; S = slough; UB = upstream backfill; DB = downstream backfill.

Methods

DPM Experimental Structures and Operations

In order to examine the impacts of restoring Everglades flow to pre-drainage flow conditions, new structures had to be built. The water inflow structure (S-152) was constructed at the northwestern end of the project and is comprised of 10 gated culverts on the L-67A levee that supply gravity drainage from WCA-3A into the experimental DPM area between the L-67A and L-67C levees known as the pocket (fig 1). Toward the south at the downstream end of the project a 3,000-foot gap was created by removing a portion of the L-67C levee. Three experimental levels of canal backfill are represented by 1,000-foot canal segments with complete, partial, and no backfill in the canal, respectively.

Construction of DPM structures and features were initiated in June 2012 and completed in October 2013, in time to allow the first of three planned high-flow events. Measured discharges through S-152 during the 2013, 2014-2015, and 2015-2016 flow releases are listed in Table 1, 2, and 3, respectively. The combined discharge capacity of approximately 250 cubic feet per second through the S-152 structure generated water velocities as high as 4 -5 centimeters per second. The L-67C levee was degraded over a period of months and then breached on 12/7/2012, allowing water to flow from the pocket into WCA-3B unimpeded at moderate to high water levels.

Prior to the first of the S-152 flow release the USGS installed instrumentation to compute continuous records of the headwater stage on the upstream side and the tail water stage on the downstream side of the structure which would serve to calibrate measured flows through S-152 (Mark Dickman, Personnel Communication, September 15, 2015). A Sontek Argonaut SW acoustic Doppler velocity meter (ADVM) was deployed inside of the downstream end of culvert pipe number 2, as counted from the north end of the structure, and a second SW ADVM was installed inside of the downstream end of pipe number 6. To develop discharge ratings, ten discharge measurements were

made on the downstream end of each culvert using a Sontek FlowTracker according to the point velocity area method outlined in the Sontek FlowTracker Technical Manual (Sontek YSI Inc., 2007). The USGS also measured continuous water temperature and specific conductance on the headwater and tail water sides of S-152, EDEN 8, and both sides of Site 69, for the purpose of determining the source of water flowing through the S-152 structure.

Table 1. Discharge measurements at the outlet, or east end, of S-152 during the 2013 experiment (National Water Information System, 2015).

Measurement number	Date and Time	Discharge, in cubic feet per second
1	11/5/2013 3:09:00 PM	303
2	11/6/2013 10:03:30 AM	299
3	11/7/2013 10:53:30 AM	308
4	11/12/2013 11:03:30 AM	291
5	11/20/2013 10:50:00 AM	260
6	11/25/2013 10:53:00 AM	266
7	12/10/2013 11:24:00 AM	267
8	12/27/2013 11:59:30 AM	255

Table 2. Discharge measurements at the outlet, or east end, of S-152 during the 2014-2015 experiment (National Water Information System, 2015).

Measurement number	Date and Time	Discharge, in cubic feet per second
1	11/4/2014 11:50:00 AM	276
2	11/4/2014 12:50:30 PM	272
3	11/4/2014 1:39:00 PM	275
4	11/7/2014 12:34:00 PM	268
5	11/7/2014 12:35:00 PM	260
6	11/13/2014 11:29:00 AM	283
7	11/25/2014 11:33:13 AM	283
8	11/25/2014 12:00:30 PM	274
9	12/8/2014 10:26:00 AM	285
10	12/22/2014 11:24:00 AM	280
11	12/22/2014 11:35:00 AM	282
12	1/13/2015 11:10:00 AM	276
13	1/26/2015 11:24:00 AM	245
14	1/26/2015 11:27:00 AM	237

Table 3. Discharge measurements at the outlet, or east end, of S-152 during the 2015-2016 experiment (National Water Information System, 2015).

Measurement number	Date and Time	Discharge, in cubic feet per second
1	11/16/2015 13:15:15 AM	242
2	11/23/2015 12:14:45 PM	276
3	11/23/2015 12:19:30 PM	301
4	12/9/2015 13:39:14 PM	359
5	12/16/2015 13:46:30 PM	339
6	12/16/2015 13:47:00 AM	323
7	1/7/2016 12:43:17 AM	324
8	1/20/2016 13:14:00 AM	367
9	1/20/2016 13:57:39 AM	337
10	2/19/2016 13:09:24 AM	544

Benchmark Elevation Surveying

Minor variations in topography are important drivers of sheet flow in the extremely flat terrain of the Everglades. Traditional ground-based surveying is impractical in the DPM research area as a result of the long distances involved, the challenging water-covered environment and the soft sediment conditions. A satellite-based survey was conducted to establish benchmark elevations at most of the DPM research sites in order to determine ground elevations and to relate the measured water levels across the project area to a common elevation datum.

Static surveys were performed using Global Navigation Satellite Systems (GNSS) techniques following general guidance (Rydlund and Densmore, 2012) to achieve Level 1 precision, i.e., the highest quality with the lowest achievable uncertainty. Surveys were conducted three times between 2012 and 2015. Elevations were determined in the NAVD 1998 datum of fixed benchmarks that were installed near the platforms at DPM sites Z51_USGS, RS1D, RS2, S1, UB1, UB2, UB3, DB2, C1, and C2. Each survey consisted of two four-hour static deployments, one each day, with the first deployment in the morning the first day and the second during the afternoon the second day to collect data from a

different set of satellites during each survey. Data files were submitted to NGS Online Positioning User Service (OPUS) program for processing. Differential gaging station leveling techniques (Kenney, 2010) were used to transfer the NAVD 88 elevation from the monument to the other reference markers at DPM research sites.

Microtopography

Small-scale topography variations (referred to as microtopography) were measured at various sites, focusing on determining the surface elevations of the flocculent organic surface of the wetland and the underlying consolidated peat along ridge to slough transects. This was accomplished by repeatedly collecting measurements of the depth from the water surface to the surface of the floc and peat, and then relating the surface water elevation to a local surveyed elevation. The water depths to floc and peat, $h_{floc,}$and h_{peat}, are measured by determining the vertical distance from the water surface to the floc and peat using a calibrated CPVC depth probe with an I-shaped foot, as described in Choi and Harvey (2013). The probe was gently placed on the floc to measure the depth to floc, and then pressure was applied to sink the probe through the floc in order to measure the depth to peat.

In 2010 and 2011, measurements were made at approximately 30 points, oriented in a large circle with a radius of roughly 100 m. At each of the 30 locations, 6 microtopography measurements were taken (6 floc surface elevations and 6 corresponding peat surface elevations). The position of the circle was chosen to include both ridge and slough topographies. Additionally, from 2010 to the 2016, water depth to floc and water depth to peat measurements were collected near the study sites, as well as along ridge to slough transects at each site. Three measurements were collected within one square meter at each sampling point to calculate an average water depth to the floc and to the peat.

The elevations of the ground surfaces, with subscript *floc* indicating the flocculent organic matter surface and *peat* indicating the consolidated peat surface, e.g., Z_{floc} or Z_{peat}, respectively, were found by subtracting the measured water depth to the floc or peat (h_{floc} or h_{peat}) from the surface water elevation (Z_{WL}) at the site for a given day and time, e.g.:

$$Z_{floc} = Z_{WL} - h_{floc} \quad (1)$$

$$Z_{peat} = Z_{WL} - h_{peat} \quad (2)$$

At sites where surface water elevation was not available, a surface water level was applied from the next closest site, if the site was within 30 meters. At such a relatively short distance water level differences are insignificant.

Surface Water and Groundwater Levels

Surface water levels were obtained using methods suggested by the USGS Office of Surface Water (Kenney, 2010) using pressure transducers with an accuracy of +/- 0.3 cm and that record water level at 5-15 minute intervals. Pressure transducers (KPSI 501 series) were deployed by emplacement in 1.5 inch PVC standpipes. The PVC standpipes were affixed with a through-bolt to a steel pipe previously driven into the bedrock. The reference marker (RM) is located at the top of the steel pipe, and the reference markers are surveyed for the elevation (Z_{RM}) by GNSS technique. Pressure transducer sensors were suspended within standpipes at a pre-determined height where the hole on the side of each sensor was close enough to the ground surface that surface water could always enter the hole, even at very low water levels. The elevation of the KPSI pressure transducer sensor (Z_{KPSI}) is determined by relating the RM elevation and measured distance between RM to KPSI senor. KPSI transducer-measured water levels, $Z_{WL\text{-}KPSI}$, were calculated by adding transducer hydrostatic pressure readings, HP_{KPSI}, to the transducer reference elevation, Z_{KPSI}:

$$Z_{WL-KPSI} = Z_{KPSI} + HP_{KPSI} \quad (3)$$

Another alternate measurement of surface water elevation using reference markers were made during site visits to serve as checks on the measurements of surface water elevation using KPSI transducers. These discrete measurements of a reference surface water elevation, ($Z_{WL\text{-}RM}$), were made by measuring as the vertical distance from the top of the reference steel pipe (*RM*) down to the surface of the water, which is referred to as a down to water measurement (*DTW*). *DTW* measurements were subtracted from the elevation of the top of the reference mark (Z_{RM}) to determine a reference water elevation ($Z_{WL\text{-}RM}$).

$$Z_{WL-RM} = Z_{RM} - DTW \quad (4)$$

The reference water levels are independent of pressure transducer data and therefore serve as a check on pressure transducer measurements. Transducer-measured water levels were compared with reference water levels to account for offset and drift of transducers. Over time the expected slope of $Z_{WL\text{-}KPSI}$ measurements plotted versus $Z_{WL\text{-}RM}$ measurements is expected to be 1 with an intercept of zero. On a given site visit no adjustment was made unless the difference of $Z_{WL\text{-}KPSI}$ and $Z_{WL\text{-}RM}$ was greater than 0.7 cm. If the difference was greater, an average of the offset measured during that visit and the offset measured during the previous visit was used for the time period between visits. USGS data on water levels from EDEN-8 (located in WCA-3A), TI-9 (located in WCA-3B), and water levels from the S-152 Headwater and S-152 Tailwater sites were included for comparison with DPM water levels.

Pressure transducers were installed at sites C1, C2, DB2, MB2, Z51_USGS, RS1D, RS2, S1, UB1, UB2 and UB3. Additionally, three sites, Z51_USGS, RS1 and UB2, had groundwater transducers installed. Groundwater transducers collected data in 15-minute intervals. Data were downloaded and instrument diagnostics performed at approximately monthly intervals. Surface water transducers began deployment in October 2010 and will remain deployed for the duration of the DPM project.

Groundwater transducers were installed in November 2012 and will also remain deployed for the remainder of the project.

Groundwater-surface water interactions were assessed by measuring the vertical hydraulic gradient, d*h*/d*L,* through the peat layer, where previously they were observed with environmental tracers and seepage meters (Harvey et al. 2004). To calculate the gradient, the measured reference elevation of surface water ($Z_{WL\text{-}RM,sw}$) from the elevation of the groundwater ($Z_{WL\text{-}RM,gw}$) and dividing that difference by the vertical distance (L) from the center of the screen of the piezometer emplaced in the peat to the peat surface.

$$\frac{dh}{dL} = \frac{\left(Z_{WL-RM,sw} - Z_{WL-RM,gw}\right)}{L} \tag{5}$$

As defined, the hydraulic gradient expresses groundwater recharge as a positive value and discharge as a negative value. Reference groundwater elevations are determined by measuring *DTW* inside the groundwater piezometer at the time of site visits. Hydraulic gradients were also analyzed using transducer-measured water levels ($Z_{WL\text{-}KPSI,sw}$ and $Z_{WL\text{-}KPSI,gw}$), with careful consideration given to correct transducer offset and drift to achieve the needed accuracy.

Surface Water Flow Velocities and Shear Stress

Flow velocity was measured in surface water at the main monitoring sites (C1, C2, Z51_USGS, RS1D, RS2, S1, UB1, UB2, UB3, DB1, DB2, DB3, MB0, MB1, and MB2) that were selected to overlap with other hydrologic and biogeochemical measurements (fig 1). Flow velocity was measured by 10 megahertz [MHz] up/down/side-looking Acoustic Doppler Velocimeters (ADV) manufactured by SonTek/YSI and by Vectrinos manufactured by Nortek. In the canal sites, MB1 and MB2, Autonomous Argonaut XRs were deployed (manufactured by SonTek). The ADV and Vectrino approach can

measure flow velocity to a resolution of 0.01 cm/s and 0.1 cm/s with an accuracy of 1% and 0.5% of measured velocity, respectively (SonTek, 2001).

The general operating procedure for ADVs outlined in Harvey et al. (2009) was followed for data collection. Continuous velocities were collected from a fixed depth at approximately the midpoint of the water column at a frequency of 10 Hz. ADV flow velocity data were recorded in one minute bursts (600 samples), and collected every 15 minutes to save battery power. Velocity datasets were filtered and edited according to standard criteria suggested by the instrument manufacturer (SonTek, 2001) as well as specific criteria developed and refined in a prior Everglades study (Riscassi and Schaffranek, 2002). To ensure data quality, ADV data had to pass a 40% minimum correlation filter with at least 70% of samples within a burst being retained (Martin et al., 2002). Data with an acoustic signal-to-noise ratio (SNR) of 5 dB or less were discarded. The ADV data collected during times when the boats were known to be present at the monitoring sites were removed. A sound-speed correction was applied to ADV data using either data from an attached Convention Temperature Device (CTD) or average temperature and salinity recorded by a nearby CTD during the deployment period. The Vectrinos also applied a sound-speed correction using an embedded thermistor and measured salinity. The 3-dimensional velocity data underwent a rotation for magnetic declination, as ADVs and Vectrinos were deployed such that the positive x-velocity direction was oriented to the direction of magnetic north. Finally, a phase space threshold despiking algorithm (Goring and Nikora, 2002) was applied to both ADV and Vectrino data. The resulting quality-assured data were used to produce hourly and daily values and statistics. Calculations of standard deviation of flow direction were performed using the Yamartino method (Yamartino, 1984).

ADVs were serviced during continuous deployments, during which data were downloaded, batteries were replaced, the compass was calibrated and diagnostics were performed on the instrument.

Between site visits, the height of the ADV sensor was adjusted to keep the sensor submerged until the next site visit. The height of each ADV sensor was adjusted to keep the sampling volume approximately at or slightly below the middle depth of the water column anticipated for the deployment period. ADVs were deployed on average for sixth months in 2010-2014 water years, centered on the operational window for flow releases (November and December).

Velocity profiles were measured vertically in the water column using Sontek ADVs as described in Harvey et al. (2009), during most monthly site visits by adjusting the height of the ADV sensors deployed for continuous monitoring. Nortek Vectrino instruments were used to measure velocity profiles at discrete sites. For the profiles, velocities were measured at 10 Hz in 1 minute bursts yielding 600 samples at each depth increment. Flow velocities were measured at 2-5 cm depth increments throughout the water column, depending on total water depth, apparent vertical variability in vegetation architecture, and overall favorability of measurement conditions and time constraints. Signal-to-noise-ratios were monitored continuously during collection of the vertical velocity profiles to determine if the sample volume was obstructed by vegetation and as an indicator of the vertical location of the top of the floc. Velocity profile data underwent the same corrections and filters as the continuous velocity data. In some cases, bursts in which fewer than 70% of samples passed the 40% correlation filter were retained if the data seemed reasonable, in order to avoid complete elimination of useful data. The large number of samples averaged for each burst and the filtering and quality assurance procedures used to edit and process the data provided confidence that the maximum possible resolution (0.01 cm s^{-1}) reported for this instrumentation (SonTek, 2001) was achieved in these measurements.

Discrete velocities were sampled along vertical water column profiles with a Sontek ADV FlowTracker at sites where no continuous ADV data were collected and where use of a Nortek Vectrino was impractical. The FlowTracker approach can measure flow velocity to a resolution of 0.01 cm/s with

an accuracy of 1% of measured velocity (SonTek, 2001). Data were recorded in one minute bursts collected at different depths; low (5cm above floc surface), middle of the water column and upper (5cm below water surface). The FlowTracker was positioned in a location with approximately 30cm of clear space around the sensor and vegetation was clipped if necessary. The operating procedure performed was followed according to the FlowTracker Handheld ADV Technical Manual (2007) and post-processing QA/QC followed the procedures described above for the ADVs.

For the velocity at the canal, acoustic doppler profilers (Argonaut-XRs) were deployed at MB0, MB1 and MB2 (Figure 1) to provide continuous records of velocity profiles. The Argonaut-XR approach can measure flow velocity to a resolution of 0.1 cm/s and 0.1 cm/s with an accuracy of 1% of measured velocity, respectively (SonTek, 2001). Argonaut-XRs were deployed in an up-looking configuration and sample vertical profiles of flow speed and direction in one-minute bursts collected every 15 minutes. Post-processing QA/QC followed the procedures described above for the ADVs. Depth-averaged flow velocities were computed directly from the profiles.

A step not yet accomplished that could improve estimates is to relate instantaneously measured velocity profiles to long-term data collected at a single point in the water column. Essentially, point velocities can be converted to depth-averaged velocities using velocity profile shape factors described in the procedures documented in Lightbody and Nepf (2007) and in Harvey et al. (2009).

Bed shear stress measurements were taken pre-release and during the flow release at 6 discrete points along the RS1U ridge-to-slough transect using a Vectrino II Profiler ADV, manufactured by Nortek. To compute bed shear stress, a Vectrino Profiler was mounted on a vertically sliding rod and deployed to sample flow immediately above the bed. Each instrument reading consisted of instantaneous velocity collected over 18 points within a 2.5-cm vertical profile, at a spacing of 2.0 mm. The instrument was operated at high power to achieve the maximum signal-to-noise ratio, with pinging

set to "max interval." Each reading was acquired over a period of 5 minutes. At the end of 5 minutes, the profiler was moved to its next location along the sliding rod (which overlapped with the first by about 0.5 cm) and again deployed. In this manner, four stacked 2.5-cm profiles were obtained near the bed. A fifth 2.5-cm profile was acquired in the middle of the water column at each site.

Raw velocity records were filtered to remove data points that did not meet standards for signal-to-noise ratio (at least 5 dB), correlation (at least 40%), or consistency in redundant measurements of the z-direction velocity component. Instrument noise spikes were removed using Goring and Nikora's (2002) threshold despiking algorithm. Following Biron et al. (2004), profiles of total stress were calculated as the sum of the total kinetic energy derived stress and laminar stress, as follows:

$$\tau_t(z) = C_1[0.5\rho(< u'^2 > + < v'^2 > + < w'^2 >)] + \mu\left(\frac{dU}{dz}\right) \quad (6)$$

where C_1 is a proportionality constant equal to 0.19, *u', v',* and *w'* are the velocity fluctuations of the streamwise, vertical and lateral components, < > denotes a temporal average, μ is dynamic viscosity [Pa·s], and *U* is the flow speed [cm/s] at a height of *z* above the bed [cm], where *U* is given as the resultant of the component-wise velocities, $(<u>^2 + <v>^2 + <w>^2)^{1/2}$. The maximum near-bed total stress was selected as the bed shear stress.

Suspended Particle Sizes and Concentrations

During both DPM flow releases in 2013, 2014, and 2015, samples were collected for analysis of suspended sediment concentration (SSC), SSC load, suspended particle size, and associated total phosphorus (TP) concentration and TP load. Water column samples were collected by peristaltic pumping at a rate of 60 ml/min through size 16 Masterflex tubing with a 500 μm Nitex screen fitted to tubing inlet. Two liters sample was collected for SSC analysis, 250mL was collected to be run in the field on the LISST-Portable, and a 60ml sample was collected for TP analysis which was preserved with

H_2SO_4 at a pH of 2 and placed on ice before shipment to the South Florida Water Management District Lab.

During the DPM high flow event beginning in November 2013 the water column samples were collected at sites RS1U, UB1, UB2, S1, DB1, DB2 and DB3 prior to the high flow (before 09:40 11/5/2013), during the flow breakthrough (09:40 11/5/2013 –11/6/2013), and during the steady high flow that followed (11/7-8/2013, 11/10/2013). During the DPM high flow event beginning in November 2014 the water column samples were collected at sites RS1U, RS1D, Z53B, RS2, S1, UB1, UB2, UB3, DB1, DB2, DB3, RS1SE, Z51 and S-152 prior to the high flow (before 09:43 11/4/2014), during the flow breakthrough (09:43 11/4/2014 – 11/5/2014), and during the steady high flow (11/7/2014, 12/4/2014, 1/21/2015) and after the closing of S-152 (3/9-10/2015). During the DPM high flow event beginning in November 2015, the water column samples were collected at sites Z51_USGS, RS1D, RS1SE, UB1, UB2, UB3, DB1, DB2, DB3 (before 09:40 11/16/2016, 12/9/2015, 1/20/2016, and 3/2/2016). During the two pulsed high-flow period, the water column samples were collected at sites Z51_USGS, RS1D, and RS1SE (09:40 to 17:00 11/16/2015, 9:00 to 17:00 11/17/2015, 09:40 to 17:00 11/19/2015, 9:00 to 17:00 11/20/2015).

Site names beginning with "RS" had paired sampling from nearby ridge and slough. At other sites samples were collected from only sloughs. At RS1U samples were collected at 2-meter spaced intervals across the transition between ridge and slough (fig 2). At the transect endpoints in the ridge and slough the samples were collected to represent the upper third, middle, and near-bed water (5cm above floc surface) water column. At RS1U locations between the transect endpoints only near-bed samples were collected. Samples from the upper water column were omitted in 2014. In 2014 sites RS1D, Z53B, RS1SE and RS2 were sampled from the low and middle water column in the ridge and slough. At

slough sites Z51_USGS, S1, UB1, UB2, UB3, DB1, DB2 and DB3, samples were collected from only the low and middle water column.

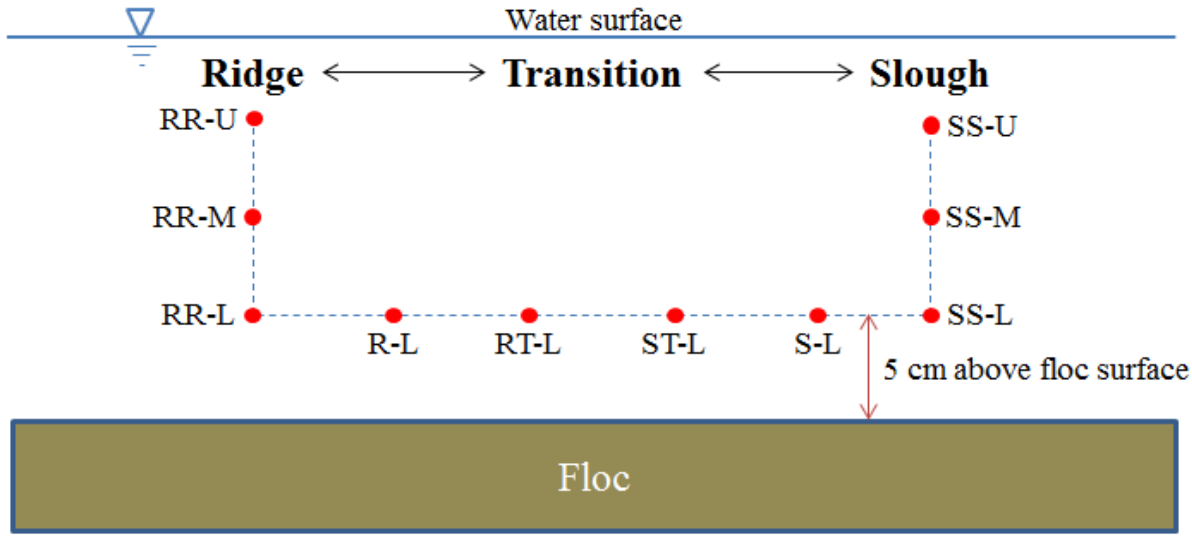

Figure 2. SSC and TP sampling scheme along the RS1U transect.

In the laboratory the volume of each suspended sediment sample was measured prior to filtration with a graduated cylinder. Each sample was then processed by vacuum filtration through a 0.7 μm filter (Whatman GF/F) (Noe et al., 2010). Filters were prepared by vacuum filtering 100mL of deionized water through the filter and then heating at 500°C for one hour to remove any present organic material. The initial dry mass of the filter was measured on an analytical balance. The sediment laden filters were oven dried at 60°C and then weighed with an analytical balance. With this information, suspended sediment concentration was calculated for each sampling time at each site by subtracting the mass of the dried filter from the mass of the sediment laden filter and dividing the difference by the volume of the sample.

Duplicate SSC and TP samples were collected on 11/5/13 at two locations (sites RS1U_RR-M and RS1U_SS-M) and on 11/8/13 at two locations (sites S1_L and UB1_L). They were also collected at sites RS1U_RR-M and RS1U_SS-M on 3/10/2015 and UB2 and DB2 on 3/9/2015. Duplicate samples were analyzed to determine the amount of error present within sampling and processing methods.

Total phosphorus concentrations (TP) of the water column samples were analyzed by the South Florida Water Management District Lab by first subjecting the samples to an acid-persulfate digestion to convert organic and inorganic phosphates into reactive phosphate. Total Phosphorus analysis is based on the formation of a blue-colored antimony-phosphomolybdate complex from the reaction of ammonium molybdate, and antimony potassium tartrate with reactive phosphate in an acidic medium followed by reduction with ascorbic acid. The blue color complex is measure by photometric analysis at 880 nm on the Lachat Flow Injection Analyzer (FIA) with a detection limit of 0.002 mg/L and detection range of 0.002 to 0.4 mg/L. The total phosphorus concentration includes phosphorus associated with sediment and dissolved in the water column.

Depth-averaged values of SSC and TP concentration were calculated at locations where vertical sampling was conducted in the water column. The total water depth was divided into water column intervals (WCI_i) where subscript i is a counter for water column intervals for which there were as many as the number of samples collected vertically in the water column. The WCI_i for a given sample was determined by summing the vertically measured half-distances to the adjacent samples above and below (or the whole distance if the sample in question is the nearest to the floc surface or water surface). The depth-averaged concentration is calculated by

$$\overline{X} = \frac{\sum_{i=1}^{n} X_i * WCI_i}{h_{floc}} \tag{7}$$

where $\overline{X}$ is the depth-averaged concentration of X_i [mg/mL], such as SSC or TP, n is the number of water column intervals [unitless], WCI_i is the water depth interval [cm] for subsample i, and the total water depth to the floc surface, h_{floc} [cm] is equal to $\sum_{i=1}^{n} WCI_i$.

Depth-averaged SSC and TP concentrations were analyzed spatially to determine distribution variation across the study area. Distances were calculated as a nominal distance along the predicted flow path. To simplify the analysis, the primary flow path direction was chosen as a linear path from the S-152 culverts to site MB2, another linear path segment from site MB2 through site DB2. Site locations were perpendicularly projected to the primary flow path to calculate the nominal distance from the S-152 culverts.

The flux of SSC and TP per unit cross sectional area of wetland was determined using velocity data collected by either a Sontek ADV or Nortek Vectrino at each sampling location and water depth where SSC was sampled. If multiple flow velocities had been measured within a water column interval, the depth-averaged velocity within that interval was applied. Load, mass flux per unit width, is calculated by:

$$L_{ssc,i} = C_{ssc,i} * u_i * WCI_i \tag{8}$$

$$L_{SSC,T} = \sum_{i=1}^{n} (L_{ssc,i}) \tag{9}$$

Where C_i = concentration [mg/cm^3], u_i = velocity [cm/s], WCI_i = water column interval [cm], $L_{ssc,i}$ is the load per unit width [mg/cm/s] for water column interval i, and $L_{SSC,T}$ is the total load per unit width [mg/cm/s] for the entire water column. The same approach for load calculations was applied for TP as for SSC. The direction of the depth-averaged load was calculated using depth-averaged east- and north-components of flow velocity and depth-averaged concentration of SSC and TP, which allows loads to be displayed as vectors.

Water column samples collected by the same method and at the same time as samples for SSC and TP were analyzed in the field to determine suspended particle size. A LISST-Portable benchtop laser diffraction particle size analyzer (Seqouia Scientific) was used to optically analyze suspended sediment to produce size distributions across a range from 0.34 - 500 μm. This instrument has a resolution of <1 mg/l an accuracy of ± 20% of measured concentration. The Three to five sample runs were averaged to determine the average particle size distribution. The analyzer also computed metrics such as median volume-weighted, D_{50} which is the grain diameter at which 50% of the sediment sample is finer. Sediment sizes D_{10} and D_{60} were also computed to quantify the 10% and 60% finer than fractions. A particle size uniformity coefficient, D_{60}/D_{10}, was calculated with larger values of D_{60}/D_{10} indicating a more poorly sorted suspended sediment sample. Depth-averaged values for D_{50} and D_{60}/D_{10} were calculated with the same using the same procedure to calculate depth-averaged SSC values.

Continuous records (on the order of days) of suspended particle size distributions were obtained at a single site using a laser diffraction particle size analyzer (LISST-100X or LISST-FLOC, Sequoia Scientific) as described in Noe et al. (2010) and Harvey et al. (2011). The Sequoia LISST instruments emit light and measure laser diffraction to estimate the in situ volume concentration and size distribution of particulates in suspension. The particle size measurement range is 1.25 - 250 μm and 7.5 - 1500 μm for the LISST-100X and LISST-FLOC, respectively, and the ranges are analyzed by dividing into 32 logarithmically spaced size-class bins. The resolution of LISST-100X and LISST-Floc is less than 1mg/L. The instruments are deployed horizontally at the mid-point of the water column and programmed to collect data in 60-second bursts every 15 minutes. The instruments can be subject to biofouling, which limits deployment to periods of up to three days.

All outputs of LISST particle size distributions from the several different instrument models are volume-weighted. To convert volume-weighted to mass-weighted values, a particle density distribution

was applied to the LISST output based on a settling column experiment using Stoke's Law to compute particle density as a function of particle size as described in Larsen et al. (2009a) and implemented in Harvey et al. (2011).

Biogeochemical Sampling

Water column, metaphyton (i.e., epiphyton and floating periphyton), and bed floc samples were collected and analyzed for particulate phosphorus, organic content, and particle size. Water column samples were collected using a peristaltic pump from the mid-point of the water column. Metaphyton samples were collected using a wet/dry vacuum to collect epiphyton from vegetation stems and periphyton at mid-water depth, as described in Larsen et al. (2009a). Bed floc samples were collected by coring the floc/peat, allowing the sample to settle, pouring off any clear liquid, and then retaining the remaining suspended sample (floc). Water column, floc and metaphyton samples were passed through 500 μm Nitex filter prior to being stored on ice and were shipped either the same day or the next day to the analytical laboratory. Particle size analyses were performed in the field on a LISST-Portable benchtop laser diffraction particle size analyzer (Sequoia Scientific) as previously described.

Samples were shipped over night to the Wetland Biological Laboratory, University of Florida, Gainesville, FL in coolers containing wet ice to maintain a sample temperature of 4°C. The following biogeochemical analyses were performed: dry weight of solids, loss on ignition (LOI), total nitrogen (TN), total phosphorus (TP) digestion and analysis, $NaHCO_3$ extraction, and $NaHCO_3$ plus chloroform extraction. For dry weight, samples were dried to a constant weight (detection limit of 0.01%), and for LOI, samples were ignited at 550±50°C in a muffle furnace. Weights were determined using scales and balances verified daily using NIST certified weights. TN was found using a Thermo

Electron FlashEA 1112. Samples for TP underwent a perchloric acid digestion and were analyzed using a Technicon Autoanalyzer AA3.

The results from $NaHCO_3$ and $NaHCO_3$ plus chloroform extraction were used to determine organic phosphorus fractions consisting of refractory, microbial and labile phosphorus (Ivanoff et al., 1998) as follows:

$$L = P_{NaHCO3} \tag{10}$$

$$M = P_{\mathrm{NaHCO3+Chloroform}} - P_{NaHCO3} \tag{11}$$

$$R = TP - (L + M) \tag{12}$$

$$L_{fraction} = \frac{L}{TP} \tag{13}$$

$$M_{fraction} = \frac{M}{TP} \tag{14}$$

$$R_{fraction} = \frac{R}{TP} \tag{15}$$

where $L(P_{NaHCO3})$ is the labile phosphorus concentration [mg/kg] removed through extraction with $NaHCO_3$ [mg/kg], M is microbial phosphorus concentration [mg/kg] which is the difference between the phosphorus extracted by $NaHCO_3$ and $NaHCO_3$+ Chloroform ($P_{NaHCO3+Chloroform}$), R is refractory phosphorus concentration [mg/kg], and TP is the total phosphorus concentration [mg/kg]. The subscript "fraction" indicates the fractionation of TP.

Vegetation Influence on Sheet Flow

Vegetation community structure is an important factor affecting the shape of velocity profiles, in determining the distribution of velocities close to the bed and in measuring entrainment and transport of suspended sediment (Harvey et al. 2009; Larsen et al., 2009b). Therefore, vegetation community composition, biomass (biovolume, including separate analysis of periphyton), and stem densities were determined by harvesting of vegetation in 0.25 m^2 clip plots and measuring the distribution of stem

diameters and frontal areas (Harvey et al., 2009; Lightbody and Nepf, 2006). Within a desired sampling area the vegetation quadrats were positioned using a stratified random sampling scheme at ridge, slough, and transition zones at all sites within the hydrologic monitoring network. Once the quadrats were situated the vegetation above the water surface was clipped and bagged as one sampling increment. Below the water surface, vegetation was sampled in 10 cm increments from 2010 - 2012 and 15 cm increments from 2013 - 2014 proceeding from the water surface to the sediment water interface. Sample increments intersecting the bed were clipped at the floc surface, bagged, and stored in the dark and on ice for transport to the laboratory for further processing.

In the lab, sample increments were spread out and categorized by species. Measurements of stem diameter and length were collected for the purpose of calculating the average diameter and the frontal area of stems, i.e. the exposed area of stem per unit volume in the water column. First the number of stems and leaves were counted for *Cephalanthus occidentalis, Cladium jamaicense, Justicia angusta, Nymphaea odorata,* and *Panicum hemitomon.* The width of 10 randomly selected stems were measured for each species, with width being measured as the distance across the middle of each stem fragment along the widest dimension (major axis) and across the narrowest dimension (minor axis) as measured using a micrometer. For every leaf (or if there were greater than 10 leaves, 10 were randomly chosen) the width, length and thickness were measured using a ruler or micrometer. Frontal area and dimensional volume were then calculated as: The following equation was used to calculate frontal area:

$$a = \left(\frac{d_{Axis1} + d_{Axis2}}{2}\right) * n \tag{16}$$

where a is projected frontal area per unit volume [cm^{-1}], d_{Axis1} is average stem diameter of Axis 1 [cm], d_{Axis2} is average stem diameter of Axis 2 [cm], and n is the number of stems per unit area [cm^{-2}]. Due to the "v" shape cross section of sawgrass, a separate equation was used to calculate its volume. The following equation was used to calculate dimensional volume for all species except sawgrass:

$$V = \pi * d_{Axis1} * \ d_{Axis2} \ * \frac{1}{4} * n \quad (17)$$

and the following equation was used for sawgrass:

$$V_{sawgrass} = d_{Axis1} * \ d_{Axis2} \ * \frac{1}{2} * n \quad (18)$$

where V is dimensional volume per unit volume [unitless], d_{Axis1} is average stem diameter of Axis 1 [cm], d_{Axis2} is the average stem diameter of Axis 2 [cm], and n is the number of stems per unit area [cm^{-2}].

Vegetation measurements were made repeatedly during the years of experimentation to establish a record of temporal variation related to seasonal and interannual variations and fire. Vegetation-flow relationships are being determined to verify empirical predictive relationships between biomass and flow resistance parameters used in hydraulic models (e.g., Harvey et al., 2009). In addition, vegetation measurements were used to help characterize how flow affects key ecological processes such as ecosystem primary production, decomposition, and nutrient cycling.

Water Quality Monitoring

Water quality parameters were monitored to quantify arrival times of conservatively transported environmental tracers and suspended sediment with the water release into the pocket by the opening of the S-152 culverts. Specific conductivity is a potentially useful tracer to quantify the relative speed of the released water in sloughs and ridges and of the rate of mixing between those waters, as well as the transport rate of suspended sediment entrained during transport.

During the high flow releases in November 2013 and November 2014 continuous measurements of specific conductivity and turbidity were collected by deploying YSI sondes at selected sites prior to the opening of the culverts and collecting them 4 days later. The turbidity probe has the range of 0 to 1000NTU, resolution of 0.1 NTU, and accuracy of +/- 2%. And the conductivity probe has the range of

0 to 100 mS/cm, resolution of 0.00 to 0.1mS/cm, and accuracy of +/- 0.5%. Sondes were deployed at sites RS1U_S, S1, UB1, DB1, DB2, and DB3 in 2013 and Z-51_USGS, RS1U_S, RS1U_R, RS1D_S, RS1D_R, Z5-3B_S, RS1-SE_S, RS1-SE_R, Z5-3NE_S, and Z5-3NE_R in 2014. Additional data were attained from USGS stations at 3A, S-152 Headwater and Tailwater, and Site 69 East and West for comparison.

To install the sondes in the water column, 1.5 inch PVC pipes were placed in the peat and the YSI sondes were attached to the exterior of the pipes such that the sensors were approximately at the midpoint of the water column. Sampling occurred autonomously on five minute intervals. The YSI turbidity probe is an optical probe with an autonomous cleaning mechanism to prevent biofouling. Before deployment, the turbidity probes were checked in deionized water and if they were not reading within +/- 2 NTU, a 3-point calibration was performed. The conductivity probes were checked in 250 µS/cm standard. If values were not within +/- 5 µS/cm, a 1-point calibration was performed. If no calibration was necessary, a 2-point check (50 and 1000 μS/cm) was performed. Immediately before deployment, all sonde readings were checked against one another in south Florida tap water.

Groundwater- Surface Water Interactions Detected using Heat as a Tracer

Groundwater-surface water interactions are often difficult to detect by hydrometric measurements. Vertical water flux through peat can be estimated from observations of the hydraulic head gradient using Darcy's Law. Vertical flux through a peat also may be detectable by deploying temperature sensors vertically in sediment and modeling heat transport to constrain the vertical flux of water. Traditional piezometers were installed with four temperature sensors in the DPM experimental footprint in the central Everglades at sites RS1D, S, UB2 and Z51-USGS. Each piezometer is made of a 0.5m long and 1 inch wide PVC pipe enclosing four TMCx Water/Soil temperature sensors connected

to a single HOBO U-12 4-channel data logger (with resolution 0.02℃ and accuracy ±0.25℃). The piezometer was inserted into the peat with temperature sensors located at the floc-peat interface (0 cm depth) and three additional depths within the peat sediment. Three depth configurations were used. Configuration 1 had probes located at 0, 5,15, and 35 cm below the peat surface. Configuration 2 had probes located at 0, 5, 10, and 15 cm below the peat surface. Configuration 3 varied by site and had a probe at the floc-surface water interface, floc-peat interface (0cm), at half of the peat thickness (69-87cm), and at the deepest possible point given the length of pipe (133-143cm). Each sensor collected temperature every 10 minutes from 9/28/2013 to 3/2/2016. Before installation, measurements in a well-mixed, warm bath were used to compare the accuracy of the sensors. For this controlled experiment, the sensors showed an accuracy of approximately 0.05℃, which is better than the accuracy reported by the manufacturer.

References Cited

Biron, P. M., C. Robson, M. F. Lapointe, and S. J. Gaskin, (2004) Comparing different methods of bed shear stress estimates in simple and complex flow fields, *Earth Surface Processes and Landforms, 29*, 1403-1415, doi: 10.1002.

Constantz, J. (2008), Heat as a Tracer to Determine Streambed Water Exchanges, *Water Resour. Res.*, *65,* doi: 10.1029/2008WR006996.

Choi, J., and J. W. Harvey (2013), Relative significance of microtopography and vegetation as controls on surface water flow on a low-gradient floodplain, *Wetlands, 34*, 101-115, doi: 10.1007/s13157-013-0489-7.

Davis, S. M., L. H. Gunderson, W. A. Park, J. R. Richardson, and J. E. Mattson (1994), Landscape dimension, composition, and function in a changing Everglades ecosystem. In: Davis SM, Ogden JC (eds) Everglades: The ecosystem and its restoration. St. Lucie, Delray Beach, pp 419–444.

Davis, S. M., D. L. Childers, J. J. Lorenz, H. R. Wanless, and T. E. Hopkins (2005), A conceptual model of ecological interactions in the mangrove estuaries of the Florida Everglades. *Wetlands, 25*, doi: 10.1672/0277-5212(2005)025[0832:ACMOEI]2.0.CO;2.

Davis, S. M., E. E. Gaiser, W. F. Loftus, and A. E. Huffman (2005), Southern Marl Prairies Conceptual Ecological Model. *Wetlands, 25*, 821-831, doi:10.1672/0277-5212(2005)025[0821:SMPCEM]2.0.CO;2.

Decomp Physical Model Science Team (DPMST) (2010), The Decomp Physical Model Science Plan. 52pp.http://www.evergladesplan.org/pm/projects/project_docs/pdp_12_decomp/060410_decomp_ea_final/april_2010_decomp_ea_app_e_bk.pdf.

Goring, D. G., and V. I. Nikora, 2002. Despiking Acoustic Doppler Velocimeter Data. *Journal of Hydraulic Engineering* Jan 2002: pp 117-126, doi: 10.1061/(ASCE)0733-9429(2002)128:1(117).

Harvey, J. W., S. L. Krupa, and J. M. Krest (2004), Ground water recharge and discharge in the central Everglades, *Groundwater*, *42*(7), 1090–1102, doi: 10.1111/j.1745-6584.2004.tb02646.x.

Harvey, J.W., R. W. Schaffranek, G. B. Noe, L. G. Larsen, D. J. Nowacki, and B. L. O'Connor (2009), Hydroecological factors governing surface-water flow on a low gradient floodplain. *Water Resourc. Res*., 45, W03421, doi:10.1029/2008WR007129.

Harvey, J. W., G. B. Noe, L. G. Larsen, D. J. Nowacki, and L. E. McPhillips (2011), *Geomorphology*. Elsevier B.V. doi: 10.1016/j.geomorph.2010.03.028.

Ivanoff, D. B., K. R. Reddy, and S. Robinson (1998), Chemical fractionation of organic phosphorus in selected histosols. *Soil Science*, *196*, 36-45, doi: 589/35400007825715.0050.

Kenney, T.A (2010), Levels at gaging stations: U.S. Geological Survey Techniques and Methods 3-A19. p 60.

Larsen, L. G., J. W. Harvey, and J. P. Crimaldi (2009a), Morphologic and transport properties of natural floc. *Water Resourc. Res*., 45, W01410, doi:10.1029/2008WR006990.

Larsen, L. G., J. W. Harvey, and J. P. Crimaldi (2009b), Predicting bed shear stress and its role in sediment dynamics and restoration potential of the Everglades and other vegetated flow systems. *Ecological Engineering* 35:1773-1785. doi: 10.1080/00221686.2012.

Lightbody, A. F., and H. M. Nepf (2006), Prediction of velocity profiles and longitudinal dispersion in emergent salt marsh vegetation. *Limnology and Oceanography, 51*(1), 218-228, doi: 10.4319/lo.2006.51.1.0218.

Light, S. S., and J.W. Dineen (1994), Water control in the Everglades: a historical perspective. In: Davis SM, Ogden JC (eds) Everglades: The ecosystem and its restoration. St. Lucie, Delray Beach, pp 47–84.

Martin, V. T. Fisher, R. Millar, and M. Quick (2002), ADV Data Analysis for Turbulent Flows: Low Correlation Problem. *Hydraulic Measurements and Experimental Methods* 2002: pp 1-10. doi: 10.1061/40655(2002)101.

Noe, G. B., J. W. Harvey, R. W. Schaffranek, and L. G. Larsen (2010), Controls of Suspended Sediment Concentration, Nutrient Content, and Transport in a Subtropical Wetland. *Wetlands, 30*, 39-54. doi:10.1007/s13157-009-0002-5.

National Water Information System, Retrieved September, 2015, from http://waterdata.usgs.gov/fl/nwis/measurements/?site_no=255154080371300&agency_cd=USGS

Ogden, J. C., J. Browder, J. H. Gentile, L. H. Gunderson, R. Fennema, and J. Wang (1999), Environmental management scenarios: ecological implications. *Urban Ecosystems* 3: pp 159–184,doi: 10.1672/0277-5212(2005)025[0810:ERASCE]2.0.CO;2.

Ogden, J. C., S. M. Davis, and L. A. Brandt (2003), Science for a regional ecosystem monitoring and assessment program: the Florida Everglades example. pp 135–160. In: D. E. Busch and J. C. Trexler (eds.) Monitoring Systems: Interdisciplinary Approaches for Evaluating Ecoregional Initiatives. Island Press, Washington, DC, USA. doi:10.1672/0277-5212(2005)025[0795:TUOCEM]2.0.CO;2.

Ogden, J. C., S. M. Davis, K. J. Jacobs, T. Barnes, and H. E. Fling (2005), The use of conceptual ecological models to guide ecosystem restoration in south Florida. *Wetlands* 25: pp 810–820, doi: 10.1672/0277-5212(2005)025.

Rudnick, D. T., P. B. Ortner, J. A. Browder, and S. M. Davis (2005), A conceptual ecological model of Florida Bay. *Wetlands*, 25: pp 870-883, doi:10.1672/0277-5212(2005)025.

Rylund, P. H., and B. K. Densmore (2012), Methods of practice and guidelines for using survey-grade global navigation satellite systems (GNSS) to establish vertical datum in the United States Geological Survey. *Techniques and Methods* 11- D1.

Science Coordination Team. 2003. The role of flow in the Everglades ridge and slough landscape. South Florida Ecosystem Restoration Working Group. http://sofia.usgs.gov/publications/papers/sct_flows/index.html. Accessed 1 Dec 2005.

SonTek. 2001. SonTek ADV Acoustic Doppler Velocimeter Technical Documentation. pp 202.

Stallman, R. (1965), Steady one-dimensional fluid flow in a semi-infinite porous medium with sinusoidal surface temperature, *J. Geophys. Res.*, *70*(12), 2821–2827.

SonTek (2007), *FlowTracker Handheld Technical Manual,* 113 pp., San Diego, Calif.

Yamartino, R. J. (1984), A Comparison of Several "Single-Pass" Estimators of the Standard Deviation of Wind Direction. *J. Climate Appl. Meteor.*, 23, pp 1362–1366. doi: http://dx.doi.org/10.1175/1520-0450(1984)023<1362:ACOSPE>2.0.CO;2.

Appendix

Data File Structure

Lettered sections A-H explain data file organization and include a copy of the metadata worksheets for each section.

A. Microtopography: Micro-scale topographic measurements.

File Name: *"Microtopography.xlsx"*, contains the following worksheets

- Metadata
- 2010 and 2011
- C1
- C2
- Z51_USGS
- RS1U
- RS1D
- RS2
- S1
- UB1
- UB2
- UB3
- DB2

Metadata Worksheet - Microtopography		
"Microtopography.xlsx" is an excel workbook presenting data as a part of the data release.		
High-Flow Field Experiments to Inform Everglades Restoration: Experimental Data 2010 to 2016		
Data were collected by USGS for USACE project "CERP: Testing and Monitoring for the Physical Model for Water Conservation Area 3 Decompartmentalization and Sheet Flow Enhancement Project", MIPR W32CS510826251		
This file contains data collected from research areas known as the Decompartmentalization Physical Model (DPM) and WCA-3A and WCA-3B, Everglades, FL		
Datum: WGS84		
Site ID	Latitude	Longitude
S152	25.8640740	-80.6208520
C1	25.8688503	-80.6107030
C2	25.8327940	-80.6351380
Z51_USGS	25.8629310	-80.6206310

Z51	25.8626030	-80.6201250
RS1D	25.8600655	-80.6204093
RS1U	25.8603442	-80.6203967
RS1SE	25.8603150	-80.6190730
Z53B	25.8585970	-80.6199950
Z53NE_2014	25.8581190	-80.6191020
Z53NE_2015	25.8596600	-80.6178700
RS2	25.8513699	-80.6221905
S1	25.8511939	-80.6170715
UB1	25.8438739	-80.6159930
UB2	25.8407041	-80.6175268
UB3	25.8376759	-80.6199131
MB0	25.8436000	-80.6142100
MB1	25.8425860	-80.6149720
MB2	25.8399780	-80.6169440
MB3	25.8366690	-80.6194060
DB1	25.8415550	-80.6138860
DB2	25.8391270	-80.6156970
DB3	25.8368580	-80.6174220

This worksheet tab, "Metadata," provides a summary of the data collection methods, defines all related variables and provides supporting calculations.

In the subsequent spreadsheet, "2010 and 2011," all data collected during those two years are presented, during which time the circle method was used.

In spreadsheets, "C1" through "DB2," data from November 2011 to March 2015 are provided for each site spreadsheet collected using the linear transect method.

Nov 2010 to Nov 2011 Data Collection Methods (Circle Method):

Topography data were collected around a circle with a 100m radius from 4 sites: C1, RS1, S1 and UB2.
At each collection location in the circle, 6 measurements were taken in a smaller circle with a 1m radius around the collection point.
Those 6 measurements were averaged to get an average measurement at that location on the 100m radius circle.
Topography is expressed as centimeters above a vertical datum.
The vertical datum for Topography Data is NAVD88.
Vertical Datum was found using a GPS survey conducted in 2012 along with levels conducted in 2013 in accordance with USGS protocol.
Period of Record for Topography Circle Data Collection: Topography was collected 11/08/2010 for UB2, 11/06/2010 for RS1 and 11/03/2011 for S1 and C1.
EDEN-8 and Site 69W are located in WCA-3A, Site 69W is in the pocket and TI-9 is located in WCA-3B.
The heading "All Observations" refers to the values calculated from all the raw measurements with no averaging.
100m refers to the values found through averaging from the 6 measurements taken at each point in the 100m circle.
1m refers to values within the 1m circle taken at each location in the 100m radius circle.
The GPS coordinates for each station located in the center of the 100m circle are located in the tab marked

"Site Locations."	
Nov 2011 to March 2016 Data Collection Methods (Linear Transect Method):	
Topography was measured at each of the following sites: C1, C2, Z51_USGS, RS1U, RS1D, S1, UB1, UB2, UB3, and DB2. **Topography measurements were taken along a linear transect.** **Measurements were taken of depth to the surface of the floc and depth to the surface of the peat.** **When possible, 3 depth-to-floc and 3 depth-to-peat measurements were taken at each point along the transect and averaged.** **Depth to floc and depth to peat were converted into elevations by using the "Down to Water Surface Elevation" and the KPSI Surface Elevations.** **Down to water surface elevations were found by subtracting the distance between a known surveyed elevation and the surface of water elevation from a benchmark elevation to get a water surface elevation.** **KPSI surface water data were adjusted with offset values before being used as a reference elevation for topography data.** **When neither DTW or KPSI elevations were available, the floc and peat depths were related (using staff gages) to the water surface elevation of the nearest site taken at the closest time to the microtopography measurements.**	
Data Columns:	
Site	Location the topography measurements were taken.
Ridge	Vegetation community primarily containing *Cladium jamaciense* (sawgrass). This zone tends to have the shallowest water depth.
Slough	Vegetation community primarily containing *Eleocharis elongata*. This zone tends to have the deepest water depth.
1-1	The first number is an indication of the location where microtopography measurements were taken at the particular site. The second number is a count of the measurements taken within that area (normally 3 repetitions are collected).
Sample Position (m)	Location of where the measurement was taken along the transect. For Ridge/Slough sites 0 starts at the Ridge. For Slough sites 0 is the measurement taken farthest East.
Date/Time	Date and time that the measurement was taken.
Depth to Floc (cm)	Distance from the surface of the water to the surface of the floc, found by resting the microtopography probe on the floc.
Depth to Peat (cm)	Distance from the surface of the water to the surface of the peat, found by pushing the probe through the floc.
Floc Thickness (cm)	Floc Thickness (cm) = Depth to Peat (cm) - Depth to Floc (cm)
KPSI Water Surface Elevations (m)	KPSI long term deployment data that has been adjusted with offset values taken at the same location, date and time as the microtopography measurements.
DTW Water Surface Elevations (m)	DTW Water Surface Elevation (m) = Surveyed Elevation Point (m) - Distance from the Surveyed Point to the Water Surface (m)
KPSI Floc Elevations (m)	KPSI Floc Elevation (m) = KPSI Water Surface Elevation (m) - Depth to Floc (m)
KPSI Peat Elevations (m)	KPSI Peat Elevation (m) = KPSI Water Surface Elevation (m) - Depth to Peat (m)
DTW Floc Elevations (m)	DTW Floc Elevation (m) = DTW Water Surface Elevation (m) - Depth to Floc (m)

DTW Peat Elevations (m)	DTW Peat Elevation (m) = DTW Water Surface Elevation (m) - Depth to Peat (m)
Difference in Peat Elevations (m)	Difference in Peat Elevations (m) = DTW Peat Elevation (m) - KPSI Peat Elevation (m)
Contact Information:	
Jay Choi	
jchoi@usgs.gov	

B. Surface Water and Groundwater Levels: Continuous measurements of water level from pressure transducers.

File Name: *"Surface Water and Groundwater Levels.xlsx"*, contains the following worksheets

- Metadata
- Water Levels

Metadata Worksheet – Surface Water and Groundwater Levels		
"Surface Water and GroundWater Levels.xlsx" is an excel workbook presenting data as a part of the data release.		
High-Flow Field Experiments to Inform Everglades Restoration: Experimental Data 2010 to 2016		
Data were collected by USGS for USACE project "CERP: Testing and Monitoring for the Physical Model for Water Conservation Area 3 Decompartmentalization and Sheet Flow Enhancement Project", MIPR W32CS510826251		
This file contains data collected from research areas known as the Decompartmentalization Physical Model (DPM) and WCA-3A and WCA-3B, Everglades, FL		
Datum: WGS84		
Site ID	Latitude	Longitude
S152	25.8640740	-80.6208520
C1	25.8688503	-80.6107030
C2	25.8327940	-80.6351380
Z51_USGS	25.8629310	-80.6206310
Z51	25.8626030	-80.6201250
RS1D	25.8600655	-80.6204093
RS1U	25.8603442	-80.6203967
RS1SE	25.8603150	-80.6190730
Z53B	25.8585970	-80.6199950
Z53NE_2014	25.8581190	-80.6191020
Z53NE_2015	25.8596600	-80.6178700
RS2	25.8513699	-80.6221905
S1	25.8511939	-80.6170715
UB1	25.8438739	-80.6159930

UB2	25.8407041	-80.6175268
UB3	25.8376759	-80.6199131
MB0	25.8436000	-80.6142100
MB1	25.8425860	-80.6149720
MB2	25.8399780	-80.6169440
MB3	25.8366690	-80.6194060
DB1	25.8415550	-80.6138860
DB2	25.8391270	-80.6156970
DB3	25.8368580	-80.6174220
This worksheet tab, "Metadata," provides a summary of the data collection methods and defines all related variables.		
In the subsequent spreadsheet, "Water Levels," the complete set of water level data is provided for the entire study period.		
Data Collection Methods:		
Surface water elevations were obtained according to the USGS Office of Surface Water standards (Kenney, 2010). **Vented KPSI pressure transducers are installed in protected surface water wells (PVC standpipes). Sites Z51_USGS, RS1D and UB2 additionally have groundwater wells.** **KPSI pressure transducers are powered by a solar panel and data are recorded in a CR10X data logger on either 5 or 15 minute intervals.** **Reference markers were installed and surveyed. During field visits surface water elevation is calculated from these reference markers and then is used to check the live sensor reading.** **Water elevation is attained from the reference marker by a hand measurement of the distance from the top of the reference marker down to the surface of the water.** **KPSI pressure transducer readings are added to the KPSI elevation to attain the water level elevation.** **If the sensor elevation differs from the water elevation measured from the reference marker, the difference is applied to the data as an offset.** **Data are downloaded from each sensor during field visits and appended to previously collected data.**		
Data Columns:		
Date	Date and Time of sampling interval	
Site Name SW	Surface water elevation at indicated site (m)	
Site Name GW	Groundwater elevation at indicated site (m)	
Contact Information:		
Jay Choi		
jchoi@usgs.gov		

C. Surface Water Flow Velocities: Discrete profile data and continuous measurements of surface water velocity.

a. File Name: *"Velocity Profiles.xlsx",* contains the following worksheets

- Metadata

- C1R
- C1S
- C2R
- C2S
- Z51_USGSR
- Z51_USGSS
- RS1UR
- RS1US
- RS1DR
- RS1DS
- RS2R
- RS2S
- S1
- UB1
- UB2
- UB3
- DB1
- DB2
- DB3
- Flow Tracker

Metadata Worksheet – Velocity Profiles		
"Velocity Profiles.xlsx" is an excel workbook presenting data as a part of the data release.		
High-Flow Field Experiments to Inform Everglades Restoration: Experimental Data 2010 to 2016		
Data were collected by USGS for USACE project "CERP: Testing and Monitoring for the Physical Model for Water Conservation Area 3 Decompartmentalization and Sheet Flow Enhancement Project", MIPR W32CS510826251		
This file contains data collected from research areas known as the Decompartmentalization Physical Model (DPM) and WCA-3A and WCA-3B, Everglades, FL		
Datum: WGS84		
Site ID	Latitude	Longitude
S152	25.8640740	-80.6208520
C1	25.8688503	-80.6107030
C2	25.8327940	-80.6351380
Z51_USGS	25.8629310	-80.6206310
Z51	25.8626030	-80.6201250
RS1D	25.8600655	-80.6204093
RS1U	25.8603442	-80.6203967
RS1SE	25.8603150	-80.6190730
Z53B	25.8585970	-80.6199950

Z53NE_2014	25.8581190	-80.6191020
Z53NE_2015	25.8596600	-80.6178700
RS2	25.8513699	-80.6221905
S1	25.8511939	-80.6170715
UB1	25.8438739	-80.6159930
UB2	25.8407041	-80.6175268
UB3	25.8376759	-80.6199131
MB0	25.8436000	-80.6142100
MB1	25.8425860	-80.6149720
MB2	25.8399780	-80.6169440
MB3	25.8366690	-80.6194060
DB1	25.8415550	-80.6138860
DB2	25.8391270	-80.6156970
DB3	25.8368580	-80.6174220
This worksheet tab, "Metadata," provides a summary of the data collection methods and defines all related variables.		
In the subsequent spreadsheets, "C1R" through "DB3," are site-specific data of all the velocity profiles collected from 2010 to March 2015 using a Sontek ADV or Nortek Vectrino.		
In the spreadsheet, "Flow Tracker," is the complete set of velocity data collected using a Sontek Flow Tracker.		
Profiles with data columns A-T are taken with a Sontek ADV. Profiles with data colums A-K are taken with a Nortek Vectrino		
ADV/Vectrino Velocity Profile Data Collection Methods:		
Velocities were measured at 10 Hz in 1 minute bursts, yielding 600 samples at each depth increment. Depth increments throughout the water column are 2-5 cm, depending on total water depth, apparent vertical variability in vegetation architecture, and overall favorability of measurement conditions and time constraints. Signal to noise ratio (SNR) was monitored continuously during collection. Samples had to pass a 40% minimum correlation filter. At least 70% of samples in a burst had to pass the filter for the burst to be retained (Martin et al., 2002). Data with SNR of 5 dB or less were discarded. The 3-dimensional velocity data underwent a rotation for magnetic declination.		
Flow Tracker Data Collection Methods:		
Sontek ADV Flow Tracker is used for discrete measurements when ADV data were not available. Data were recorded in one minute bursts collected at depths; low (5cm above floc surface), middle of the water column, and upper (5 cm below the water surface). The probe head is positioned in a location with approximately 30 cm of clear space around the sensor. Vegetation was clipped if necessary.		
Sontek ADV Data Columns:		
Profile depth	Arbitrary depth marked on the ADV cradle (cm)	
Height	Height of receivers above the top of peat (cm), sampling volume is 5 or 10 cm below the probe depending on the probe type	

Burst	Burst number
V-x/V-E	Burst-averaged velocity (cm/sec) in x/E direction
V-y/V-N	Burst-averaged velocity (cm/sec) in y/N direction
V-z/V-U	Burst-averaged velocity (cm/sec) in z/U direction
Speed	Magnitude of horizontal velocity vector (cm/sec)
Direction	Angle (degree in clockwise) from North
COR0_0	A ratio of the coherent portion of the acoustic pulse signal to the total power: $S_x^2/(S_x^2+N_x^2)$ where S_x and N_x are signal and random noise in beam x
COR1_0	A ratio of the coherent portion of the acoustic pulse signal to the total power: $S_y^2/(S_y^2+N_y^2)$ where Sx and Nx are signal and random noise in beam y
COR2_0	A ratio of the coherent portion of the acoustic pulse signal to the total power: $S_z^2/(S_z^2+N_z^2)$ where Sx and Nx are signal and random noise in beam z
SNR0_0	Burst-averaged ratio of signal to noise in x/E probe
SNR1_0	Burst-averaged ratio of signal to noise in y/N probe
SNR2_0	Burst-averaged ratio of signal to noise in z/U probe
AMP0_0	Burst-averaged signal strength for acoustic receiver (x/E) in units of counts
AMP1_0	Burst-averaged signal strength for acoustic receiver (y/N) in units of counts
AMP2_0	Burst-averaged signal strength for acoustic receiver (z/U) in units of counts
STD_SPD	Burst-averaged standard deviation of horizontal speed (cm/sec)
Samp_Pass	Number of samples passed the 40% minimum correlation filter
Nortek Vectrino Data Columns:	
Profile depth	Arbitrary depth marked on the ADV cradle (cm)
Depth (cm)	Distance (cm) from water surface
Burst	Burst number
V-x (cm/s)	Burst-averaged velocity (cm/sec) in x direction
V-y (cm/s)	Burst-averaged velocity (cm/sec) in y direction
v-z (cm/s)	Burst-averaged velocity (cm/sec) in z direction
Speed (cm/s)	Magnitude of horizontal velocity vector (cm/sec)
STD speed	Standard deviation of speed
Direction	Angle (degree in clockwise) from North
STD Dir	Standard deviation of direction
Flow Tracker Data Columns:	
Flow tracker data from all sites are together in the spreadsheet "Flow Tracker"	
Site	Location where the measurement was taken.
Ridge	Vegetation community primarily containing *Cladium jamaciense* (sawgrass). This zone tends to have the shallowest water depth.

Slough	Vegetation community primarily containing *Eleocharis elongata*. This zone tends to have the deepest water depth.
Date	Date the measurement was taken.
Time	Time the measurement was taken.
Total Depth (cm)	Depth from the surface of the water to the top of the floc layer.
Depth from Surface (cm)	Depth from the surface of the water to the location of the flow tracker probe as the measurement as performed.
Low	Sampling location positioned approximately 5cm above the floc surface.
Mid	Sampling location positioned in the approximate center of the water column.
High	Sampling location positioned approximately 5cm from the water surface.
Vx (cm/s)	Velocity in the positive east direction.
Vy (cm/s)	Velocity in the positive north direction.
Vz (cm/s)	Velocity in the upward direction.
Sontek, 2001. *SonTek/YSI ADVField/Hydra Acoustic Doppler Velocimeter (Field) Technical Documentation*	
Sontek, 1997. *Pulse Coherent Doppler Processing and the ADV Correlation Coefficient*, Technical Notes.	
Contact Information:	
Jay Choi	
jchoi@usgs.gov	

b. File Name *"Continuous Flow Velocity.xlsx",* contains the following worksheets

- Metadata
- C1R-ADV
- C1S-ADV
- C2S-ADV
- Z51_USGSR-ADV
- Z51_USGSS-ADV
- RS1UR-Vectrino
- RS1US-Vectrino
- RS1DR-ADV
- RS1DS-ADV
- RS2R-ADV
- RS2S-ADV
- S1-ADV
- UB1-ADV
- UB2-ADV
- UB3-ADV
- UB3-Vectrino
- DB1-ADV

- DB2-ADV
- DB3-ADV
- MB0-XR
- MB1-XR
- MB2-XR

Metadata Worksheet – Continuous Flow Velocity		
"Continuous Flow Velocity.xlsx" is an excel workbook presenting data as a part of the data release.		
High-Flow Field Experiments to Inform Everglades Restoration: Experimental Data 2010 to 2016		
Data were collected by USGS for USACE project "CERP: Testing and Monitoring for the Physical Model for Water Conservation Area 3 Decompartmentalization and Sheet Flow Enhancement Project", MIPR W32CS510826251		
This file contains data collected from research areas known as the Decompartmentalization Physical Model (DPM) and WCA-3A and WCA-3B, Everglades, FL		
Datum: WGS84		
Site ID	Latitude	Longitude
S152	25.8640740	-80.6208520
C1	25.8688503	-80.6107030
C2	25.8327940	-80.6351380
Z51_USGS	25.8629310	-80.6206310
Z51	25.8626030	-80.6201250
RS1D	25.8600655	-80.6204093
RS1U	25.8603442	-80.6203967
RS1SE	25.8603150	-80.6190730
Z53B	25.8585970	-80.6199950
Z53NE_2014	25.8581190	-80.6191020
Z53NE_2015	25.8596600	-80.6178700
RS2	25.8513699	-80.6221905
S1	25.8511939	-80.6170715
UB1	25.8438739	-80.6159930
UB2	25.8407041	-80.6175268
UB3	25.8376759	-80.6199131
MB0	25.8436000	-80.6142100
MB1	25.8425860	-80.6149720
MB2	25.8399780	-80.6169440
MB3	25.8366690	-80.6194060
DB1	25.8415550	-80.6138860
DB2	25.8391270	-80.6156970
DB3	25.8368580	-80.6174220

This worksheet tab, "ADV and Vectrino Metadata," provides a summary of the data collection methods specific to the Sontek ADV and Nortek Vectrino equipment, and defines all related variables.	
In the subsequent spreadsheet, "XR Metadata," is a summary of the data collection methods specific to the Sontek XR equipment, and definitions of all related variables.	
In the spreadsheets "C1R-ADV" and "C1S-ADV" are ADV data for C1 Ridge and C1 Slough.	
In the spreadsheet "C2S-ADV" are ADV data for C2 Slough.	
In the spreadsheets "Z51_USGSR-ADV" and "Z51_USGSS-ADV" are ADV data for Z51_USGS Ridge and Z51_USGS Slough.	
In the spreadsheets "RS1UR-Vectrino," "RS1US-Vectrino," "RS1DR-ADV," and "RS1DS-ADV" are Vectrino data for RS1U ridge, Vectrino data for RS1U slough, ADV data for RS1D ridge and ADV data for RS1D slough (respectively).	
In the spreadsheets "RS2R-ADV" and "RS2S-ADV" are ADV data for RS2 ridge and RS2 slough.	
In the spreadsheet "S1-ADV" are ADV data for S1.	
In the spreadsheets "UB1-ADV," "UB2-ADV," "UB3-ADV" and "UB3-Vectrino" are ADV data for UB1, ADV data for UB2, ADV data for UB3 and Vectrino data for UB3 (respectively).	
In the spreadsheets "DB1-ADV," DB2-ADV" and "DB3-ADV" are ADV data for DB1, DB2 and DB3 (respectively).	
In the spreadsheets "MB0-XR," "MB1-XR" and "MB2-XR"are main cell XR data for MB0, main cell XR data for MB1 and main cells XR data for MB2 (respectively).	
Velocity Continuous Data Collection Methods:	
Velocity was measured at the midpoint of the water column at a frequency of 10 Hz. Data were recorded in one minute bursts (600 samples) collected every 15 minutes to save battery power. Datasets were filtered and edited according to standard criteria suggested by the manufacturer (SonTek, 2001) as well as specific criteria developed and refined in a prior Everglades study (Riscassi and Schaffranek, 2002). Samples had to pass a 40% minimum correlation filter with at least 70% of samples within a burst being retained (Martin et al., 2002). Data with acoustic signal-to-noise ratio (SNR) of 5 dB or less was discarded. The ADVs and Vectrinos were deployed such that the positive x-velocity direction was oriented to the direction of magnetic north and positive y-velocity direction points west. A phase space threshold despiking algorithm (Goring and Nikora, 2002) was applied to ADV and Vectrino data.	
XR Data Collection Methods:	
The argonaut XR is installed on the floor and in the center of the canal in an up-looking configuration and samples vertical profiles of flow speed and direction. Velocity data are collected for a 120 second interval every 900 seconds. The size of the main cell is determined in the field from the surface water depth. The number of individual cells is determined in the field based off surface water depth.	
Data Columns from Sontek ADV:	
ADV data are presented as daily averaged values with standard deviation for speed and direction.	
Year	**Year (yyyy)**
Month	Month (mm)
Day	Day (dd)
V-x (N) (cm/s)	Velocity in the x direction (north)

V-y (W) (cm/s)	Velocity in the y direction (west)
V-z (Up) (cm/s)	Velocity in the z direction (up)
Speed (cm/s)	Speed is found through the calculation: Speed = sqrt(vx^2 + vy^2)
StdDev Speed	Standard deviation of speed
Direction (degrees)	Direction of velocity vector in degrees
StdDev Dir	Standard deviation of the direction
Data Columns from Nortek Vectrino:	
RS1UR Vectrino data were collected from 11/3/2014 to 11/6/2014	
RS1US Vectrino data were collected from 11/3/2014 to 11/6/2014	
UB3 Vectrino data were collected from 11/6/2014 to 11/7/2014	
The Vectrino has four beams, and collected velocity data in four directions	
Beam 1 is the x-direction	
Beam 2 is the y-direction	
Beam 3 is the z-direction	
Beam 4 is the z2-direction	
Time (s)	Time in seconds starting at 0
V-x (m/s)	Velocity data in the x direction in m/s (beam 1)
V-y (m/s)	Velocity data in the y direction in m/s (beam 2)
V-z (m/s)	Velocity data in the z direction in m/s (beam 3)
V-z2 (m/s)	Velocity data in the z2 direction in m/s (beam 4)
Amplitude of Beam 1 (counts)	The amplitude of Beam 1 measured in counts
Amplitude of Beam 2 (counts)	The amplitude of Beam 2 measured in counts
Amplitude of Beam 3 (counts)	The amplitude of Beam 3 measured in counts
Amplitude of Beam 4 (counts)	The amplitude of Beam 4 measured in counts
SNR of Beam 1 (dB)	The Signal to Noise Ratio in dB of Beam 1
SNR of Beam 2 (dB)	The Signal to Noise Ratio in dB of Beam 2
SNR of Beam 3 (dB)	The Signal to Noise Ratio in dB of Beam 3
SNR of Beam 4 (dB)	The Signal to Noise Ratio in dB of Beam 4
Correlation of Beam 1 (%)	Correlation of Beam 1 as a percentage
Correlation of Beam 2 (%)	Correlation of Beam 2 as a percentage
Correlation of Beam 3 (%)	Correlation of Beam 3 as a percentage
Correlation of Beam 4 (%)	Correlation of Beam 4 as a percentage
XR Main Cell Data Columns:	
All data described below are daily averaged values.	
Year	Year of collection
Month	Month of collection

Day	Day of collection
VelocityE	Velocity (cm/sec) in x/E direction
VelocityN	Velocity (cm/sec) in y/N direction
VelocityU	Velocity (cm/sec) in z/U direction
StdError1	Standard error of beam 1
StdError2	Standard error of beam 2
StdError3	Standard error of beam 3
SNR1	Signal to noise ratio of beam 1
SNR2	Signal to noise ratio of beam 2
SNR3	Signal to noise ratio of beam 3
SignalAmp1	Signal amplitude of beam 1
SignalAmp2	Signal amplitude of beam 2
SignalAmp3	Signal amplitude of beam 3
Noise1	Noise beam 1
Noise2	Noise beam 2
Noise3	Noise beam 3
IceDetection	Indicator of ice coverage
Heading	Magnetic heading
Pitch	Rotation about the y-axis
Roll	Rotation about the x-axis
StdDevHeading	Standard deviation of the heading
StdDevPitch	Standard deviation of the pitch
StdDevRoll	Standard deviation of the roll
Temperature	Temperature degrees C
Pressure	Pressure in Bars
StdDevPressure	Standard deviation of the pressure
Voltage	Battery Voltage
CellBegin	Distance from the sensor that the main cell begins
CellEnd	Distance from the sensor that the main cell ends
Speed	Magnitude of horizontal velocity vector (cm/sec)
Direction	Angle (degree in clockwise) from North
Sontek, 2001. ***SonTek/YSI ADVField/Hydra Acoustic Doppler Velocimeter (Field) Technical Documentation***	
Sontek, 1997. ***Pulse Coherent Doppler Processing and the ADV Correlation Coefficient*****, Technical Notes.**	
Contact Information:	
Jay Choi	
jchoi@usgs.gov	

D. Suspended Particle Sizes and Concentrations: Discrete measurements of suspended sediment and total phosphorus concentration, load and flux.

File Name: *"Suspended Particle Sizes and Concentrations.xlsx",* contains the following worksheets

- Metadata
- SSC Discrete
- SSC Depth Average
- SSC Interval Load&Flux
- SSC D-Avg Load&Flux
- P Discrete
- P Depth Average
- P Interval Load&Flux
- P D-Avg Load&Flux

Metadata Worksheet – Suspended Particle Sizes		
"Suspended Particle Sizes and Concentrations.xlsx" is an excel workbook presenting data as a part of the data release.		
High-Flow Field Experiments to Inform Everglades Restoration: Experimental Data 2010 to 2016		
Data were collected by USGS for USACE project "CERP: Testing and Monitoring for the Physical Model for Water Conservation Area 3 Decompartmentalization and Sheet Flow Enhancement Project", MIPR W32CS510826251		
This file contains data collected from research areas known as the Decompartmentalization Physical Model (DPM) and WCA-3A and WCA-3B, Everglades, FL		
Datum: WGS84		
Site ID	Latitude	Longitude
S152	25.8640740	-80.6208520
C1	25.8688503	-80.6107030
C2	25.8327940	-80.6351380
Z51_USGS	25.8629310	-80.6206310
Z51	25.8626030	-80.6201250
RS1D	25.8600655	-80.6204093
RS1U	25.8603442	-80.6203967
RS1SE	25.8603150	-80.6190730
Z53B	25.8585970	-80.6199950
Z53NE_2014	25.8581190	-80.6191020
Z53NE_2015	25.8596600	-80.6178700
RS2	25.8513699	-80.6221905
S1	25.8511939	-80.6170715

UB1	25.8438739	-80.6159930
UB2	25.8407041	-80.6175268
UB3	25.8376759	-80.6199131
MB0	25.8436000	-80.6142100
MB1	25.8425860	-80.6149720
MB2	25.8399780	-80.6169440
MB3	25.8366690	-80.6194060
DB1	25.8415550	-80.6138860
DB2	25.8391270	-80.6156970
DB3	25.8368580	-80.6174220

This worksheet tab, "Metadata," provides a summary of the data collection methods, defines all related variables and provides supporting calculations.

The subsequent spreadsheet, "SSC Discrete," includes discrete suspended sediment concentrations and particle size data for all sites over the entire study period.

The spreadsheet "SSC Depth Average" includes depth-averaged suspended sediment concentrations and particle size data for all sites over the entire study period.

The spreadsheet "SSC Interval Load&Flux" includes suspended sediment concentrations, particle size data, velocity data and suspended sediment load and flux results for all sites over the entire study period.

The spreadsheet "SSC D-Avg Load&Flux" includes depth-averaged suspended sediment concentrations, depth-averaged particle size data, depth-averaged velocity data and depth-averaged suspended sediment load and flux results for all sites over the entire study period.

The spreadsheet "P Discrete" includes discrete phosphorus concentrations for all sites over the entire study period.

The spreadsheet "P Depth Average" includes depth-averaged phosphorus concentrations for all sites over the entire study period.

The spreadsheet "P Interval Load&Flux" includes phosphorus concentrations, velocity data and phosphorus load and flux results for all sites over the entire study period.

The spreadsheet "P D-Avg Load&Flux" includes depth-averaged phosphorus concentrations, depth-averaged velocity data and depth-averaged phosphorus load and flux results for all sites over the entire study period.

Data Collection Methods:

Suspended sediment and phosphorus samples were collected using peristaltic pumps at a rate of 60mL/min and filtered through a 500 micron Nitex screen.
2 liter samples were collected for SSC analysis, 250 mL samples were run on the LISST portable to obtain grainsize data and 60mL were collected for phosphorus analysis.
Phosphorus analysis was done by the South Florida Water Management District Lab.
Suspended sediment concentrations were found by measuring the exact volume before filtering the suspended sediment sample via vacuum filtration.
The pre-weight of the filter was compared to the weight after the suspended sediment sample had been run through it, to find the mass of sediment. Mass of sediment and volume of sample were used to calculate suspended sediment concentration.
By examining concentrations, velocities and water depths, load and flux values could be calculated. Calculations are included in the following data column descriptions.

SSC (suspended sediment concentration) Data Columns:

Sample

2013 Sample Naming Convention	Sample naming convention: RS1U-RR_L = "Site" - "Sampling location"_"Sample Depth"
	RS1U-ridge designates a vertical profile of low (L), mid (M) and upper (U) sampling locations.
	RS1U-slough designates a vertical profile of low (L), mid (M) and upper (U) sampling locations.
	"RR" indicates the ridge end of the transect, "R" indicates ridge characteristics, "S" indicates slough, "SS" indicates the slough end of the transect and "T" indicates transition.
	"dup" indicates duplicate samples taken at a the same time and location as the primary sample (for error calculation purposes).
	"M" indicates a sample taken in the middle of the water column, "L" indicates a sample collected approximately 5cm above the floc and "U" indicates 5cm below the water surface.
	"grab" refers to a sample that was collected without pumping, and instead was scooped from the water using a nalgene bottle.
2014 Sample Naming Convention	Sample naming convention: T1-RS1D-2-RM = "Time of Sample" - "Site" - "Sample Number" - "Sampling location" "Sample Depth"
	R= Ridge, S = Slough
	Time of Sample:
	Pre Pre-Flow Release (before November 5th 2014)
	T1 Transition 1 (Nov 4th 9:43 to Nov 5th 9:43)
	T2 Transition 2 (Nov 5th 9:43 to Nov 6th 9:43)
	Samples without a time (or with a month) were taken during Steady Flow conditions (steady flow begins after Nov 6th, 9:43)
	For ridge/slough locations, R designates ridge and S designates slough
	Sample Depth is either "M" for middle of the water column, or "L" for lower water column (5cm above the surface of the floc)
	Upper water column sampling points were not collected for flow release 2014
	For RS1U:
	Sampling locations: RS1U = A-H
	B, C, D, E, F, and G are the lower (Near bed) sampling points along the transect; A and H are the middle of the water column sampling points; see figure 3 for reference
	RS1U-ridge designates vertical profile of A and B sampling locations
	RS1U-slough designates vertical profile of H and G sampling locations
	RS1U: A=RR_M, B=RR_L, C=R_L, D=RT_L, E=ST_L, F=S_L, G=SS_L, H=SS_M (Sampling location: L - Lower, M - Middle)
	Duplicate samples ("dup") were taken for error analysis in March 2015 for sites RS1U-R, RS1U-S, UB2 and DB2.
2015 Sample Naming Convention	Sample Naming
	R = Ridge, S = Slough
	M = Mid location in the water column, L = Low location in the water column (approximately 5cm above the bed).
	Time of Sample:
	PRE
	T Pre-Flow Release (before November 16th 2015)

	T1	T stands for "transient flow" defined as when the system is rapidly changing. "Transient flow" begins the moment right before the culvert opening, and ends when a steady-state condition is reached.
	T2	Pulse 1 (Nov 16th 9:40)
	T2-1	Pulse 2 (Nov 19th 9:40)
	T1-X	At Z51_USGS an extra sampling round was added at 9:40 on the 16th and at 9:43 on the 19th (T2-X)
	DEC	Round 1 sample collected for the Pulse 2 event.
	JAN	Samples collected in December, 2015
	MAR	Samples collected in January, 2016
	Example Name:	Samples collected in March, 2016
	T1-4-Z51_USGS-SL	
	Example Meaning:	
	Pulse **1**, Round **4**, Site **Z51_USGS**, **S**lough, **L**ow sampling location in the water column.	
	Duplicate samples ("dup") were taken for error analysis in March 2016 for sites RS1D-R, RS1D-S, UB2 and DB2.	
Date/Time	The date and time at which the sampling event occurred.	
Flow Release 2013	Name used to describe the opening of the culvert at L67-A. The zero flow release date and time used is 11052013 @ 09:40.	
Flow Release 2014	Name used to describe the opening of the culvert at L67-A. The zero flow release date and time used is 11042014 @ 09:43.	
Flow Release 2015 Pulse 1	Name used to describe the opening of the culvert at L67-A. The zero flow release date and time used is 11162015 @ 09:40.	
Flow Release 2015 Pulse 2	Name used to describe the opening of the culvert at L67-A. The zero flow release date and time used is 11192015 @ 09:40.	
Distance from Floc (cm)	Measured distance from floc boundary on day of sampler installation.	
Water Depth (cm)	Measured value or calculated from available depth to floc, staff gage and down to water measurement data.	
Sediment mass (g)	Calculated sediment mass ((filter mass + sediment mass) - filter mass)	
Volume (mL)	Measured volume of collected SSC sample	
Sediment Concentration (µg/L)	Calculated sediment concentration ((sediment mass)/(volume)) and units converted from g/mL to µg/L (result * 1000000000)	
Depth Average SSC (µg/L)	Weighted average of samples in a vertical profile. (ex. (((SSC_1) x (water column interval_1) + (SSC_2) x (water column interval_2) + (SSC_3) x (water column interval_3))/(total water depth))	
	Locations with 1 sampling point intervals were not depth-averaged.	
Water Column Interval (cm)	Calculated vertical water column length from which a specific sample was collected (ex. RS1U-A interval is the distance from the sample to the floc + half the distance from the sample to the RS1U-B sampling point. The RS1U-B interval is half the distance from B to A + half the distance from B to C. RS1U-C is the half the distance from C to B + the distance from the sample to the water surface).	
Mass Weighted Particle Size	*Calculation*: 29.3138 *(Volume Concentration in a specific Bin)^-1.1235, Bins are cumulatively summed to determine statistical particle size fractions of D_{10}, D_{50}, D_{60} and D_{90}; Density calculations from Larsen et al, 2009a	
D_{50} (µm)	Median mass weighted size of suspended particles in a specific sample	

	(collected by running an aliquot of a sample through the LISST portable)
Depth Average D_{50} (µm)	Weighted average of mass weighted D_{50} values from the LISST portable. (ex. ((D_{50}_1) x (water column interval_1) + (D_{50}_2) x (water column interval_2) + (D_{50}_3) x (water column interval_3))/(total water depth))
D_{60}/D_{10}	Mass weighted particle size uniformity coefficient of suspended sediment in a specific sample (collected by running an aliquot of a sample through the LISST portable)
Depth Average D_{60}/D_{10}	Weighted average of mass D_{60}/D_{10} values from the LISST portable. (ex. ((D_{60}/D_{10}_1) x (water column interval_1) + (D_{60}/D_{10}_2) x (water column interval_2) + (D_{60}/D_{10}_3) x (water column interval_3))/(total water depth))
	In this file and in the report particle sizes are displayed as mass weighted values.
Lower	Sampling location positioned 5cm from the floc surface on the day of sampler installation. Also referred to as 'Near bed'
Middle	Sampling location positioned in the center of the water column on the day of sampler installation.
Upper	Sampling location positioned 5cm from the water surface on the day of sampler installation.
Ridge	Vegetation community primarily containing *Cladium jamaciense* (sawgrass). This zone tends to have the shallowest water depth.
Transition	Vegetation community containing a mixture of *Cladium jamaciense* (sawgrass) and *Eleocharis elongata*. This zone tends to have medium water depth.
Slough	Vegetation community primarily containing *Eleocharis elongata*. This zone tends to have the deepest water depth.
Load and Flux Data Set:	
Vx(cm/s)	Burst-averaged velocity in x/E direction
Vy(cm/s)	Burst-averaged velocity in y/N direction
Water column interval velocity (cm/s)	Velocity averaged across specific water column interval
Vx_depth avg(cm/s)	Total depth averaged burst-averaged velocity in x/E direction
Vy_depth avg(cm/s)	Total depth averaged burst-averaged velocity in y/N direction
Water column average velocity (cm/s)	Total depth-averaged velocity in sampled water column
SSC Flux_U (µg/cm^2*s)	SSC flux in upper water column interval (SSC * Interval velocity)
SSC Flux_M (µg/cm^2*s)	SSC flux in middle water column interval (SSC * Interval velocity)
SSC Flux_L (µg/cm^2*s)	SSC flux in lower water column interval (SSC * Interval velocity)
SSC Total Flux (µg/cm^2*s)	Total SSC flux in sampled water column ((Depth-average SSC)*(water column average velocity))
SSC Loading_U (µg/cm*s)	SSC load in upper water column interval (SSC * Interval velocity * Water column interval)
SSC Loading_M (µg/cm*s)	SSC load in middle water column interval (SSC * Interval velocity * Water column interval)
SSC Loading_L (µg/cm*s)	SSC load in lower water column interval (SSC * Interval velocity * Water column interval)
SSC Total Loading (µg/cm*s)	Total SSC load in sampled water column ((Depth-average SSC)*(total depth speed))

P Flux_U (mg/cm^2*s)	Phosphorus flux in upper water column interval (P Concentration * Interval velocity)
P Flux_M (mg/cm^2*s)	Phosphorus flux in middle water column interval (P Concentration * Interval velocity)
P Flux_L (mg/cm^2*s)	Phosphorus flux in lower water column interval (P Concentration * Interval velocity)
P Total Flux (mg/cm^2*s)	Total Phosphorus flux in sampled water column ((Depth-average P Concentration)*(total depth speed))
P Loading_U (mg/cm*s)	Phosphorus load in upper water column interval (P Concentration * Interval velocity * Water column interval)
P Loading_M (mg/cm*s)	Phosphorus load in middle water column interval (P Concentration * Interval velocity * Water column interval)
P Loading_L (mg/cm*s)	Phosphorus load in lower water column interval (P Concentration * Interval velocity * Water column interval)
P Total Load (mg/cm*s)	Total Phosphorus load in sampled water column ((Depth-average P Concentration)*(total depth speed))
Contact Information:	
Jay Choi	
jchoi@usgs.gov	

E. Biogeochemical Sampling: Discrete measurements of phosphorus fractionation, nitrogen and ash free dry weight from samples of floc, metaphyton and water column.
File Name: *"Biogeochemical Sampling.xlsx",* contains the following worksheets

- Metadata
- Floc
- Metaphyton
- Water Column

Metadata Worksheet – Biogeochemical Sampling		
"Biogeochemical Sampling.xlsx" is an excel workbook presenting data as a part of the data release.		
High-Flow Field Experiments to Inform Everglades Restoration: Experimental Data 2010 to 2016		
Data were collected by USGS for USACE project "CERP: Testing and Monitoring for the Physical Model for Water Conservation Area 3 Decompartmentalization and Sheet Flow Enhancement Project", MIPR W32CS510826251		
This file contains data collected from research areas known as the Decompartmentalization Physical Model (DPM) and WCA-3A and WCA-3B, Everglades, FL		
Datum: WGS84		
Site ID	Latitude	Longitude
S152	25.8640740	-80.6208520
C1	25.8688503	-80.6107030
C2	25.8327940	-80.6351380
Z51_USGS	25.8629310	-80.6206310
Z51	25.8626030	-80.6201250

RS1D	25.8600655	-80.6204093
RS1U	25.8603442	-80.6203967
RS1SE	25.8603150	-80.6190730
Z53B	25.8585970	-80.6199950
Z53NE_2014	25.8581190	-80.6191020
Z53NE_2015	25.8596600	-80.6178700
RS2	25.8513699	-80.6221905
S1	25.8511939	-80.6170715
UB1	25.8438739	-80.6159930
UB2	25.8407041	-80.6175268
UB3	25.8376759	-80.6199131
MB0	25.8436000	-80.6142100
MB1	25.8425860	-80.6149720
MB2	25.8399780	-80.6169440
MB3	25.8366690	-80.6194060
DB1	25.8415550	-80.6138860
DB2	25.8391270	-80.6156970
DB3	25.8368580	-80.6174220

This worksheet tab, "Metadata," provides a summary of the data collection methods, defines all related variables and provides supporting calculations.

The subsequent spreadsheet, "Floc," includes all biogeochemistry data and phosphorus fractionation for the floc samples collected throughout the entire study period.

The spreadsheet, "Metaphyton," includes all biogeochemistry data and phosphorus fractionation for the metaphyton samples collected throughout the entire study period.

The spreadsheet, "Water Column," includes all biogeochemistry data and phosphorus fractionation for the water column samples collected throughout the entire study period.

Data Collection and Lab Analysis Methods:

Samples of floc, metaphyton and water column were collected at sites S152 (water column only), C1R, C1S, C2R, C2S, Z51_USGSR, Z51_USGSS, RS1DR, RSDS, RS2R, RS2S, RS1SER, S1, UB1, UB2, UB3, DB1, DB2 and DB3 for biogeochemical analysis.
Floc was collected by taking a core sample, allowing the floc material to settle, decanting the water, and then pouring out the floc into a 125mL Nalgene bottle.
Metaphyton samples were obtained by using a wet/dry vacuum to collect epiphyton from vegetation stems at mid-water depth, allowing the sample to settle, and decanting the excess water.
Water column samples were collected at mid-water depth using a peristaltic pump.
Metaphyton and water column samples were filtered through a 500 micron Nitex prior to particle size and biogeochemical analysis. Floc samples were filtered through a 500 micron filter prior to particle size analysis.
Samples in 2010 and 2011 were analyzed by DB Environmental. Samples in 2012, 2013, 2014 and 2015 analyzed by the Wetland Biogeochemistry Laboratory at the University of Florida.

Parameters	Methods
TP Ashing	WBL SP-008,SM4500P F

Total Nitrogen	WBL AN-10
Total Carbon	WBL AN-10
All soil, sediment, and plant data calculated based on dry weight.	
All particle size measurements analyzed in the field by project personnel using a LISST-Portable.	
Data Columns:	
Site	Site name: Refers to the platform name within the DPM footprint
RIDGE	Vegetation community primarily containing *Cladium jamaciense* (sawgrass). This zone tends to have the shallowest water depth.
SLOUGH	Vegetation community primarily containing *Eleocharis elongata*. This zone tends to have the deepest water depth.
DRYWT (g)	Dry weight of the sample in g, after drying in a drying oven
AFDW (%) or LOI (%, starting 2012)	For the 2010-2011 data, ash-free dry weight (mass percent), for data starting in 2012, loss on ignition (mass percent)
TPP (mg/kg)	Total particulate phosphorus (mg/kg sample collected)
Labile P (mg/kg)	Labile phosphorus (mg/kg sample collected), defined as the phosphorus removed through extraction with NaHCO3
Microbial P (mg/kg)	Microbial phosphorus (mg/kg sample collected), defined as the phosphorus removed through extraction with NaHCO3 + chloroform, minus the labile phosphorus fraction
TPN (g/kg)	Total particulate nitrogen (g/kg sample collected)
TPC (g/kg)	Total particulate carbon (g/kg sample collected)
Refractory P (mg/kg)	Refractory phosphorus (mg/kg sample collected), calculated by subtracting labile and microbial phosphorus fractions from total phosphorus
Labile P	Labile phosphorus, expressed as a fraction of total phosphorus
Microbial P	Microbial phosphorus, expressed as a fraction of total phosphorus
Refractory P	Refractory phosphorus, expressed as a fraction of total phosphorus
TPN/TPP	Total particulate nitrogen to total particulate phosphorus ratio
Mass-Weighted Mean size, um	Mass-weighted mean particle size, determined by multiplying the mass fraction of material in each LISST-Portable size class bin by the bin centroid. Masses are calculated from the volumetric information provided by the LISST-Portable by multiplying by density, calculated from previous settling column experiments
Mass concentration (mg/L)	Mass concentration of suspended material found by multiplying the total volume concentration of particles by their estimated density distribution (found through previous experiments on Everglades particle samples)
Contact Information	
Jay Choi	
jchoi@usgs.gov	

F. Vegetation Influence on Sheet Flow: Discrete measurements of vegetative frontal area and dimensional volume.
File Name: *"Vegetative Influence on Sheet Flow.xlsx",* contains the following worksheets
- Metadata
- 2010 with epi

- 2010 no epi
- 2011 with epi
- 2012 with epi
- 2013 with epi
- 2014 with epi

Metadata Worksheet – Vegetation Influence on Sheet Flow		
"Vegetation Influence on Sheet Flow.xlsx" is an excel workbook presenting data as a part of the data release.		
High-Flow Field Experiments to Inform Everglades Restoration: Experimental Data 2010 to 2016		
Data were collected by USGS for USACE project "CERP: Testing and Monitoring for the Physical Model for Water Conservation Area 3 Decompartmentalization and Sheet Flow Enhancement Project", MIPR W32CS510826251		
This file contains data collected from research areas known as the Decompartmentalization Physical Model (DPM) and WCA-3A and WCA-3B, Everglades, FL		
Datum: WGS84		
Site ID	Latitude	Longitude
S152	25.8640740	-80.6208520
C1	25.8688503	-80.6107030
C2	25.8327940	-80.6351380
Z51_USGS	25.8629310	-80.6206310
Z51	25.8626030	-80.6201250
RS1D	25.8600655	-80.6204093
RS1U	25.8603442	-80.6203967
RS1SE	25.8603150	-80.6190730
Z53B	25.8585970	-80.6199950
Z53NE_2014	25.8581190	-80.6191020
Z53NE_2015	25.8596600	-80.6178700
RS2	25.8513699	-80.6221905
S1	25.8511939	-80.6170715
UB1	25.8438739	-80.6159930
UB2	25.8407041	-80.6175268
UB3	25.8376759	-80.6199131
MB0	25.8436000	-80.6142100
MB1	25.8425860	-80.6149720
MB2	25.8399780	-80.6169440
MB3	25.8366690	-80.6194060
DB1	25.8415550	-80.6138860
DB2	25.8391270	-80.6156970
DB3	25.8368580	-80.6174220

This worksheet tab, "Metadata," provides a summary of the data collection methods and defines all related variables.	
The subsequent spreadsheet, "2010 with epi," includes data from vegetation samples collected in 2010 that included epiphyton.	
The spreadsheet, "2010 no epi," includes data from vegetation samples collected in 2010 with the epiphyton removed.	
The spreadsheets "2011 with epi," "2012 with epi," "2013 with epi" and "2014 with epi" contain data from vegetation samples collected in 2011, 2012, 2013 and 2014 (respectively) that included epiphyton.	
Data Collection and Measurement Methods:	
Vegetation was harvested within a 0.25 m^2 area that was positioned at ridge, slough and transition sites using a stratified random sampling scheme. **Once the quadrats were positioned, the vegetation above the water surface was clipped, and below the water surface the vegetation was sampled in 10cm increments (2010-2012) and 15cm increments (2013-2014).** **Vegetative data refer to only stems and leaves greater than 15 cm in length with epiphyton collected in September and November of 2010, November 2011, November 2012, August 2013 and August 2014. Both live and dead materials were included. Measurements are integrated values for depth increments above floc-surface (0 cm) to water-surface. Above-water measurements were recorded at a height equal to 0.5 * average stem length above water-surface.**	
Data are processed including and excluding floating epiphyton matter (with epi and no epi). **Site codes R, S, and T denote vegetative community: 'R' - ridge, 'T' – ridge/slough transition, and 'S' – slough.** **Site codes ADV and LAI denote proximity to an autonomous ADV deployment or where PAR measurements were taken to get leaf area index respectively.** **Raw data were sorted based on three levels in descending order: Site > Lower Depth > Species** **Calculations were made to obtain values for each site > depth > species sub-category that exists in the data set.**	
n: number of stems per unit area (cm-1)	
average stem/leaf diameter (mm): an average of all values weighted by n	
average diam1 (mm): an average of all values weighted by n	
average diam2 (mm): an average of all values weighted by n	
Frontal area (cm^{-1}): calculated using n value and average stem/leaf diameter previously determined.	
Formula:	$a = n*(d_{axis1} + d_{axis2})/2$
a	Projected frontal area per unit volume (cm^{-1})
n	Number of stems per unit area (cm-1)
d_{axis1}	Average stem diameter of axis 1 (cm)
d_{axis2}	Average stem diameter of axis 2 (cm)
Dimensional volume (fraction): calculated either using the triangle model for sawgrass or the ellipse model for everything else. Calculated using the n value, average diam1 and average diam2 previously determined.	
Formula (sawgrass only):	$V = d_{axis1} * d_{axis2} * (1/2) * n$
Formula (all other species):	$V = pi * d_{axis1} * d_{axis2} * (1/4) * n$
V	Dimensional volume per unit volume

Categories were further consolidated to obtain values for each site and depth sub-category that exists in the data set. **Categories were further consolidated to obtain *summed* values for each site that exists in the data set (values represent a sum of depth increments in quadrat).** **Categories were again consolidated to obtain *averaged* values for each site that exists in the data set (values represent an average of depth increments in quadrat).**			
vegetative community	dominant species in descending order		
Ridge (R)	*Cladium jamaciense*	*Typha latifolia*	*Crinum americanum*
Transition (T)	*Cladium jamaciense*	*Eleocharis elongata*	*Eleocharis cellulosa*
Slough (S)	*Eleocharis elongata*	*Eleocharis cellulosa*	*Nymphaea odorata*
Data Columns:			
Site	Location with indication of type of community		
Collection Date	Collection date		
Canopy Height (cm)	Distance in cm down to the peat		
Water Surface	Depth of the water surface to the peat		
Stem Diameter (cm)	Lab measured diameter of the vegetation		
Vegetative Frontal Area (cm^2)	Lab measured frontal area of the vegetation		
Dimensional Volume (fraction of bulk volume)	Calculated volume from dimensional lab measurements		
Contact Information:			
Jay Choi			
jchoi@usgs.gov			

G. Water Quality Monitoring: Turbidity and specific conductivity measurements collected continuously using YSI Sondes.

File Name: *"Water Quality Monitoring.xlsx",* contains the following worksheets

- Metadata
- 2013
- 2014
- 2015

Metadata Worksheet – Water Quality Monitoring
"Water Quality Monitoring.xlsx" is an excel workbook presenting data as a part of the data release.
High-Flow Field Experiments to Inform Everglades Restoration: Experimental Data 2010 to 2016
Data were collected by USGS for USACE project "CERP: Testing and Monitoring for the Physical Model for Water Conservation Area 3 Decompartmentalization and Sheet Flow Enhancement Project", MIPR W32CS510826251

This file contains data collected from research areas known as the Decompartmentalization Physical Model (DPM) and WCA-3A and WCA-3B, Everglades, FL		
Datum: WGS84		
Site ID	Latitude	Longitude
S152	25.8640740	-80.6208520
C1	25.8688503	-80.6107030
C2	25.8327940	-80.6351380
Z51_USGS	25.8629310	-80.6206310
Z51	25.8626030	-80.6201250
RS1D	25.8600655	-80.6204093
RS1U	25.8603442	-80.6203967
RS1SE	25.8603150	-80.6190730
Z53B	25.8585970	-80.6199950
Z53NE_2014	25.8581190	-80.6191020
Z53NE_2015	25.8596600	-80.6178700
RS2	25.8513699	-80.6221905
S1	25.8511939	-80.6170715
UB1	25.8438739	-80.6159930
UB2	25.8407041	-80.6175268
UB3	25.8376759	-80.6199131
MB0	25.8436000	-80.6142100
MB1	25.8425860	-80.6149720
MB2	25.8399780	-80.6169440
MB3	25.8366690	-80.6194060
DB1	25.8415550	-80.6138860
DB2	25.8391270	-80.6156970
DB3	25.8368580	-80.6174220
Eden 8	25.8700000	-80.6800000
Site 69	25.9100000	-80.5900000
This worksheet tab, "Metadata," provides a summary of the data collection methods and defines all related variables.		
The spreadsheet, "2013," includes water quality data collected during the 2013 flow release across the study area.		
The spreadsheet, "2014," includes water quality data collected during the 2014 flow release across the study area.		
The spreadsheet, "2015," includes water quality data collected during the 2015 flow release across the study area.		
Collection Methods:		

Specific conductivity, turbidity and DO probes were calibrated according to YSI standards in the lab prior to being taken to the field. **If the specific conductivity probe was reading inaccurately, a 1-point calibration was performed using a standard of 250 uS/cm. This calibration was checked with 50, 250 and 1000 uS/cm standards. If the turbidity probe was reading inaccurately, a 3-point calibration was performed using 0 (DI water), 100 and 1000 NTU standards. The DO probe was calibrated with a 1-pt calibration using the local barometric pressure and sensor reading at 100% saturation.** **Probes were checked in Florida tap water one day before installation. After data collection was complete, turbidity values were corrected according to the Florida tap water measurements. Adjustments were also made to compensate for drift in the sensor readings.** **Sondes were deployed for 7 to over 30 days at a time, depending on the site and time constraints in the field. Measurements were recorded every 5-30 minutes, depending on how long they were deployed for. For longer time periods 30 minute intervals were used to lengthen the battery life.** **YSI sondes were installed such that the turbidity, SC and DO probes were located at the midpoint of the water column.**
Data Columns:

Turbid+	Turbidity (NTU)
SC	Specific Conductivity (mS/cm)
DO	Dissolved Oxygen (mg/L)

Contact Information:
Jay Choi
jchoi@usgs.gov

H. Groundwater-Surface Water Interactions Detected using Heat as a Tracer: Continuous measurements of temperature along a vertical profile below the peat surface.

File Name: *"Groundwater-Surface Water Interactions Detected using Heat as a Tracer.xlsx"*, contains the following worksheets

- Metadata
- UB2_2013
- UB2_2014
- UB2_2015
- RS1D_2013
- RS1D_2014
- RS1D_2015
- S1_2014
- Z51_USGS_2015

Metadata Worksheet – Groundwater – Surface Water Interactions using Heat as a Tracer
"Heat Tracer Detection of GW-SW Interactions.xlsx" is an excel workbook presenting data as a part of the data release.
High-Flow Field Experiments to Inform Everglades Restoration: Experimental Data 2010 to 2016
Data were collected by USGS for USACE project "CERP: Testing and Monitoring for the Physical Model for Water Conservation Area 3 Decompartmentalization and Sheet Flow Enhancement Project", MIPR

W32CS510826251		
This file contains data collected from research areas known as the Decompartmentalization Physical Model (DPM) and WCA-3A and WCA-3B, Everglades, FL		
Datum: WGS84		
Site ID	Latitude	Longitude
S152	25.8640740	-80.6208520
C1	25.8688503	-80.6107030
C2	25.8327940	-80.6351380
Z5-1	25.8626030	-80.6201250
RS1D	25.8600655	-80.6204093
RS1U	25.8603442	-80.6203967
RS1-SE	25.8603150	-80.6190730
Z5-3B	25.8585970	-80.6199950
Z5-3NE	25.8581190	-80.6191020
RS2	25.8513699	-80.6221905
S1	25.8511939	-80.6170715
UB1	25.8438739	-80.6159930
UB2	25.8407041	-80.6175268
UB3	25.8376759	-80.6199131
MB1	25.8425860	-80.6149720
MB2	25.8399780	-80.6169440
MB3	25.8366690	-80.6194060
DB1	25.8415550	-80.6138860
DB2	25.8391270	-80.6156970
DB3	25.8368580	-80.6174220
This worksheet tab, "Metadata," provides a summary of the data collection methods and defines all related variables.		
The spreadsheet, "S1_2014," contains temperature data collected at S1 from November 2014 through March 2015.		
The spreadsheet, "UB2_2013," contains temperature data collected at UB2 from September 2013 to November 2014.		
The spreadsheet, "UB2_2014," contains temperature data collected at UB2 from November 2014 through March 2015.		
The spreadsheet, "UB2_2015," contains temperature data collected at UB2 from August 2015 to March 2016.		
The spreadsheet, "RS1D_2013," contains temperature data collected at RS1D from September 2013 to November 2014.		
The spreadsheet, "RS1D_2014," contains temperature data collected at RS1D from November 2014 through March 2015.		
The spreadsheet, "RS1D_2015," contains temperature data collected at RS1D from August 2015 to March 2016.		

The spreadsheet, "S1_2014," contains temperature data collected at S1 from November 2014 through March 2015.	
The spreadsheet, "Z51_USGS_2015," contains temperature data collected at Z51_USGS from August 2015 to March 2016.	
Temperature Data Collection Methods:	
Temperature data were measured in degrees Celsius. **Traditional piezometers with four temperature sensors were set up at varying depths below the peat.** **Each piezometer is made of a 0.5m long PVC pipe containing four TMCx Water/Soil temperature sensors connected to a single HOBO U-12-4-channel data logger.** **HOBO U-12-4-channel data logger has 0.02 resolution and 0.25 accuracy, http://www.onsetcomp.com.** **Temperature sensors were located at the peat-floc interface (0 cm depth) and three additional depths within the peat sediment. Three configurations were used. Configuration 1 had probes located at 5, 15, and 35 cm below the peat. Configuration 2 had probes located at 5, 10, and 15 cm below the peat. Configuration 3 varied depending on the location and had a probe located at the floc-surface water interface, floc-peat interace (0cm), half of the peat depth (69-87cm) and as deepa s possible given the length of pipe (133-143 cm).** **Temperature data were collected every 10 minutes for a time period spanning September 28, 2013 to March 3, 2016.**	
Data Columns:	
Date	Date and time of measurement collection.
Shallow Configuration	For August 2015 to March 2016 two configurations were deployed. Shallow refers to configuration 2 (described above).
Deep Configuration	For August 2015 to March 2016 two configurations were deployed. Deep refers to configuration 3 (described above).
Air Temperature	For August 2015 to March 2016 at Z51_USGS air temperature data were collected using a HOBO temperature pendant.
T1	Temperature in degrees Celsius at the first depth interval.
T2	Temperature in degrees Celsius at the second depth interval.
T3	Temperature in degrees Celsius at the third depth interval.
T4	Temperature in degrees Celsius at the last depth interval.
Contact Information:	
Jay Choi	
jchoi@usgs.gov	

Figures and Tables

A. Microtopography

2010 and 2011 Topography Data

Table A-1 Mean and Variability of Peat Elevations in DPM, 2010 and 2011

Site	**Class of Site (All, Ridge, or Slough)**	**Mean** Elevation (cm)	**SD** Elevation (cm)	**Mean** Elevation of plots (cm)	**SD** Elevation of plots (cm)	**Mean SD** Elevation at plots (cm)	**SD of SD** Elevation at plots (cm)
		All Observ-ations	**All Observ-ations**	**100m**	**100m**	**1m**	**1m**
C1	All	173.03	7.08	173.03	6.62	2.73	1.24
C1	Ridge	177.80	4.30	177.80	3.05	3.20	1.22
C1	Slough	166.05	3.77	166.05	5.37	2.06	1.01
C1	Mean Difference (ridge - slough)			11.74			
RS1	All	175.52	9.79	175.82	9.01	3.44	1.65
RS1	Ridge	181.67	6.62	181.84	5.39	4.00	1.14
RS1	Slough	165.51	4.26	165.98	2.42	2.53	1.97
RS1	Mean Difference (ridge - slough)			15.87			
S1	All	168.91	4.59	168.91	4.17	2.09	0.86
S1	Ridge	171.35	3.53	171.35	2.84	2.25	0.84
S1	Slough	165.00	3.17	165.00	2.68	1.83	0.89
S1	Mean Difference (ridge - slough)			6.36			
UB2	All	168.25	12.01	168.42	11.03	2.37	1.11
UB2	Ridge	174.71	8.41	174.71	6.55	2.41	0.88
UB2	Slough	154.50	4.69	154.59	3.07	2.30	1.64
UB2	Mean Difference (ridge - slough)			20.13			

Table A-2 Mean and Variability of Floc Thickness in DPM, 2010 and 2011.

Site	**Class of Site (All, Ridge, or Slough)**	**Mean** Elevation of plots (cm)	**SD** Elevation of plots (cm)	**Mean** Thickness at plots (cm)	**Mean SD** Elevation at plots (cm)	**SD of SD** Elevation at plots (cm)
		100m	**100m**	**100m**	**1m**	**1m**
C1	All	176.27	7.94	3.25	3.01	1.47
C1	Ridge	182.12	3.48	4.32	3.57	1.14
C1	Slough	167.73	6.35	1.68	2.23	1.61
C1	Mean Difference (ridge - slough)	14.39				
RS1	All	188.86	8.96	13.03	4.02	1.72
RS1	Ridge	195.12	3.90	13.28	3.72	1.68
RS1	Slough	178.61	3.56	12.63	5.06	1.73
RS1	Mean Difference (ridge - slough)	16.51				
S1	All	172.45	4.54	3.54	2.24	0.96
S1	Ridge	175.11	2.99	3.76	2.20	1.01
S1	Slough	168.19	3.11	3.20	2.29	0.92
S1	Mean Difference (ridge - slough)	6.92				
UB2	All	180.74	8.83	12.32	2.05	0.80
UB2	Ridge	185.97	4.39	11.26	1.96	0.63
UB2	Slough	169.24	3.22	14.57	2.25	1.16
UB2	Mean Diference (ridge - slough)	16.73				

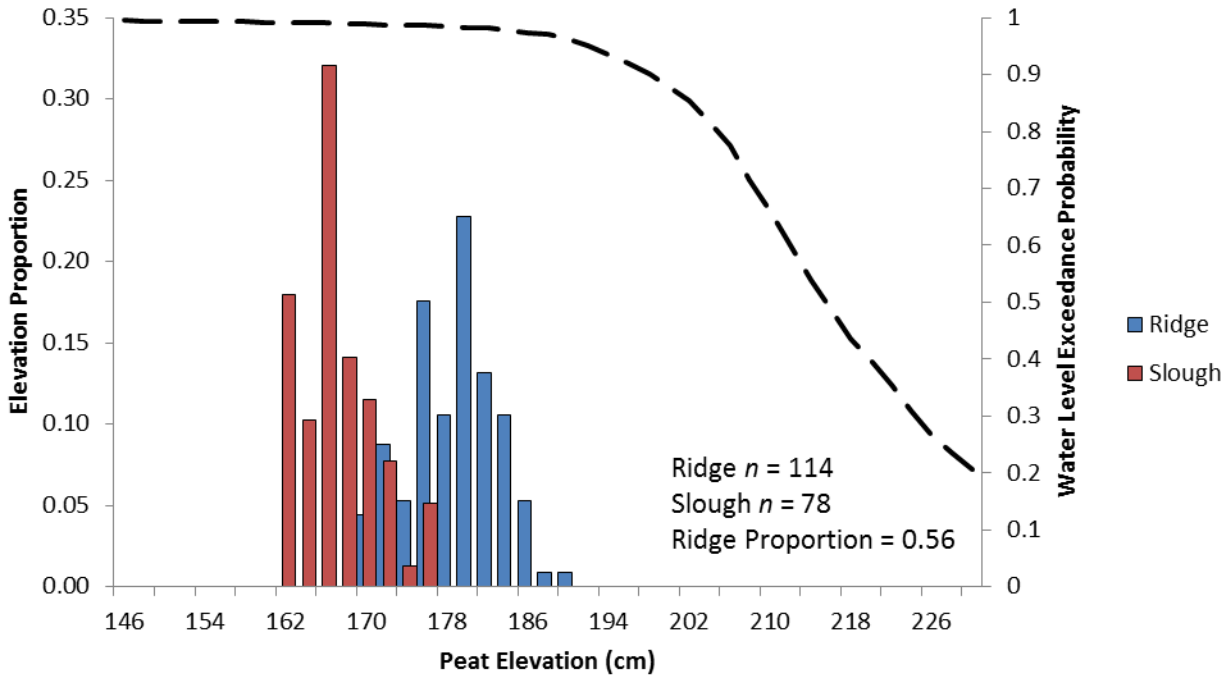

Figure A-1 Site C1 distribution of peat surface elevation and vegetation type contrasted with water level exceedance probability at EDEN site 69E.

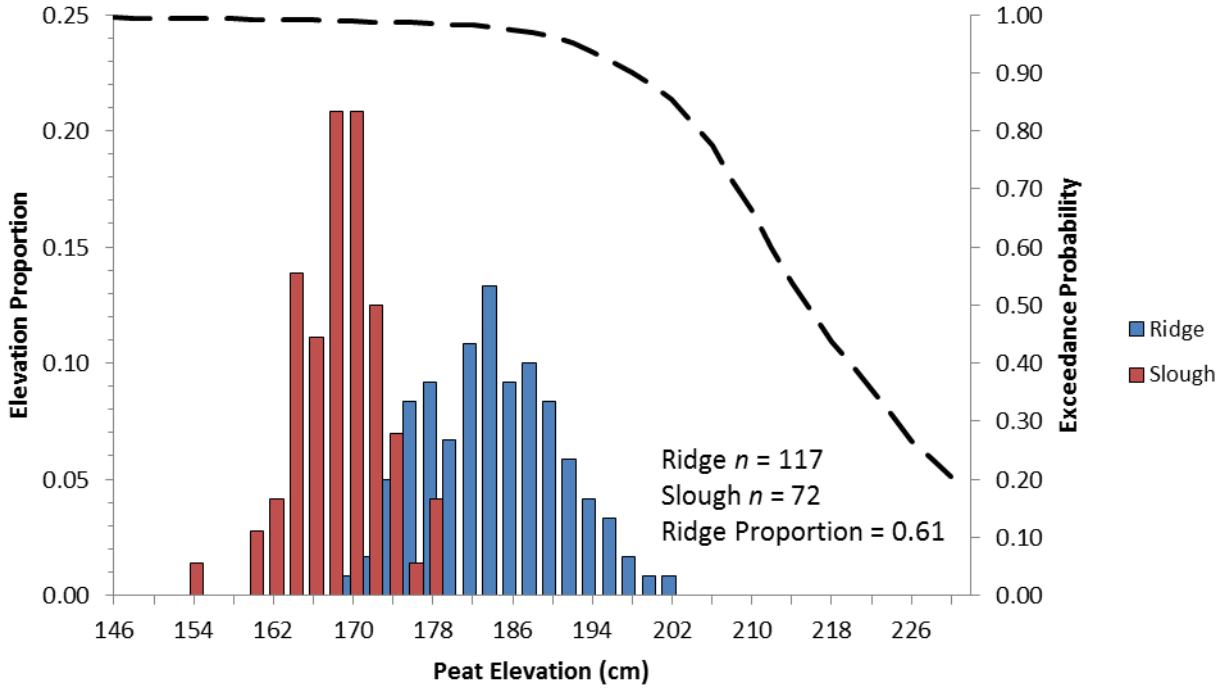

Figure A-2 Site RS1 distribution of peat surface elevation and vegetation type contrasted with water level exceedance probability at EDEN site 69E.

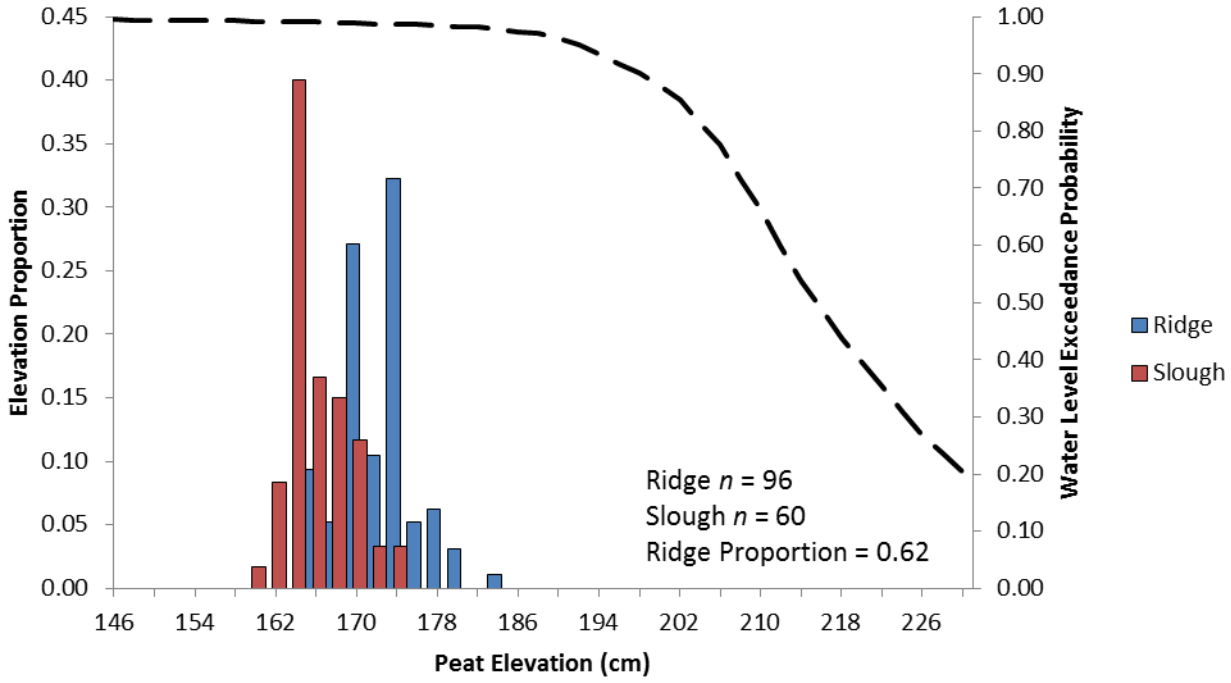

Figure A-3 Site S1 distribution of peat surface elevation and vegetation type contrasted with water level exceedance probability at EDEN site 69E.

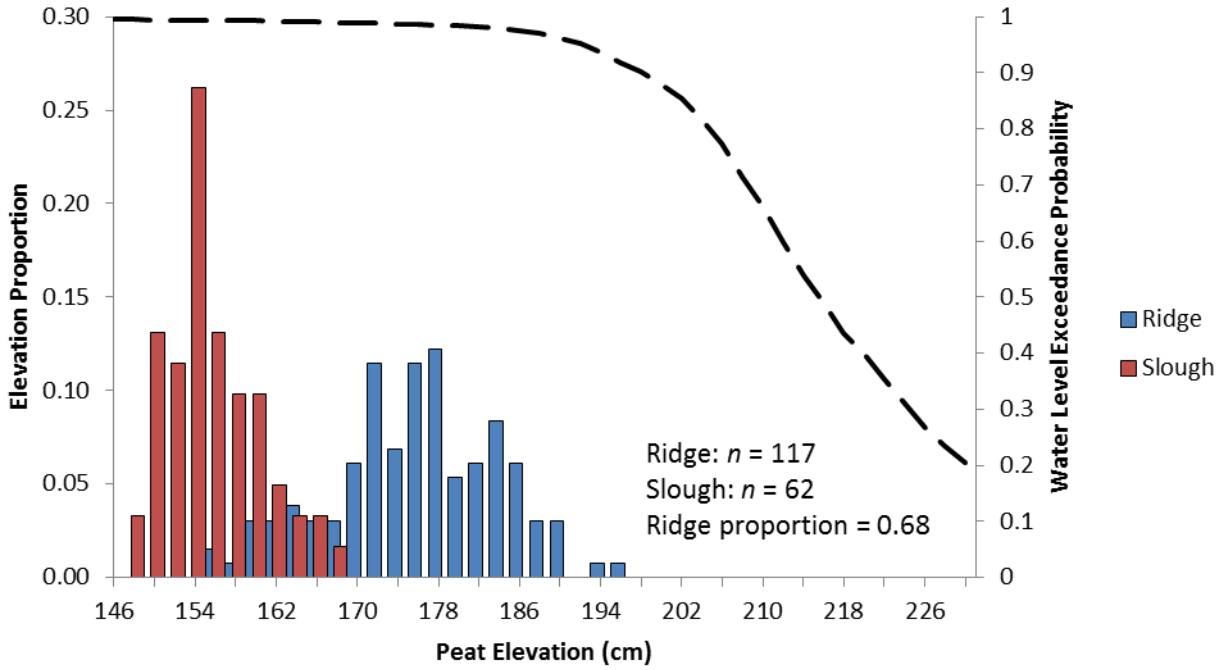

Figure A-4 Site UB2 distribution of peat surface elevation and vegetation type contrasted with water level exceedance probability at EDEN site 69E.

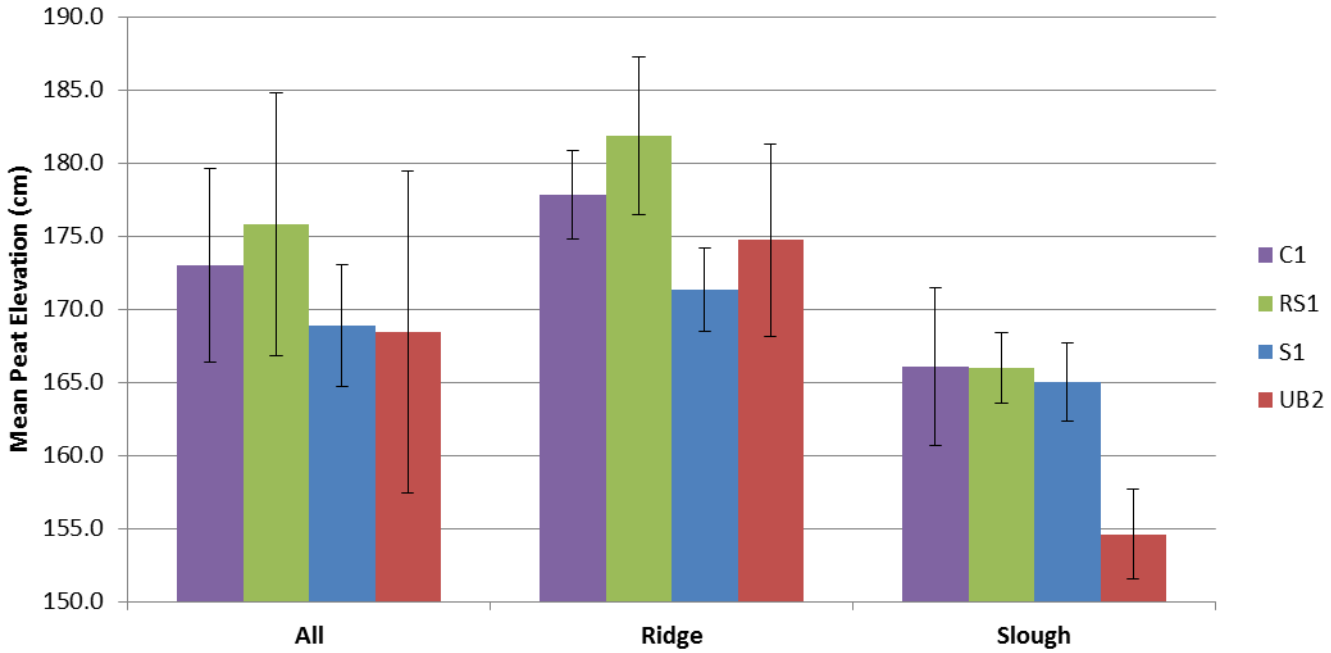

Figure A-5 Comparison of mean peat elevations for DPM data collected in 2010 and 2011. Sites labeled "transition" were classified as ridge.

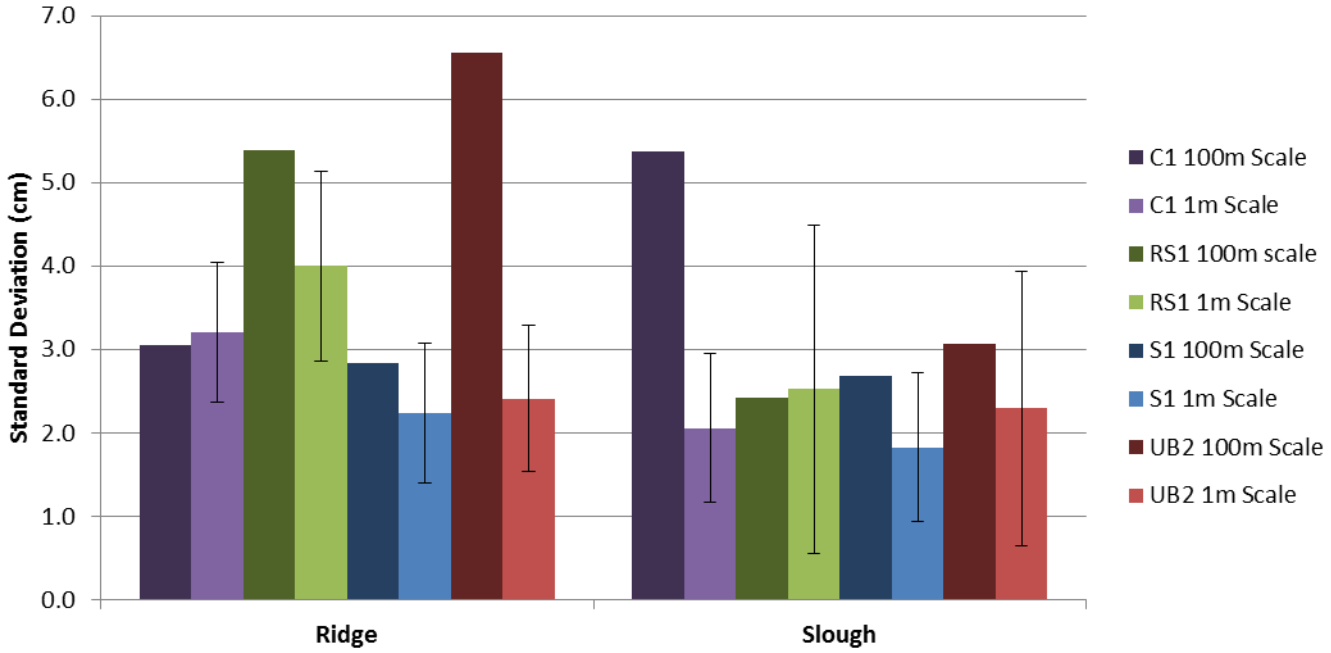

Figure A-6 Comparison of the standard deviations for ridge and slough DPM data collected in 2010 and 2011. Each site has a standard deviation for all observed values (100m Scale) plotted with a standard deviation found through averaging the standard deviations calculated from each plot (1m Scale) in the microtopography circle.

Temporal Microtopography Figures of Sloughs

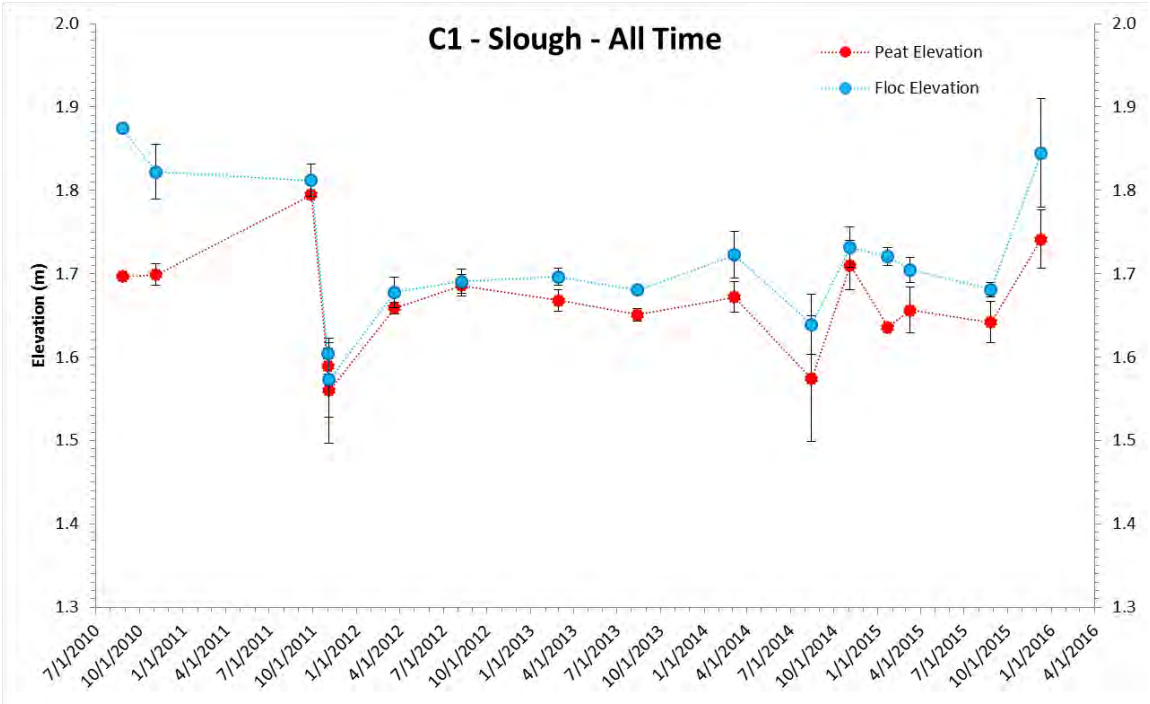

Figure A-7 Time series of averaged microtopography elevations collected near the KPSI piezometer at site C1 slough. Values without error bars are single point measurements.

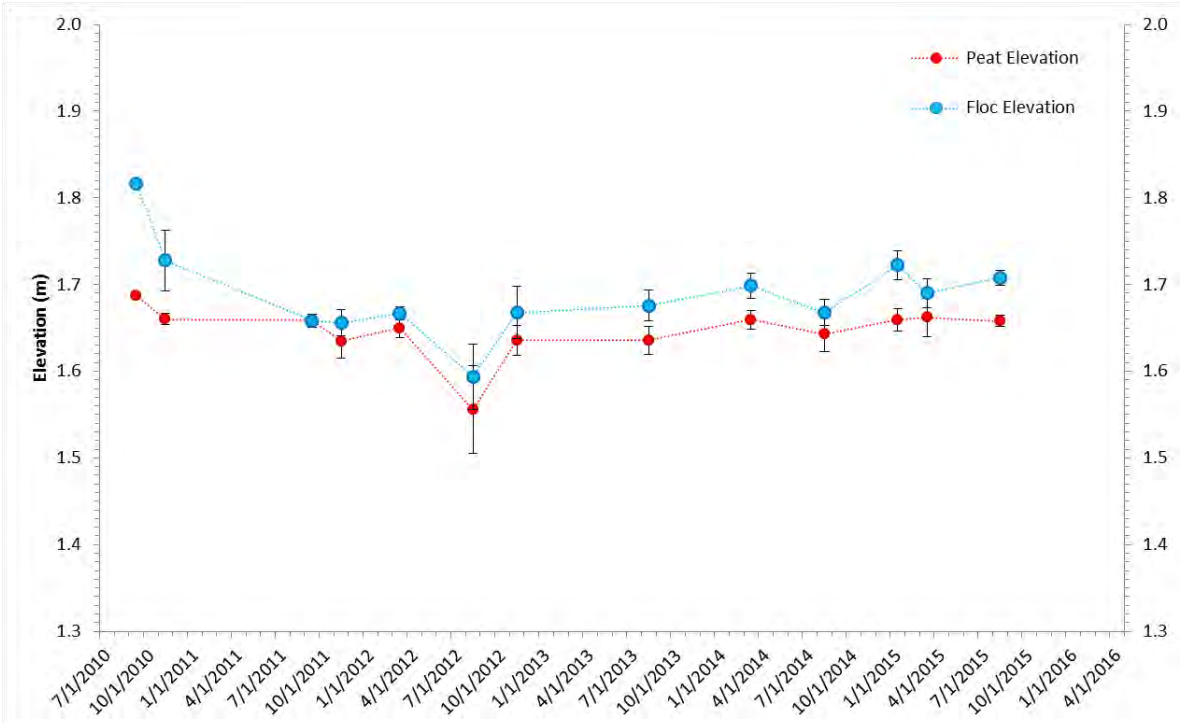

Figure A-8 Time series of averaged microtopography elevations collected near the KPSI piezometer at site C2 slough. Values without error bars are single point measurements.

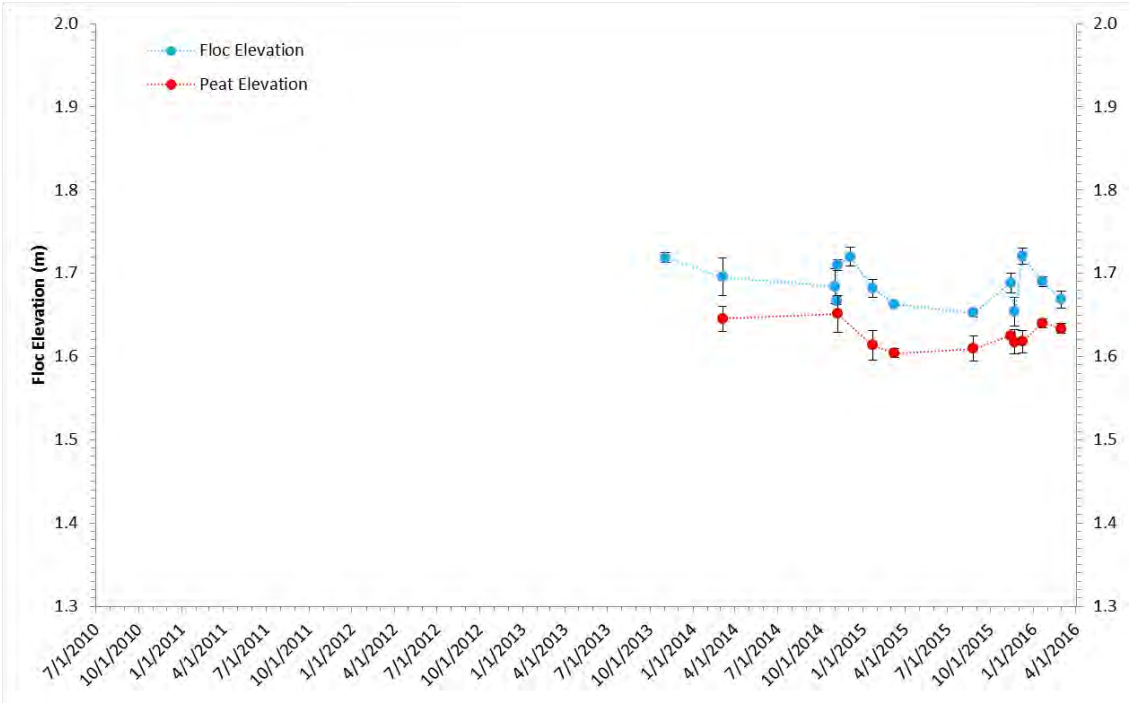

Figure A-9 Time series of averaged microtopography elevations collected near the KPSI piezometer at site RS1U slough. Values without error bars are single point measurements.

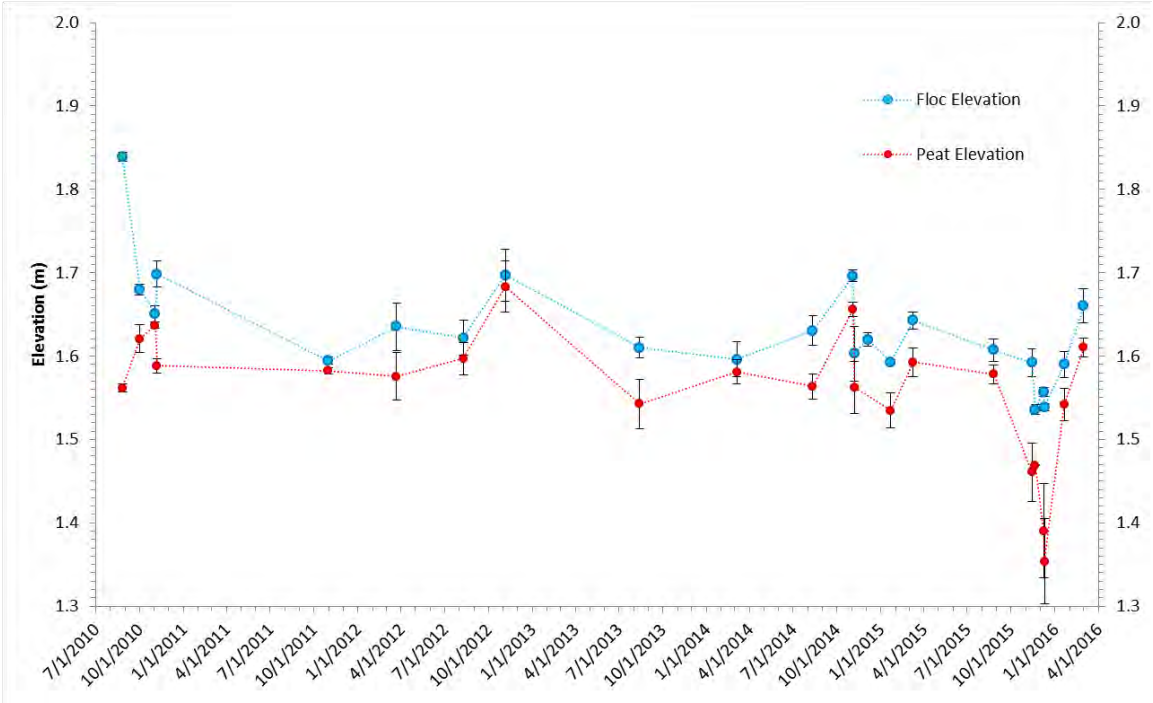

Figure A-10 Time series of averaged microtopography elevations collected near the KPSI piezometer at site RS1D slough. Values without error bars are single point measurements.

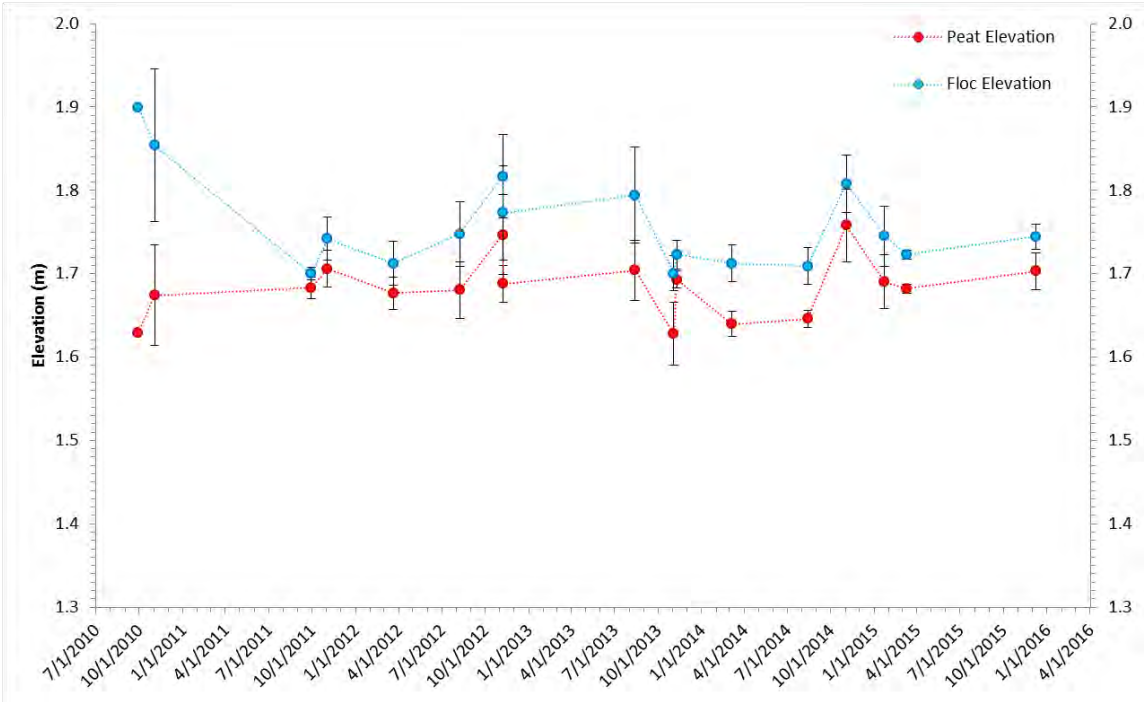

Figure A-11 Time series of averaged microtopography elevations collected near the KPSI piezometer at site RS2 slough. Values without error bars are single point measurements.

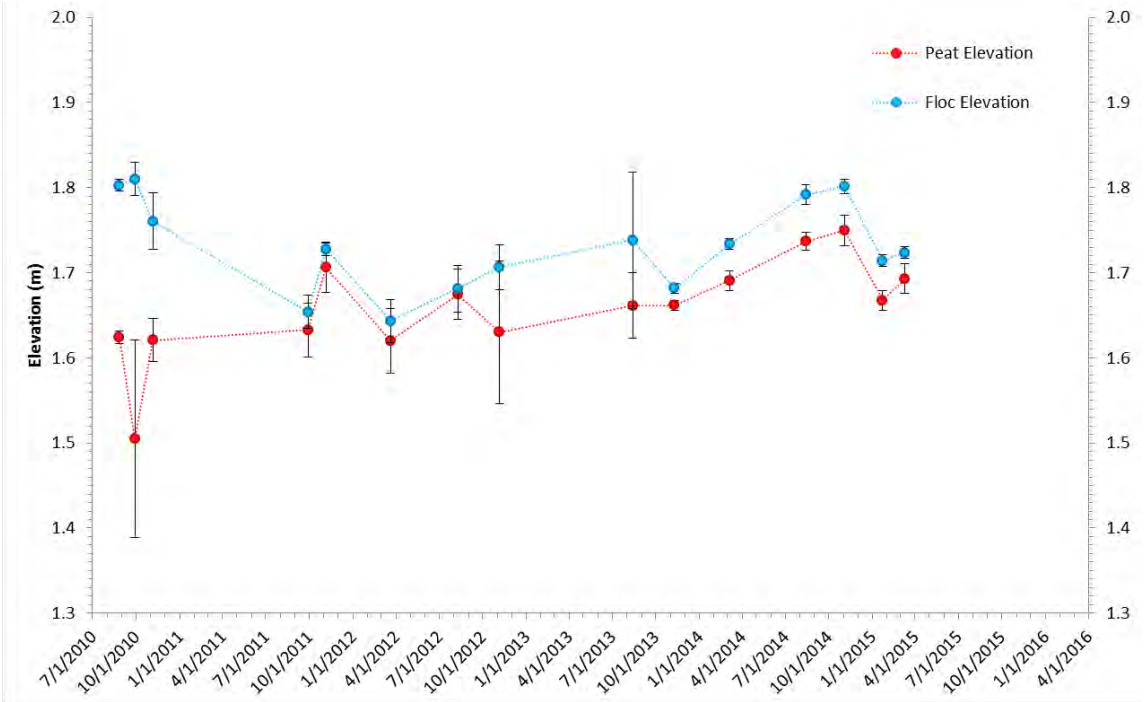

Figure A-12 Time series of averaged microtopography elevations collected near the KPSI piezometer at site S1. Values without error bars are single point measurements.

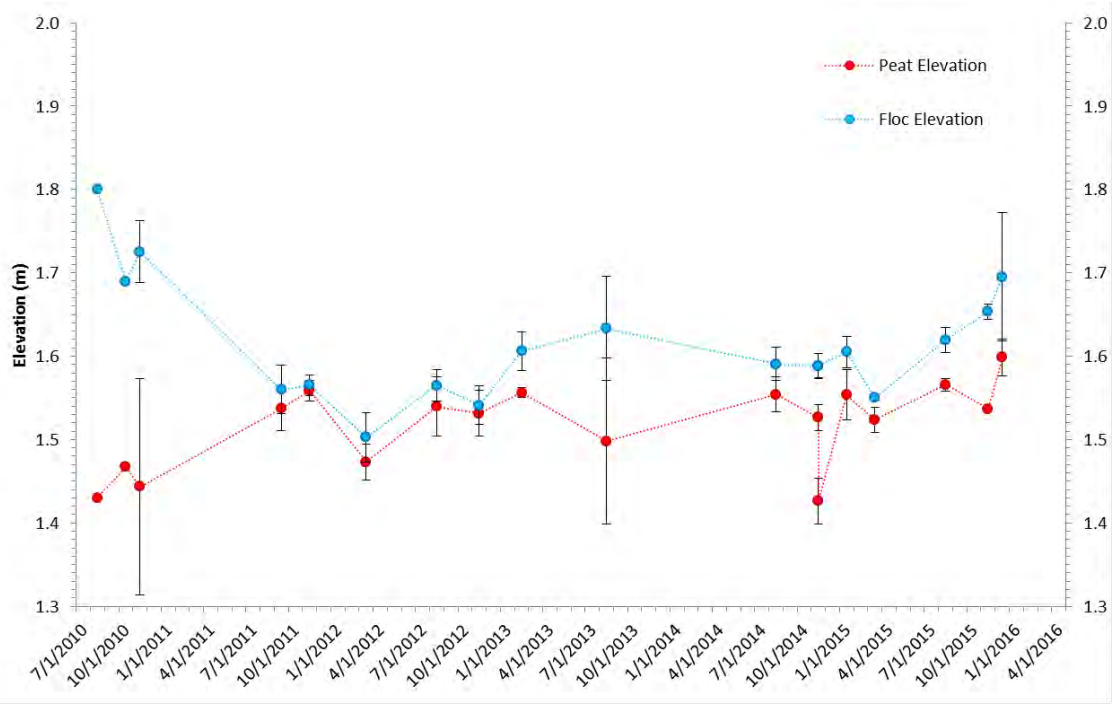

Figure A-13 Time series of averaged microtopography elevations collected near the KPSI piezometer at site UB1. Values without error bars are single point measurements.

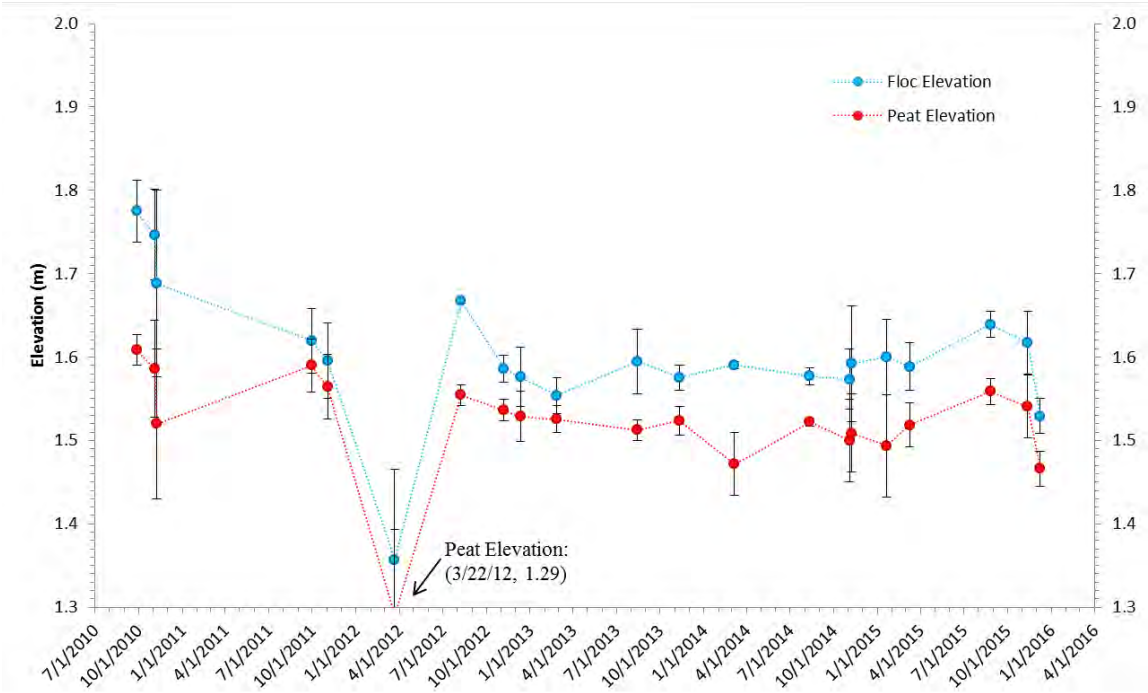

Figure A-14 Time series of averaged microtopography elevations collected near the KPSI piezometer at site UB2. Values without error bars are single point measurements.

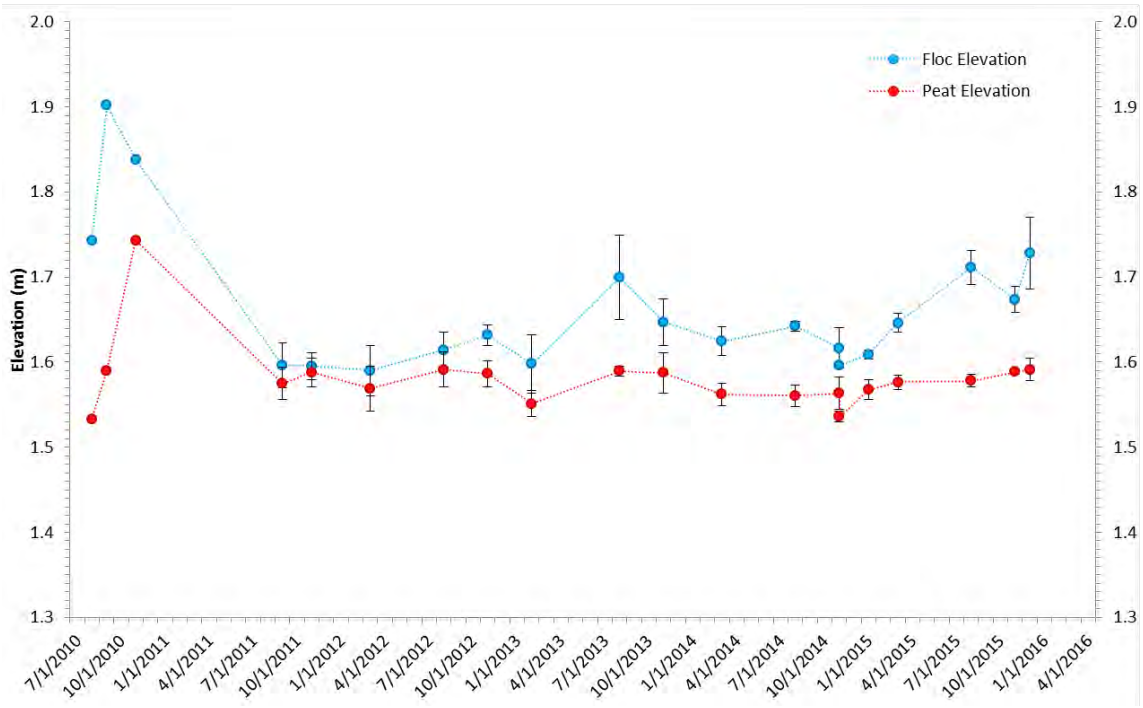

Figure A-15 Time series of averaged microtopography elevations collected near the KPSI piezometer at site UB3. Values without error bars are single point measurements.

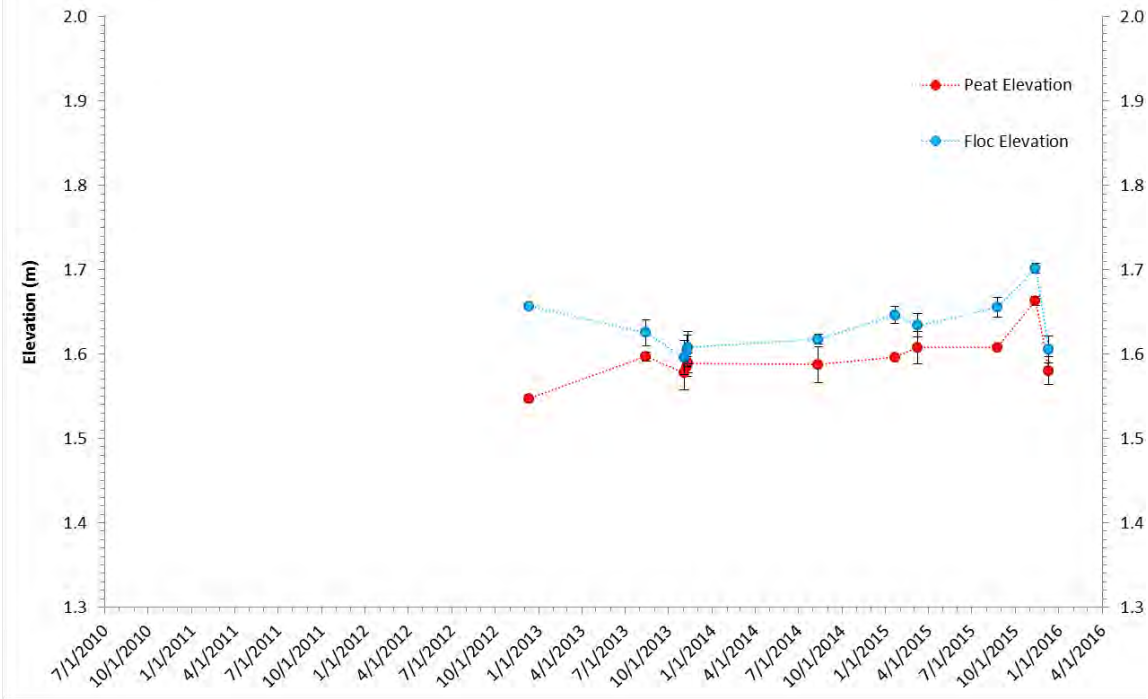

Figure A-16 Time series of averaged microtopography elevations collected near the KPSI piezometer at site DB2. Values without error bars are single point measurements.

Transect Plots

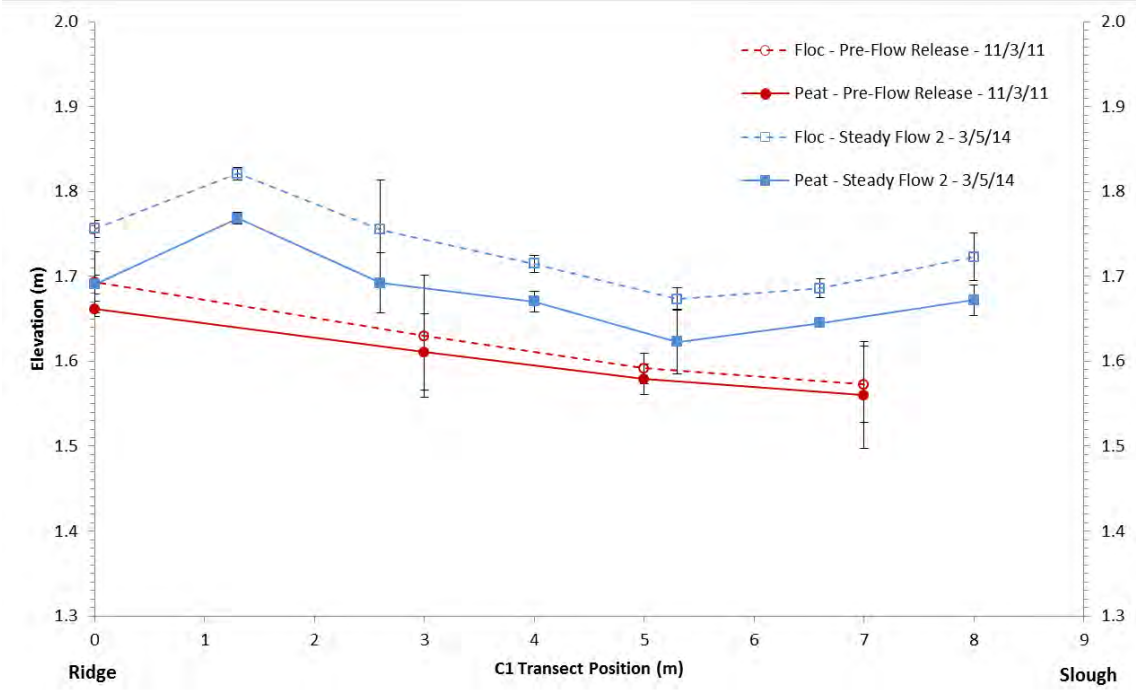

Figure A-17. Elevation transect of floc and peat microtopography measurements collected prior to and after the Nov 5th 2013 flow release at site C1.

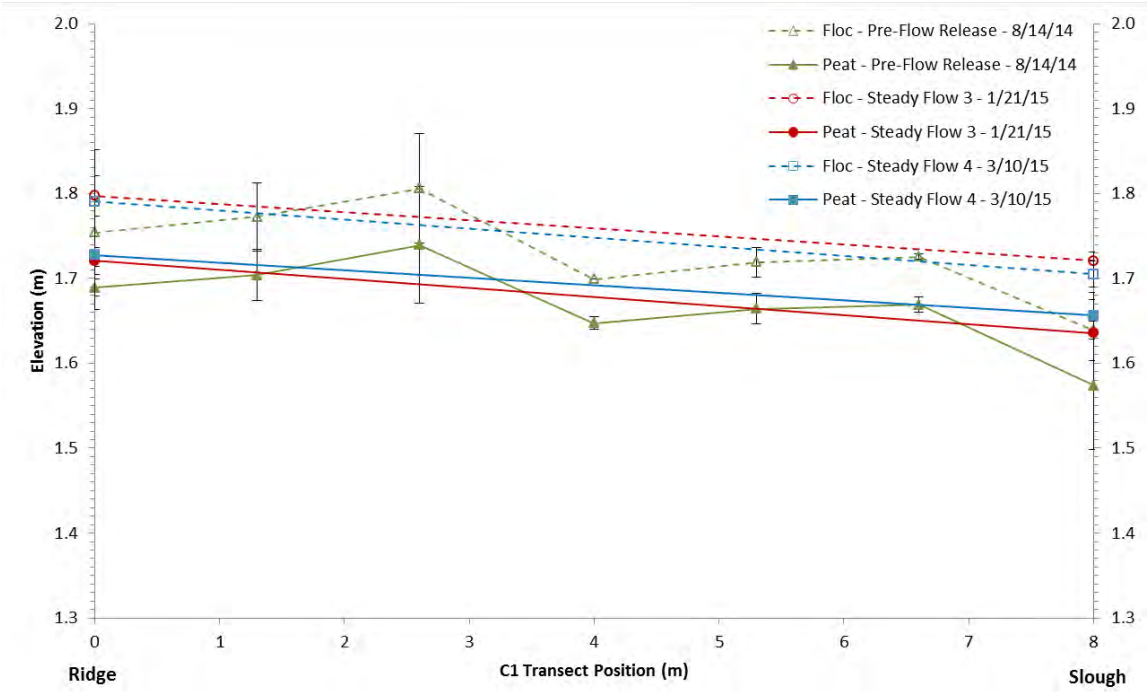

Figure A-18 Elevation transect of floc and peat microtopography measurements collected prior to and after the Nov 4th 2014 flow release at site C1. Values without error bars are single point measurements.

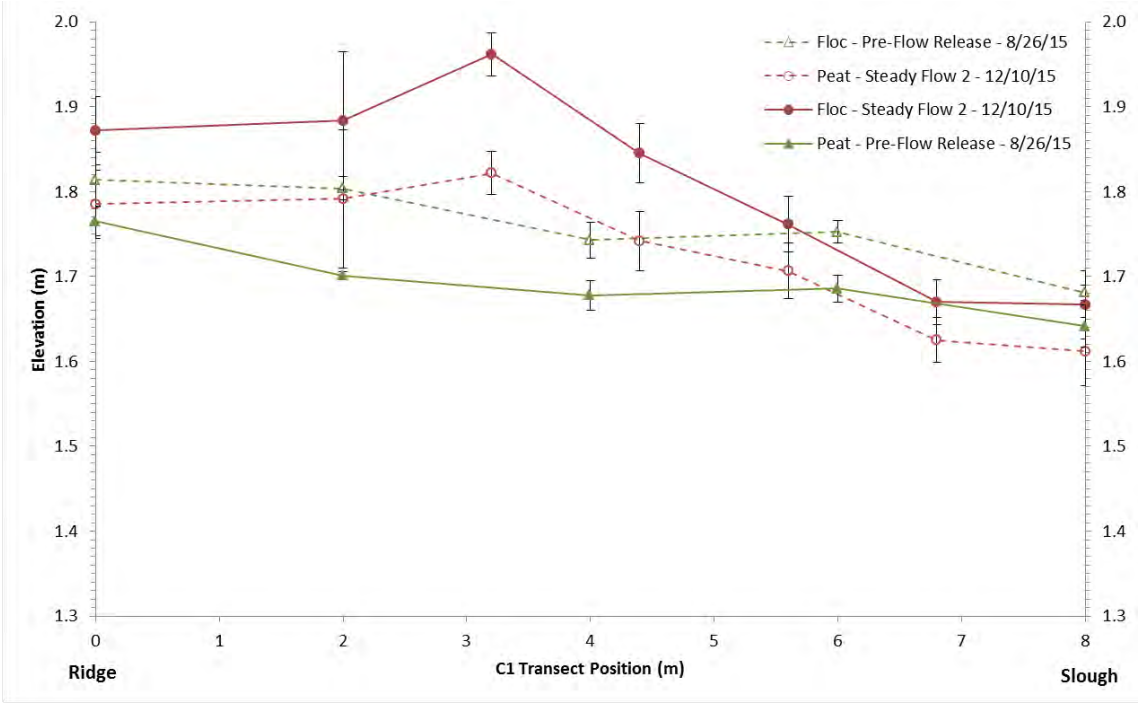

Figure A-19 Elevation transect of floc and peat microtopography measurements collected prior to and after the Nov 4th 2014 flow release at site C1. Values without error bars are single point measurements.

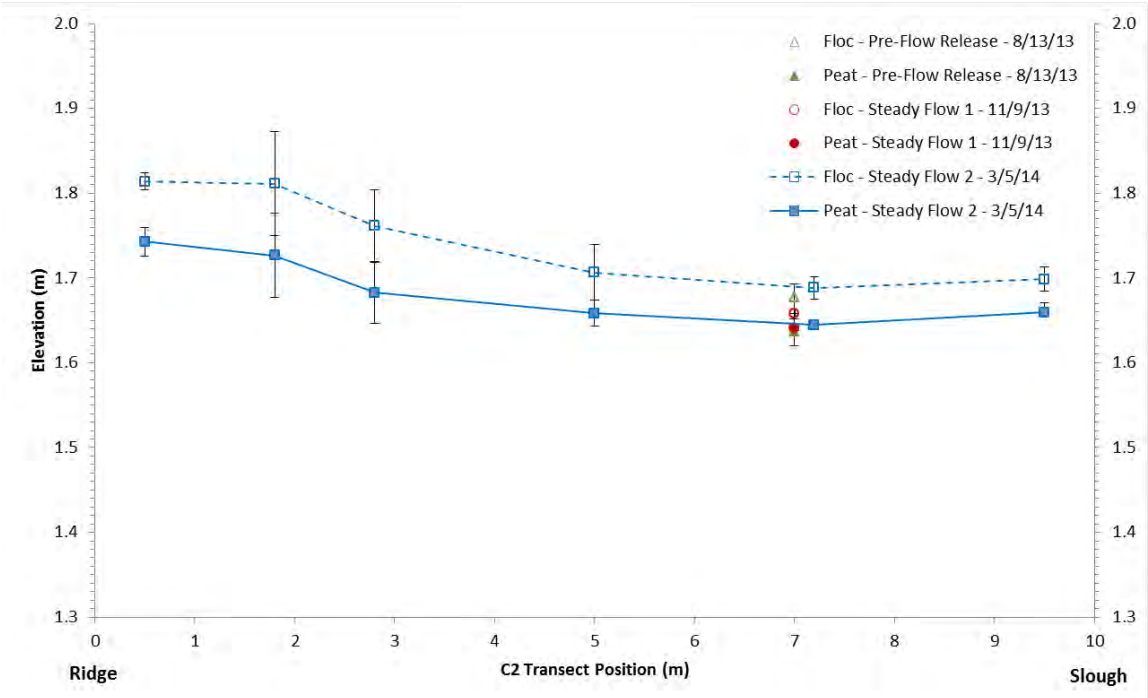

Figure A-20 Elevation transect of floc and peat microtopography measurements collected prior to and after the Nov 5th 2013 flow release at site C2. Values without error bars are single point measurements.

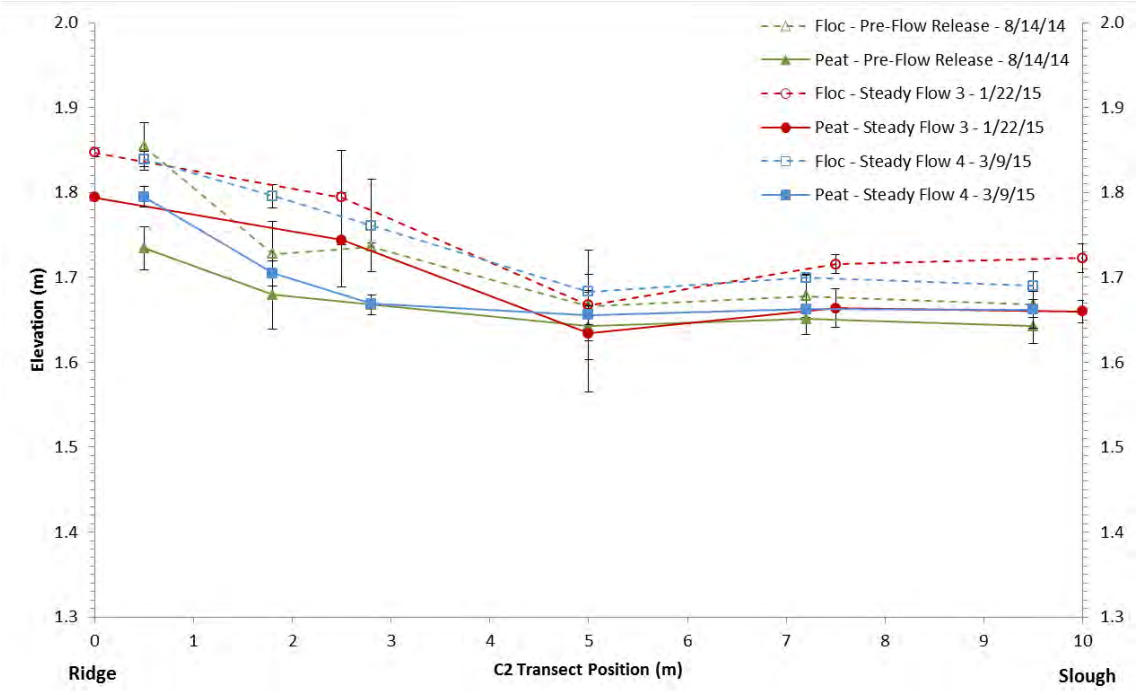

Figure A-21 Elevation transect of floc and peat microtopography measurements collected prior to and after the Nov 4th 2014 flow release at site C2. Values without error bars are single point measurements.

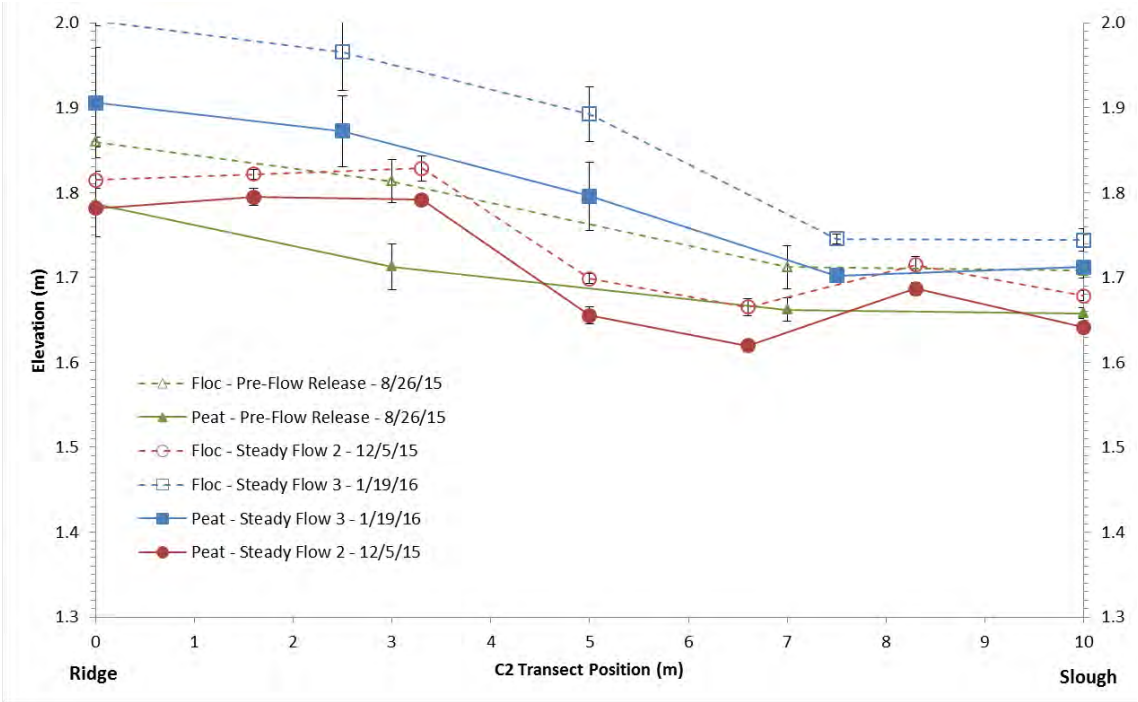

Figure A-22 Elevation transect of floc and peat microtopography measurements collected prior to and after the Nov 4th 2014 flow release at site C2. Values without error bars are single point measurements.

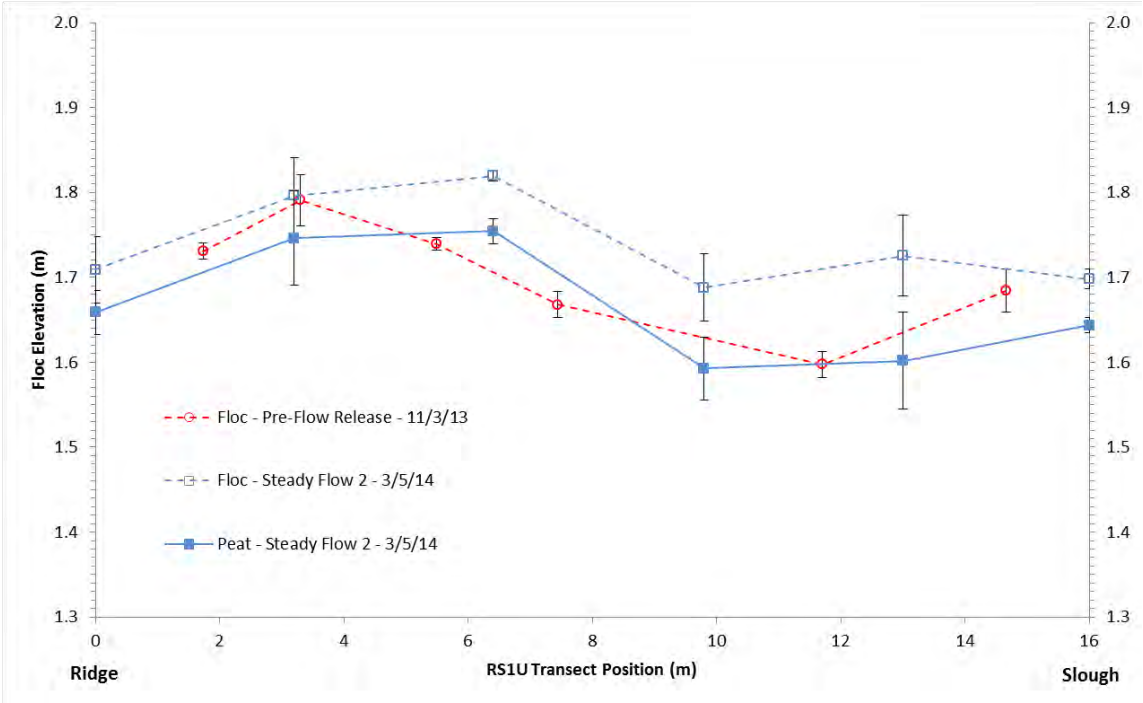

Figure A-23 Elevation transect of floc and peat microtopography measurements collected prior to and after the Nov 5th 2013 flow release at site RS1U. Values without error bars are single point measurements.

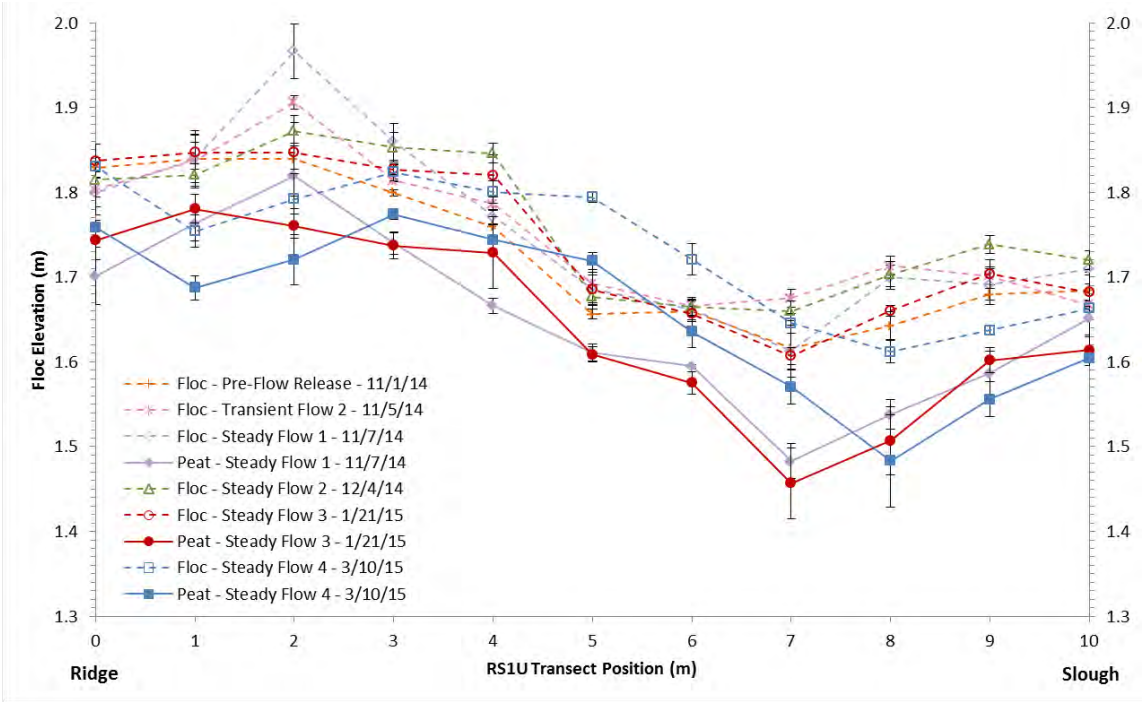

Figure A-24 Elevation transect of floc and peat microtopography measurements collected prior to and after the Nov 4th 2014 flow release at site RS1U. Values without error bars are single point measurements.

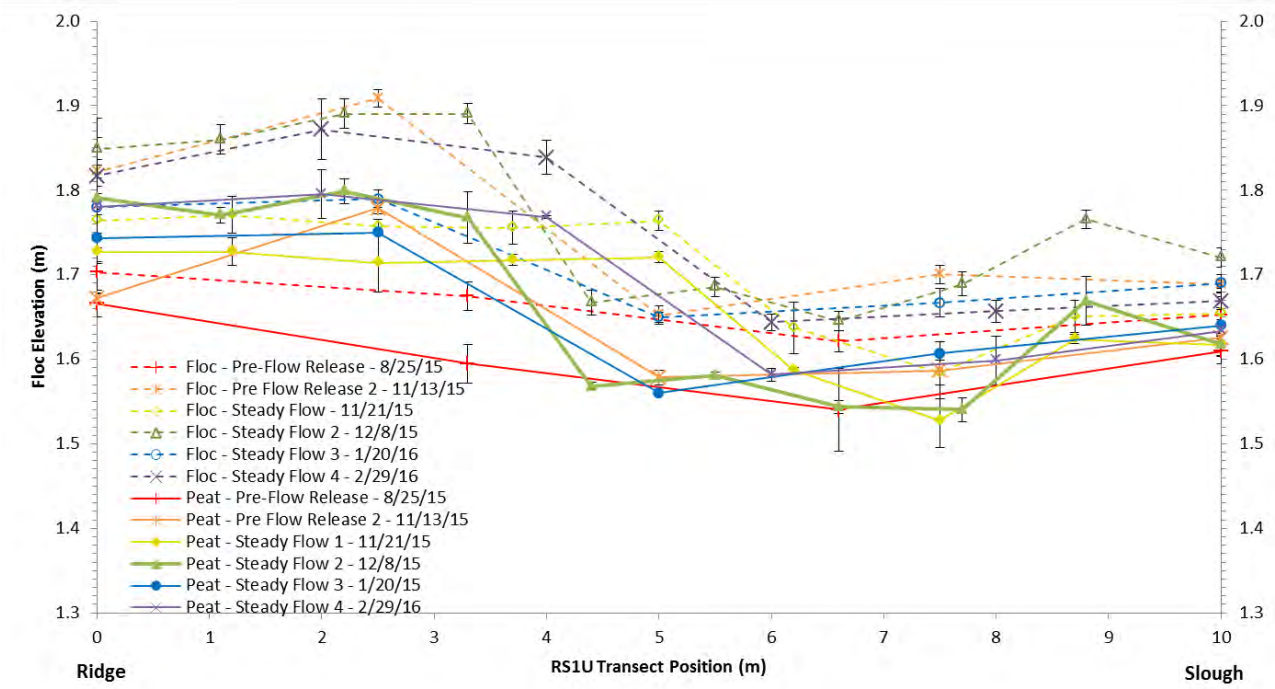

Figure A-25 Elevation transect of floc and peat microtopography measurements collected prior to and after the Nov 4th 2014 flow release at site RS1U. Values without error bars are single point measurements.

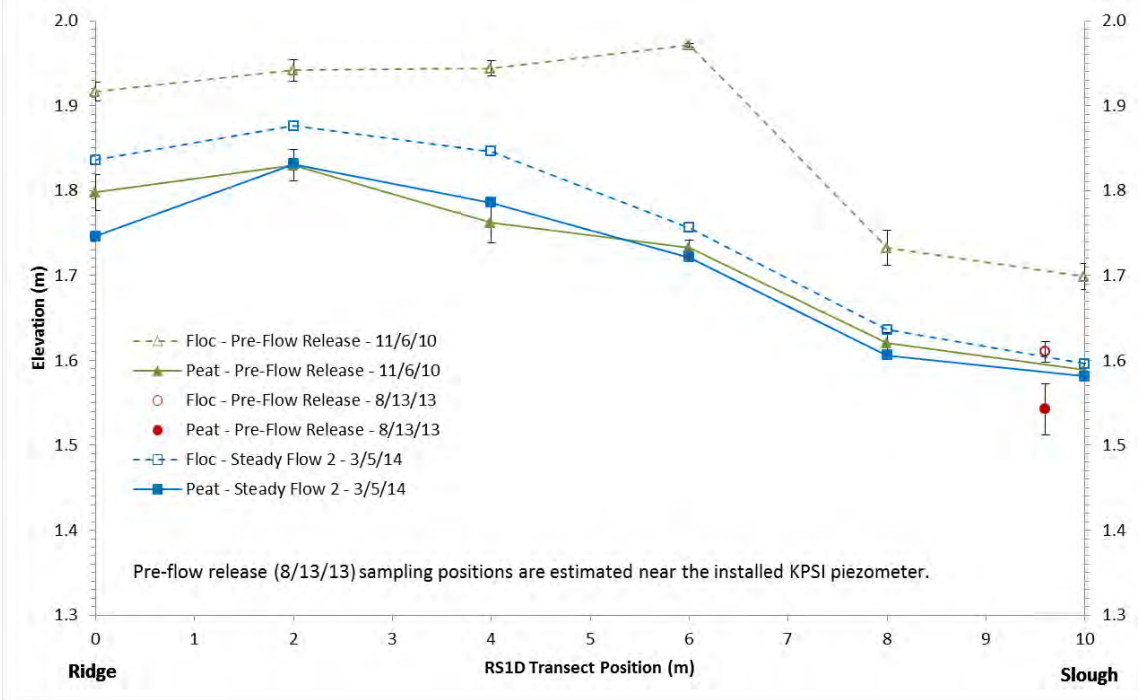

Figure A-26 Elevation transect of floc and peat microtopography measurements collected prior to and after the Nov 5th 2013 flow release at site RS1D. Values without error bars are single point measurements.

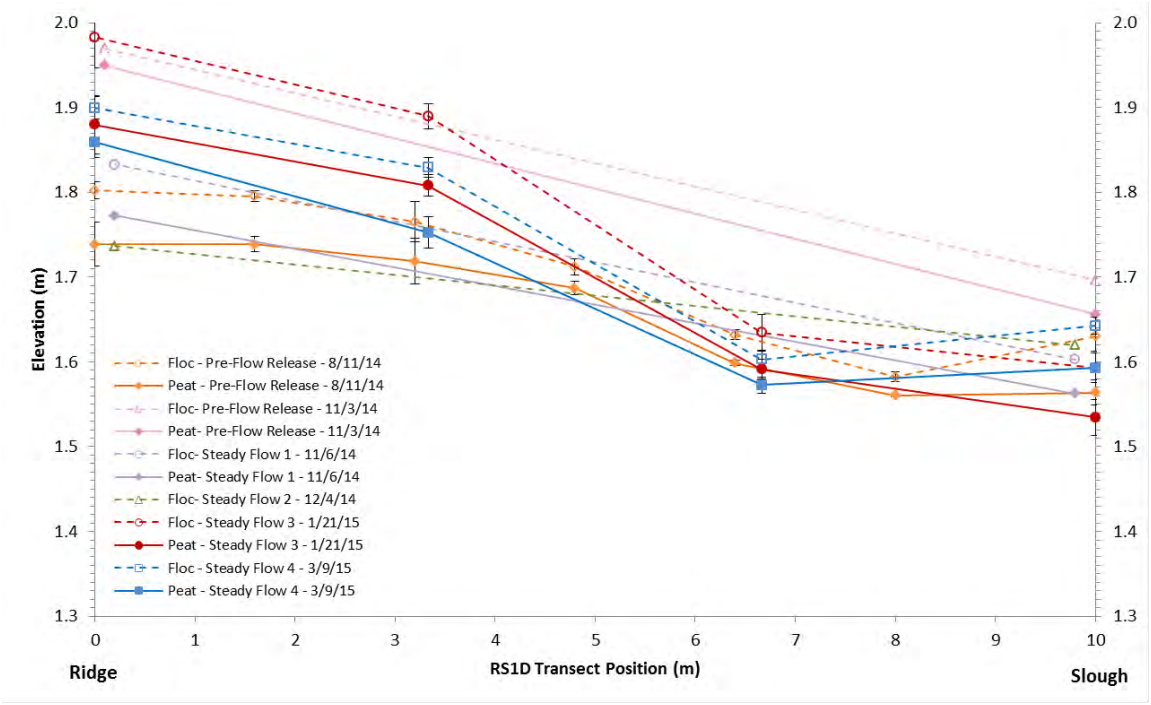

Figure A-27 Elevation transect of floc and peat microtopography measurements collected prior to and after the Nov 4th 2014 flow release at site RS1D. Values without error bars are single point measurements.

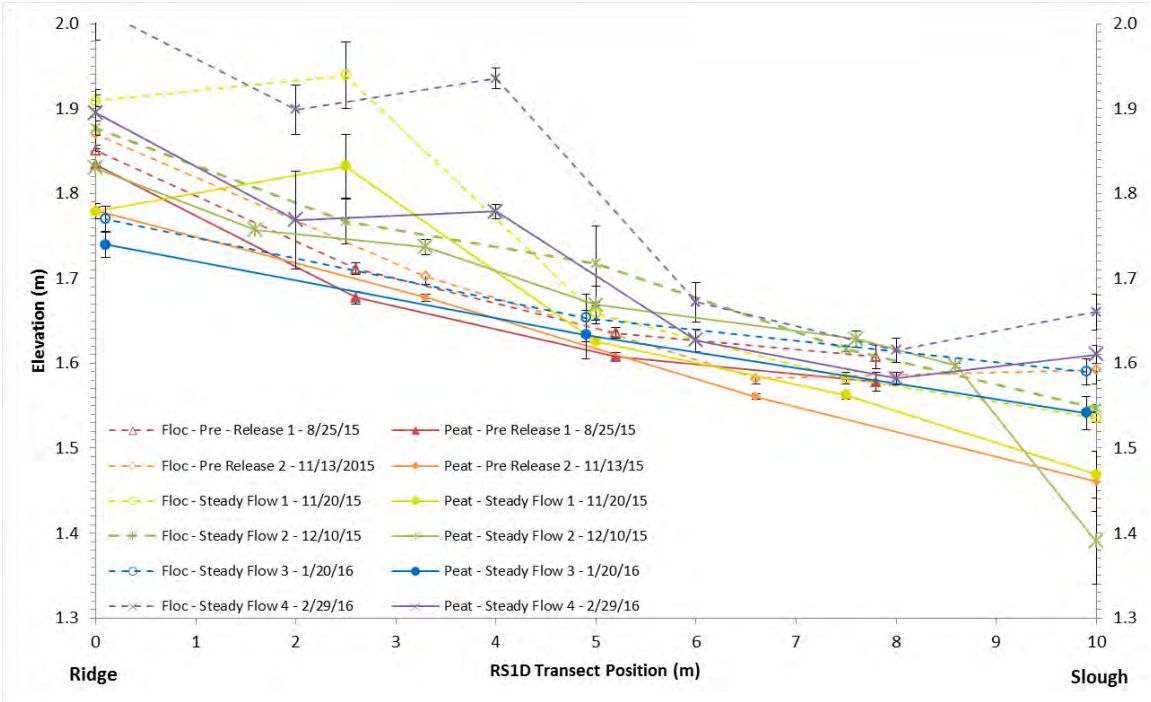

Figure A-28 Elevation transect of floc and peat microtopography measurements collected prior to and after the Nov 16th 2015 flow release at site RS1D.

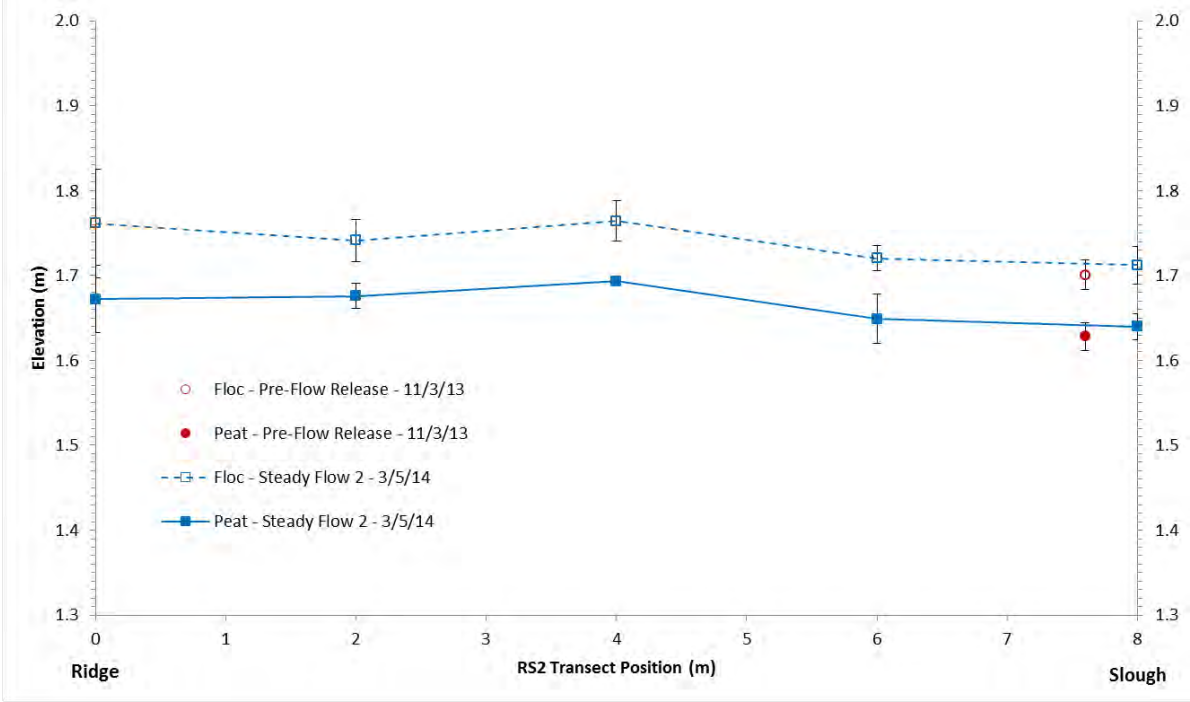

Figure A-29 Elevation transect of floc and peat microtopography measurements collected prior to and after the Nov 5th 2013 flow release at site RS2. Values without error bars are single point measurements.

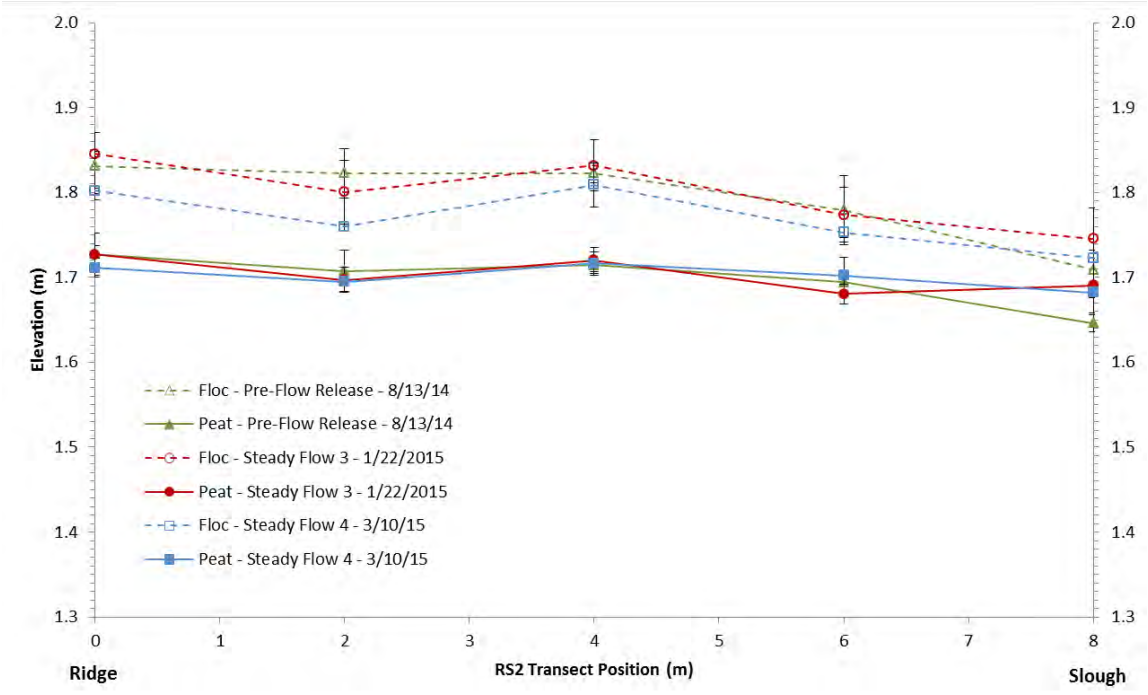

Figure A-30 Elevation transect of floc and peat microtopography measurements collected prior to and after the Nov 4th 2014 flow release at site RS2. Values without error bars are single point measurements.

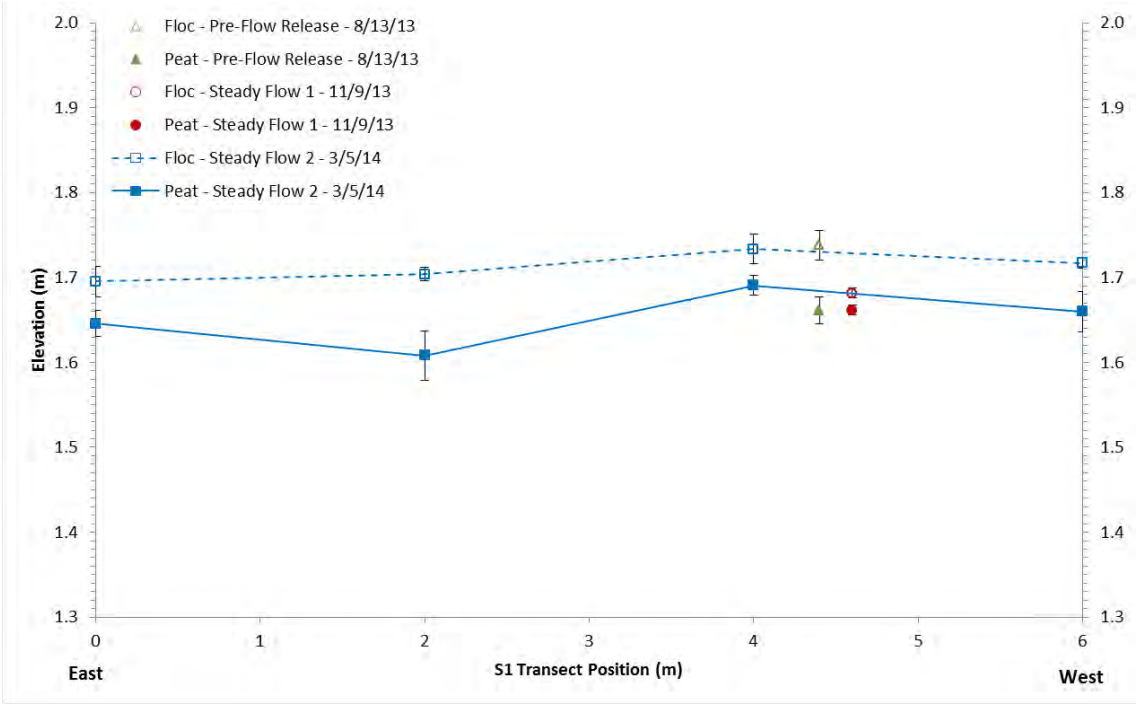

Figure A-31 Elevation transect of floc and peat microtopography measurements collected prior to and after the Nov 5th 2013 flow release at site S1. Values without error bars are single point measurements.

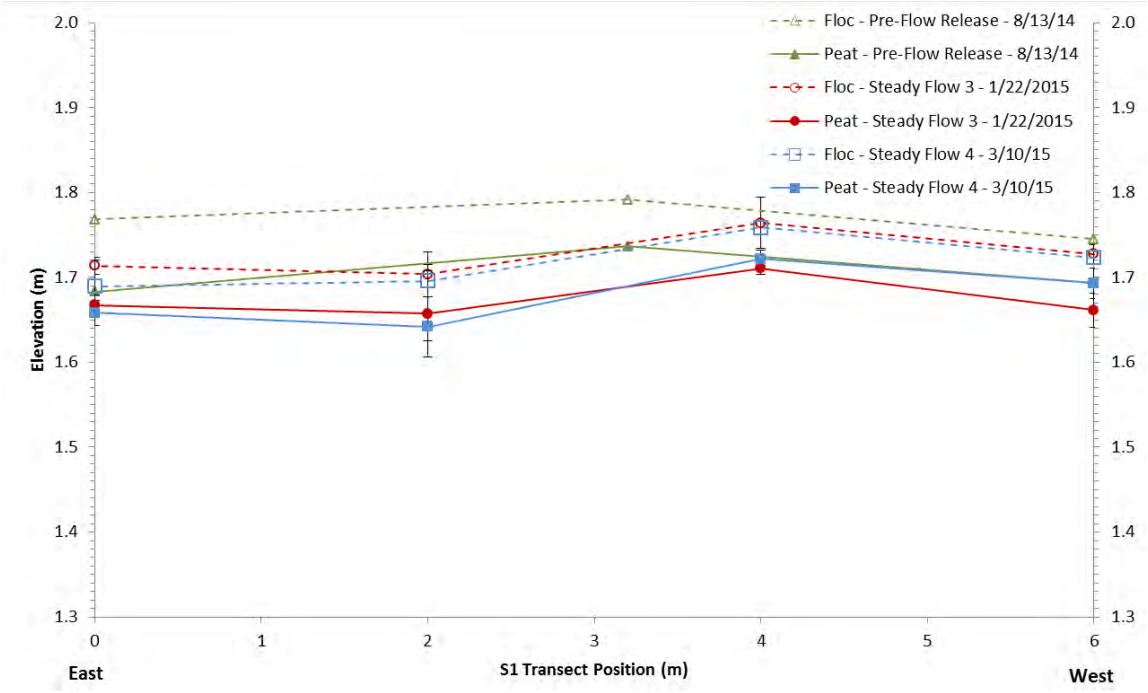

Figure A-32 Elevation transect of floc and peat microtopography measurements collected prior to and after the Nov 4th 2014 flow release at site S1. Values without error bars are single point measurements.

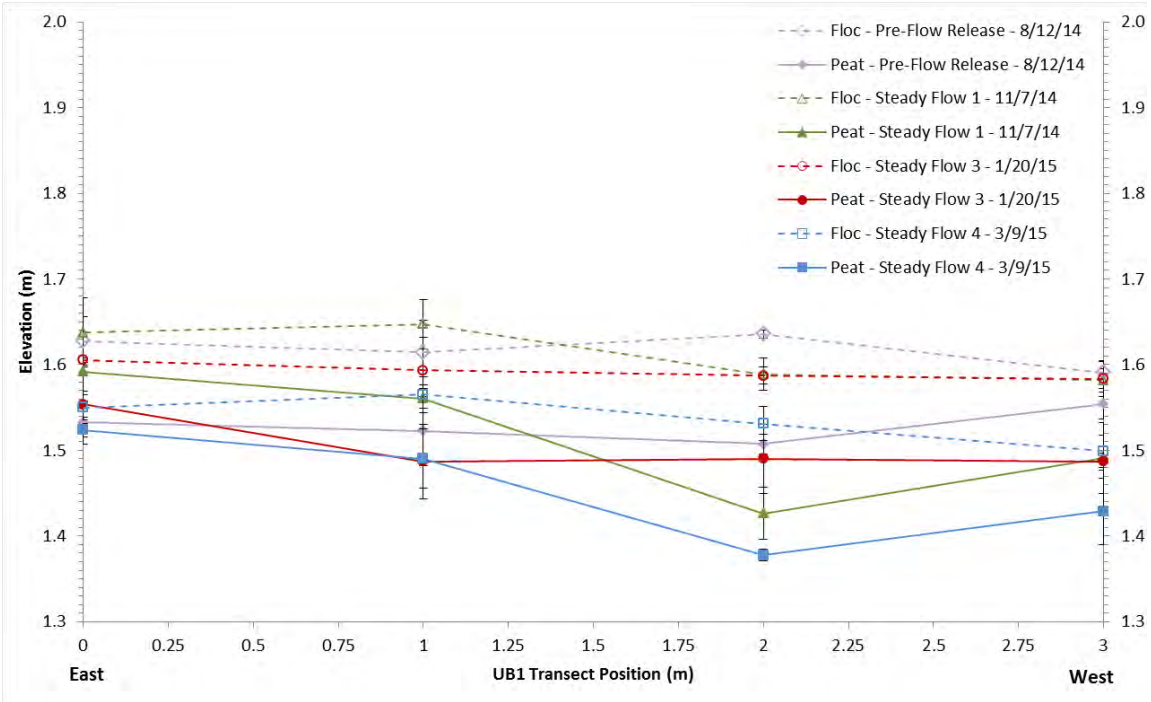

Figure A-33 Elevation transect of floc and peat microtopography measurements collected prior to and after the Nov 4th 2014 flow release at site UB1. Values without error bars are single point measurements.

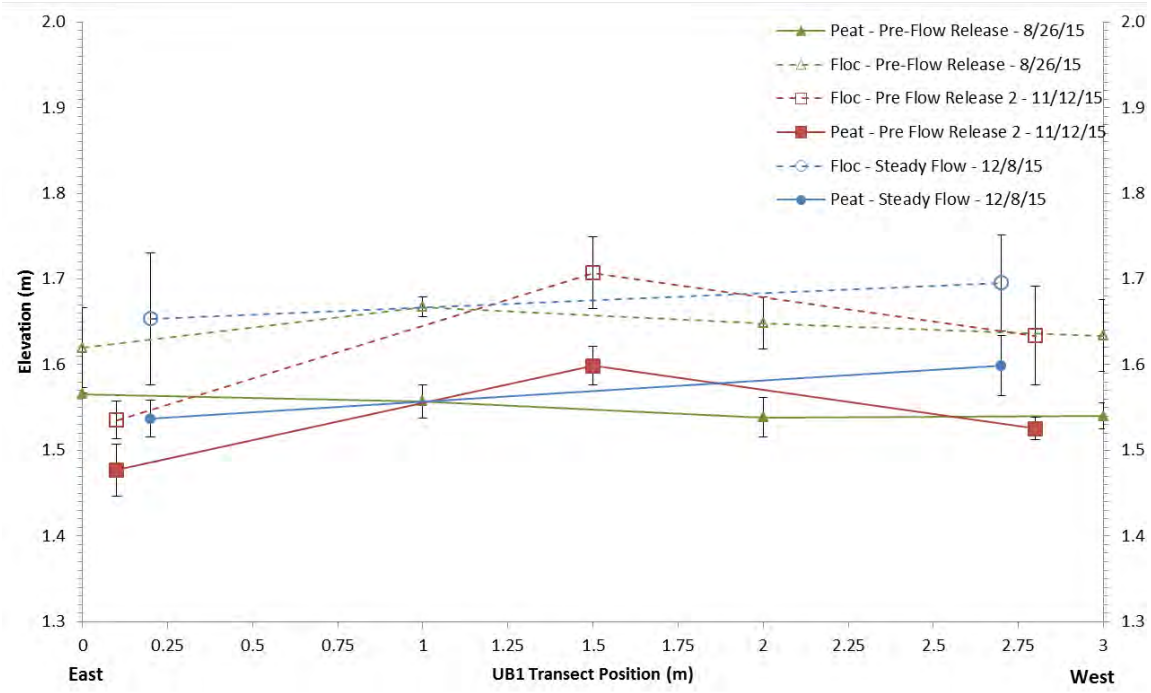

Figure A-34 Elevation transect of floc and peat microtopography measurements collected prior to and after the Nov 16th 2015 flow release at site UB1.

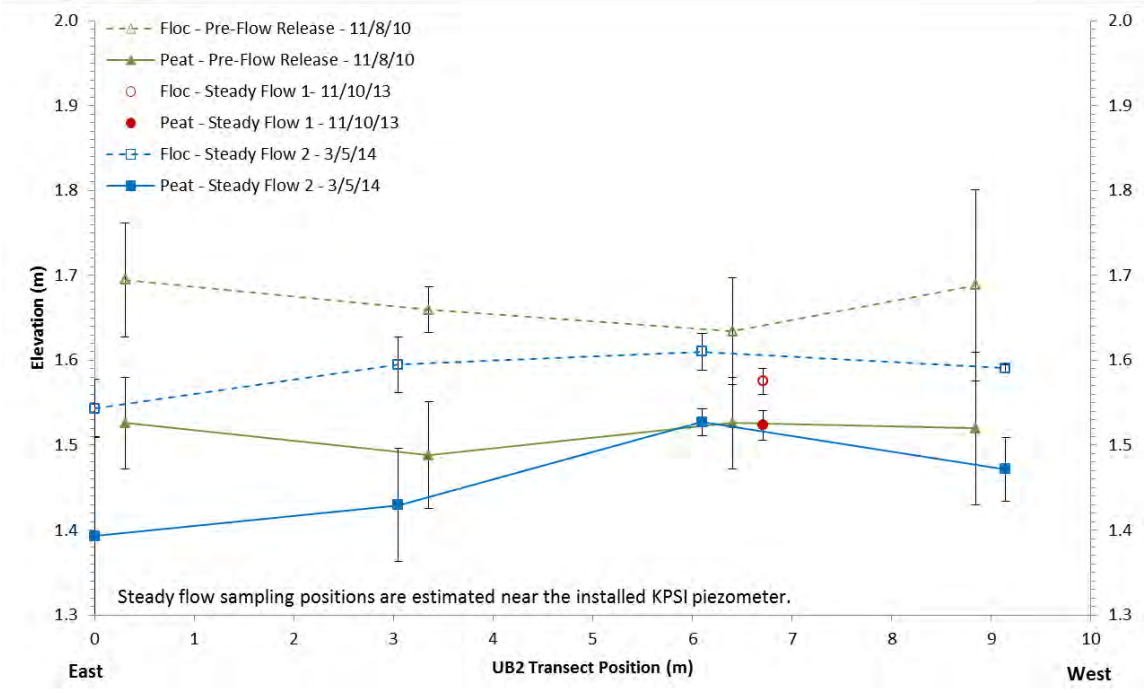

Figure A-35 Elevation transect of floc and peat microtopography measurements collected prior to and after the Nov 5th 2013 flow release at site UB2. Values without error bars are single point measurements.

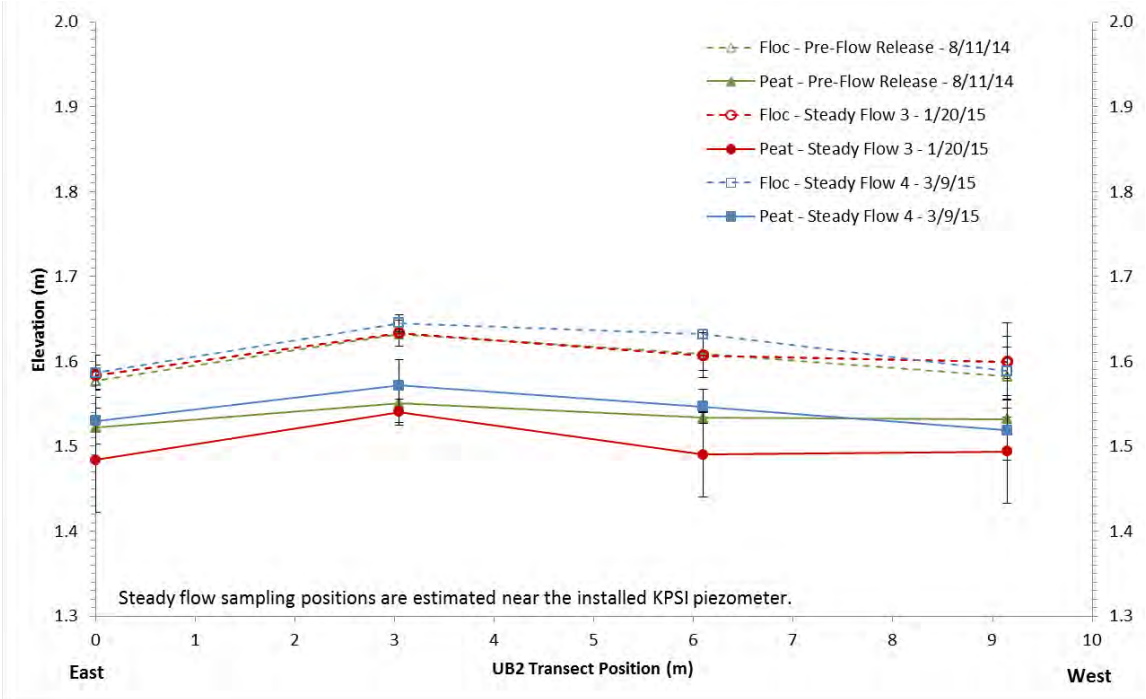

Figure A-36 Elevation transect of floc and peat microtopography measurements collected prior to and after the Nov 4th 2014 flow release at site UB2. Values without error bars are single point measurements.

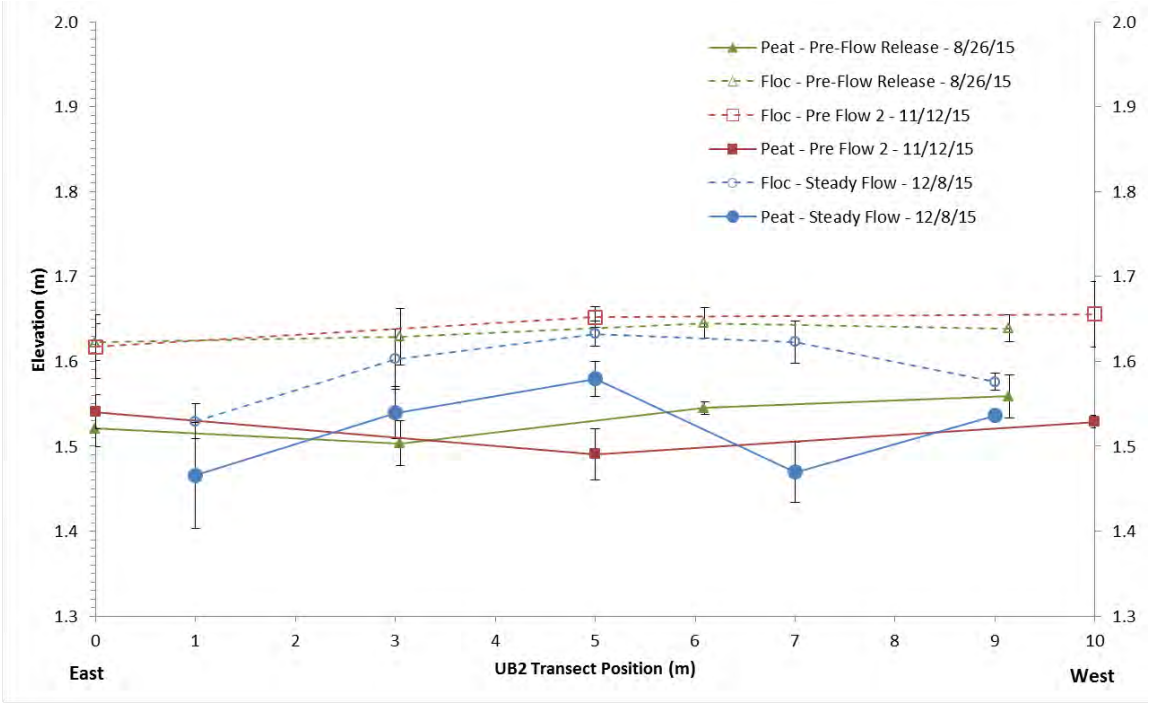

Figure A-37 Elevation transect of floc and peat microtopography measurements collected prior to and after the Nov 16th 2015 flow release at site UB2. Values without error bars are single point measurements.

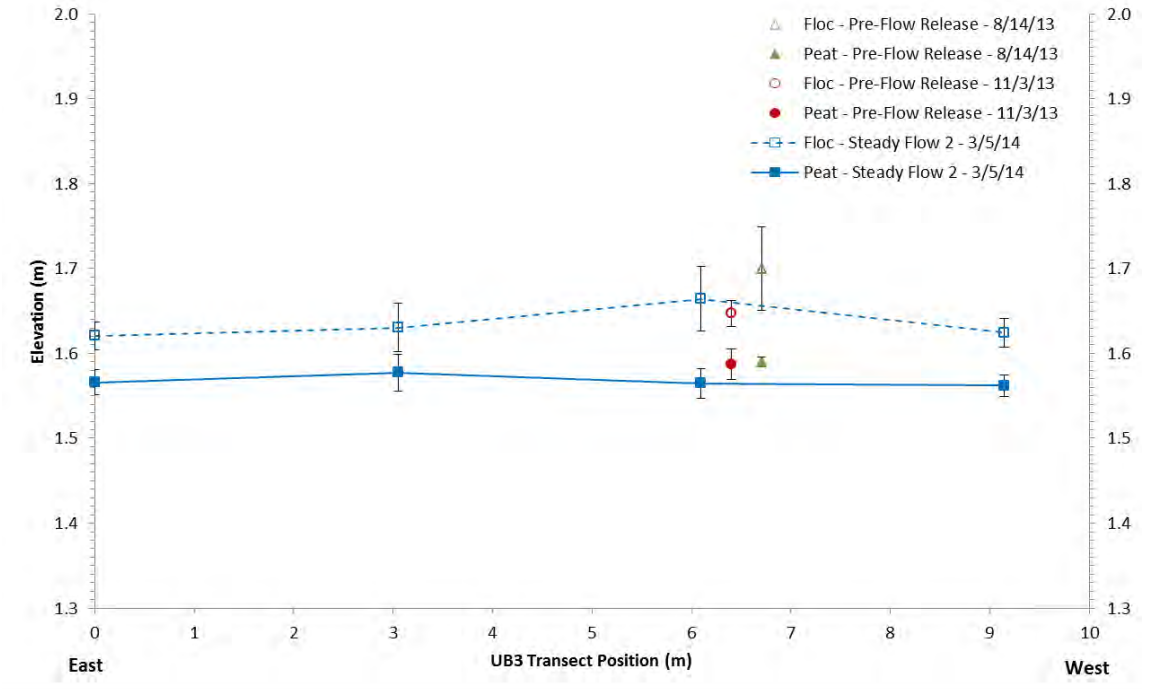

Figure A-38 Elevation transect of floc and peat microtopography measurements collected prior to and after the Nov 5th 2013 flow release at site UB3. Values without error bars are single point measurements.

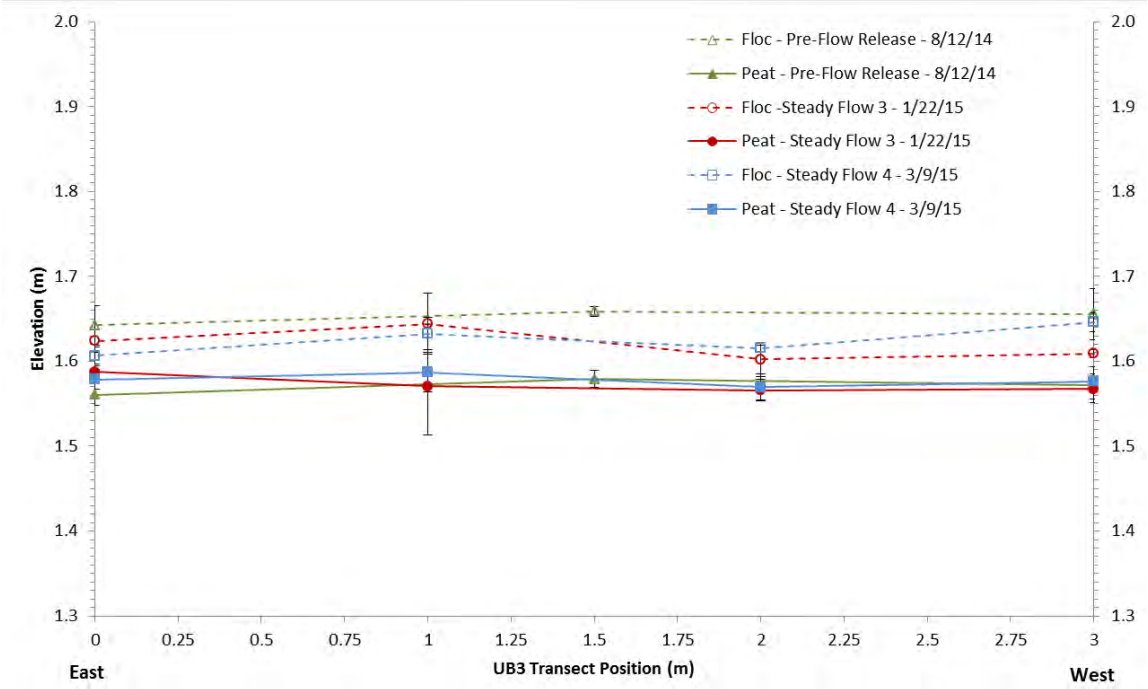

Figure A-39 Elevation transect of floc and peat microtopography measurements collected prior to and after the Nov 4th 2014 flow release at site UB3. Values without error bars are single point measurements.

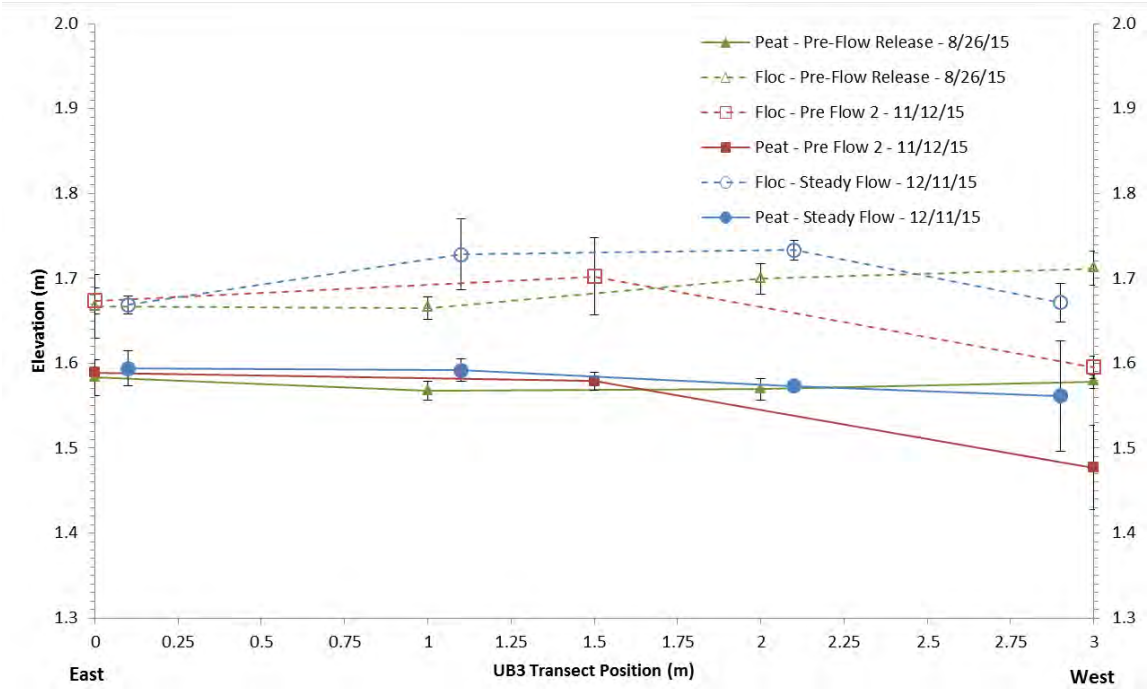

Figure A-40 Elevation transect of floc and peat microtopography measurements collected prior to and after the Nov 16th 2015 flow release at site UB3. Values without error bars are single point measurements.

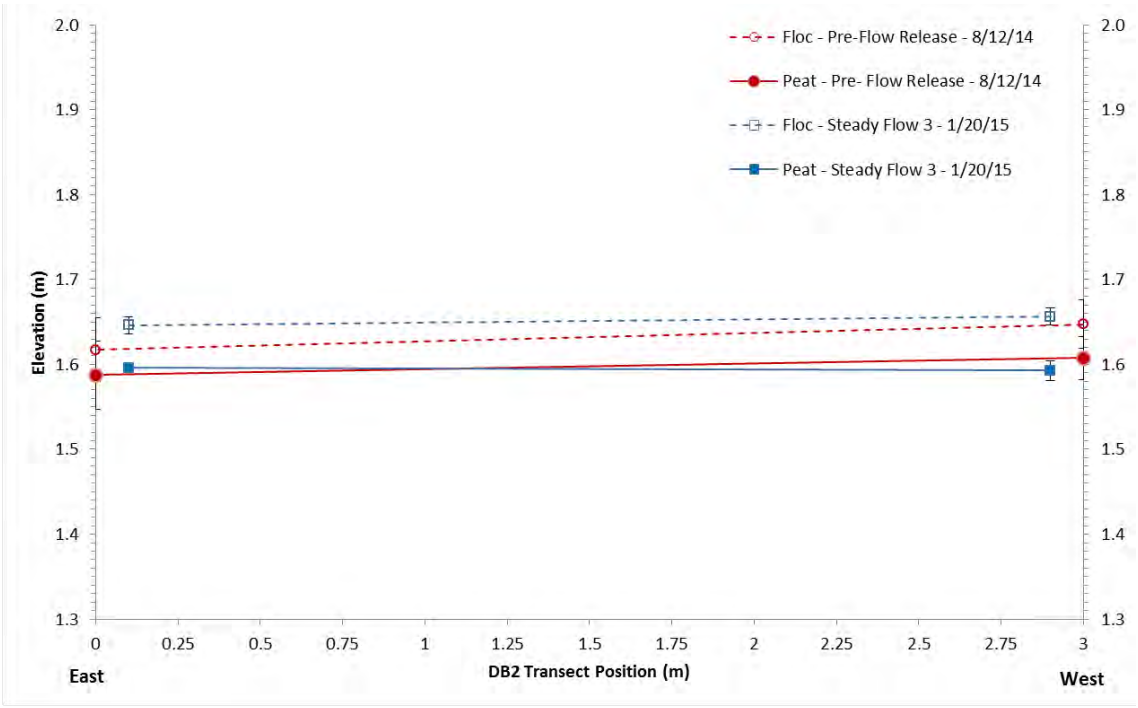

Figure A-41 Elevation transect of floc and peat microtopography measurements collected prior to and after the Nov 4th 2014 flow release at site DB2. Values without error bars are single point measurements.

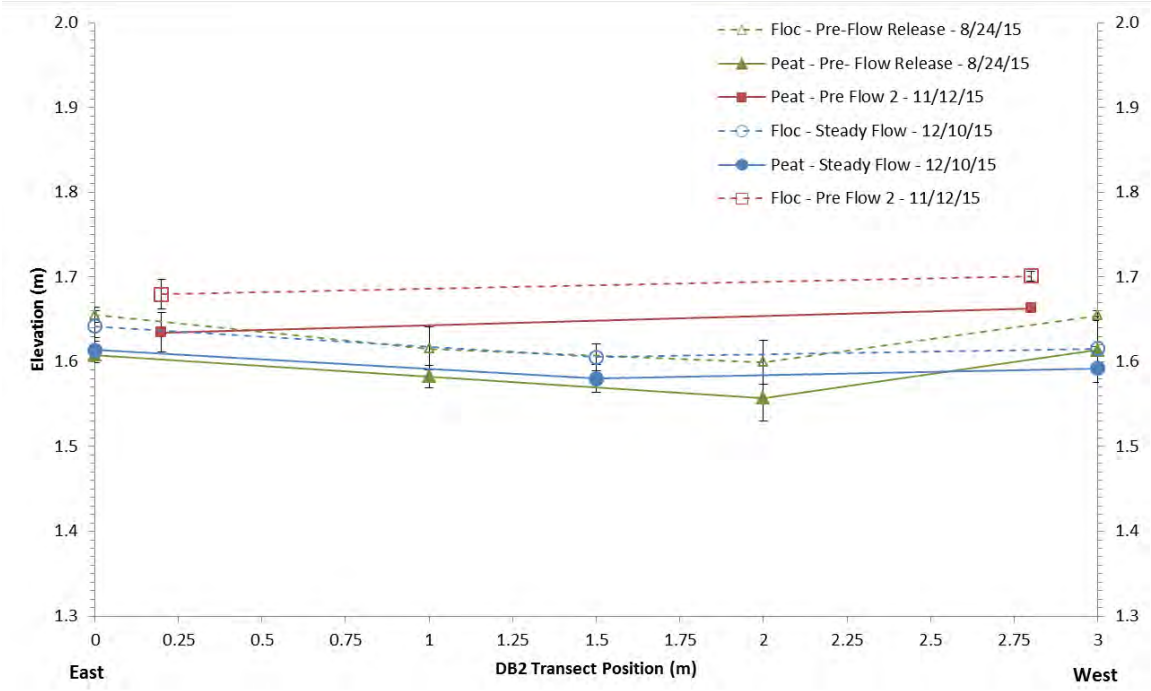

Figure A-42 Elevation transect of floc and peat microtopography measurements collected prior to and after the Nov 16th 2015 flow release at site DB2. Values without error bars are single point measurements.

B. Surface Water and Groundwater Levels

Complete Continuous Water Levels

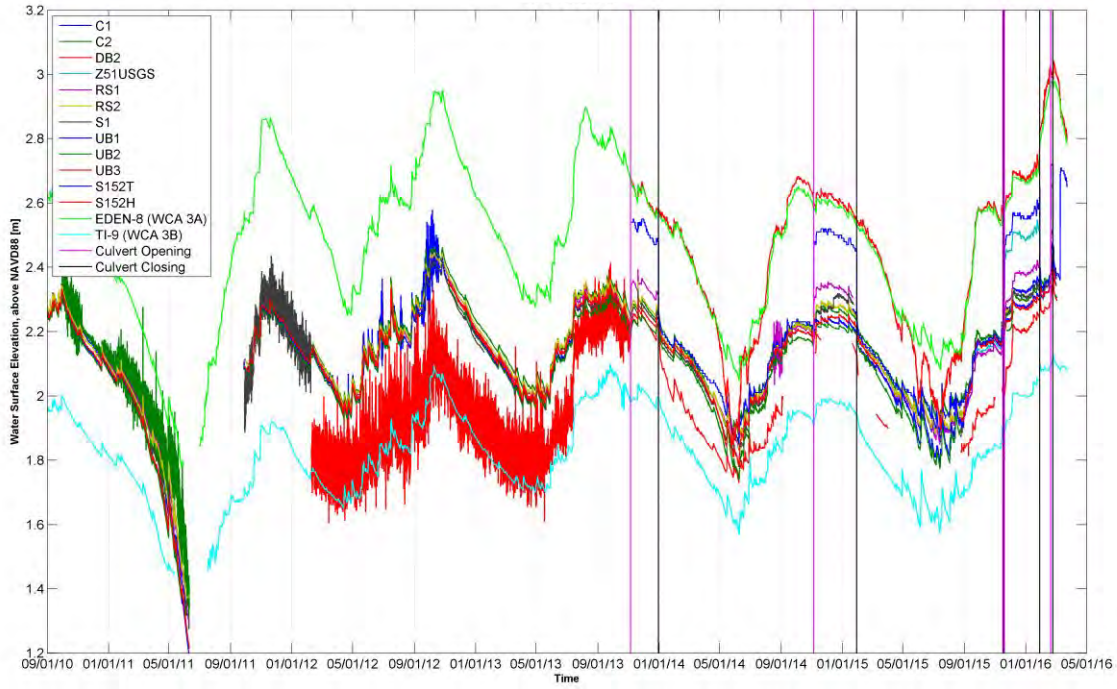

Figure B-1 Water level elevation at all of the sites in DPM.

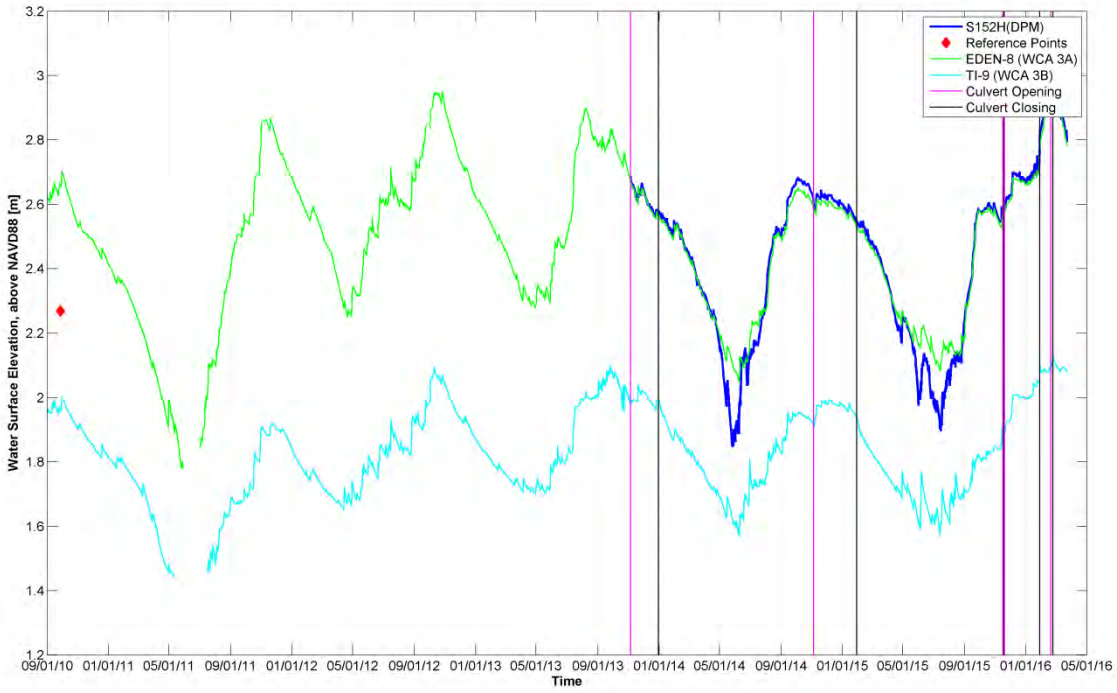

Figure B-2 Water level elevation at DPM site S152 Headwater.

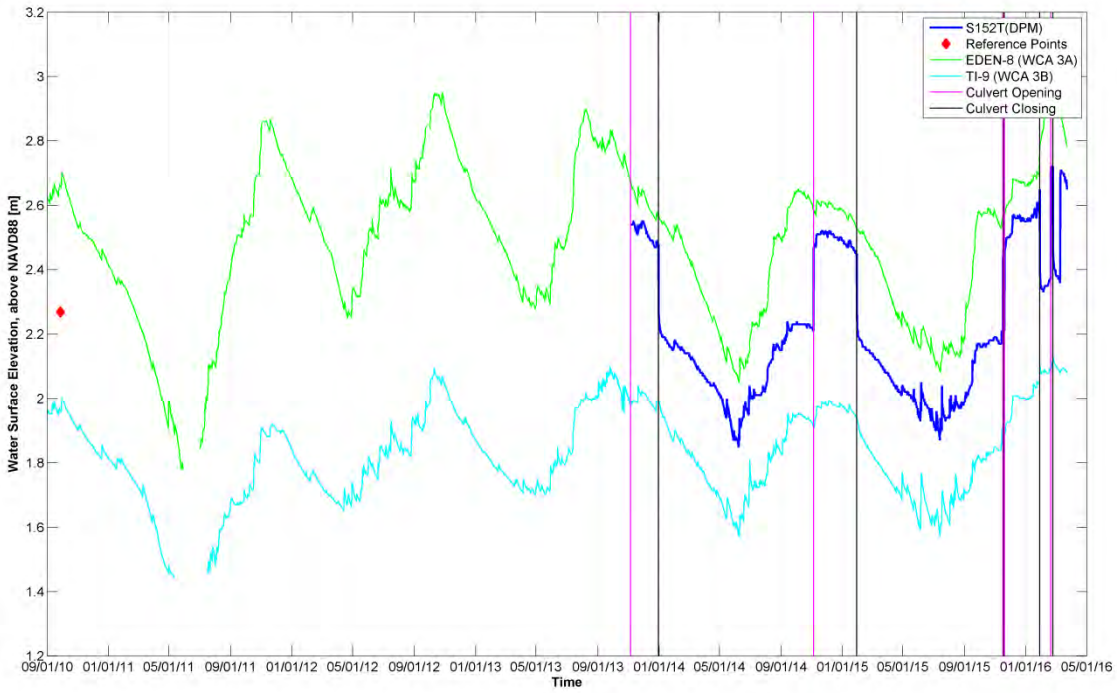

Figure B-3 Water level elevation at DPM site S152 Tailwater.

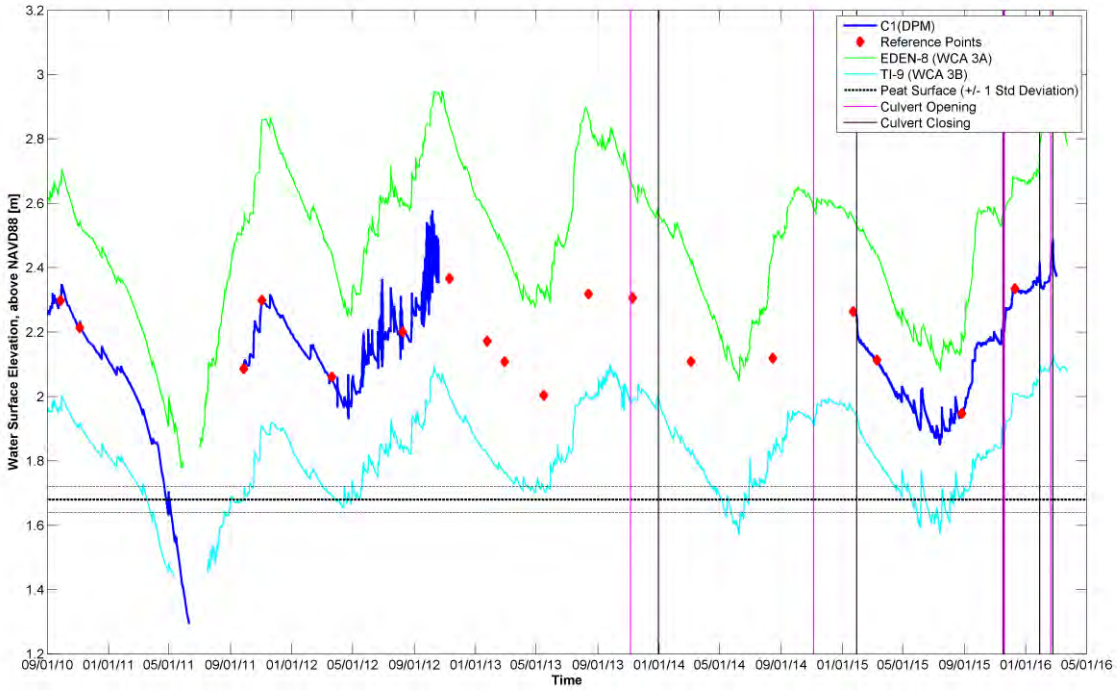

Figure B-4 Water level and ground surface elevation at DPM site C1. The mean ground surface elevation ± 1 standard deviation is shown for nearby areas of ridge and slough vegetation.

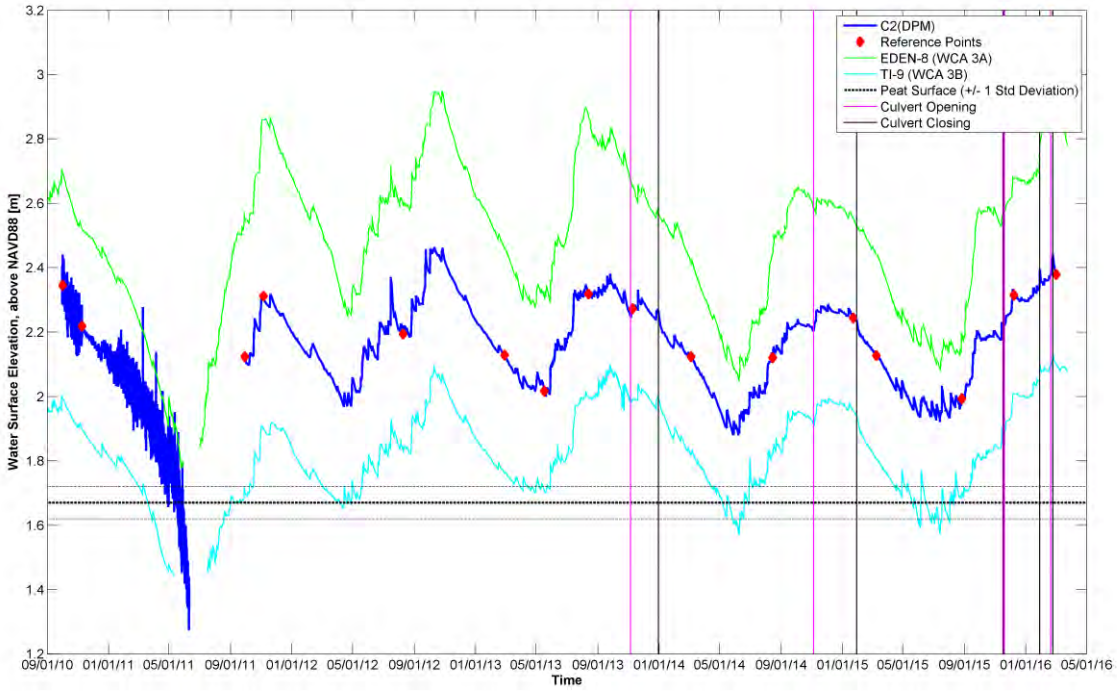

Figure B-5 Water level and ground surface elevation at DPM site C2. The mean ground surface elevation ± 1 standard deviation is shown for nearby areas of ridge and slough vegetation.

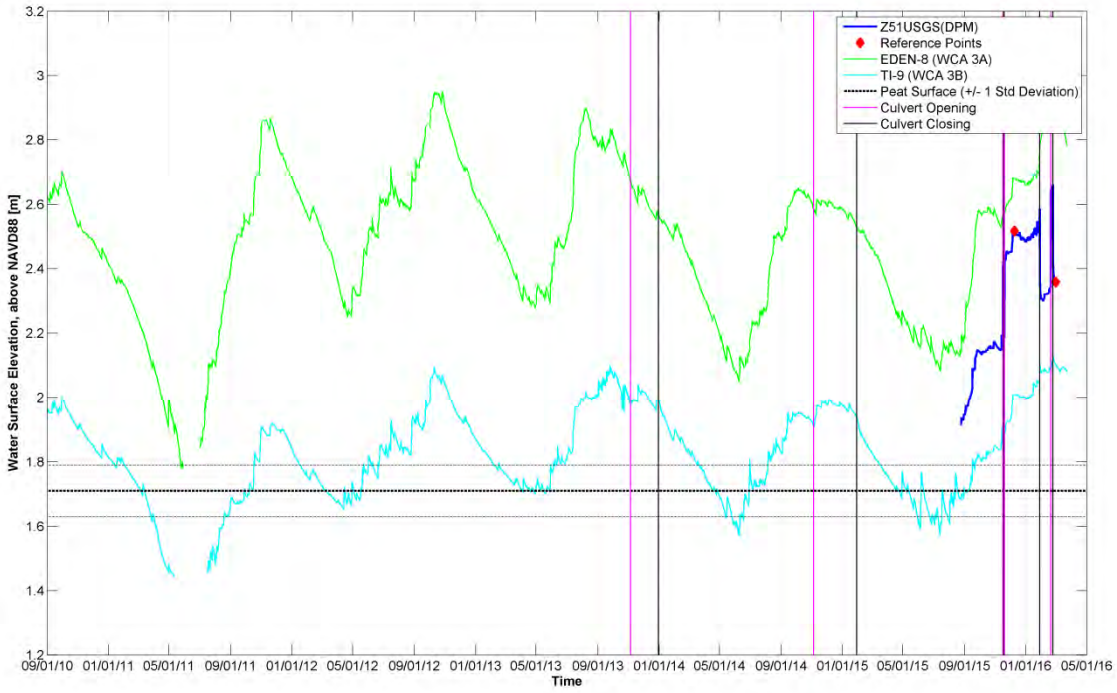

Figure B-6 Water level and ground surface elevation at DPM site Z51_USGS. The mean ground surface elevation ± 1 standard deviation is shown for nearby areas of ridge and slough vegetation.

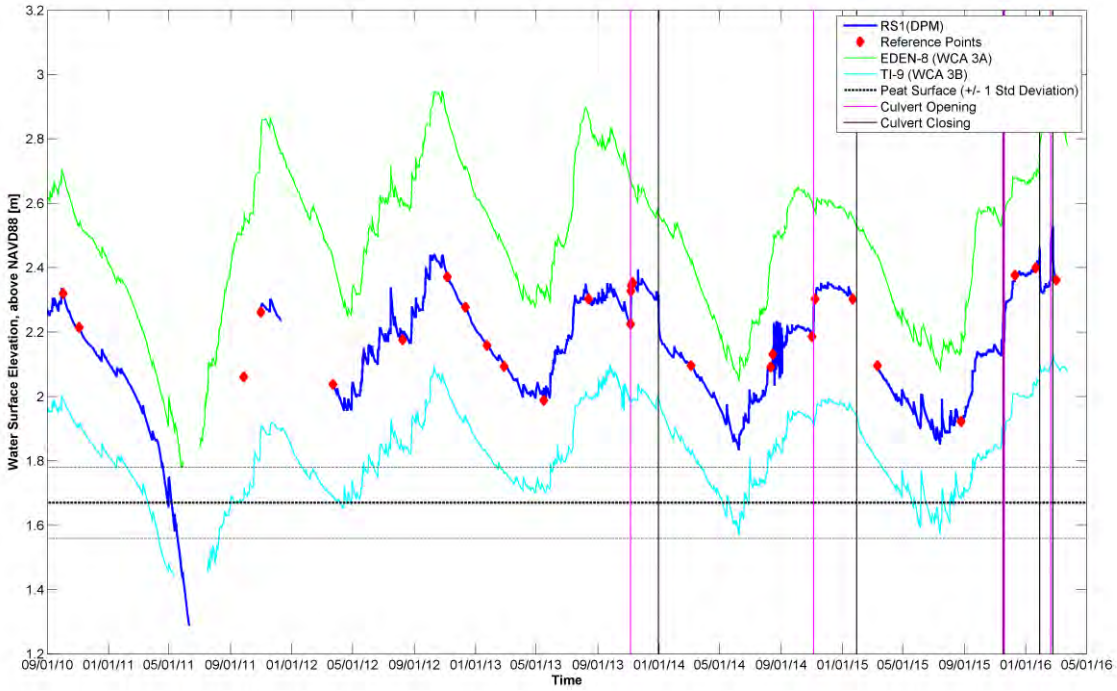

Figure B-7 Water level and ground surface elevation at DPM site RS1. The mean ground surface elevation ± 1 standard deviation is shown for nearby areas of ridge and slough vegetation.

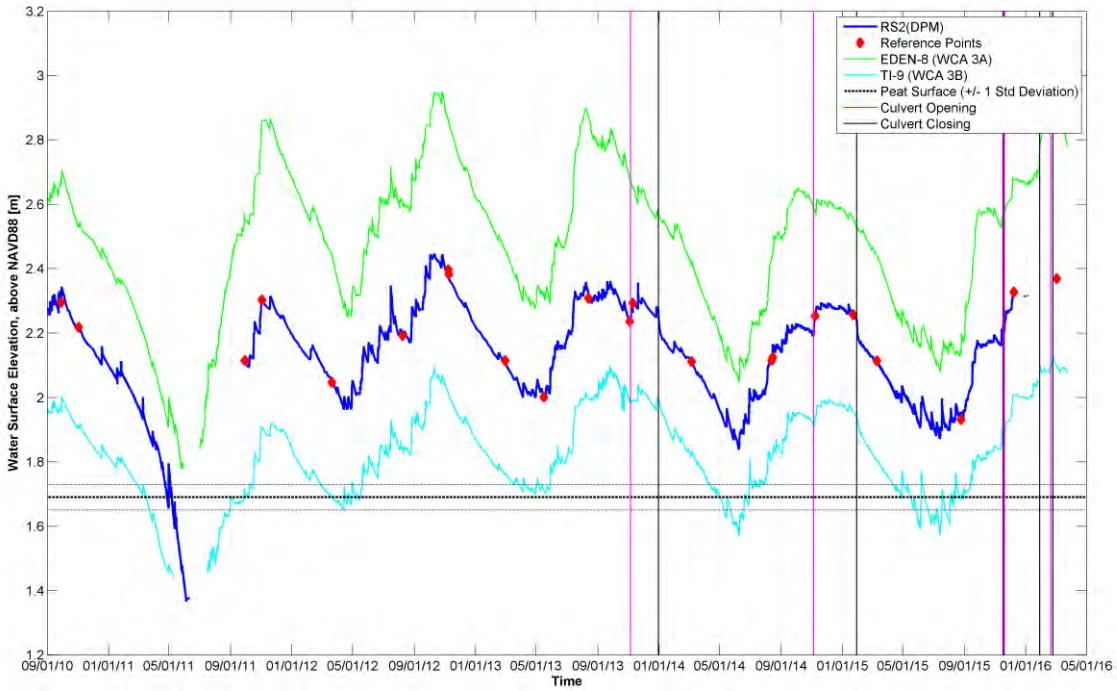

Figure B-8 Water level and ground surface elevation at DPM site RS2. The mean ground surface elevation ± 1 standard deviation is shown for nearby areas of ridge and slough vegetation.

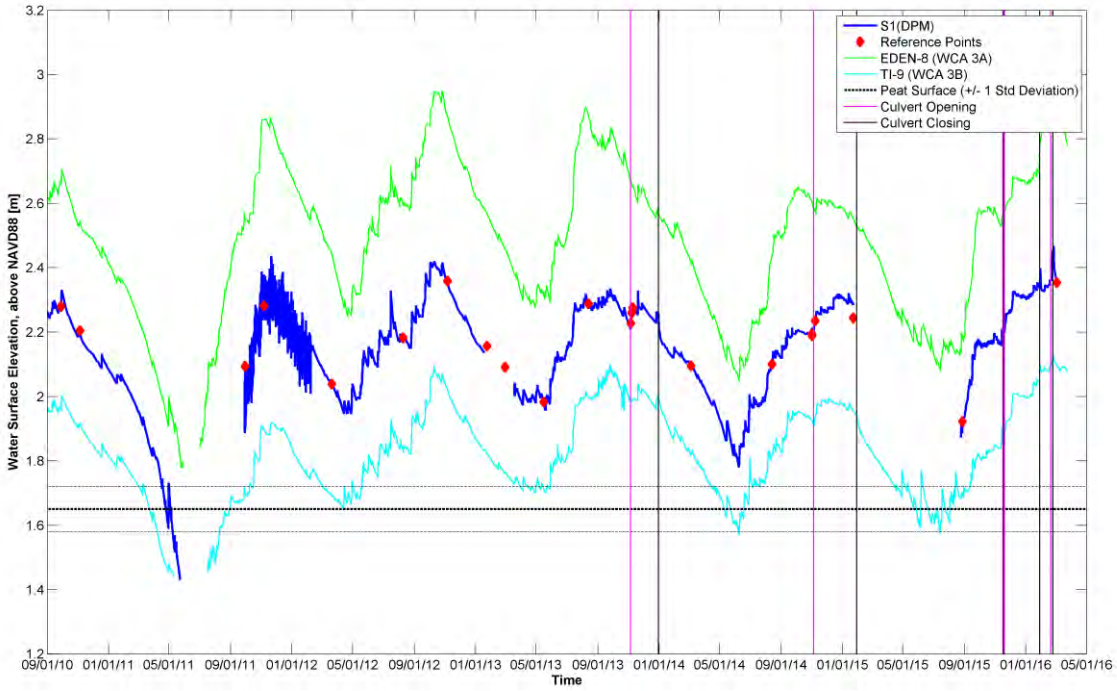

Figure B-9 Water level and ground surface elevation at DPM site S1. The mean ground surface elevation ± 1 standard deviation is shown for nearby areas of ridge and slough vegetation.

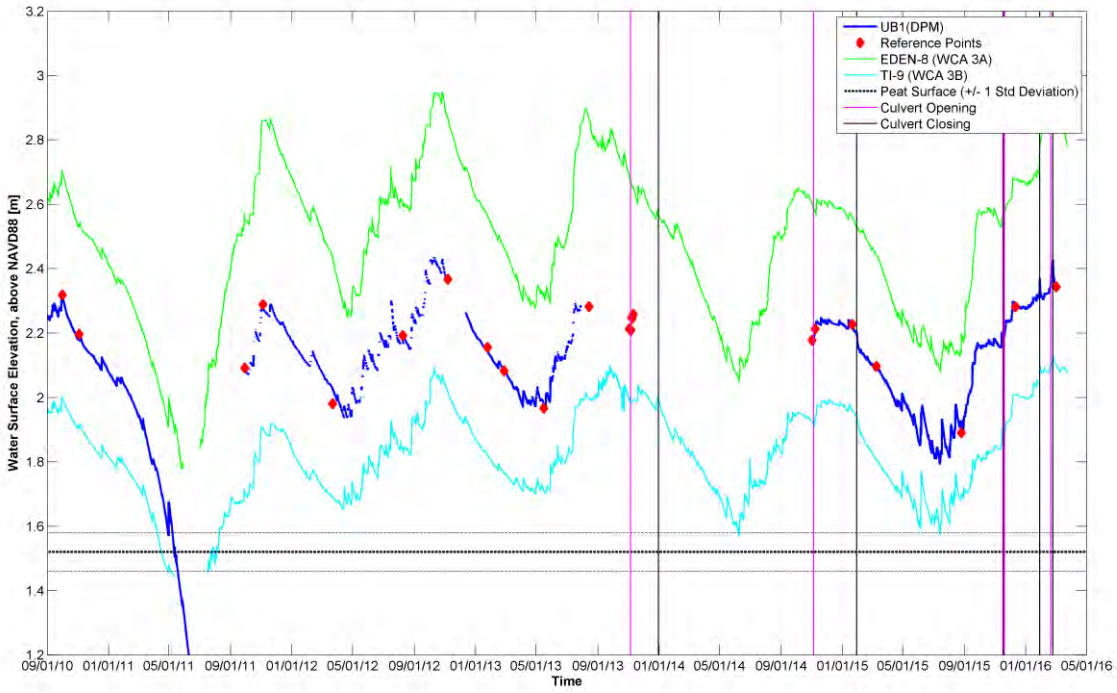

Figure B-10 Water level and ground surface elevation at DPM site UB1. The mean ground surface elevation ± 1 standard deviation is shown for nearby areas of ridge and slough vegetation.

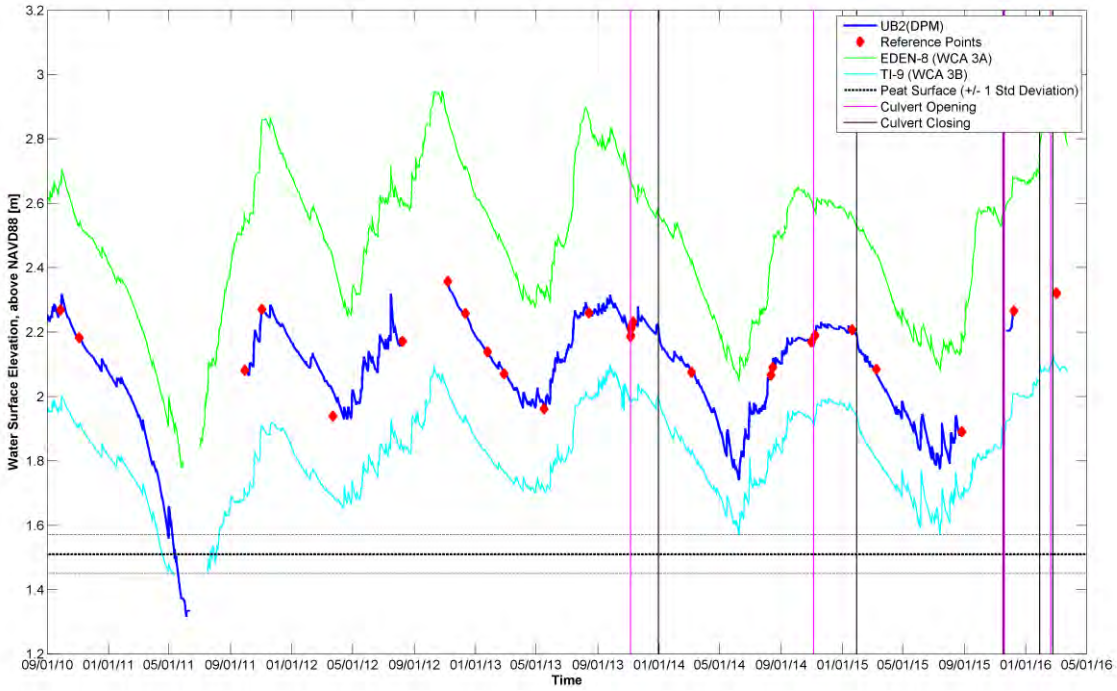

Figure B-11 Water level and ground surface elevation at DPM site UB2. The mean ground surface elevation ± 1 standard deviation is shown for nearby areas of ridge and slough vegetation.

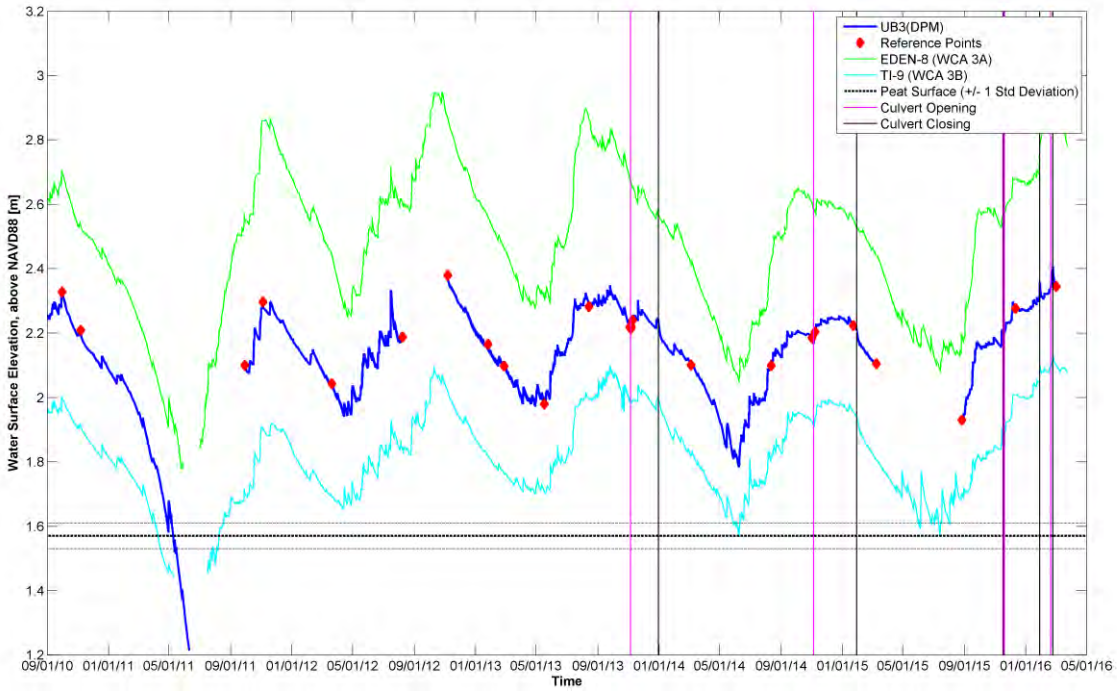

Figure B-12 Water level and ground surface elevation at DPM site UB3. The mean ground surface elevation ± 1 standard deviation is shown for nearby areas of ridge and slough vegetation.

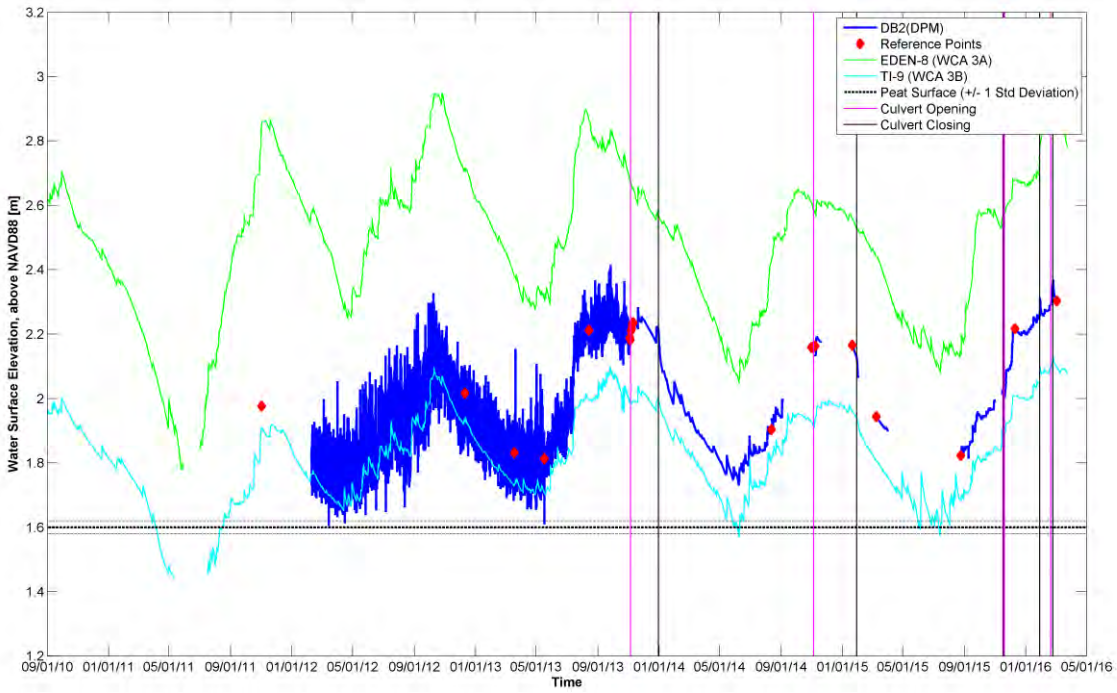

Figure B-13 Water level and ground surface elevation at DPM site DB2. The mean ground surface elevation ± 1 standard deviation is shown for nearby areas of ridge and slough vegetation.

Groundwater Surface Water Comparisons

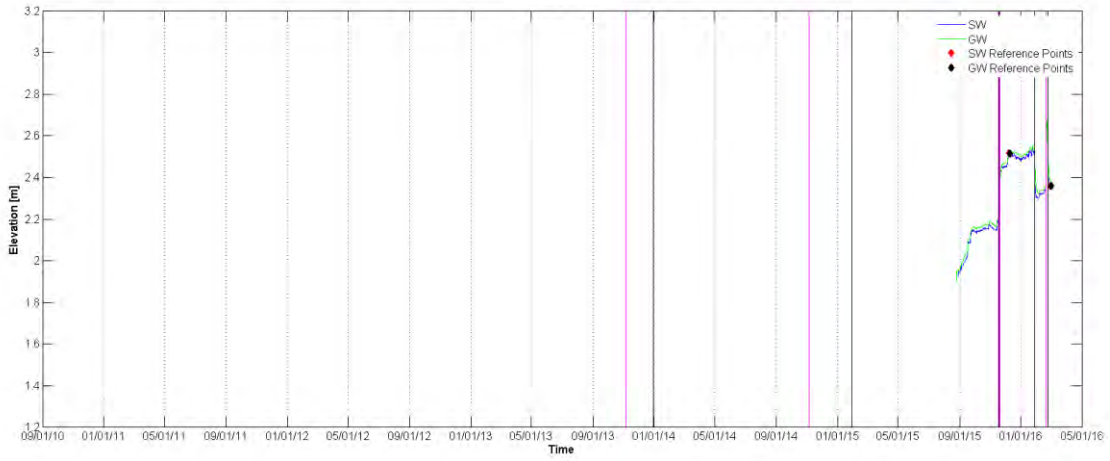

Figure B-14 Surface water and groundwater in DPM at site Z51_USGS.

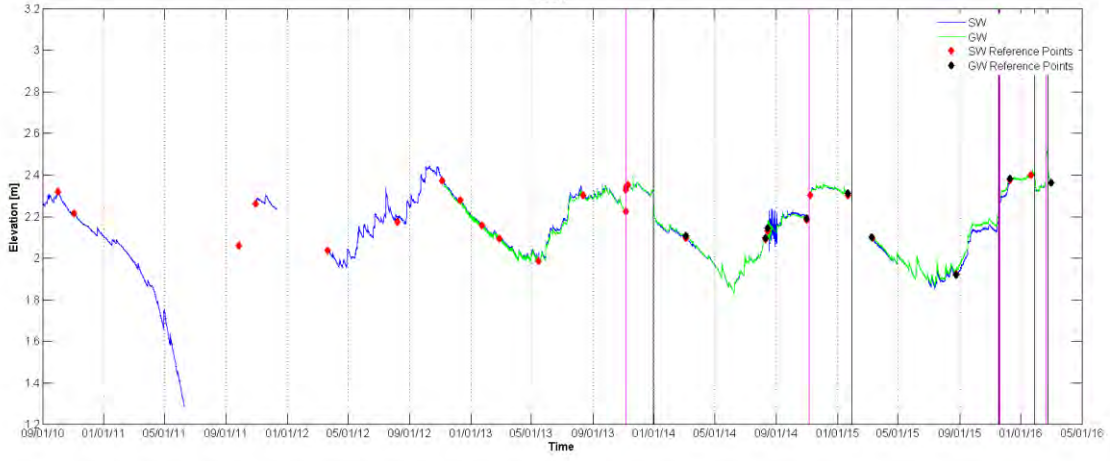

Figure B-15 Surface water and groundwater at DPM site RS1D.

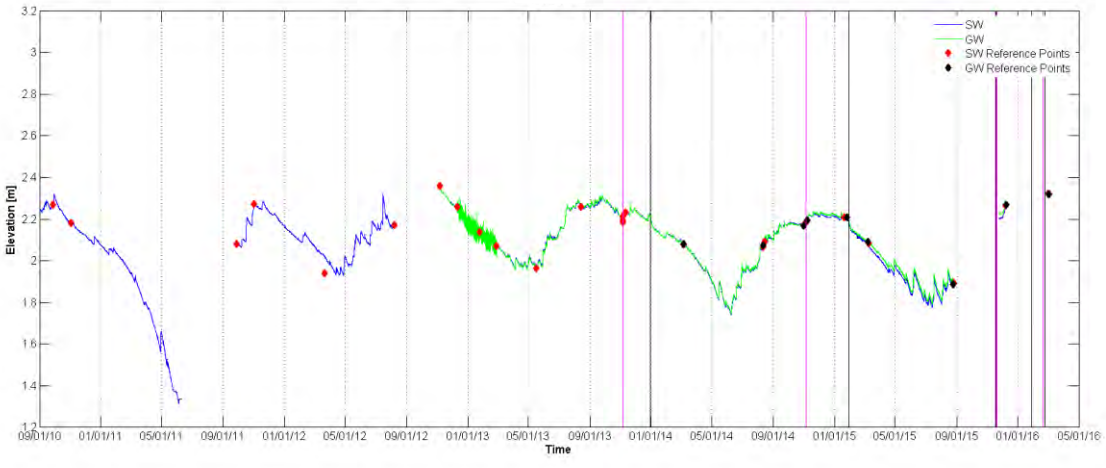

Figure B-16 Surface water and groundwater at DPM site UB2.

2013 Flow Release Water Levels

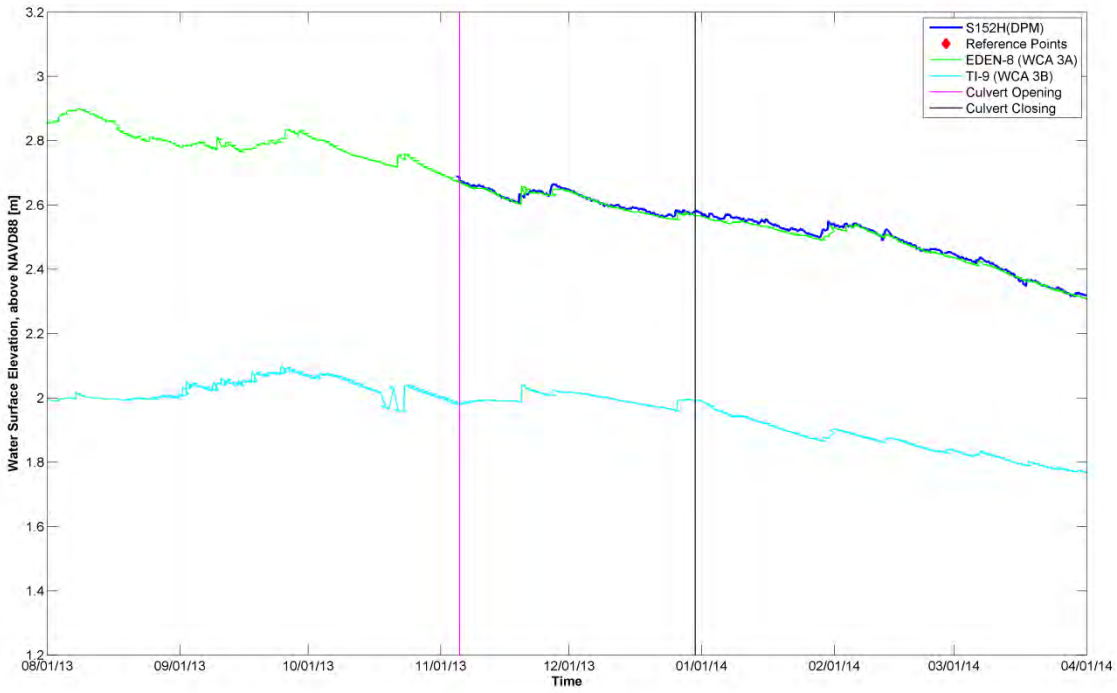

Figure B-17 Water levels at C1 in DPM for the period of the 2013 flow release.

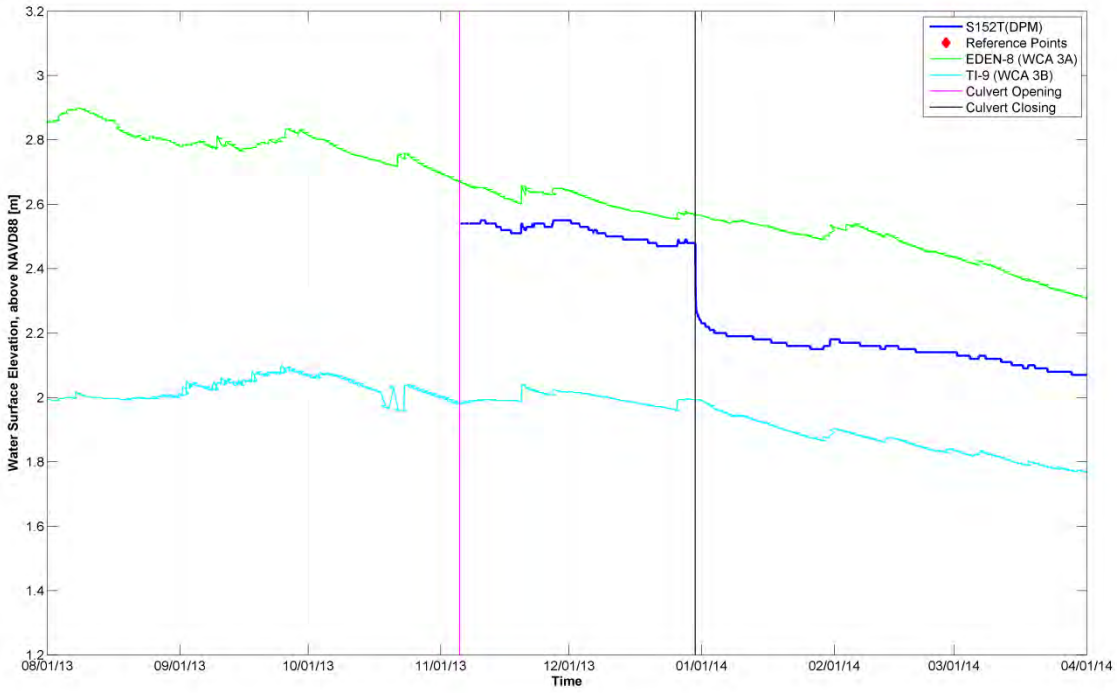

Figure B-18 Water levels at C2 in DPM for the period of the 2013 flow release.

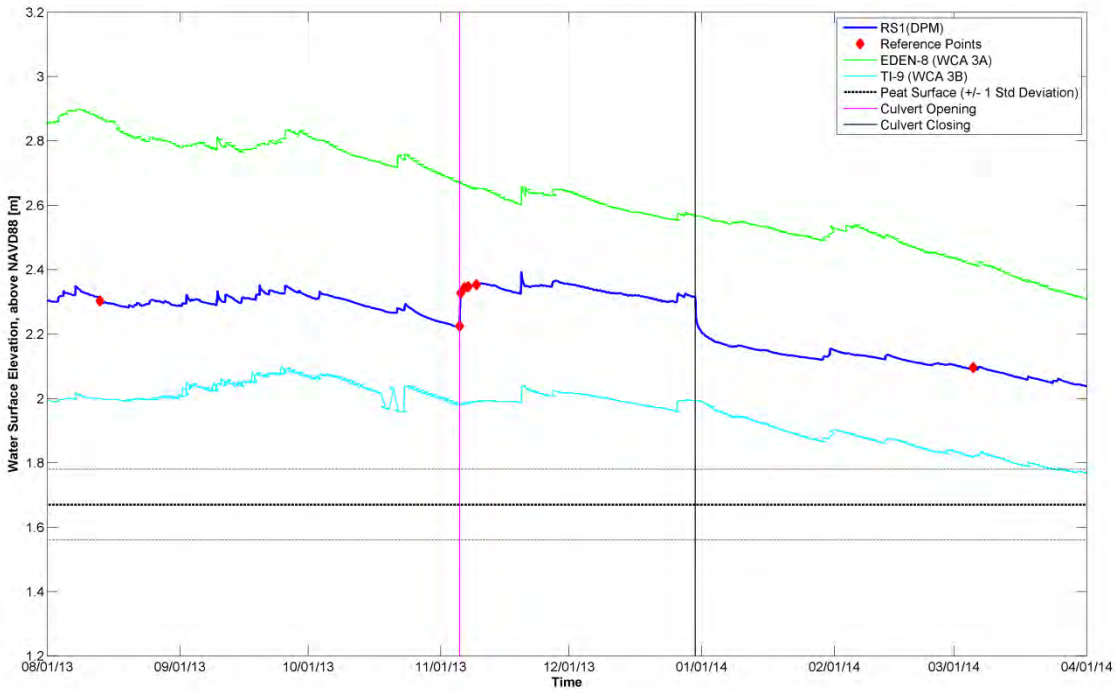

Figure B-19 Water levels at RS1 in DPM for the period of the 2013 flow release.

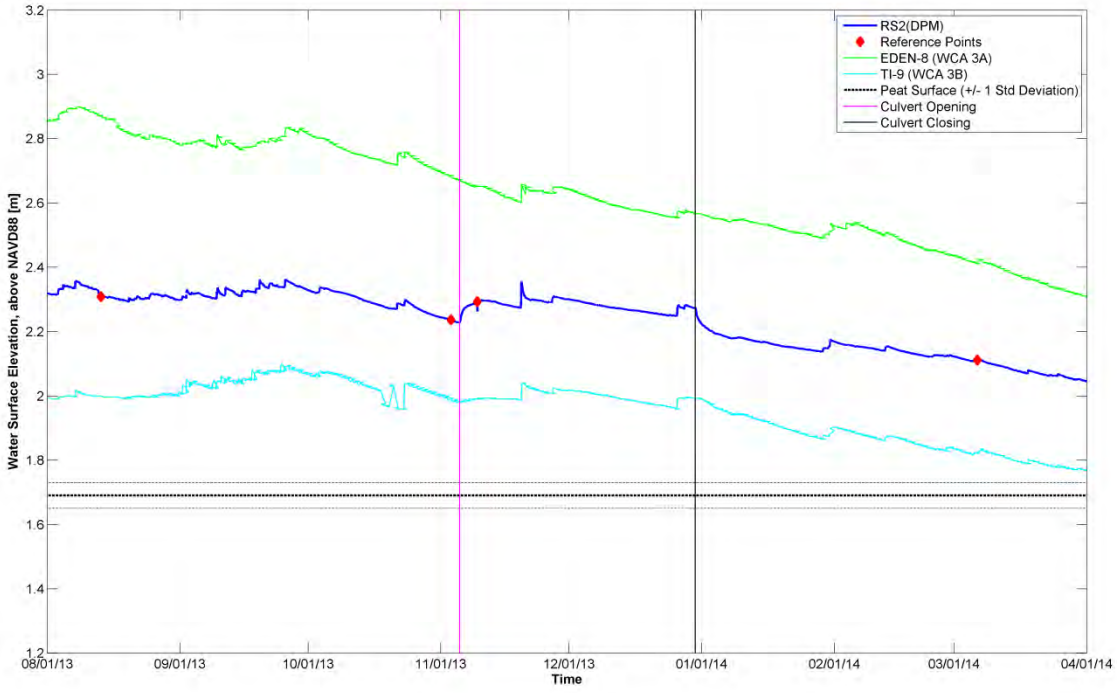

Figure B-20 Water levels at RS2 in DPM for the period of the 2013 flow release.

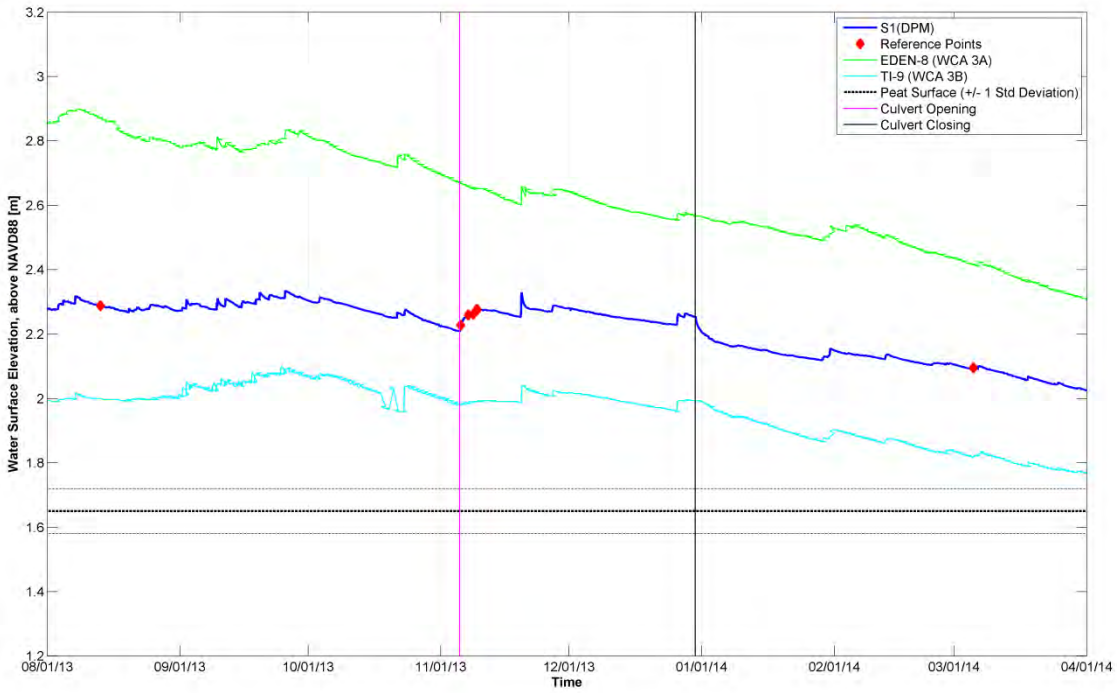

Figure B-21 Water levels at S1 in DPM for the period of the 2013 flow release.

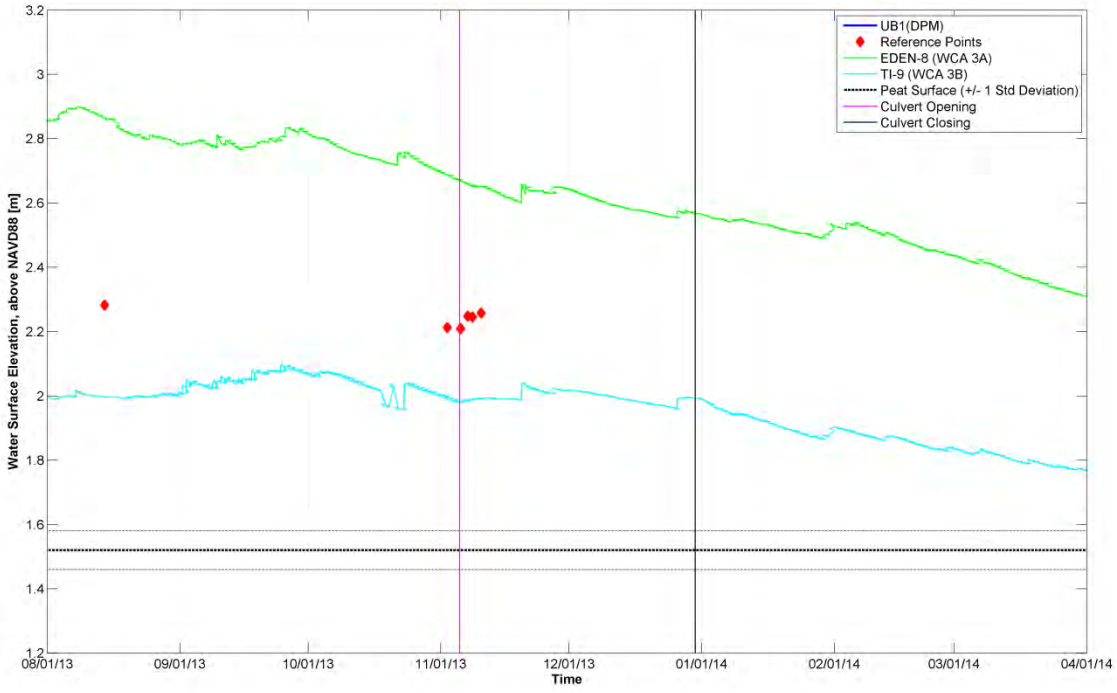

Figure B-22 Water levels at UB1 in DPM for the period of the 2013 flow release.

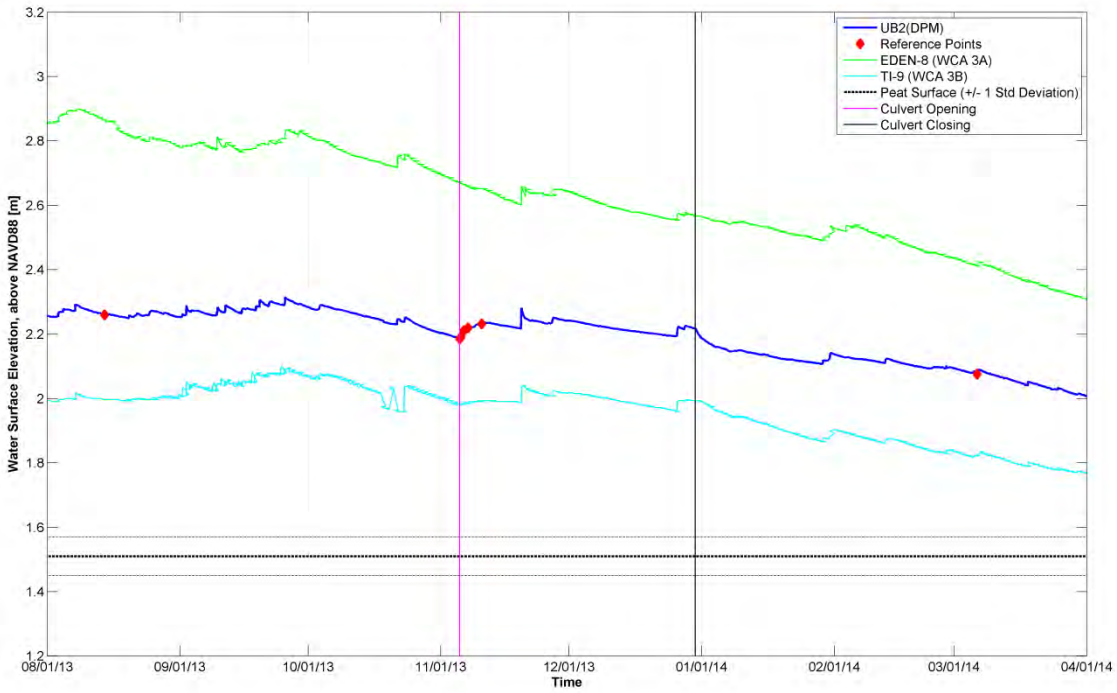

Figure B-23 Water levels at UB2 in DPM for the period of the 2013 flow release.

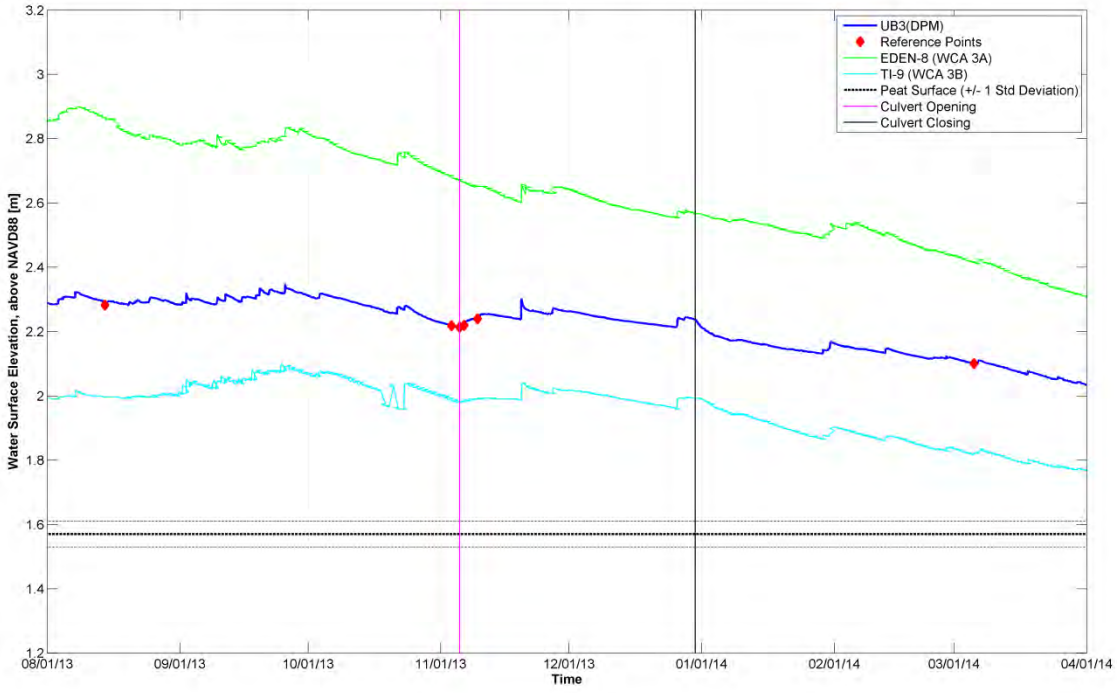

Figure B-24 Water levels at UB3 in DPM for the period of the 2013 flow release.

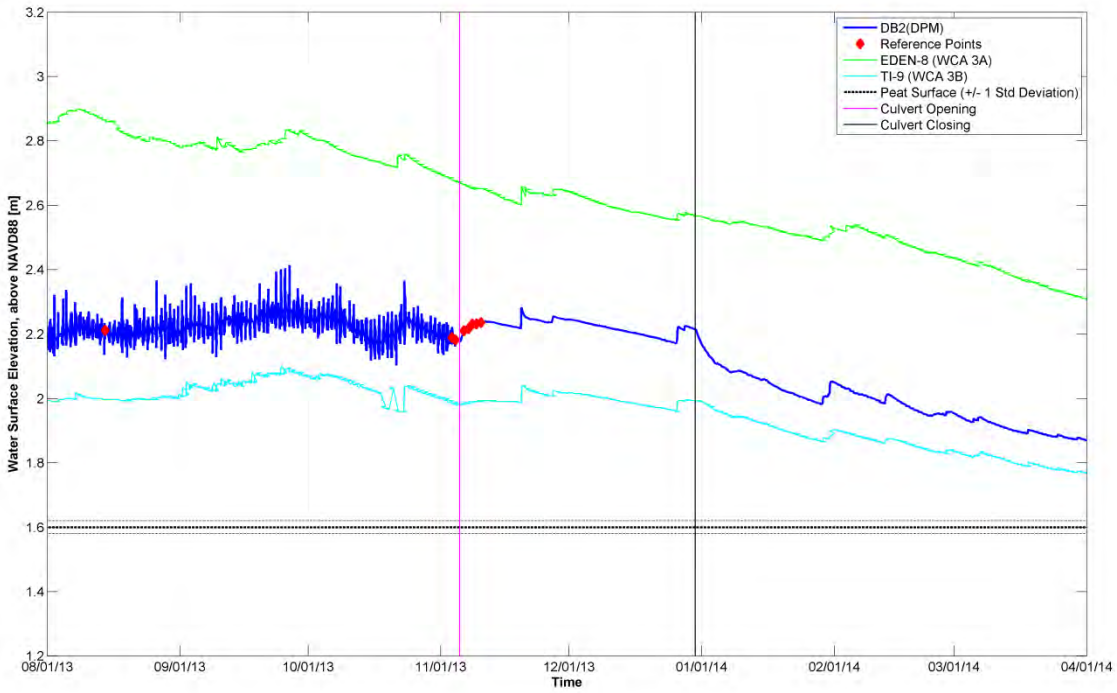

Figure B-25 Water levels at DB2 in DPM for the period of the 2013 flow release.

Groundwater Surface Water Comparisons for 2013 Flow Release

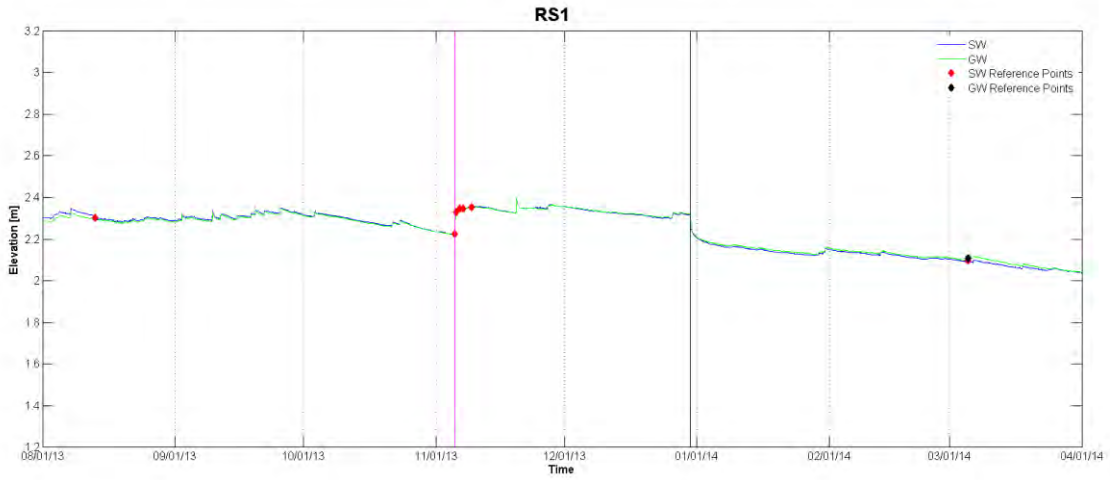

Figure B-26 Surface water and groundwater at DPM site RS1D for the period of the 2013 flow release.

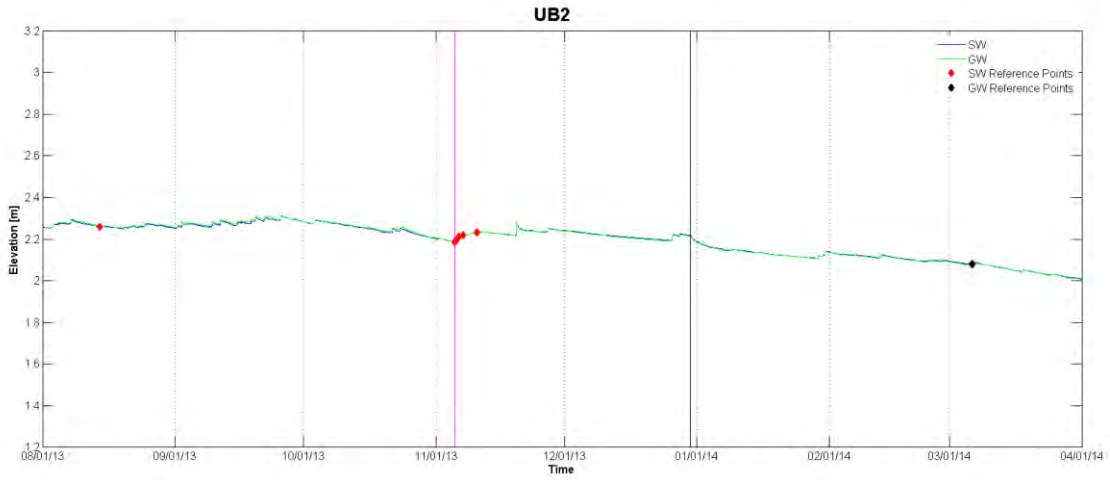

Figure B-27 Surface water and groundwater at DPM site RS1D for the period of the 2013 flow release.

2014 Flow Release Water Levels

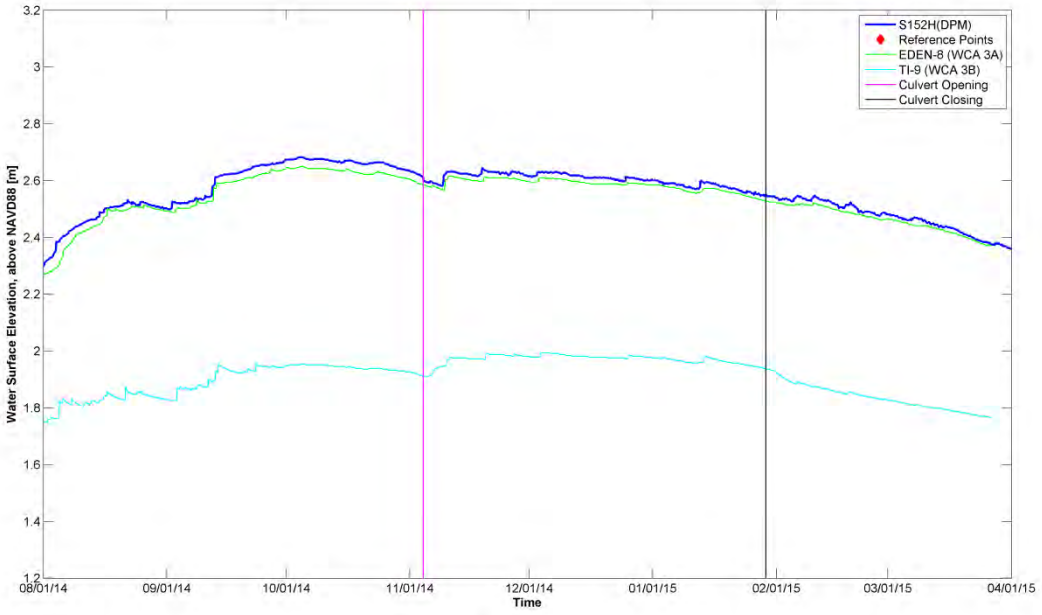

Figure B-28 Water levels at S152 Headwater in DPM for the period of the 2014 flow release.

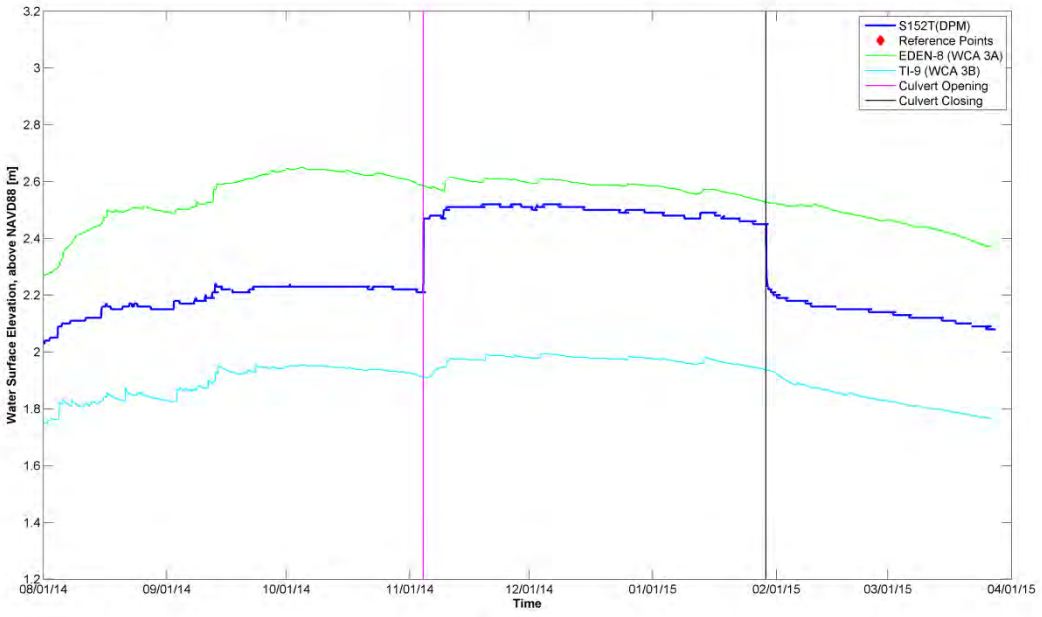

Figure B-29 Water levels at S152 Tailwater in DPM for the period of the 2014 flow release.

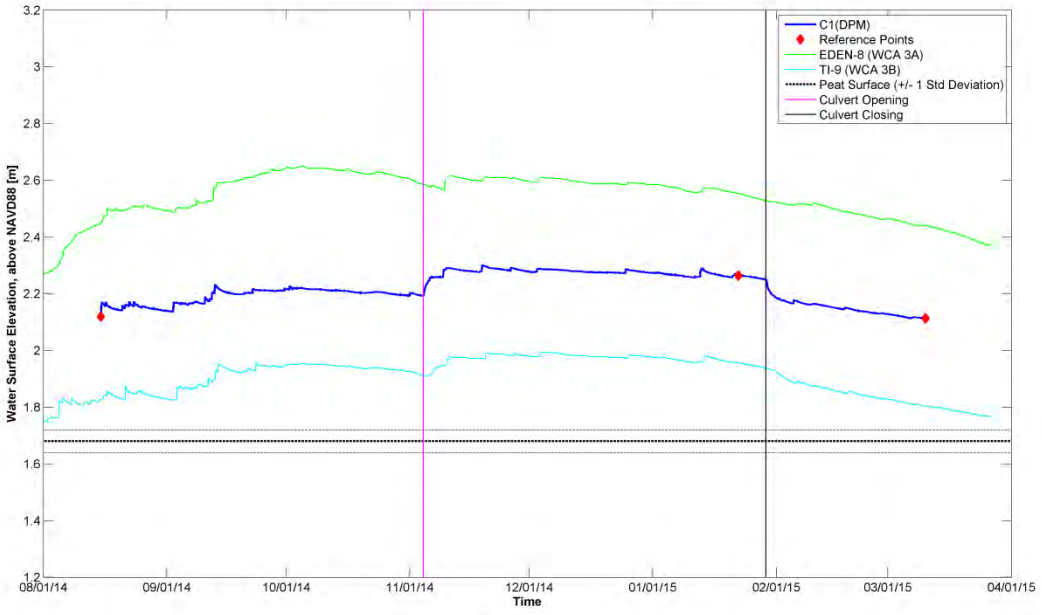

Figure B-30 Water levels at C1 in DPM for the period of the 2014 flow release.

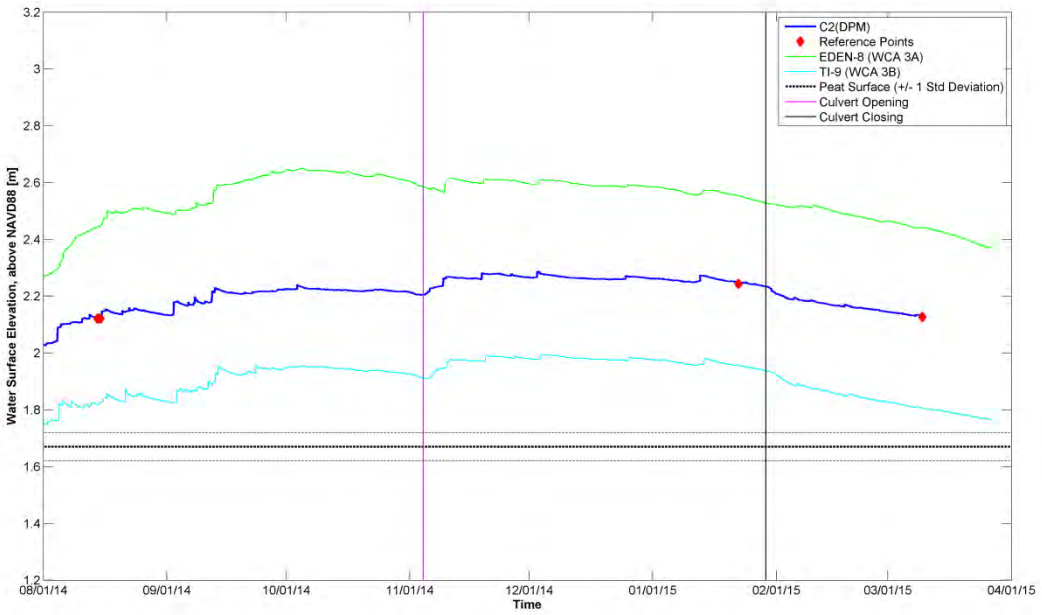

Figure B-31 Water levels at C2 in DPM for the period of the 2014 flow release.

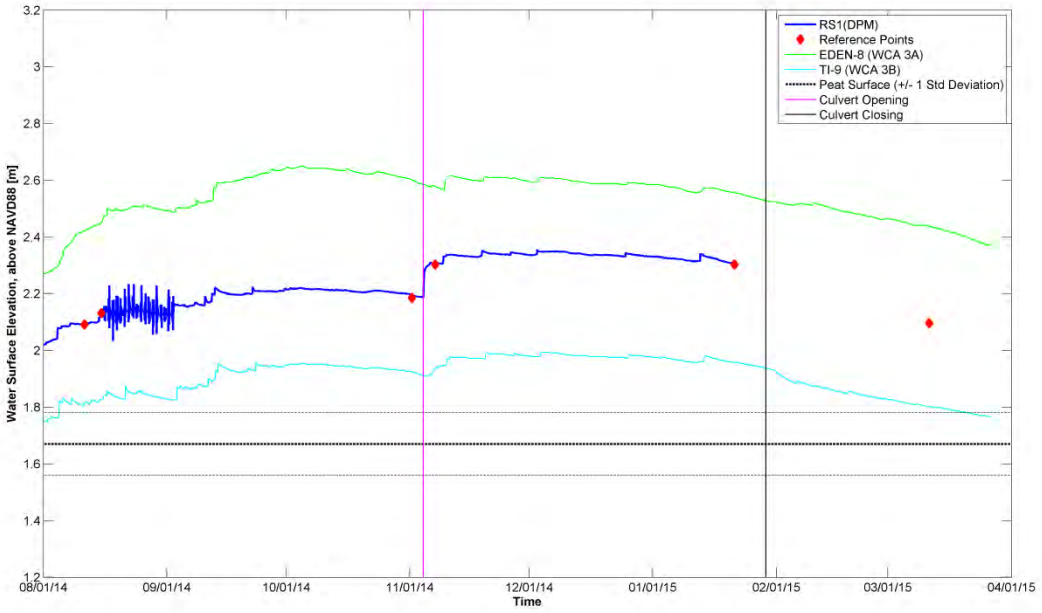

Figure B-32 Water levels at RS1 in DPM for the period of the 2014 flow release.

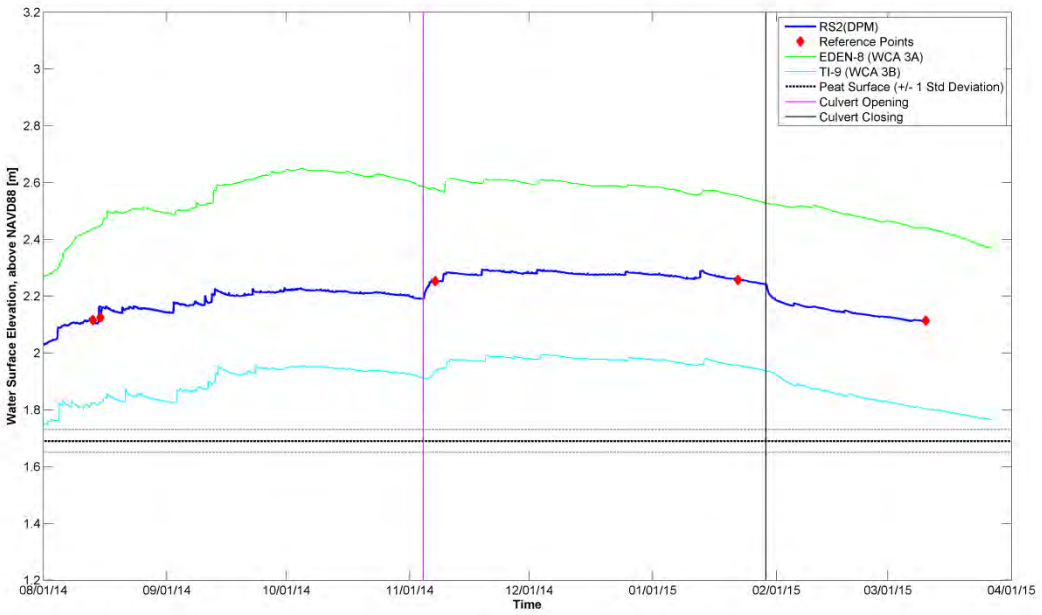

Figure B-33 Water levels at RS2 in DPM for the period of the 2014 flow release.

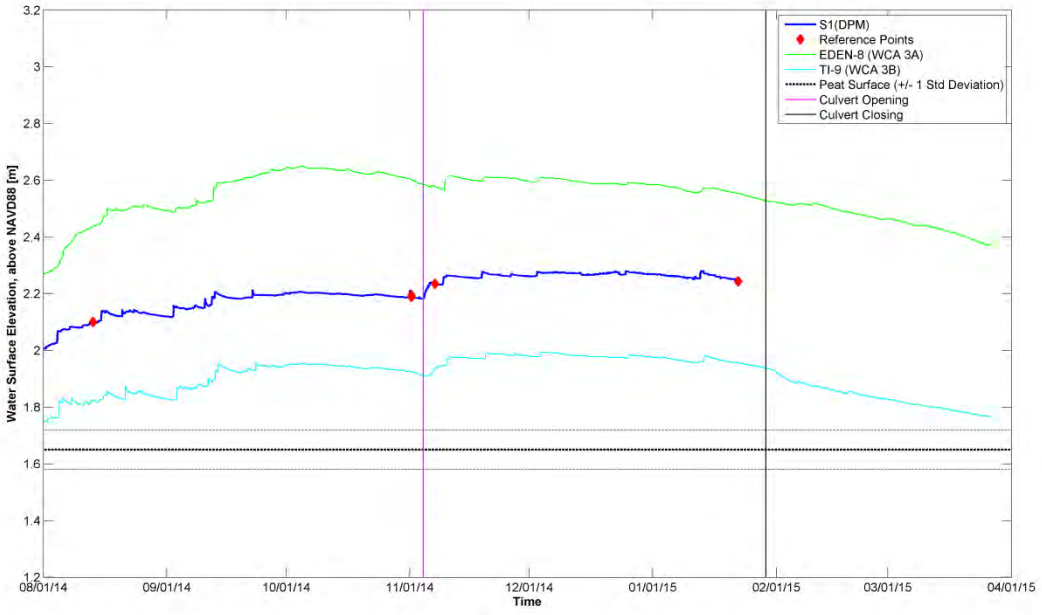

Figure B-34 Water levels at S1 in DPM for the period of the 2014 flow release.

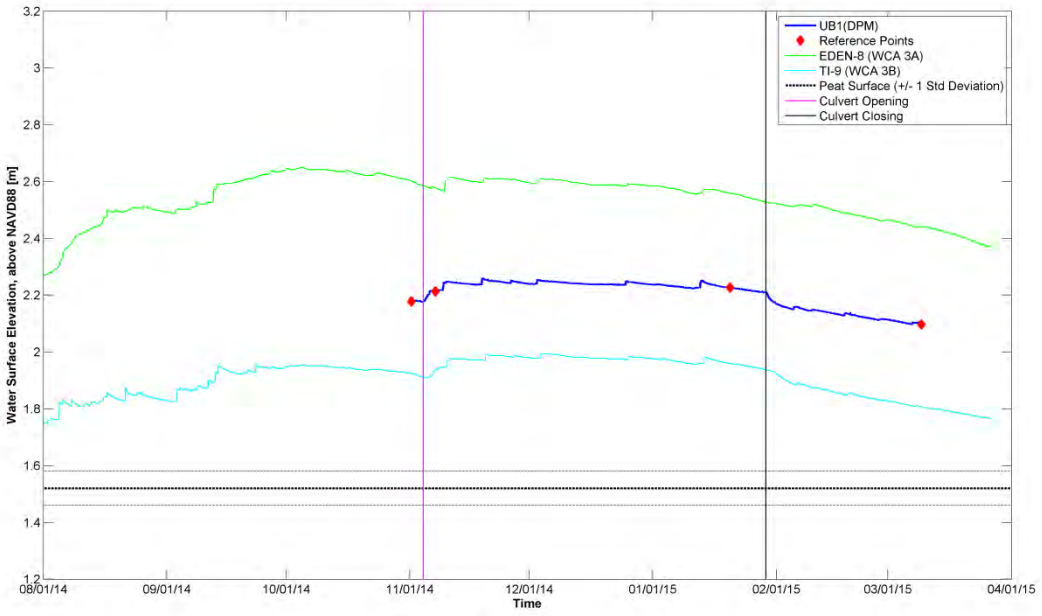

Figure B-35 Water levels at UB1 in DPM for the period of the 2014 flow release.

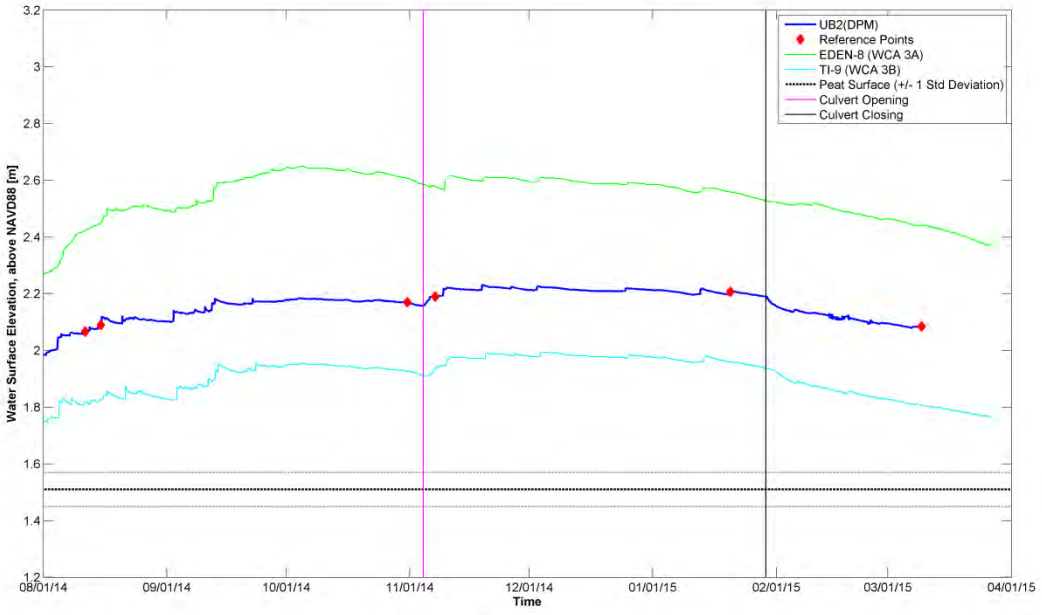

Figure B-36 Water levels at UB2 in DPM for the period of the 2014 flow release.

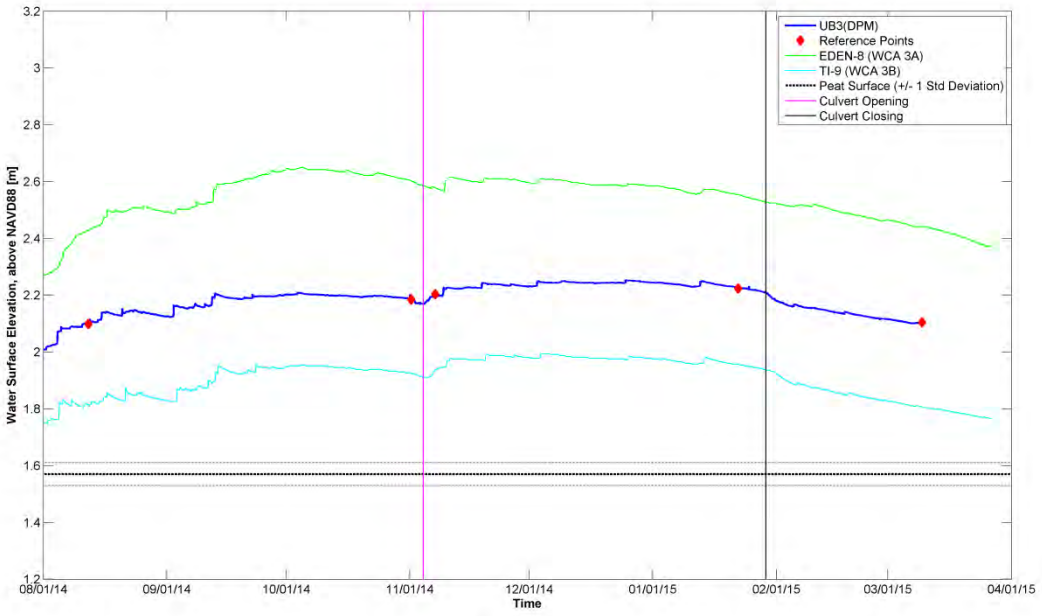

Figure B-37 Water levels at UB3 in DPM for the period of the 2014 flow release.

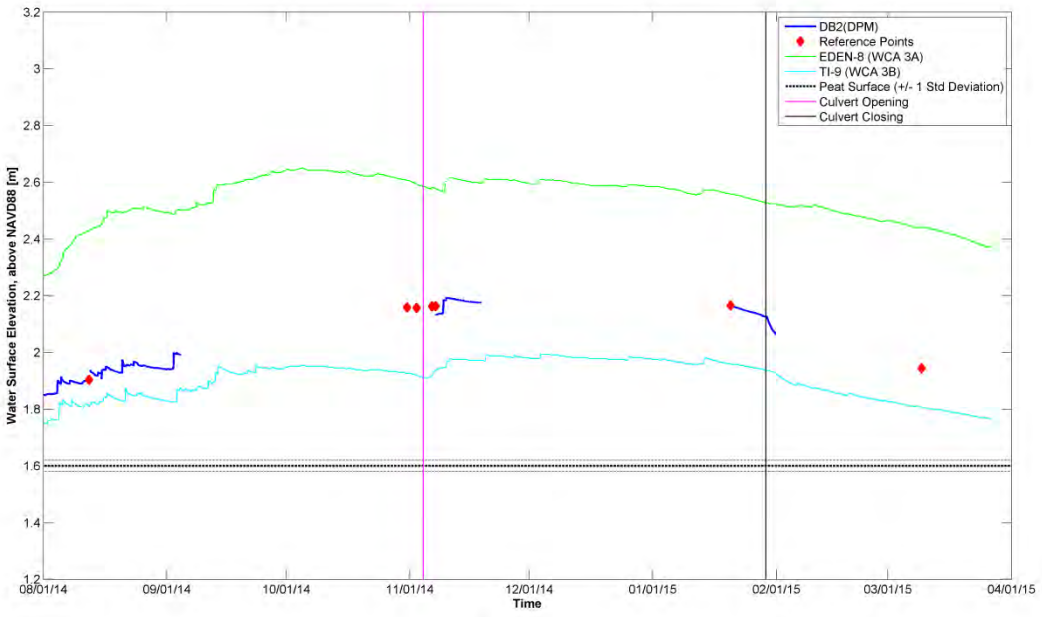

Figure B-38 Water levels at DB2 in DPM for the period of the 2014 flow release.

Groundwater Surface Water Comparisons for 2014 Flow Release

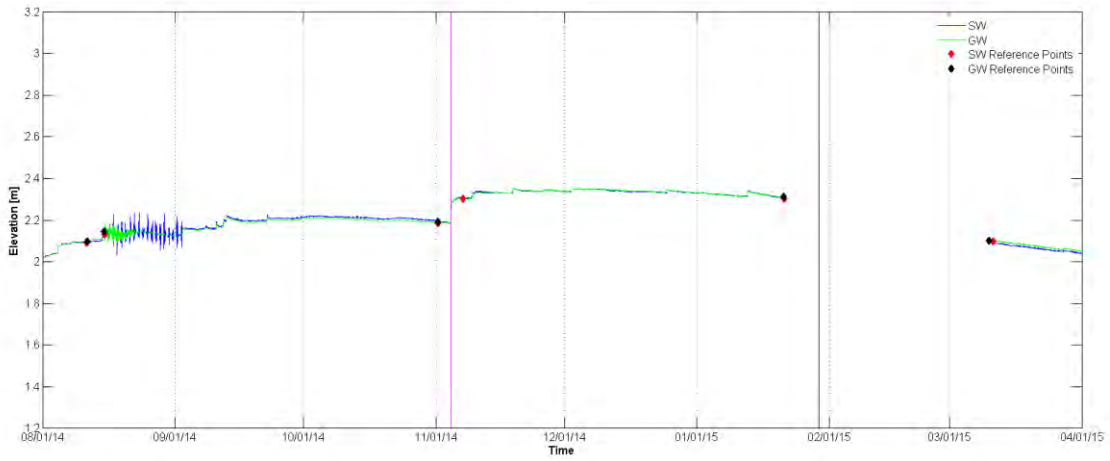

Figure B-39 Surface water and groundwater in DPM at site RS1D for the period of the 2014 flow release.

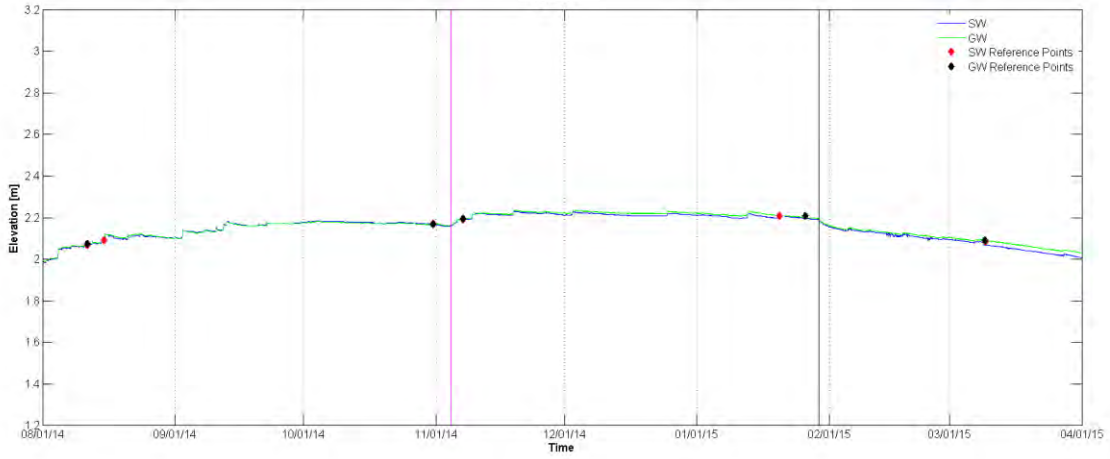

Figure B-40 Surface water and groundwater in DPM at site UB2 for the period of the 2014 flow release.

2015 Flow Release Water Levels

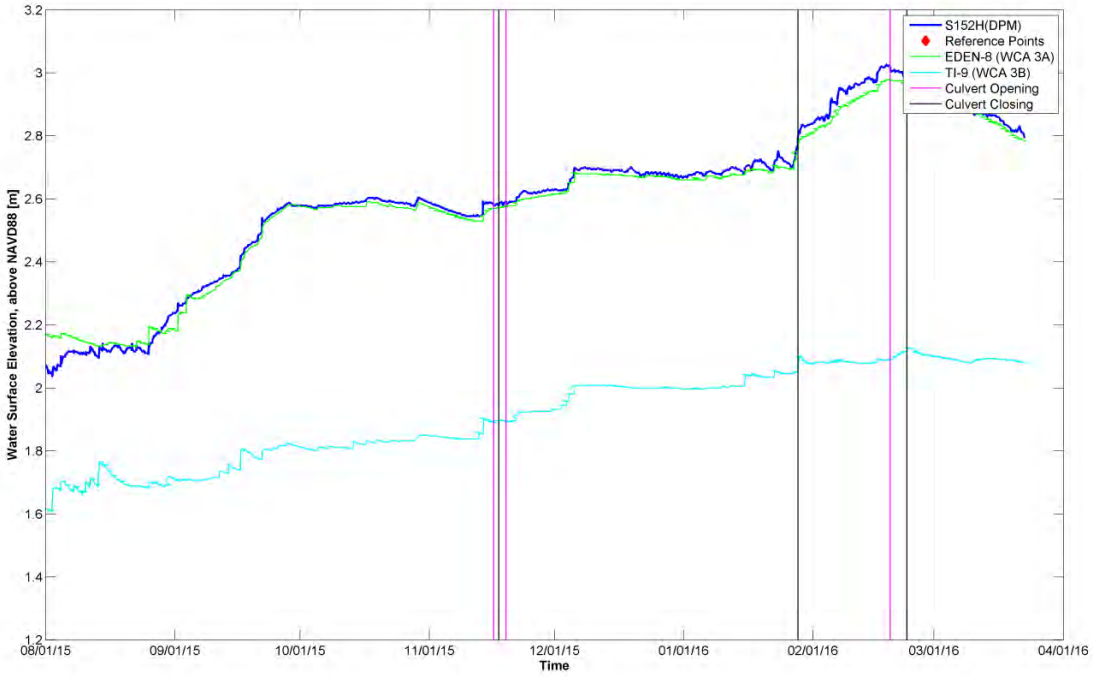

Figure B-41 Surface water and groundwater in DPM at site S152 Headwater for the period of the 2015 flow release.

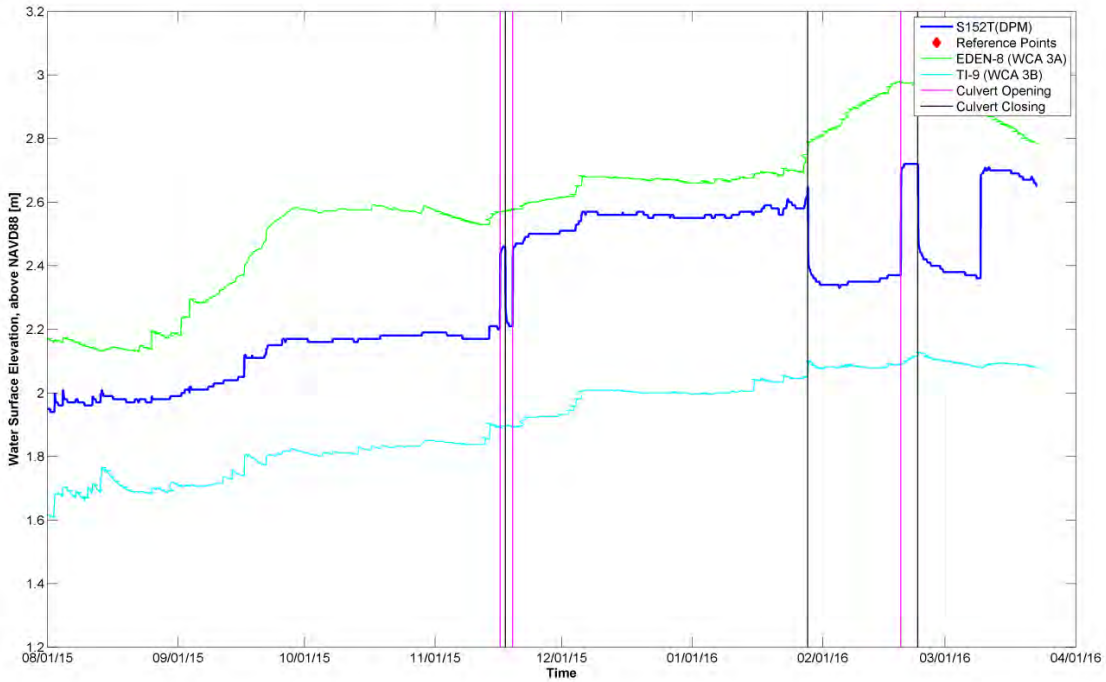

Figure B-42 Surface water and groundwater in DPM at site S152 Headwater for the period of the 2015 flow release.

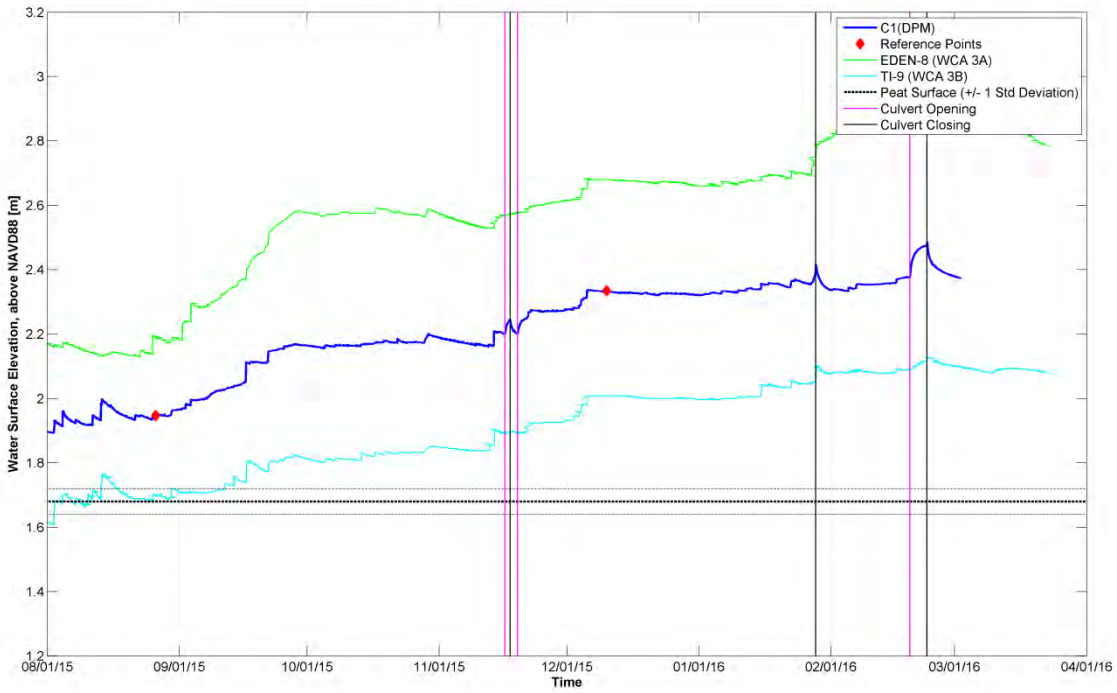

Figure B-43 Surface water and groundwater in DPM at site C1 for the period of the 2015 flow release.

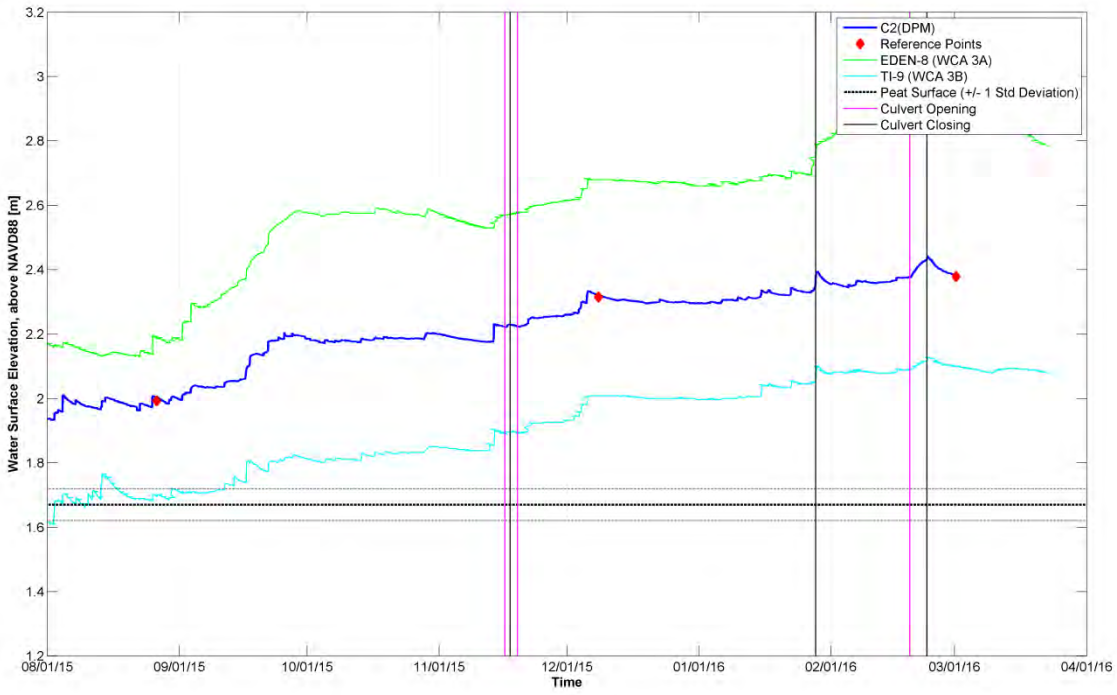

Figure B-44 Surface water and groundwater in DPM at site C2 for the period of the 2015 flow release.

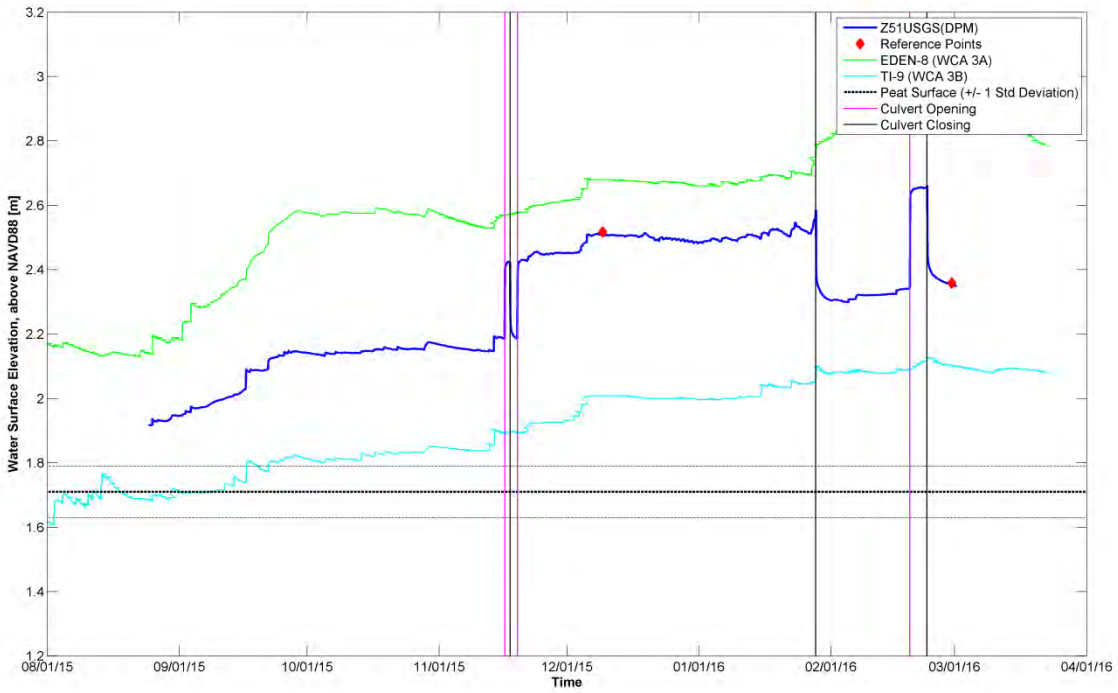

Figure B-45 Surface water and groundwater in DPM at site Z51_USGS for the period of the 2015 flow release.

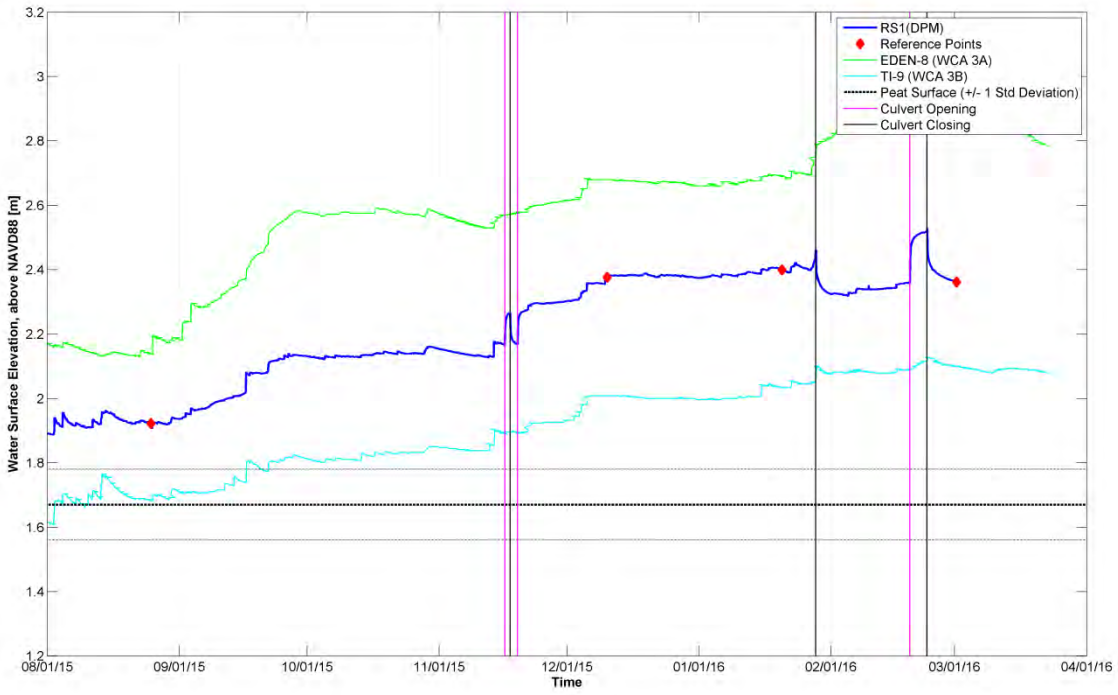

Figure B-46 Surface water and groundwater in DPM at site RS1D for the period of the 2015 flow release.

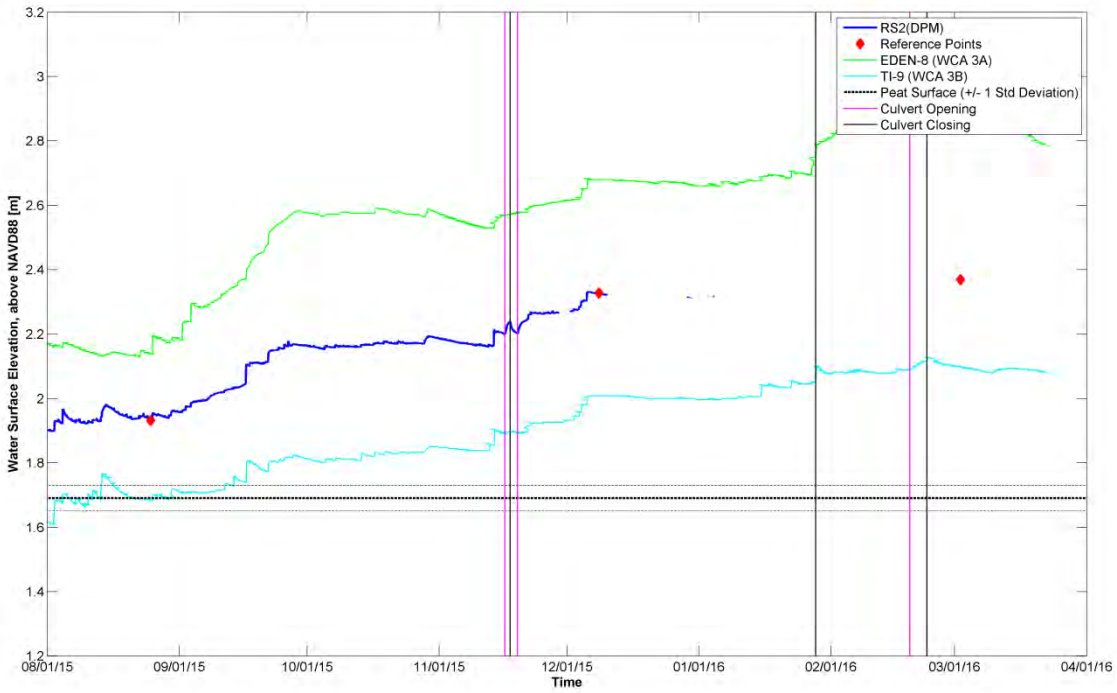

Figure B-47 Surface water and groundwater in DPM at site RS2 for the period of the 2015 flow release.

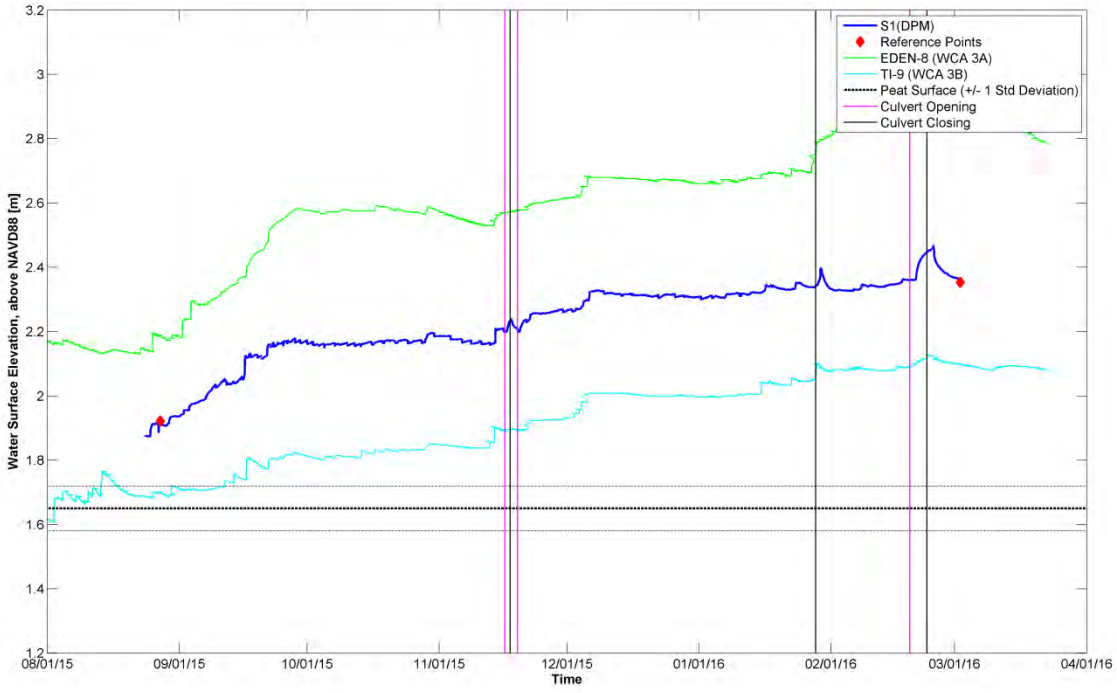

Figure B-48 Surface water and groundwater in DPM at site S1 for the period of the 2015 flow release.

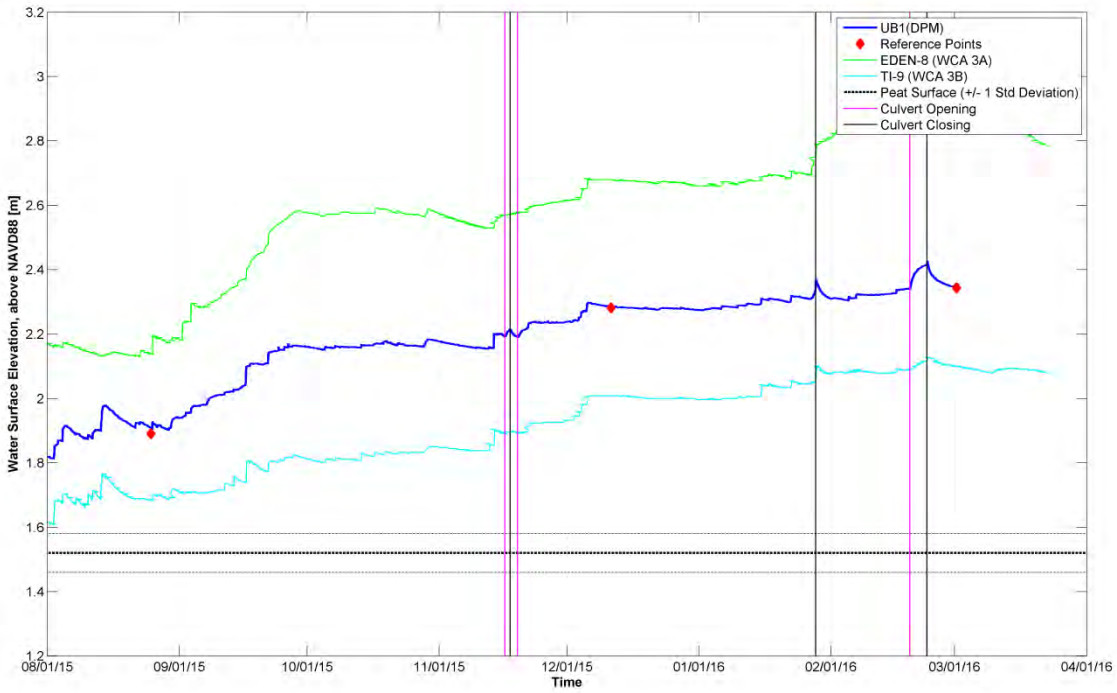

Figure B-49 Surface water and groundwater in DPM at site UB1 for the period of the 2015 flow release.

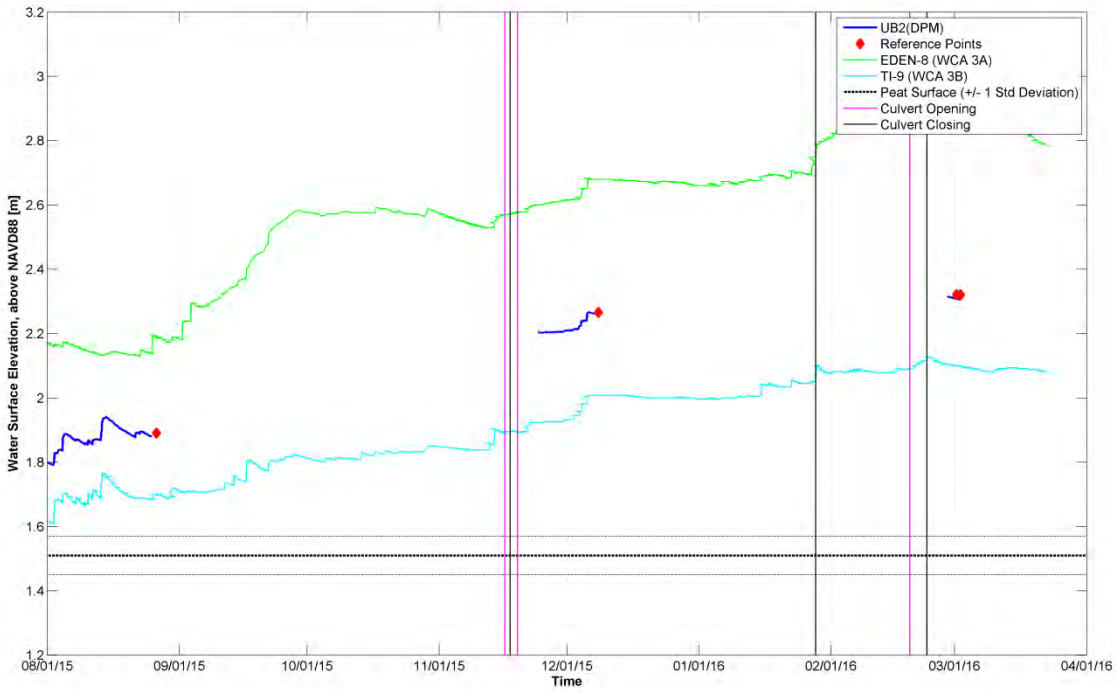

Figure B-50 Surface water and groundwater in DPM at site UB2 for the period of the 2015 flow release.

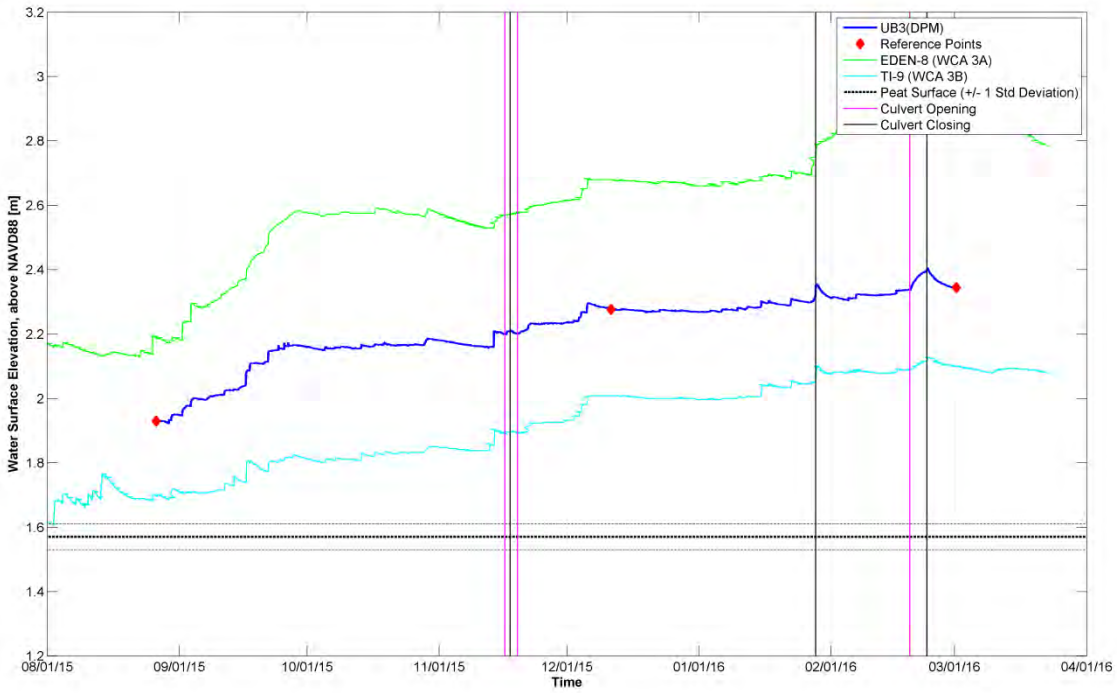

Figure B-51 Surface water and groundwater in DPM at site UB3 for the period of the 2015 flow release.

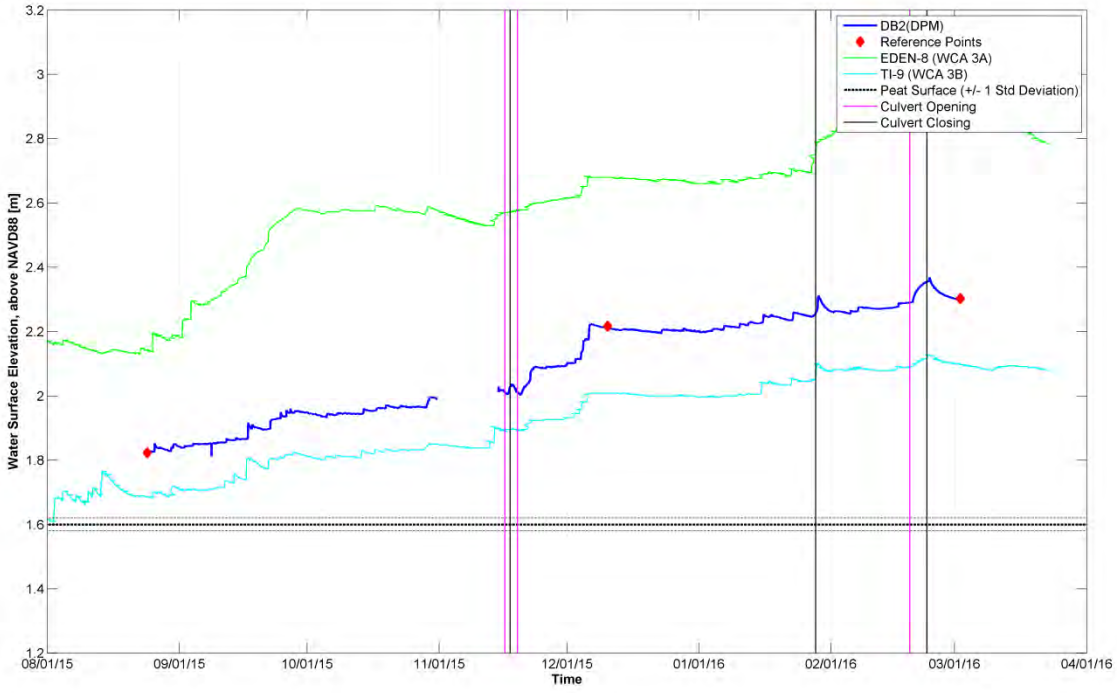

Figure B-52 Surface water and groundwater in DPM at site DB2 for the period of the 2015 flow release.

Groundwater Surface Water Comparisons for 2015 Flow Release

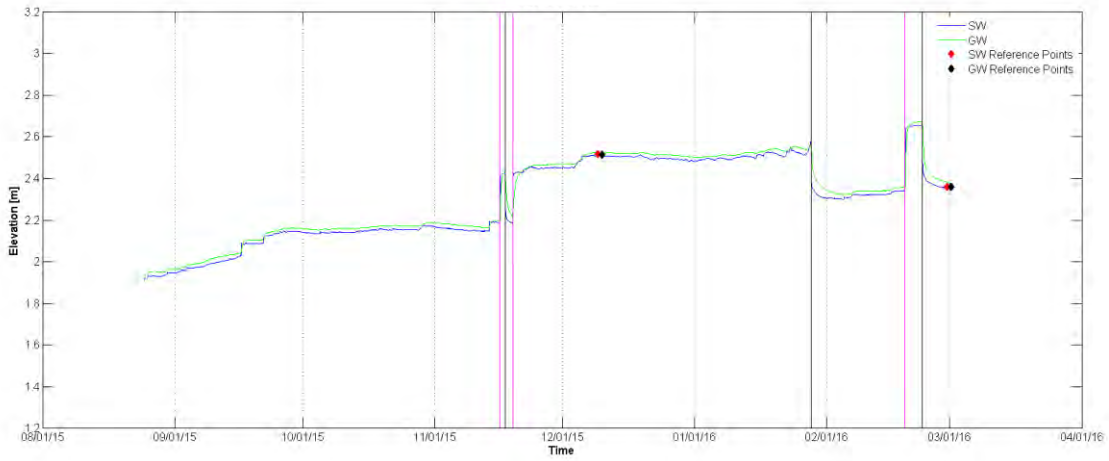

Figure B-53 Surface water and groundwater in DPM at site Z51_USGS for the period of the 2015 flow release.

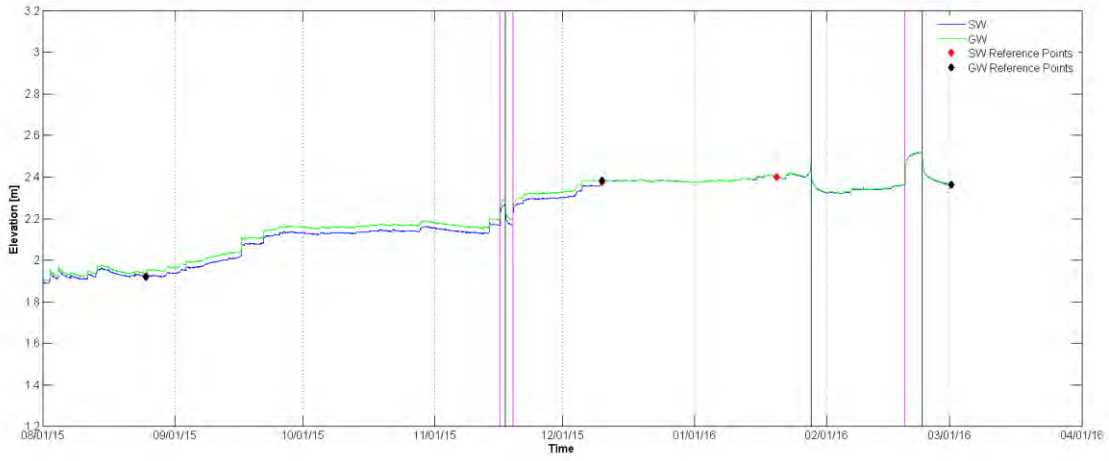

Figure B-54 Surface water and groundwater in DPM at site RS1D for the period of the 2015 flow release.

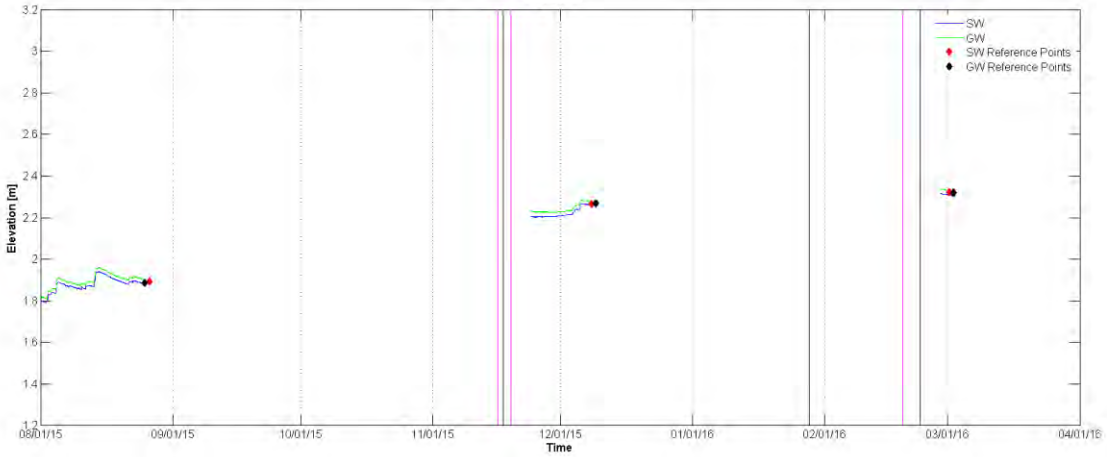

Figure B-55 Surface water and groundwater in DPM at site UB2 for the period of the 2015 flow release.

C. Surface Flow Velocities and Shear Stress

Velocity Statistics and Site Averages

Table C-1 Monthly Flow Velocity Statistics for continuously sampled ADV sites.

Site	Year	Month	V-X (N) (cm/s)	V-Y (W) (cm/s)	V-Z (Up) (cm/s)	I (X)	I (Y)	I (Z)	Speed (cm/s)	STD Speed	Dir.	STD Dir.	TKE	STD TKE
C1R	2011	11	-0.23	-0.31	-0.09	-1.17	-0.81	-1.54	0.4	0.25	126.2	44.4	0.08	0.08
C1S	2010	11	-0.08	-0.15	-0.18	-2.56	-1.29	-0.53	0.25	0.15	116.7	65.8	0.04	0.04
C1S	2011	9	-0.23	-0.43	-0.09	-0.87	-0.47	-2.12	0.49	0.2	118	26.5	0.06	0.06
C1S	2011	10	-0.15	-0.34	-0.05	-1.42	-0.62	-3.16	0.37	0.21	114.5	38.2	0.06	0.06
C2S	2015	11	-0.36	0.06	-0.00	-1.48	4.08	-45.11	0.36	0.52	190.26	70.93	0.18	0.35
C2S	2015	12	-0.12	0.01	-0.01	-2.42	18.19	-7.47	0.11	0.28	185.84	88.24	0.17	0.12
C2S	2016	1	-0.05	0.04	-0.00	-4.64	6.20	-27.14	0.07	0.24	218.37	94.40	0.06	0.10
C2S	2016	2	0.00	0.03	-0.01	41.90	8.42	-8.87	0.04	0.27	278.26	102.30	0.06	0.14
Z51_USGSR	2015	11	-4.07	0.01	-0.97	-0.28	114.14	-0.58	4.18	1.12	180.11	16.24	1.20	1.74
Z51_USGSR	2015	12	-1.13	-0.96	0.09	-0.72	-0.47	4.36	1.49	0.68	139.65	21.76	0.50	0.92
Z51_USGSR	2016	1	0.69	-2.28	-0.06	1.42	-0.33	-4.92	2.39	0.76	73.21	23.65	0.80	0.84
Z51_USGSR	2016	2	0.83	-1.08	-0.10	1.39	-1.30	-3.69	1.36	1.31	52.46	67.78	1.72	1.61
Z51_USGSS	2015	11	-6.86	-9.36	-0.33	-0.52	-0.58	-5.15	11.61	4.82	126.23	30.60	22.31	22.23
Z51_USGSS	2015	12	-9.57	-5.44	-0.65	-0.67	-0.75	-2.32	11.03	5.96	150.38	47.89	30.38	22.77
Z51_USGSS	2016	1	-0.18	-0.15	-0.02	-7.72	-8.13	-14.35	0.23	1.30	139.52	100.70	1.70	13.01
Z51_USGSS	2016	2	-0.20	-0.20	-0.06	-2.40	-2.44	-2.10	0.29	0.47	134.16	79.10	0.24	0.25
RS1DR	2010	7	-0.17	-0.26	-0.02	-1.23	-1.05	-3.8	0.31	0.25	124	55.3	0.06	0.06
RS1DR	2010	8	-0.11	-0.22	-0.01	-2.04	-1.24	-11.62	0.25	0.27	117	63.3	0.07	0.07
RS1DR	2010	9	-0.19	-0.36	-0.03	-1.07	-0.68	-2.83	0.41	0.23	117.5	33.3	0.05	0.09
RS1DR	2010	10	-0.12	-0.15	-0.01	-1.09	-1.15	-6.37	0.2	0.16	128.7	50.5	0.03	0.03
RS1DR	2010	11	-0.13	-0.19	-0.11	-0.74	-0.6	-0.21	0.26	0.1	124.7	29.9	0.01	0.01
RS1DR	2011	9	-0.16	-0.2	-0.17	-1.01	-0.8	-0.6	0.31	0.15	128.5	41.5	0.03	0.03
RS1DR	2011	10	NaN	NaN	NaN	NaN	NaN	NaN	0.25	0.15	NaN	NaN	0.04	0.04
RS1DR	2011	11	NaN	NaN	NaN	NaN	NaN	NaN	0.32	0.17	NaN	NaN	0.06	0.06
RS1DR	2012	8	-0.09	-0.01	-0.02	-2.39	-19.83	-2.98	0.1	0.21	173.7	85.35	0.05	0.05
RS1DR	2012	9	-0.09	0.01	-0.02	-2.87	21.11	-3.3	0.09	0.24	187.46	89.07	0.06	0.07
RS1DR	2012	10	-0.02	-0.02	-0.01	-7.51	-9.33	-7.19	0.03	0.18	141.48	96.76	0.03	0.05
RS1DR	2012	11	-0.01	-0.01	-0.01	-15.1	-12.01	-5.17	0.02	0.14	126.94	98.13	0.02	0.05
RS1DR	2012	12	-0.02	-0.03	-0.01	-9.07	-7.58	-5.17	0.03	0.18	129.8	96.79	0.04	0.06
RS1DR	2013	1	-0.14	-0.08	-0.02	-2.03	-3.34	-4.25	0.17	0.28	150.05	77.29	0.08	0.09
RS1DR	2013	2	-0.08	-0.08	-0.05	-2.55	-2.58	-2.1	0.12	0.19	133.7	82.32	0.05	0.06
RS1DR	2013	8	-0.23	0	-0.02	-1.04	-340.55	-5.01	0.23	0.24	179.82	61.99	0.07	0.07

RS1DR	2013	9	-0.09	0.01	-0.01	-2.97	28.61	-5.99	0.09	0.27	186.49	88.15	0.08	0.13
RS1DR	2013	10	-0.15	-0.17	-0.04	-1.7	-1.5	-3.28	0.23	0.25	130.66	65.11	0.08	0.08
RS1DR	2013	10	-0.15	-0.17	-0.04	-1.70	-1.50	-3.28	0.23	0.25	130.66	65.11	0.08	0.08
RS1DR	2013	11	-1.63	0.10	-0.33	-0.48	5.39	-0.72	1.67	0.76	183.57	30.35	0.48	0.48
RS1DR	2013	12	-1.94	0.03	-0.37	-0.33	15.37	-0.78	1.97	0.62	181.02	20.18	0.38	0.41
RS1DR	2014	1	-0.03	-0.07	-0.03	-9.46	-4.79	-3.83	0.08	0.33	115.40	92.23	0.12	0.14
RS1DR	2014	2	-0.01	-0.02	-0.01	-22.60	-14.96	-10.17	0.03	0.31	121.76	100.38	0.10	0.27
RS1DR	2014	3	-0.01	0.00	-0.01	-31.81	-73.85	-12.22	0.01	0.29	155.44	102.16	0.11	0.15
RS1DR	2014	11	-1.03	-0.22	-0.31	-0.40	-1.39	-0.43	1.10	0.39	168.03	21.44	0.14	0.15
RS1DS	2010	7	-0.39	0.15	-0.04	-0.53	1.43	-2.11	0.42	0.21	201.1	32.1	0.05	0.06
RS1DS	2010	8	-0.25	-0.02	-0.04	-0.89	-9.91	-2.24	0.26	0.22	174.9	55.3	0.05	0.06
RS1DS	2010	9	-0.59	-0.1	-0.01	-0.43	-1.87	-10.3	0.6	0.25	170.1	24.7	0.06	0.06
RS1DS	2010	10	-0.83	-0.02	0	-0.38	-10.7	26.23	0.83	0.31	178.4	20.7	0.09	0.08
RS1DS	2010	11	-1.13	-0.15	-0.01	-0.31	-1.9	-10.79	1.14	0.35	172.4	17.2	0.11	0.13
RS1DS	2010	12	-1.17	-0.29	-0.08	-0.37	-1.17	-2.27	1.21	0.43	166	21.9	0.17	0.18
RS1DS	2011	9	-0.28	-0.02	-0.09	-0.61	-7.16	-0.93	0.29	0.16	175.4	40.1	0.03	0.03
RS1DS	2011	10	-0.3	-0.05	-0.09	-0.66	-3.72	-1.55	0.31	0.19	170.9	41.3	0.04	0.05
RS1DS	2011	11	-0.26	-0.17	-0.04	-1.1	-1.72	-3.25	0.31	0.29	147.2	57.3	0.09	0.12
RS1DS	2012	9	-0.42	-0.05	-0.02	-0.81	-4.58	-5.32	0.43	0.34	173.33	47.4	0.09	0.1
RS1DS	2012	10	-0.51	-0.04	-0.01	-0.51	-6.02	-8.41	0.51	0.26	175.9	31.85	0.06	0.08
RS1DS	2012	11	-0.17	-0.03	-0.06	-1.86	-9.33	-2.4	0.18	0.3	169.53	80.13	0.1	0.11
RS1DS	2012	12	-0.23	-0.02	-0.03	-1.2	-10.35	-4.32	0.24	0.28	174.4	66.12	0.07	0.08
RS1DS	2013	8	-0.49	-0.12	-0.06	-0.81	-2.96	-1.72	0.51	0.4	166.22	51.71	0.15	0.14
RS1DS	2013	9	-0.52	-0.11	-0.06	-0.79	-3.29	-1.82	0.53	0.4	168.28	49.86	0.15	0.15
RS1DS	2013	10	-0.6	-0.16	-0.06	-0.62	-2.1	-1.96	0.63	0.37	165.33	40.76	0.13	0.14
RS1DS	2013	11	-3.75	-1.27	-0.24	-0.48	-0.65	-2.62	3.96	1.72	161.22	16.72	2.15	2.21
RS1DS	2013	12	-3.29	-0.70	0.06	-0.49	-1.30	12.09	3.36	1.60	167.99	26.61	1.97	1.85
RS1DS	2014	1	-0.38	-0.18	-0.04	-1.38	-3.09	-4.00	0.42	0.53	154.87	63.42	0.30	0.69
RS1DS	2014	2	-0.54	-0.28	-0.09	-0.78	-1.28	-1.87	0.62	0.41	152.20	45.73	0.17	0.18
RS1DS	2014	3	-0.21	-0.11	-0.05	-1.78	-2.60	-2.63	0.24	0.34	151.34	77.30	0.12	0.18
RS1DS	2014	8	-0.47	0.06	0.06	-0.69	5.73	4.19	0.47	0.32	186.90	43.56	0.14	0.21
RS1DS	2014	9	-0.57	0.09	-0.10	-0.63	3.78	-2.86	0.59	0.36	188.77	41.35	0.16	0.17
RS1DS	2014	10	-0.32	0.04	-0.05	-1.32	7.89	-4.43	0.32	0.42	187.11	73.75	0.16	0.20
RS1DS	2014	11	-2.23	-0.73	-0.25	-0.70	-1.90	-2.14	2.36	1.54	161.82	38.06	2.33	3.07
RS1DS	2014	12	-3.95	-1.02	-0.75	-0.38	-1.24	-1.01	4.15	1.47	165.55	21.35	2.21	2.36
RS1DS	2015	1	-2.48	-0.72	-0.42	-0.50	-1.40	-1.65	2.62	1.20	163.75	24.96	1.51	1.50
RS1DS	2015	2	-0.27	0.05	-0.05	-1.31	7.43	-4.06	0.27	0.34	189.68	67.69	0.14	0.17
RS1DS	2015	3	-0.16	0.03	-0.03	-2.12	9.83	-6.93	0.17	0.35	190.99	81.08	0.13	0.19

RS1DS	2015	11	-1.95	-0.89	-0.14	-0.59	-0.85	-2.97	2.15	1.09	155.33	23.37	1.03	0.98
RS1DS	2015	12	-3.32	-2.49	-0.22	-0.35	-0.54	-3.78	4.16	1.23	143.08	15.23	1.92	1.89
RS1DS	2016	1	-2.43	-1.68	-0.28	-0.55	-0.69	-2.00	2.97	1.28	145.29	22.79	1.74	1.55
RS1DS	2016	2	-1.07	-0.72	-0.03	-1.43	-1.22	-13.51	1.29	1.36	145.87	29.80	1.62	4.71
RS2R	2014	10	-0.17	-0.11	-0.04	-1.53	-2.41	-1.95	0.21	0.26	147.96	69.95	0.07	0.07
RS2R	2014	11	-0.74	-0.05	0.01	-0.73	-6.09	14.31	0.74	0.54	176.25	42.72	0.20	0.17
RS2R	2015	11	-1.31	-0.37	-0.17	-0.54	-0.64	-1.24	1.37	0.68	164.37	22.14	0.30	0.26
RS2R	2015	12	-2.05	-0.41	-0.22	-0.14	-0.59	-0.86	2.10	0.29	168.62	7.25	0.09	.011
RS2R	2016	1	-1.97	-0.47	-0.23	-0.27	-0.47	-0.70	2.04	0.51	166.59	8.89	0.18	0.31
RS2R	2016	2	-0.94	-0.32	-0.14	-0.70	-0.59	-1.08	1.00	0.62	161.02	16.90	0.24	0.38
RS2S	2014	10	-0.23	-0.16	0.01	-0.78	-1.69	15.99	0.28	0.21	145.65	52.63	0.05	0.07
RS2S	2014	11	-0.39	-0.19	0.11	-0.68	-1.54	1.58	0.45	0.27	153.68	41.00	0.09	0.07
S1	2010	7	-0.05	-0.15	-0.01	-4.23	-1.29	-6.6	0.16	0.19	108.02	67.25	0.04	0.05
S1	2010	8	-0.05	-0.14	-0.02	-3.81	-1.28	-3.37	0.15	0.18	108.94	66.49	0.04	0.05
S1	2010	9	-0.09	-0.19	-0.04	-2.04	-0.95	-2.1	0.21	0.18	117.1	55.48	0.04	0.04
S1	2010	10	-0.12	-0.2	-0.04	-1.4	-0.87	-2.06	0.24	0.17	121.51	49.38	0.03	0.03
S1	2010	11	0.09	-0.14	-0.05	2.21	-1.43	-1.8	0.18	0.2	56.51	68.06	0.05	0.05
S1	2010	12	0.12	-0.11	-0.04	2.04	-2.25	-2.64	0.17	0.24	42.99	73.71	0.07	0.08
S1	2012	8	-0.13	-0.16	-0.02	-1.8	-1.44	-5.16	0.21	0.24	129.23	64.9	0.06	0.07
S1	2012	9	-0.04	-0.05	-0.01	-4.83	-4.28	-7.08	0.07	0.22	131.02	90.96	0.05	0.06
S1	2012	10	-0.03	-0.01	-0.01	-7.19	-12.62	-5.54	0.03	0.18	150.39	97.02	0.04	0.06
S1	2012	11	-0.01	-0.01	0	-12.01	-13.16	-11.6	0.02	0.18	135.85	99.22	0.03	0.05
S1	2013	8	-0.22	-0.15	-0.01	-1.2	-2.01	-13.94	0.26	0.27	145.19	58.39	0.09	0.11
S1	2013	9	-0.09	-0.03	-0.02	-2.42	-7.22	-4.02	0.09	0.21	160.74	86.41	0.05	0.07
S1	2013	10	-0.02	-0.01	-0.01	-8.66	-28.31	-5.34	0.02	0.14	161.4	98.41	0.02	0.05
S1	2013	11	-0.51	-0.71	-0.08	-0.73	-0.78	-2.50	0.88	0.50	125.71	37.08	0.24	0.31
S1	2013	12	-0.66	-0.22	0.00	-0.64	-1.83	44.97	0.69	0.42	161.12	40.45	0.19	0.23
S1	2014	1	-0.21	-0.26	-0.03	-1.50	-1.43	-3.99	0.33	0.35	128.39	62.11	0.12	0.13
S1	2014	2	-0.22	-0.16	-0.06	-1.39	-2.01	-2.91	0.28	0.30	143.23	58.63	0.11	0.15
S1	2014	3	-0.05	-0.08	-0.06	-7.28	-5.65	-3.84	0.11	0.38	124.68	94.91	0.20	0.19
UB1	2010	11	-0.05	-0.08	-0.01	-6.14	-3.32	-7.52	0.1	0.28	119	87.1	0.08	0.1
UB1	2010	12	-0.04	-0.06	-0.01	-6.94	-4.42	-8.71	0.07	0.27	122.8	90.5	0.08	0.1
UB1	2011	1	-0.05	-0.05	-0.01	-5.48	-5.65	-4.87	0.07	0.27	135.6	91.3	0.08	0.1
UB1	2011	11	0.06	-0.1	-0.09	3.45	-2.07	-1.29	0.15	0.18	60.3	76.7	0.05	0.06
UB1	2012	8	-0.03	-0.12	-0.08	-5.65	-1.54	-0.91	0.15	0.17	104.25	71.33	0.04	0.05
UB1	2012	9	-0.03	-0.14	-0.08	-5.71	-1.49	-0.98	0.16	0.18	103.65	71.73	0.04	0.04
UB1	2012	10	-0.04	-0.14	-0.06	-5.55	-1.54	-1.1	0.15	0.2	104.57	72.81	0.04	0.05
UB1	2012	11	0	-0.16	-0.06	-52.46	-1.34	-1.28	0.17	0.2	91.48	69.84	0.05	0.05

UB1	2012	12	-0.08	-0.31	-0.07	-2.85	-0.89	-1.43	0.32	0.26	103.94	54.09	0.06	0.06
UB1	2013	1	-0.07	-0.33	-0.03	-2.81	-0.87	-2.26	0.34	0.28	101.85	54.77	0.06	0.05
UB1	2013	2	-0.02	-0.04	-0.01	-6.02	-4.14	-3.18	0.04	0.14	123.24	93.68	0.02	0.03
UB1	2013	8	-0.33	-0.15	-0.09	-0.78	-1.61	-1.04	0.37	0.24	155.74	46.55	0.06	0.07
UB1	2013	9	-0.13	-0.07	-0.05	-1.84	-3.22	-1.37	0.16	0.23	153.2	77.06	0.06	0.06
UB1	2013	10	-0.14	-0.05	-0.03	-1.62	-3.94	-1.94	0.15	0.22	160.62	76.15	0.05	0.06
UB1	2013	11	-0.48	-0.19	-0.10	-0.86	-2.17	-1.48	0.53	0.41	158.68	52.97	0.18	0.19
UB1	2013	12	-0.32	-0.17	-0.06	-1.37	-2.53	-2.24	0.37	0.43	152.20	67.72	0.20	0.19
UB1	2014	1	-0.25	-0.34	-0.07	-1.60	-1.19	-1.57	0.42	0.39	126.53	58.52	0.16	0.17
UB1	2014	8	-0.08	-0.05	-0.04	-2.51	-4.48	-2.58	0.10	0.19	148.79	83.62	0.05	0.07
UB1	2014	9	-0.12	-0.13	-0.04	-2.01	-2.08	-3.66	0.18	0.25	132.47	72.42	0.08	0.09
UB1	2014	10	-0.17	-0.08	-0.03	-1.52	-3.48	-4.77	0.19	0.26	155.15	71.04	0.09	0.10
UB1	2014	11	-0.52	0.07	-0.06	-0.67	4.71	-3.08	0.53	0.35	187.91	42.85	0.14	0.15
UB1	2014	12	-0.50	-0.03	-0.05	-0.60	-9.50	-3.10	0.50	0.30	176.26	39.24	0.11	0.13
UB1	2015	1	-0.37	-0.09	-0.05	-0.71	-3.00	-3.13	0.38	0.26	166.03	46.53	0.08	0.09
UB1	2015	2	-0.12	-0.24	-0.03	-1.97	-1.08	-3.54	0.27	0.25	116.42	58.90	0.06	0.06
UB1	2015	3	-0.07	-0.09	-0.04	-2.74	-2.34	-2.02	0.13	0.20	127.78	80.39	0.05	0.05
UB2	2010	8	0.04	0	-0.02	1.61	15.7	-1.07	0.04	0.06	354.45	74.48	0	0
UB2	2010	9	-0.01	-0.07	-0.01	-30.12	-3.23	-10.44	0.07	0.23	95.5	91.2	0.05	0.09
UB2	2010	10	-0.01	-0.09	-0.01	-22.27	-3.53	-5.94	0.09	0.32	98.5	88.8	0.1	0.13
UB2	2010	11	0.02	-0.03	-0.01	14.16	-10.45	-15.73	0.04	0.3	55.7	97.9	0.09	0.13
UB2	2011	11	-0.04	-0.09	-0.03	-6.27	-2.66	-3.31	0.11	0.24	114.5	86.4	0.07	0.07
UB2	2012	8	-0.06	-0.07	-0.04	-2.93	-2.9	-2.13	0.1	0.18	133.88	81.43	0.04	0.05
UB2	2012	9	-0.07	-0.06	-0.05	-2.7	-3.35	-1.54	0.11	0.17	141.06	79.63	0.04	0.05
UB2	2012	10	-0.01	-0.02	-0.03	-11.59	-8.83	-1.32	0.04	0.08	127.48	97.75	0.02	0.03
UB2	2012	11	-0.02	-0.02	-0.01	-7.52	-7.22	-2.19	0.03	0.1	133.72	94.4	0.01	0.04
UB2	2012	12	0.38	-0.51	-0.04	0.83	-0.62	-2.23	0.64	0.32	53.24	34.97	0.1	0.11
UB2	2013	1	0.1	-0.26	-0.01	2.81	-1.13	-9.52	0.28	0.29	68.63	61.05	0.09	0.1
UB2	2013	2	0.08	-0.21	0.01	4.1	-1.47	6.36	0.22	0.31	69.54	73.09	0.1	0.09
UB2	2013	8	-0.53	-0.35	0.08	-0.66	-0.95	2.18	0.64	0.35	146.7	37.8	0.13	0.12
UB2	2013	9	-0.61	-0.34	0.04	-0.56	-0.98	4.4	0.69	0.34	150.95	33.31	0.12	0.11
UB2	2013	10	-0.36	-0.11	0	-0.98	-2.56	-61.11	0.38	0.35	163.4	58.18	0.11	0.1
UB2	2013	11	-0.63	-0.13	0.04	-0.65	-3.03	3.89	0.65	0.41	168.37	41.84	0.18	0.18
UB2	2013	12	-0.57	-0.12	0.07	-0.78	-3.44	2.13	0.59	0.44	168.45	49.31	0.19	0.19
UB2	2014	1	-0.04	-0.18	-0.01	-8.25	-2.01	-6.67	0.18	0.35	103.71	77.97	0.13	0.15
UB2	2014	2	-0.02	-0.02	-0.01	-14.63	-11.68	-5.01	0.03	0.21	128.23	98.34	0.05	0.09
UB2	2014	3	-0.01	-0.01	-0.01	-23.58	-31.87	-6.48	0.02	0.22	143.38	100.86	0.07	0.11
UB2	2014	10	-0.01	0.00	-0.01	-34.80	-53.80	-8.62	0.01	0.18	145.61	101.61	0.05	0.13

UB2	2014	11	-0.03	-0.02	0.00	-37.03	-39.38	-54.25	0.04	0.95	138.63	101.96	0.92	1.24
UB2	2014	12	-0.01	-0.01	0.00	-62.88	-94.39	-42.07	0.02	0.78	144.98	102.31	0.68	1.12
UB2	2015	1	-0.01	-0.01	0.00	-36.94	-59.50	-20.53	0.02	0.43	145.94	101.92	0.22	0.56
UB2	2015	2	-0.05	0.02	0.03	-25.90	54.15	9.32	0.07	1.14	205.64	102.17	1.79	1.72
UB2	2015	3	0.00	-0.02	0.01	392.71	-64.77	40.16	0.02	1.17	80.77	103.43	1.54	1.41
UB2	2015	11	-0.47	0.21	-0.06	-1.04	1.70	-2.56	0.52	0.46	204.44	61.38	0.19	0.17
UB2	2015	12	-0.95	0.39	-0.08	-0.53	0.83	-2.04	1.03	0.48	201.99	28.10	0.19	0.19
UB2	2016	1	-0.63	0.31	-0.05	-0.68	0.95	-2.16	0.71	0.40	205.96	35.67	0.14	0.12
UB2	2016	2	-0.26	0.08	-0.02	-1.21	2.46	-4.79	0.27	0.30	197.79	65.70	0.07	0.09
UB3	2010	11	0.01	-0.06	0.01	40.82	-7.18	11.53	0.06	0.44	80.5	96.1	0.19	0.24
UB3	2010	12	0.02	-0.06	0.01	23.44	-7.78	9.89	0.06	0.45	72.8	95.6	0.21	0.25
UB3	2011	11	-0.06	-0.11	-0.03	-3.78	-2.07	-3.27	0.13	0.22	118.4	78.3	0.06	0.06
UB3	2012	8	-0.01	-0.11	-0.25	-17.27	-1.76	-0.55	0.27	0.15	94.97	74.86	0.04	0.05
UB3	2012	9	-0.02	-0.11	-0.28	-10.92	-1.82	-0.52	0.3	0.15	98.56	76.72	0.05	0.06
UB3	2012	10	0.01	-0.13	-0.3	23.18	-1.81	-0.52	0.32	0.17	85.65	78.42	0.07	0.07
UB3	2012	11	0.03	-0.06	-0.45	6.86	-3.28	-0.4	0.46	0.18	64.86	88.83	0.06	0.05
UB3	2012	12	0.02	-0.06	-0.49	10.98	-3.53	-0.29	0.5	0.15	71.88	90.8	0.05	0.06
UB3	2013	8	-0.04	-0.45	0.03	-3.98	-0.76	2.85	0.46	0.34	95.25	45	0.08	0.07
UB3	2013	9	-0.27	-0.69	0.04	-1.02	-0.82	2.27	0.74	0.53	111.24	45.09	0.2	0.14
UB3	2013	10	-0.1	-0.27	0.02	-1.84	-1.14	2.61	0.29	0.3	110.56	57.48	0.07	0.09
UB3	2013	11	-0.50	-0.73	0.06	-0.82	-0.59	2.43	0.88	0.42	124.31	31.95	0.18	0.17
UB3	2013	12	-0.09	-0.14	0.00	-2.64	-2.08	12.99	0.17	0.27	123.81	81.81	0.07	0.11
UB3	2014	1	-0.03	-0.02	-0.02	-6.70	-9.73	-2.51	0.04	0.19	145.24	96.62	0.05	0.06
UB3	2014	2	-0.06	-0.13	-0.07	-4.94	-2.32	-1.48	0.16	0.28	115.29	83.52	0.10	0.10
UB3	2014	3	-0.10	-0.03	-0.02	-2.95	-8.25	-2.61	0.11	0.28	160.58	87.88	0.08	0.08
DB1	2014	8	-1.33	-0.68	-0.14	-0.51	-0.97	-1.35	1.51	0.67	152.93	30.26	0.47	0.42
DB1	2014	9	-0.63	-0.85	0.03	-0.77	-0.73	5.81	1.06	0.57	126.57	35.07	0.33	0.31
DB1	2014	10	-0.61	-0.70	-0.06	-0.82	-0.88	-3.51	0.93	0.57	130.76	41.89	0.33	0.30
DB1	2014	11	-1.08	-1.46	-0.05	-0.68	-0.74	-5.51	1.82	0.97	126.56	39.30	0.89	0.73
DB1	2014	12	-0.40	-0.63	-0.02	-1.29	-1.30	-13.57	0.75	0.74	122.76	59.24	0.49	0.62
DB1	2015	1	-0.80	-0.80	-0.09	-0.70	-0.77	-2.40	1.13	0.59	134.79	39.72	0.37	0.31
DB1	2015	2	-0.88	-0.22	-0.07	-0.48	-1.76	-2.55	0.91	0.42	166.04	27.91	0.18	0.16
DB1	2015	3	-0.25	-0.01	-0.02	-1.16	-29.73	-5.41	0.25	0.28	177.81	64.96	0.09	0.11
DB2	2014	8	-0.01	0.00	-0.01	-10.76	-14.23	-3.25	0.01	0.06	141.24	97.12	0.00	0.01
DB2	2014	9	-0.27	-0.14	-0.04	-1.76	-1.94	-1.99	0.31	0.43	151.69	76.52	0.15	0.29
DB2	2014	10	-1.31	-0.41	-0.18	-0.38	-0.99	-1.14	1.39	0.49	162.57	18.62	0.23	0.23
DB2	2014	11	-1.95	-0.48	-0.06	-0.59	-1.04	-8.13	2.00	1.13	166.07	35.14	0.91	0.86
DB2	2014	12	-1.40	-0.35	-0.42	-0.67	-1.16	-1.15	1.50	0.89	166.10	42.07	0.64	0.58

DB2	2015	1	-1.25	-0.27	-0.51	-0.55	-1.48	-0.84	1.37	0.64	167.66	31.97	0.40	0.32
DB2	2015	2	-0.04	-0.09	-0.17	-8.12	-1.84	-0.63	0.20	0.14	112.69	83.47	0.07	0.08
DB2	2015	3	0.29	-0.15	-0.10	0.58	-1.09	-0.99	0.34	0.16	28.20	34.04	0.03	0.06
DB3	2014	8	0.00	-1.52	-0.06	-76.51	-0.31	-2.53	1.52	0.47	90.14	13.04	0.16	0.17
DB3	2014	9	-0.19	-1.40	-0.22	-1.66	-0.43	-1.03	1.43	0.59	97.87	19.66	0.26	0.27
DB3	2014	10	-0.05	-0.25	-0.06	-3.57	-2.00	-2.04	0.26	0.48	101.33	81.92	0.15	0.29
DB3	2014	11	-1.29	-1.15	-0.21	-0.38	-0.40	-0.96	1.74	0.47	138.22	16.26	0.25	0.26
DB3	2014	12	-0.78	-0.99	-0.18	-0.84	-0.55	-0.87	1.27	0.58	128.33	29.60	0.37	1.90
DB3	2015	1	-0.85	-1.22	-0.33	-0.64	-0.36	-0.54	1.52	0.47	124.93	21.06	0.26	0.88
DB3	2015	2	0.07	-1.18	-0.09	6.27	-0.39	-2.38	1.19	0.46	86.69	23.86	0.22	0.20
DB3	2015	3	0.36	-0.79	0.09	0.68	-0.32	1.38	0.87	0.25	65.13	17.83	0.07	0.07

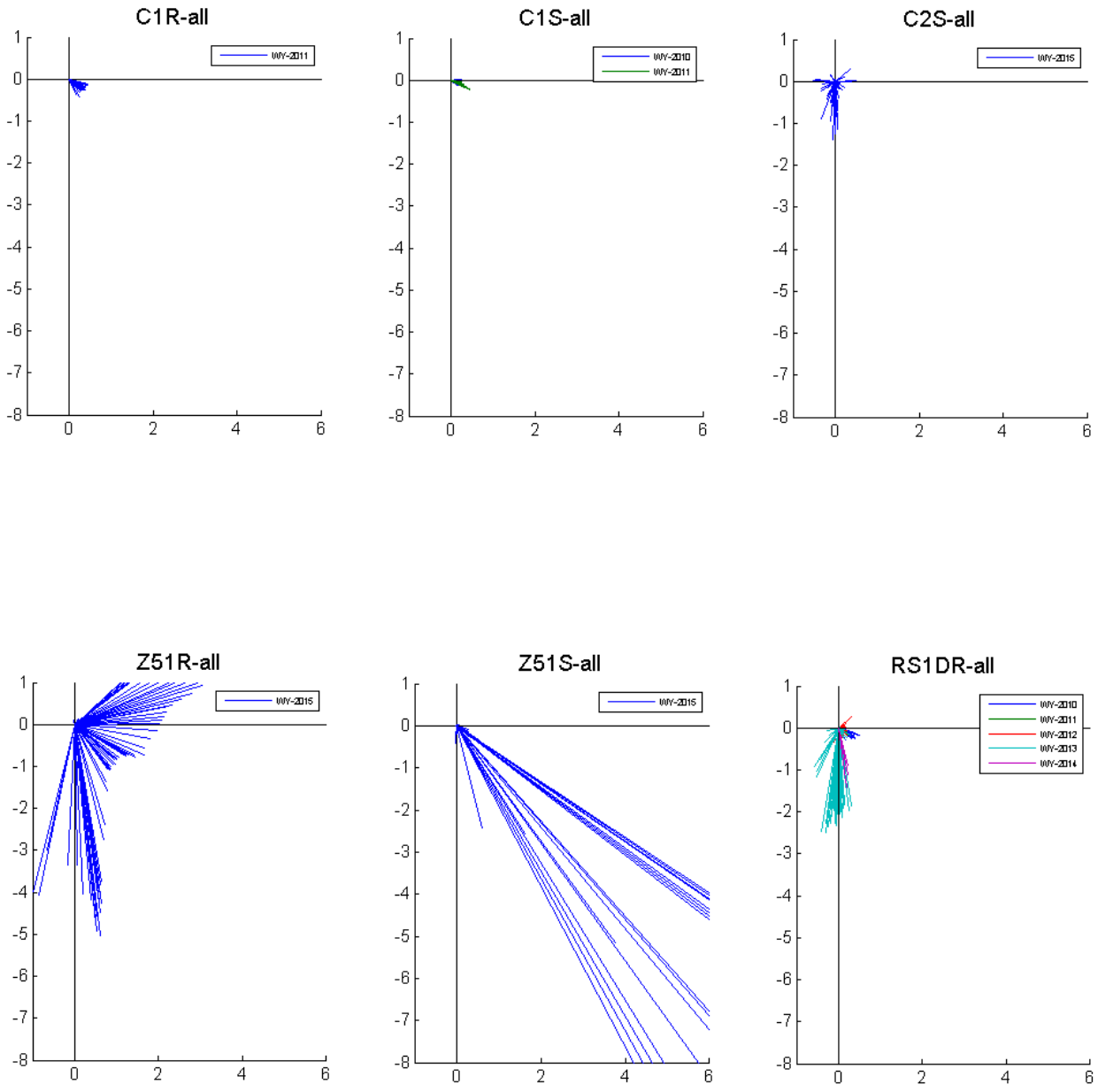

Figure C-1 Daily average ADV flow vectors (cm/s) recorded at continuously sampled DPM sites during water years 2010 through 2015. The axes represent cardinal directions with true north at the top of each plot.

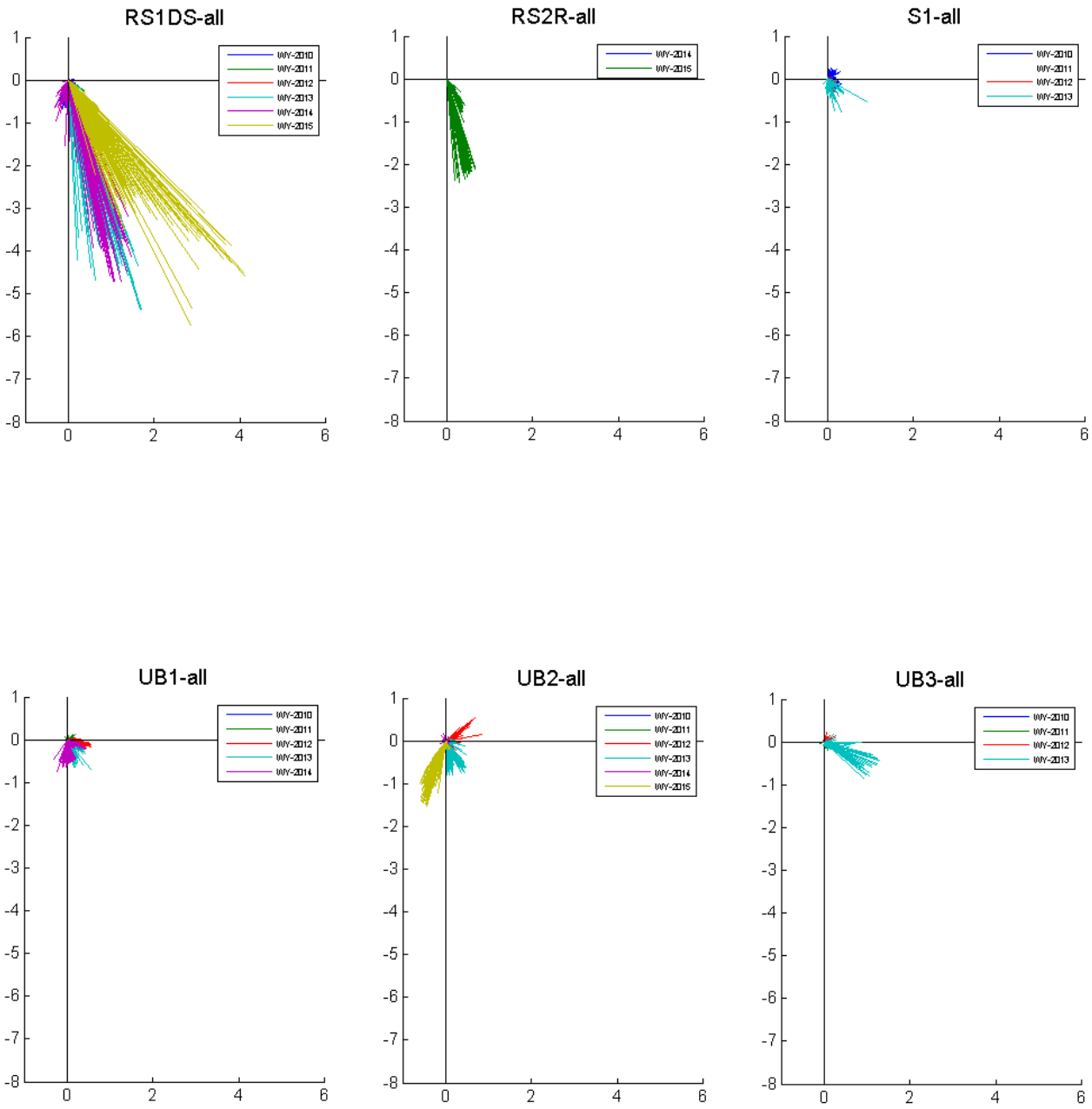

Figure C-2 Daily average ADV flow vectors (cm/s) recorded at continuously sampled DPM sites during water years 2010 through 2015. The axes represent cardinal directions with true north at the top of each plot.

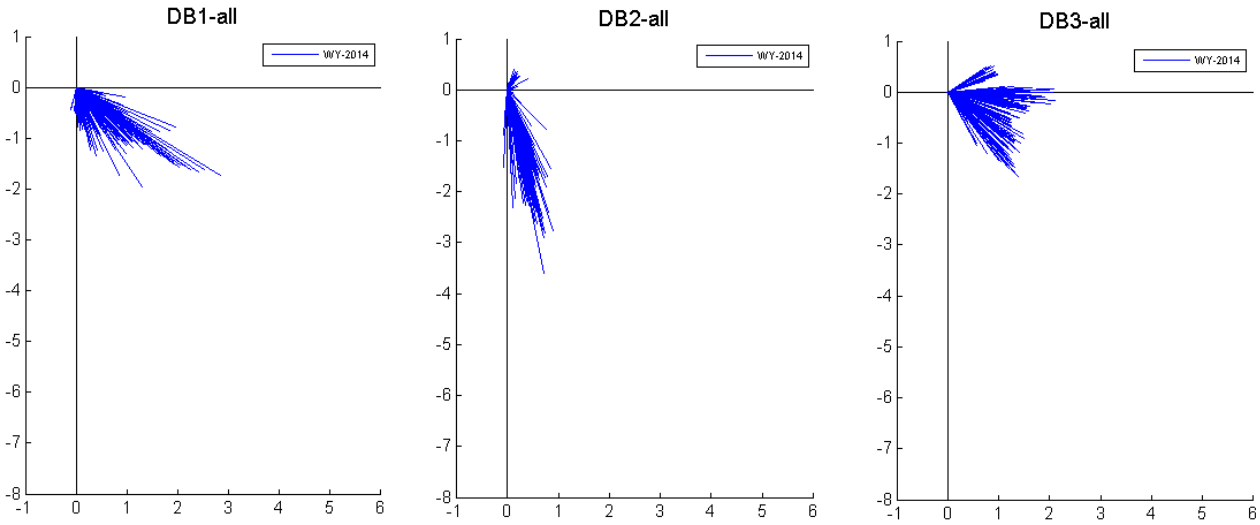

Figure C-3 Daily average ADV flow vectors (cm/s) recorded at continuously sampled DPM sites during water years 2010 through 2015. The axes represent cardinal directions with true north at the top of each plot.

Continuous ADV Data

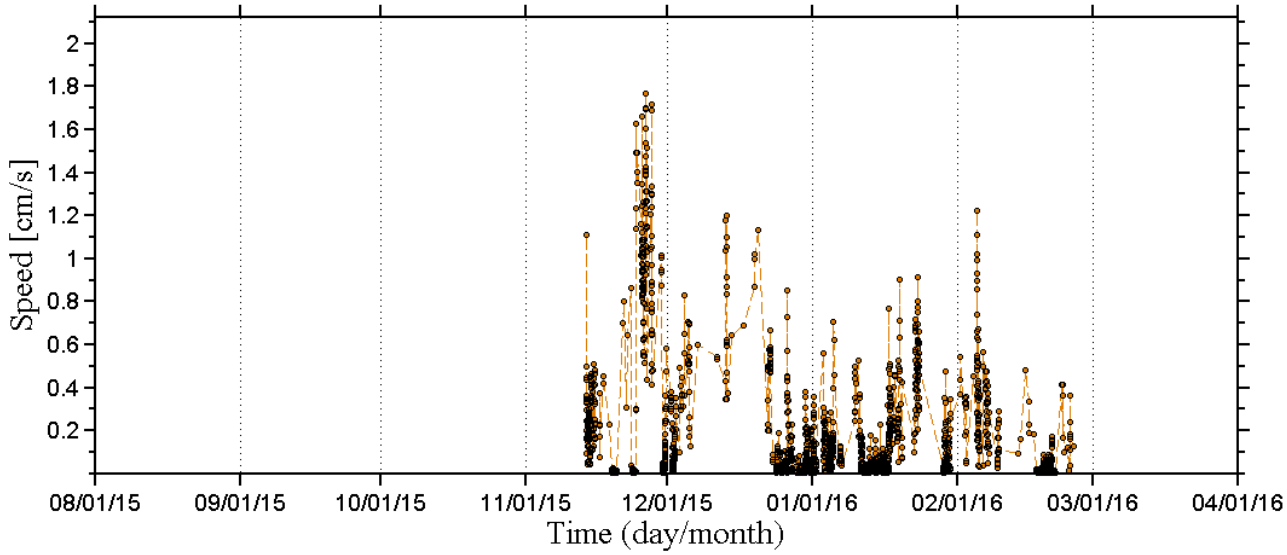

Figure C-4 Continuously sampled burst average ADV flow speed (cm/s) recorded at C2S site during water year 2015 (8/1/2015 – 3/31/2016).

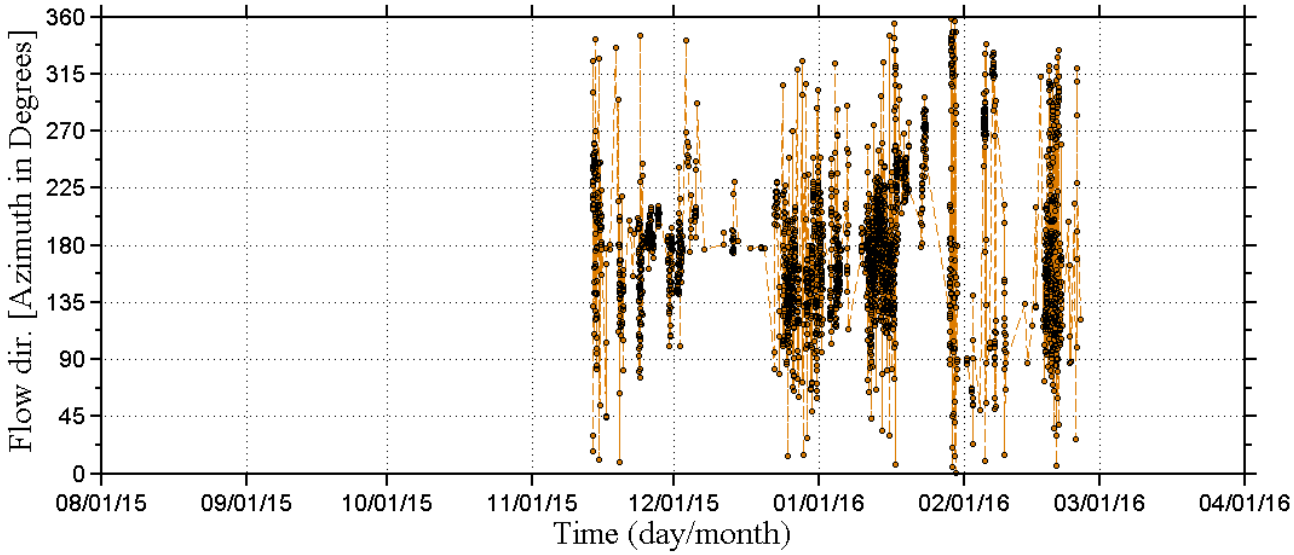

Figure C-5 Continuously sampled burst average ADV flow direction (clockwise degree from North) recorded at C2S site during water year 2015 (8/1/2015 – 3/31/2016).

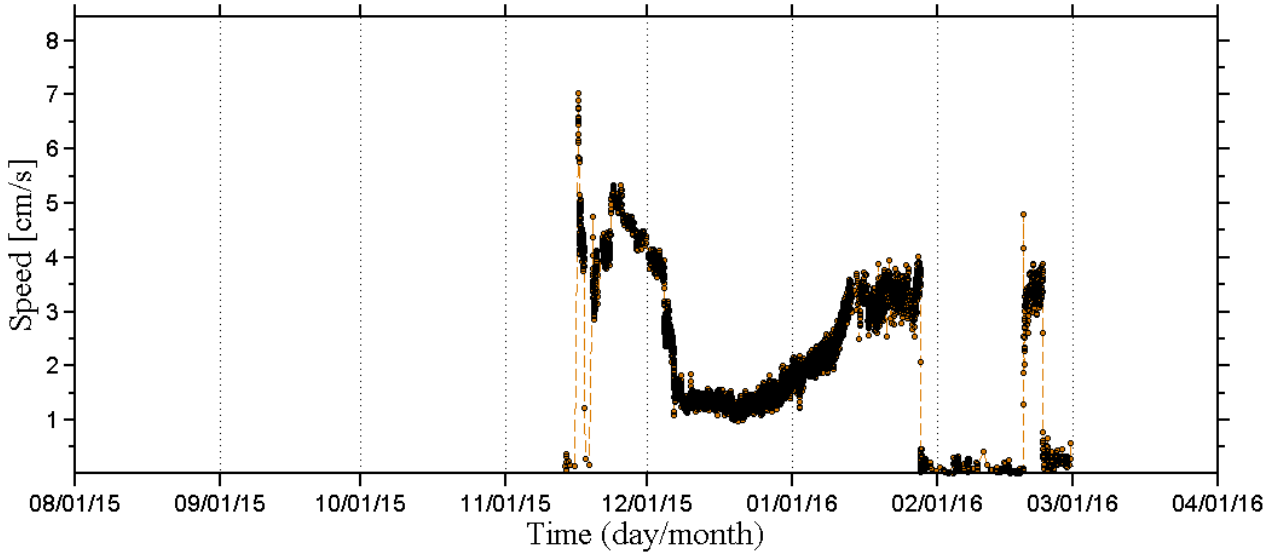

Figure C-6 Continuously sampled burst average ADV flow speed (cm/s) recorded at Z51_USGS R site during water year 2015 (8/1/2015 – 3/31/2016).

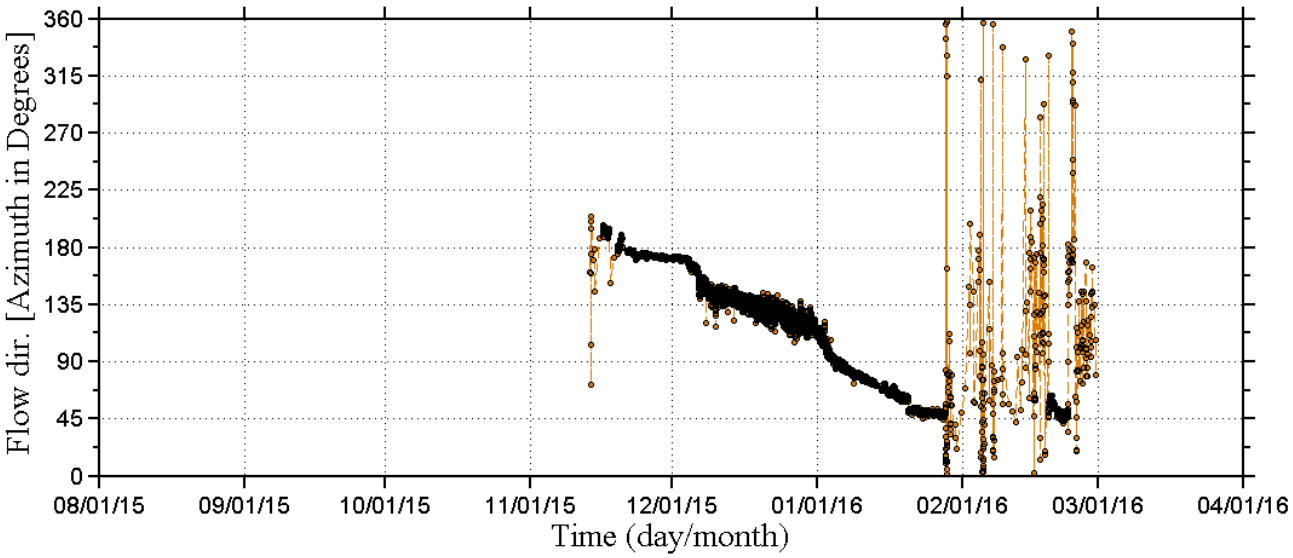

Figure C-7 Continuously sampled burst average ADV flow direction (clockwise degree from North) recorded at Z51_USGS R site during water year 2015 (8/1/2015 – 3/31/2016).

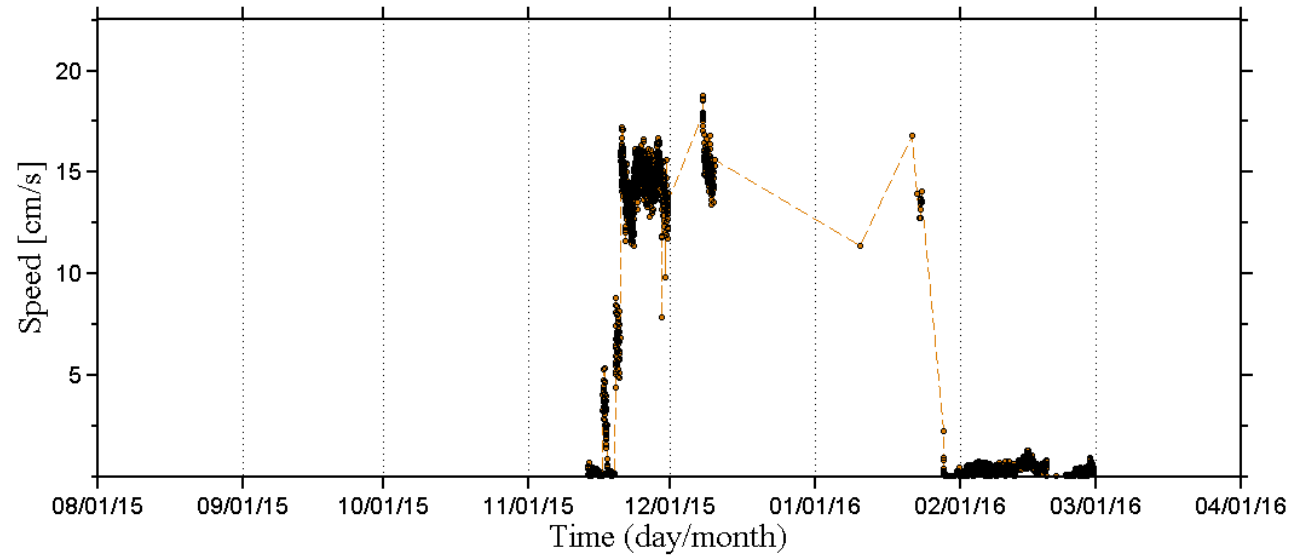

Figure C-8 Continuously sampled burst average ADV flow speed (cm/s) recorded at Z51_USGS S site during water year 2015 (8/1/2015 – 3/31/2016).

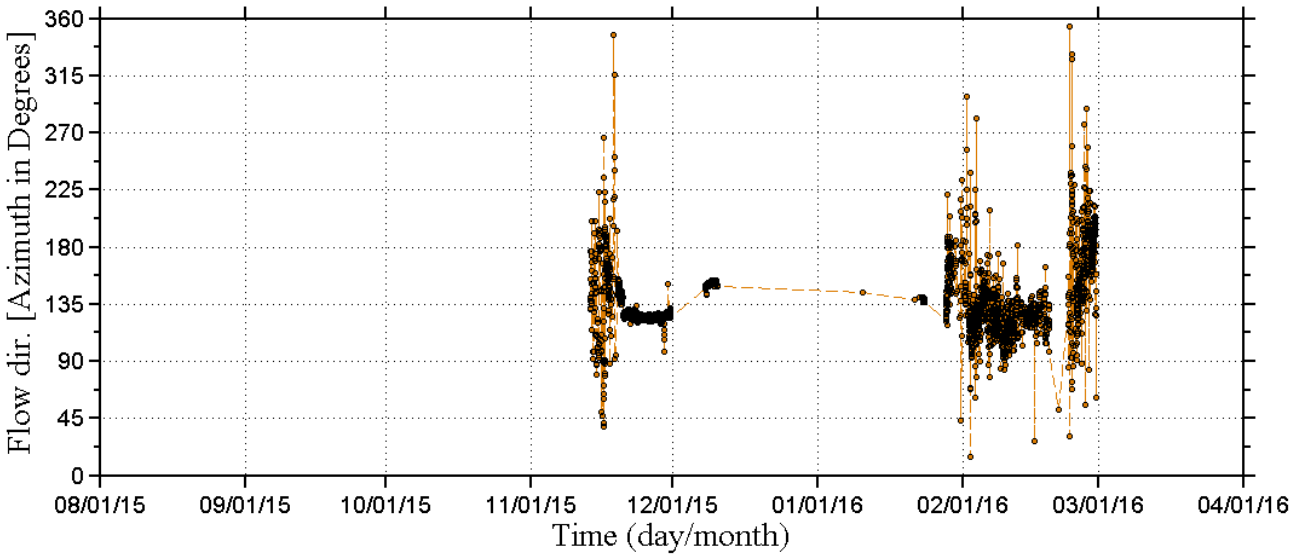

Figure C-9 Continuously sampled burst average ADV flow direction (clockwise degree from North) recorded at Z51_USGS S site during water year 2015 (8/1/2015 – 3/31/2016).

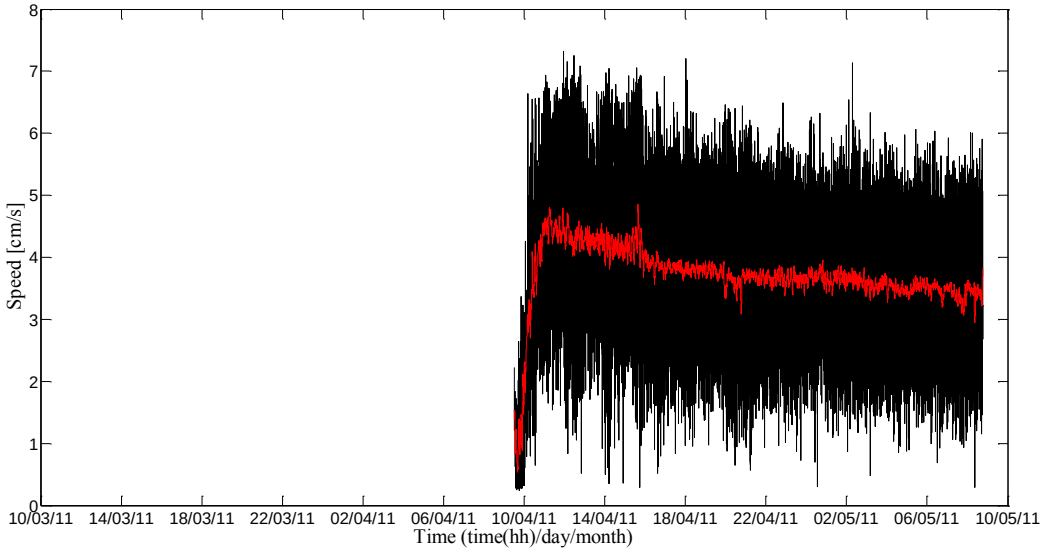

Figure C-10 Continuously sampled Vectrino flow speed (cm/s) recorded at RS1UR site during water year 2014 (11/3/2014 – 11/6/2014).

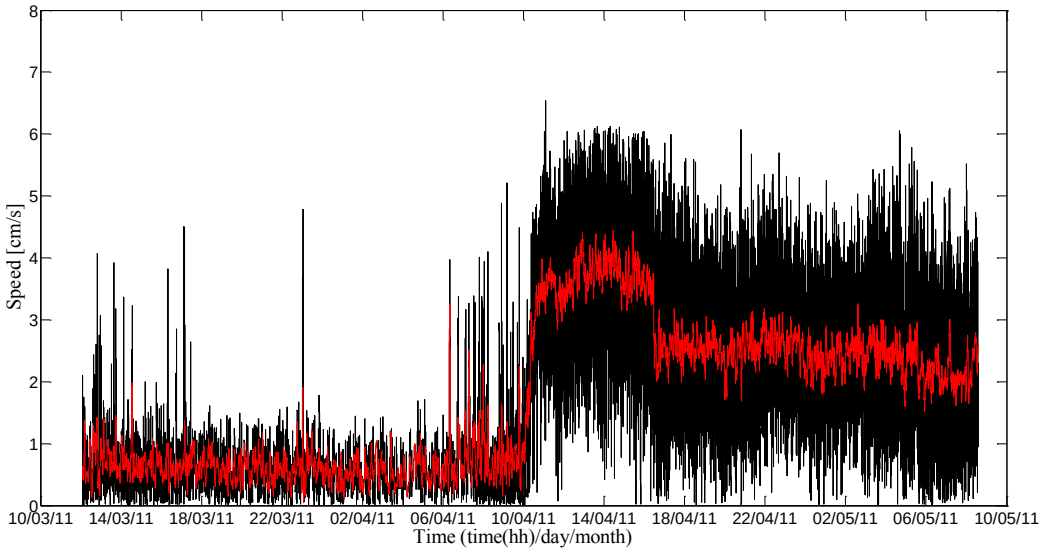

Figure C-11 Continuously sampled Vectrino flow speed (cm/s) recorded at RS1US site during water year 2014 (11/3/2014 – 11/6/2014).

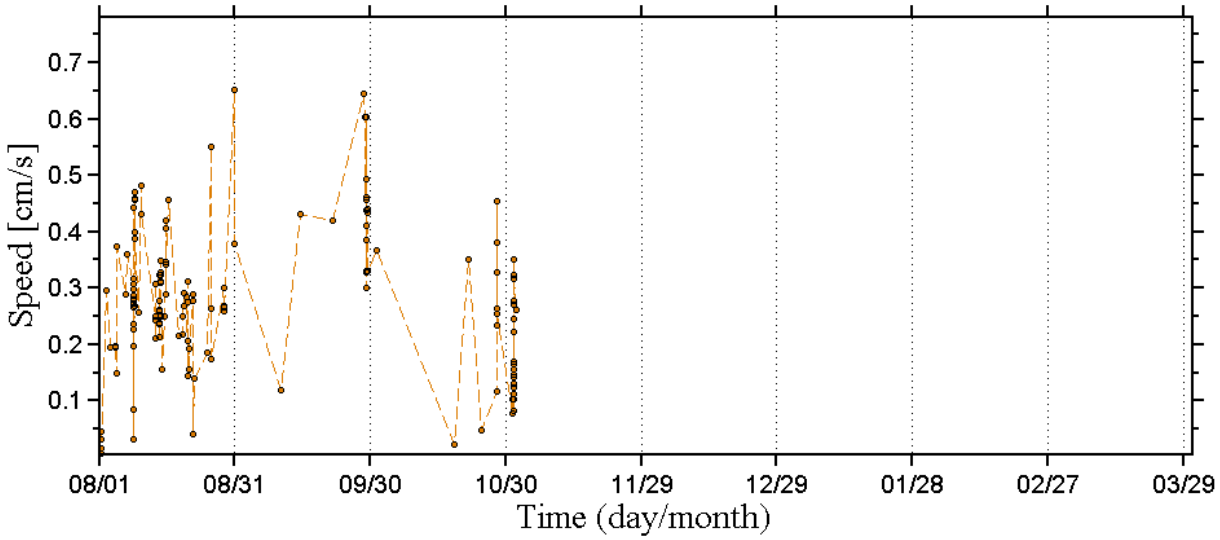

Figure C-12 Continuously sampled burst average ADV flow speed (cm/s) recorded at RS1DR site during water year 2010 (8/1/2010 – 3/31/2011).

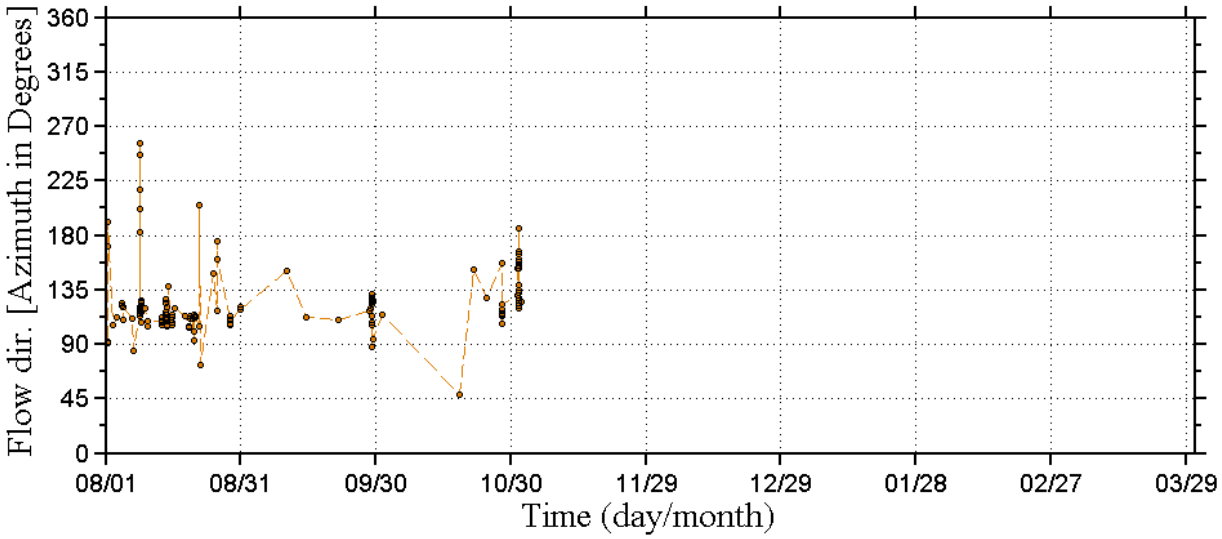

Figure C-13 Continuously sampled burst average ADV flow direction (clockwise degree from North) recorded at RS1DR site during water year 2010 (8/1/2010 – 3/31/2011).

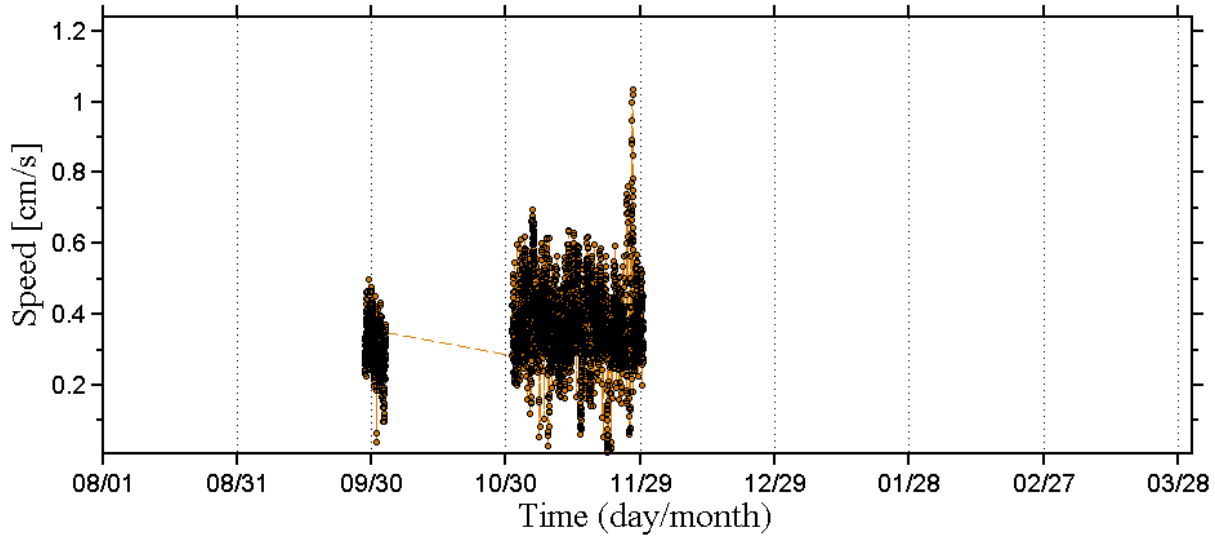

Figure C-14 Continuously sampled burst average ADV flow speed (cm/s) recorded at RS1DR site during water year 2011 (8/1/2011 – 3/31/2012).

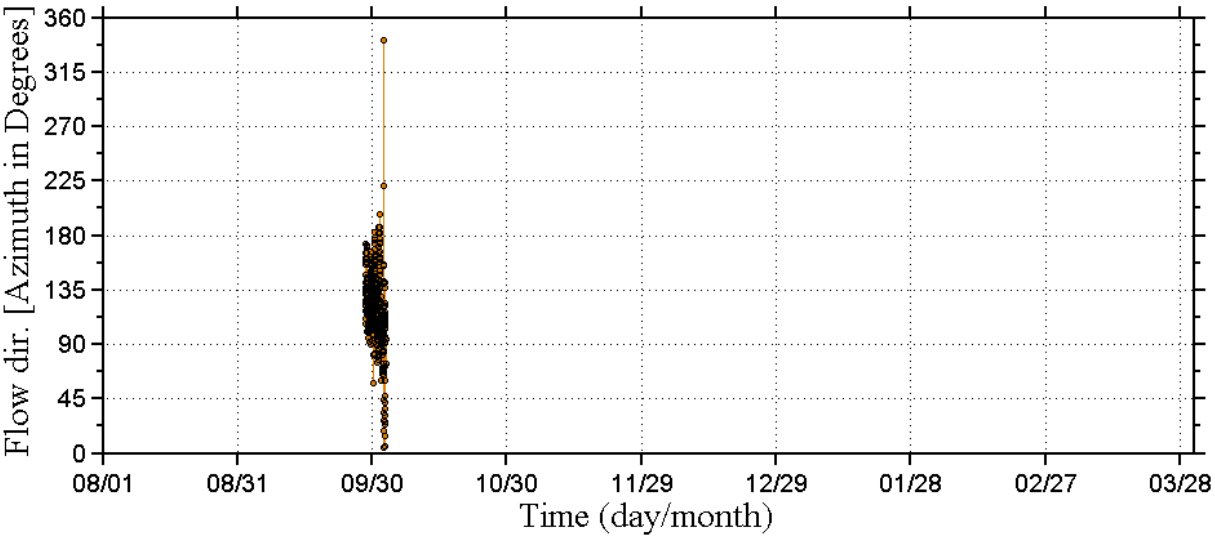

Figure C-15. Continuously sampled burst average ADV flow direction (clockwise degree from North) recorded at RS1DR site during water year 2011 (8/1/2011 – 3/31/2012).

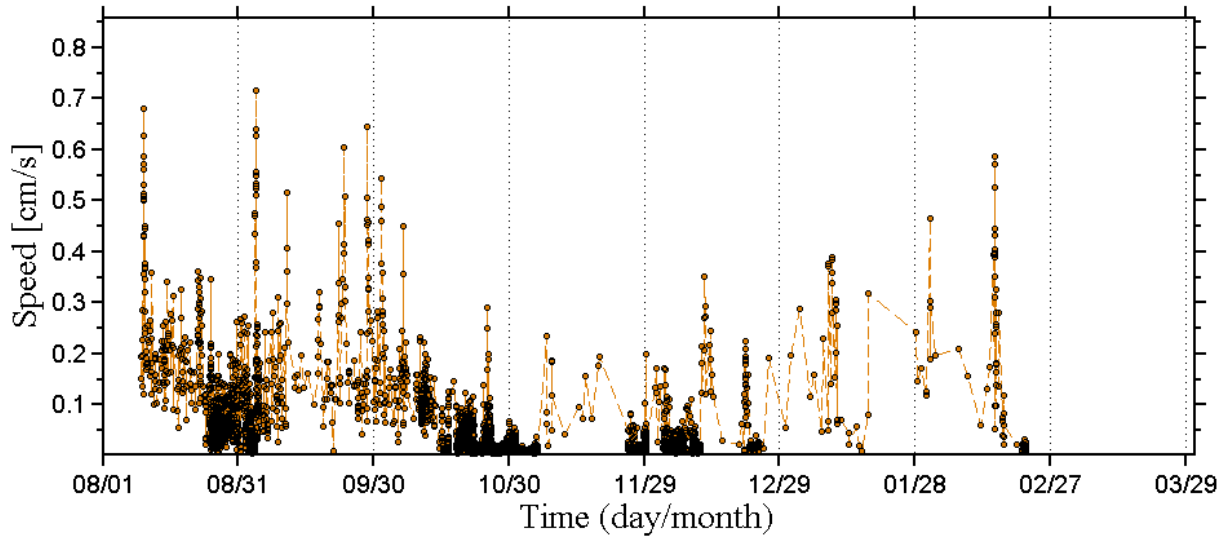

Figure C-16 Continuously sampled burst average ADV flow speed (cm/s) recorded at RS1DR site during water year 2012 (8/1/2012 – 3/31/2013).

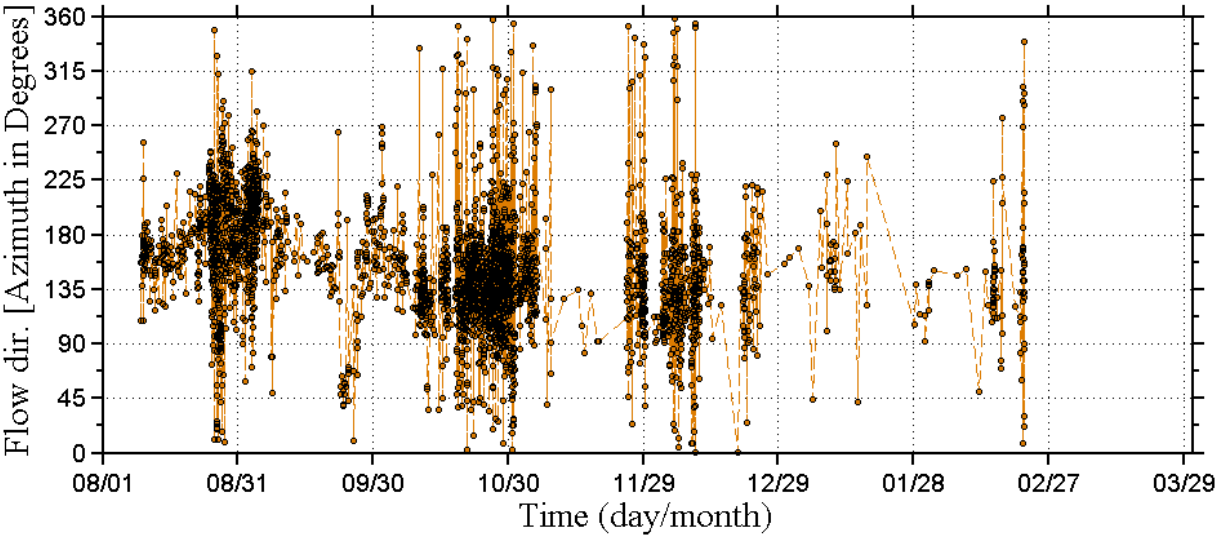

Figure C-17 Continuously sampled burst average ADV flow direction (clockwise degree from North) recorded at RS1DR site during water year 2012 (8/1/2012 – 3/31/2013).

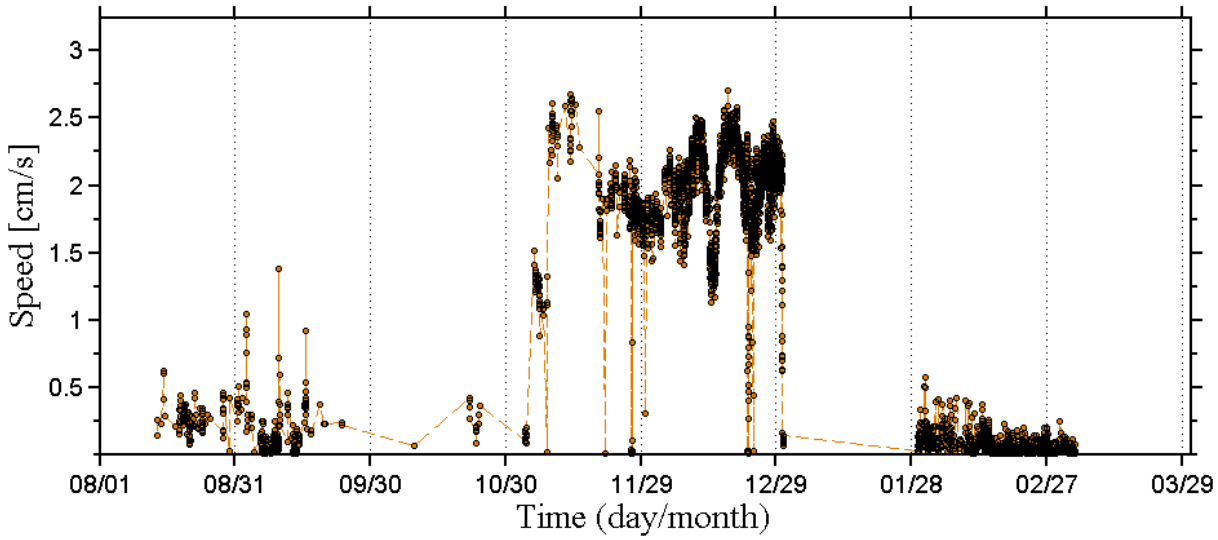

Figure C-18 Continuously sampled burst average ADV flow speed (cm/s) recorded at RS1DR site during water year 2013 (8/1/2013 – 3/31/2014).

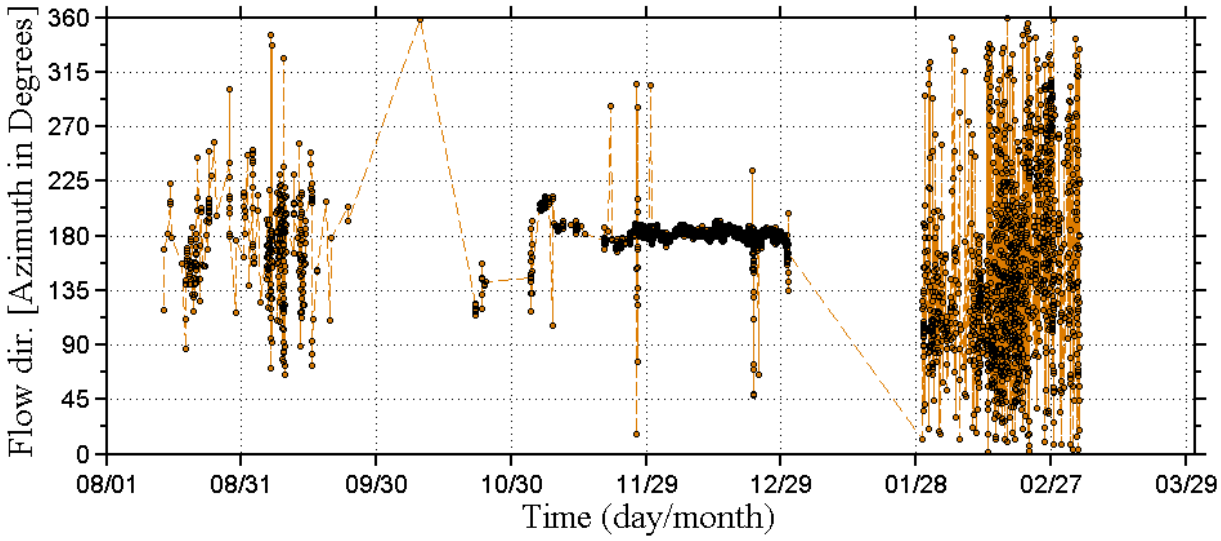

Figure C-19 Continuously sampled burst average ADV flow direction (clockwise degree from North) recorded at RS1DR site during water year 2013 (8/1/2013 – 3/31/2014).

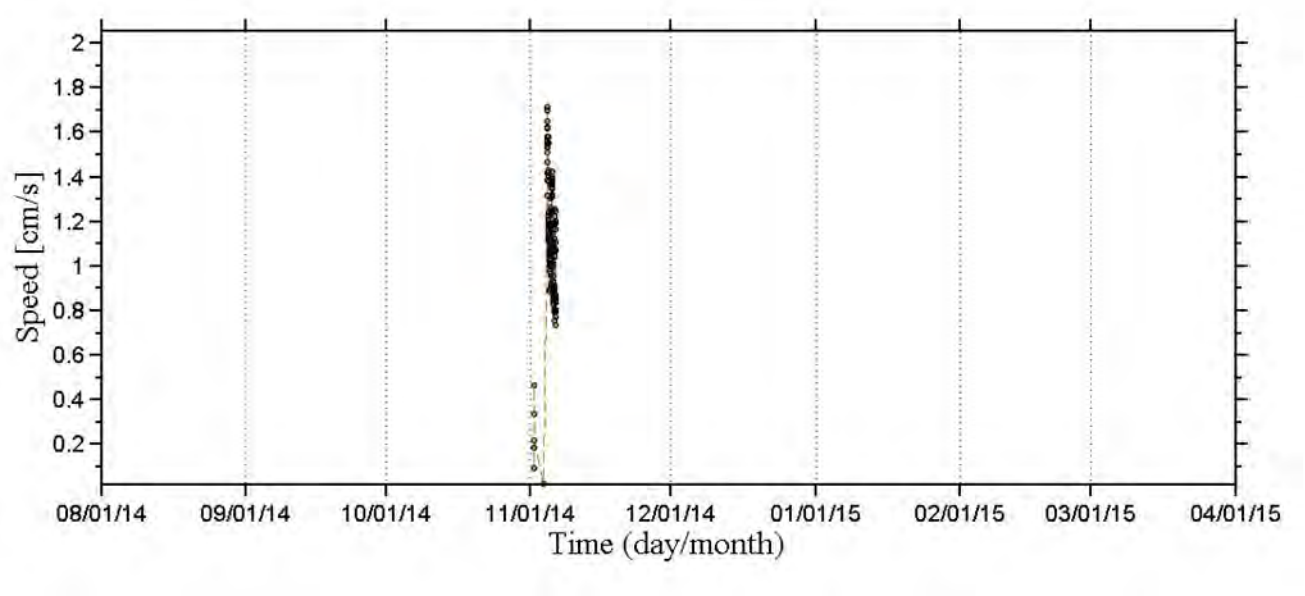

Figure C-20 Continuously sampled burst average ADV flow speed (cm/s) recorded at RS1DR site during water year 2014 (8/1/2014 – 3/31/2015).

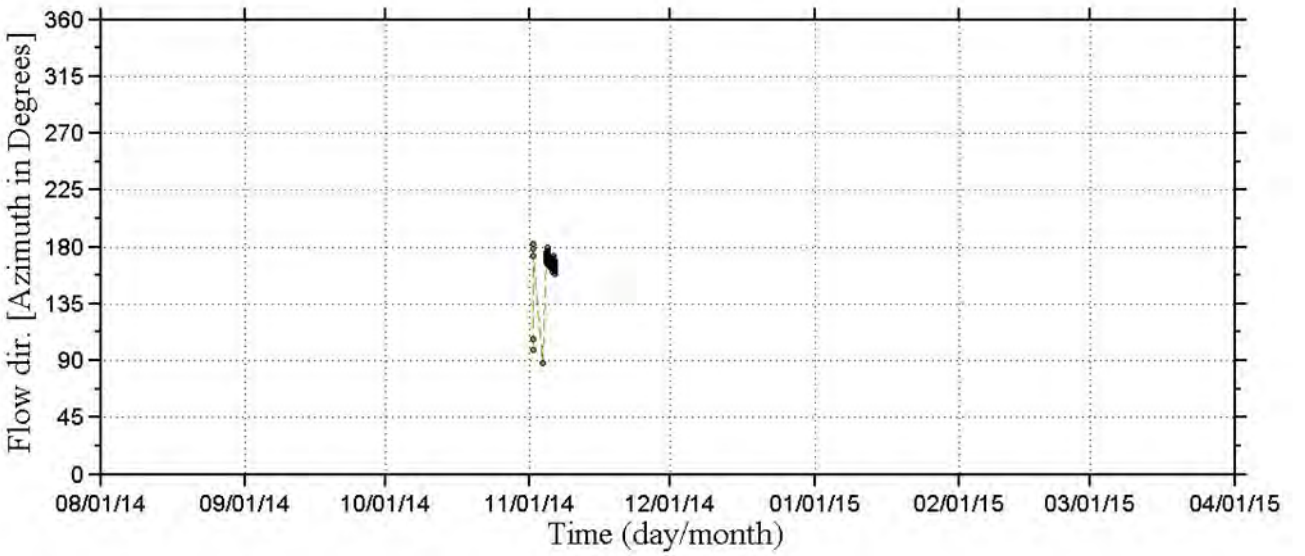

Figure C-21 Continuously sampled burst average ADV flow direction (clockwise degree from North) recorded at RS1DR site during water year 2014 (8/1/2014 – 3/31/2015).

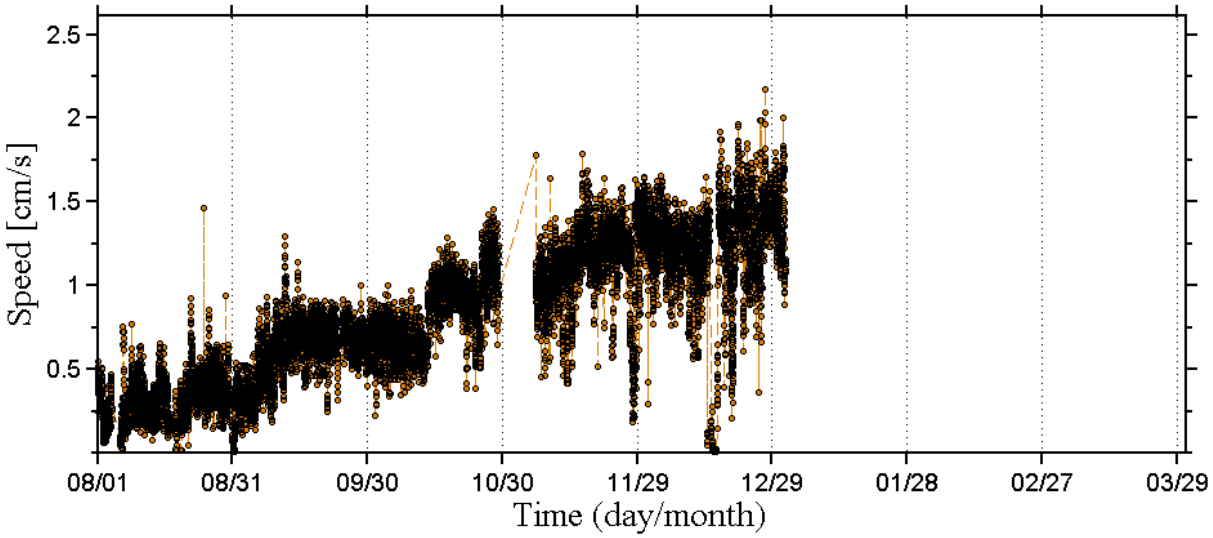

Figure C-22 Continuously sampled burst average ADV flow speed (cm/s) recorded at RS1DS site during water year 2010 (8/1/2010 – 3/31/2011).

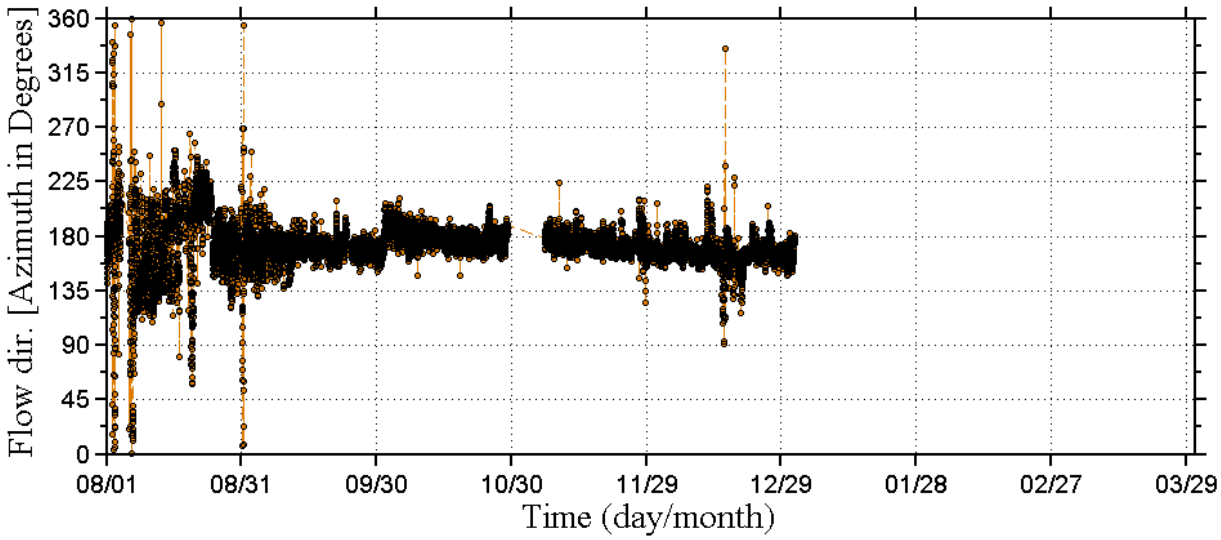

Figure C-23 Continuously sampled burst average ADV flow direction (clockwise degree from North) recorded at RS1DS site during water year 2010 (8/1/2010 – 3/31/2011).

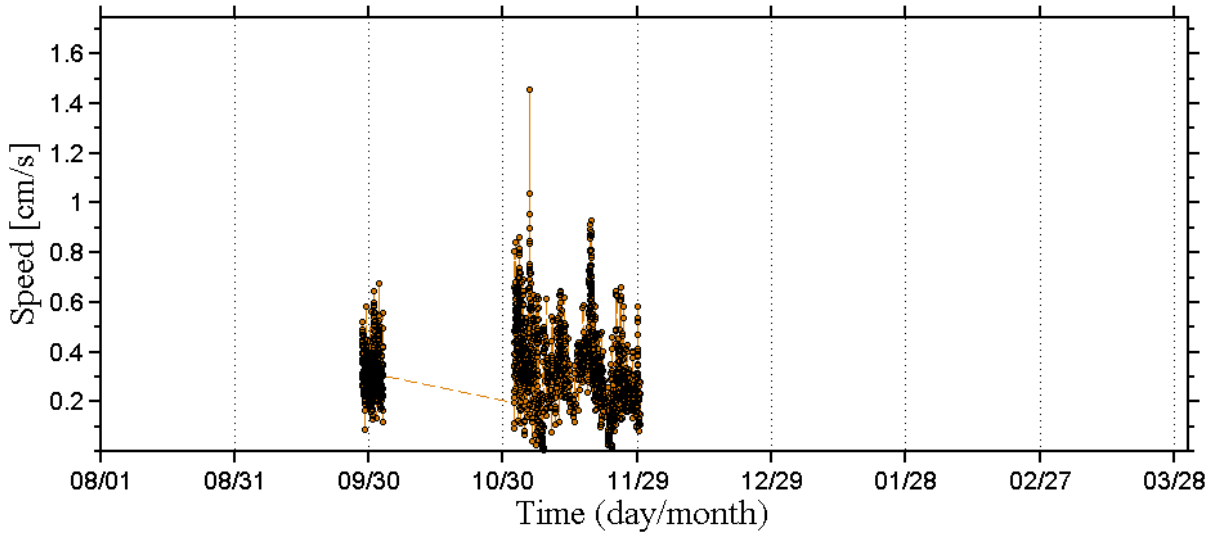

Figure C-24 Continuously sampled burst average ADV flow speed (cm/s) recorded at RS1DS site during water year 2011 (8/1/2011 – 3/31/2012).

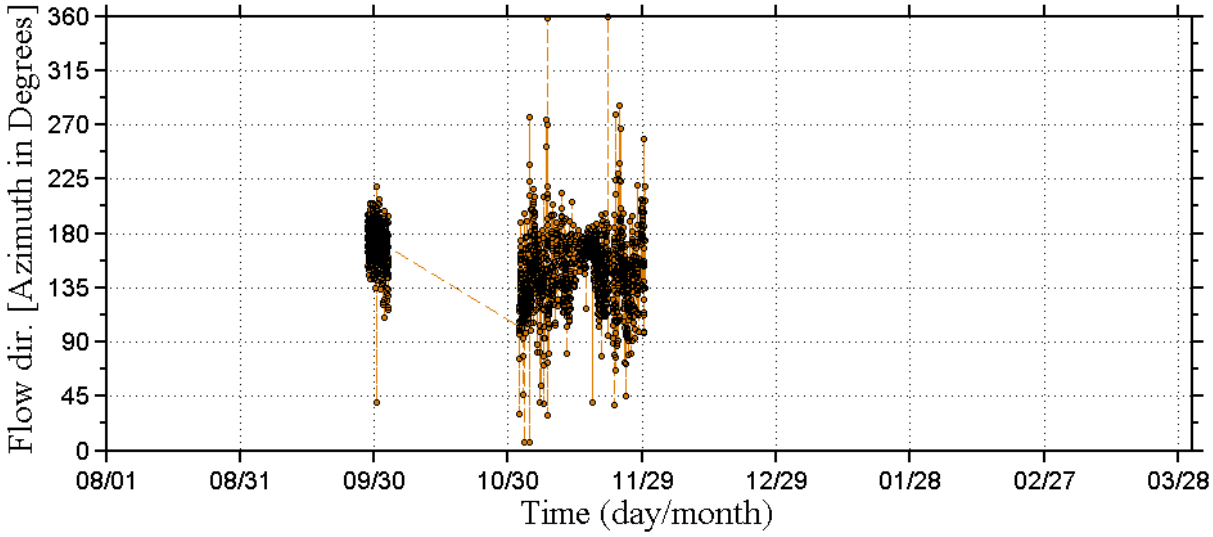

Figure C-25 Continuously sampled burst average ADV flow direction (clockwise degree from North) recorded at RS1DS site during water year 2011 (8/1/2011 – 3/31/2012).

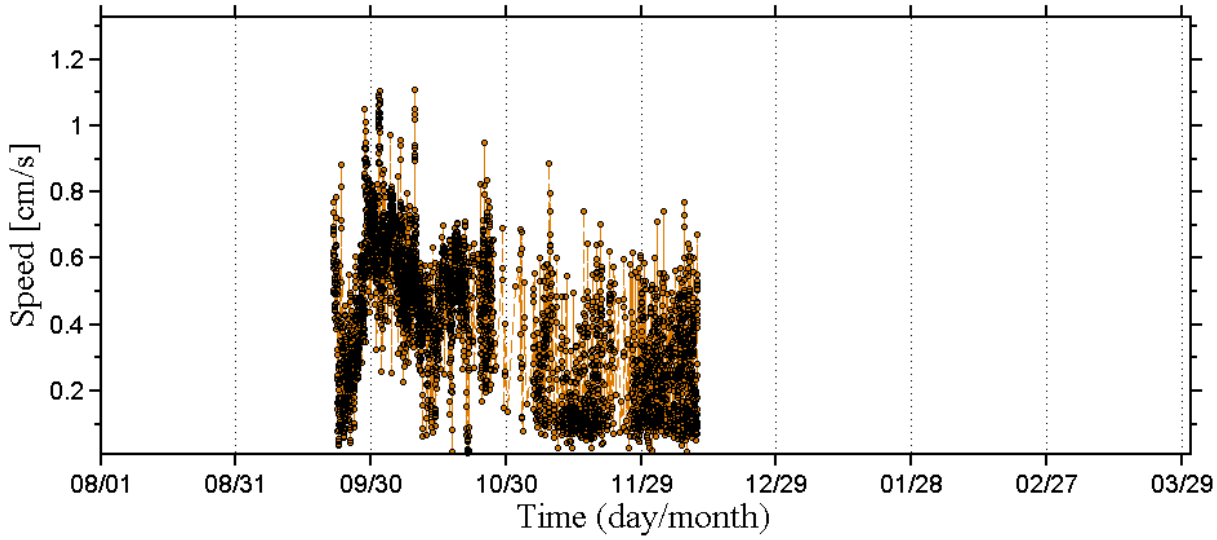

Figure C-26 Continuously sampled burst average ADV flow speed (cm/s) recorded at RS1DS site during water year 2012 (8/1/2012 – 3/31/2013).

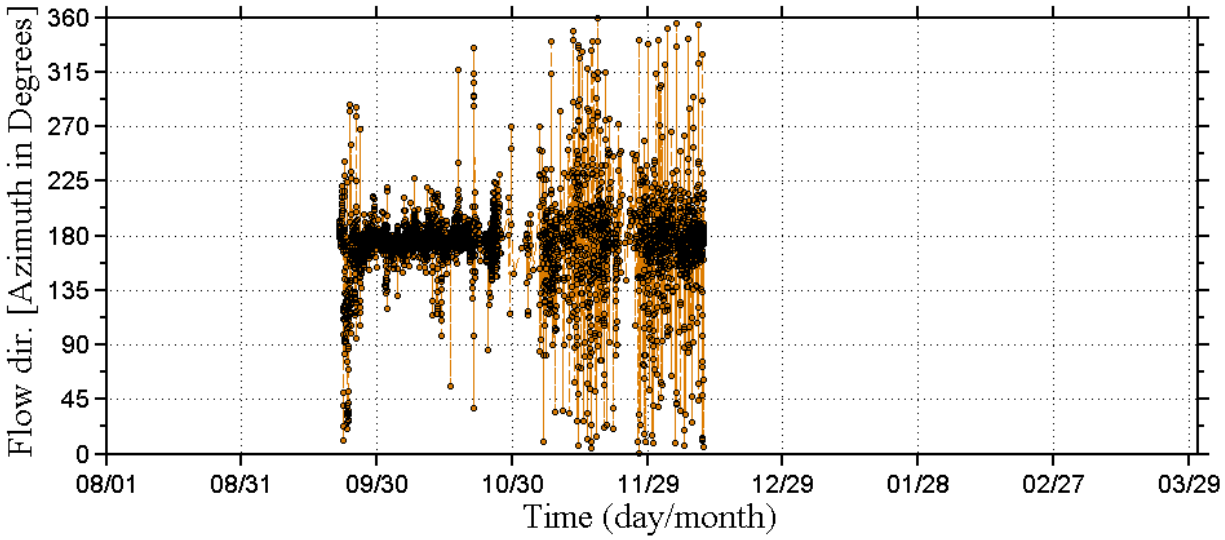

Figure C-27 Continuously sampled burst average ADV flow direction (clockwise degree from North) recorded at RS1DS site during water year 2012 (8/1/2012 – 3/31/2013).

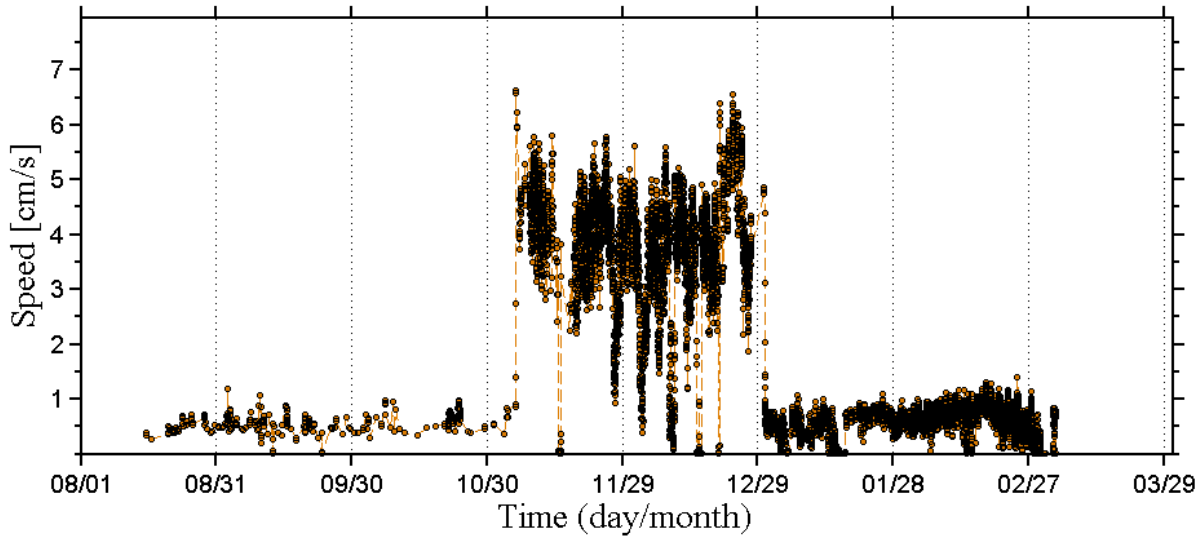

Figure C-28 Continuously sampled burst average ADV flow speed (cm/s) recorded at RS1DS site during water year 2013 (8/1/2013 – 3/31/2014).

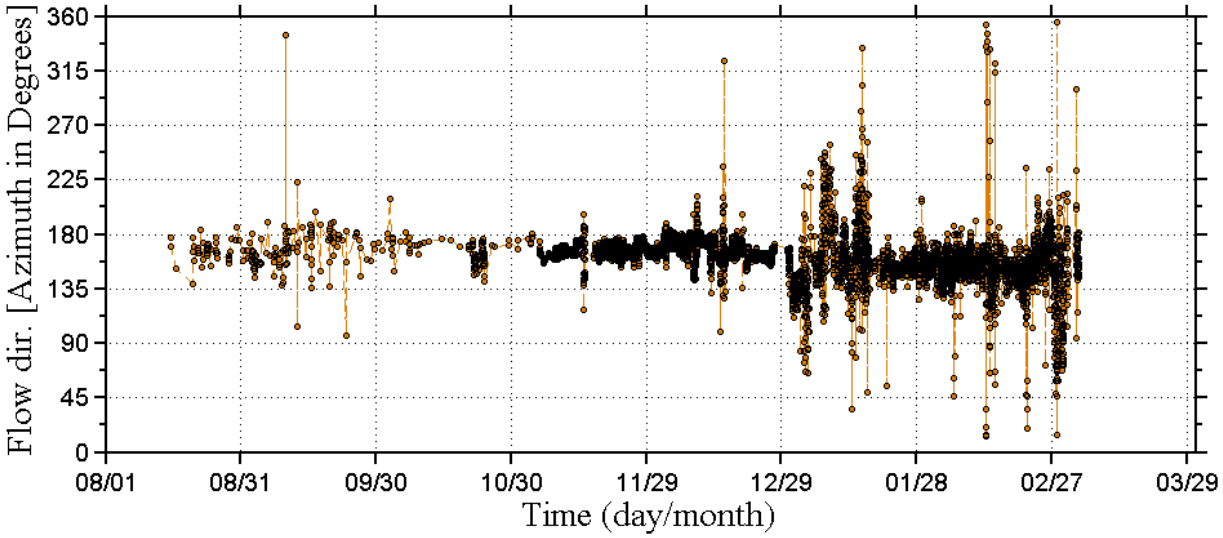

Figure C-29 Continuously sampled burst average ADV flow direction (clockwise degree from North) recorded at RS1DS site during water year 2013 (8/1/2013 – 3/31/2014).

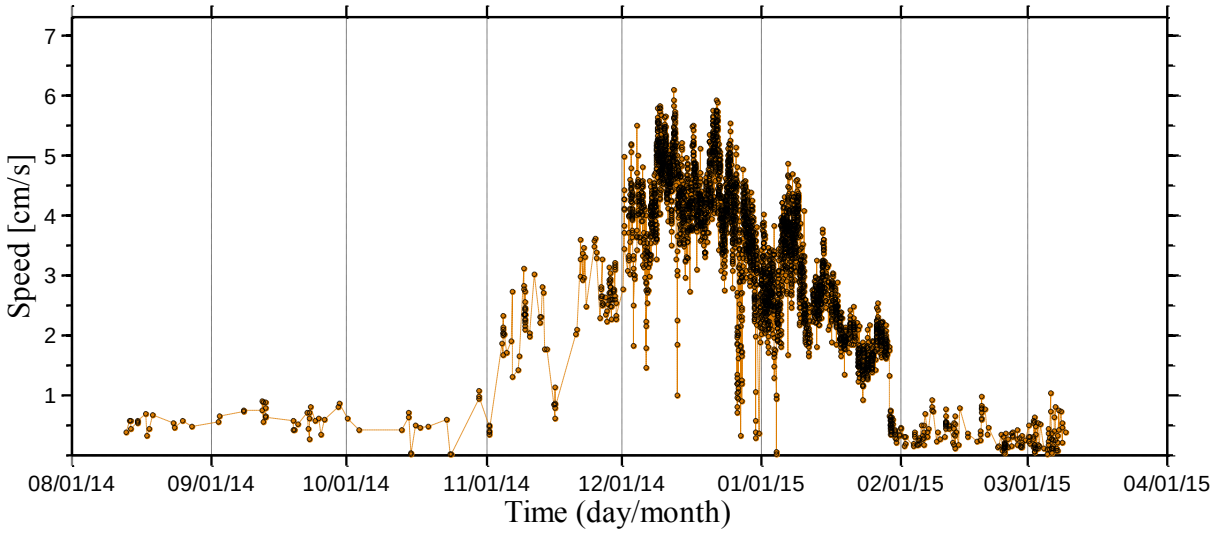

Figure C-30 Continuously sampled burst average ADV flow speed (cm/s) recorded at RS1DS site during water year 2014 (8/1/2014 – 3/31/2015).

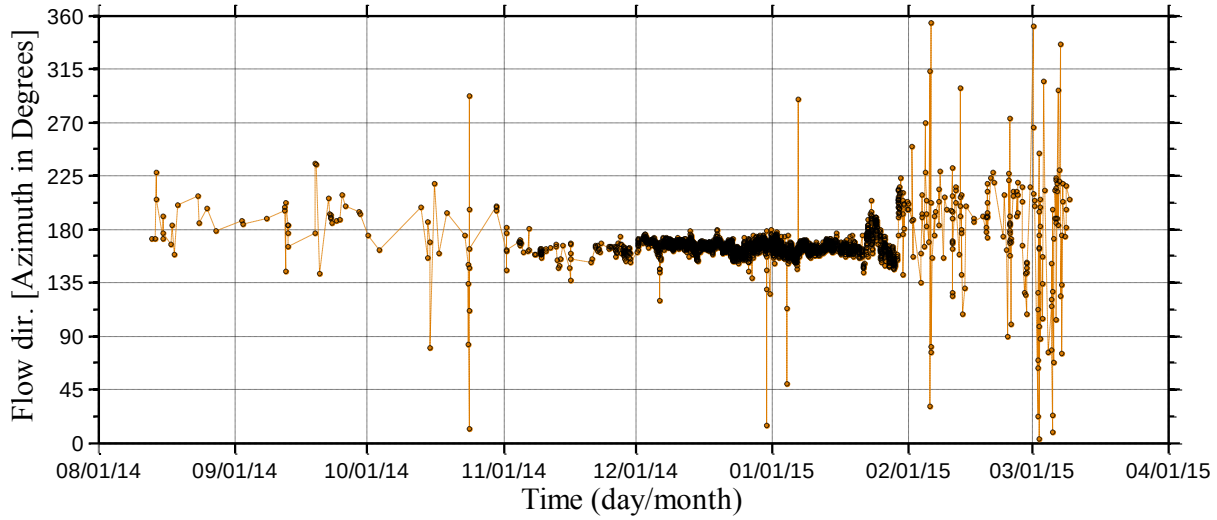

Figure C-31 Continuously sampled burst average ADV flow direction (clockwise degree from North) recorded at RS1DS site during water year 2014 (8/1/2014 – 3/31/2015).

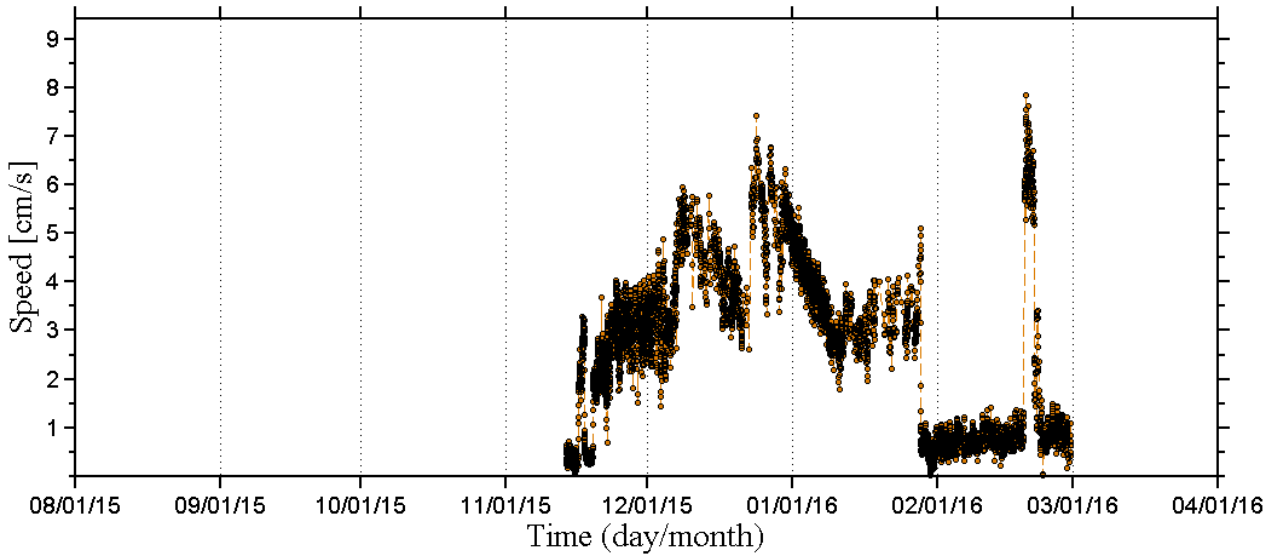

Figure C-32 Continuously sampled burst average ADV flow speed (cm/s) recorded at RS1DS site during water year 2015 (8/1/2015 – 3/31/2016).

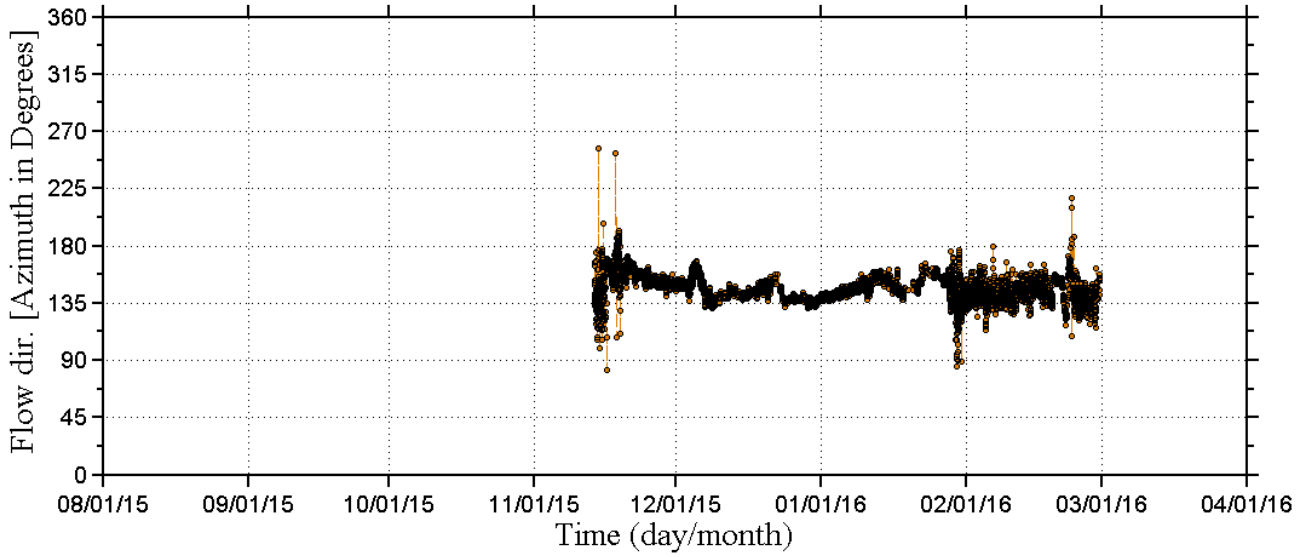

Figure C-33 Continuously sampled burst average ADV flow direction (clockwise degree from North) recorded at RS1DS site during water year 2015 (8/1/2015 – 3/31/2016).

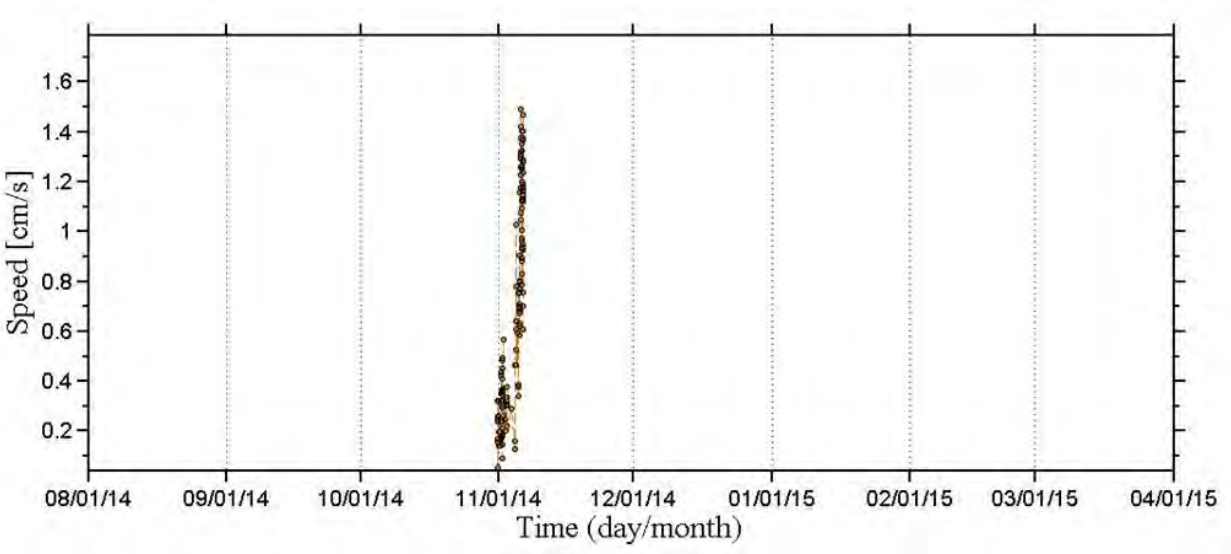

Figure C-34 Continuously sampled burst average ADV flow speed (cm/s) recorded at RS2R site during water year 2014 (8/1/2014 – 3/31/2015).

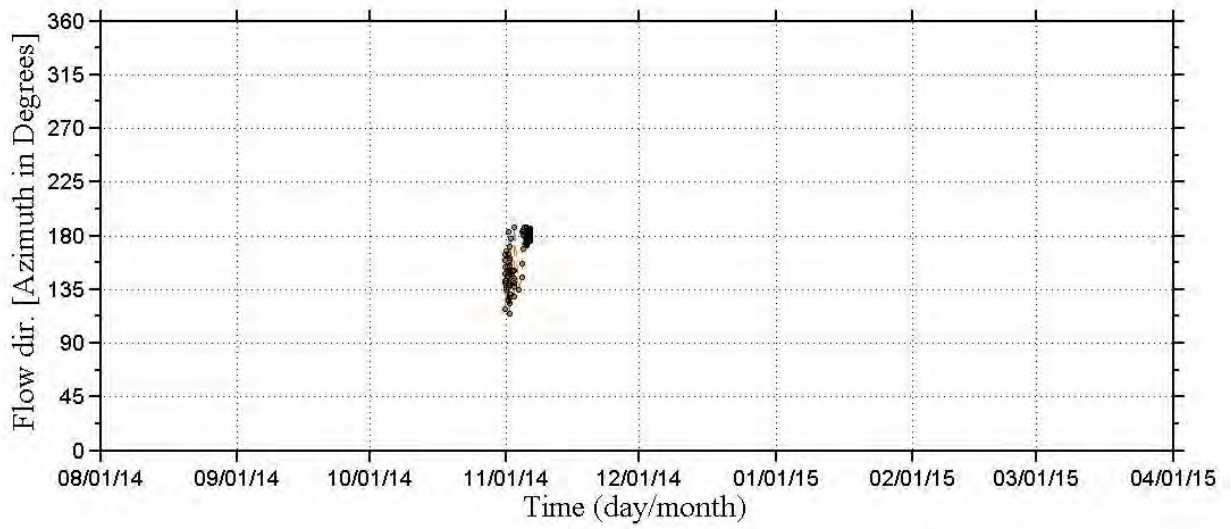

Figure C-35 Continuously sampled burst average ADV flow direction (clockwise degree from North) recorded at RS2R site during water year 2014 (8/1/2014 – 3/31/2015).

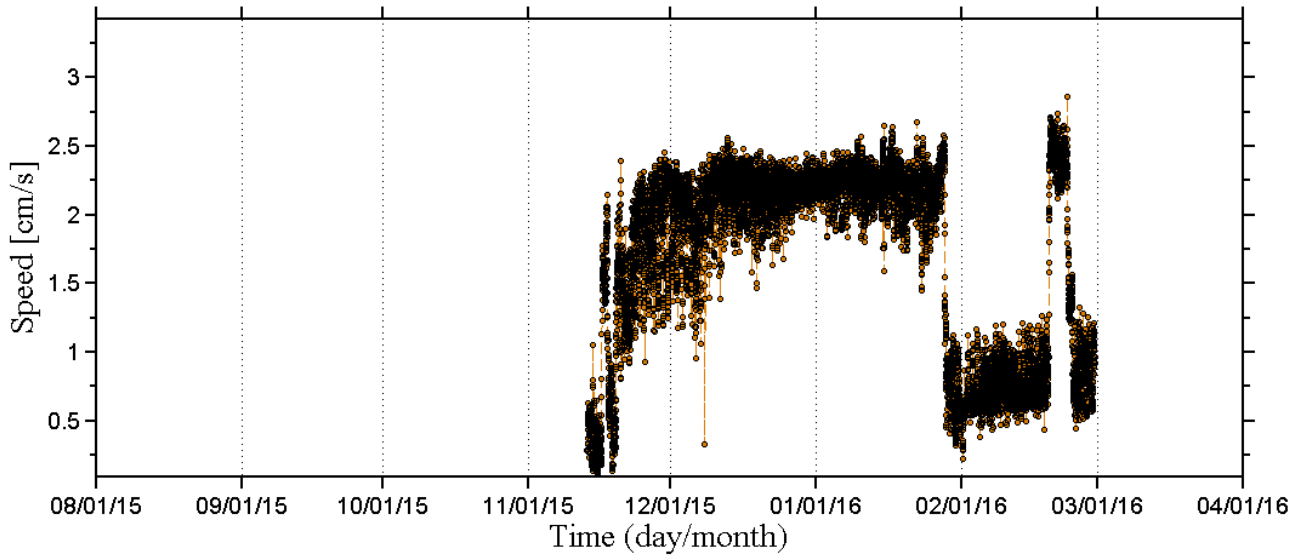

Figure C-36 Continuously sampled burst average ADV flow speed (cm/s) recorded at RS2R site during water year 2015 (8/1/2015 – 3/31/2016).

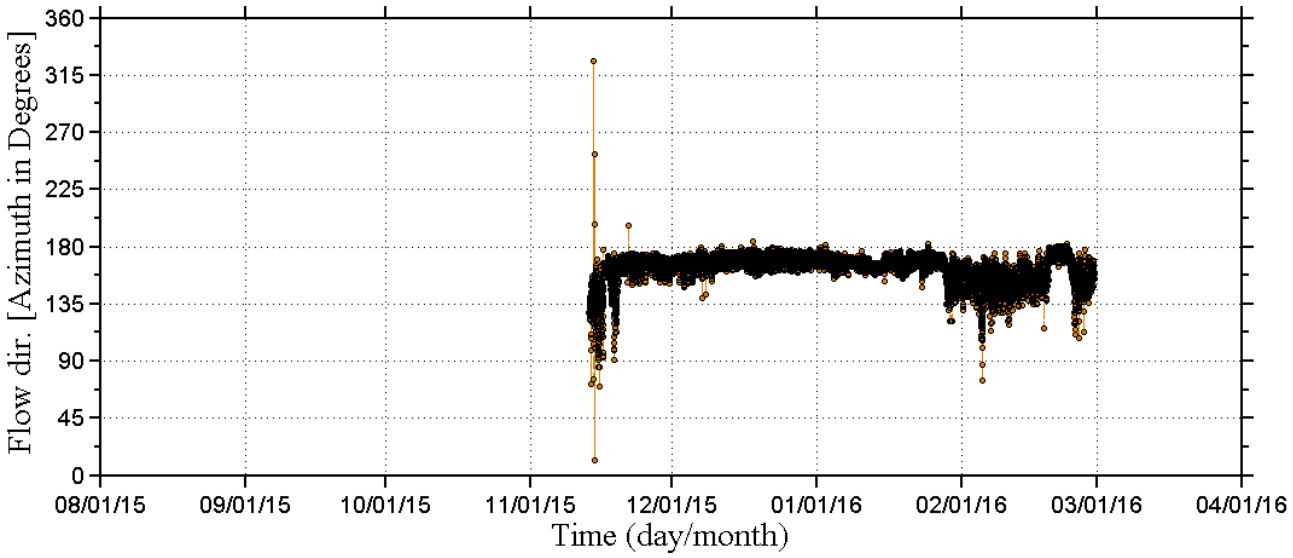

Figure C-37 Continuously sampled burst average ADV flow direction (clockwise degree from North) recorded at RS2R site during water year 2015 (8/1/2015 – 3/31/2016).

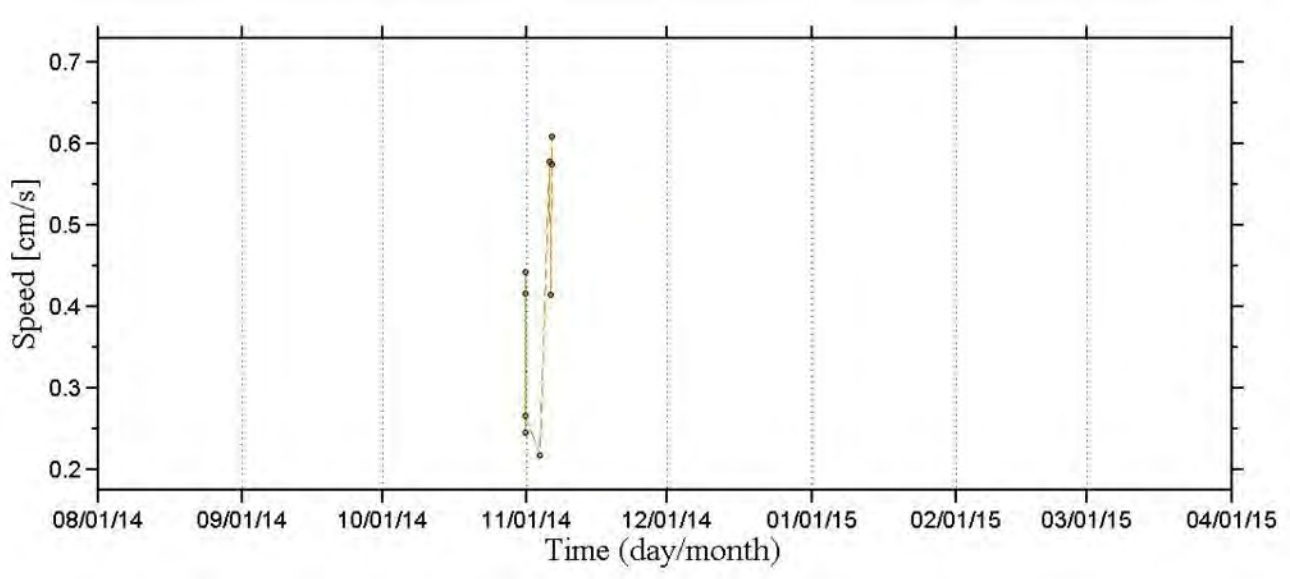

Figure C-38 Continuously sampled burst average ADV flow speed (cm/s) recorded at RS2S site during water year 2014 (8/1/2014 – 3/31/2015).

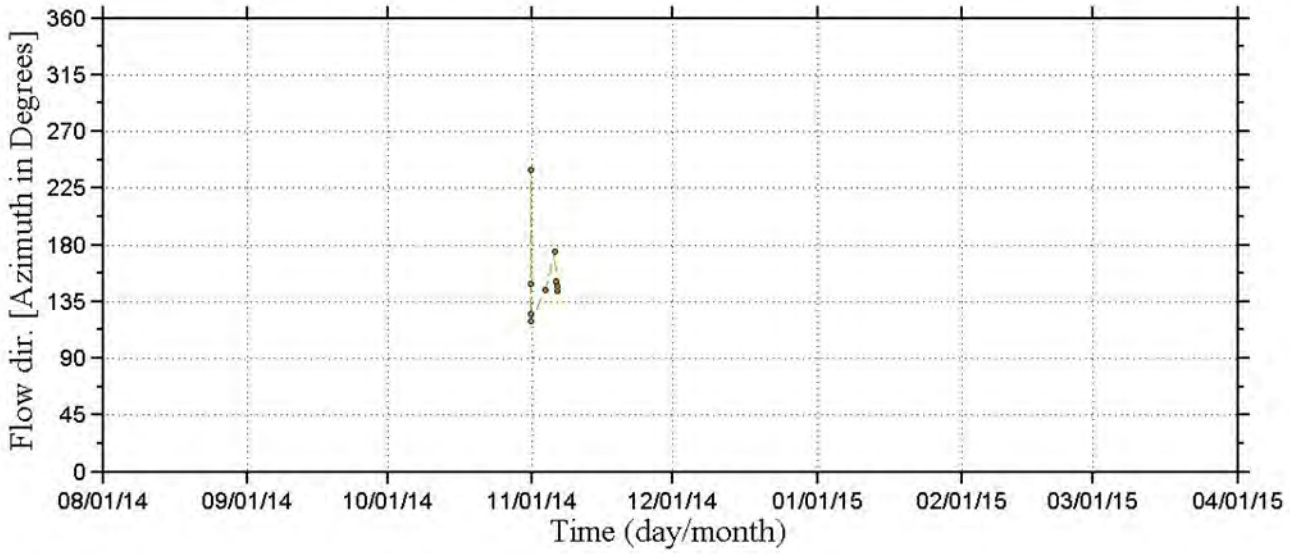

Figure C-39 Continuously sampled burst average ADV flow direction (clockwise degree from North) recorded at RS2S site during water year 2014 (8/1/2014 – 3/31/2015).

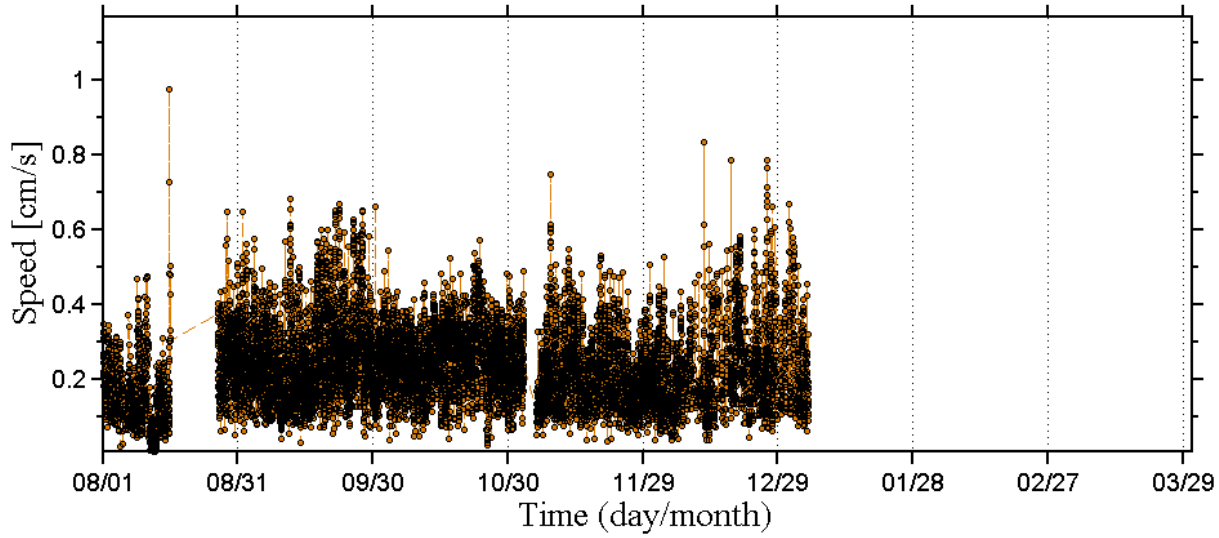

Figure C-40 Continuously sampled burst average ADV flow speed (cm/s) recorded at S1 site during water year 2010 (8/1/2010 – 3/31/2011).

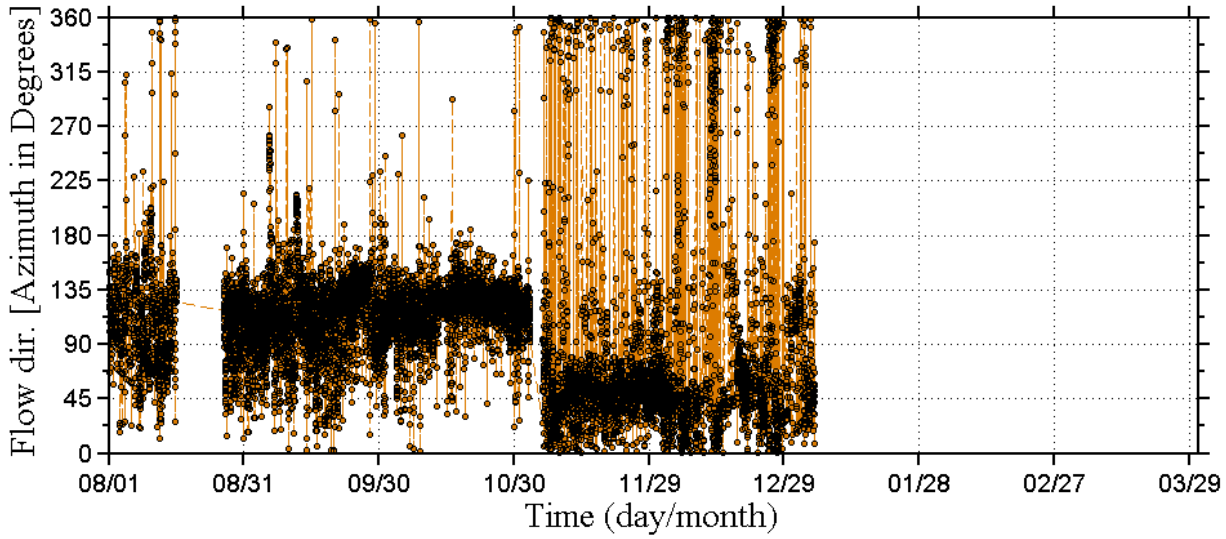

Figure C-41 Continuously sampled burst average ADV flow direction (clockwise degree from North) recorded at S1 site during water year 2010 (8/1/2010 – 3/31/2011).

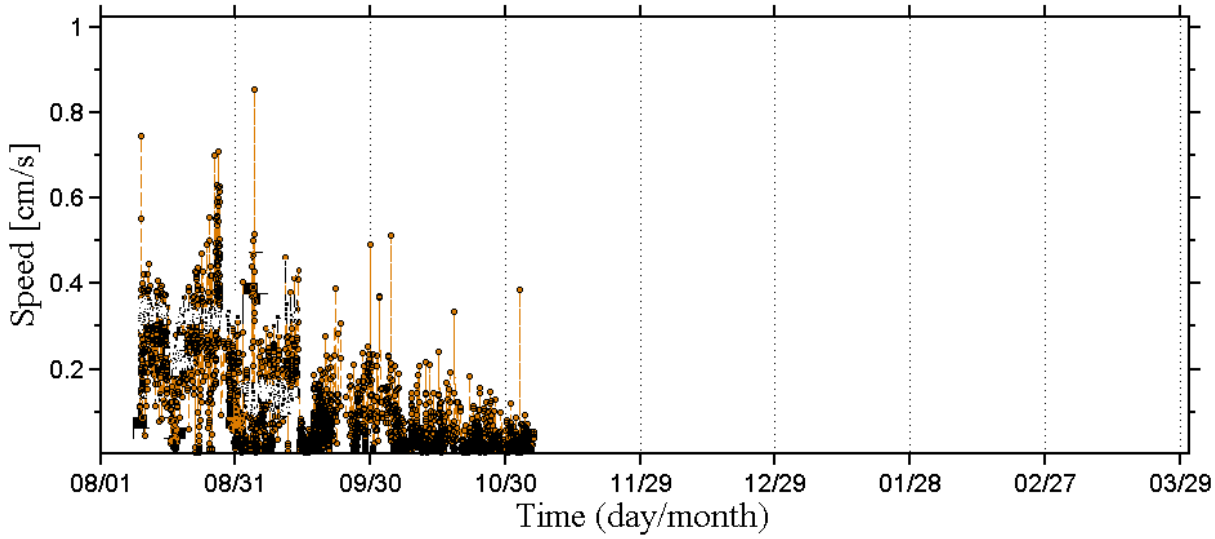

Figure C-42 Continuously sampled burst average ADV flow speed (cm/s) recorded at S1 site during water year 2012 (8/1/2012 – 3/31/2013).

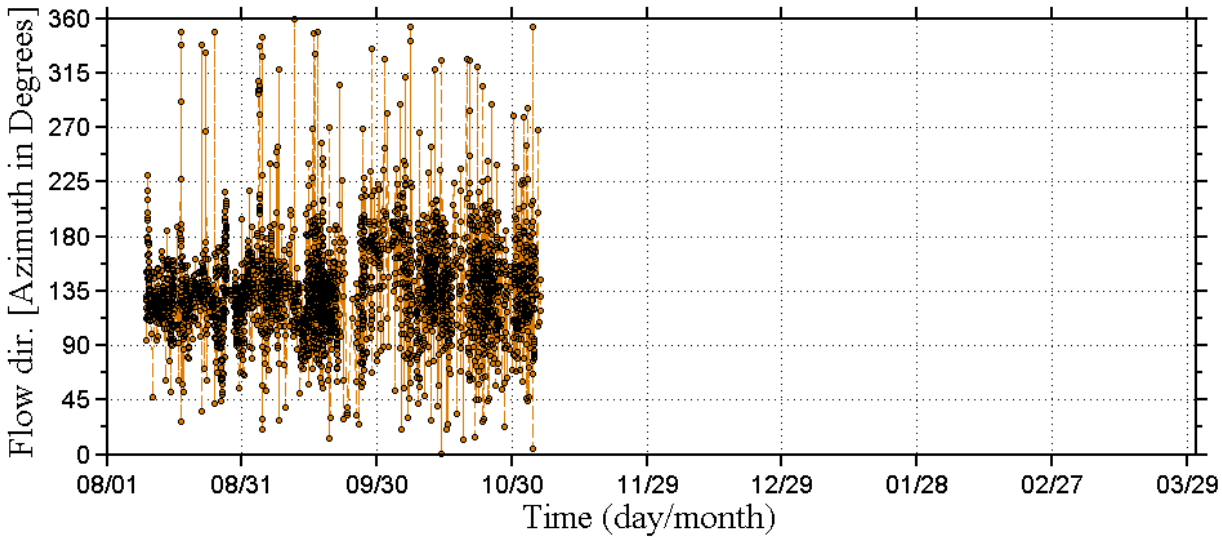

Figure C-43 Continuously sampled burst average ADV flow direction (clockwise degree from North) recorded at S1 site during water year 2012 (8/1/2012 – 3/31/2013).

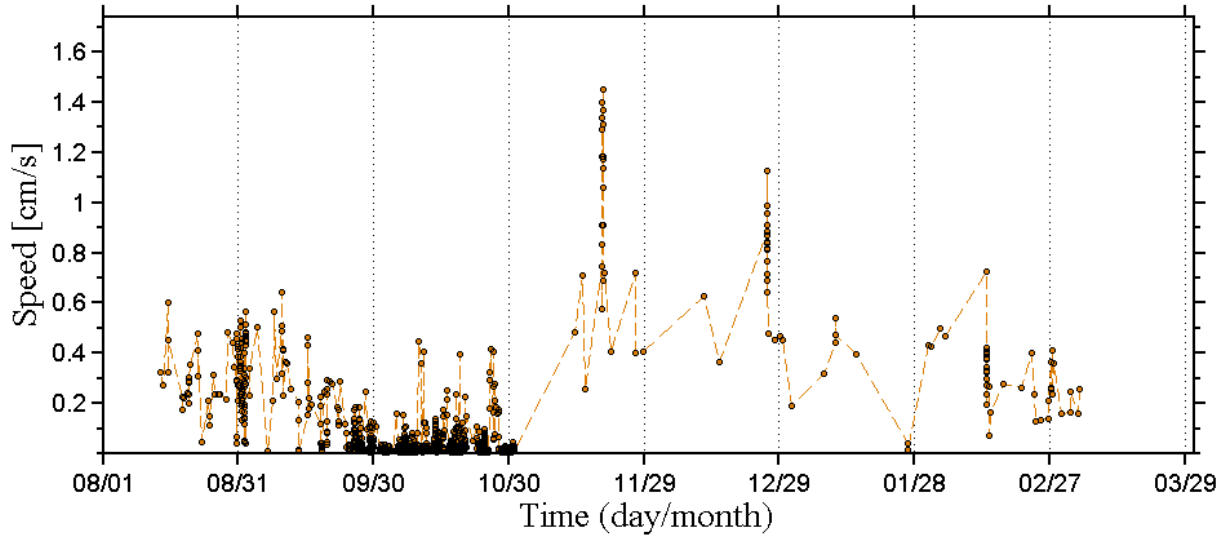

Figure C-44 Continuously sampled burst average ADV flow speed (cm/s) recorded at S1 site during water year 2013 (8/1/2013 – 3/31/2014).

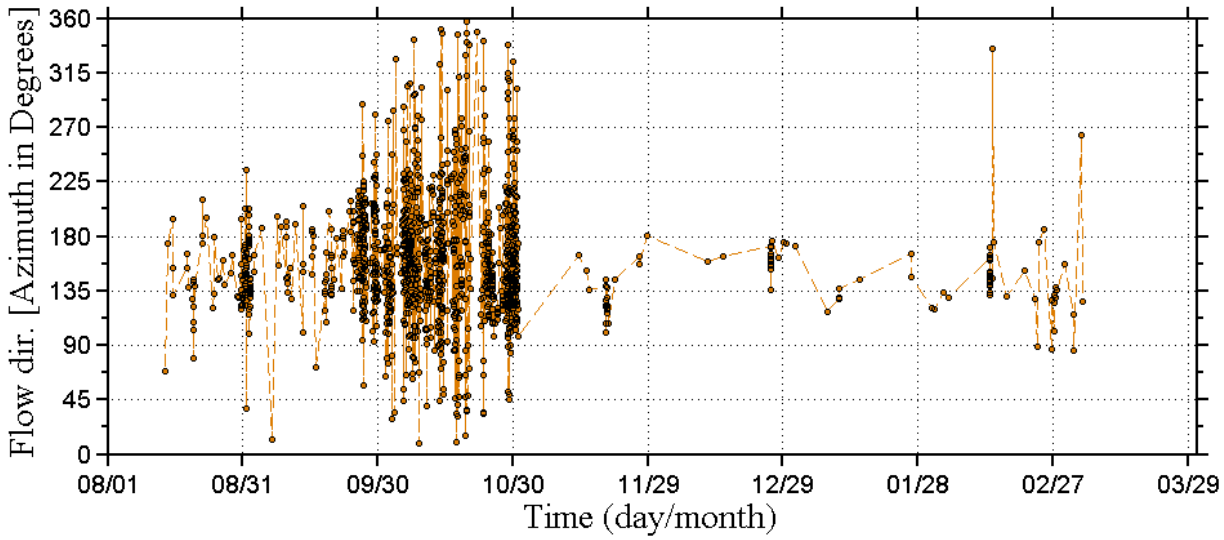

Figure C-45 Continuously sampled burst average ADV flow direction (clockwise degree from North) recorded at S1 site during water year 2013 (8/1/2013 – 3/31/2014).

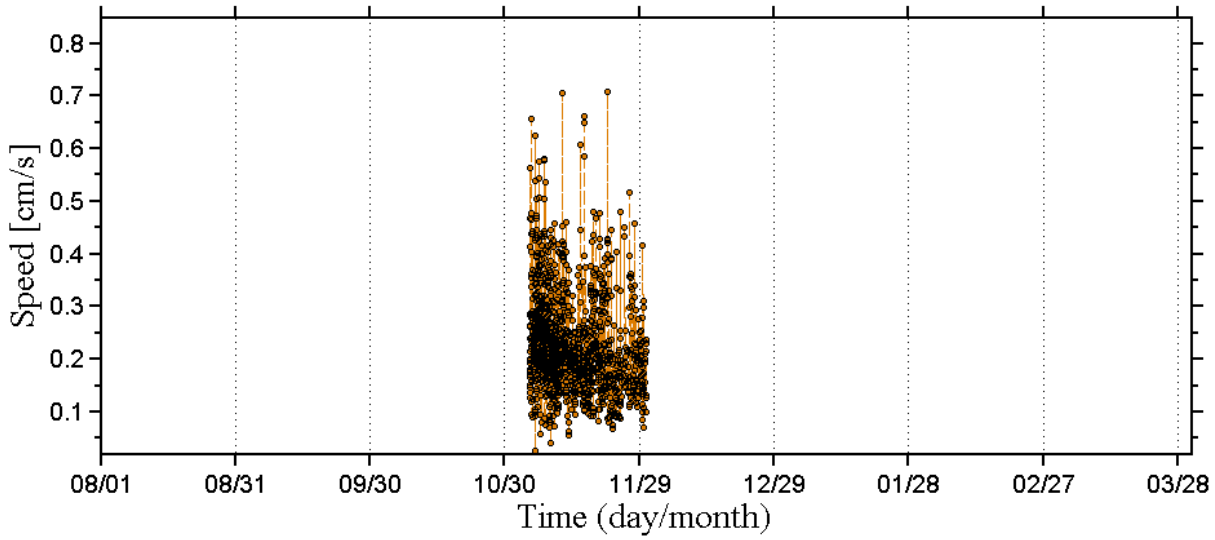

Figure C-46 Continuously sampled burst average ADV flow speed (cm/s) recorded at UB1 site during water year 2011 (8/1/2011 – 3/31/2012).

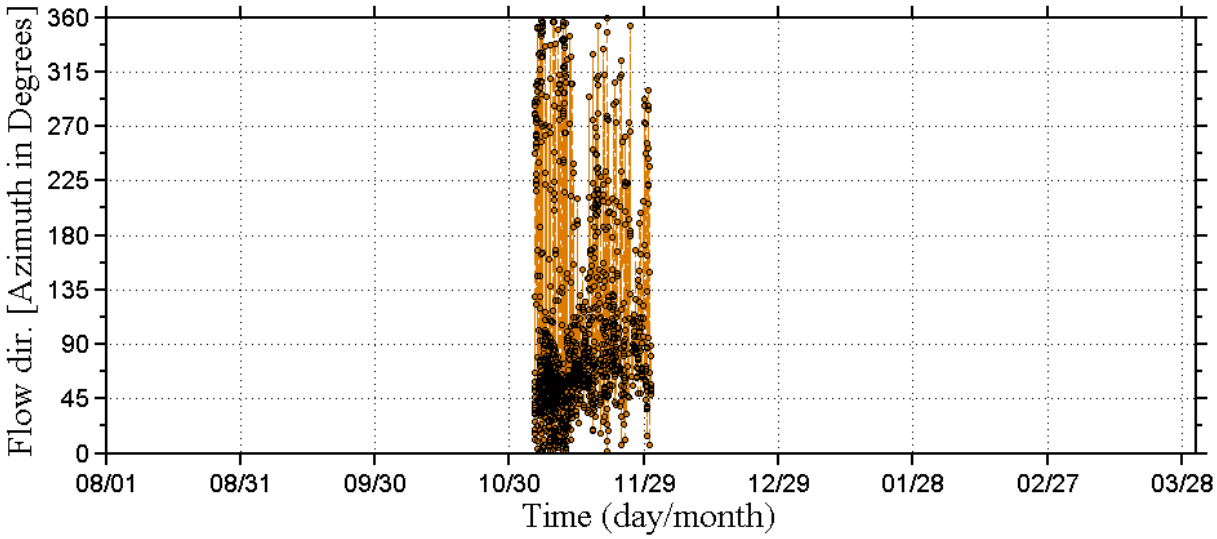

Figure C-47 Continuously sampled burst average ADV flow direction (clockwise degree from North) recorded at UB1 site during water year 2011 (8/1/2011 – 3/31/2012).

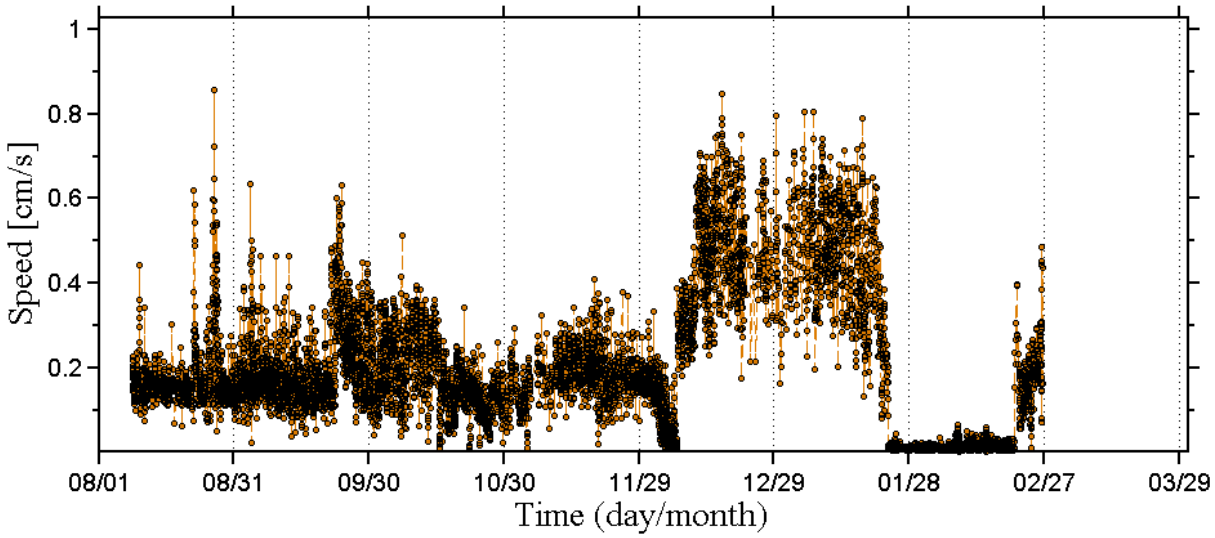

Figure C-48 Continuously sampled burst average ADV flow speed (cm/s) recorded at UB1 site during water year 2012 (8/1/2012– 3/31/2013).

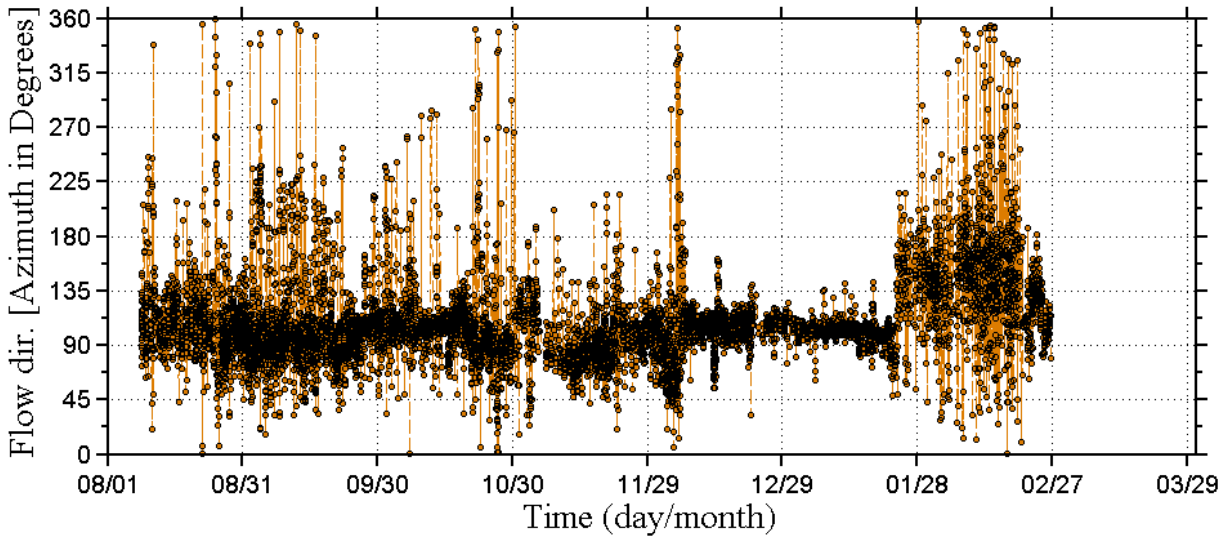

Figure C-49. Continuously sampled burst average ADV flow direction (clockwise degree from North) recorded at UB1 site during water year 2012 (8/1/2012 – 3/31/2013).

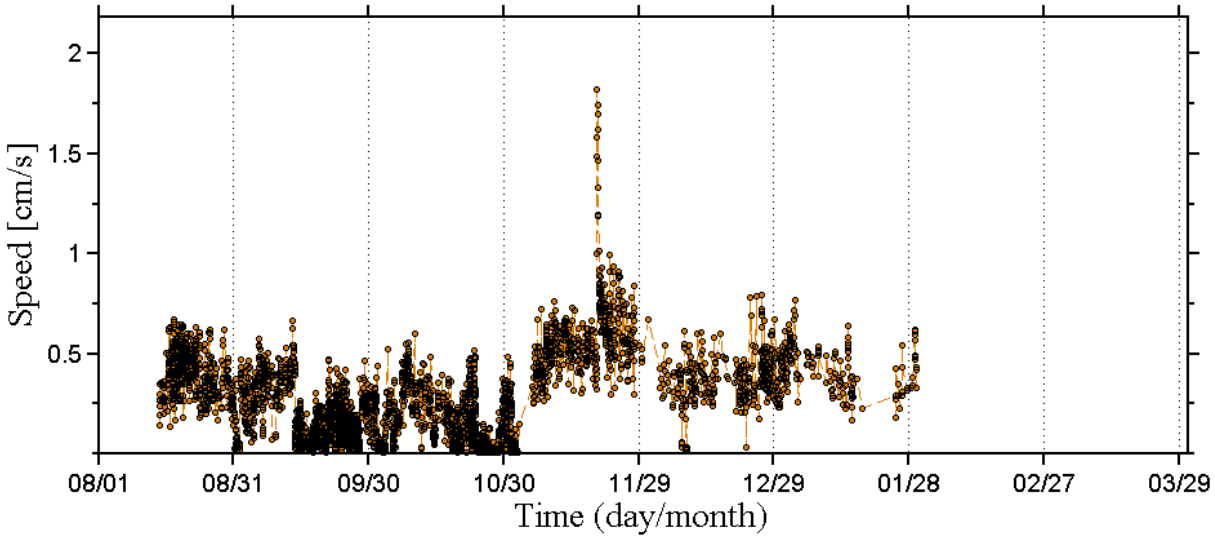

Figure C-50 Continuously sampled burst average ADV flow speed (cm/s) recorded at UB1 site during water year 2013 (8/1/2013 – 3/31/2014).

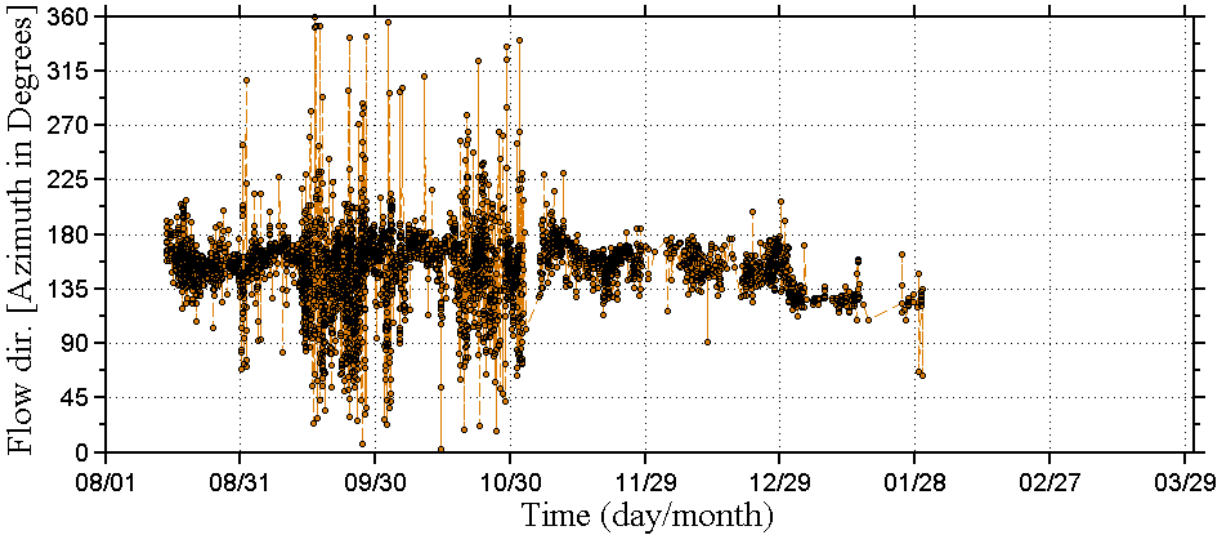

Figure C-51 Continuously sampled burst average ADV flow direction (clockwise degree from North) recorded at UB1 site during water year 2013 (8/1/2013 – 3/31/2014).

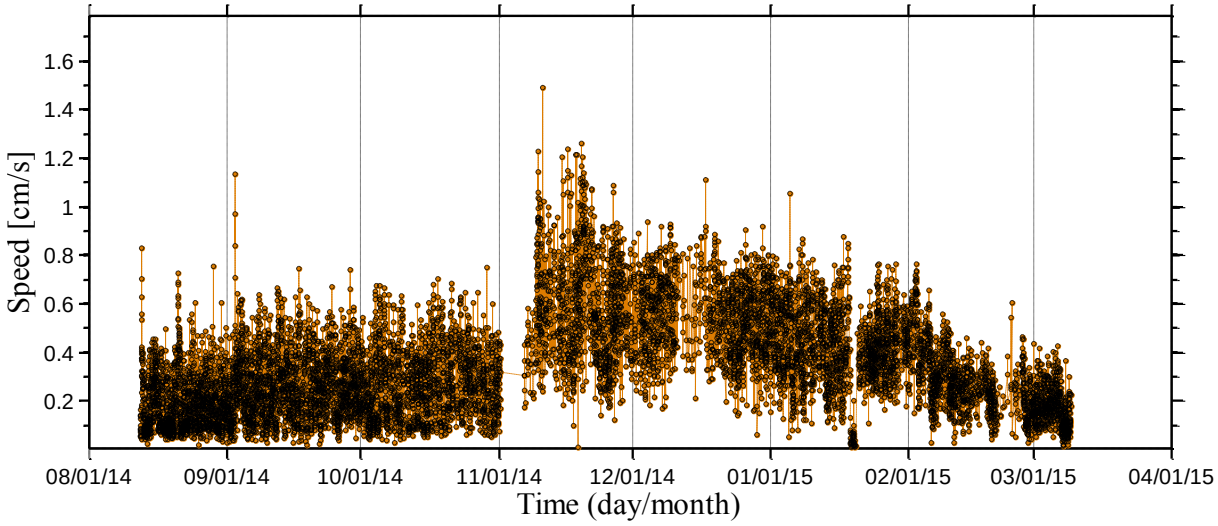

Figure C-52 Continuously sampled burst average ADV flow speed (cm/s) recorded at UB1 site during water year 2014 (8/1/2014 – 3/31/2015).

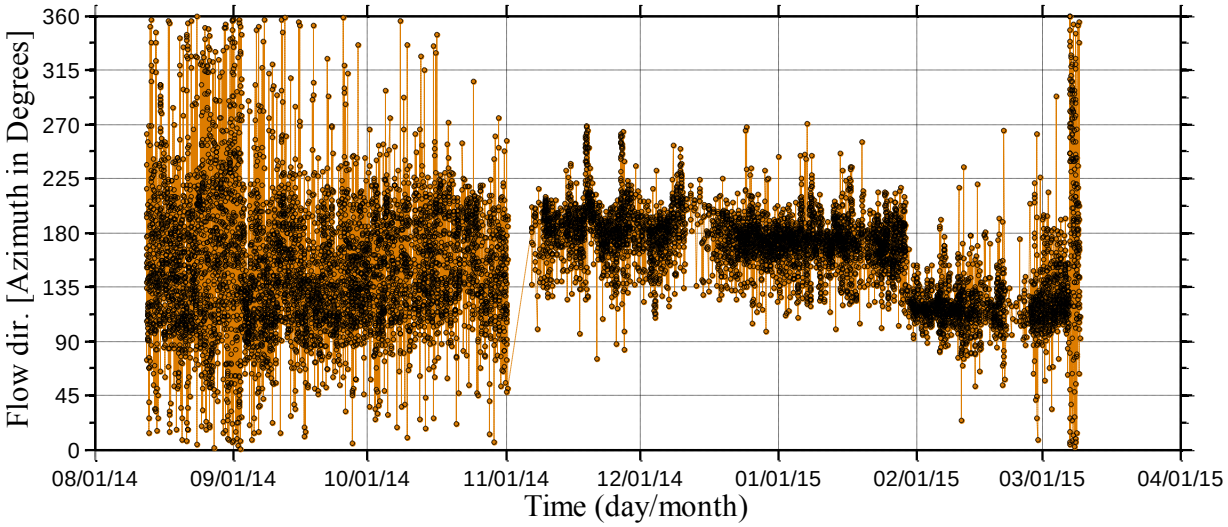

Figure C-53 Continuously sampled burst average ADV flow direction (clockwise degree from North) recorded at UB1 site during water year 2014 (8/1/2014 – 3/31/2015).

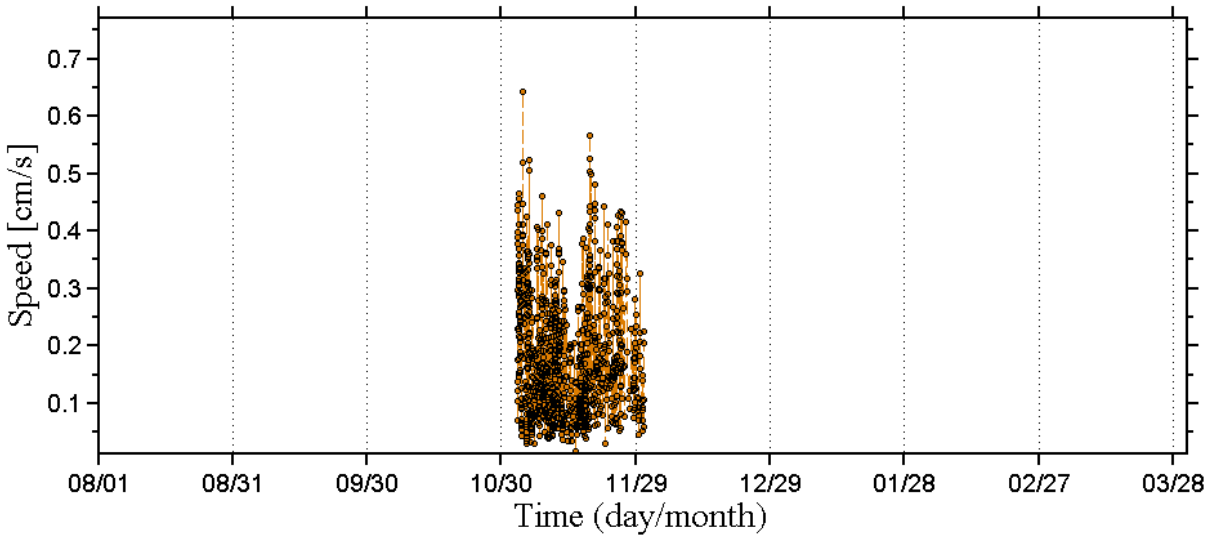

Figure C-54 Continuously sampled burst average ADV flow speed (cm/s) recorded at UB2 site during water year 2011 (8/1/2011 – 3/31/2012).

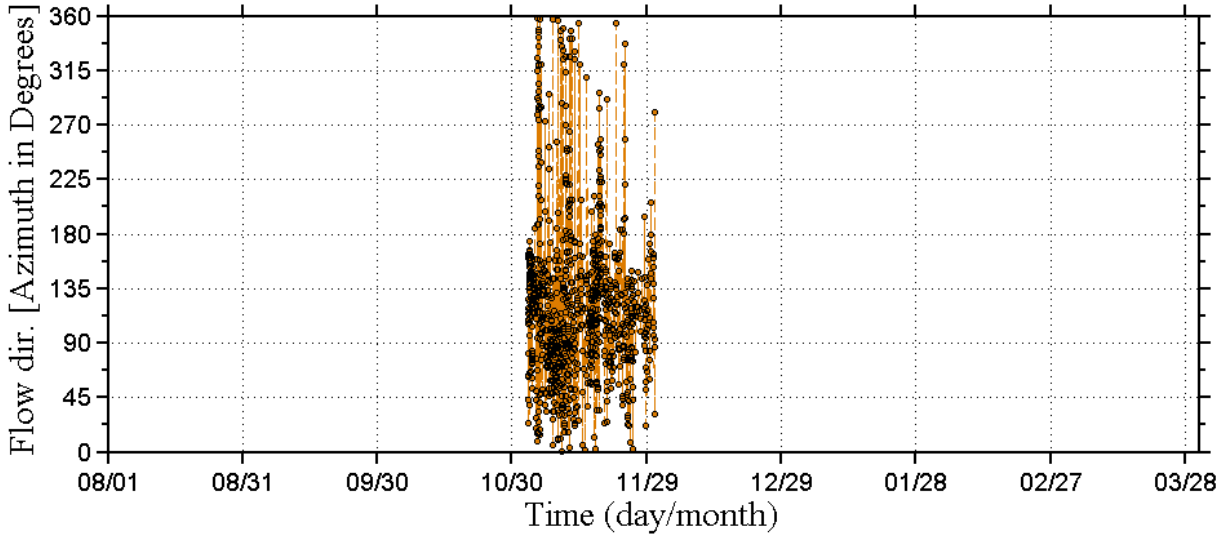

Figure C-55 Continuously sampled burst average ADV flow direction (clockwise degree from North) recorded at UB2 site during water year 2011 (8/1/2011 – 3/31/2012).

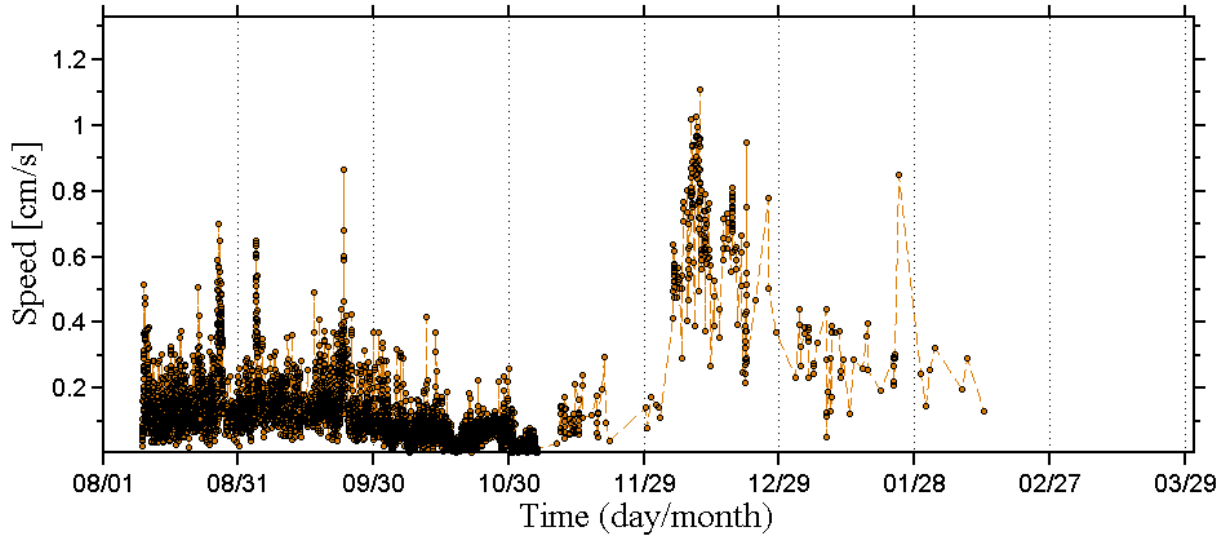

Figure C-56 Continuously sampled burst average ADV flow speed (cm/s) recorded at UB2 site during water year 2012 (8/1/2012 – 3/31/2013).

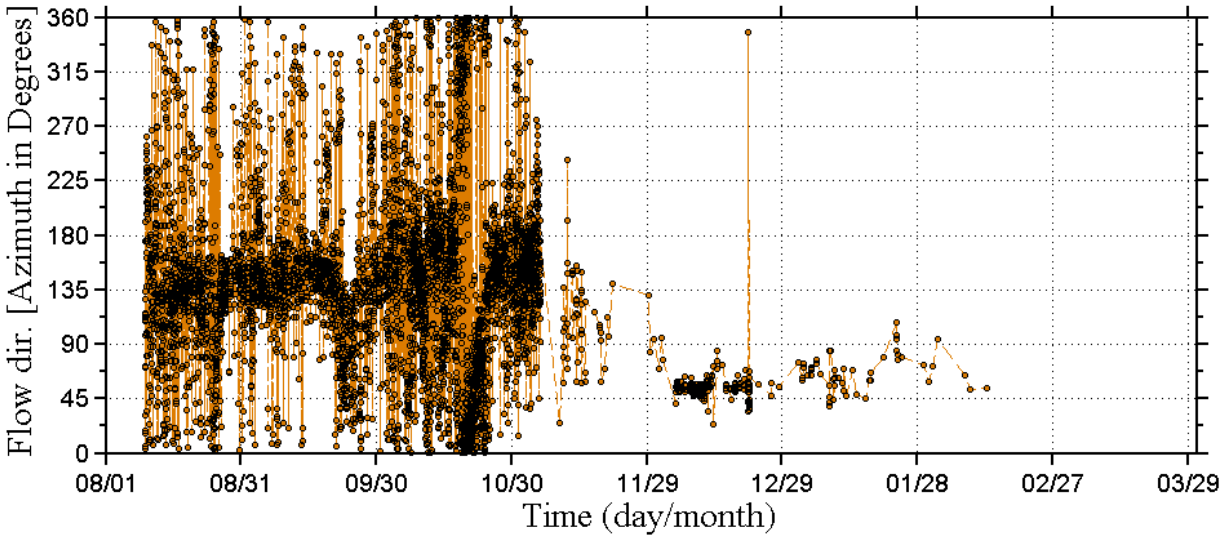

Figure C-57 Continuously sampled burst average ADV flow direction (clockwise degree from North) recorded at UB2 site during water year 2012 (8/1/2012 – 3/31/2013).

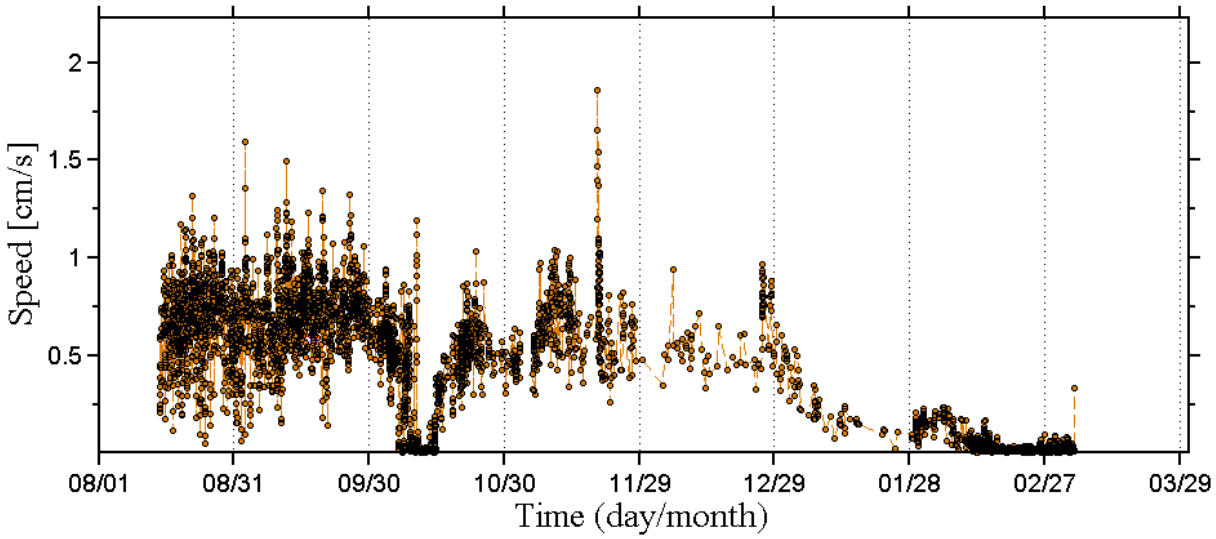

Figure C-58 Continuously sampled burst average ADV flow speed (cm/s) recorded at UB2 site during water year 2013 (8/1/2013 – 3/31/2014).

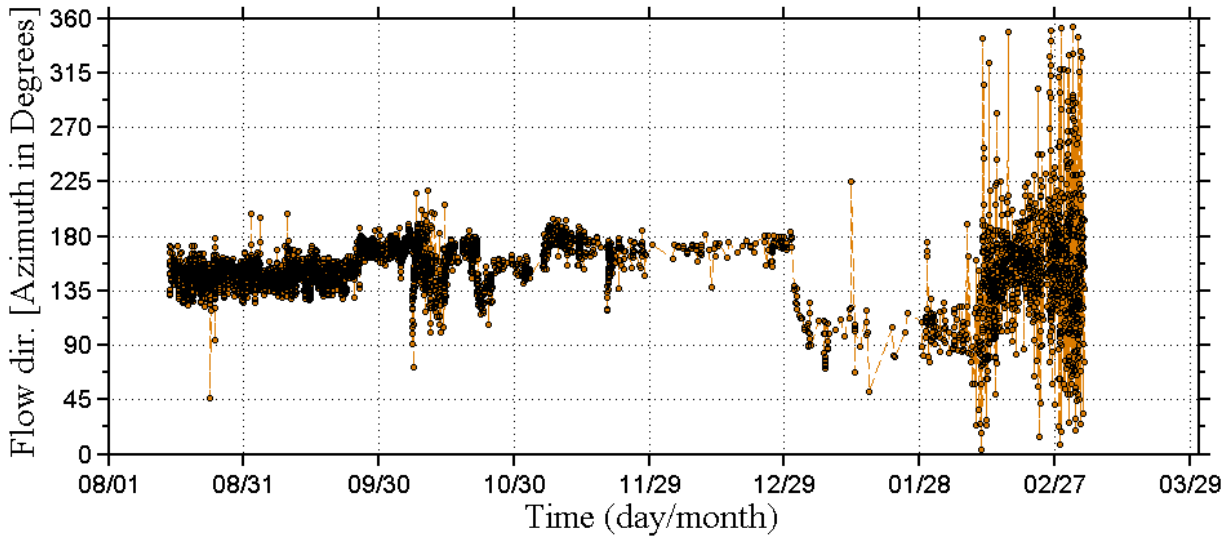

Figure C-59 Continuously sampled burst average ADV flow direction (clockwise degree from North) recorded at UB2 site during water year 2013 (8/1/2013 – 3/31/2014).

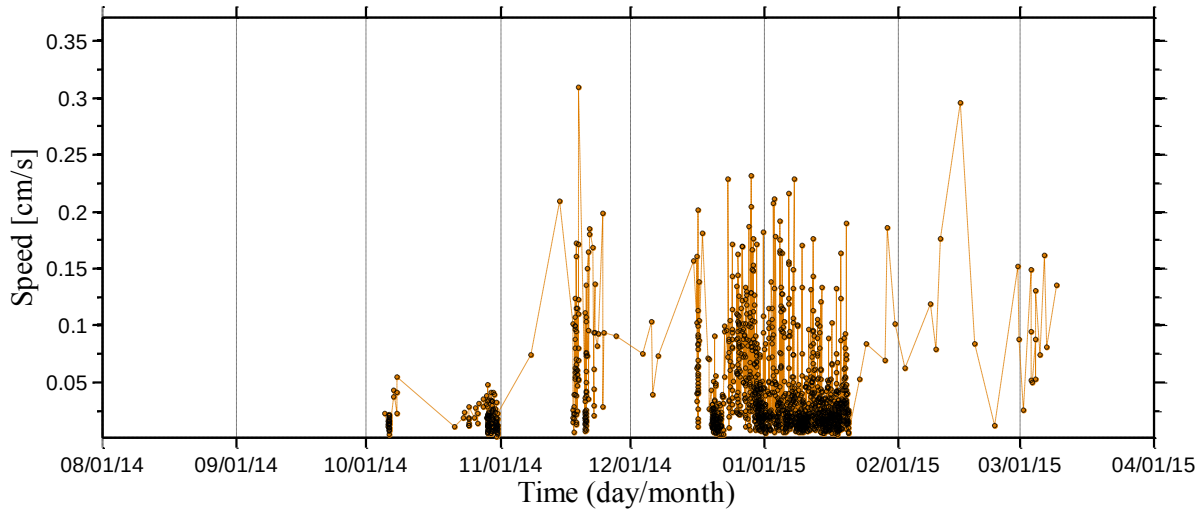

Figure C-60 Continuously sampled burst average ADV flow speed (cm/s) recorded at UB2 site during water year 2014 (8/1/2014 – 3/31/2015).

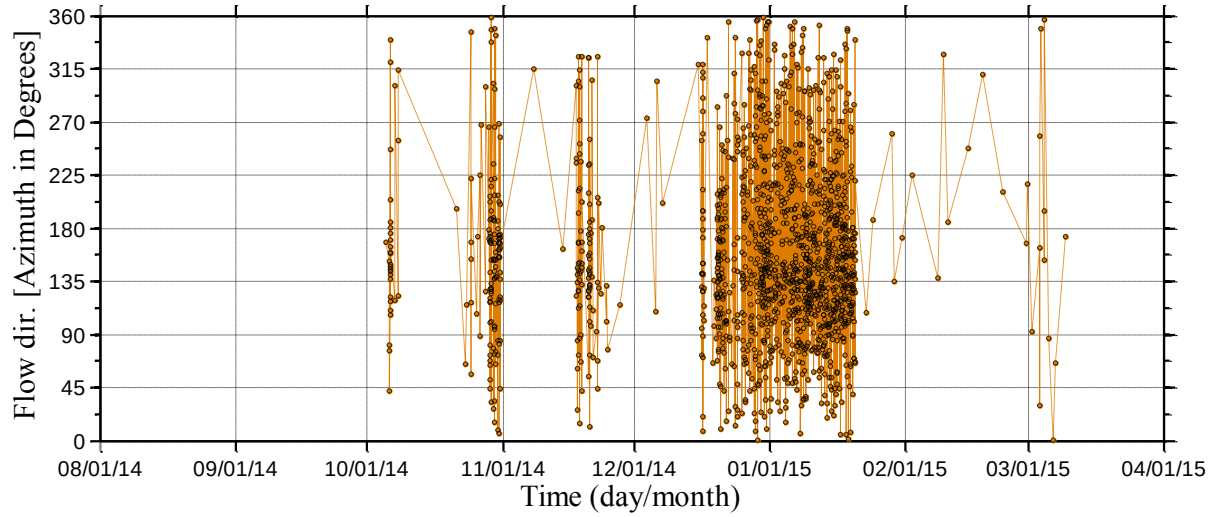

Figure C-61 Continuously sampled burst average ADV flow direction (clockwise degree from North) recorded at UB2 site during water year 2014 (8/1/2014 – 3/31/2015).

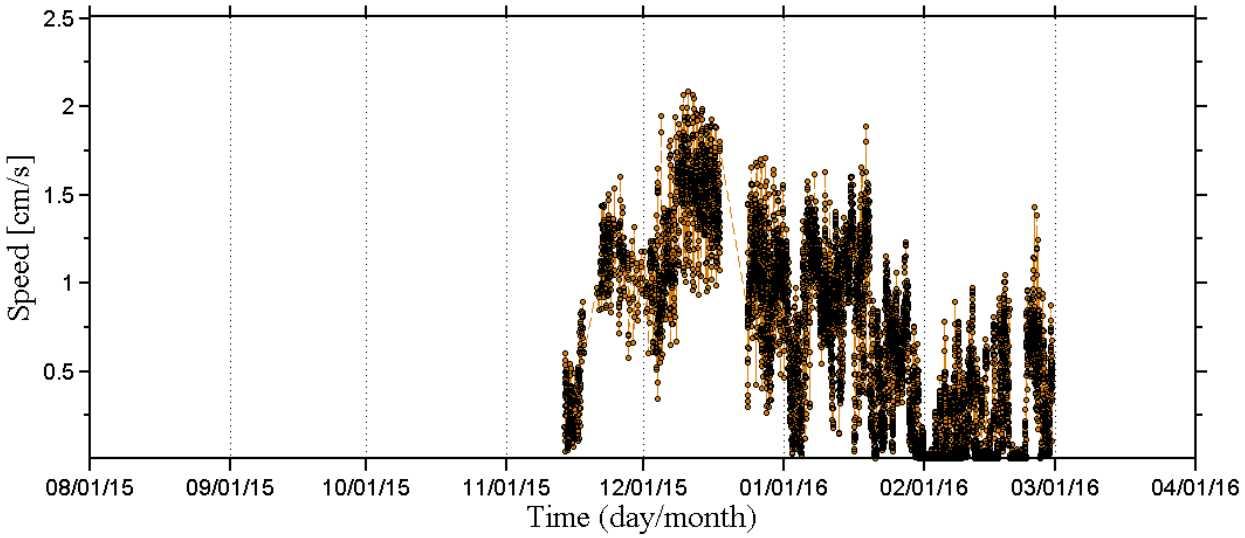

Figure C-62 Continuously sampled burst average ADV flow speed (cm/s) recorded at UB2 site during water year 2015 (8/1/2015 – 3/31/2016).

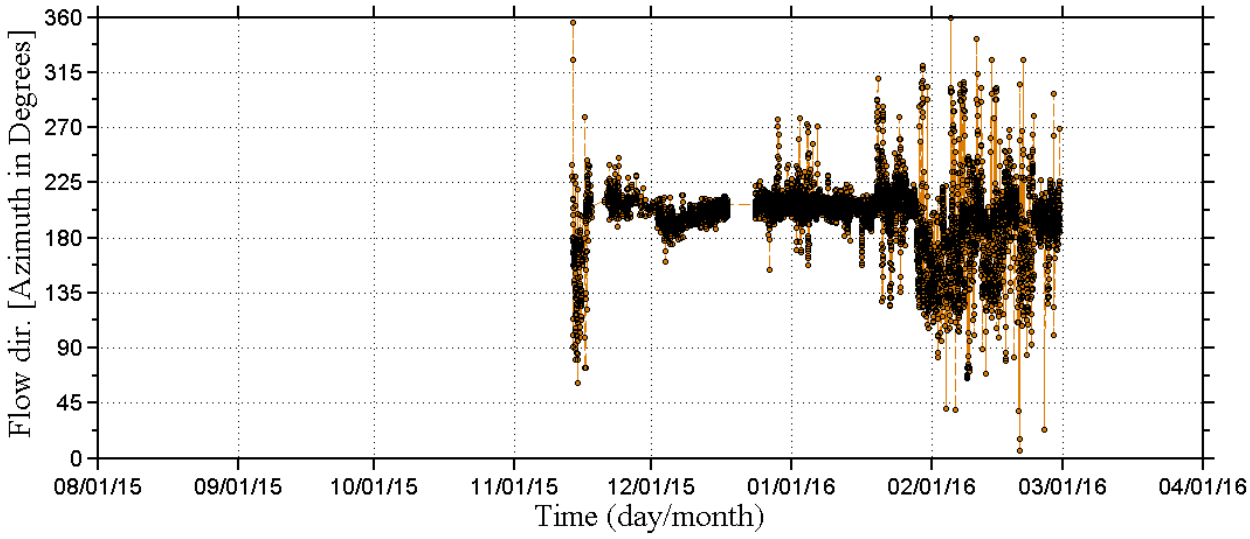

Figure C-63 Continuously sampled burst average ADV flow direction (clockwise degree from North) recorded at UB2 site during water year 2015 (8/1/2015 – 3/31/2016).

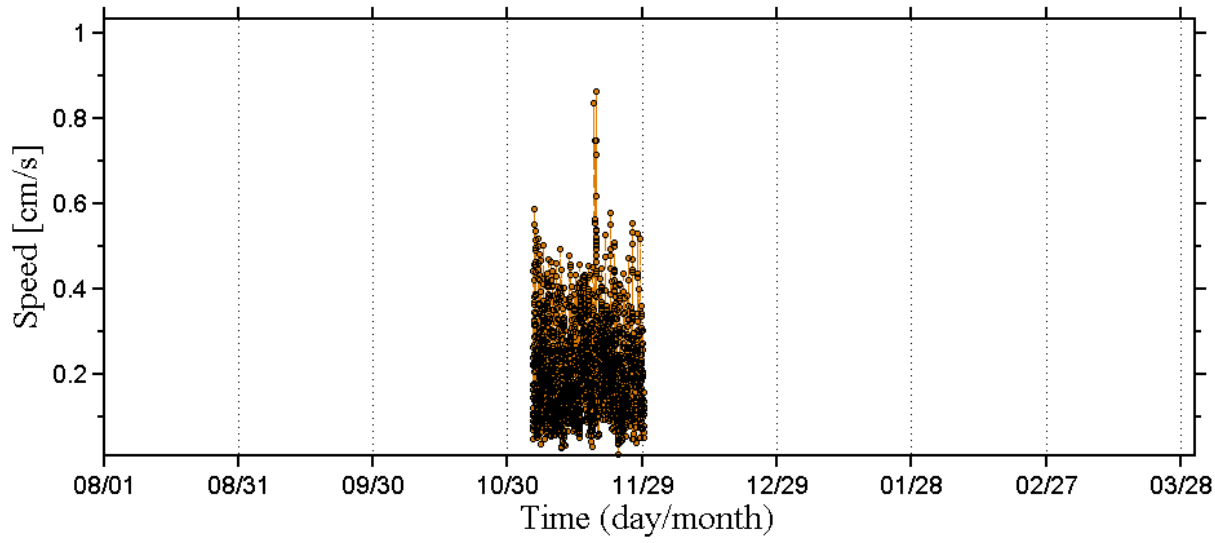

Figure C-64 Continuously sampled burst average ADV flow speed (cm/s) recorded at UB3 site during water year 2011 (8/1/2011 – 3/31/2012).

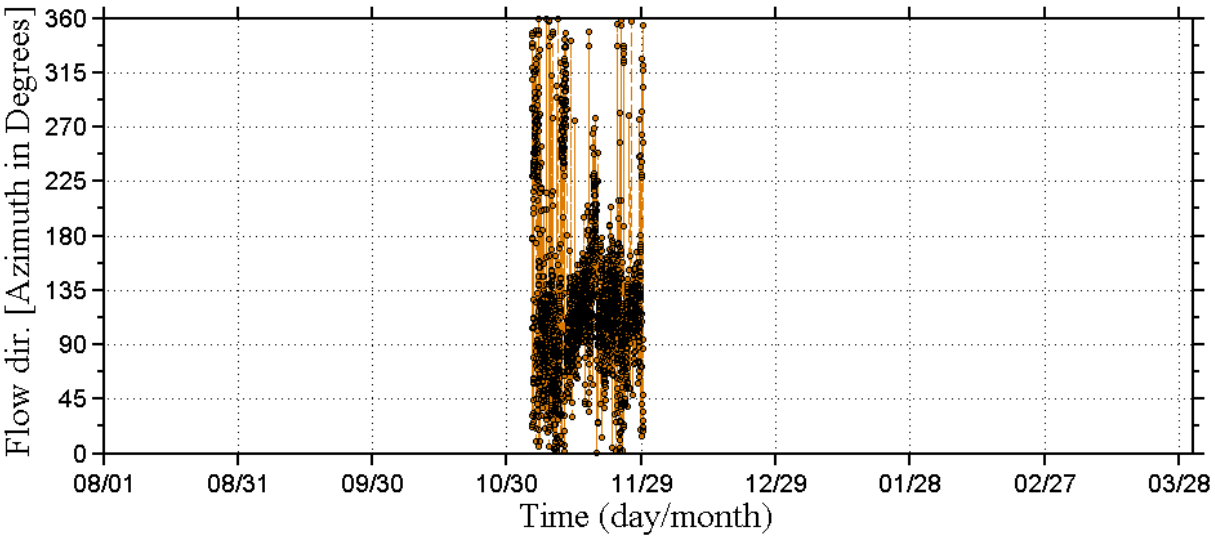

Figure C-65 Continuously sampled burst average ADV flow direction (clockwise degree from North) recorded at UB3 site during water year 2011 (8/1/2011 – 3/31/2012).

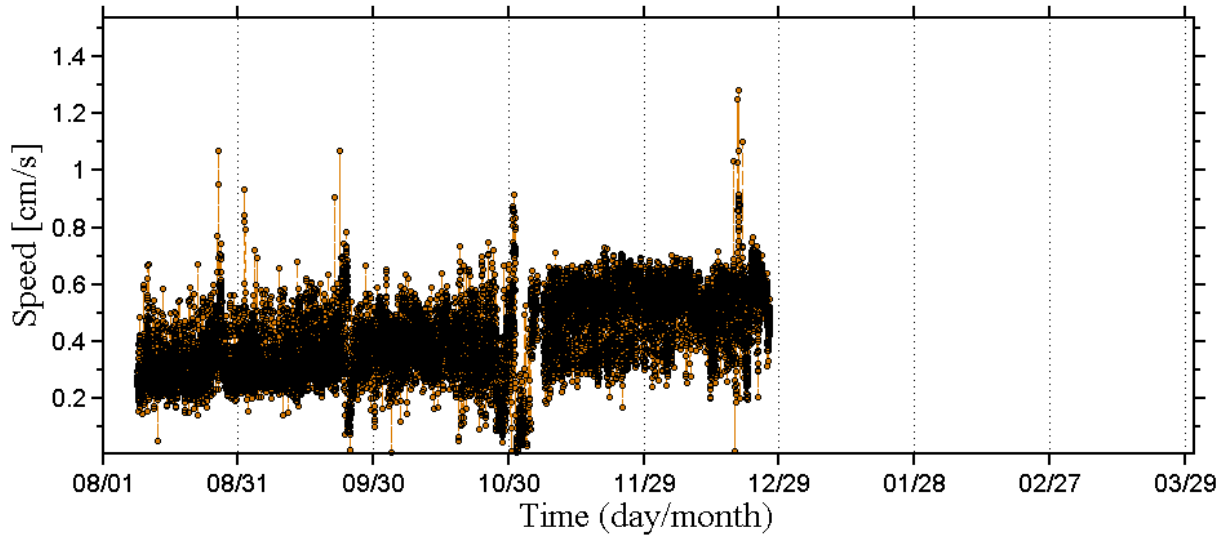

Figure C-66 Continuously sampled burst average ADV flow speed (cm/s) recorded at UB3 site during water year 2012 (8/1/2012 – 3/31/2013).

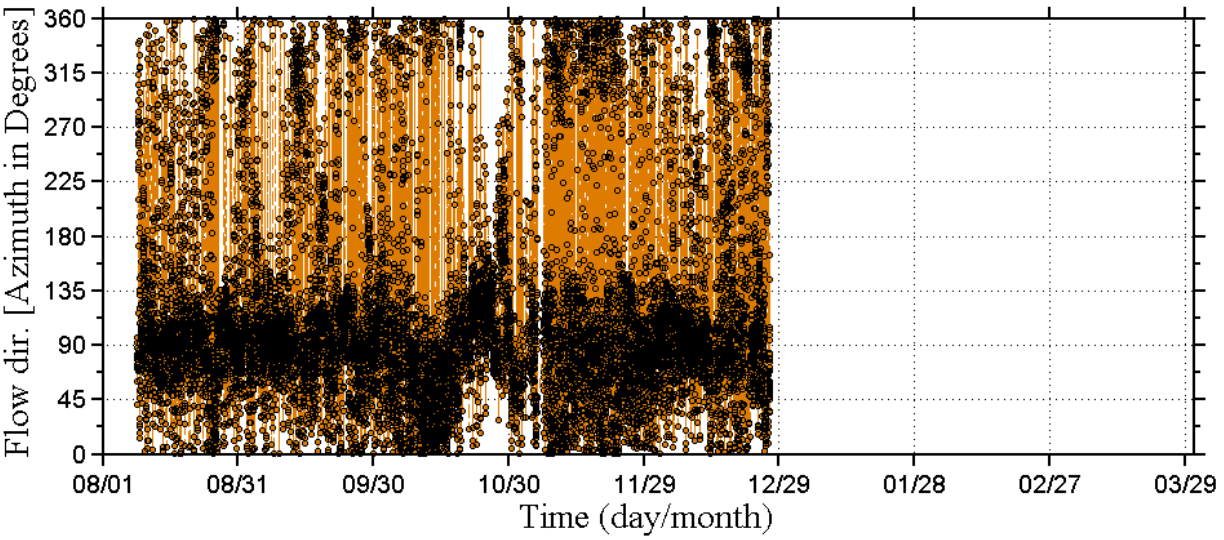

Figure C-67 Continuously sampled burst average ADV flow direction (clockwise degree from North) recorded at UB3 site during water year 2012 (8/1/2012 – 3/31/2013).

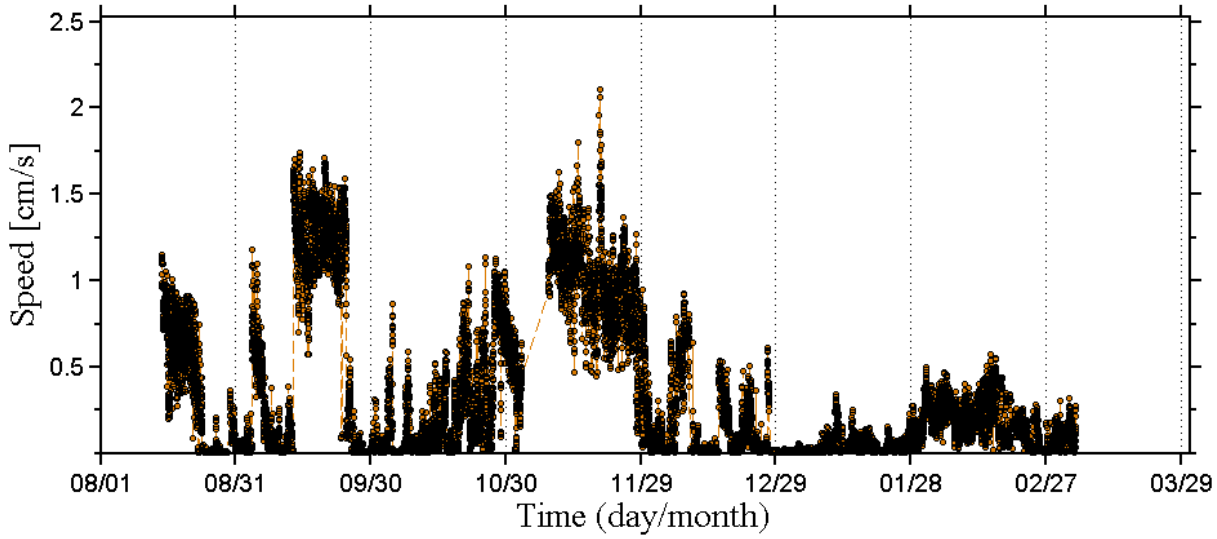

Figure C-68 Continuously sampled burst average ADV flow speed (cm/s) recorded at UB3 site during water year 2013 (8/1/2013 – 3/31/2014).

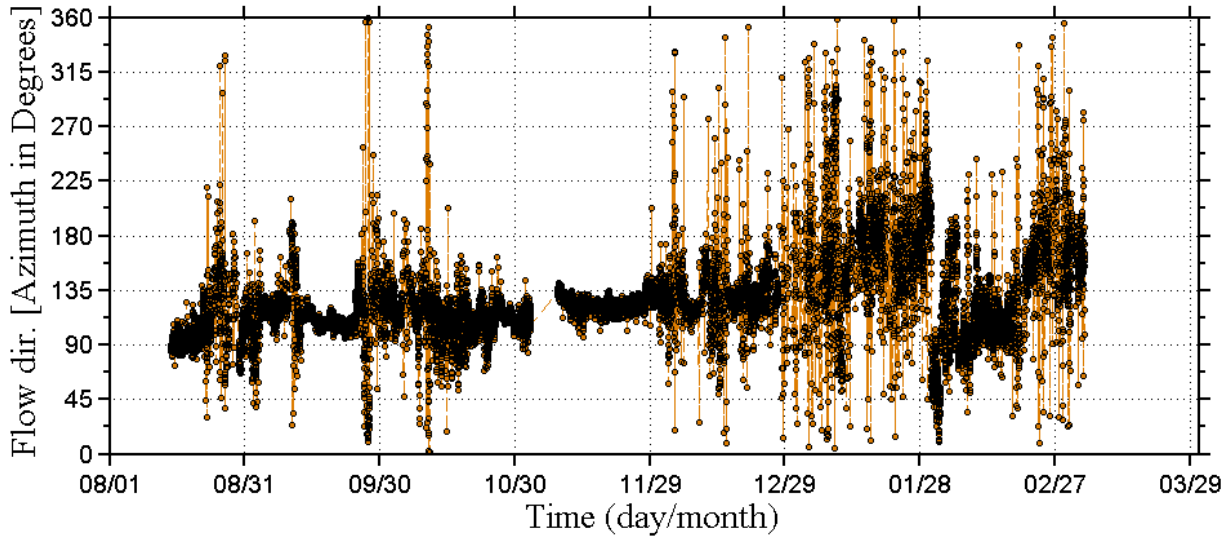

Figure C-69 Continuously sampled burst average ADV flow direction (clockwise degree from North) recorded at UB3 site during water year 2013 (8/1/2013 – 3/31/2014).

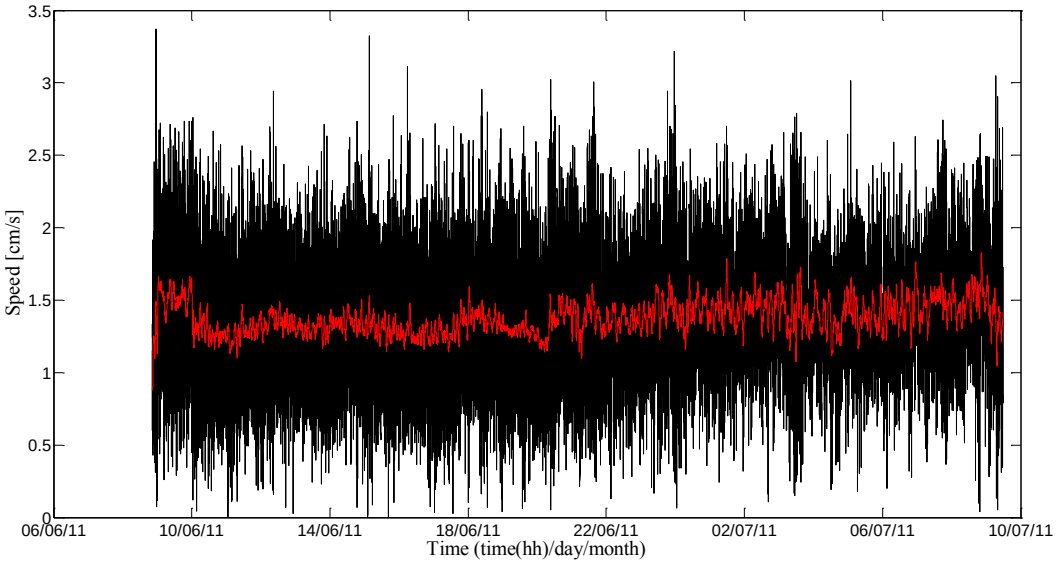

Figure C-70 Continuously sampled Vectrino flow speed (cm/s) recorded at UB3 site during water year 2014 (11/6/2014 – 11/7/2014).

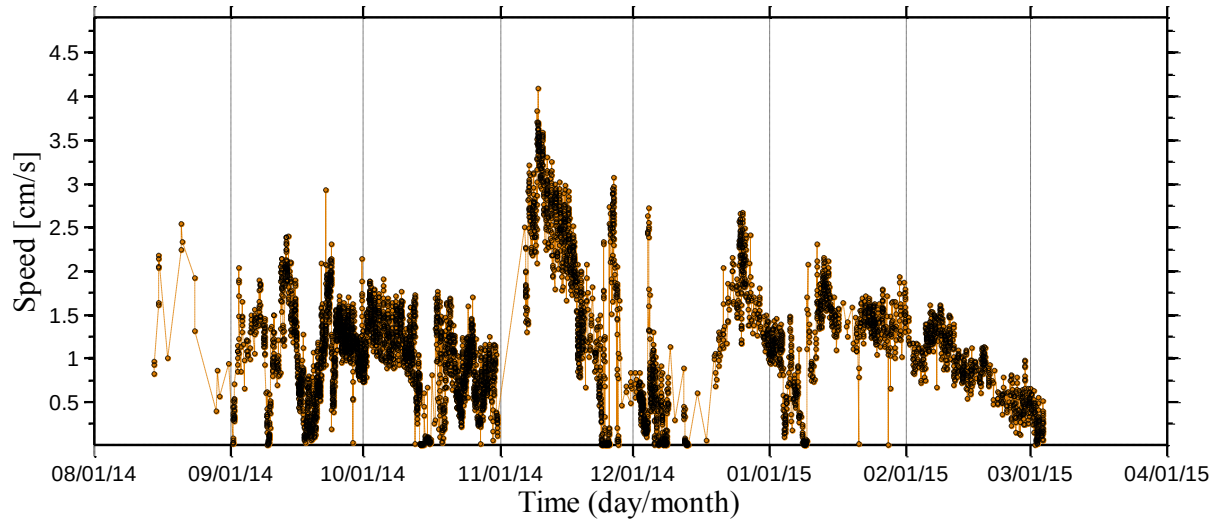

Figure C-71 Continuously sampled burst average ADV flow speed (cm/s) recorded at DB1 site during water year 2014 (8/1/2014 – 3/31/2015).

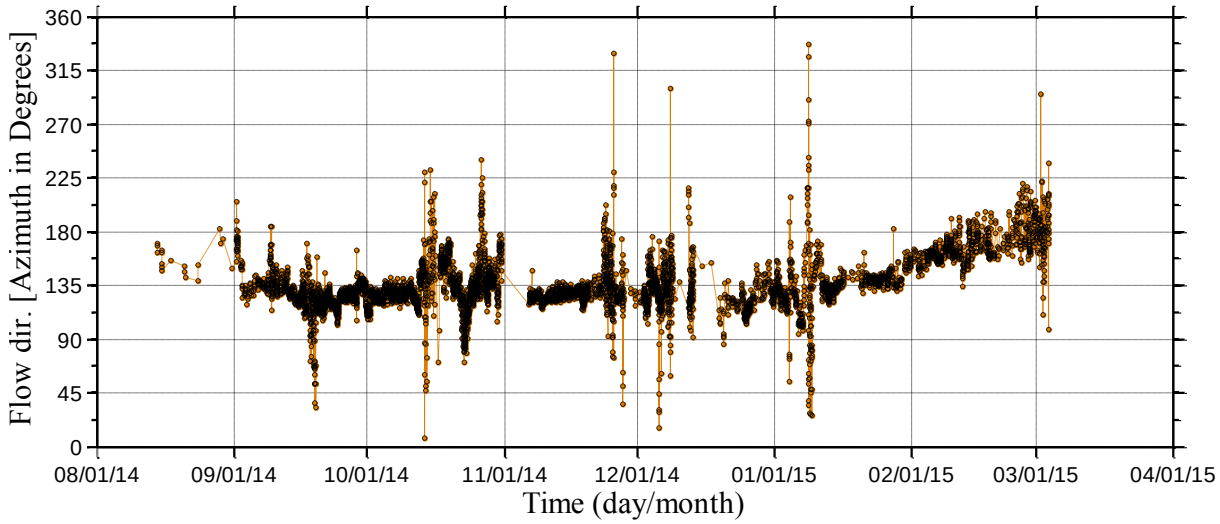

Figure C-72 Continuously sampled burst average ADV flow direction (clockwise degree from North) recorded at DB1 site during water year 2014 (8/1/2014 – 3/31/2014).

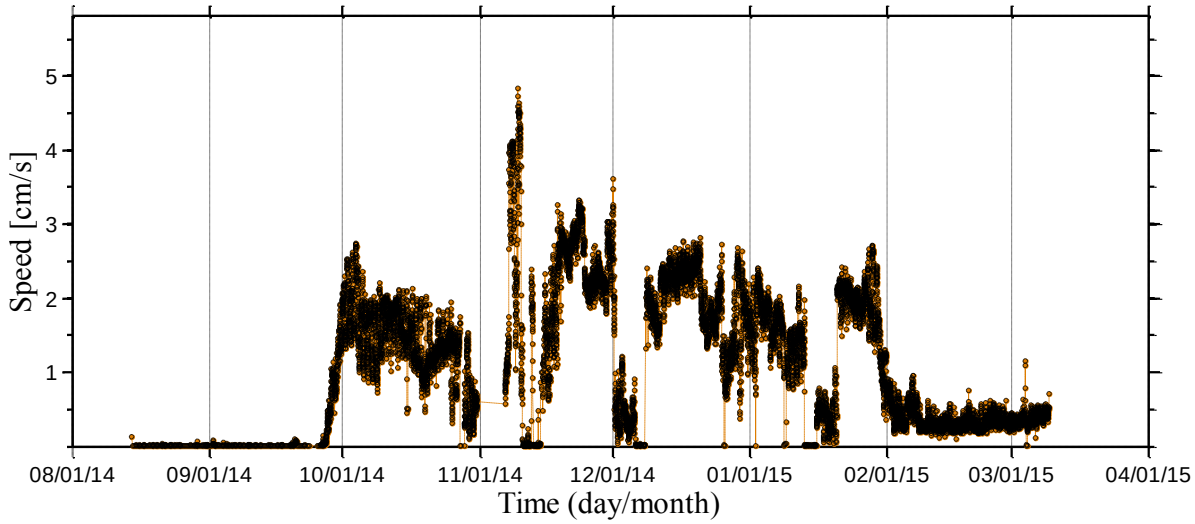

Figure C-73 Continuously sampled burst average ADV flow speed (cm/s) recorded at DB2 site during water year 2014 (8/1/2014 – 3/31/2015).

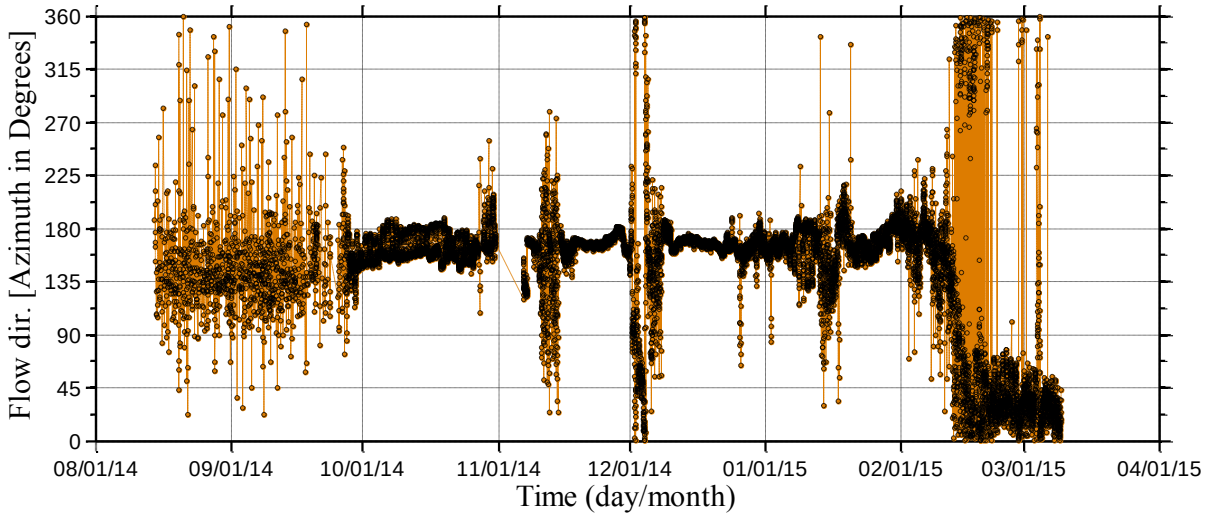

Figure C-74 Continuously sampled burst average ADV flow direction (clockwise degree from North) recorded at DB2 site during water year 2014 (8/1/2014 – 3/31/2015).

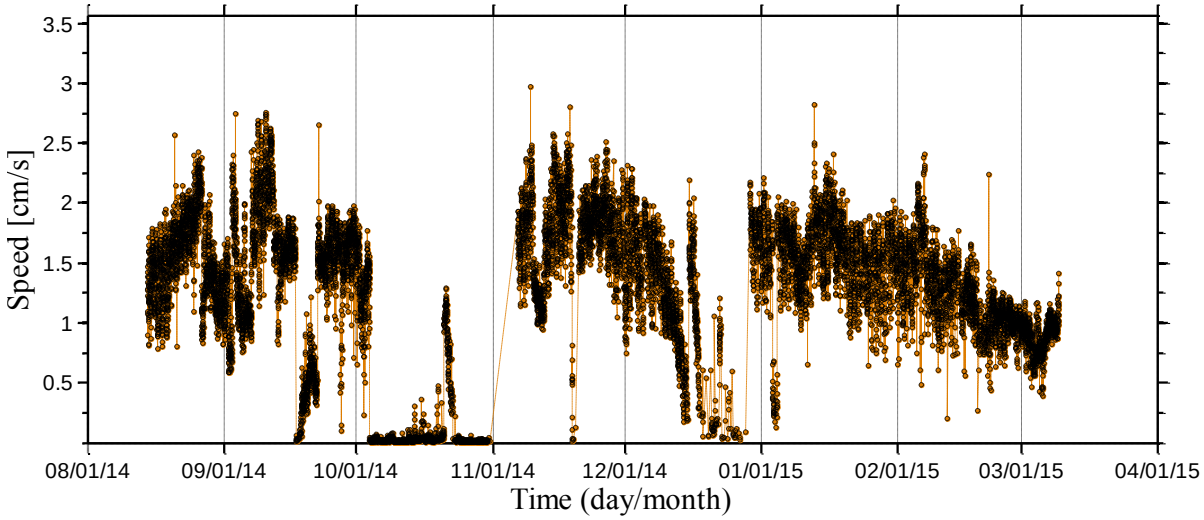

Figure C-75 Continuously sampled burst average ADV flow speed (cm/s) recorded at DB3 site during water year 2014 (8/1/2014 – 3/31/2015).

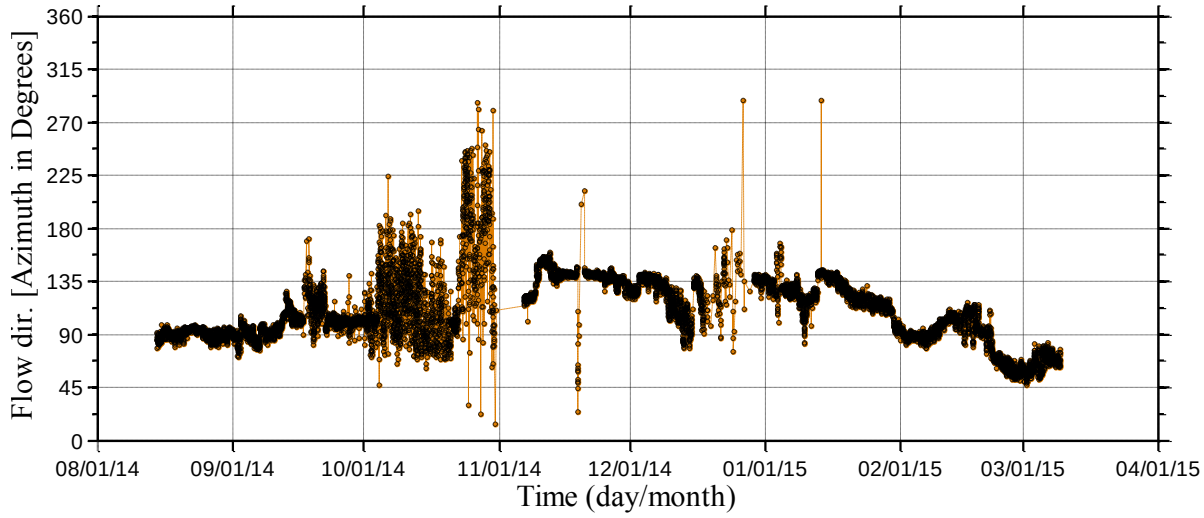

Figure C-76 Continuously sampled burst average ADV flow direction (clockwise degree from North) recorded at DB3 site during water year 2014 (8/1/2014 – 3/31/2015).

Continuous Argonaut XR Data

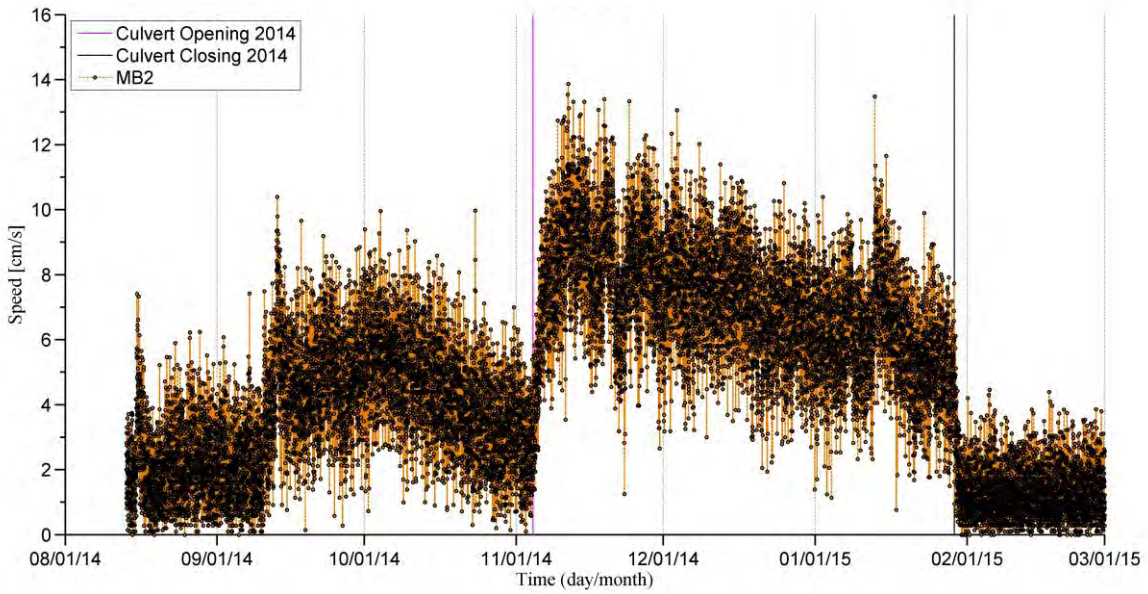

Figure C-77 Continuously sampled burst average Argonaut XR flow speed at canal site MB1 in L67C canal during water year 2014 (8/1/2014 – 3/31/2015).

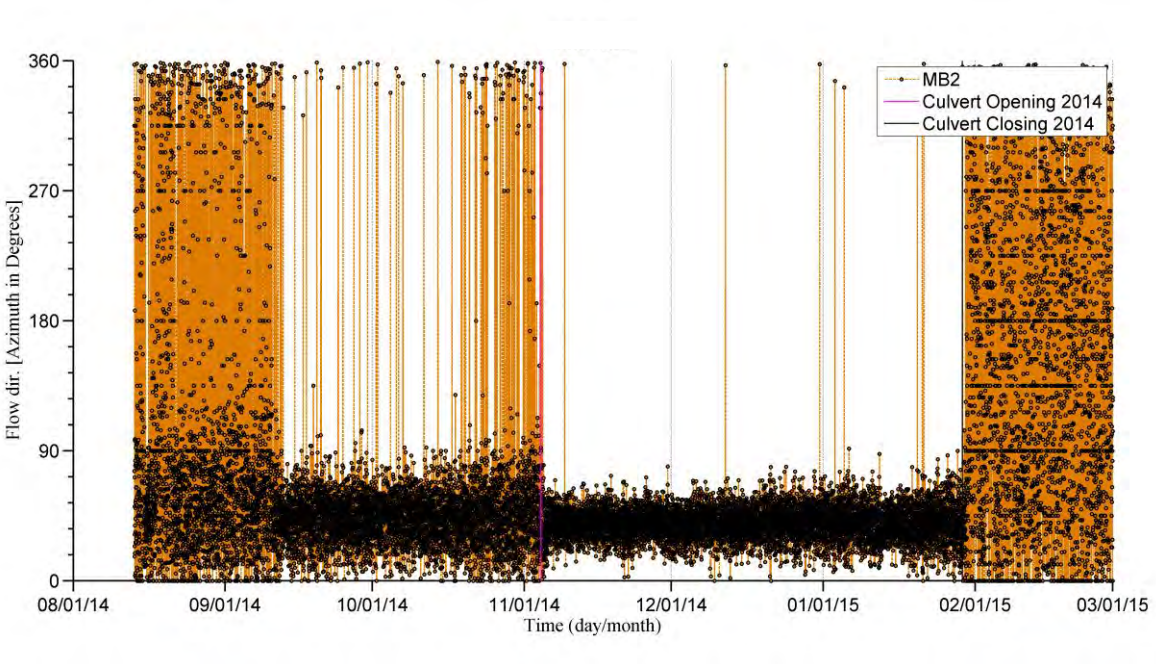

Figure C-78 Continuously sampled burst average Argonaut XR flow direction at canal site MB1 in L67C canal during water year 2014 (8/1/2014 – 3/31/2015).

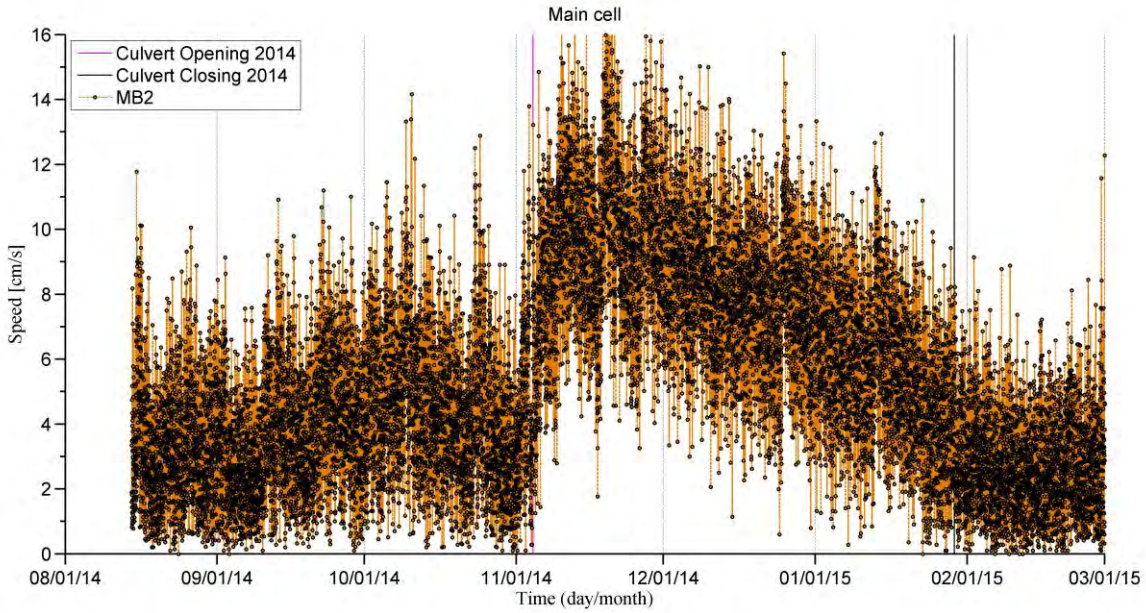

Figure C-79 Continuously sampled burst average Argonaut XR flow speed at canal site MB2 in L67C canal during water year 2014 (8/1/2014 – 3/31/2015).

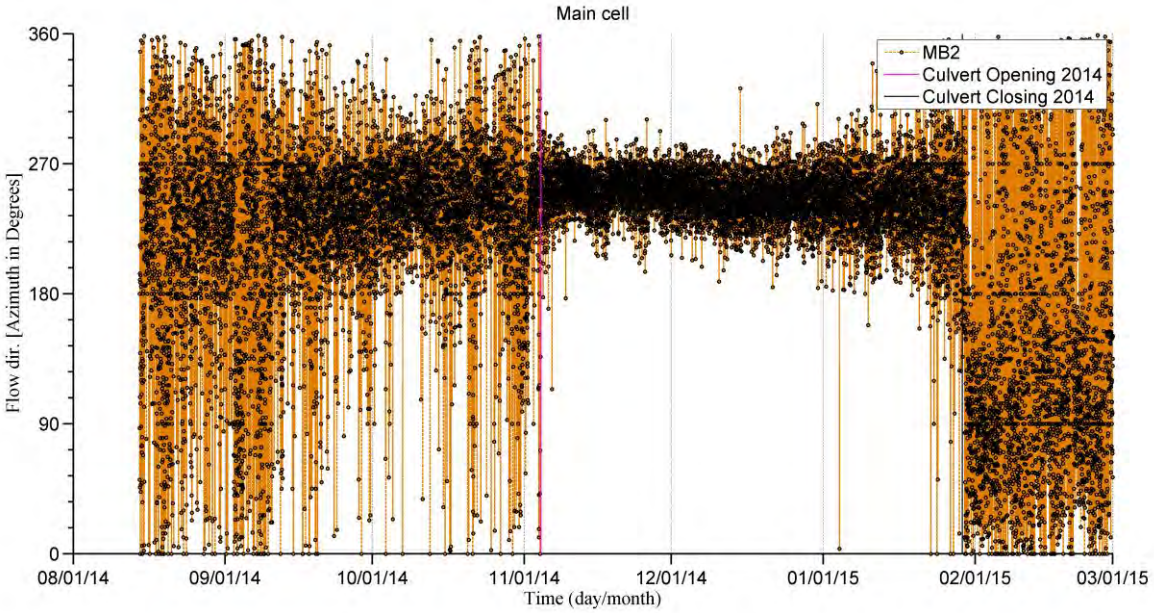

Figure C-80 Continuously sampled burst average Argonaut XR flow direction at canal site MB2 in L67C canal during water year 2014 (8/1/2014 – 3/31/2015).

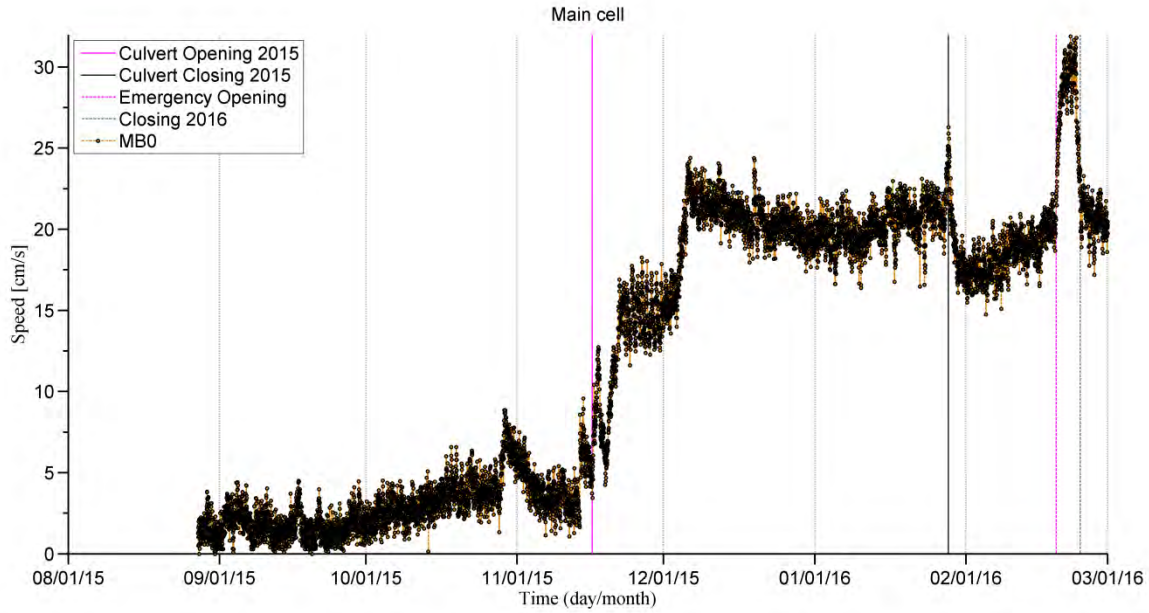

Figure C-81 Continuously sampled burst average Argonaut XR flow speed at canal site MB0 in L67C canal during water year 2015 (8/1/2015 – 3/1/2016).

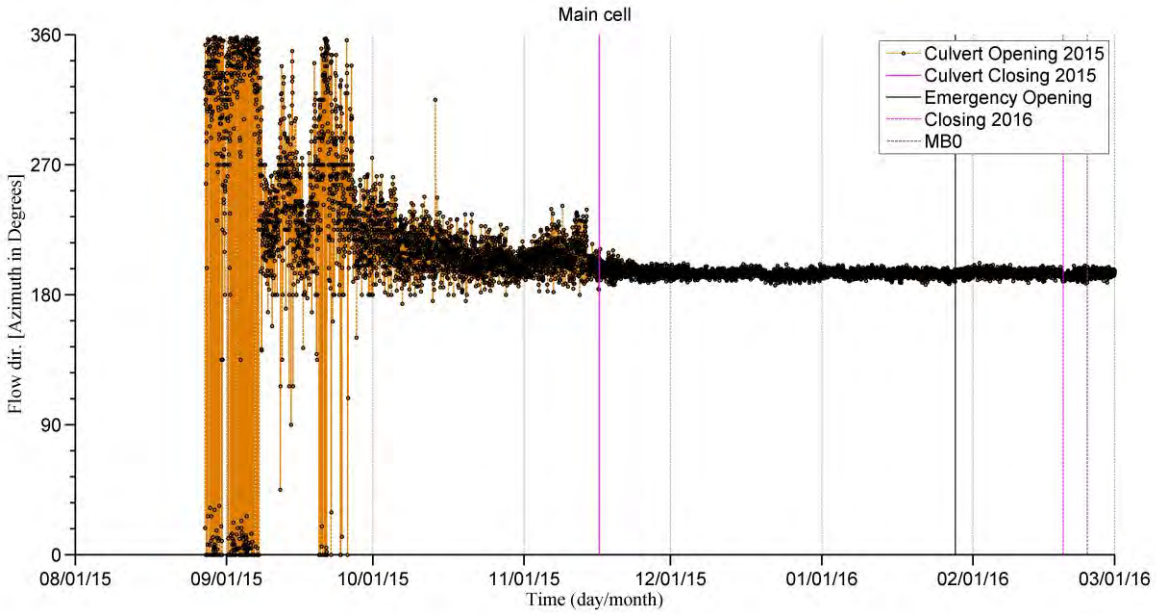

Figure C-82 Continuously sampled burst average Argonaut XR flow direction at canal site MB0 in L67C canal during water year 2015 (8/1/2015 – 3/1/2016).

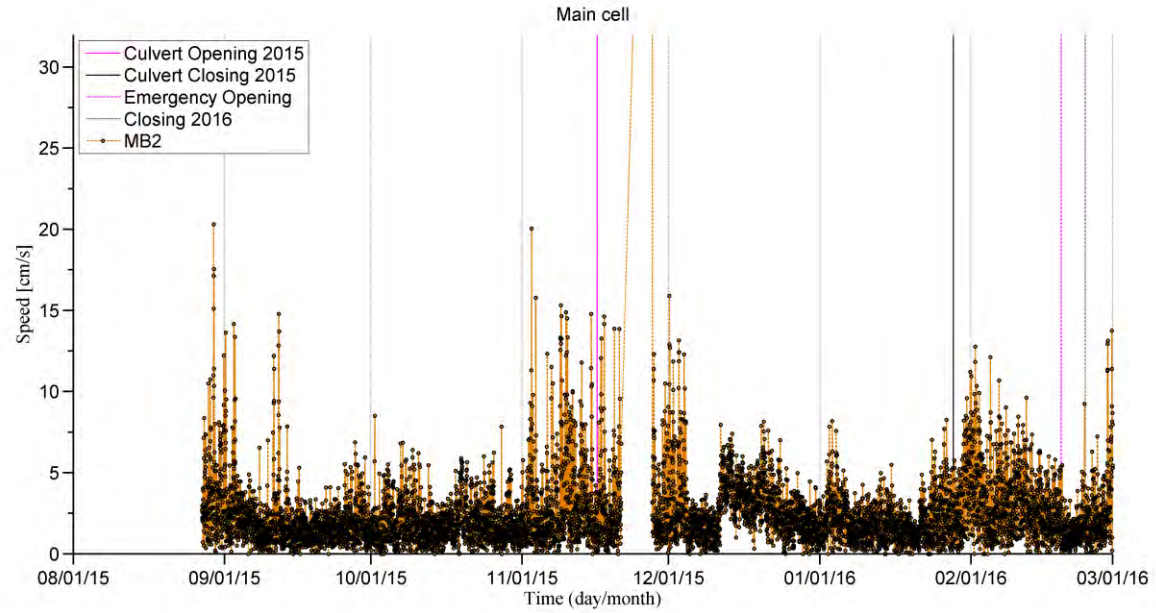

Figure C-83 Continuously sampled burst average Argonaut XR flow speed at canal site MB2 in L67C canal during water year 2015 (8/1/2015 – 3/1/2016).

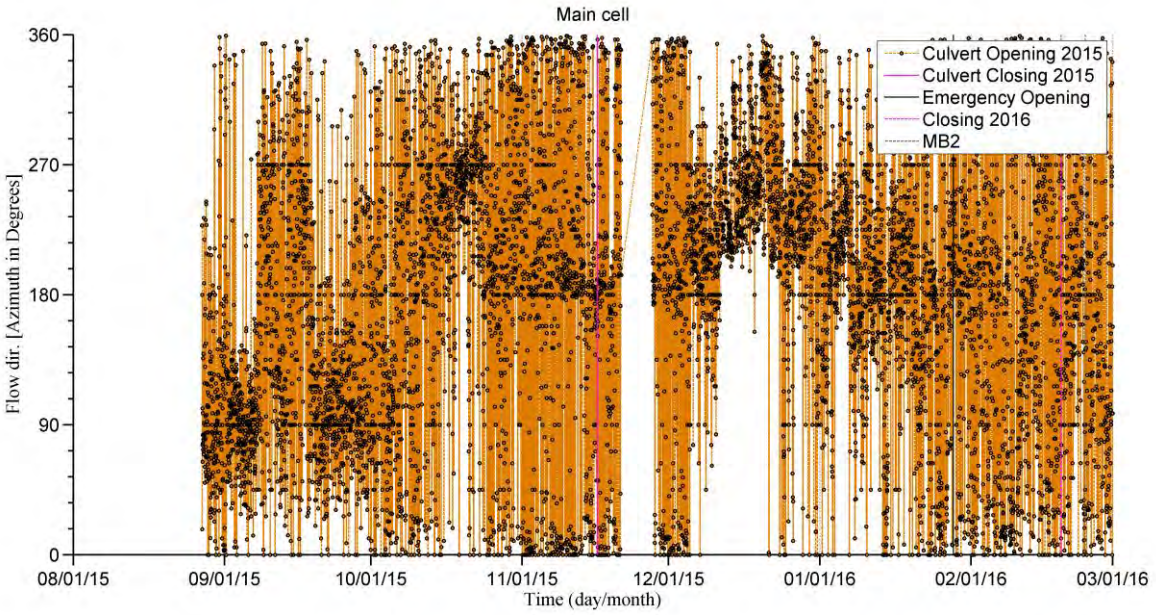

Figure C-84 Continuously sampled burst average Argonaut XR flow direction at canal site MB2 in L67C canal during water year 2015 (8/1/2015 – 3/1/2016).

ADV Discrete Profile Data

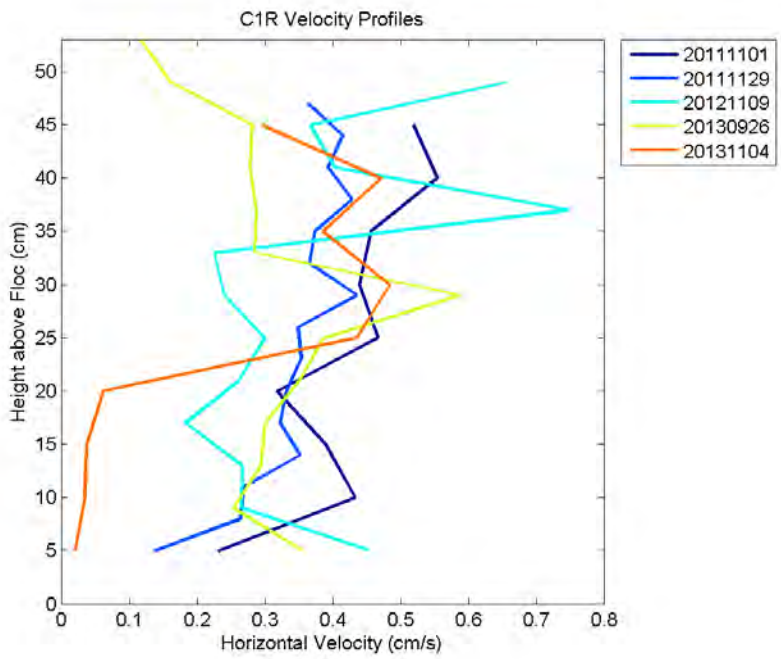

Figure C-85 All ADV velocity profiles recorded at DPM site C1 Ridge. Horizontal velocities in cm/s are shown. Dates are given in the format yyyymmdd.

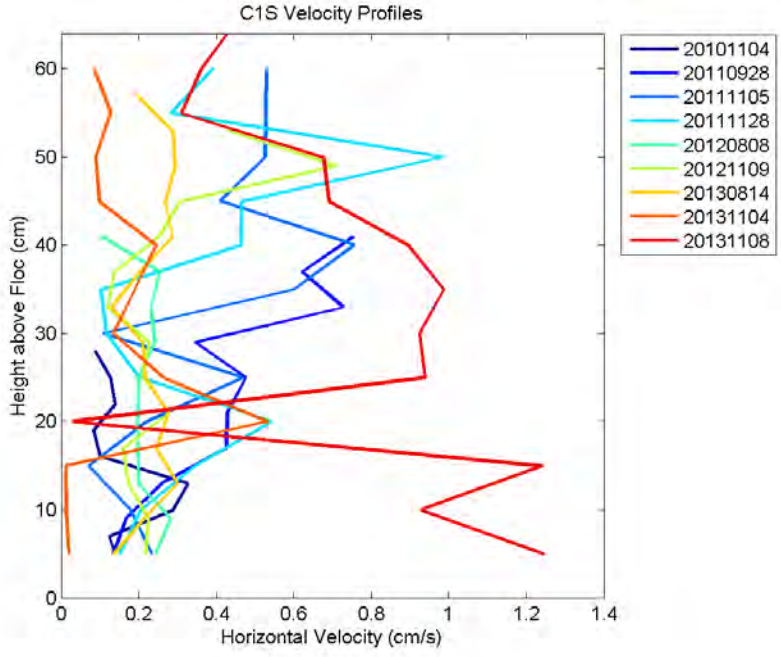

Figure C-86 All ADV velocity profiles recorded at DPM site C1 Slough. Horizontal velocities in cm/s are shown. Dates are given in the format yyyymmdd.

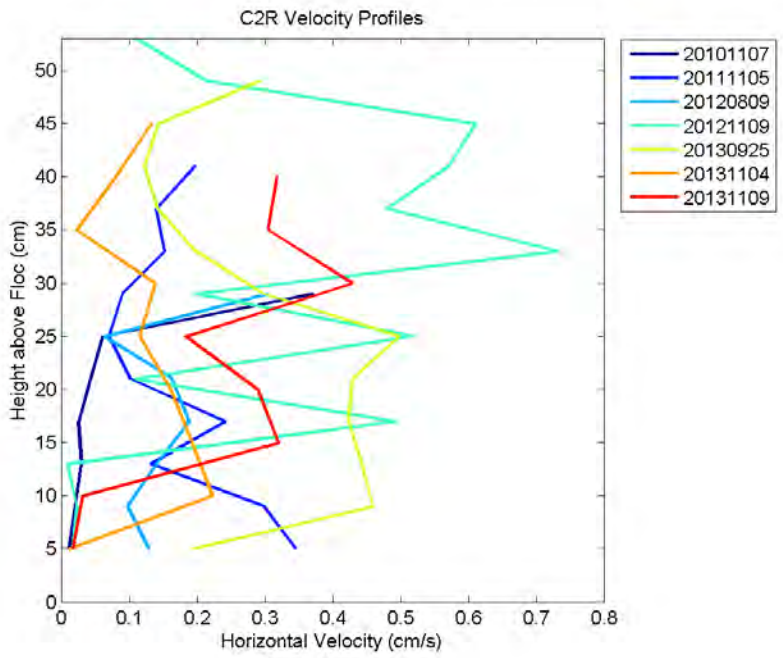

Figure C-87 All ADV velocity profiles recorded at DPM site C2 Ridge. Horizontal velocities in cm/s are shown. Dates are given in the format yyyymmdd.

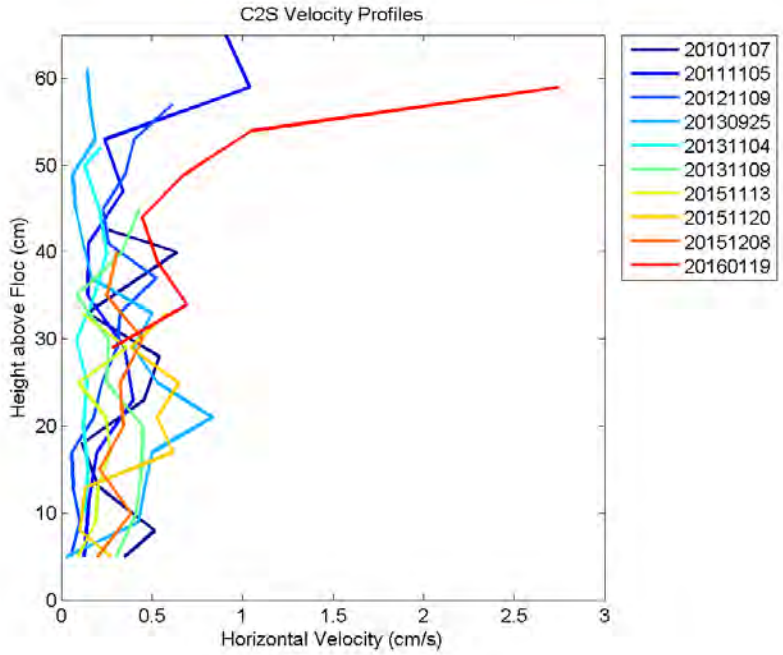

Figure C-88 All ADV velocity profiles recorded at DPM site C2 Slough. Horizontal velocities in cm/s are shown. Dates are given in the format yyyymmdd.

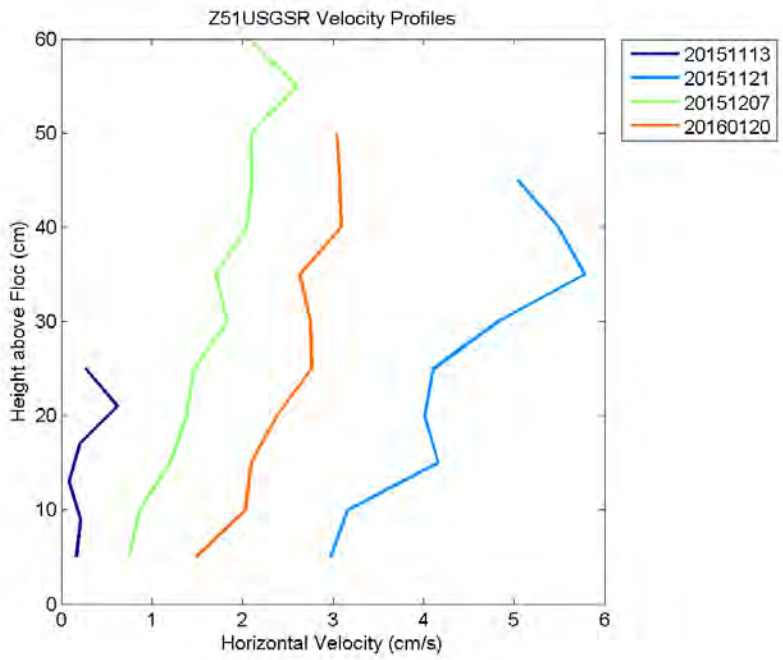

Figure C-89 All ADV velocity profiles recorded at DPM site Z51_USGS Ridge. Horizontal velocities in cm/s are shown. Dates are given in the format yyyymmdd.

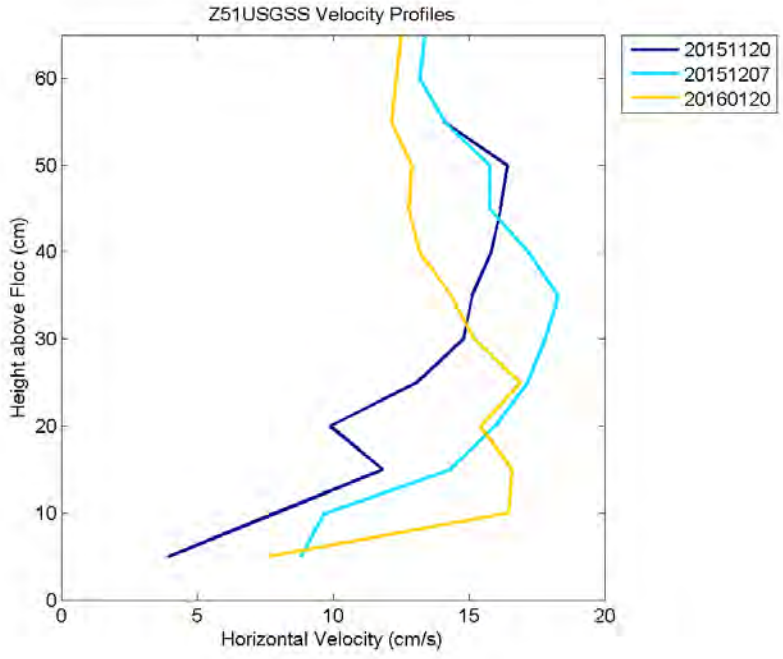

Figure C-90 All ADV velocity profiles recorded at DPM site Z51_USGS Slough. Horizontal velocities in cm/s are shown. Dates are given in the format yyyymmdd.

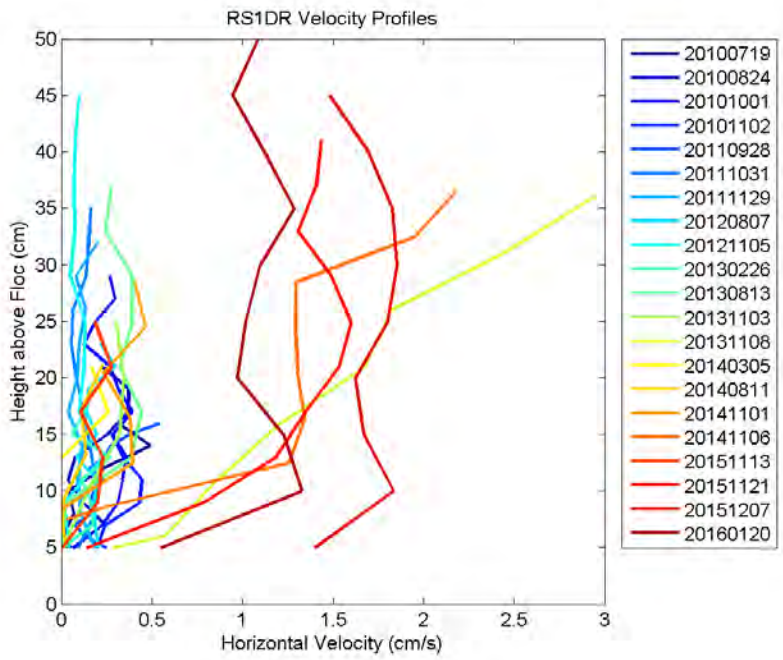

Figure C-91 All ADV velocity profiles recorded at DPM site RS1D Ridge. Horizontal velocities in cm/s are shown. Dates are given in the format yyyymmdd.

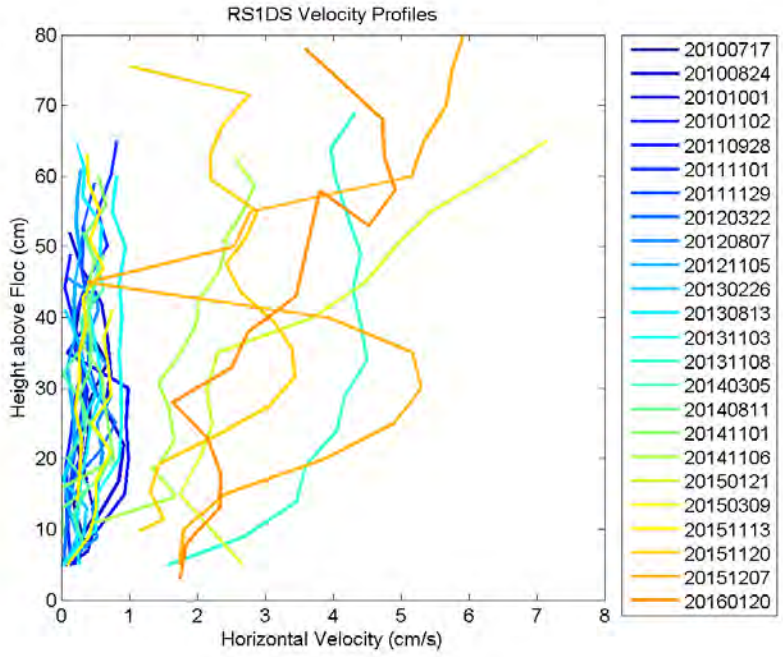

Figure C-92 All ADV velocity profiles recorded at DPM site RS1D Slough. Horizontal velocities in cm/s are shown. Dates are given in the format yyyymmdd.

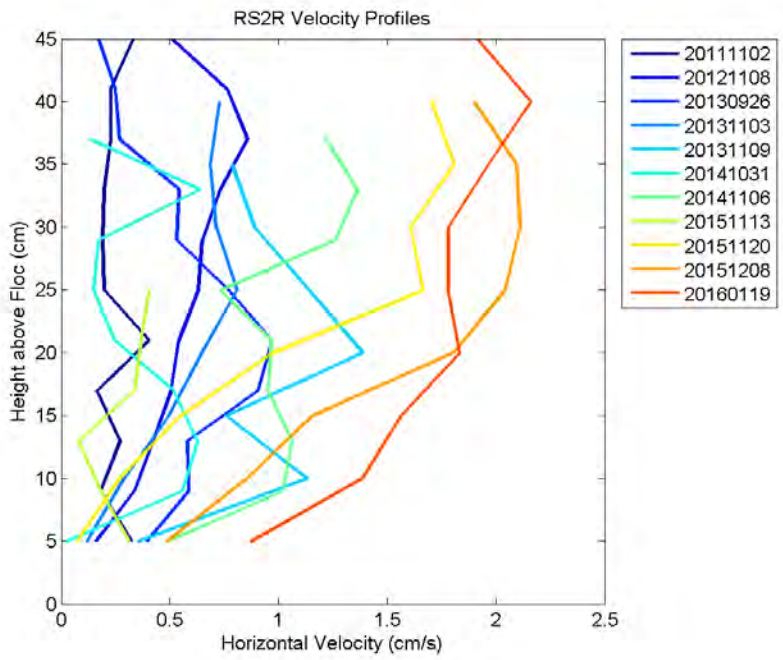

Figure C-93 All ADV velocity profiles recorded at DPM site RS2 Ridge. Horizontal velocities in cm/s are shown. Dates are given in the format yyyymmdd.

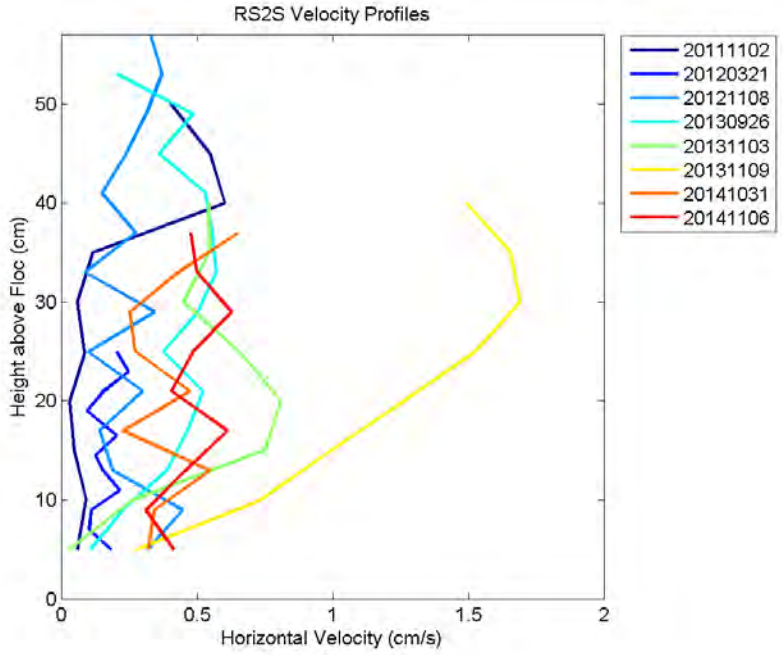

Figure C-94 All ADV velocity profiles recorded at DPM site RS2 Slough. Horizontal velocities in cm/s are shown. Dates are given in the format yyyymmdd.

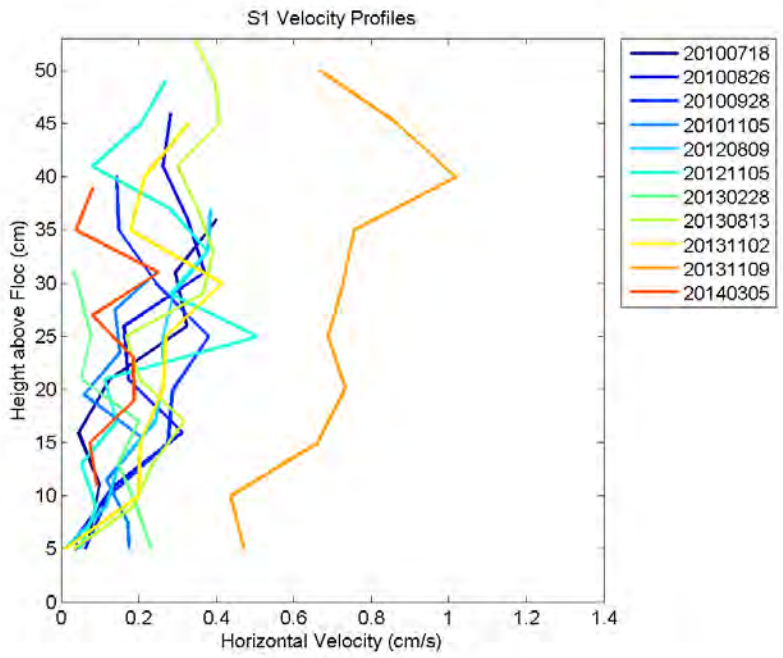

Figure C-95 All ADV velocity profiles recorded at DPM site S1. Horizontal velocities in cm/s are shown. Dates are given in the format yyyymmdd.

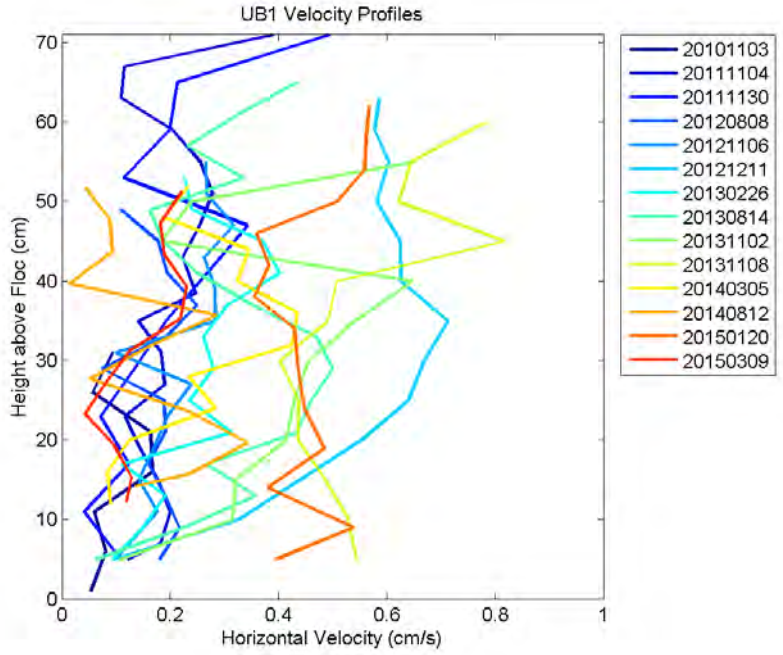

Figure C-96 All ADV velocity profiles recorded at DPM site UB1. Horizontal velocities in cm/s are shown. Dates are given in the format yyyymmdd.

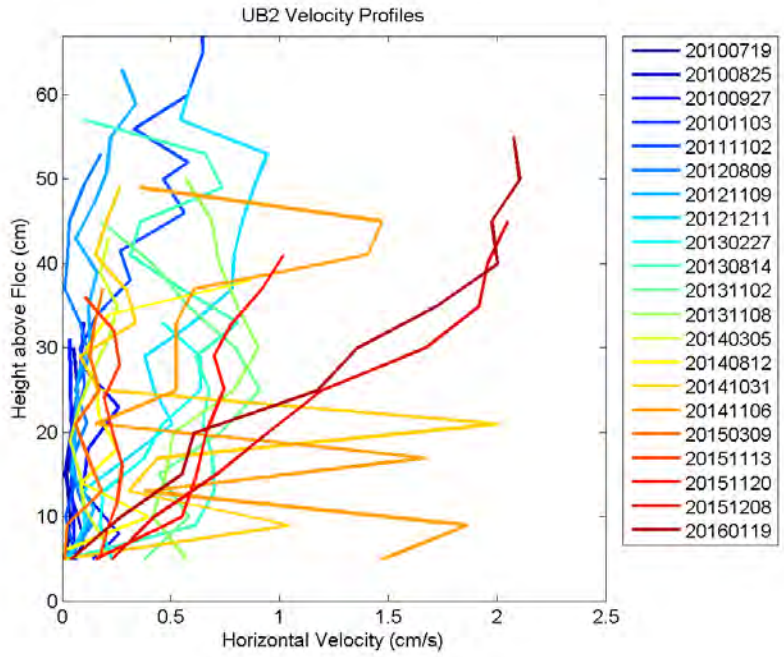

Figure C-97 All ADV velocity profiles recorded at DPM site UB2. Horizontal velocities in cm/s are shown. Dates are given in the format yyyymmdd.

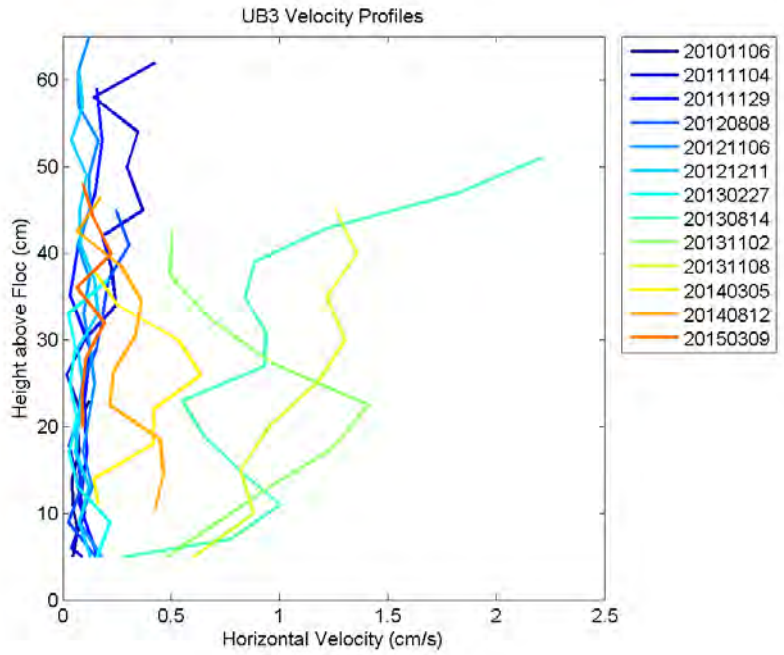

Figure C-98 All ADV velocity profiles recorded at DPM site UB3. Horizontal velocities in cm/s are shown. Dates are given in the format yyyymmdd.

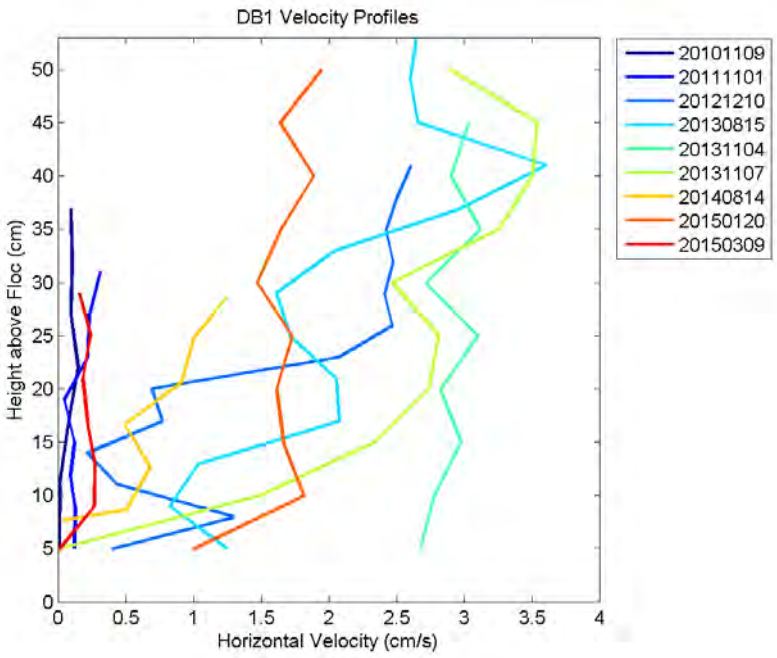

Figure C-99 All ADV velocity profiles recorded at DPM site DB1. Horizontal velocities in cm/s are shown. Dates are given in the format yyyymmdd.

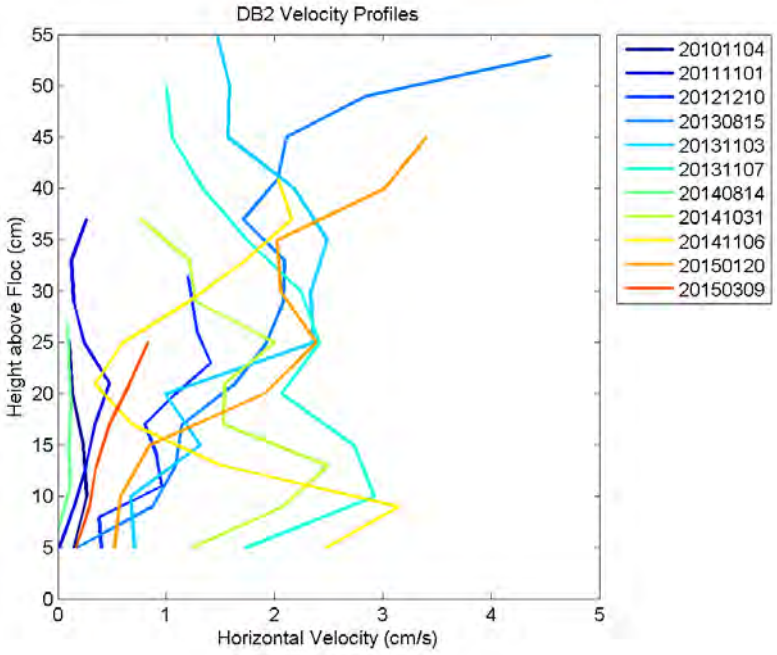

Figure C-100 All ADV velocity profiles recorded at DPM site DB2. Horizontal velocities in cm/s are shown. Dates are given in the format yyyymmdd.

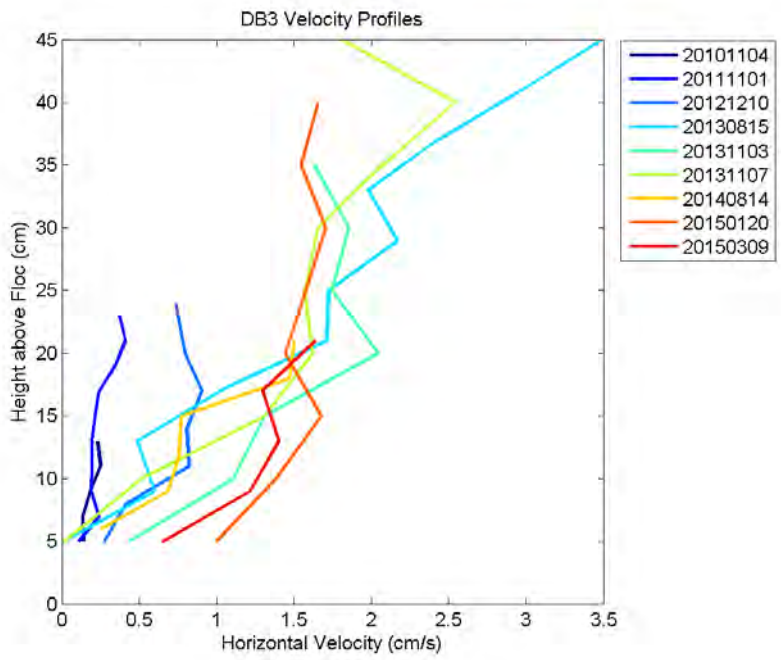

Figure C-101 All ADV velocity profiles recorded at DPM site DB3. Horizontal velocities in cm/s are shown. Dates are given in the format yyyymmdd.

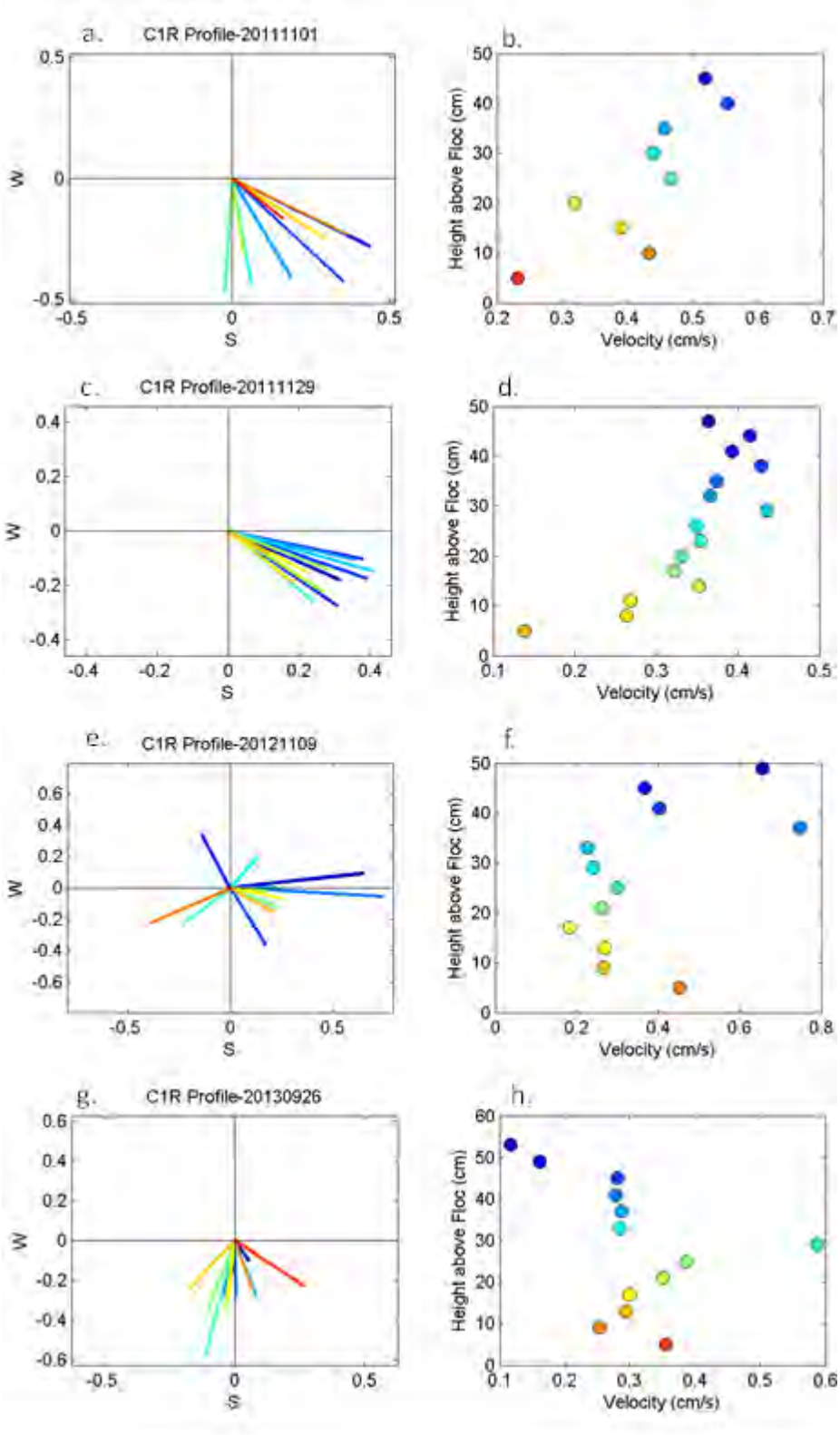
a.
C1R Profile-20111101
W
S
b.
Height above Floc (cm)
Velocity (cm/s)
c.
C1R Profile-20111129
W
S
d.
Height above Floc (cm)
Velocity (cm/s)
e.
C1R Profile-20121109
W
S
f.
Height above Floc (cm)
Velocity (cm/s)
g.
C1R Profile-20130926
W
S
h.
Height above Floc (cm)
Velocity (cm/s)

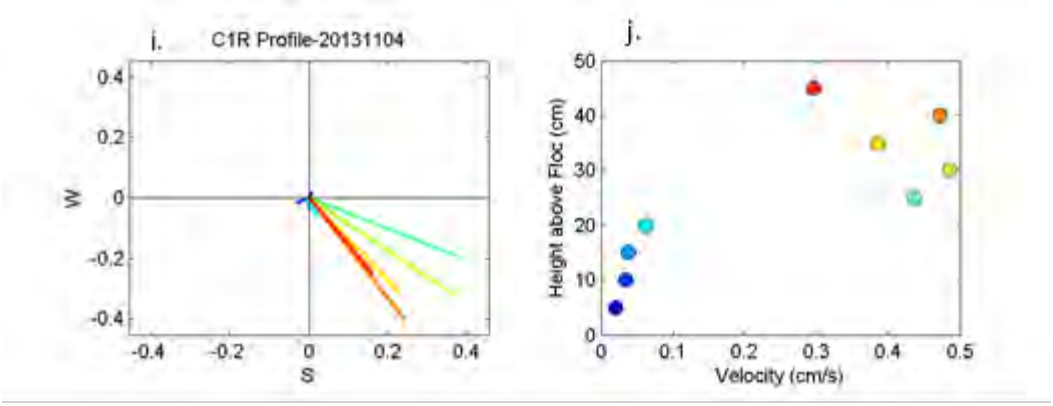

Figure C-102 ADV velocity profiles recorded at DPM site C1 Ridge. Profiles recorded on (a-b) Nov. 01, 2011, (c-d) Nov. 29, 2011, (e-f) Nov. 09, 2012, (g-h) Sept. 26, 2013, (i-j) Nov. 04, 2013. Panels (a), (c), (e), (g) and (i) show velocity vectors (cm/s) with the axes representing cardinal directions, such that the top of the plot is true north. Panels (b), (d), (f), (h) and (j) show horizontal velocities (cm/s). Dates are given in the format yyyymmdd.

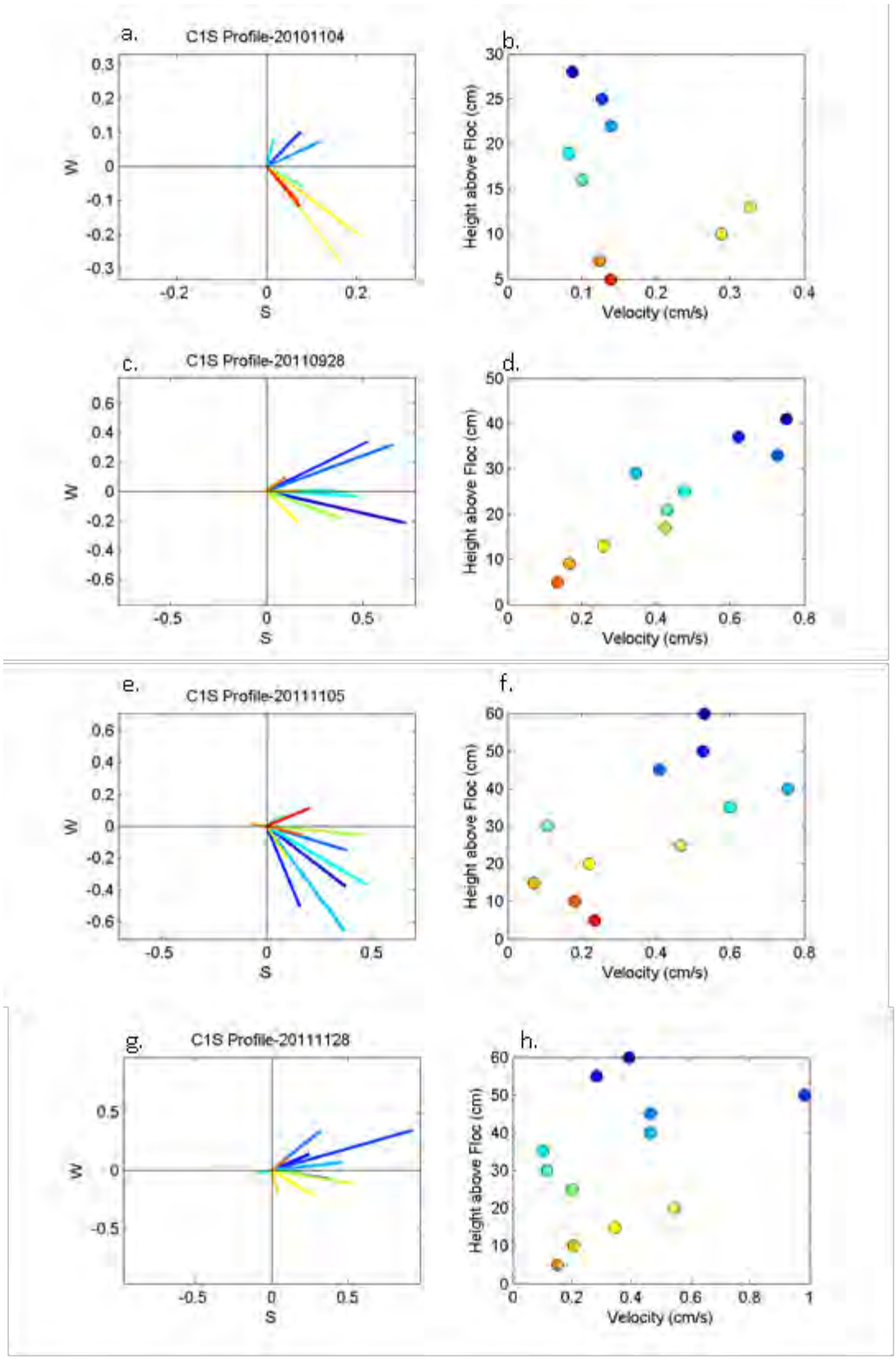
a.
C1S Profile-20101104
W
S
b.
Height above Floc (cm)
Velocity (cm/s)
c.
C1S Profile-20110928
W
S
d.
Height above Floc (cm)
Velocity (cm/s)
e.
C1S Profile-20111105
W
S
f.
Height above Floc (cm)
Velocity (cm/s)
g.
C1S Profile-20111128
W
S
h.
Height above Floc (cm)
Velocity (cm/s)

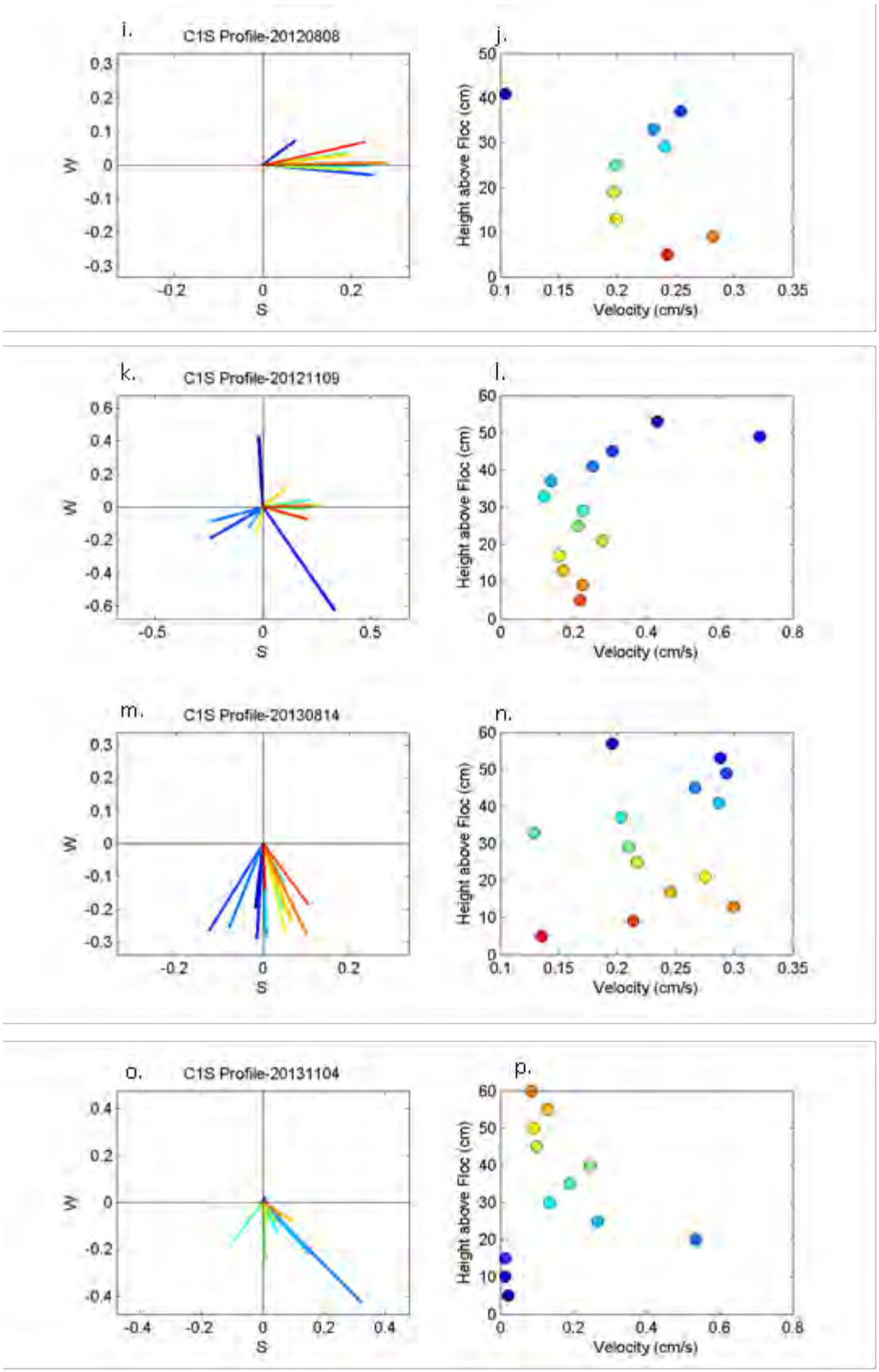
i.
C1S Profile-20120808
W
S
j.
Height above Floc (cm)
Velocity (cm/s)
k.
C1S Profile-20121109
W
S
l.
Height above Floc (cm)
Velocity (cm/s)
m.
C1S Profile-20130814
W
S
n.
Height above Floc (cm)
Velocity (cm/s)
o.
C1S Profile-20131104
W
S
p.
Height above Floc (cm)
Velocity (cm/s)

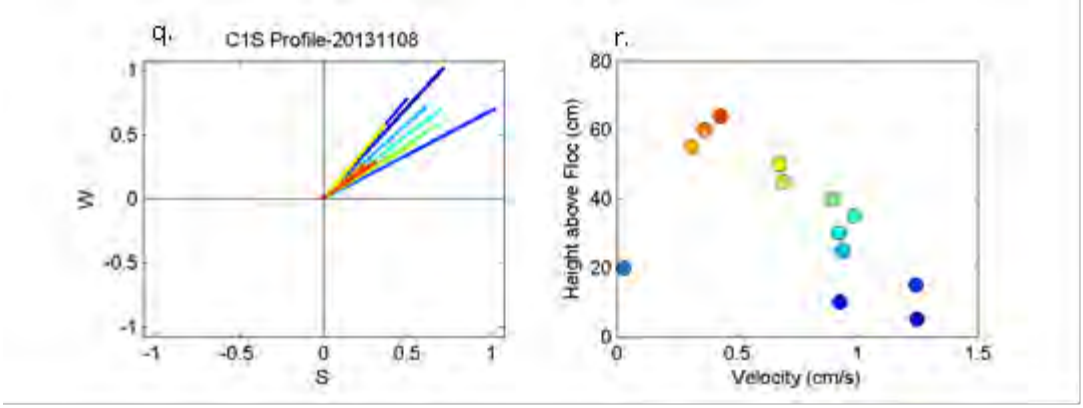

Figure C-103 ADV velocity profiles recorded at DPM site C1 Slough. Profiles recorded on (a-b) Nov. 04, 2010, (c-d) Sep. 28, 2011, (e-f) Nov. 5, 2011, (g-h) Nov. 28, 2011, (i-j) Aug. 8, 2012, (k-l) Nov. 9, 2012, (m-n) Aug. 14, 2013, (o-p) Nov. 04, 2013, (q-r) Nov. 8, 2013. Panels (a), (c), (e), (g), (i), (k), (m), (o) and (q) show velocity vectors (cm/s) with the axes representing cardinal directions, such that the top of the plot is true north. Panels (b), (d), (f), (h), (j), (l), (n), (p) and (r) show horizontal velocities (cm/s). Dates are given in the format yyyymmdd.

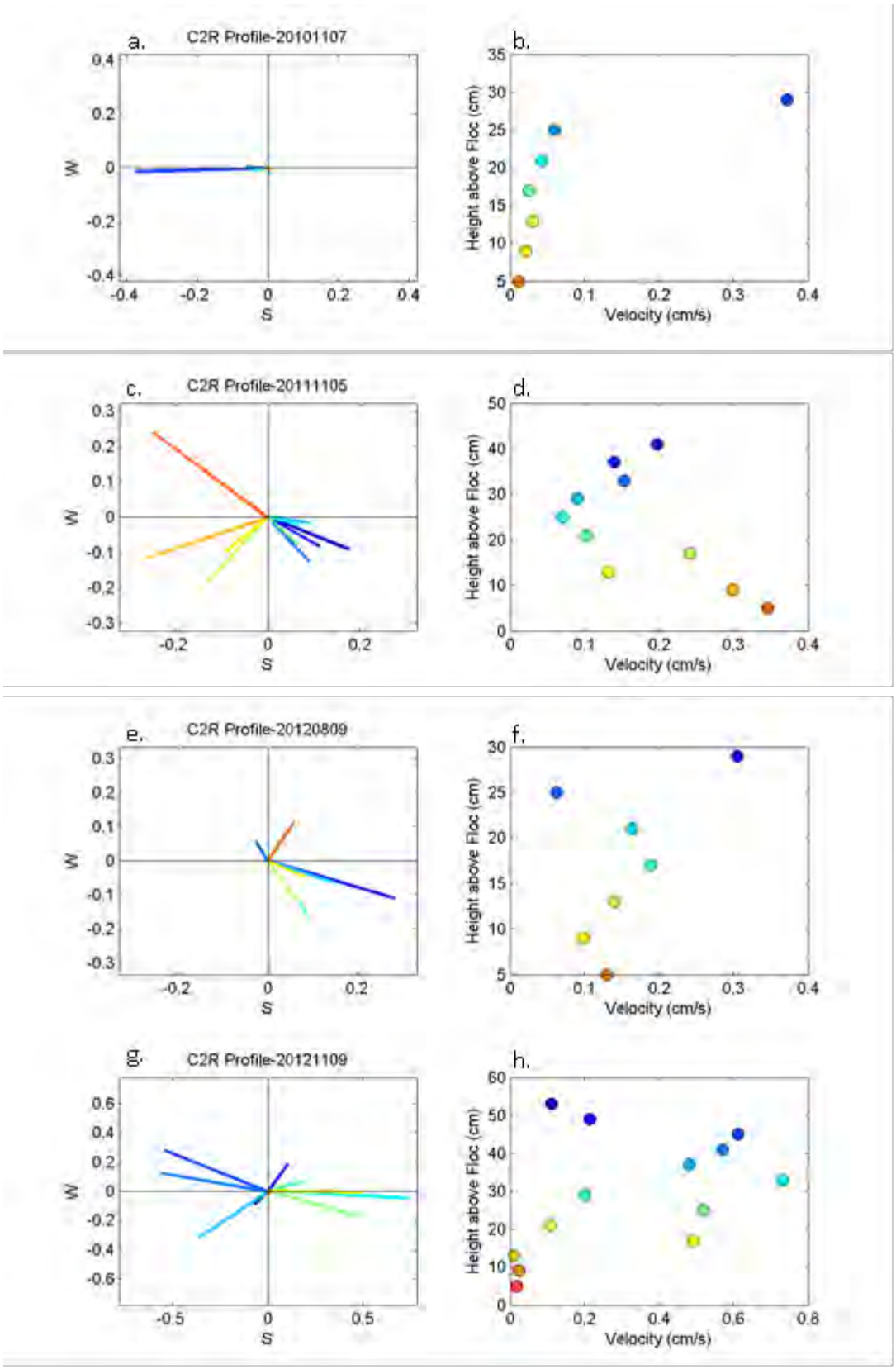
a.
C2R Profile-20101107
W
S
b.
Height above Floc (cm)
Velocity (cm/s)
c.
C2R Profile-20111105
W
S
d.
Height above Floc (cm)
Velocity (cm/s)
e.
C2R Profile-20120809
W
S
f.
Height above Floc (cm)
Velocity (cm/s)
g.
C2R Profile-20121109
W
S
h.
Height above Floc (cm)
Velocity (cm/s)

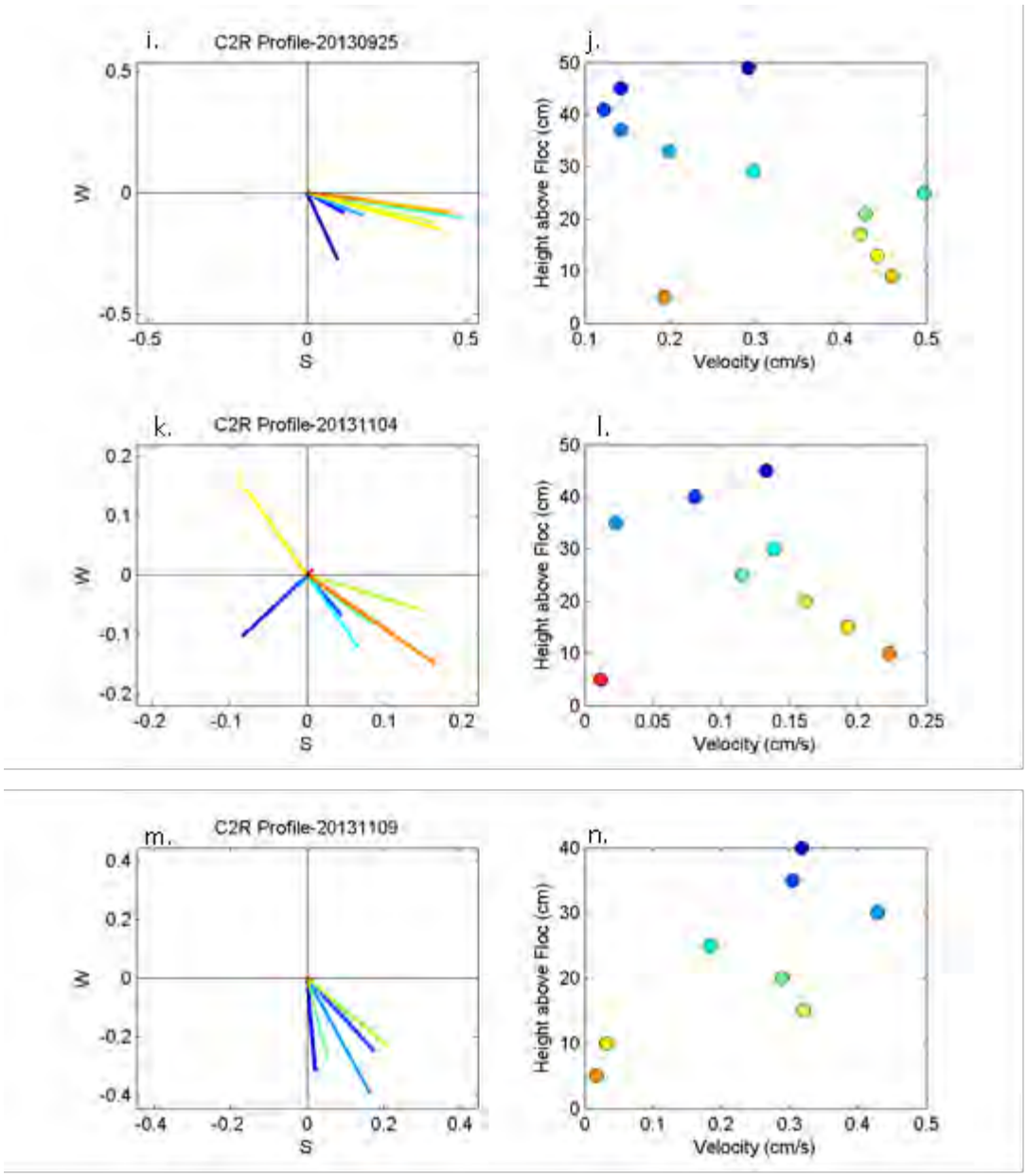

Figure C-104 ADV velocity profiles recorded at DPM site C2 Ridge. Profiles recorded on (a-b) Nov. 7, 2010, (c-d) Nov. 5, 2011, (e-f) Aug. 9, 2012, (g-h) Nov. 9, 2012, (i-j) Sep. 25, 2013, (k-l) Nov. 4, 2013, and (m-n) Nov. 9, 2013. Panels (a), (c), (e), (g), (i), (k), and (m) show velocity vectors (cm/s) with the axes representing cardinal directions, such that the top of the plot is true north. Panels (b), (d), (f), (h), (j), (l), and (n) show horizontal velocities (cm/s). Dates are given in the format yyyymmdd.

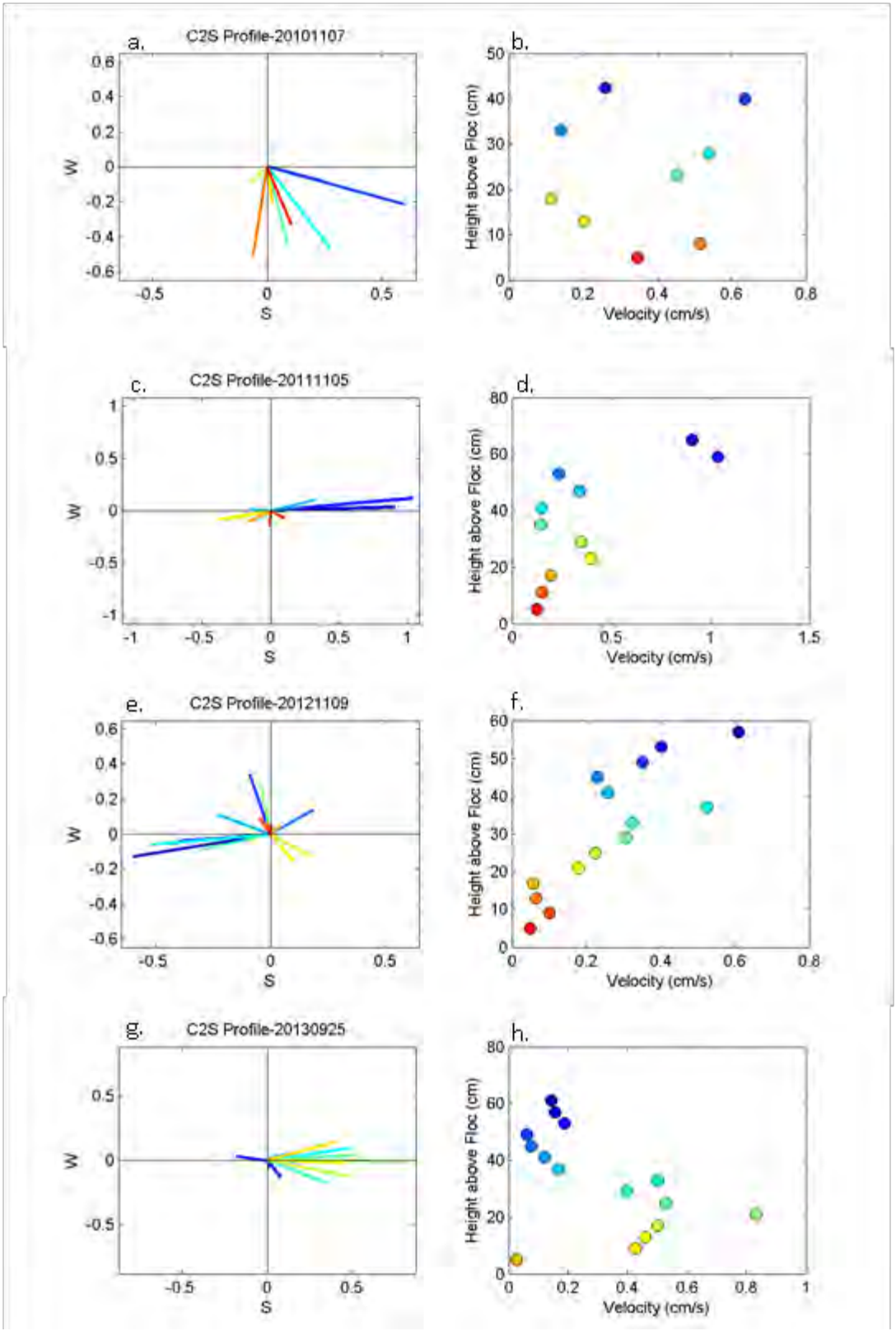
a.
C2S Profile-20101107
W
S
b.
Height above Floc (cm)
Velocity (cm/s)
c.
C2S Profile-20111105
d.
e.
C2S Profile-20121109
f.
g.
C2S Profile-20130925
h.

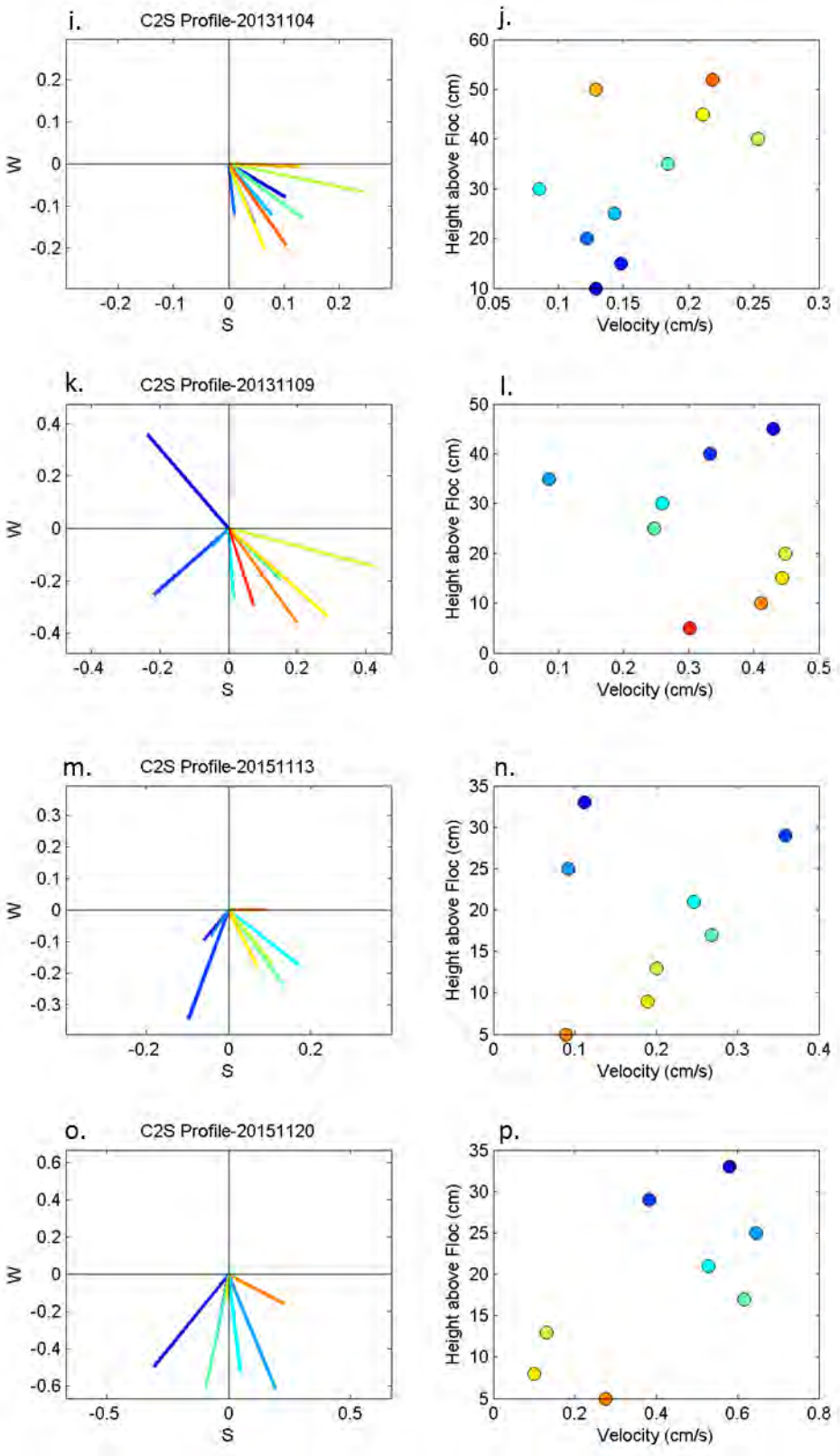
i.
C2S Profile-20131104
W
S
j.
Height above Floc (cm)
Velocity (cm/s)
k.
C2S Profile-20131109
W
S
l.
Height above Floc (cm)
Velocity (cm/s)
m.
C2S Profile-20151113
W
S
n.
Height above Floc (cm)
Velocity (cm/s)
o.
C2S Profile-20151120
W
S
p.
Height above Floc (cm)
Velocity (cm/s)

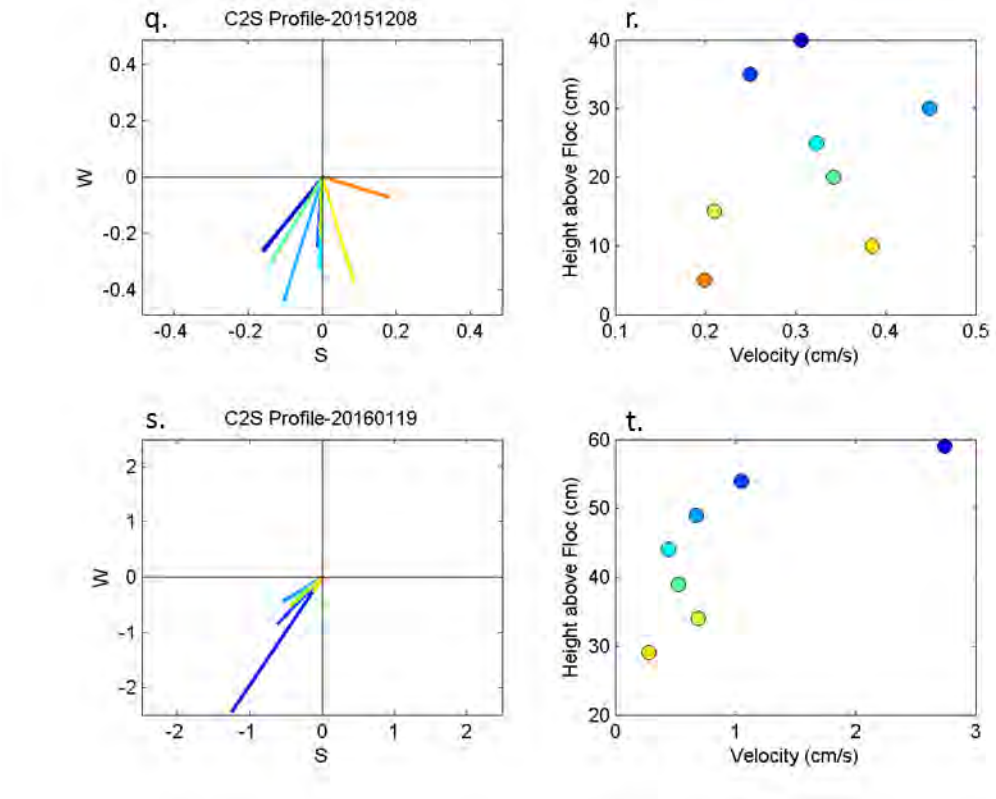

Figure C-105 ADV velocity profiles recorded at DPM site C2 Slough. Profiles recorded on (a-b) Nov. 7, 2010, (c-d) Nov. 5, 2011, (e-f) Nov. 9, 2012, (g-h) Sep. 25, 2013, (i-j) Nov. 4, 2013, (k-l) Nov. 9, 2013, (m-n) Nov. 13, 2015, (o-p) Nov. 20, 2015, (q-r) Dec. 8, 2015, and (s-t) Jan. 19, 2016. Panels (a), (c), (e), (g), (i), (k), (m), (o), (q) and (s) show velocity vectors (cm/s) with the axes representing cardinal directions, such that the top of the plot is true north. Panels (b), (d), (f), (h), (j), (l), (n), (p), (r) and (t) show horizontal velocities (cm/s). Dates are given in the format yyyymmdd.

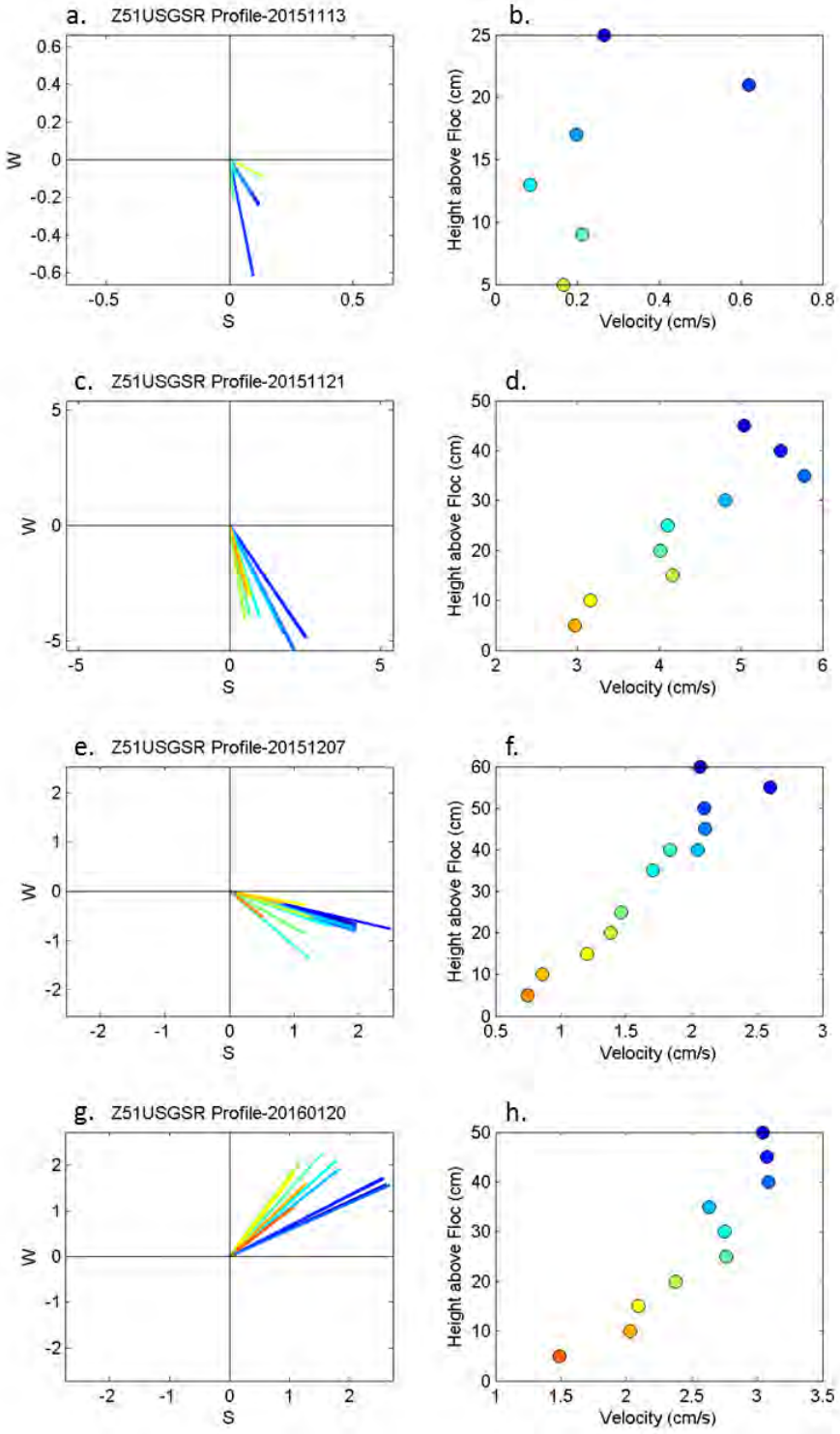

Figure C-106 ADV velocity profiles recorded at DPM site Z51_USGS Ridge. Profiles recorded on (a-b) Nov. 13, 2015, (c-d) Nov. 21, 2015, (e-f) Dec. 7, 2015, and (g-h) Jan. 20, 2016. Panels (a), (c), (e), and (g) show velocity vectors (cm/s) with the axes representing cardinal directions, such that the top of the plot is true north. Panels (b), (d), (f), and (h) show horizontal velocities (cm/s). Dates are given in the format yyyymmdd.

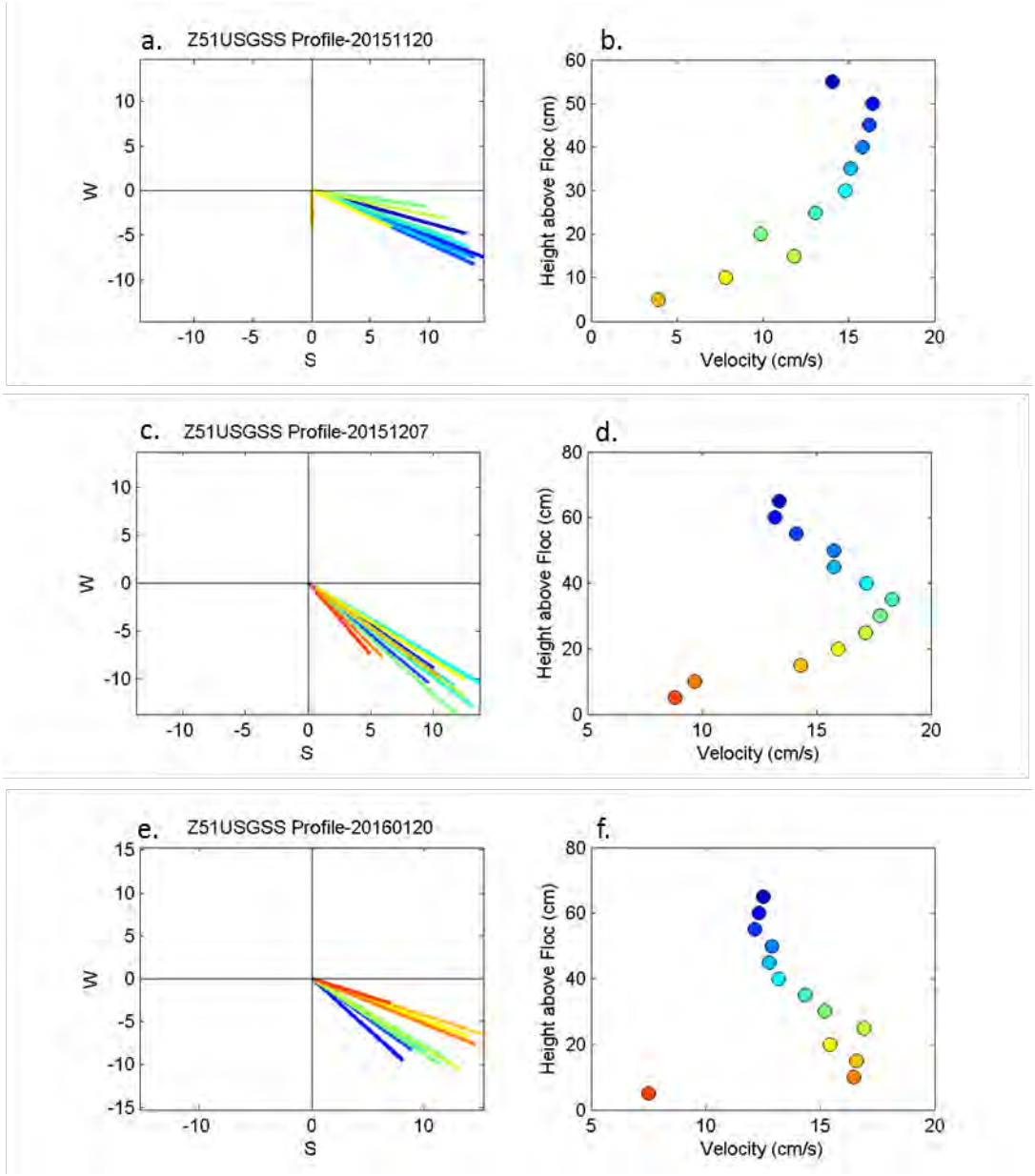

Figure C-107 ADV velocity profiles recorded at DPM site Z51_USGS Slough. Profiles recorded on (a-b) Nov. 20, 2015, (c-d) Dec. 7, 2015, and (e-f) Jan. 20, 2016. Panels (a), (c), and (e) show velocity vectors (cm/s) with the axes representing cardinal directions, such that the top of the plot is true north. Panels (b), (d), and (f) show horizontal velocities (cm/s). Dates are given in the format yyyymmdd.

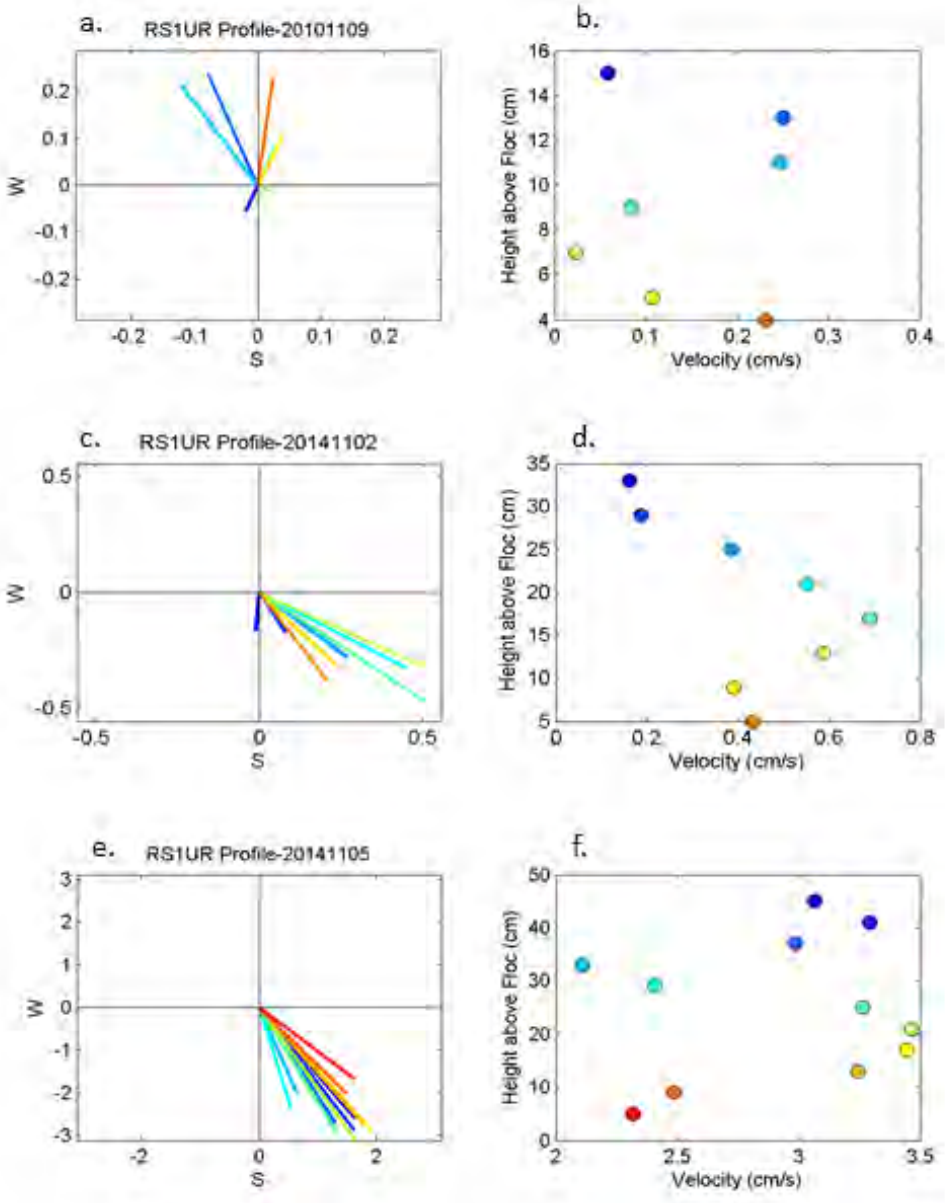

Figure C-108 ADV velocity profiles recorded at site RS1U Ridge. Profiles recorded on (a-b) Nov. 9, 2010, (c-d) Nov. 2, 2014 and (e-f) Nov. 5, 2014. Panels (a), (c), and (e) show velocity vectors (cm/s) with the axes representing cardinal directions, such that the top of the plot is true north. Panels (b), (d) and (f) show horizontal velocities (cm/s). Dates are given in the format yyyymmdd.

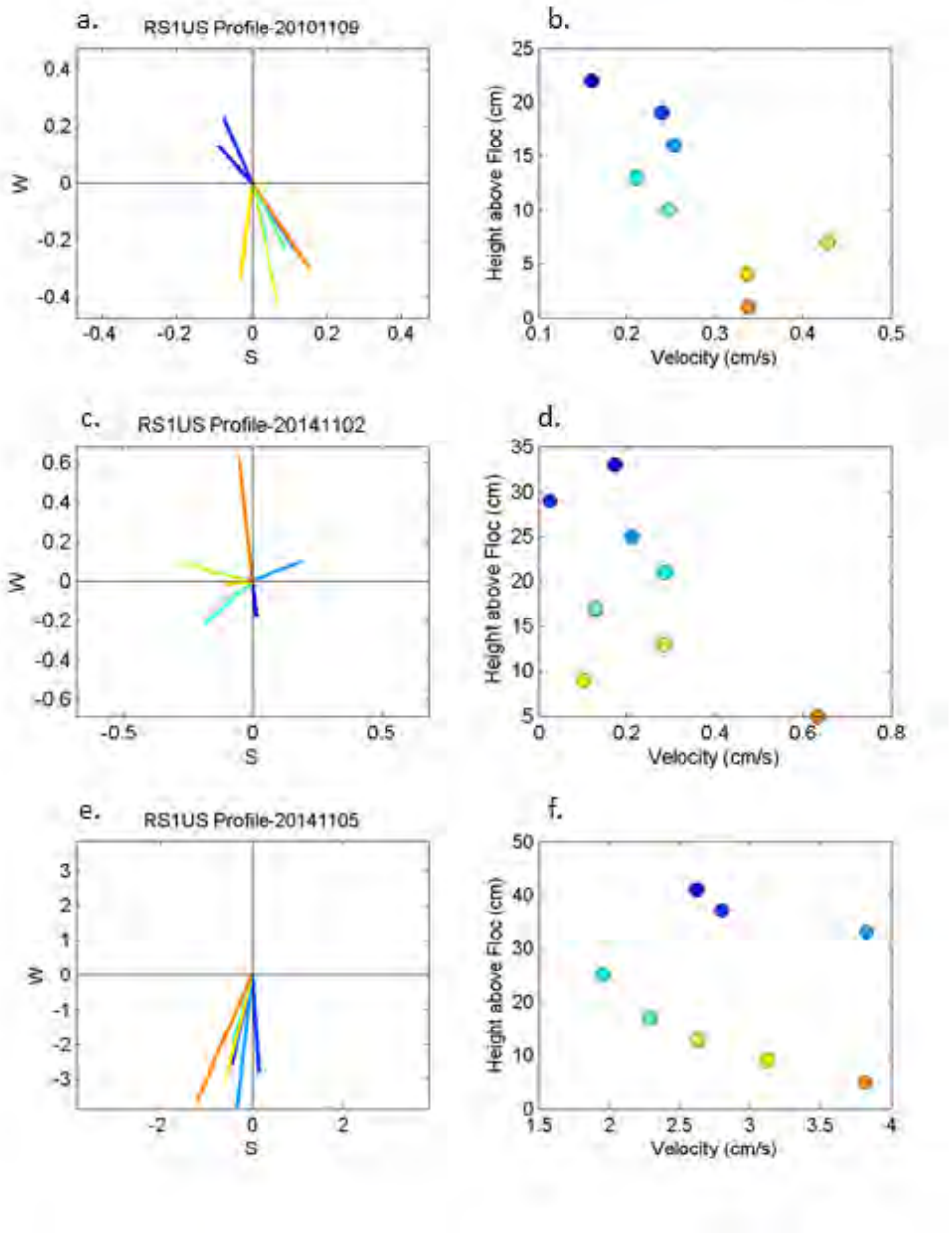

Figure C-109 ADV velocity profiles recorded at site RS1U Slough. Profiles recorded on (a-b) Nov. 9, 2010, (c-d) Nov. 2, 2014 and (e-f) Nov. 5, 2014. Panels (a), (c), and (e) show velocity vectors (cm/s) with the axes representing cardinal directions, such that the top of the plot is true north. Panels (b), (d) and (f) show horizontal velocities (cm/s). Dates are given in the format yyyymmdd.

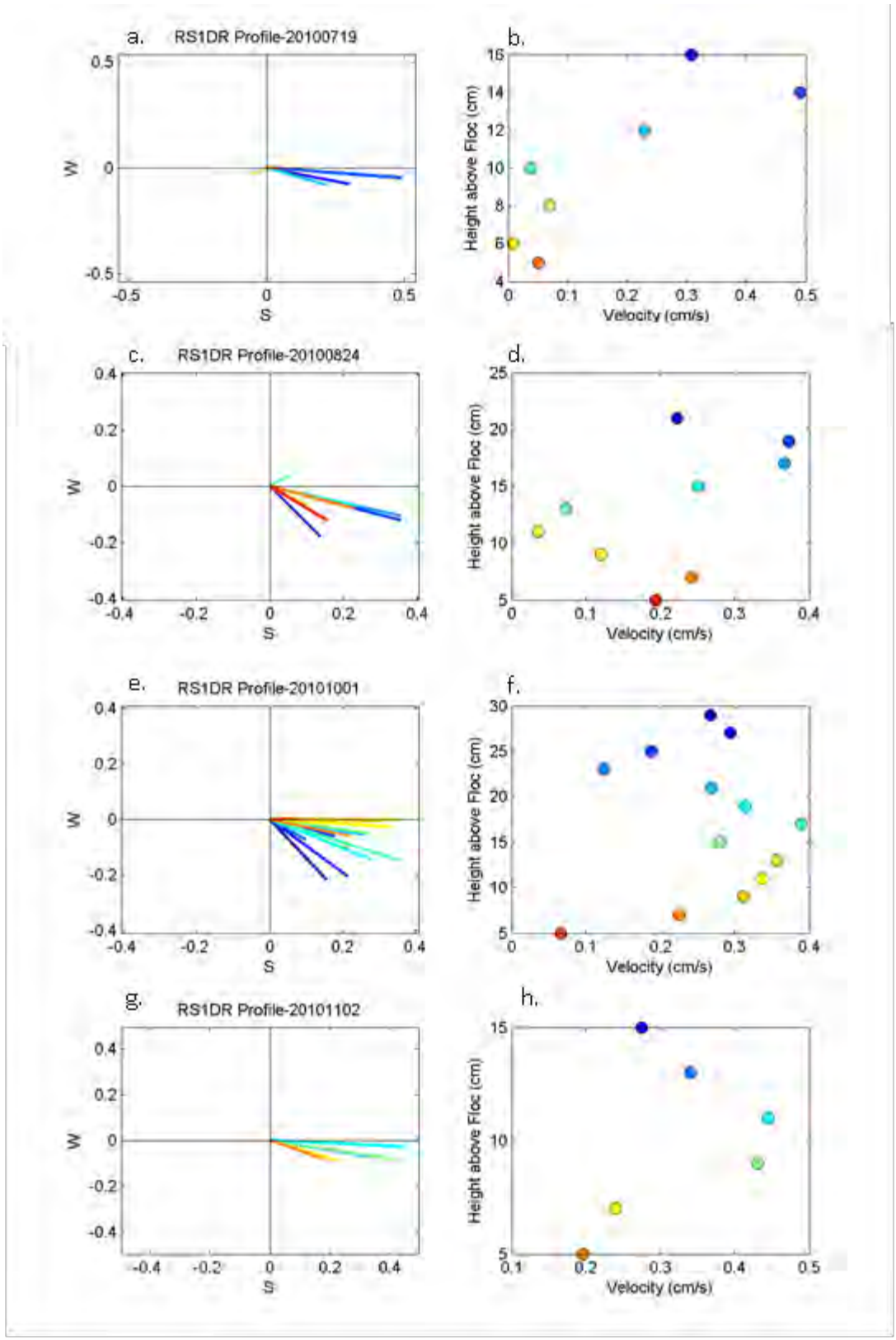
a.
RS1DR Profile-20100719
W
S
b.
Height above Floc (cm)
Velocity (cm/s)
c.
RS1DR Profile-20100824
d.
e.
RS1DR Profile-20101001
f.
g.
RS1DR Profile-20101102
h.

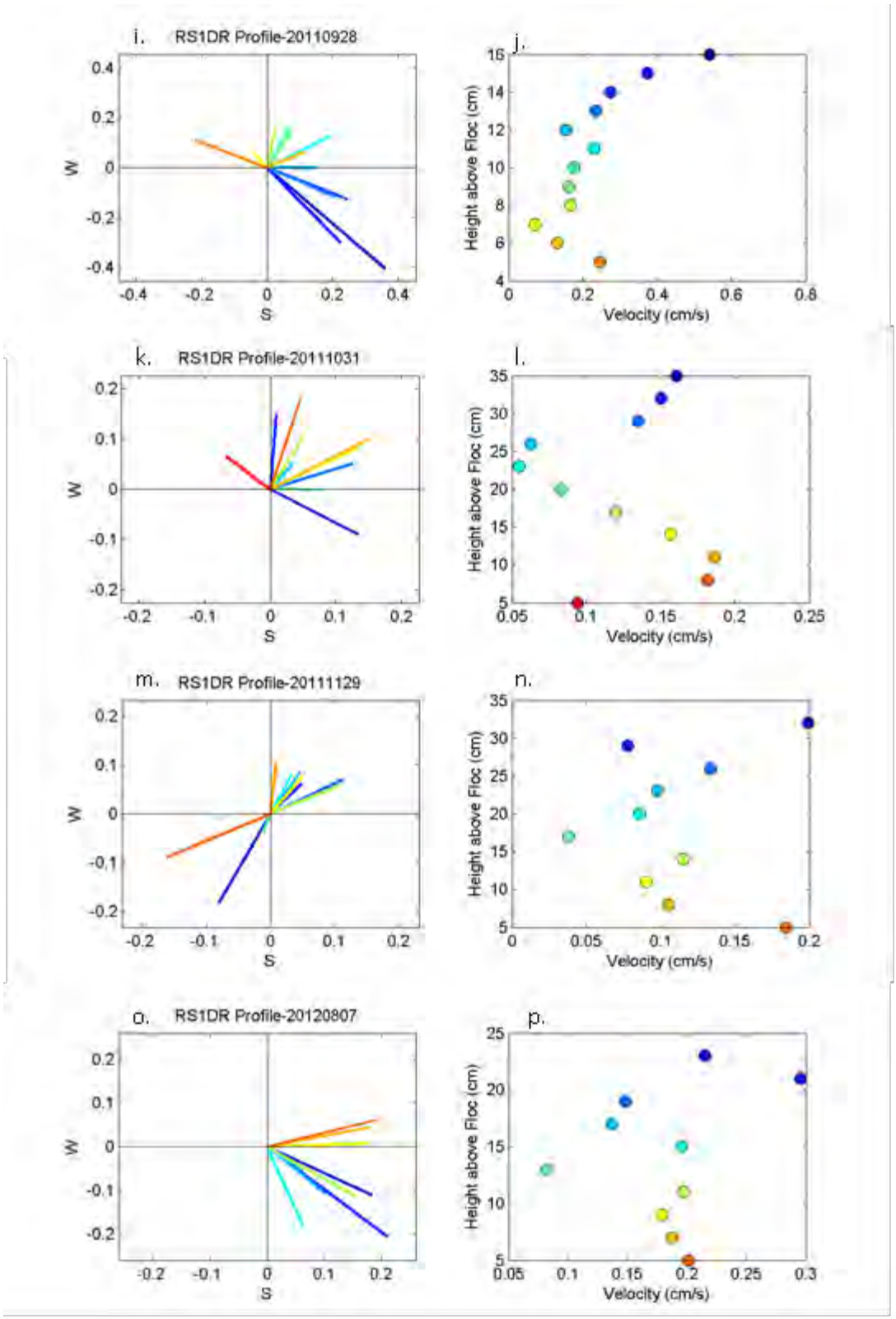
i.
RS1DR Profile-20110928
W
S
j.
Height above Floc (cm)
Velocity (cm/s)
k.
RS1DR Profile-20111031
W
S
l.
Height above Floc (cm)
Velocity (cm/s)
m.
RS1DR Profile-20111129
W
S
n.
Height above Floc (cm)
Velocity (cm/s)
o.
RS1DR Profile-20120807
W
S
p.
Height above Floc (cm)
Velocity (cm/s)

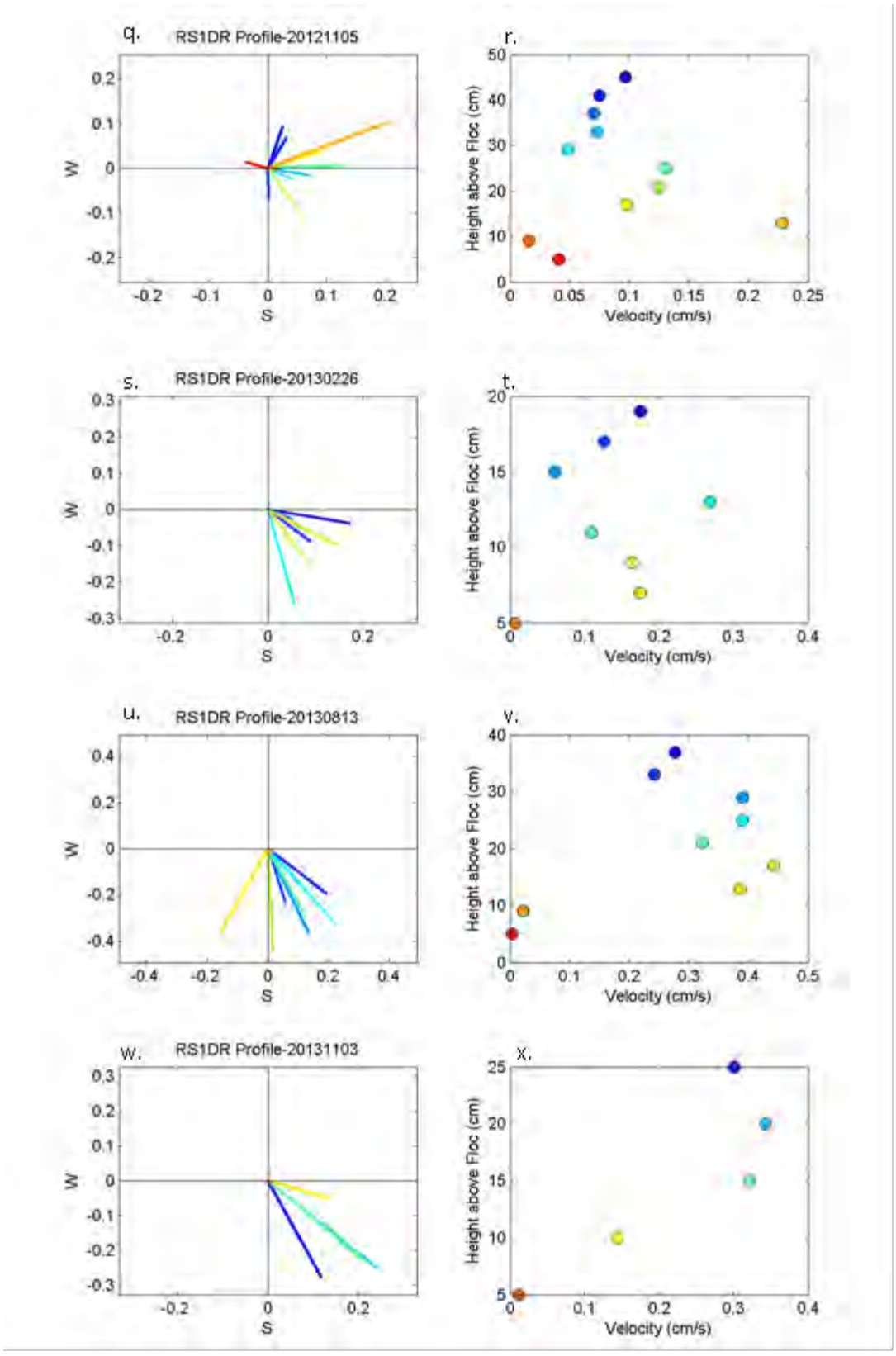
q.
RS1DR Profile-20121105
W
S
r.
Height above Floc (cm)
Velocity (cm/s)
s.
RS1DR Profile-20130226
W
S
t.
Height above Floc (cm)
Velocity (cm/s)
u.
RS1DR Profile-20130813
W
S
v.
Height above Floc (cm)
Velocity (cm/s)
w.
RS1DR Profile-20131103
W
S
x.
Height above Floc (cm)
Velocity (cm/s)

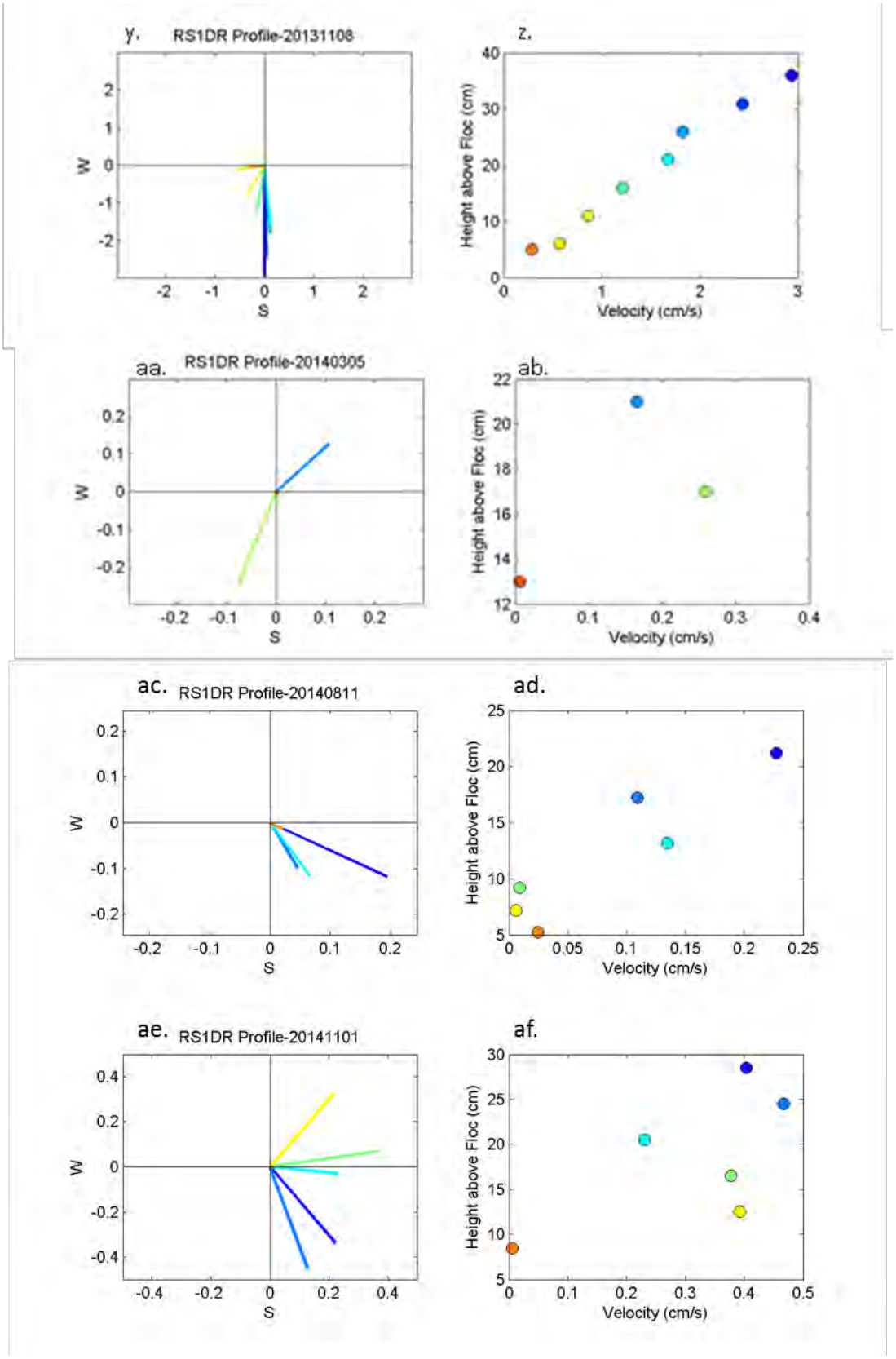
y.
RS1DR Profile-20131108
W
S
z.
Height above Floc (cm)
Velocity (cm/s)
aa.
RS1DR Profile-20140305
ab.
ac.
RS1DR Profile-20140811
ad.
ae.
RS1DR Profile-20141101
af.

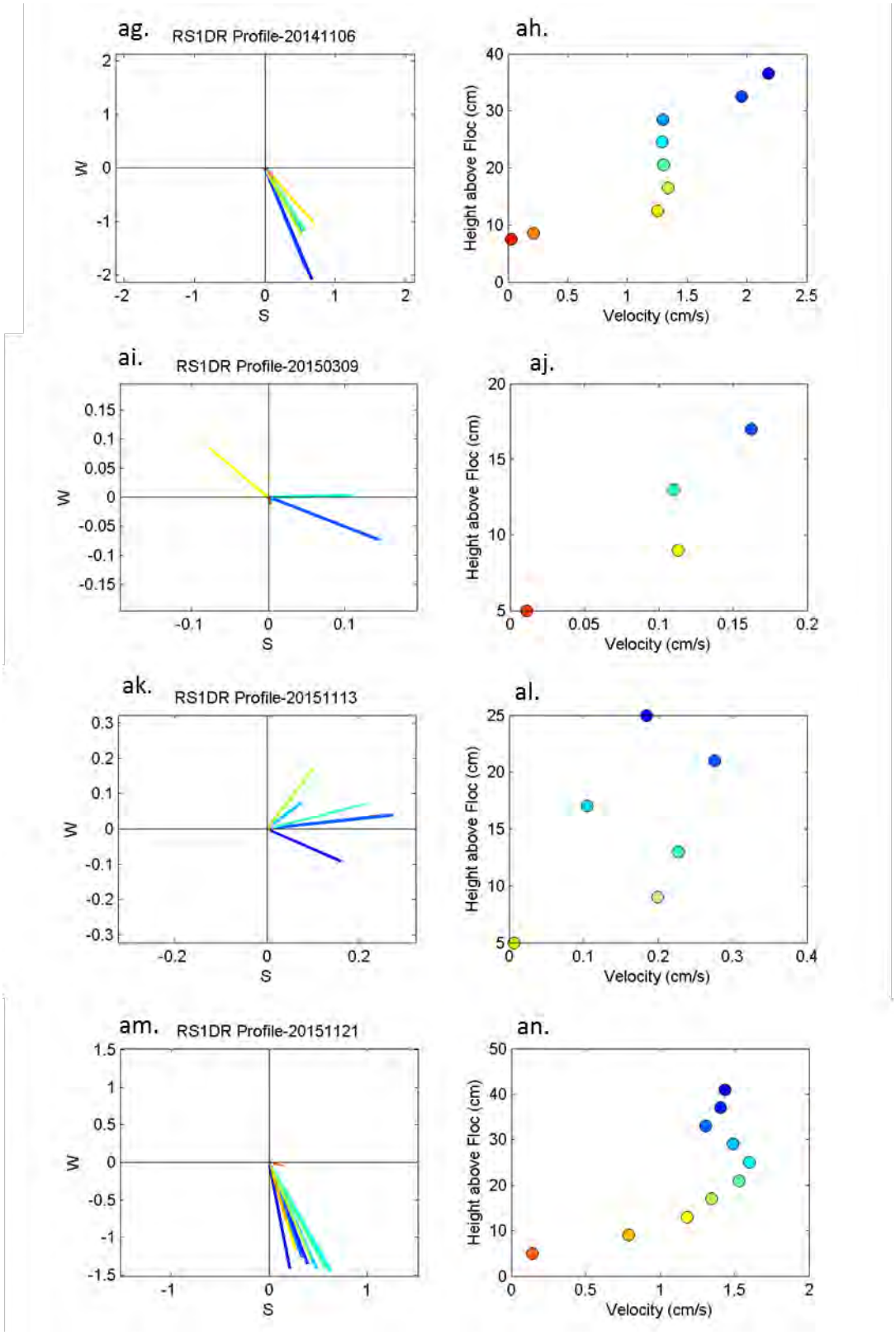
ag.
RS1DR Profile-20141106
W
S
ah.
Height above Floc (cm)
Velocity (cm/s)
ai.
RS1DR Profile-20150309
aj.
ak.
RS1DR Profile-20151113
al.
am.
RS1DR Profile-20151121
an.

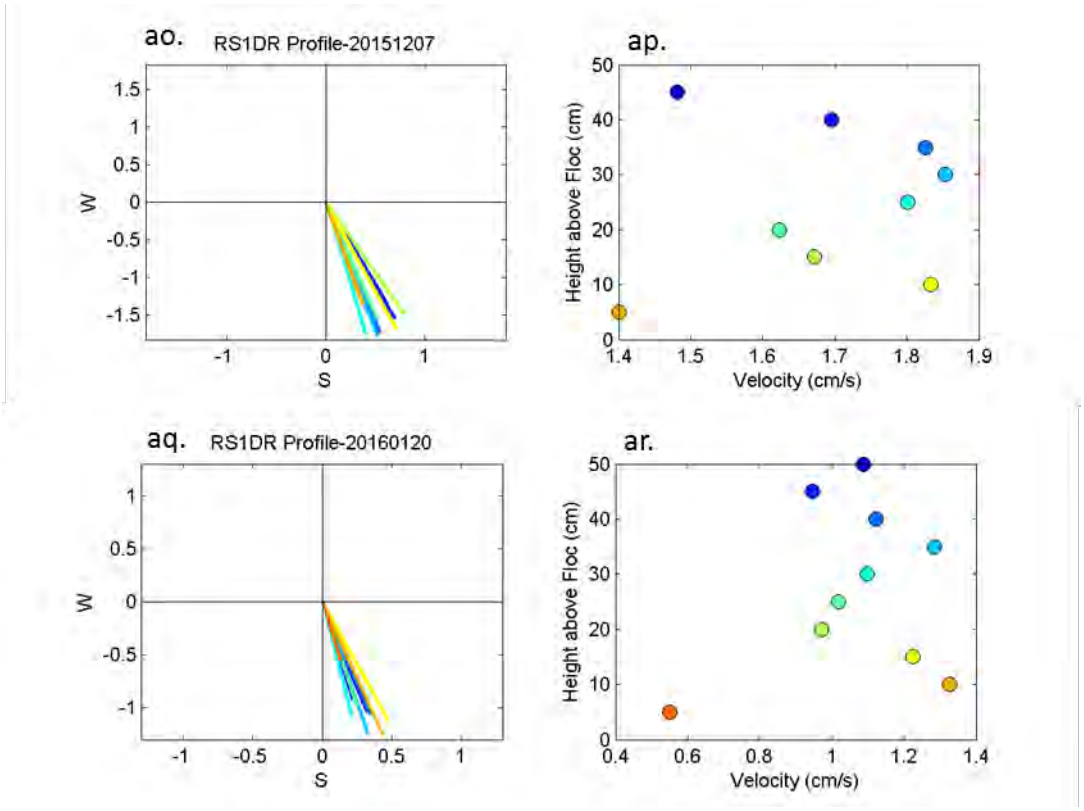

Figure C-110 ADV velocity profiles recorded at site RS1D Ridge. Profiles recorded on (a-b) Jul. 19, 2010, (c-d) Aug. 24, 2010, (e-f) Oct. 1, 2010, (g-h) Nov. 2, 2010, (i-j) Sep. 28, 2011, (k-l) Oct. 31, 2011, (m-n) Nov. 29, 2011, (o-p) Aug. 7, 2012, (q-r) Nov. 5, 2012, and (s-t) Feb. 26, 2013, (u-v), Aug. 13, 2013, (w-x) Nov. 03, 2013, (y-z) Nov. 8, 2013, (aa-ab) Mar. 5, 2014, (ac-ad), Aug. 11, 2014, (ae-af), Nov.1, 2014, (ag-ah) Nov. 6 2014, (ai-aj) Mar. 9, 2015, (ak-al) Nov. 13, 2015, (am-an) Nov. 21, 2015, (ao-ap) Dec. 7, 2015, and (aq-ar) Jan 20, 2016. Panels (a), (c), (e), (g), (i), (k), (m), (o), (q), (s), (u), (w), (y), (aa), (ac), (ae), (ag), (ai), (ak), (am), (ao) and (aq) show velocity vectors (cm/s) with the axes representing cardinal directions, such that the top of the plot is true north. Panels (b), (d), (f), (h), (j), (l), (n), (p), (r), (t), (v), (x), (z), (ab), (ad), (af), (ah), (aj), (al), (an), (ap), and (ar) show horizontal velocities (cm/s). Dates are given in the format yyyymmdd.

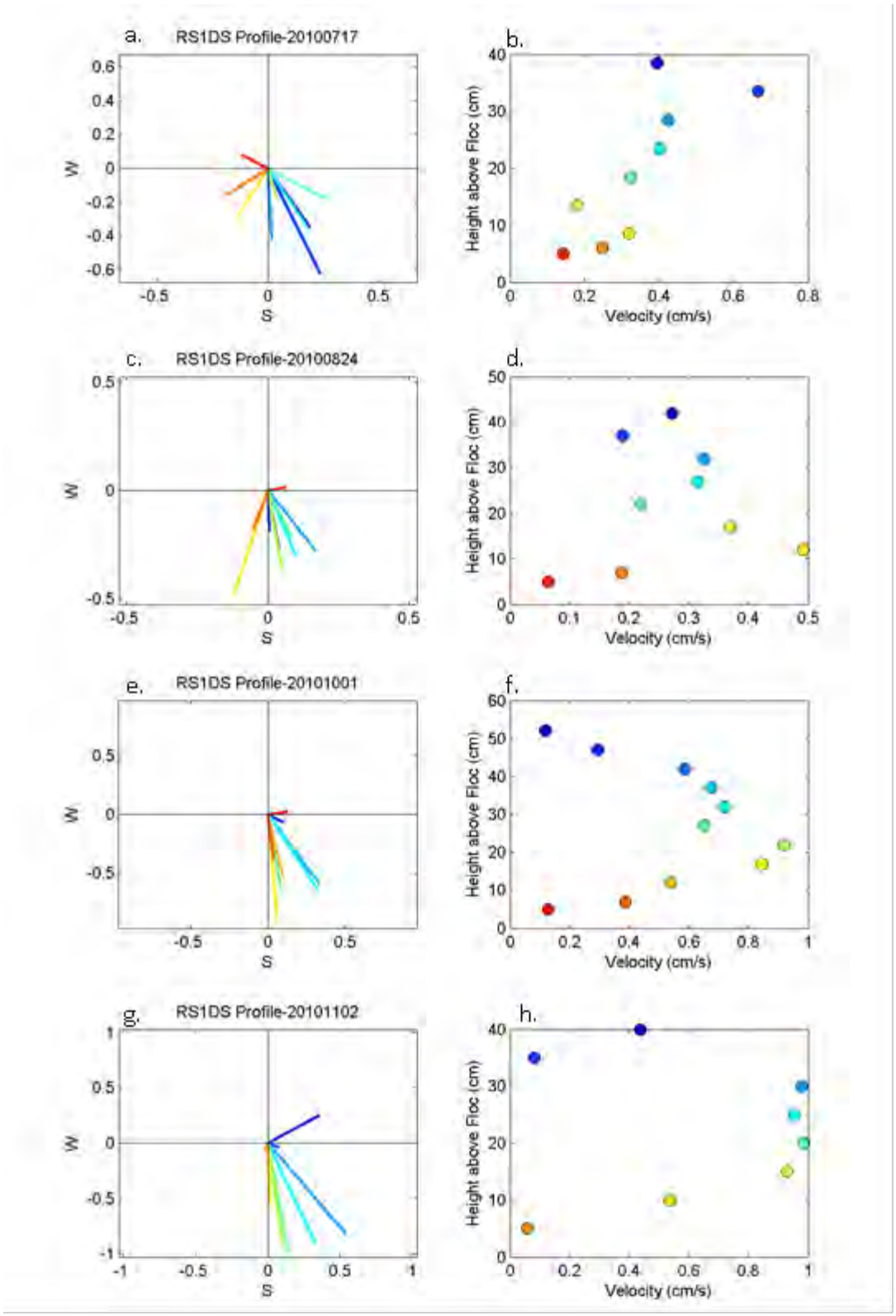
a.
RS1DS Profile-20100717
W
S
b.
Height above Floc (cm)
Velocity (cm/s)
c.
RS1DS Profile-20100824
d.
e.
RS1DS Profile-20101001
f.
g.
RS1DS Profile-20101102
h.

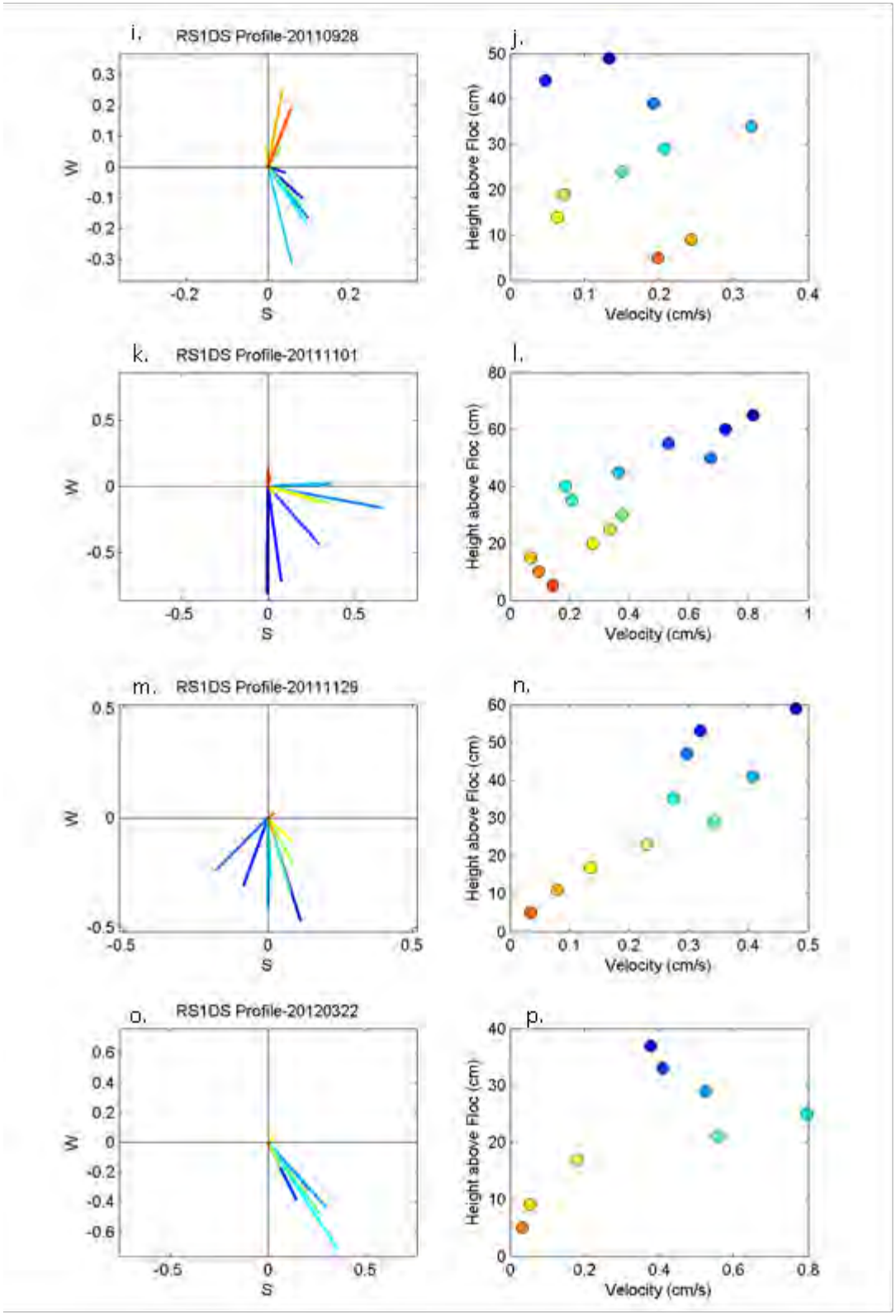
i.
RS1DS Profile-20110928
W
S
j.
Height above Floc (cm)
Velocity (cm/s)
k.
RS1DS Profile-20111101
l.
m.
RS1DS Profile-20111129
n.
o.
RS1DS Profile-20120322
p.

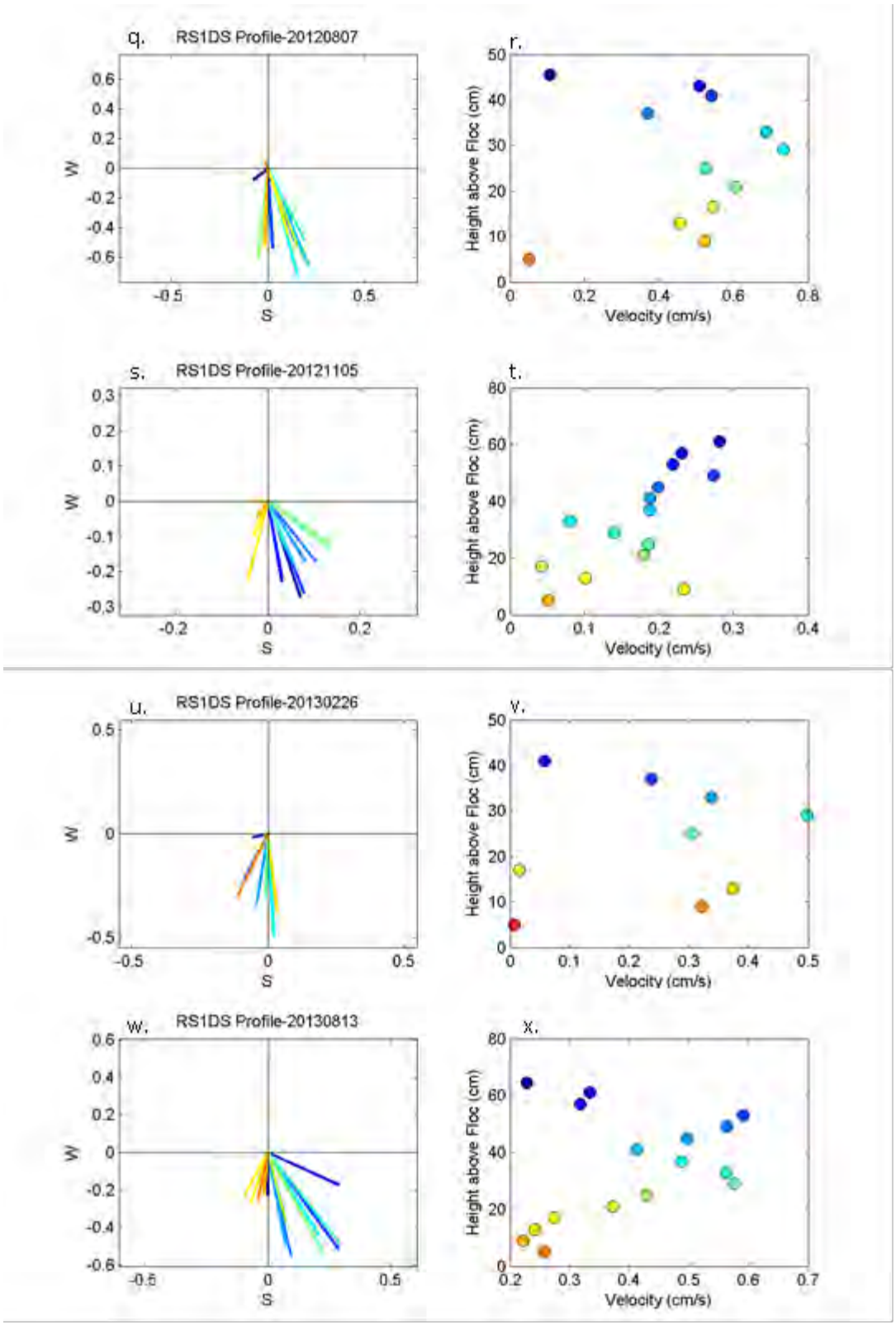
q.
RS1DS Profile-20120807
W
S
r.
Height above Floc (cm)
Velocity (cm/s)
s.
RS1DS Profile-20121105
W
S
t.
Height above Floc (cm)
Velocity (cm/s)
u.
RS1DS Profile-20130226
W
S
v.
Height above Floc (cm)
Velocity (cm/s)
w.
RS1DS Profile-20130813
W
S
x.
Height above Floc (cm)
Velocity (cm/s)

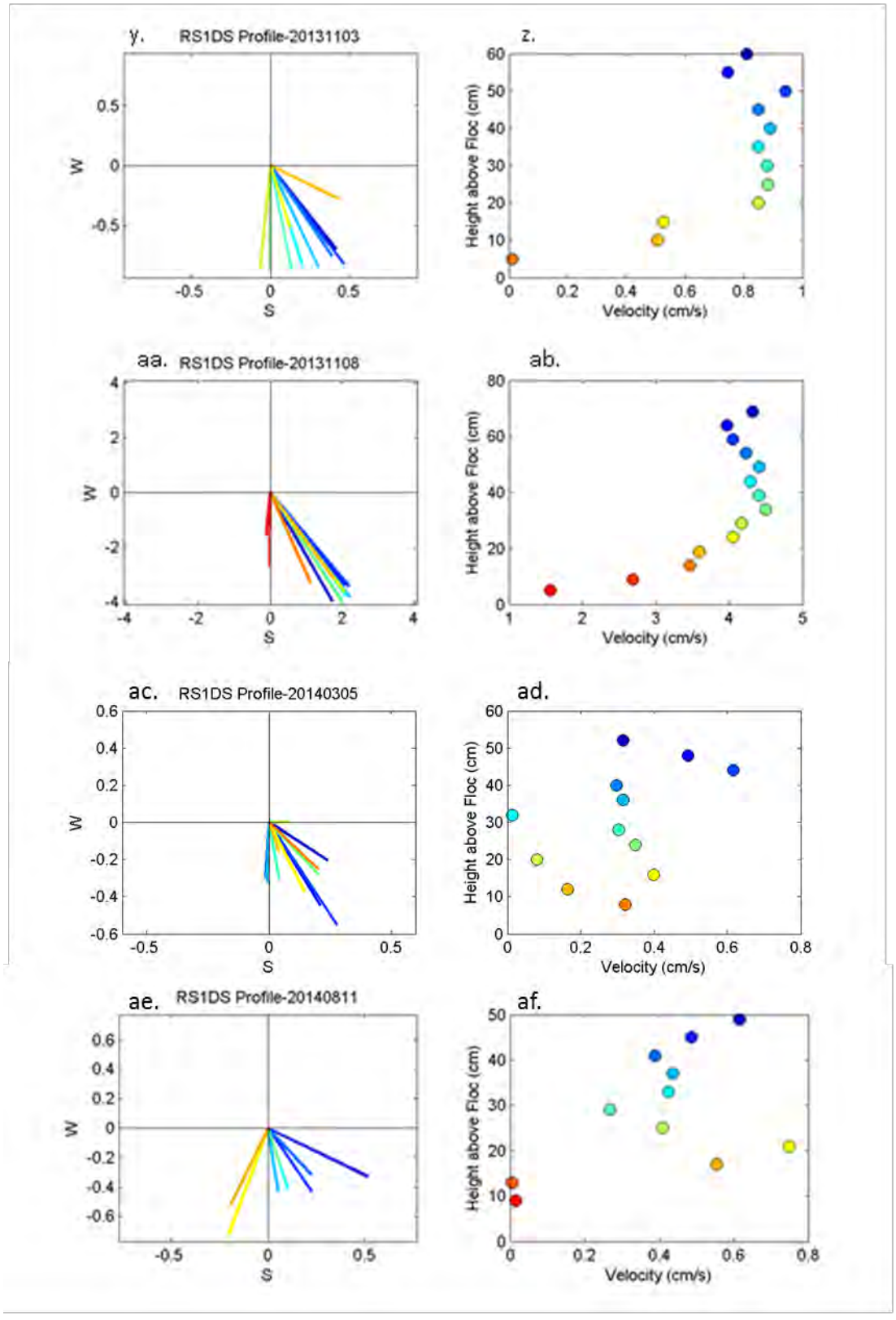
y.
RS1DS Profile-20131103
W
S
z.
Height above Floc (cm)
Velocity (cm/s)
aa.
RS1DS Profile-20131108
ab.
ac.
RS1DS Profile-20140305
ad.
ae.
RS1DS Profile-20140811
af.

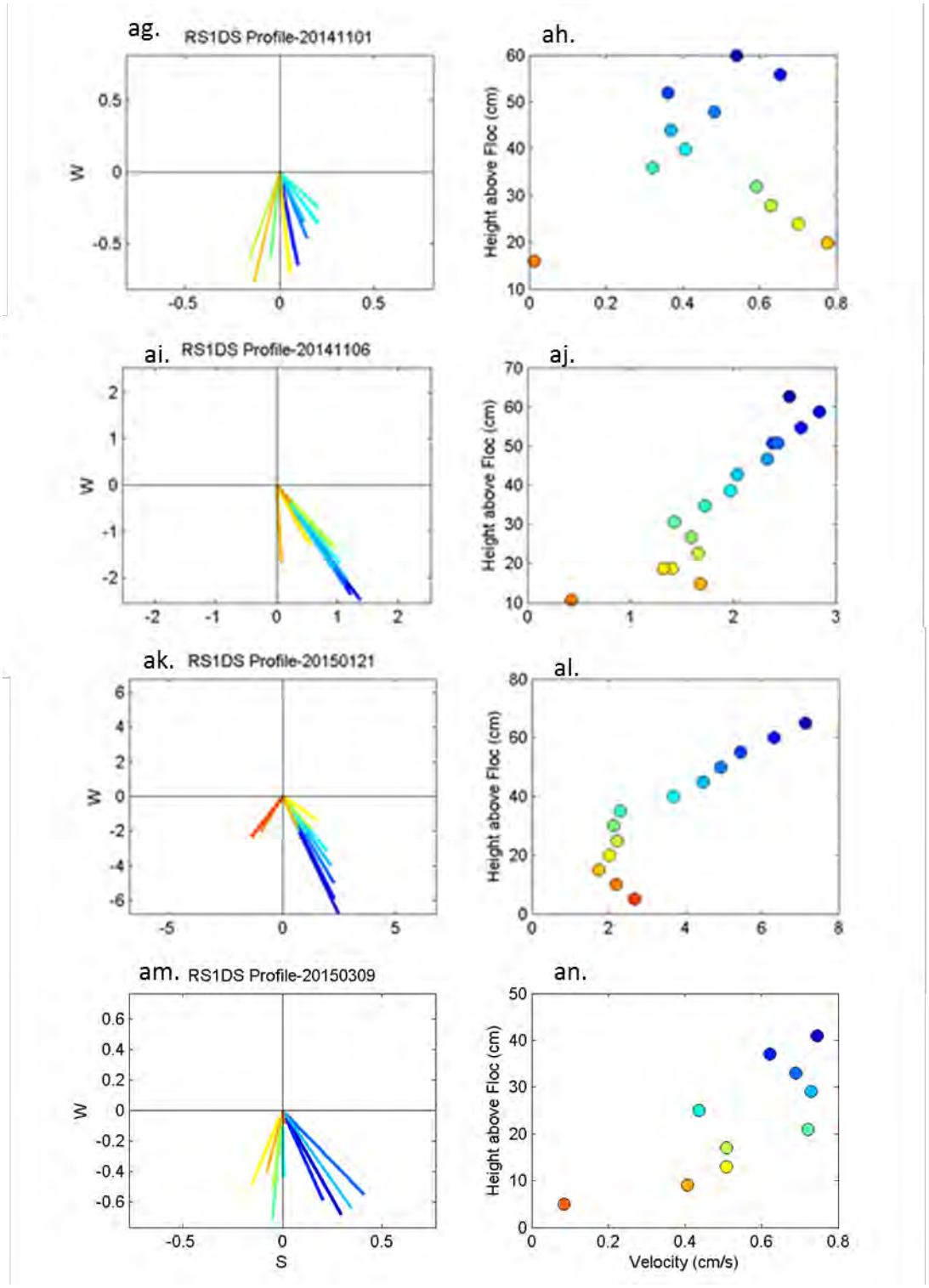
ag.
RS1DS Profile-20141101
W
ah.
Height above Floc (cm)
ai.
RS1DS Profile-20141106
W
aj.
Height above Floc (cm)
ak.
RS1DS Profile-20150121
W
al.
Height above Floc (cm)
am.
RS1DS Profile-20150309
W
S
an.
Height above Floc (cm)
Velocity (cm/s)

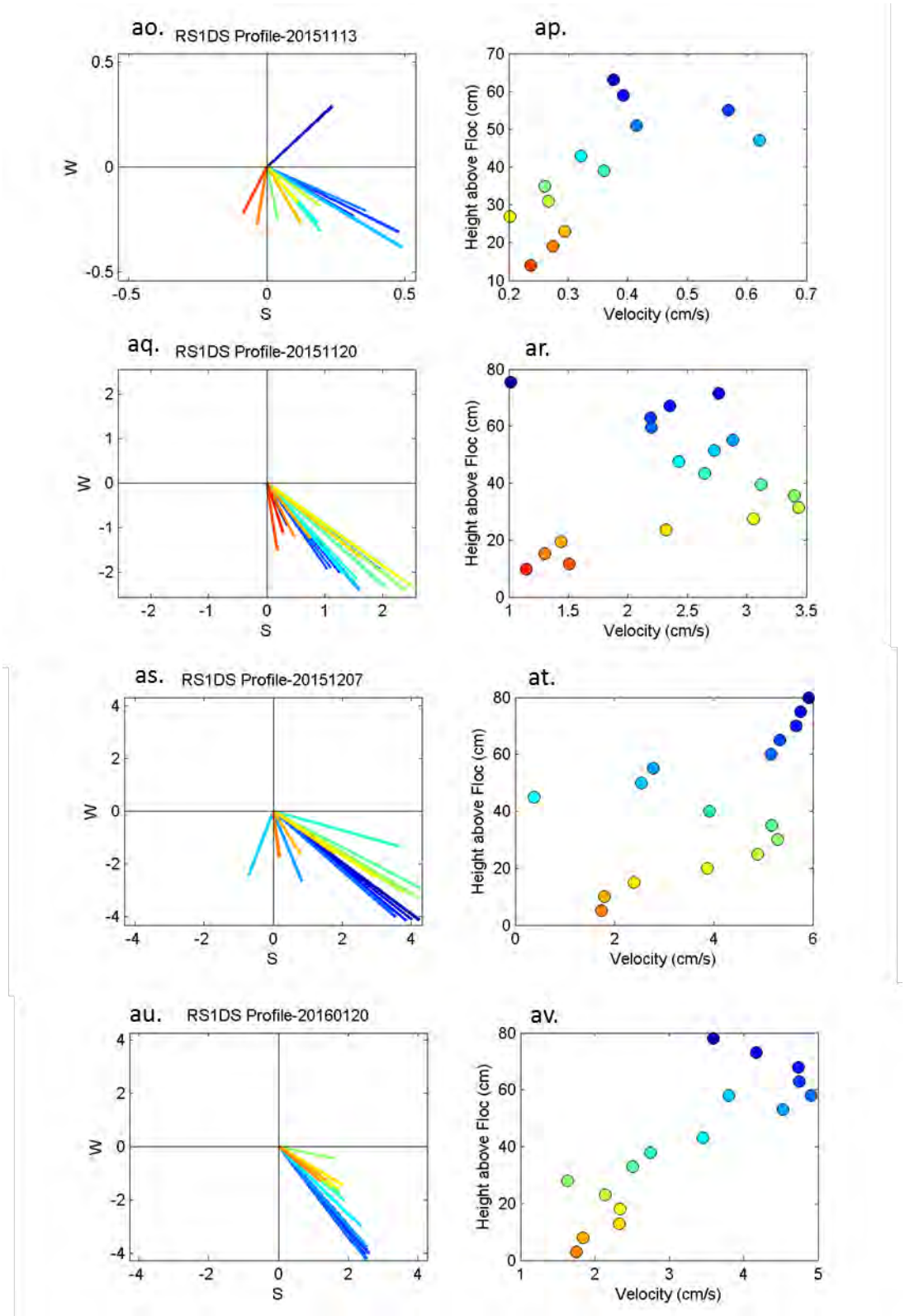

Figure C-111 ADV velocity profiles recorded at DPM site RS1D Slough. Profiles recorded on (a-b) Jul. 17, 2010, (c-d) Aug. 24, 2010, (e-f) Oct. 1, 2010, (g-h) Nov. 2, 2010, (i-j) Sep. 28, 2011, (k-l) Nov. 1, 2011, (m-n)

Nov. 29, 2011, (o-p) Mar. 22, 2012, (q-r) Aug. 7, 2012, (s-t) Nov. 5, 2012, and (u-v) Feb. 26, 2013, (w-x) Aug. 13, 2013, (y-z) Nov. 03, 2013, (aa-ab) Nov. 08, 2013, (ac-ad) Mar. 05, 2014, (ae-af) Aug. 11,2014, (ag-ah) Nov. 1, 2014, (ai-aj) Nov. 6, 2014, (ak-al) Jan. 21, 2015, (am-an) Mar. 9, 2015, (ao-ap) Nov. 13, 2015, (aq-ar) Nov. 20, 2015, (as-at) Dec. 7, 2015 and (au-av) Jan. 20, 2016. Panels (a), (c), (e), (g), (i), (k), (m), (o), (q), (s), (u), (w), (y), (aa), (ac), (ae), (ag), (ai), (ak), (am), (ao), (aq), (as) and (au) show velocity vectors (cm/s) with the axes representing cardinal directions, such that the top of the plot is true north. Panels (b), (d), (f), (h), (j), (l), (n), (p), (r), (t), (v), (x), (z), (ab), (ad), (af), (ah), (aj), (al), (an), (ap), (ar), (at), and (av) show horizontal velocities (cm/s). Dates are given in the format yyyymmdd.

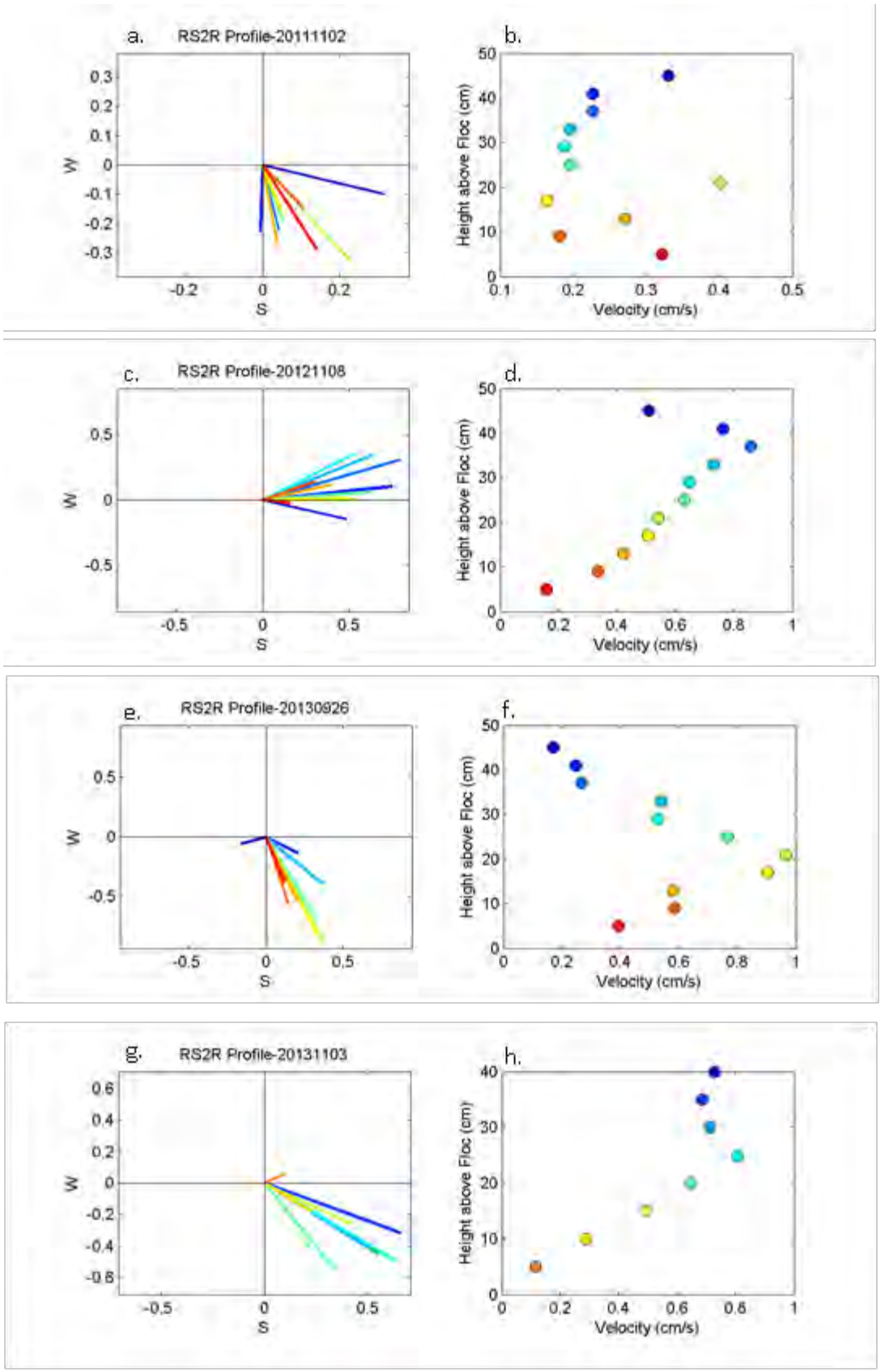
a.
RS2R Profile-20111102
W
S
b.
Height above Floc (cm)
Velocity (cm/s)
c.
RS2R Profile-20121108
d.
e.
RS2R Profile-20130926
f.
g.
RS2R Profile-20131103
h.

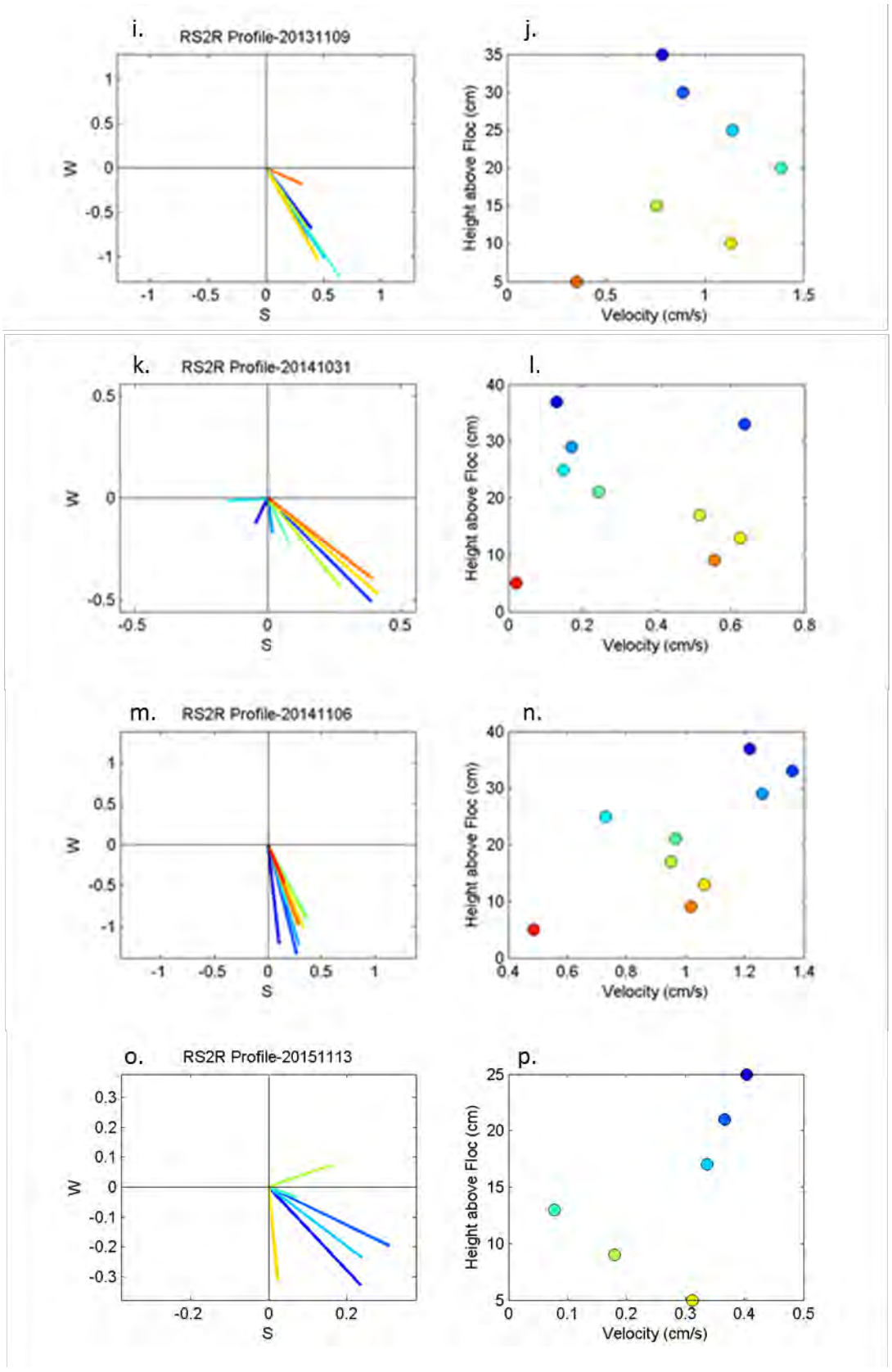
i.
RS2R Profile-20131109
W
S
j.
Height above Floc (cm)
Velocity (cm/s)
k.
RS2R Profile-20141031
W
S
l.
Height above Floc (cm)
Velocity (cm/s)
m.
RS2R Profile-20141106
W
S
n.
Height above Floc (cm)
Velocity (cm/s)
o.
RS2R Profile-20151113
W
S
p.
Height above Floc (cm)
Velocity (cm/s)

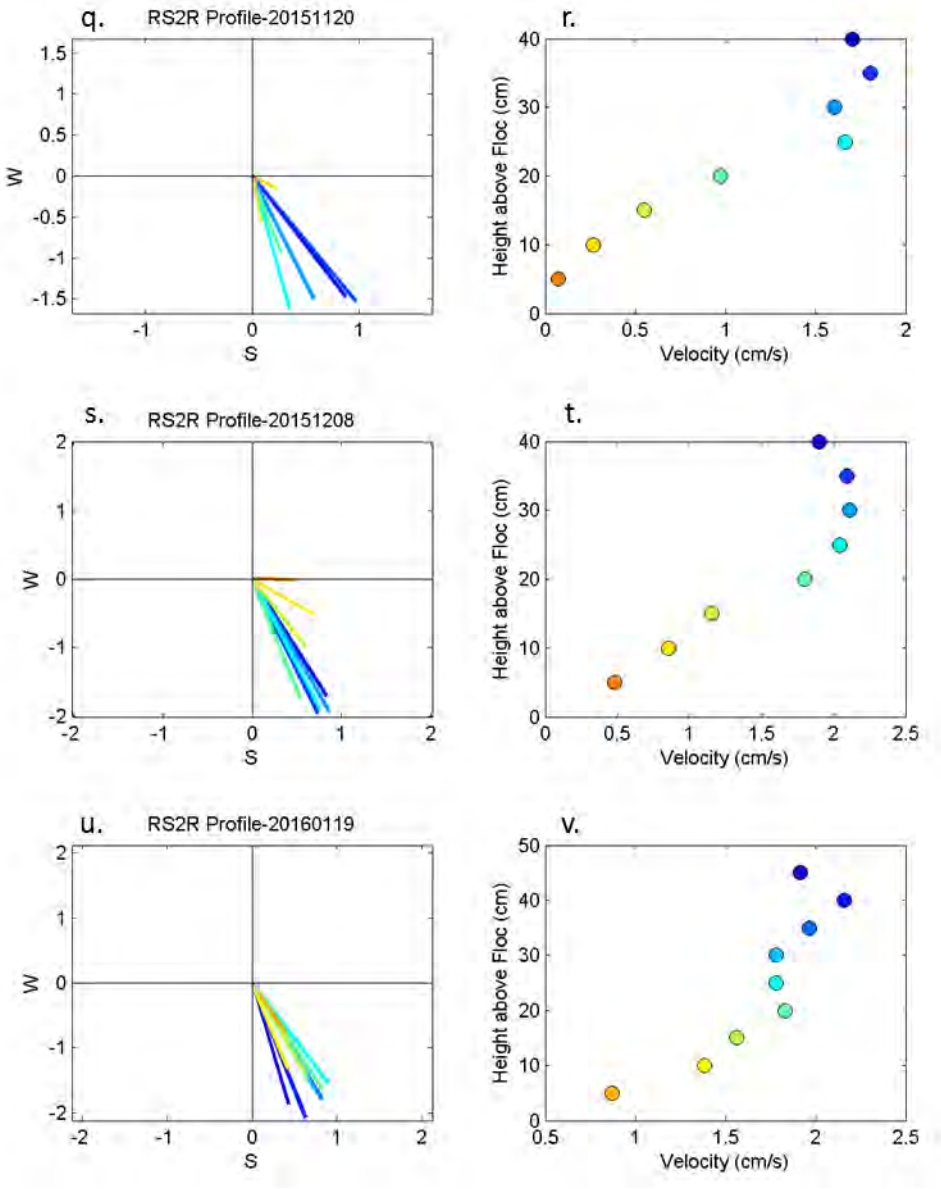

Figure C-112 ADV velocity profiles recorded at DPM site RS2 Ridge. Profiles recorded on (a-b) Nov. 2, 2011, (c-d) Nov. 8, 2012, (e-f) Sep. 26, 2013, (g-h) Nov. 3, 2013, (i-j) Nov. 9, 2013, (k-l) Oct. 31, 2014, (m-n) Nov. 6, 2014, (o-p) Nov. 13, 2015, (q-r) Nov. 20,2015, (s-t) Dec. 8, 2015, and (u-v) Jan. 19, 2016. Panels (a), (c), (e), (g), (i), (k), (m), (o), (q), (s) and (u) show velocity vectors (cm/s) with the axes representing cardinal directions, such that the top of the plot is true north. Panels (b), (d), (f), (h), (j), (l), (n), (p), (r), (t), and (v) show horizontal velocities (cm/s). Dates are given in the format yyyymmdd.

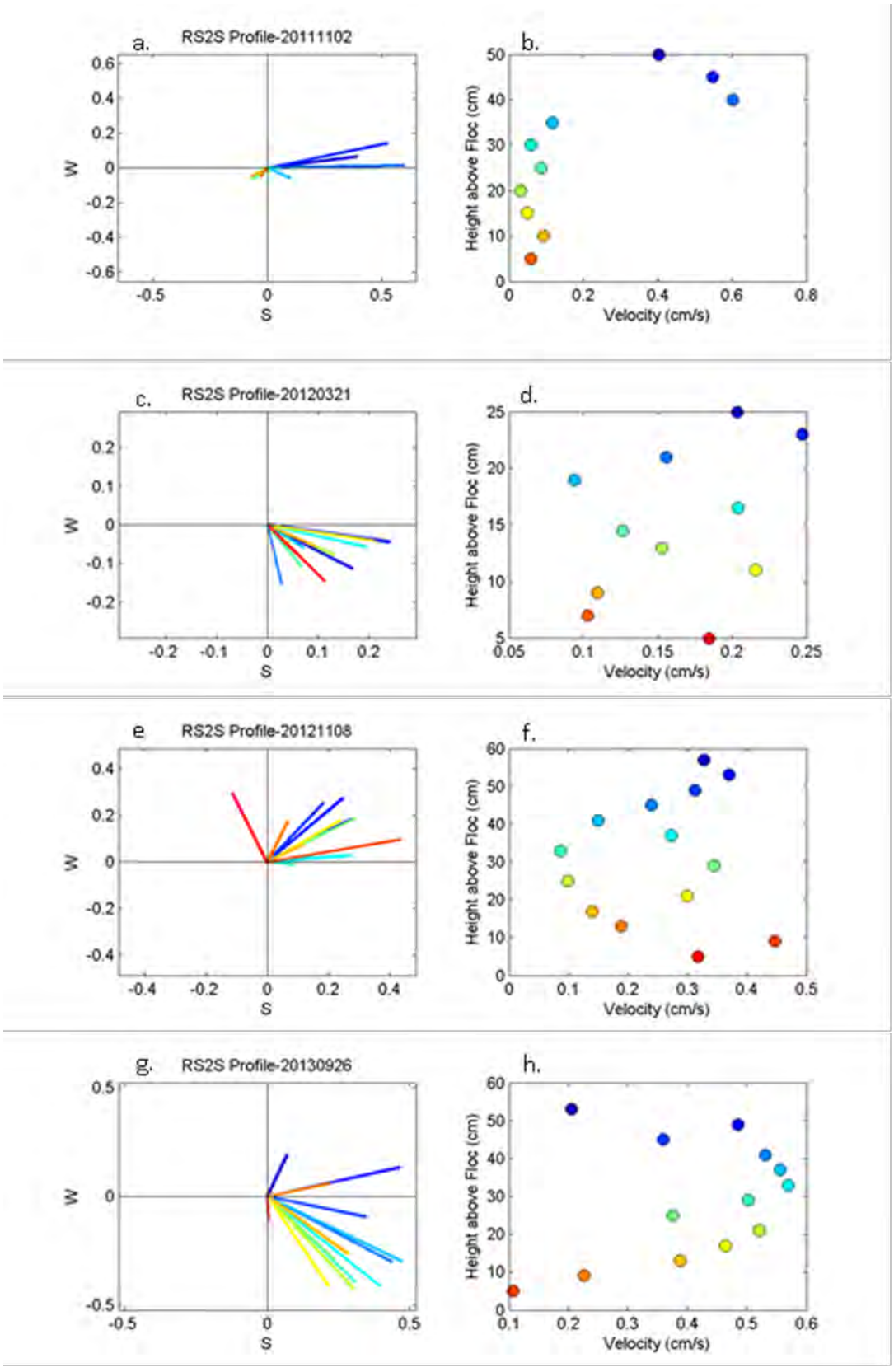
a.
RS2S Profile-20111102
W
S
b.
Height above Floc (cm)
Velocity (cm/s)
c.
RS2S Profile-20120321
d.
e
RS2S Profile-20121108
f.
g.
RS2S Profile-20130926
h.

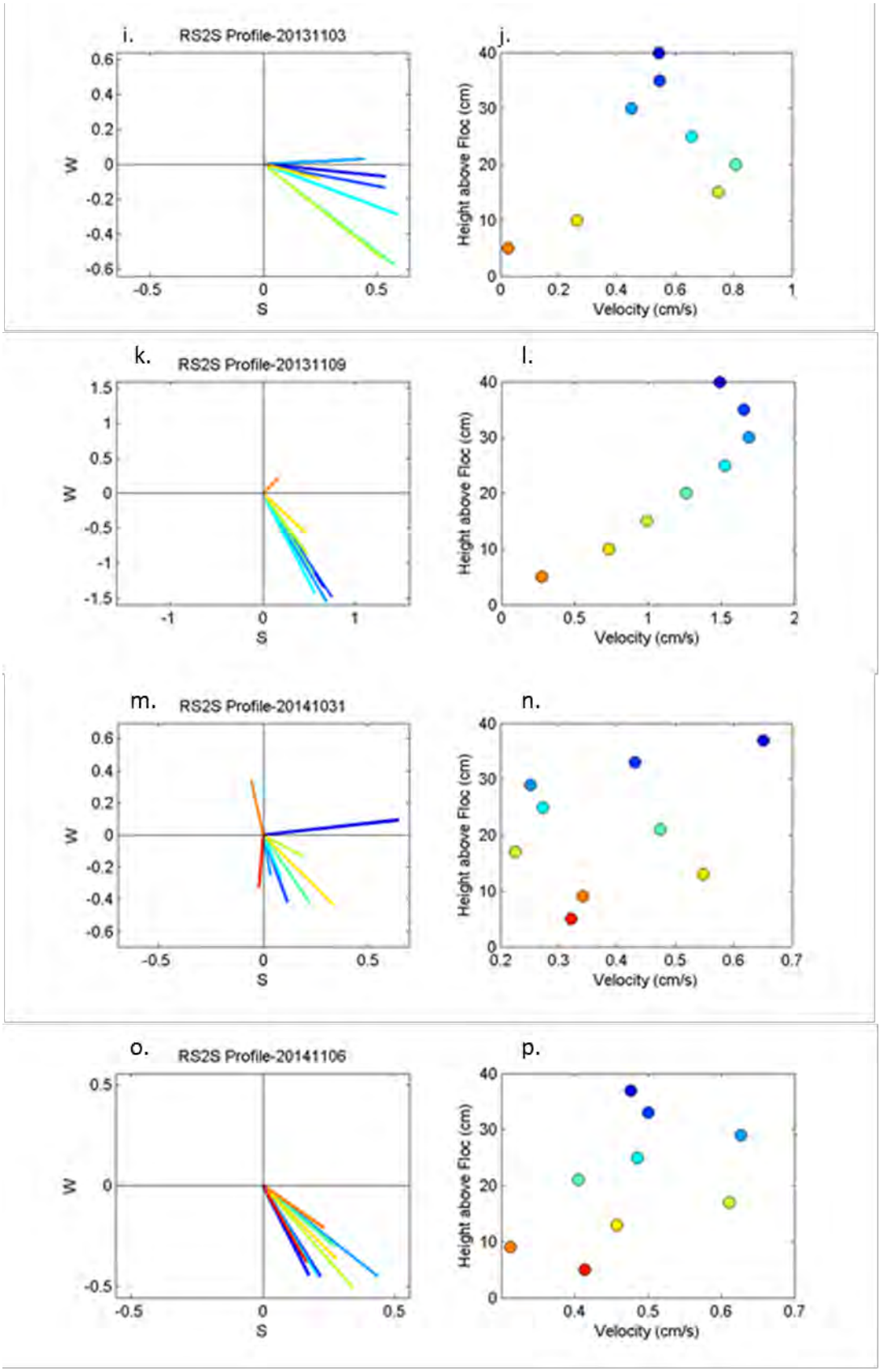
i.
RS2S Profile-20131103
W
S
j.
Height above Floc (cm)
Velocity (cm/s)
k.
RS2S Profile-20131109
W
S
l.
Height above Floc (cm)
Velocity (cm/s)
m.
RS2S Profile-20141031
W
S
n.
Height above Floc (cm)
Velocity (cm/s)
o.
RS2S Profile-20141106
W
S
p.
Height above Floc (cm)
Velocity (cm/s)

Figure C-113 ADV velocity profiles recorded at DPM site RS2 Slough. Profiles recorded on (a-b) Nov. 2, 2011, (c-d) Mar. 21, 2012, (e-f) Nov. 8, 2012, (g-h) Sep. 26, 2013, (i-j) Nov. 3, 2013, (k-l) Nov. 9, 2013, (m-n) Oct. 31, 2014, and (o-p) Nov. 6, 2014. Panels (a), (c), (e), (g), (i), (k), (m), and (o) show velocity vectors (cm/s) with the axes representing cardinal directions, such that the top of the plot is true north. Panels (b), (d), (f), (h), (j), (l), (n), and (p) show horizontal velocities (cm/s). Dates are given in the format yyyymmdd.

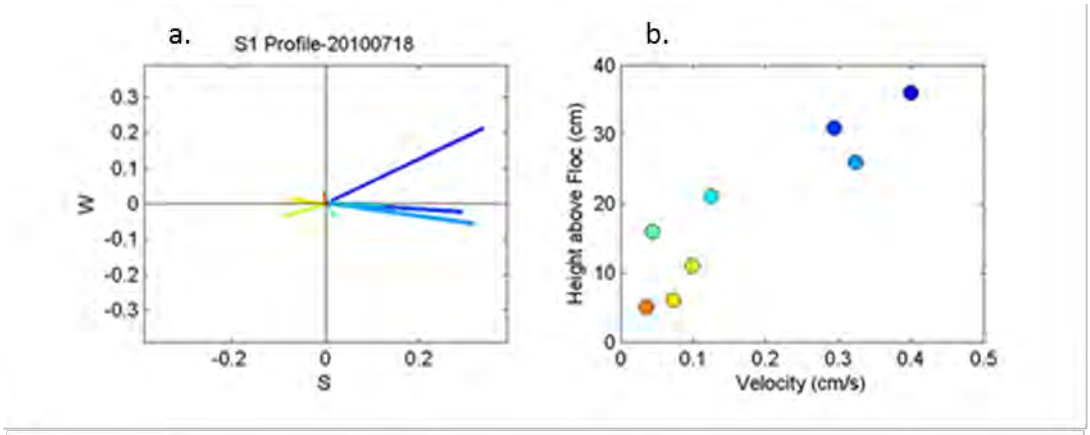
a.
S1 Profile-20100718
W
S
b.
Height above Floc (cm)
Velocity (cm/s)

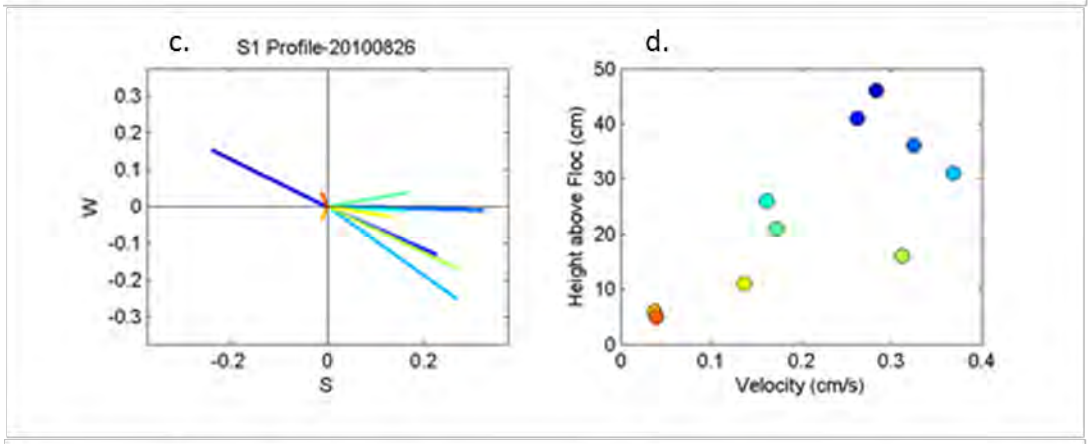
c.
S1 Profile-20100826
W
S
d.
Height above Floc (cm)
Velocity (cm/s)

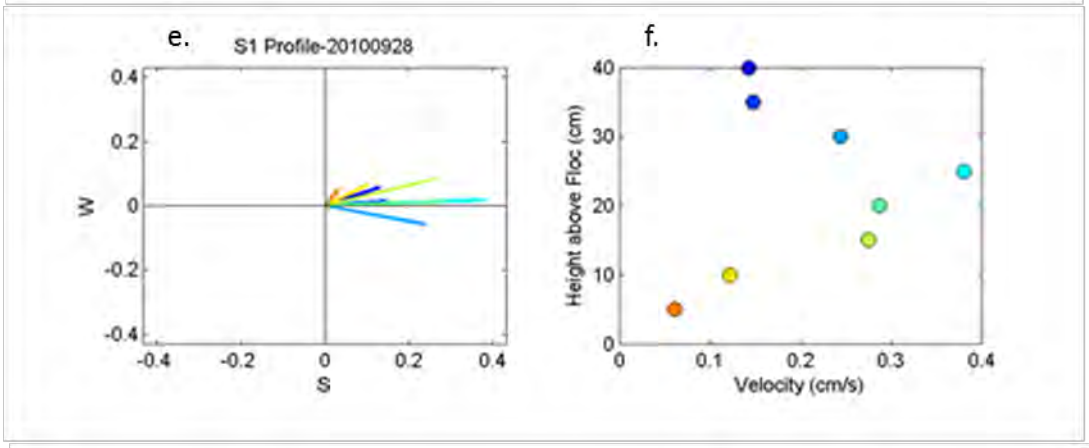
e.
S1 Profile-20100928
W
S
f.
Height above Floc (cm)
Velocity (cm/s)

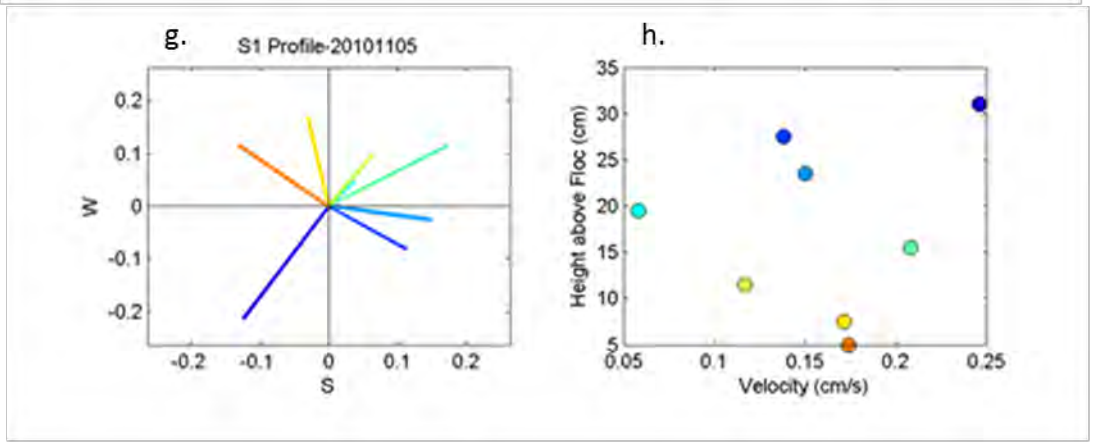
g.
S1 Profile-20101105
W
S
h.
Height above Floc (cm)
Velocity (cm/s)

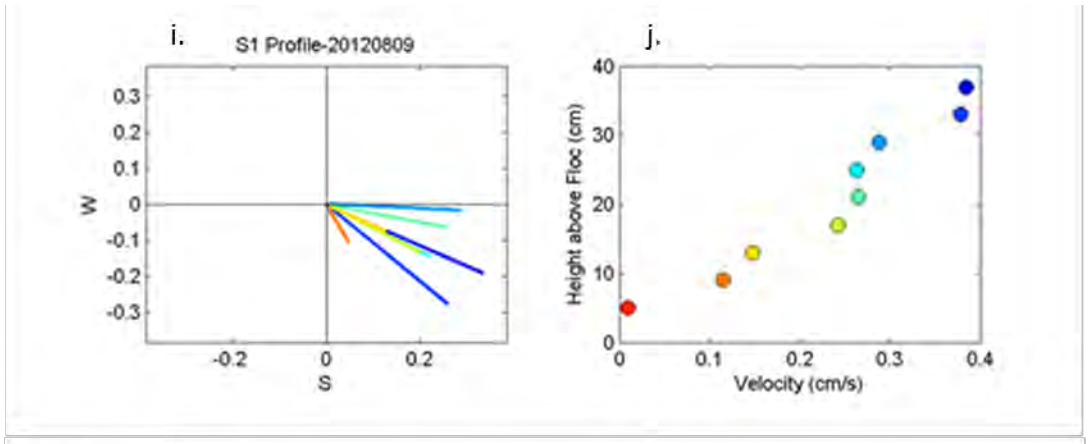
i.
S1 Profile-20120809
W
S
j.
Height above Floc (cm)
Velocity (cm/s)

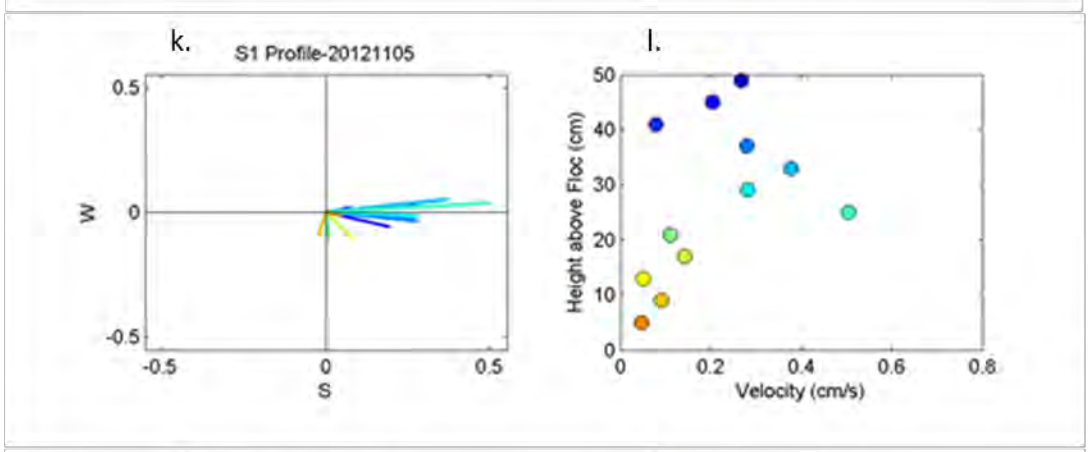
k.
S1 Profile-20121105
W
S
l.
Height above Floc (cm)
Velocity (cm/s)

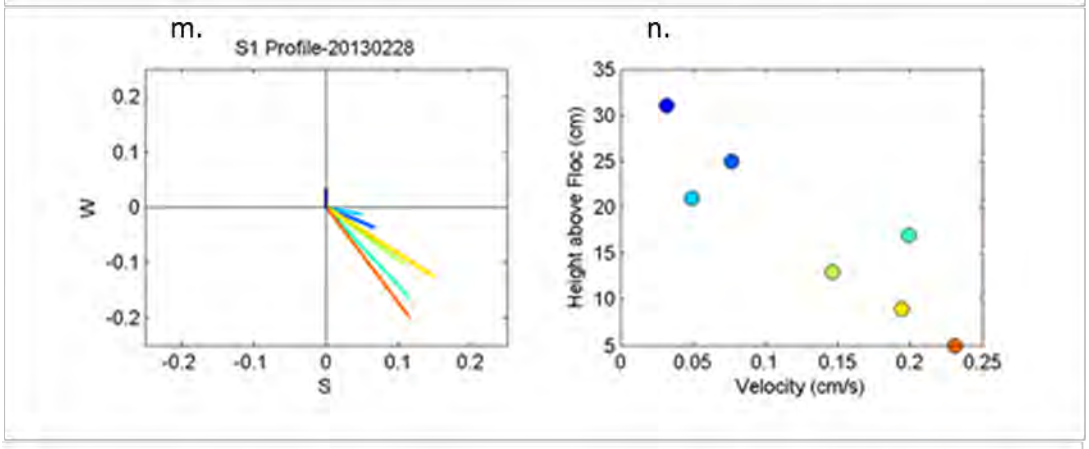
m.
S1 Profile-20130228
W
S
n.
Height above Floc (cm)
Velocity (cm/s)

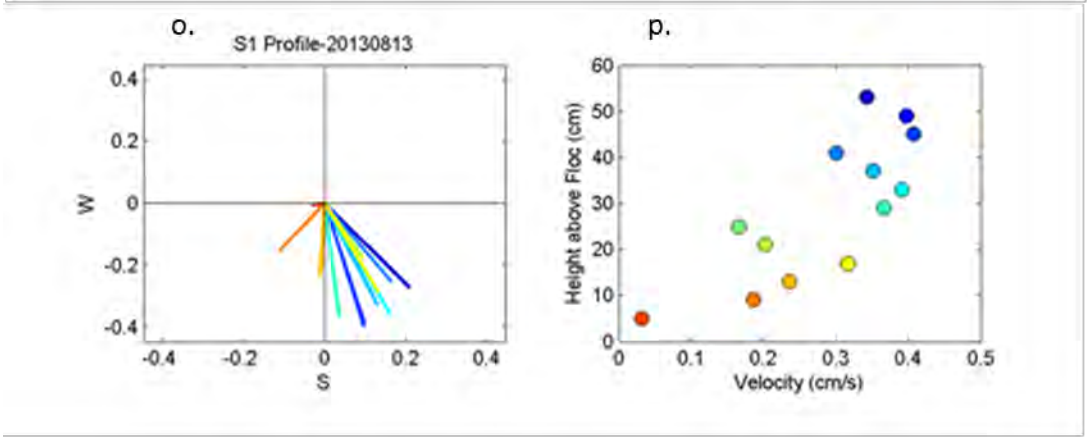
o.
S1 Profile-20130813
W
S
p.
Height above Floc (cm)
Velocity (cm/s)

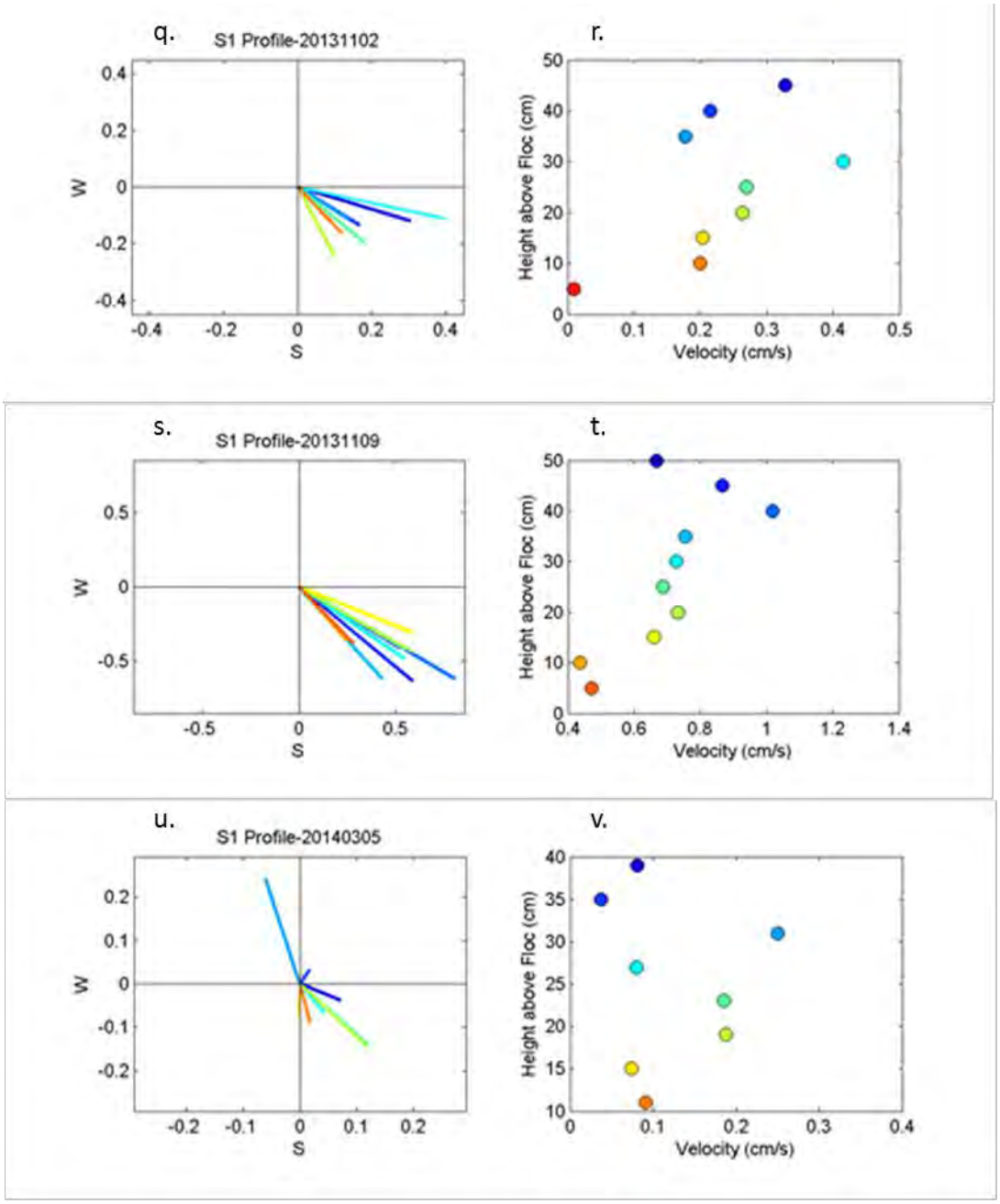

Figure C-114 ADV velocity profiles recorded at DPM site S1. Profiles recorded on (a-b) Jul. 18, 2010, (c-d) Aug. 26, 2010, (e-f) Sep. 28, 2010, (g-h) Nov. 5, 2010, (i-j) Aug. 9, 2012, (k-l) Nov. 5, 2012, and (m-n) Feb. 28, 2013, (o-p) Aug. 13, 2013, (q-r) Nov. 02, 2013, (s-t) Nov. 09, 2013, and (u-v) Mar. 05, 2014. Panels (a), (c), (e), (g), (i), (k), (m), (o), (q), (s) and (u) show velocity vectors (cm/s) with the axes representing cardinal directions, such that the top of the plot is true north. Panels (b), (d), (f), (h), (j), (l), (n), (p), (r), (t) and (v) show horizontal velocities (cm/s). Dates are given in the format yyyymmdd.

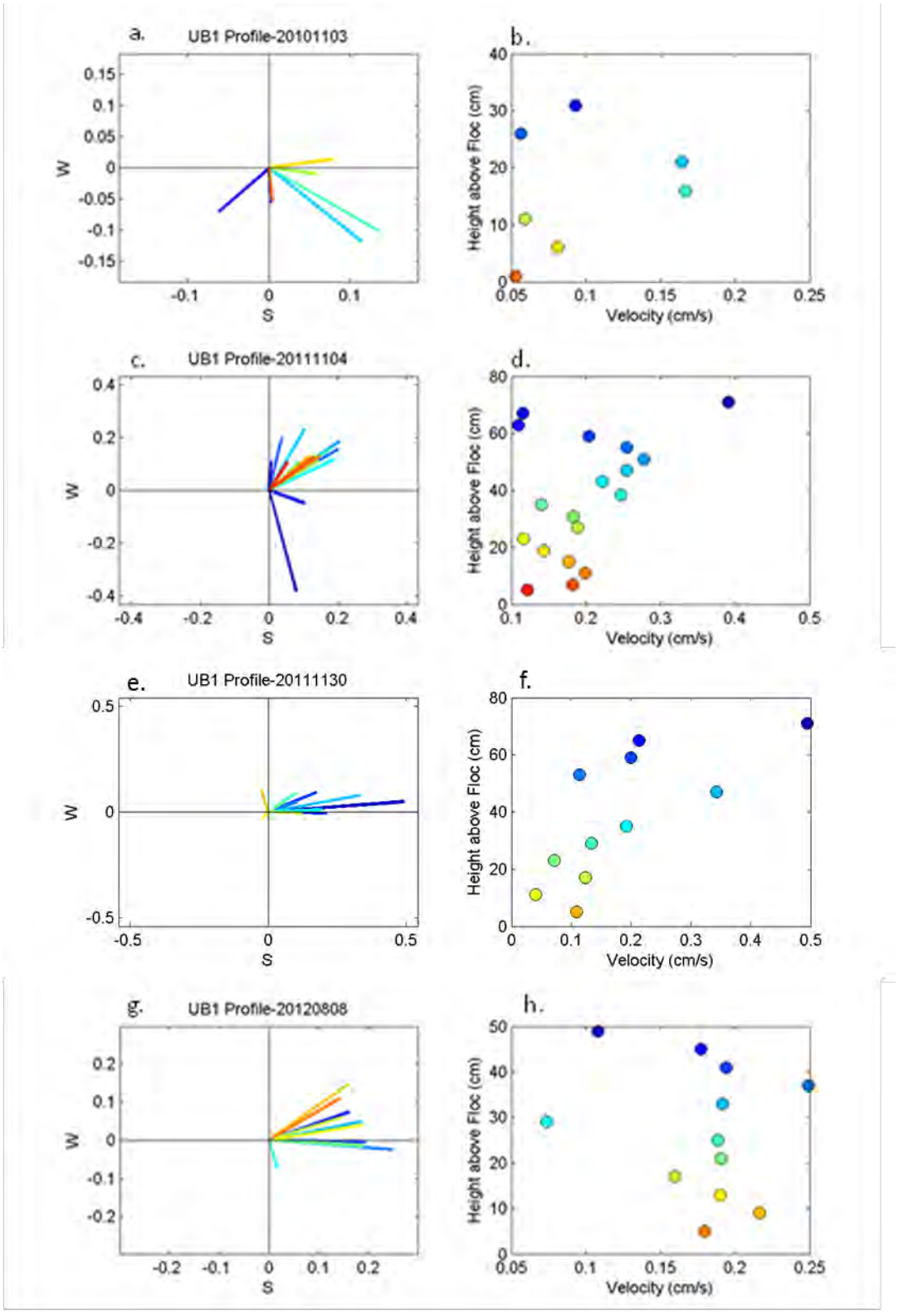
a.
UB1 Profile-20101103
W
S
b.
Height above Floc (cm)
Velocity (cm/s)
c.
UB1 Profile-20111104
W
S
d.
Height above Floc (cm)
Velocity (cm/s)
e.
UB1 Profile-20111130
W
S
f.
Height above Floc (cm)
Velocity (cm/s)
g.
UB1 Profile-20120808
W
S
h.
Height above Floc (cm)
Velocity (cm/s)

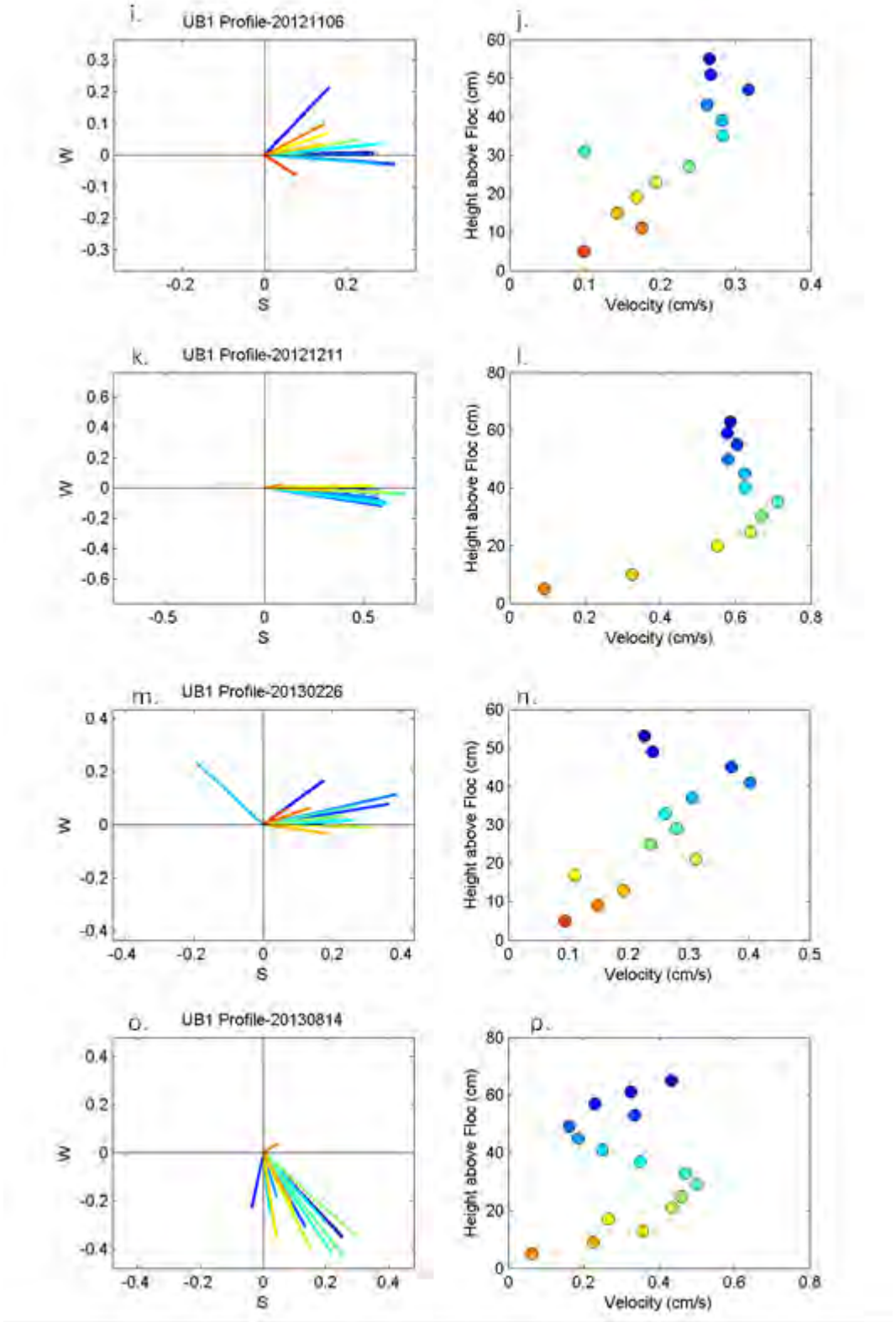
i.
UB1 Profile-20121106
W
S
j.
Height above Floc (cm)
Velocity (cm/s)
k.
UB1 Profile-20121211
W
S
l.
Height above Floc (cm)
Velocity (cm/s)
m.
UB1 Profile-20130226
W
S
n.
Height above Floc (cm)
Velocity (cm/s)
o.
UB1 Profile-20130814
W
S
p.
Height above Floc (cm)
Velocity (cm/s)

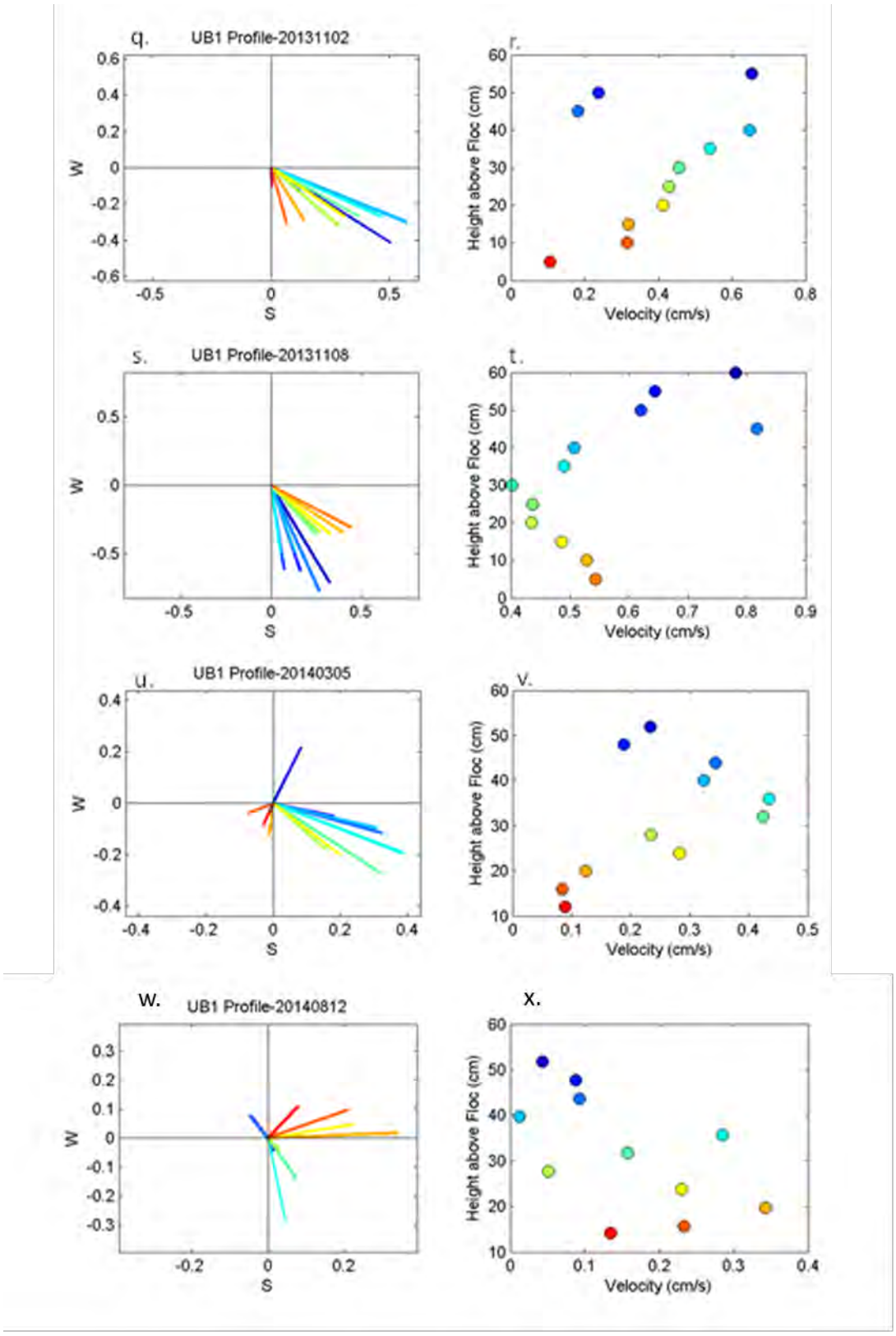
q.
UB1 Profile-20131102
W
S
r.
Height above Floc (cm)
Velocity (cm/s)
s.
UB1 Profile-20131108
t.
u.
UB1 Profile-20140305
v.
w.
UB1 Profile-20140812
x.

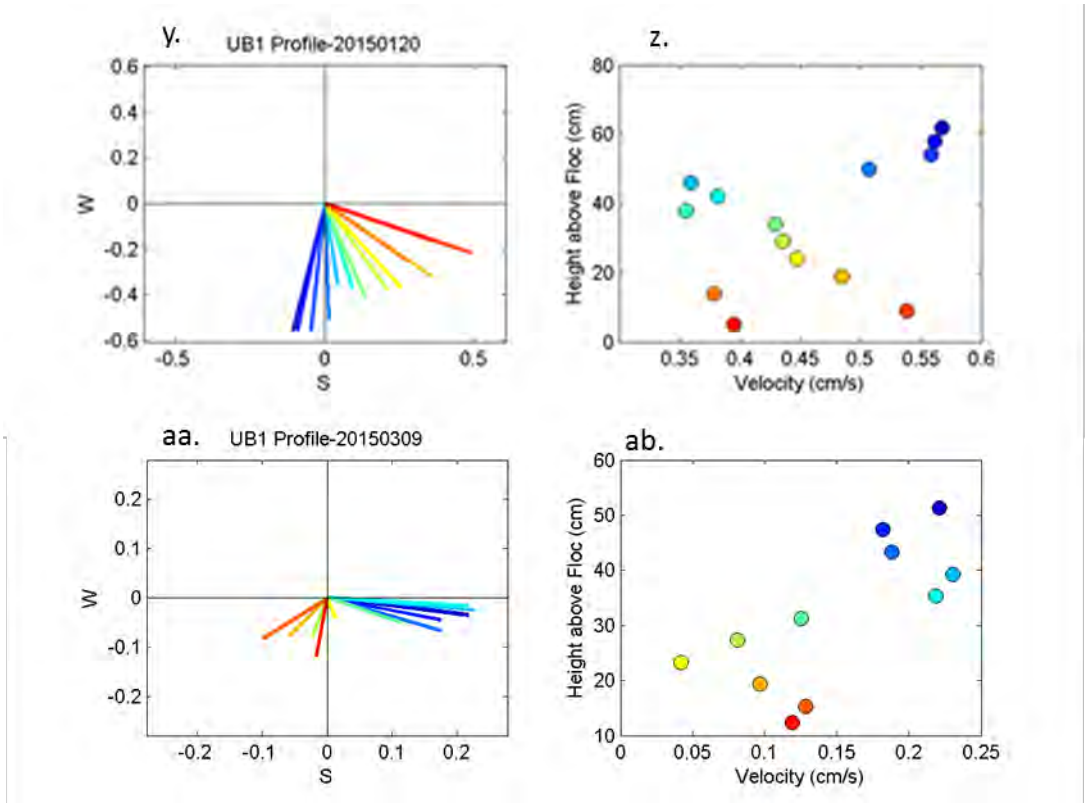

Figure C-115 ADV velocity profiles recorded at DPM site UB1. Profiles recorded on (a-b) Nov. 3, 2010, (c-d) Nov. 4, 2011, and (e-f) Nov. 30, 2011, (g-h) Aug. 8, 2012, (i-j) Nov. 6, 2012, (k-l) Dec. 11, 2012, (m-n) Feb. 26, 2013, (o-p) Aug. 14, 2013, (q-r) Nov. 02, 2013, (s-t) Nov. 08, 2013, (u-v) Mar. 05, 2014, (w-x) Aug. 12, 2014, (y-z) Jan. 20, 2015 and (aa-ab) Mar. 9, 2015. Panels (a), (c), (e), (g), (i), (k), (m), (o), (q), (s), (u), (w), (y) and (aa) show velocity vectors (cm/s) with the axes representing cardinal directions, such that the top of the plot is true north. Panels (b), (d), (f), (h), (j), (l), (n), (p), (r), (t), (v), (x), (z) and (ab) show horizontal velocities (cm/s). Dates are given in the format yyyymmdd.

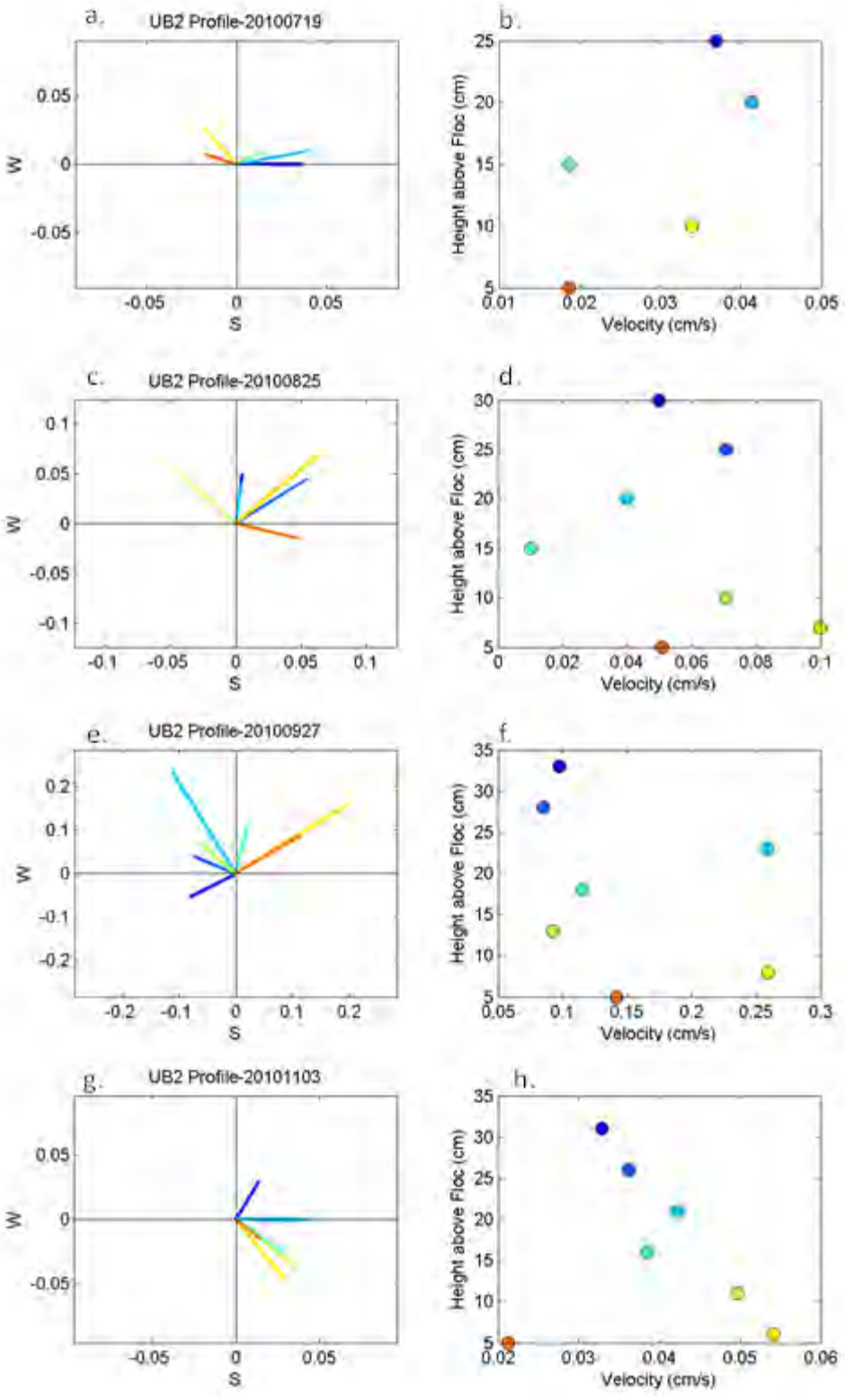
a.
UB2 Profile-20100719
W
S
b.
Height above Floc (cm)
Velocity (cm/s)
c.
UB2 Profile-20100825
d.
e.
UB2 Profile-20100927
f.
g.
UB2 Profile-20101103
h.

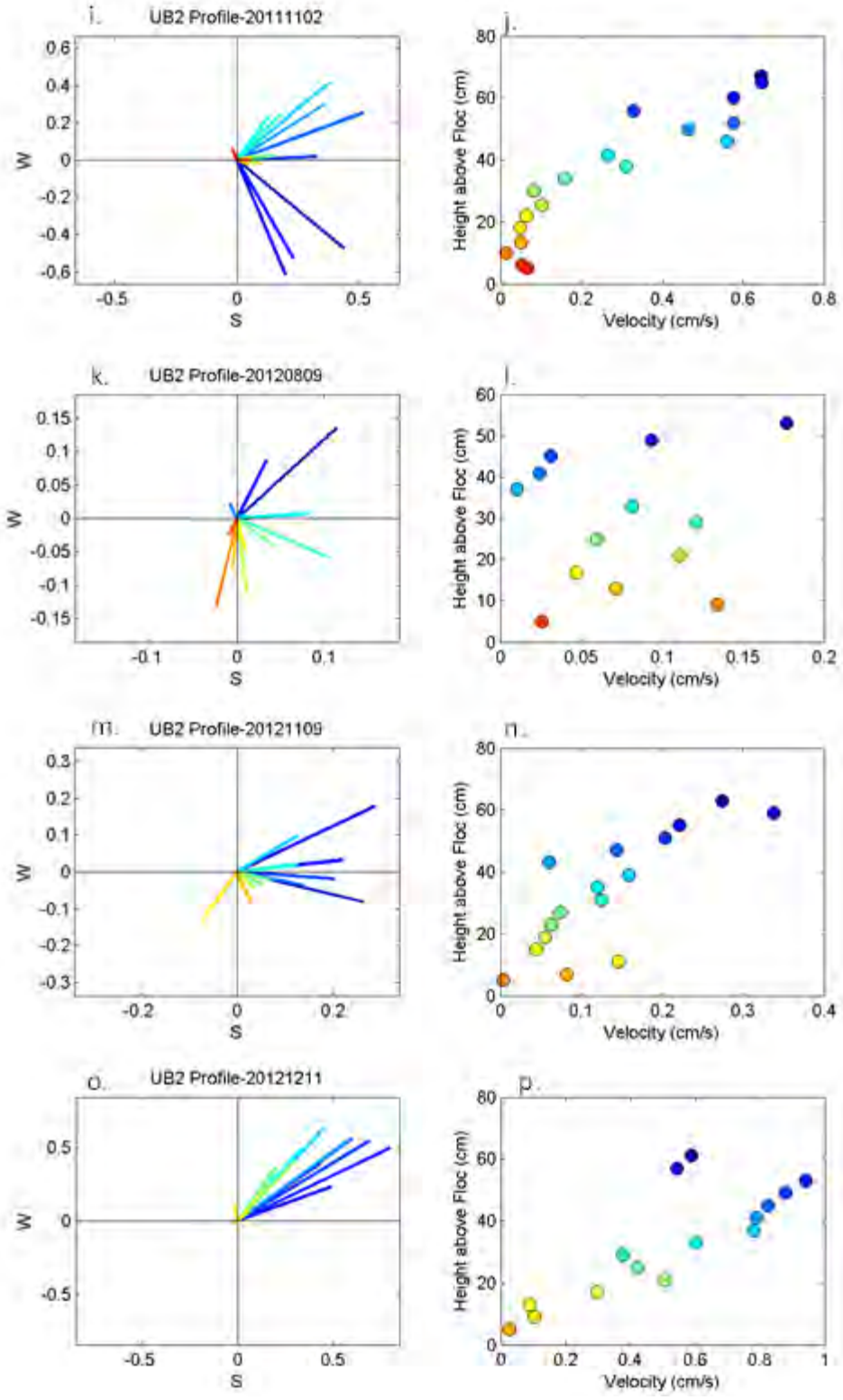
i.
UB2 Profile-20111102
W
S
j.
Height above Floc (cm)
Velocity (cm/s)
k.
UB2 Profile-20120809
W
S
l.
Height above Floc (cm)
Velocity (cm/s)
m.
UB2 Profile-20121109
W
S
n.
Height above Floc (cm)
Velocity (cm/s)
o.
UB2 Profile-20121211
W
S
p.
Height above Floc (cm)
Velocity (cm/s)

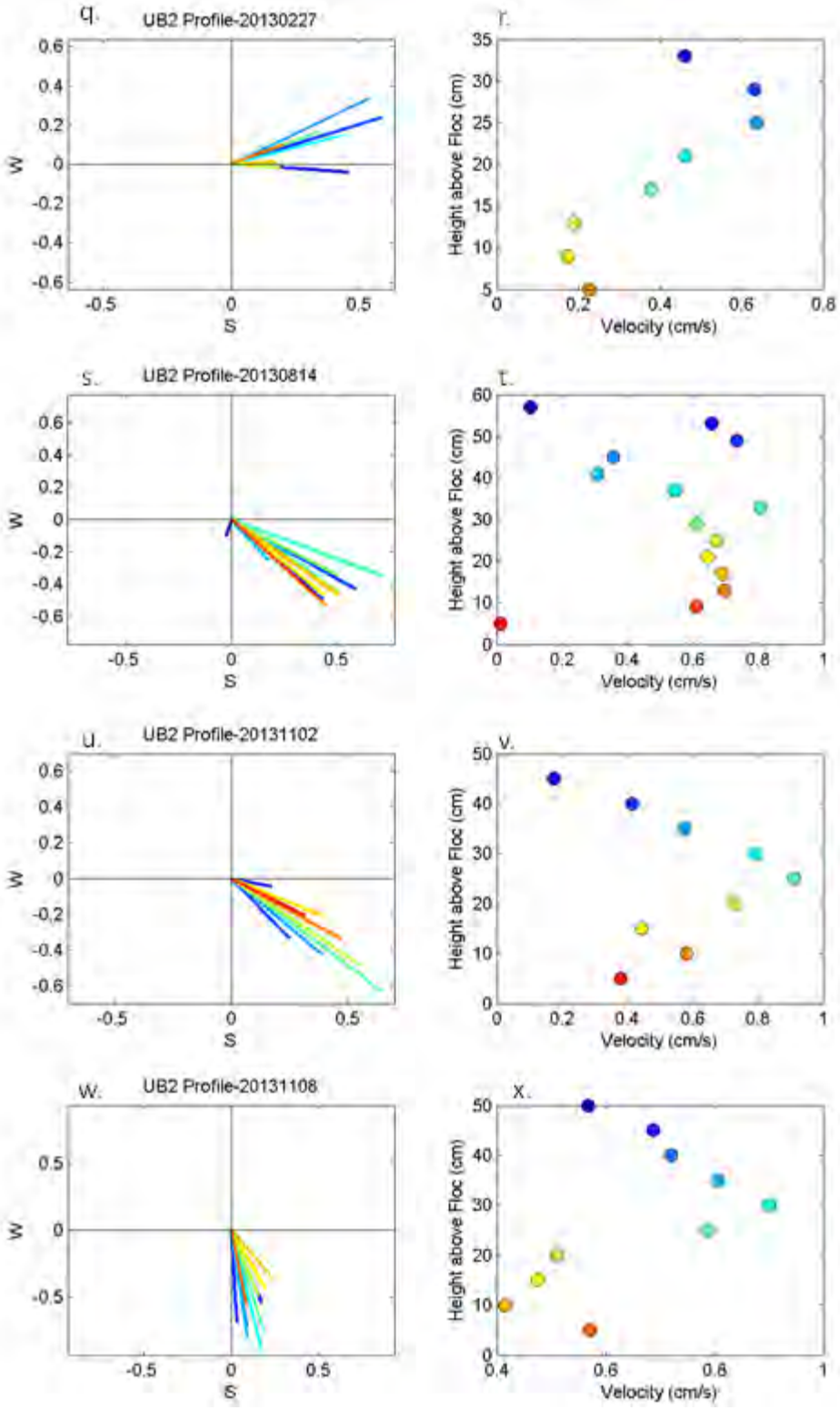
q.
UB2 Profile-20130227
W
S
r.
Height above Floc (cm)
Velocity (cm/s)
s.
UB2 Profile-20130814
t.
u.
UB2 Profile-20131102
v.
w.
UB2 Profile-20131108
x.

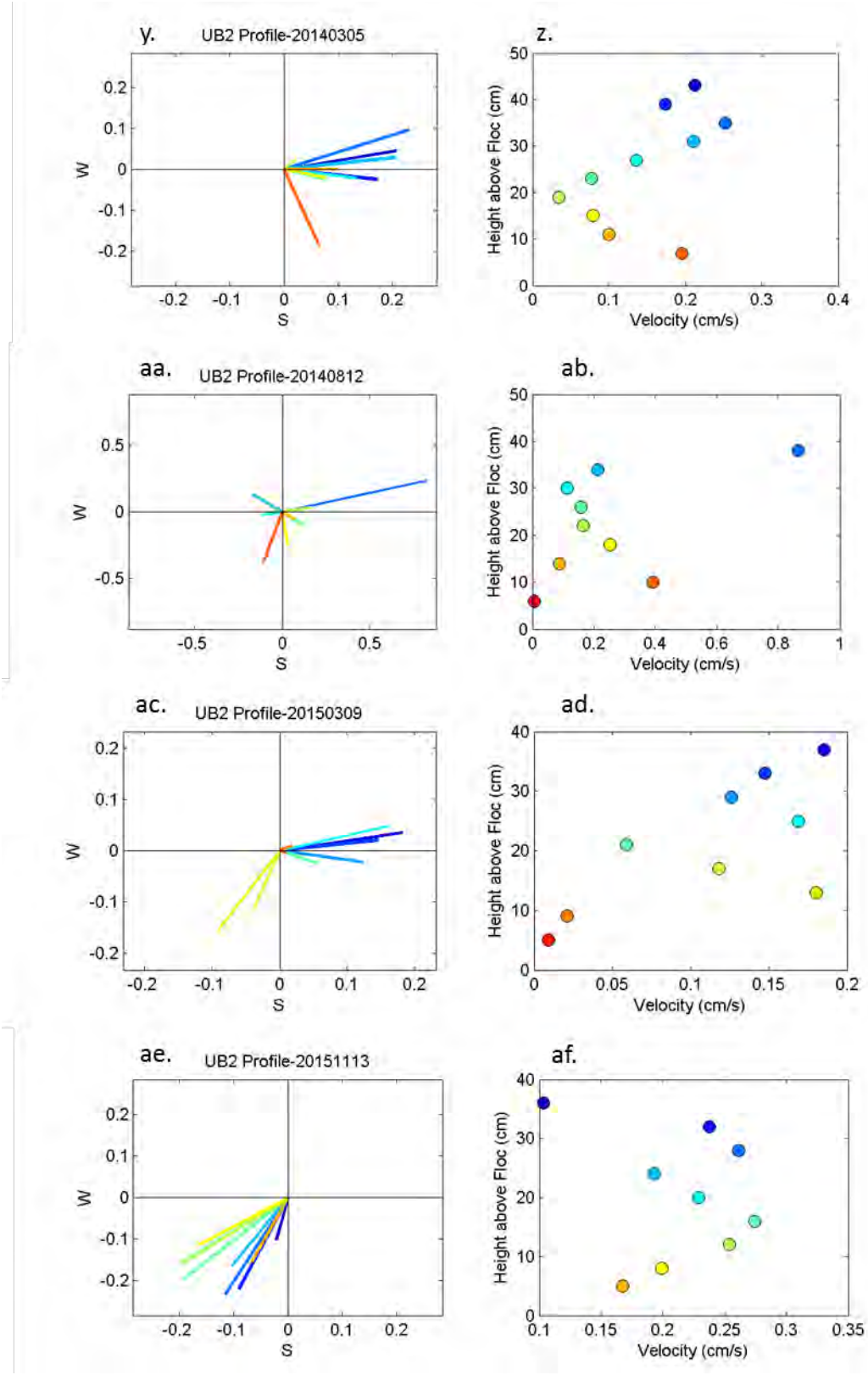
y.
UB2 Profile-20140305
W
S
z.
Height above Floc (cm)
Velocity (cm/s)
aa.
UB2 Profile-20140812
ab.
ac.
UB2 Profile-20150309
ad.
ae.
UB2 Profile-20151113
af.

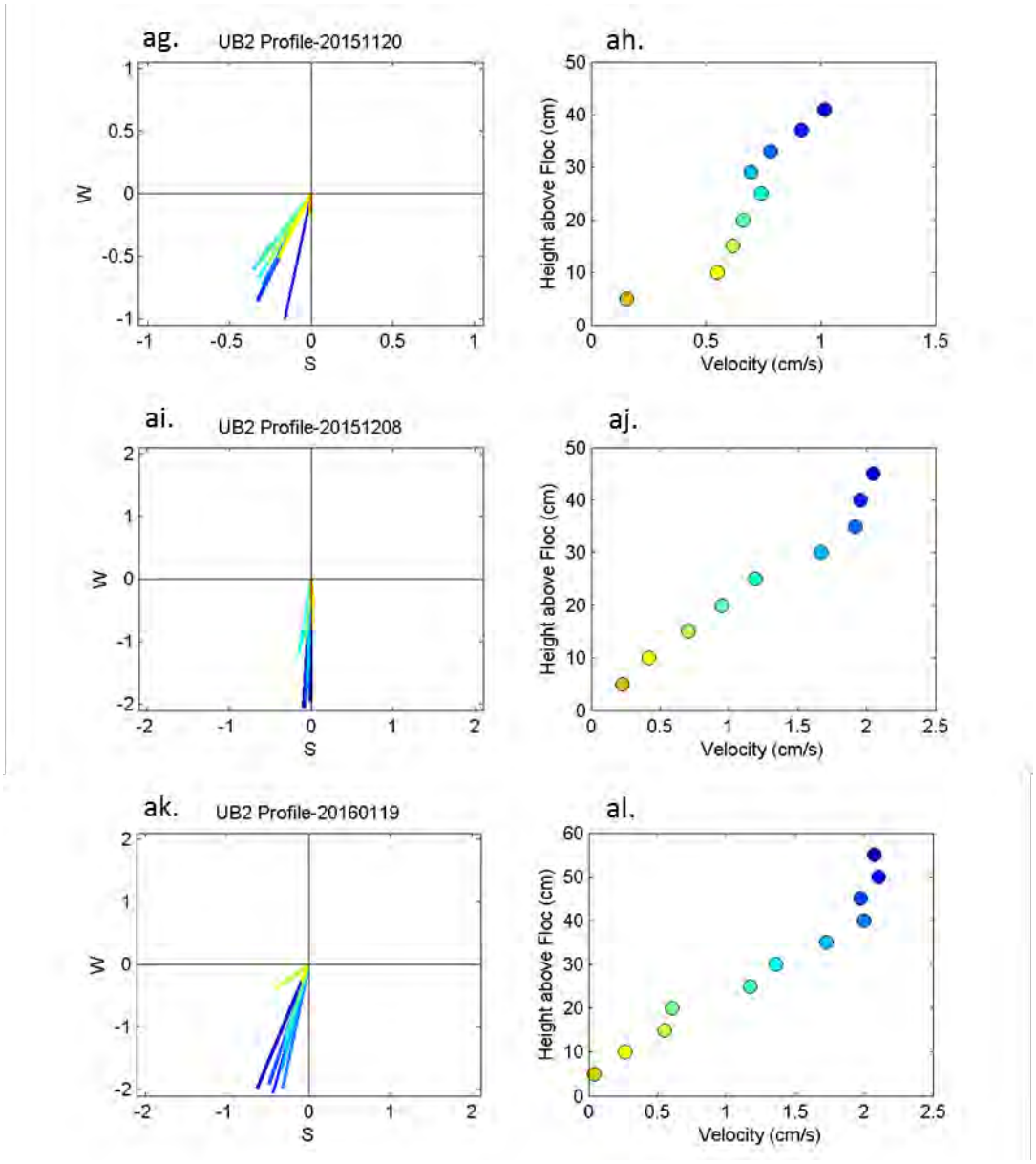

Figure C-116 ADV velocity profiles recorded at DPM site UB2. Profiles recorded on (a-b) Jul. 19, 2010, (c-d) Aug. 25, 2010, (e-f) Sep. 27, 2010, (g-h) Nov. 3, 2010, (i-j) Nov. 2, 2011, (k-l) Aug. 9, 2012, (m-n) Nov. 9, 2012, (o-p) Dec. 11, 2012, (q-r) Feb. 27, 2013, (s-t) Aug. 14, 2013, (u-v) Nov. 02, 2013, (w-x) Nov. 08, 2013, (y-z) Mar. 05, 2014, (aa-ab) Aug. 12, 2014, (ac-ad) Mar. 9, 2015, (ae-af) Nov. 13, 2015, (ag-ah) Nov. 20, 2015, (ai-aj) Dec. 8, 2015, and (ak-al) Jan. 19, 2016. Panels (a), (c), (e), (g), (i), (k), (m), (o), (q), (s), (u), (w), (y), (aa), (ac), (ae), (ag), (ai), and (ak) show velocity vectors (cm/s) with the axes representing cardinal directions, such that the top of the plot is true north. Panels (b), (d), (f), (h), (j), (l), (n), (p), (r), (t), (v), (x), (z), (ab), (ad), (af), (ah), (aj), and (al) show horizontal velocities (cm/s). Dates are given in the format yyyymmdd.

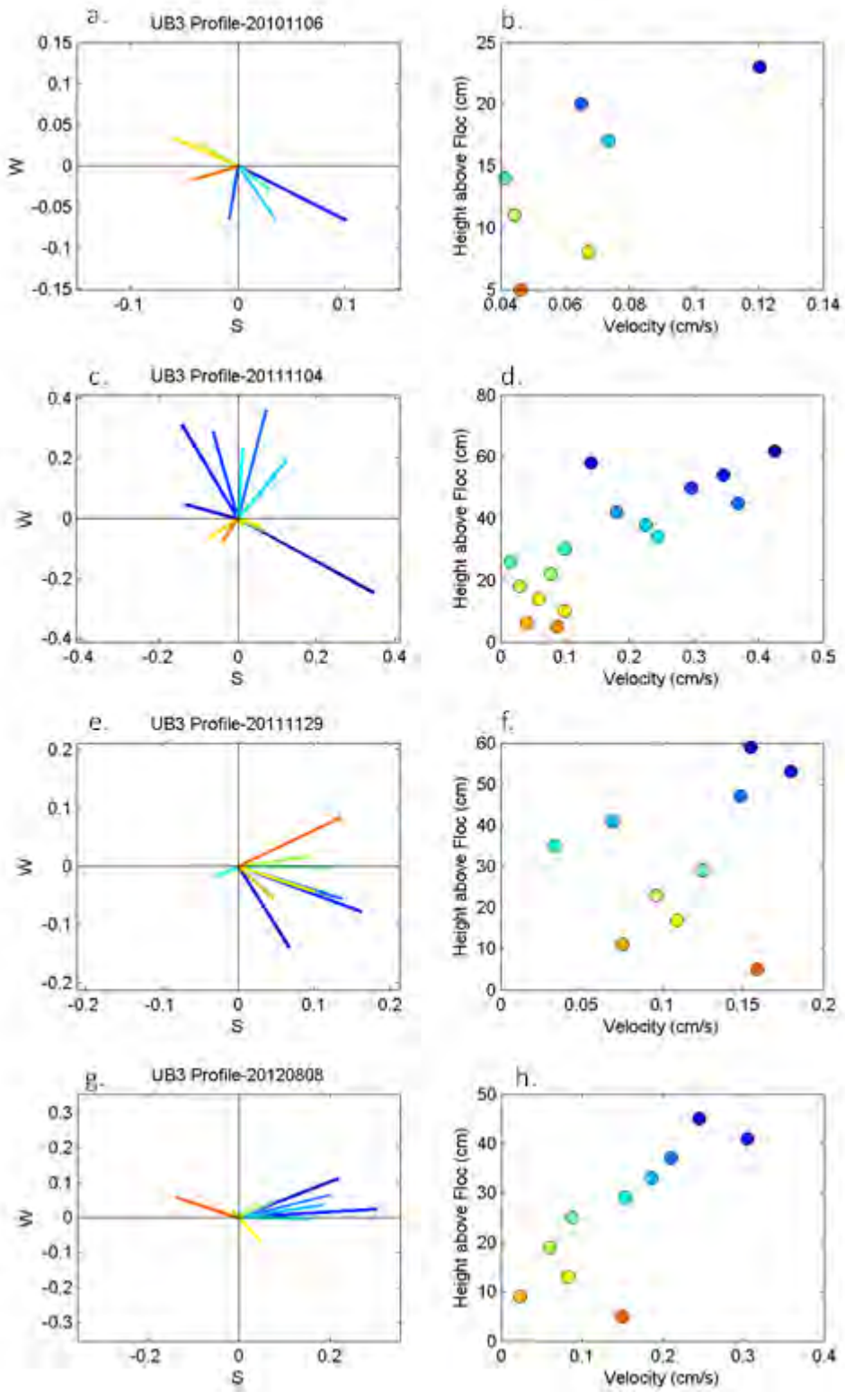
a.
UB3 Profile-20101106
W
S
b.
Height above Floc (cm)
Velocity (cm/s)
c.
UB3 Profile-20111104
W
S
d.
Height above Floc (cm)
Velocity (cm/s)
e.
UB3 Profile-20111129
W
S
f.
Height above Floc (cm)
Velocity (cm/s)
g.
UB3 Profile-20120808
W
S
h.
Height above Floc (cm)
Velocity (cm/s)

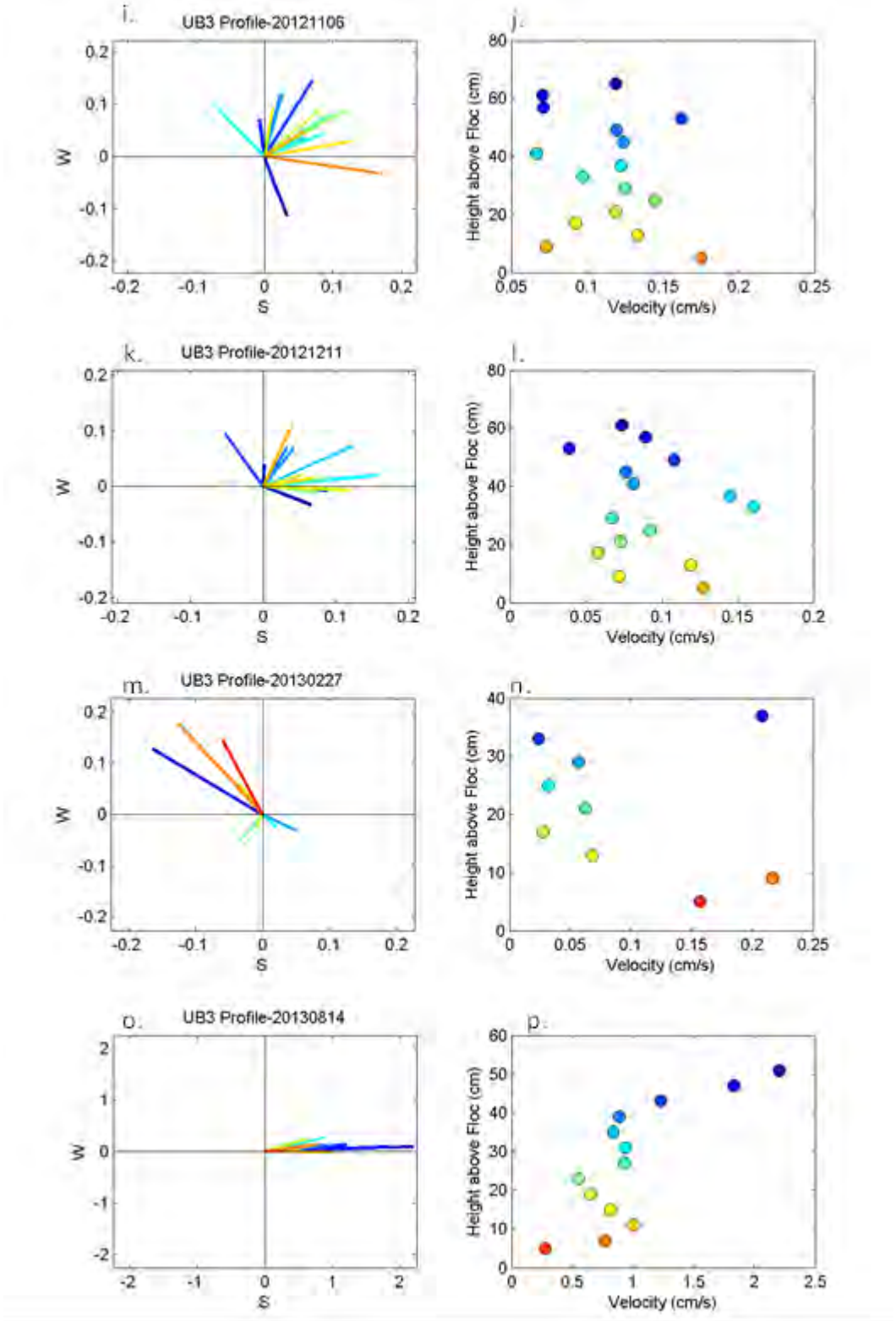
i.
UB3 Profile-20121106
W
S
j.
Height above Floc (cm)
Velocity (cm/s)
k.
UB3 Profile-20121211
W
S
l.
Height above Floc (cm)
Velocity (cm/s)
m.
UB3 Profile-20130227
W
S
n.
Height above Floc (cm)
Velocity (cm/s)
o.
UB3 Profile-20130814
W
S
p.
Height above Floc (cm)
Velocity (cm/s)

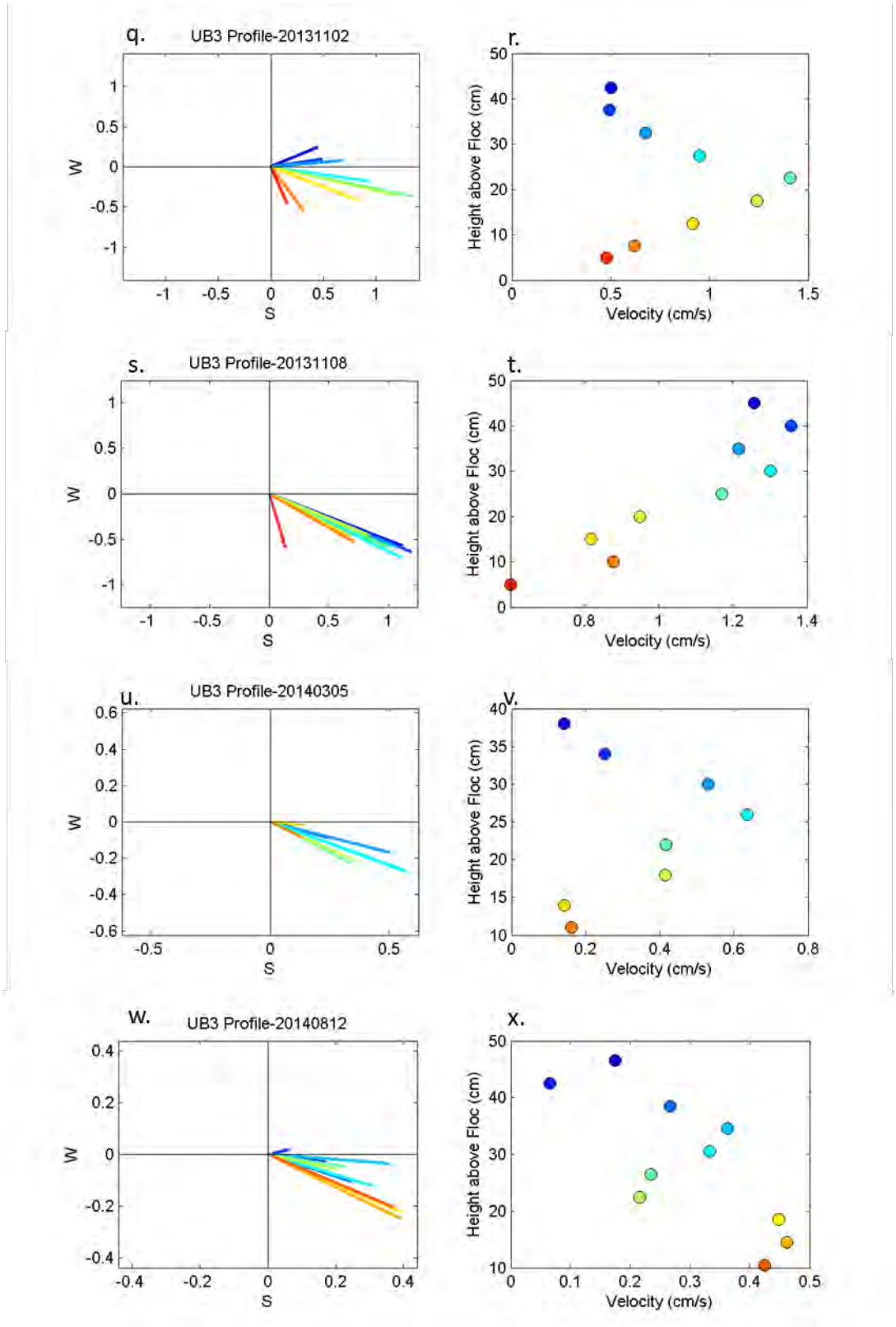
q.
UB3 Profile-20131102
W
S
r.
Height above Floc (cm)
Velocity (cm/s)
s.
UB3 Profile-20131108
W
S
t.
Height above Floc (cm)
Velocity (cm/s)
u.
UB3 Profile-20140305
W
S
v.
Height above Floc (cm)
Velocity (cm/s)
w.
UB3 Profile-20140812
W
S
x.
Height above Floc (cm)
Velocity (cm/s)

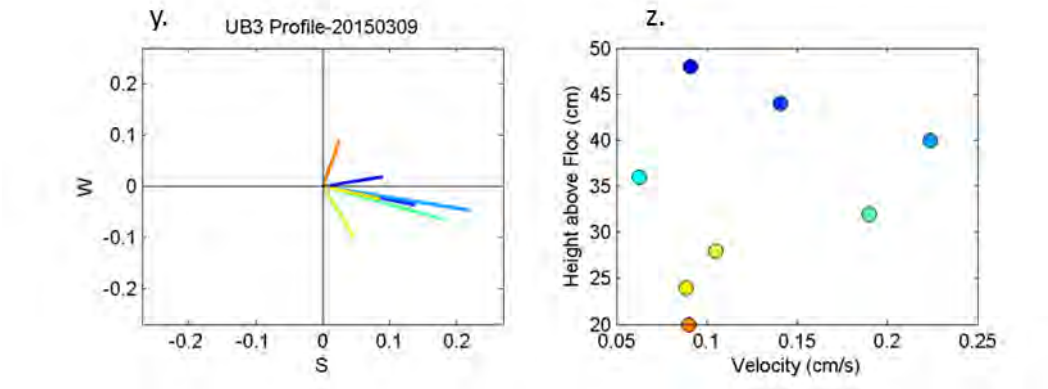

Figure C-117 ADV velocity profiles recorded at DPM site UB3. Profiles recorded on (a-b) Nov. 6, 2010, (c-d) Nov. 4, 2011, (e-f) Nov. 29, 2011, (g-h) Aug. 8, 2012, (i-j) Nov. 6, 2012, (k-l) Dec. 11, 2012, and (m-n) Feb. 27, 2013, (o-p) Aug. 14, 2013, (q-r) Nov. 02, 2013, (s-t) Nov. 08, 2013, (u-v) Mar. 05, 2014, (w-x) Aug. 12, 2014 and (y-z) Mar. 9, 2015. Panels (a), (c), (e), (g), (i), (k), (m), (o), (q), (s), (u), (w) and (y) show velocity vectors (cm/s) with the axes representing cardinal directions, such that the top of the plot is true north. Panels (b), (d), (f), (h), (j), (l), (n), (p), (r), (t), (v), (x) and (z) show horizontal velocities (cm/s). Dates are given in the format yyyymmdd.

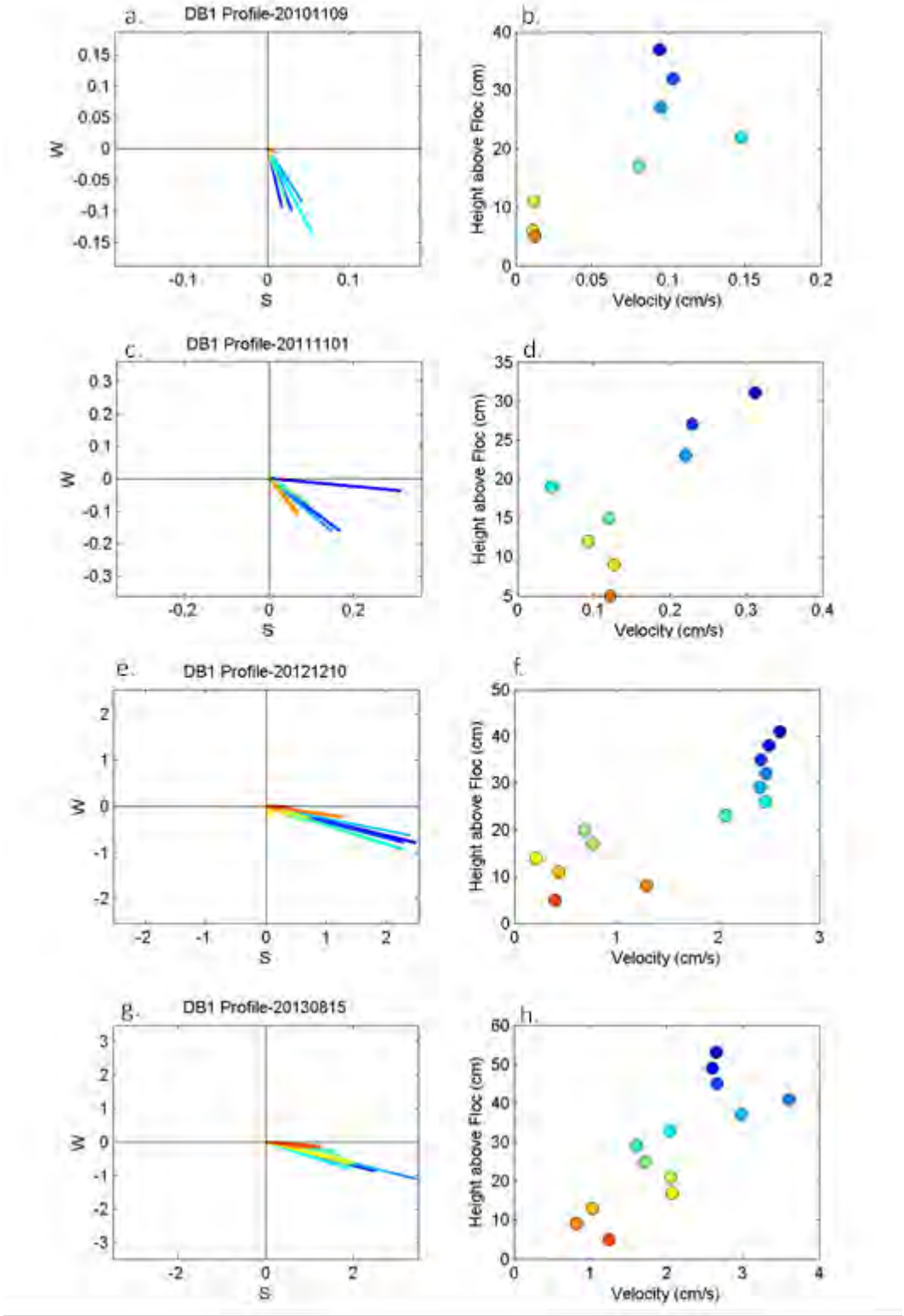
a.
DB1 Profile-20101109
W
S
b.
Height above Floc (cm)
Velocity (cm/s)
c.
DB1 Profile-20111101
d.
e.
DB1 Profile-20121210
f.
g.
DB1 Profile-20130815
h.

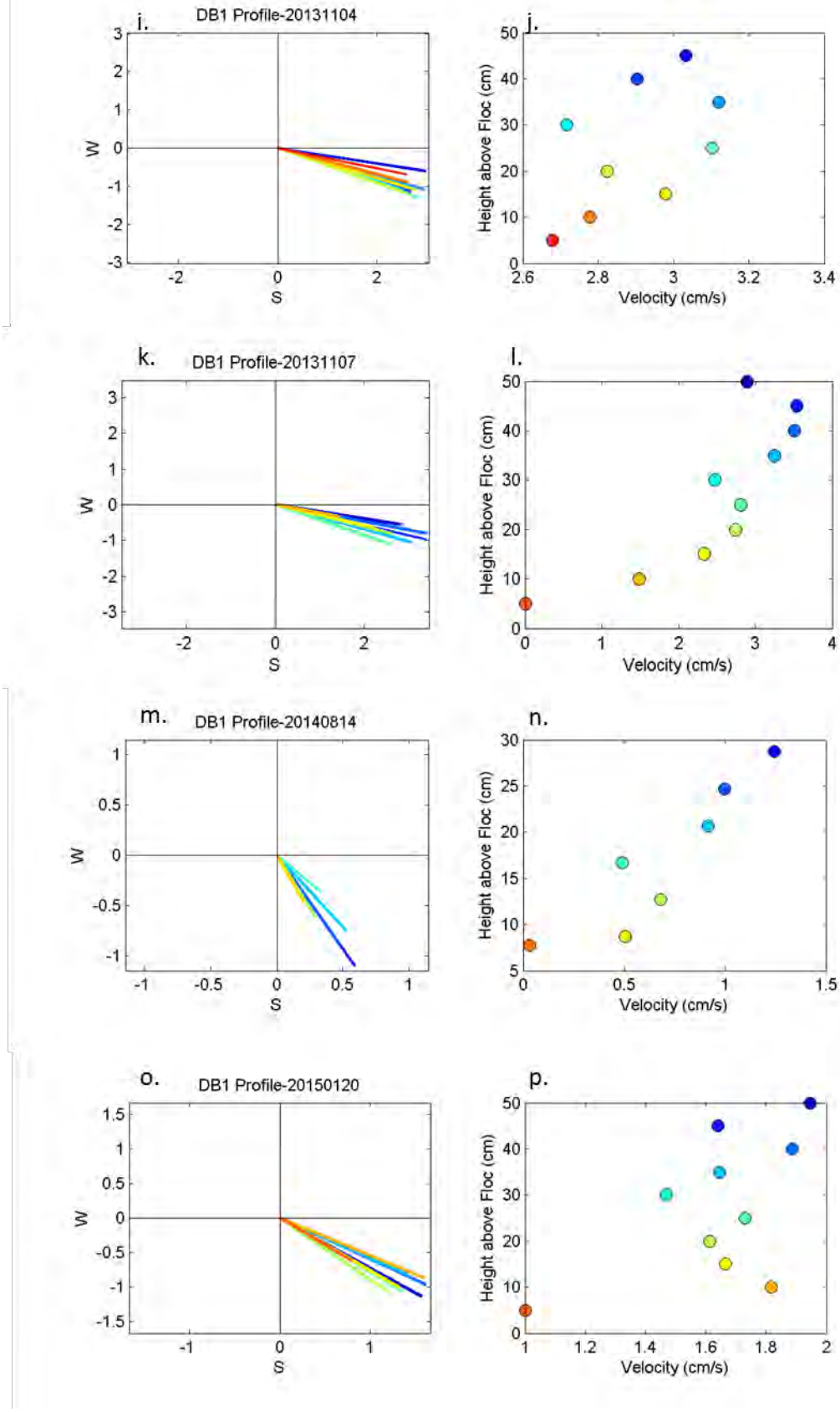
i.
DB1 Profile-20131104
W
S
j.
Height above Floc (cm)
Velocity (cm/s)
k.
DB1 Profile-20131107
W
S
l.
Height above Floc (cm)
Velocity (cm/s)
m.
DB1 Profile-20140814
W
S
n.
Height above Floc (cm)
Velocity (cm/s)
o.
DB1 Profile-20150120
W
S
p.
Height above Floc (cm)
Velocity (cm/s)

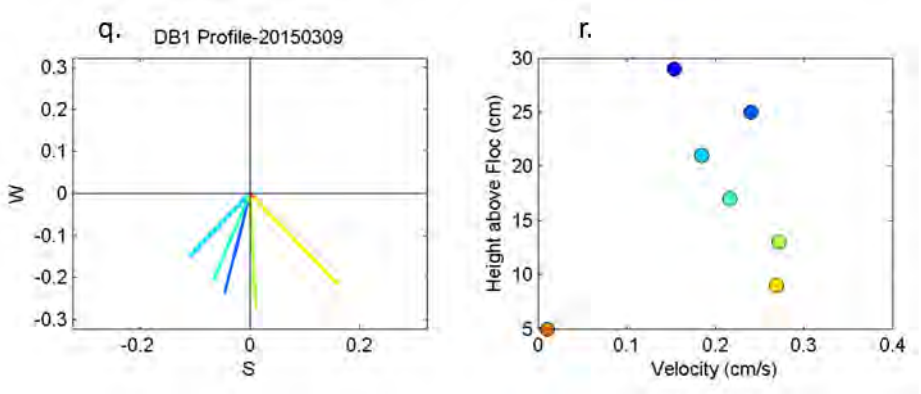

Figure C-118 ADV velocity profiles recorded at DPM site DB1. Profiles recorded on (a-b) Nov. 9, 2010, (c-d) Nov. 1, 2011, (e-f) Dec. 10, 2012, (g-h) Aug. 15, 2013, (i-j) Nov. 04, 2013, (k-l) Nov. 07, 2013, (m-n) Aug. 14, 2014, (o-p) Jan. 20, 2015 and (q-r) Mar. 9, 2015. Panels (a), (c), (e), (g), (i), (k), (m), (o) and (q) show velocity vectors (cm/s) with the axes representing cardinal directions, such that the top of the plot is true north. Panels (b), (d), (f), (h), (i), (l), (n), (p) and (r) show horizontal velocities (cm/s). Dates are given in the format yyyymmdd.

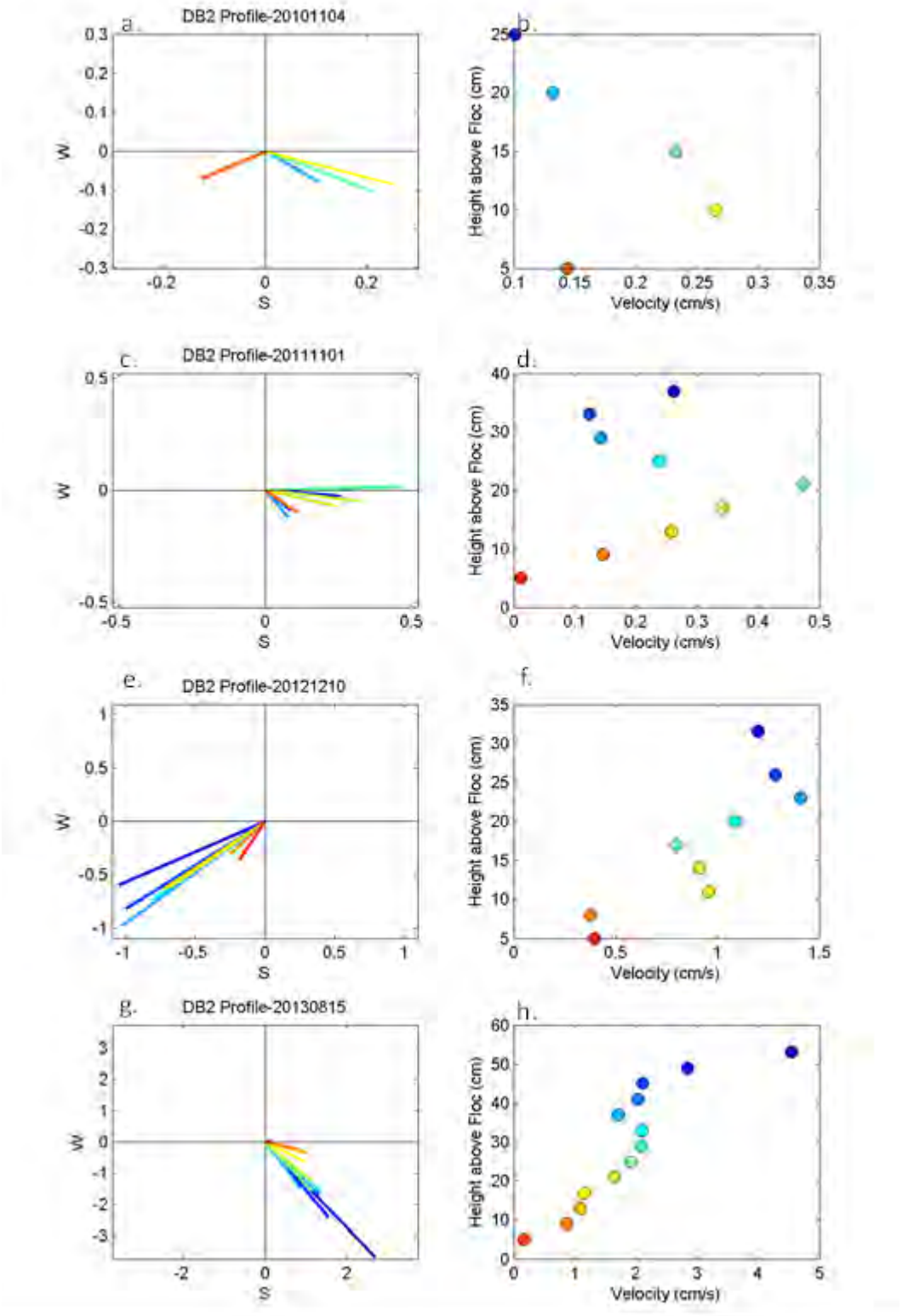
a.
DB2 Profile-20101104
W
S
b.
Height above Floc (cm)
Velocity (cm/s)
c.
DB2 Profile-20111101
W
S
d.
Height above Floc (cm)
Velocity (cm/s)
e.
DB2 Profile-20121210
W
S
f.
Height above Floc (cm)
Velocity (cm/s)
g.
DB2 Profile-20130815
W
S
h.
Height above Floc (cm)
Velocity (cm/s)

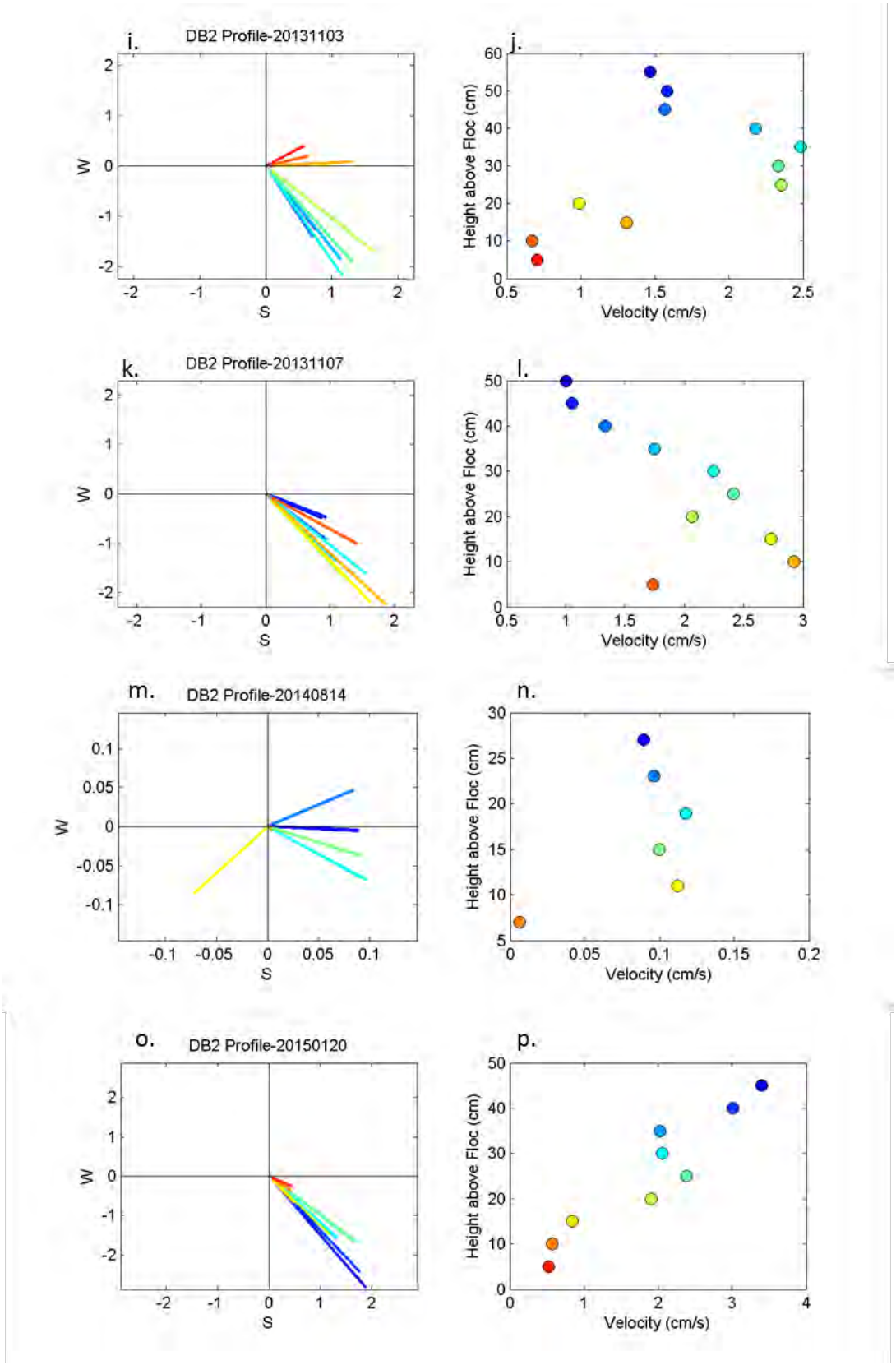
i.
DB2 Profile-20131103
W
S
j.
Height above Floc (cm)
Velocity (cm/s)
k.
DB2 Profile-20131107
W
S
l.
Height above Floc (cm)
Velocity (cm/s)
m.
DB2 Profile-20140814
W
S
n.
Height above Floc (cm)
Velocity (cm/s)
o.
DB2 Profile-20150120
W
S
p.
Height above Floc (cm)
Velocity (cm/s)

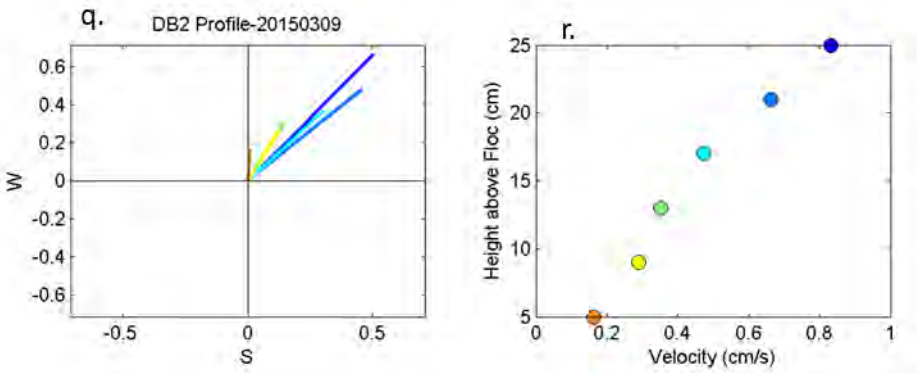

Figure C-119 ADV velocity profiles recorded at DPM site DB2. Profiles recorded on (a-b) Nov. 4, 2010, (c-d) Nov. 1, 2011, (e-f) Dec. 10, 2012, (g-h) Aug. 15, 2013, (i-j) Nov. 03, 2013, (k-l) Nov. 07, 2013, (m-n) Aug. 14, 2014, (o-p) Jan. 20, 2015 and (q-r) Mar. 9, 2015. Panels (a), (c), (e), (g), (i), (k), (m), (o) and (q)show velocity vectors (cm/s) with the axes representing cardinal directions, such that the top of the plot is true north. Panels (b), (d), (f), (h), (i), (l), (n), (p) and (r) show horizontal velocities (cm/s). Dates are given in the format yyyymmdd.

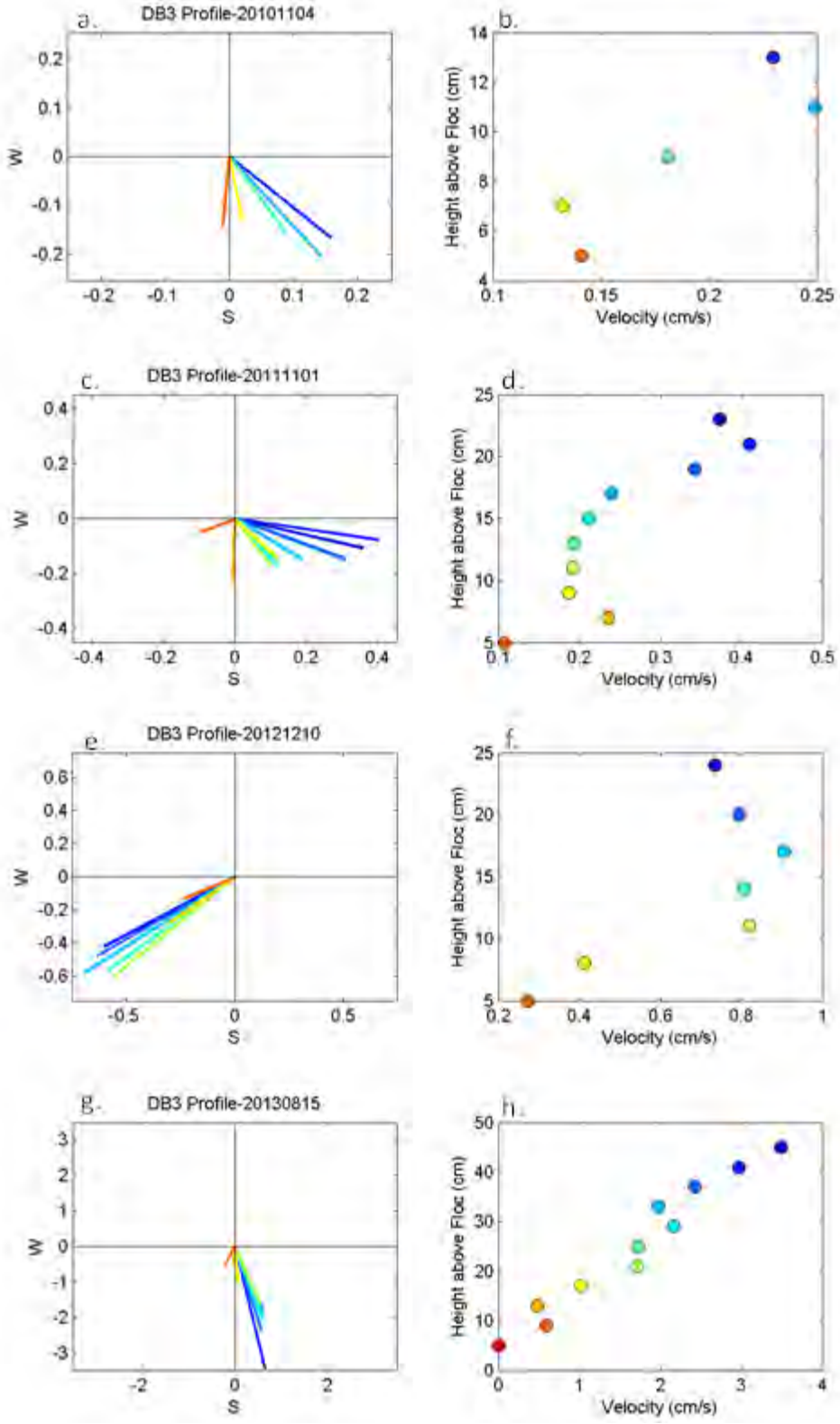
a.
DB3 Profile-20101104
W
S
b.
Height above Floc (cm)
Velocity (cm/s)
c.
DB3 Profile-20111101
W
S
d.
Height above Floc (cm)
Velocity (cm/s)
e.
DB3 Profile-20121210
W
S
f.
Height above Floc (cm)
Velocity (cm/s)
g.
DB3 Profile-20130815
W
S
h.
Height above Floc (cm)
Velocity (cm/s)

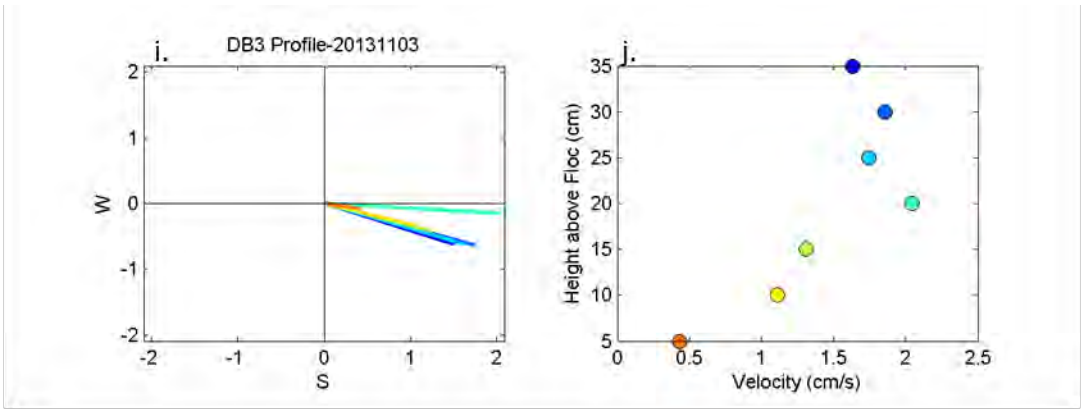
i.
DB3 Profile-20131103
W
S
j.
Height above Floc (cm)
Velocity (cm/s)

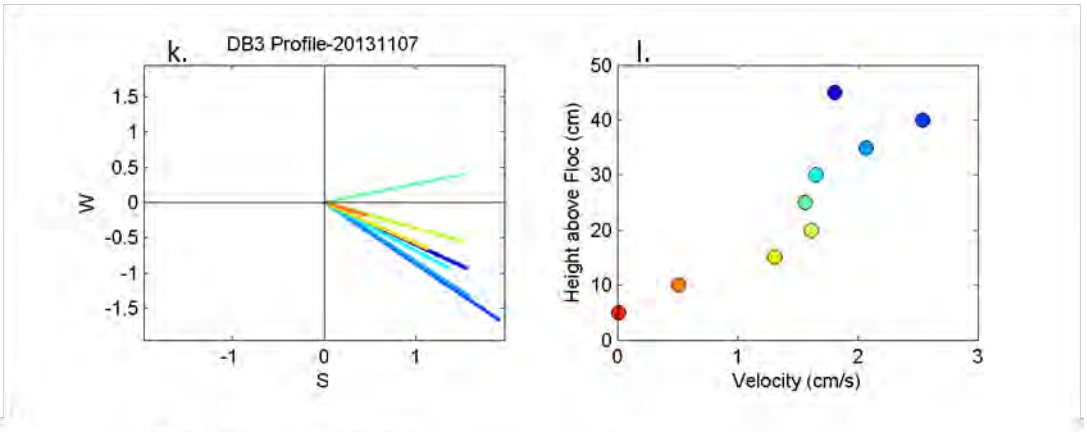
k.
DB3 Profile-20131107
W
S
l.
Height above Floc (cm)
Velocity (cm/s)

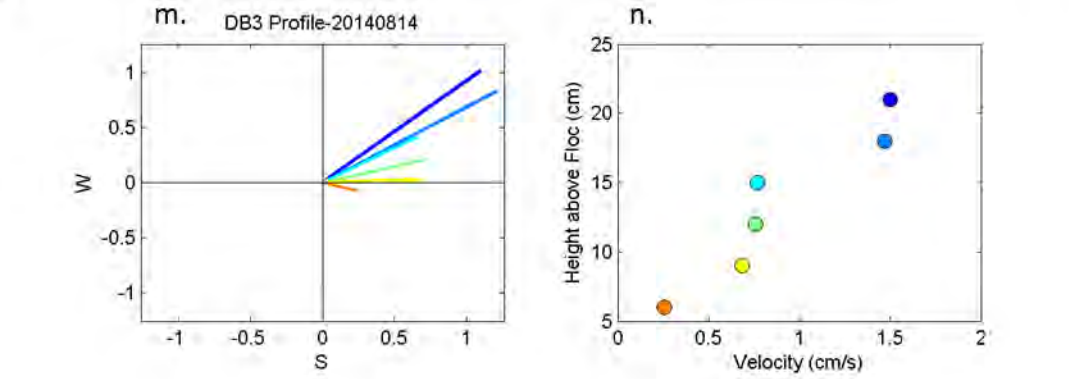
m.
DB3 Profile-20140814
W
S
n.
Height above Floc (cm)
Velocity (cm/s)

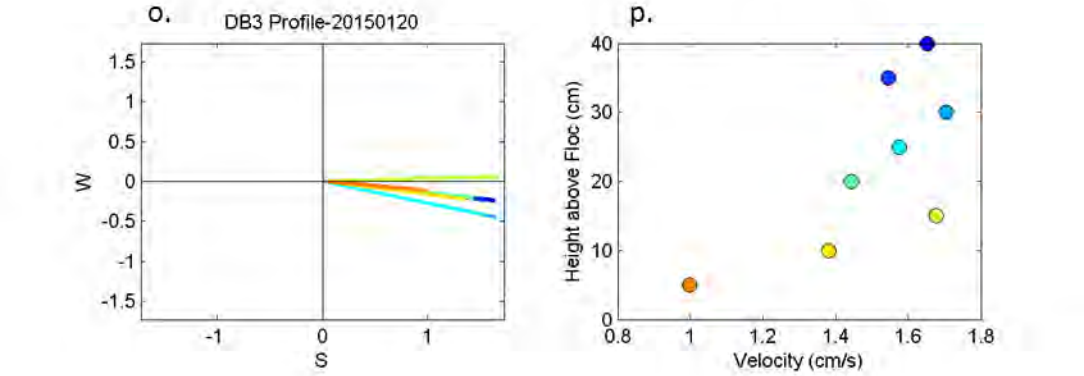
o.
DB3 Profile-20150120
W
S
p.
Height above Floc (cm)
Velocity (cm/s)

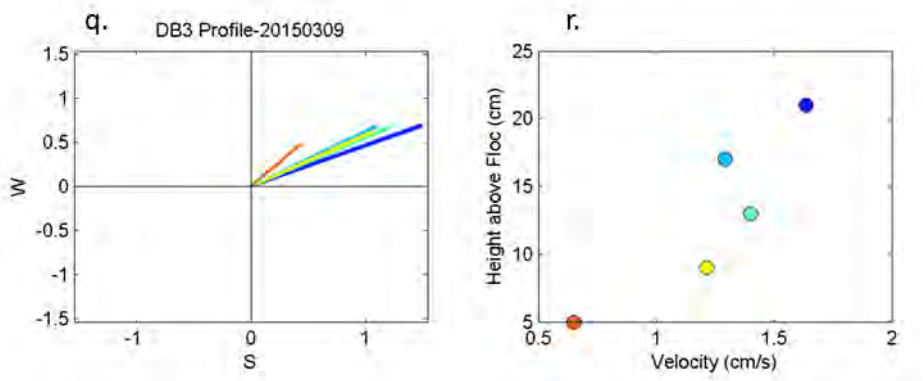

Figure C-120 ADV velocity profiles recorded at DPM site DB3. Profiles recorded on (a-b) Nov. 4, 2010, (c-d) Nov. 1, 2011, (e-f) Dec. 10, 2012, (g-h) Aug. 15, 2013, (i-j) Nov. 03, 2013, (k-l) Nov. 07, 2013, (m-n) Aug. 14, 2014, (o-p) Jan. 20, 2015 and (q-r) Mar. 9, 2015. Panels (a), (c), (e), (g), (i), (k), (m), (o) and (q)show velocity vectors (cm/s) with the axes representing cardinal directions, such that the top of the plot is true north. Panels (b), (d), (f), (h), (i), (l), (n), (p) and (r) show horizontal velocities (cm/s). Dates are given in the format yyyymmdd.

2013 Flow Release Profiles

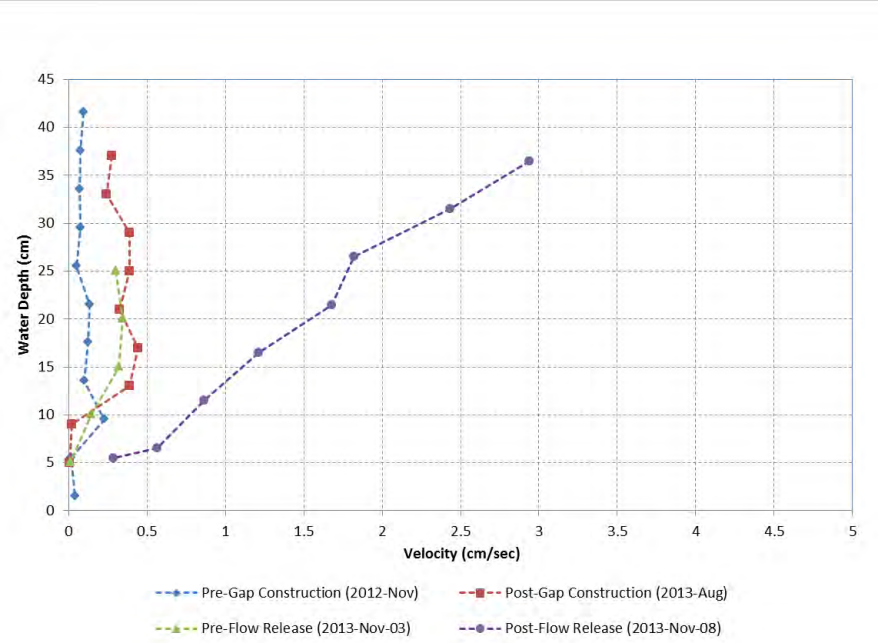

Figure C-121. Flow Release 2013 ADV velocity profiles recorded at DPM site RS1D Ridge. Horizontal velocities in cm/s are shown.

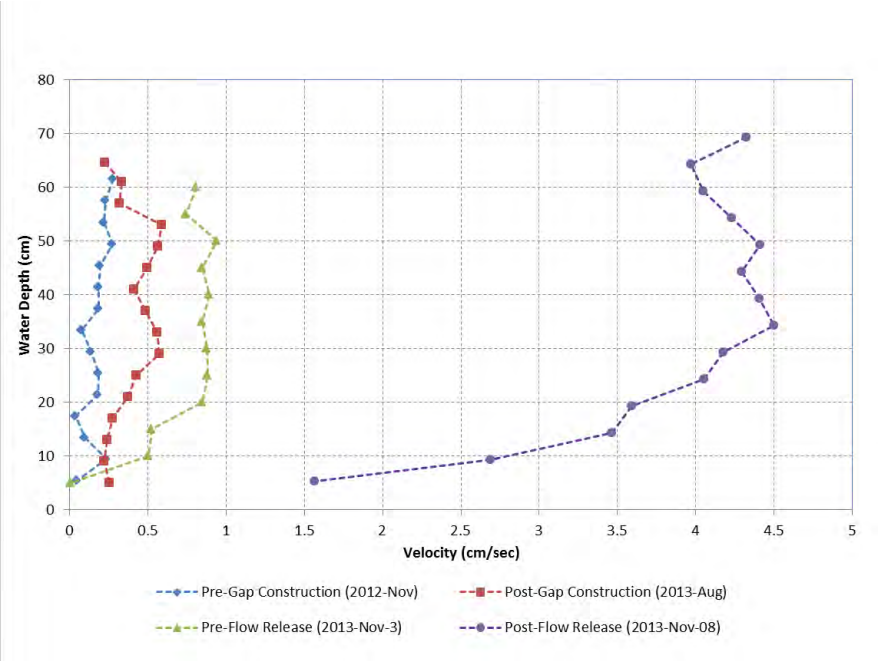

Figure C-122 Flow Release 2013 ADV velocity profiles recorded at DPM site RS1D Slough. Horizontal velocities in cm/s are shown.

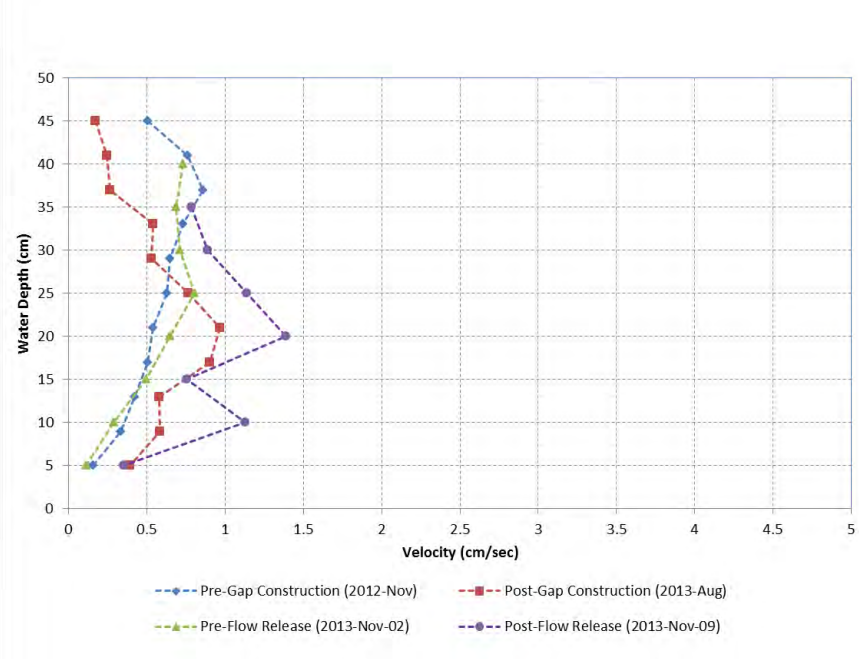

Figure C-123 Flow Release 2013 ADV velocity profiles recorded at DPM site RS2 Ridge. Horizontal velocities in cm/s are shown.

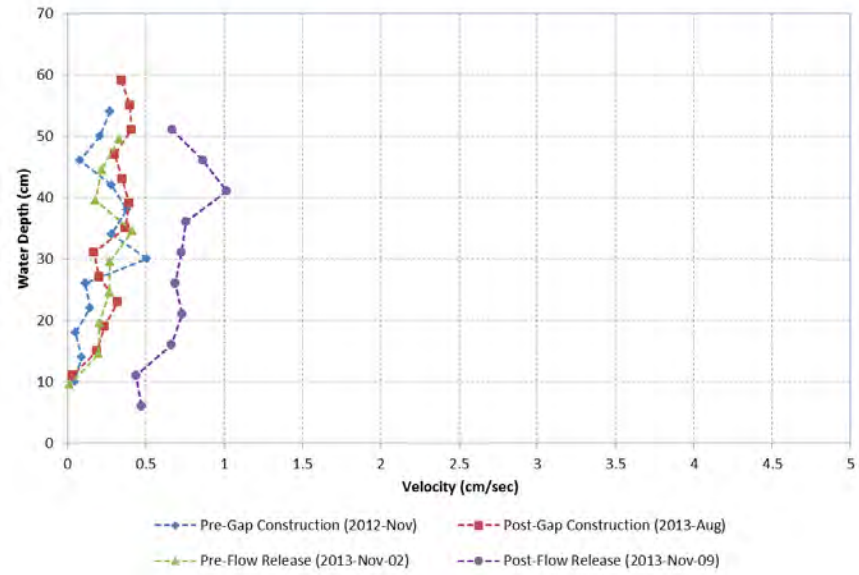

Figure C-124. Flow Release 2013 ADV velocity profiles recorded at DPM site S1. Horizontal velocities in cm/s are shown.

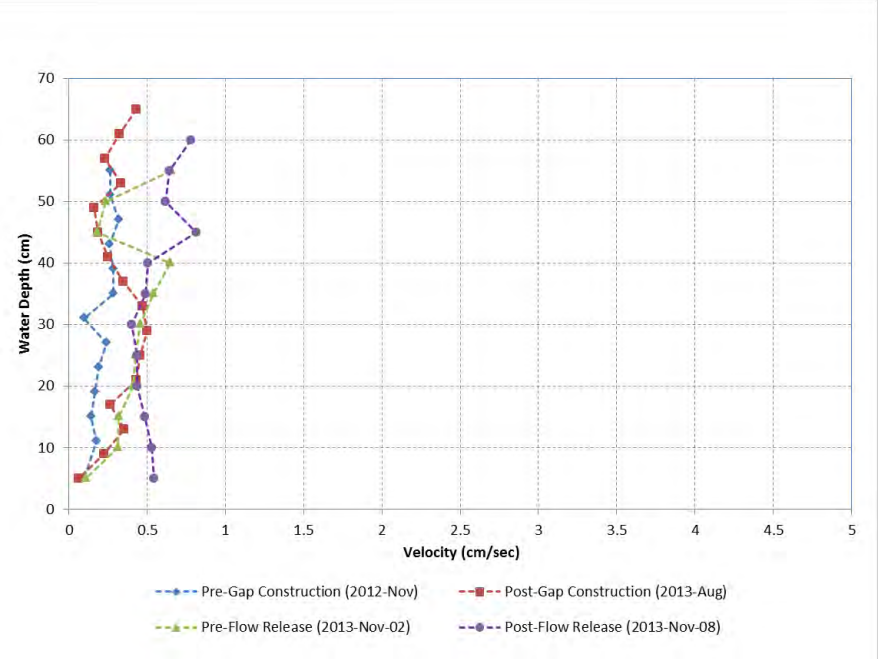

Figure C-125 Flow Release 2013 ADV velocity profiles recorded at DPM site UB1. Horizontal velocities in cm/s are shown.

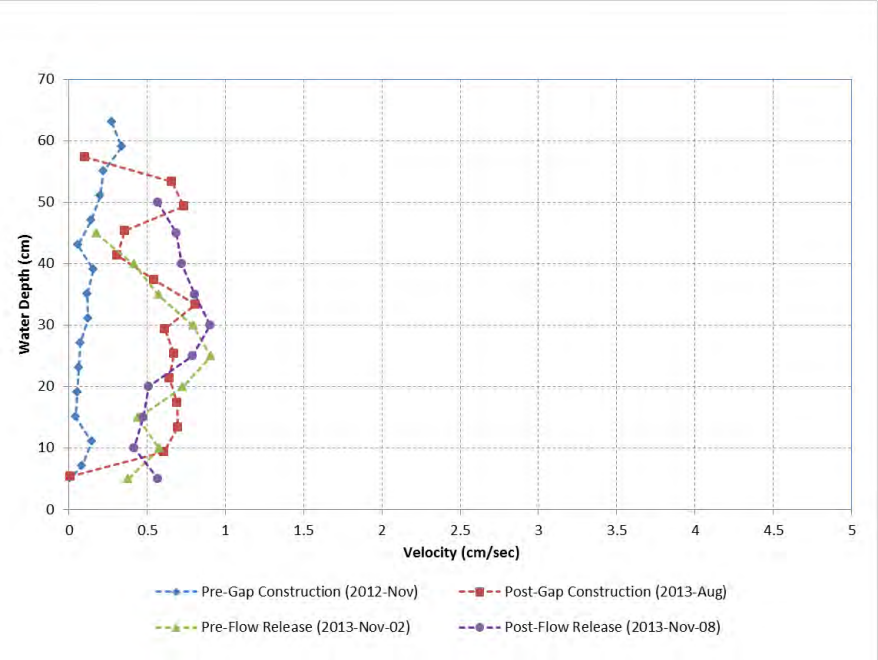

Figure C-126 Flow Release 2013 ADV velocity profiles recorded at DPM site UB2. Horizontal velocities in cm/s are shown.

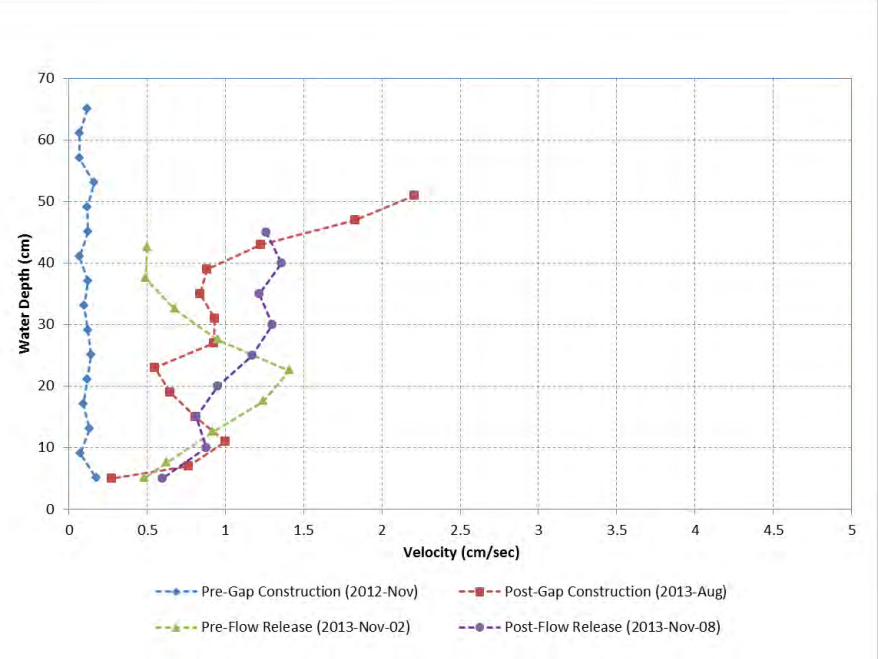

Figure C-127 Flow Release 2013 ADV velocity profiles recorded at DPM site UB3. Horizontal velocities in cm/s are shown.

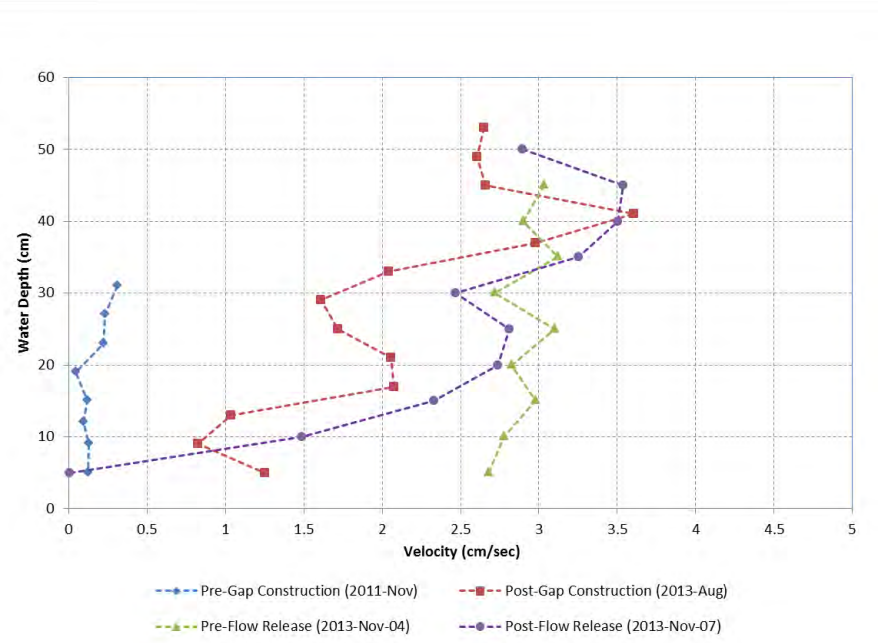

Figure C-128 Flow Release 2013 ADV velocity profiles recorded at DPM site DB1. Horizontal velocities in cm/s are shown.

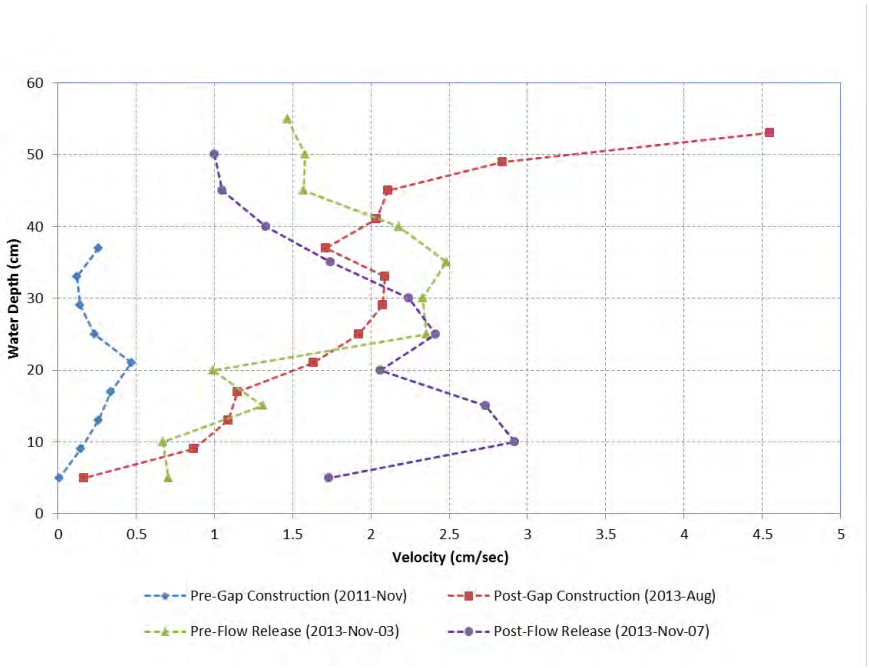

Figure C-129 Flow Release 2013 ADV velocity profiles recorded at DPM site DB2. Horizontal velocities in cm/s are shown.

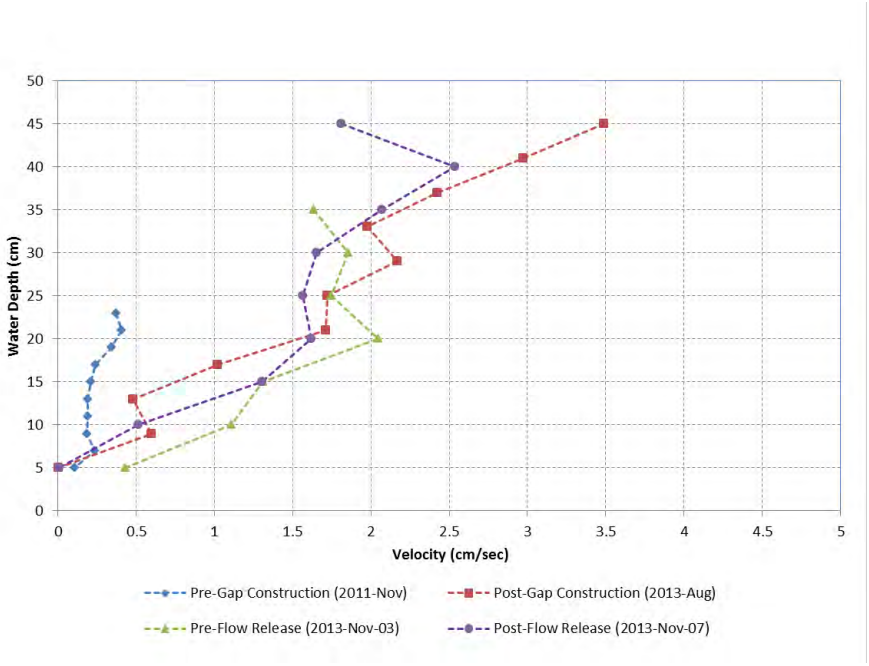

Figure C-130 Flow Release 2013 ADV velocity profiles recorded at DPM site DB3. Horizontal velocities in cm/s are shown.

2014 Flow Release Profiles

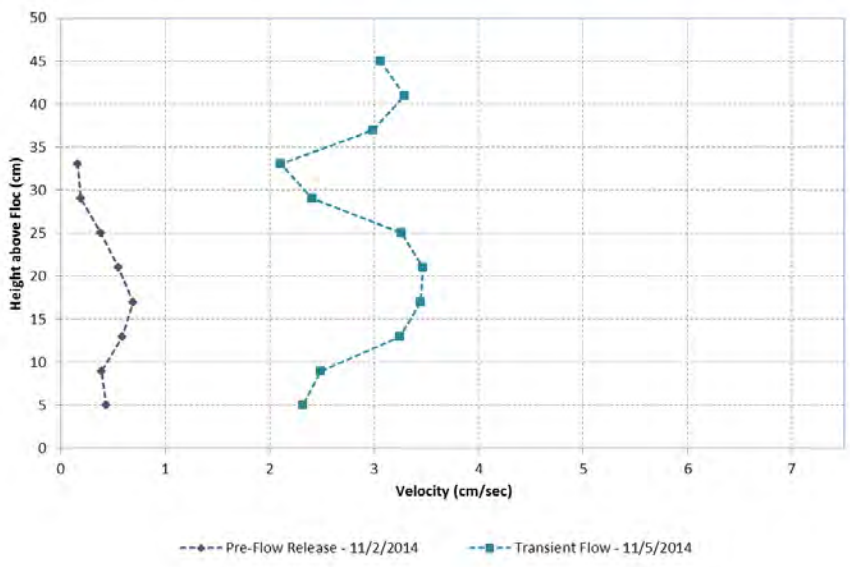

Figure C-131. Flow Release 2014 ADV velocity profiles recorded at DPM site RS1U Ridge. Horizontal velocities in cm/s are shown.

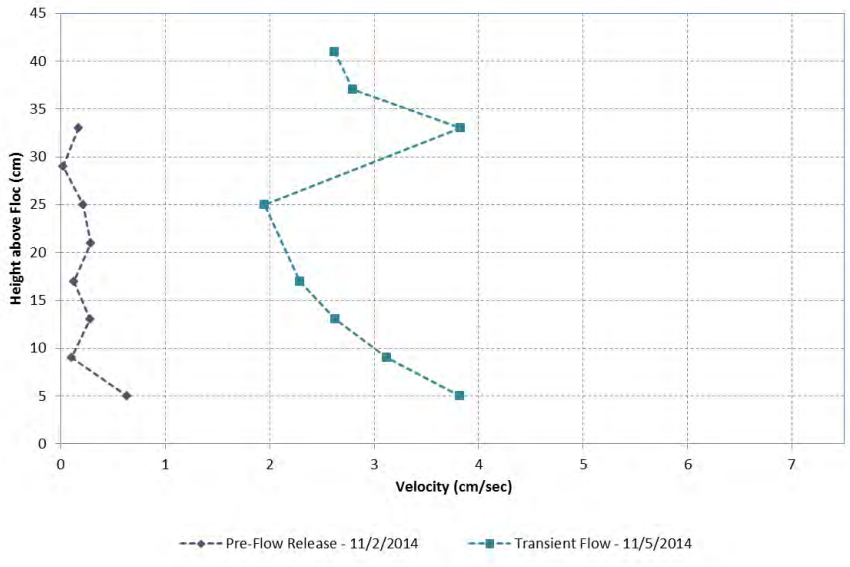

Figure C-132 Flow Release 2014 ADV velocity profiles recorded at DPM site RS1U Slough. Horizontal velocities in cm/s are shown.

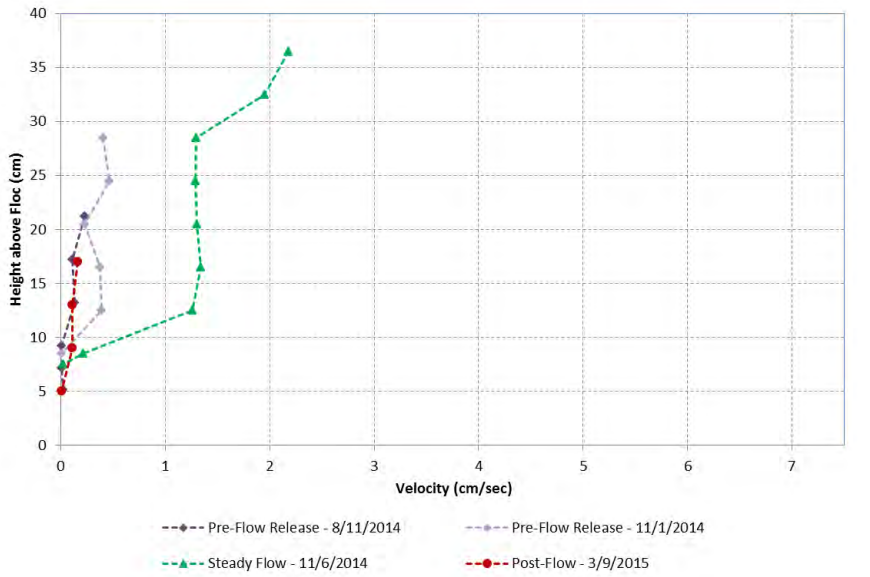

Figure C-133 Flow Release 2014 ADV velocity profiles recorded at DPM site RS1D Ridge. Horizontal velocities in cm/s are shown.

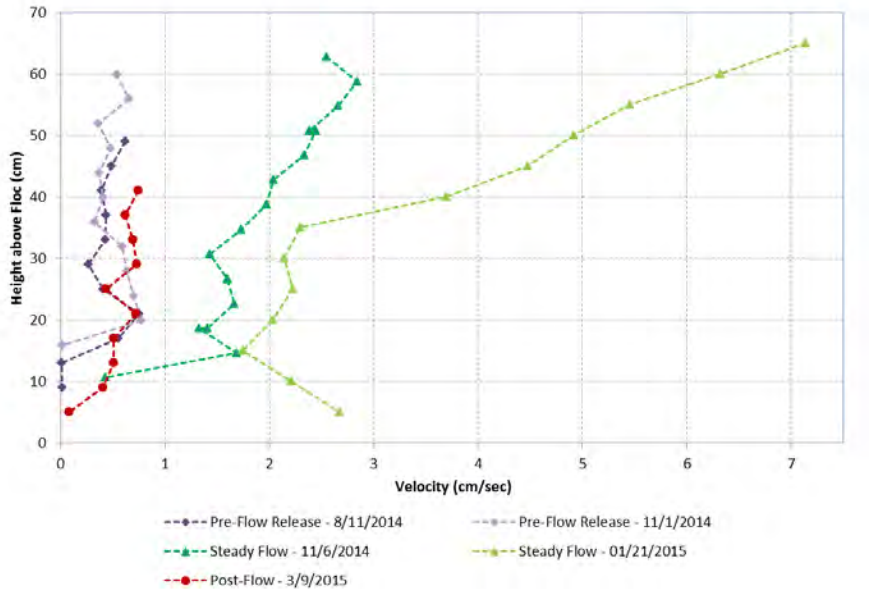

Figure C-134 Flow Release 2014 ADV velocity profiles recorded at DPM site RS1D Slough. Horizontal velocities in cm/s are shown.

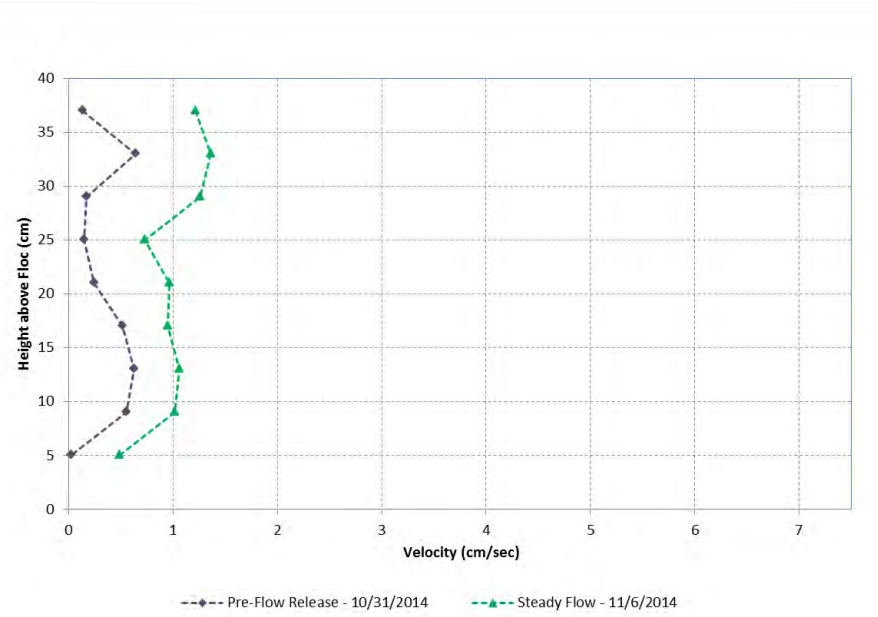

Figure C-135 Flow Release 2014 ADV velocity profiles recorded at DPM site RS2 Ridge. Horizontal velocities in cm/s are shown.

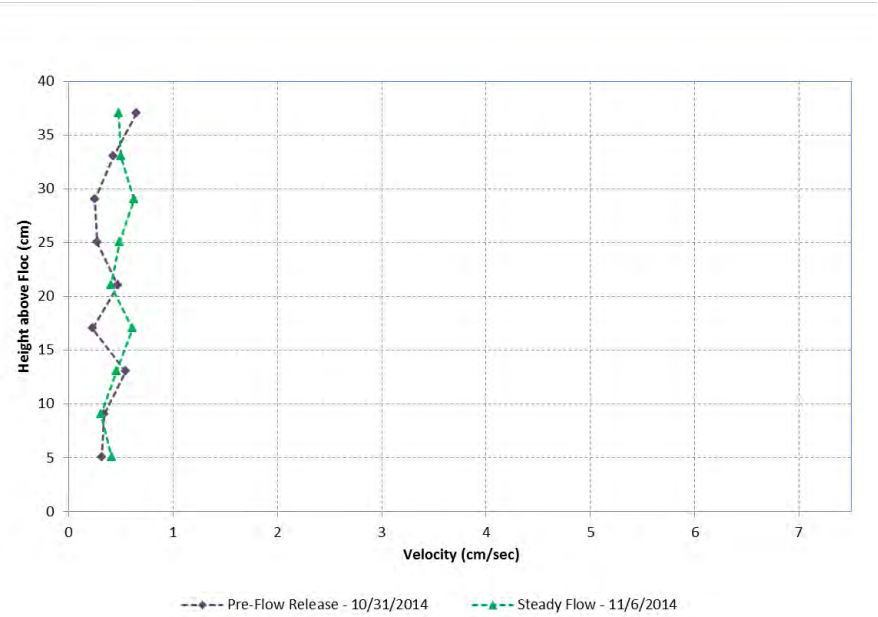

Figure C-136 Flow Release 2014 ADV velocity profiles recorded at DPM site RS2 Slough. Horizontal velocities in cm/s are shown.

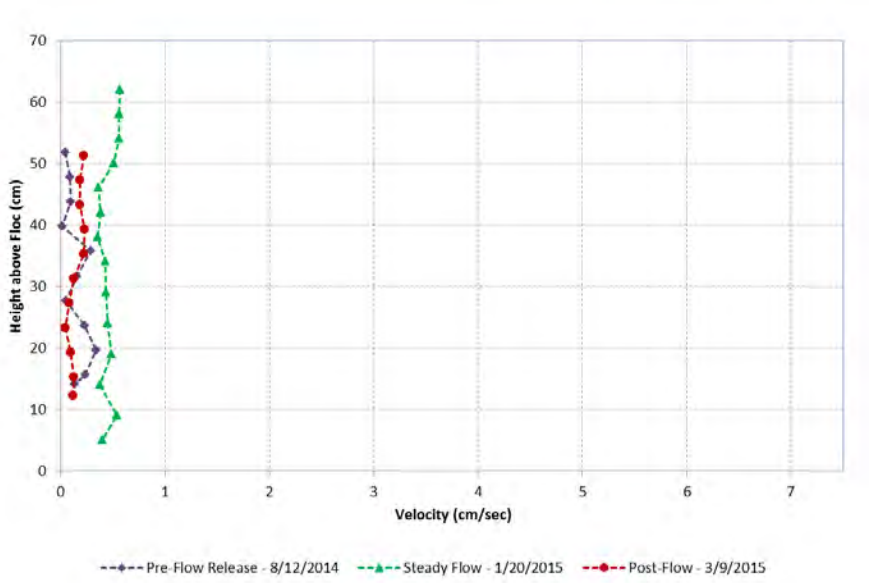

Figure C-137 Flow Release 2014 ADV velocity profiles recorded at DPM site UB1. Horizontal velocities in cm/s are shown.

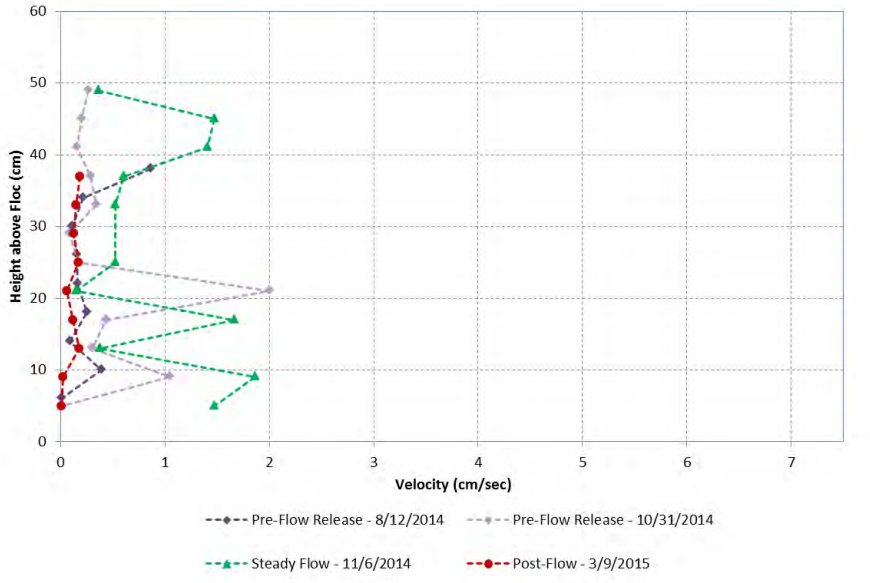

Figure C-138 Flow Release 2014 ADV velocity profiles recorded at DPM site UB2. Horizontal velocities in cm/s are shown.

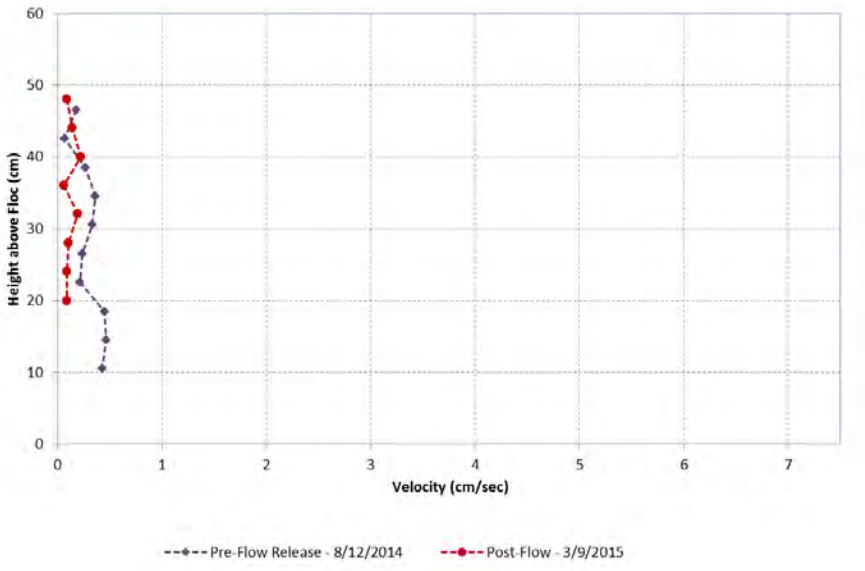

Figure C-139 Flow Release 2014 ADV velocity profiles recorded at DPM site UB3. Horizontal velocities in cm/s are shown.

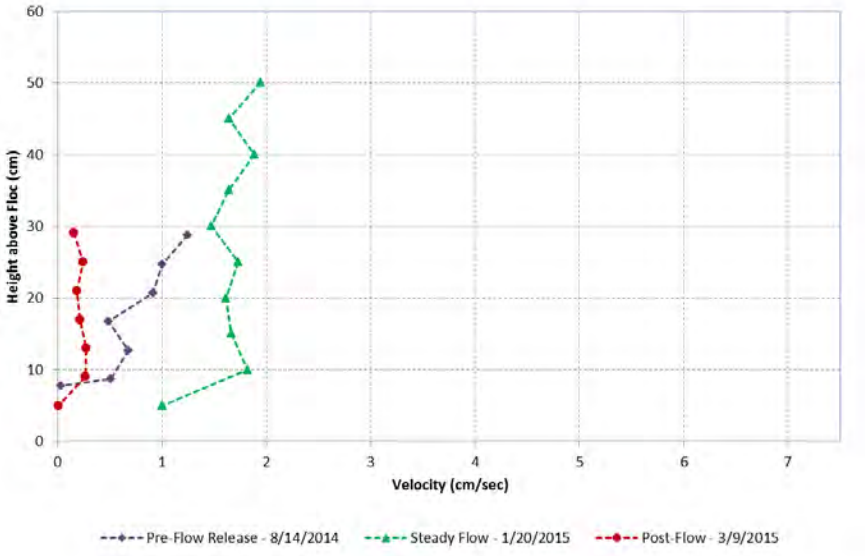

Figure C-140 Flow Release 2014 ADV velocity profiles recorded at DPM site DB1. Horizontal velocities in cm/s are shown.

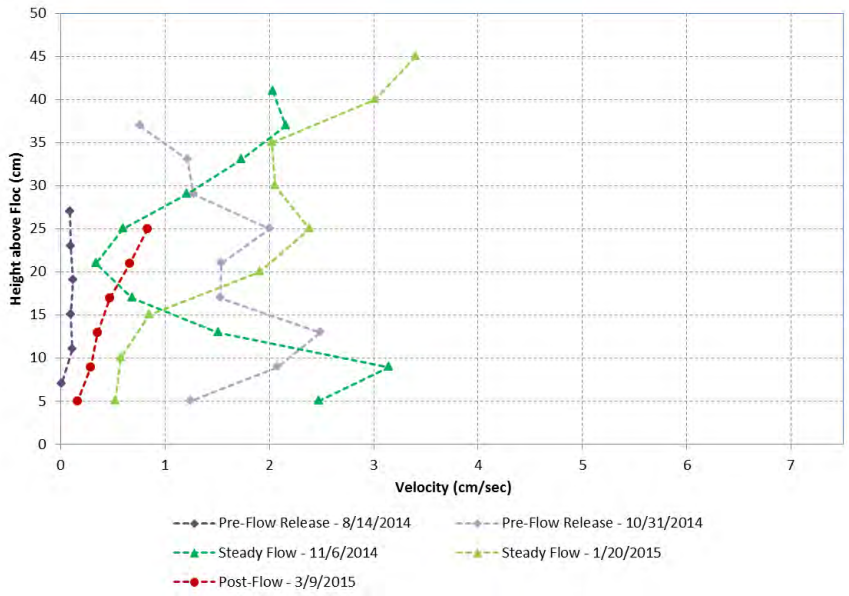

Figure C-141 Flow Release 2014 ADV velocity profiles recorded at DPM site DB2. Horizontal velocities in cm/s are shown.

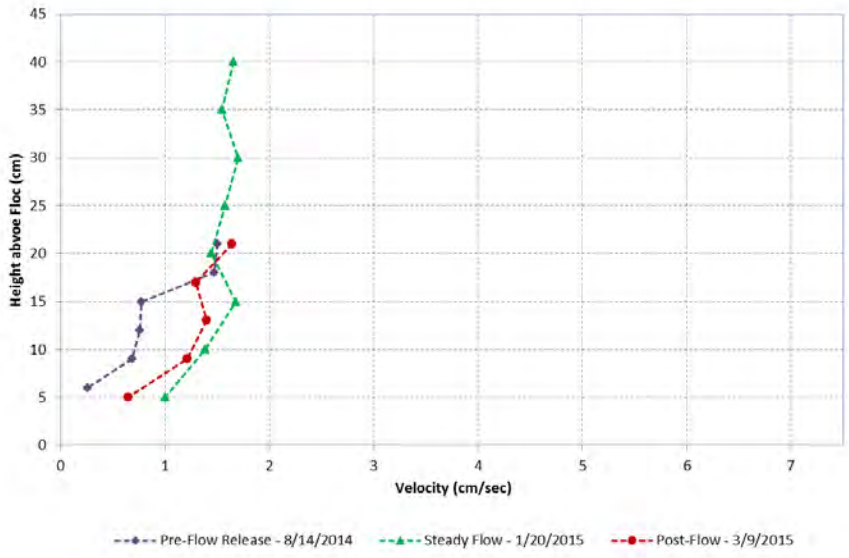

Figure C-142 Flow Release 2014 ADV velocity profiles recorded at DPM site DB3. Horizontal velocities in cm/s are shown.

2015 Flow Release Profiles

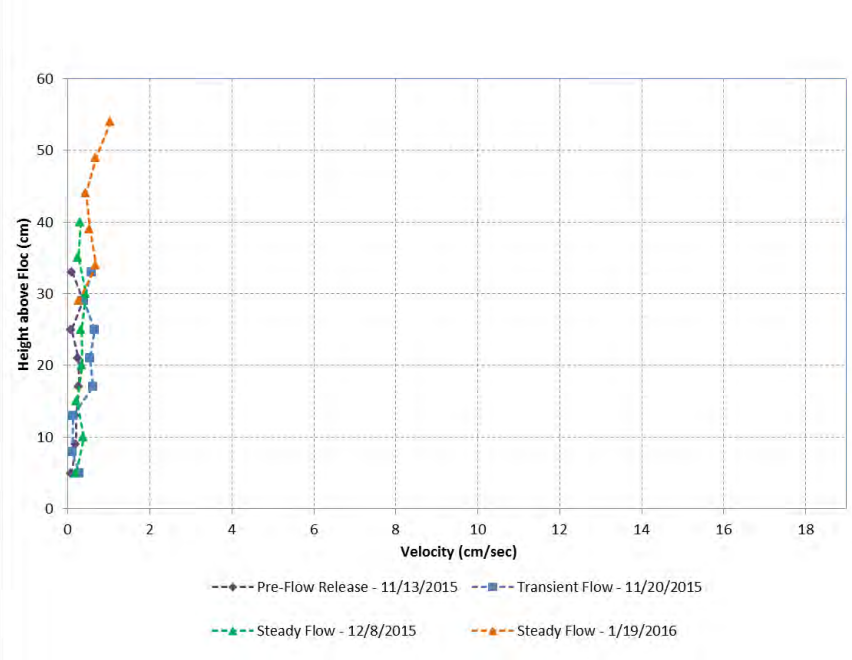

Figure C-143. Flow Release 2015 ADV velocity profiles recorded at DPM site C2 Slough. Horizontal velocities in cm/s are shown.

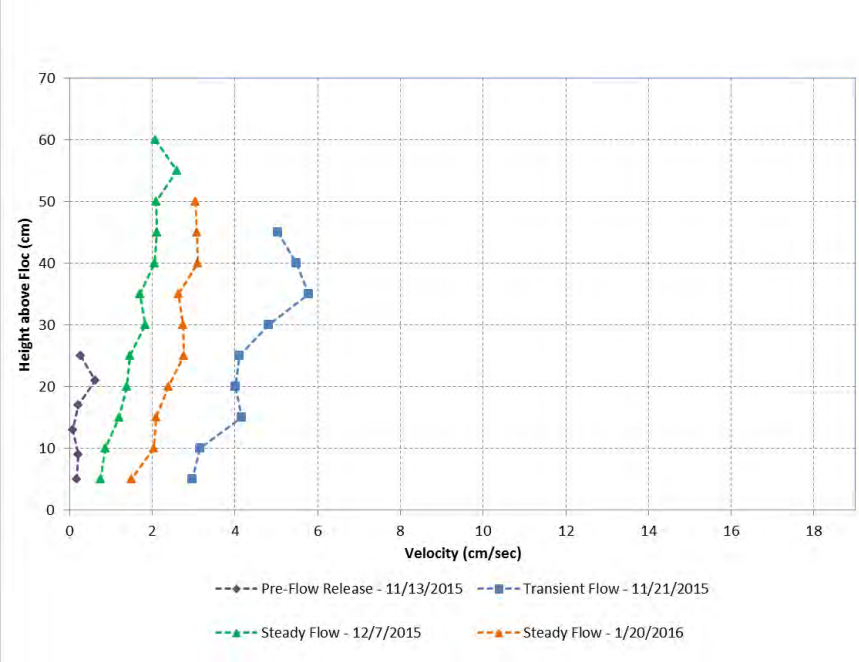

Figure C-144 Flow Release 2015 ADV velocity profiles recorded at DPM site Z51_USGS Ridge. Horizontal velocities in cm/s are shown.

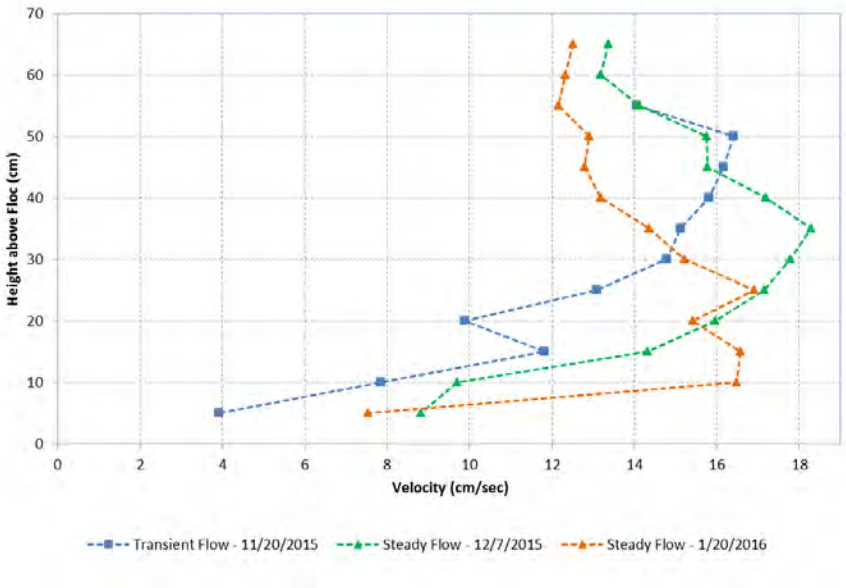

Figure C-145 Flow Release 2015 ADV velocity profiles recorded at DPM site Z51_USGS Slough. Horizontal velocities in cm/s are shown.

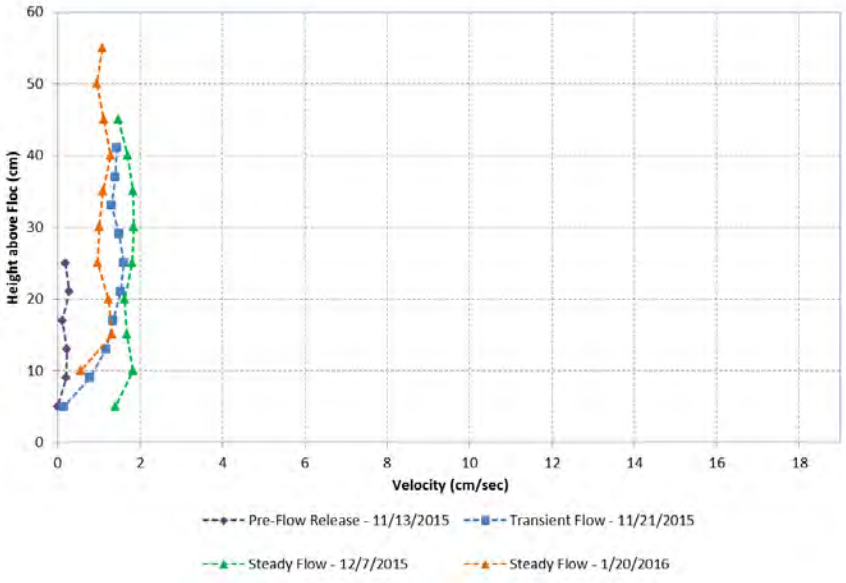

Figure C-146 Flow Release 2015 ADV velocity profiles recorded at DPM site RS1D Ridge. Horizontal velocities in cm/s are shown.

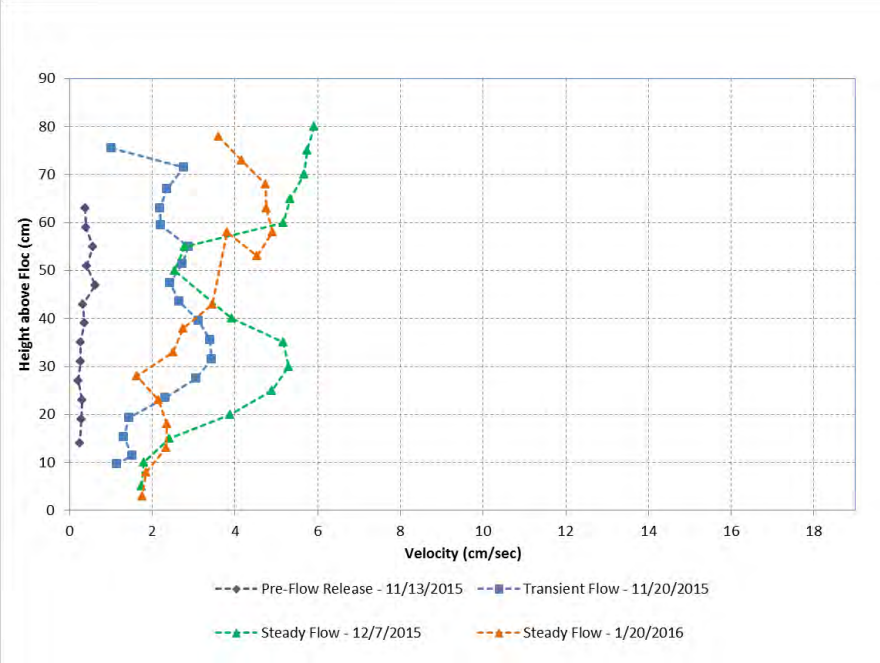

Figure C-147 Flow Release 2015 ADV velocity profiles recorded at DPM site RS1D Slough. Horizontal velocities in cm/s are shown.

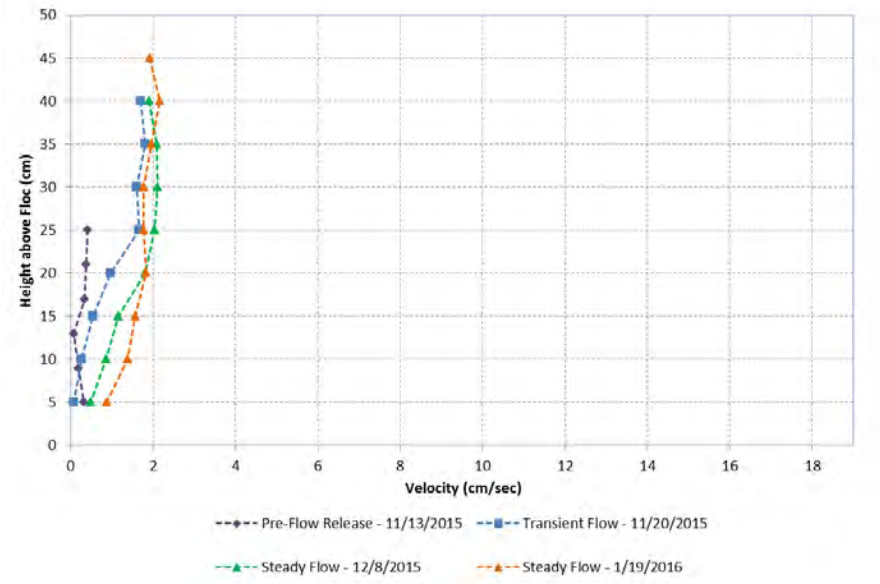

Figure C-148 Flow Release 2015 ADV velocity profiles recorded at DPM site RS2 Ridge. Horizontal velocities in cm/s are shown.

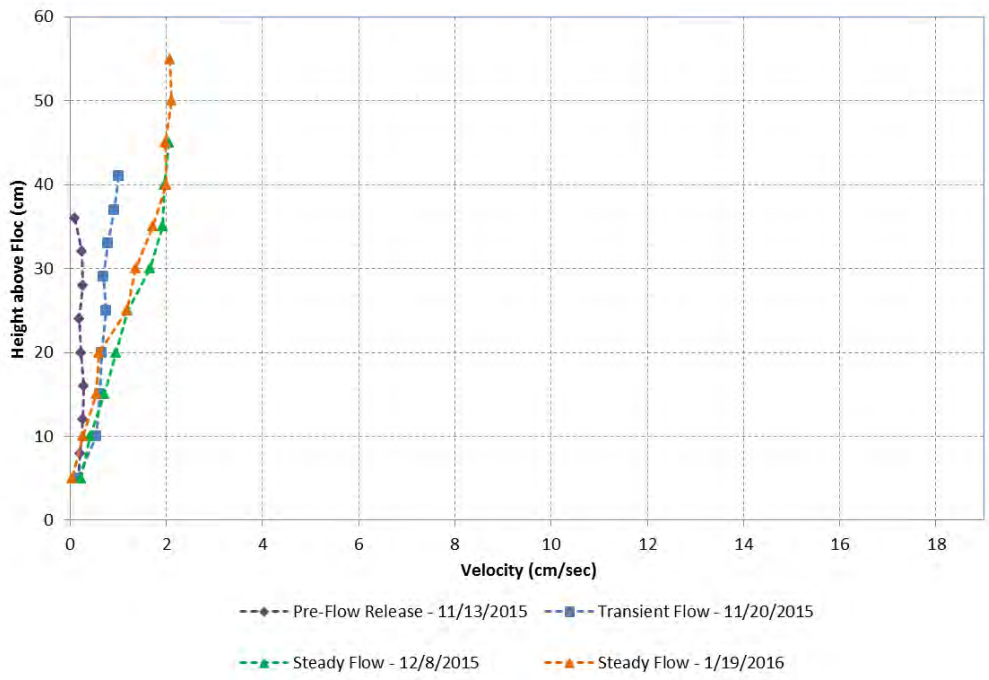

Figure C-149 Flow Release 2015 ADV velocity profiles recorded at DPM site UB2. Horizontal velocities in cm/s are shown.

Flow Tracker Profile Velocity for the 2014 Flow Release Year

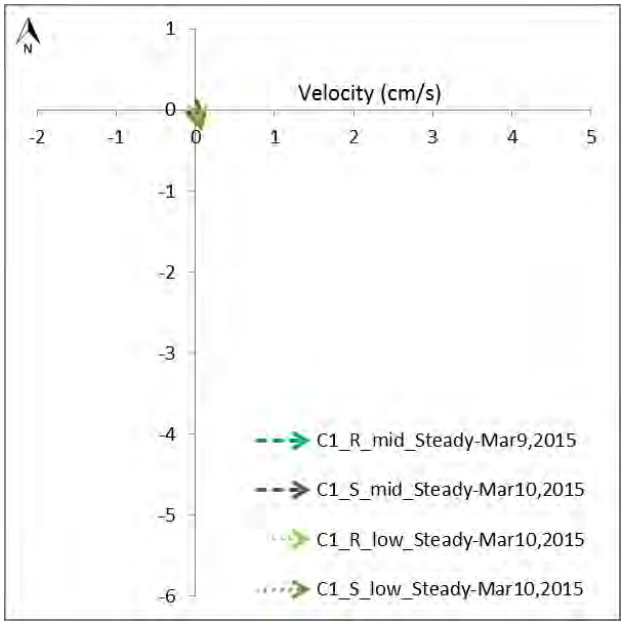

Figure C-150 Velocities at C1 from Flow Tracker measurements. “Low,” “mid” and “high” indicate samples taken approximately 5 cm above the floc, in the middle of the water column and 5 cm below the water surface.

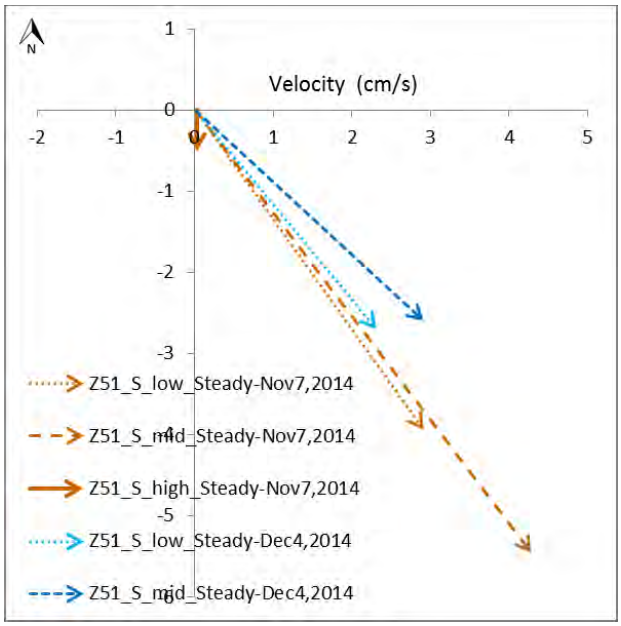

Figure C-151 Velocities at Z51 Slough from Flow Tracker measurements. “Low,” “mid” and “high” indicate samples taken approximately 5 cm above the floc, in the middle of the water column and 5 cm below the water surface.

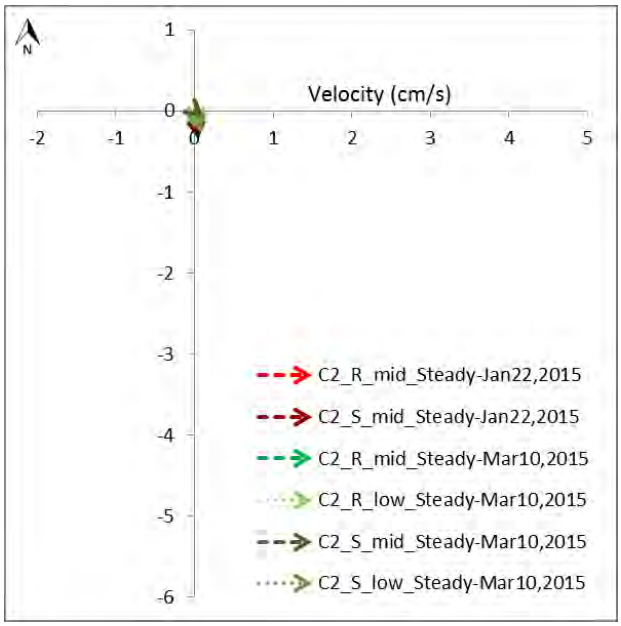

Figure C-152 Velocities at C2 from Flow Tracker measurements. “Low,” “mid” and “high” indicate samples taken approximately 5 cm above the floc, in the middle of the water column and 5 cm below the water surface.

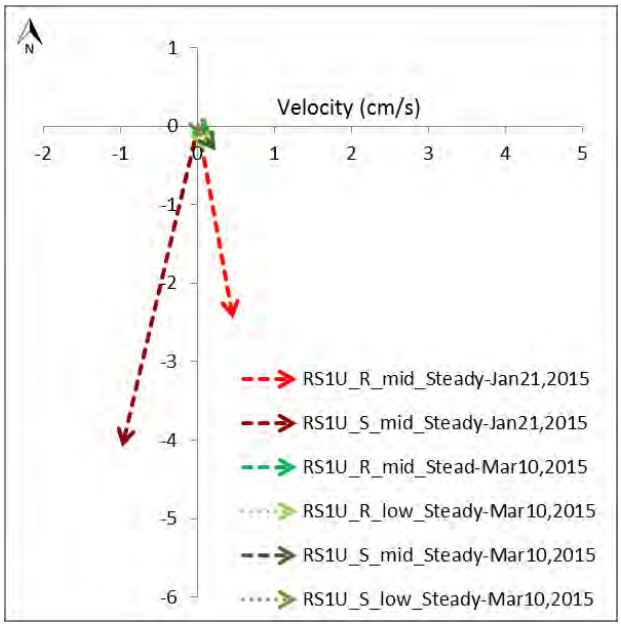

Figure C-153 Velocities at RS1U Ridge and Slough from Flow Tracker measurements. “Low,” “mid” and “high” indicate samples taken approximately 5 cm above the floc, in the middle of the water column and 5 cm below the water surface.

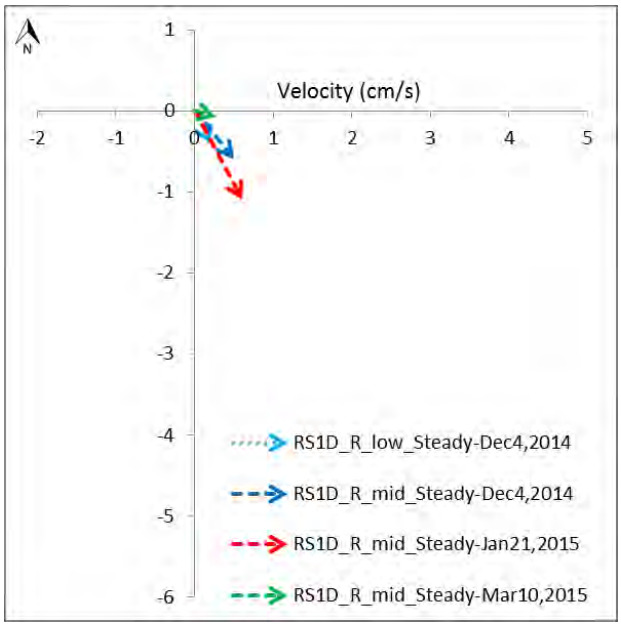

Figure C-154 Velocities at RS1D Ridge from Flow Tracker measurements. “Low,” “mid” and “high” indicate samples taken approximately 5 cm above the floc, in the middle of the water column and 5 cm below the water surface.

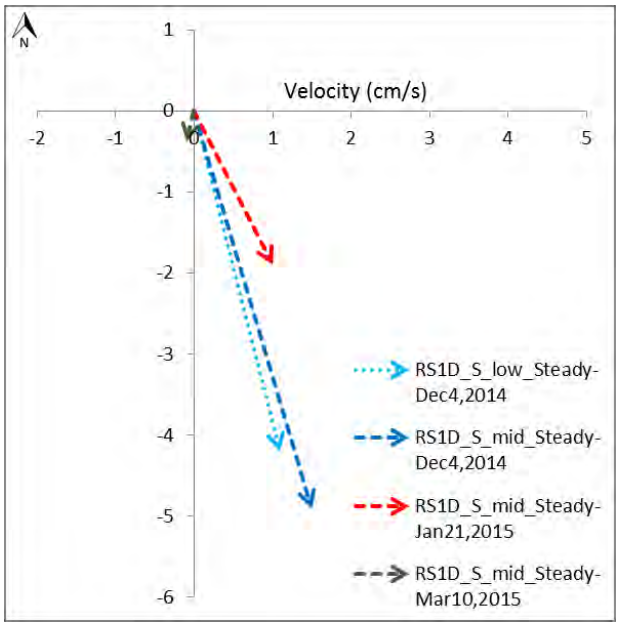

Figure C-155 Velocities at RS1D Slough from Flow Tracker measurements. “Low,” “mid” and “high” indicate samples taken approximately 5 cm above the floc, in the middle of the water column and 5 cm below the water surface.

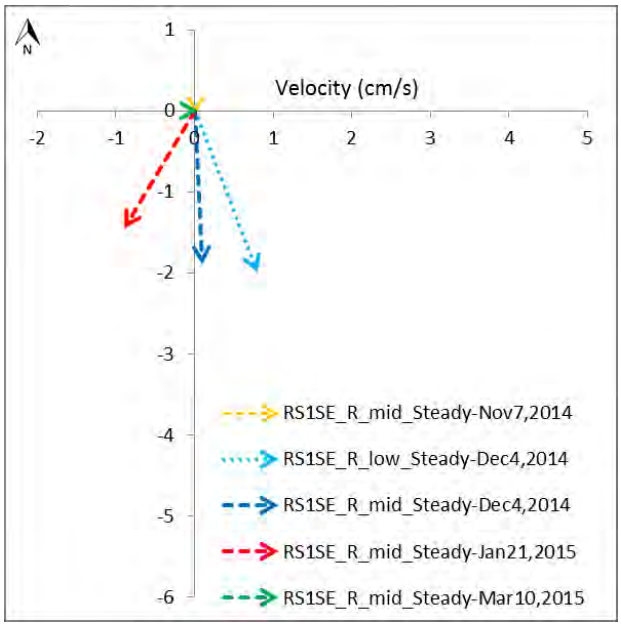

Figure C-156 Velocities at RS1SE Ridge from Flow Tracker measurements. “Low,” “mid” and “high” indicate samples taken approximately 5 cm above the floc, in the middle of the water column and 5 cm below the water surface.

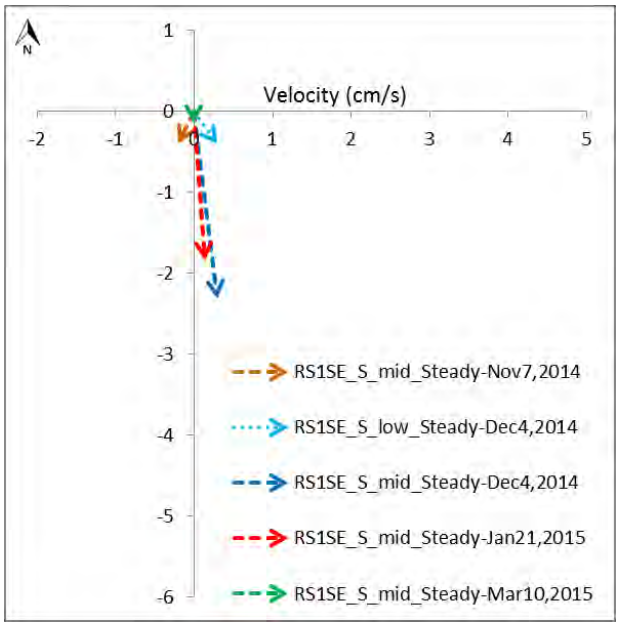

Figure C-157 Velocities at RS1SE Slough from Flow Tracker measurements. “Low,” “mid” and “high” indicate samples taken approximately 5 cm above the floc, in the middle of the water column and 5 cm below the water surface.

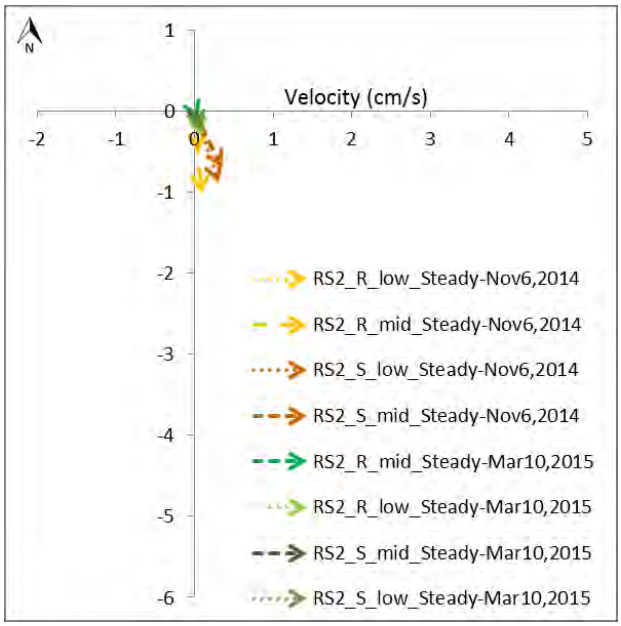

Figure C-158 Velocities at RS2 Ridge and Slough from Flow Tracker measurements. “Low,” “mid” and “high” indicate samples taken approximately 5 cm above the floc, in the middle of the water column and 5 cm below the water surface.

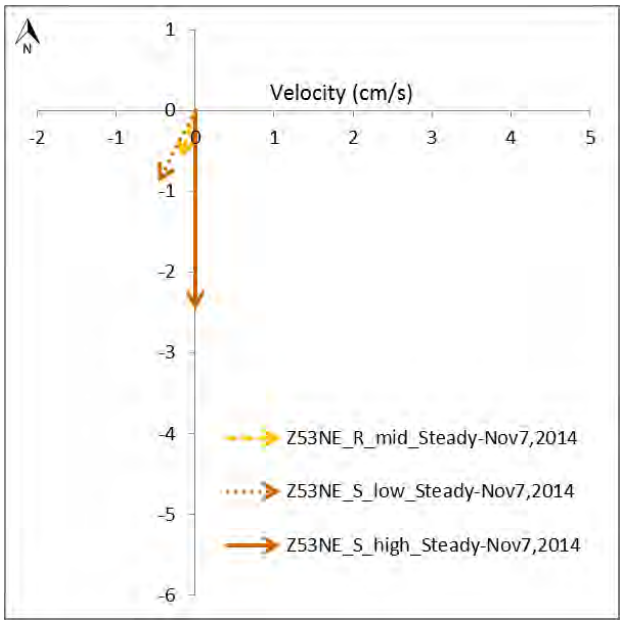

Figure C-159 Velocities at Z53NE_2014 Ridge and Slough from Flow Tracker measurements. “Low,” “mid” and “high” indicate samples taken approximately 5 cm above the floc, in the middle of the water column and 5 cm below the water surface.

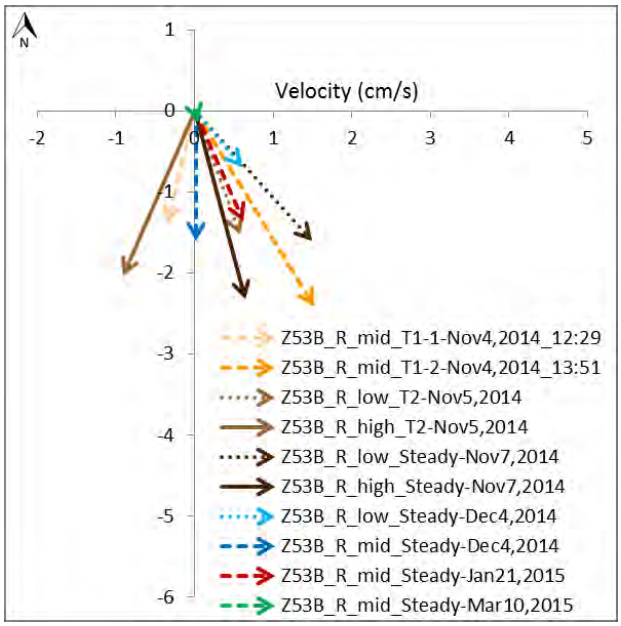

Figure C-160 Velocities at Z53B Ridge from Flow Tracker measurements. “Low,” “mid” and “high” indicate samples taken approximately 5 cm above the floc, in the middle of the water column and 5 cm below the water surface.

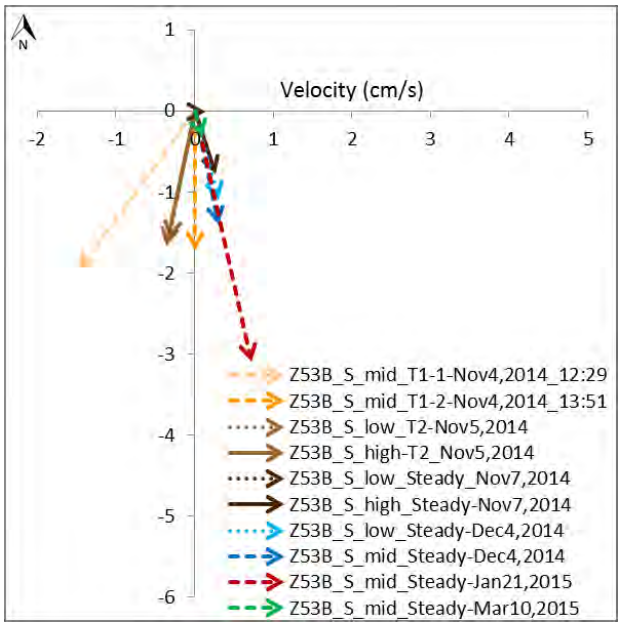

Figure C-161 Velocities at Z53B Slough from Flow Tracker measurements. “Low,” “mid” and “high” indicate samples taken approximately 5 cm above the floc, in the middle of the water column and 5 cm below the water surface.

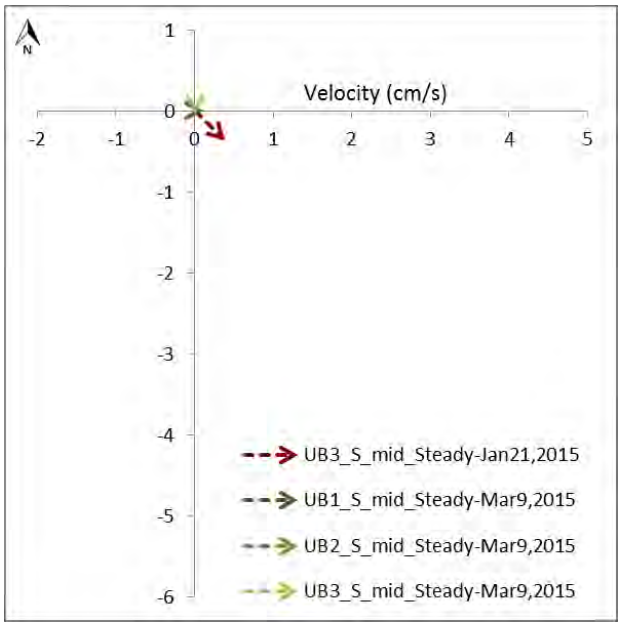

Figure C-162 Velocities at UB1, UB2 and UB3 Slough from Flow Tracker measurements. “Low,” “mid” and “high” indicate samples taken approximately 5 cm above the floc, in the middle of the water column and 5 cm below the water surface.

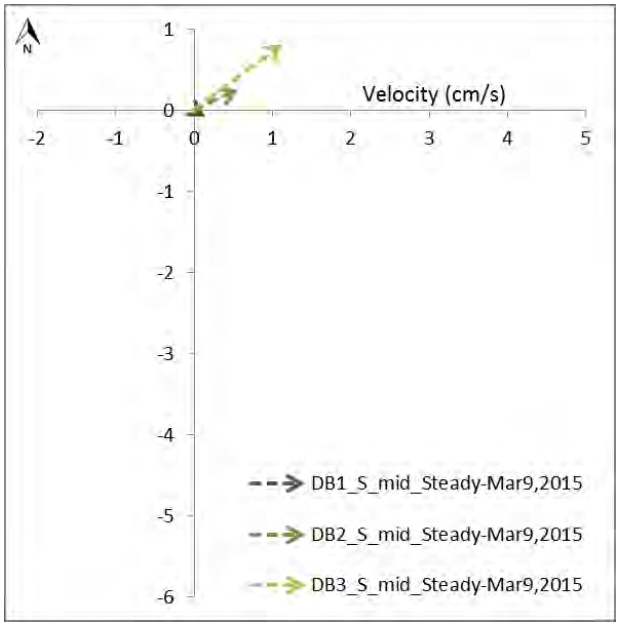

Figure C-163 Velocities at DB1, DB2 and DB3 Slough from Flow Tracker measurements. “Low,” “mid” and “high” indicate samples taken approximately 5 cm above the floc, in the middle of the water column and 5 cm below the water surface.

Flow Tracker Profile Velocity for the 2015 Flow Release Year

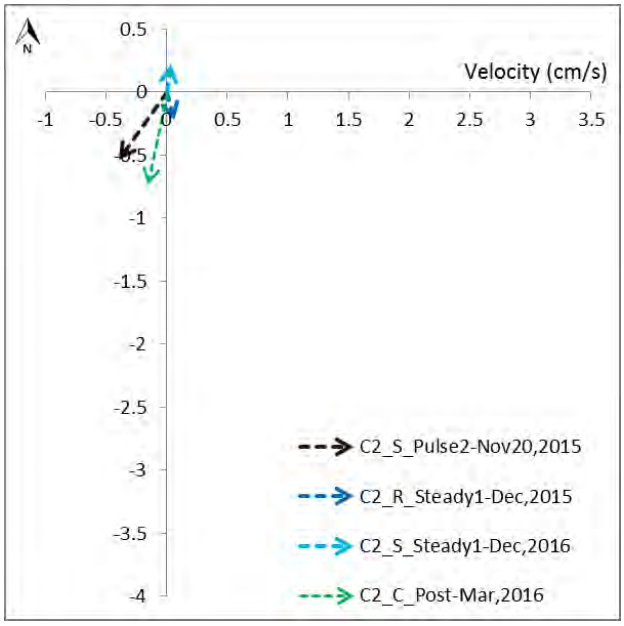

Figure C-164 Velocit**ies** at C2 from Flow Tracker measurements**.**

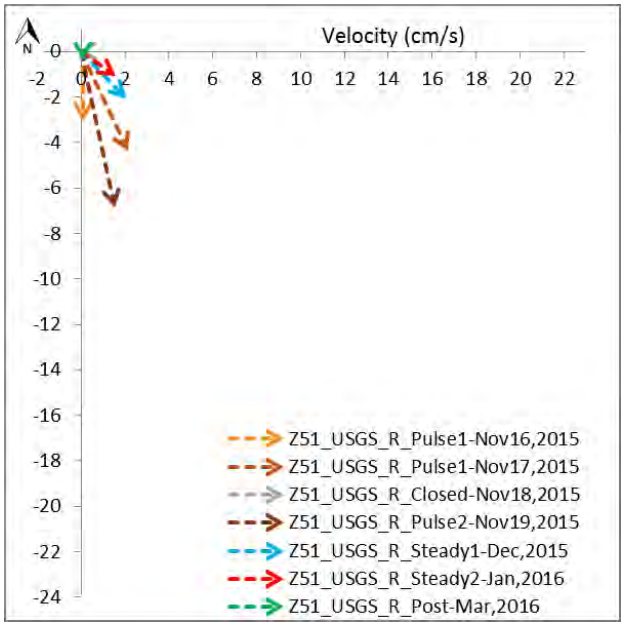

Figure C-165 Velocities at Z51_USGS Ridge from Flow Tracker measurements.

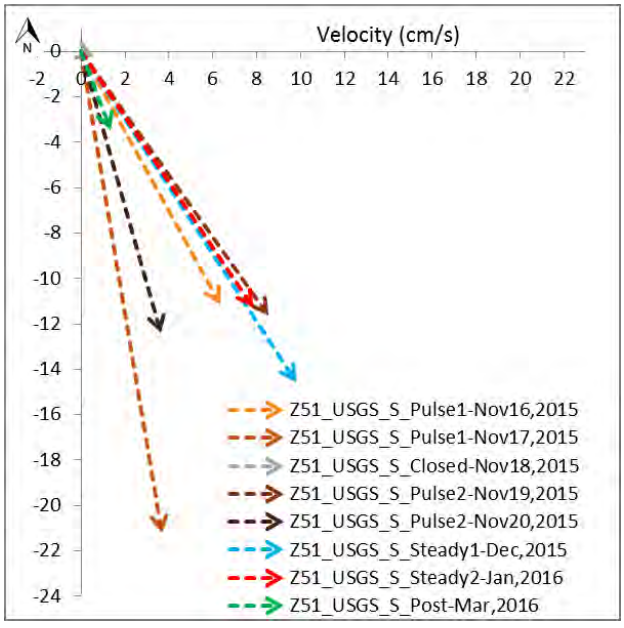

Figure C-166 Velocities at Z51_USGS Slough from Flow Tracker measurements.

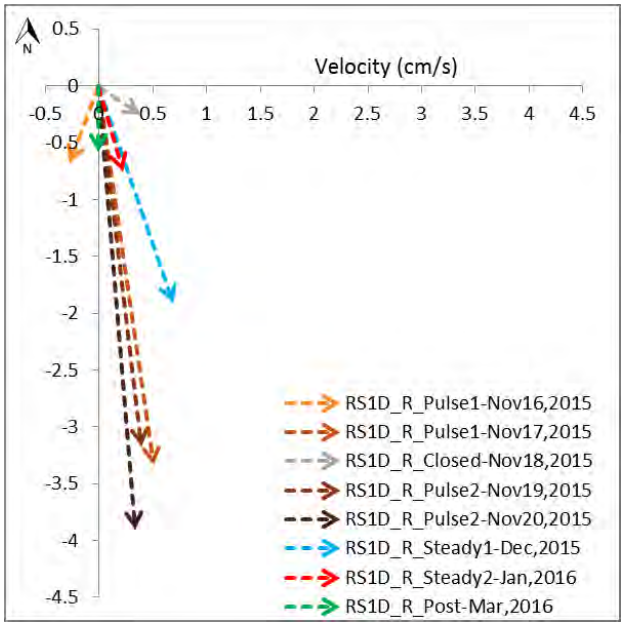

Figure C-167 Velocities at RS1D Ridge from Flow Tracker measurements.

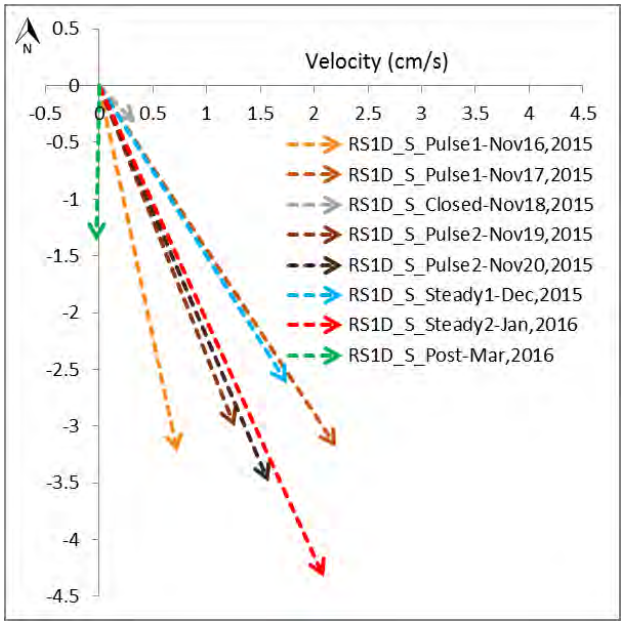

Figure C-168 Velocities at RS1D Slough from Flow Tracker measurements.

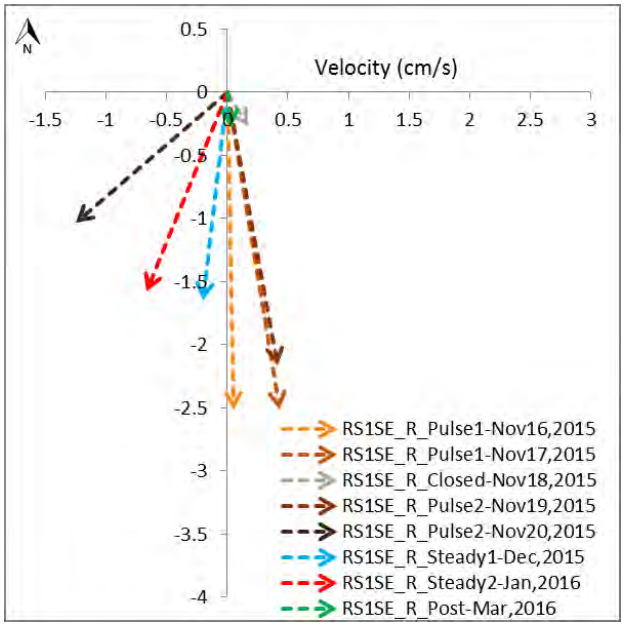

Figure C-169 Velocitie at RS1SE Ridge from Flow Tracker measurements.

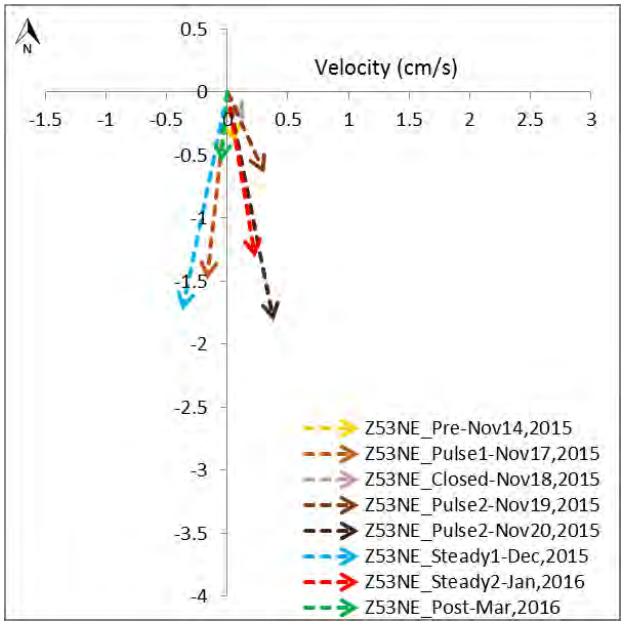

Figure C-170 Velocitie at Z53NE Ridge from Flow Tracker measurements.

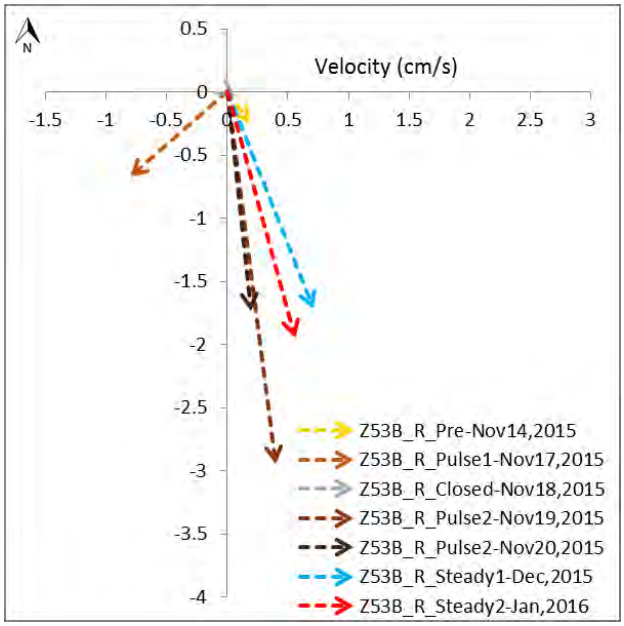

Figure C-171 Velocities at Z53B Ridge from Flow Tracker measurements.

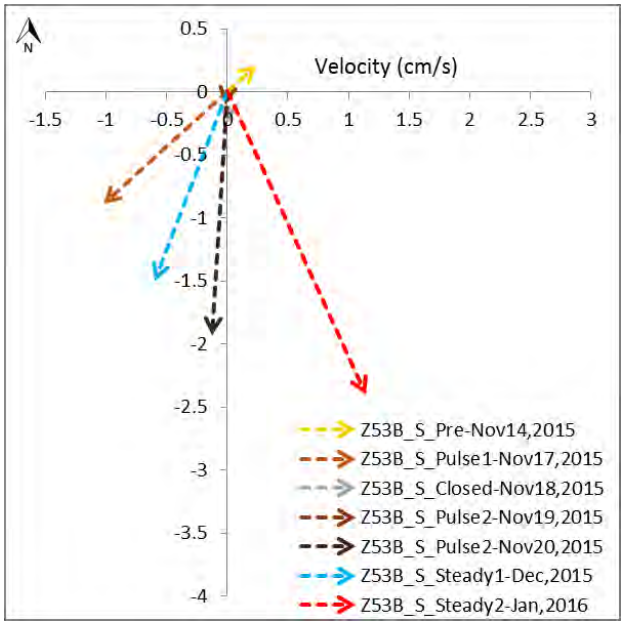

Figure C-172 Velocities at Z53B Slough from Flow Tracker measurements.

.

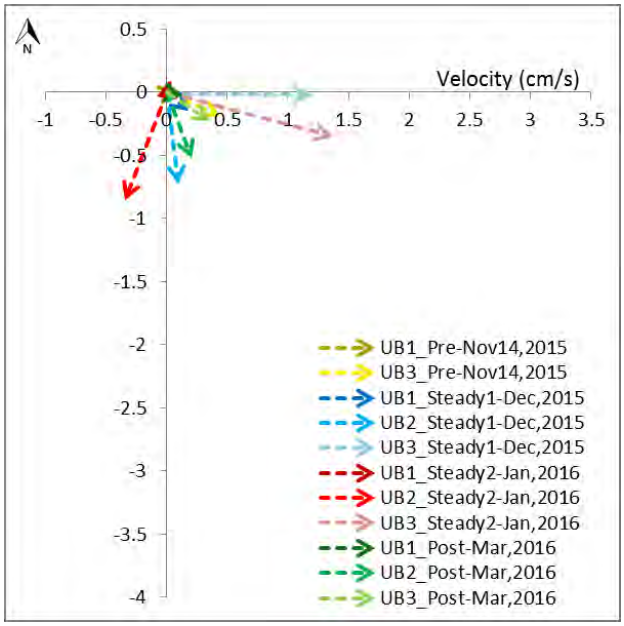

Figure C-173 Velocities at UB1, UB2 and UB3 Slough from Flow Tracker measurements.

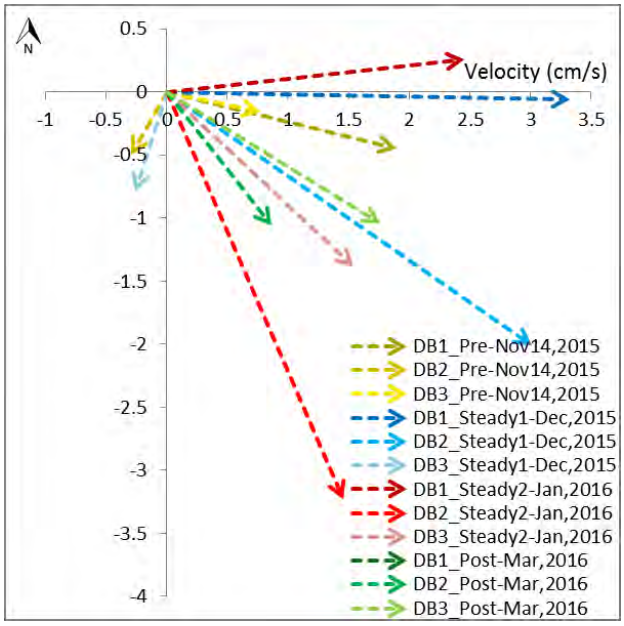

Figure C-174 Velocities at DB1, DB2 and DB3 Slough from Flow Tracker measurements.

Bed Shear Stress

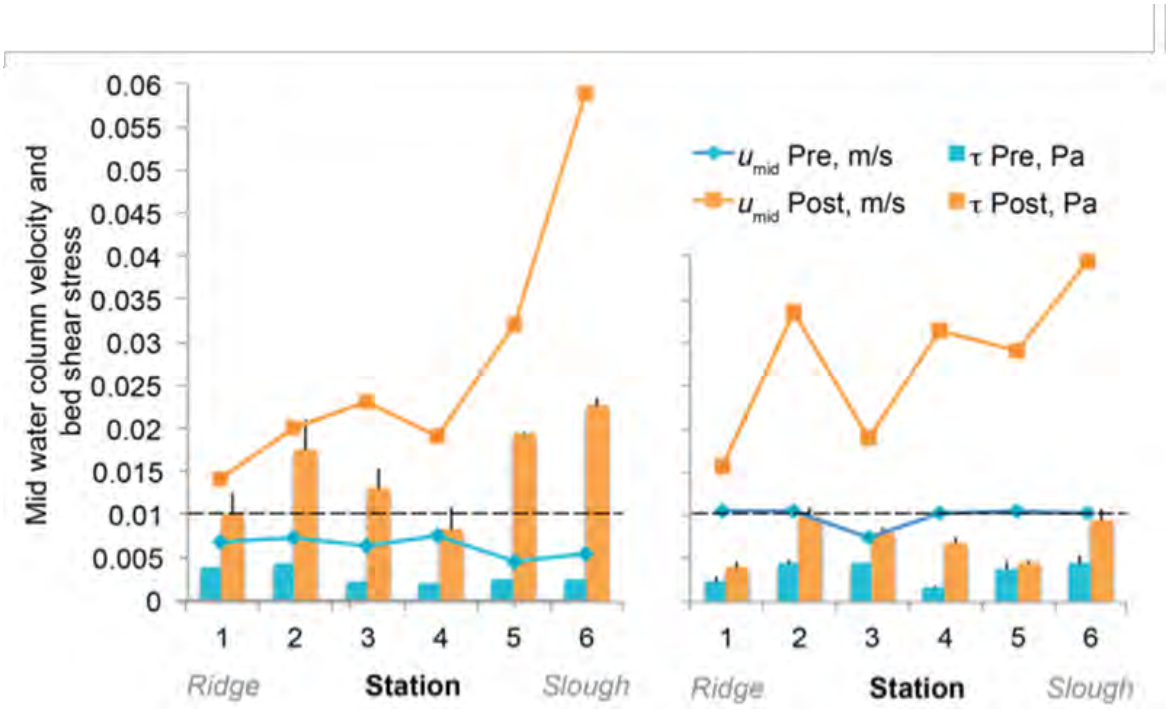

Figure C-175 Velocity and bed shear stress values in the mid water column before and just after the opening of the culverts at RS1U. 2013 is depicted on the left and 2014 on the right.

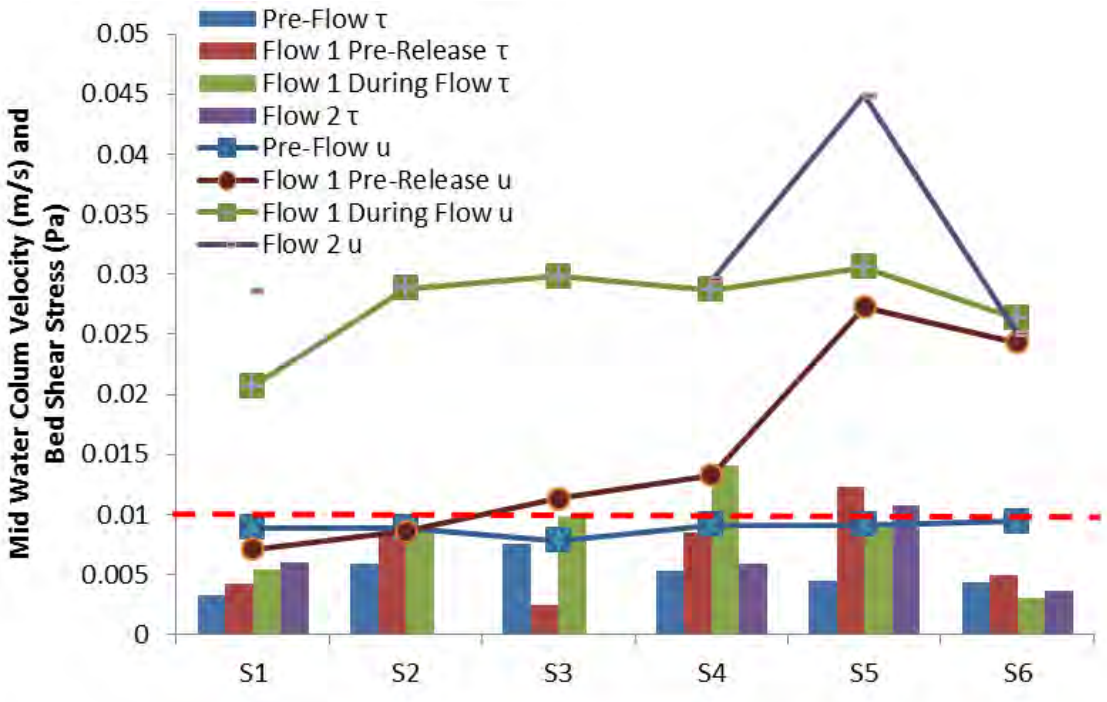

Figure C-176 Mid-water column velocity (u, m/s) and bed shear stress (τ, Pa) for different flow conditions at RS1U in November 2015.

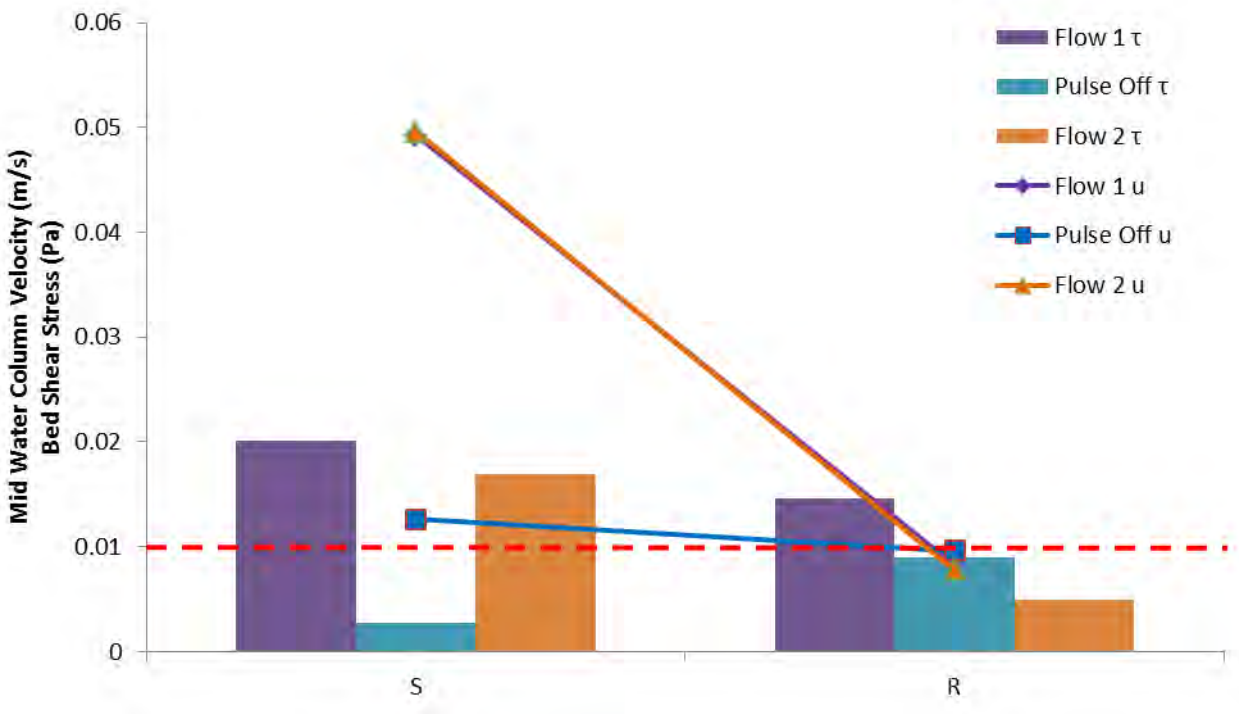

Figure C-177 Mid-water column velocity (u, m/s) and bed shear stresses (τ, Pa) for different flow conditions at RS1D in November 2015.

D. Suspended Particle Sizes and Concentrations

2013 Suspended Sediment and Phosphorus

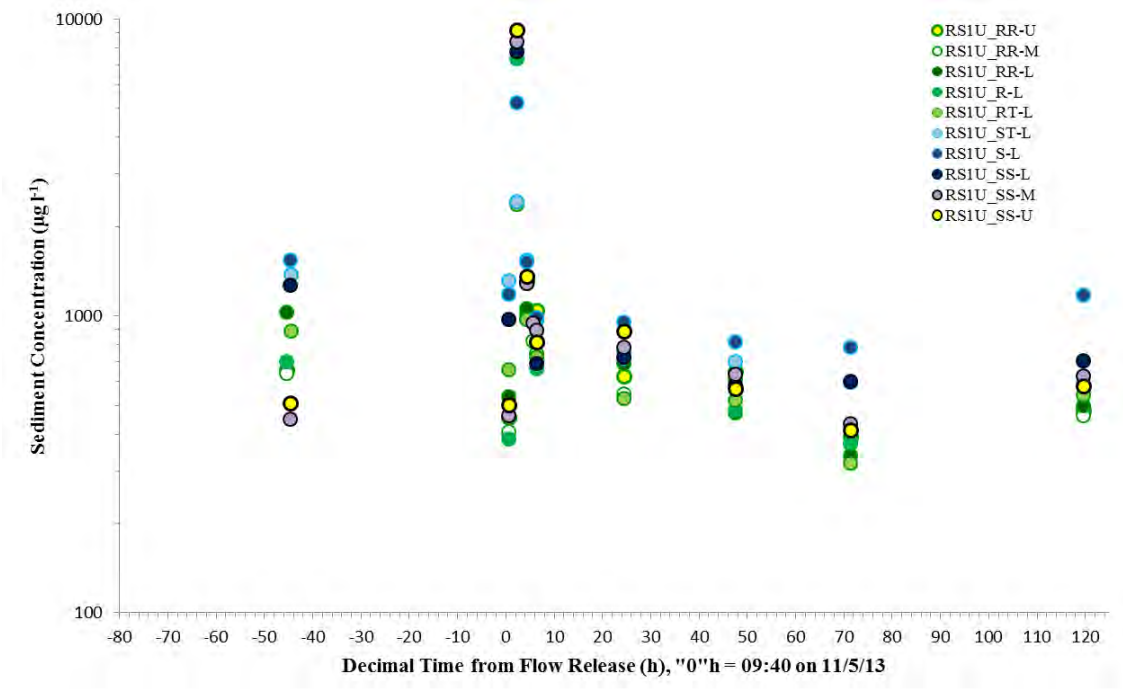

Figure D-1 Time series of suspended sediment concentration at site RS1U during the November 5th, 2013 flow release.

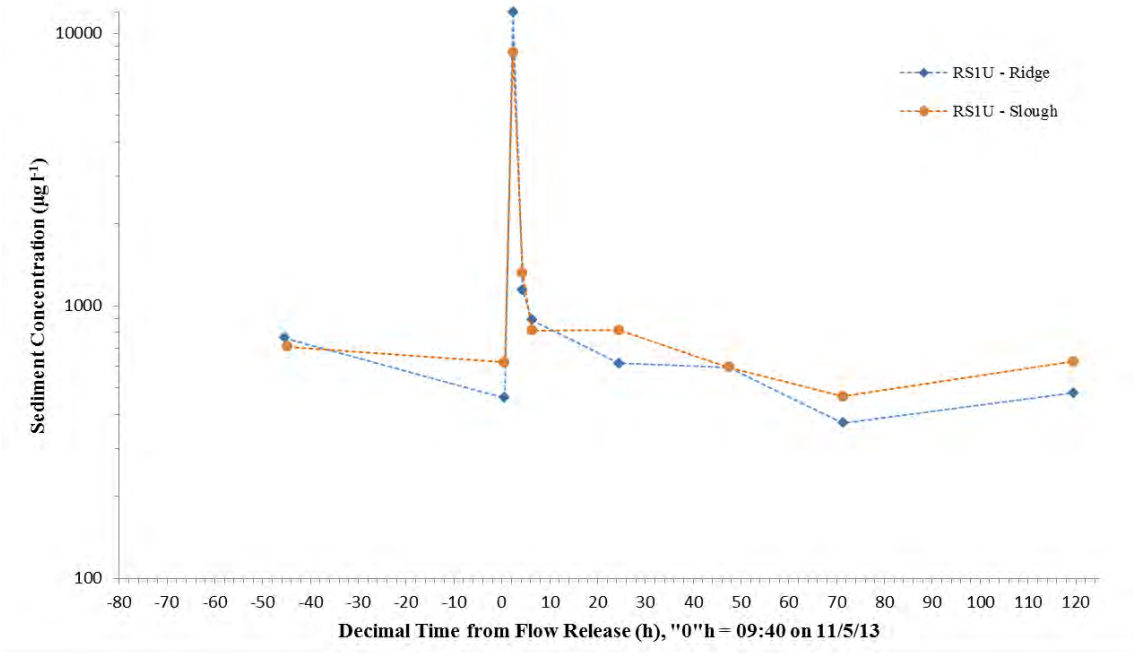

Figure D-2 Time series of depth-averaged suspended sediment concentration at site RS1U during the November 5th, 2013 flow release.

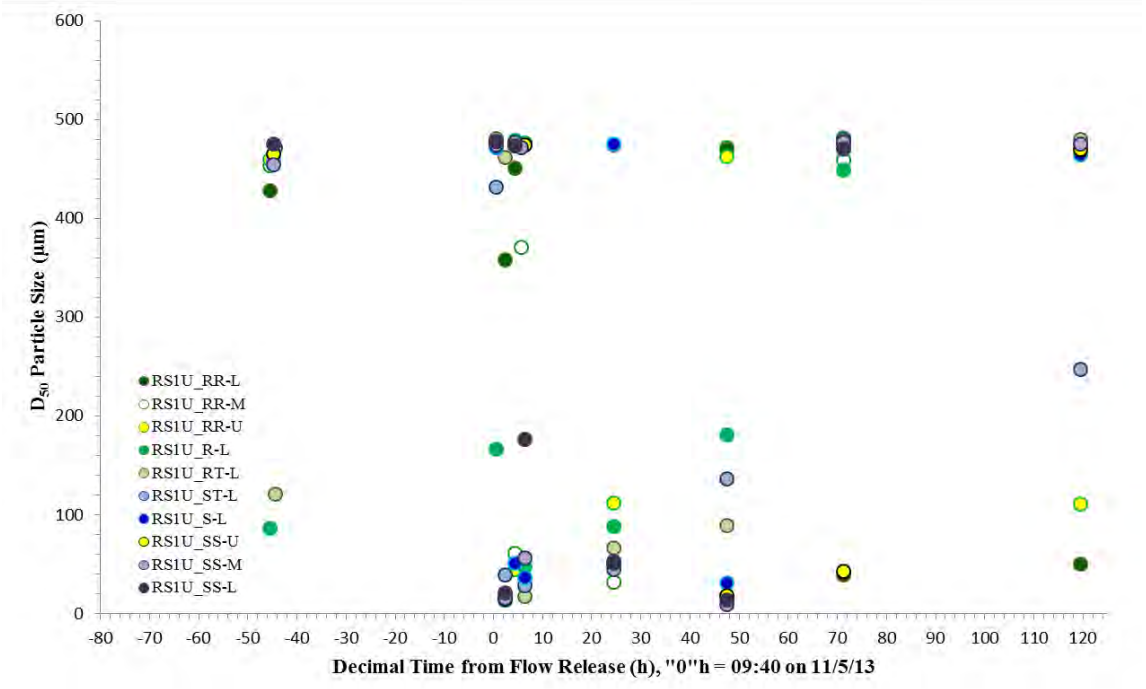

Figure D-3 Time series of D_{50} (median mass weighted size) of suspended particles at site RS1U during the November 5th, 2013 flow release.

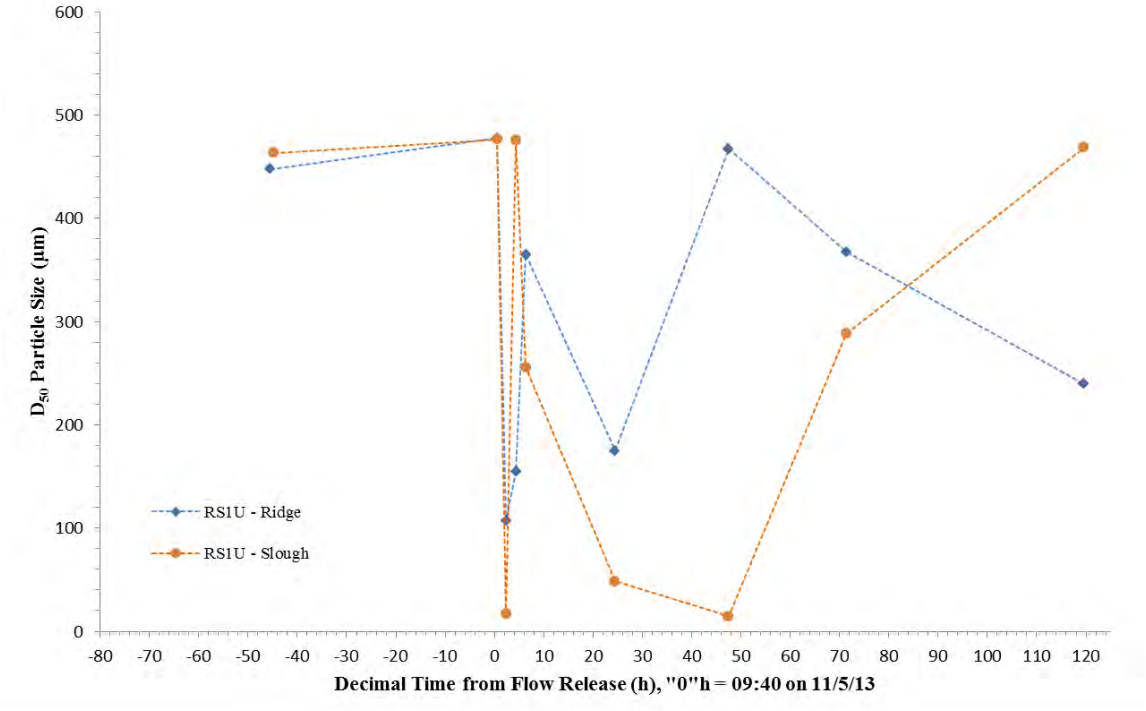

Figure D-4 Time series of depth-averaged D_{50} (median mass weighted size) of suspended particles at site RS1U during the November 5th, 2013 flow release.

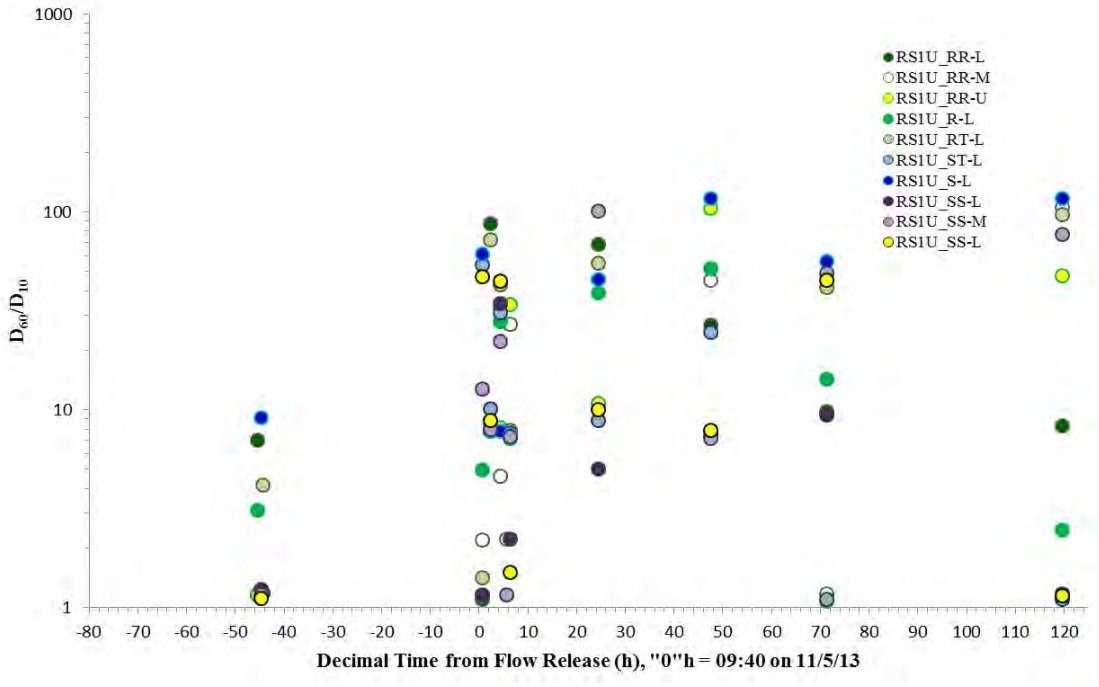

Figure D-5 Time series of D_{60}/D_{10} (particle size uniformity coefficient) of suspended sediment at site RS1U during the November 5th, 2013 flow release.

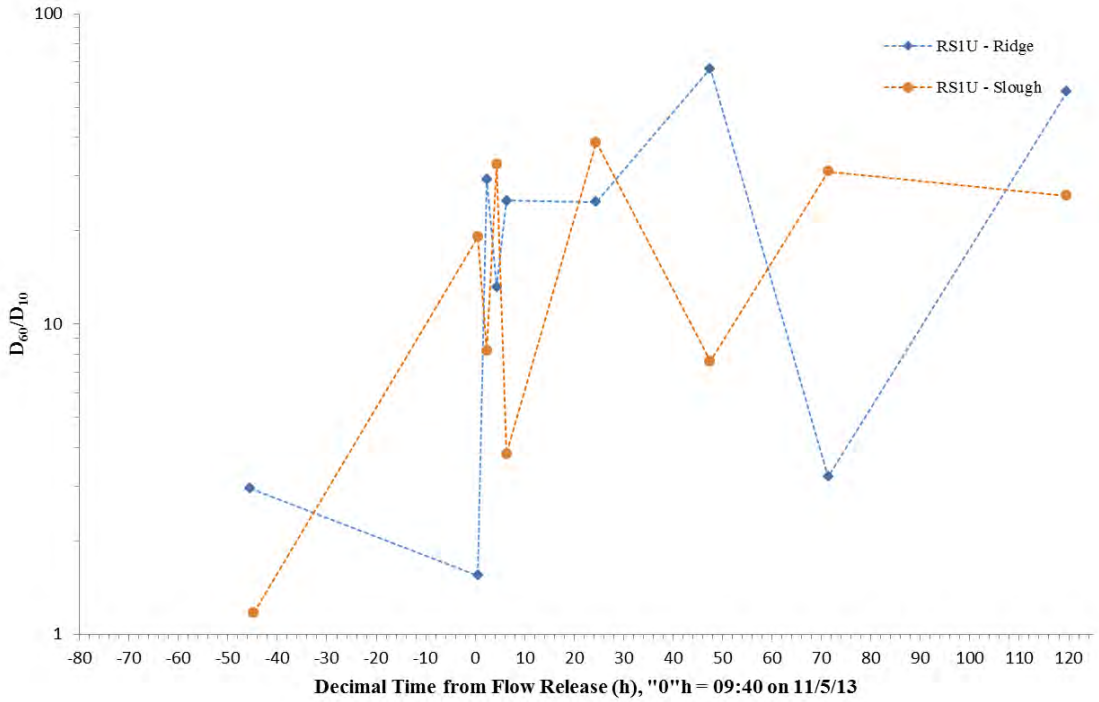

Figure D-6 Time series of depth-averaged D_{60}/D_{10} (particle size uniformity coefficient) of suspended sediment at site RS1U during the November 5th, 2013 flow release.

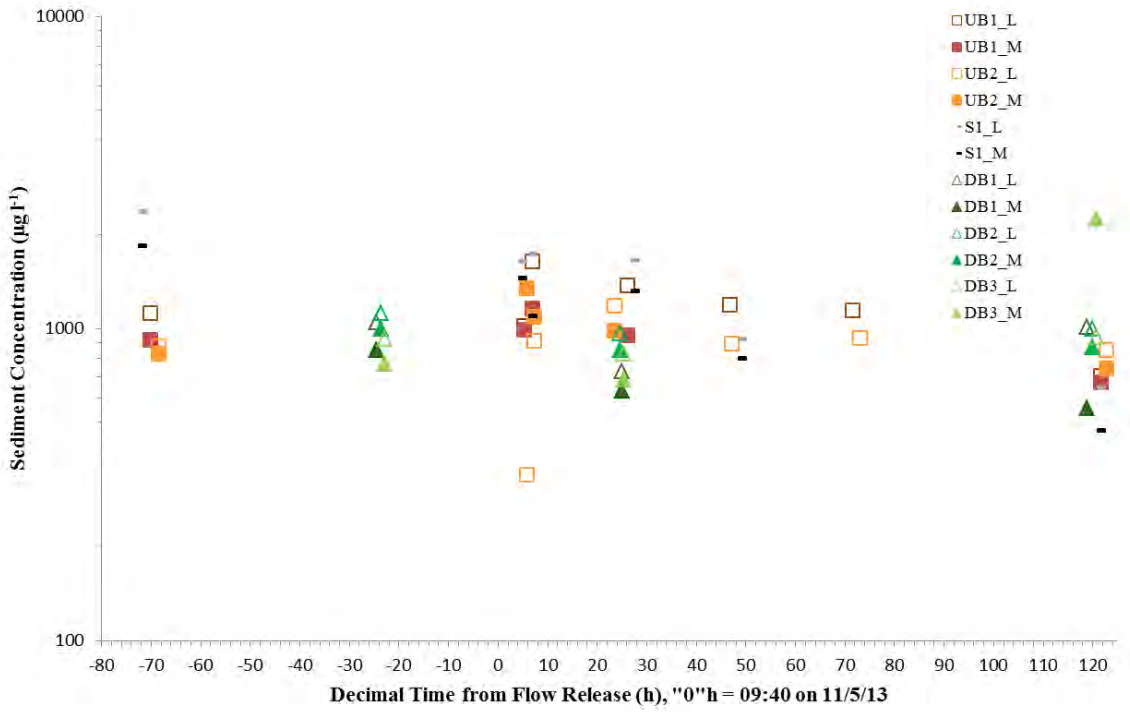

Figure D-7 Time series of suspended sediment concentration at sites S1, UB1, UB2, DB1, DB2, and DB3 during the November 5th, 2013 flow release.

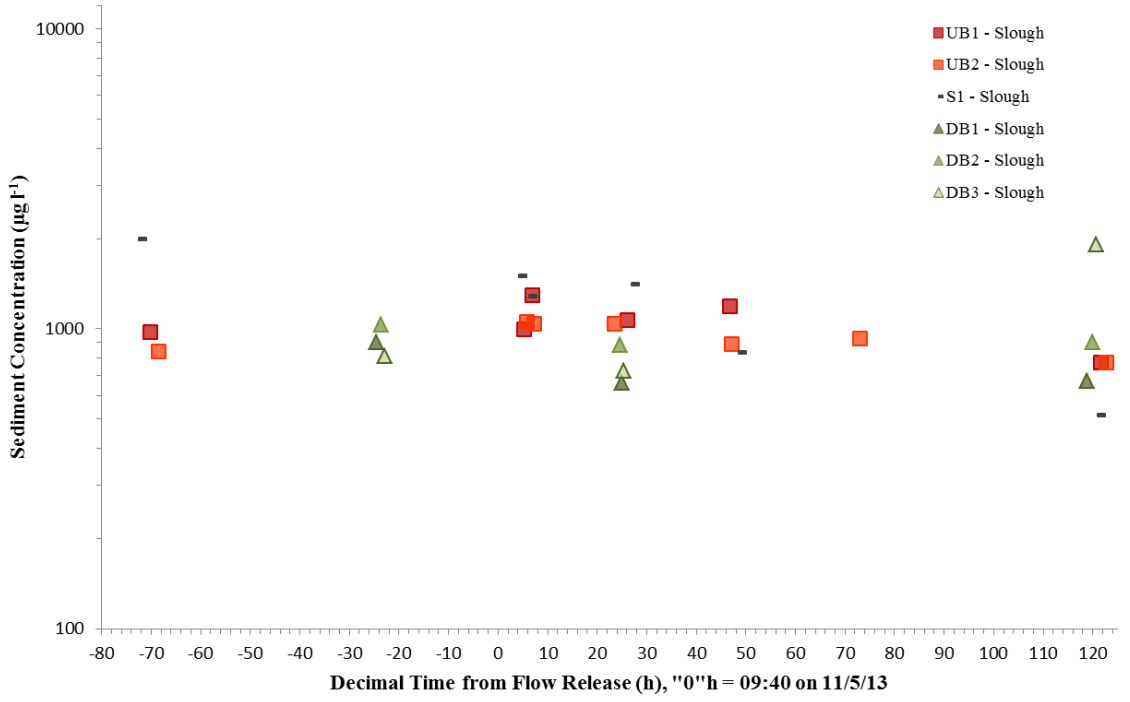

Figure D-8 Time series of depth-averaged suspended sediment concentration at sites S1, UB1, UB2, DB1, DB2, and DB3 during the November 5th, 2013 flow release.

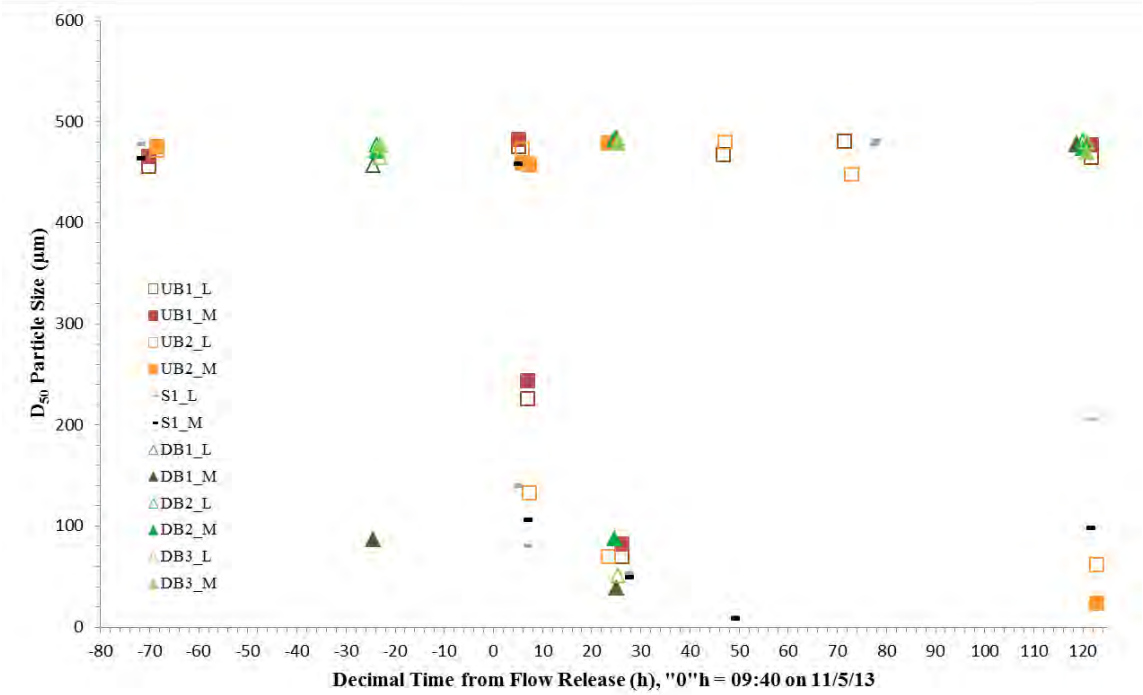

Figure D-9 Time series of D_{50} (median mass weighted size) of suspended particles at sites S1, UB1, UB2, DB1, DB2, and DB3 during the November 5th, 2013 flow release.

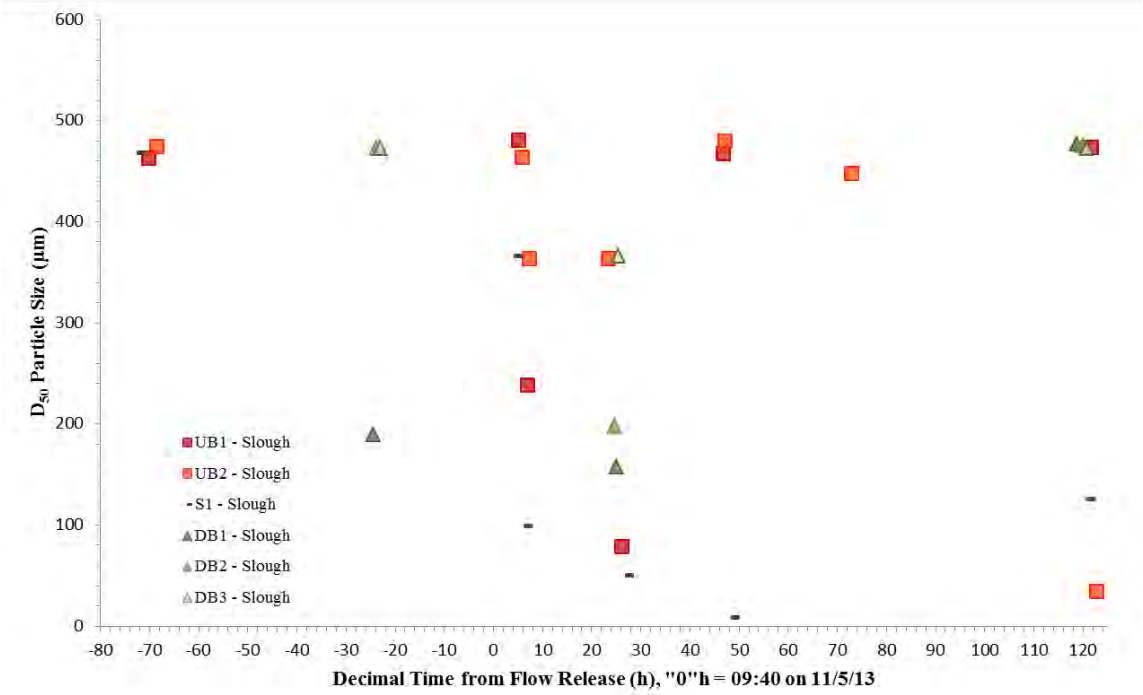

Figure D-10 Time series of depth-averaged D_{50} (median mass weighted size) of suspended particles at sites S1, UB1, UB2, DB1, DB2, and DB3 during the November 5th, 2013 flow release.

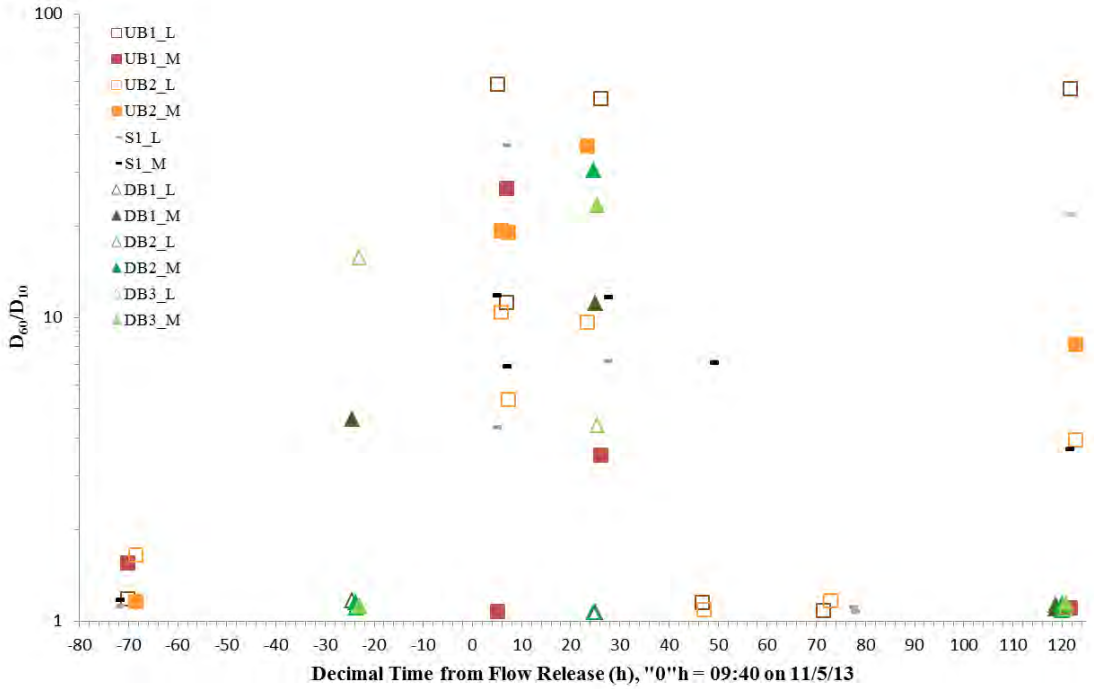

Figure D-11 Time series of D_{60}/D_{10} (particle size uniformity coefficient) of suspended sediment at sites S1, UB1, UB2, DB1, DB2, and DB3 during the November 5th, 2013 flow release.

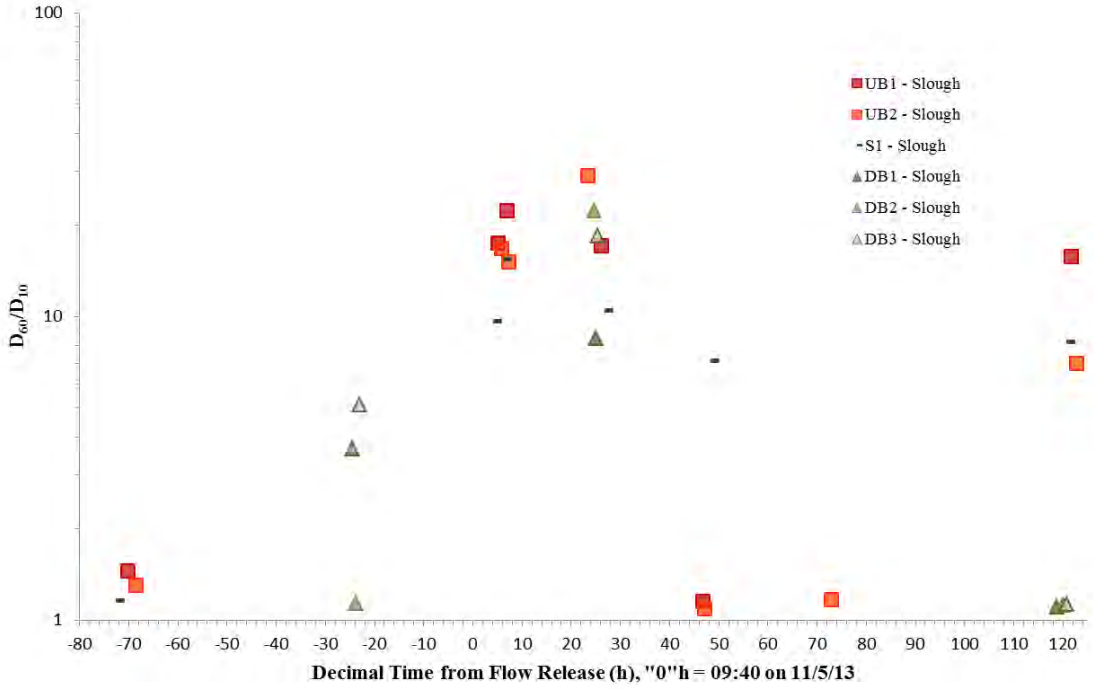

Figure D-12 Time series of depth-averaged D_{60}/D_{10} (particle size uniformity coefficient) of suspended sediment at sites S1, UB1, UB2, DB1, DB2, and DB3 during the November 5th, 2013 flow release.

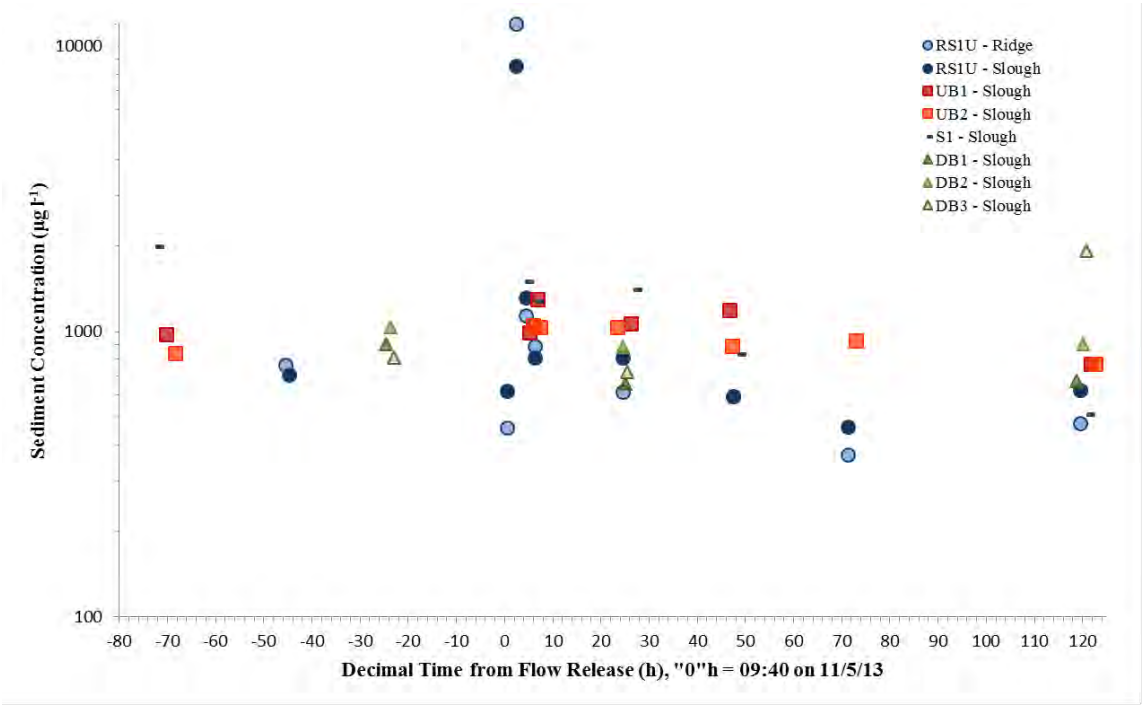

Figure D-13 Time series of depth-averaged suspended sediment concentration at all sites during the November 5th, 2013 flow release.

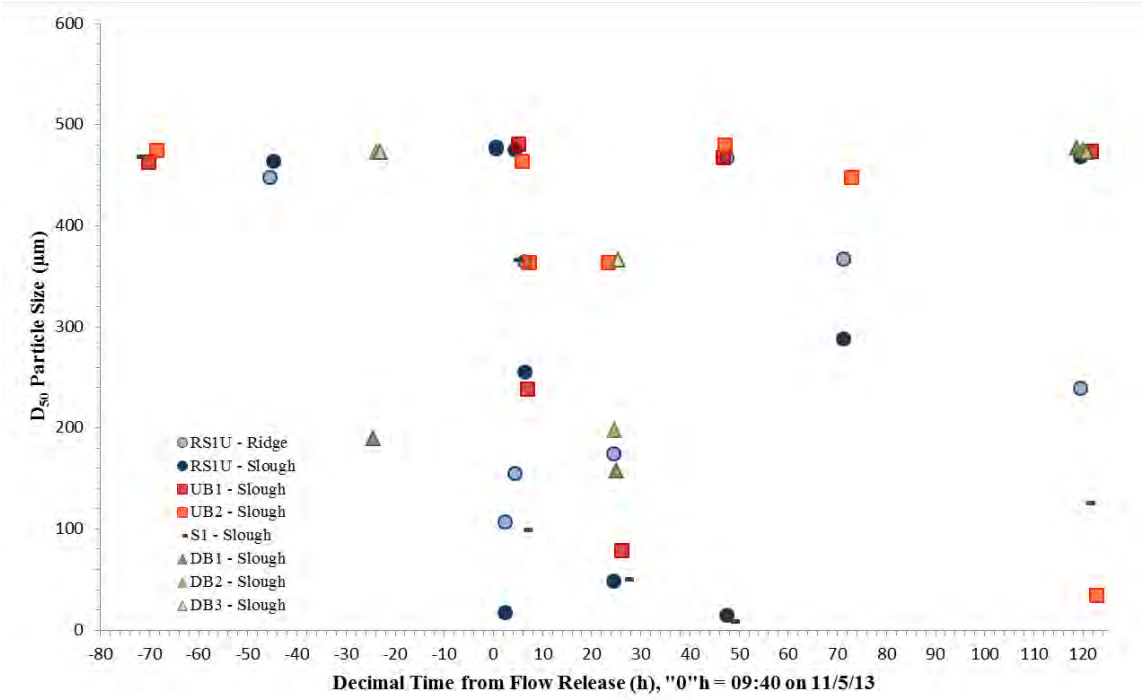

Figure D-14 Time series of depth-averaged D_{50} (median mass weighted size) of suspended particles at all sites during the November 5th, 2013 flow release.

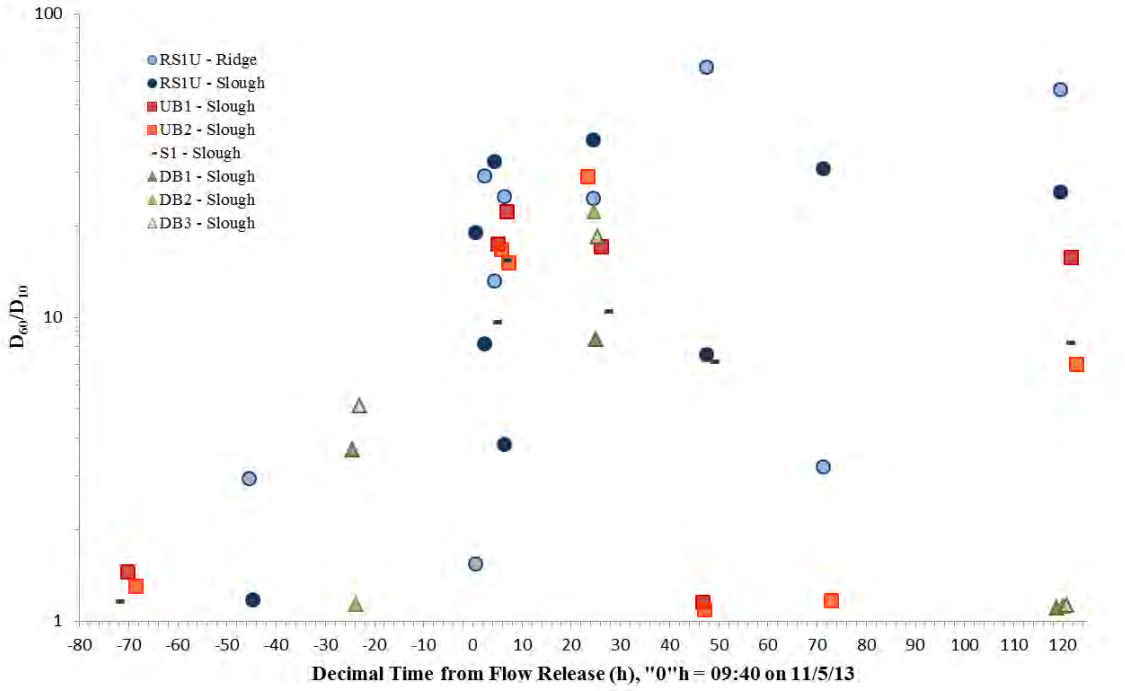

Figure D-15 Time series of depth-averaged D_{60}/D_{10} (particle size uniformity coefficient) of suspended sediment at all sites during the November 5th, 2013 flow release.

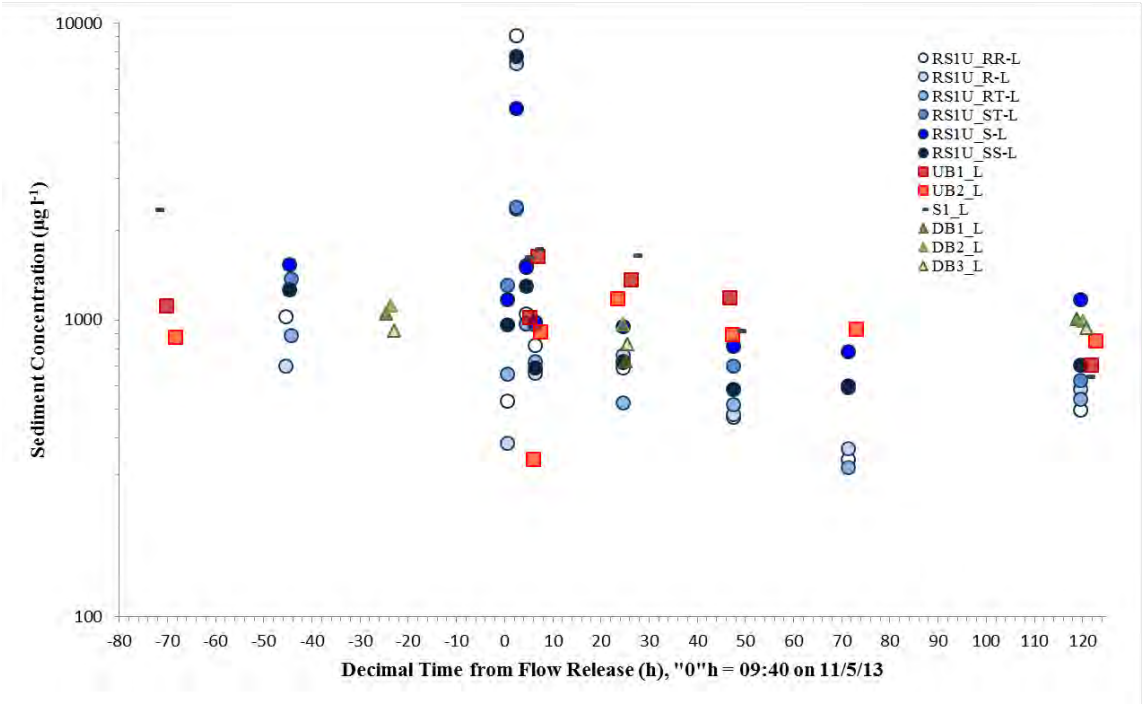

Figure D-16 Time series of suspended sediment concentration near the bed (5cm) at all sites during the November 5th, 2013 flow release.

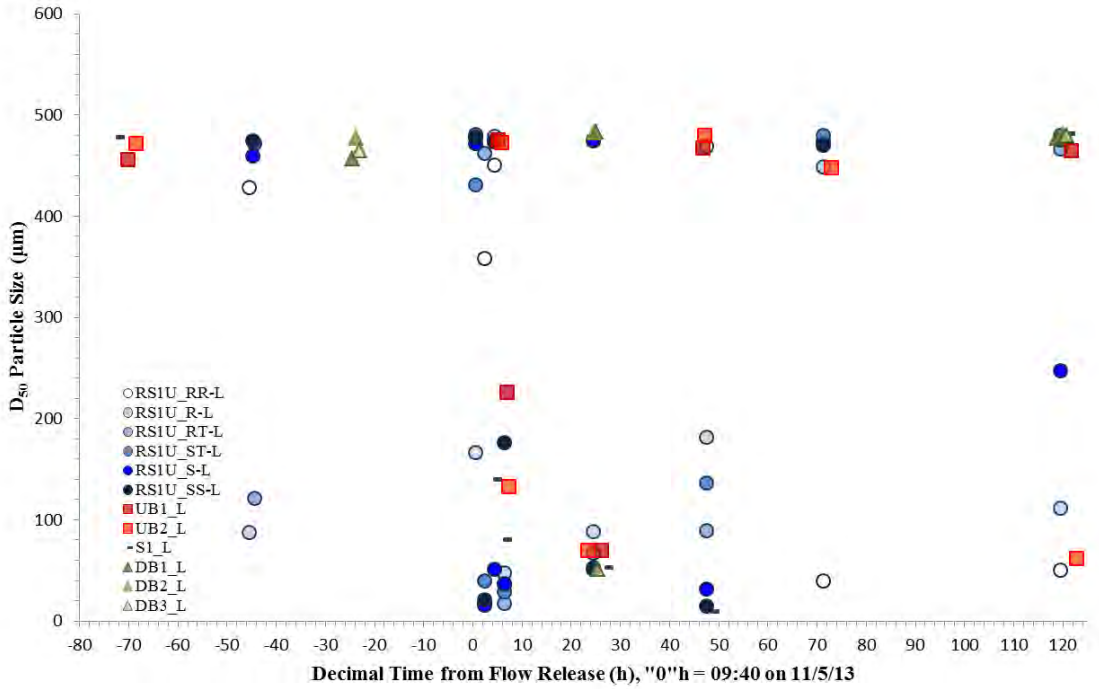

Figure D-17 Time series of D_{50} (median mass weighted size) of suspended particles near the bed (5cm) at all sites during the November 5th, 2013 flow release.

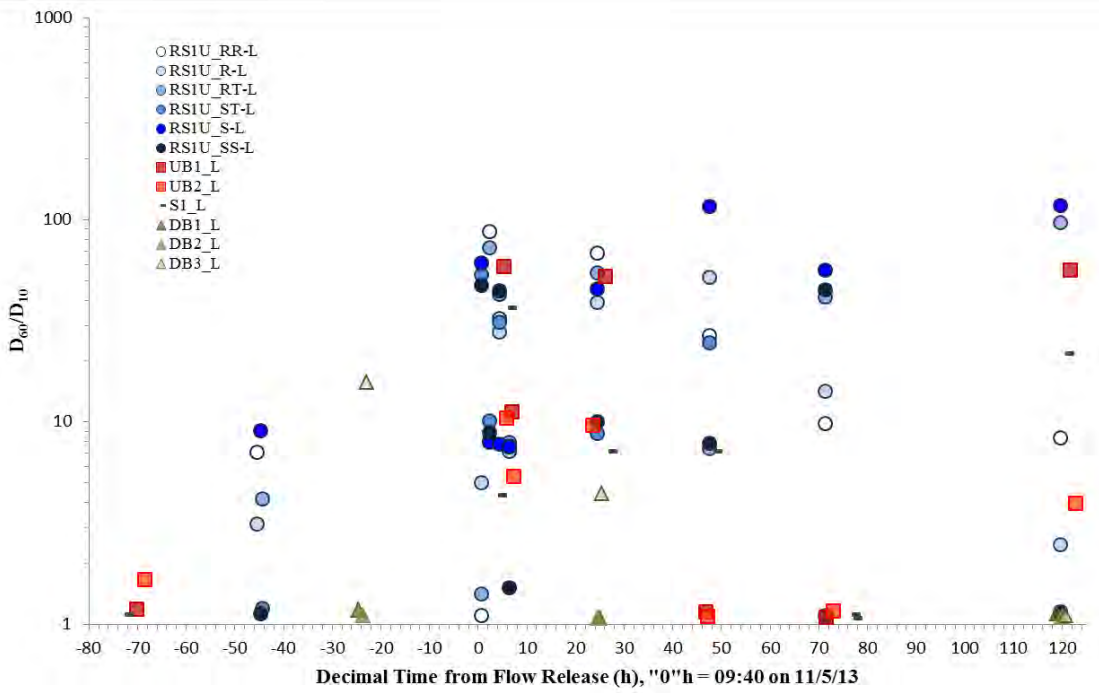

Figure D-18 Time series of D_{60}/D_{10} (particle size uniformity coefficient) of suspended sediment near the bed (5cm) at all sites during the November 5th, 2013 flow release.

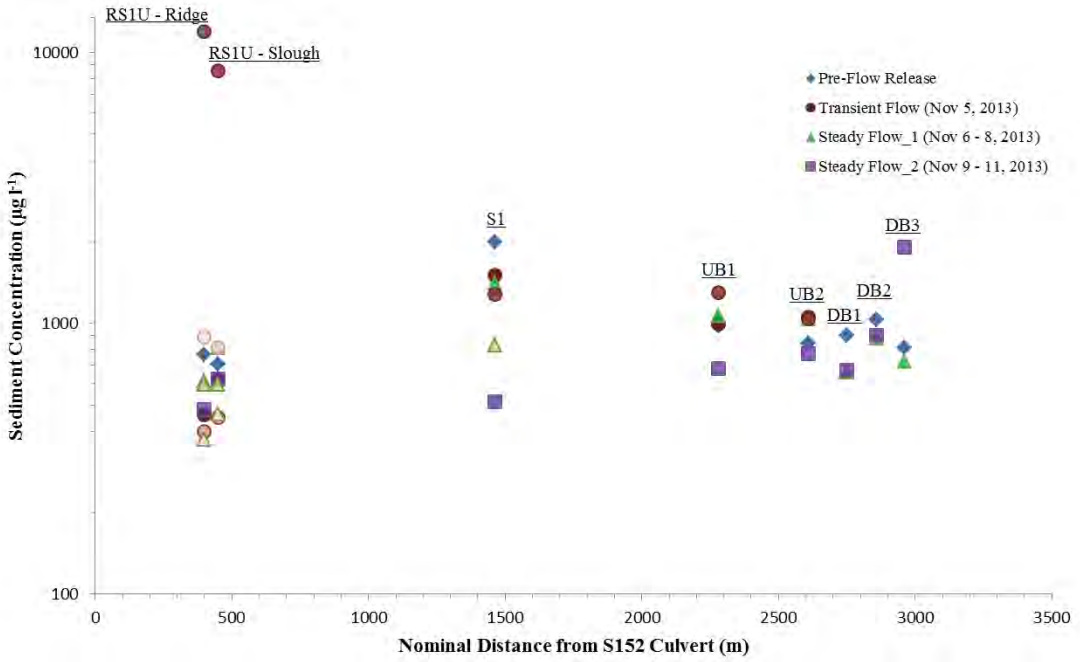

Figure D-19 Spatial distribution of depth-averaged suspended sediment concentration at all sites during the November 5th, 2013 flow release. RS1U ridge and slough are geographically co-located, data have been separated for clarity. Color intensity of each symbol decreases with time..

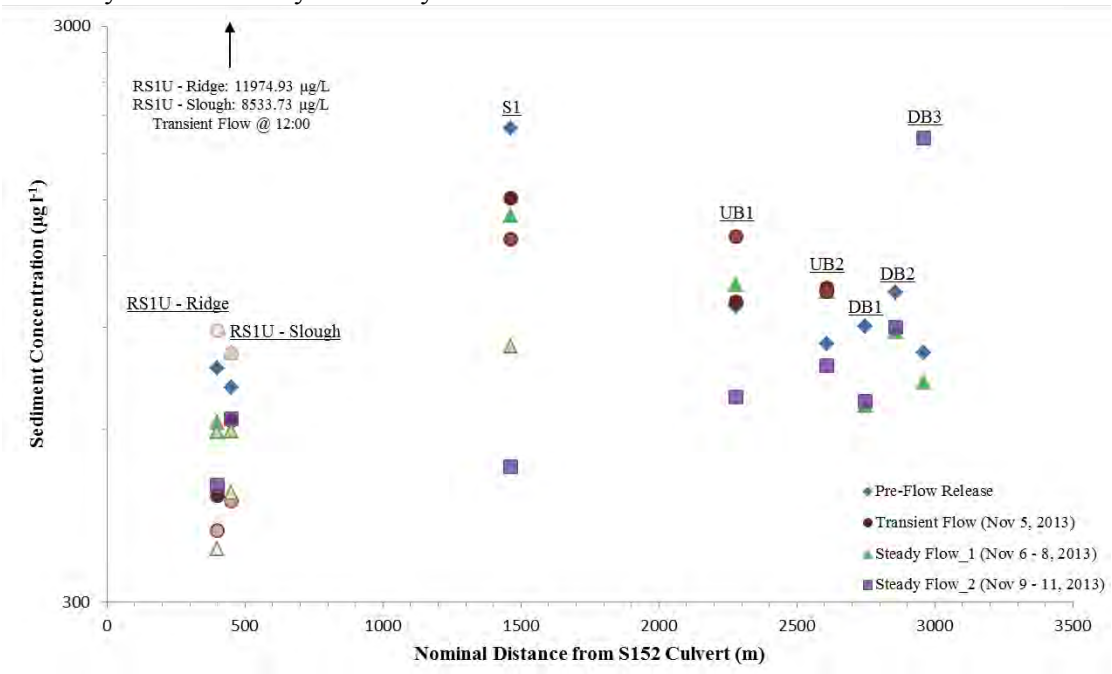

Figure D-20 Spatial distribution of depth-averaged suspended sediment concentration at all sites (condensed scale on Y-axis) during the November 5th, 2013 flow release. RS1U ridge and slough are geographically co-located, data have been separated for clarity. Color intensity of each symbol decreases with time.

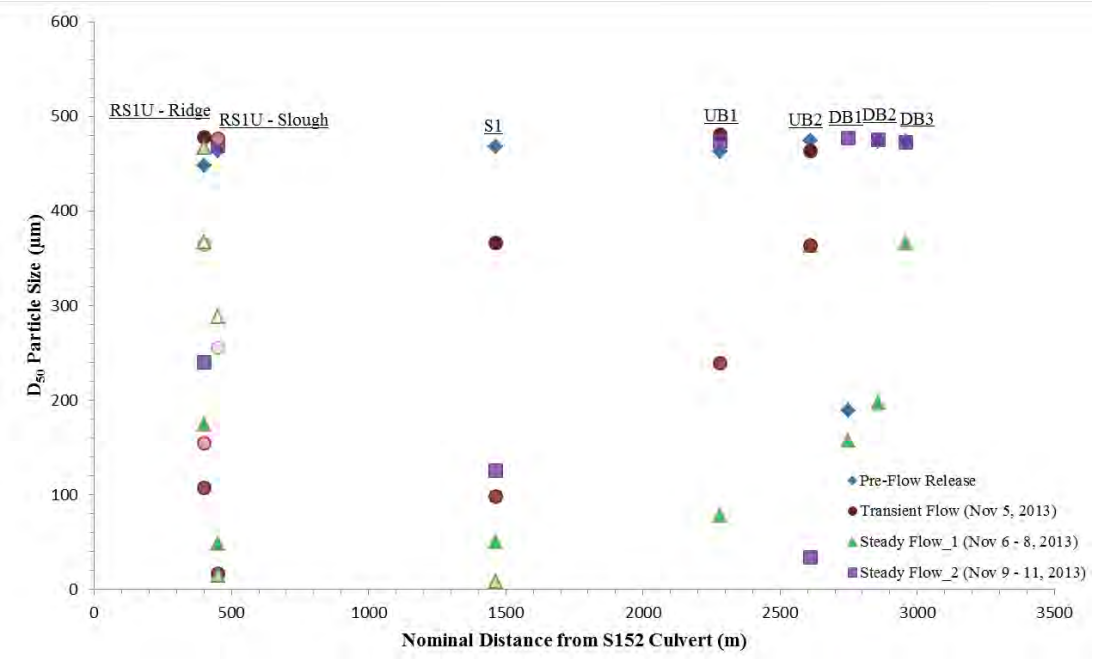

Figure D-21 Spatial distribution of depth-averaged D_{50} (median mass weighted size) of suspended particles at all sites during the November 5th, 2013 flow release. RS1U ridge and slough are geographically co-located, data have been separated for clarity. Color intensity of each symbol decreases with time.

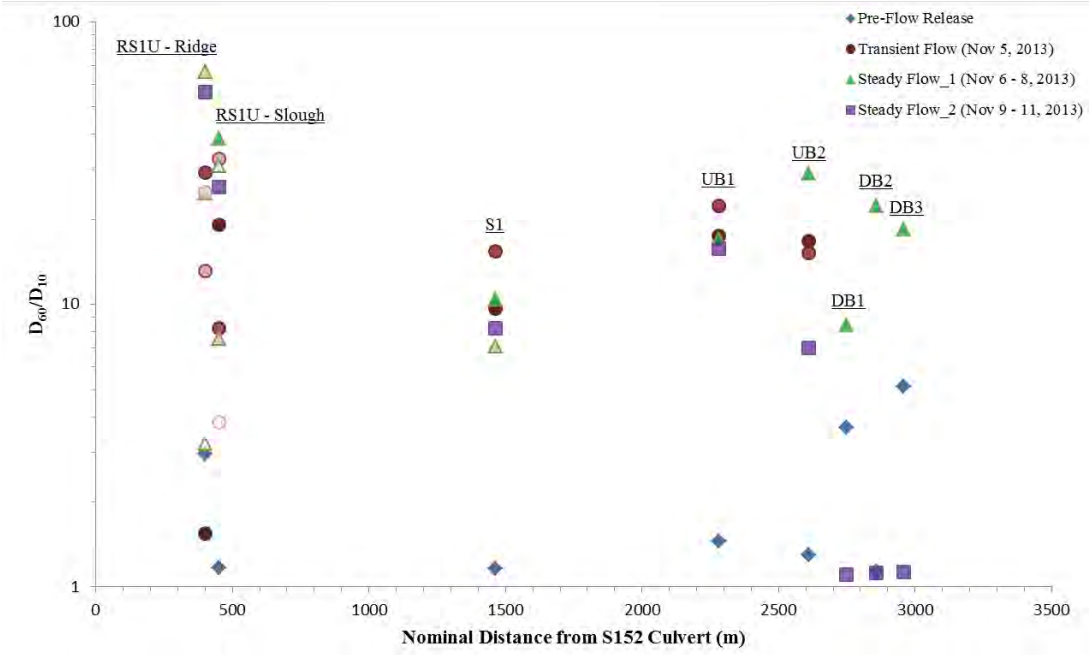

Figure D-22 Spatial distribution of depth-averaged D_{60}/D_{10} (particle size uniformity coefficient) of suspended sediment at all sites during the November 5th, 2013 flow release. RS1U ridge and slough are geographically co-located, data have been separated for clarity. Color intensity of each symbol decreases with time.

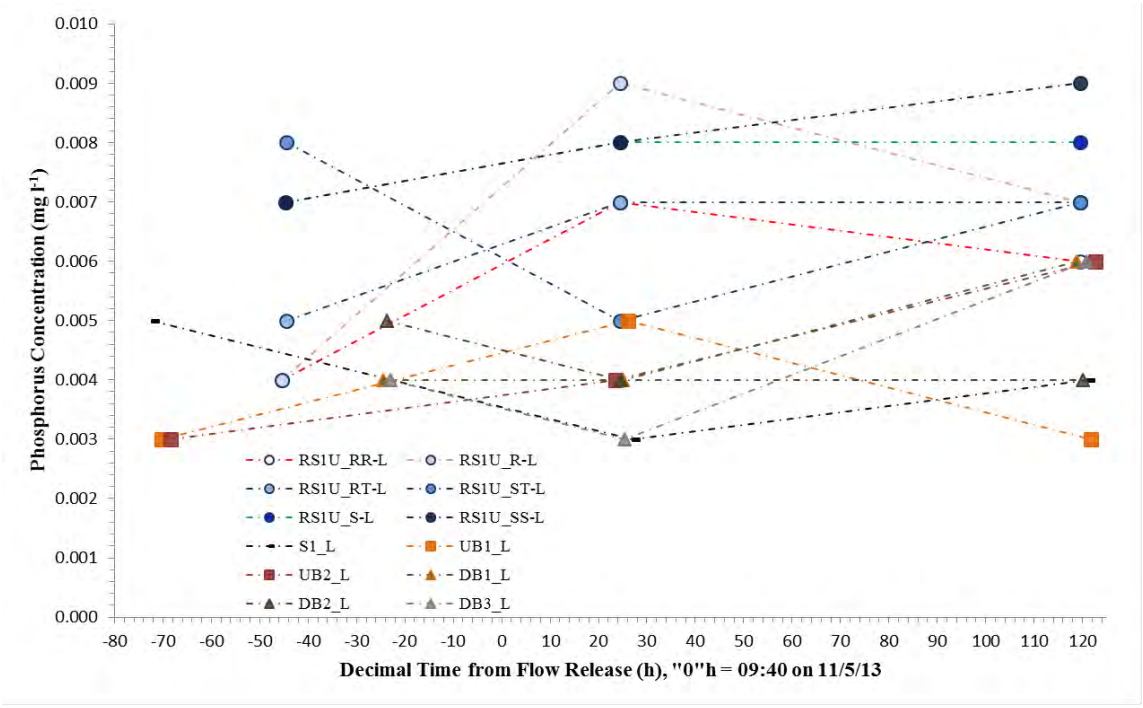

Figure D-23 Time series of phosphorus concentration near the bed (5cm) at all sites during the November 5th, 2013 flow release.

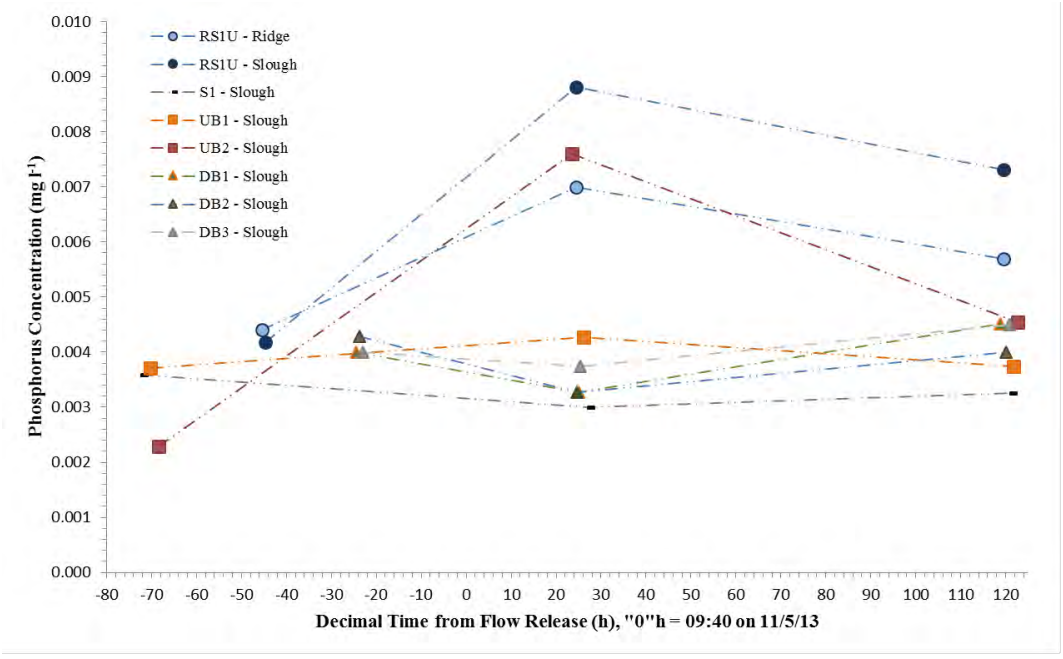

Figure D-24 Time series of depth-averaged phosphorus concentration at all sites during the November 5th, 2013 flow release.

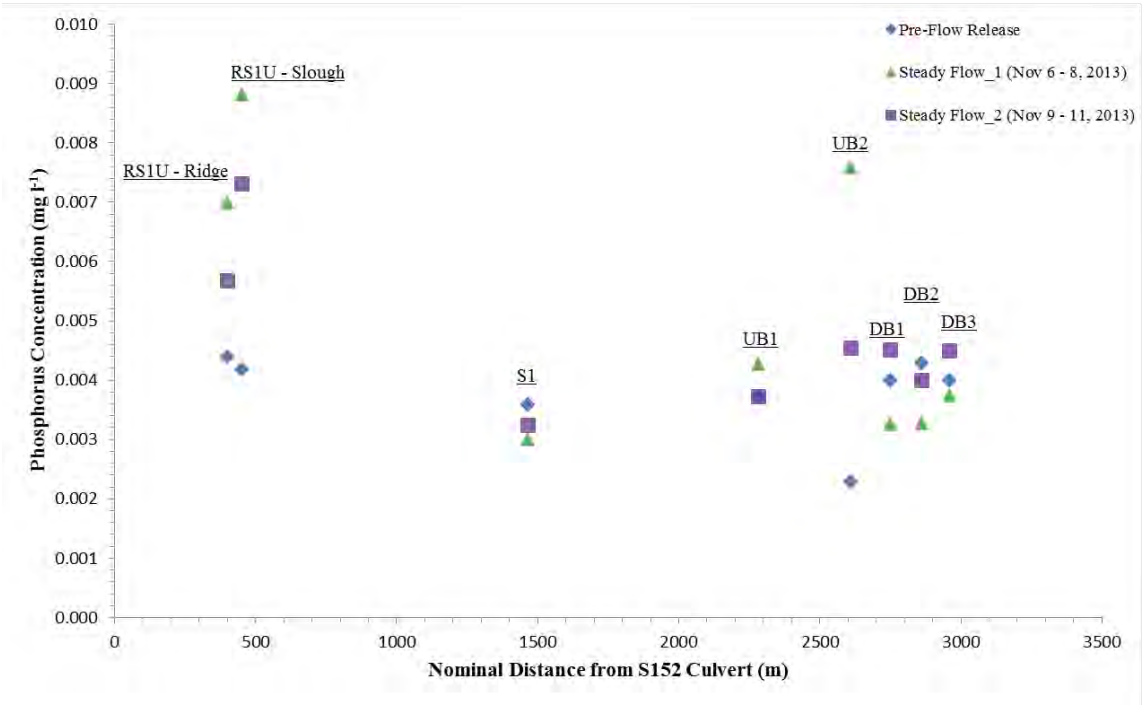

Figure D-25 Spatial distribution of depth-averaged phosphorus concentration at all sites. RS1U ridge and slough are geographically co-located, data have been separated for clarity during the November 5th, 2013 flow release.

2013 Load

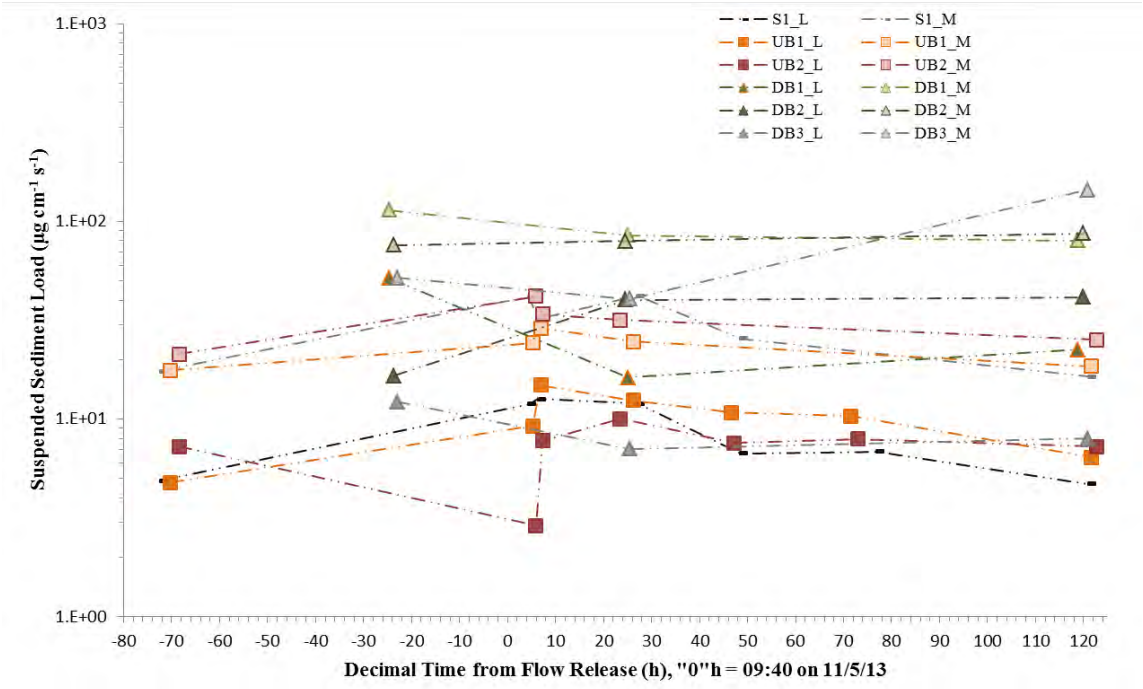

Figure D-26 Time series of suspended sediment load in each water column interval at sites S1, UB1, UB2, DB1, DB2, and DB3 during the November 5th, 2013 flow release.

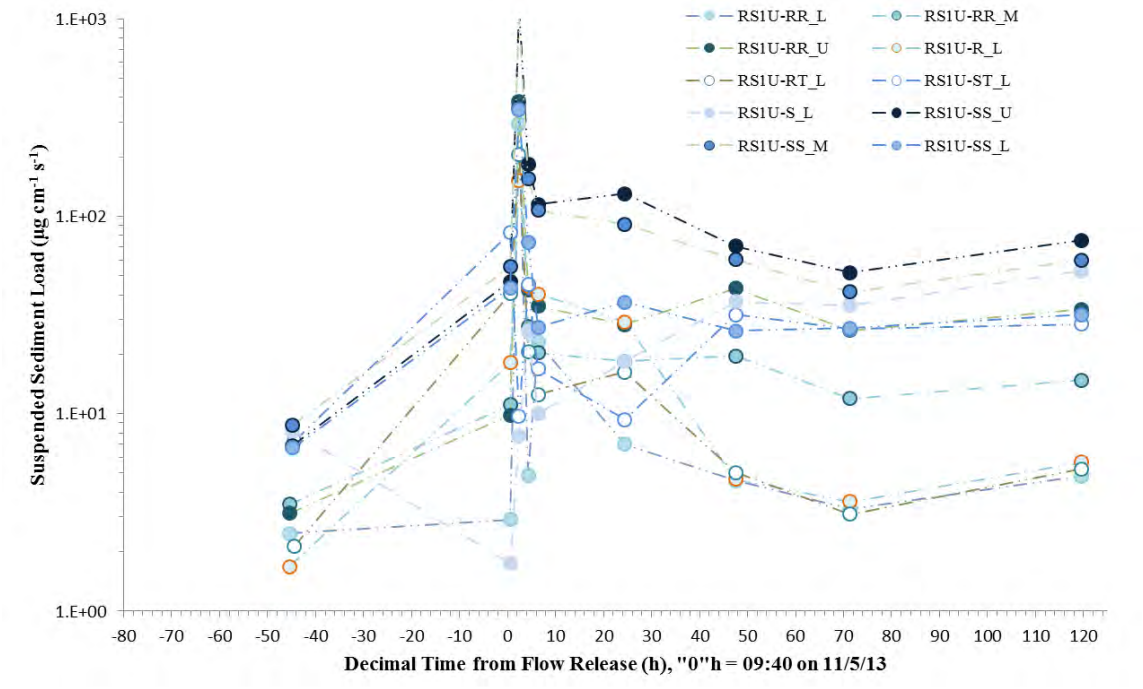

Figure D-27 Time series of suspended sediment load in each water column interval at site RS1U during the November 5th, 2013 flow release.

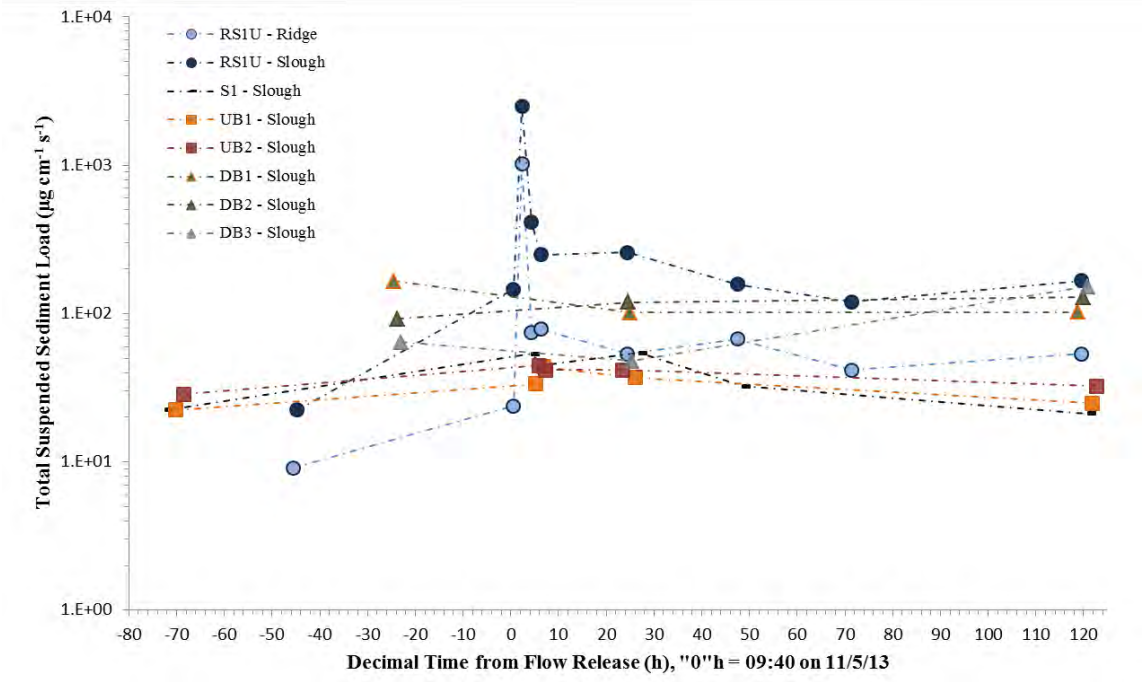

Figure D-28 Time series of total suspended sediment load at all sites during the November 5th, 2013 flow release.

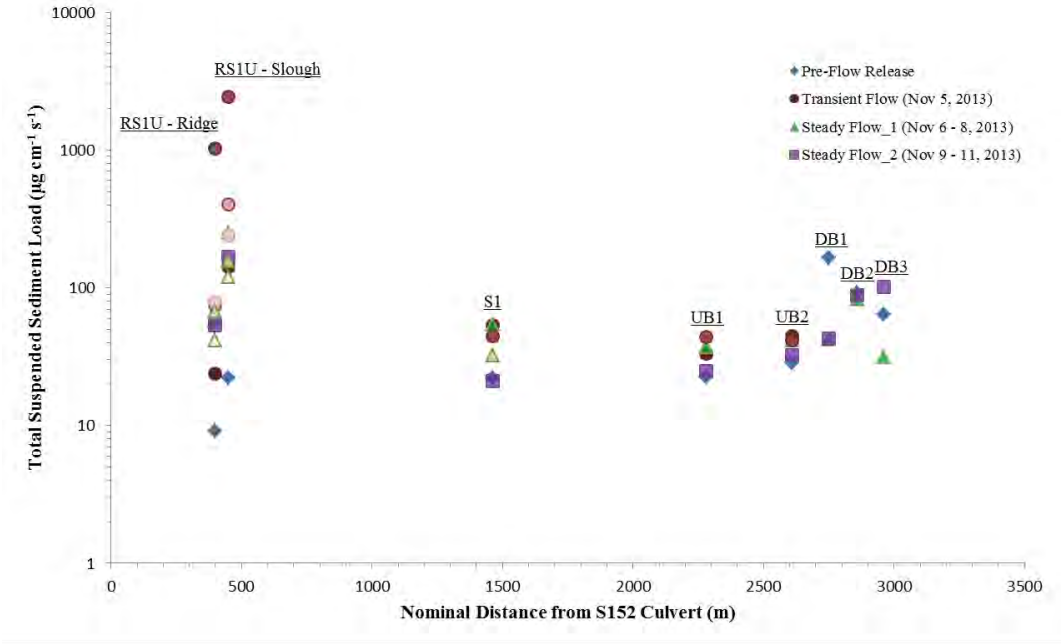

Figure D-29 Spatial distribution of total suspended sediment load at all sites during the November 5th, 2013 flow release. RS1U ridge and slough are geographically co-located, data have been separated for clarity. Color intensity of each symbol decreases with time.

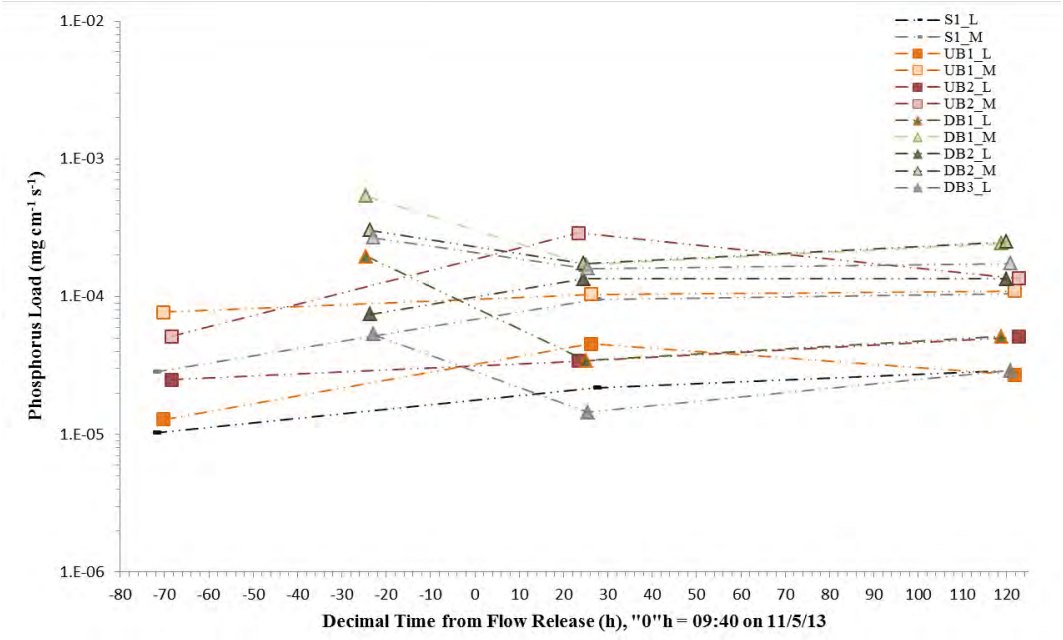

Figure D-30 Time series of phosphorus load in each water column interval at sites S1, UB1, UB2, DB1, DB2, and DB3 during the November 5th, 2013 flow release.

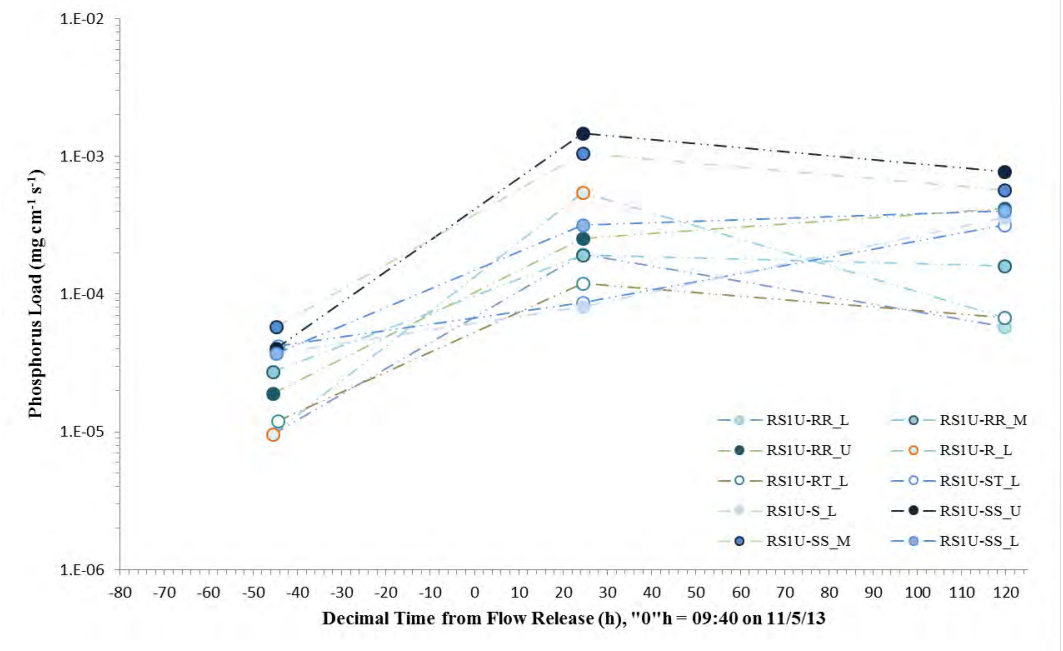

Figure D-31 Time series of phosphorus load in each water column interval at site RS1U during the November 5th, 2013 flow release.

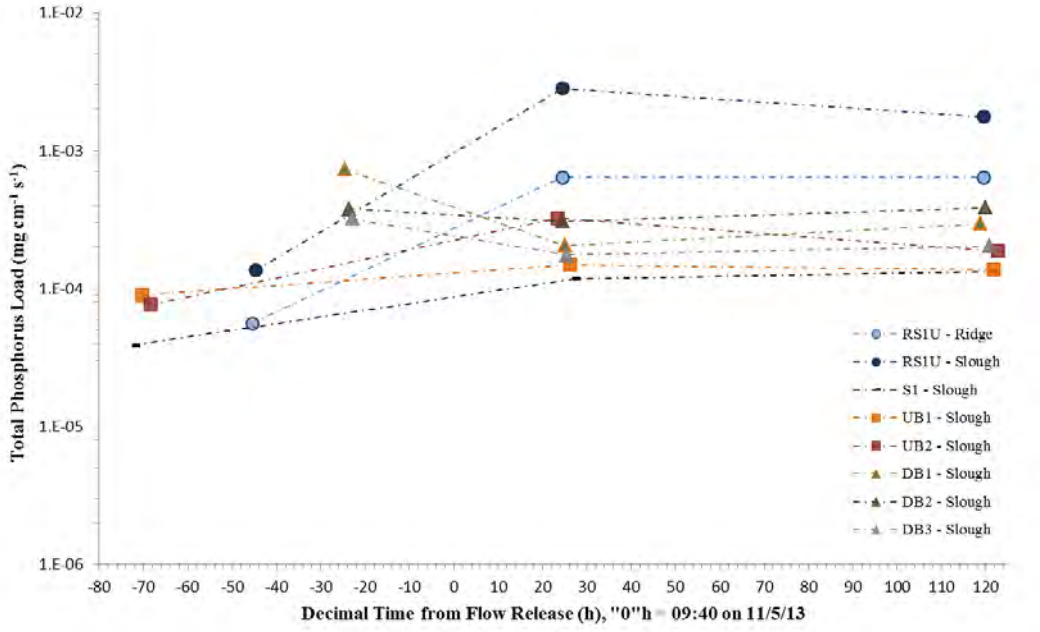

Figure D-32 Time series of total phosphorus load at all sites during the November 5th, 2013 flow release.

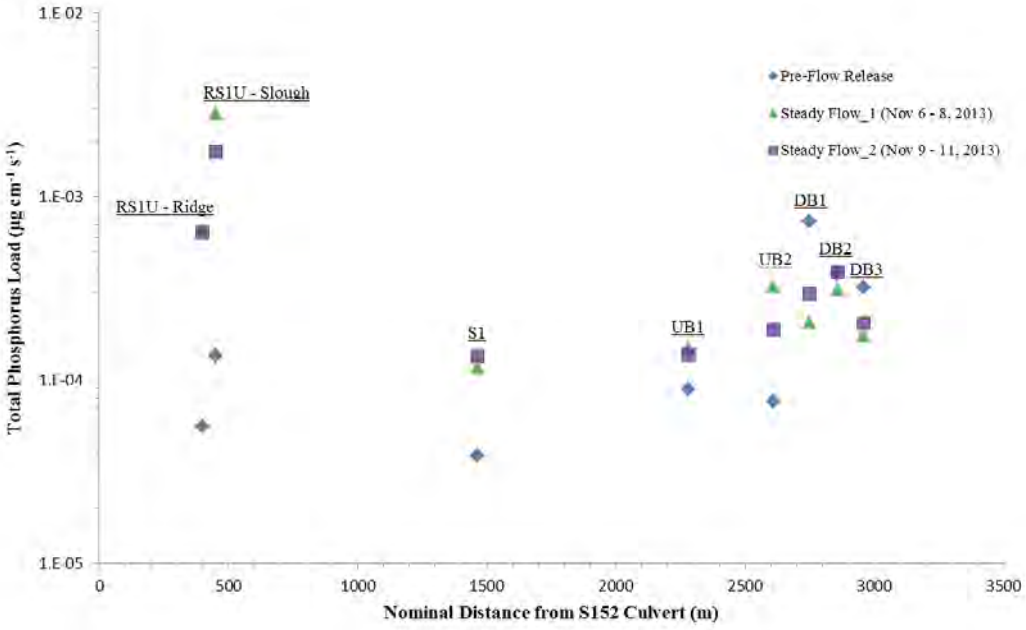

Figure D-33 Spatial distribution of total phosphorus load at all sites during the November 5th, 2013 flow release. RS1U ridge and slough are geographically co-located, data have been separated for clarity.

Table D-1 SSC calculated error.

		SSC (µg/L)	D_{50} (µm)	D_{60}/D_{10}
RS1U_RR-M	Mean (µg/L):	784.0	216.16	3.41
	Standard Deviation (µg/L):	36.5	154.96	1.19
	Coefficient of Variation (%):	4.7	71.69	34.96
RS1U_SS-M	Mean (µg/L):	919.3	474.46	11.64
	Standard Deviation (µg/L):	26.3	2.93	10.48
	Coefficient of Variation (%):	2.9	0.62	90.01
S1_L	Mean (µg/L):	786.3	480.05	1.09
	Standard Deviation (µg/L):	157.1	1.76	0.02
	Coefficient of Variation (%):	20.0	0.37	1.56
UB1_L	Mean (µg/L):	970.7	472.83	1.14
	Standard Deviation (µg/L):	170.7	7.71	0.06
	Coefficient of Variation (%):	17.6	1.63	5.24

2014 Suspended Sediment and Phosphorus

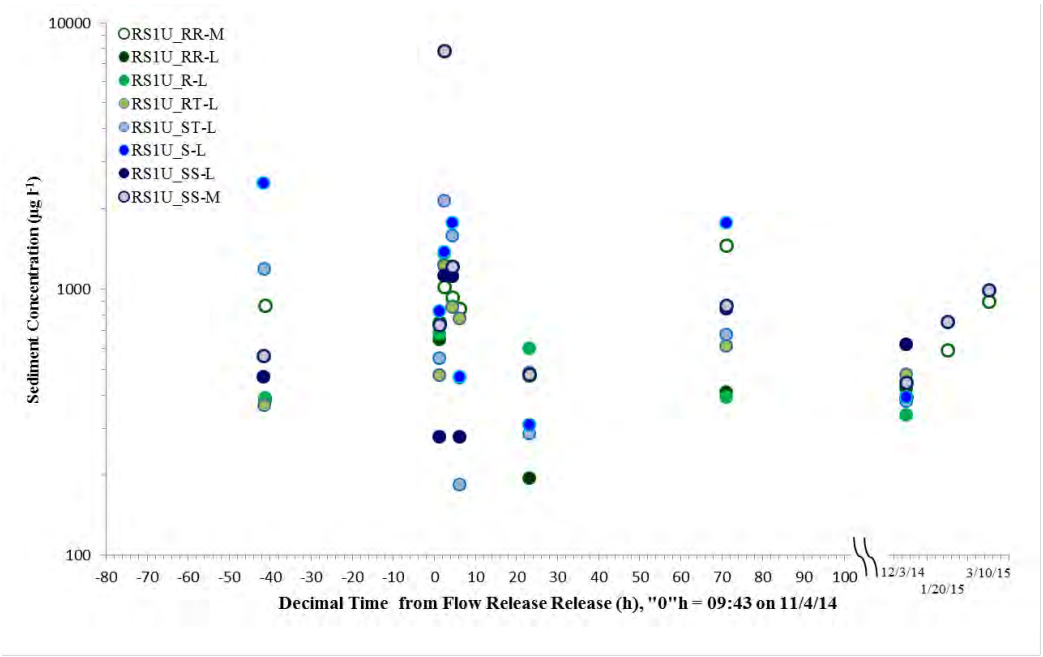

Figure D-34 Time series of suspended sediment concentration at site RS1U during the November 4th, 2014 flow release.

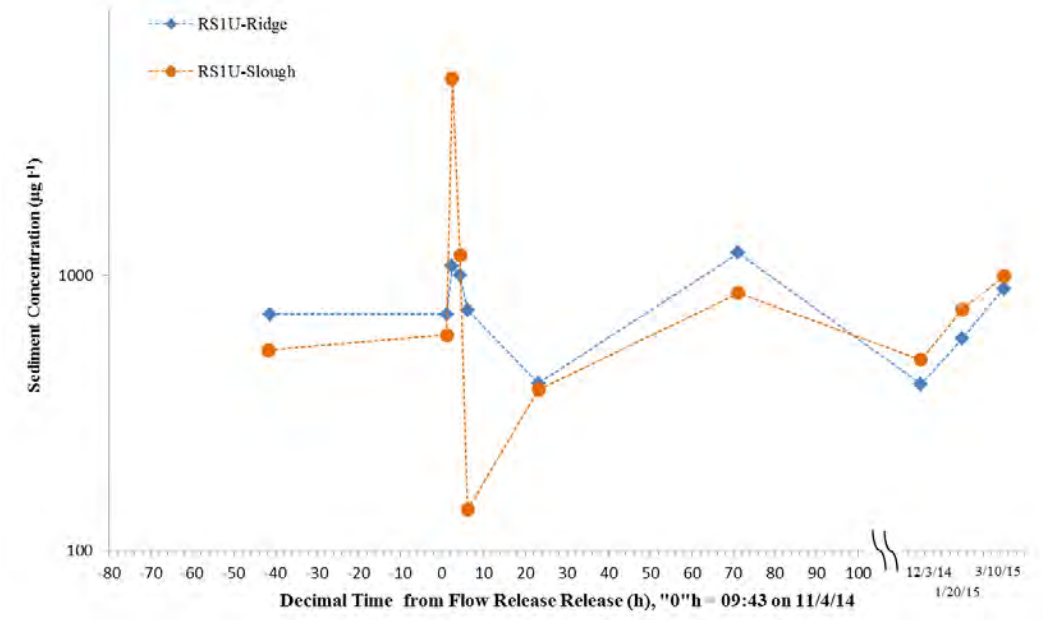

Figure D-35 Time series of depth-averaged suspended sediment concentration at site RS1U during the November 4th, 2014 flow release.

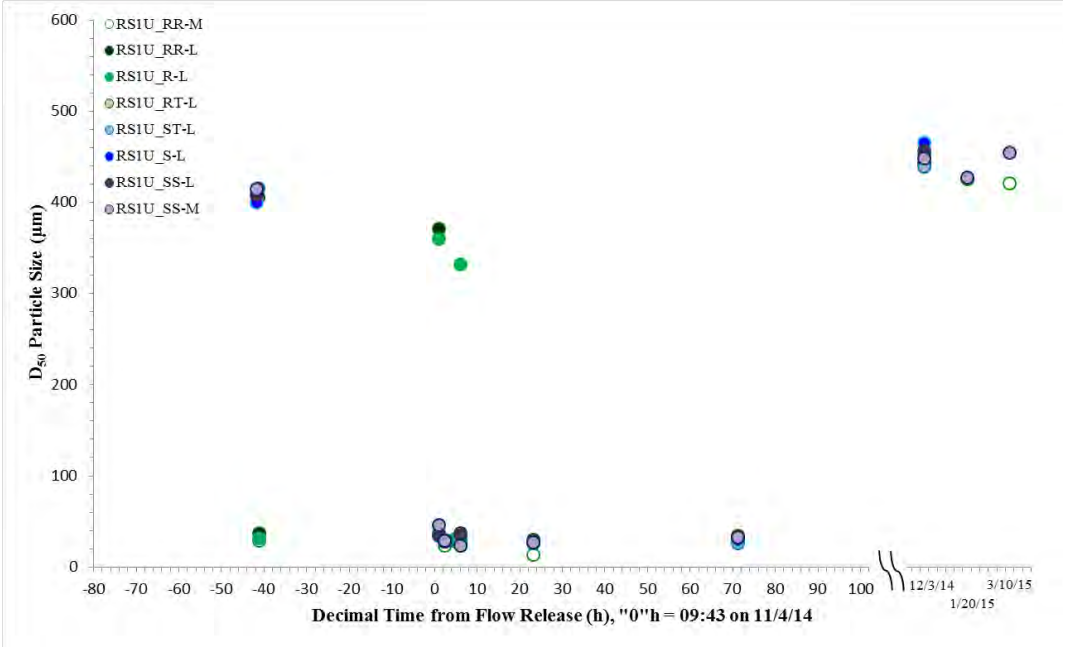

Figure D-36 Time series of D_{50} (median mass weighted size) of suspended particles at the site RS1U during the November 4th, 2014 flow release.

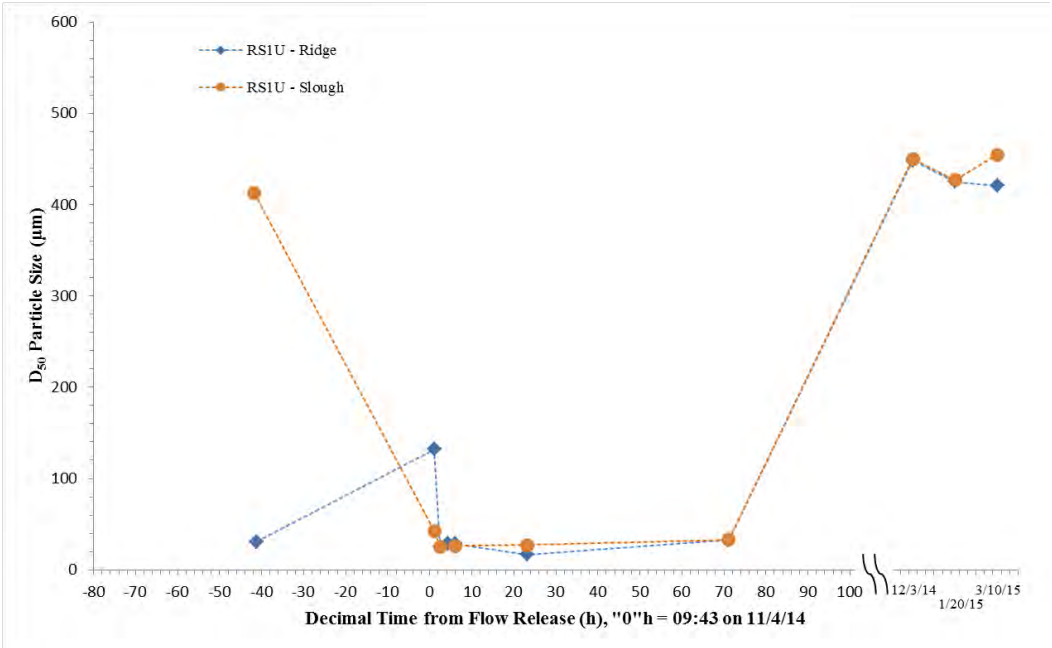

Figure D-37 Time series of depth-averaged D_{50} (median mass weighted size) of suspended particles at the site RS1U during the November 4th, 2014 flow release.

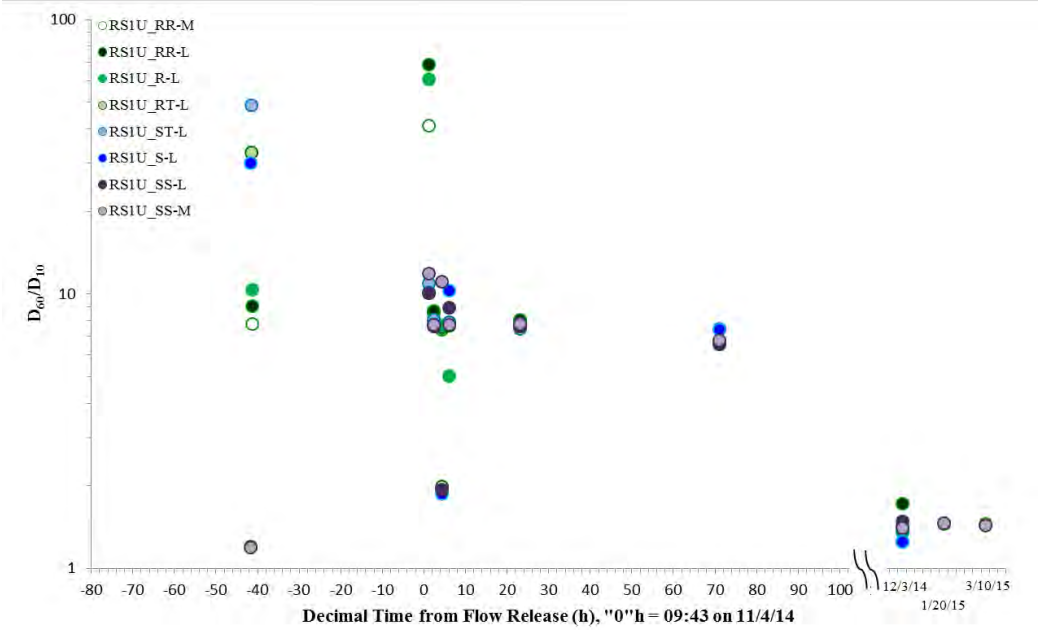

Figure D-38 Time series of D_{60}/D_{10} (particle size uniformity coefficient) of suspended particles at the site RS1U during the November 4th, 2014 flow release.

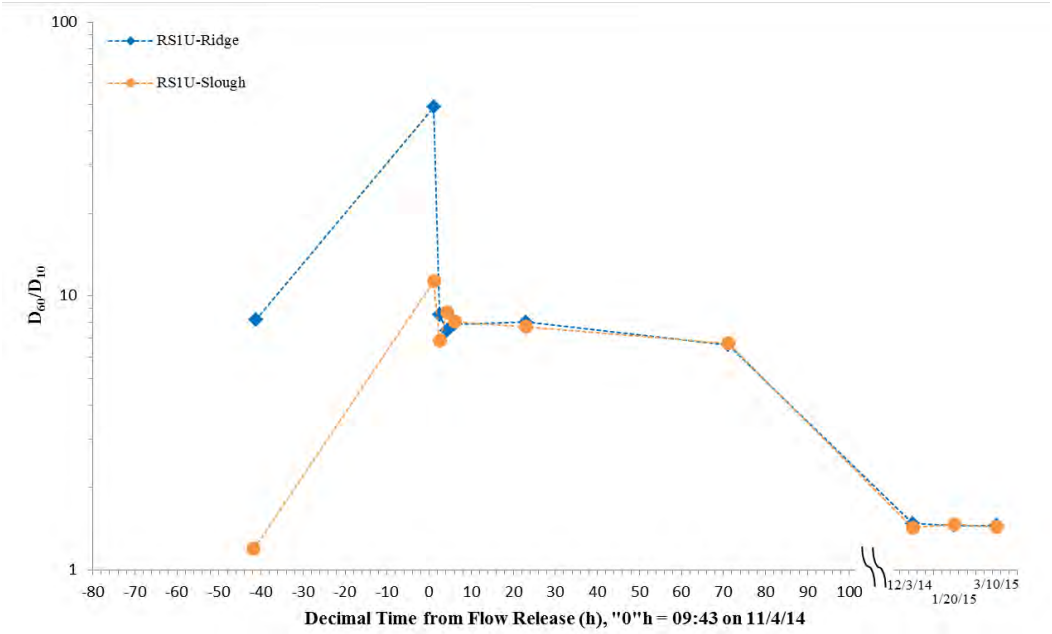

Figure D-39 Time series of depth-averaged D_{60}/D_{10} (particle size uniformity coefficient) of suspended particles at the site RS1U during the November 4th, 2014 flow release.

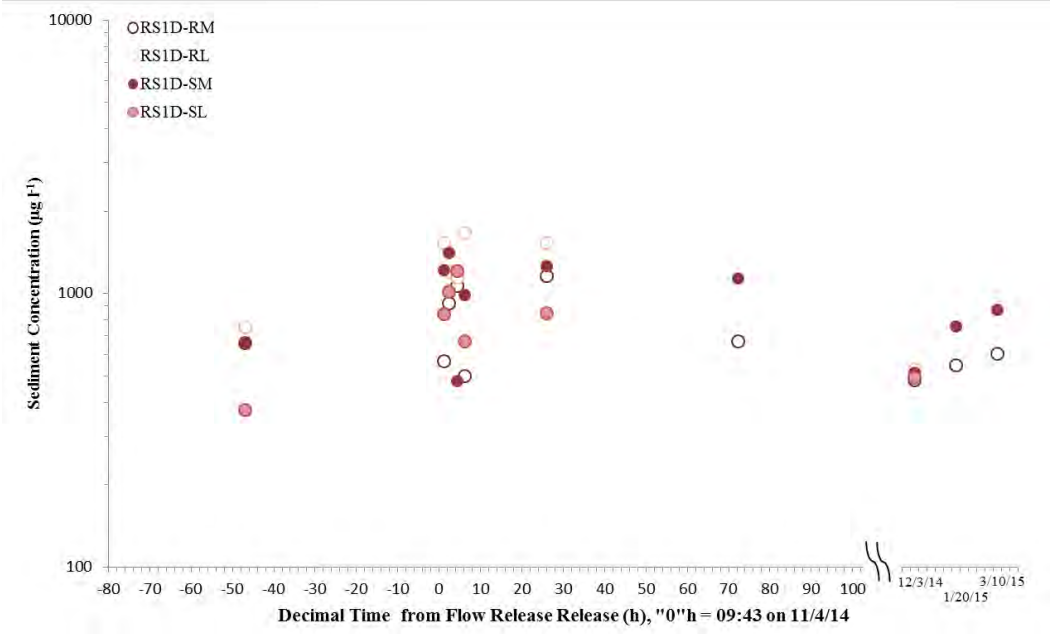

Figure D-40 Time series of suspended sediment concentration at site RS1D during the November 4th, 2014 flow release.

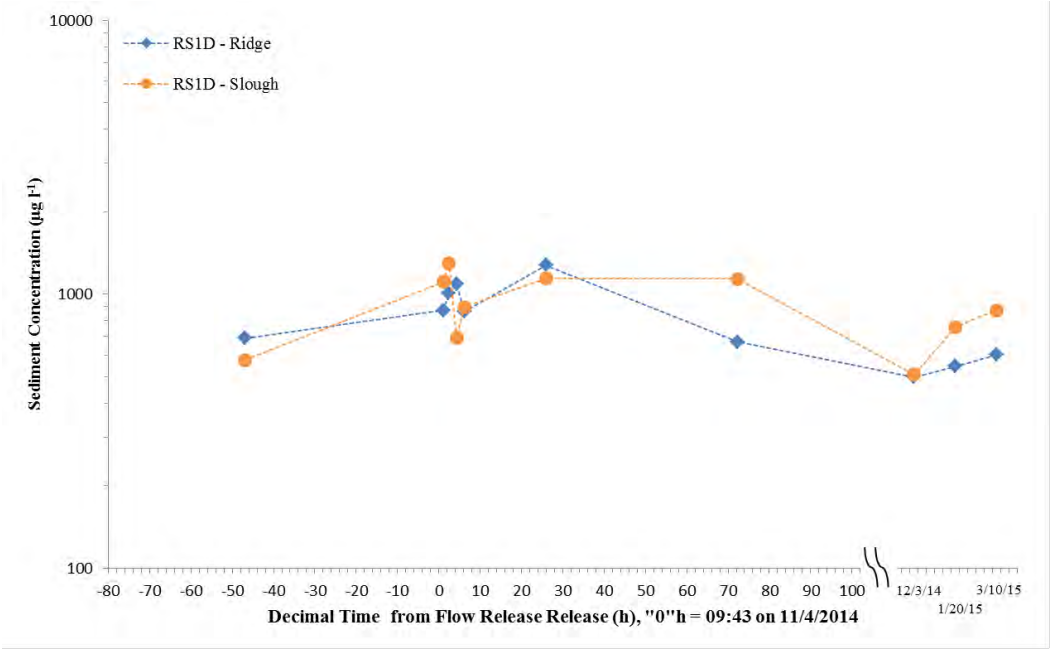

Figure D-41 Time series of depth-averaged suspended sediment concentration at site RS1D during the November 4th, 2014 flow release.

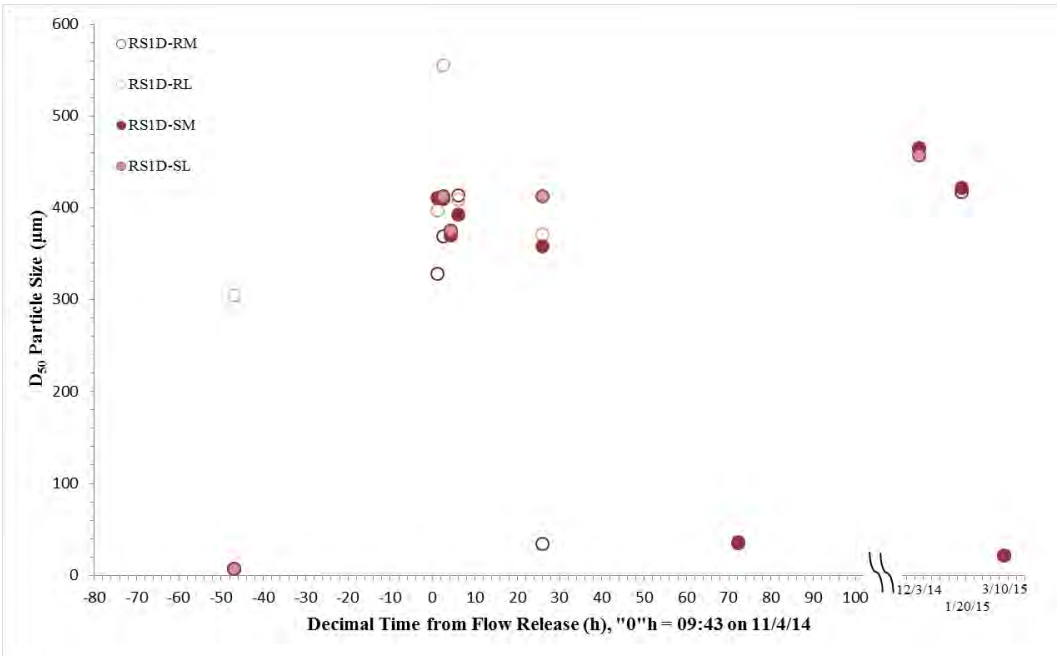

Figure D-42 Time series of D_{50} (median mass weighted size) of suspended particles at the site RS1D during the November 4th, 2014 flow release.

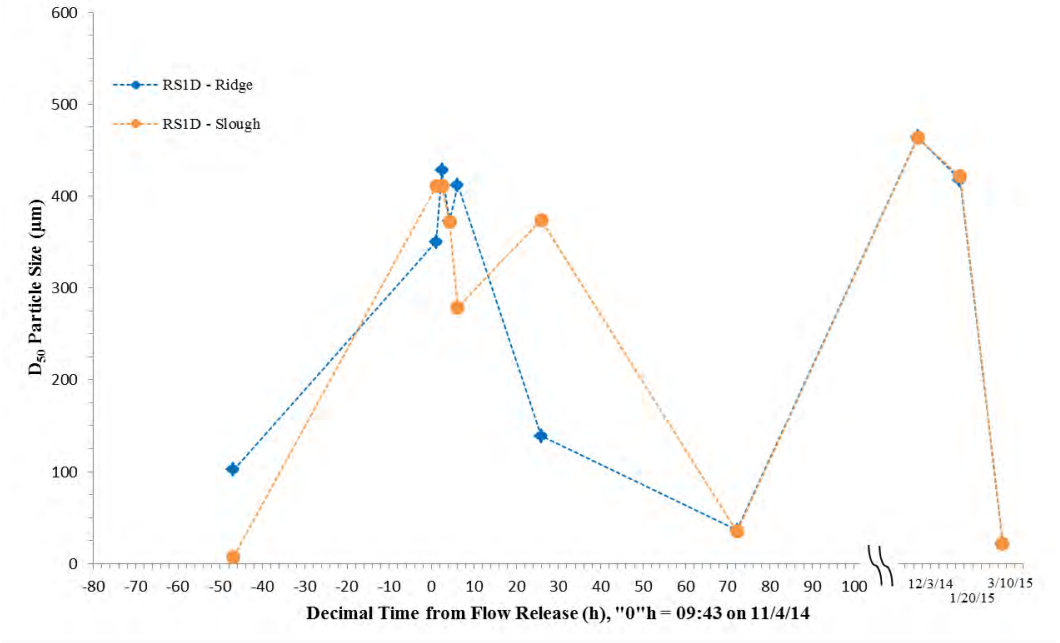

Figure D-43 Time series of depth-averaged D_{50} (median mass weighted size) of suspended particles at the site RS1D during the November 4th, 2014 flow release.

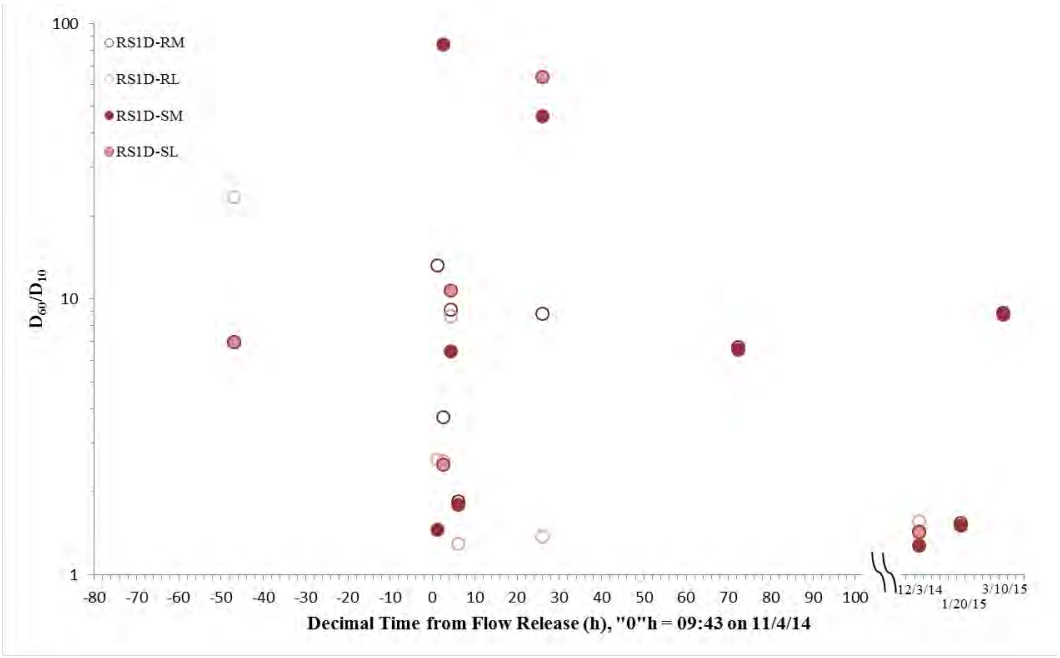

Figure D-44 Time series of D_{60}/D_{10} (particle size uniformity coefficient) of suspended particles at the site RS1D during the November 4th, 2014 flow release.

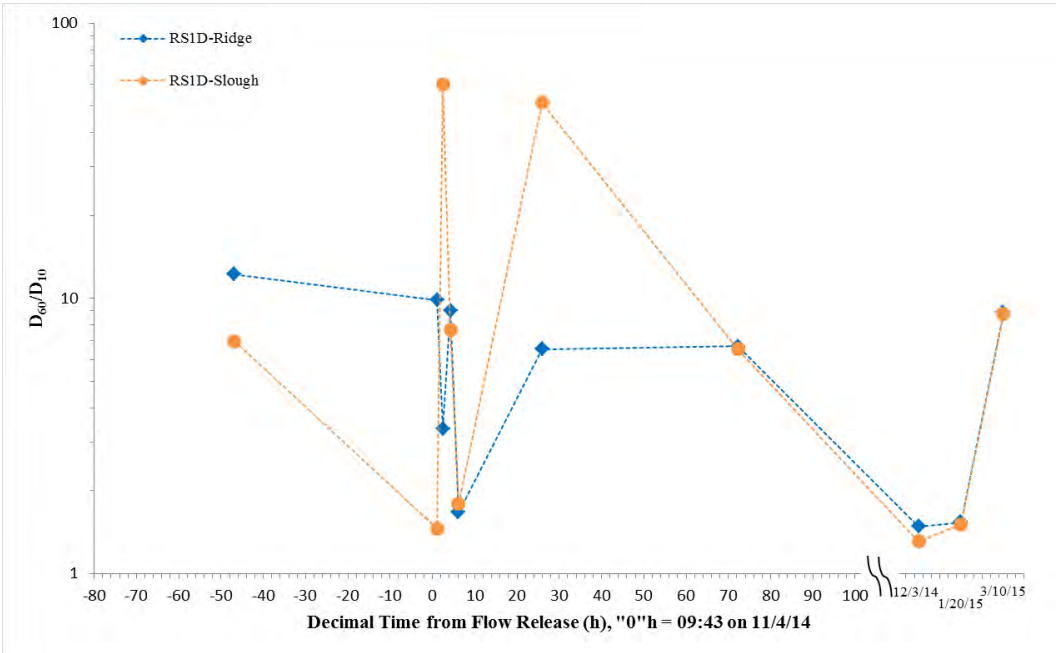

Figure D-45 Time series of depth-averaged D_{60}/D_{10} (particle size uniformity coefficient) of suspended particles at the site RS1D during the November 4th, 2014 flow release.

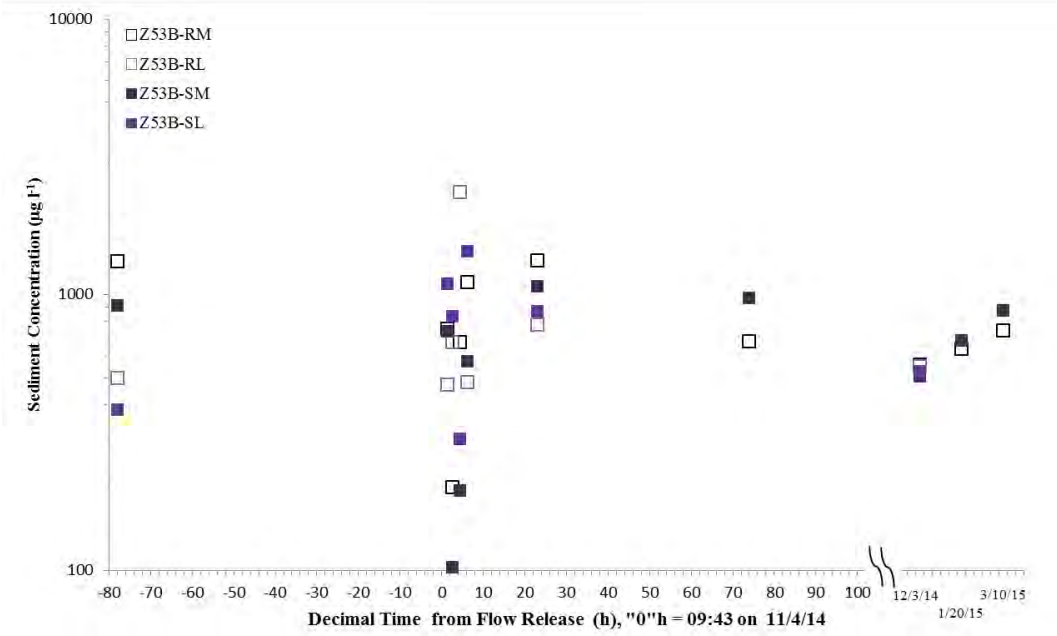

Figure D-46 Time series of suspended sediment concentration at site Z53B during the November 4th, 2014 flow release.

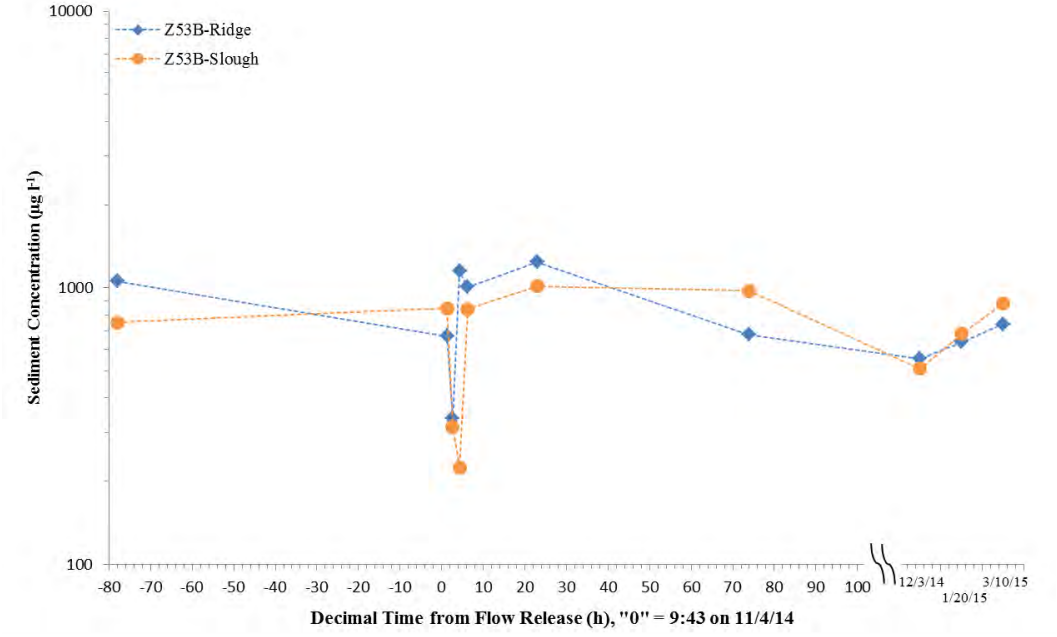

Figure D-47 Time series of depth-averaged suspended sediment concentration at site Z53B during the November 4th, 2014 flow release.

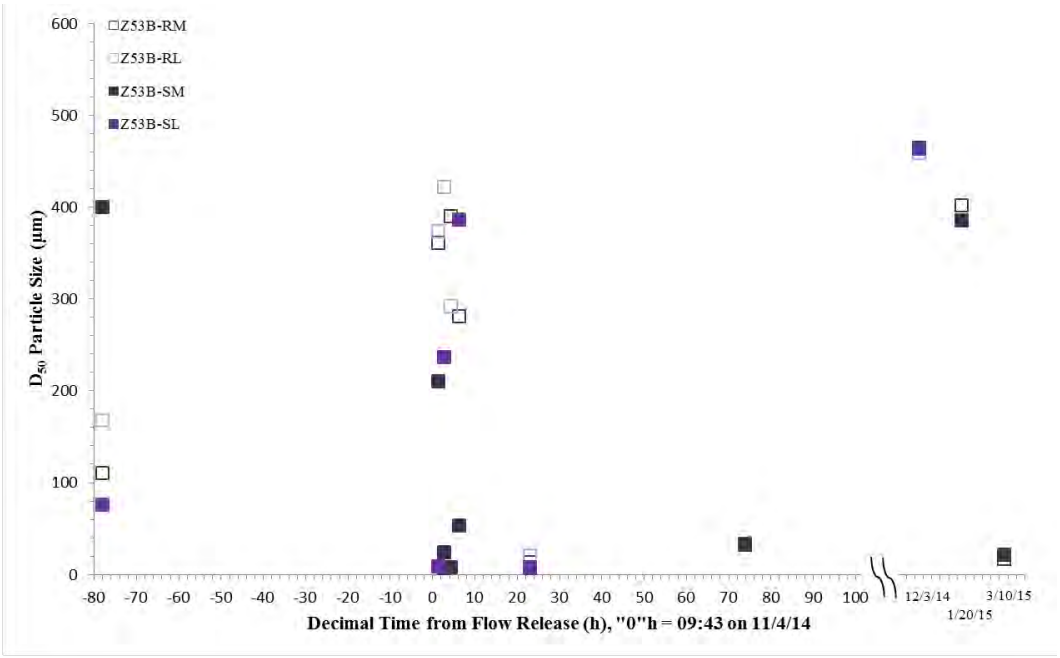

Figure D-48 Time series of D_{50} (median mass weighted size) of suspended particles at the site Z53B during the November 4th, 2014 flow release.

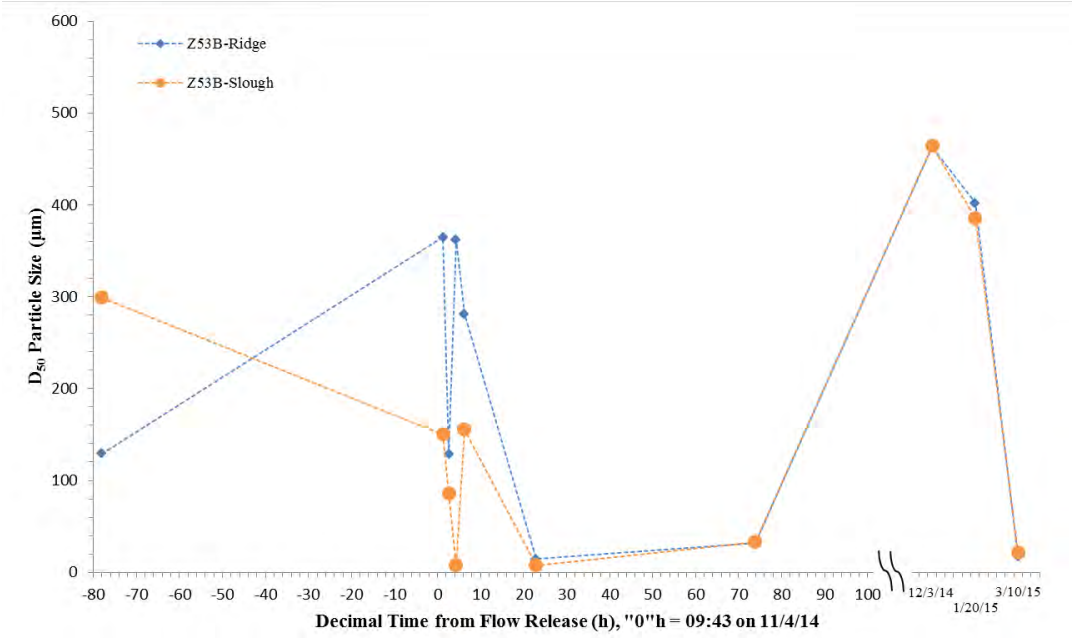

Figure D-49 Time series of depth-averaged D_{50} (median mass weighted size) of suspended particles at the site Z53B during the November 4th, 2014 flow release.

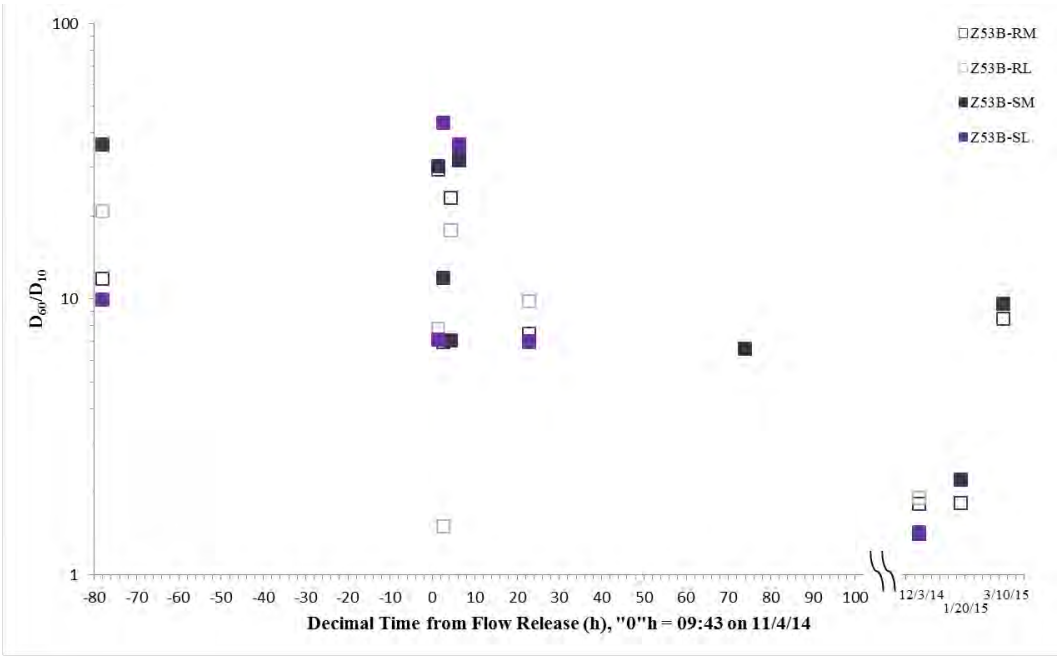

Figure D-50 Time series of D_{60}/D_{10} (particle size uniformity coefficient) of suspended particles at the site Z53B during the November 4th, 2014 flow release.

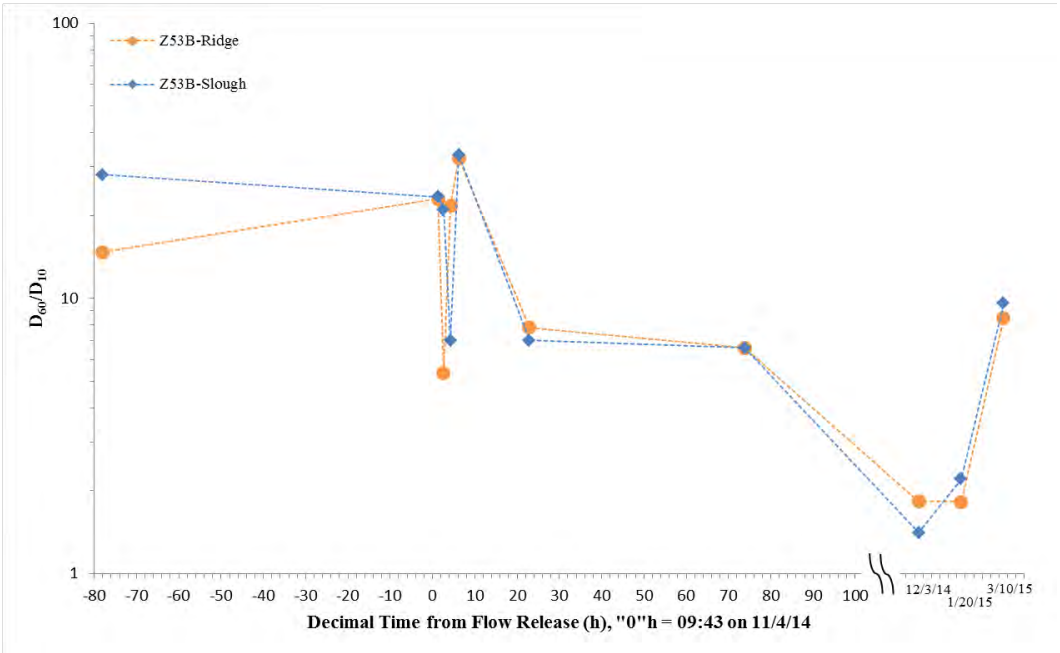

Figure D-51 Time series of depth-averaged D_{60}/D_{10} (particle size uniformity coefficient) of suspended particles at the site Z53B during the November 4th, 2014 flow release.

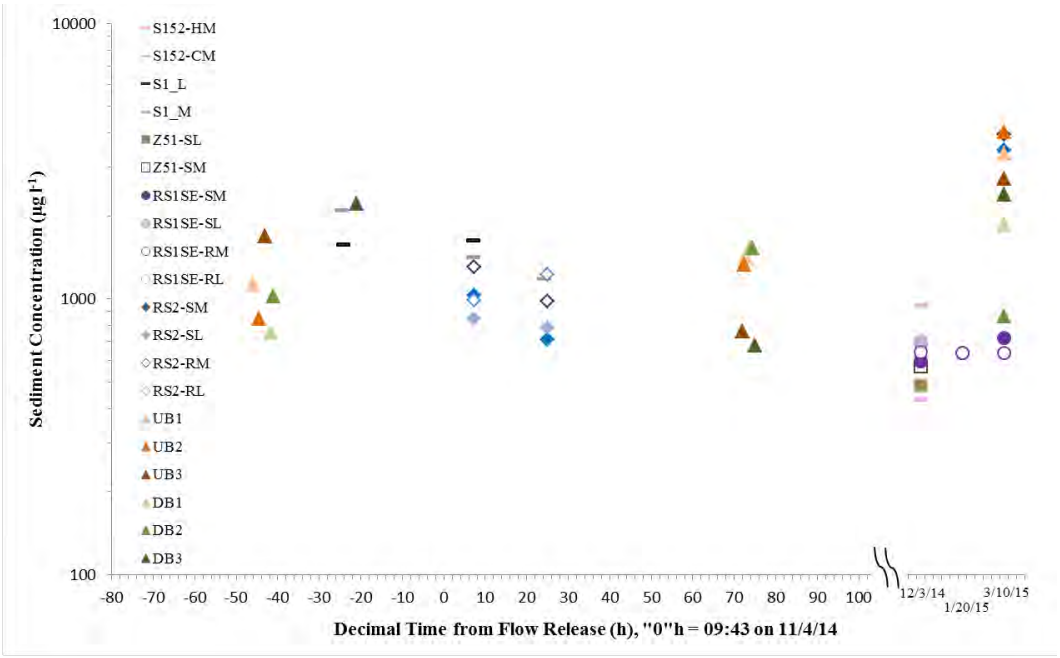

Figure D-52 Time series of suspended sediment concentration at sites S152, S1, Z51, RS1SE, RS2, UB1, UB2, UB3, DB1, DB2 and DB3 during the November 4th, 2014 flow release.

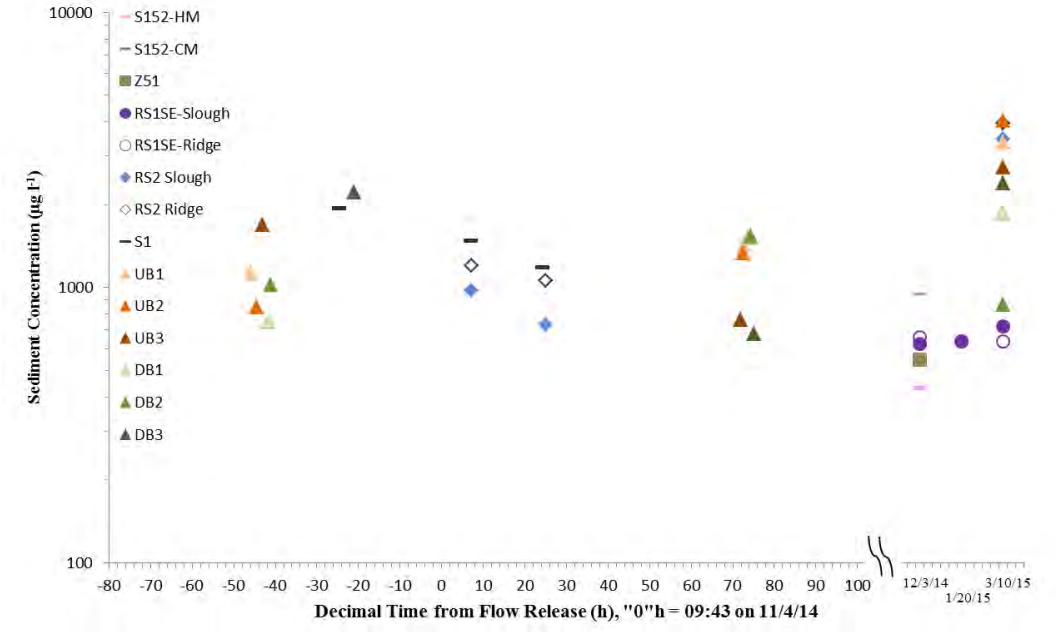

Figure D-53 Time series of depth-averaged suspended sediment concentration at sites S152, S1, Z51, RS1SE, RS2, UB1, UB2, UB3, DB1, DB2 and DB3 during the November 4th, 2014 flow release.

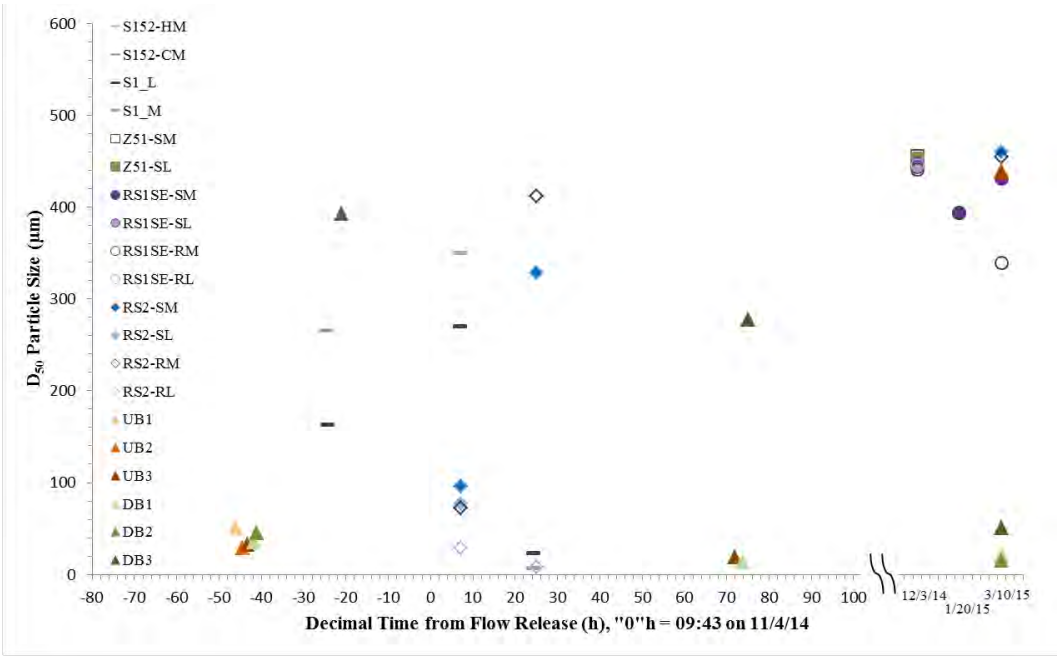

Figure D-54 Time series of D_{50} (median mass weighted size) of suspended particles at the sites S152, S1, Z51, RS1SE, RS2, UB1, UB2, UB3, DB1, DB2 and DB3 during the November 4th, 2014 flow release.

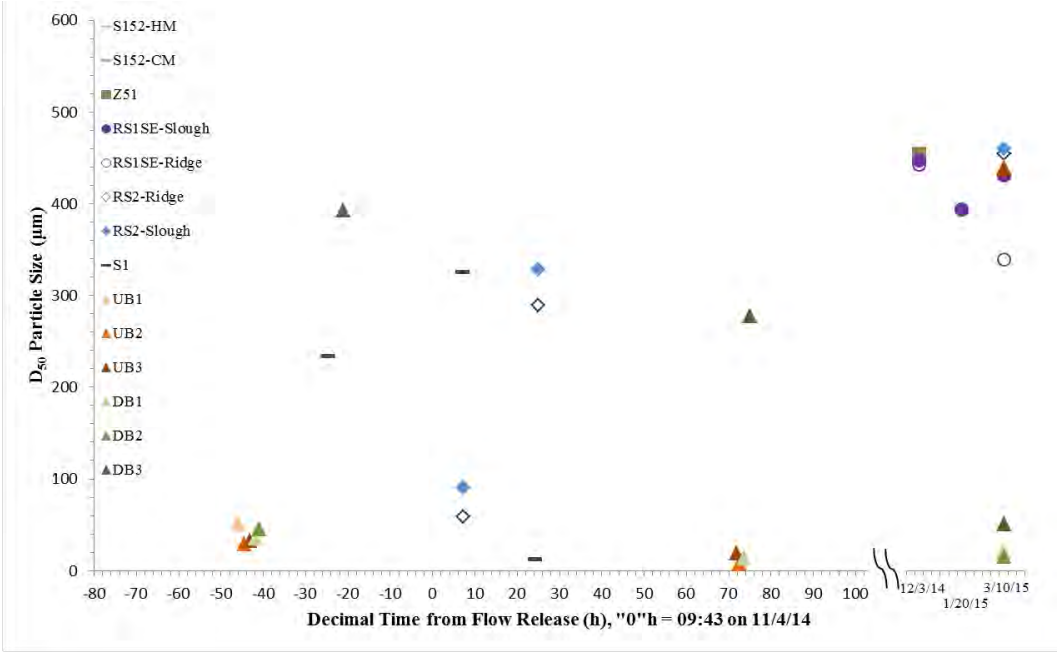

Figure D-55 Time series of depth-averaged D_{50} (median mass weighted size) of suspended particles at the sites S152, S1, Z51, RS1SE, RS2, UB1, UB2, UB3, DB1, DB2 and DB3 during the November 4th, 2014 flow release.

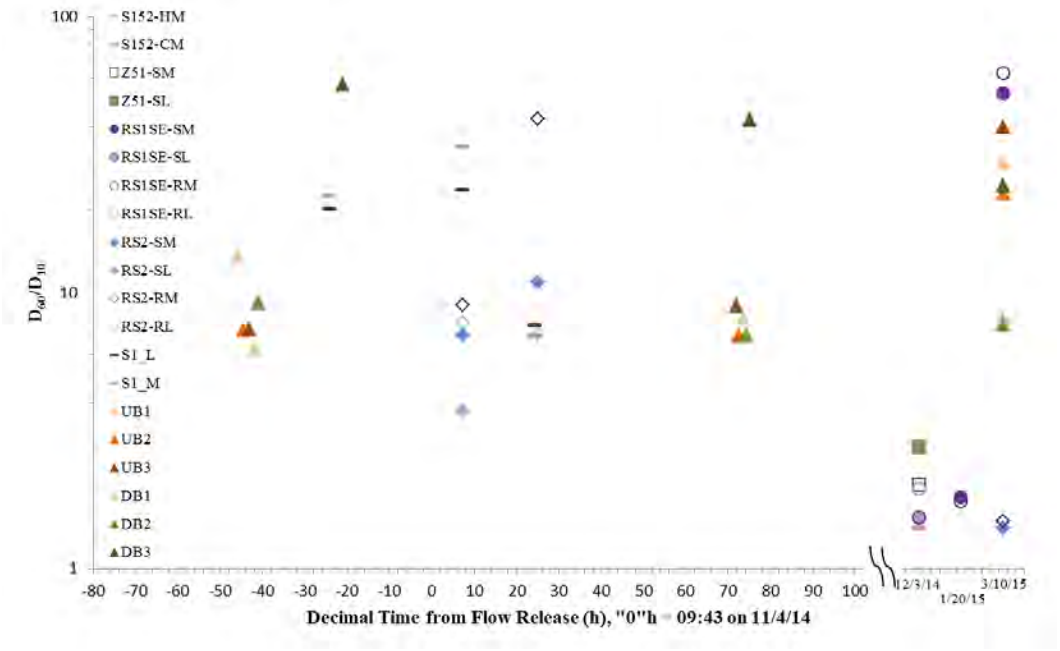

Figure D-56 Time series of D_{60}/D_{10} (particle size uniformity coefficient) of suspended particles at the sites S152, S1, Z51, RS1SE, RS2, UB1, UB2, UB3, DB1, DB2 and DB3 during the November 4th, 2014 flow release.

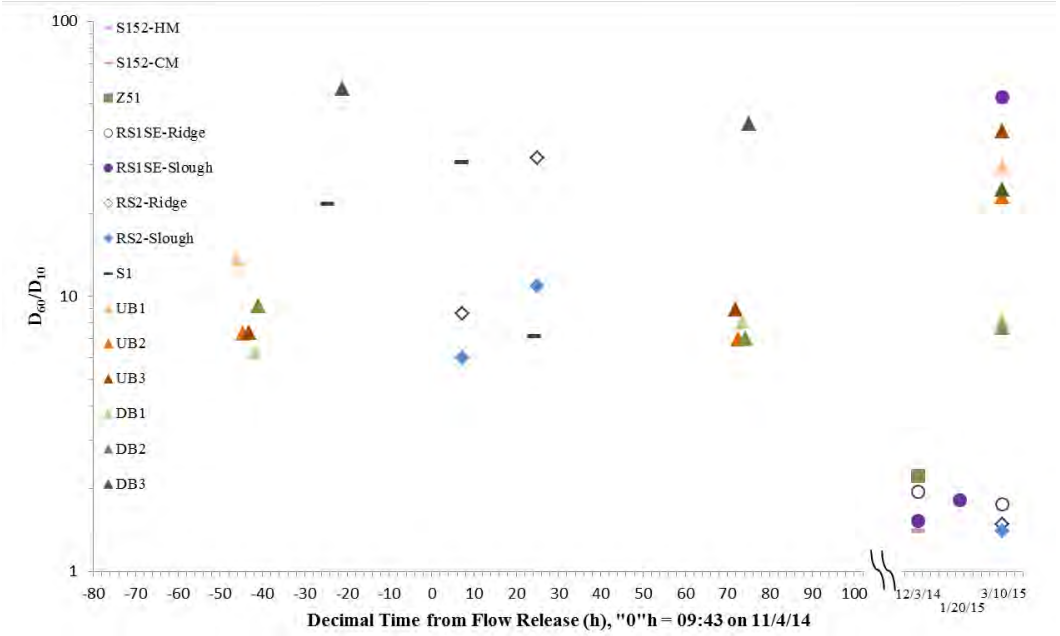

Figure D-57 Time series of depth-averaged D_{60}/D_{10} (particle size uniformity coefficient) of suspended particles at the sites S152, S1, Z51, RS1SE, RS2, UB1, UB2, UB3, DB1, DB2 and DB3 during the November 4th, 2014 flow release.

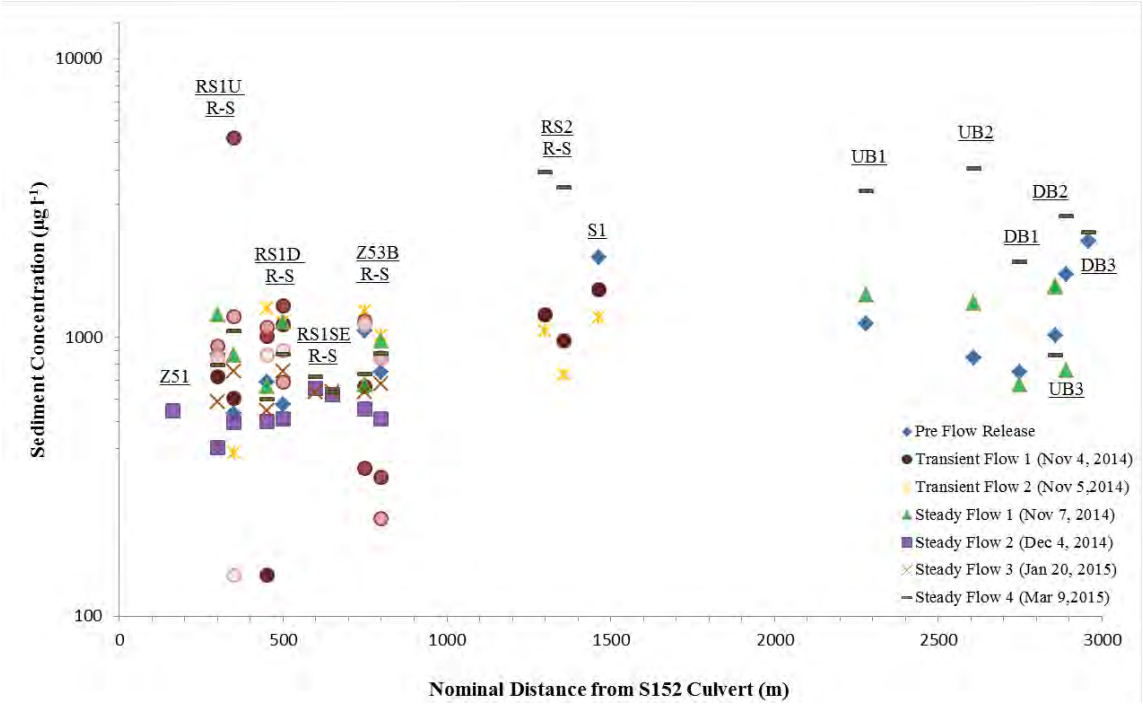

Figure D-58 Spatial distribution of depth-averaged suspended sediment concentration at all sites during the November 4th, 2014 flow release. RS1U ridge and slough are geographically co-located, data have been separated for clarity. Symbol color intensity decreases with time for Transient Flow 1.

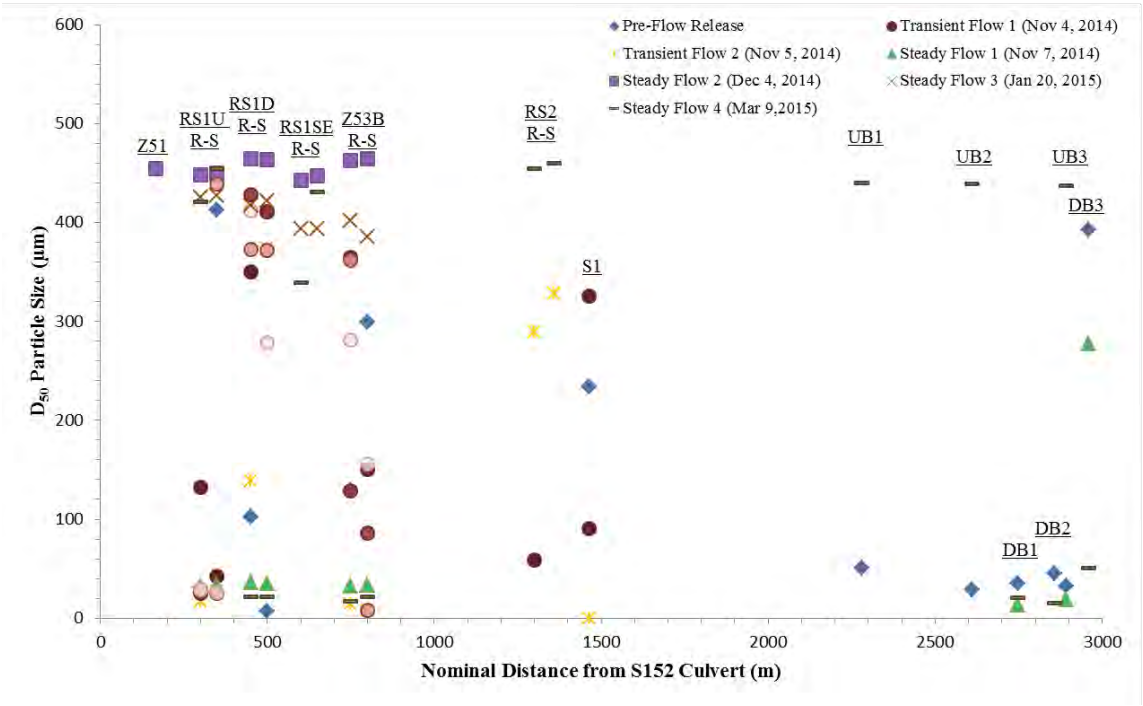

Figure D-59 Spatial distribution of depth-averaged D_{50} (median mass weighted size) of suspended particles at all sites during the November 4th, 2014 flow release. RS1U ridge and slough are geographically co-located, data have been separated for clarity. Symbol color intensity decreases with time for Transient Flow 1.

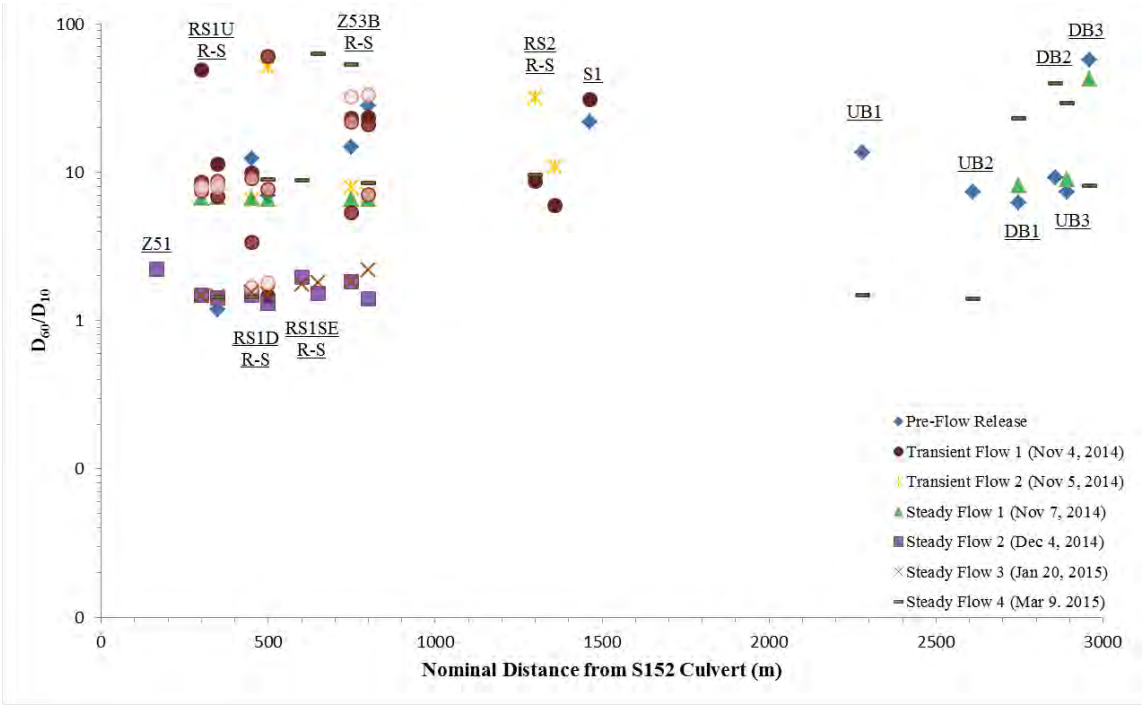

Figure D-60 Spatial distribution of depth-averaged D_{60}/D_{10} (particle size uniformity coefficient) of suspended sediment at all sites during the November 4th, 2014 flow release. RS1U ridge and slough are geographically co-located, data have been separated for clarity. Symbol color intensity decreases with time for Transient Flow 1.

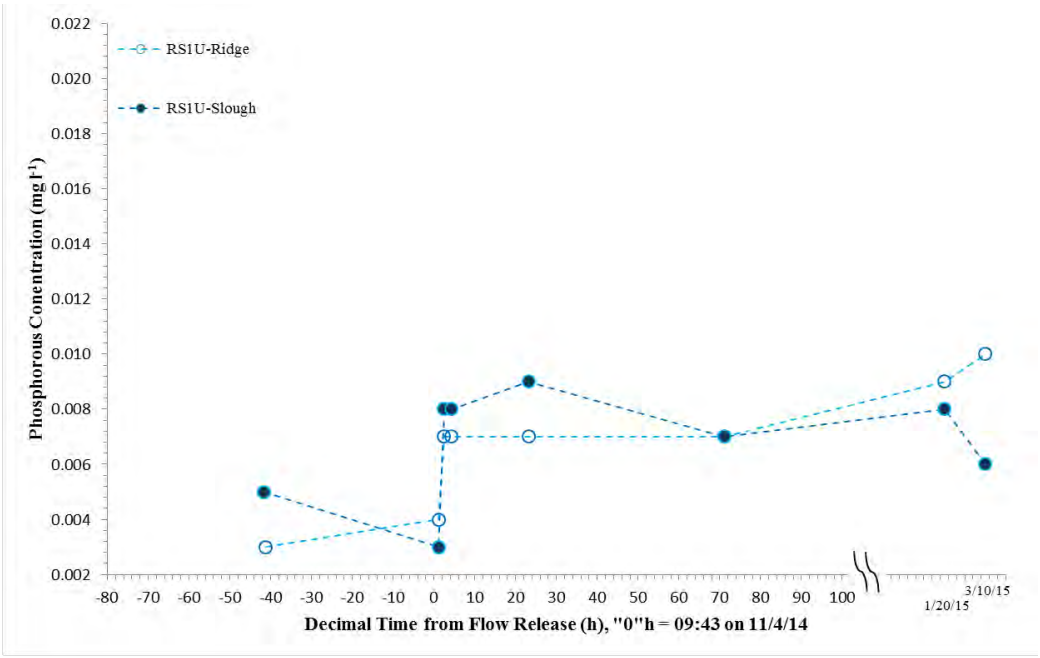

Figure D-61 Time series of depth-averaged phosphorus concentration at site RS1U during the November 4th, 2014 flow release.

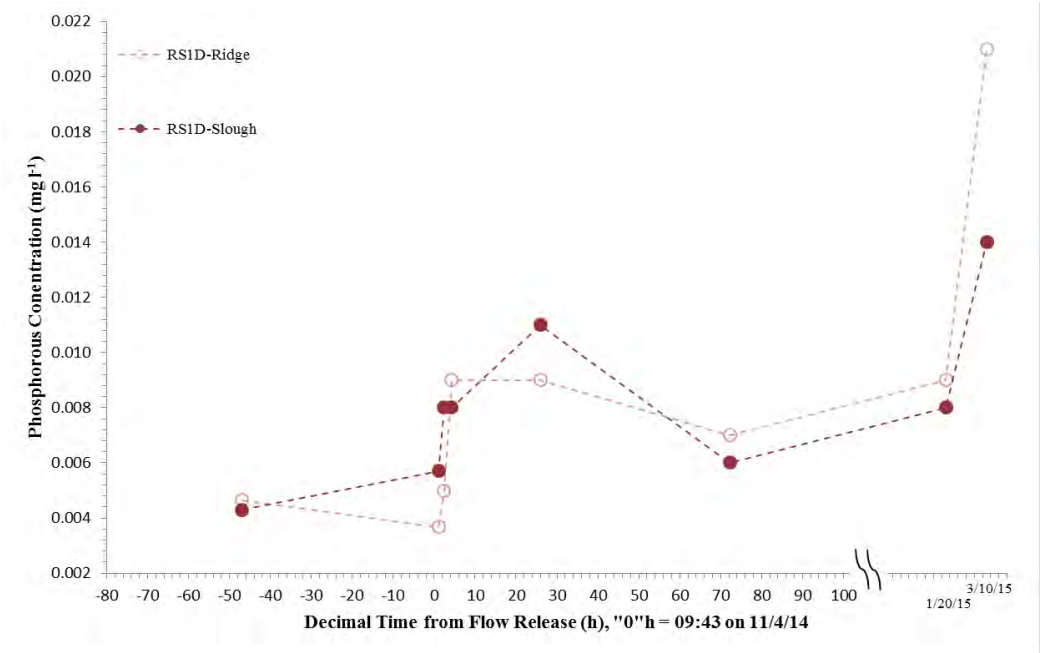

Figure D-62 Time series of depth-averaged phosphorus concentration at site RS1D during the November 4th, 2014 flow release.

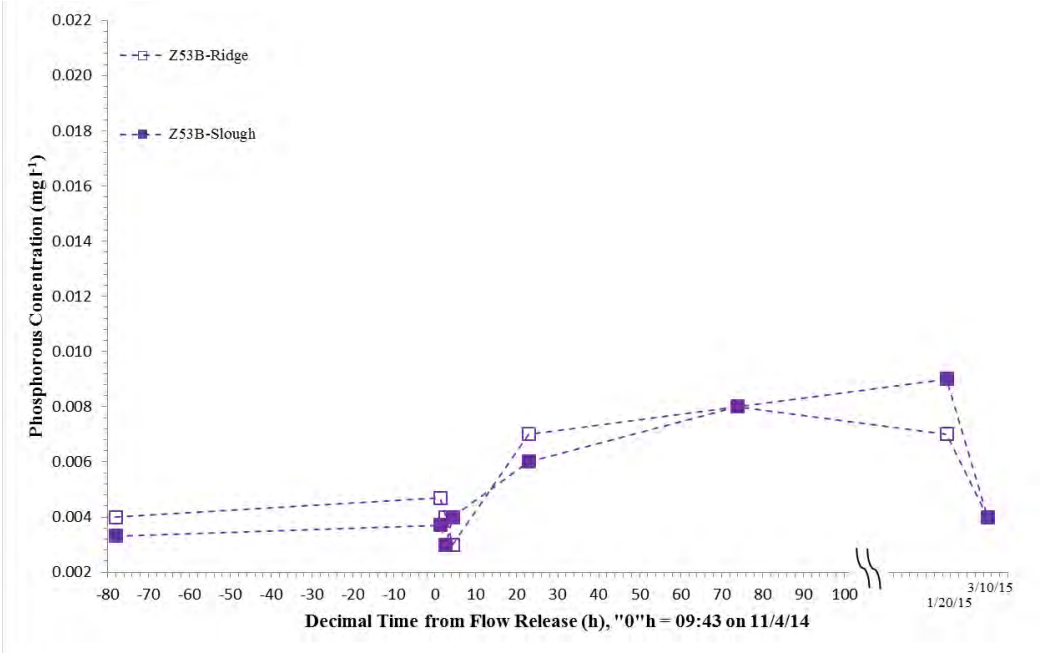

Figure D-63 Time series of depth-averaged phosphorus concentration at site Z53B during the November 4th, 2014 flow release.

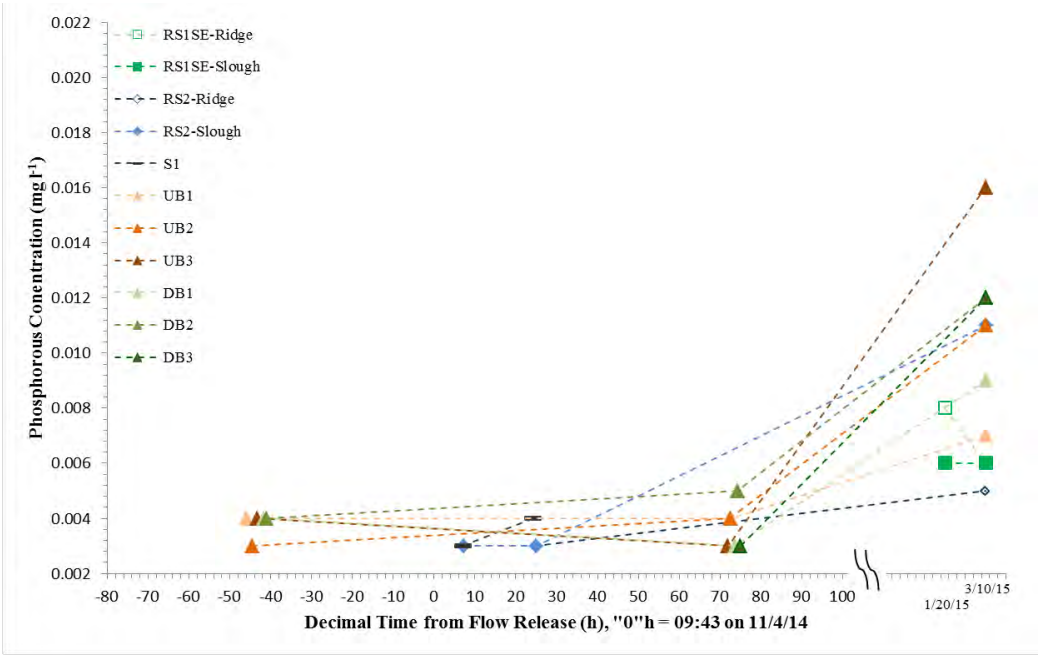

Figure D-64 Time series of depth-averaged phosphorus concentration at the sites S1, RS1SE, RS2, UB1, UB2, UB3, DB1, DB2 and DB3 during the November 4th, 2014 flow release.

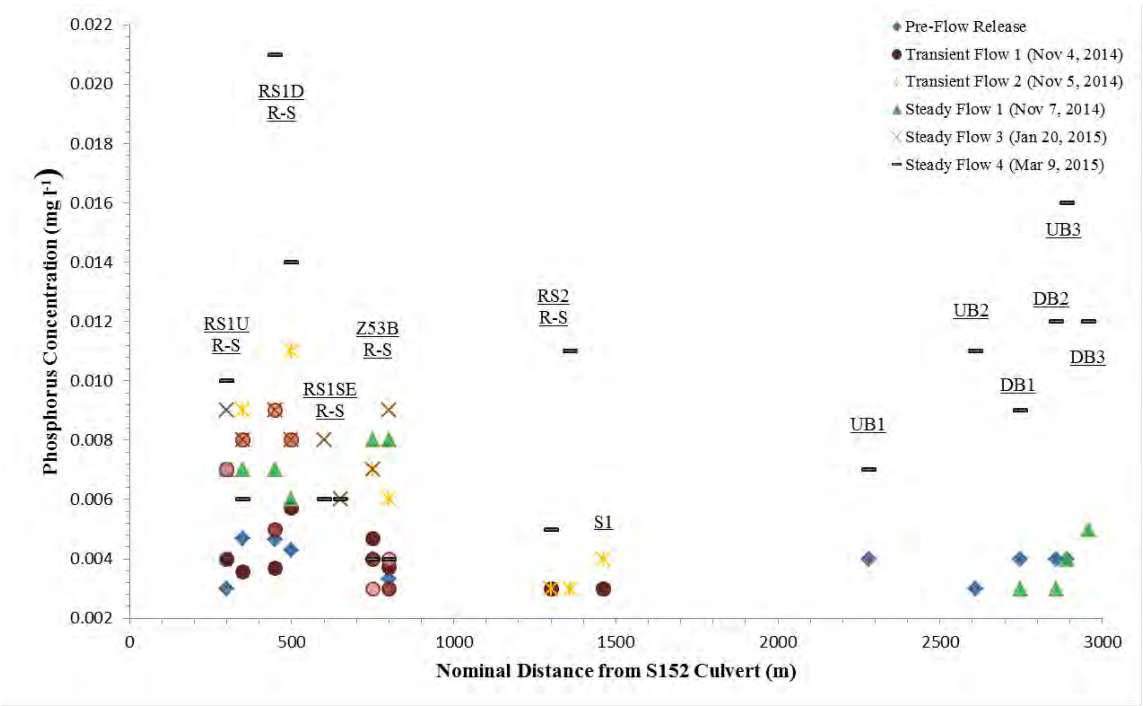

Figure D-65 Spatial distribution of depth-averaged phosphorus concentration at all sites during the November 4th, 2014 flow release. RS1U ridge and slough are geographically co-located, data have been separated for clarity. Symbol color intensity decreases with time for Transient Flow 1.

2014 Load

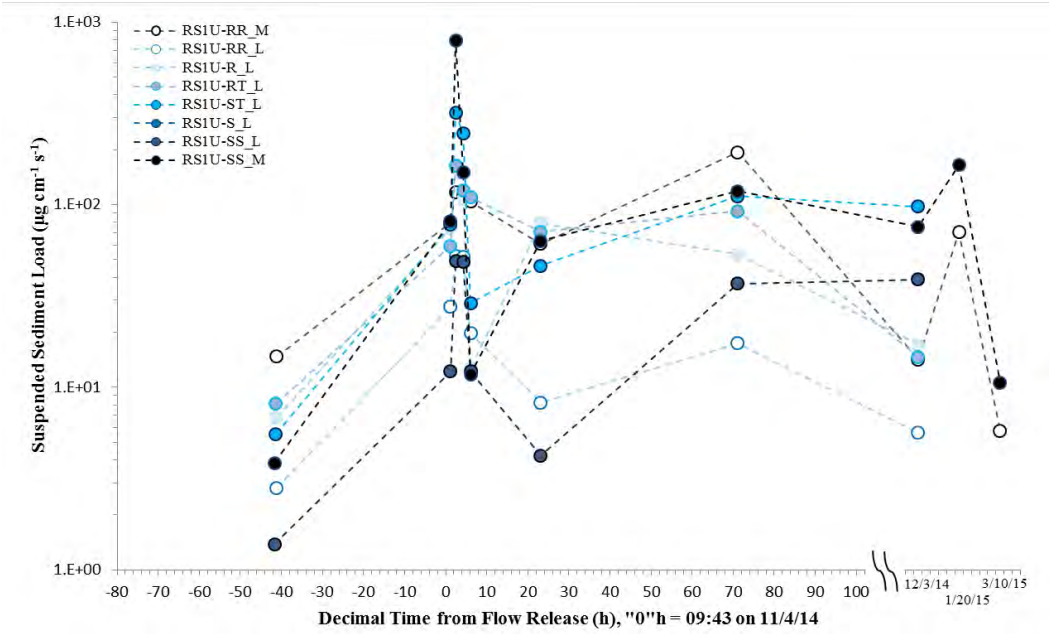

Figure D-66 Time series of suspended sediment load in each water column interval at site RS1U during the November 4th, 2014 flow release.

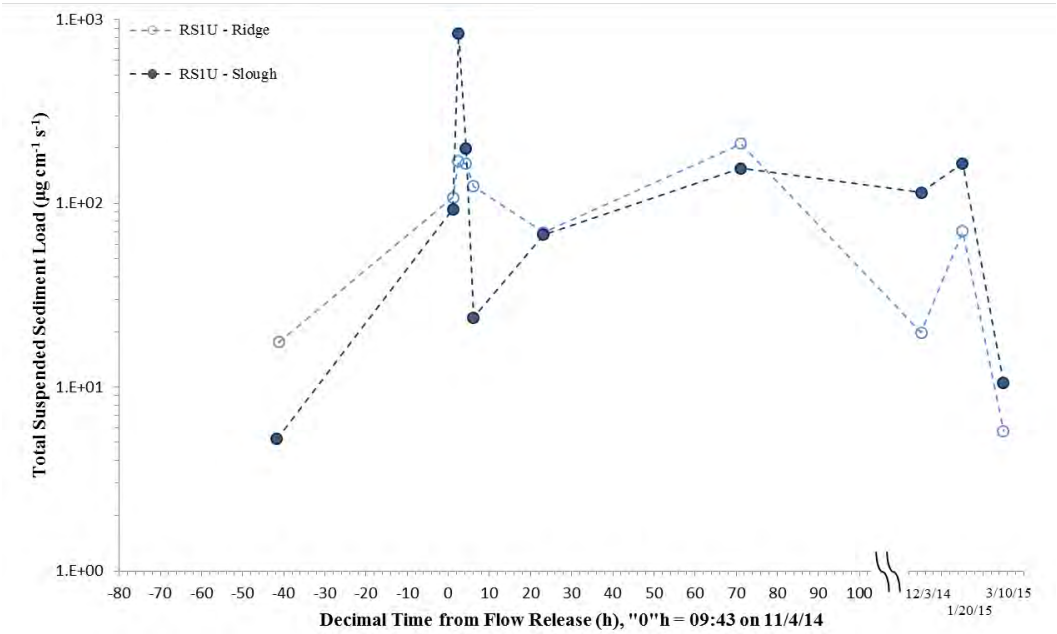

Figure D-67 Time series of total suspended sediment load at site RS1U during the November 4th, 2014 flow release.

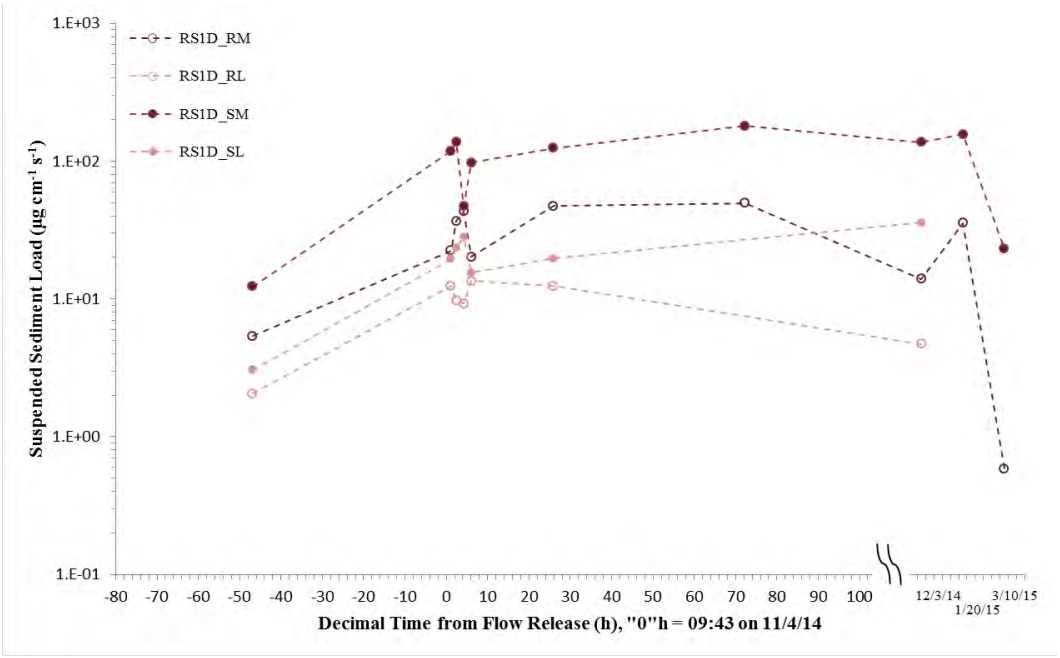

Figure D-68 Time series of suspended sediment load in each water column interval at site RS1D during the November 4th, 2014 flow release.

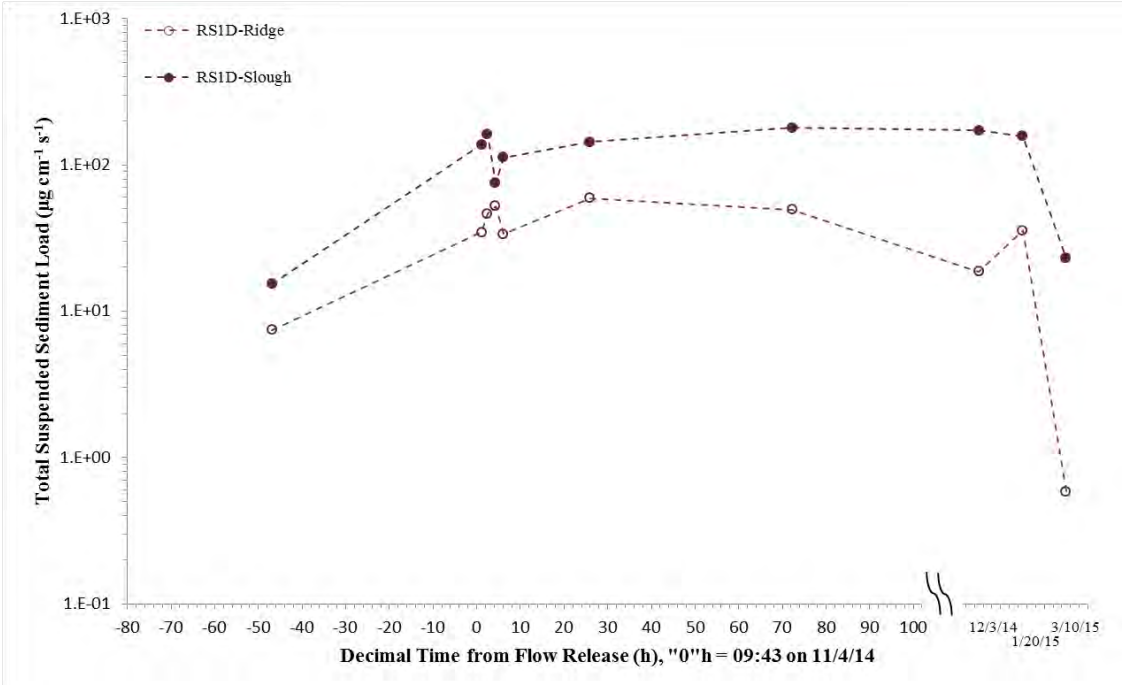

Figure D-69 Time series of total suspended sediment load at site RS1D during the November 4th, 2014 flow release.

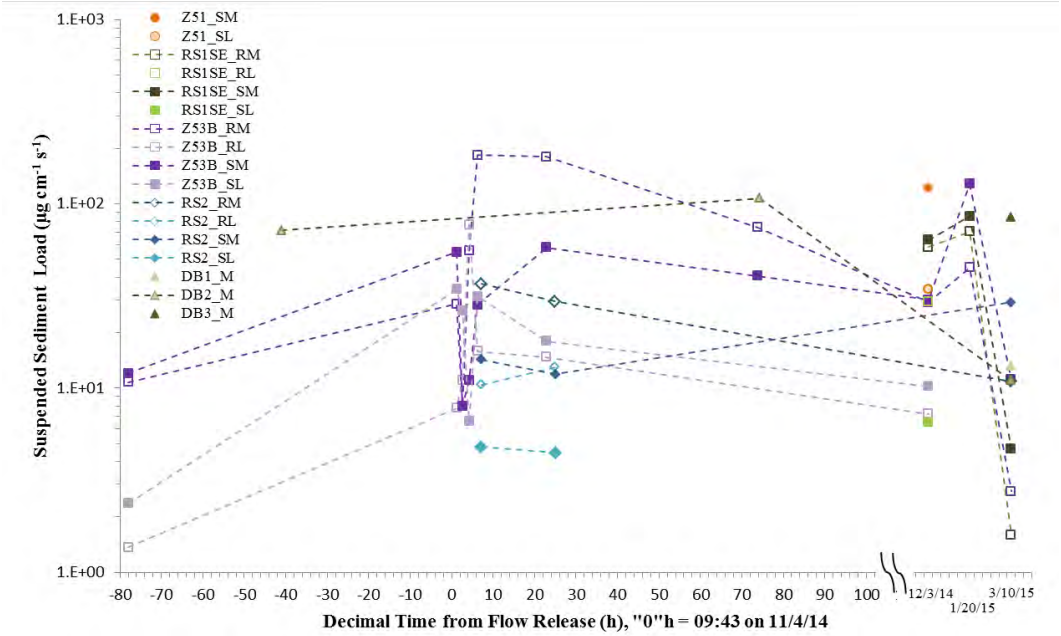

Figure D-70 Time series of suspended sediment load in each water column interval at sites Z51, RS1SE, Z53B, RS2, DB1, DB2 and DB3 during the November 4th, 2014 flow release.

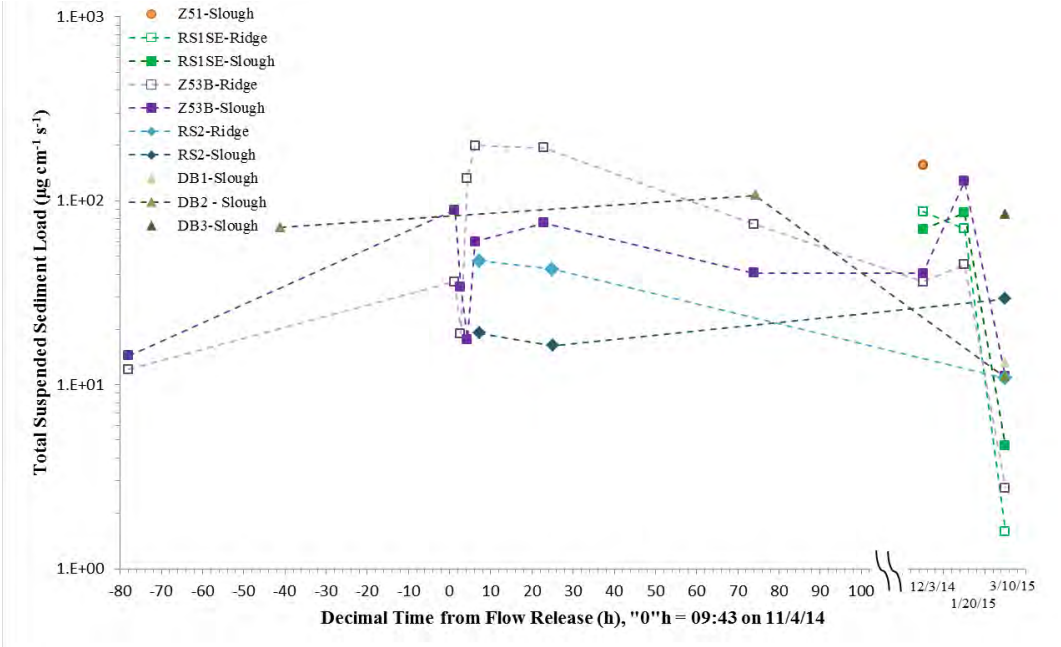

Figure D-71 Time series of total suspended sediment load sites Z51, RS1SE, Z53B, RS2, DB1, DB2 and DB3 during the November 4th, 2014 flow release.

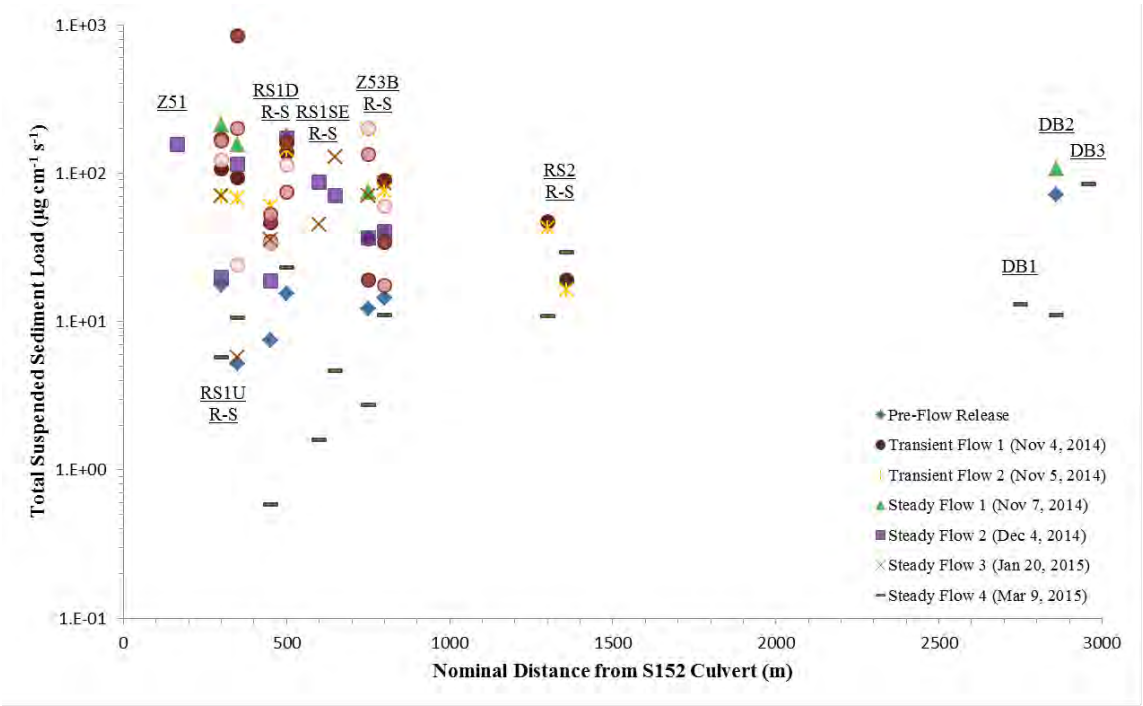

Figure D-72 Spatial distribution of total suspended sediment load at all sites during the November 4th, 2014 flow release. RS1U ridge and slough are geographically co-located, data have been separated for clarity. Symbol color intensity decreases with time for Transient Flow 1.

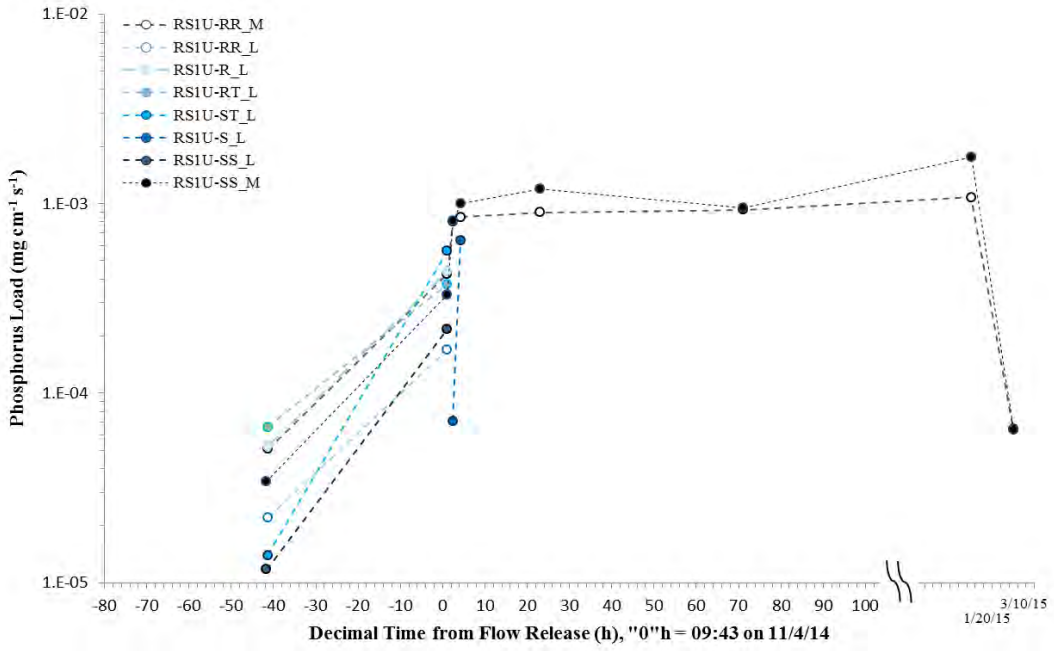

Figure D-73 Time series of phosphorus load in each water column interval at site RS1U during the November 4th, 2014 flow release.

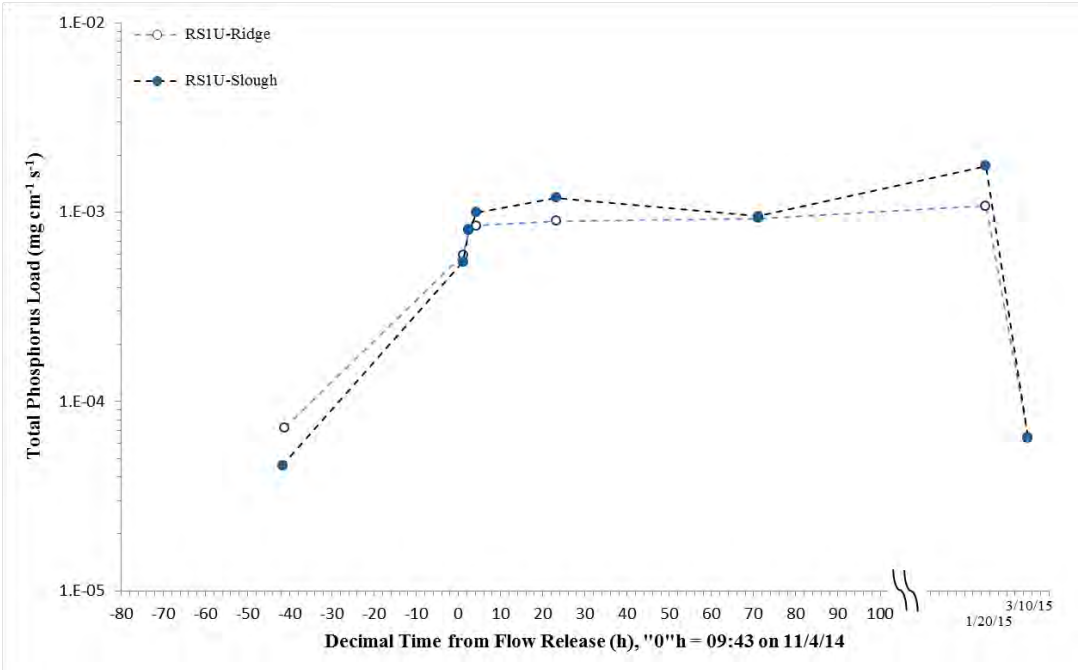

Figure D-74 Time series of total phosphorus load at site RS1U during the November 4th, 2014 flow release.

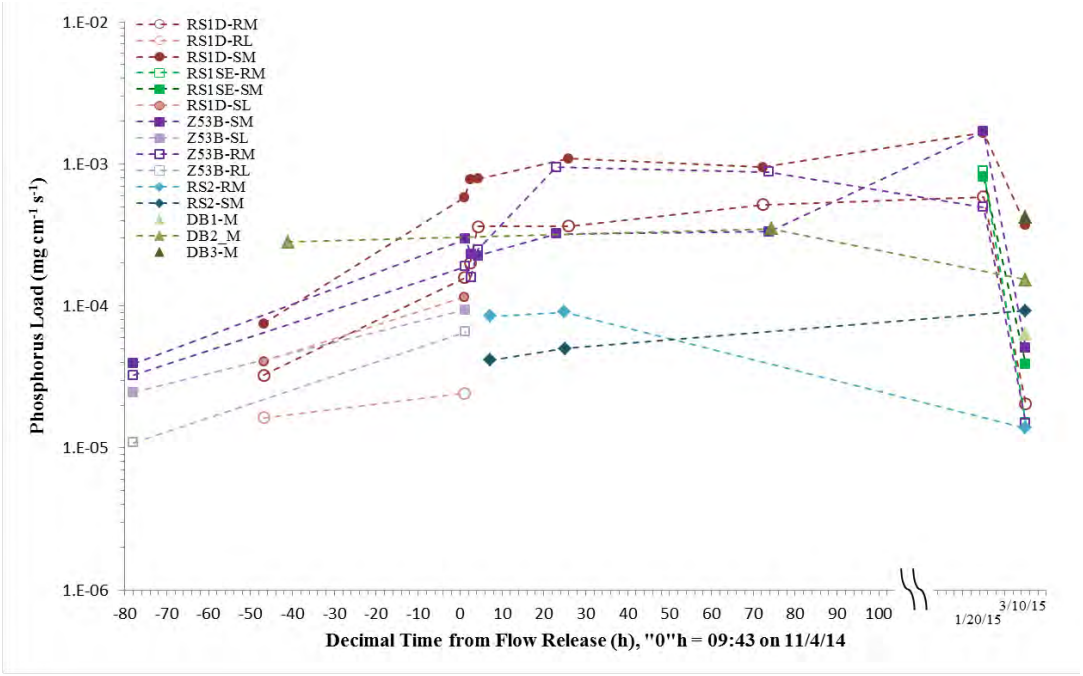

Figure D-75 Time series of phosphorus load in each water column interval at sites RS1D, RS1SE, DB2, RS2, and Z53B during the November 4th, 2014 flow release.

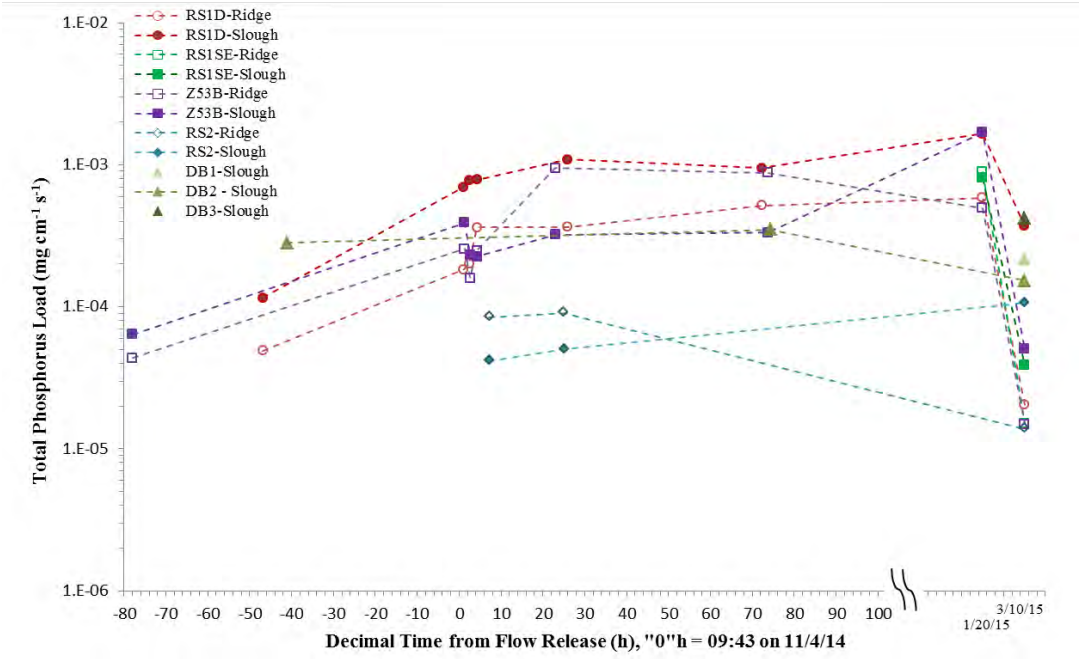

Figure D-76 Time series of total phosphorus load at sites RS1D, RS1SE, DB2, RS2, and Z53B during the November 4th, 2014 flow release.

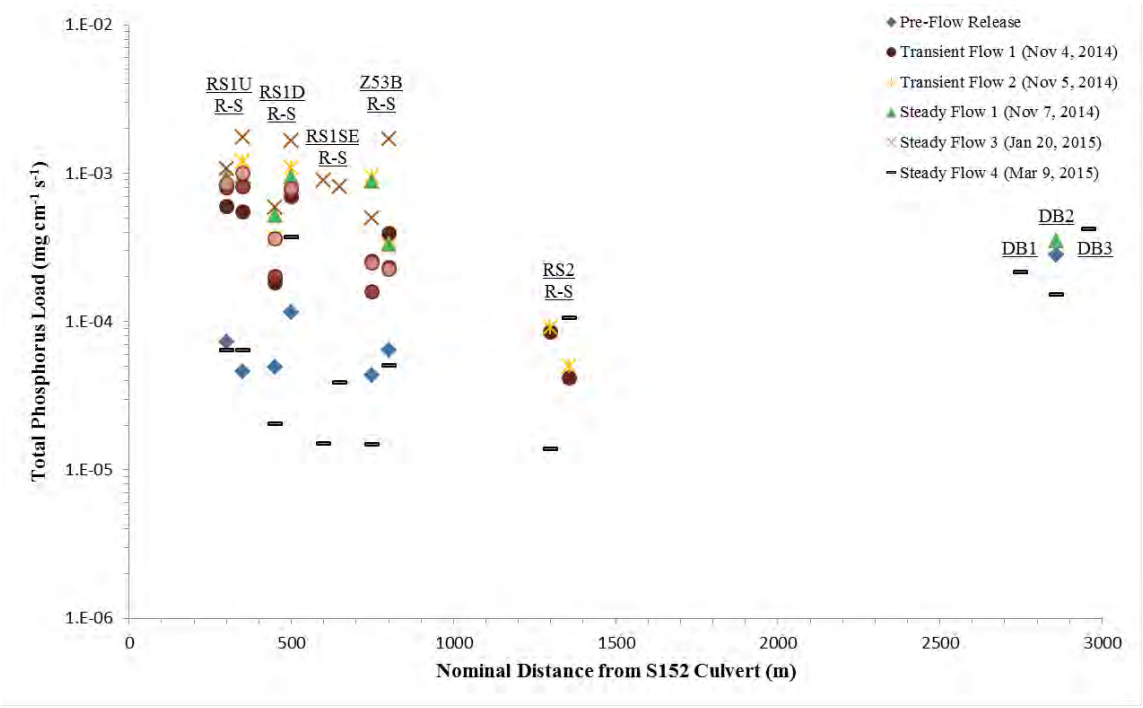

Figure D-77 Spatial distribution of total phosphorus load at all sites during the November 4th, 2014 flow release. RS1U ridge and slough are geographically co-located, data have been separated for clarity. Symbol color intensity decreases with time for Transient Flow 1.

Table D-2 Error analysis performed using duplicate samples taken March 9-10, 2015.

RS1U_RR-M	Mean (µg/L):	847.79
	Standard Deviation (µg/L):	49.49
	Coefficient of Variation (%):	5.84
RS1U_SS-M	Mean (µg/L):	1026.98
	Standard Deviation (µg/L):	32.89
	Coefficient of Variation (%):	3.20
UB2_SS-M	Mean (µg/L):	2789.51
	Standard Deviation (µg/L):	1243.41
	Coefficient of Variation (%):	44.57
DB2_SS-M	Mean (µg/L):	928.366
	Standard Deviation (µg/L):	64.67
	Coefficient of Variation (%):	6.97

2015 Suspended Sediment and Phosphorus

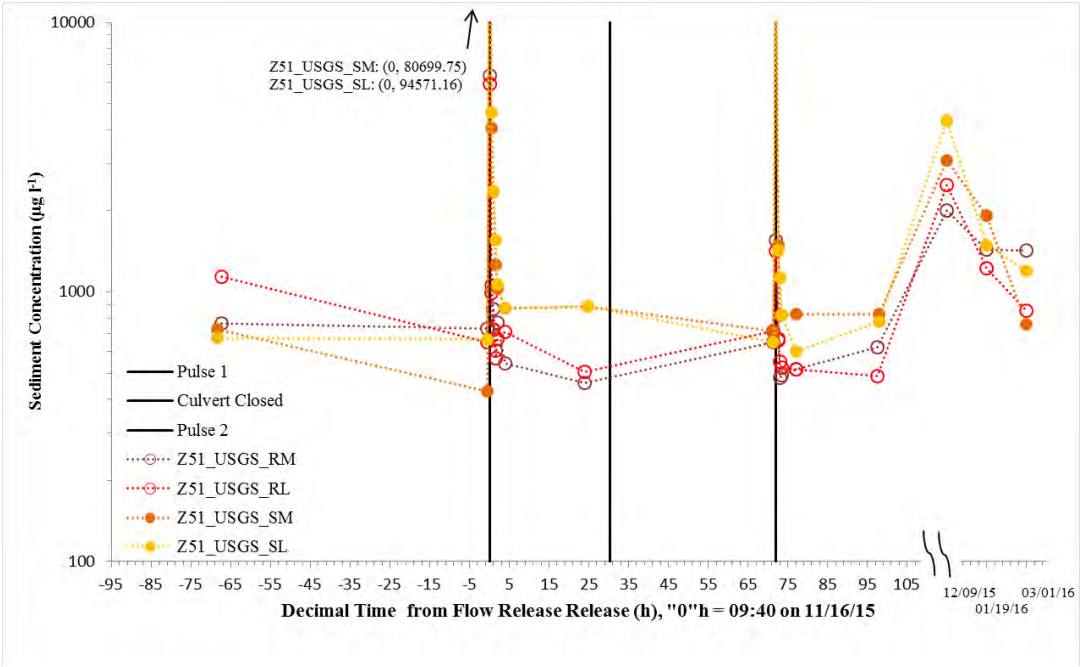

Figure D-78 Time series of suspended sediment concentration at site Z51_USGS during the November, 2015 flow release. The culvert was opened on November 16th (Pulse 1), closed on November 17th, and opened again November 19th (Pulse 2).

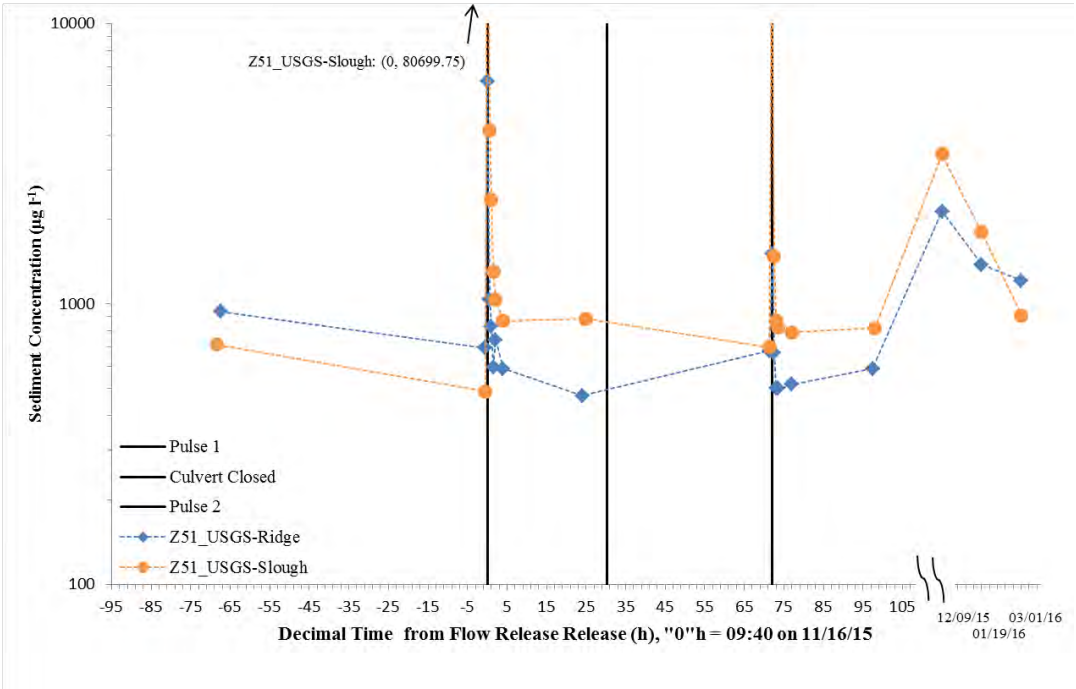

Figure D-79 Time series of depth-averaged suspended sediment concentration at site Z51_USGS during the November, 2015 flow release. The culvert was opened on November 16th (Pulse 1), closed on November 17th, and opened again November 19th (Pulse 2).

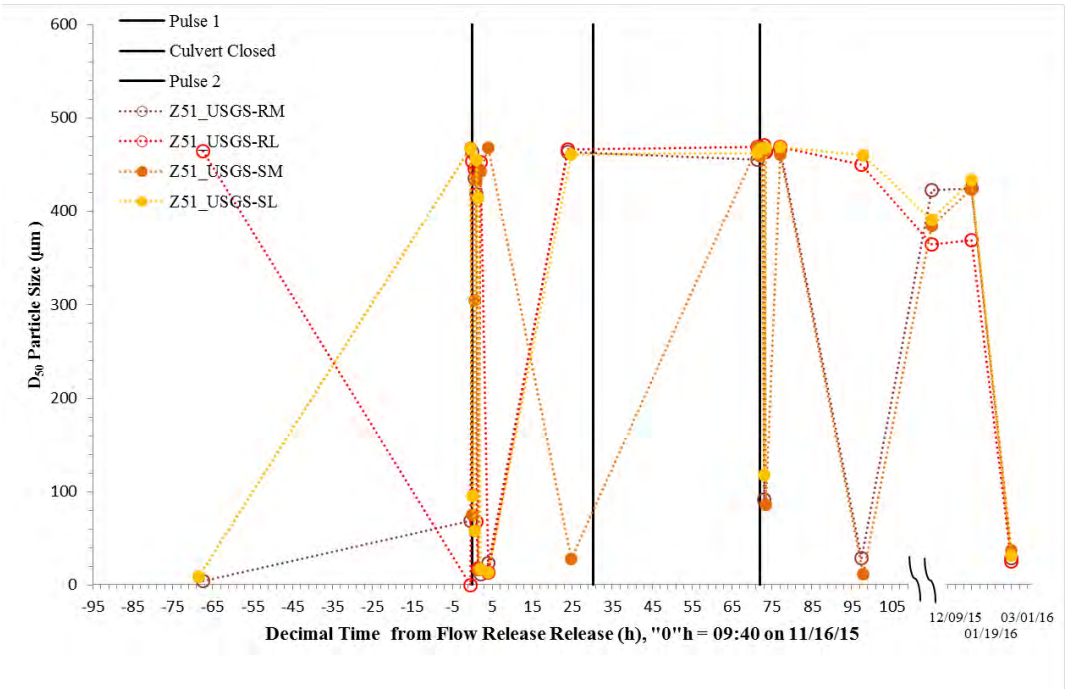

Figure D-80 Time series of D_{50} (median mass weighted size) of suspended particles at the site Z51_USGS during the November, 2015 flow release. The culvert was opened on November 16th (Pulse 1), closed on November 17th, and opened again November 19th (Pulse 2).

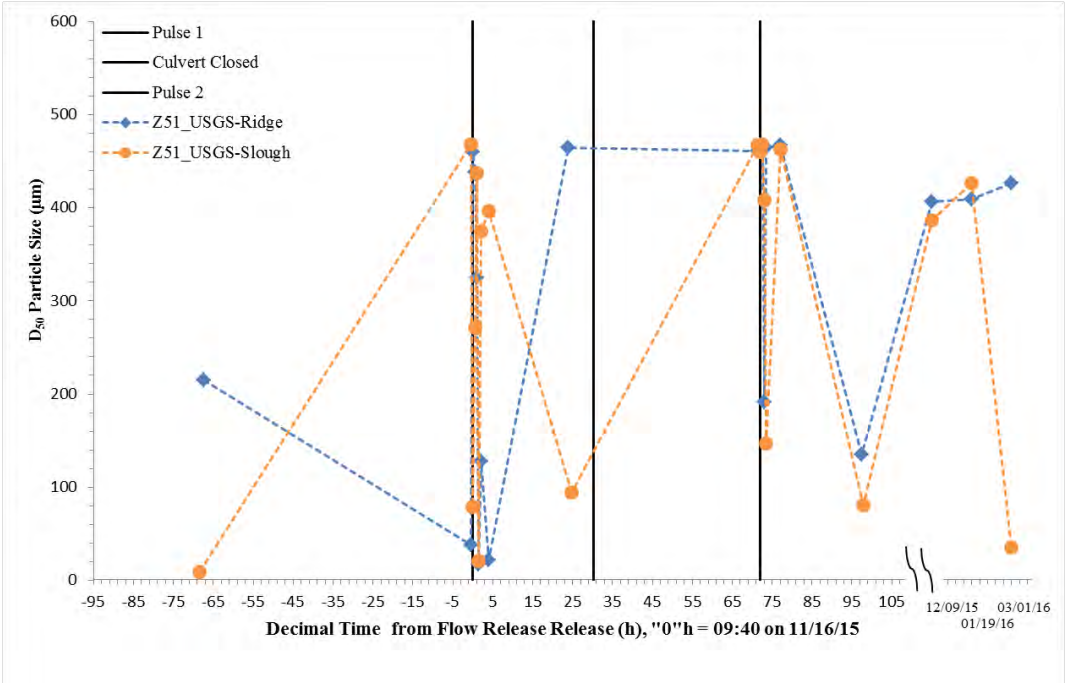

Figure D-81 Time series of depth-averaged D_{50} (median mass weighted size) of Z51_USGS during the November, 2015 flow release. The culvert was opened on November 16th (Pulse 1), closed on November 17th, and opened again November 19th (Pulse 2).

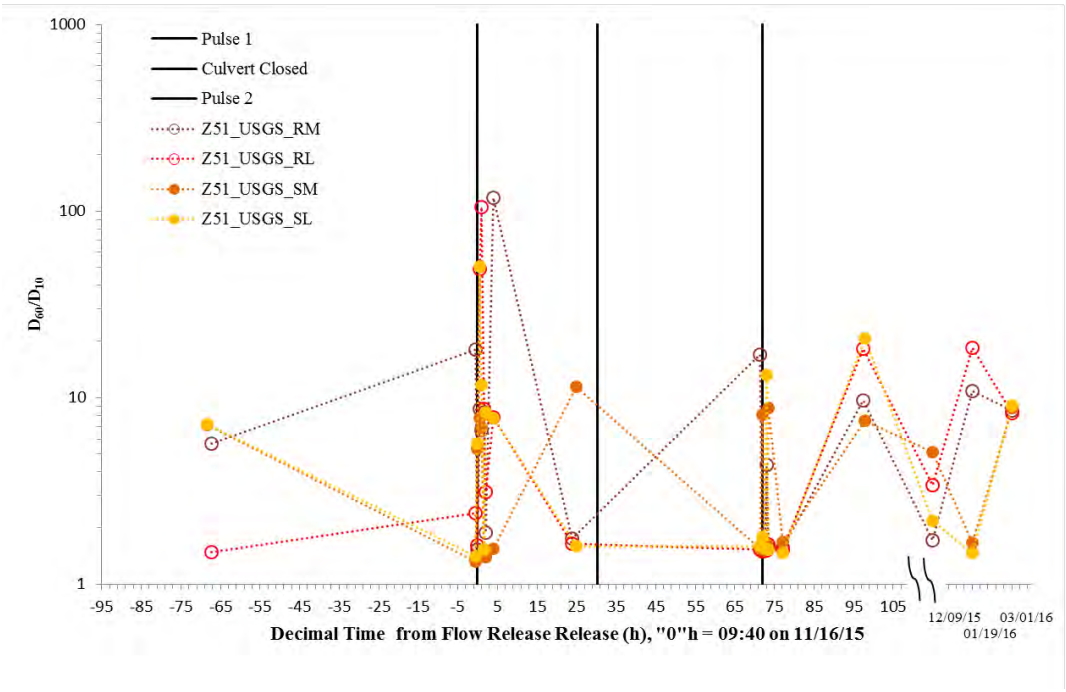

Figure D-82 Time series of D_{60}/D_{10} (particle size uniformity coefficient) of suspended particles at the site Z51_USGS during the November, 2015 flow release. The culvert was opened on November 16th (Pulse 1), closed on November 17th, and opened again November 19th (Pulse 2).

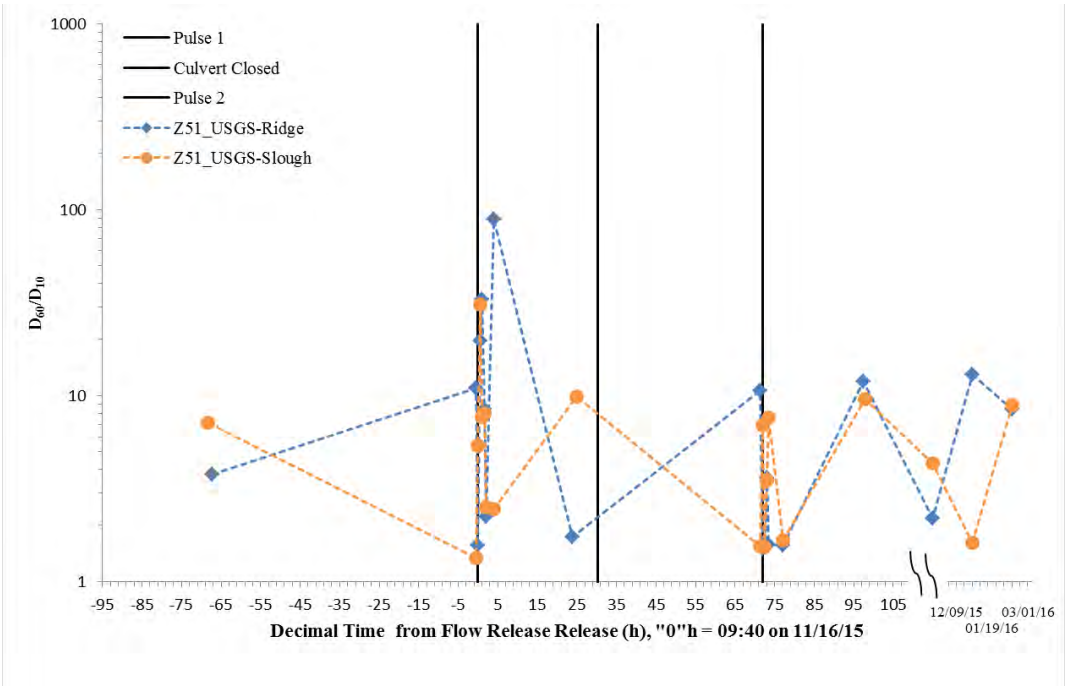

Figure D-83 Time series of depth-averaged D_{60}/D_{10} (particle size uniformity coefficient) of suspended particles at the site Z51_USGS during the November, 2015 flow release. The culvert was opened on November 16th (Pulse 1), closed on November 17th, and opened again November 19th (Pulse 2).

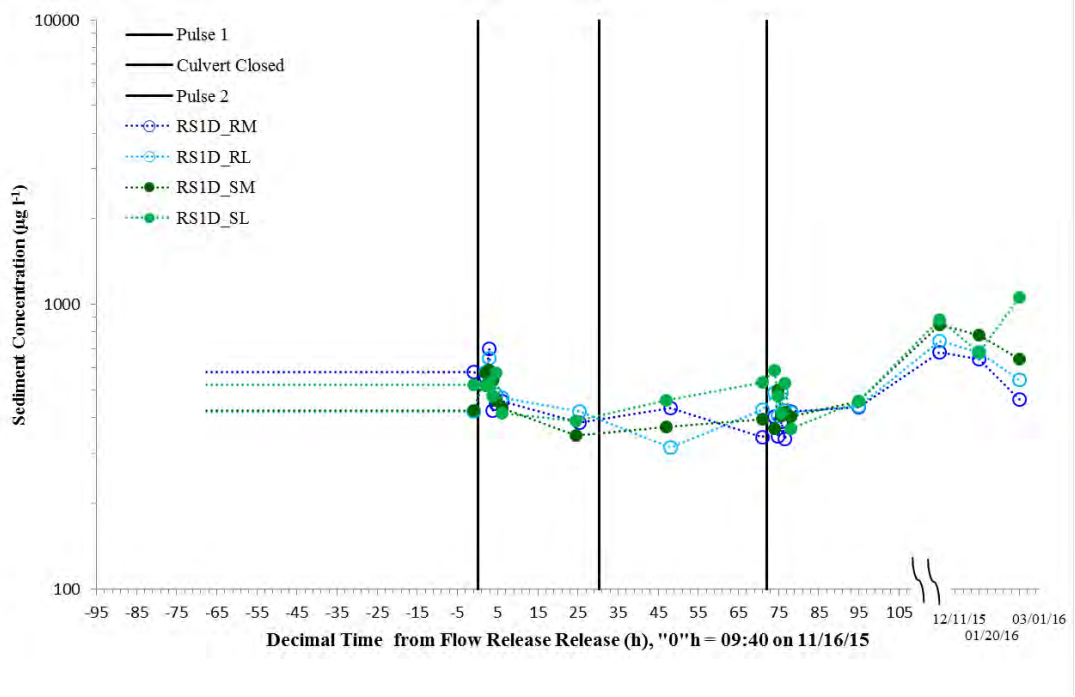

Figure D-84 Time series of suspended sediment concentration at site RS1D during the November, 2015 flow release. The culvert was opened on November 16th (Pulse 1), closed on November 17th, and opened again November 19th (Pulse 2).

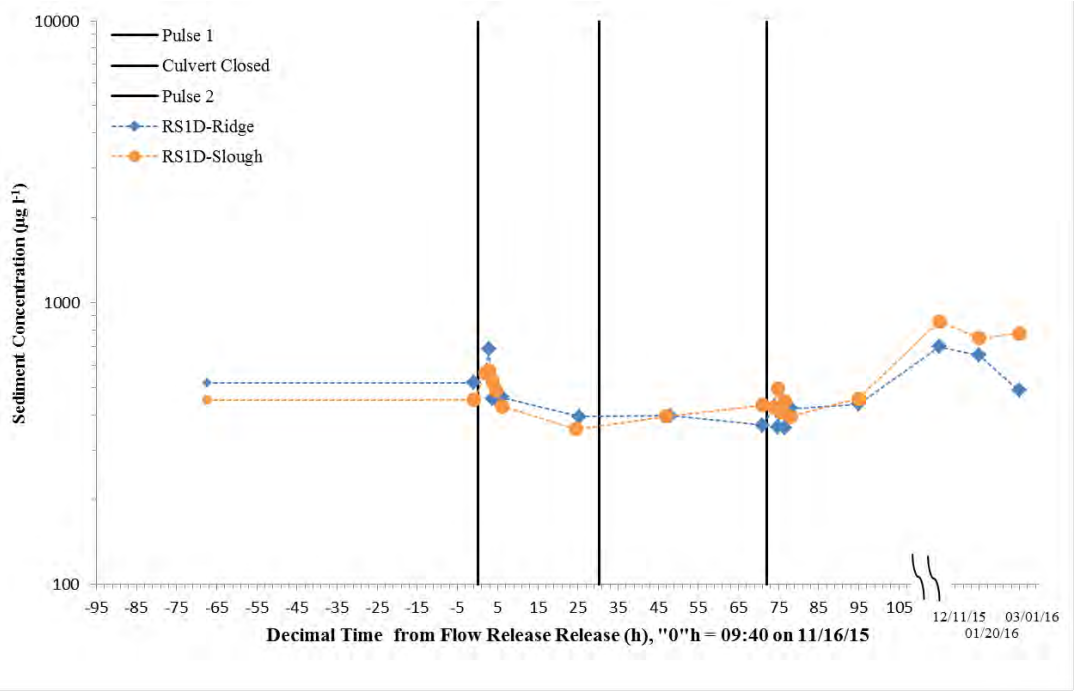

Figure D-85 Time series of depth-averaged suspended sediment concentration at site RS1D during the November, 2015 flow release. The culvert was opened on November 16th (Pulse 1), closed on November 17th, and opened again November 19th (Pulse 2).

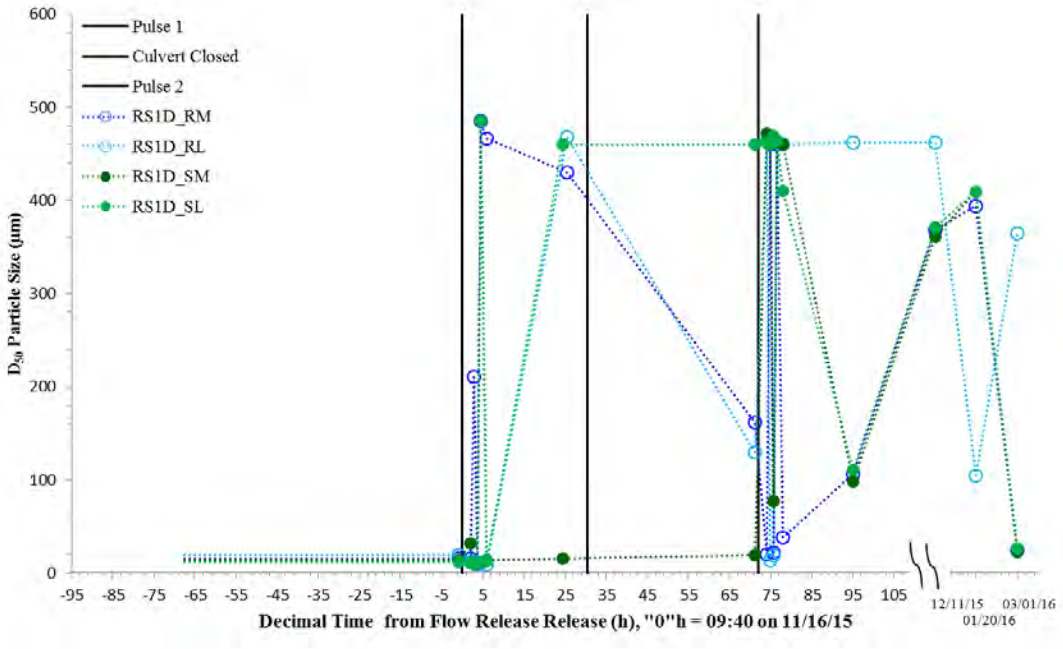

Figure D-86 Time series of D_{50} (median mass weighted size) of suspended particles at the site RS1D during the November, 2015 flow release. The culvert was opened on November 16th (Pulse 1), closed on November 17th, and opened again November 19th (Pulse 2).

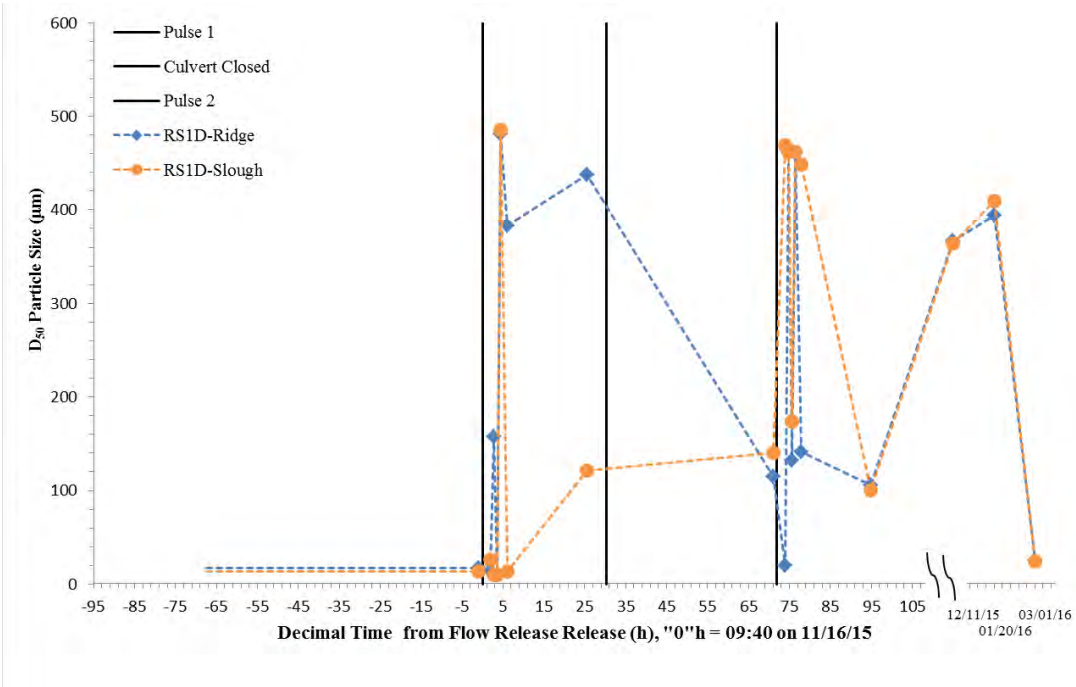

Figure D-87 Time series of depth-averaged D_{50} (median mass weighted size) of suspended particles at the site RS1D during the November, 2015 flow release. The culvert was opened on November 16th (Pulse 1), closed on November 17th, and opened again November 19th (Pulse 2).

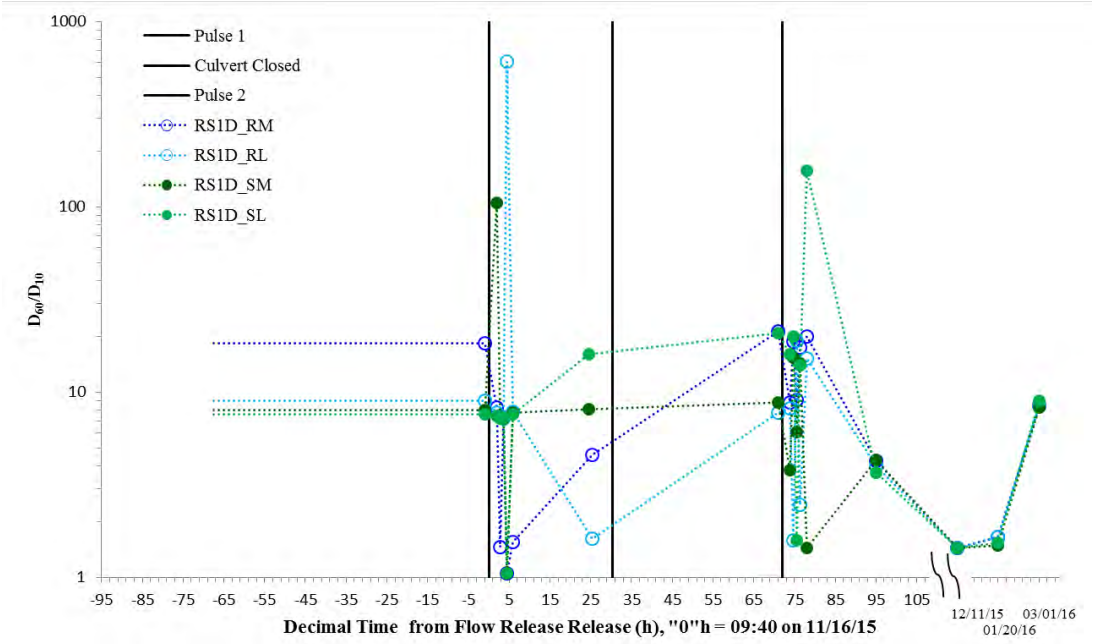

Figure D-88 Time series of D_{60}/D_{10} (particle size uniformity coefficient) of suspended particles at the site RS1D during the November, 2015 flow release. The culvert was opened on November 16th (Pulse 1), closed on November 17th, and opened again November 19th (Pulse 2).

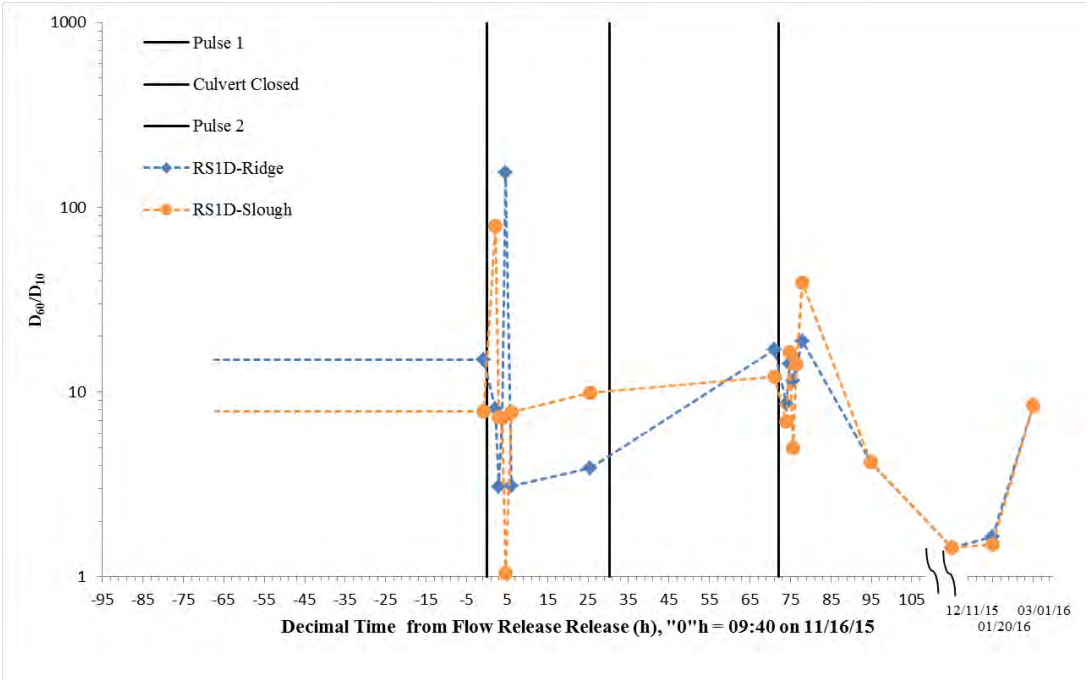

Figure D-89 Time series of depth-averaged D_{60}/D_{10} (particle size uniformity coefficient) of suspended particles at the site RS1D during the November, 2015 flow release. The culvert was opened on November 16th (Pulse 1), closed on November 17th, and opened again November 19th (Pulse 2).

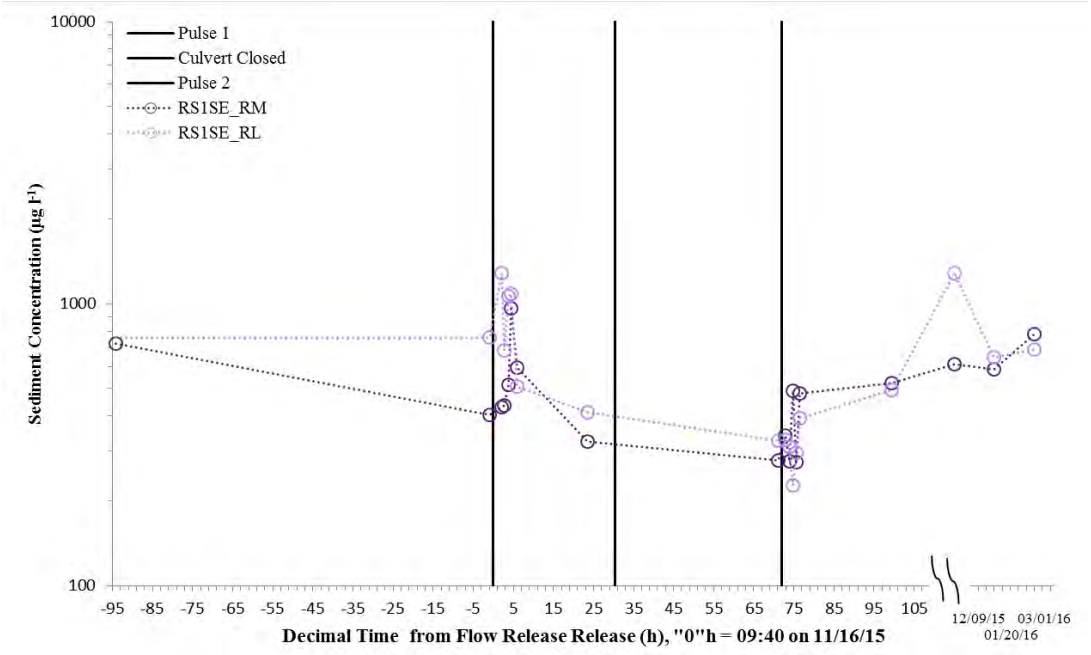

Figure D-90 Time series of suspended sediment concentration at site RS1SE during the November, 2015 flow release. The culvert was opened on November 16th (Pulse 1), closed on November 17th, and opened again November 19th (Pulse 2).

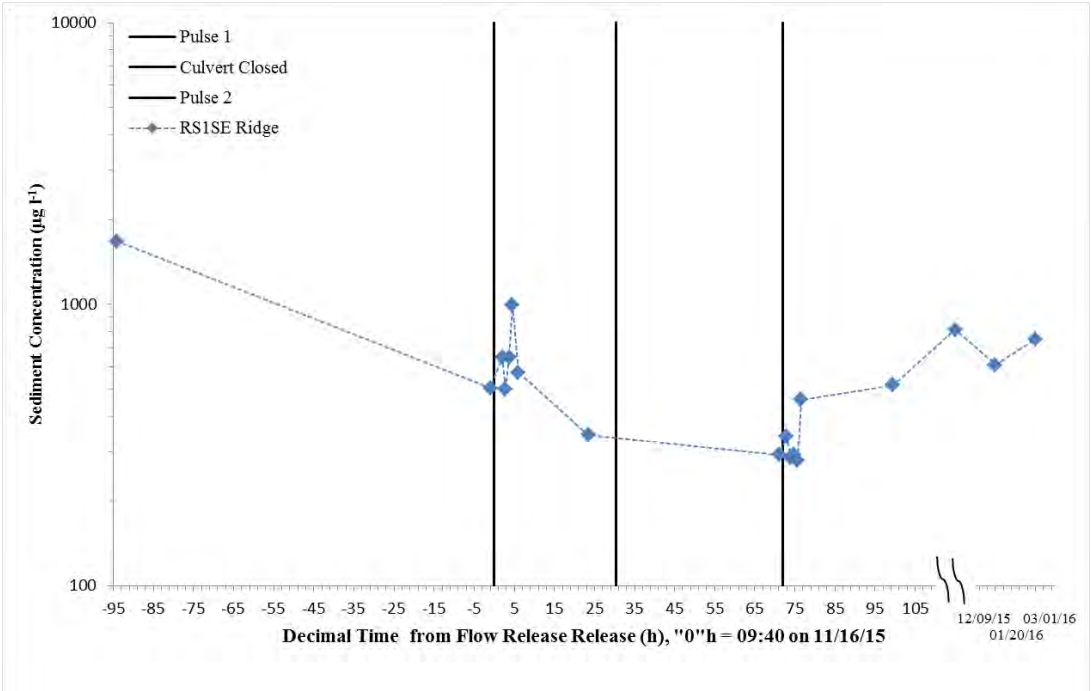

Figure D-91 Time series of depth-averaged suspended sediment concentration at site RS1SE during the November, 2015 flow release. The culvert was opened on November 16th (Pulse 1), closed on November 17th, and opened again November 19th (Pulse 2).

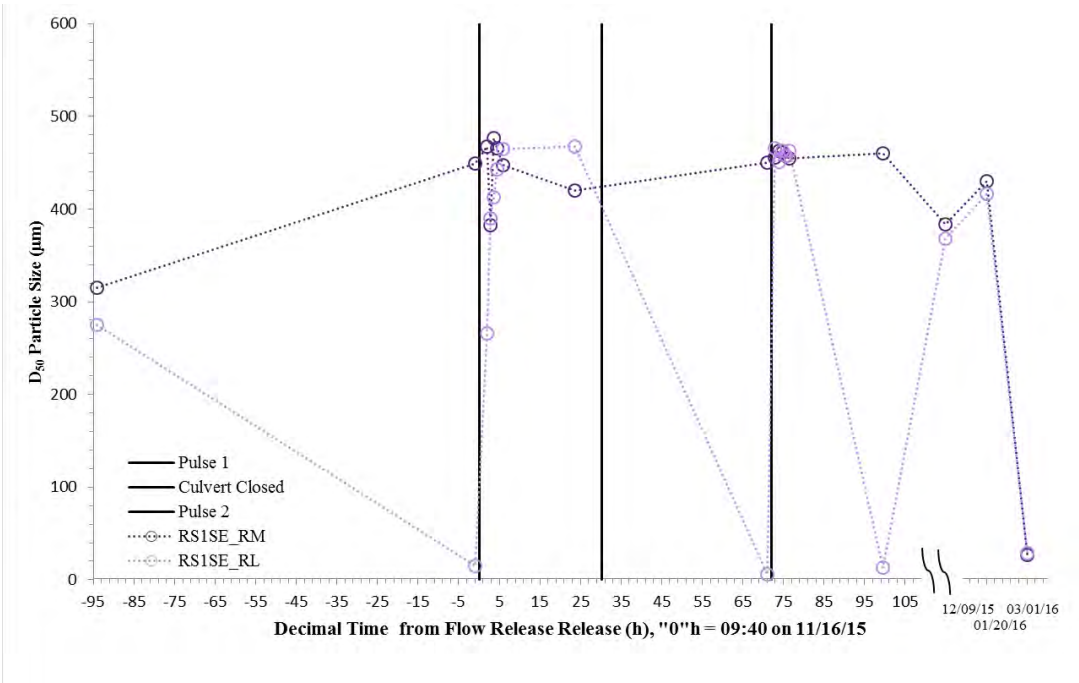

Figure D-92 Time series of D_{50} (median mass weighted size) of suspended particles at the site RS1SE during the November, 2015 flow release. The culvert was opened on November 16th (Pulse 1), closed on November 17th, and opened again November 19th (Pulse 2).

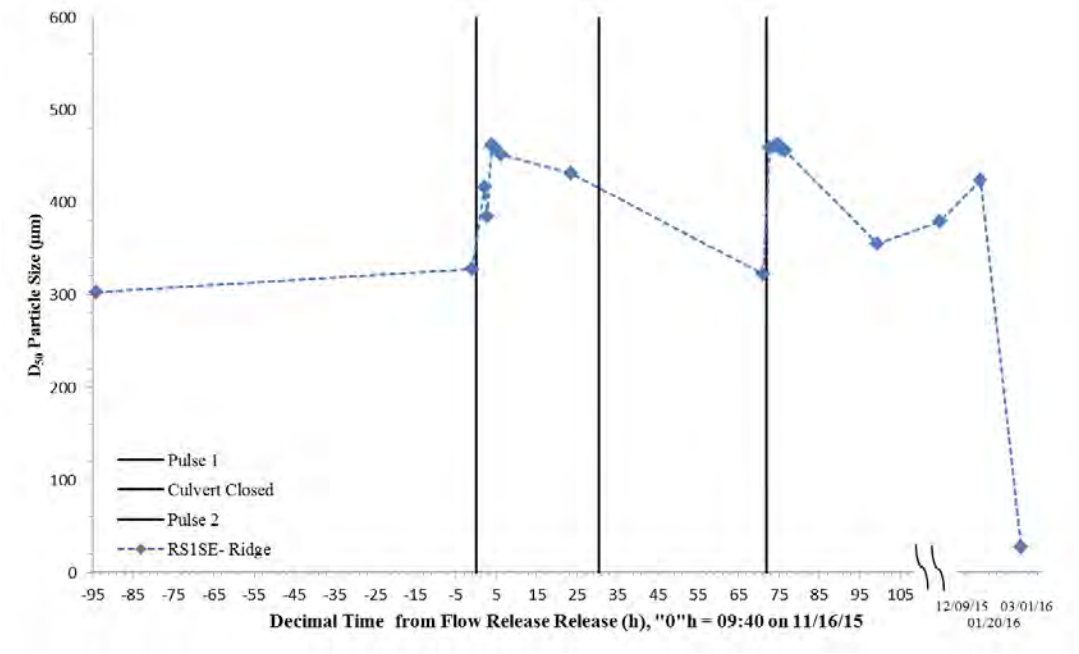

Figure D-93 Time series of depth-averaged D_{50} (median mass weighted size) of suspended particles at the site RS1SE during the November, 2015 flow release. The culvert was opened on November 16th (Pulse 1), closed on November 17th, and opened again November 19th (Pulse 2).

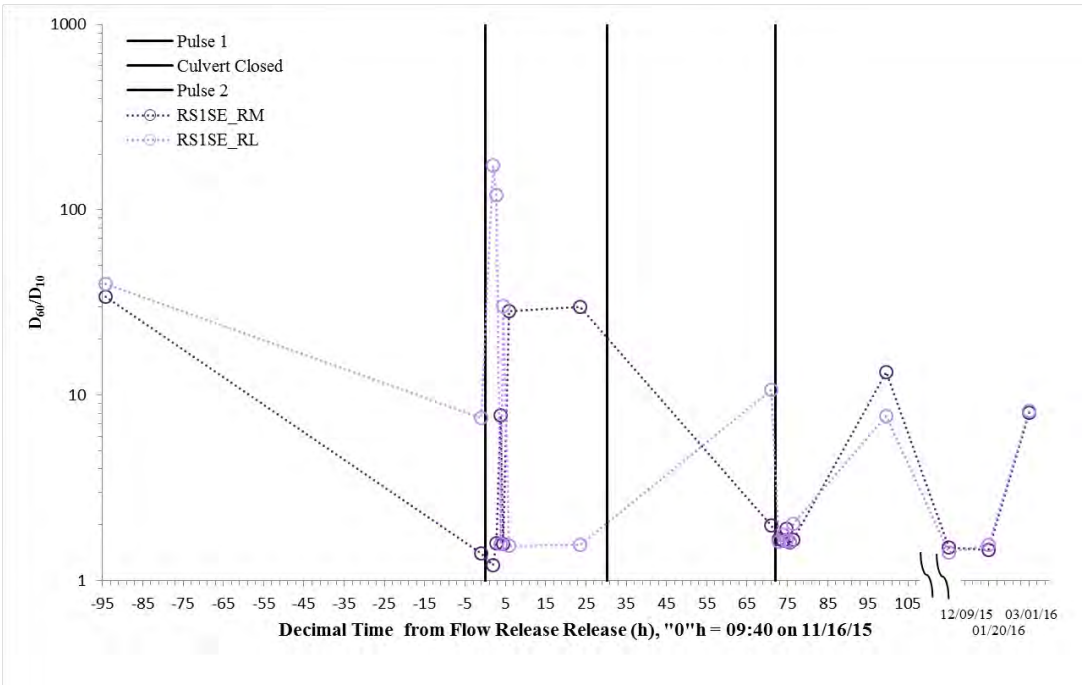

Figure D-94 Time series of D_{60}/D_{10} (particle size uniformity coefficient) of suspended particles at the site RS1SE during the November, 2015 flow release. The culvert was opened on November 16th (Pulse 1), closed on November 17th, and opened again November 19th (Pulse 2).

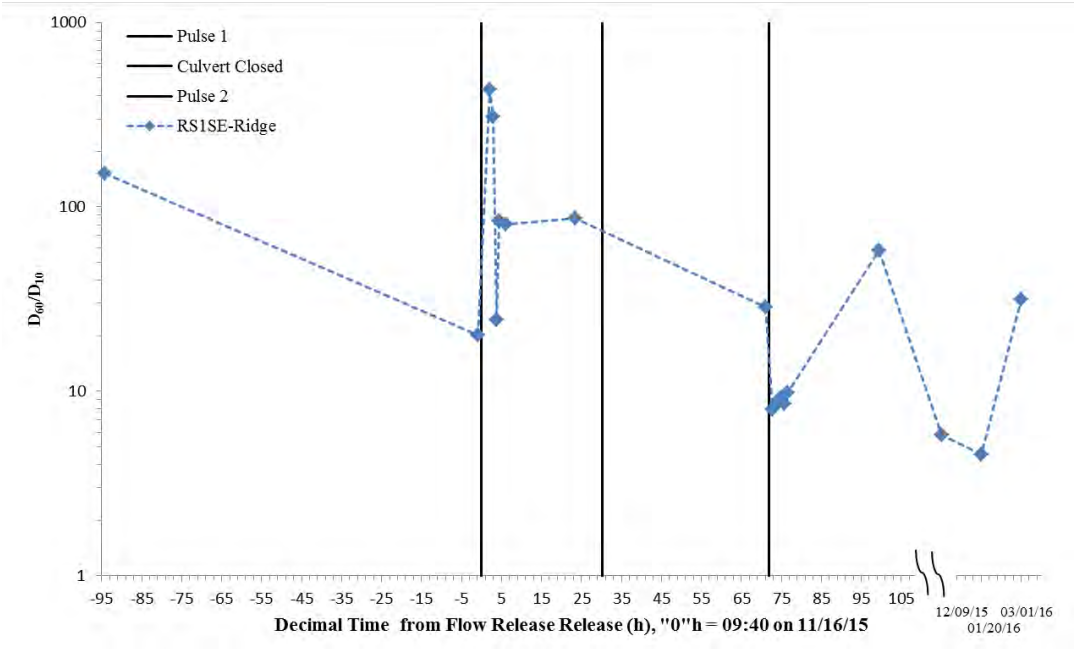

Figure D-95 Time series of depth-averaged D_{60}/D_{10} (particle size uniformity coefficient) of suspended particles at the site RS1SE during the November, 2015 flow release. The culvert was opened on November 16th (Pulse 1), closed on November 17th, and opened again November 19th (Pulse 2).

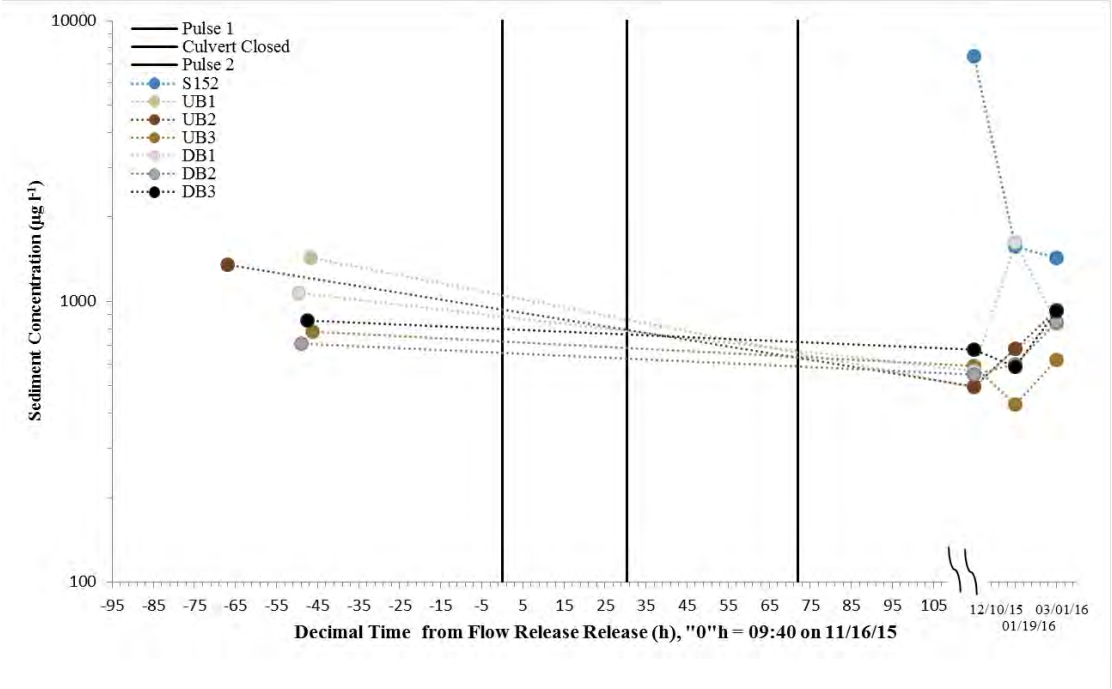

Figure D-96 Time series of suspended sediment concentration at sites UB1, UB2, UB3, DB1, DB2, DB3 and S152 during the November, 2015 flow release. The culvert was opened on November 16th (Pulse 1), closed on November 17th, and opened again November 19th (Pulse 2).

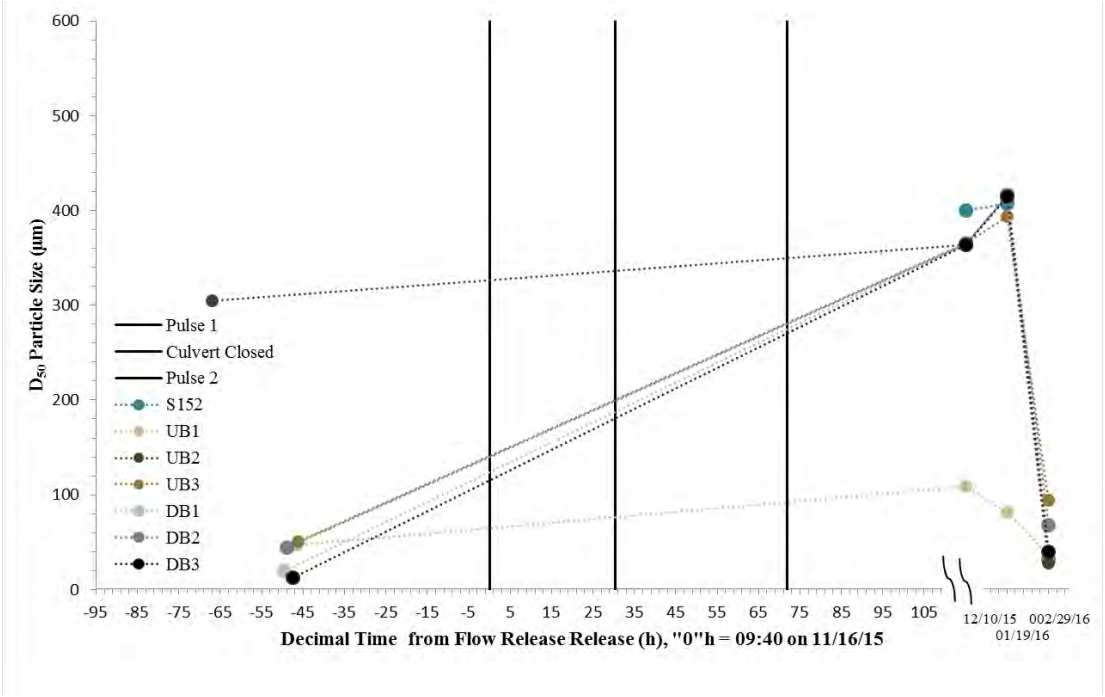

Figure D-97 Time series of D_{50} (median mass weighted size) of suspended particles at the sites UB1, UB2, UB3, DB1, DB2, DB3 and S152 during the November, 2015 flow release. The culvert was opened on November 16th (Pulse 1), closed on November 17th, and opened again November 19th (Pulse 2).

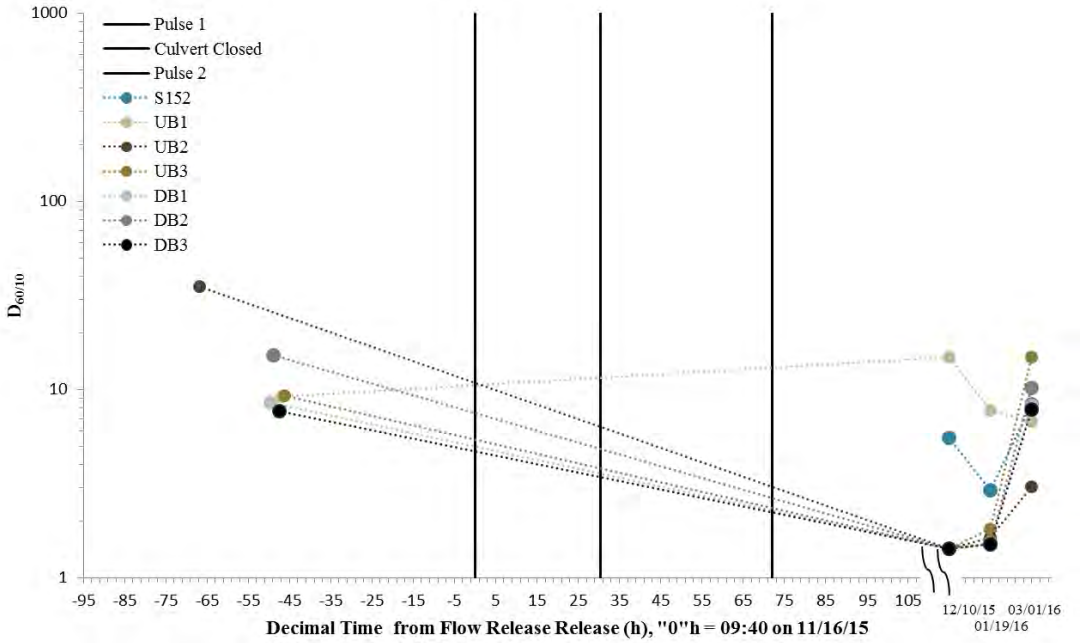

Figure D-98 Time series of D_{60}/D_{10} (particle size uniformity coefficient) of suspended particles at the sites UB1, UB2, UB3, DB1, DB2, DB3 and S152 during the November, 2015 flow release. The culvert was opened on November 16th (Pulse 1), closed on November 17th, and opened again November 19th (Pulse 2).

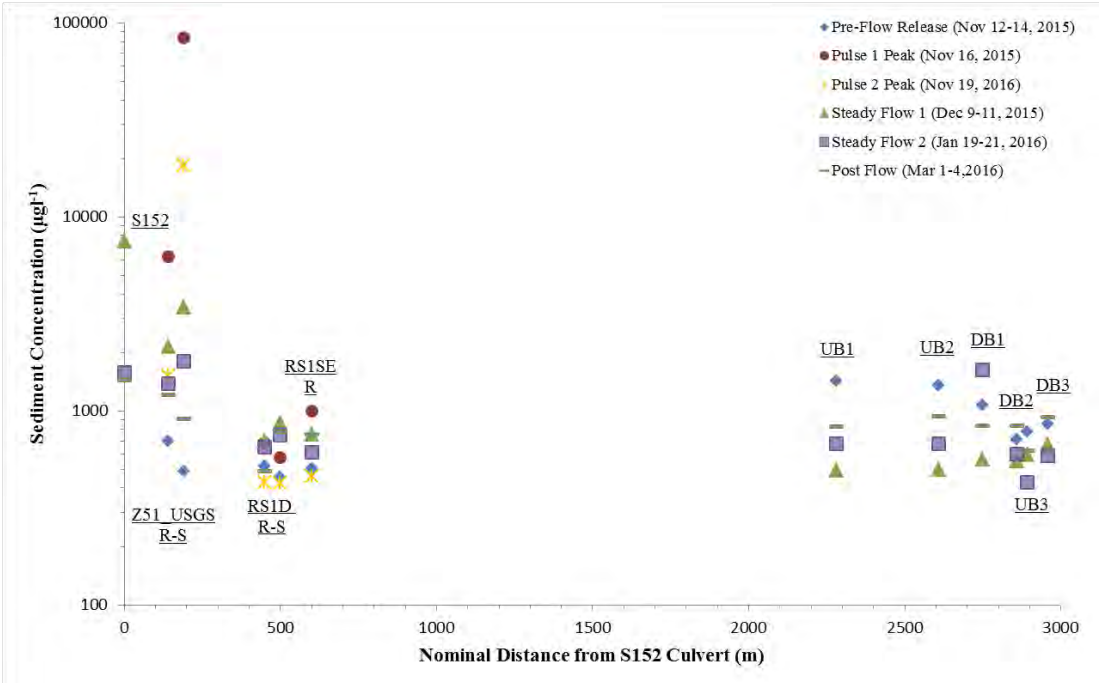

Figure D-99 Spatial distribution of depth-averaged suspended sediment concentration at all sites during the November, 2015 flow release. The culvert was opened on November 16th (Pulse 1), closed on November 17th, and opened again November 19th (Pulse 2).

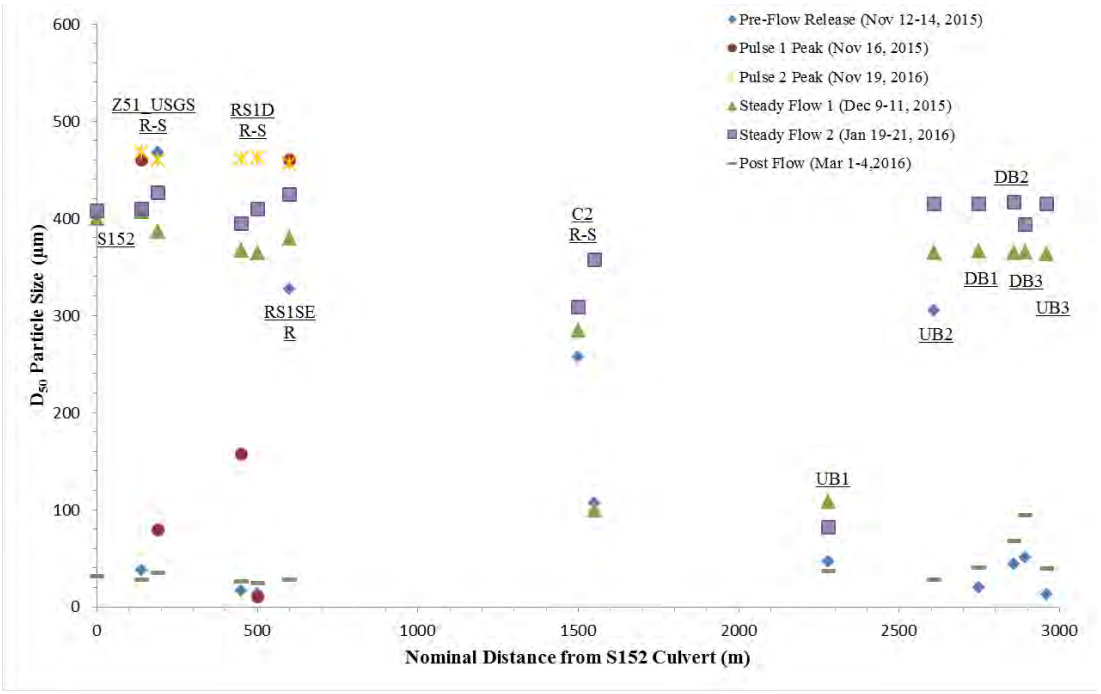

Figure D-100 Spatial distribution of depth-averaged D_{50} (median mass weighted size) of suspended particles at all sites during the November, 2015 flow release. The culvert was opened on November 16th (Pulse 1), closed on November 17th, and opened again November 19th (Pulse 2).

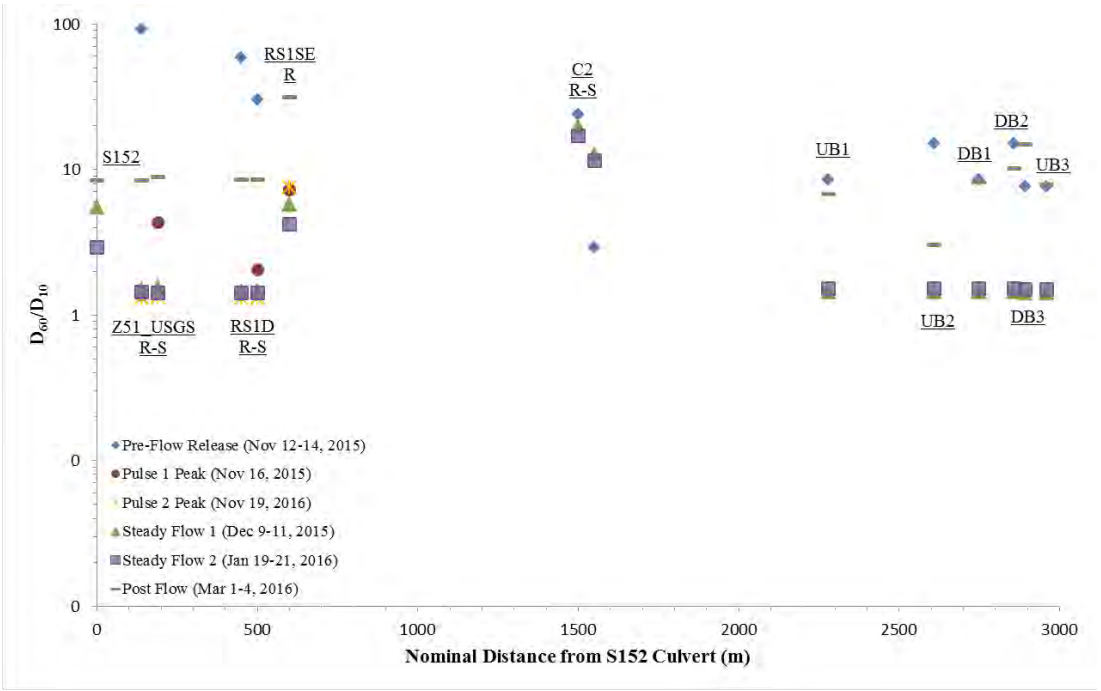

Figure D-101 Spatial distribution of depth-averaged D_{60}/D_{10} (particle size uniformity coefficient) of suspended sediment at all sites during the November, 2015 flow release. The culvert was opened on November 16th (Pulse 1), closed on November 17th, and opened again November 19th (Pulse 2).

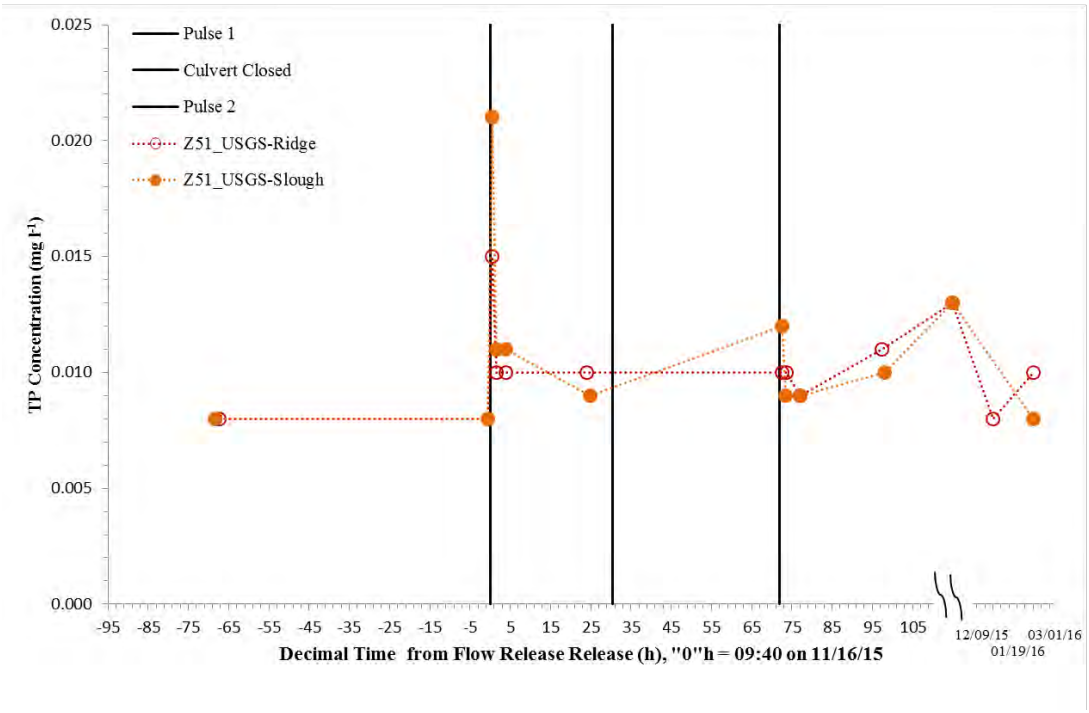

Figure D-102 Time series of total phosphorus concentration at site Z51USGS during the November, 2015 flow release. The culvert was opened on November 16th (Pulse 1), closed on November 17th, and opened again November 19th (Pulse 2).

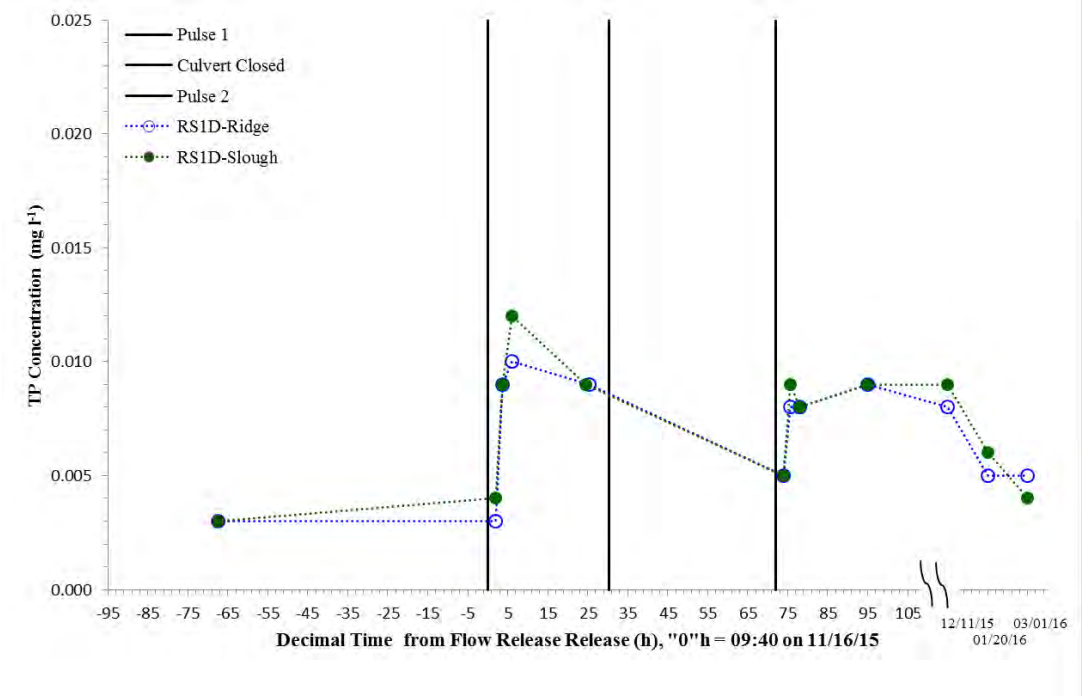

Figure D-103 Time series of total phosphorus concentration at site RS1D during the November, 2015 flow release. The culvert was opened on November 16th (Pulse 1), closed on November 17th, and opened again November 19th (Pulse 2).

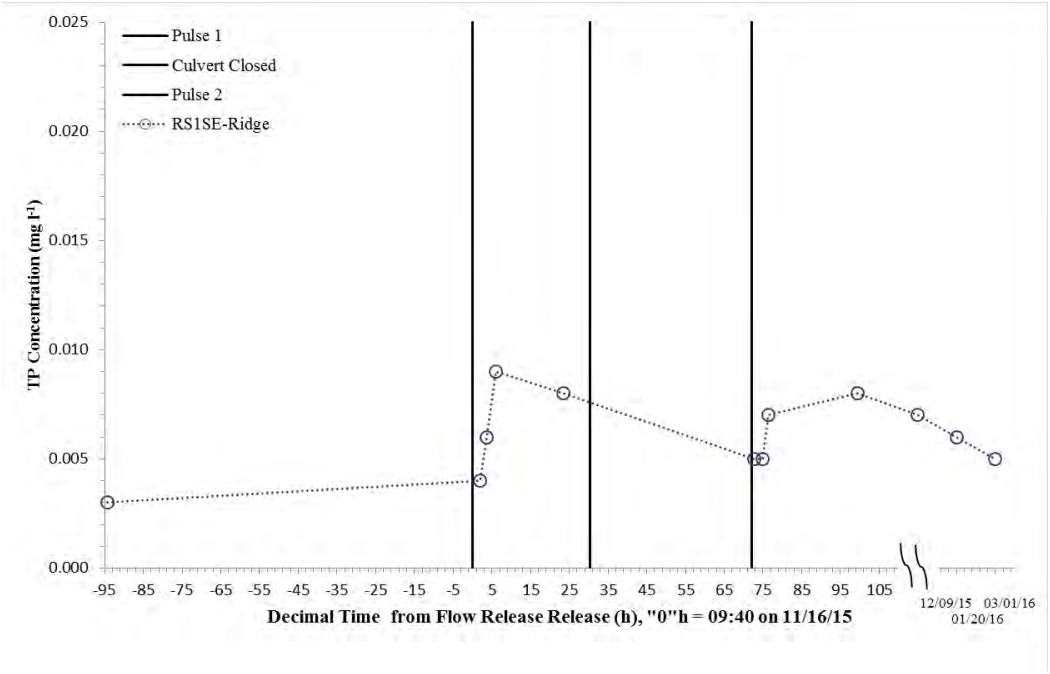

Figure D-104 Time series of total phosphorus concentration at site RS1SE during the November, 2015 flow release. The culvert was opened on November 16th (Pulse 1), closed on November 17th, and opened again November 19th (Pulse 2).

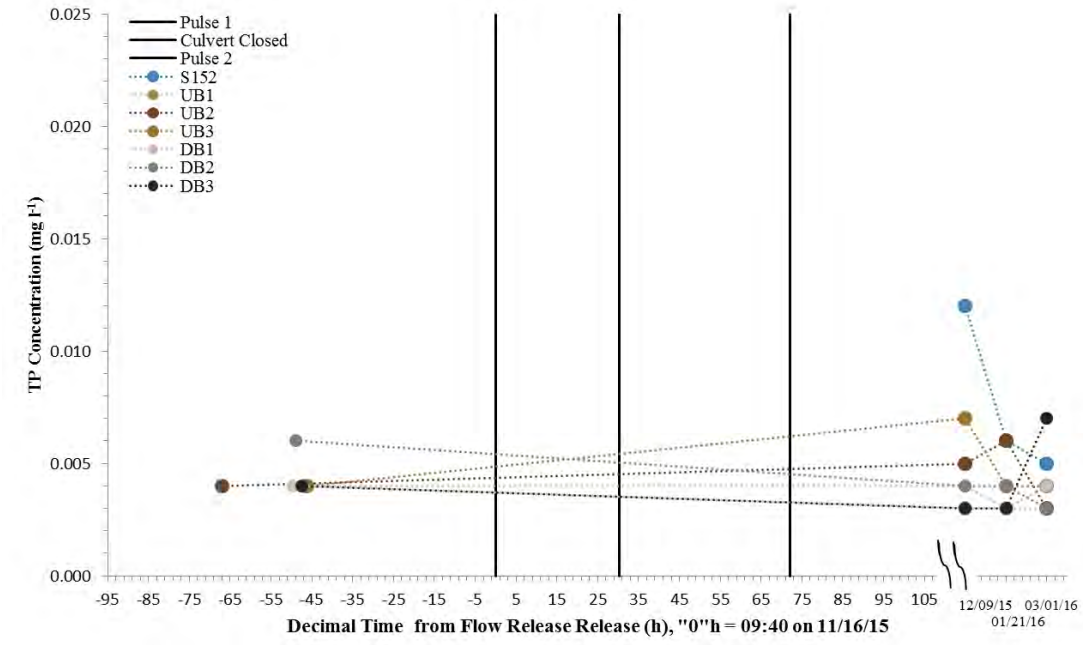

Figure D-105 Time series of total phosphorus concentration at sites UB1, UB2, UB3, DB1, DB2, DB3 and S152 during the November, 2015 flow release. The culvert was opened on November 16th (Pulse 1), closed on November 17th, and opened again November 19th (Pulse 2).

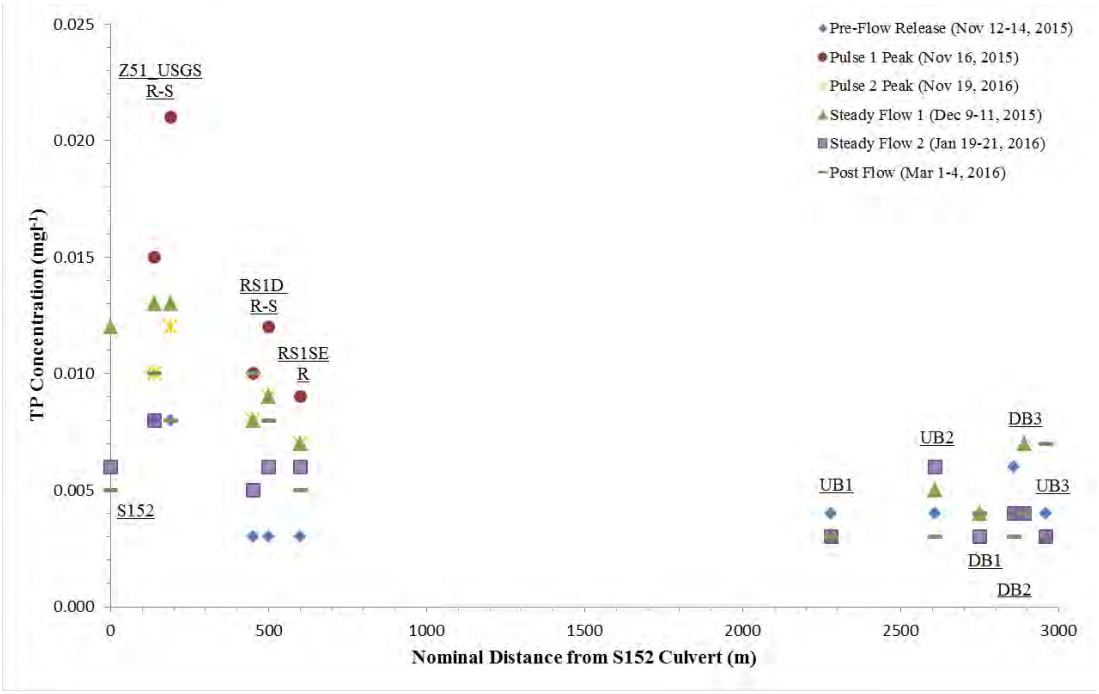

Figure D-106 Spatial distribution of depth-averaged phosphorus concentration at all sites during the November, 2015 flow release. The culvert was opened on November 16th (Pulse 1), closed on November 17th, and opened again November 19th (Pulse 2).

2015 Load

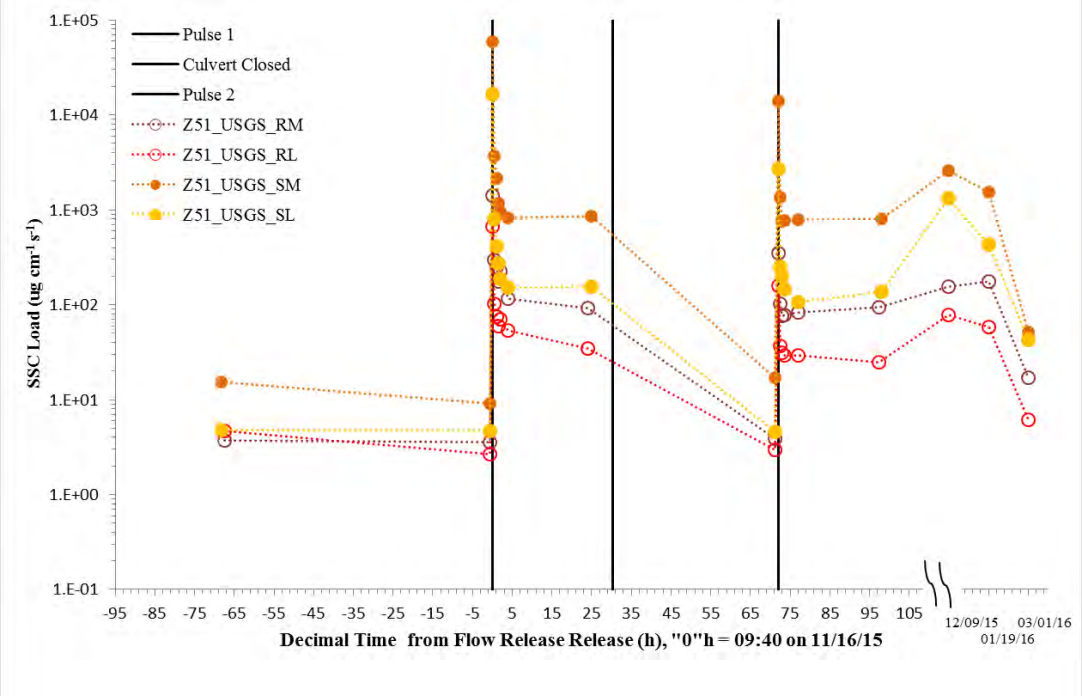

Figure D-107 Time series of suspended sediment load in each water column interval at site Z51_USGS during the November, 2015 flow release. The culvert was opened on November 16th (Pulse 1), closed on November 17th, and opened again November 19th (Pulse 2).

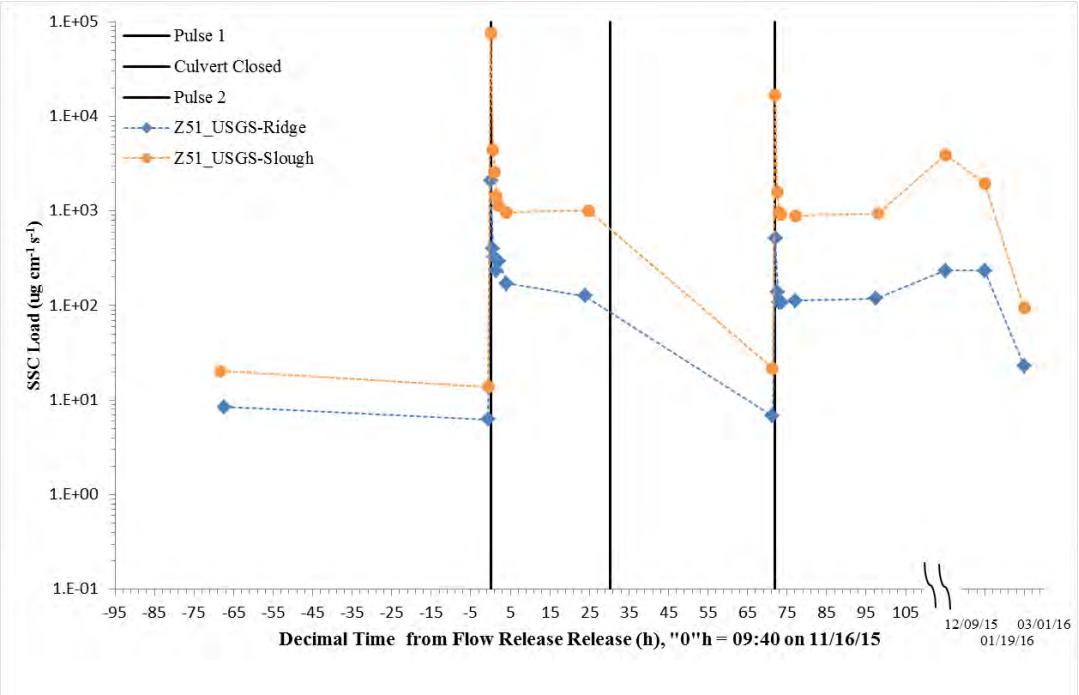

Figure D-108 Time series of total suspended sediment load at site Z51_USGS during the November, 2015 flow release. The culvert was opened on November 16th (Pulse 1), closed on November 17th, and opened again November 19th (Pulse 2).

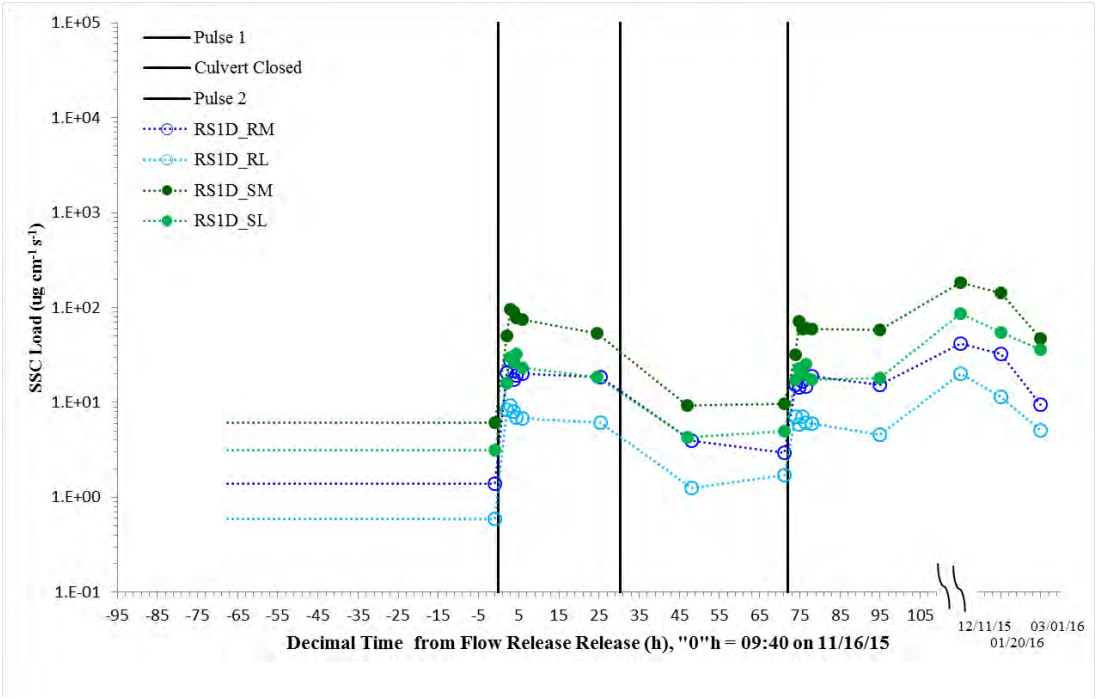

Figure D-109 Time series of suspended sediment load in each water column interval at site RS1D during the November, 2015 flow release. The culvert was opened on November 16th (Pulse 1), closed on November 17th, and opened again November 19th (Pulse 2).

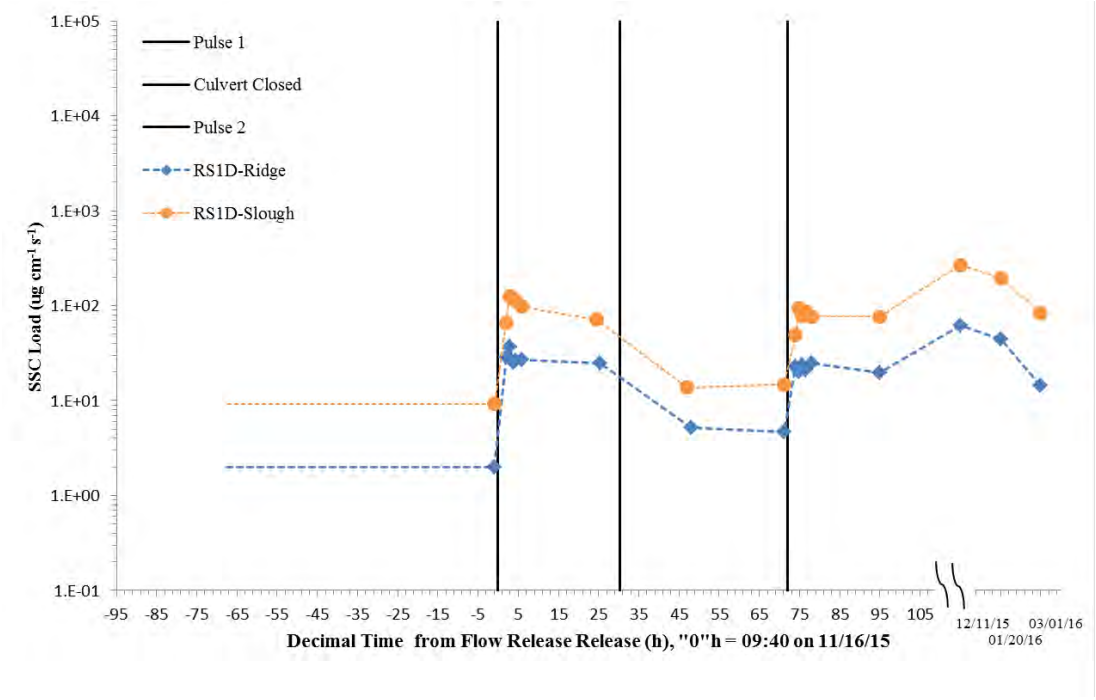

Figure D-110 Time series of total suspended sediment load at site RS1D during the November, 2015 flow release. The culvert was opened on November 16th (Pulse 1), closed on November 17th, and opened again November 19th (Pulse 2).

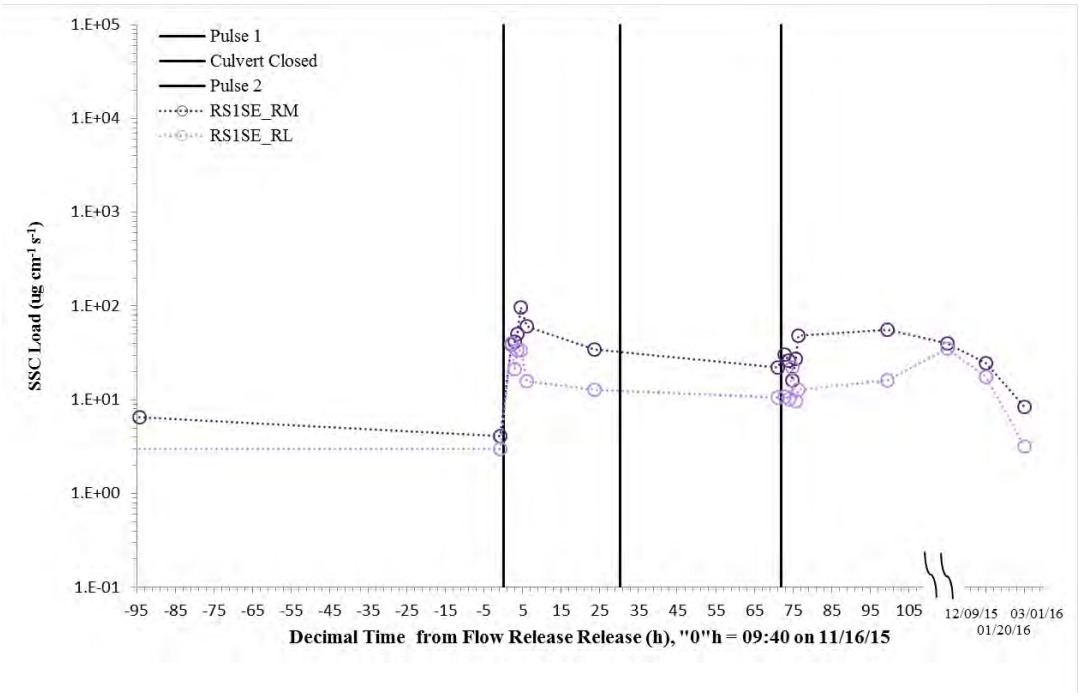

Figure D-111 Time series of suspended sediment load in each water column interval at site RS1SE during the November, 2015 flow release. The culvert was opened on November 16th (Pulse 1), closed on November 17th, and opened again November 19th (Pulse 2).

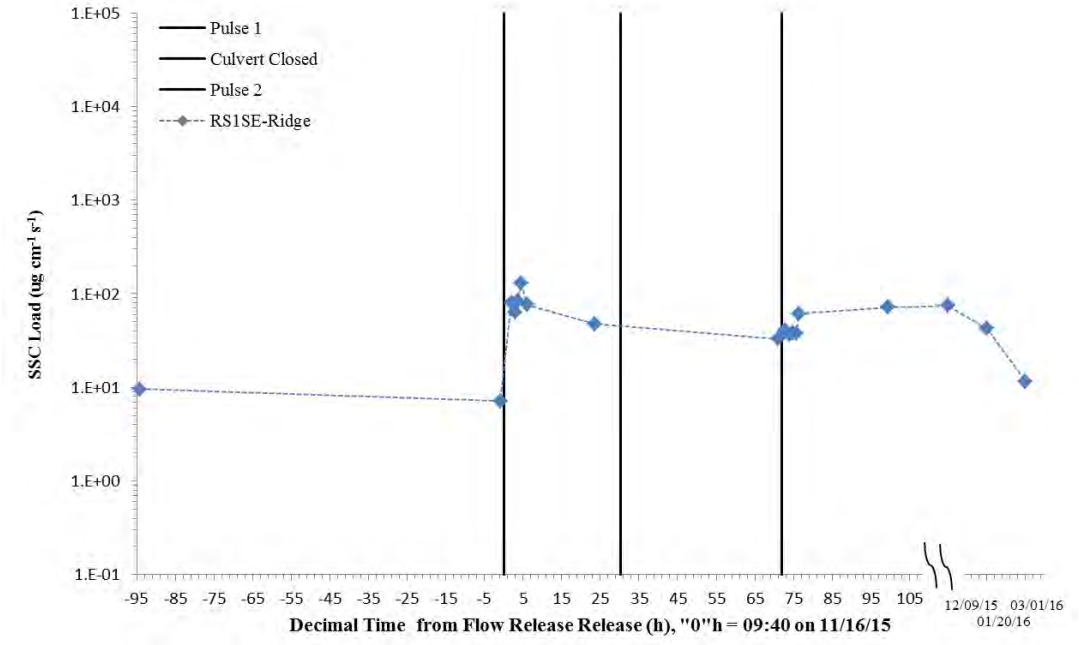

Figure D-112 Time series of total suspended sediment load at site RS1SE during the November, 2015 flow release. The culvert was opened on November 16th (Pulse 1), closed on November 17th, and opened again November 19th (Pulse 2).

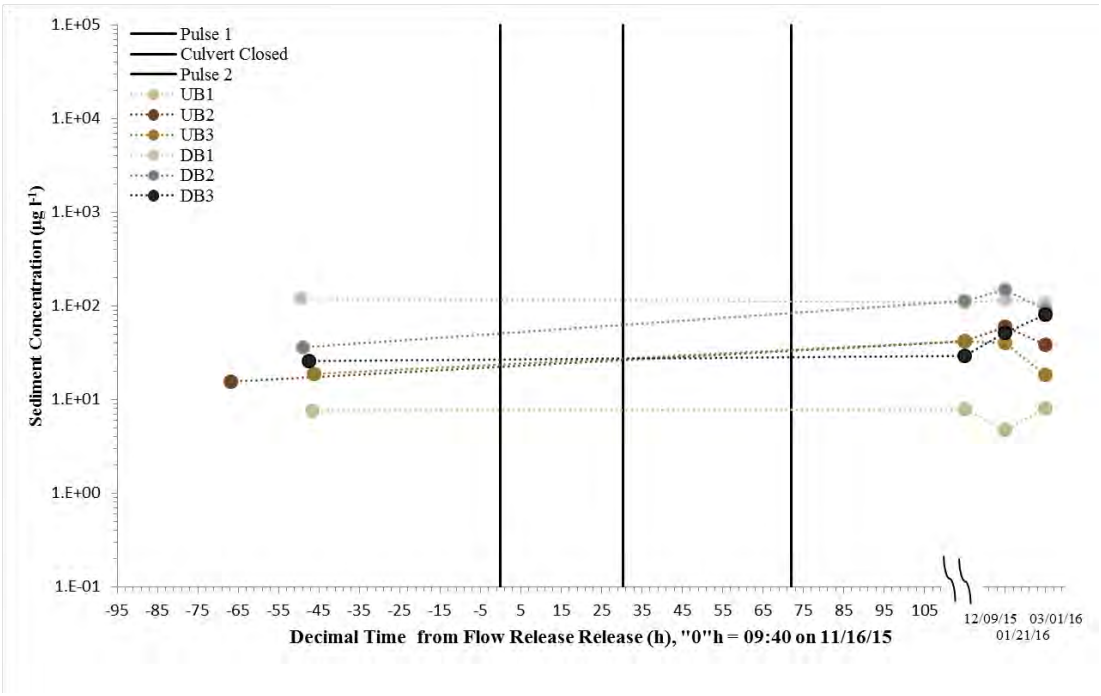

Figure D-113 Time series of total suspended sediment load at sites UB1, UB2, UB3, DB1, DB2, DB3 and S152 during the November, 2015 flow release. The culvert was opened on November 16th (Pulse 1), closed on November 17th, and opened again November 19th (Pulse 2).

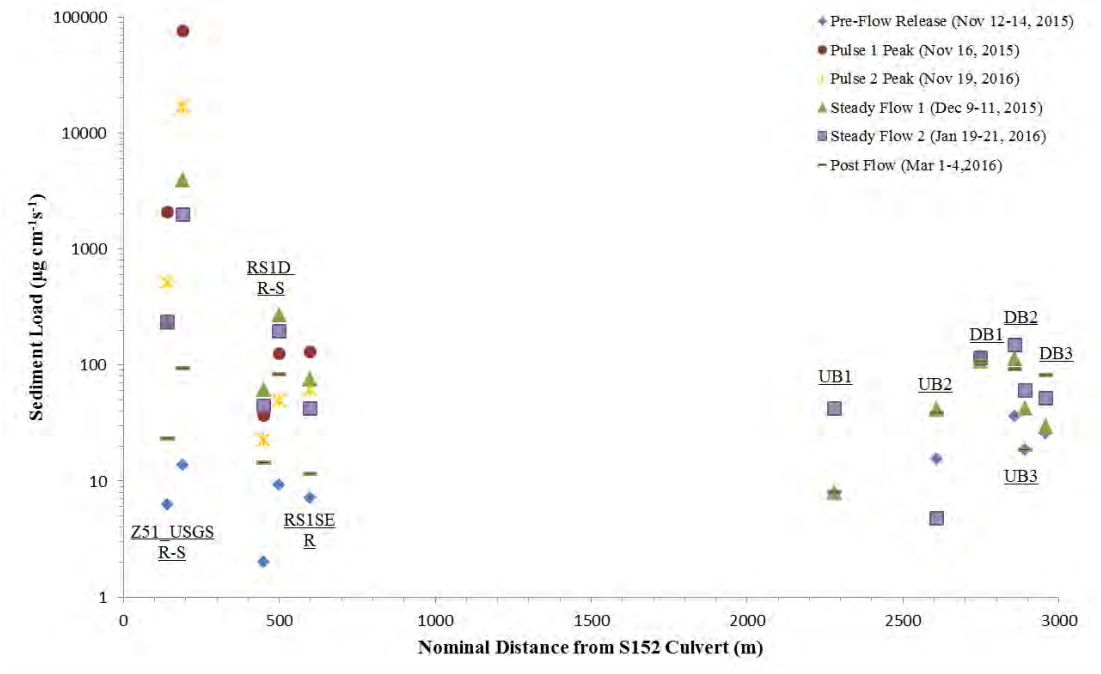

Figure D-114 Spatial distribution of total suspended sediment load at all sites during the November, 2015 flow release. The culvert was opened on November 16th (Pulse 1), closed on November 17th, and opened again November 19th (Pulse 2).

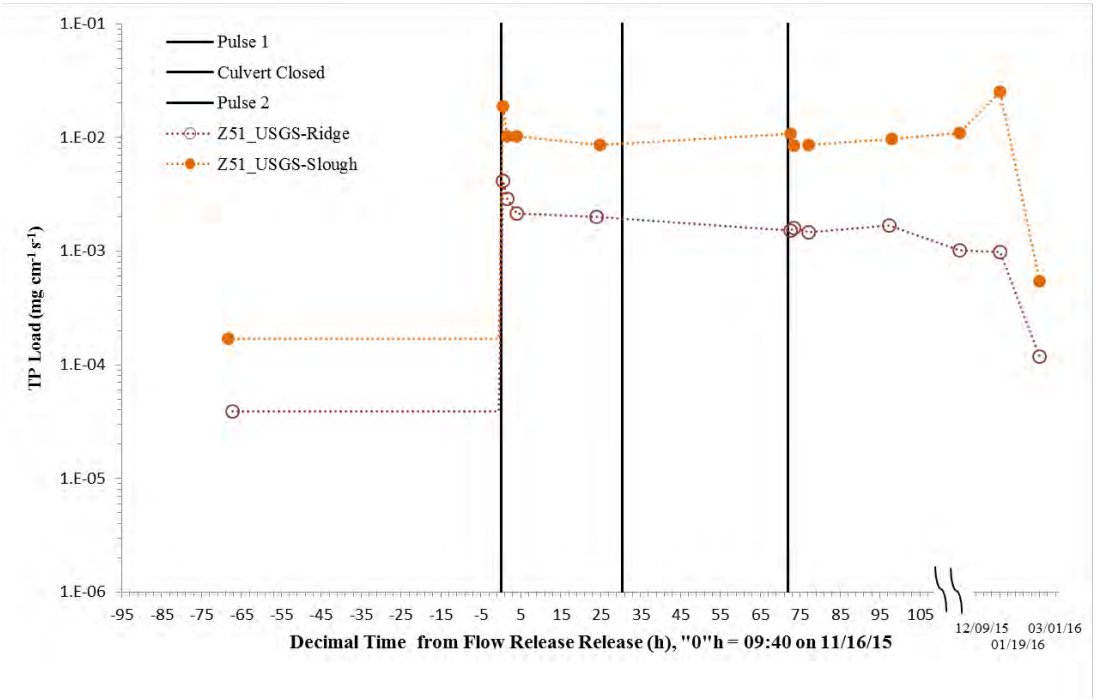

Figure D-115 Time series of total phosphorus load at site Z51_USGS during the November, 2015 flow release. The culvert was opened on November 16th (Pulse 1), closed on November 17th, and opened again November 19th (Pulse 2).

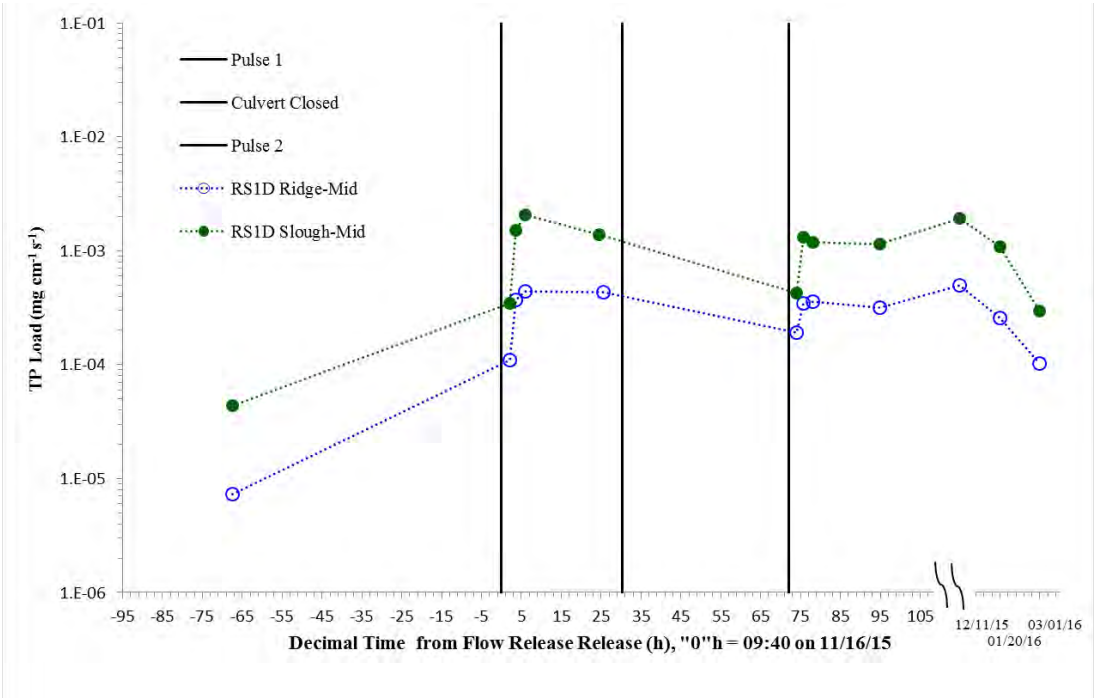

Figure D-116 Time series of total phosphorus load at site RS1D during the November, 2015 flow release. The culvert was opened on November 16th (Pulse 1), closed on November 17th, and opened again November 19th (Pulse 2).

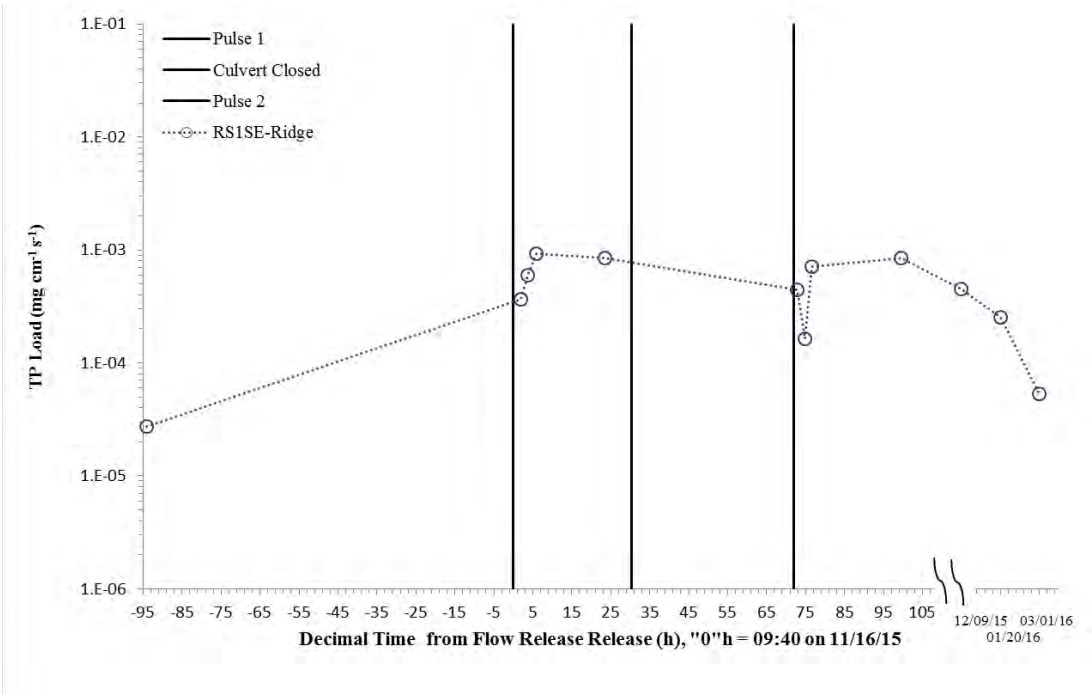

Figure D-117 Time series of total phosphorus load at site RS1SE during the November, 2015 flow release. The culvert was opened on November 16th (Pulse 1), closed on November 17th, and opened again November 19th (Pulse 2).

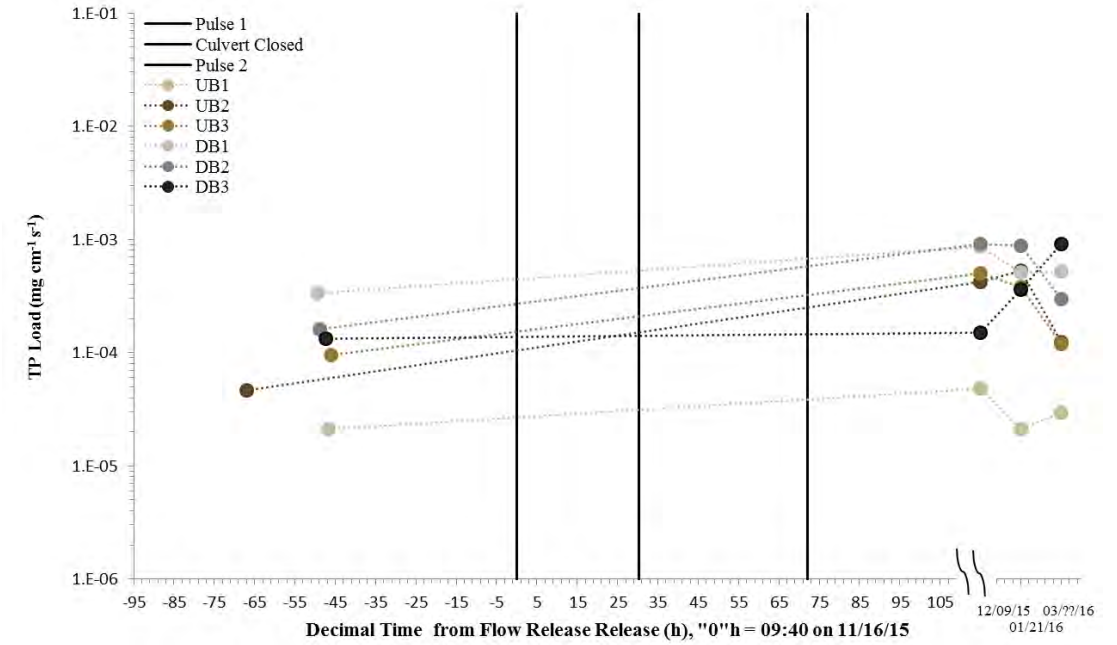

Figure D-118 Time series of total phosphorus load at sites UB1, UB2, UB3, DB1, DB2, DB3 and S152 during the November, 2015 flow release. The culvert was opened on November 16th (Pulse 1), closed on November 17th, and opened again November 19th (Pulse 2).

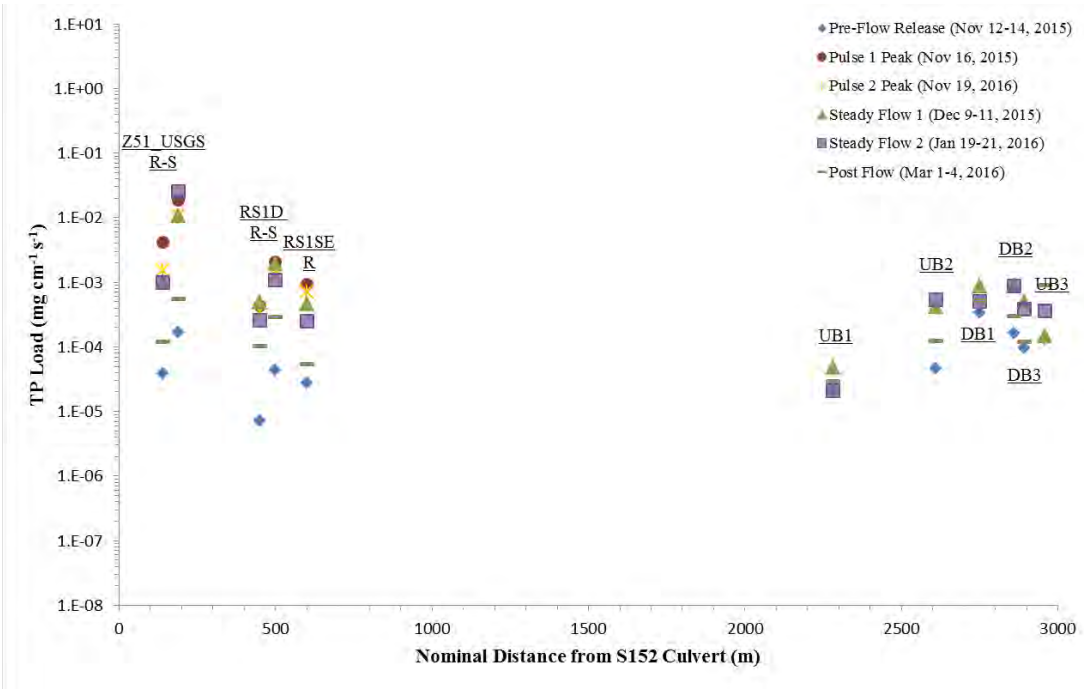

Figure D-119 Spatial distribution of total phosphorus load at all sites during the November, 2015 flow release. The culvert was opened on November 16th (Pulse 1), closed on November 17th, and opened again November 19th (Pulse 2).

Table D-3 Error analysis performed using duplicate samples taken March 1-3, 2016.

RS1D-RM	Mean (µg/L):	482.26
	Standard Deviation (µg/L):	19.39
	Coefficient of Variation (%):	4.02
RS1D-RL	Mean (µg/L):	684.90
	Standard Deviation (µg/L):	139.58
	Coefficient of Variation (%):	20.38
RS1D-SM	Mean (µg/L):	617.84
	Standard Deviation (µg/L):	26.49
	Coefficient of Variation (%):	4.29
RS1D-SL	Mean (µg/L):	1034.44
	Standard Deviation (µg/L):	27.72
	Coefficient of Variation (%):	2.68
UB2-M	Mean (µg/L):	848.34
	Standard Deviation (µg/L):	86.34
	Coefficient of Variation (%):	10.18
DB2-M	Mean (µg/L):	852.95
	Standard Deviation (µg/L):	11.48
	Coefficient of Variation (%):	1.35

2013 Flow Release Vector Maps

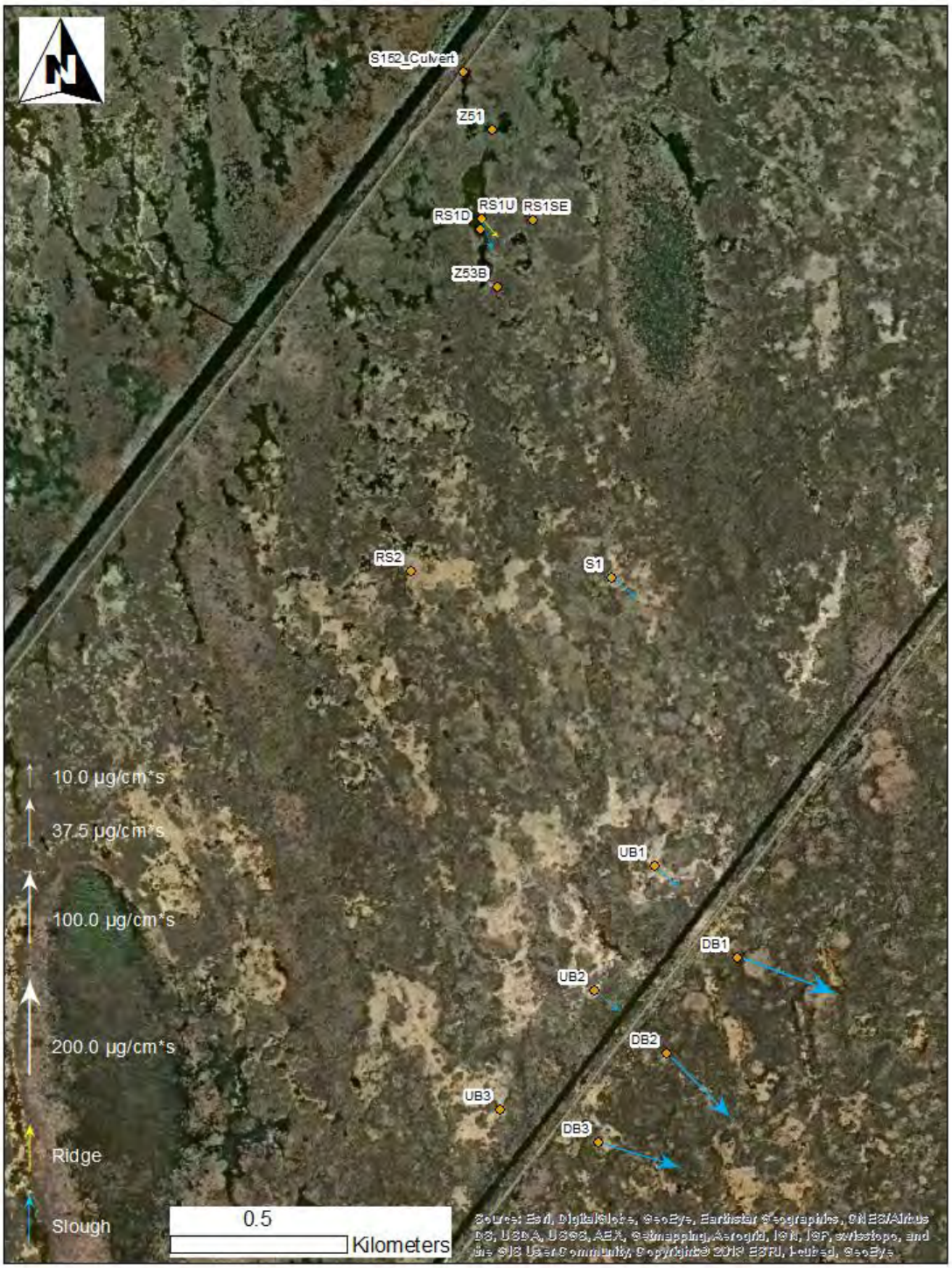

Figure D-120 Pre-release Suspended Sediment Load. Samples collected Nov. 2, 2013.

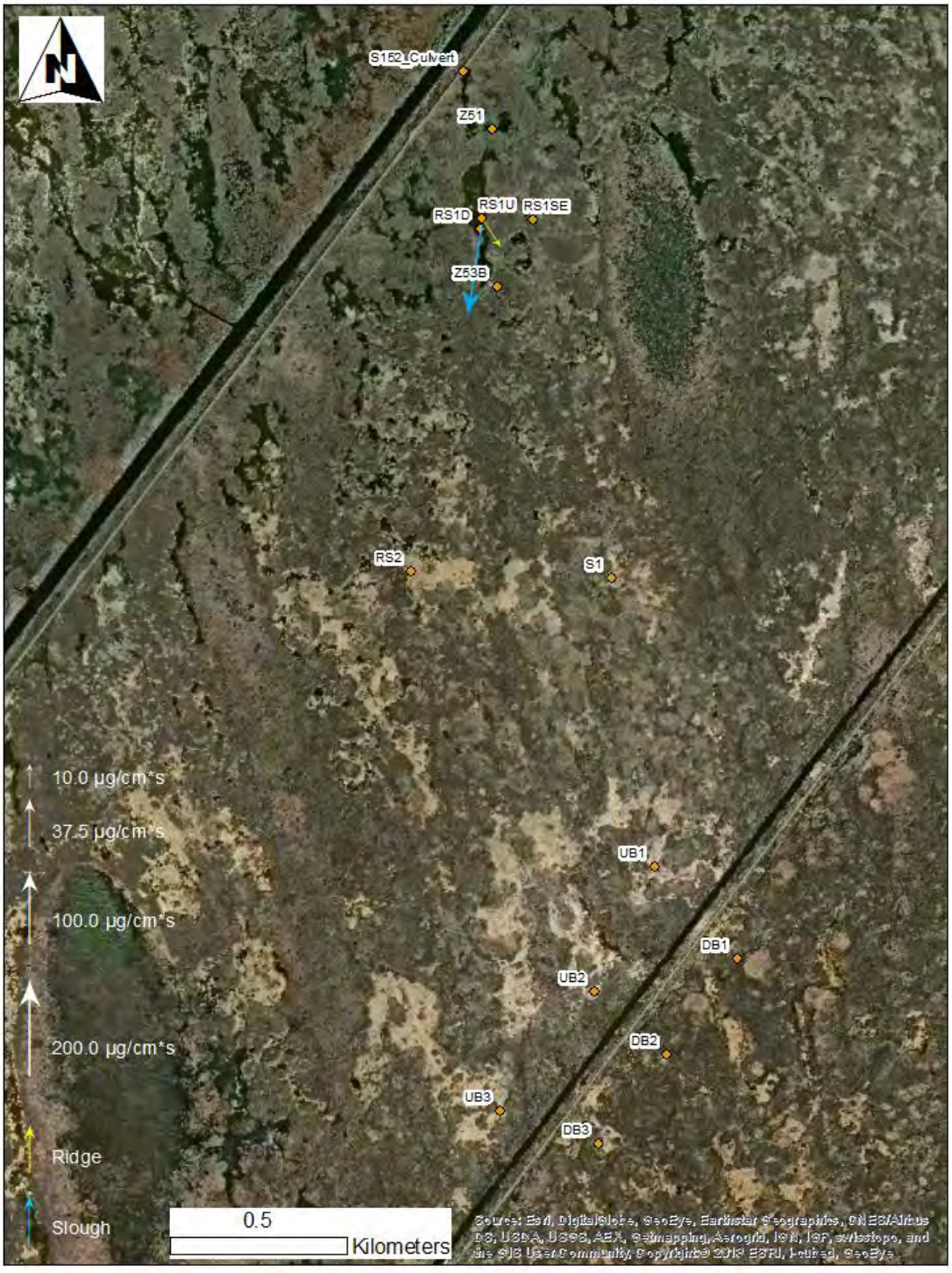

Figure D-121 Transient Flow 1 Suspended Sediment Load. Samples collected Nov. 5, 2013 at 10:15.

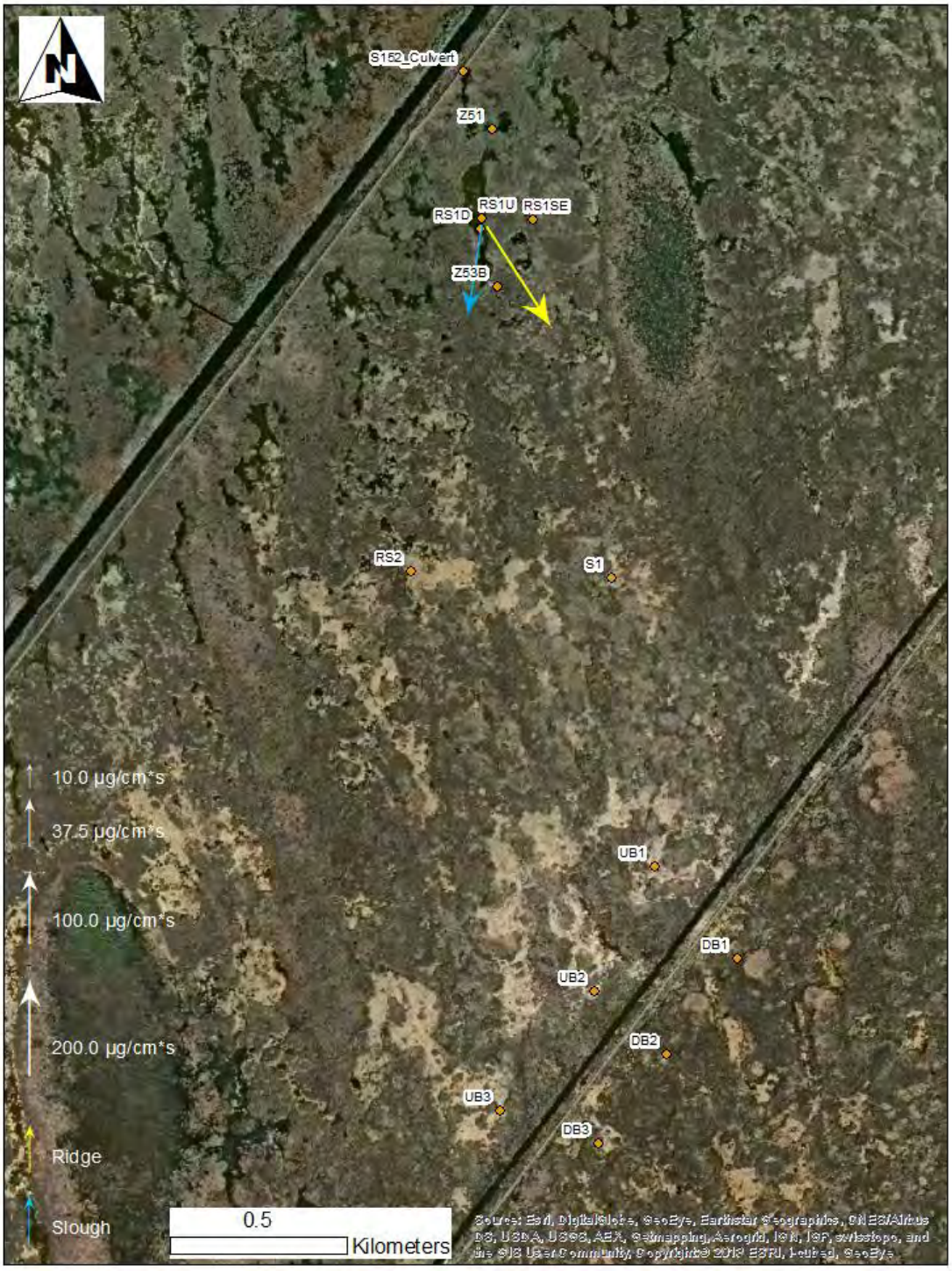

Figure D-122 Transient Flow 1 Suspended Sediment Load. Samples collected Nov. 5, 2013 at 12:00.

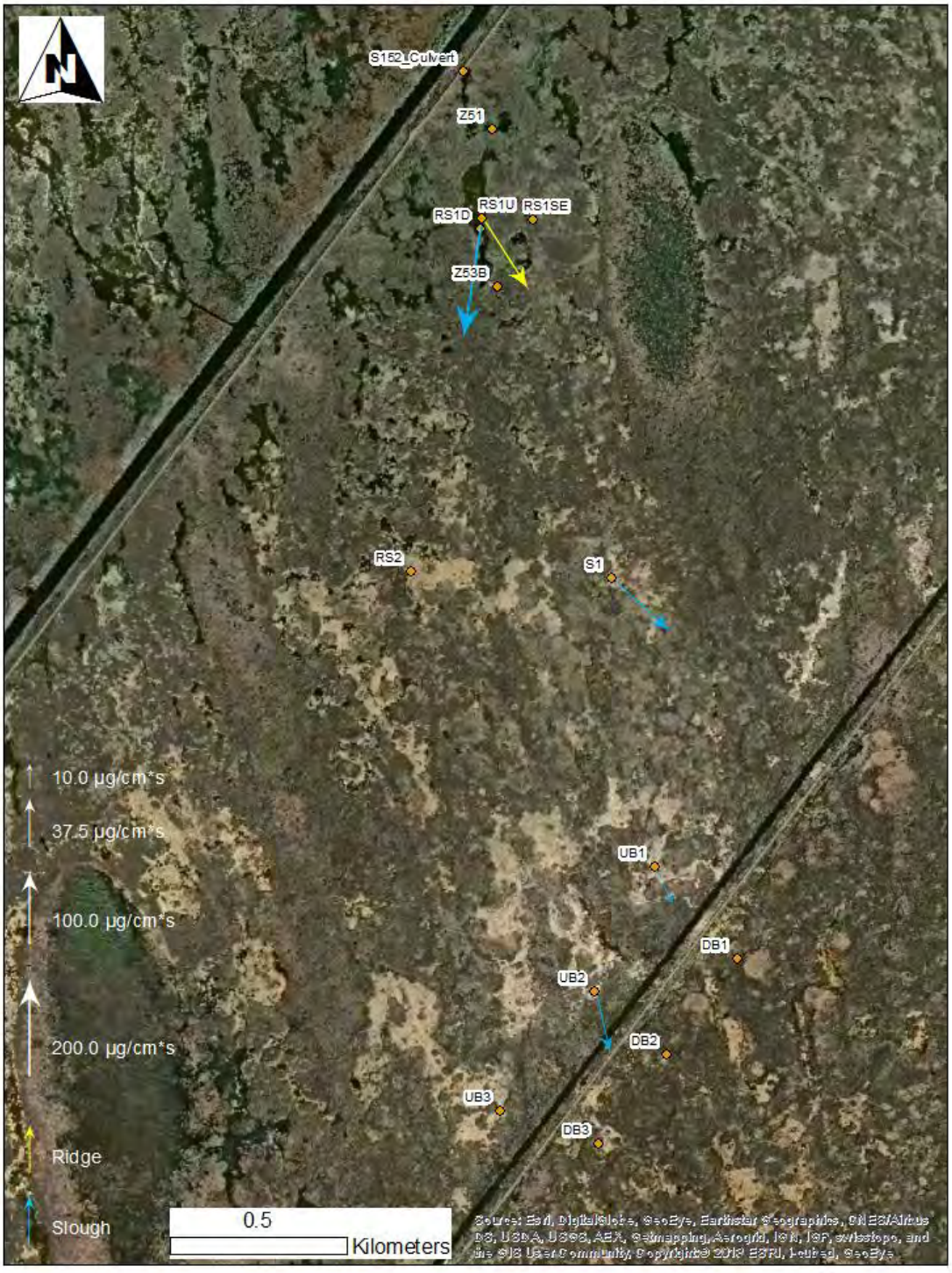

Figure D-123 Transient Flow 1 Suspended Sediment Load. Samples collected Nov. 5, 2013 at 14:00.

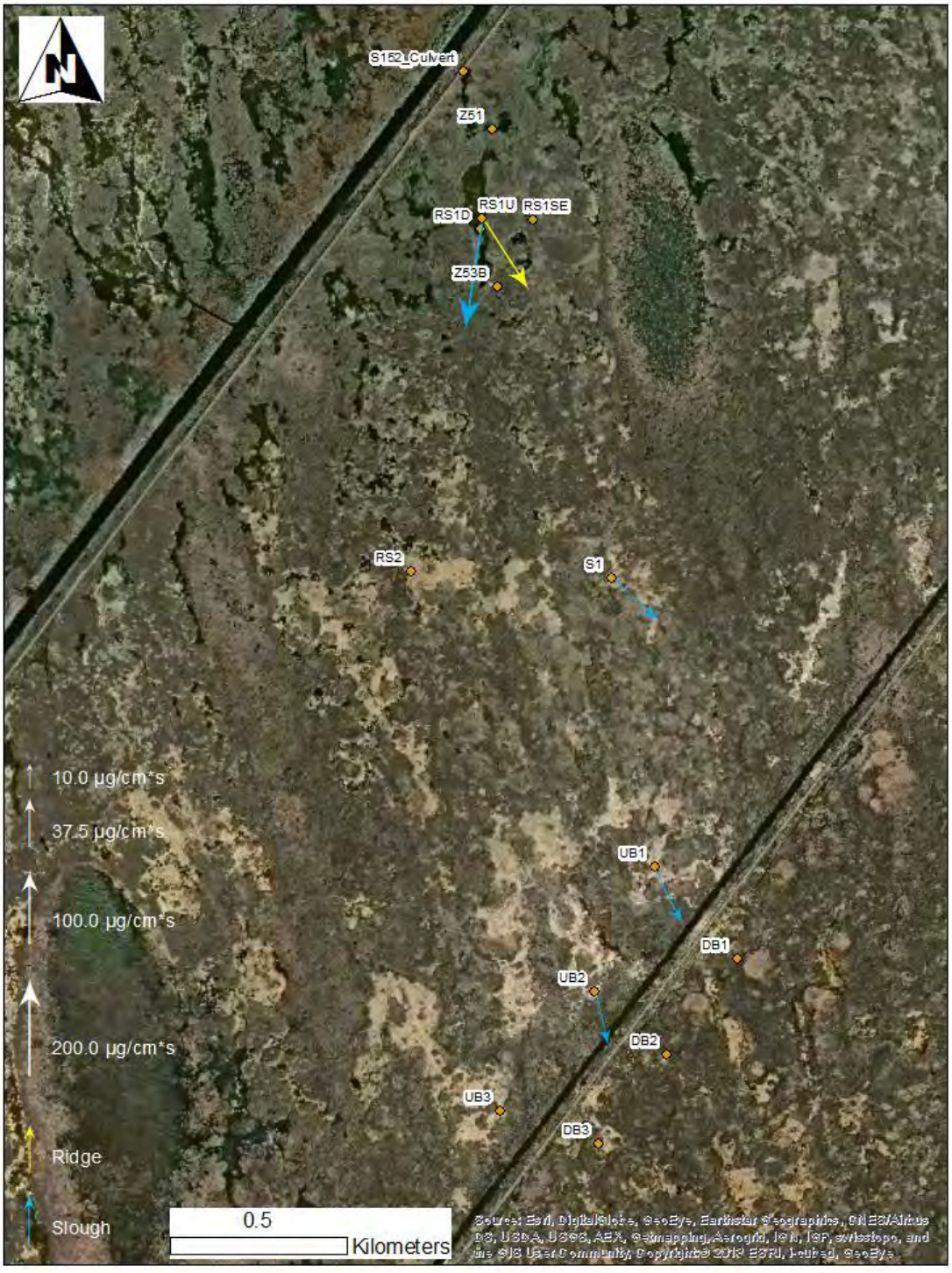

Figure D-124 Transient Flow 1 Suspended Sediment Load. Samples collected Nov. 5, 2013 at 16:00.

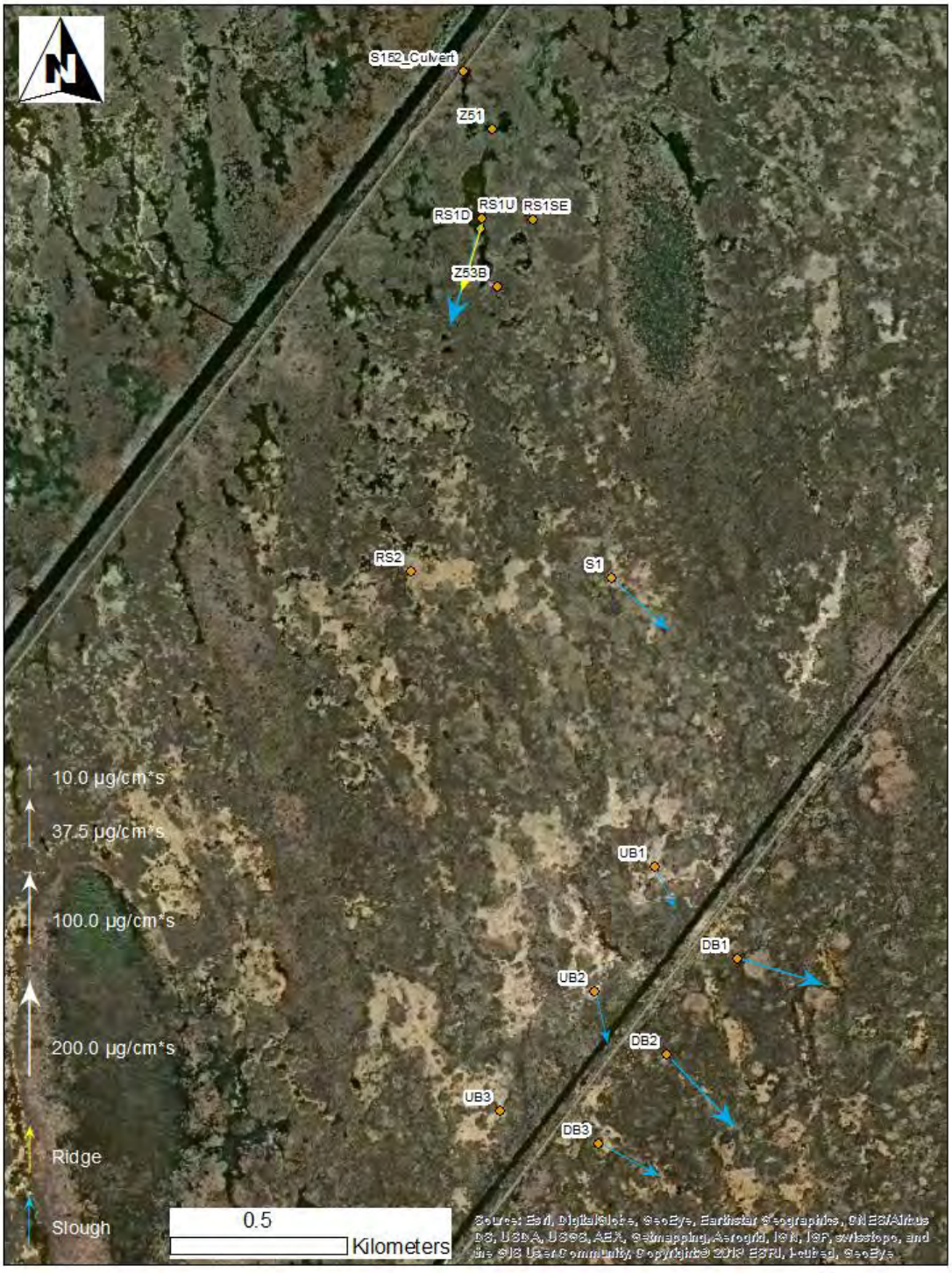

Figure D-125 Transient Flow 2 Suspended Sediment Load. Samples collected Nov. 6, 2013.

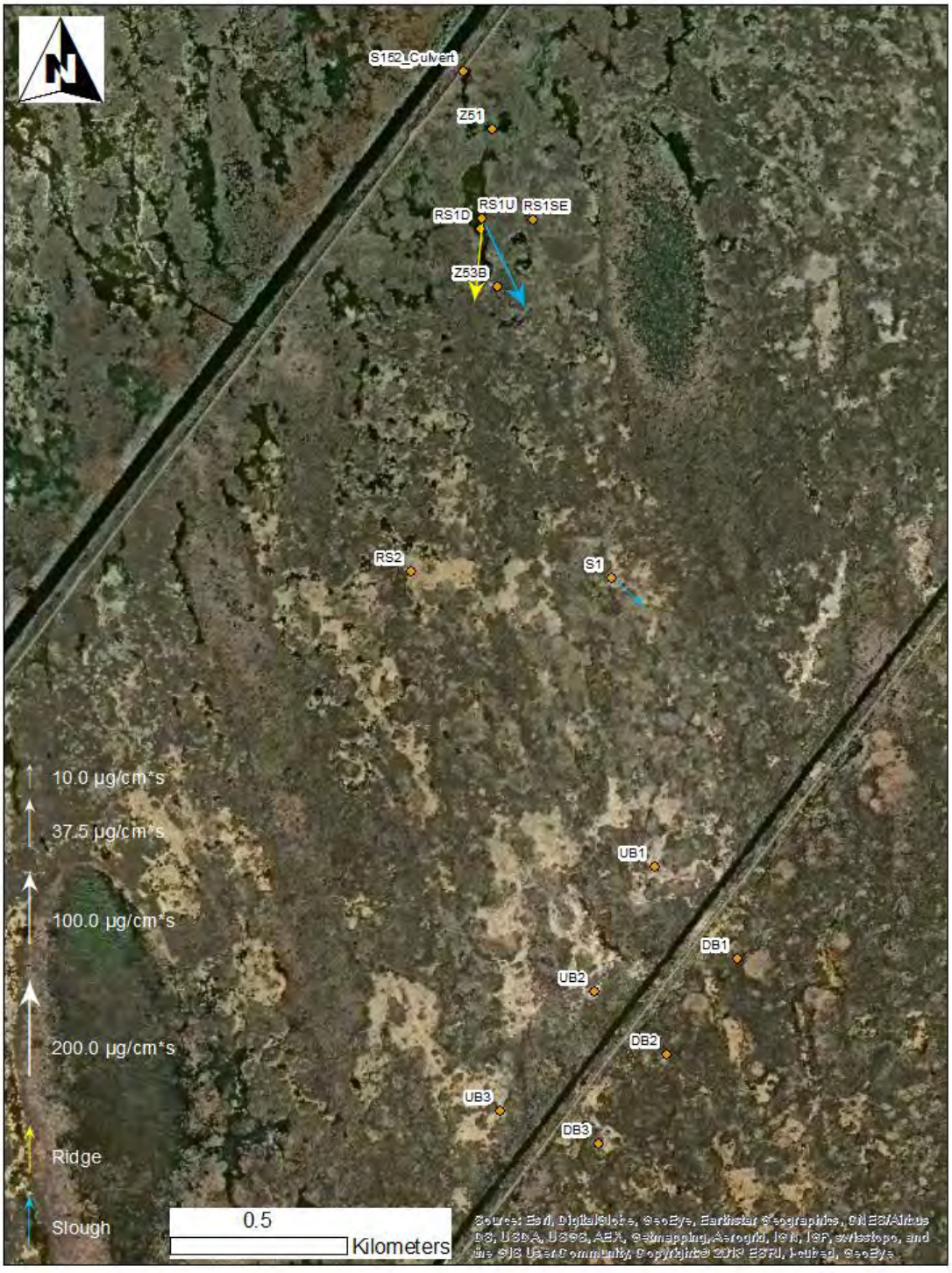

Figure D-126 Steady Flow 1 Suspended Sediment Load. Samples collected Nov. 7, 2013.

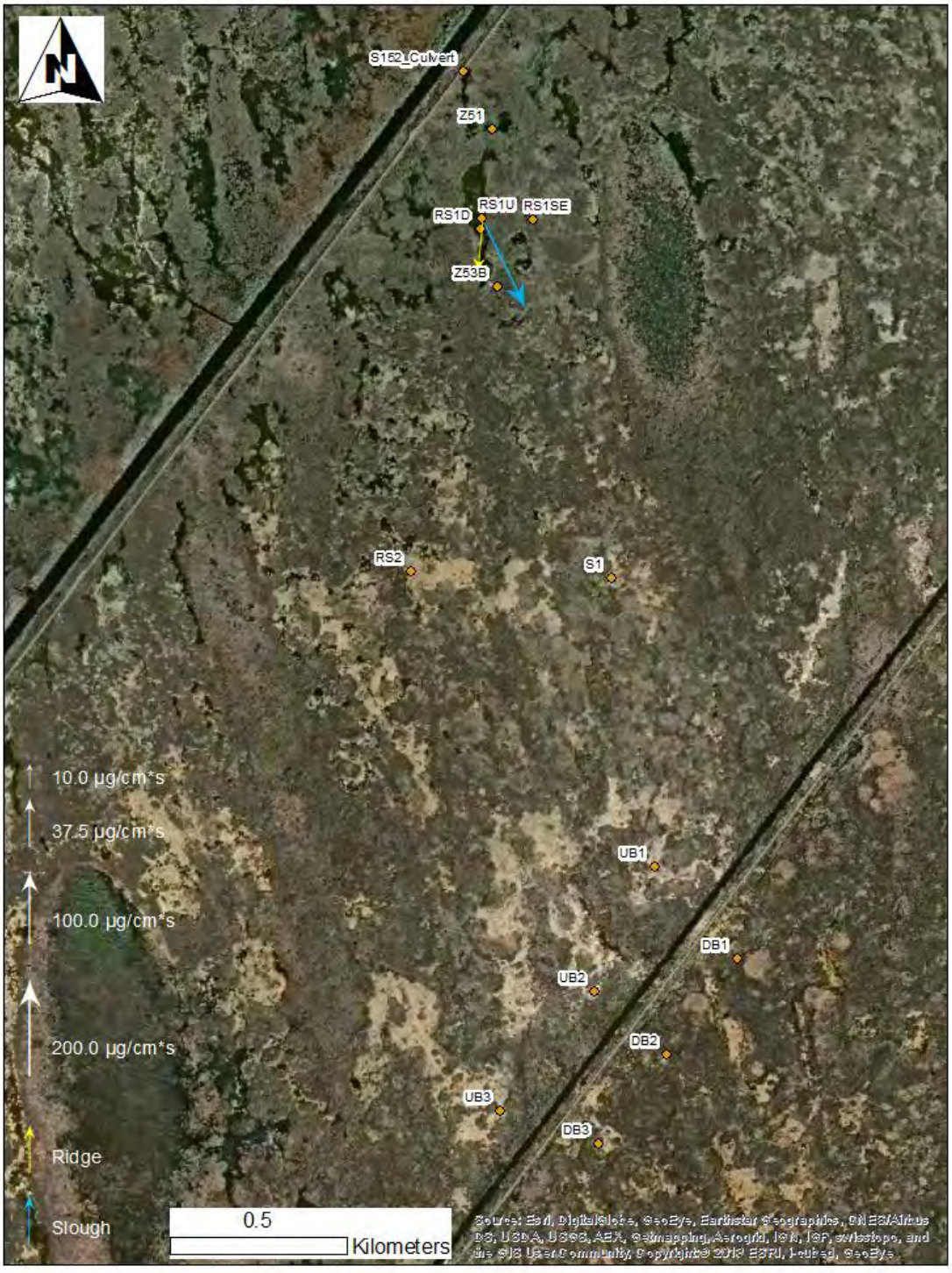

Figure D-127 Steady Flow 1 Suspended Sediment Load. Samples collected Nov. 8, 2013.

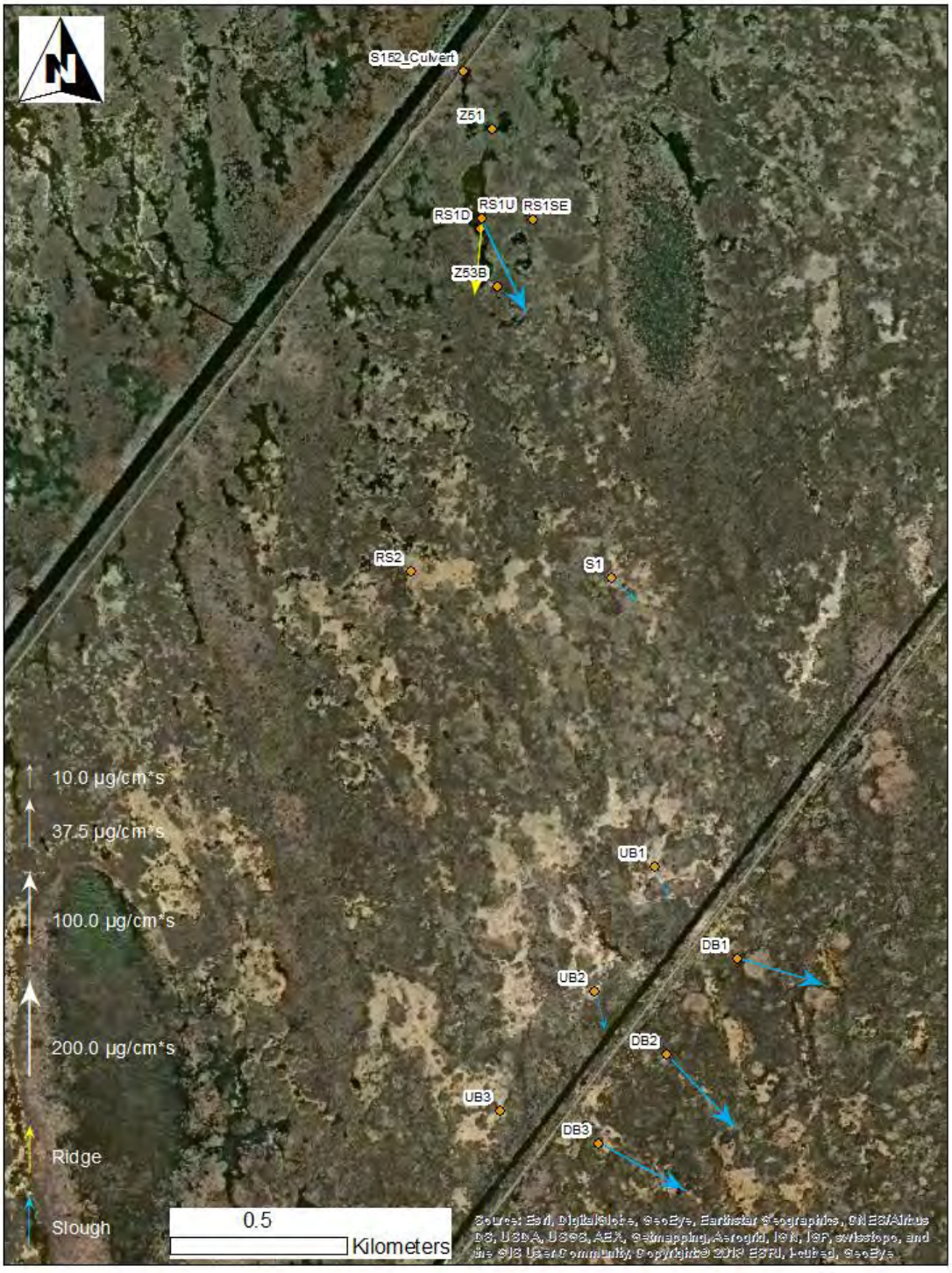

Figure D-128 Steady Flow 1 Suspended Sediment Load. Samples collected Nov. 10, 2013.

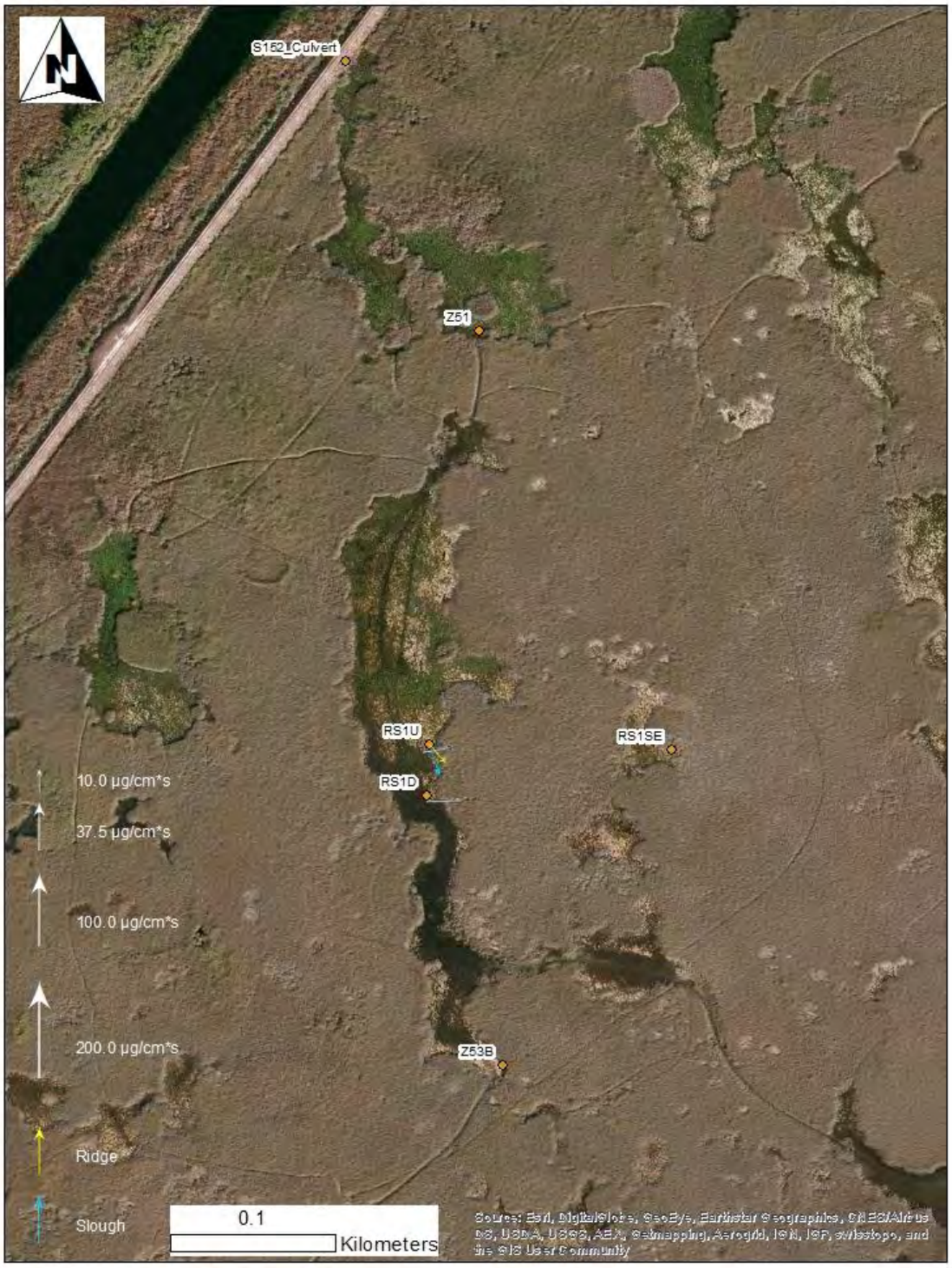

Figure D-129 Pre-release Suspended Sediment Load. Samples collected Nov. 2, 2013.

Figure D-130 Transient Flow 1 Suspended Sediment Load. Samples collected Nov. 5, 2013 at 10:15.

Figure D-131 Transient Flow 1 Suspended Sediment Load. Samples collected Nov. 5, 2013 at 12:00.

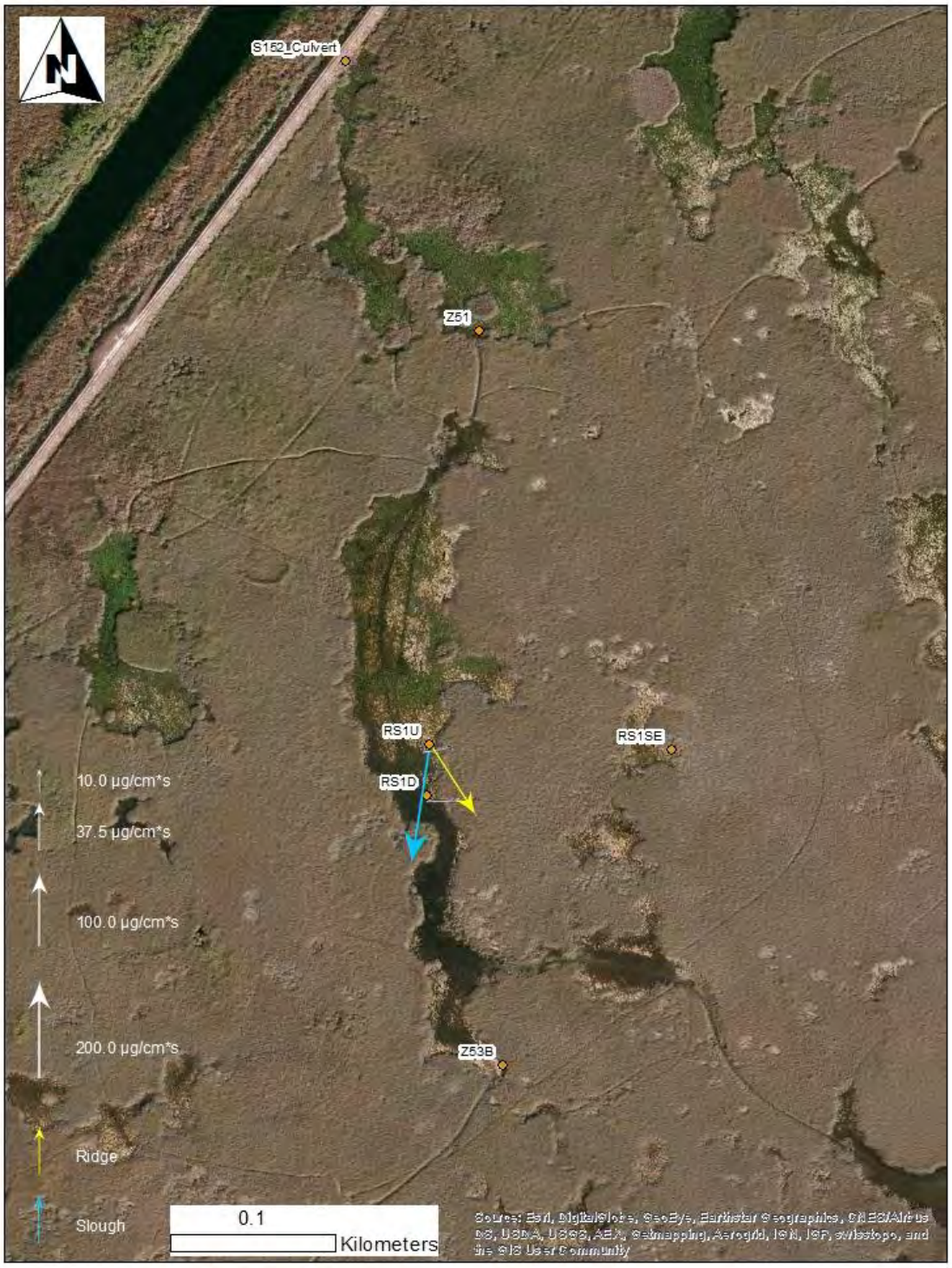

Figure D-132 Transient Flow 1 Suspended Sediment Load. Samples collected Nov. 5, 2013 at 14:00.

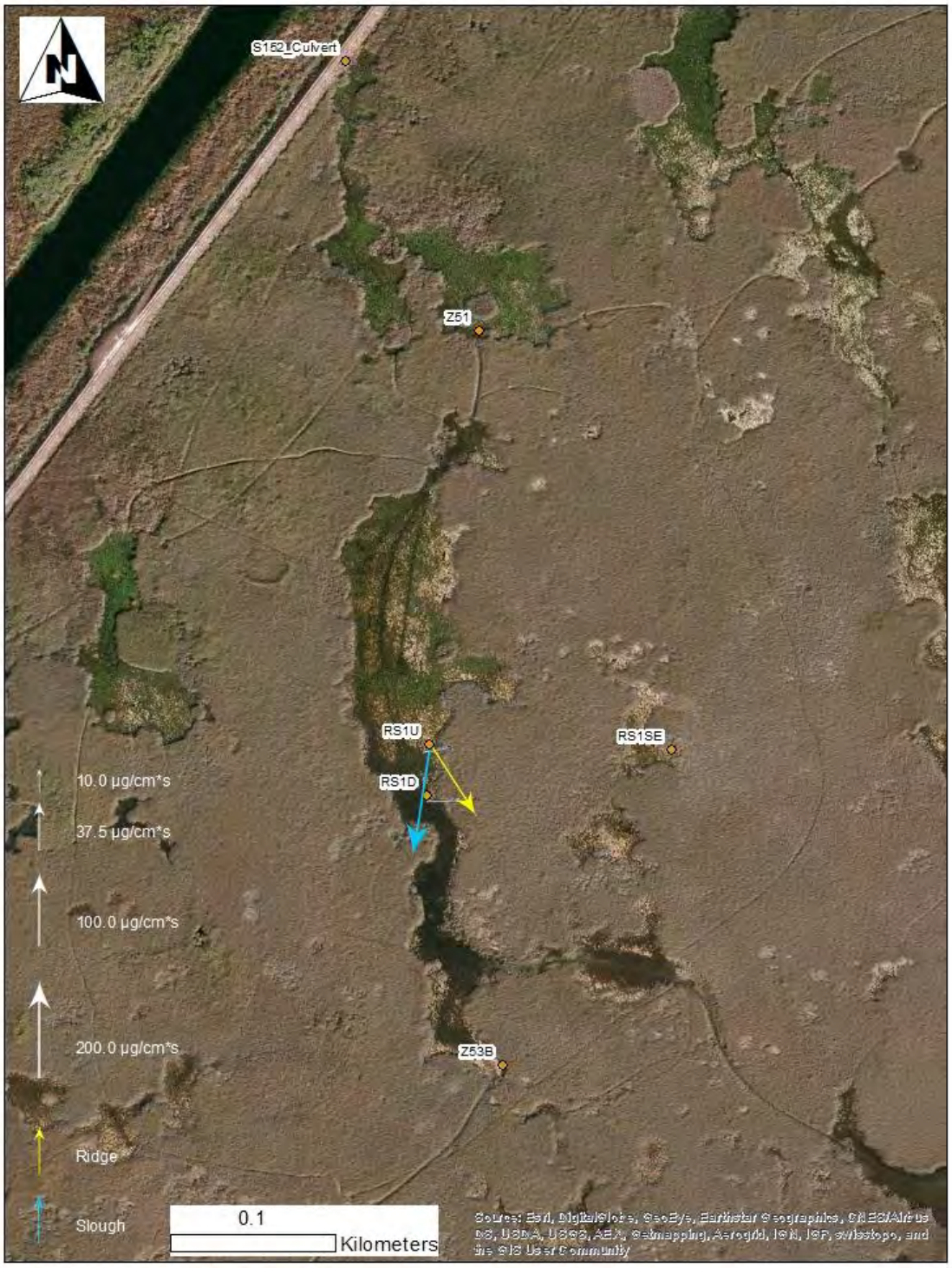

Figure D-133 Transient Flow 1 Suspended Sediment Load. Samples collected Nov. 5, 2013 at 16:00.

Figure D-134 Transient Flow 2 Suspended Sediment Load. Samples collected Nov. 6, 2013.

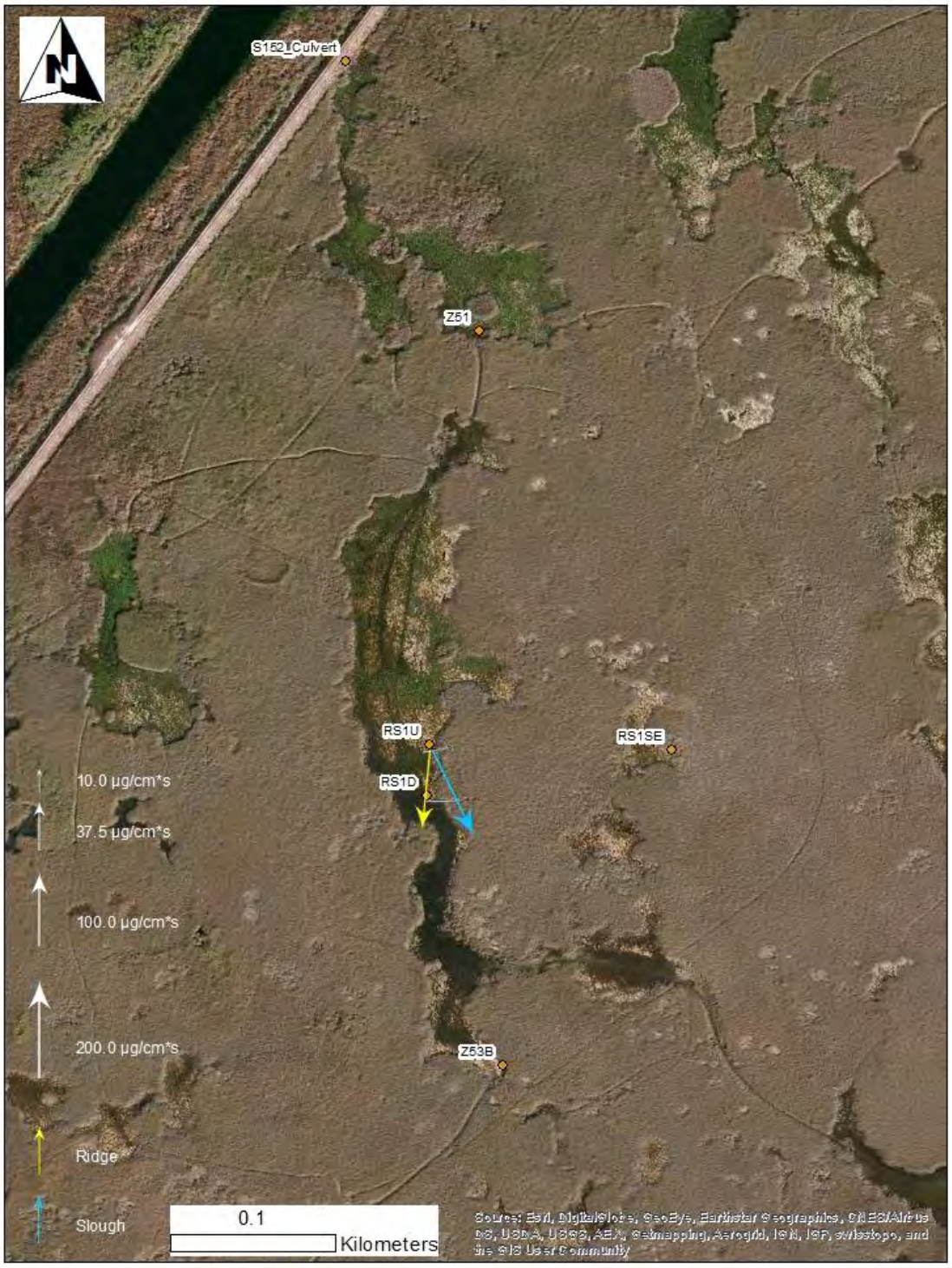

Figure D-135 Steady Flow 1 Suspended Sediment Load. Samples collected Nov. 7, 2013.

Figure D-136 Steady Flow 1 Suspended Sediment Load. Samples collected Nov. 8. 2013.

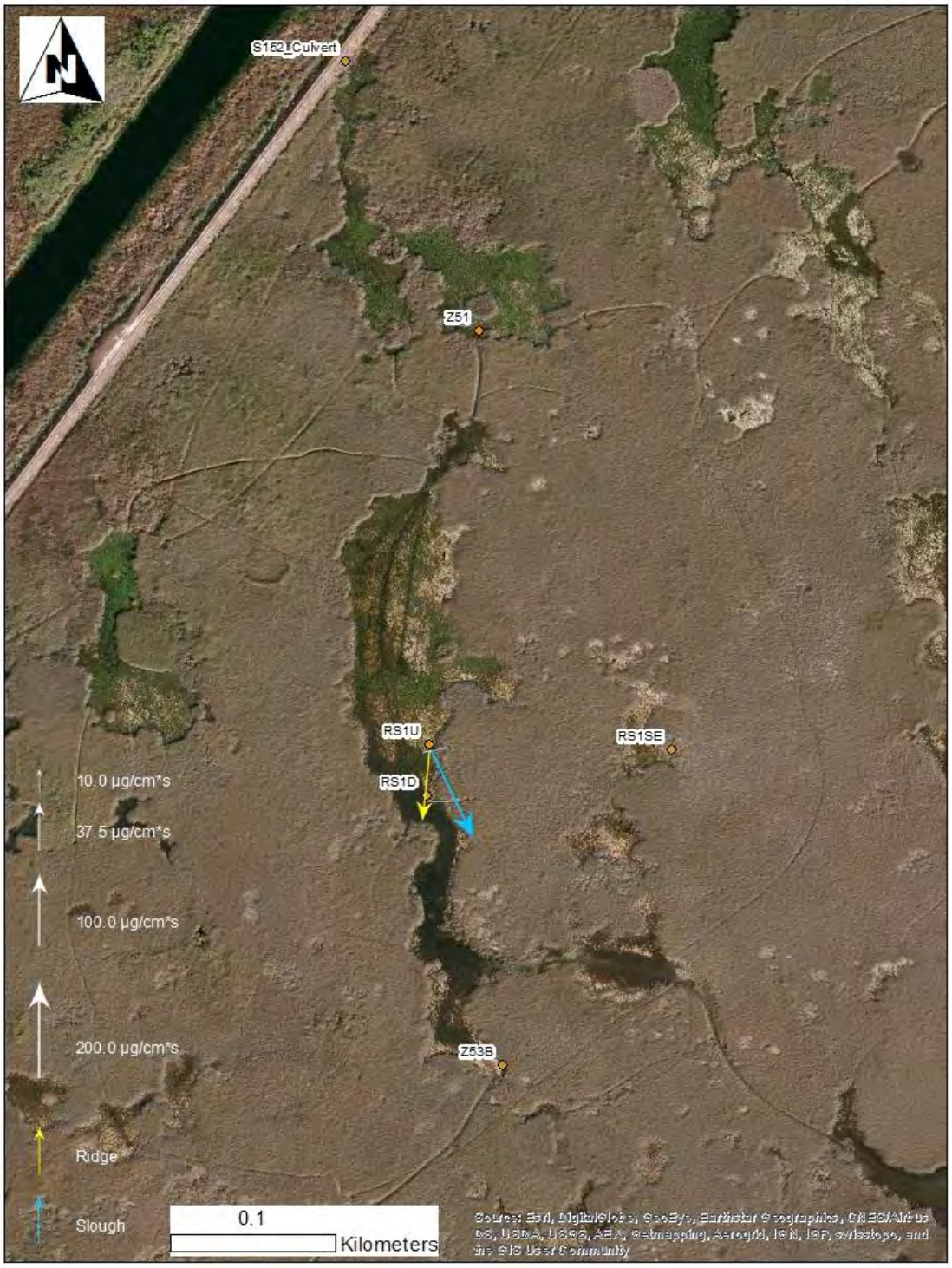

Figure D-137 Steady Flow 1 Suspended Sediment Load. Samples collected Nov. 10, 2013.

Figure D-138 Pre-release Phosphorus Load. Samples collected Nov. 2 - Nov. 4, 2013.

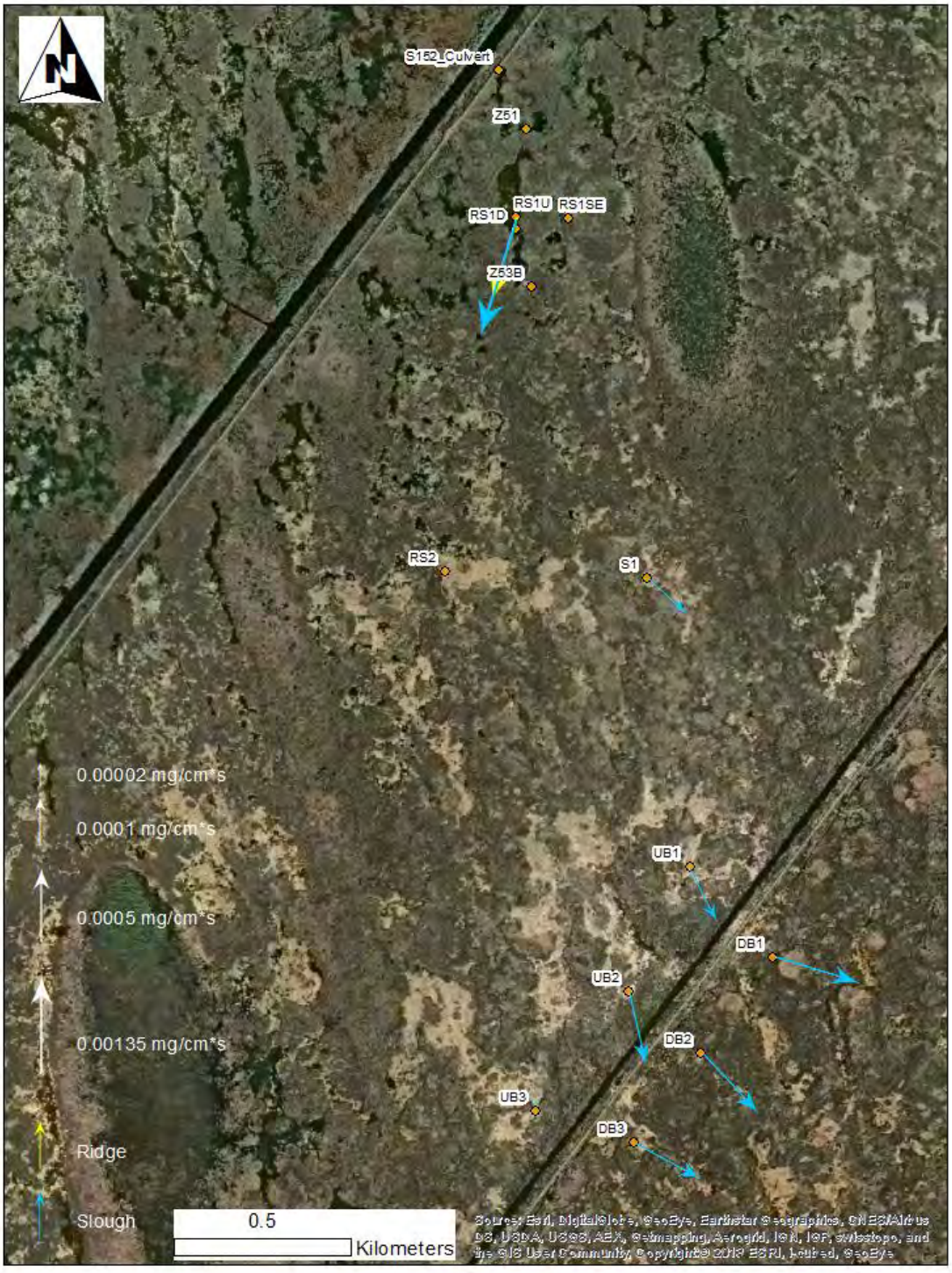

Figure D-139 Transient Flow 2 Phosphorus Load. Samples collected Nov. 6, 2013.

Figure D-140 Steady Flow 1 Phosphorus Load. Samples collected Nov. 10, 2013.

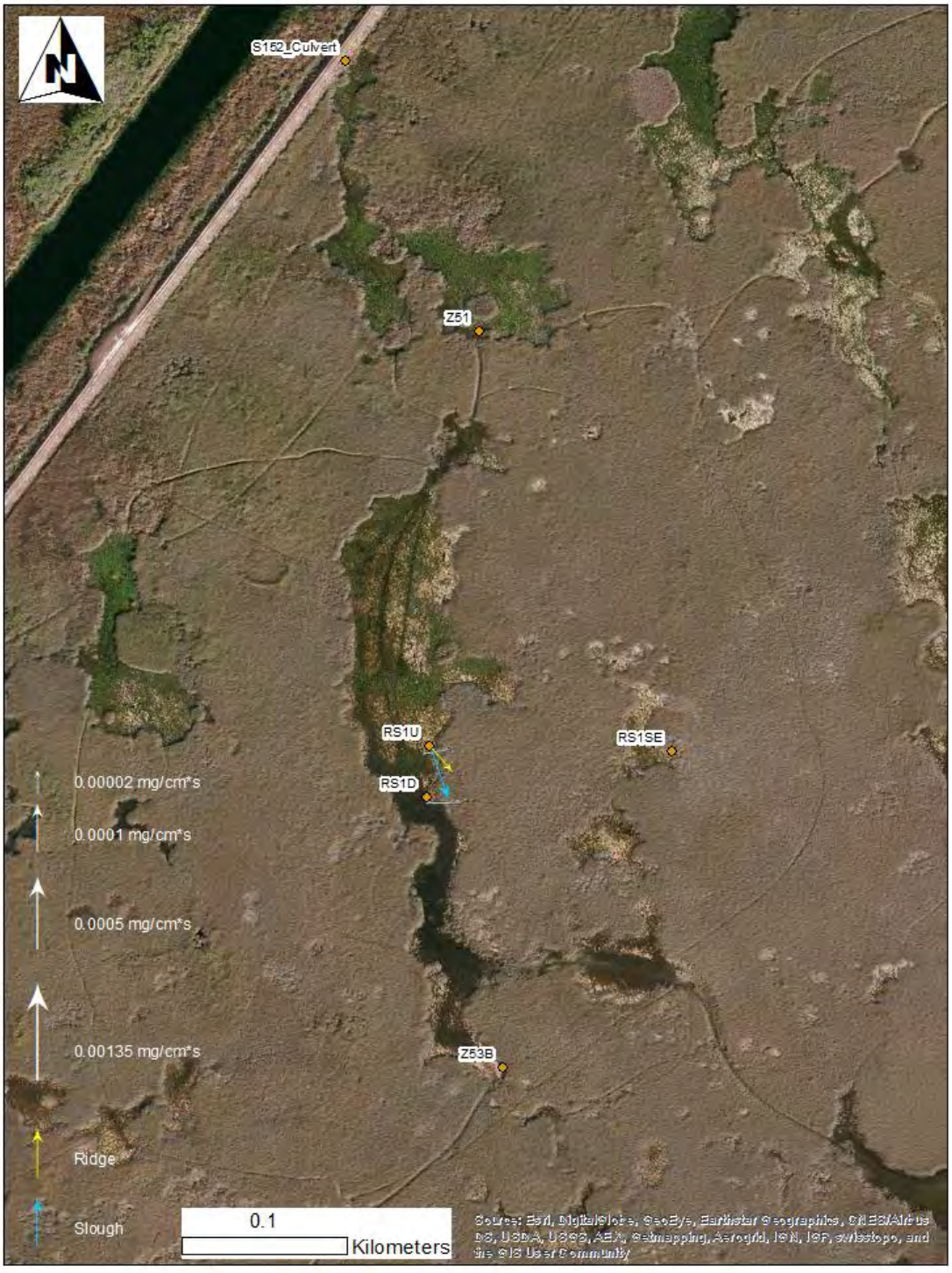

Figure D-141 Pre-release Phosphorus Load. Samples collected Nov. 2 - Nov. 4, 2013.

Figure D-142 Transient Flow 2 Phosphorus Load. Samples collected Nov. 6, 2013.

Figure D-143 Steady Flow 1 Phosphorus Load. Samples collected Nov. 10, 2013.

2014 Flow Release Vector Maps

Figure D-144 Pre-release Suspended Sediment Load. Samples collected Oct. 31 – Nov. 3, 2014.

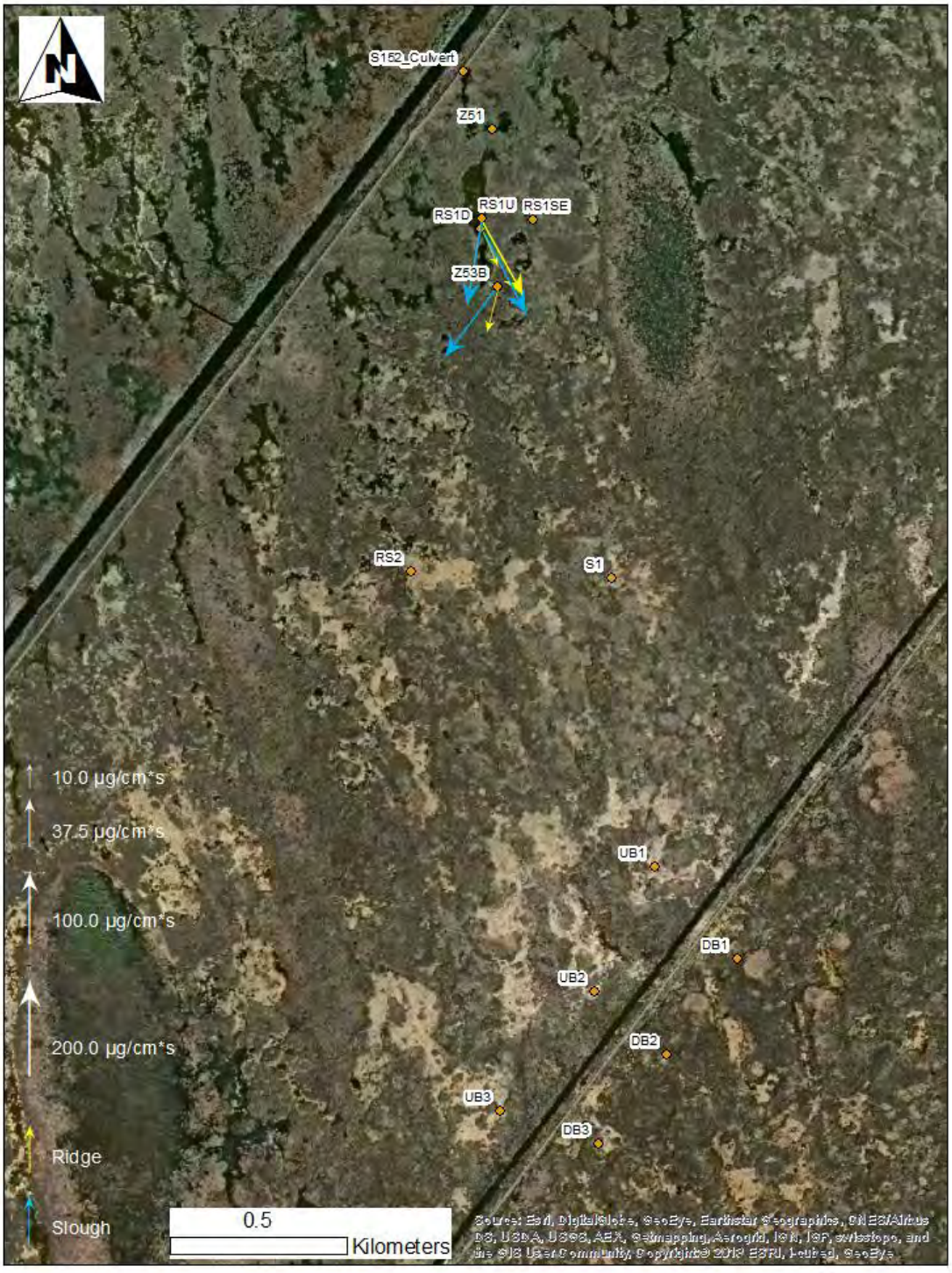

Figure D-145 Transient Flow 1 Suspended Sediment Load. Samples collected Nov. 4, 2014 at 10:50.

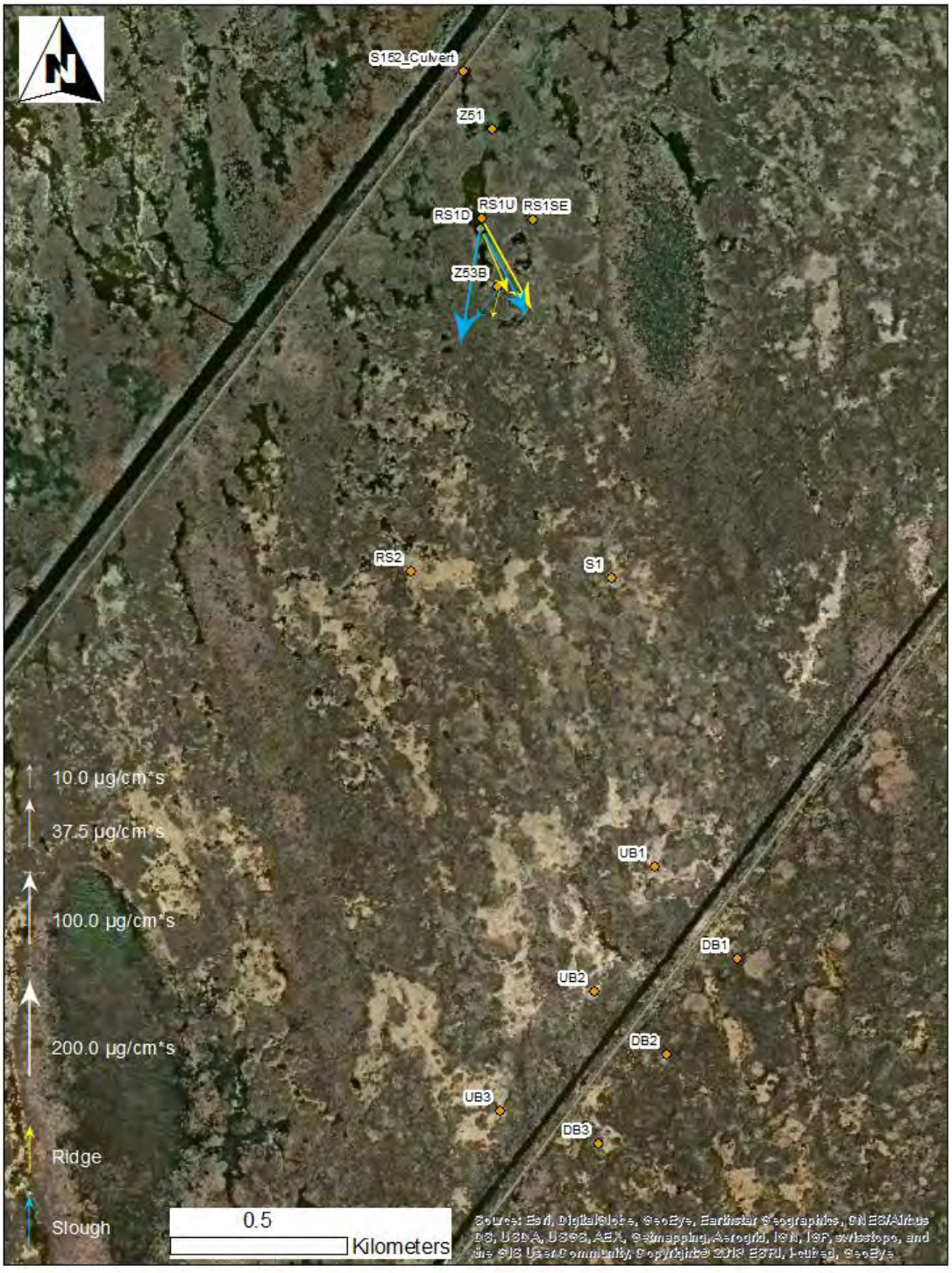

Figure D-146 Transient Flow 1 Suspended Sediment Load. Samples collected Nov. 4, 2014 at 12:00.

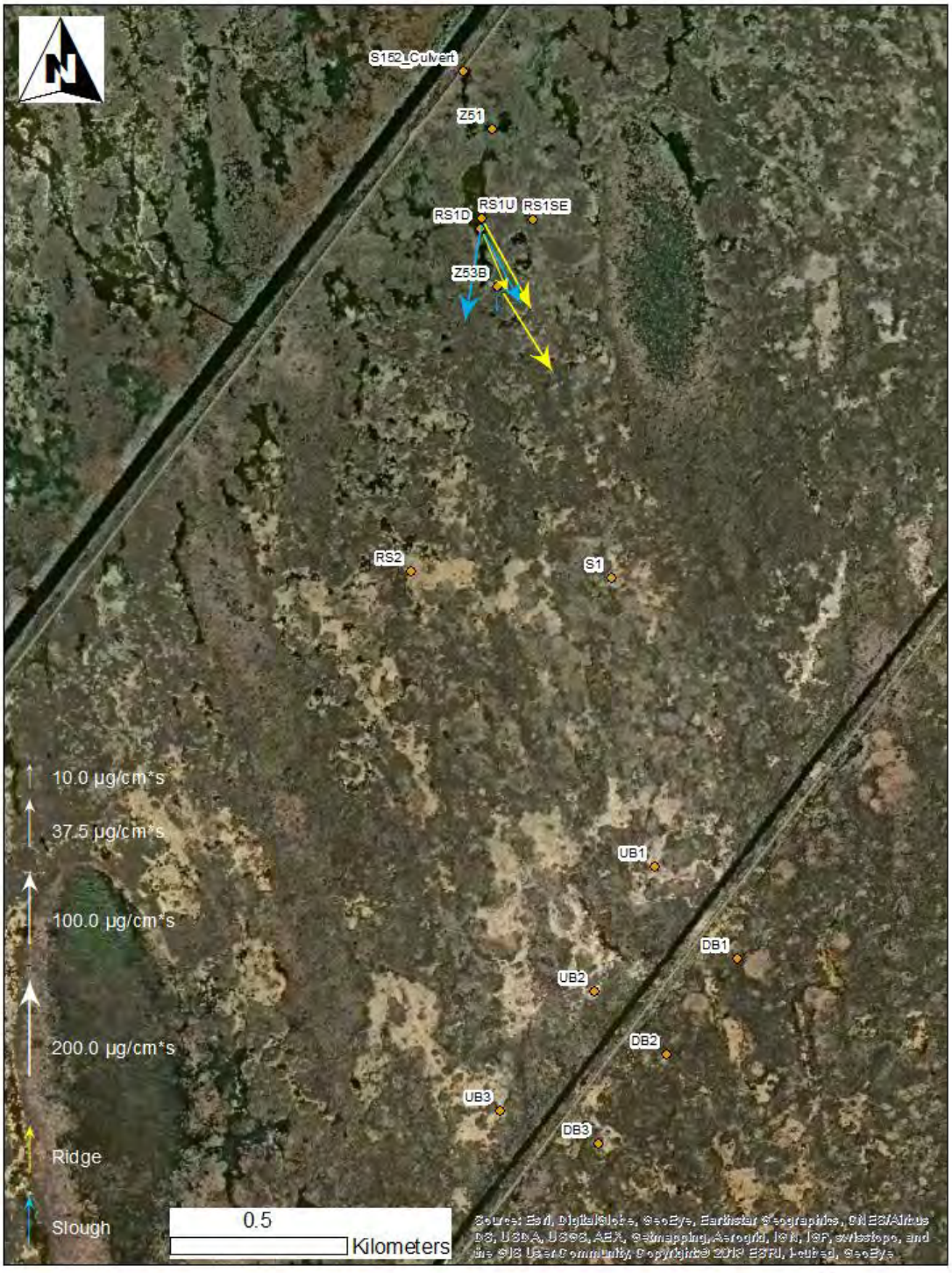

Figure D-147 Transient Flow 1 Suspended Sediment Load. Samples collected Nov. 4, 2014 at 14:00.

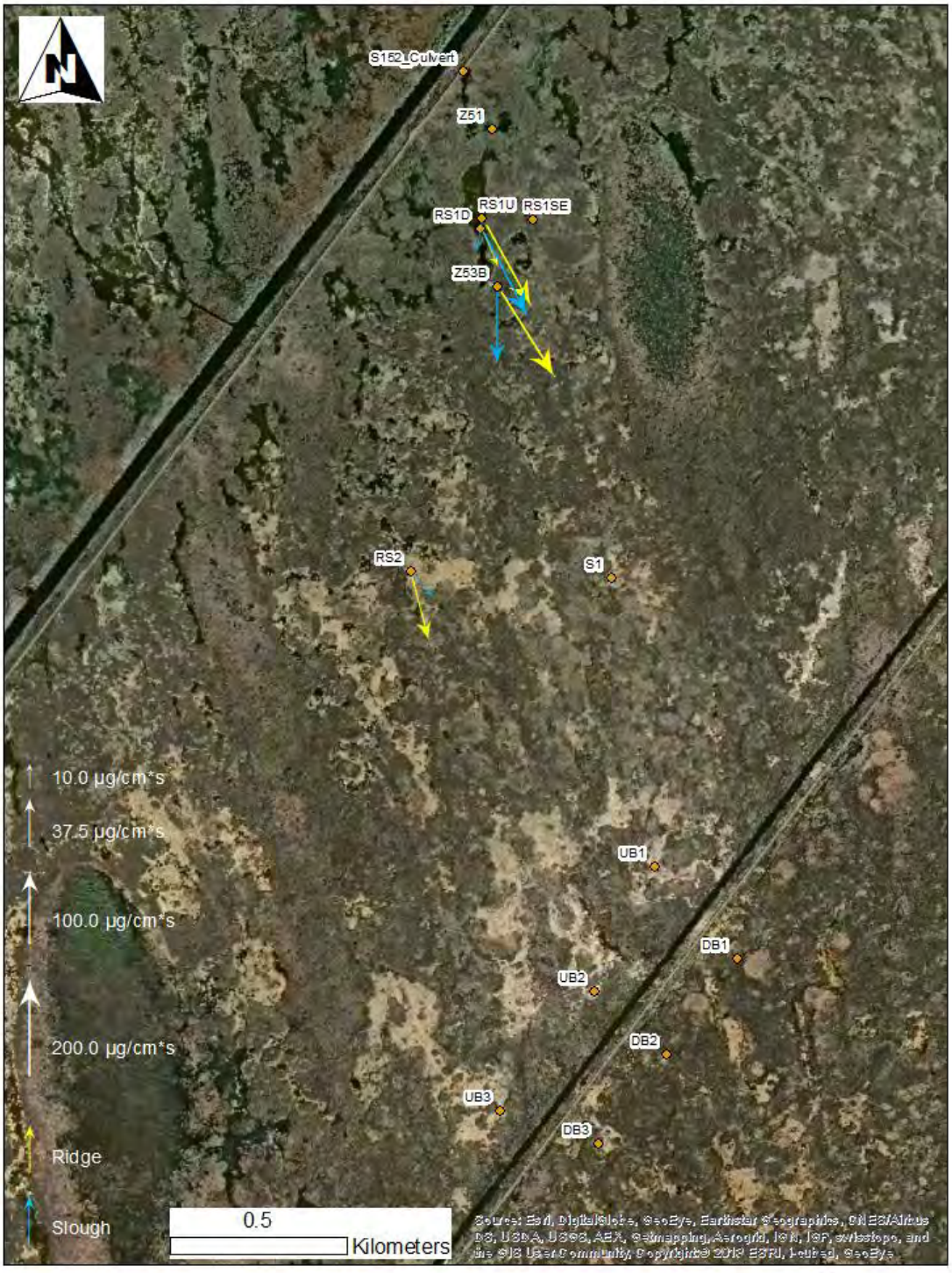

Figure D-148 Transient Flow 1 Suspended Sediment Load. Samples collected Nov. 4, 2014 at 16:00.

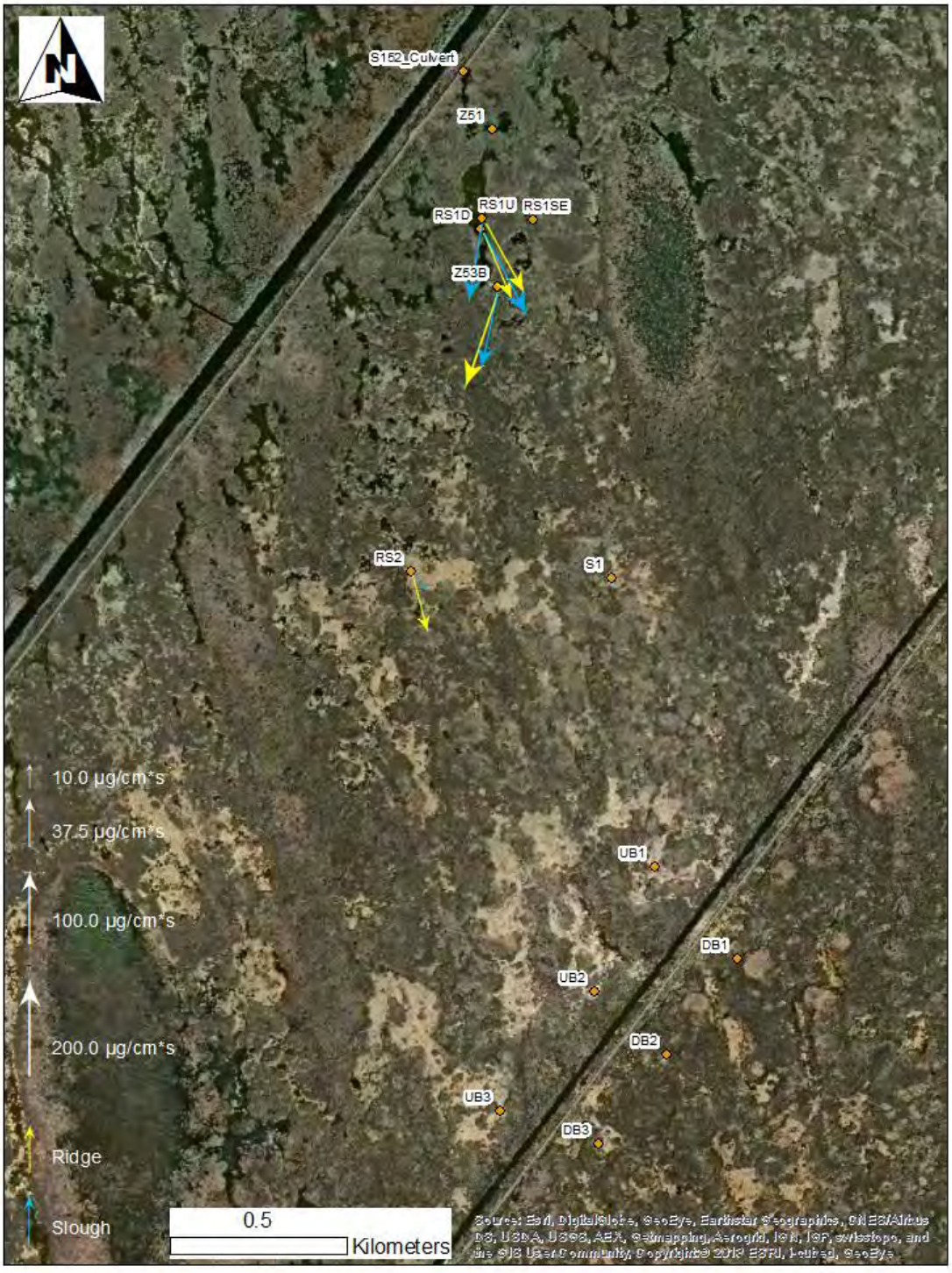

Figure D-149 Transient Flow 2 Suspended Sediment Load. Samples collected Nov. 5, 2014.

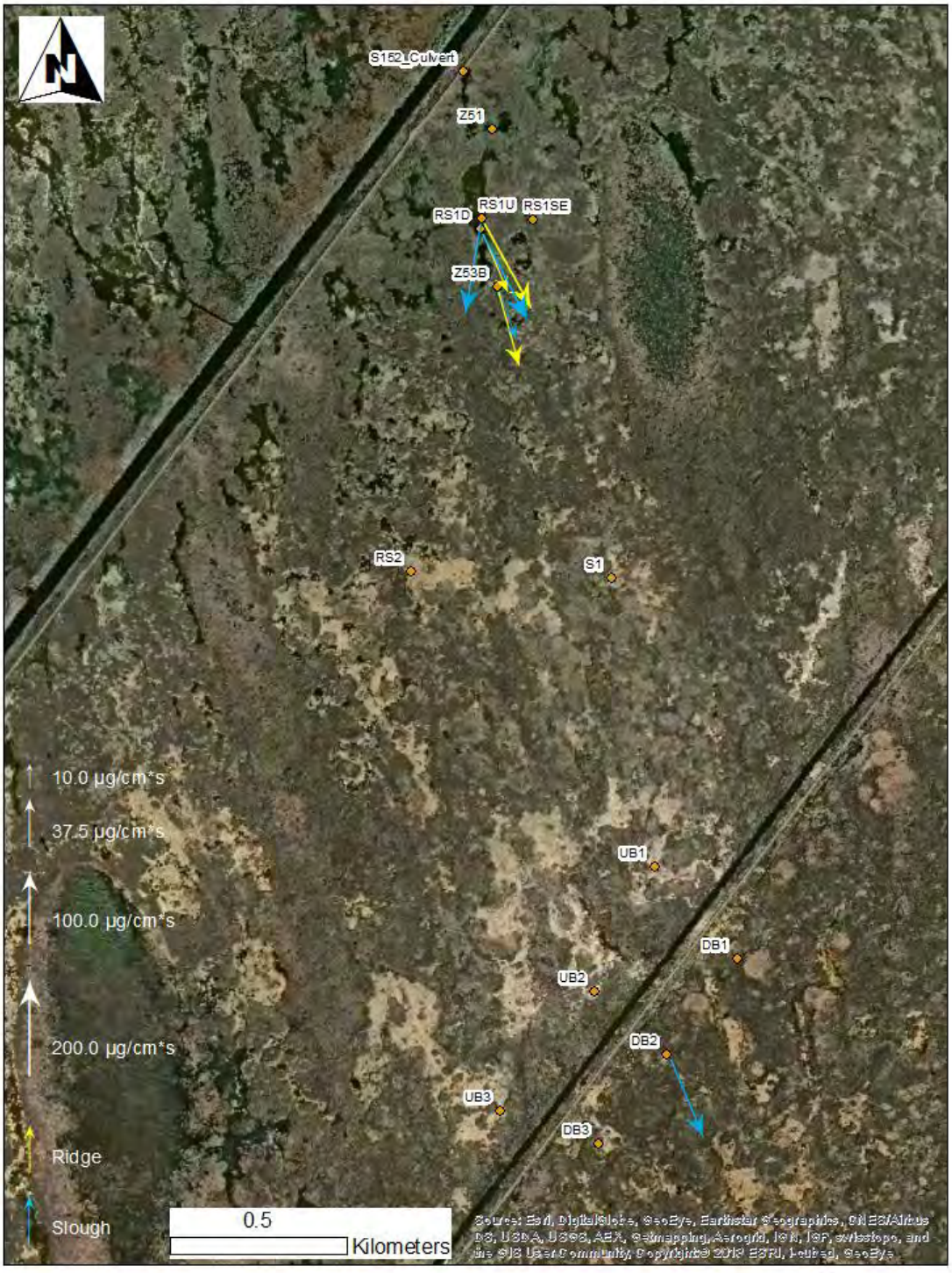

Figure D-150 Steady Flow 1 Suspended Sediment Load. Samples collected Nov. 7, 2014.

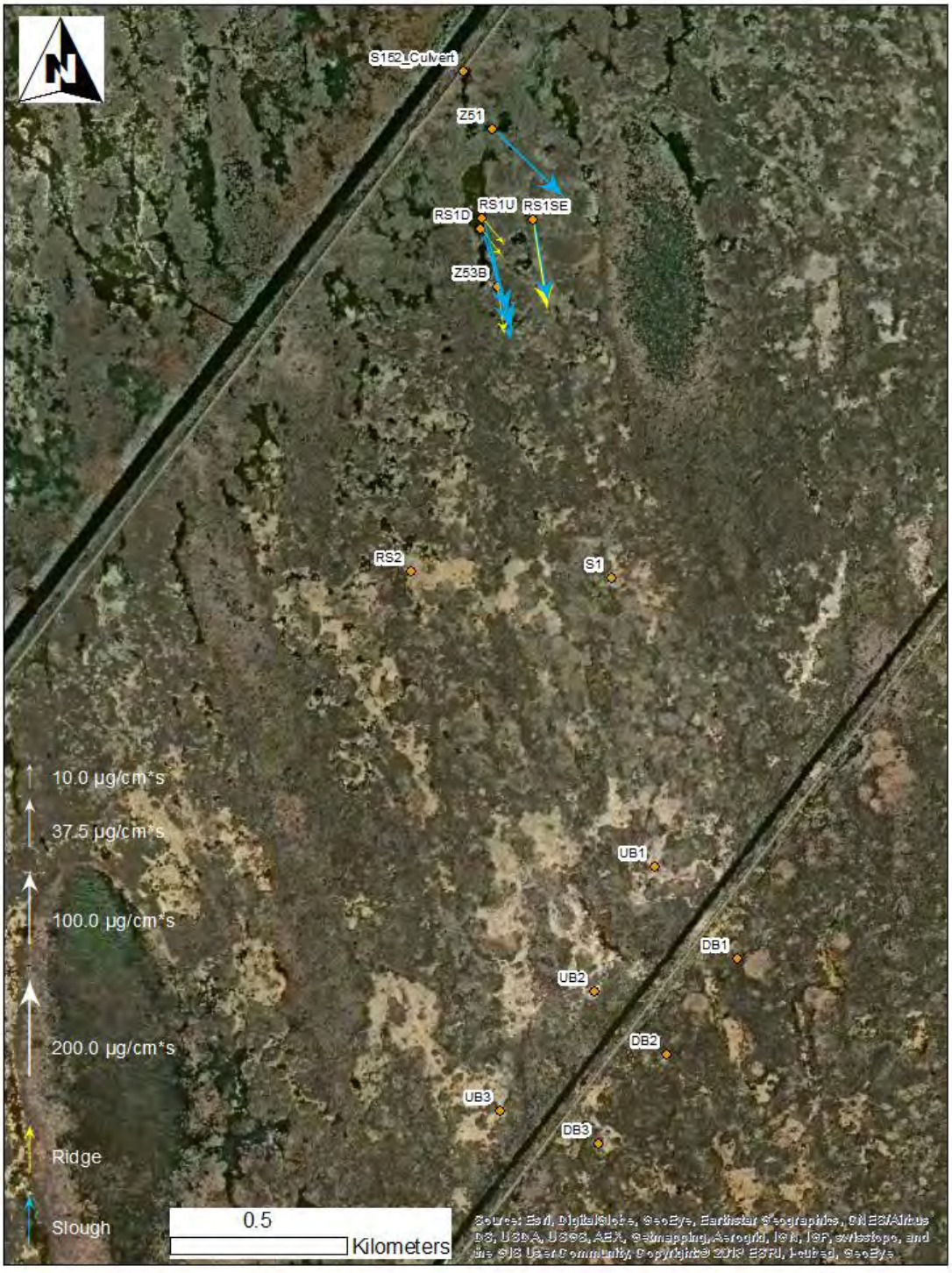

Figure D-151 Steady Flow 2 Suspended Sediment Load. Samples collected Dec 2 -3, 2014.

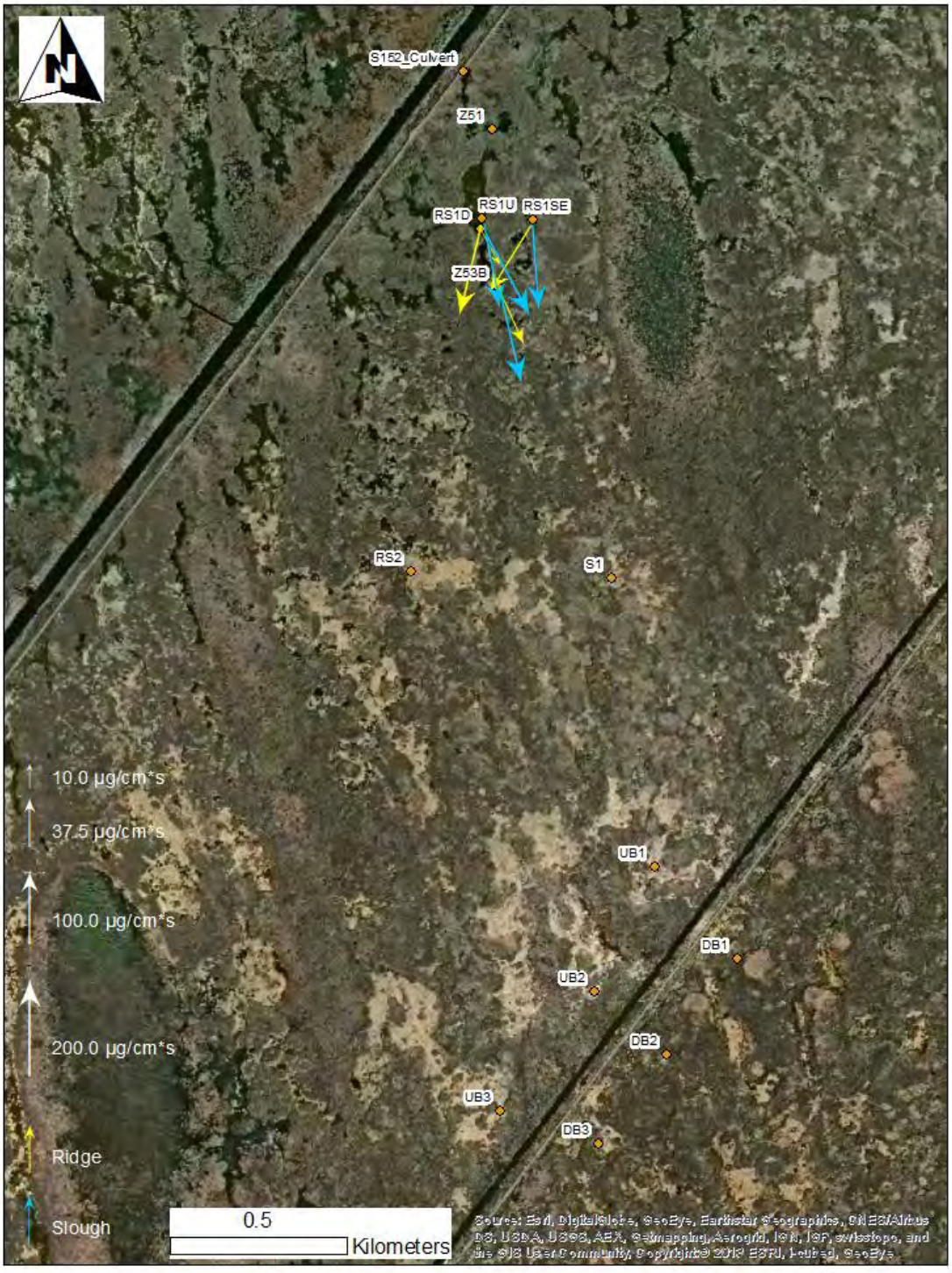

Figure D-152 Steady Flow 3 Suspended Sediment Load. Samples collected Jan. 19 - Jan. 22, 2015.

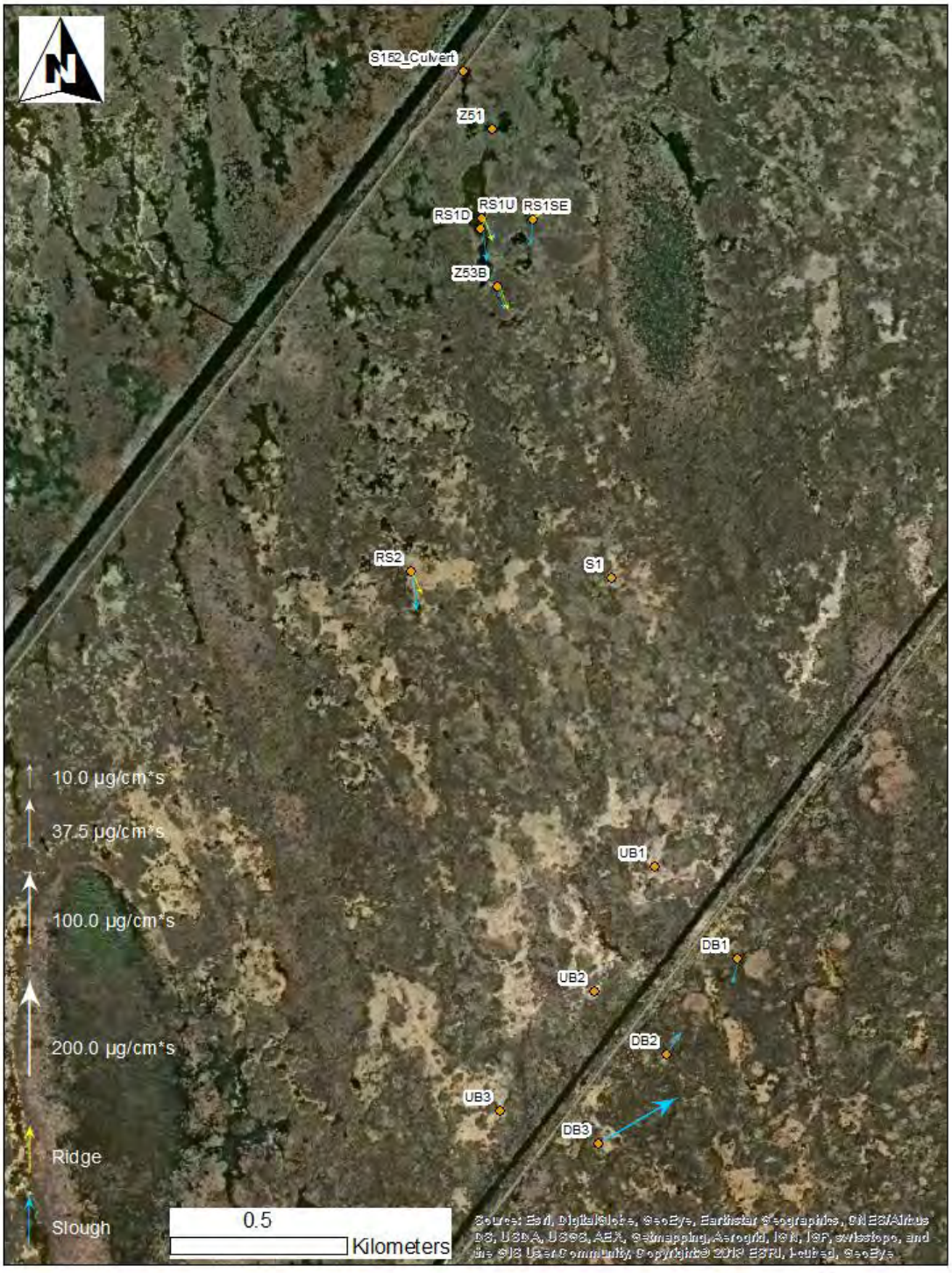

Figure D-153 Steady Flow 4 Suspended Sediment Load. Samples collected Mar. 9 - Mar. 10, 2015.

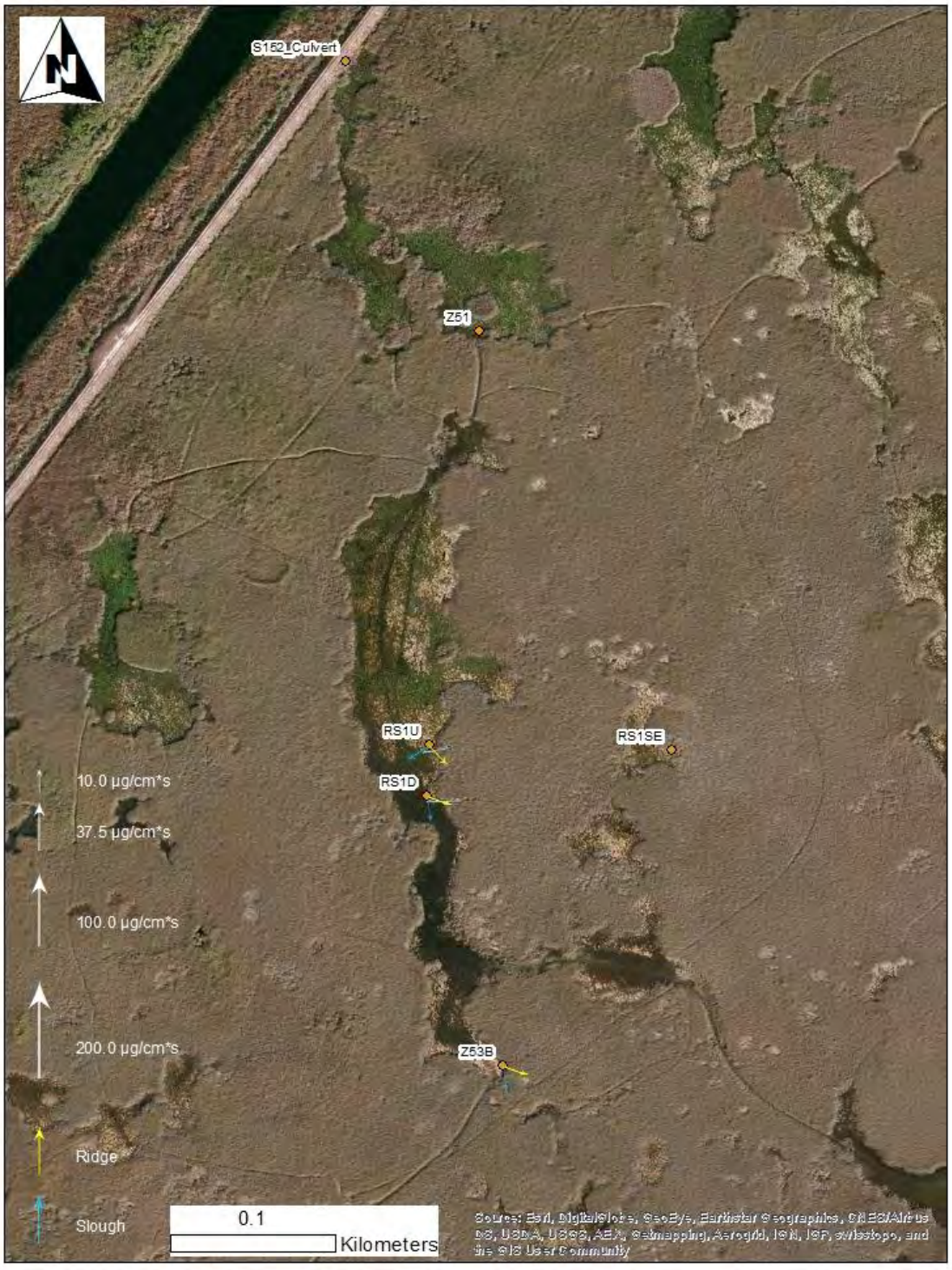

Figure D-154 Pre-release Suspended Sediment Load. Samples collected Oct. 31 – Nov. 3, 2014.

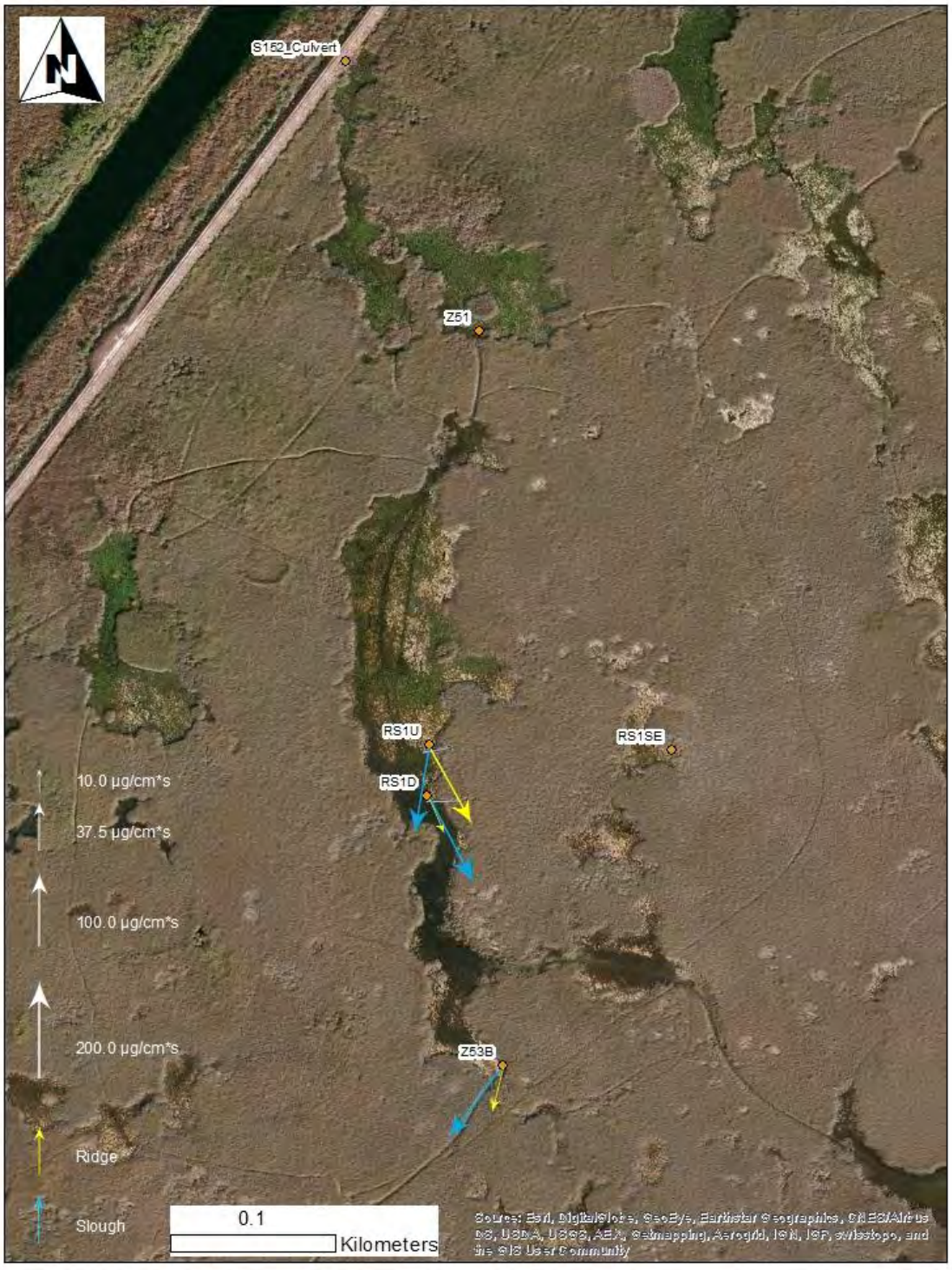

Figure D-155 Transient Flow 1 Suspended Sediment Load. Samples collected Nov. 4, 2014 at 10:50.

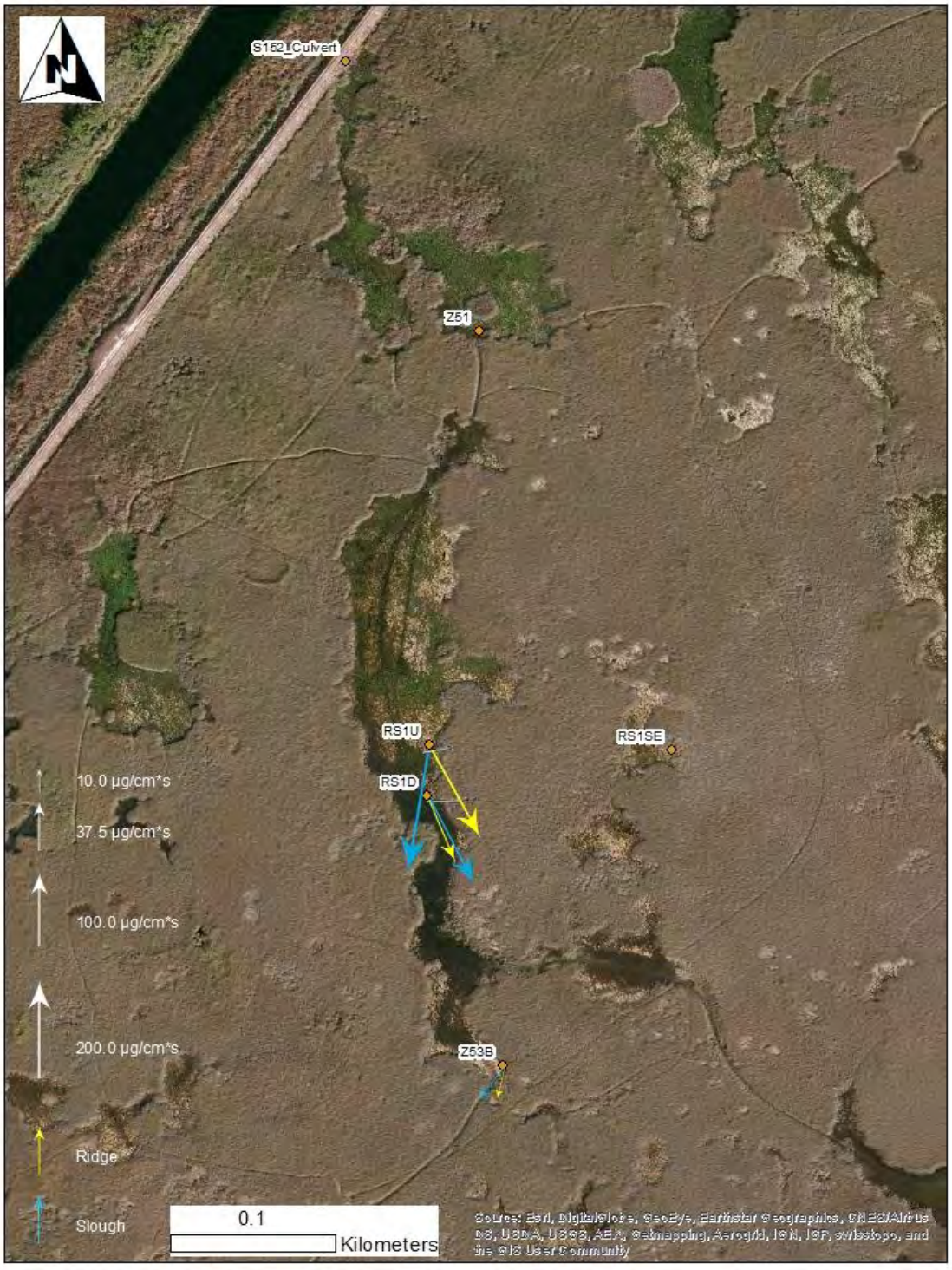

Figure D-156 Transient Flow 1 Suspended Sediment Load. Samples collected Nov. 4, 2014 at 12:00.

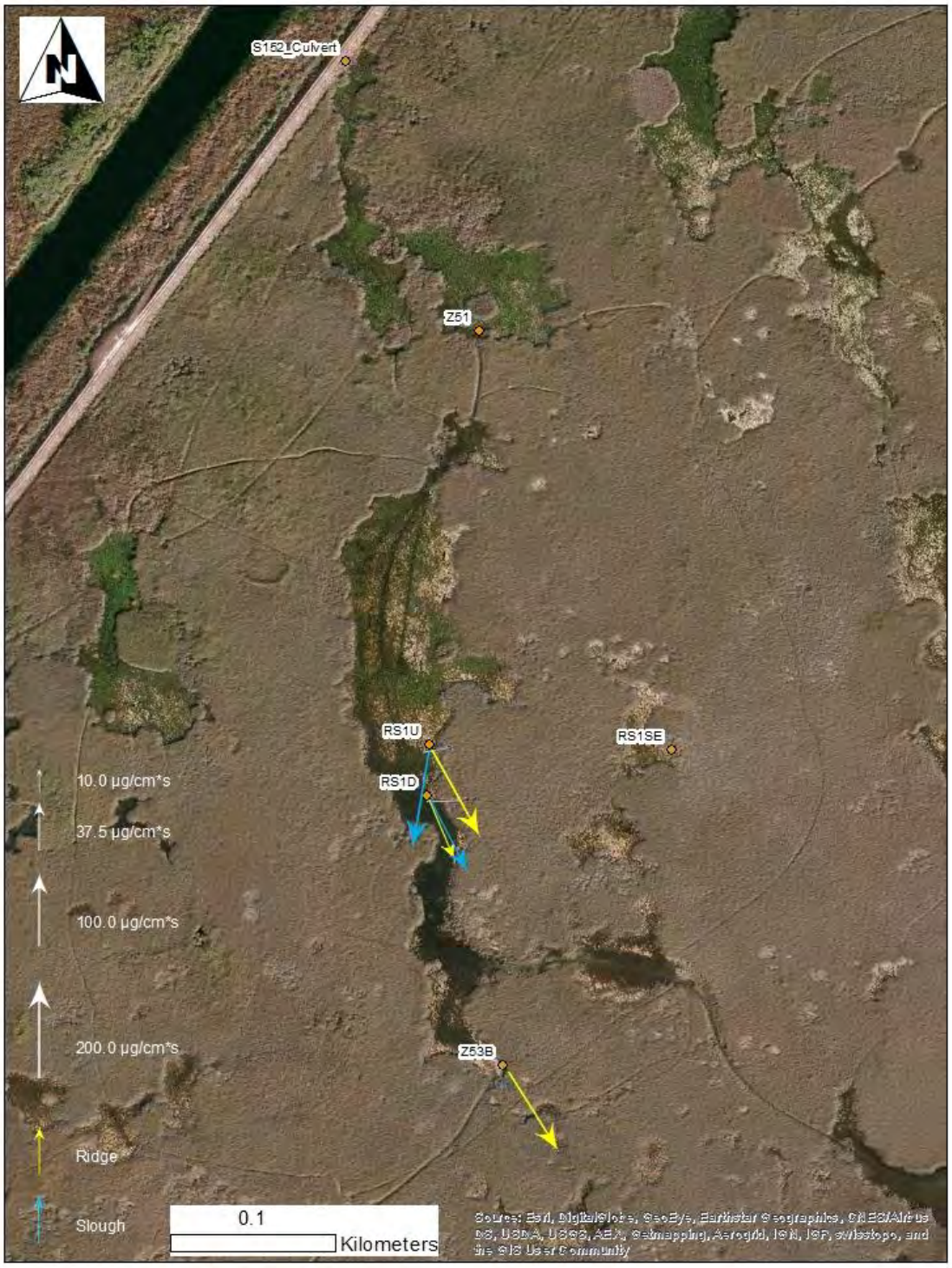

Figure D-157 Transient Flow 1 Suspended Sediment Load. Samples collected Nov. 4, 2014 at 14:00.

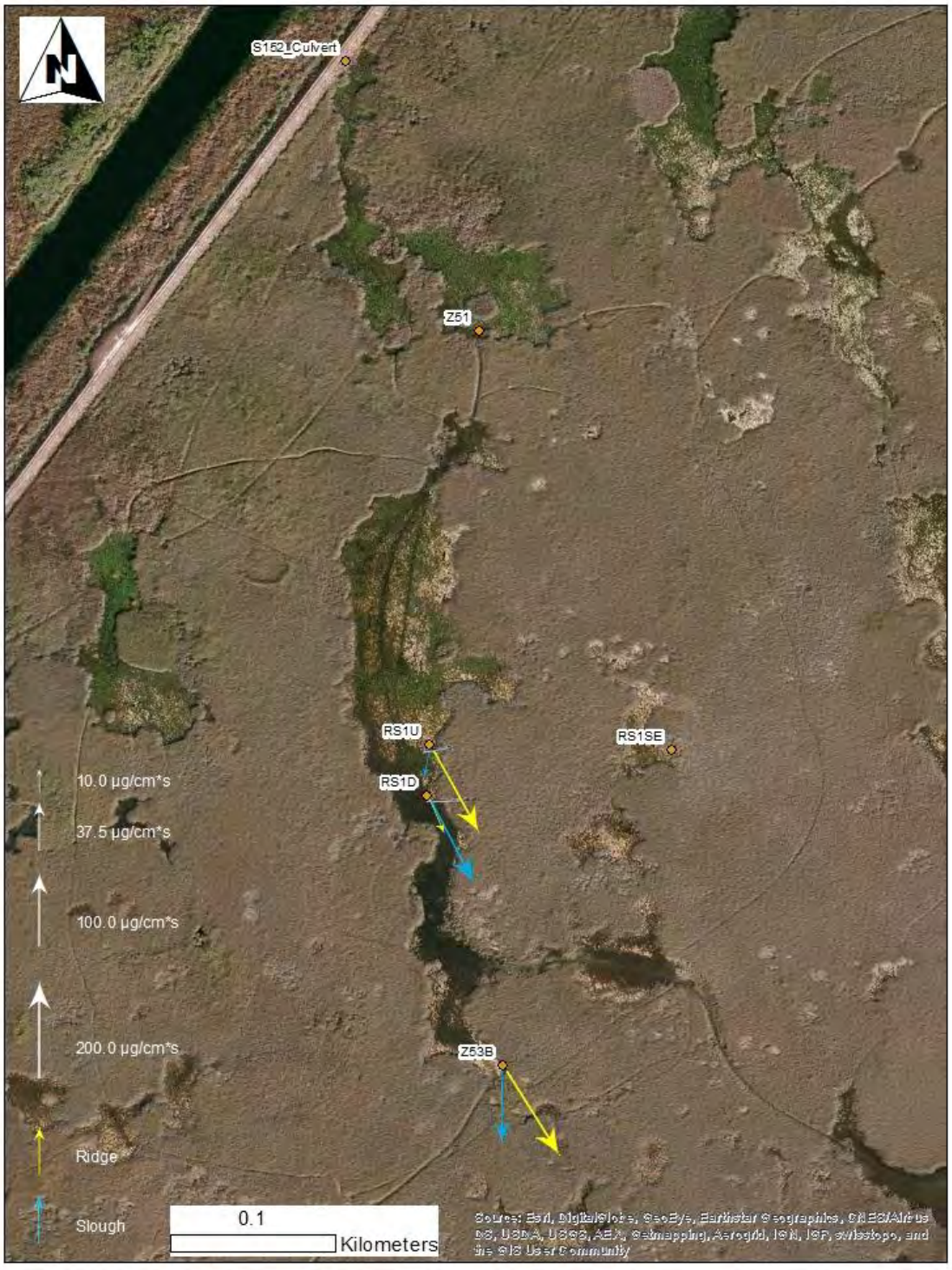

Figure D-158 Transient Flow 1 Suspended Sediment Load. Samples collected Nov. 4, 2014 at 16:00.

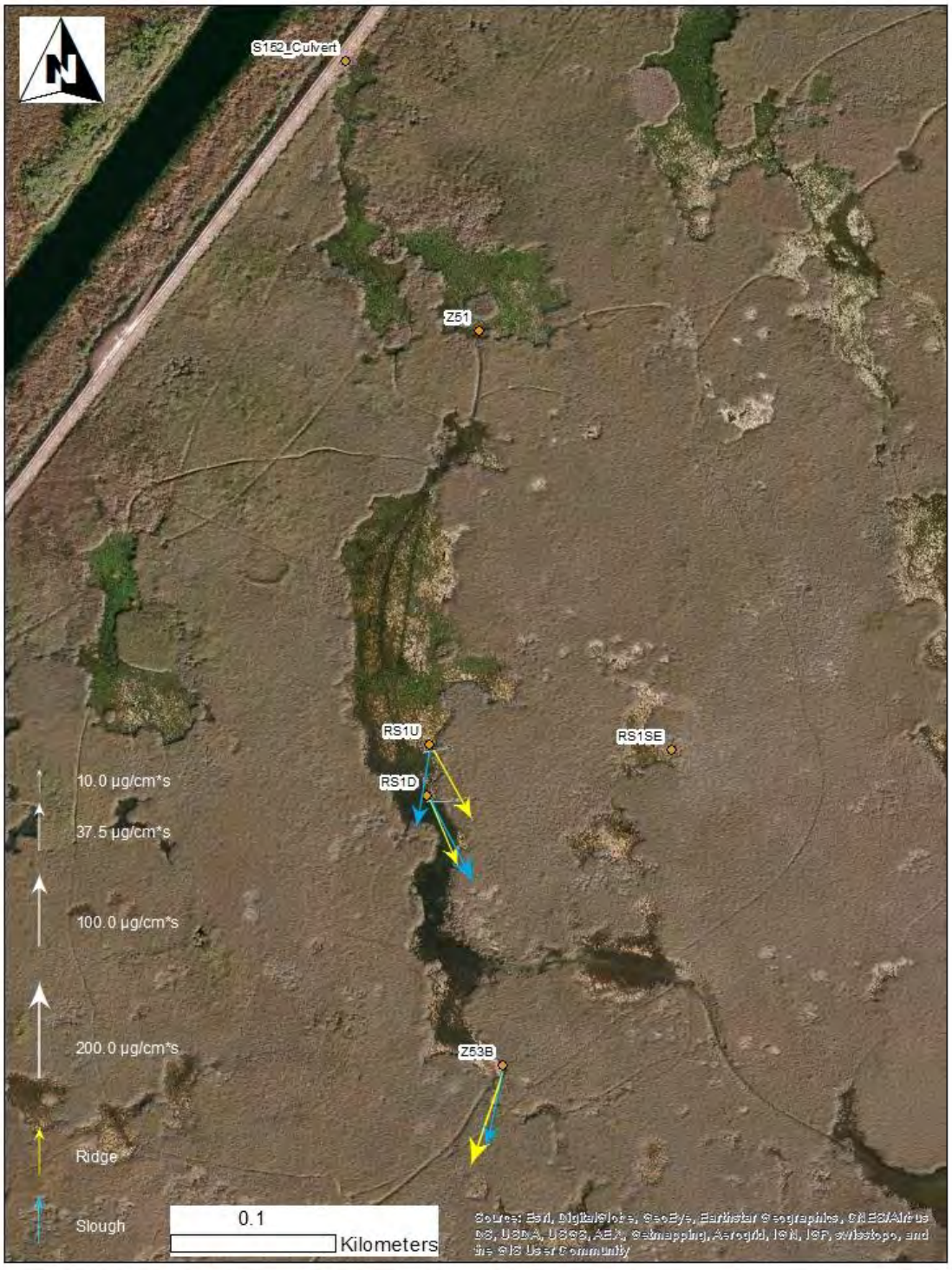

Figure D-159 Transient Flow 2 Suspended Sediment Load. Samples collected Nov. 5, 2014.

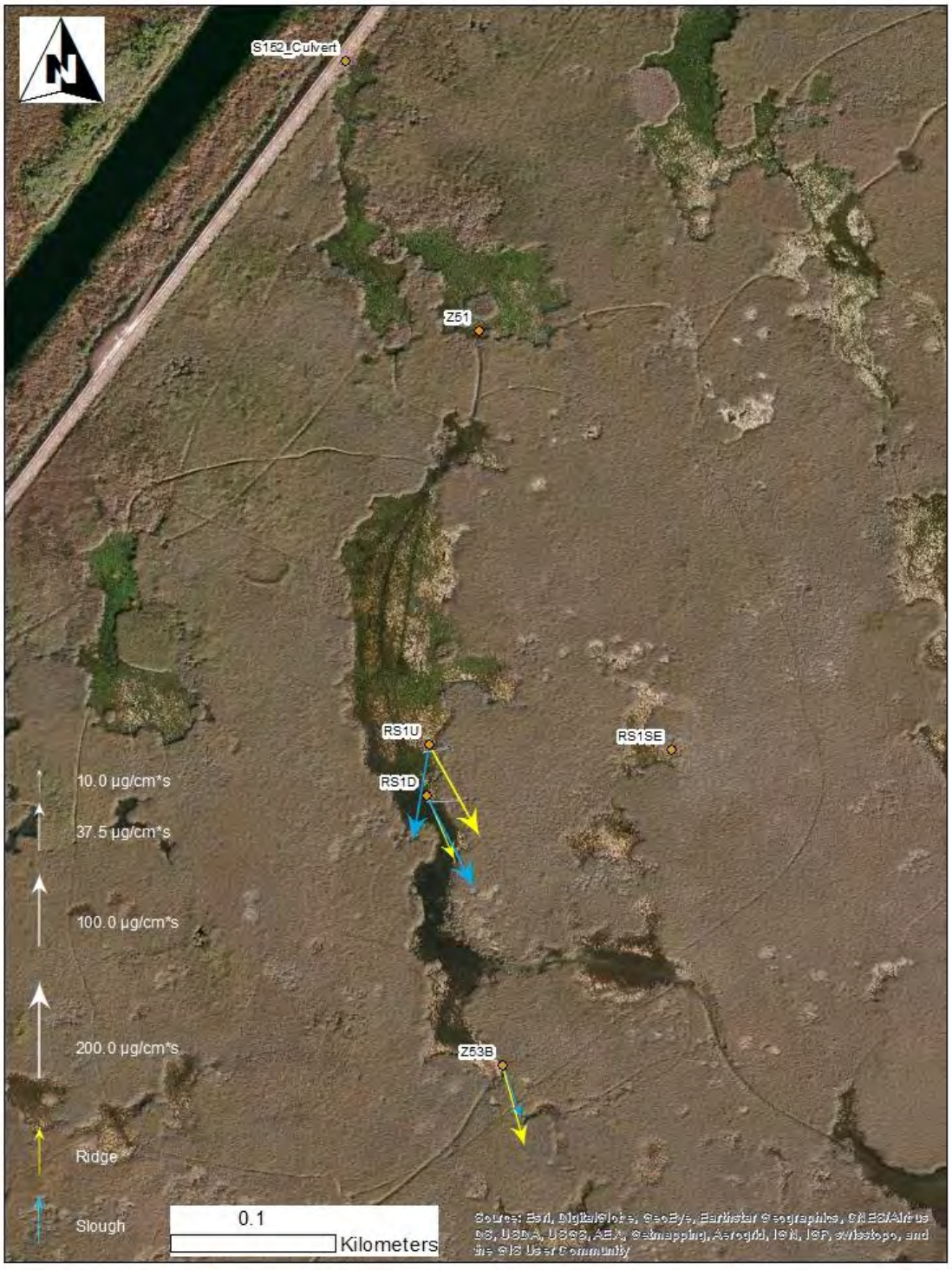

Figure D-160 Steady Flow 1 Suspended Sediment Load. Samples collected Nov. 7, 2014.

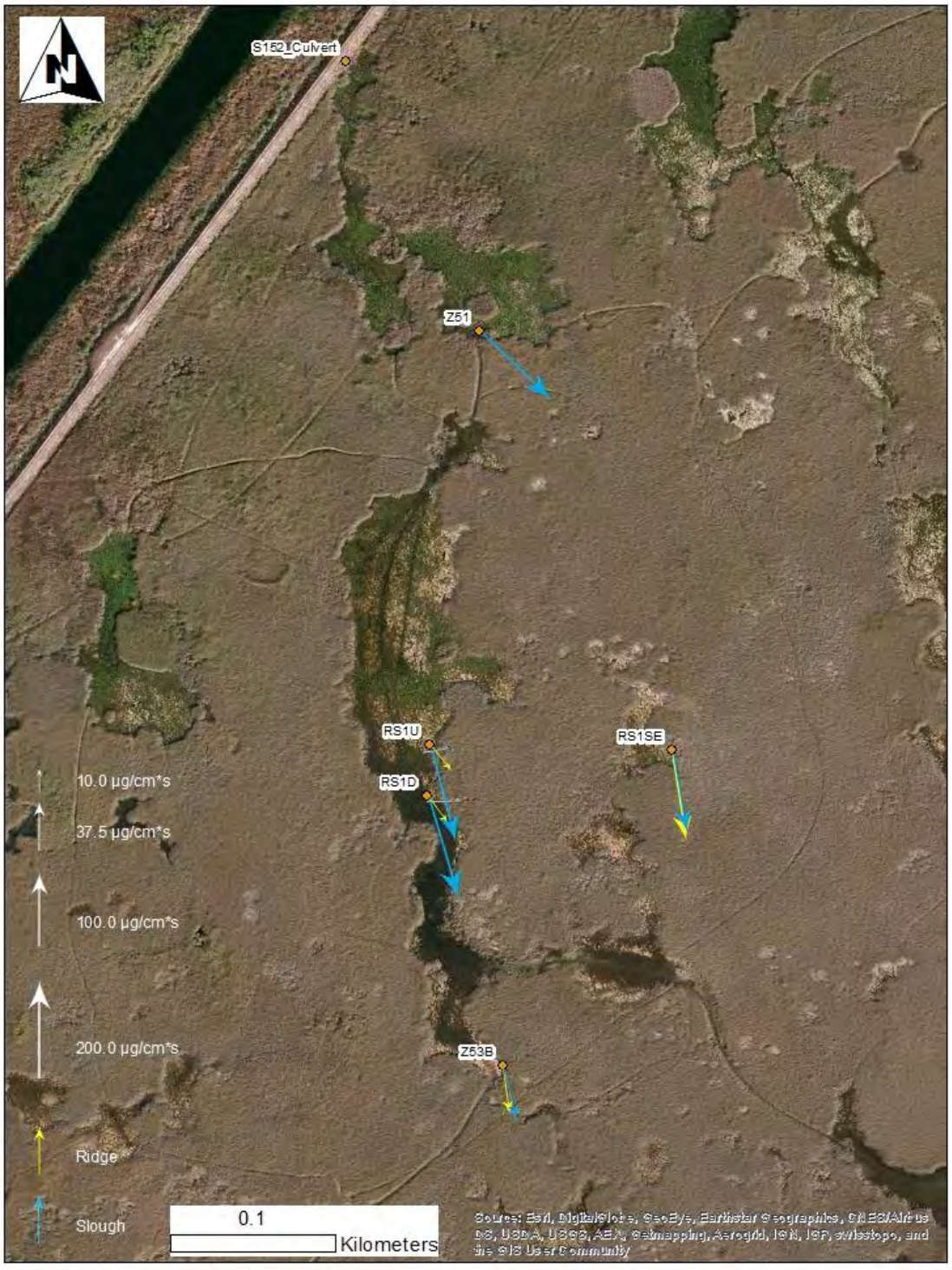

Figure D-161 Steady Flow 2 Suspended Sediment Load. Samples collected Dec 2 -3, 2014.

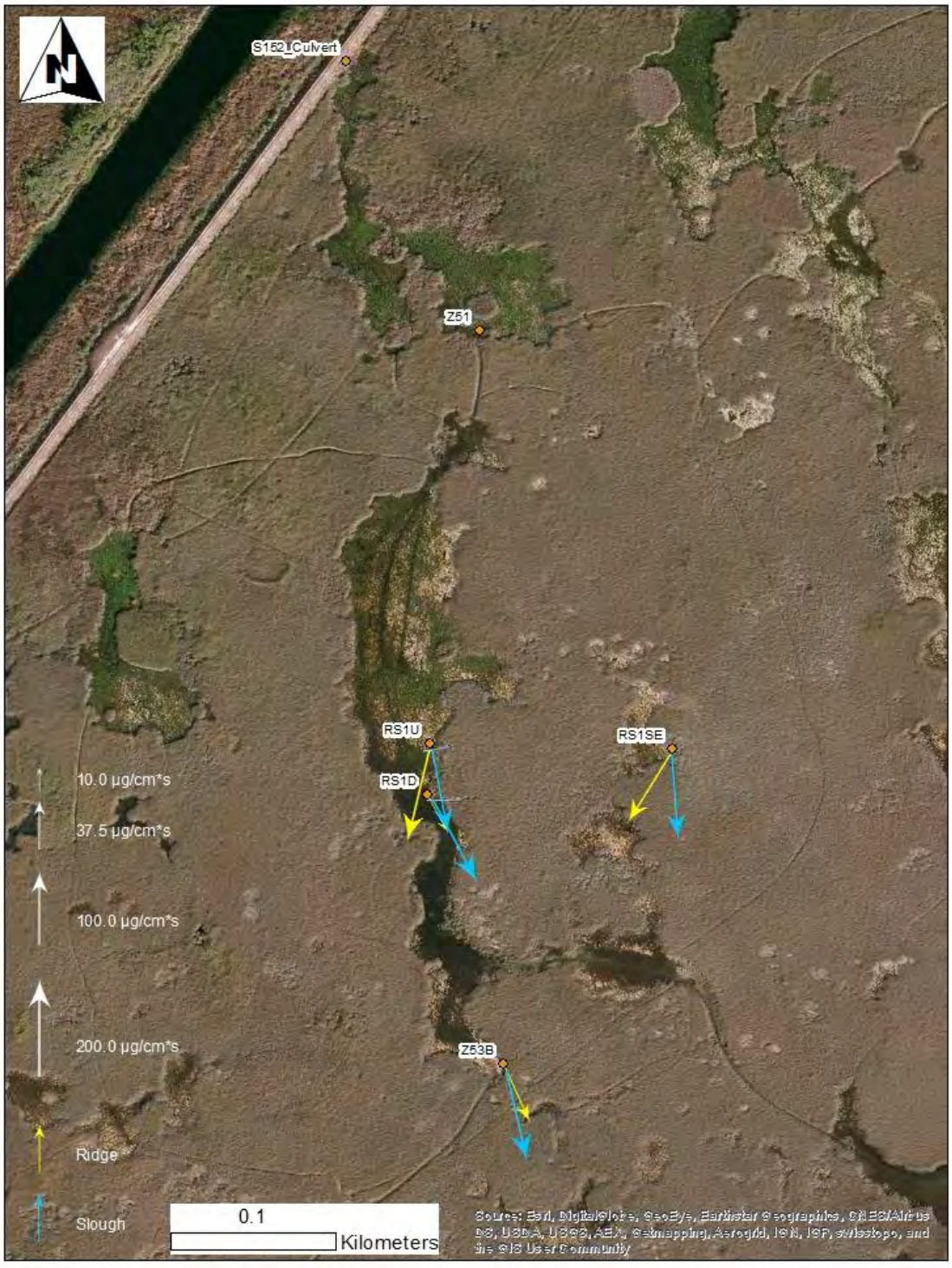

Figure D-162 Steady Flow 3 Suspended Sediment Load. Samples collected Jan. 19 - Jan. 22, 2015

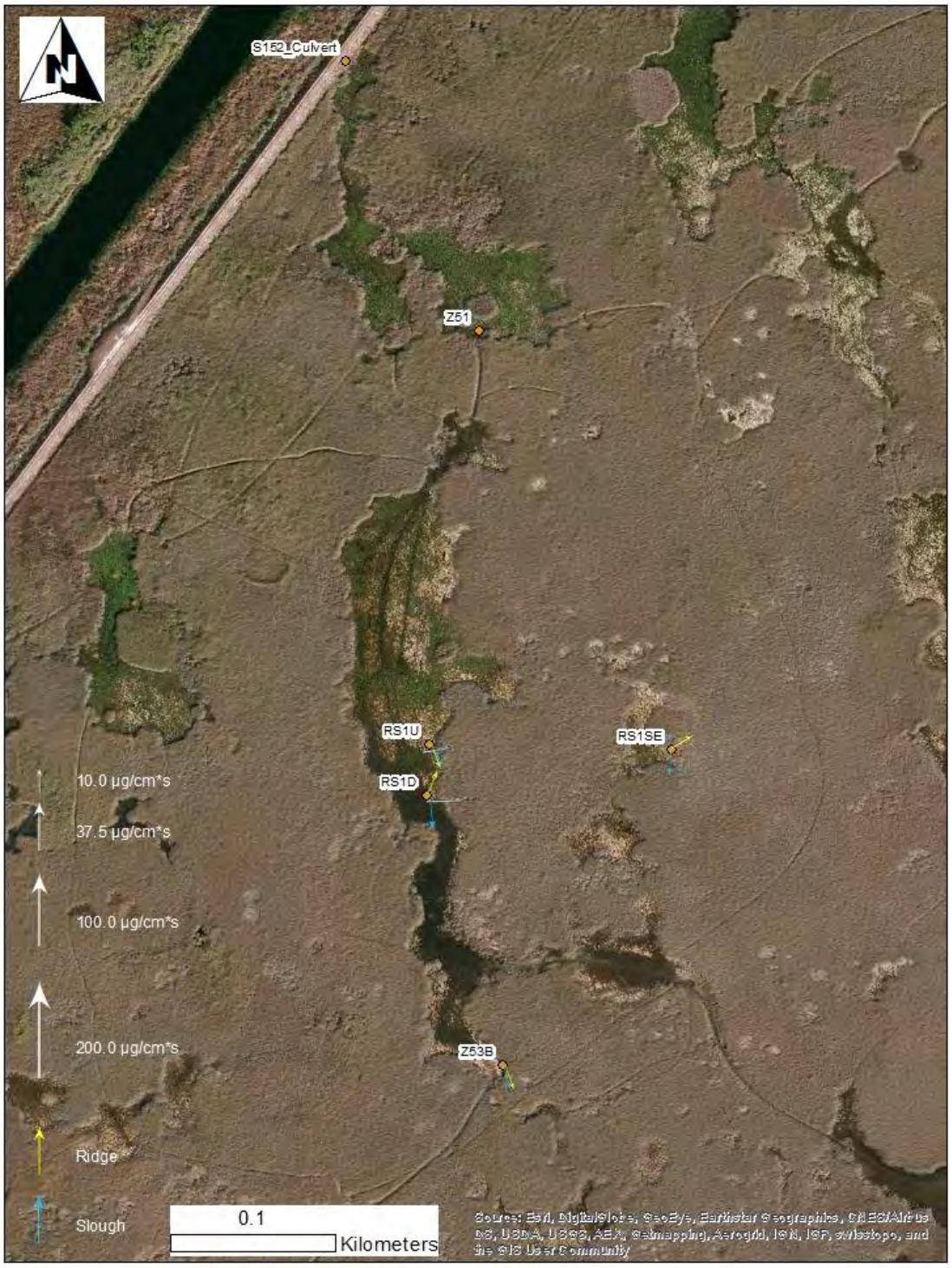

Figure D-163 Steady Flow 4 Suspended Sediment Load. Samples collected Mar. 9 - Mar. 11, 2015.

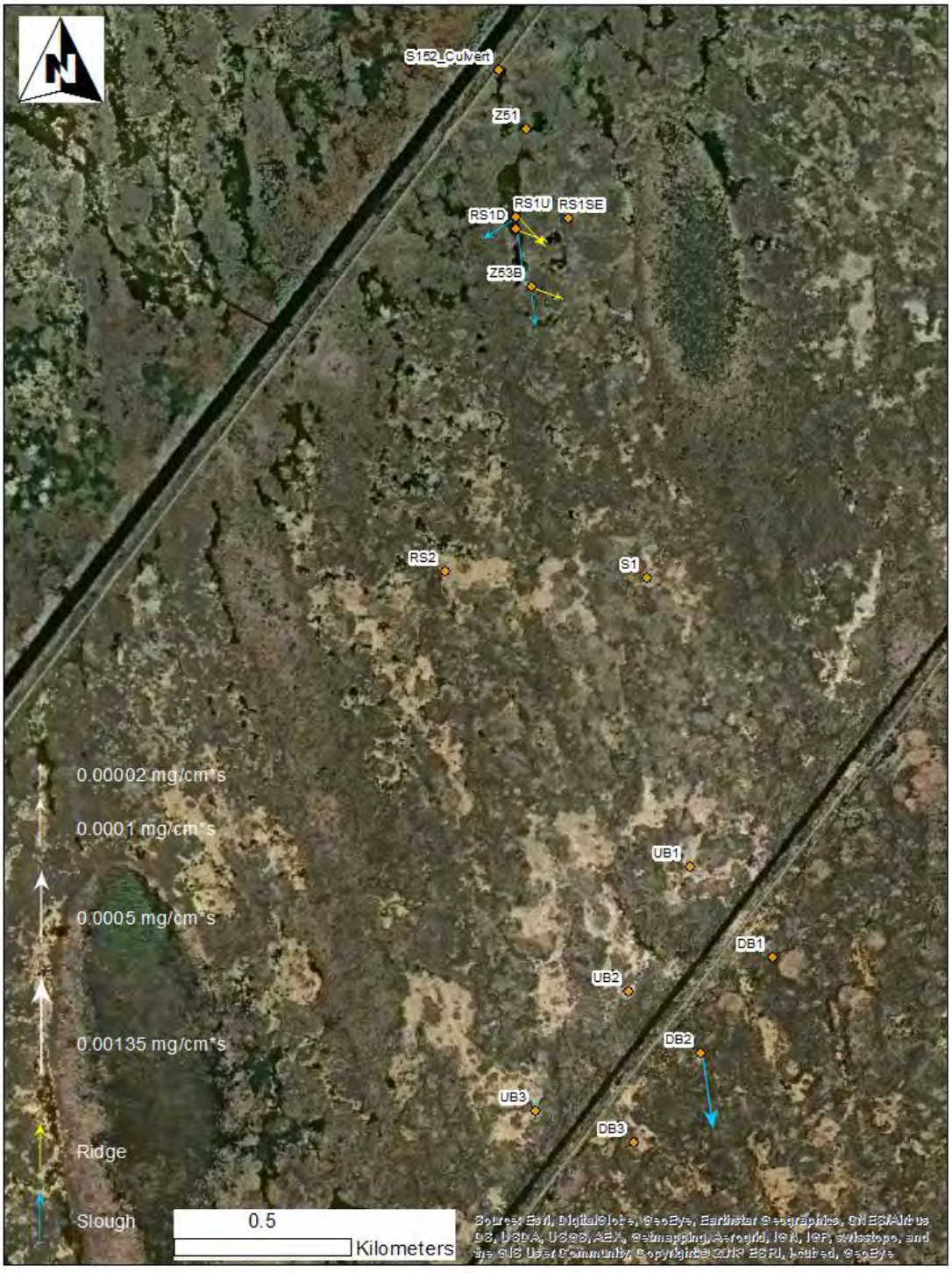

Figure D-164 Pre-release Phosphorus Load. Samples collected Oct. 31 - Nov. 3, 2014.

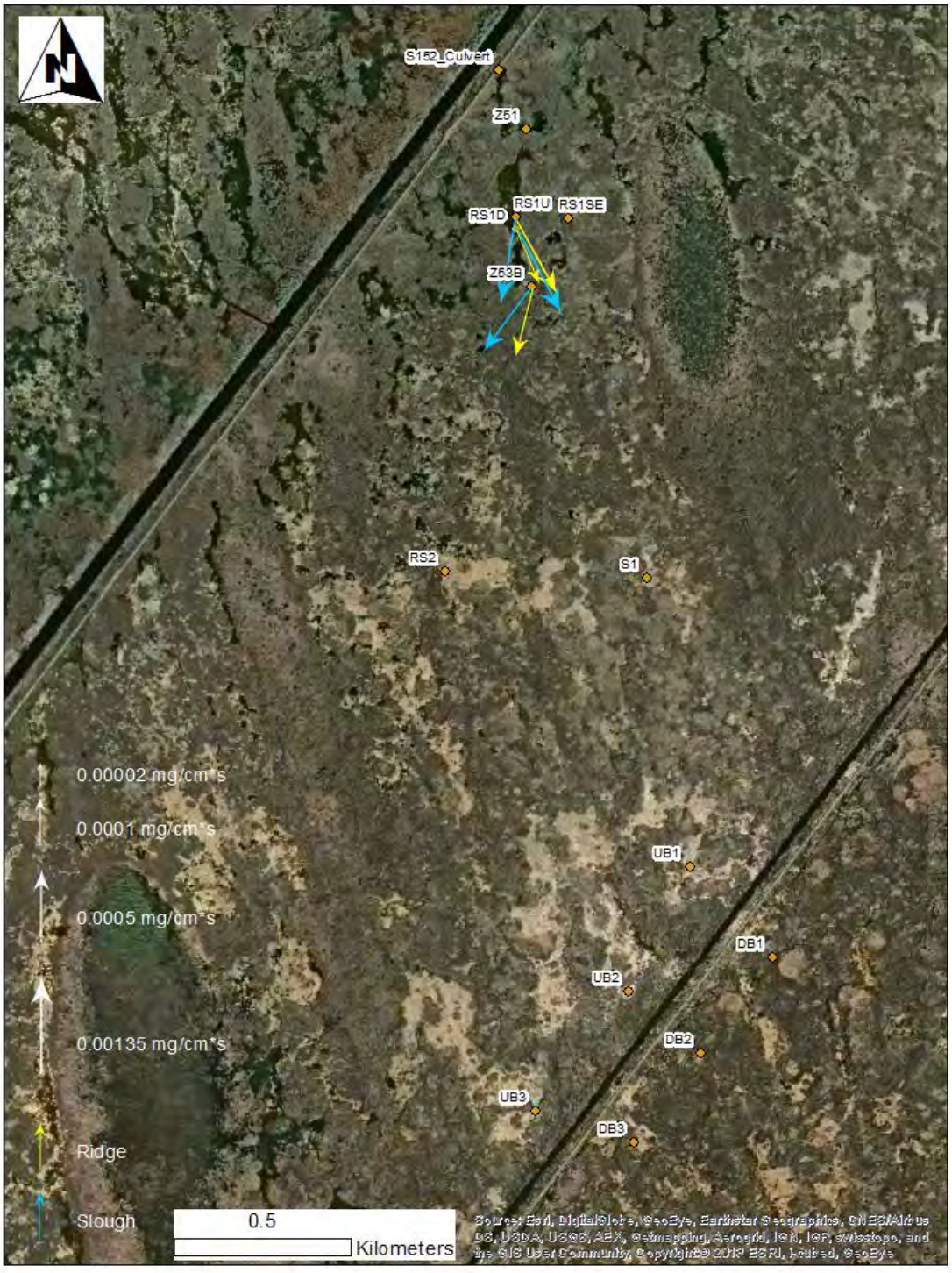

Figure D-165 Transient Flow 1 Phosphorus Load. Samples collected Nov. 4, 2014 at 11:10.

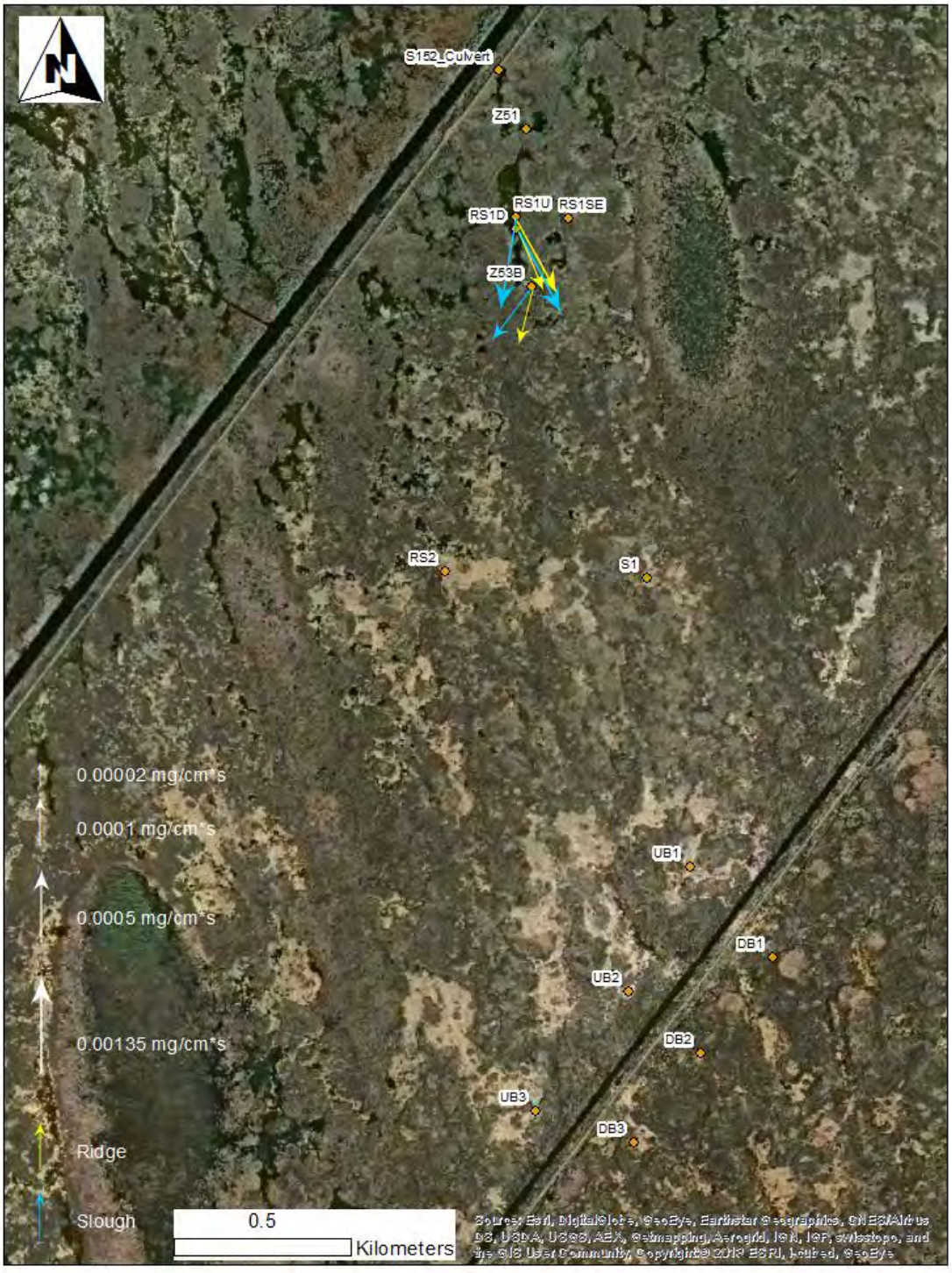

Figure D-166 Transient Flow 1 Phosphorus Load. Samples collected Nov. 4, 2014 at 12:30.

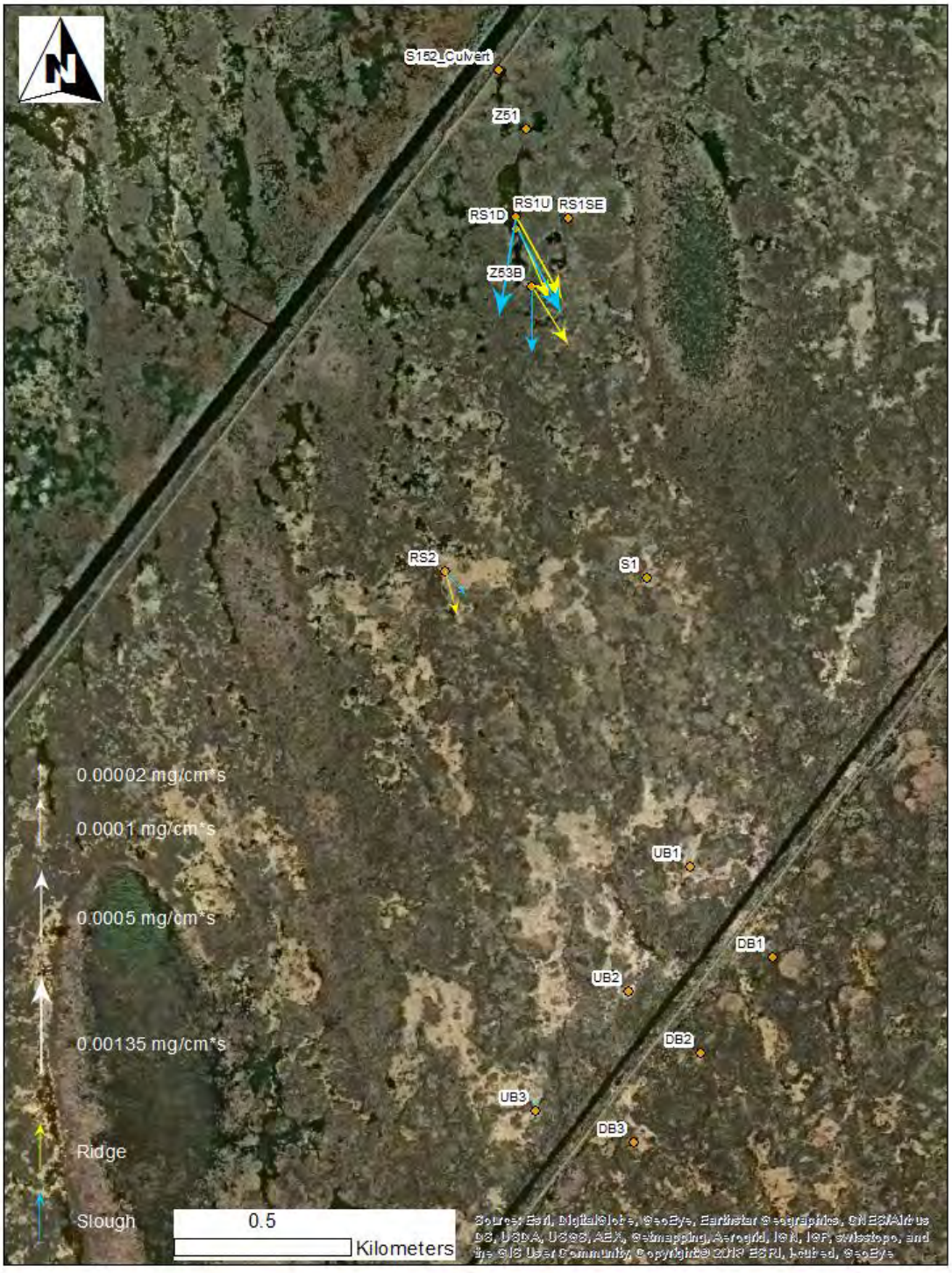

Figure D-167 Transient Flow 1 Phosphorus Load. Samples collected Nov. 4, 2014 from 14:20.

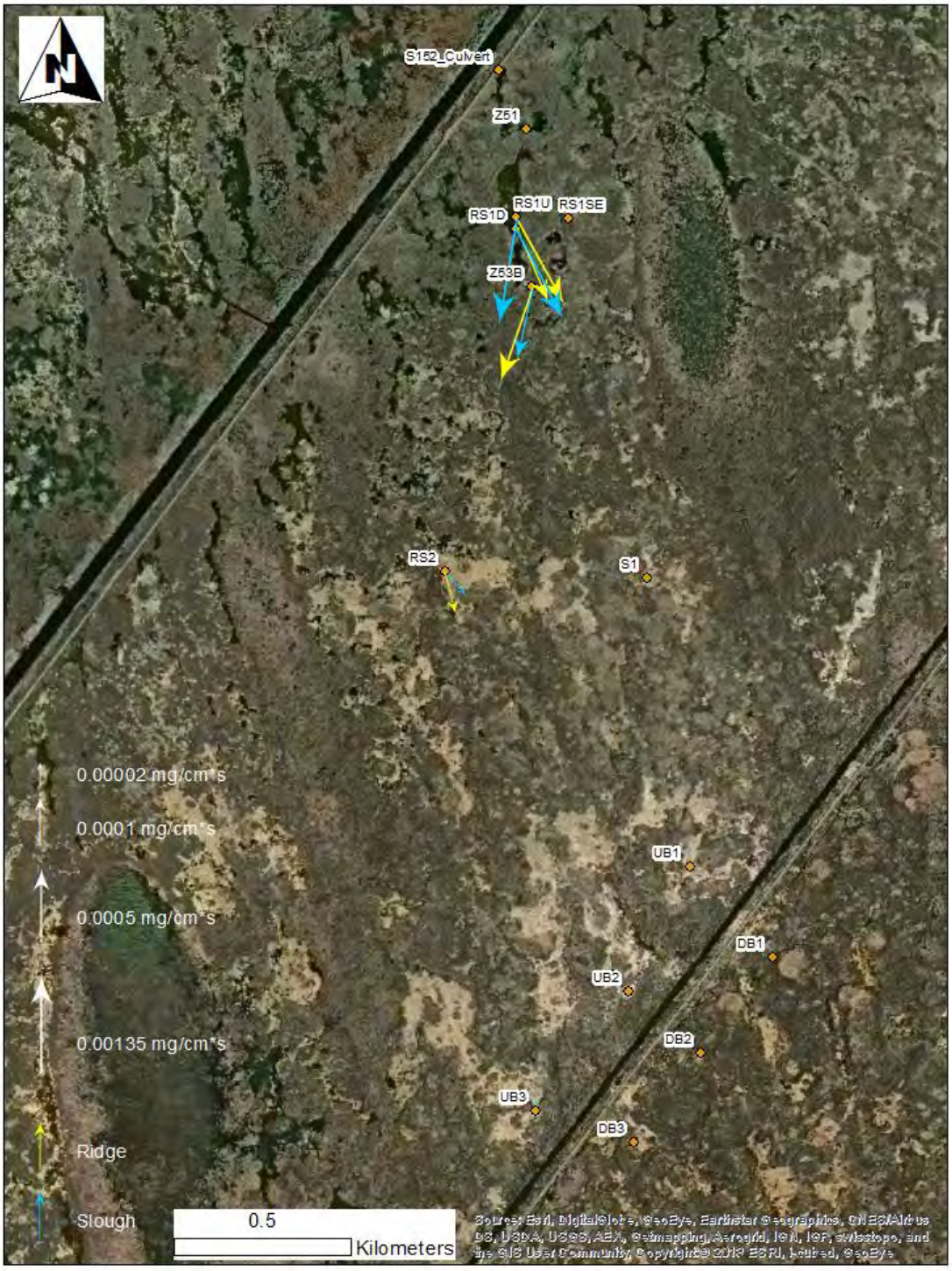

Figure D-168 Transient Flow 2 Phosphorus Load. Samples collected Nov. 5, 2014.

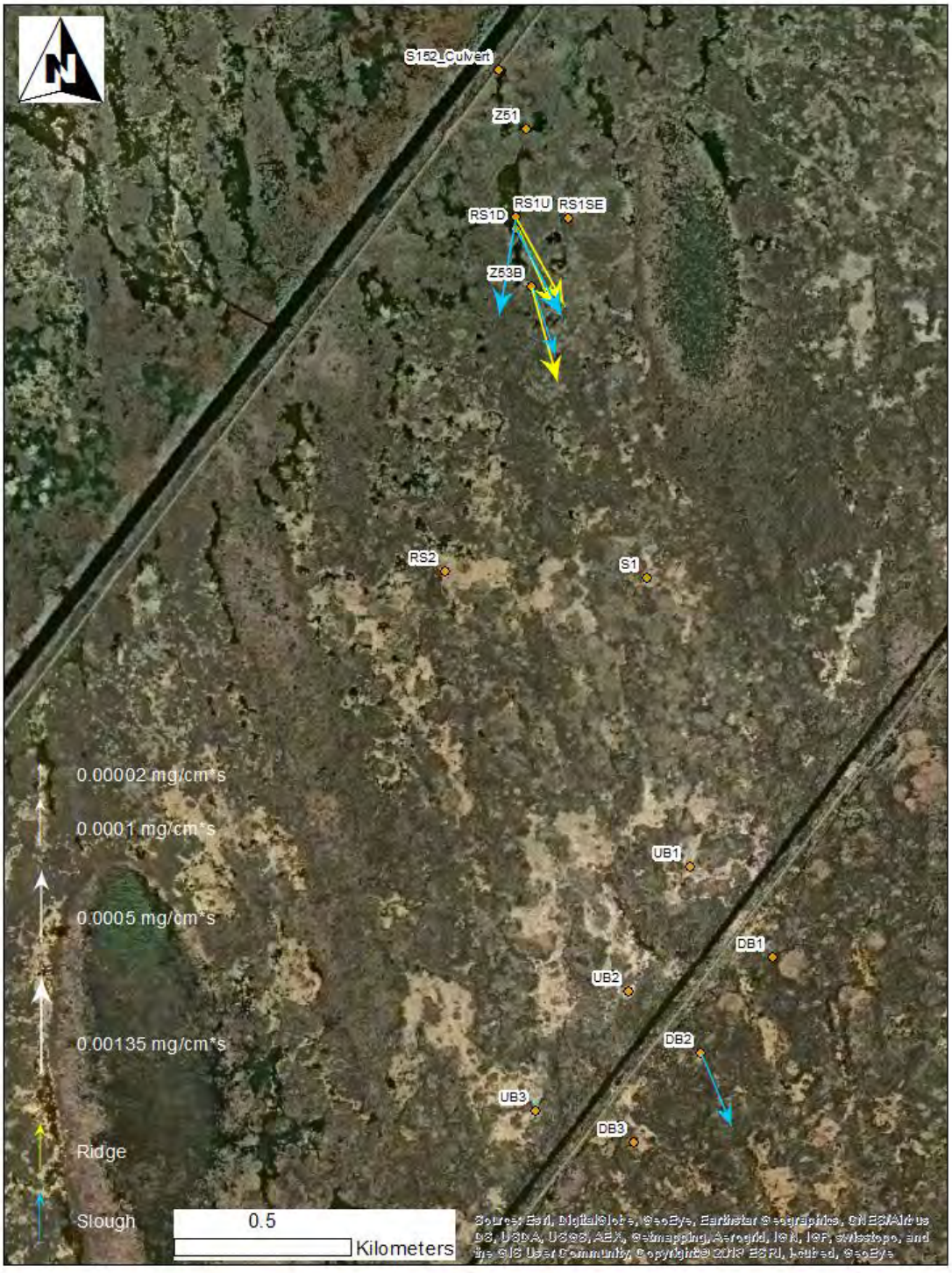

Figure D-169 Steady Flow 1 Phosphorus Load. Samples collected Nov. 7, 2014.

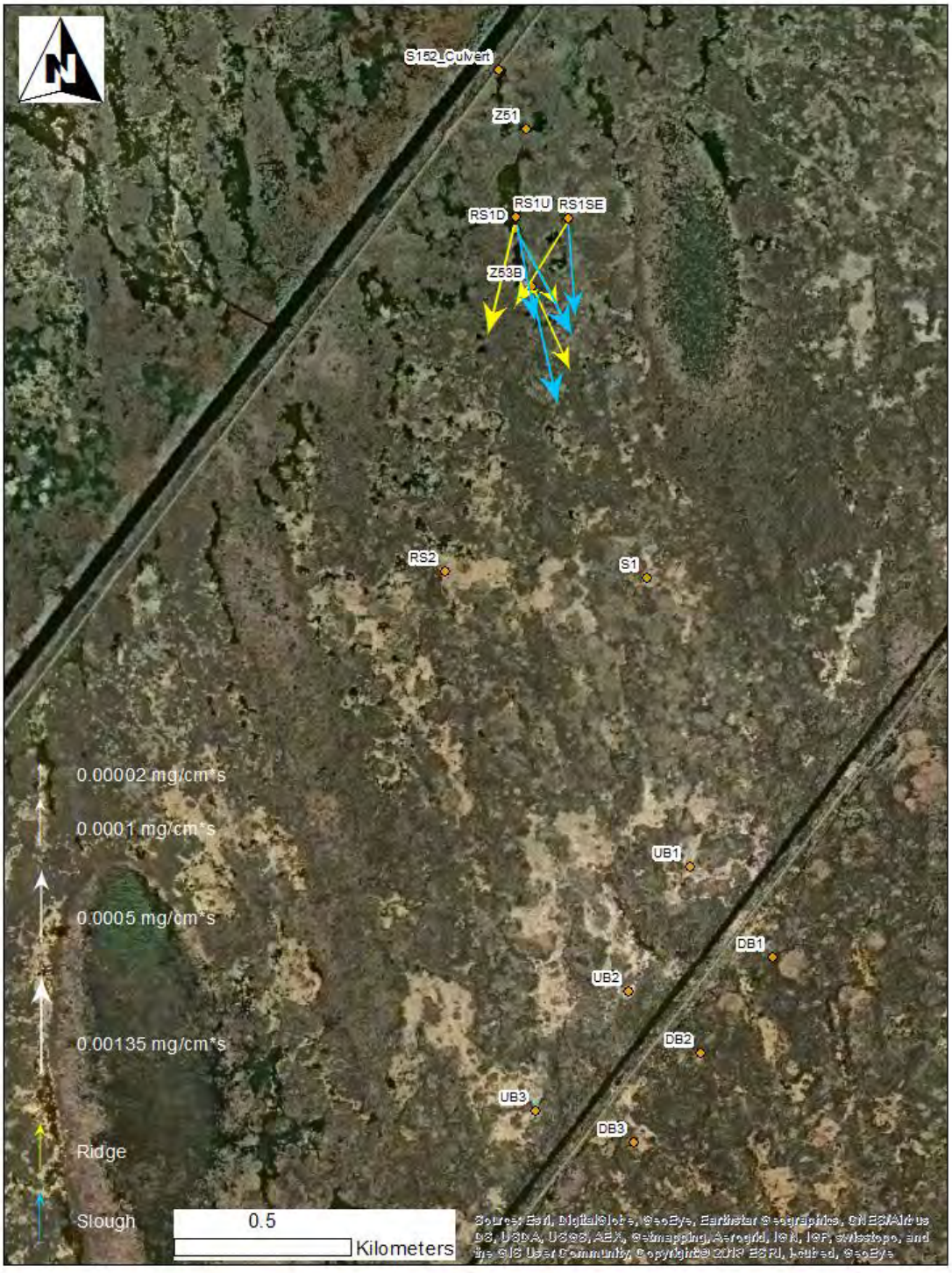

Figure D-170 Steady Flow 3 Phosphorus Load. Samples collected Jan. 19 – Jan. 22, 2015.

Figure D-171 Steady Flow 4 Phosphorus Load. Samples collected Mar. 9 – Mar. 11, 2015.

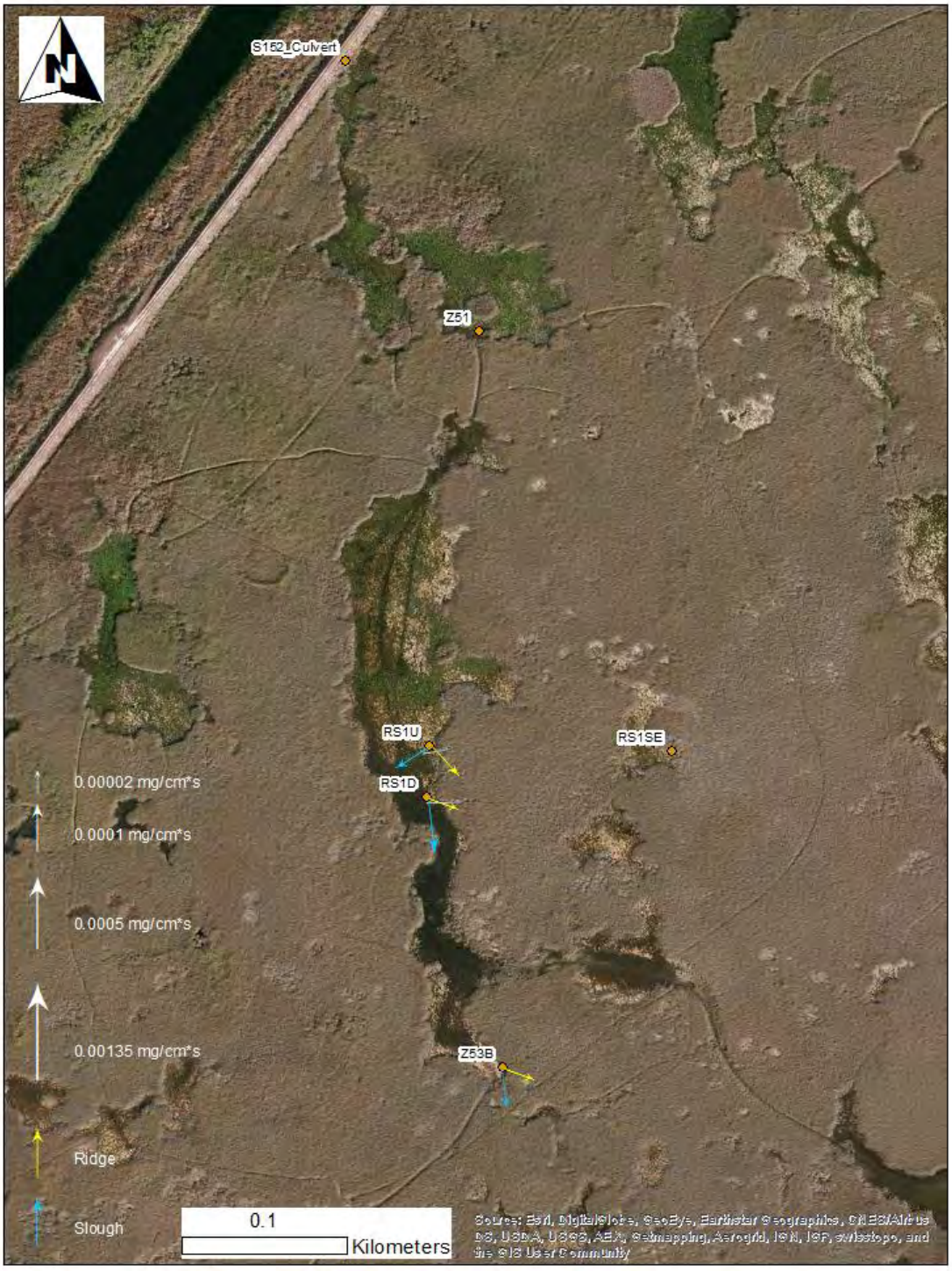

Figure D-172 Pre-release Phosphorus Load. Samples collected Oct. 31 - Nov. 3, 2014.

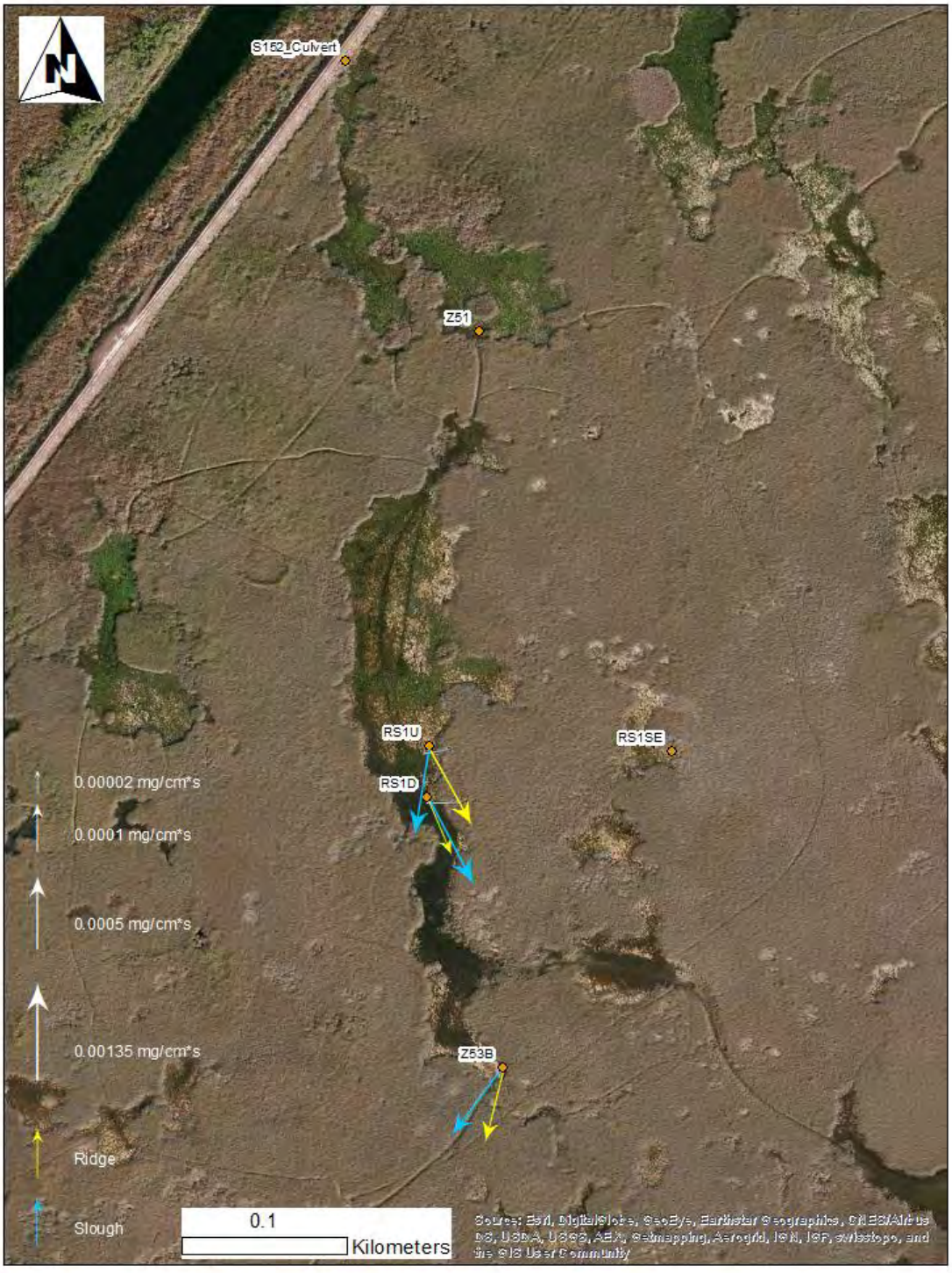

Figure D-173 Transient Flow 1 Phosphorus Load. Samples collected Nov. 4, 2014 at 11:10.

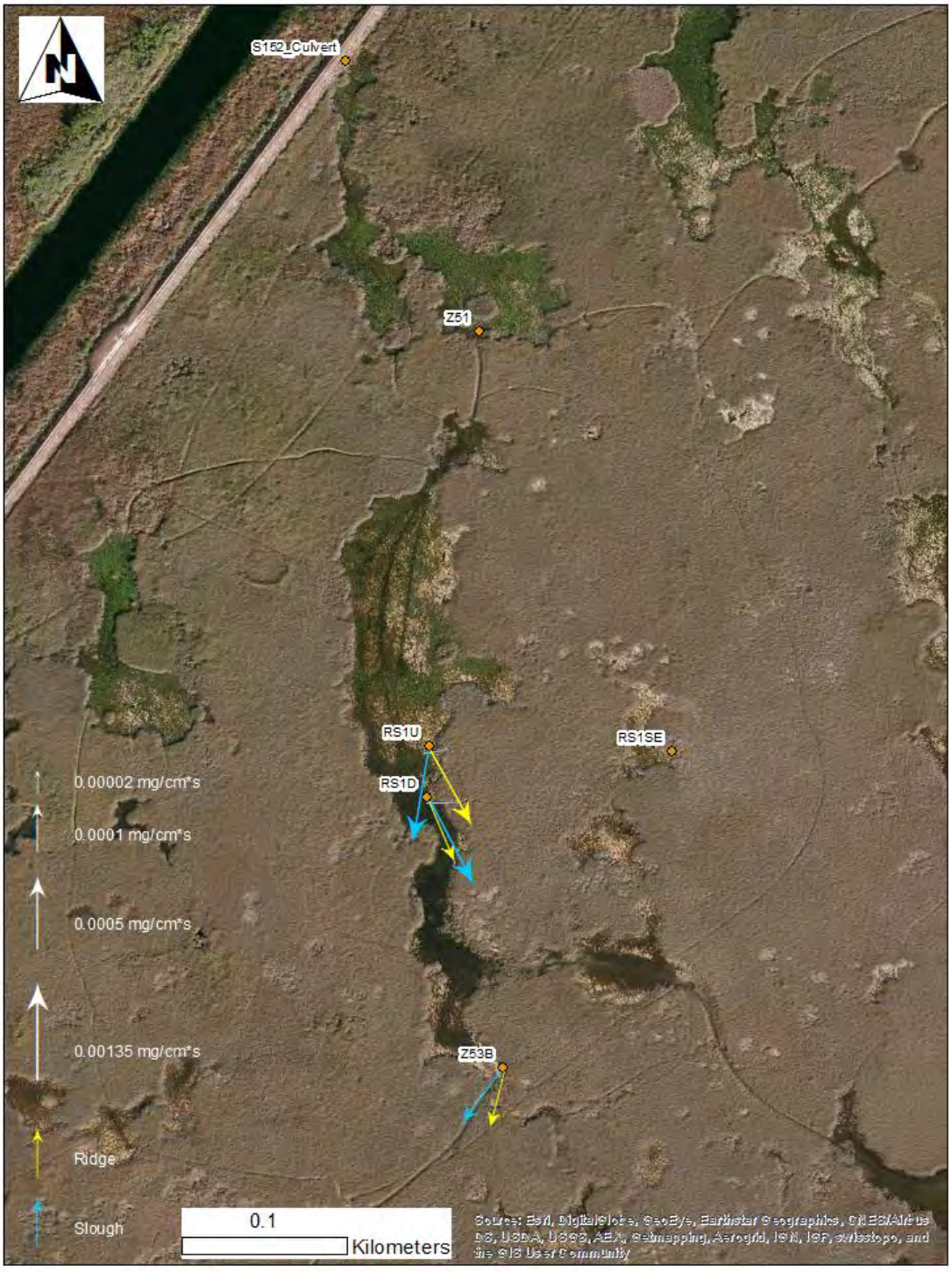

Figure D-174 Transient Flow 1 Phosphorus Load. Samples collected Nov. 4, 2014 at 12:30.

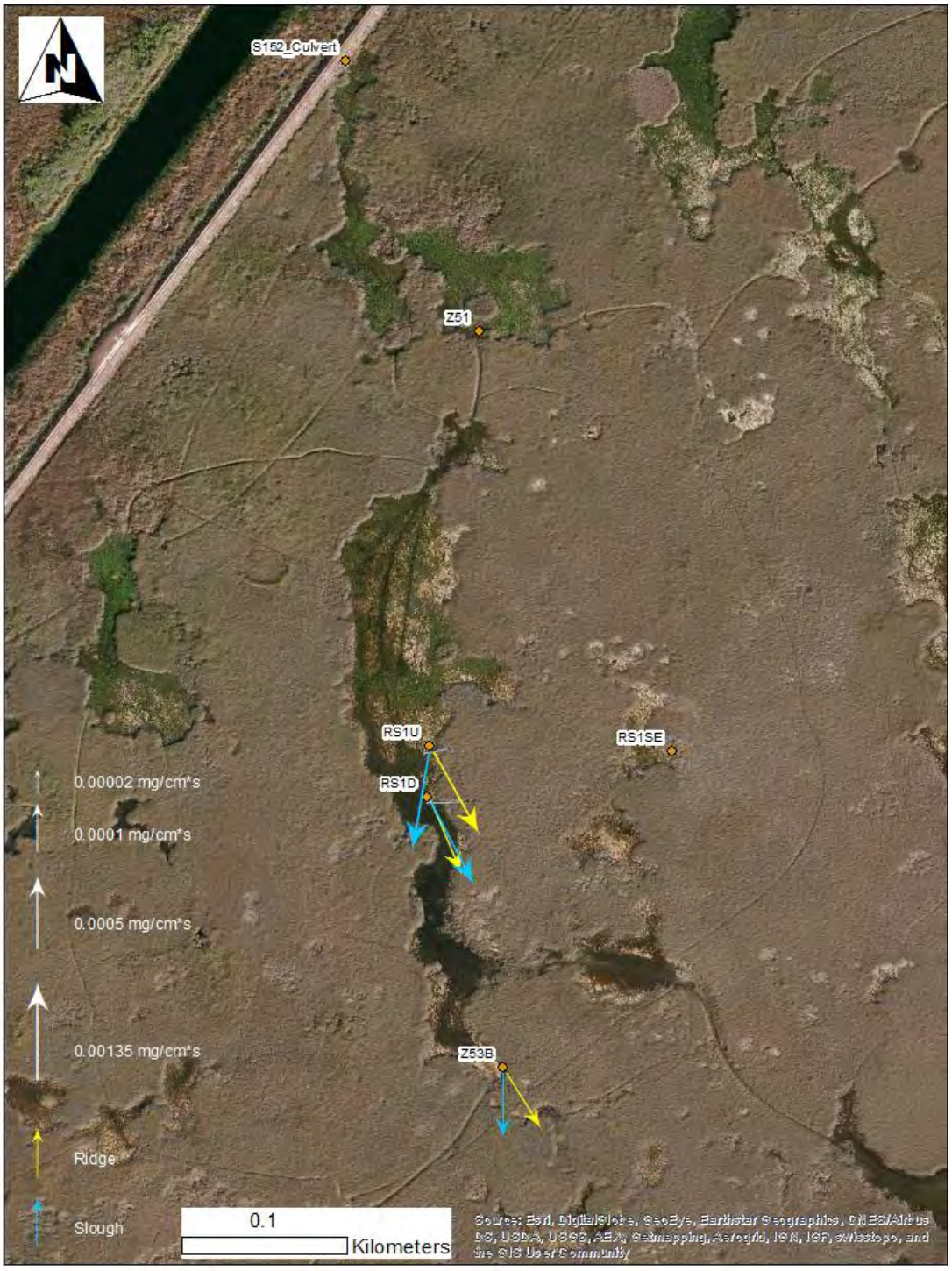

Figure D-175 Transient Flow 1 Phosphorus Load. Samples collected Nov. 4, 2014 from 14:20.

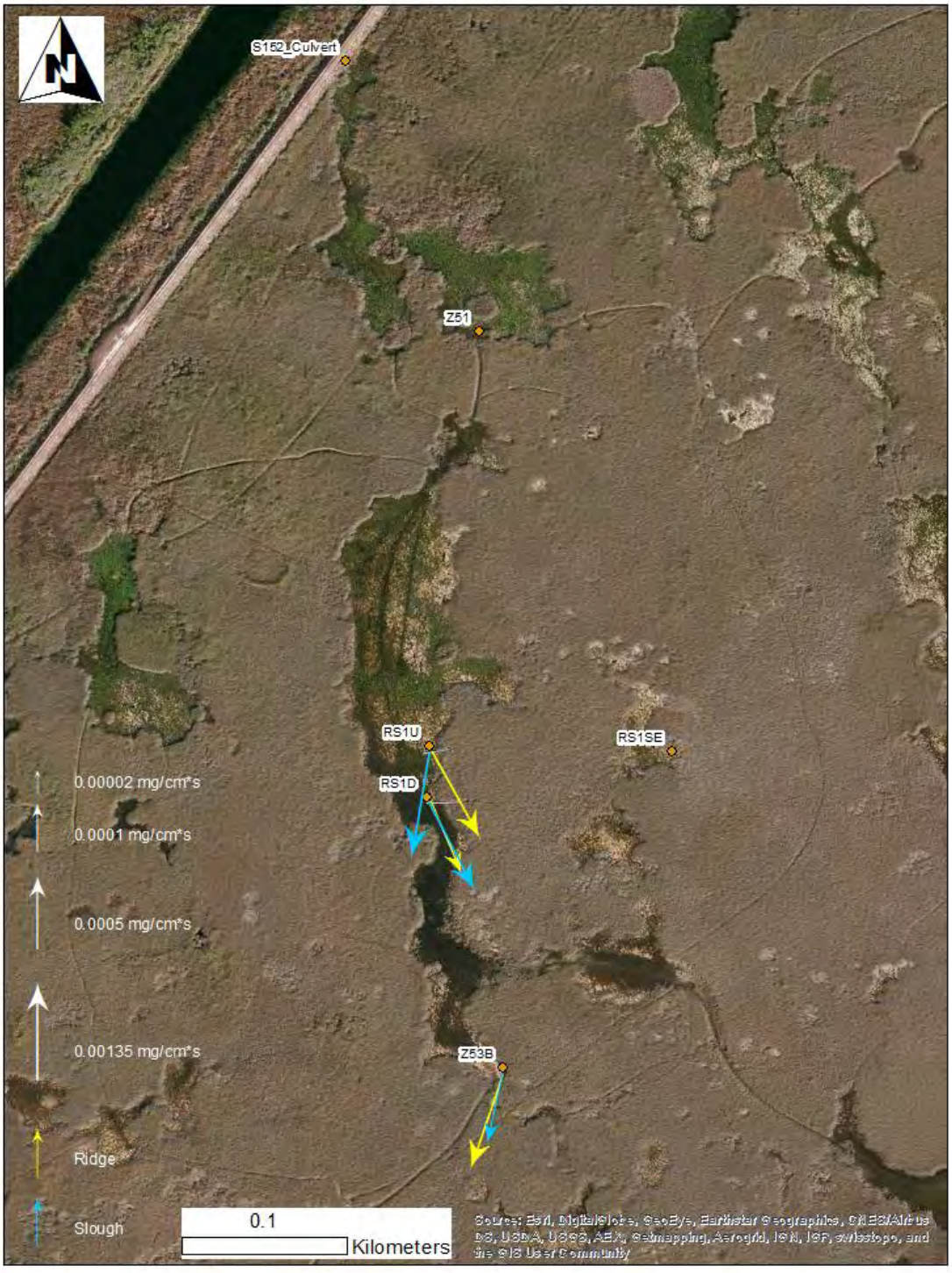

Figure D-176 Transient Flow 2 Phosphorus Load. Samples collected Nov. 5, 2014.

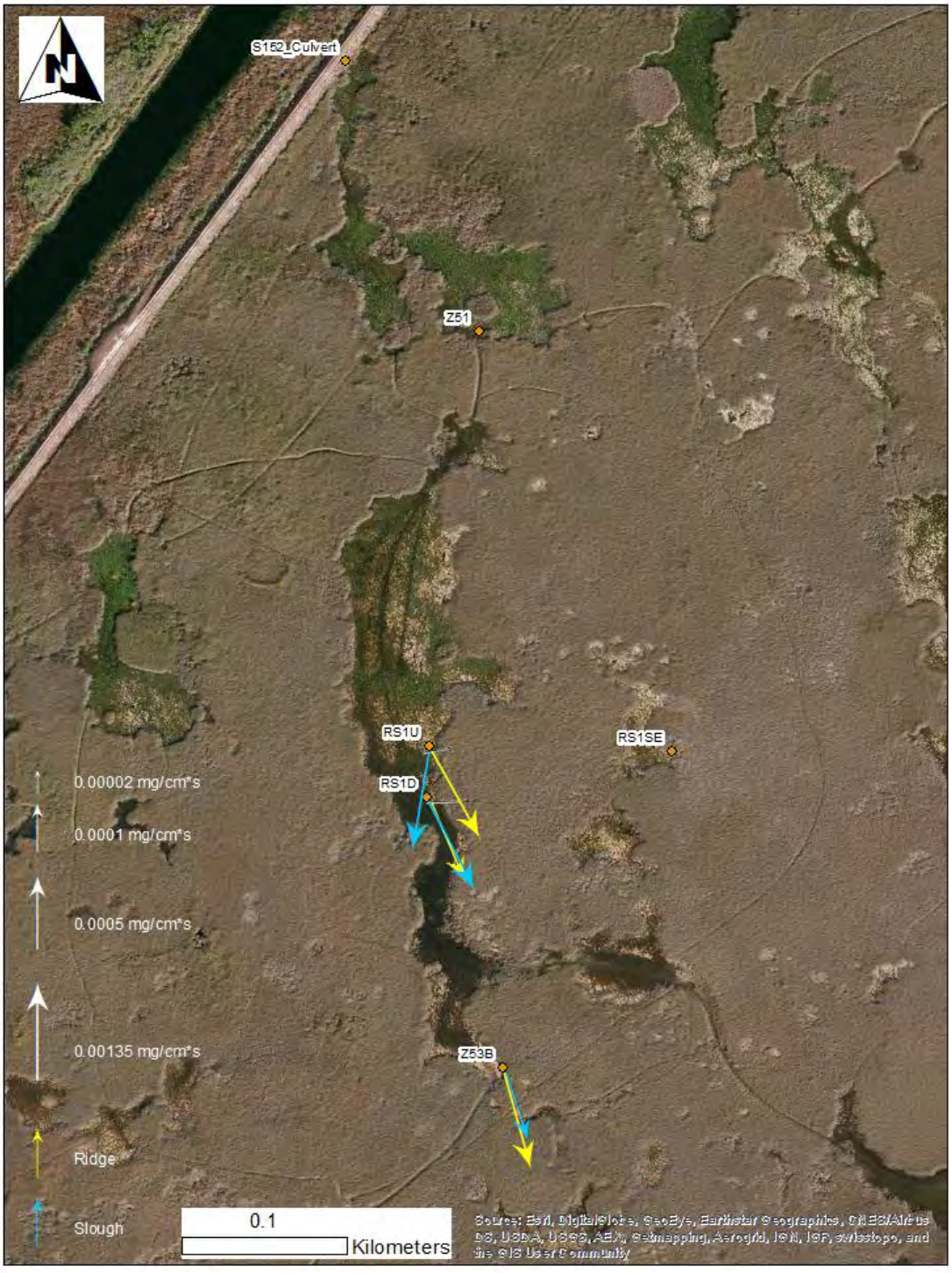

Figure D-177 Steady Flow 1 Phosphorus Load. Samples collected Nov. 7, 2014.

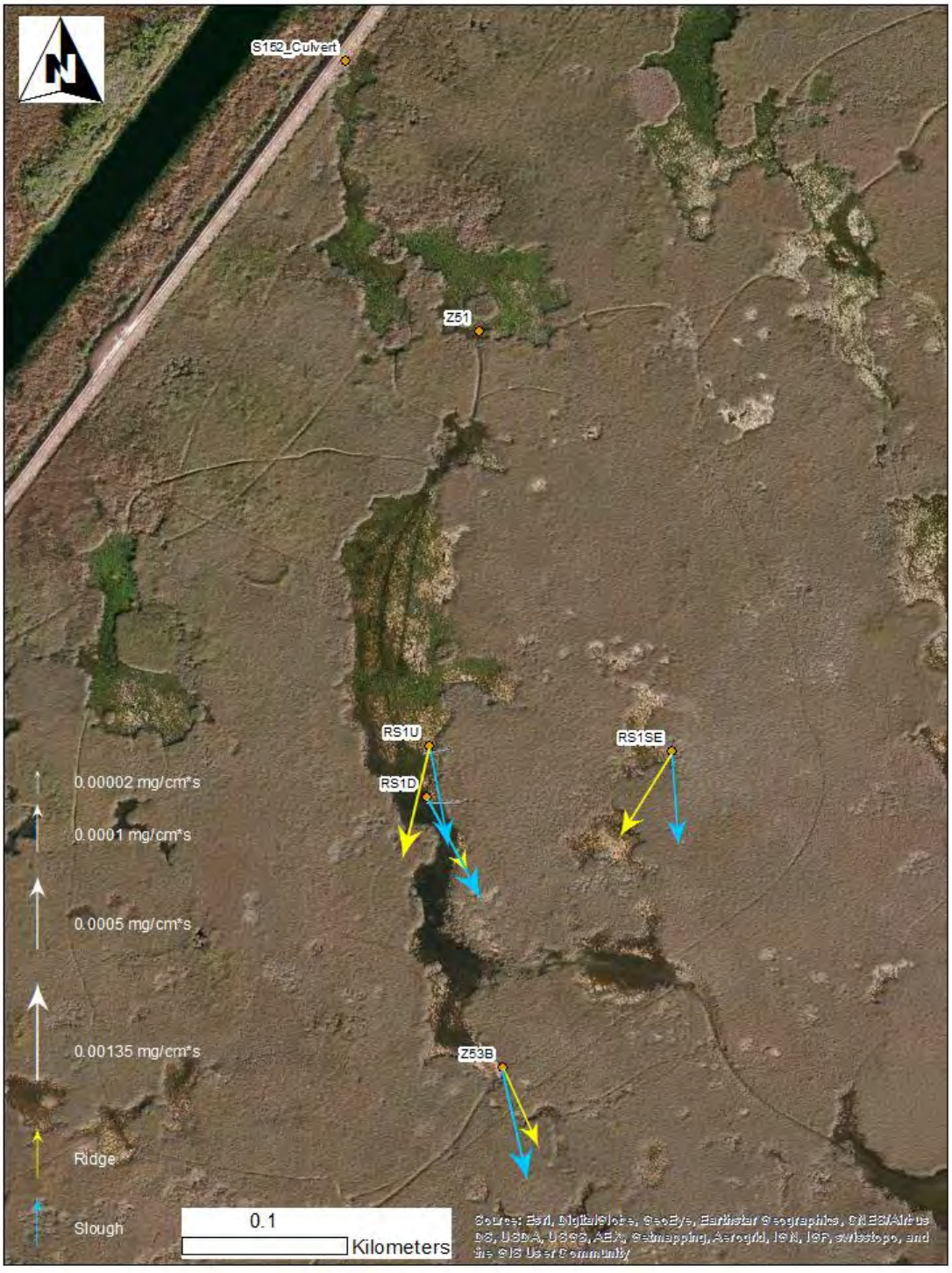

Figure D-178 Steady Flow 3 Phosphorus Load. Samples collected Jan. 19 – Jan. 22, 2015.

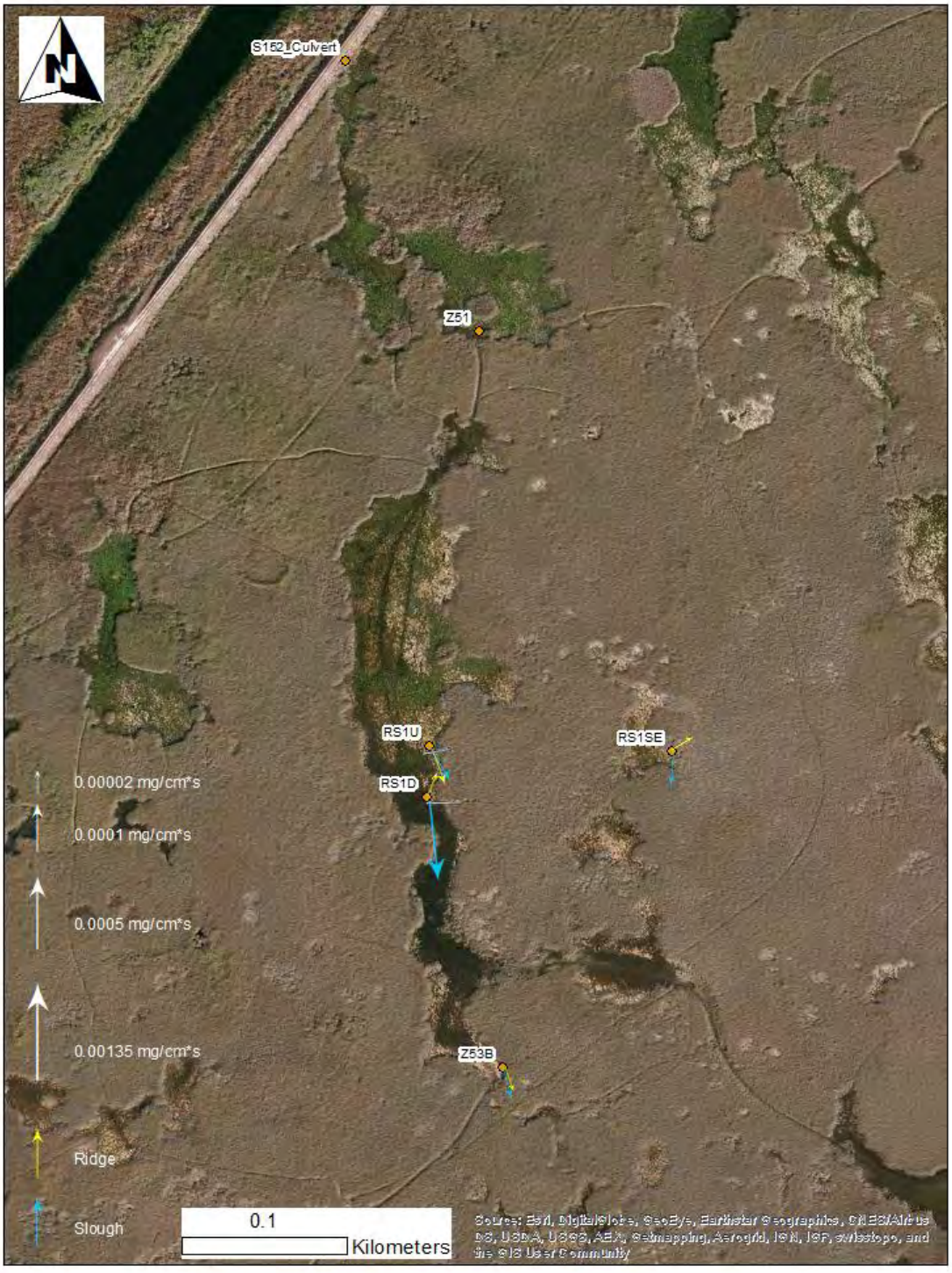

Figure D-179 Steady Flow 4 Phosphorus Load. Samples collected Mar. 9 – Mar. 11, 2015.

2015 Flow Release Vector Maps

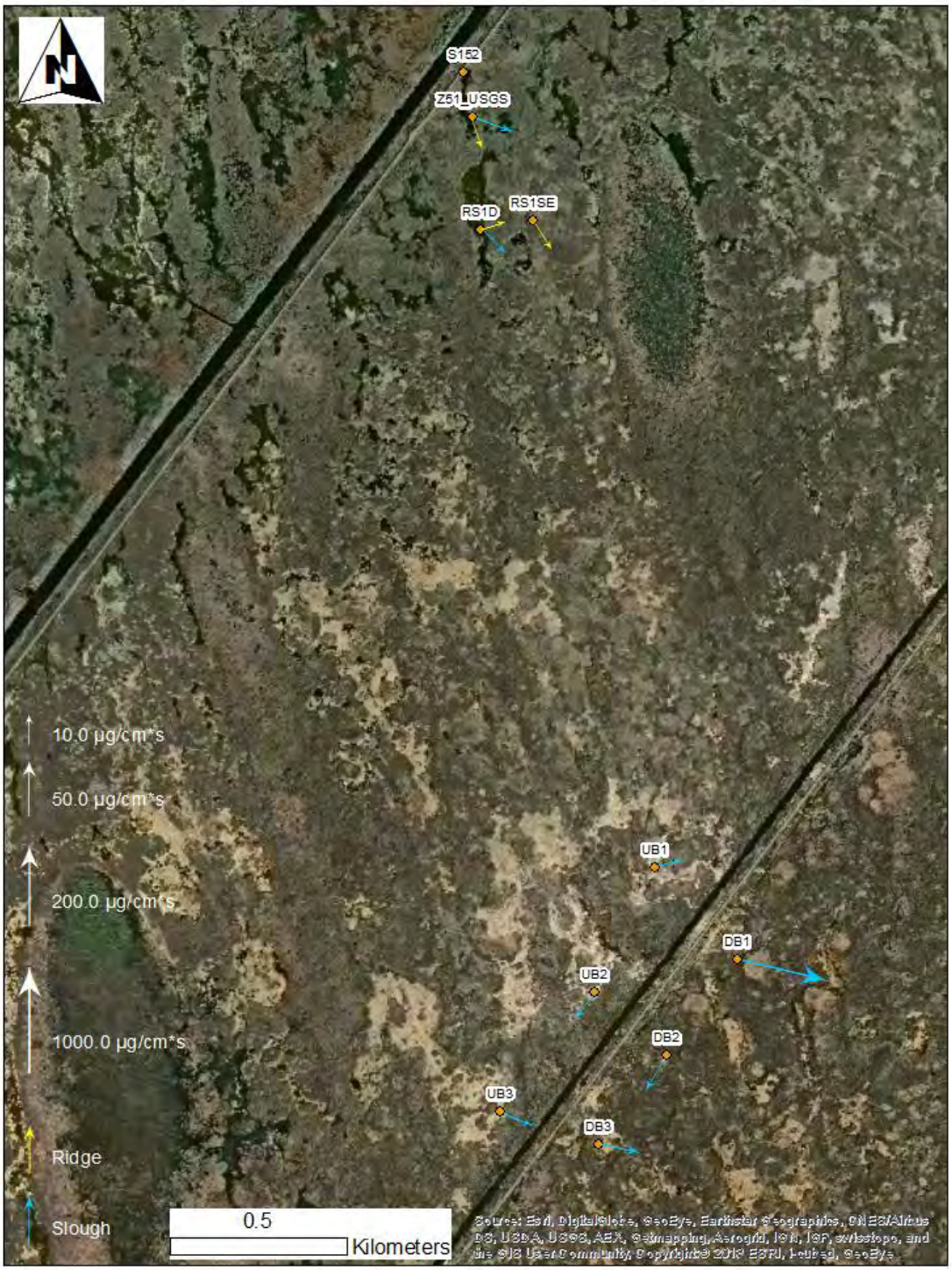

Figure D-180 Pre flow release suspended sediment load. Samples collected Nov. 12 - 14, 2015.

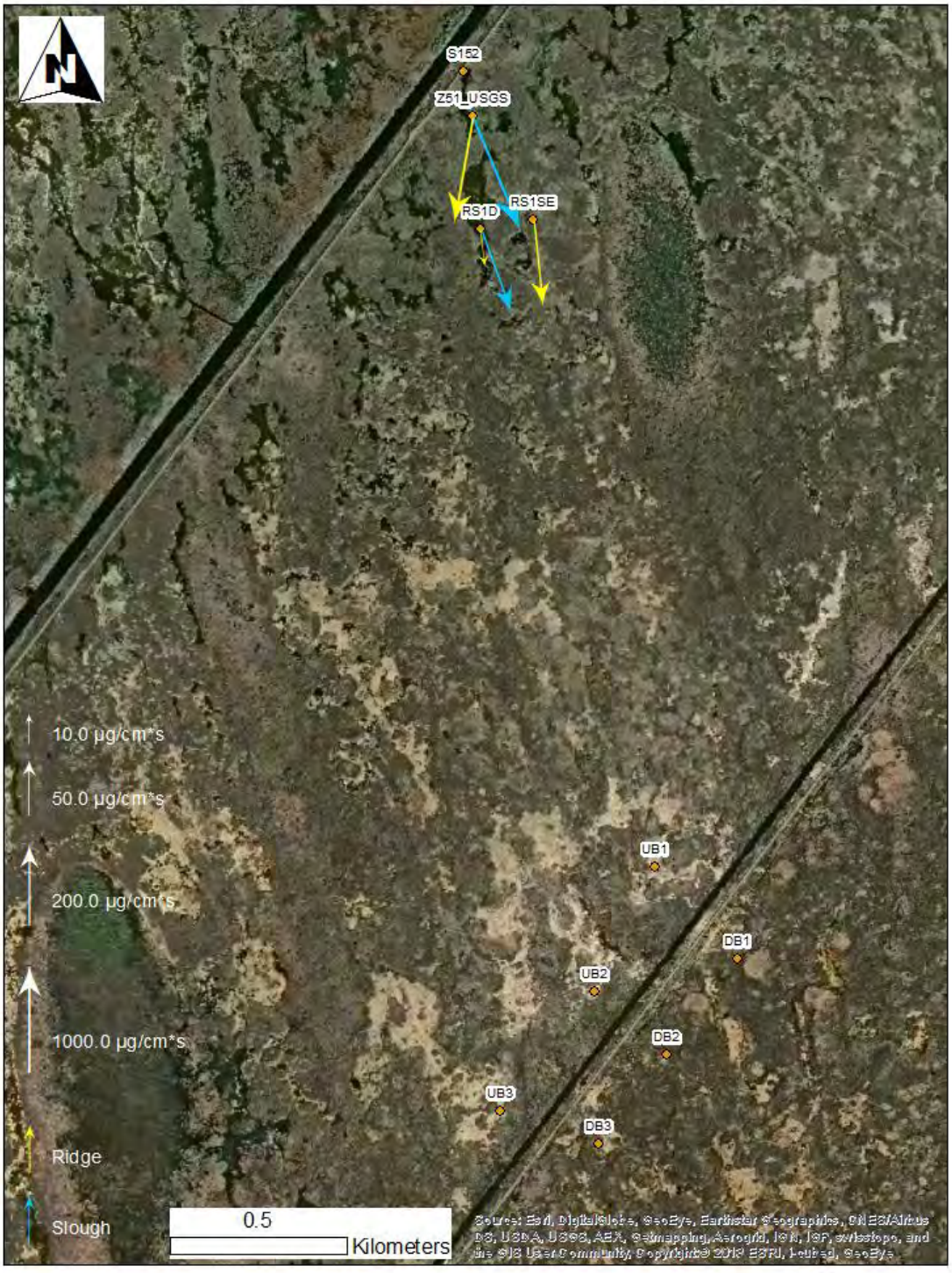

Figure D-181 Pulse 1 peak suspended sediment load. Samples collected Nov. 16th, 2015 at 9:40 at Z51_USGS, 12:30 at RS1D and 14:10 at RS1SE.

Figure D-182 Post pulse 1 suspended sediment load (during which the culvert was closed). Samples collected Nov. 19, 2015 at 8:57 at Z51_USGS and 8:45 at RS1D and RS1SE.

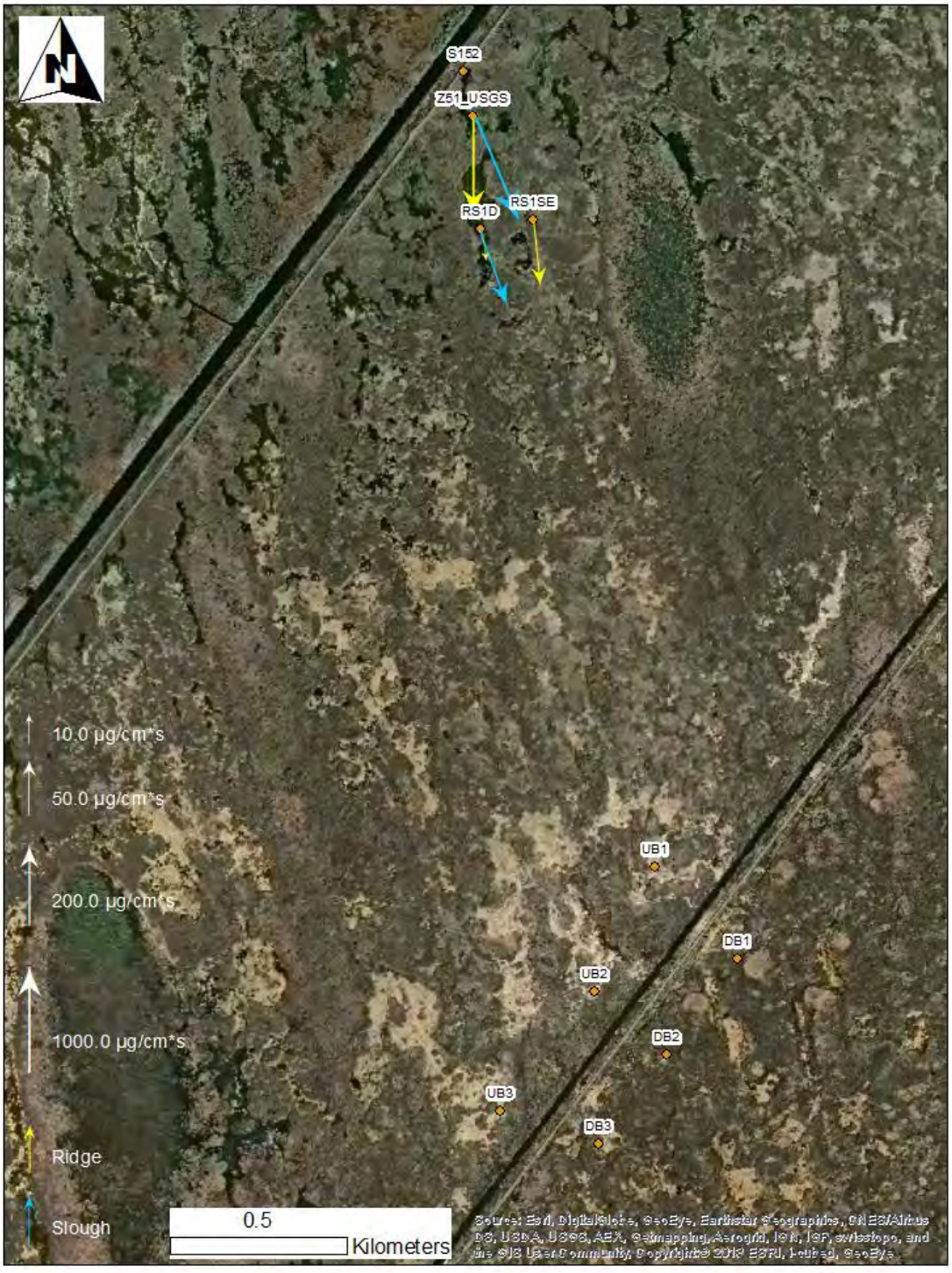

Figure D-183 Pulse 2 peak suspended sediment load. Samples collected Nov. 19th, 2015 at 9:43 at Z51_USGS, 12:29 at RS1D and 14:10 at RS1SE.

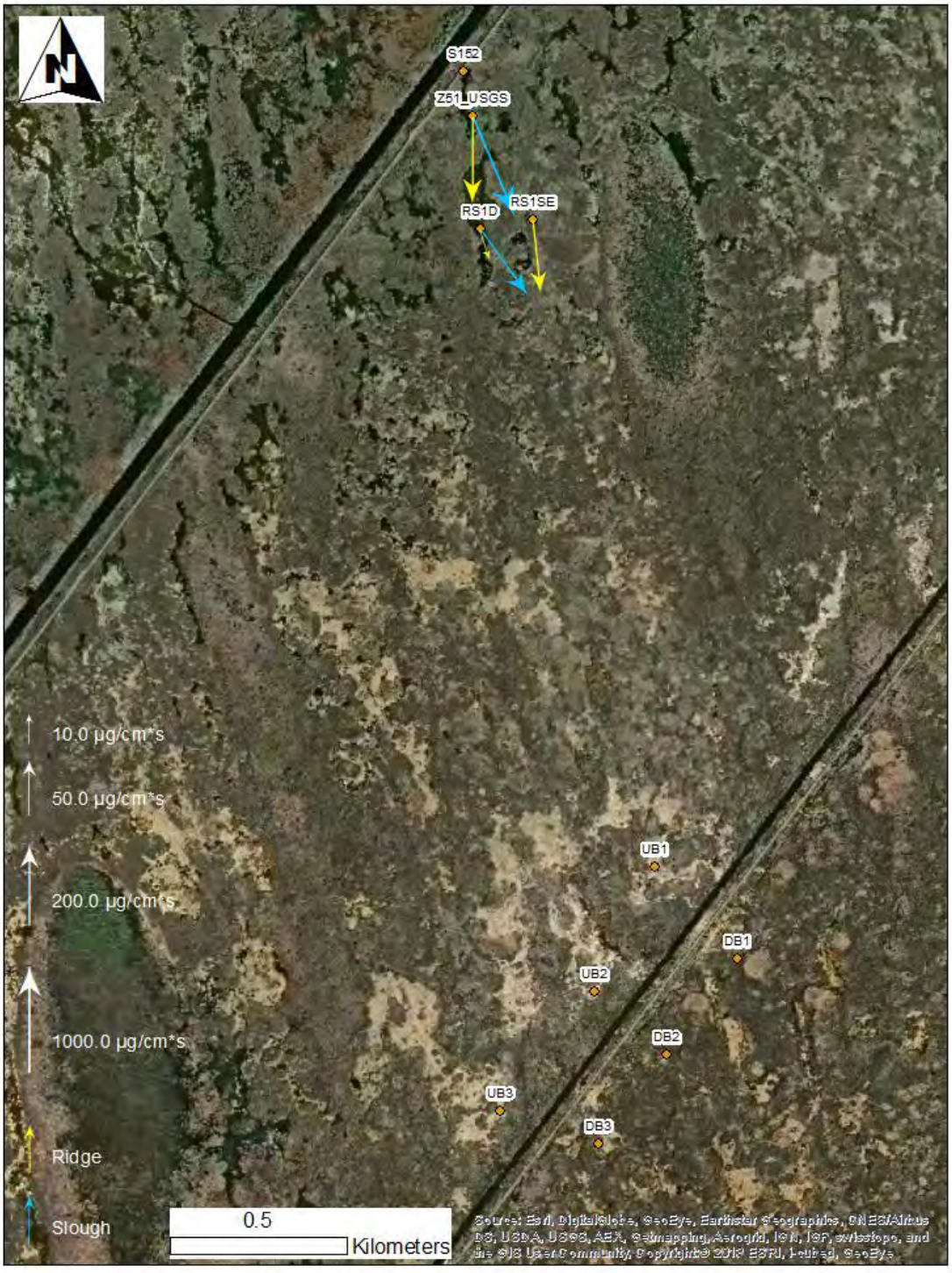

Figure D-184 Transient flow following pulse 2 suspended sediment load. Samples collected Nov. 20th, 2015 at 11:06 at Z51_USGS, 8:38 at RS1D and 13:09 at RS1SE.

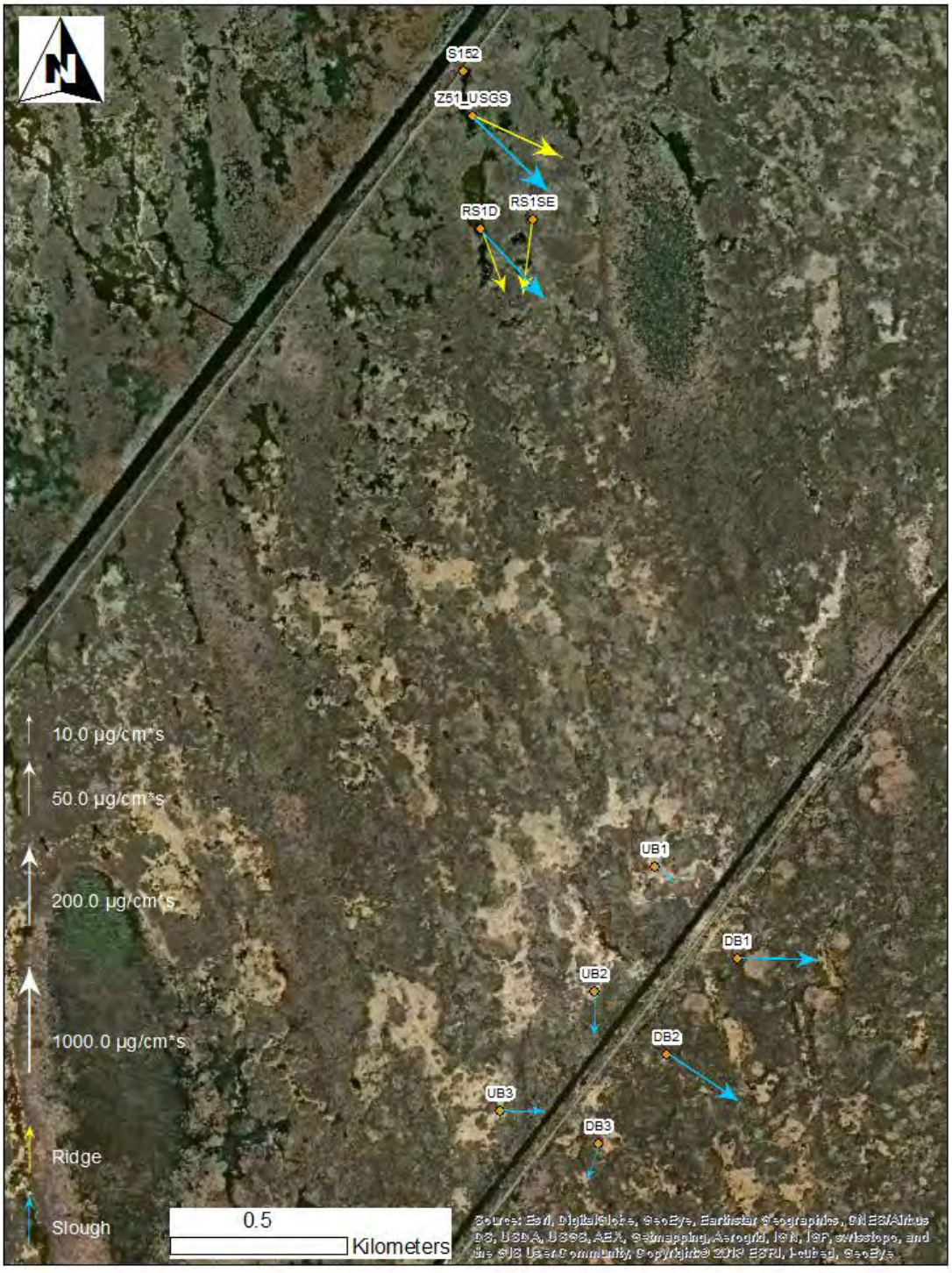

Figure D-185 Steady flow suspended sediment load. Samples collected Dec. 9 - 11, 2015.

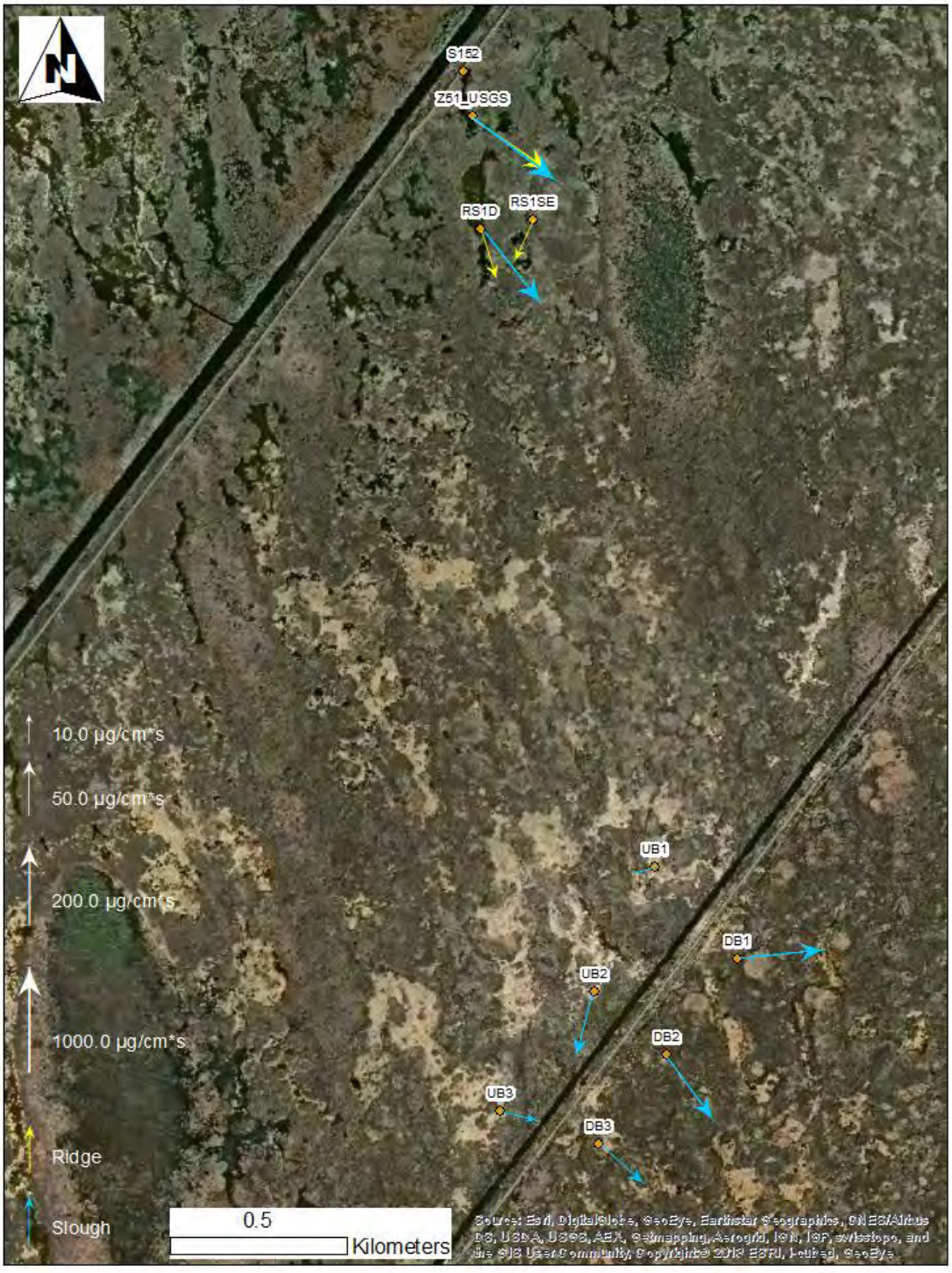

Figure D-186 Steady flow suspended sediment load. Samples collected Jan. 19 - 21, 2016.

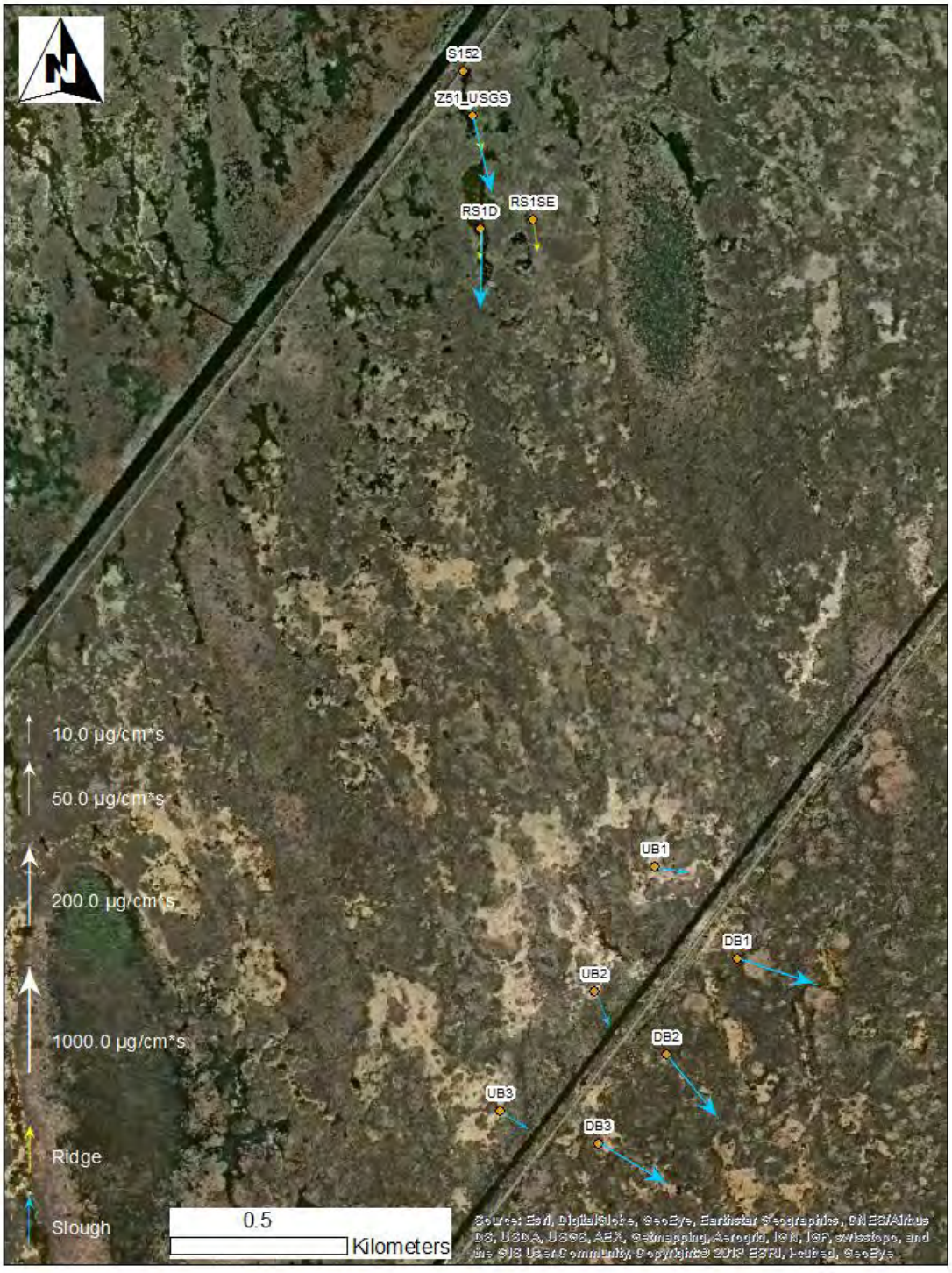

Figure D-187 Steady flow suspended sediment load. Samples collected Mar. 1 - 4, 2016.

Figure D-188 Pre flow release suspended sediment load. Samples collected Nov. 12 - 14, 2015.

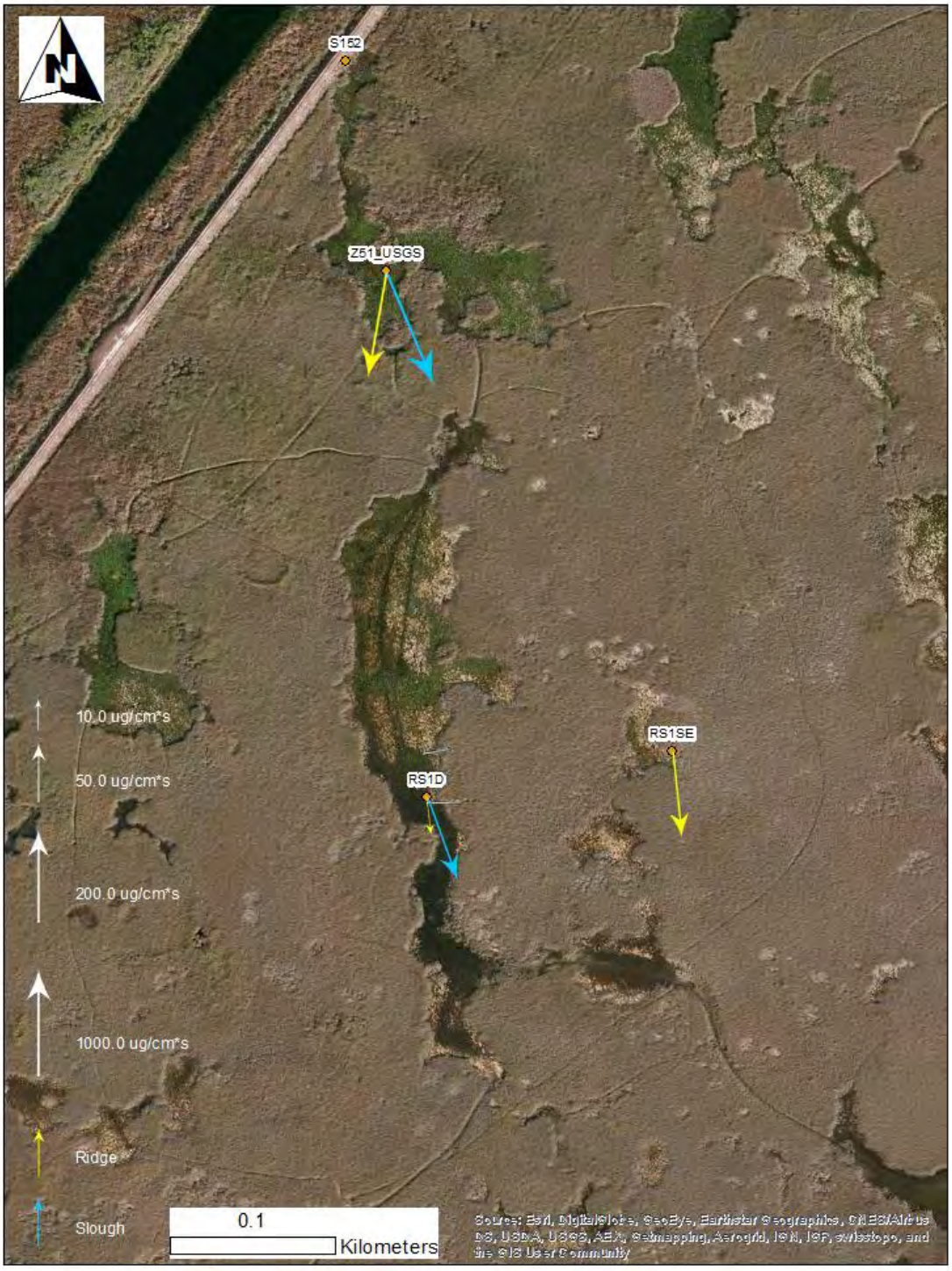

Figure D-189 Pulse 1 peak suspended sediment load. Samples collected Nov. 16th, 2015 at 9:40 at Z51_USGS, 12:30 at RS1D and 14:10 at RS1SE.

Figure D-190 Post pulse 1 suspended sediment load (during which time the culvert was closed). Samples collected Nov. 19, 2015 at 8:57 at Z51_USGS and 8:45 at RS1D and RS1SE.

Figure D-191 Pulse 2 peak suspended sediment load. Samples collected Nov. 19th, 2015 at 9:43 at Z51_USGS, 12:29 at RS1D and 14:10 at RS1SE.

Figure D-192 Transient flow following pulse 2 suspended sediment load. Samples collected Nov. 20th, 2015 at 11:06 at Z51_USGS, 8:38 at RS1D and 13:09 at RS1SE.

Figure D-193 Steady flow suspended sediment load. Samples collected Dec. 9 - 11, 2015.

Figure D-194 Steady flow suspended sediment load. Samples collected Jan. 19 - 21, 2016.

Figure D-195 Steady flow suspended sediment load. Samples collected Mar. 1 - 4, 2016.

Figure D-196 Pre pulse 1 total phosphorus load. Samples collected Nov. 13 - 14, 2015.

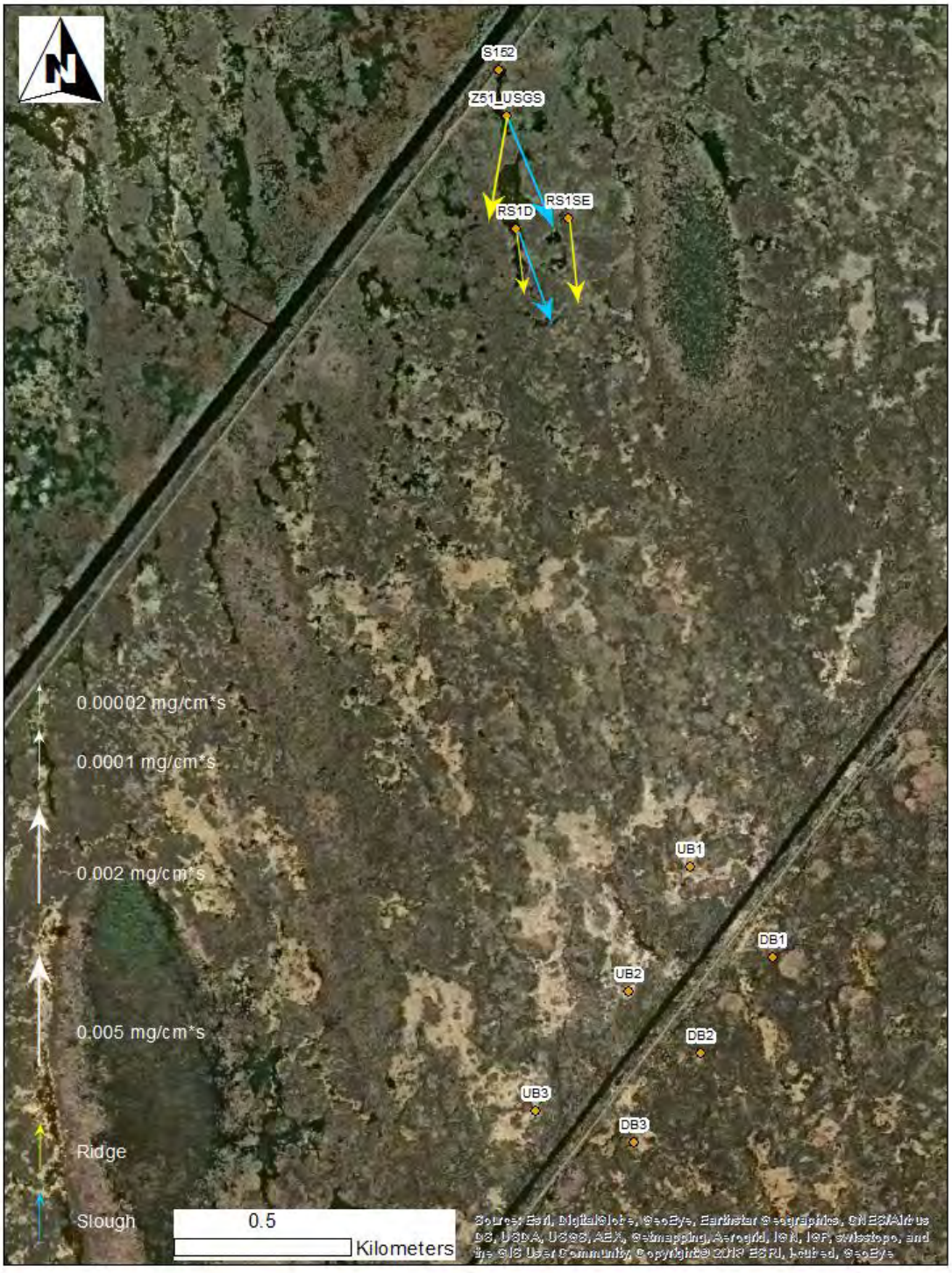

Figure D-197 Pulse 1 peak total phosphorus load. Samples collected Nov. 16th at 10:15 at Z51_USGS, 15:40 at RS1D and 15:40 at RS1SE.

Figure D-198 Pulse 2 peak total phosphorus load. Samples collected Nov. 19th at 10:14 at Z51_USGS, 13:19 at RS1D and 14:10 at RS1SE.

Figure D-199 Transient flow following pulse 2 total phosphorus load. Samples collected Nov. 20th at 11:06 at Z51_USGS, 8:38 at RS1D and 13:09 at RS1SE.

Figure D-200 Steady flow total phosphorus load. Samples collected Dec. 9 - 11, 2015.

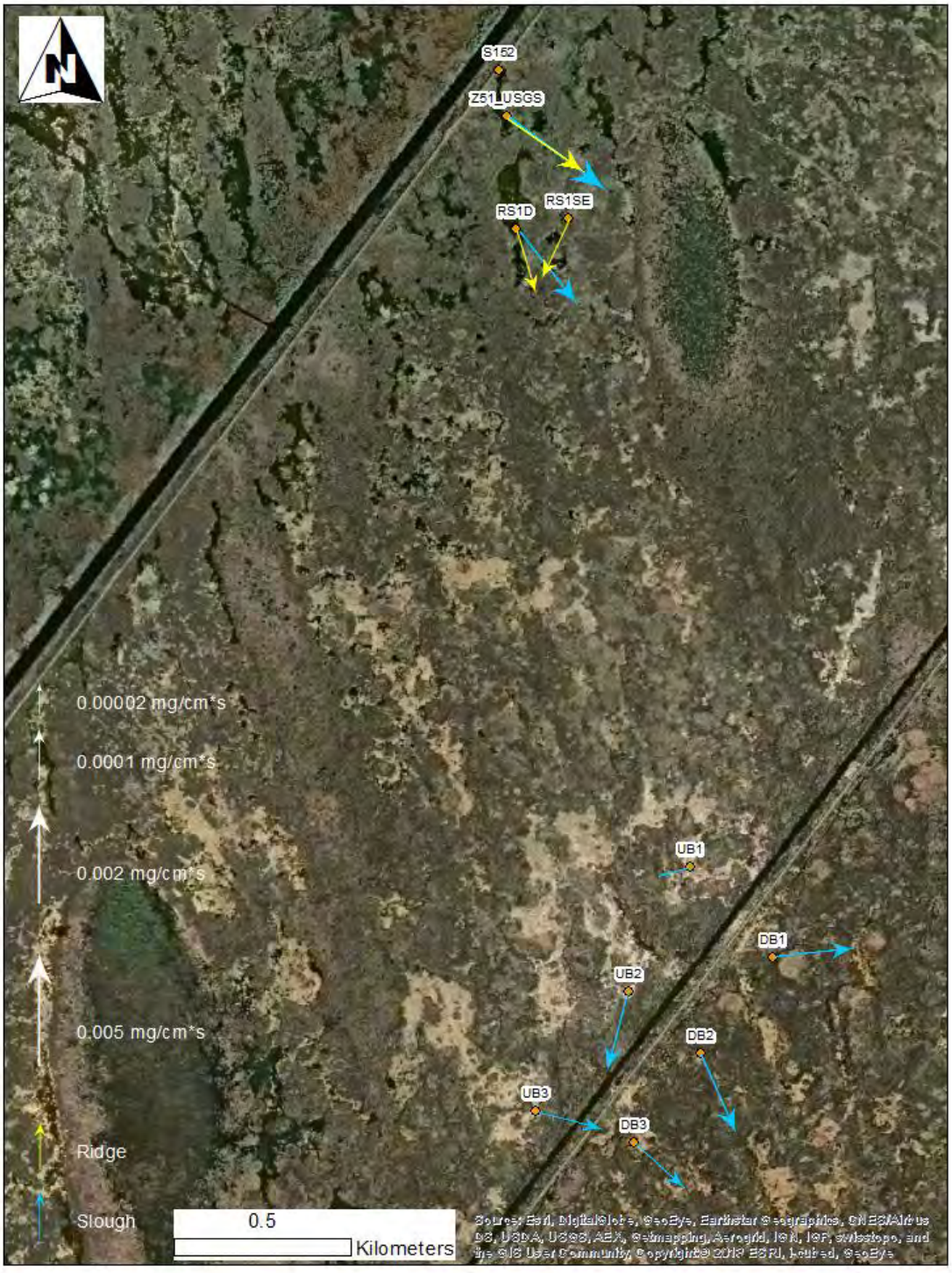

Figure D-201 Steady flow total phosphorus load. Samples collected Jan. 19 - 20, 2016.

Figure D-202 Steady flow total phosphorus load. Samples collected Mar. 1 - 4, 2016.

Figure D-203 Pre pulse 1 total phosphorus load. Samples collected Nov. 13 14, 2015.

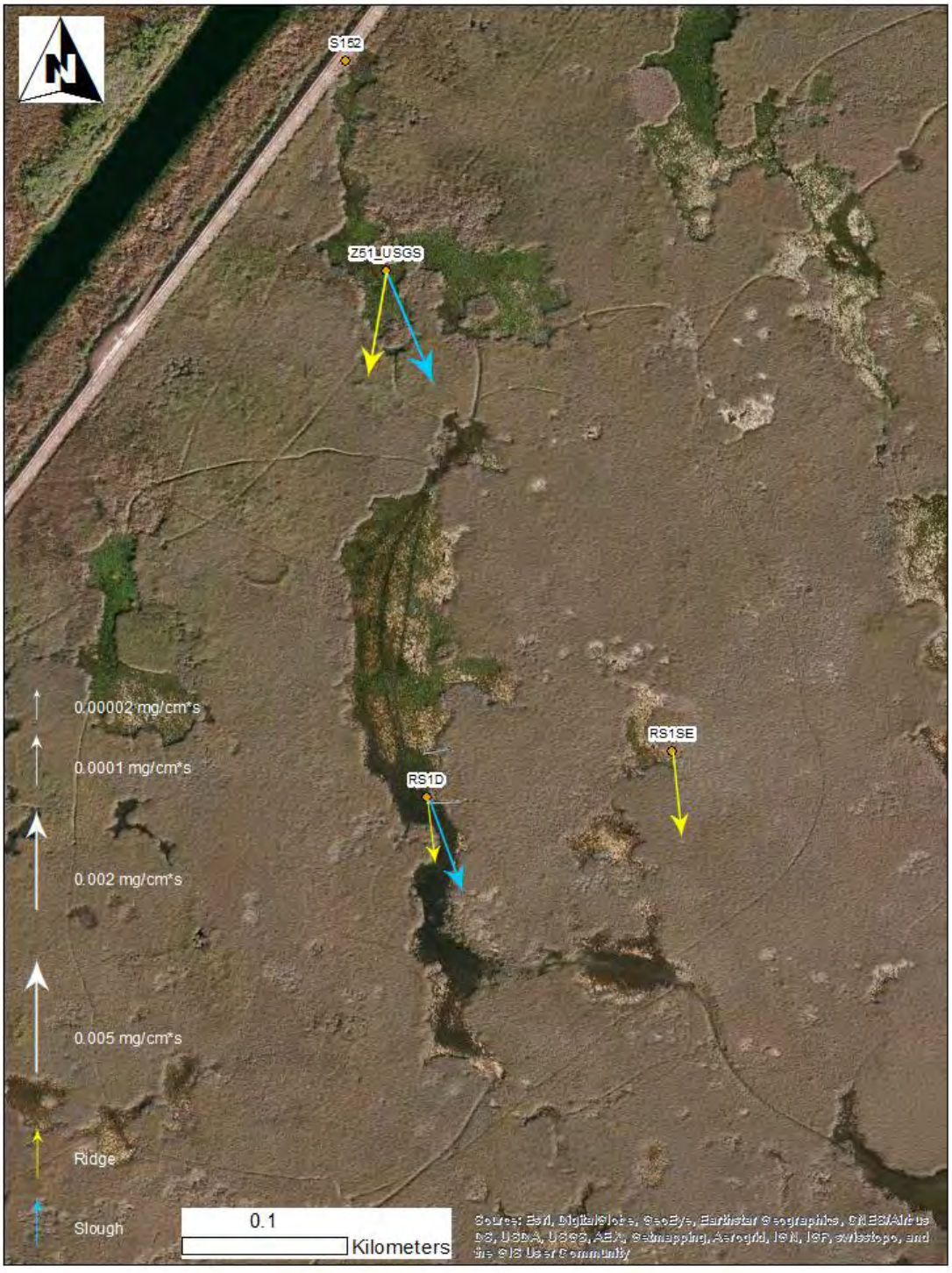

Figure D-204 Pulse 1 peak total phosphorus load. Samples collected Nov. 16th at 10:15 at Z51_USGS, 15:40 at RS1D and 15:40 at RS1SE.

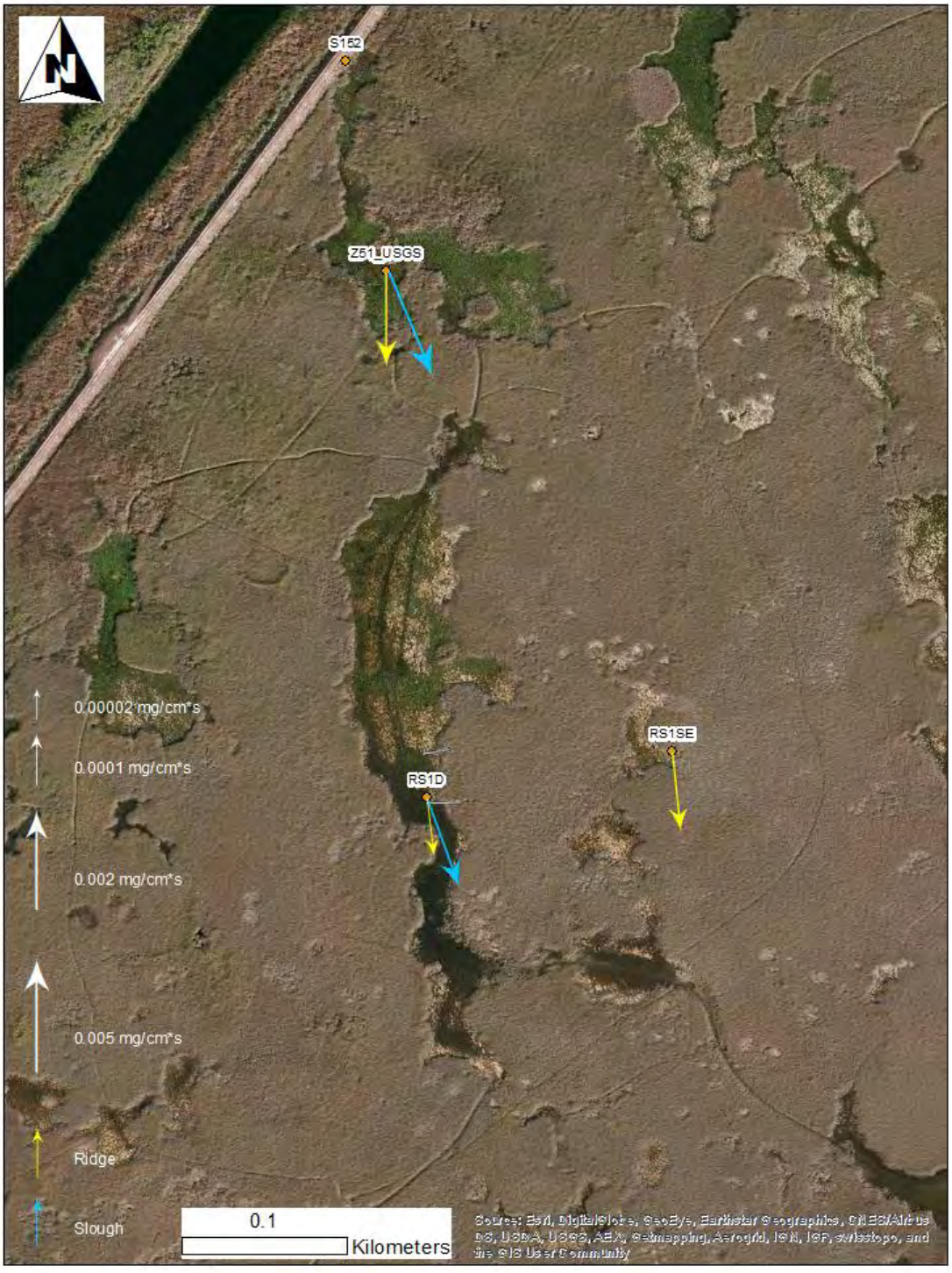

Figure D-205 Pulse 2 peak total phosphorus load. Samples collected Nov. 19th at 10:14 at Z51_USGS, 13:19 at RS1D and 14:10 at RS1SE.

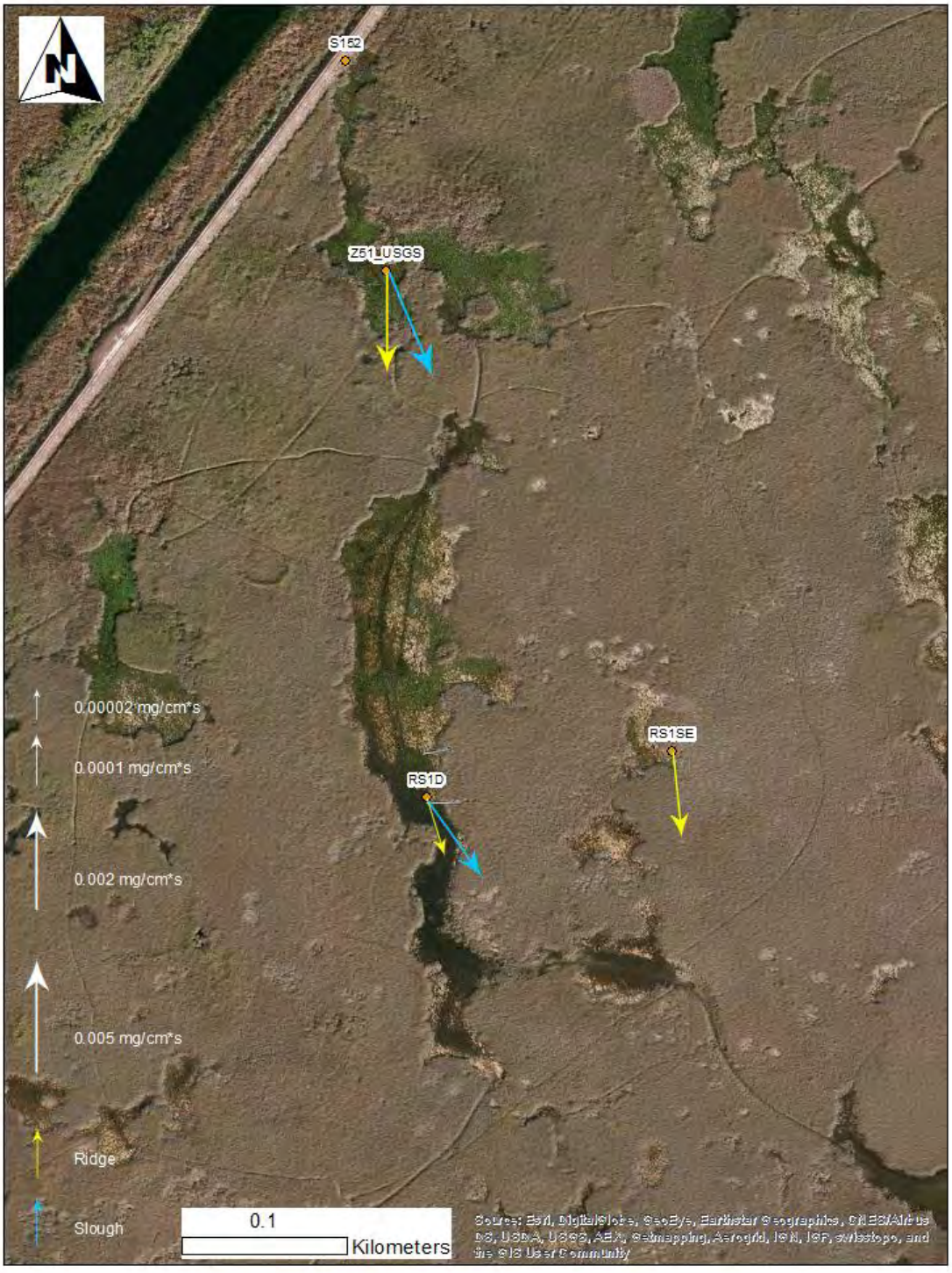

Figure D-206 Transient flow following pulse 2 total phosphorus load. Samples collected Nov. 20th at 11:06 at Z51_USGS, 8:38 at RS1D and 13:09 at RS1SE.

Figure D-207 Steady flow total phosphorus load. Samples collected Dec. 9 - 11, 2015.

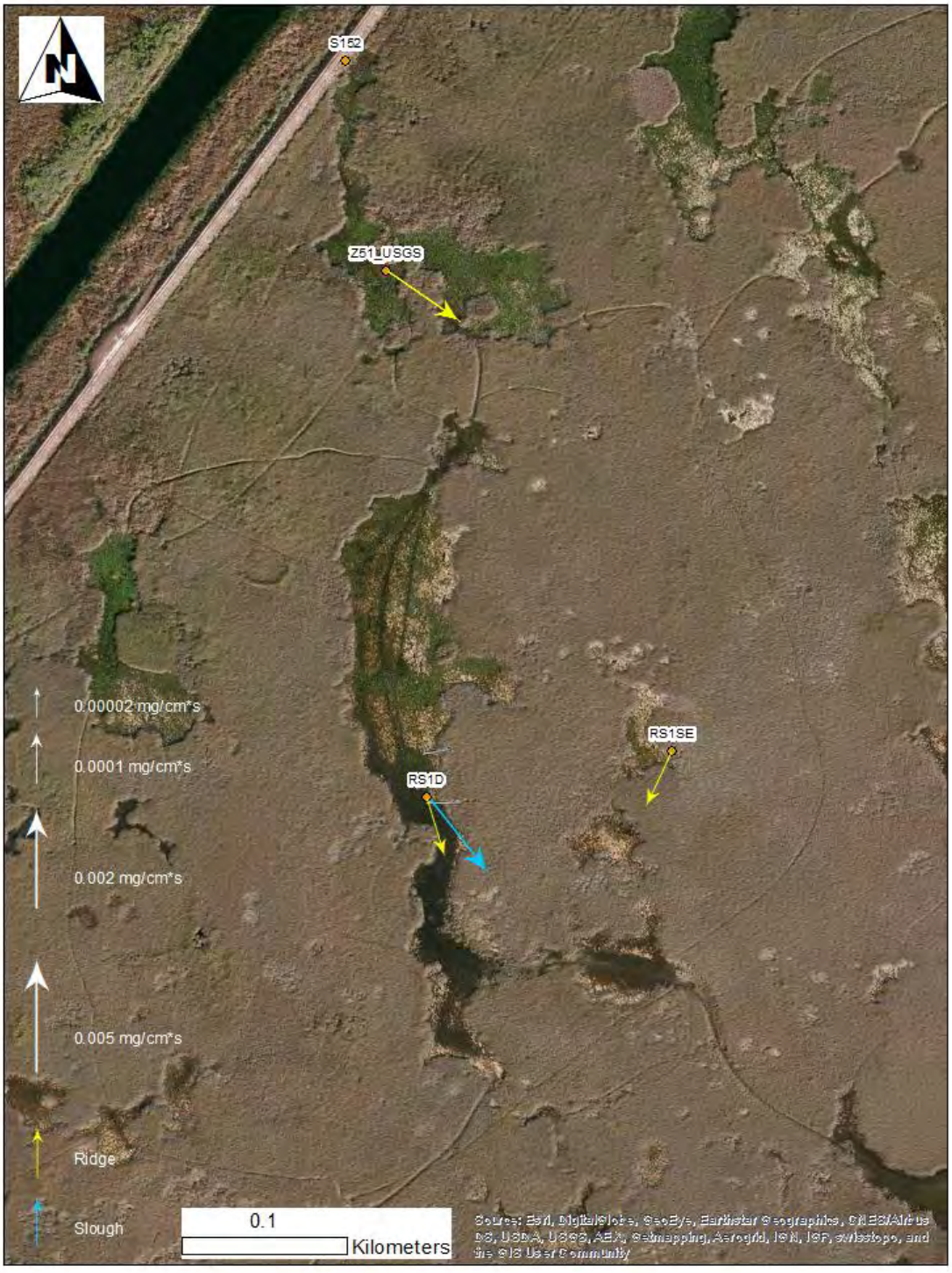

Figure D-208 Steady flow total phosphorus load. Samples collected Jan. 19 - 20, 2016.

Figure D-209 Steady flow total phosphorus load. Samples collected Mar. 1 - 4, 2016.

Particle Grain Size Analysis: LISST Continuous Grain Size Data

2010 November

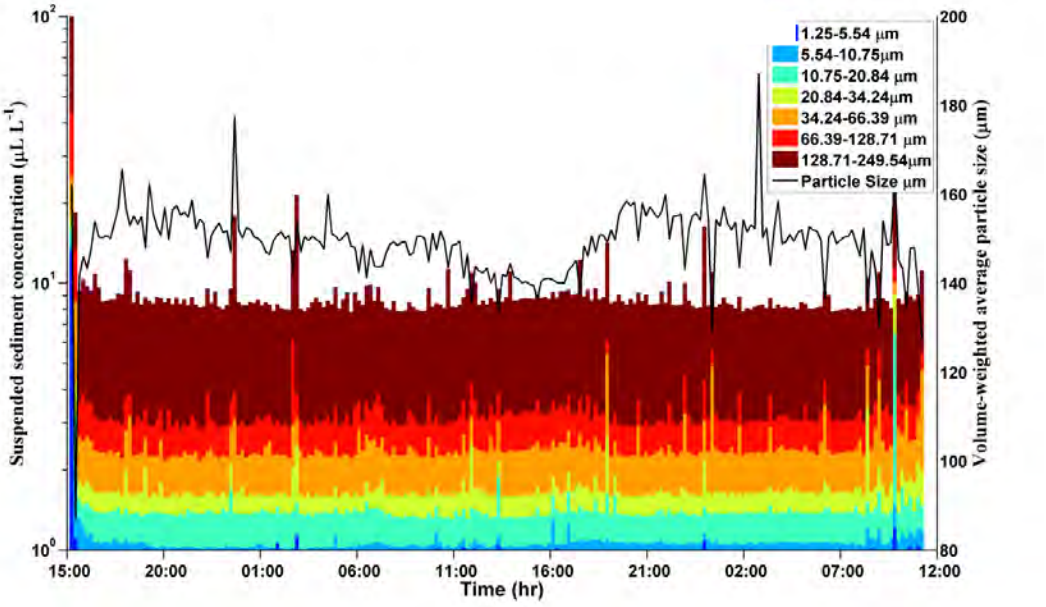

Figure D-210 Stacked time series of particle size distribution and volume-weighted particle size distributions at RS1D Ridge site. Data were binned into 32 size categories from 1.25 to 250 microns. Deployed period is November 9, 2010 15:14 to November 11, 2010 11:29. Data baseline set to 10^0.

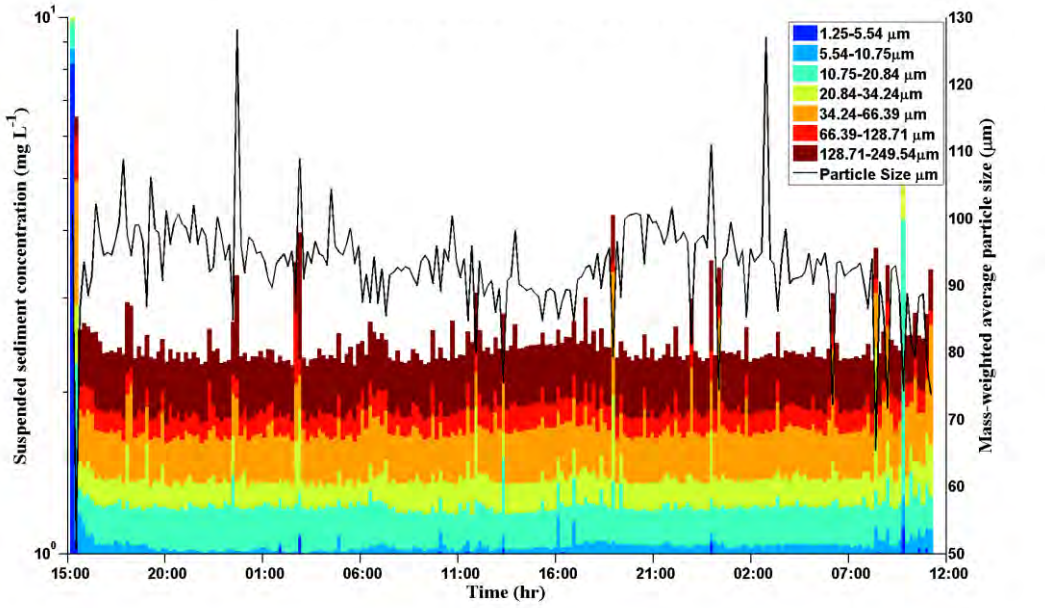

Figure D-211 Stacked time series of particle size distribution and mass-weighted particle size distributions at RS1D Ridge site. Data were binned into 32 size categories from 1.25 to 250 microns. Deployed period is November 9, 2010 15:14 to November 11, 2010 11:29. Data baseline set to 10^0.

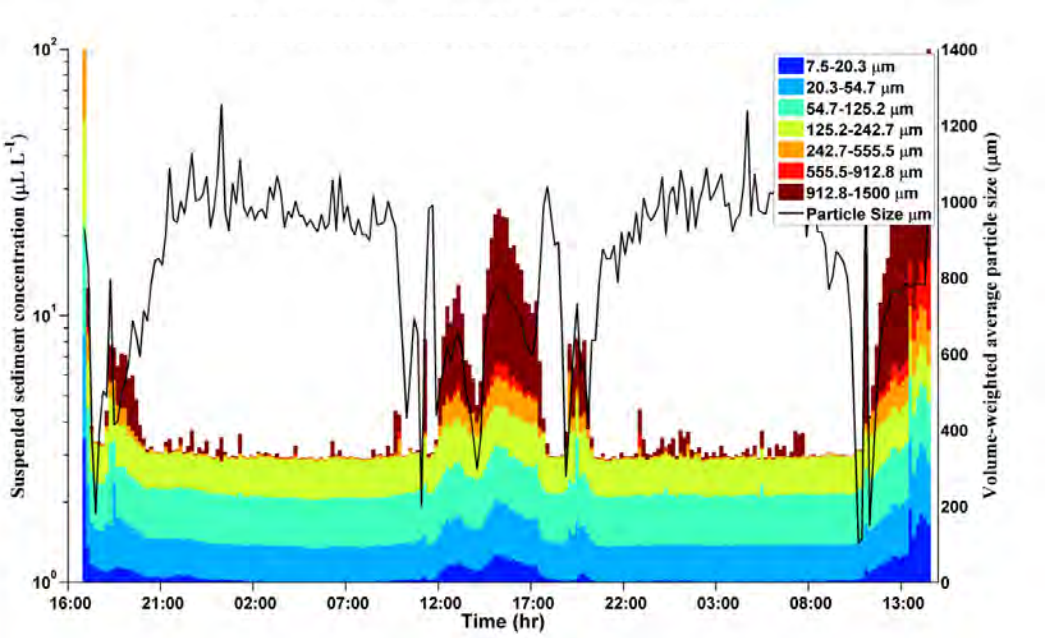

Figure D-212 Stacked time series of particle size distribution and volume-weighted particle size distributions at RS1D Ridge site. Data were binned into 32 size categories from 7.5 to 1500 microns. Deployed period is November 7, 2010 16:53 to November 9, 2010 14:42. Data baseline set to 10^0.

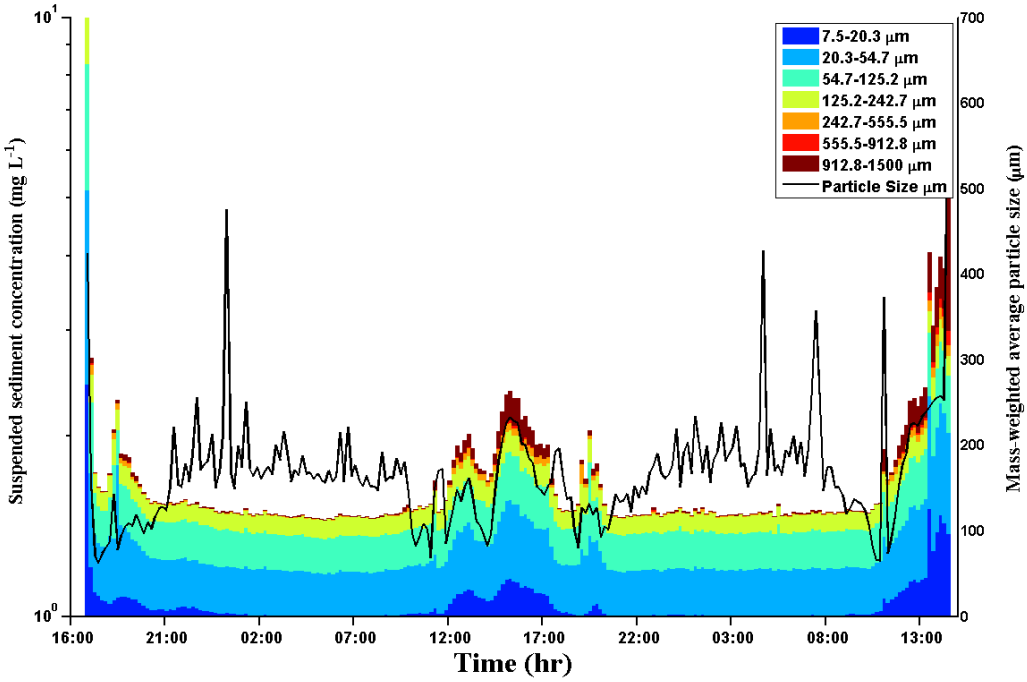

.

Figure D-213 Stacked time series of particle size distribution and mass-weighted particle size distributions at RS1D Ridge site. Data were binned into 32 size categories from 7.5 to 1500 microns. Deployed period is November 7, 2010 16:53 to November 9, 2010 14:42. Data baseline set to 10^0.

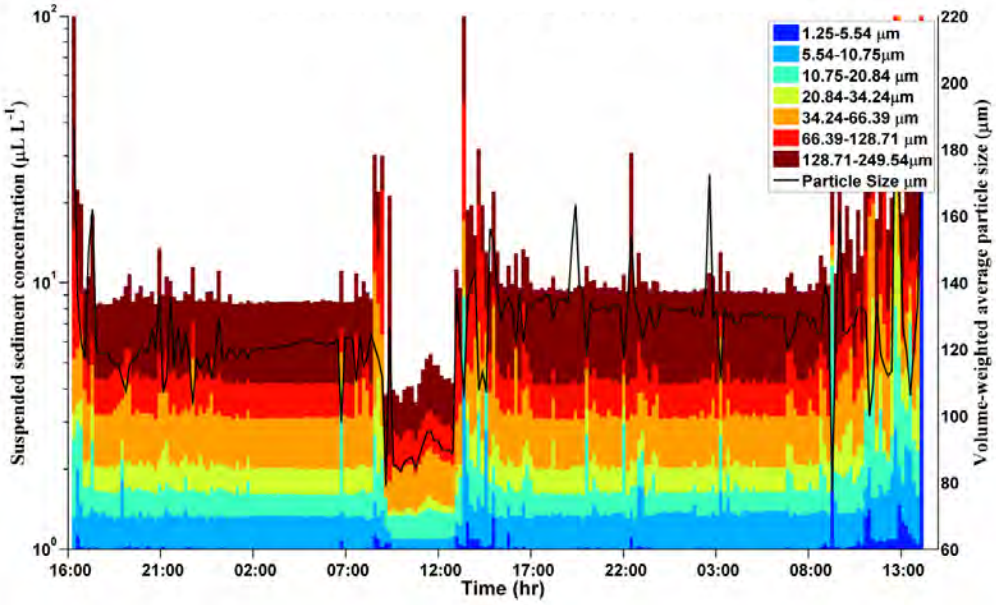

Figure D-214 Stacked time series of particle size distribution and volume-weighted particle size distributions at RS1D Slough site. Data were binned into 32 size categories from 1.25 to 250 microns. Deployed period is November 7, 2010 16:18 to November 9, 2010 14:20. Data baseline set to 10^0.

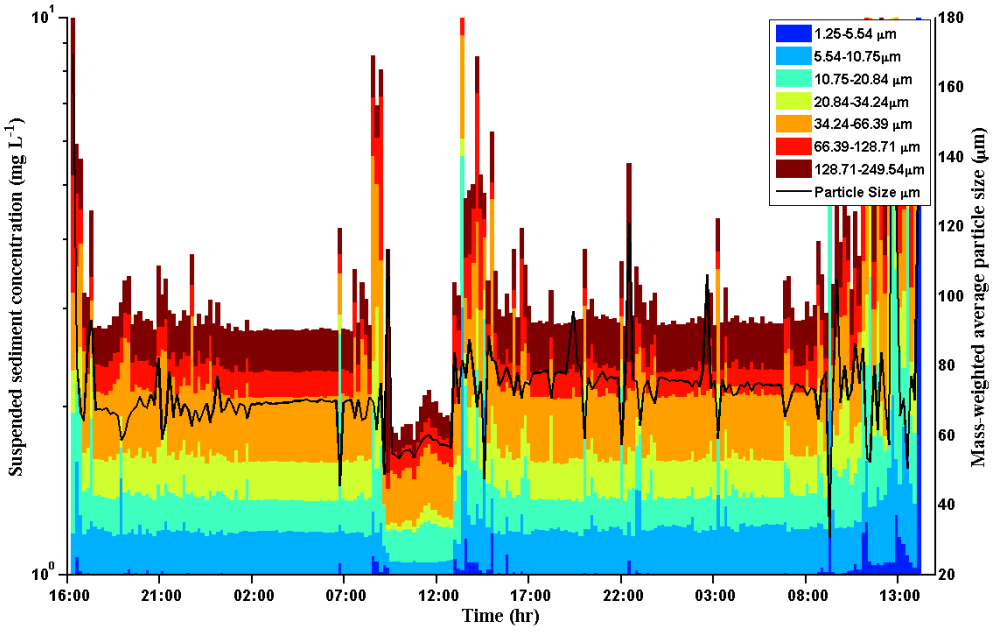

Figure D-215 Stacked time series of particle size distribution and mass-weighted particle size distributions at RS1D Slough site. Data were binned into 32 size categories from 1.25 to 250 microns. . Deployed period is November 7, 2010 16:18 to November 9, 2010 14:20. Data baseline set to 10^0.

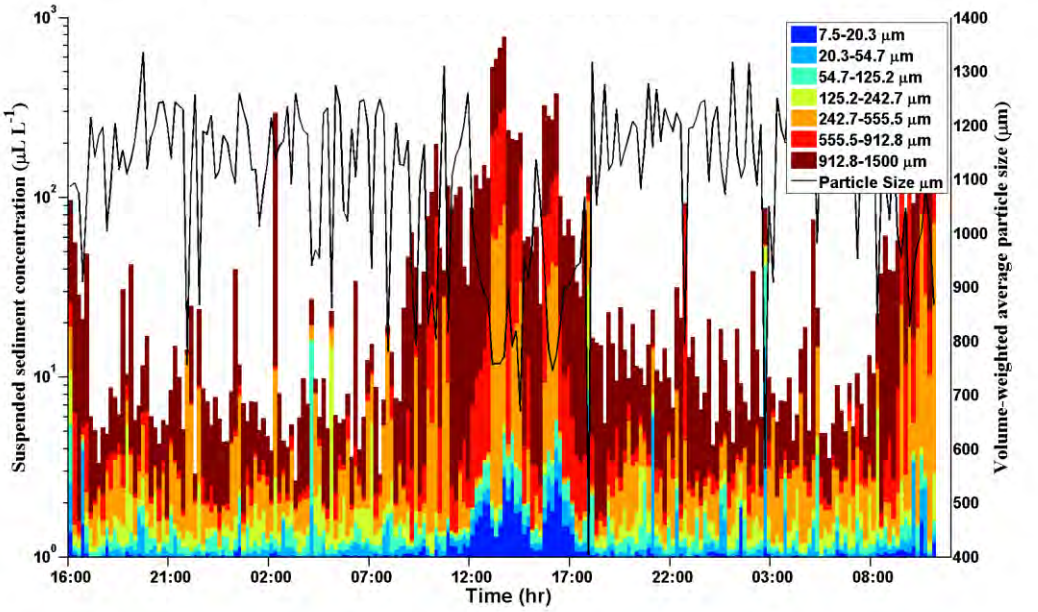

Figure D-216 Stacked time series of particle size distribution and volume-weighted particle size distributions at RS1D Slough site. Data were binned into 32 size categories from 7.5 to 1500 microns. Deployed period is November 9, 2010 16:08 to November 11, 2010 11:30. Data baseline set to 10^0.

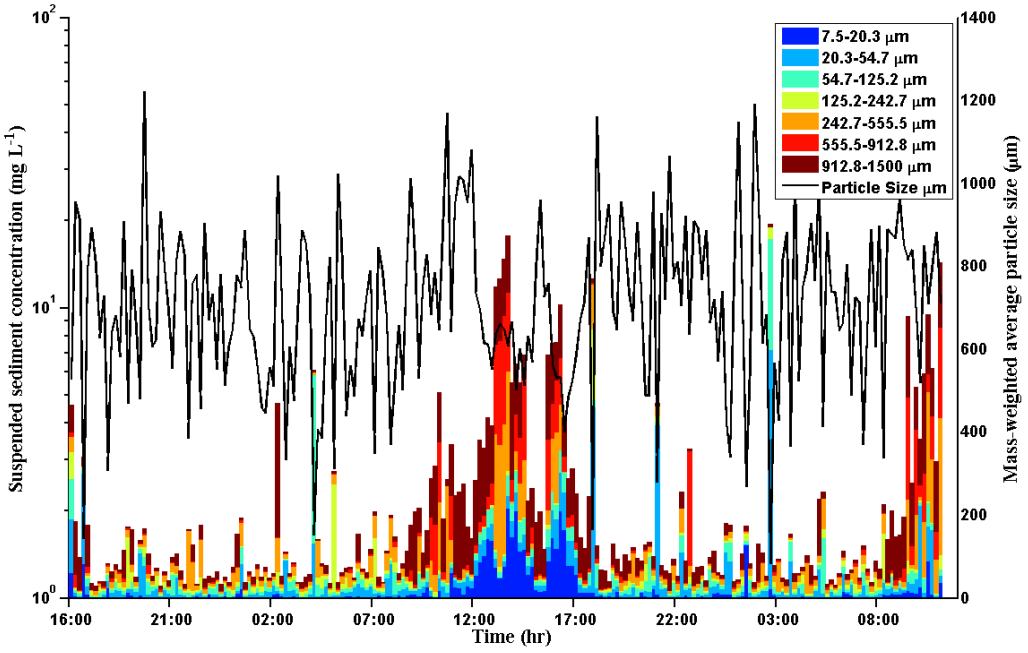

Figure D-217 Stacked time series of particle size distribution and mass-weighted particle size distributions at RS1D Slough site. Data were binned into 32 size categories from 7.5 to 1500 microns. Deployed period is November 9, 2010 16:08 to November 11, 2010 11:30. Data baseline set to 10^0.

2012 August

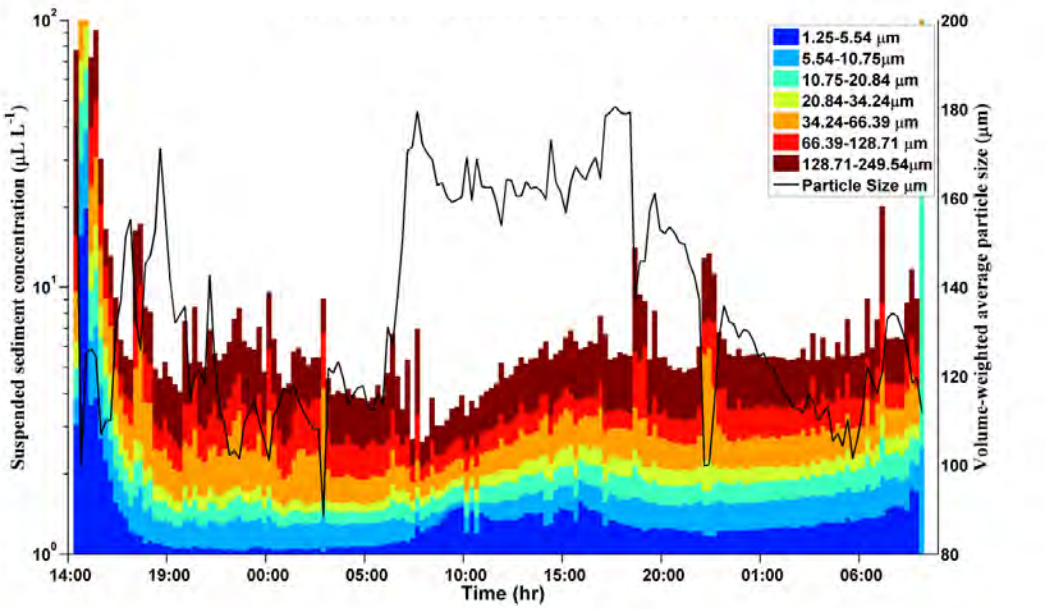

Figure D-218 Stacked time series of particle size distribution and volume-weighted particle size distributions at RS1D Ridge site. Data were binned into 32 size categories from 1.25 to 250 microns. Deployed period is August 7, 2012 14:24 to August 9, 2012 09:11. Data baseline set to 10^0.

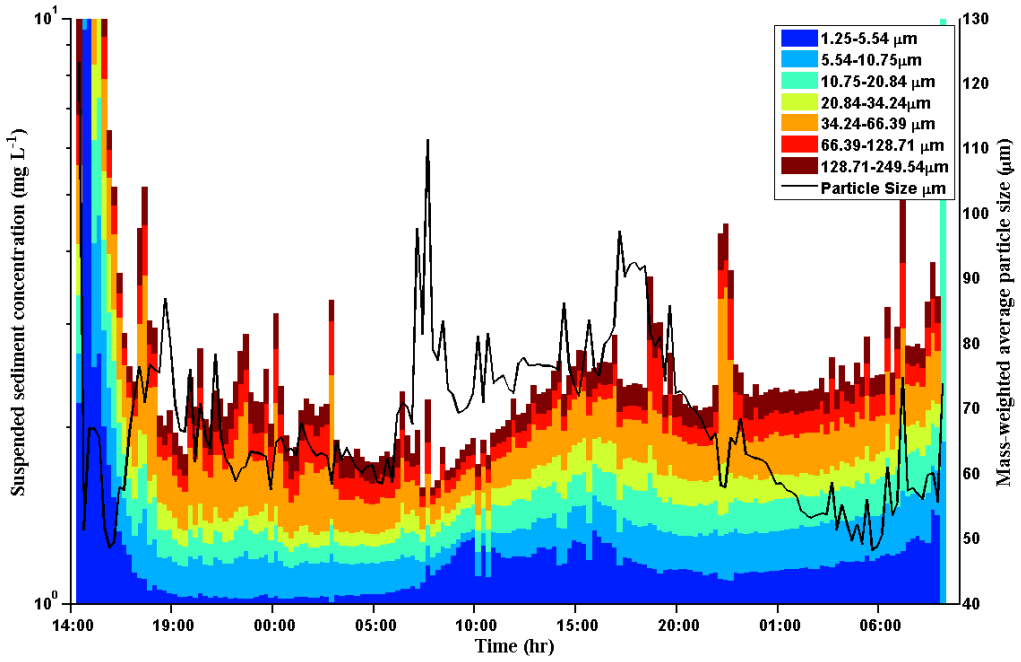

Figure D-219 Stacked time series of particle size distribution and mass-weighted particle size distributions at RS1D Ridge site. Data were binned into 32 size categories from 1.25 to 250 microns. . Deployed period is August 7, 2012 14:24 to August 9, 2012 09:11. Data baseline set to 10^0.

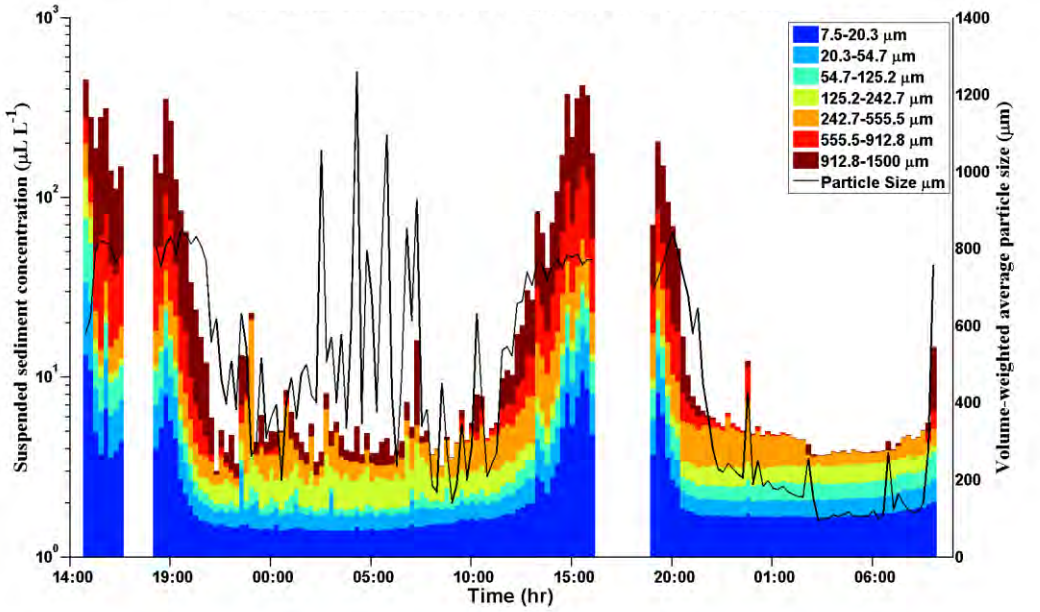

Figure D-220 Stacked time series of particle size distribution and volume-weighted particle size distributions at RS1D Slough site. Data were binned into 32 size categories from 7.5 to 1500 microns. Deployed period is August 7, 2012 14:24 to August 9, 2012 09:11. Data baseline set to 10^0.

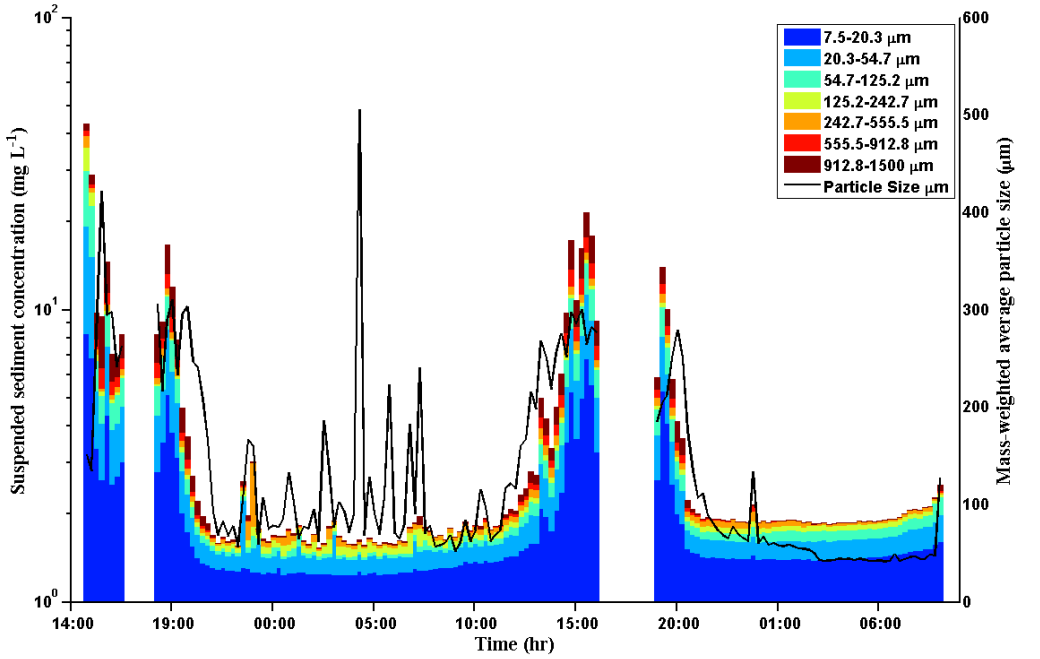

Figure D-221 Stacked time series of particle size distribution and mass-weighted particle size distributions at RS1D Slough site. Data were binned into 32 size categories from 7.5 to 1500 microns. Deployed period is August 7, 2012 14:24 to August 9, 2012 09:11. Data baseline set to 10^0.

2012 November

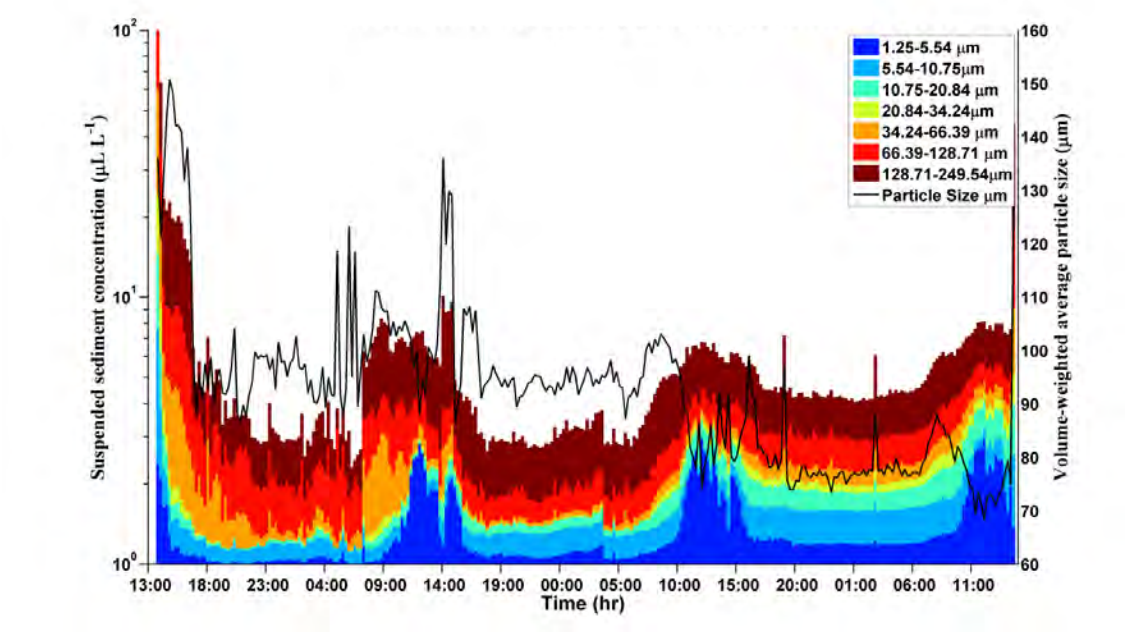

Figure D-222 Stacked time series of particle size distribution and volume-weighted particle size distributions at RS1D Ridge site. Data were binned into 32 size categories from 1.25 to 250 microns. Deployed period is November 5, 2012 13:47 to November 8, 2012 14:18. Data baseline set to 10^0.

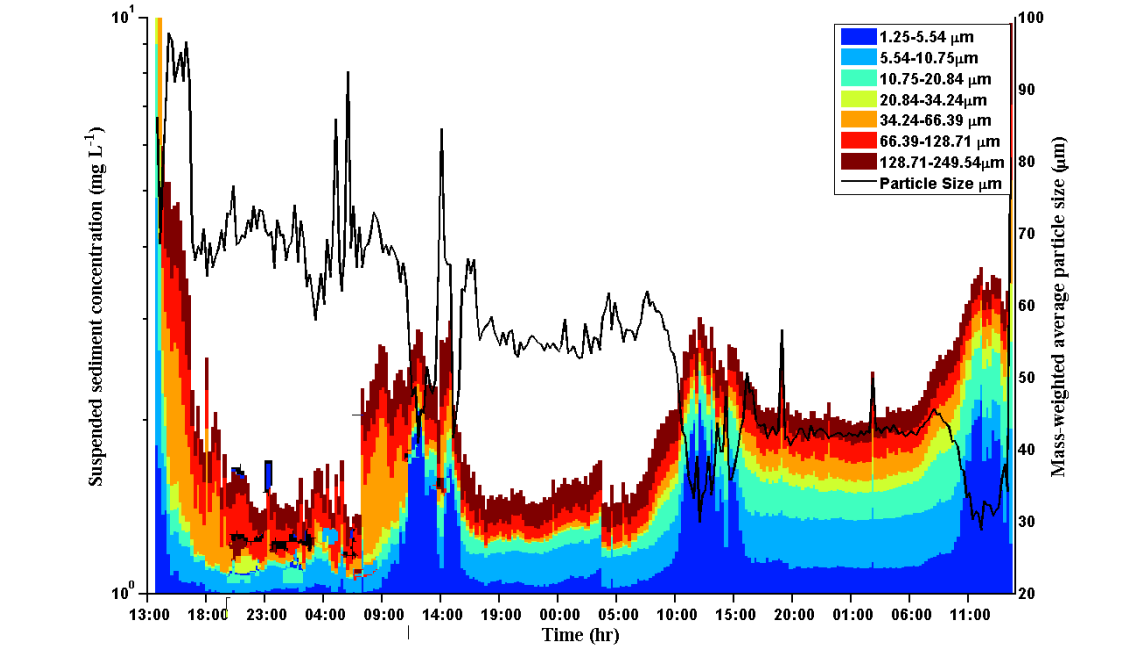

Figure D-223 Stacked time series of particle size distribution and mass-weighted particle size distributions at RS1D Ridge site. Data were binned into 32 size categories from 1.25 to 250 microns. Deployed period is November 5, 2012 13:47 to November 8, 2012 14:18. Data baseline set to 10^0.

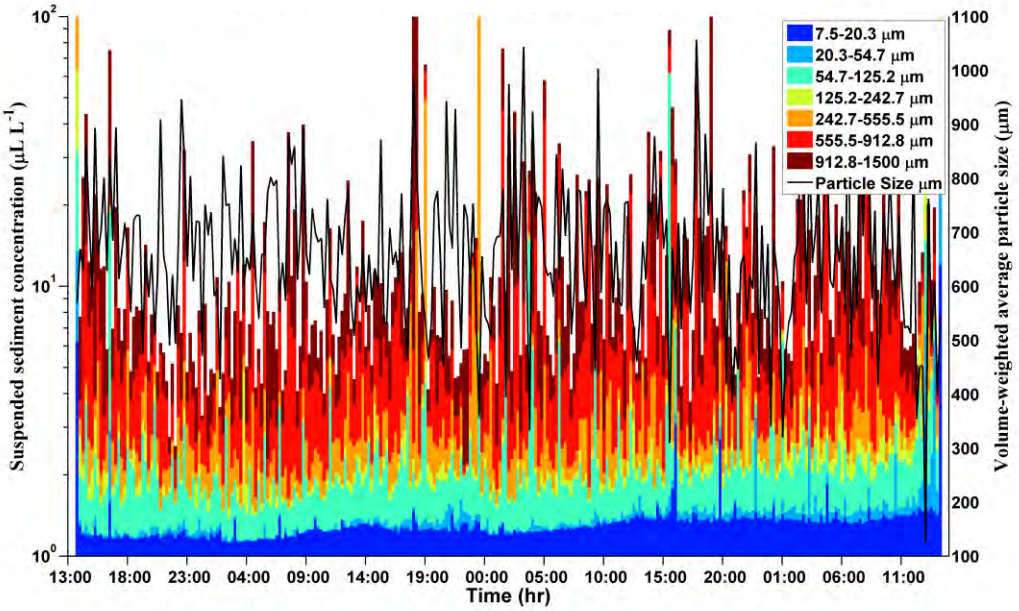

Figure D-224 Time series of particle size distribution and volume-weighted particle size distributions at RS1D Slough site. Data were binned into 32 size categories from 7.5 to 1500 microns. Deployed period is November 5, 2012 13:50 to November 8, 2012 14:52. Data baseline set to 10^0.

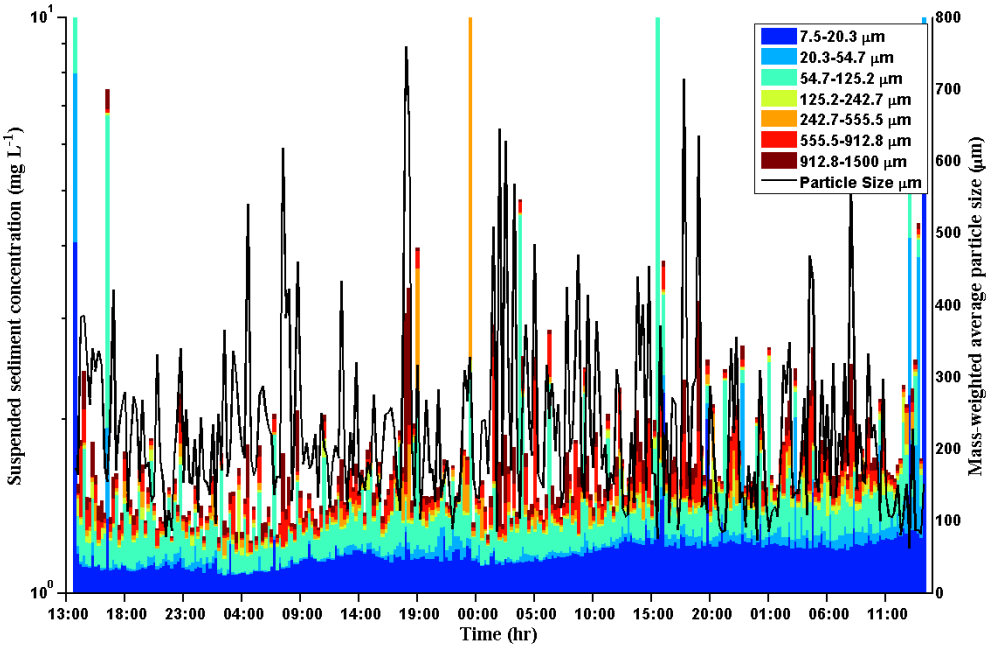

Figure D-225 Stacked time series of particle size distribution and mass-weighted particle size distributions at RS1D Slough site. Data were binned into 32 size categories from 7.5 to 1500 microns. Deployed period is November 5, 2012 13:50 to November 8, 2012 14:52. Data baseline set to 10^0.

2013 February

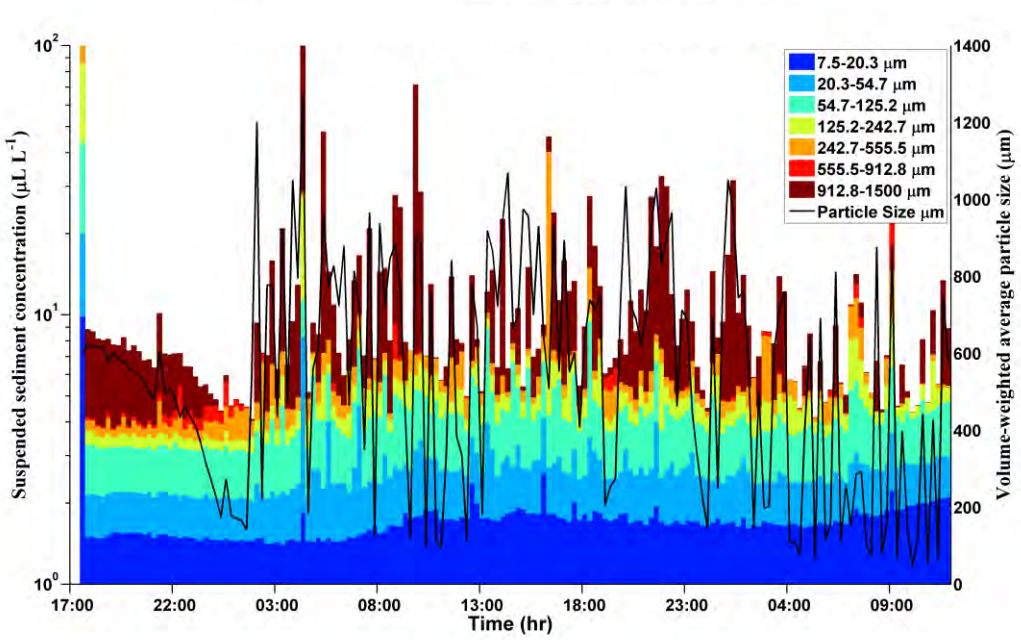

Figure D-226 Stacked time series of particle size distribution and volume-weighted particle size distributions at UB1 site. Data were binned into 32 size categories from 7.5 to 1500 microns. Deployed period is February 26, 2013 17:40 to February 28, 2013 12:05. Data baseline set to 10^0.

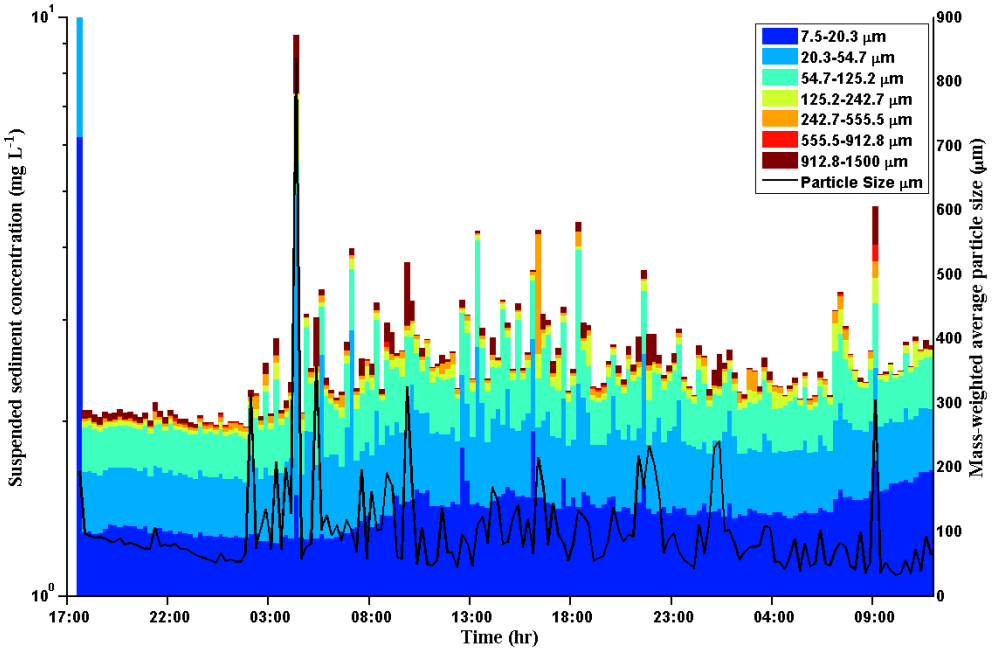

Figure D-227 Stacked time series of particle size distribution and mass-weighted particle size distributions at UB1 site. Data were binned into 32 size categories from 7.5 to 1500 microns. Deployed period is February 26, 2013 17:40 to February 28, 2013 12:05. Data baseline set to 10^0.

2013 August

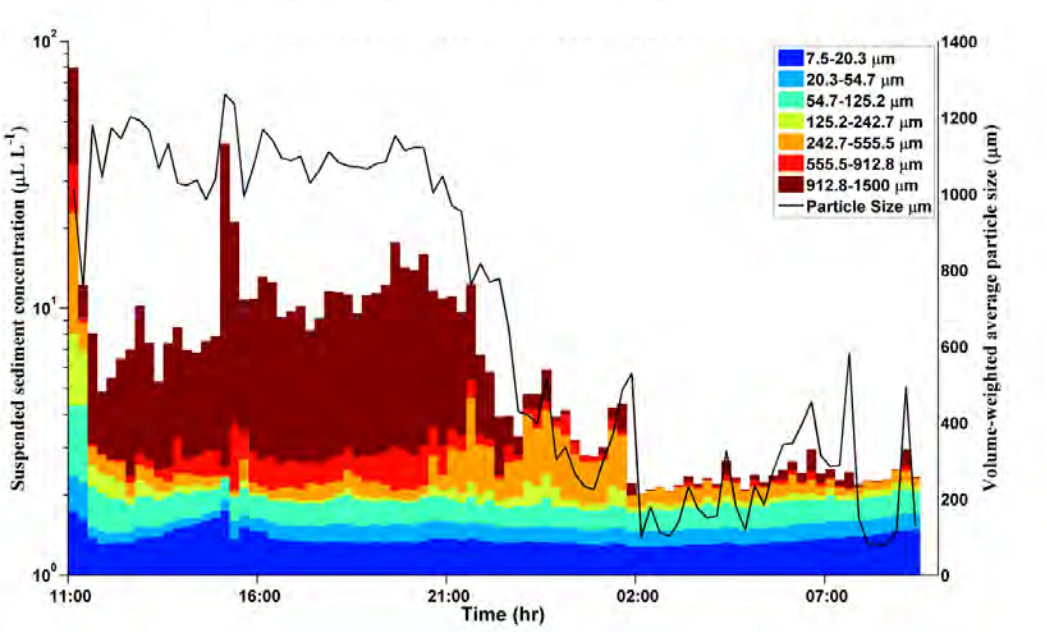

Figure D-228 Stacked time series of particle size distribution and volume-weighted particle size distributions at RS1D Slough site. Data were binned into 32 size categories from 7.5 to 1500 microns. Deployed period is August 14, 2013 11:08 to August 15, 2013 09:24. Data baseline set to 10^0.

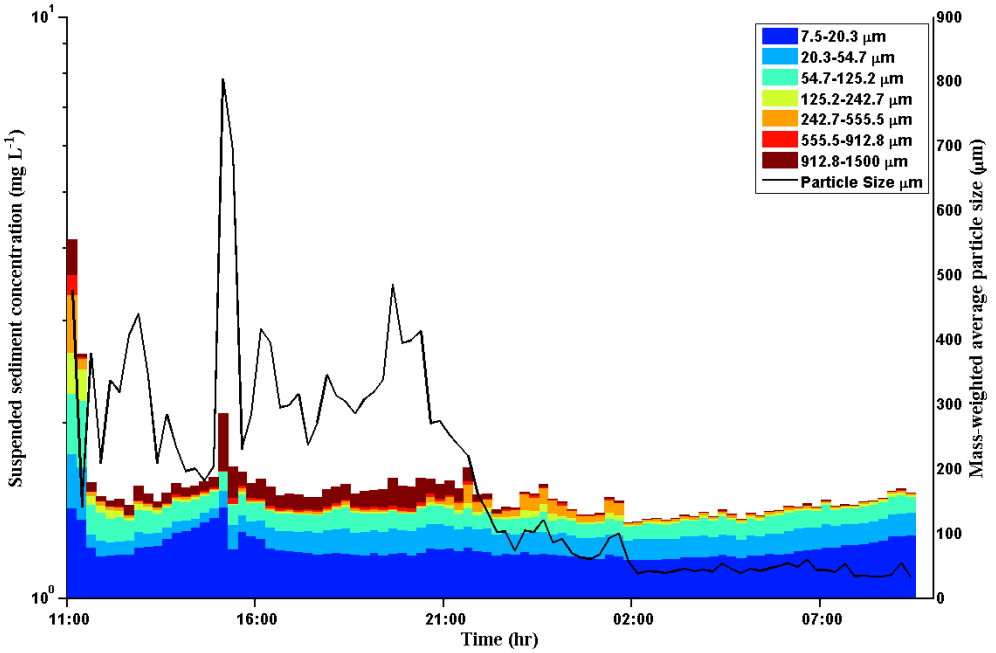

Figure D-229 Stacked time series of particle size distribution and mass-weighted particle size distributions at RS1D Slough site. Data were binned into 32 size categories from 7.5 to 1500 microns. Deployed period is August 14, 2013 11:08 to August 15, 2013 09:24. Data baseline set to 10^0.

2013 September

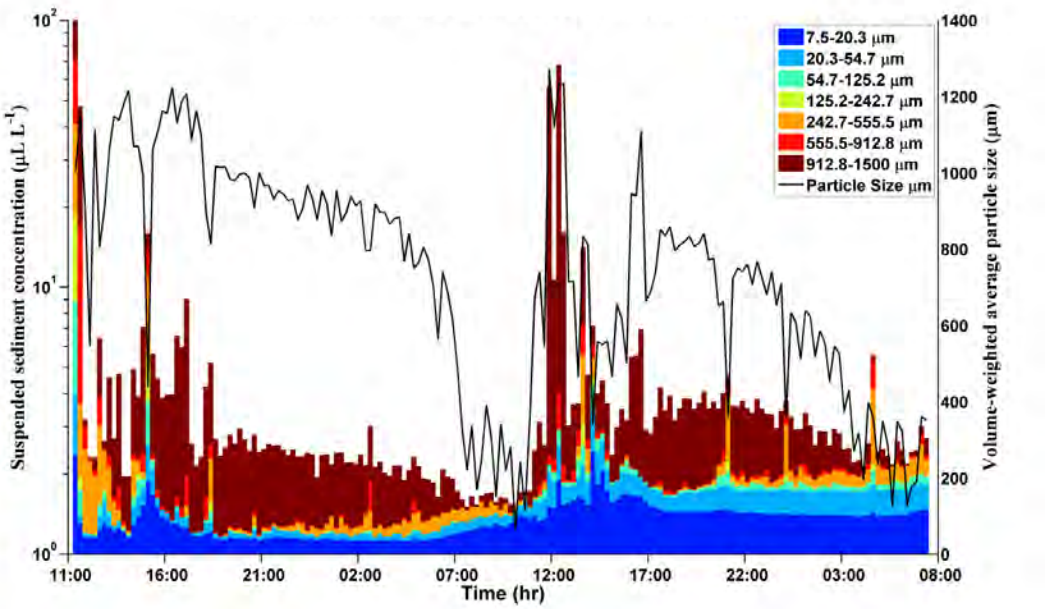

Figure D-230 Stacked time series of particle size distribution and volume-weighted particle size distributions at UB2 site. Data were binned into 32 size categories from 7.5 to 1500 microns. Deployed period is September 24, 2013 11:22 to September 26, 2013 07:39. Data baseline set to 10^0.

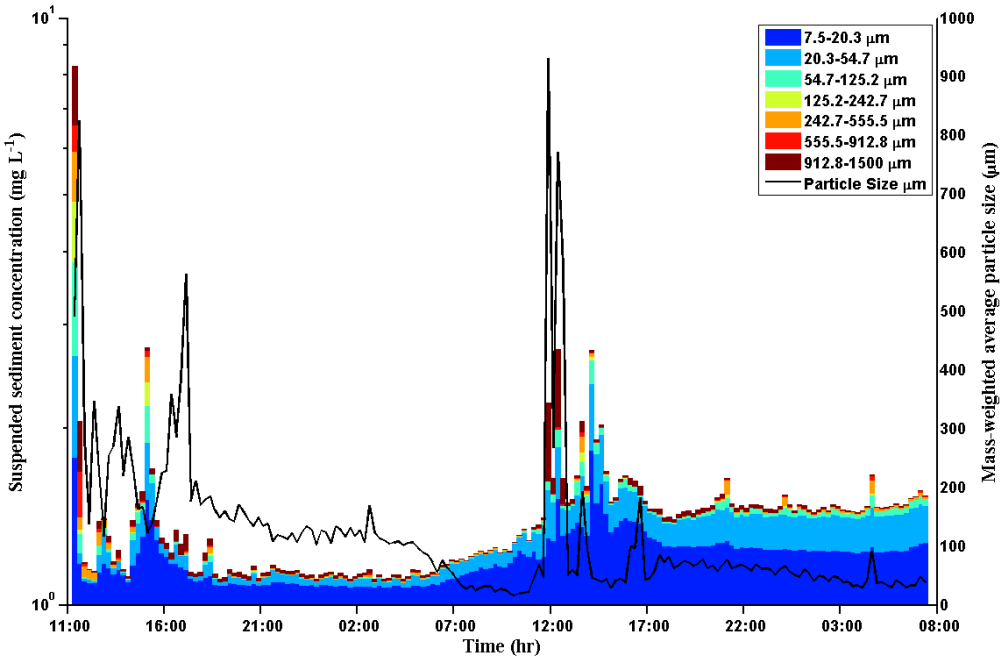

Figure D-231 Stacked time series of particle size distribution and mass-weighted particle size distributions at UB2 site. Data were binned into 32 size categories from 7.5 to 1500 microns. Deployed period is September 24, 2013 11:22 to September 26, 2013 07:39. Data baseline set to 10^0.

2013 November

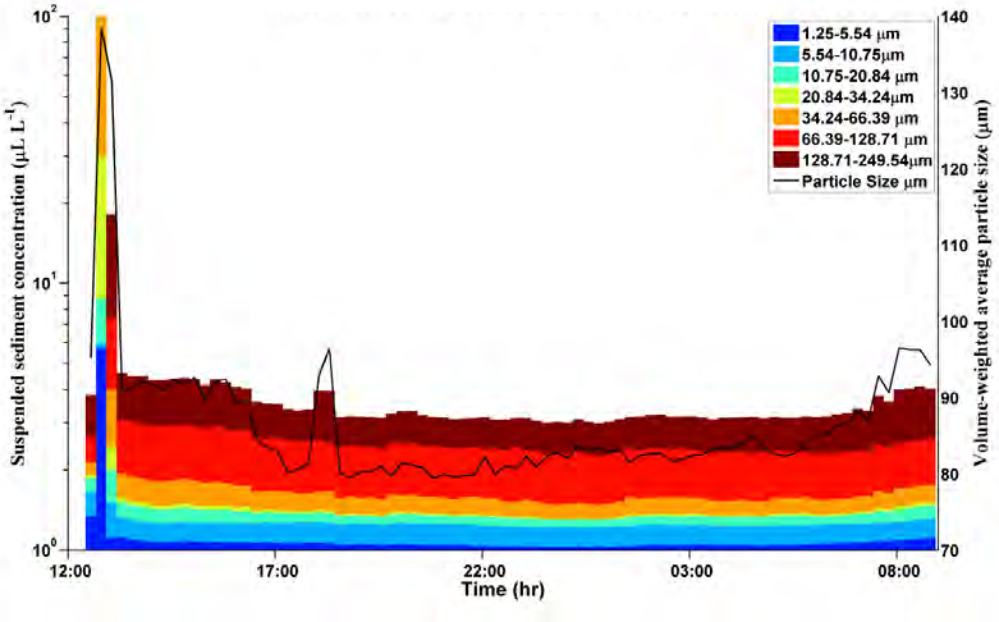

Figure D-232 Stacked time series of particle size distribution and volume-weighted particle size distributions at RS1D Ridge site. Data were binned into 32 size categories from 1.25 to 250 microns. Deployed period is November 4, 2013 13:30 to November 5, 2013 09:00 (Pre-Flow). Data baseline set to 10^0.

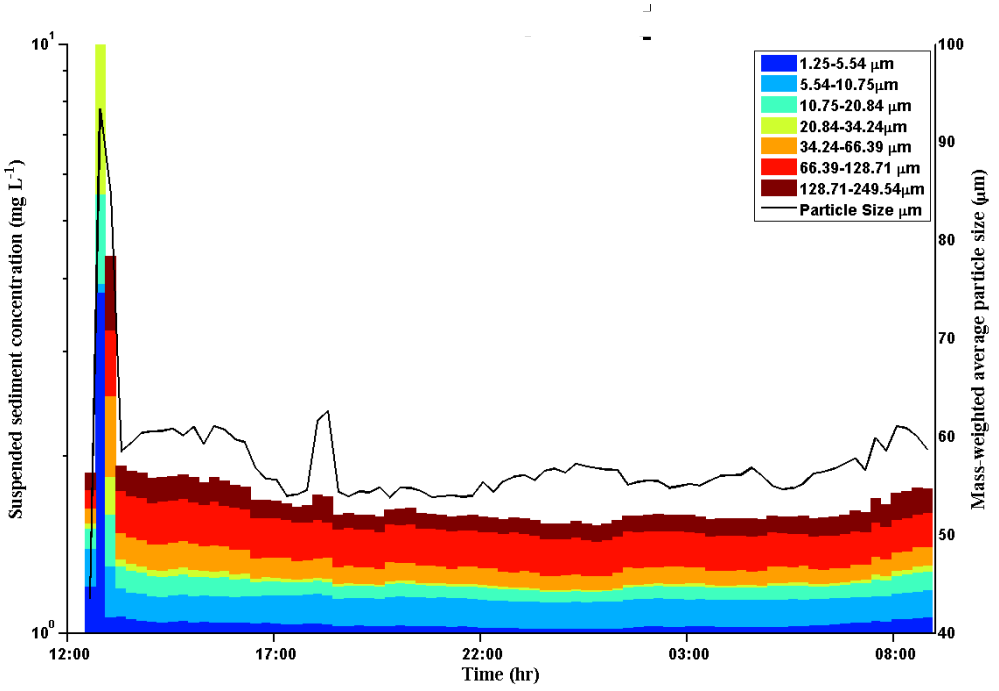

Figure D-233 Stacked time series of particle size distribution and mass-weighted particle size distributions at RS1D Ridge site. Data were binned into 32 size categories from 1.25 to 250 microns. Deployed period is November 4, 2013 13:30 to November 5, 2013 09:00 (Pre-Flow). Data baseline set to 10^0.

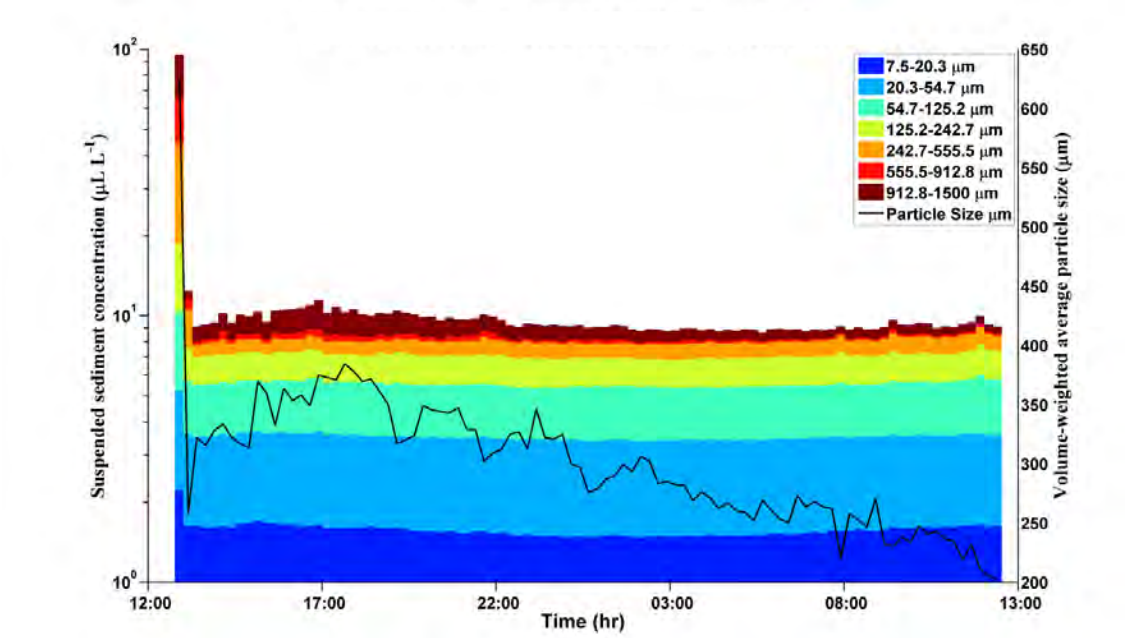

Figure D-234 Stacked time series of particle size distribution and volume-weighted particle size distributions at RS1D Ridge site. Data were binned into 32 size categories from 7.5 to 1500 microns. Deployed period is November 3, 2013 12:54 to November 4, 2013 12:30 (Pre-Flow). Data baseline set to 10^0.

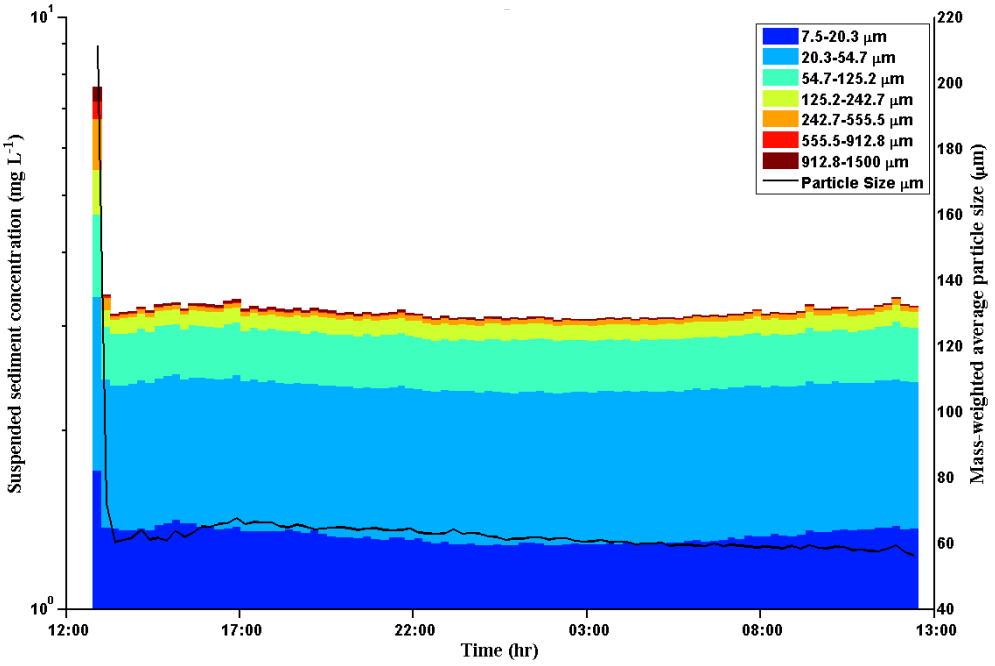

Figure D-235 Stacked time series of particle size distribution and mass-weighted particle size distributions at RS1D Ridge site. Data were binned into 32 size categories from 7.5 to 1500 microns. Deployed period is November 3, 2013 12:54 to November 4, 2013 12:30 (Pre-Flow). Data baseline set to 10^0.

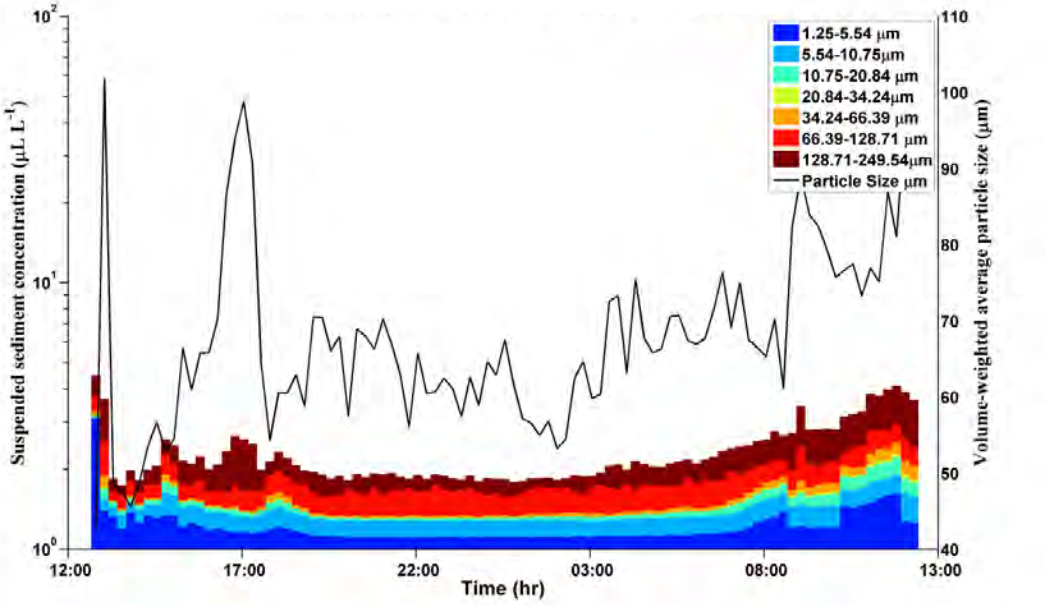

Figure D-236 Stacked time series of particle size distribution and volume-weighted particle size distributions at RS1D Slough site. Data were binned into 32 size categories from 1.25 to 250 microns. Deployed period is November 3, 2013 12:47 to November 4, 2013 12:30 (Pre-Flow). Data baseline set to 10^0.

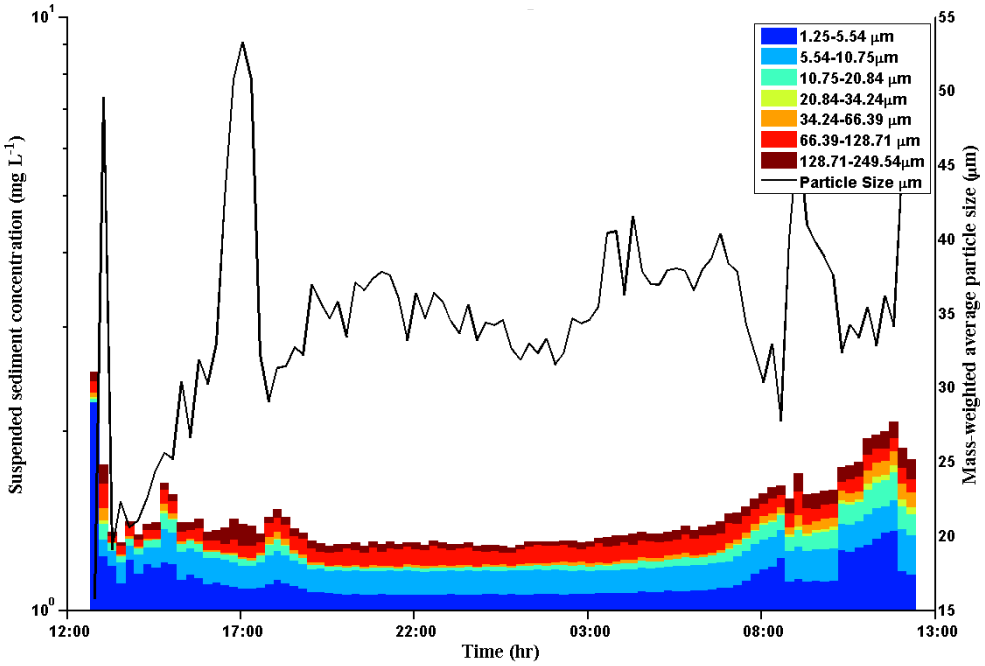

Figure D-237 Stacked time series of particle size distribution and mass-weighted particle size distributions at RS1D Slough site. Data were binned into 32 size categories from 1.25 to 250 microns. Deployed period is November 3, 2013 12:47 to November 4, 2013 12:30 (Pre-Flow). Data baseline set to 10^0.

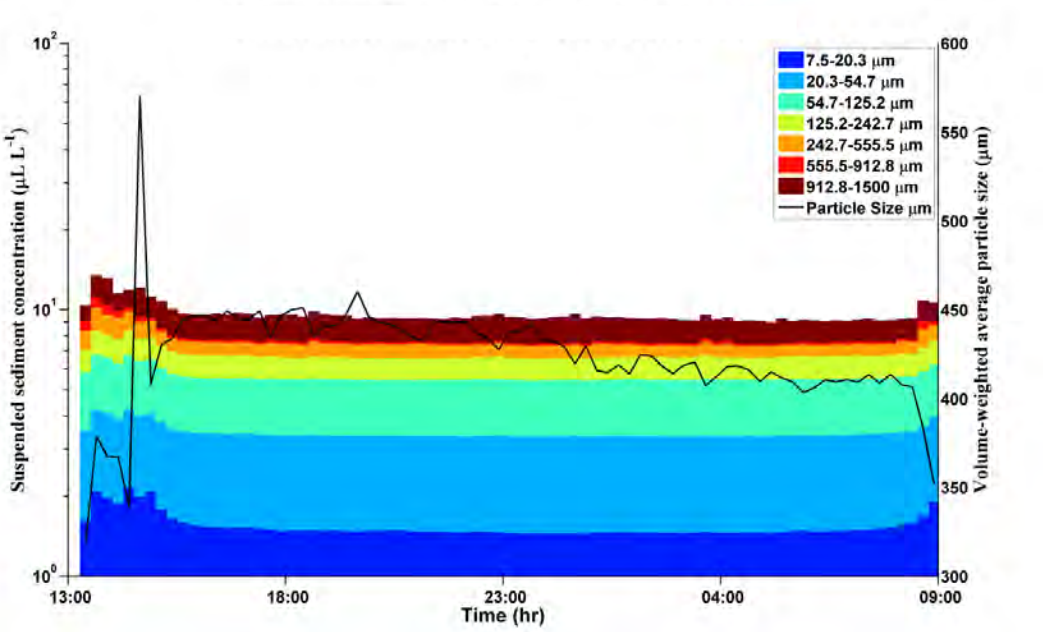

Figure D-238 Stacked time series of particle size distribution and volume-weighted particle size distributions at RS1D Slough site. Data were binned into 32 size categories from 7.5 to 1500 microns. Deployed period is November 4, 2013 13:30 to November 5, 2013 09:00 (Pre-Flow). Data baseline set to 10^0.

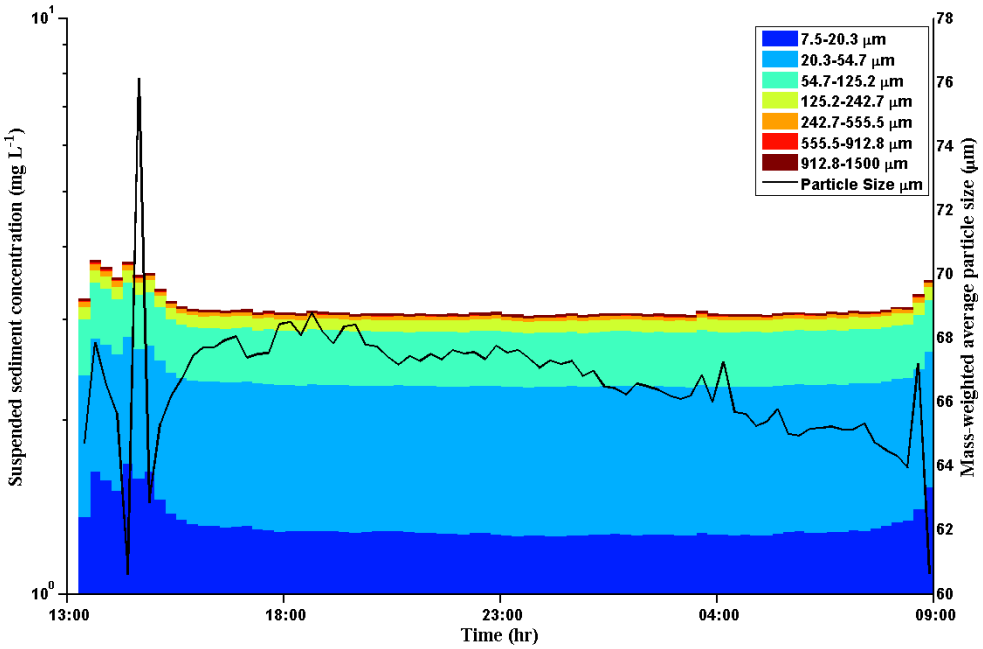

Figure D-239 Stacked time series of particle size distribution and mass-weighted particle size distributions at RS1D Slough site. Data were binned into 32 size categories from 7.5 to 1500 microns. Deployed period is November 4, 2013 13:30 to November 5, 2013 09:00 (Pre-Flow). Data baseline set to 10^0.

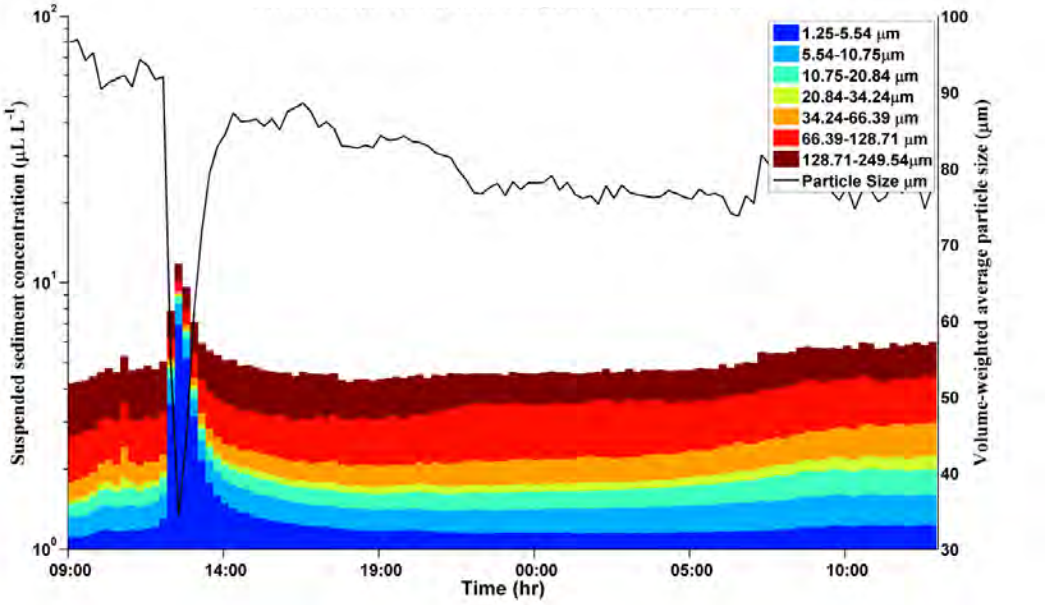

Figure D-240 Stacked time series of particle size distribution and volume-weighted particle size distributions at RS1D Ridge site. Data were binned into 32 size categories from 1.25 to 250 microns. Deployed period is November 5, 2013 09:00 to November 6, 2013 13:00 (Transient). Data baseline set to 10^0.

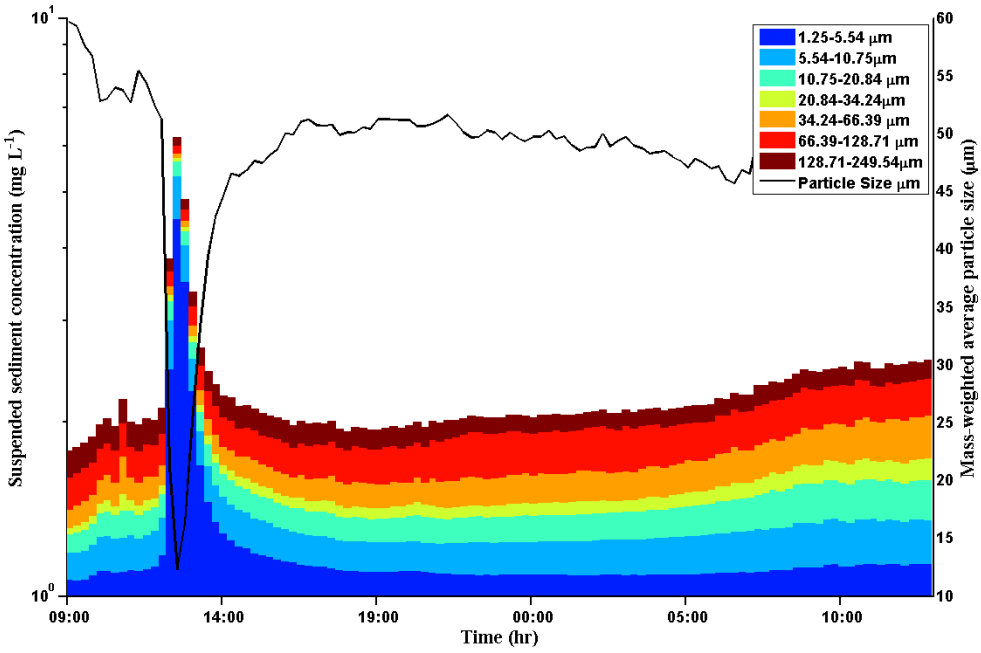

Figure D-241 Stacked time series of particle size distribution and mass-weighted particle size distributions at RS1D Ridge site. Data were binned into 32 size categories from 1.25 to 250 microns. Deployed period is November 5, 2013 09:00 to November 6, 2013 13:00 (Transient). Data baseline set to 10^0.

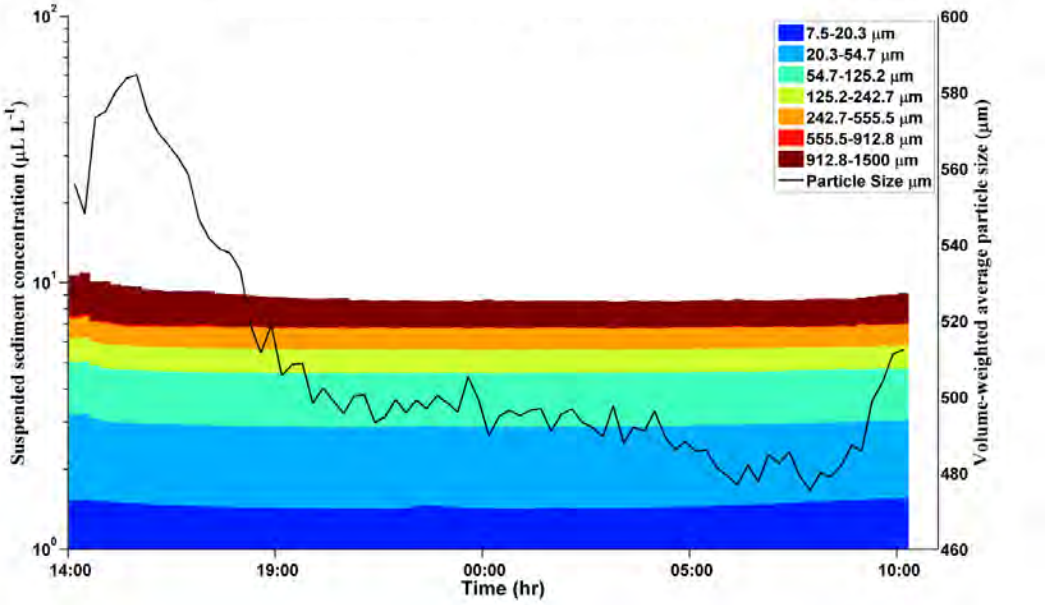

Figure D-242 Stacked time series of particle size distribution and volume-weighted particle size distributions at RS1D Ridge site. Data were binned into 32 size categories from 7.5 to 1500 microns. Deployed period is November 6, 2013 14:00 to November 7, 2013 10:00 (Transient). Data baseline set to 10^0.

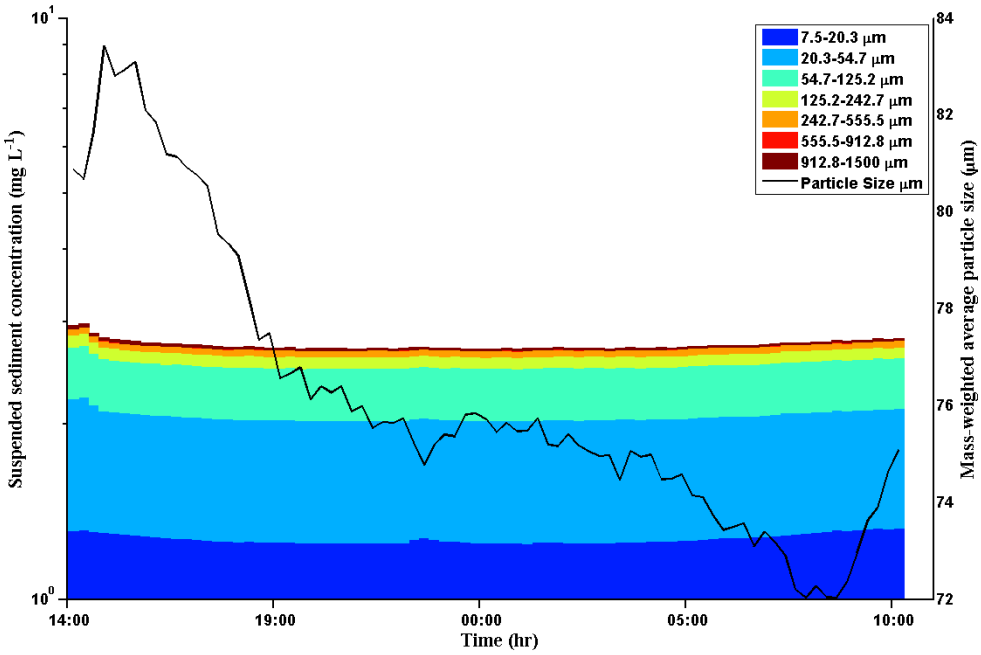

Figure D-243 Stacked time series of particle size distribution and mass-weighted particle size distributions at RS1D Ridge site. Data were binned into 32 size categories from 7.5 to 1500 microns. Deployed period is November 6, 2013 14:00 to November 7, 2013 10:00 (Transient). Data baseline set to 10^0.

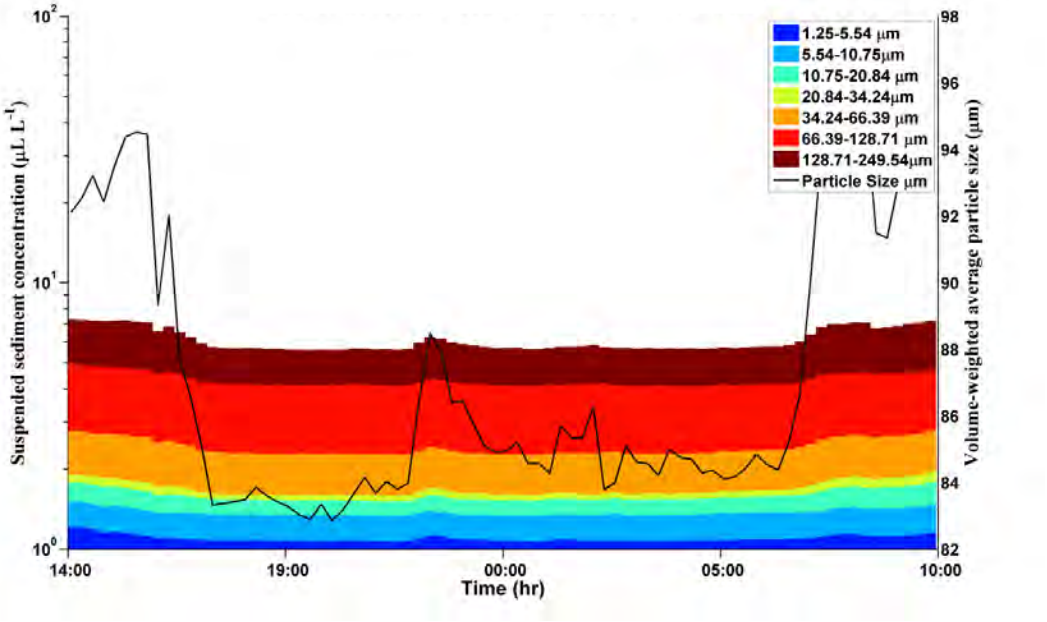

Figure D-244 Stacked time series of particle size distribution and volume-weighted particle size distributions at RS1D Slough site. Data were binned into 32 size categories from 1.25 to 250 microns. Deployed period is November 6, 2013 14:00 to November 7, 2013 10:00 (Transient). Data baseline set to 10^0.

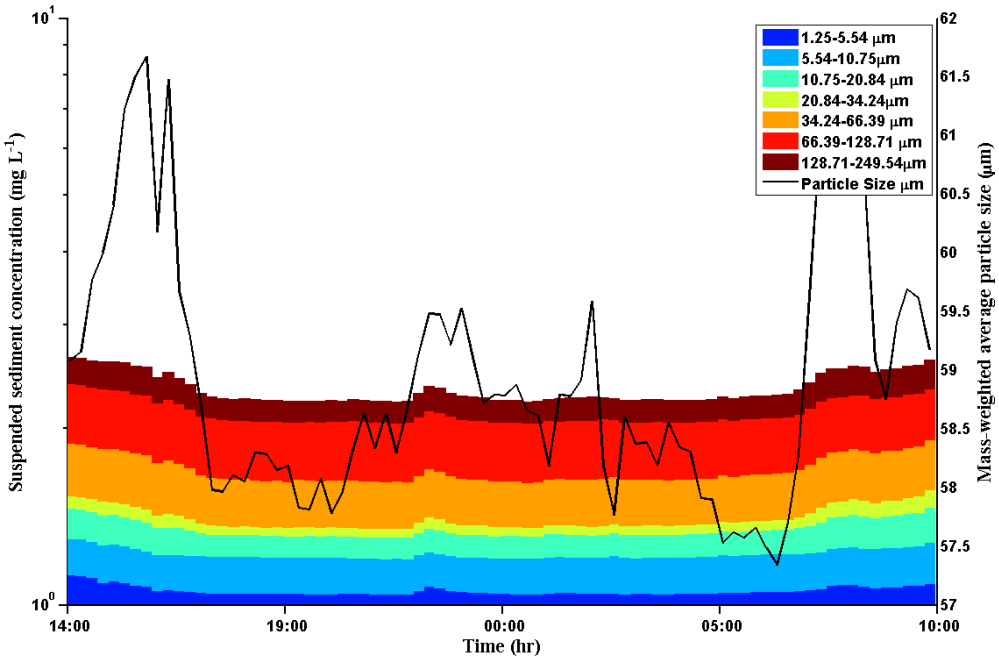

Figure D-245 Stacked time series of particle size distribution and mass-weighted particle size distributions at RS1D Slough site. Data were binned into 32 size categories from 1.25 to 250 microns. Deployed period is November 6, 2013 14:00 to November 7, 2013 10:00 (Transient). Data baseline set to 10^0.

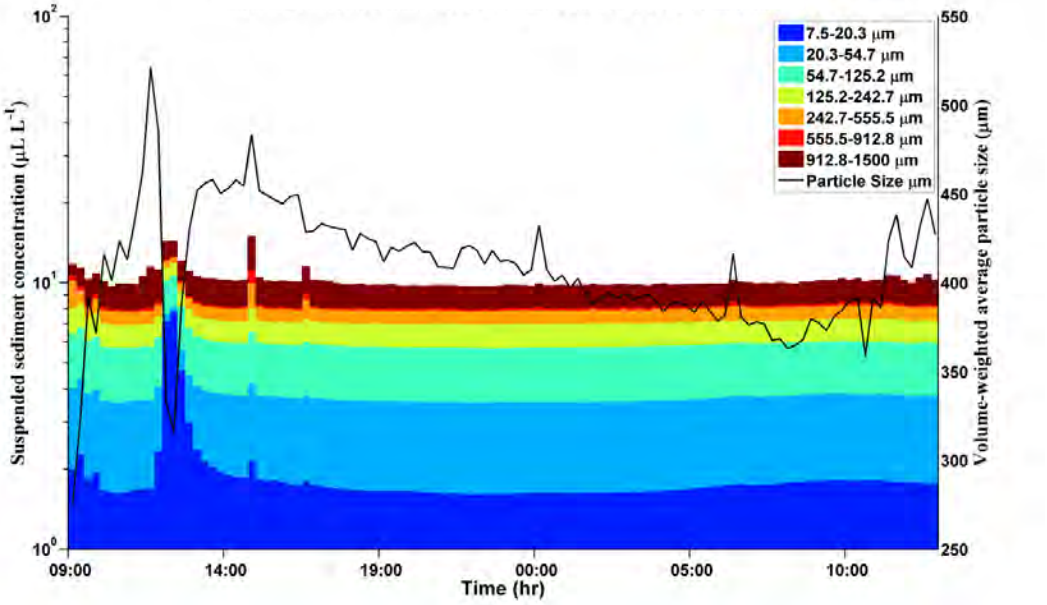

Figure D-246 Stacked time series of particle size distribution and volume-weighted particle size distributions at RS1D Slough site. Data were binned into 32 size categories from 7.5 to 1500 microns. Deployed period is November 5, 2013 09:00 to November 6, 2013 13:00 (Transient). Data baseline set to 10^0.

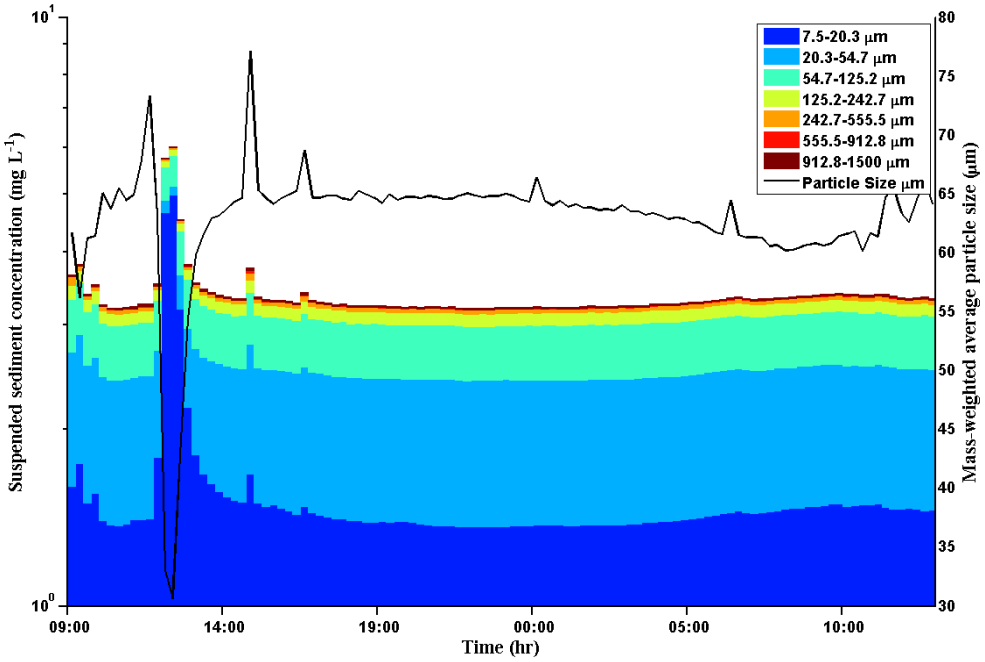

Figure D-247 Stacked time series of particle size distribution and mass-weighted particle size distributions at RS1D Slough site. Data were binned into 32 size categories from 7.5 to 1500 microns. Deployed period is November 5, 2013 09:00 to November 6, 2013 13:00 (Transient). Data baseline set to 10^0.

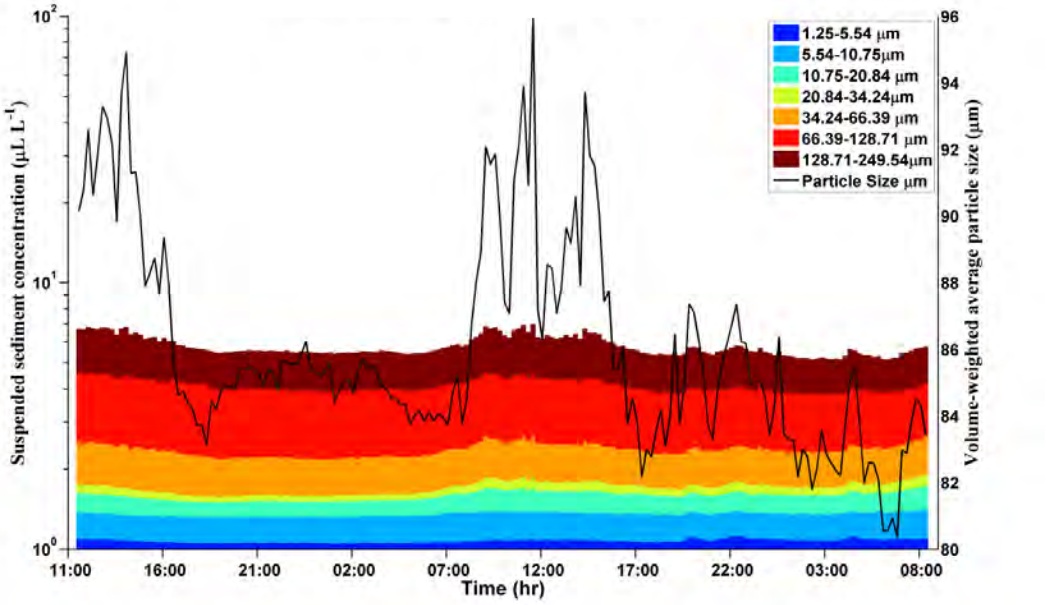

Figure D-248 Stacked time series of particle size distribution and volume-weighted particle size distributions at RS1D Ridge site. Data were binned into 32 size categories from 1.25 to 250 microns. Deployed period is November 7, 2013 11:30 to November 9, 2013 08:30 (Steady Flow). Data baseline set to 10^0.

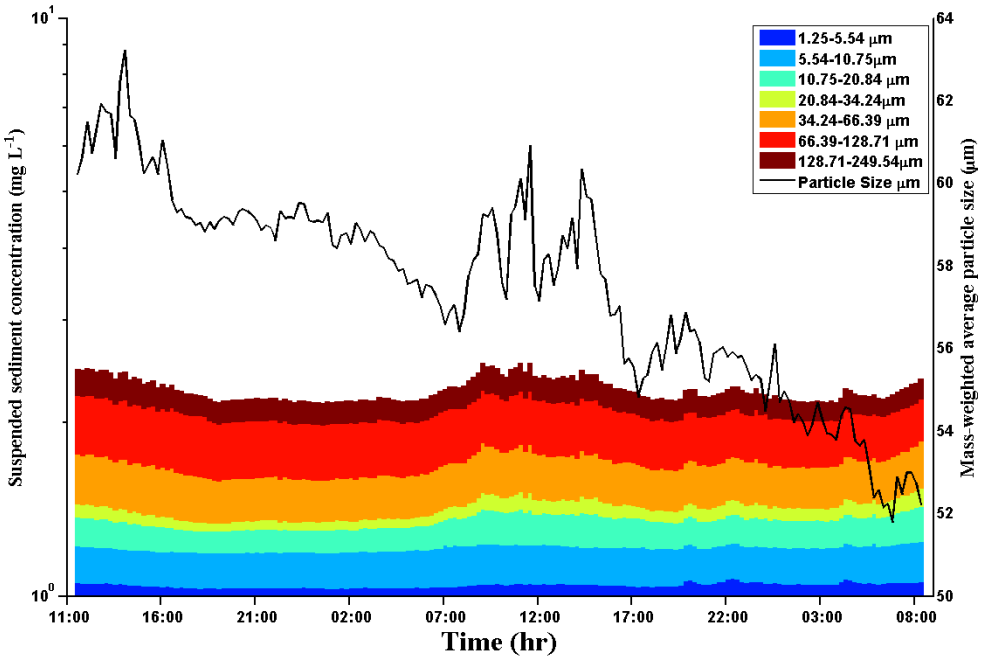

Figure D-249 Stacked time series of particle size distribution and mass-weighted particle size distributions at RS1D Ridge site. Data were binned into 32 size categories from 1.25 to 250 microns. Deployed period is November 7, 2013 11:30 to November 9, 2013 08:30 (Steady Flow). Data baseline set to 10^0.

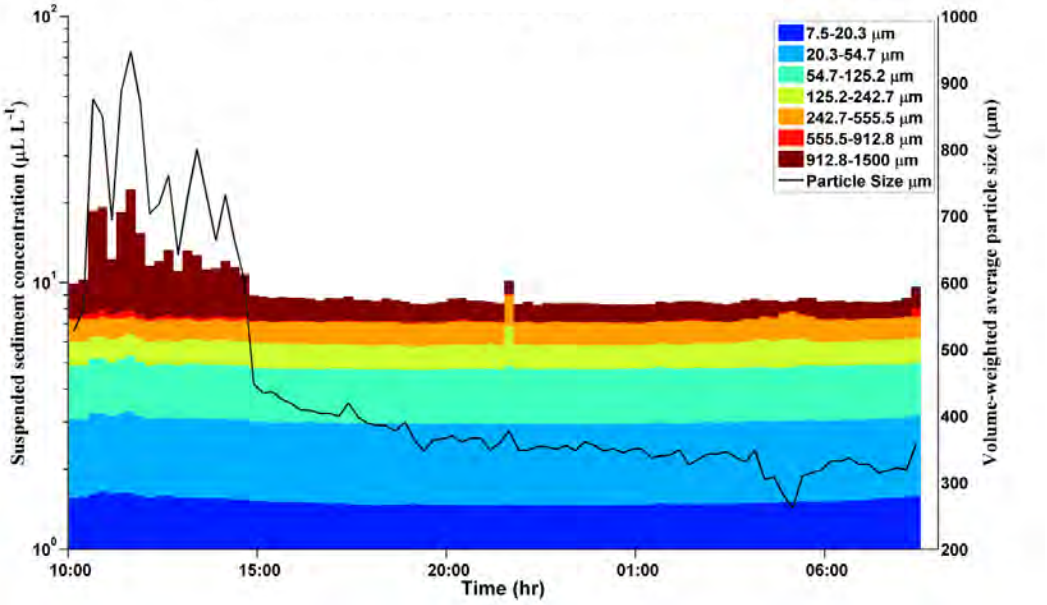

Figure D-250 Stacked time series of particle size distribution and volume-weighted particle size distributions at RS1D Ridge site. Data were binned into 32 size categories from 7.5 to 1500 microns. Deployed period is November 9, 2013 10:00 to November 10, 2013 08:30 (Steady Flow). Data baseline set to 10^0.

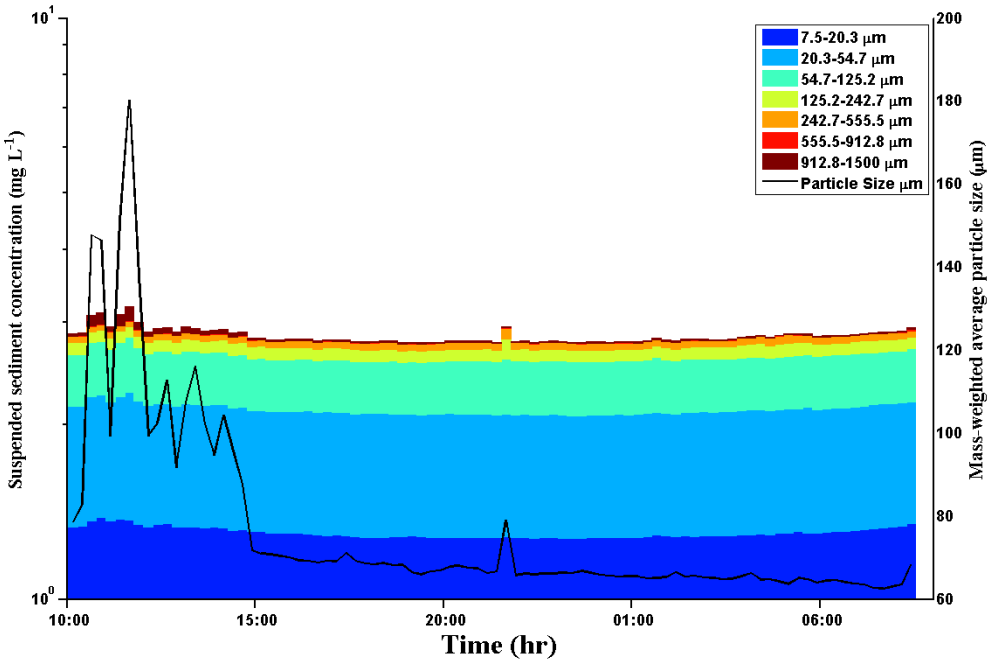

Figure D-251 Stacked time series of particle size distribution and mass-weighted particle size distributions at RS1D Ridge site. Data were binned into 32 size categories from 7.5 to 1500 microns. Deployed period is November 9, 2013 10:00 to November 10, 2013 08:30 (Steady Flow). Data baseline set to 10^0.

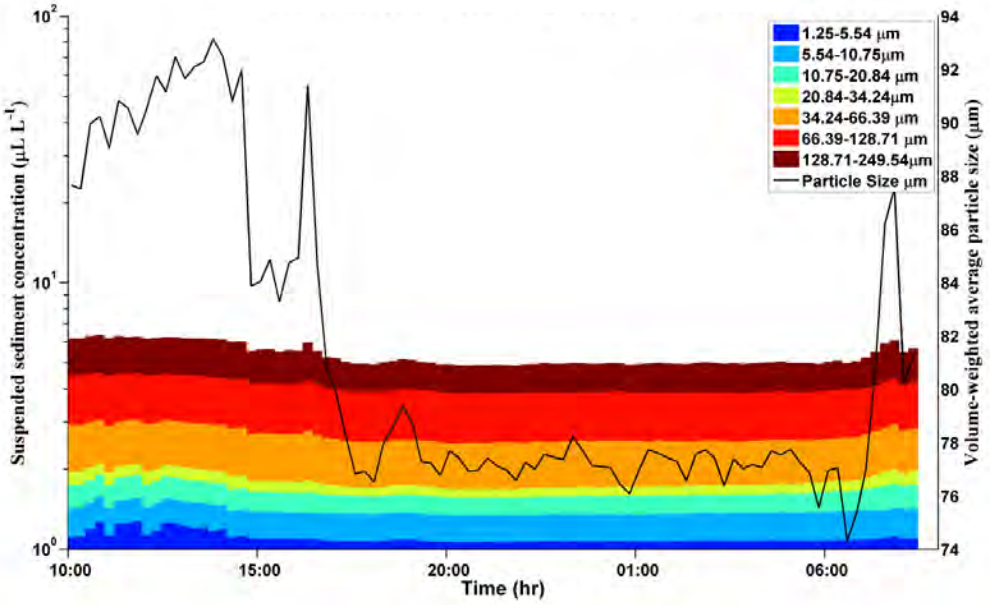

Figure D-252 Stacked time series of particle size distribution and volume-weighted particle size distributions at RS1D Slough site. Data were binned into 32 size categories from 1.25 to 250 microns. Deployed period is November 9, 2013 10:00 to November 10, 2013 08:30 (Steady Flow). Data baseline set to 10^0.

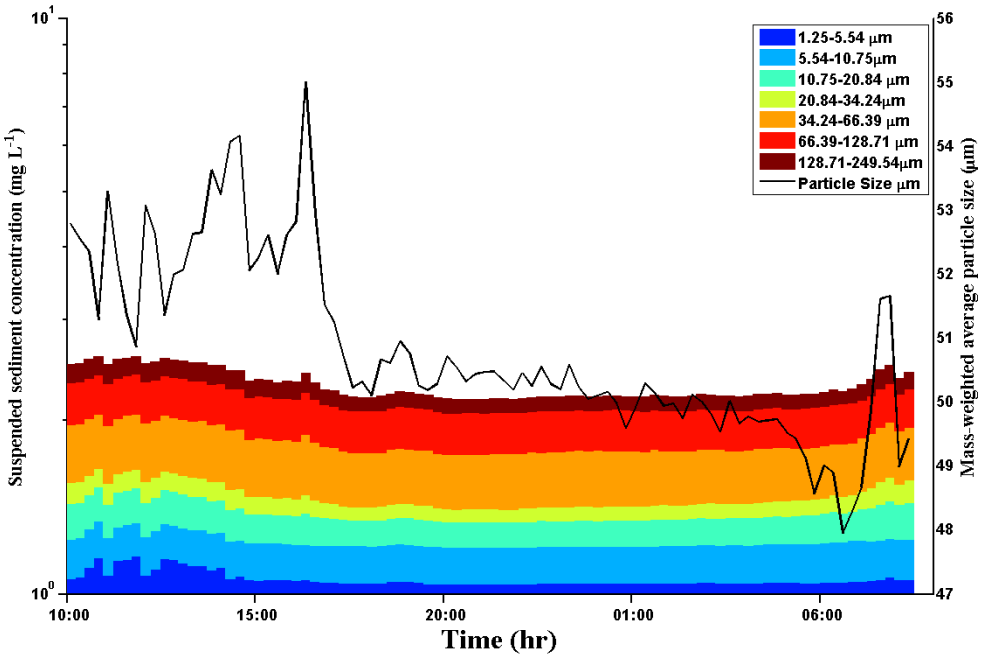

Figure D-253 Stacked time series of particle size distribution and mass-weighted particle size distributions at RS1D Slough site. Data were binned into 32 size categories from 1.25 to 250 microns. Deployed period is November 9, 2013 10:00 to November 10, 2013 08:30 (Steady Flow). Data baseline set to 10^0.

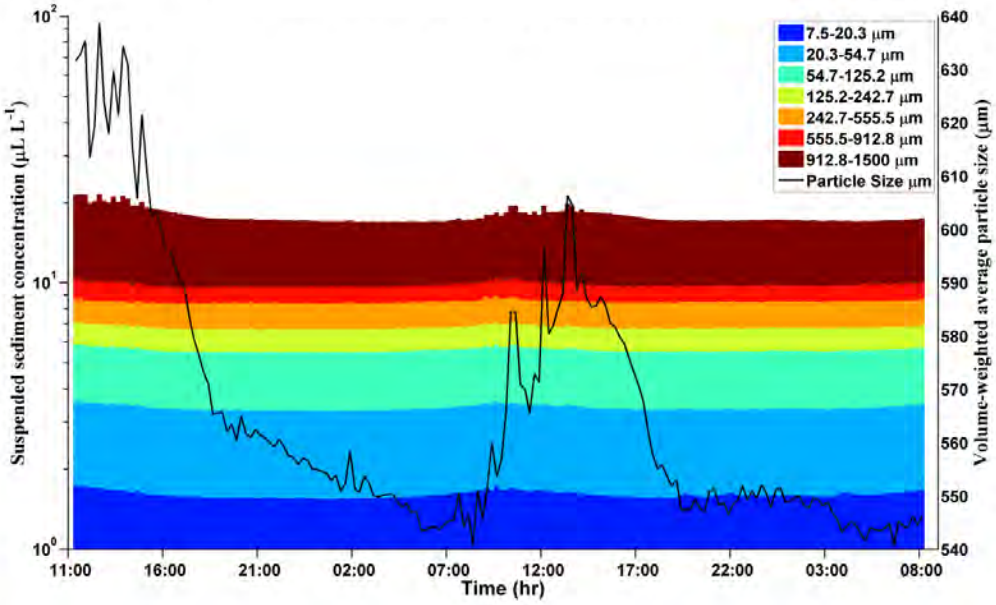

Figure D-254 Stacked time series of particle size distribution and volume-weighted particle size distributions at RS1D Slough site. Data were binned into 32 size categories from 7.5 to 1500 microns. Deployed period is November 7, 2013 11:30 to November 9, 2013 08:30 (Steady Flow). Data baseline set to 10^0.

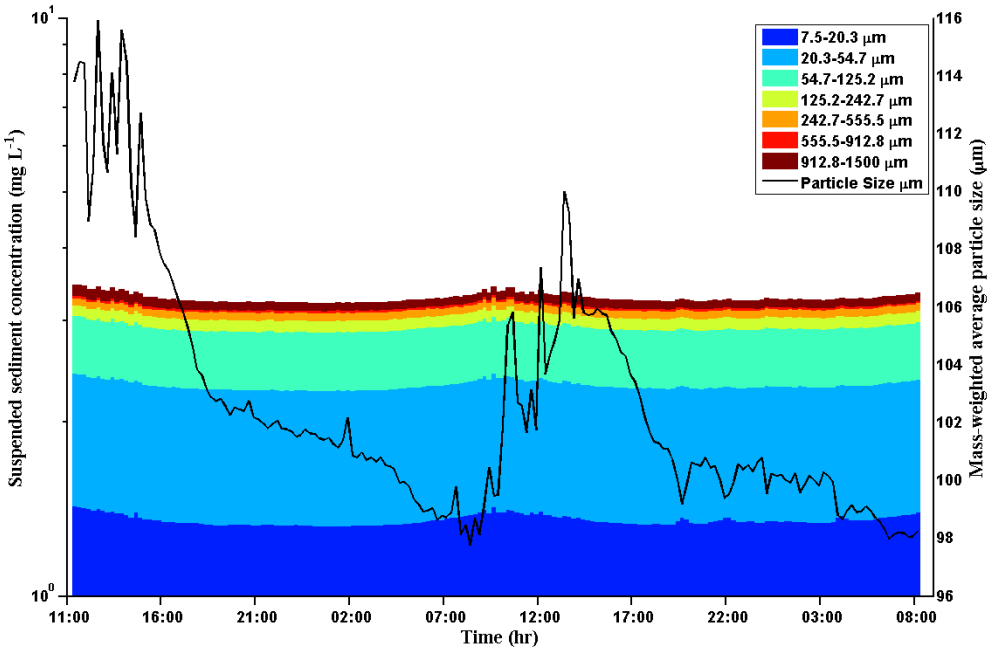

Figure D-255 Stacked time series of particle size distribution and mass-weighted particle size distributions at RS1D Slough site. Data were binned into 32 size categories from 7.5 to 1500 microns. Deployed period is November 7, 2013 11:30 to November 9, 2013 08:30 (Steady Flow). Data baseline set to 10^0.

2014 November

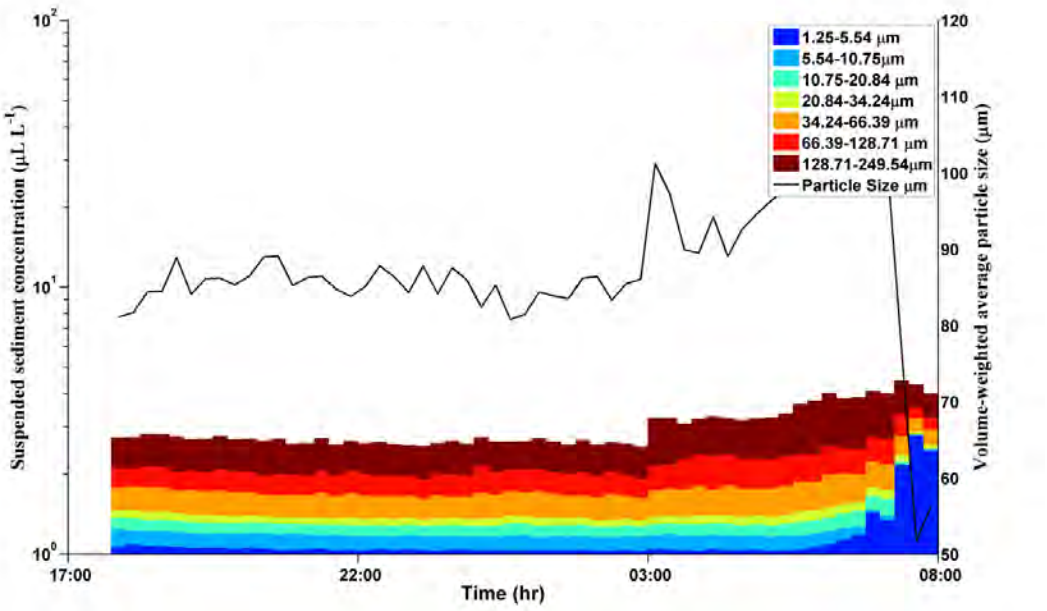

Figure D-256 Stacked time series of particle size distribution and volume-weighted particle size distributions at RS1D Ridge site. Data were binned into 32 size categories from 1.25 to 250 microns. Deployed period is November 2, 2014 18:00 to November 3, 2014 08:00 (Pre-Flow). Data baseline set to 10^0.

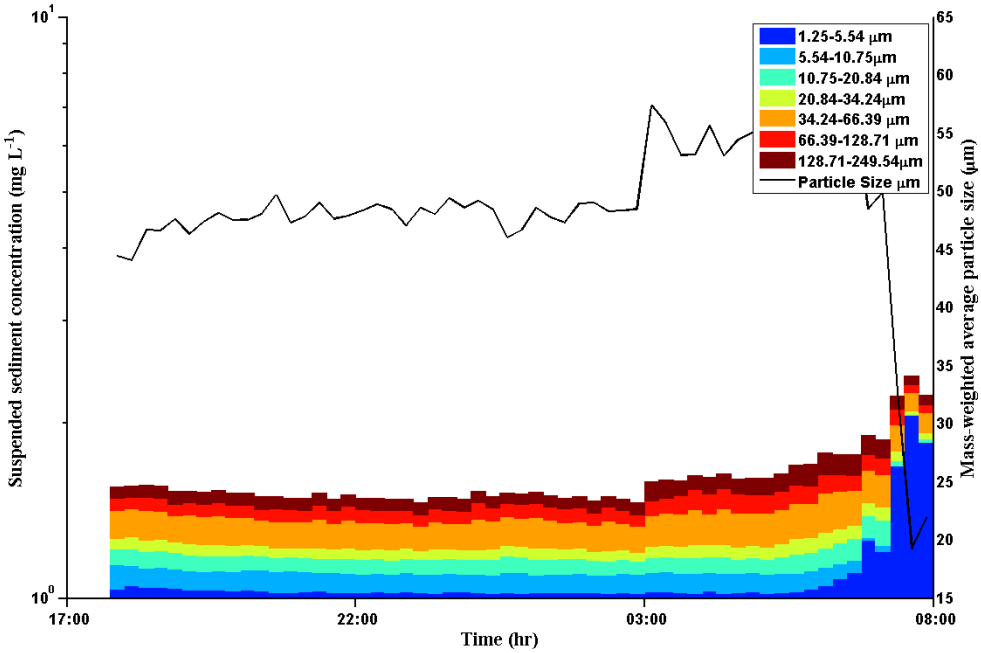

Figure D-257 Stacked time series of particle size distribution and mass-weighted particle size distributions at RS1D Ridge site. Data were binned into 32 size categories from 1.25 to 250 microns. Deployed period is November 2, 2014 18:00 to November 3, 2014 08:00 (Pre-Flow). Data baseline set to 10^0.

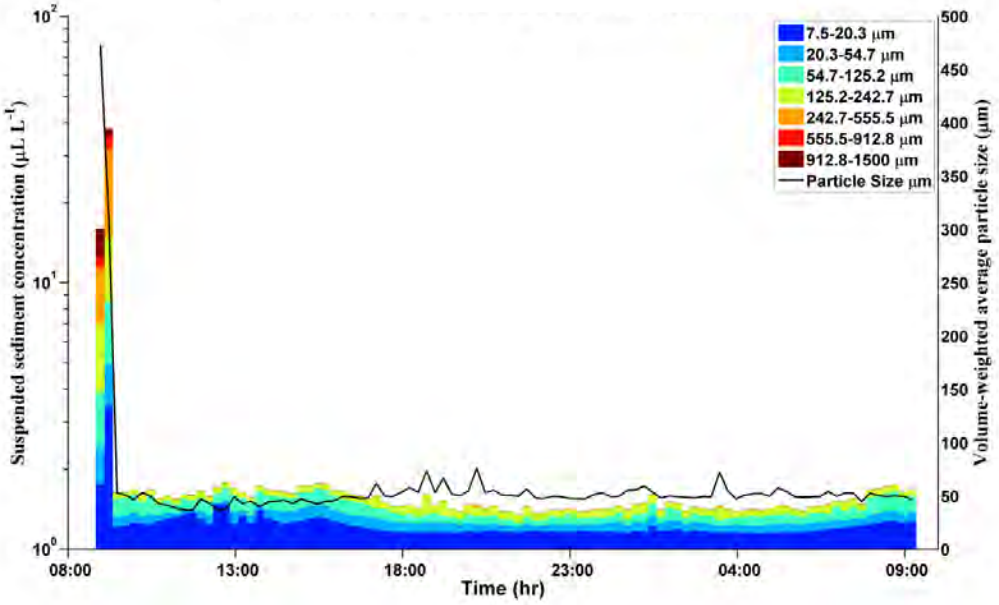

Figure D-258 Stacked time series of particle size distribution and volume-weighted particle size distributions at RS1D Ridge site. Data were binned into 32 size categories from 7.5 to 1500 microns. Deployed period is November 3, 2014 09:00 to November 4, 2014 09:30 (Pre-Flow). Data baseline set to 10^0.

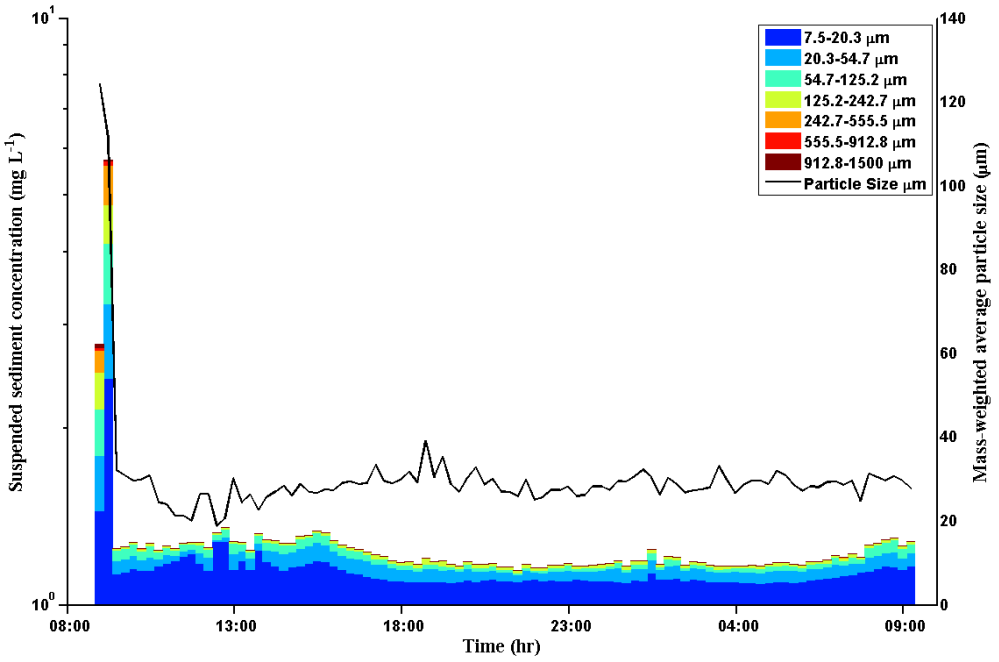

Figure D-259 Stacked time series of particle size distribution and mass-weighted particle size distributions at RS1D Ridge site. Data were binned into 32 size categories from 7.5 to 1500 microns. Deployed period is November 3, 2014 09:00 to November 4, 2014 09:30 (Pre-Flow). Data baseline set to 10^0.

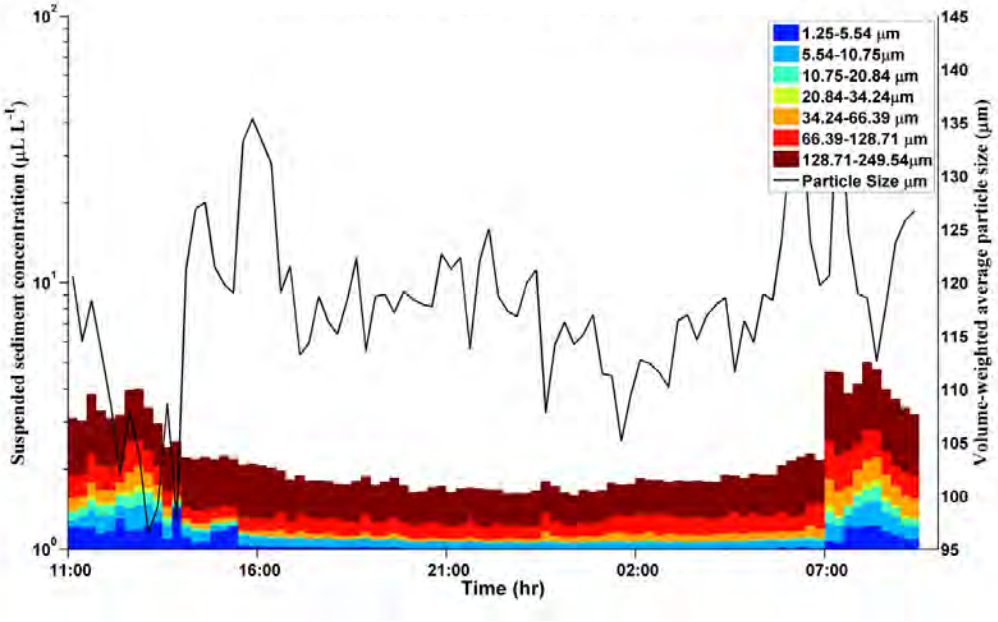

Figure D-260 Stacked time series of particle size distribution and volume-weighted particle size distributions at RS1D Slough site. Data were binned into 32 size categories from 1.25 to 250 microns. Deployed period is November 3, 2014 11:00 to November 4, 2014 09:30 (Pre-Flow). Data baseline set to 10^0.

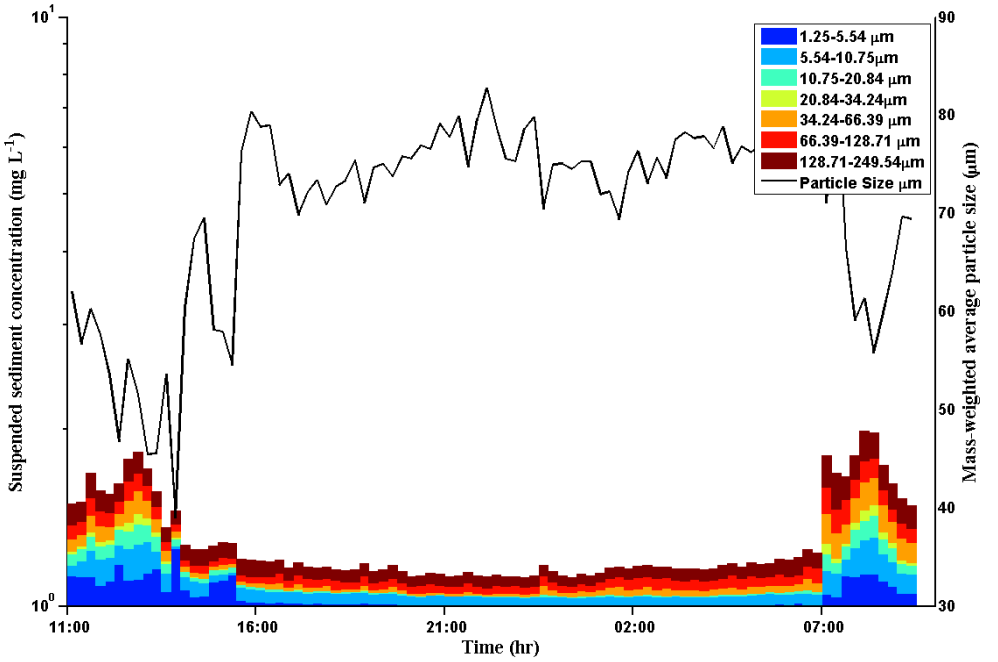

Figure D-261 Stacked time series of particle size distribution and mass-weighted particle size distributions at RS1D Slough site. Data were binned into 32 size categories from 1.25 to 250 microns. Deployed period is November 3, 2014 11:00 to November 4, 2014 09:30 (Pre-Flow). Data baseline set to 10^0.

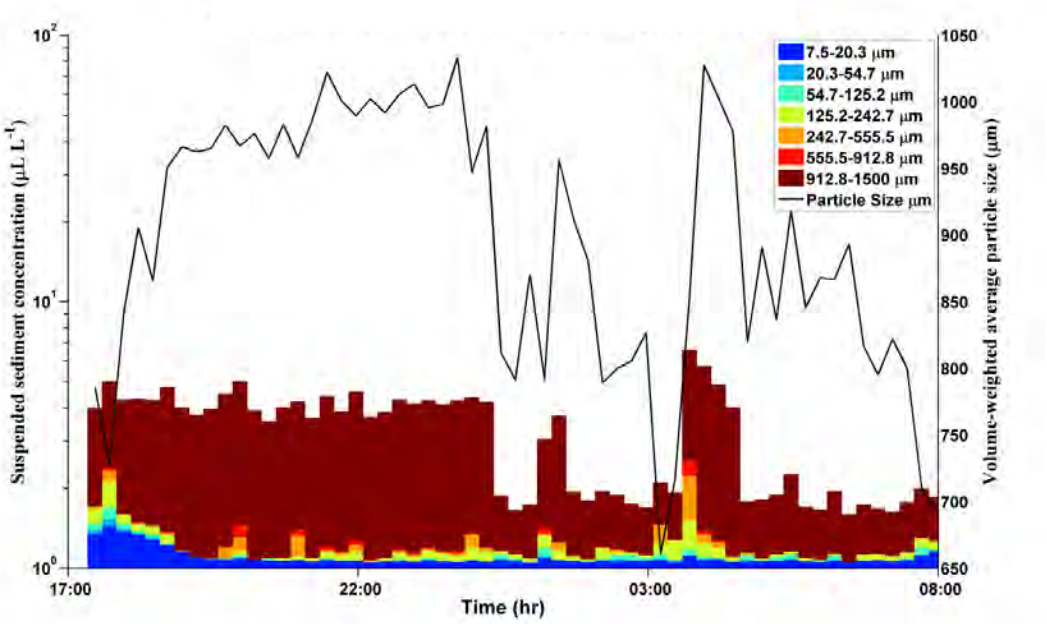

Figure D-262 Stacked time series of particle size distribution and volume-weighted particle size distributions at RS1D Slough site. Data were binned into 32 size categories from 7.5 to 1500 microns. Deployed period is November 2, 2014 18:00 to November 3, 2014 08:00 (Pre-Flow). Data baseline set to 10^0.

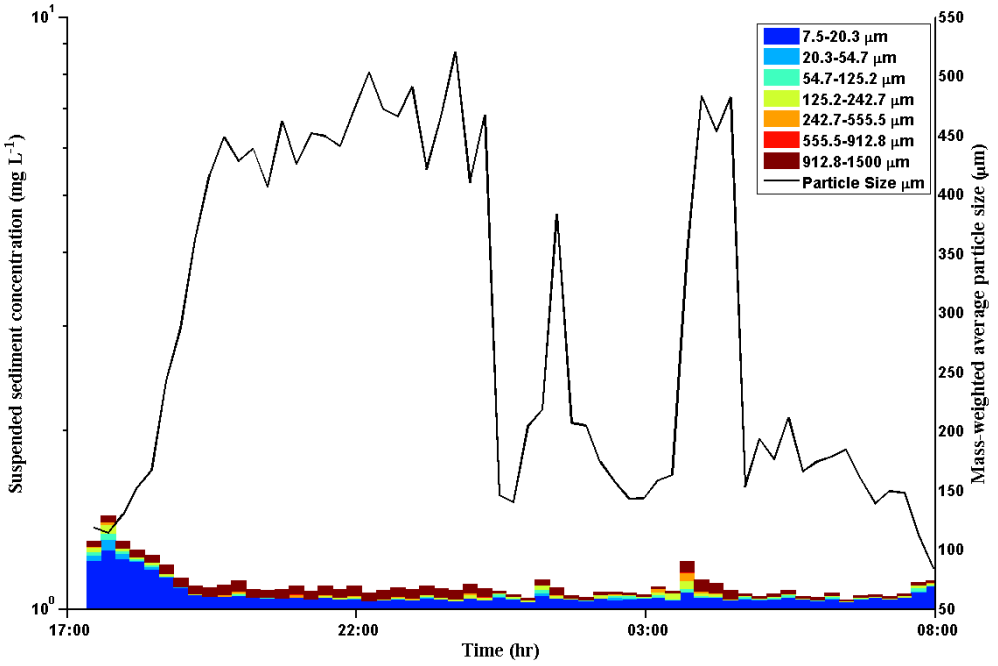

Figure D-263 Stacked time series of particle size distribution and mass-weighted particle size distributions at RS1D Slough site. Data were binned into 32 size categories from 7.5 to 1500 microns. Deployed period is November 2, 2014 18:00 to November 3, 2014 08:00 (Pre-Flow). Data baseline set to 10^0.

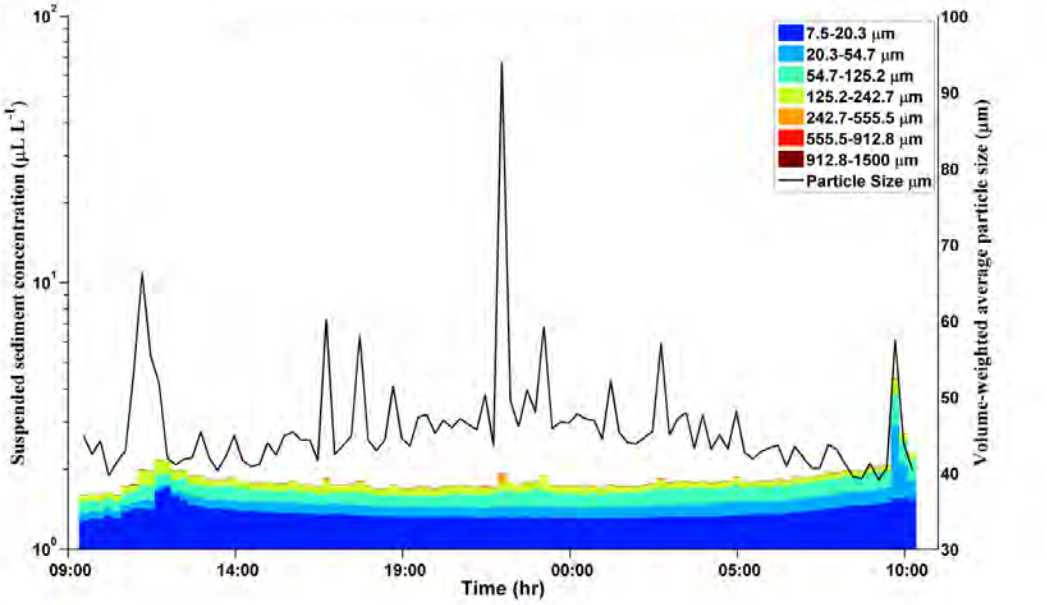

Figure D-264 Stacked time series of particle size distribution and volume-weighted particle size distributions at RS1D Ridge site. Data were binned into 32 size categories from 7.5 to 1500 microns. Deployed period is November 4, 2014 09:30 to November 5, 2014 10:15 (Transient). Data baseline set to 10^0.

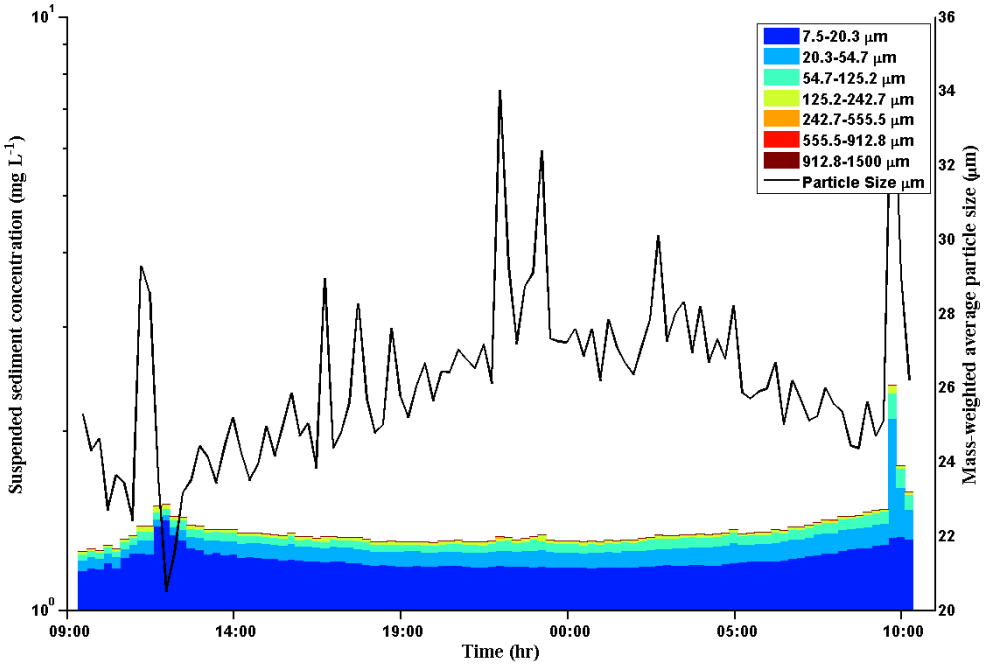

Figure D-265 Stacked time series of particle size distribution and mass-weighted particle size distributions at RS1D Ridge site. Data were binned into 32 size categories from 7.5 to 1500 microns. Deployed period is November 4, 2014 09:30 to November 5, 2014 10:15 (Transient). Data baseline set to 10^0.

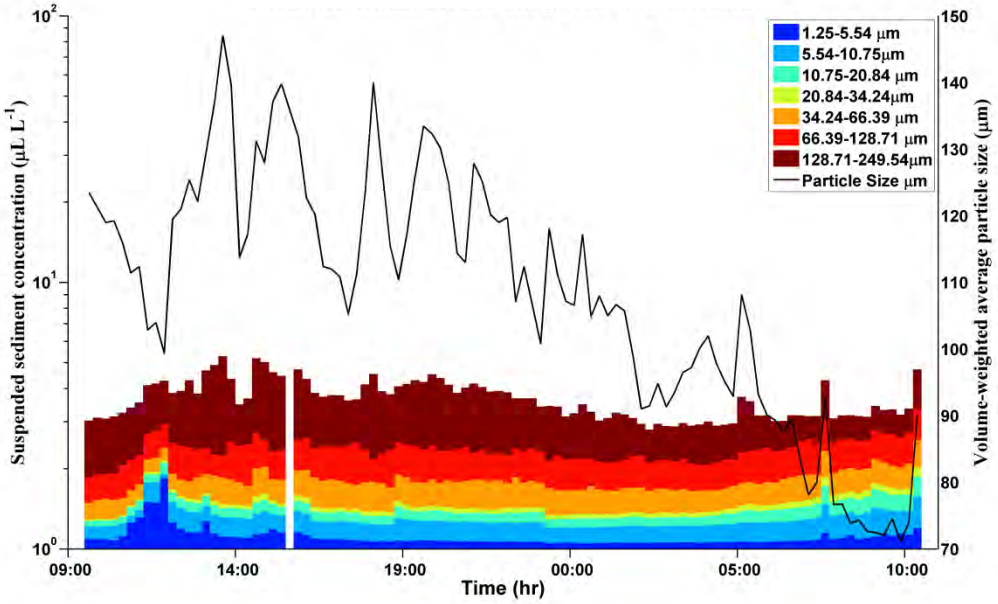

Figure D-266 Stacked time series of particle size distribution and volume-weighted particle size distributions at RS1D Slough site. Data were binned into 32 size categories from 1.25 to 250 microns. Deployed period is November 4, 2014 09:30 to November 5, 2014 10:15 (Transient). Data baseline set to 10^0.

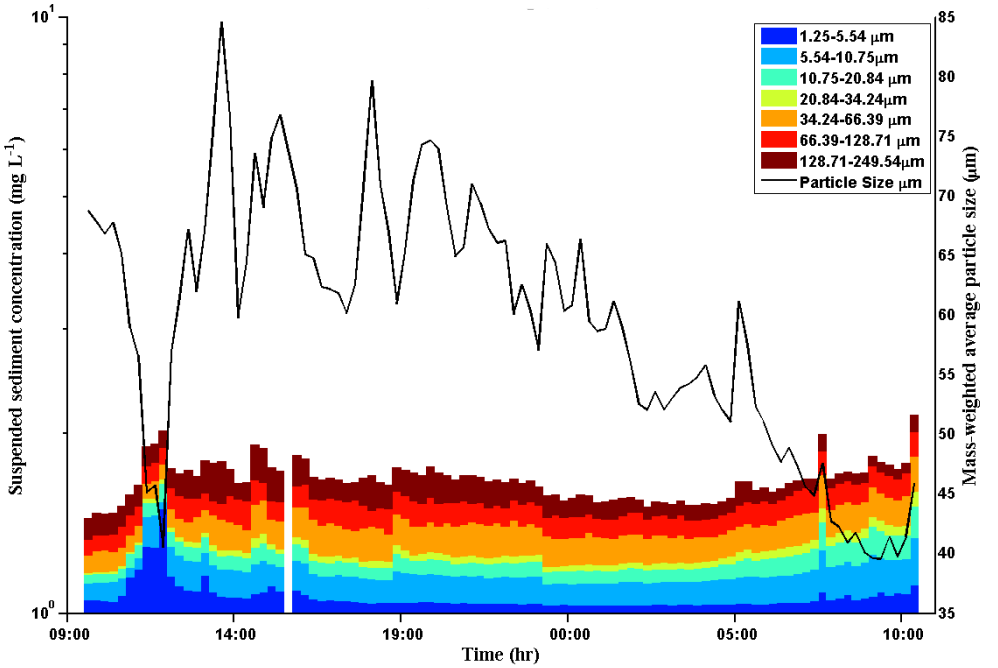

Figure D-267 Stacked time series of particle size distribution and mass-weighted particle size distributions at RS1D Slough site. Data were binned into 32 size categories from 1.25 to 250 microns. Deployed period is November 4, 2014 09:30 to November 5, 2014 10:15 (Transient). Data baseline set to 10^0.

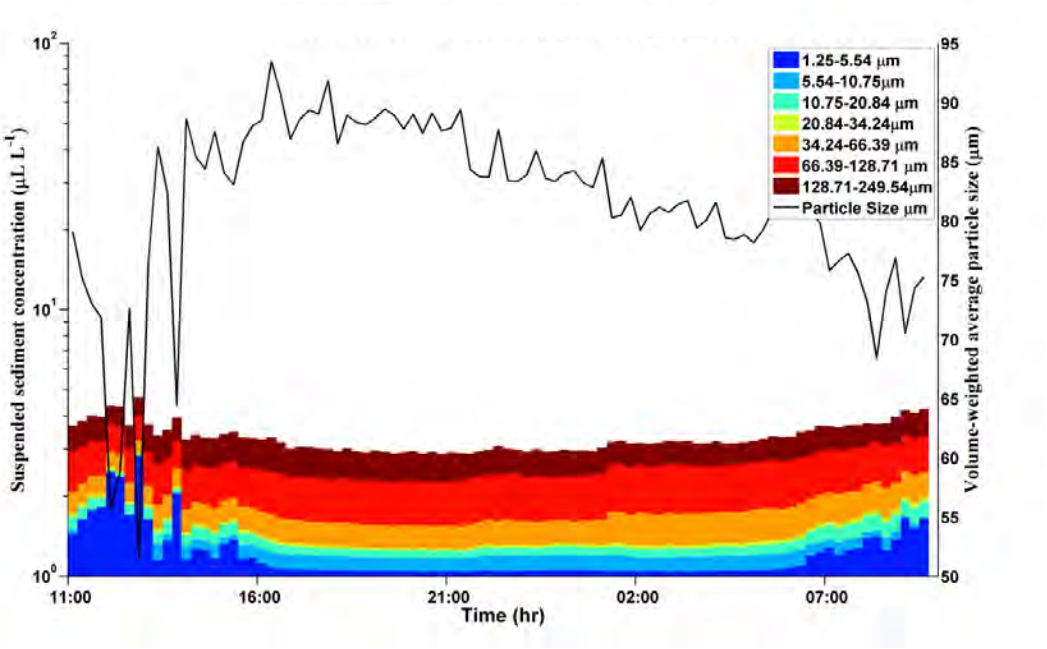

Figure D-268 Stacked time series of particle size distribution and volume-weighted particle size distributions at RS1D Ridge site. Data were binned into 32 size categories from 1.25 to 250 microns. Deployed period is November 5, 2014 11:00 to November 6, 2014 10:00 (Steady Flow). Data baseline set to 10^0.

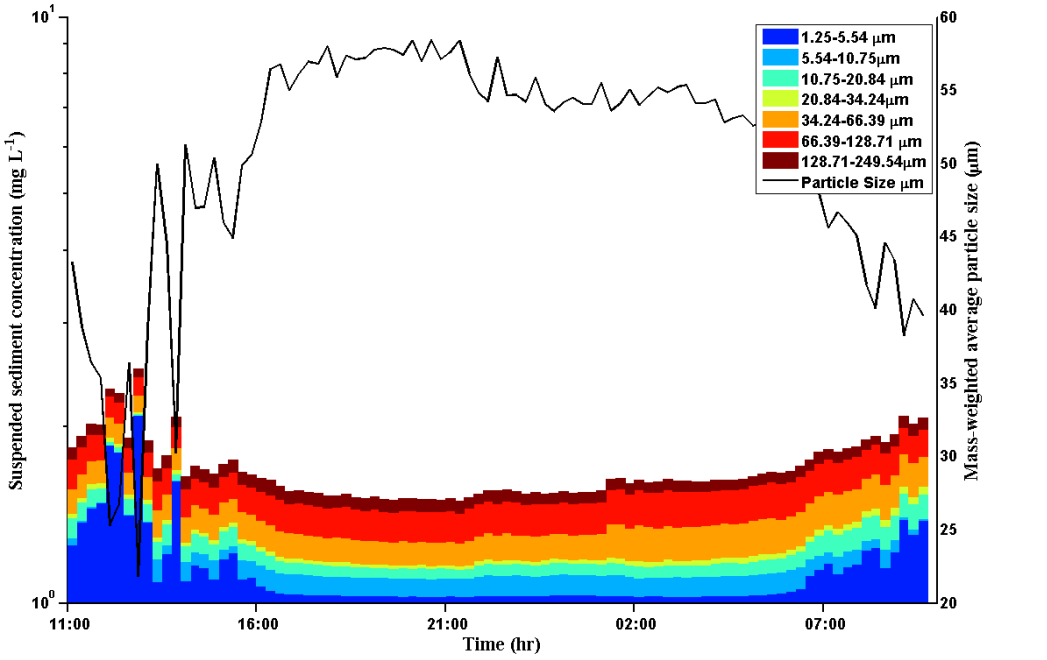

Figure D-269 Stacked time series of particle size distribution and mass-weighted particle size distributions at RS1D Ridge site. Data were binned into 32 size categories from 1.25 to 250 microns. Deployed period is November 5, 2014 11:00 to November 6, 2014 10:00 (Steady Flow). Data baseline set to 10^0.

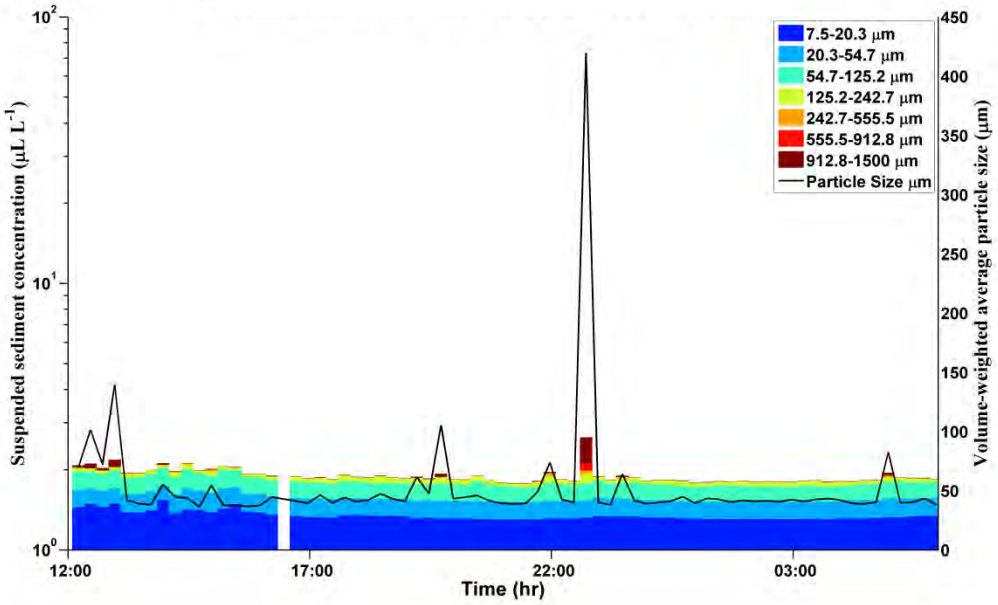

Figure D-270 Stacked time series of particle size distribution and volume-weighted particle size distributions at RS1D Slough site. Data were binned into 32 size categories from 7.5 to 1500 microns. Deployed period is November 5, 2014 12:00 to November 6, 2014 08:00 (Steady Flow). Data baseline set to 10^0.

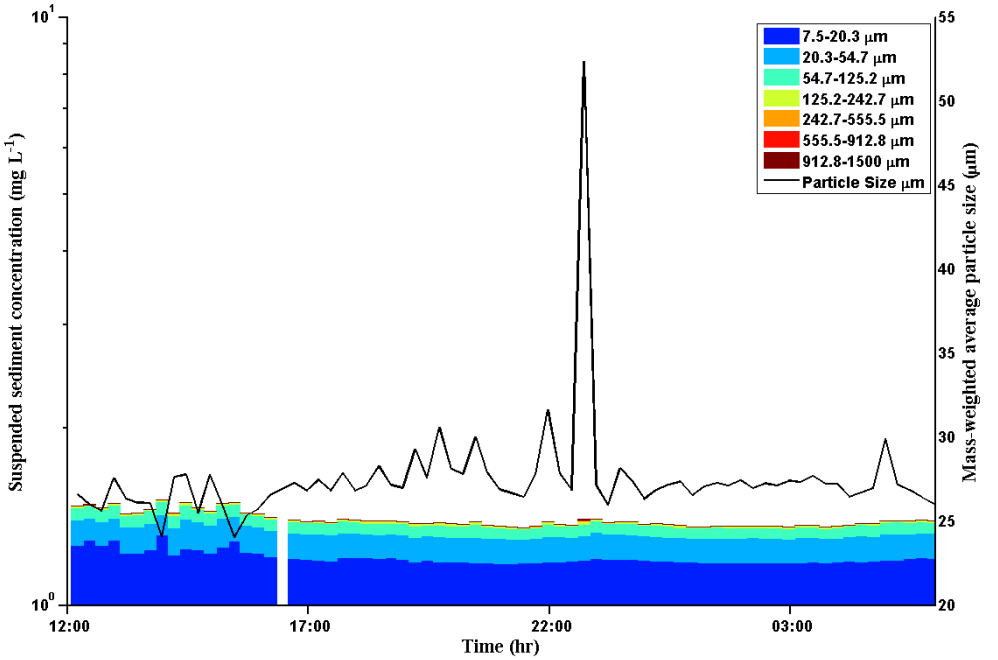

Figure D-271 Stacked time series of particle size distribution and mass-weighted particle size distributions at RS1D Slough site. Data were binned into 32 size categories from 7.5 to 1500 microns. Deployed period is November 5, 2014 12:00 to November 6, 2014 08:00 (Steady Flow). Data baseline set to 10^0.

2015 November

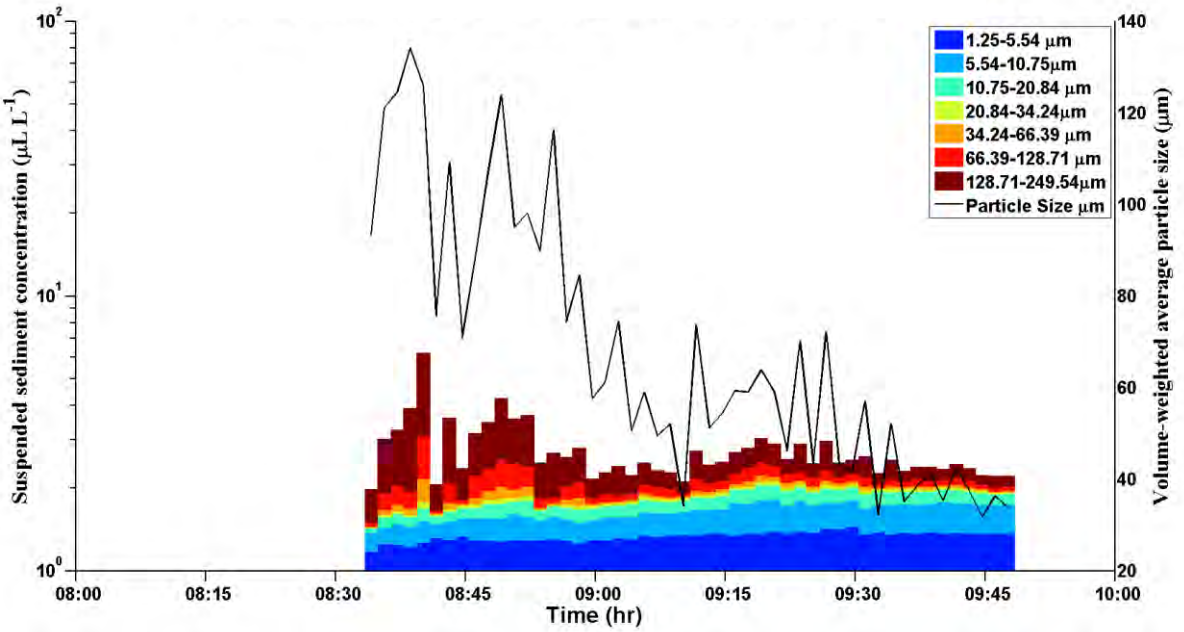

Figure D-272 Stacked time series of particle size distribution and volume-weighted particle size distributions at RS1D Slough site. Data were binned into 32 size categories from 1.25 to 250 microns. Deployed period is November 16, 2015 8:00 to November 16, 2015 09:40 (Pre-Pulse1). Data baseline set to 10^0.

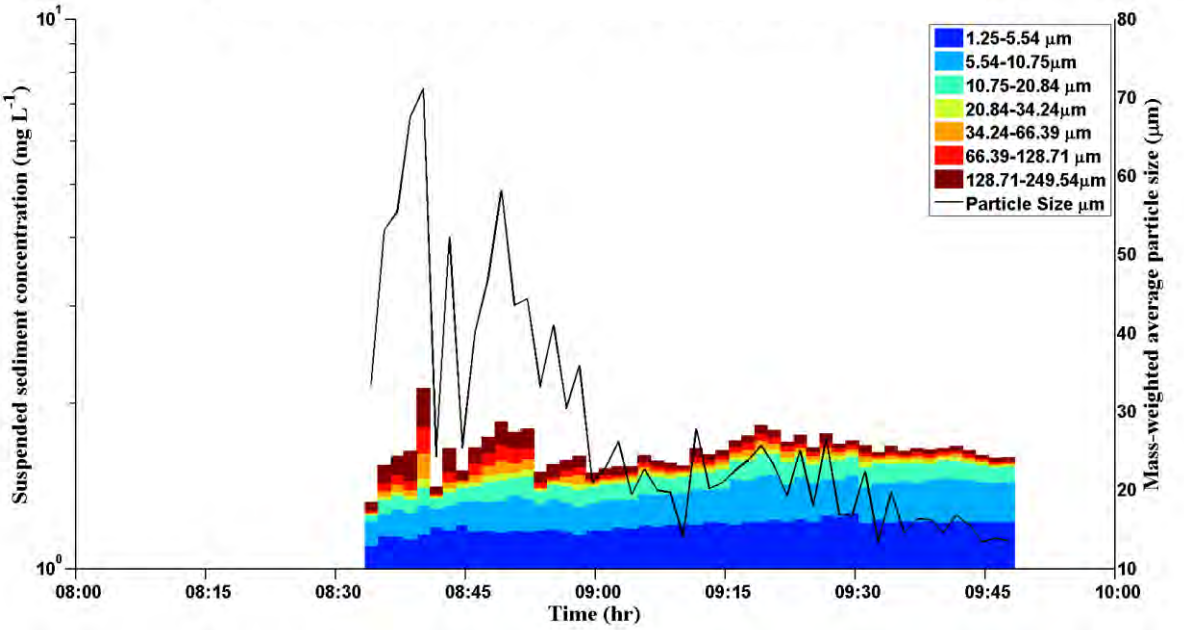

Figure D-273 Stacked time series of particle size distribution and mass-weighted particle size distributions at RS1D Slough site. Data were binned into 32 size categories from 1.25 to 250 microns. Deployed period is November 16, 2015 8:00 to November 16, 2015 09:40 (Pre-Pulse1). Data baseline set to 10^0.

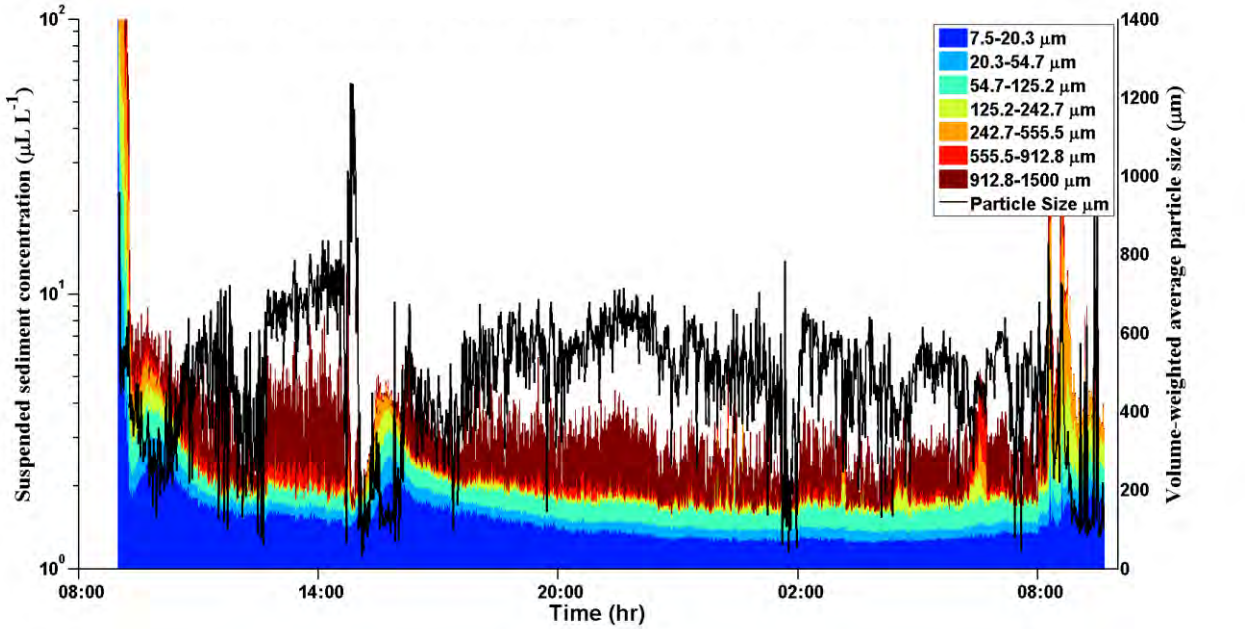

Figure D-274 Stacked time series of particle size distribution and volume-weighted particle size distributions at RS1D Slough site. Data were binned into 32 size categories from 7.5 to 1500 microns. Deployed period is November 15, 2015 9:00 to November 16, 2015 09:40 (Pre-Pulse1). Data baseline set to 10^0.

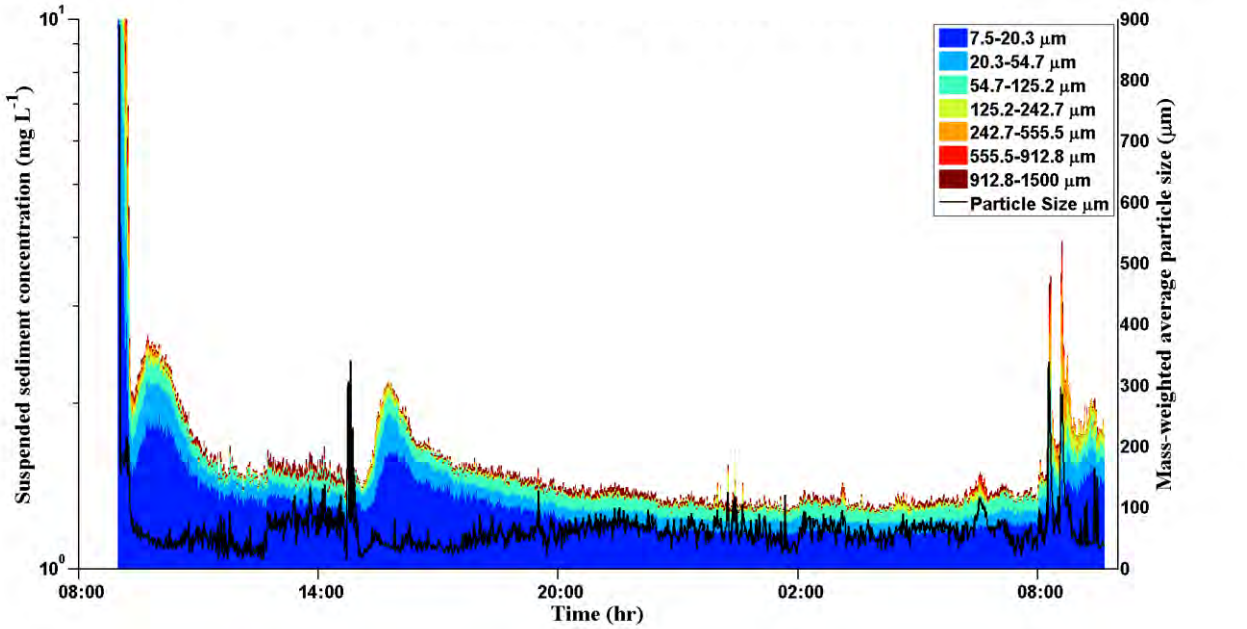

Figure D-275 Stacked time series of particle size distribution and mass-weighted particle size distributions at RS1D Slough site. Data were binned into 32 size categories from 7.5 to 1500 microns. Deployed period is November 15, 2015 9:00 to November 16, 2015 09:40 (Pre-Pulse1). Data baseline set to 10^0.

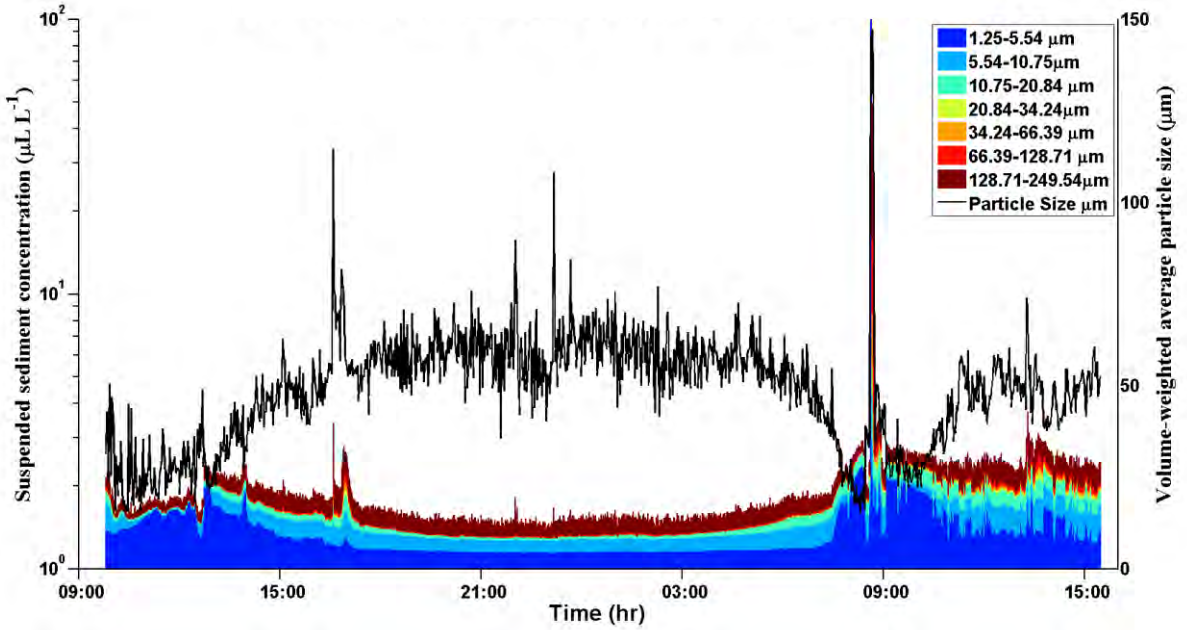

Figure D-276 Stacked time series of particle size distribution and volume-weighted particle size distributions at RS1D Slough site. Data were binned into 32 size categories from 1.25 to 250 microns. Deployed period is November 16, 2015 09:40 to November 17, 2015 15:30 (Pulse 1). Data baseline set to 10^0.

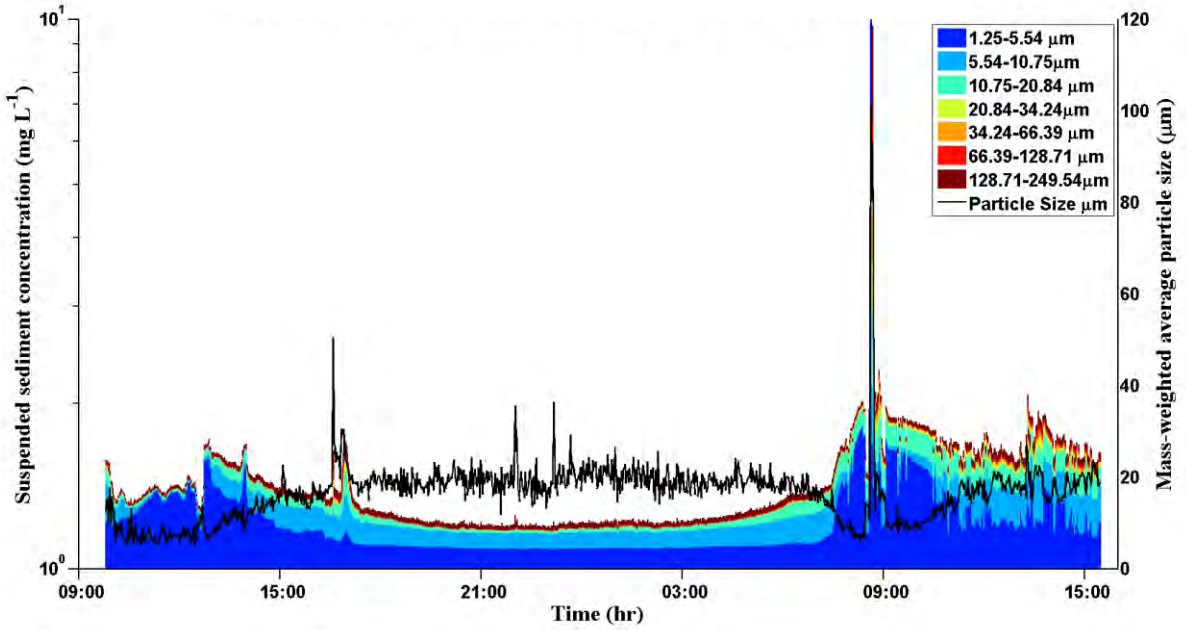

Figure D-277 Stacked time series of particle size distribution and mass-weighted particle size distributions at RS1D Slough site. Data were binned into 32 size categories from 1.25 to 250 microns. Deployed period is November 16, 2015 09:40 to November 17, 2015 15:30 (Pulse 1). Data baseline set to 10^0.

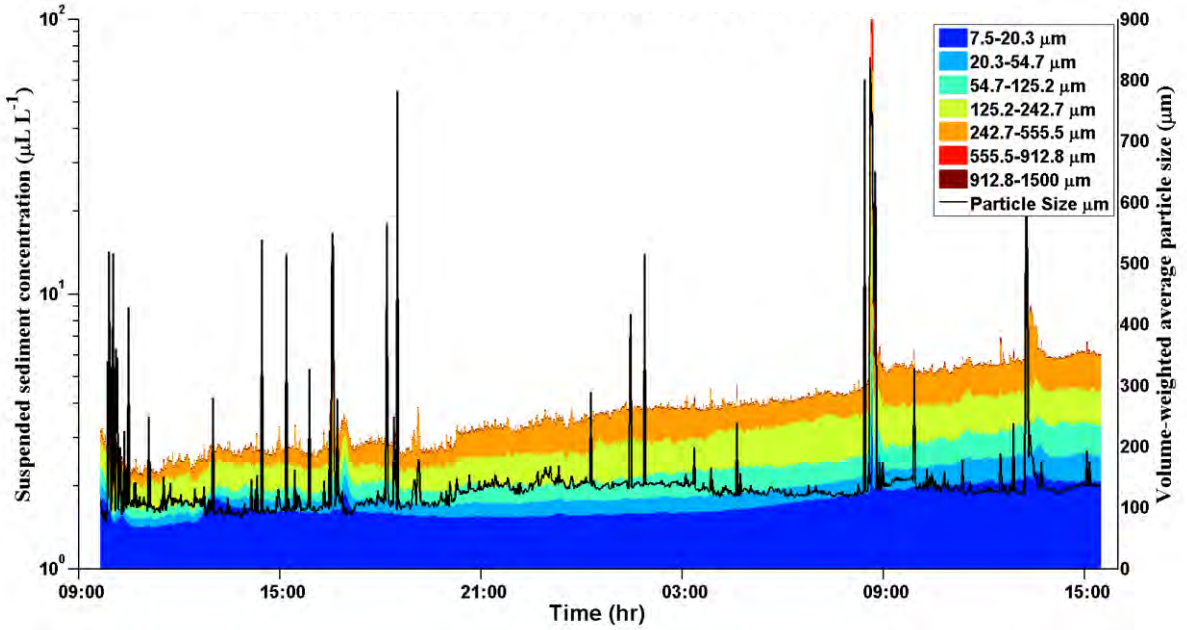

Figure D-278 Stacked time series of particle size distribution and volume-weighted particle size distributions at RS1D Slough site. Data were binned into 32 size categories from 7.5 to 1500 microns. Deployed period is November 16, 2015 09:40 to November 17, 2015 15:30 (Pulse 1). Data baseline set to 10^0.

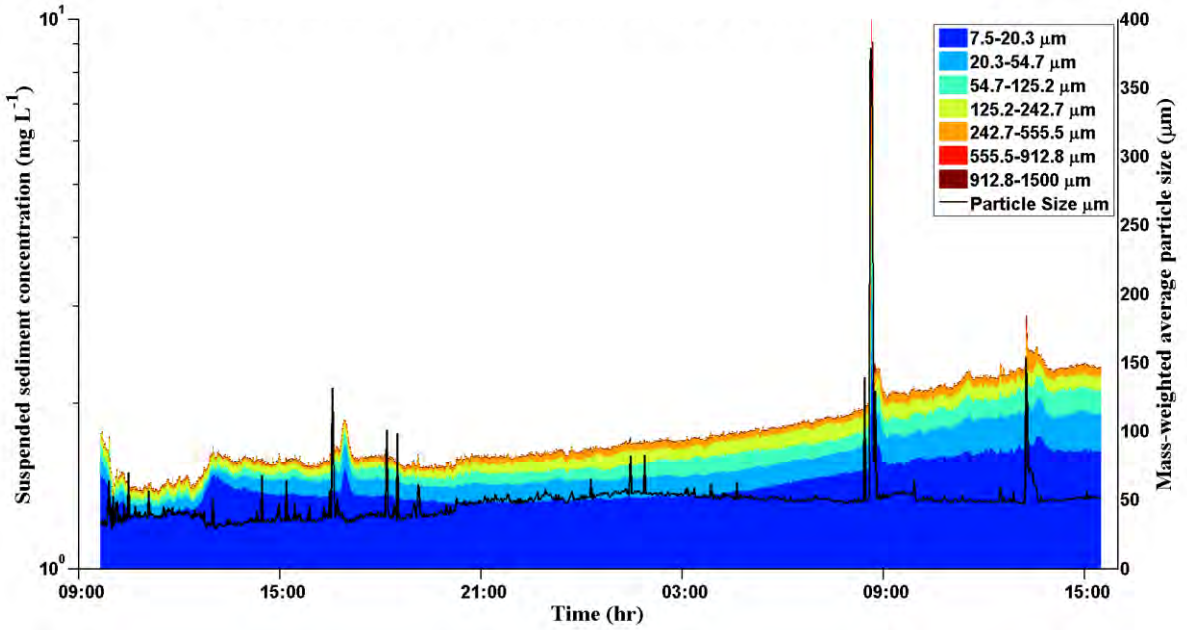

Figure D-279 Stacked time series of particle size distribution and mass-weighted particle size distributions at RS1D Slough site. Data were binned into 32 size categories from 7.5 to 1500 microns. Deployed period is November 16, 2015 09:40 to November 17, 2015 15:30 (Pulse 1). Data baseline set to 10^0.

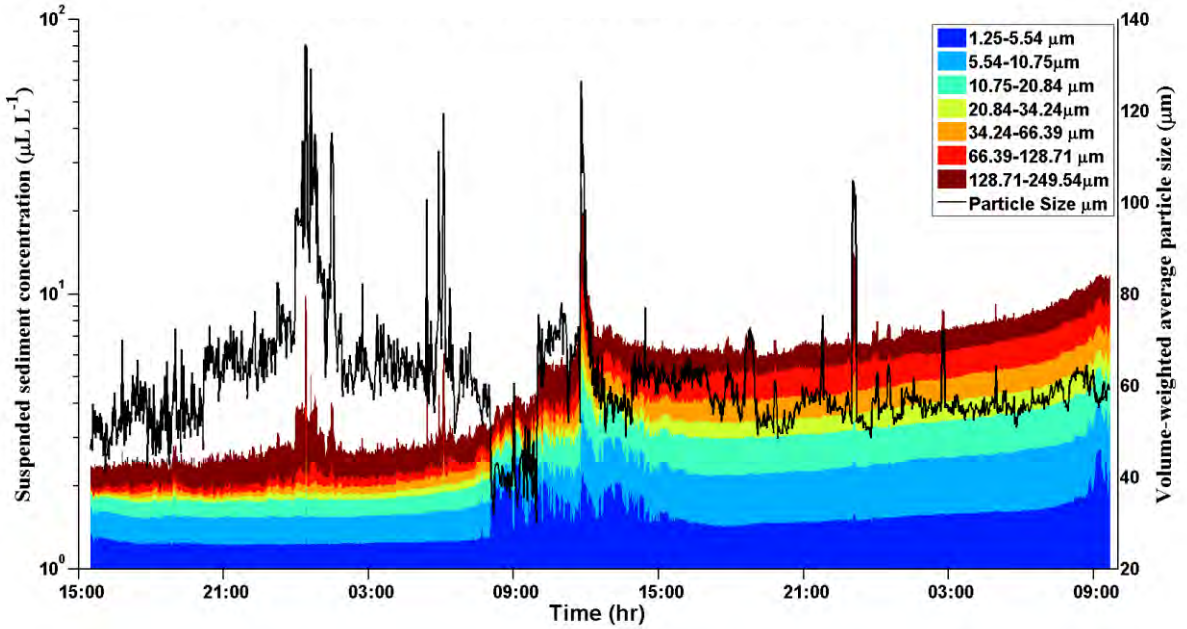

Figure D-280 Stacked time series of particle size distribution and volume-weighted particle size distributions at RS1D Slough site. Data were binned into 32 size categories from 1.25 to 250 microns. Deployed period is November 17, 2015 15:30 to November 19, 2015 9:40 (Pre-Pulse 2). Data baseline set to 10^0.

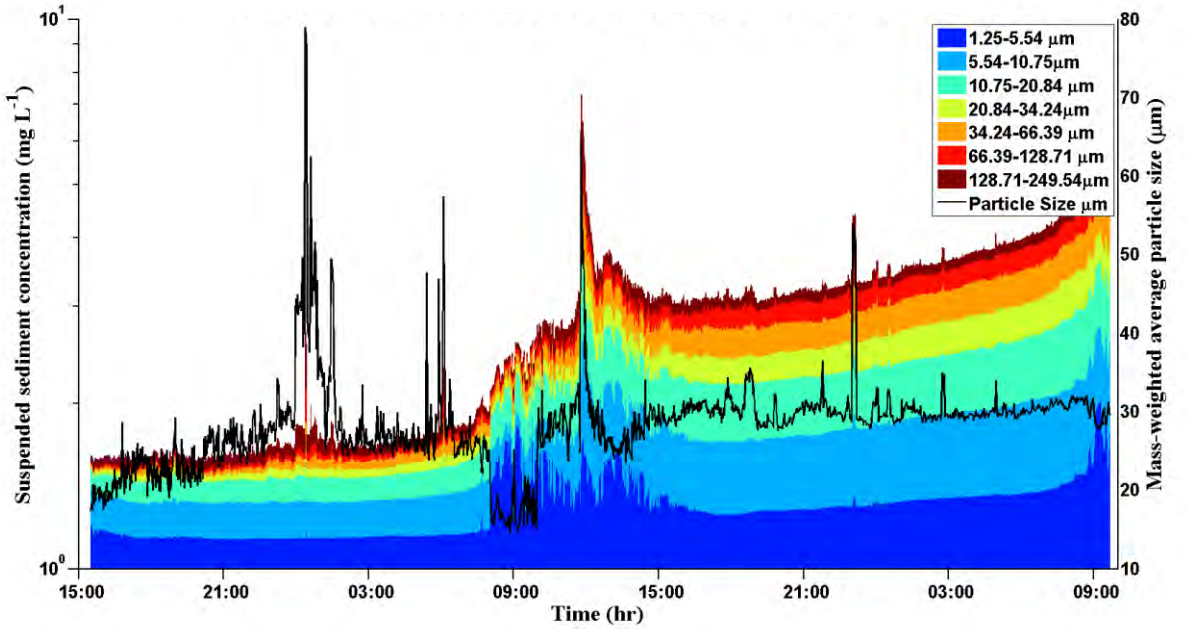

Figure D-281 Stacked time series of particle size distribution and mass-weighted particle size distributions at RS1D Slough site. Data were binned into 32 size categories from 1.25 to 250 microns. Deployed period is November 17, 2015 15:30 to November 19, 2015 9:40 (Pre-Pulse 2). Data baseline set to 10^0.

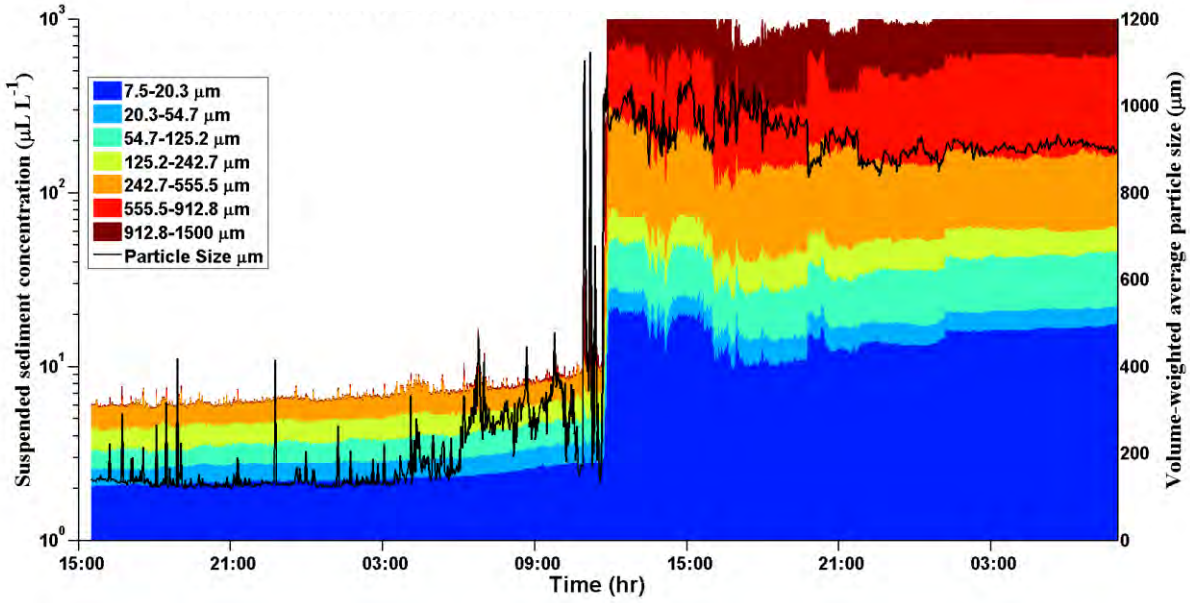

Figure D-282 Stacked time series of particle size distribution and volume-weighted particle size distributions at RS1D Slough site. Data were binned into 32 size categories from 7.5 to 1500 microns. Deployed period is November 17, 2015 15:30 to November 19, 2015 9:40 (Pre-Pulse 2). Data baseline set to 10^0.

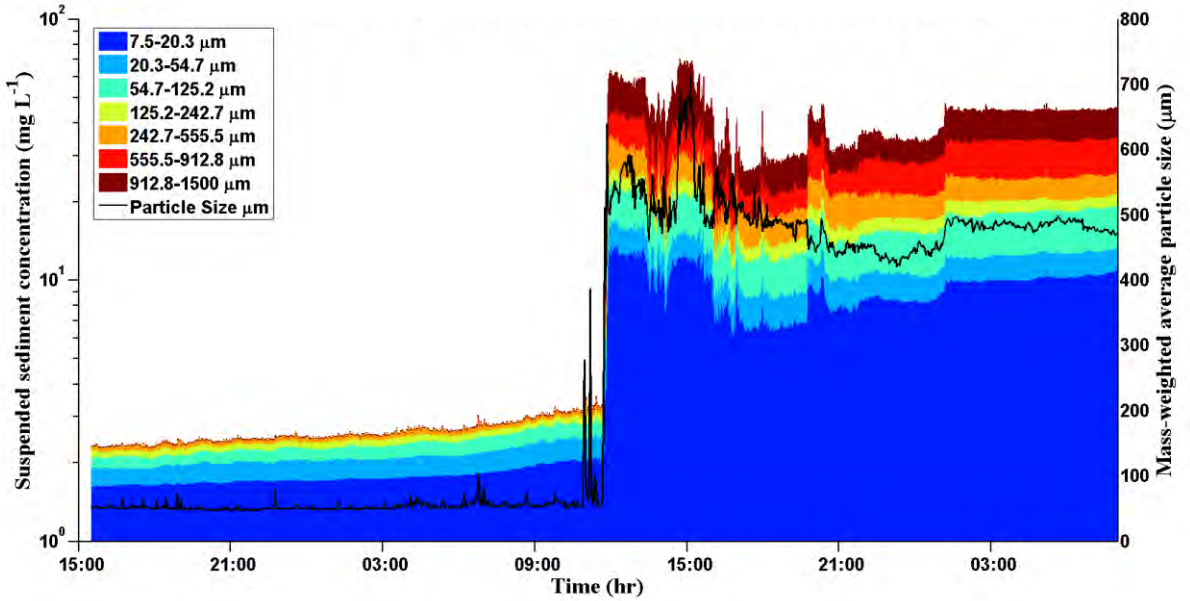

Figure D-283 Stacked time series of particle size distribution and mass-weighted particle size distributions at RS1D Slough site. Data were binned into 32 size categories from 7.5 to 1500 microns. Deployed period is November 17, 2015 15:30 to November 19, 2015 9:40 (Pre-Pulse 2). Data baseline set to 10^0.

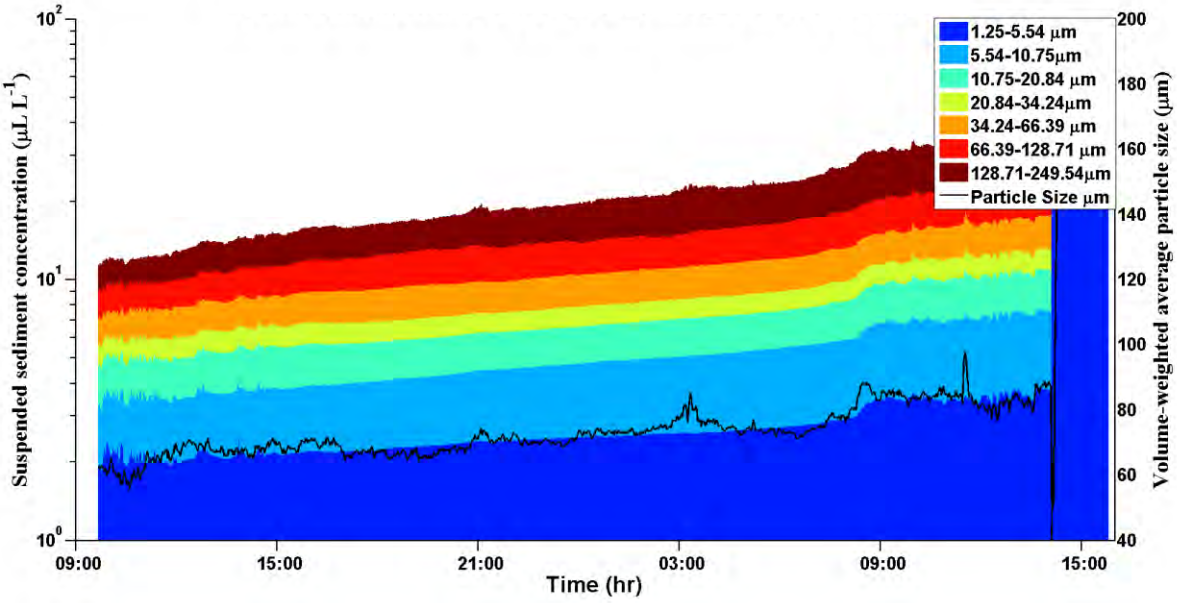

Figure D-284 Stacked time series of particle size distribution and volume-weighted particle size distributions at RS1D Slough site. Data were binned into 32 size categories from 1.25 to 250 microns. Deployed period is November 19, 2015 9:40 to November 20, 2015 16:00 (Pulse 2). Data baseline set to 10^0.

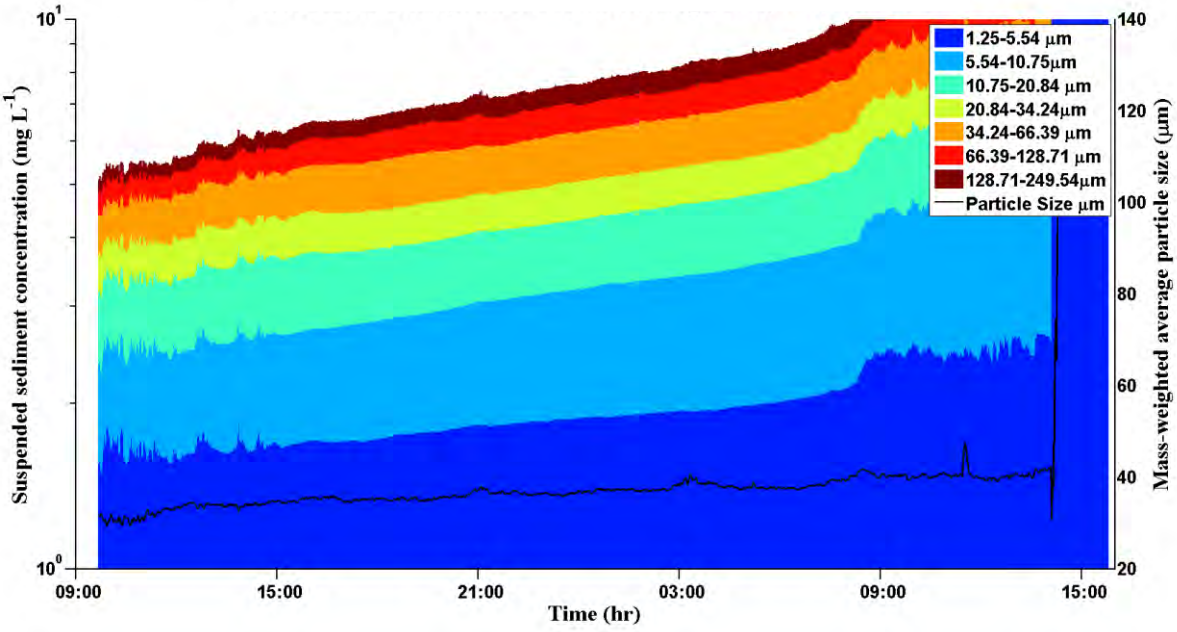

Figure D-285 Stacked time series of particle size distribution and mass-weighted particle size distributions at RS1D Slough site. Data were binned into 32 size categories from 1.25 to 250 microns. Deployed period is November 5, 2014 11:00 to November 20, 2015 16:00 (Pulse 2). Data baseline set to 10^0.

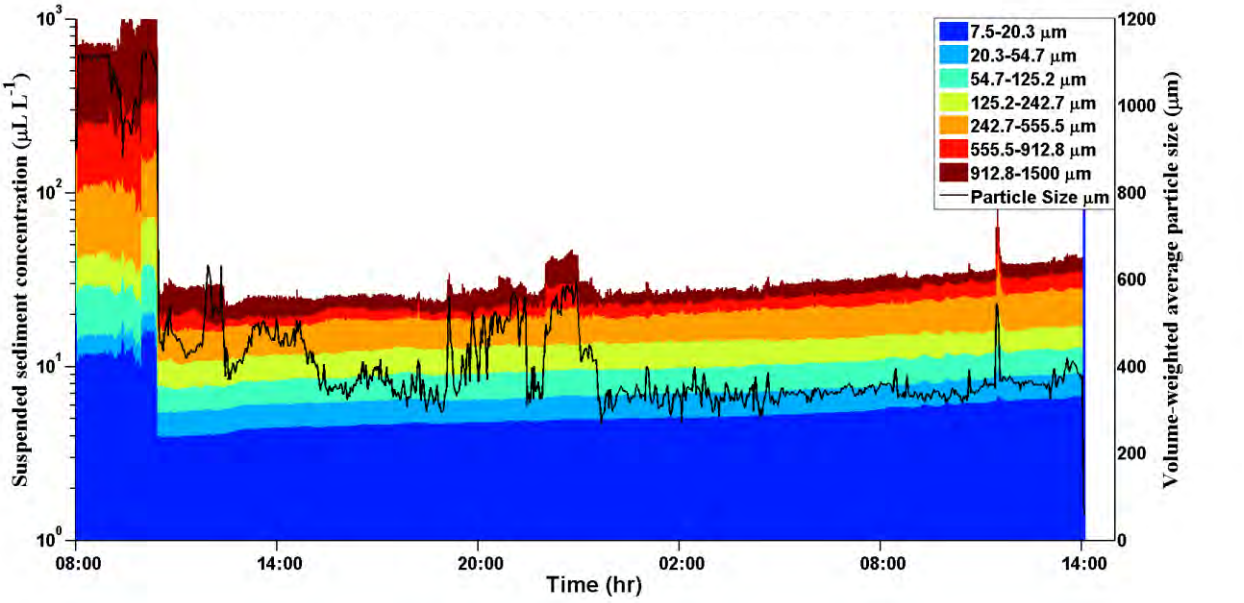

Figure D-286 Stacked time series of particle size distribution and volume-weighted particle size distributions at RS1D Slough site. Data were binned into 32 size categories from 7.5 to 1500 microns. Deployed period is November 5, 2014 11:00 to November 20, 2015 14:00 (Pulse 2). Data baseline set to 10^0.

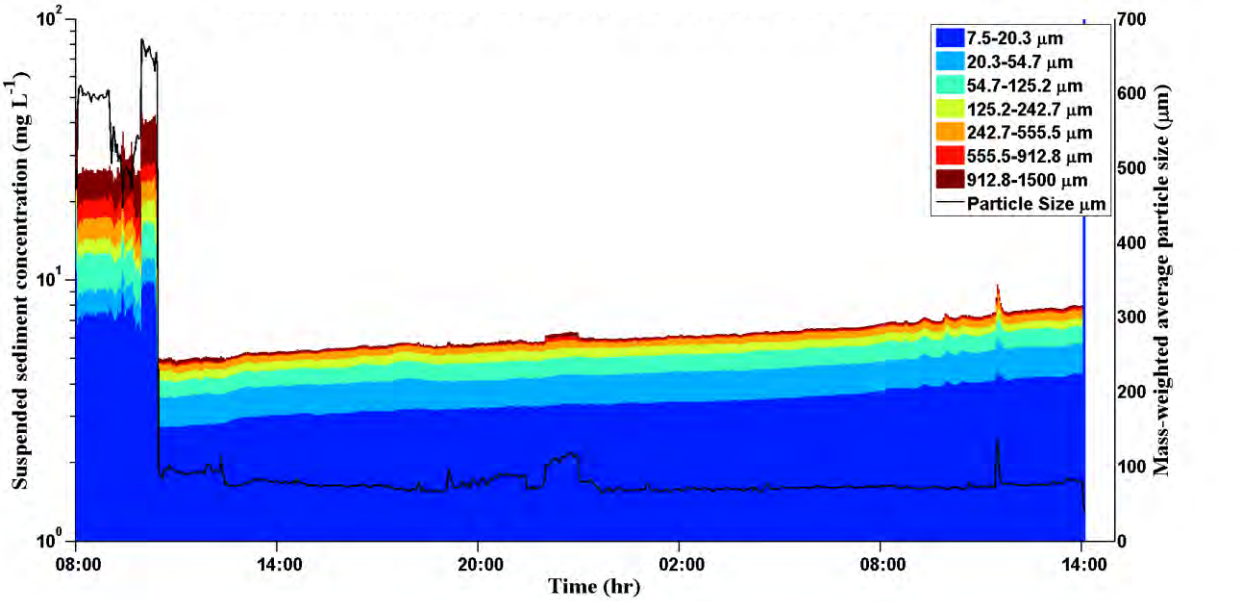

Figure D-287 Stacked time series of particle size distribution and mass-weighted particle size distributions at RS1D Slough site. Data were binned into 32 size categories from 7.5 to 1500 microns. Deployed period is November 5, 2014 11:00 to November 20, 2015 14:00 (Pulse 2). Data baseline set to 10^0.

LISST_Histograms
2010 November

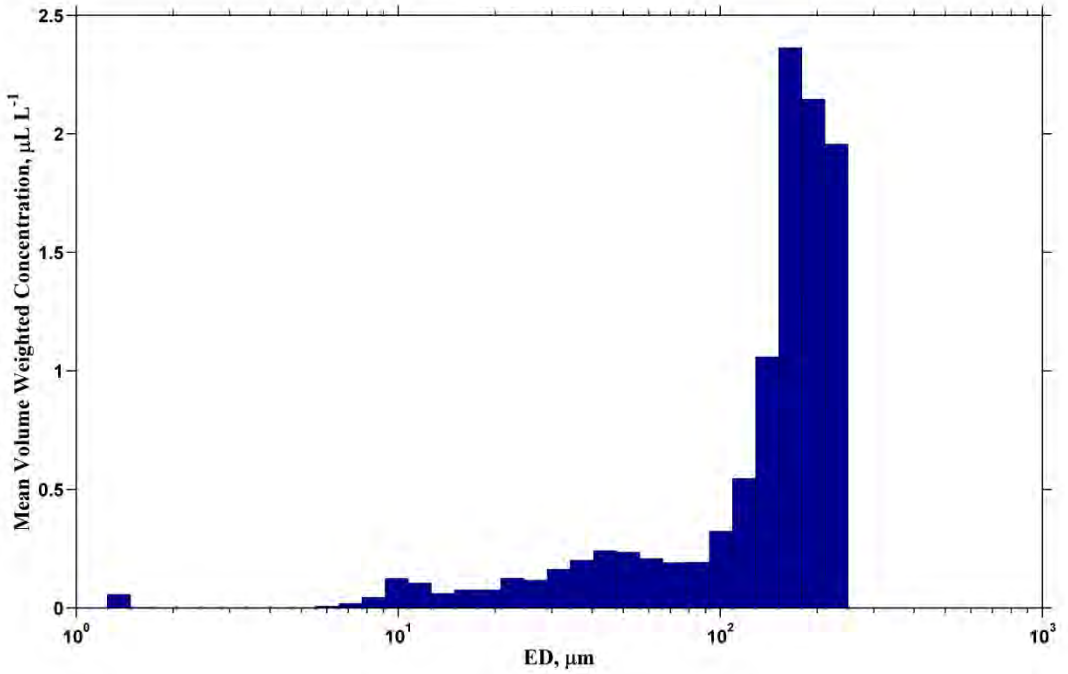

Figure D-288 Mean volume-weighted concentration histogram. Deployment period is November 9, 2010 15:14 to November 11, 2010 11:29.

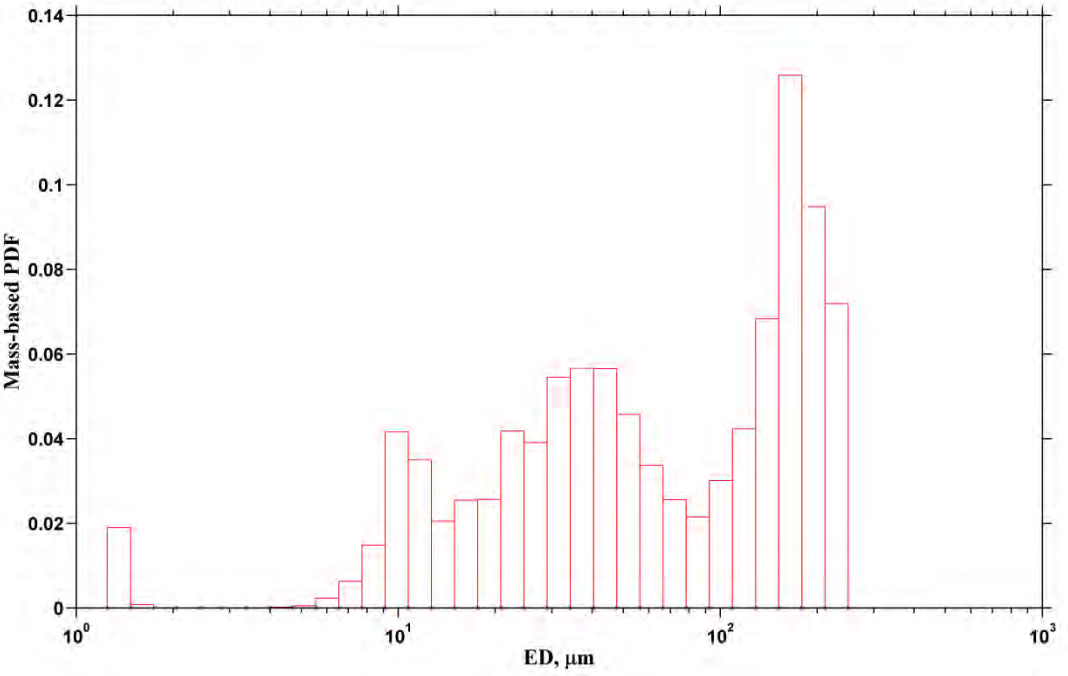

Figure D-289 Mass contribution of each grain-size bin to total calculated mass. Deployment period is November 9, 2010 15:14 to November 11, 2010 11:29.

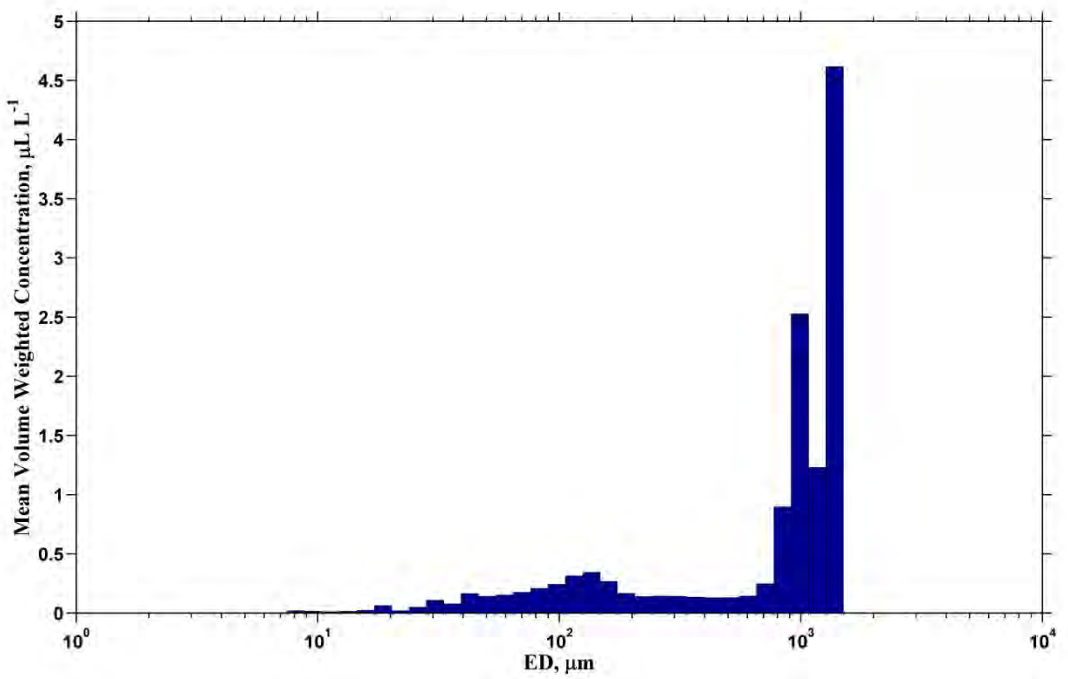

Figure D-290 Mean volume-weighted concentration histogram. Deployment period is November 7, 2010 16:53 to November 9, 2010 14:42.

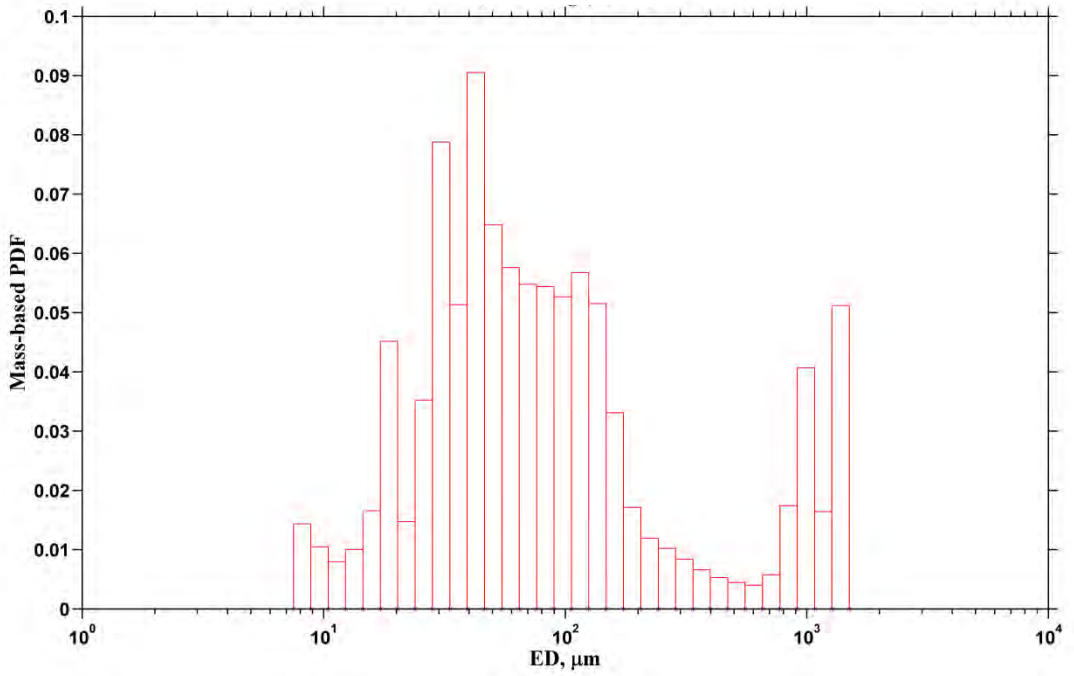

Figure D-291 Mass contribution of each grain-size bin to total calculated mass. Deployment period is November 7, 2010 16:53 to November 9, 2010 14:42.

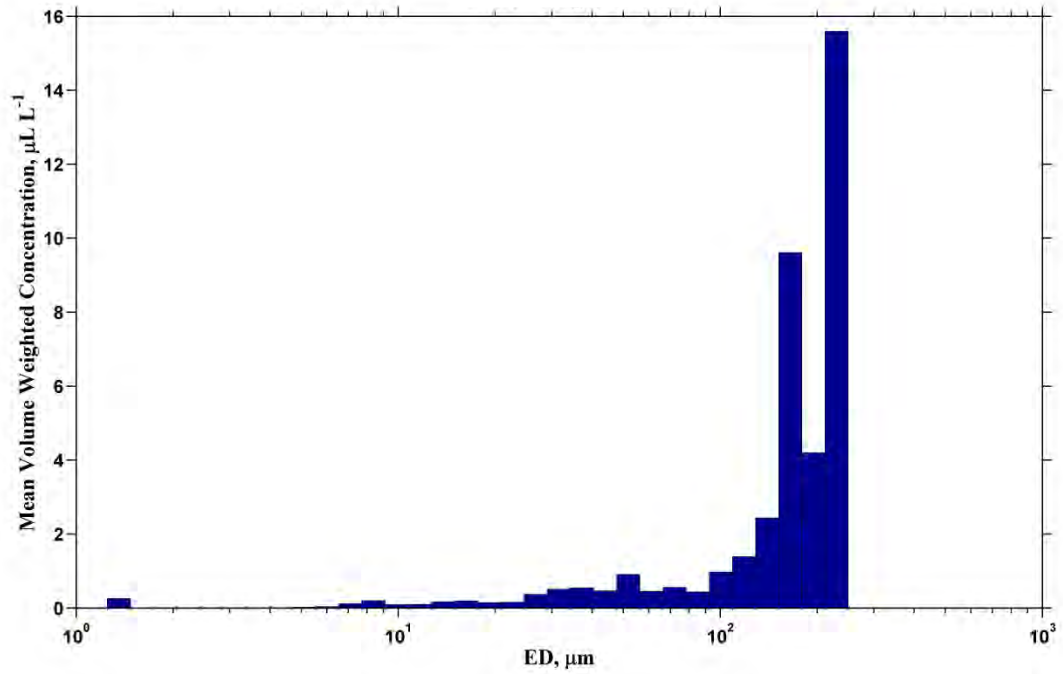

Figure D-292 Mean volume-weighted concentration histogram. Deployment period is November 7, 2010 16:18 to November 9, 2010 14:20.

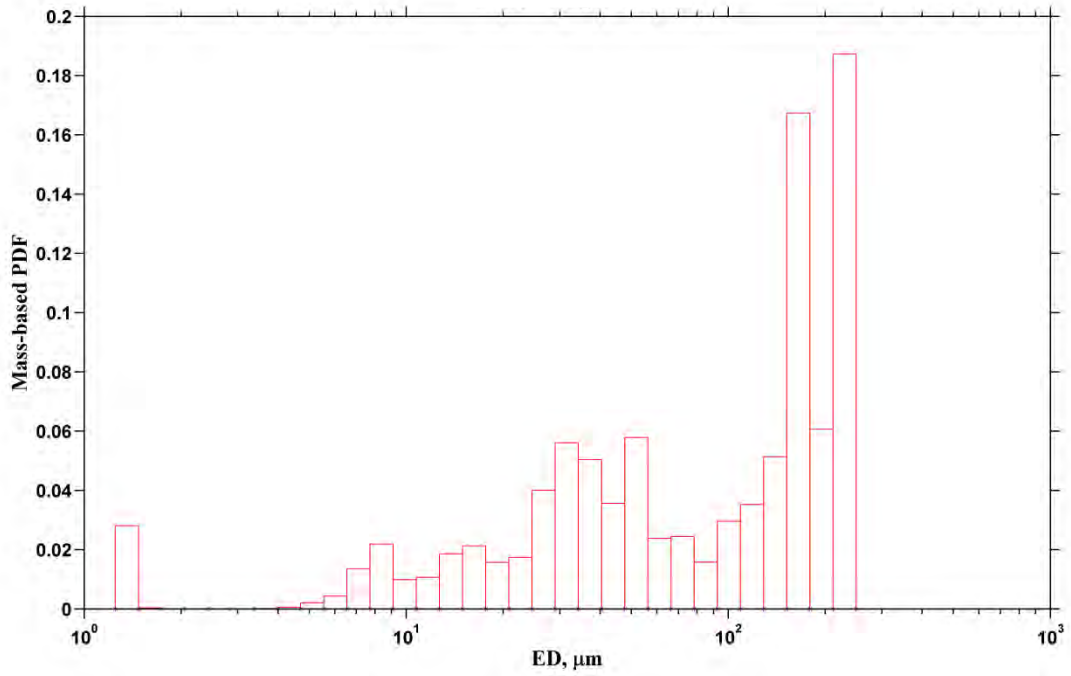

Figure D-293 Mass contribution of each grain-size bin to total calculated mass. Deployment period is November 7, 2010 16:18 to November 9, 2010 14:20.

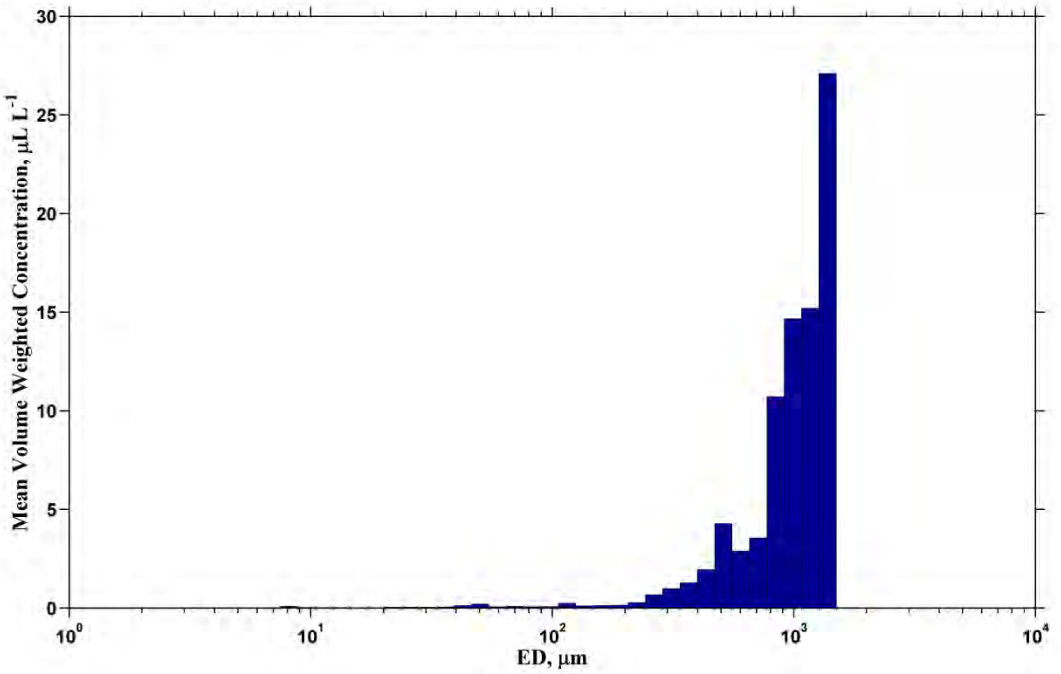

Figure D-294 Mean volume-weighted concentration histogram. Deployment period is November 9, 2010 16:08 to November 11, 2010 11:30.

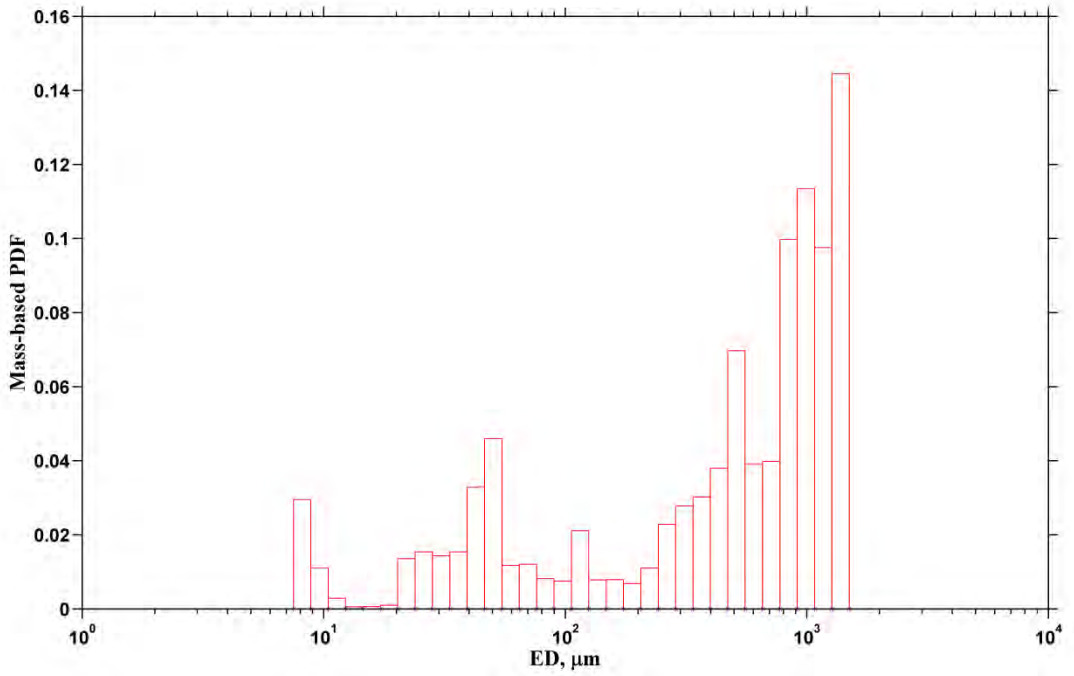

Figure D-295 Mass contribution of each grain-size bin to total calculated mass. Deployment period is November 9, 2010 16:08 to November 11, 2010 11:30.

2012 August

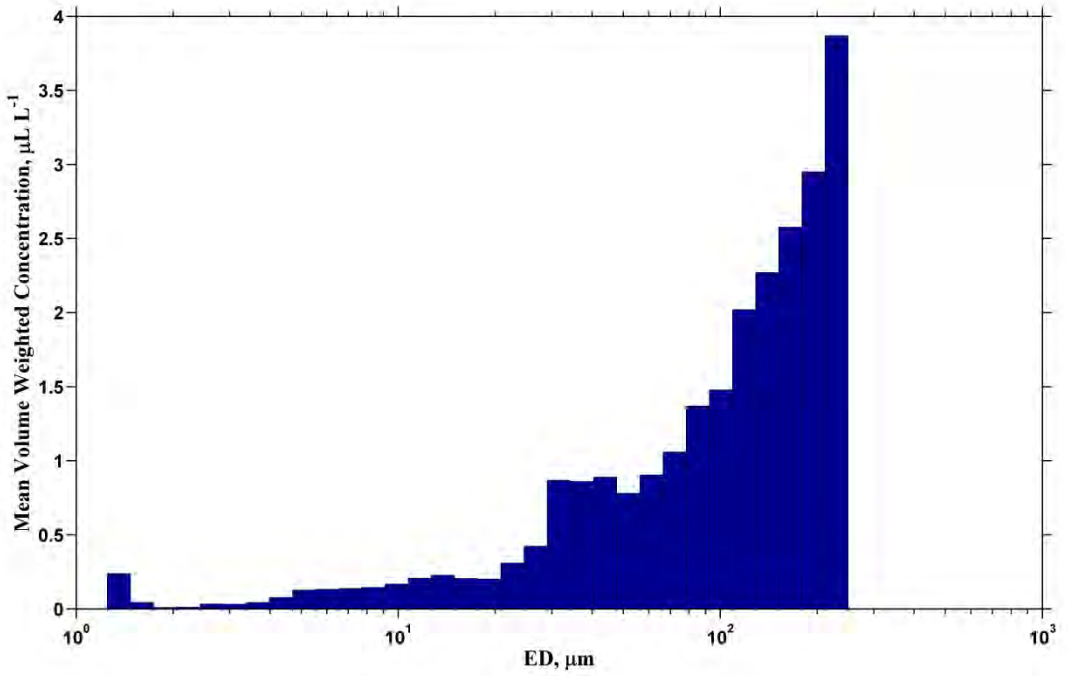

Figure D-296 Mean volume-weighted concentration histogram. Deployment period is August 7, 2012 14:24 to August 9, 2012 09:11.

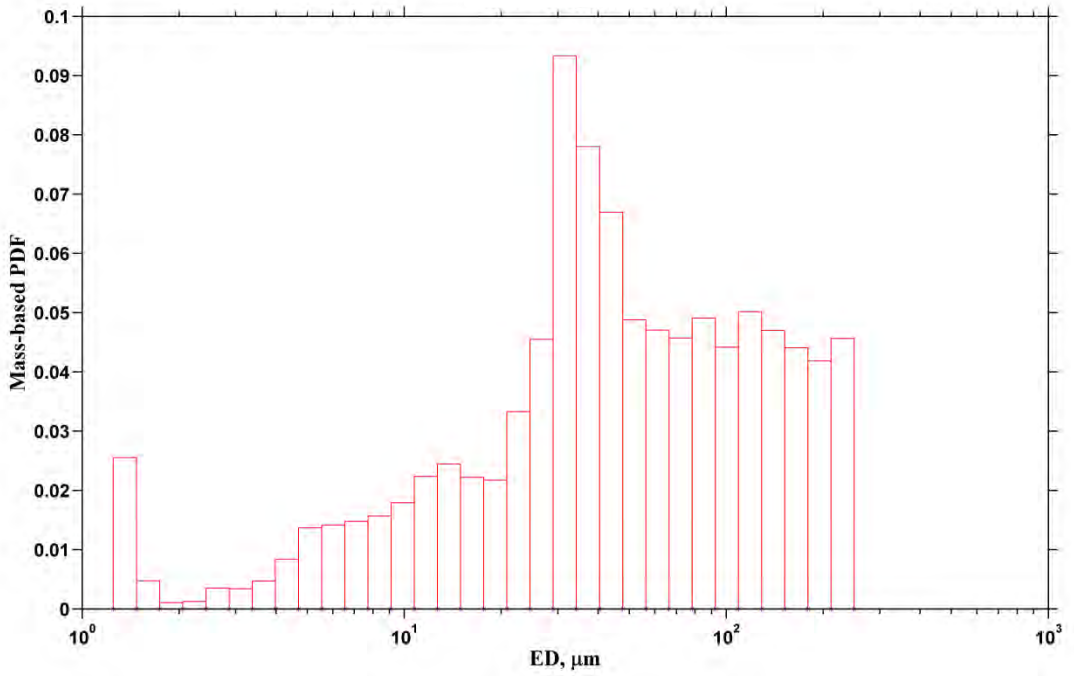

Figure D-297 Mass contribution of each grain-size bin to total calculated mass. Deployment period is August 7, 2012 14:24 to August 9, 2012 09:11.

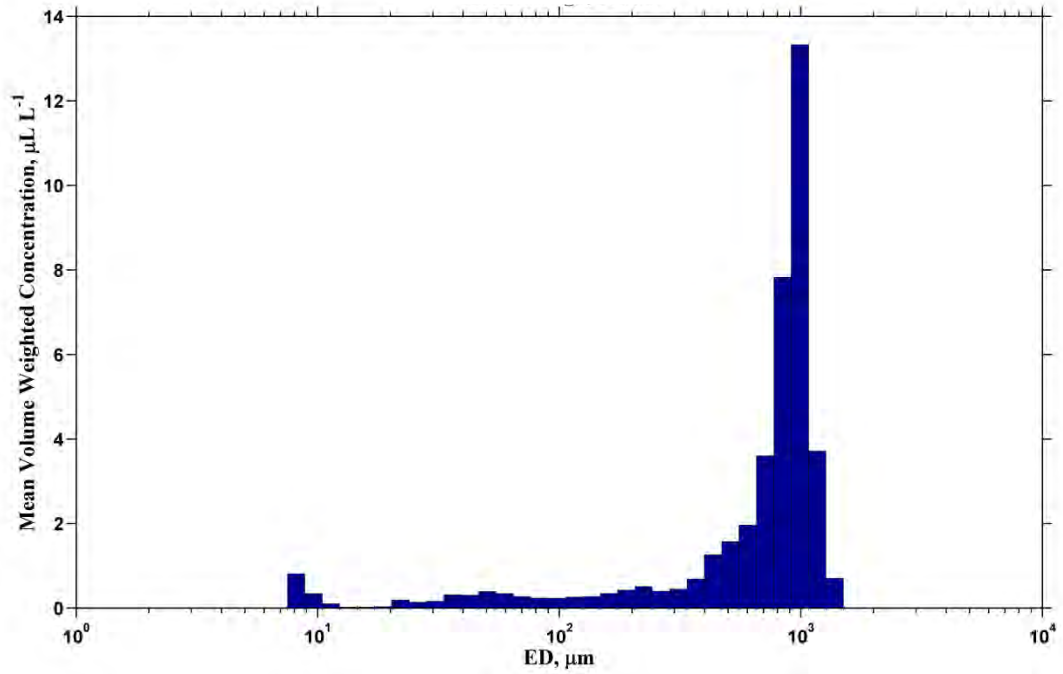

Figure D-298 Mean volume-weighted concentration histogram. Deployment period is August 7, 2012 14:24 to August 9, 2012 09:11.

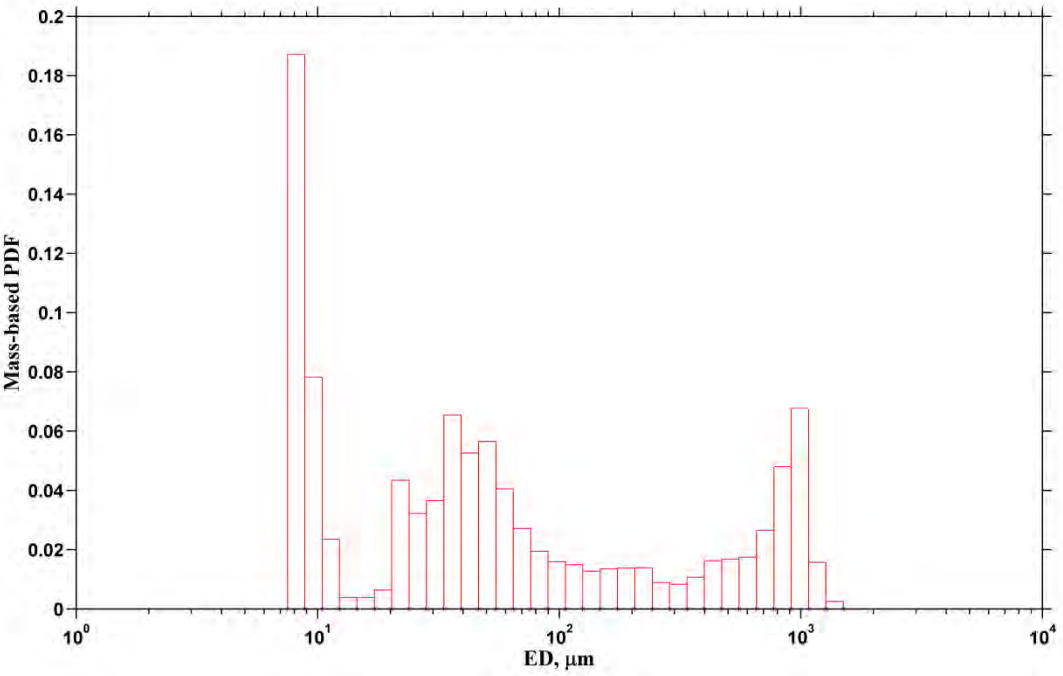

Figure D-299 Mass contribution of each grain-size bin to total calculated mass. Deployment period is August 7, 2012 14:24 to August 9, 2012 09:11.

2012 November

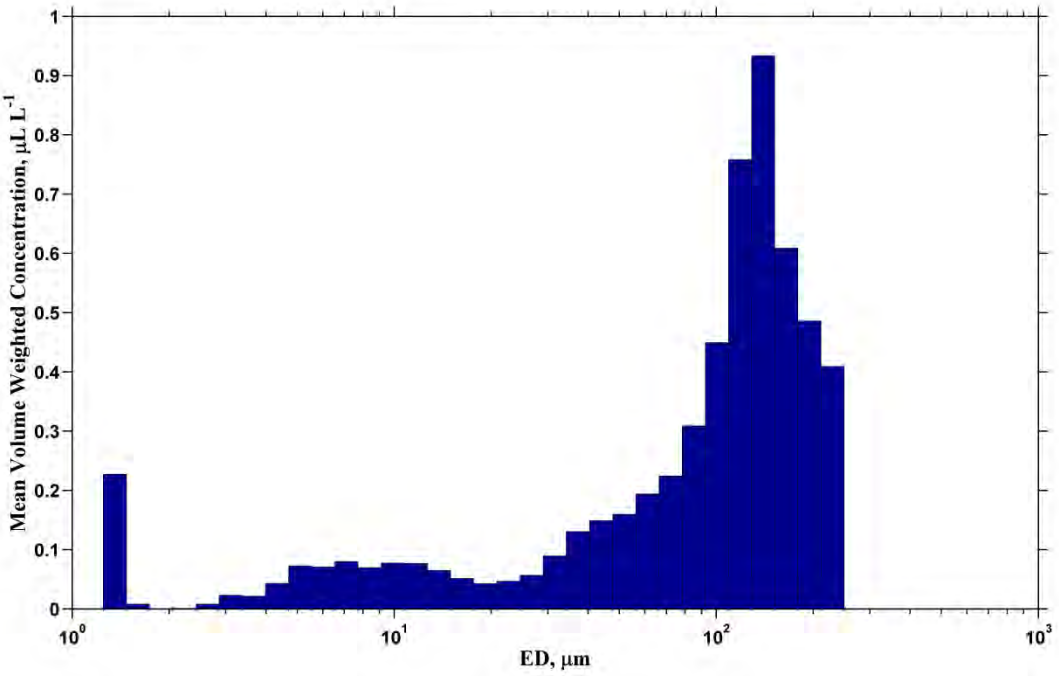

Figure D-300 Mean volume-weighted concentration histogram. Deployment period is November 5, 2012 13:47 to November 8, 2012 14:18.

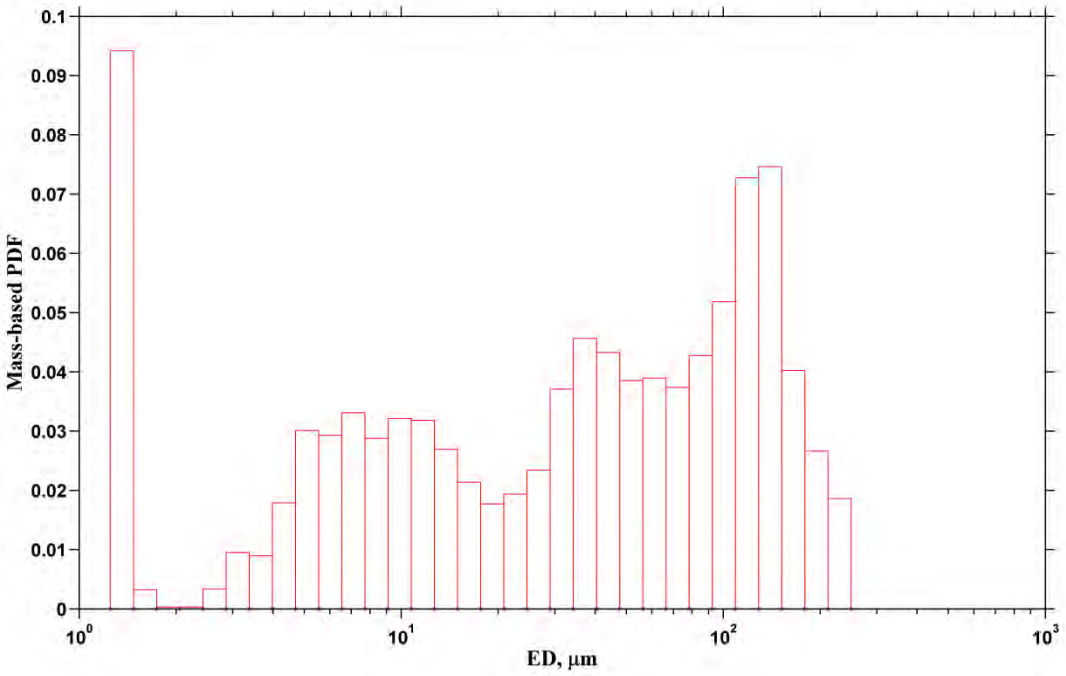

Figure D-301 Mass contribution of each grain-size bin to total calculated mass. Deployment period is November 5, 2012 13:47 to November 8, 2012 14:18.

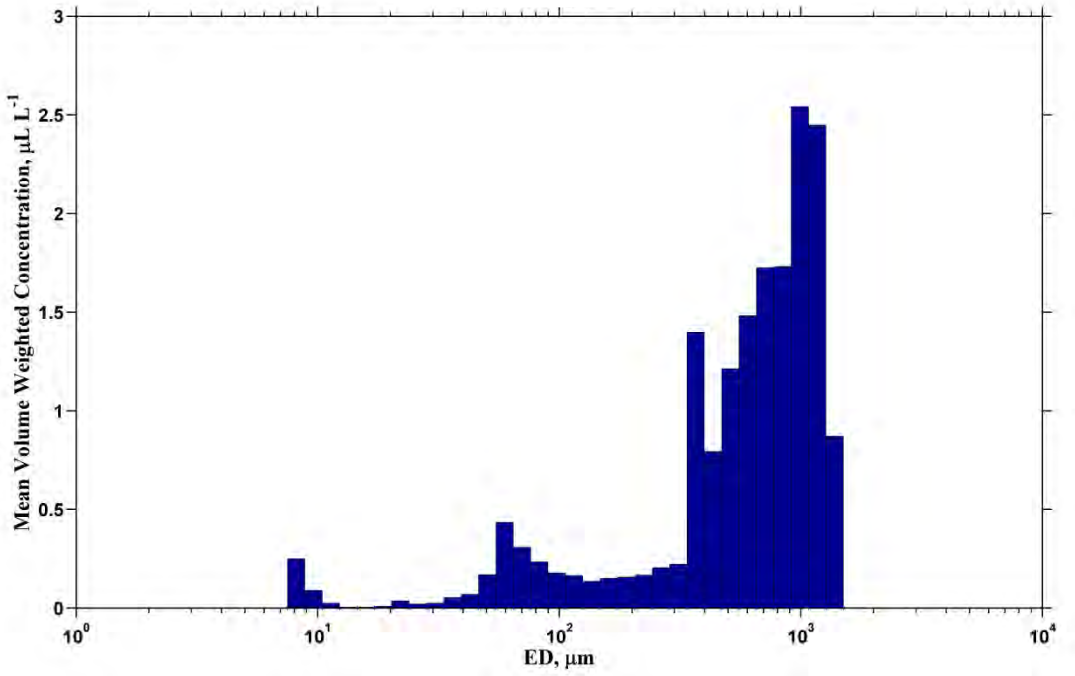

Figure D-302 Mean volume-weighted concentration histogram. Deployment period is November 5, 2012 13:50 to November 8, 2012 14:52.

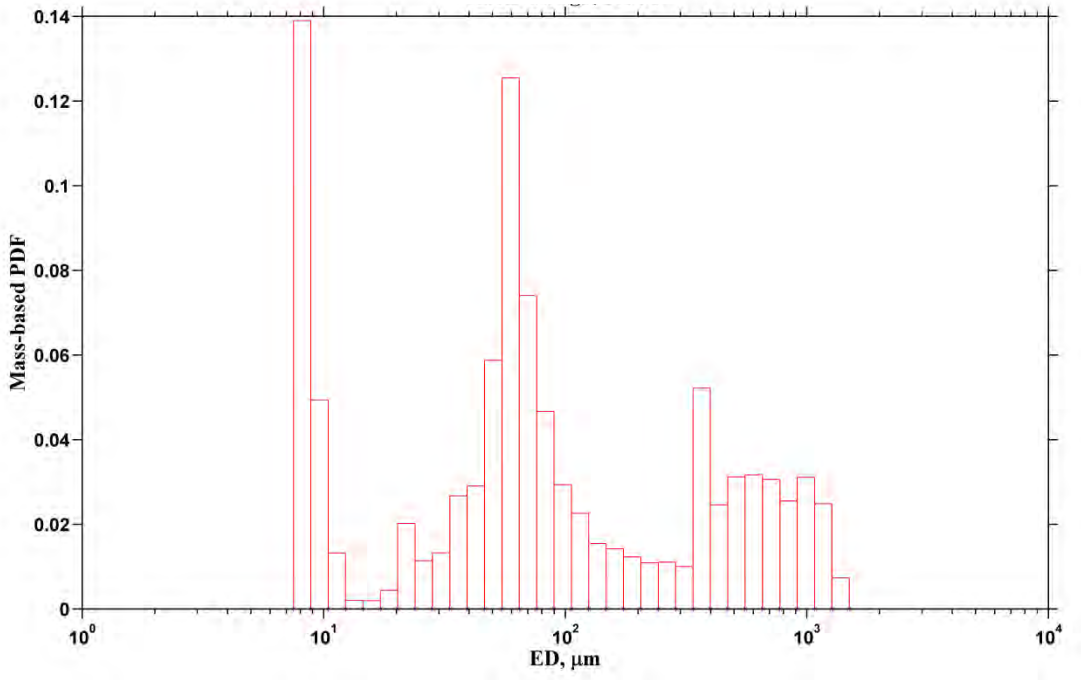

Figure D-303 Mass contribution of each grain-size bin to total calculated mass. Deployment period is November 5, 2012 13:50 to November 8, 2012 14:52.

2013 February

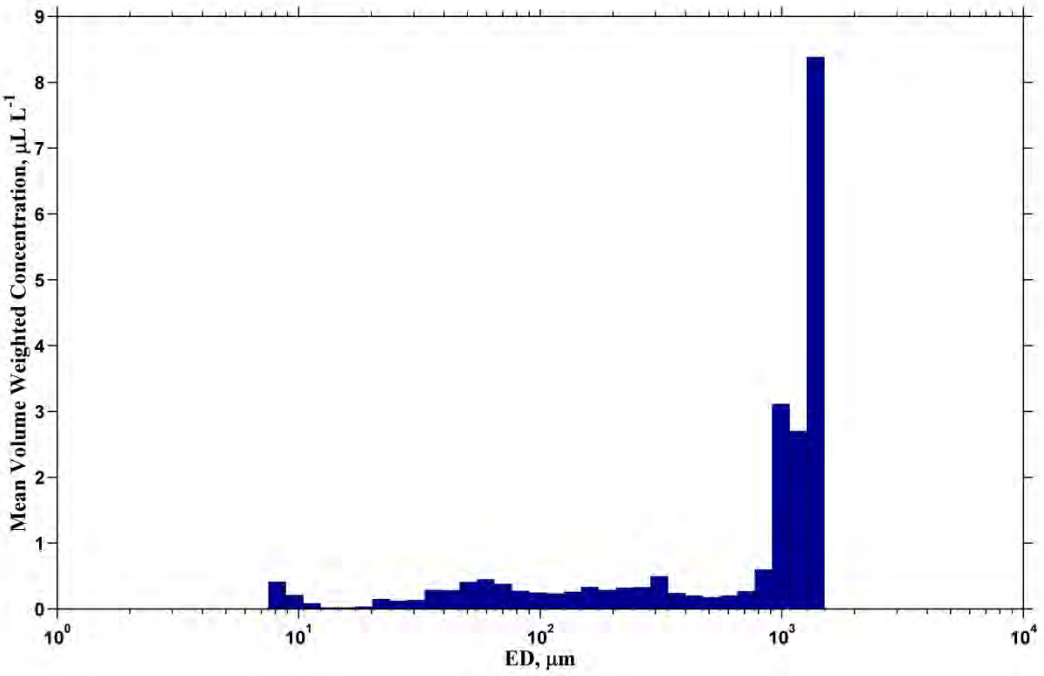

Figure D-304 Mean volume-weighted concentration histogram. Deployment period is February 26, 2013 17:40 to February 28, 2013 12:05.

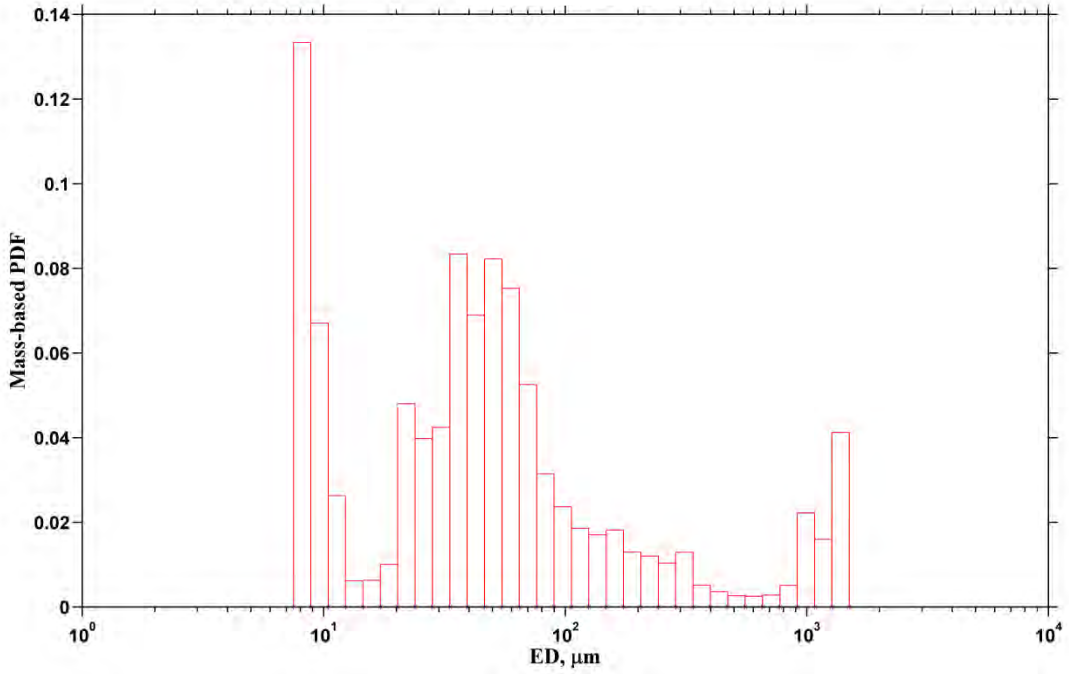

Figure D-305 Mass contribution of each grain-size bin to total calculated mass. Deployment period is February 26, 2013 17:40 to February 28, 2013 12:05.

2013 August

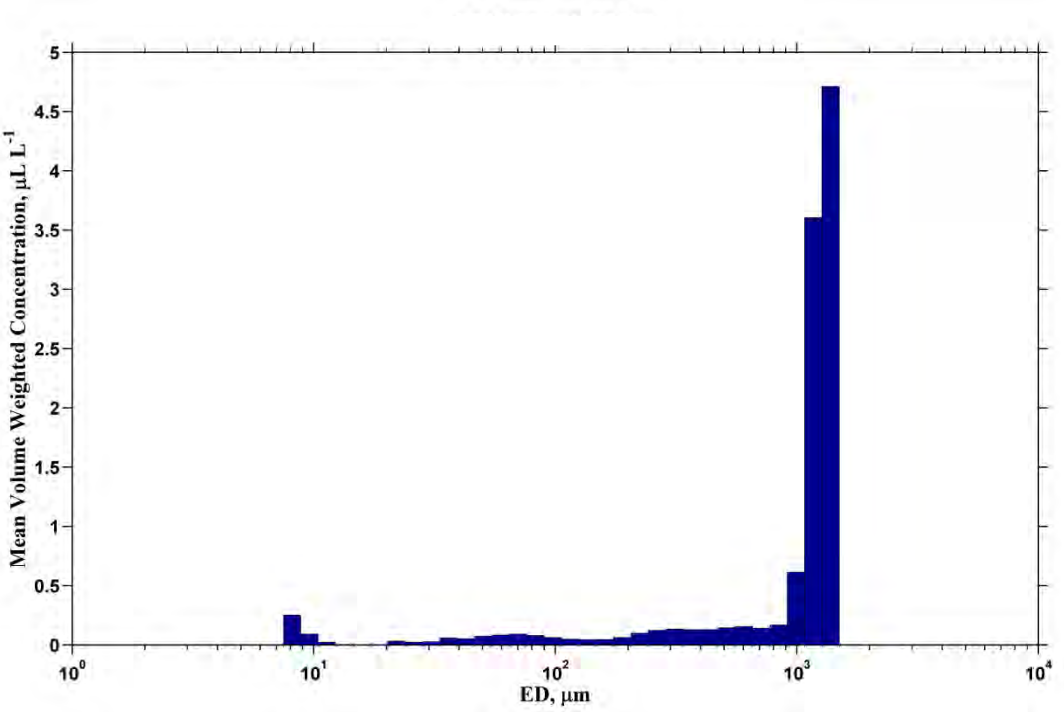

Figure D-306 Mean volume-weighted concentration histogram. Deployment period is August 14, 2013 11:08 to August 15, 2013 09:24.

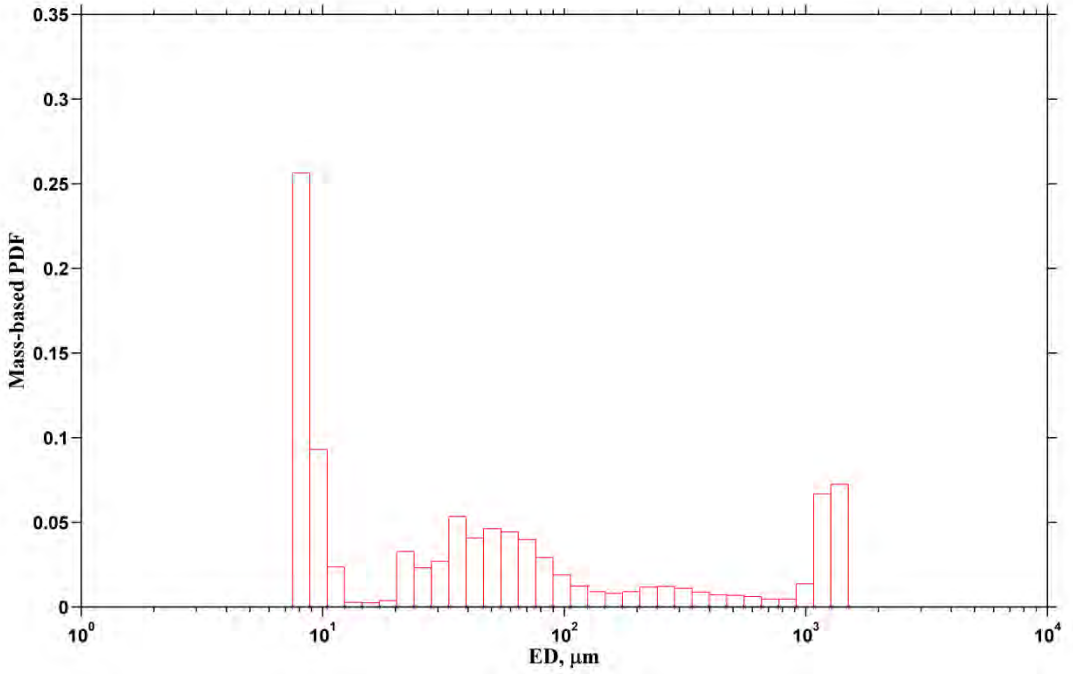

Figure D-307 Mass contribution of each grain-size bin to total calculated mass. Deployment period is August 14, 2013 11:08 to August 15, 2013 09:24.

2013 September

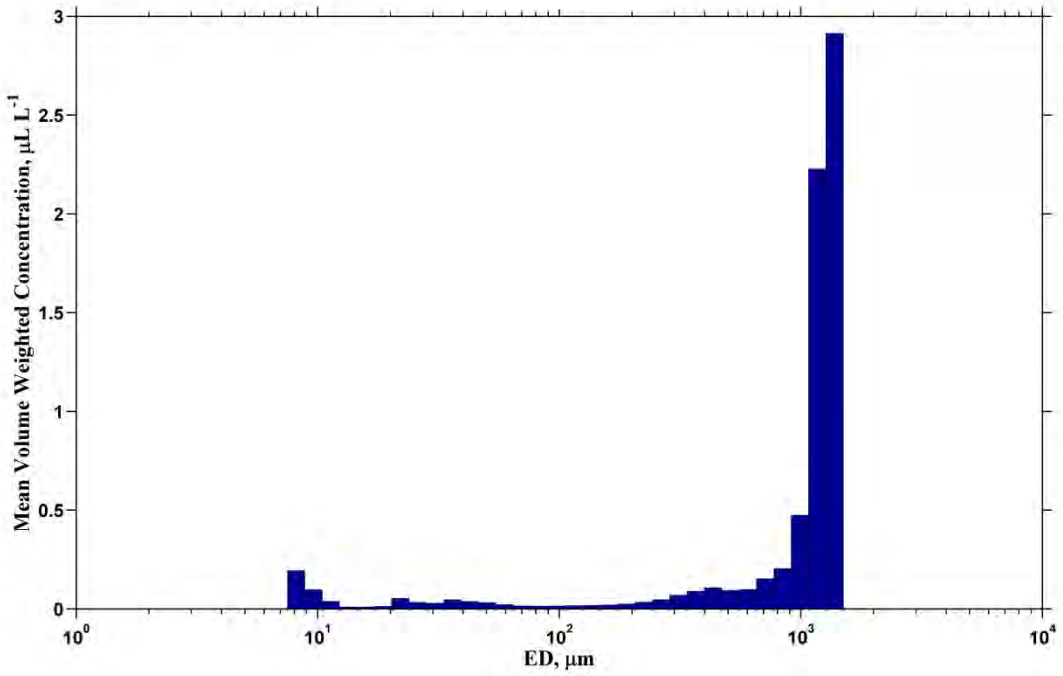

Figure D-308 Mean volume-weighted concentration histogram. Deployment period is September 24, 2013 11:22 to September 26, 2013 07:39.

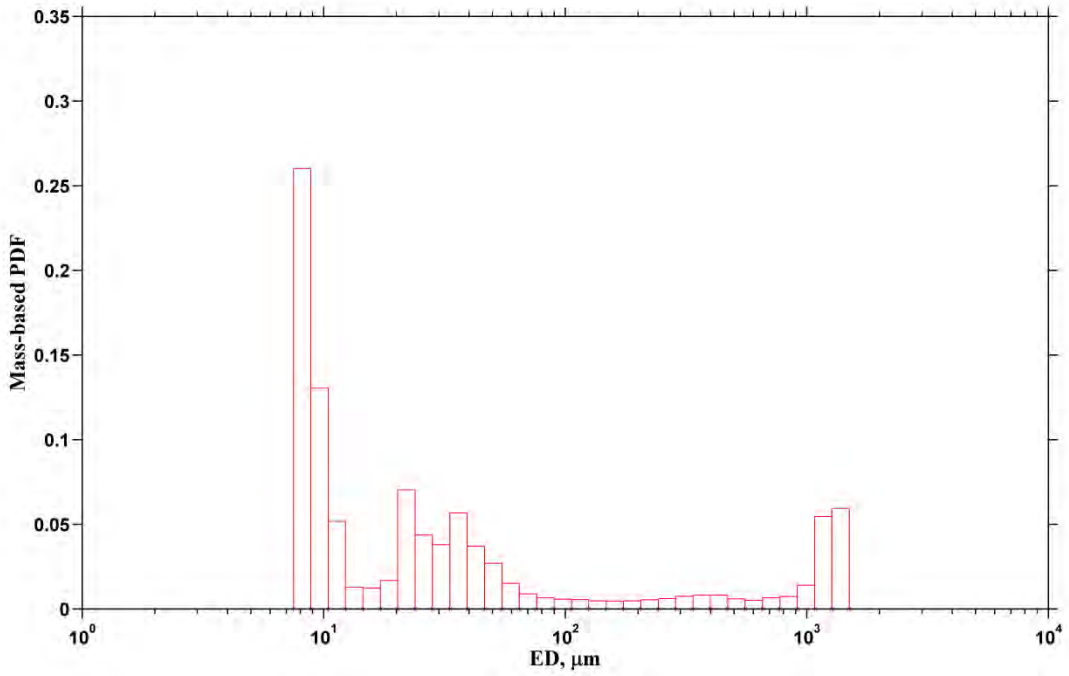

Figure D-309 Mass contribution of each grain-size bin to total calculated mass. Deployment period is September 24, 2013 11:22 to September 26, 2013 07:39.

2013 November

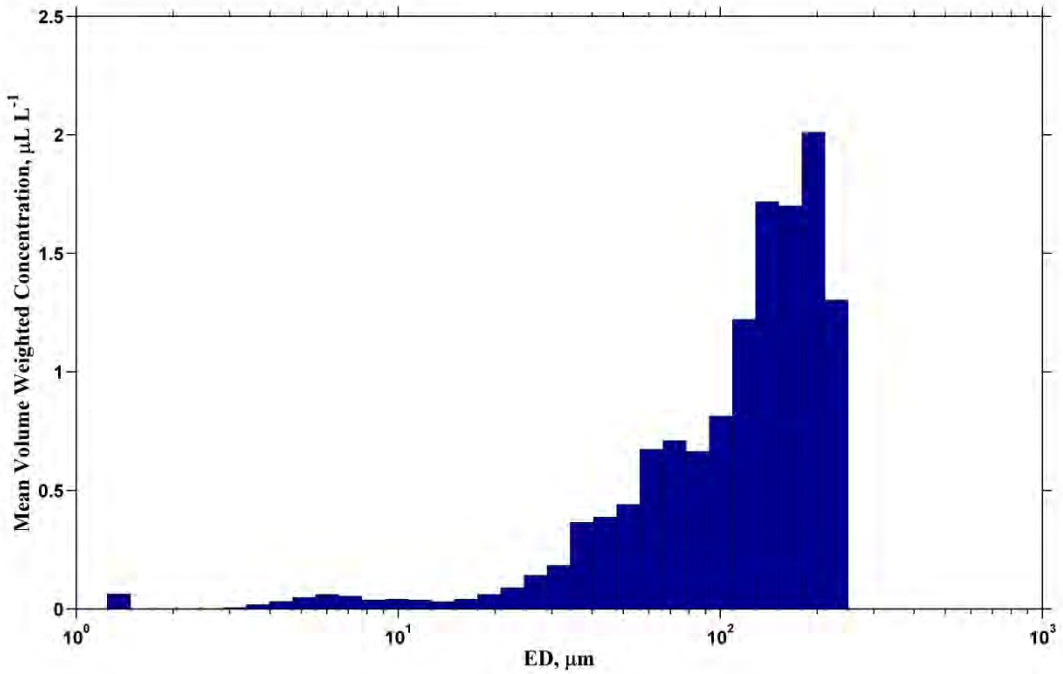

Figure D-310 Mean volume-weighted concentration histogram. Deployment period is November 4, 2013 13:30 to November 5, 2013 09:00 (Pre-Flow).

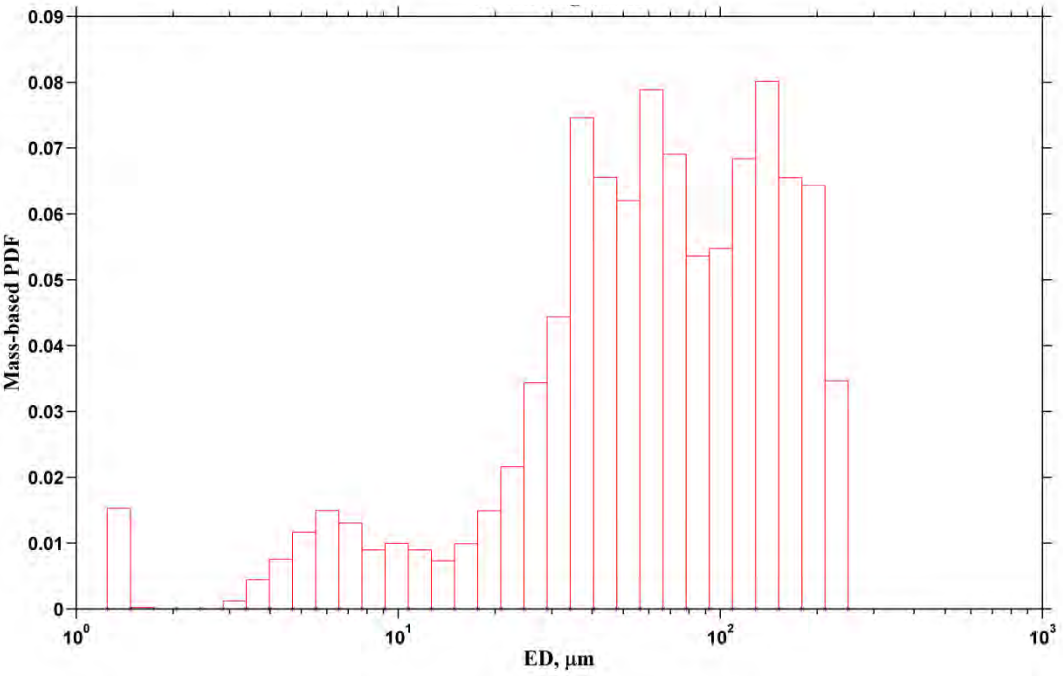

Figure D-311 Mass contribution of each grain-size bin to total calculated mass. Deployment period is November 4, 2013 13:30 to November 5, 2013 09:00 (Pre-Flow).

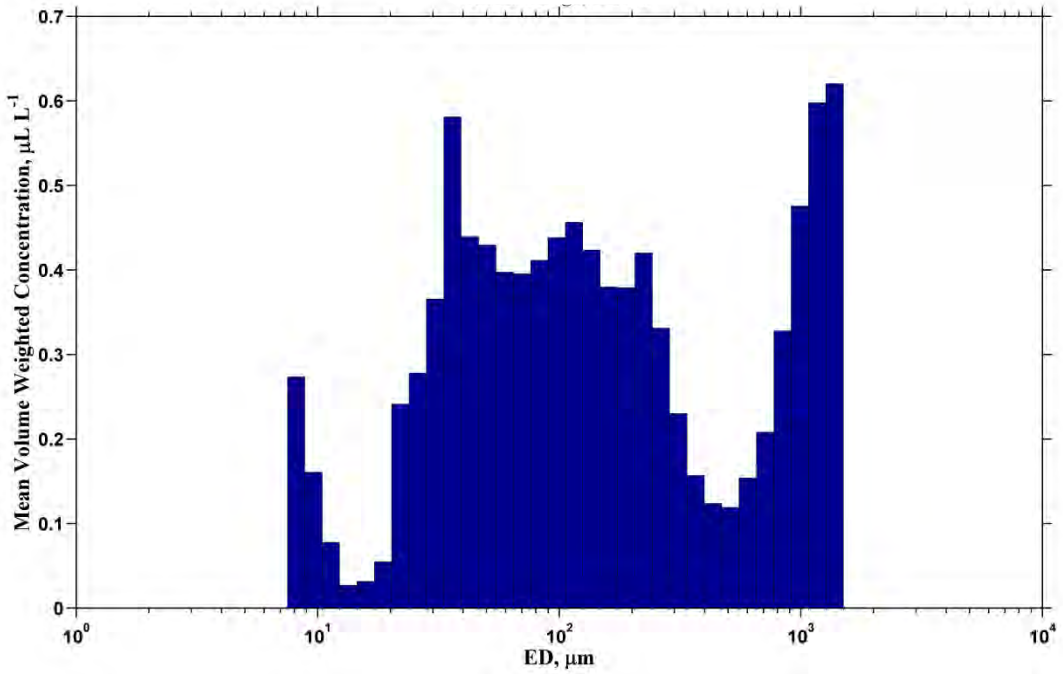

Figure D-312 Mean volume-weighted concentration histogram. Deployment period is November 3, 2013 12:54 to November 4, 2013 12:30 (Pre-Flow).

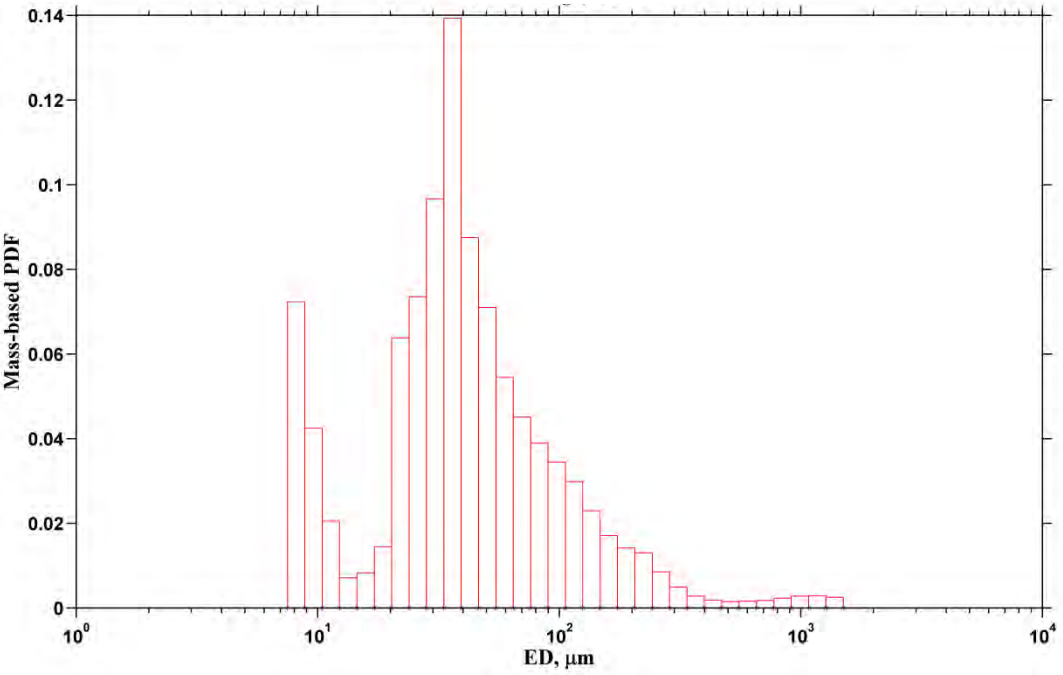

Figure D-313 Mass contribution of each grain-size bin to total calculated mass. Deployment period is November 3, 2013 12:54 to November 4, 2013 12:30 (Pre-Flow).

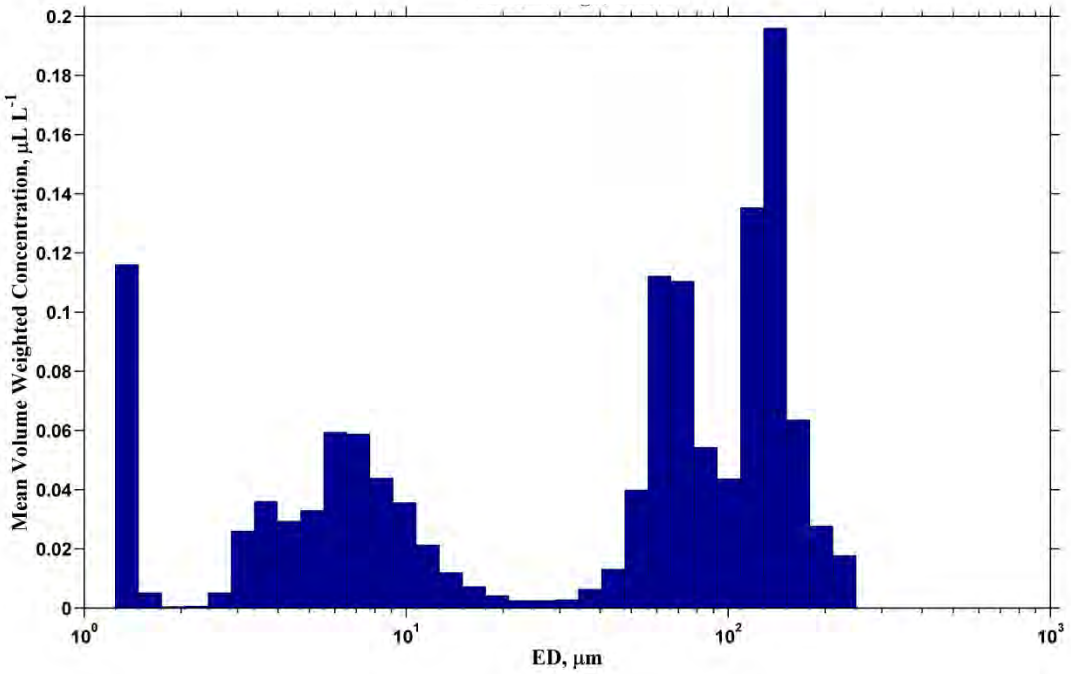

Figure D-314 Mean volume-weighted concentration histogram. Deployment period is November 3, 2013 12:47 to November 4, 2013 12:30 (Pre-Flow).

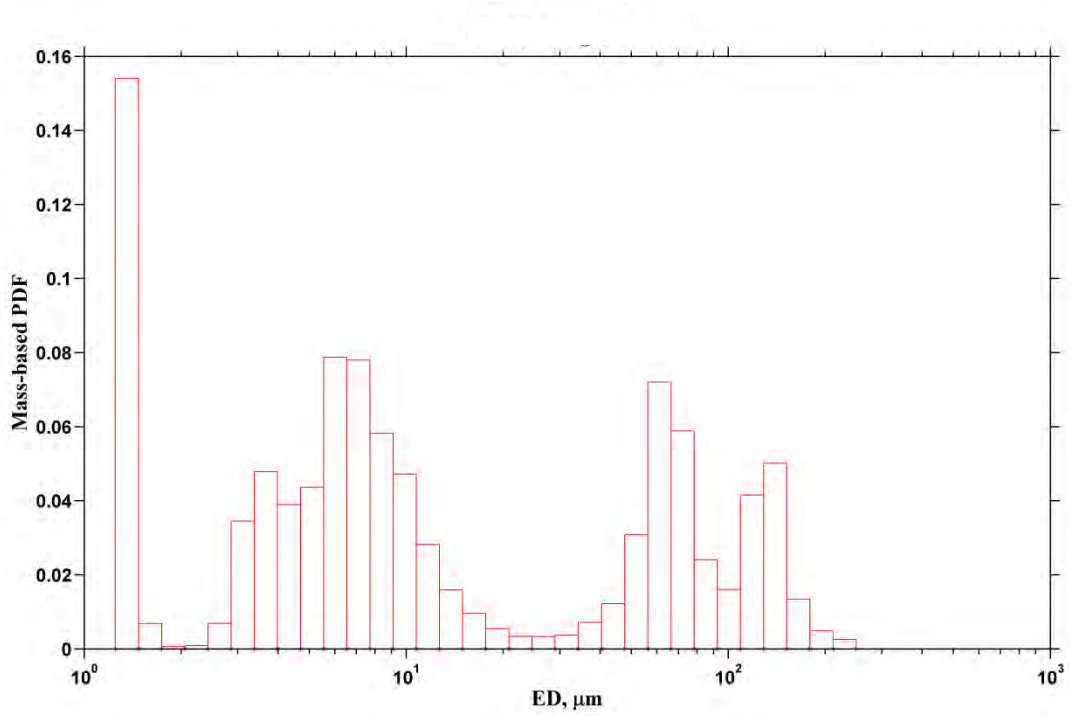

Figure D-315 Mass contribution of each grain-size bin to total calculated mass. Deployment period is November 3, 2013 12:47 to November 4, 2013 12:30 (Pre-Flow).

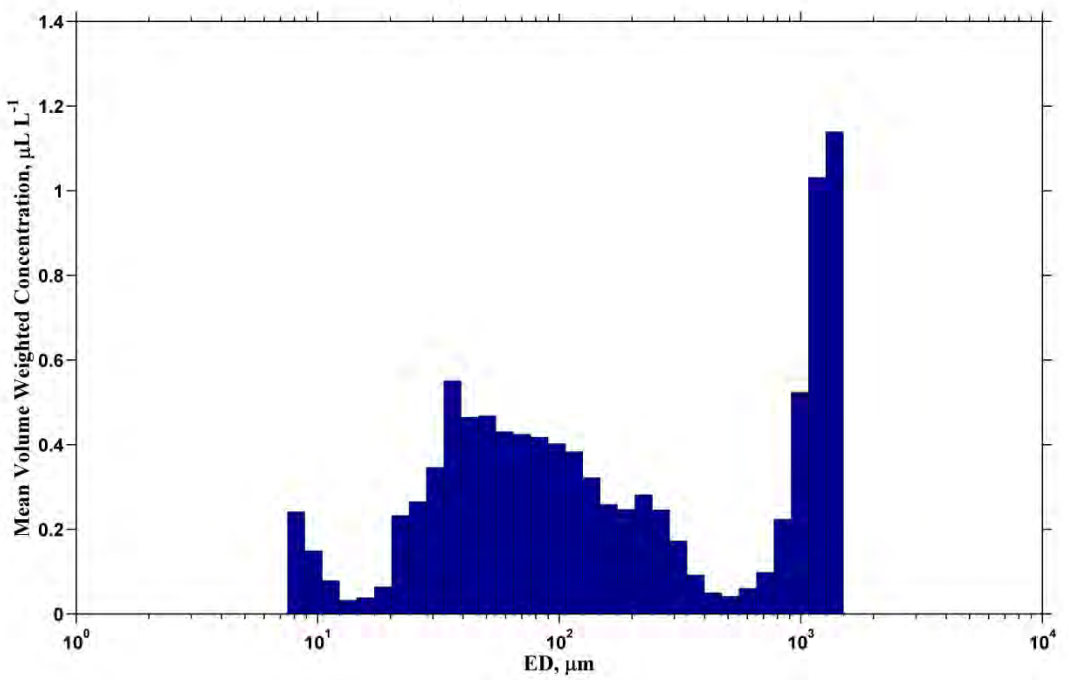

Figure D-316 Mean volume-weighted concentration histogram. Deployment period is November 4, 2013 13:30 to November 5, 2013 09:00 (Pre-Flow).

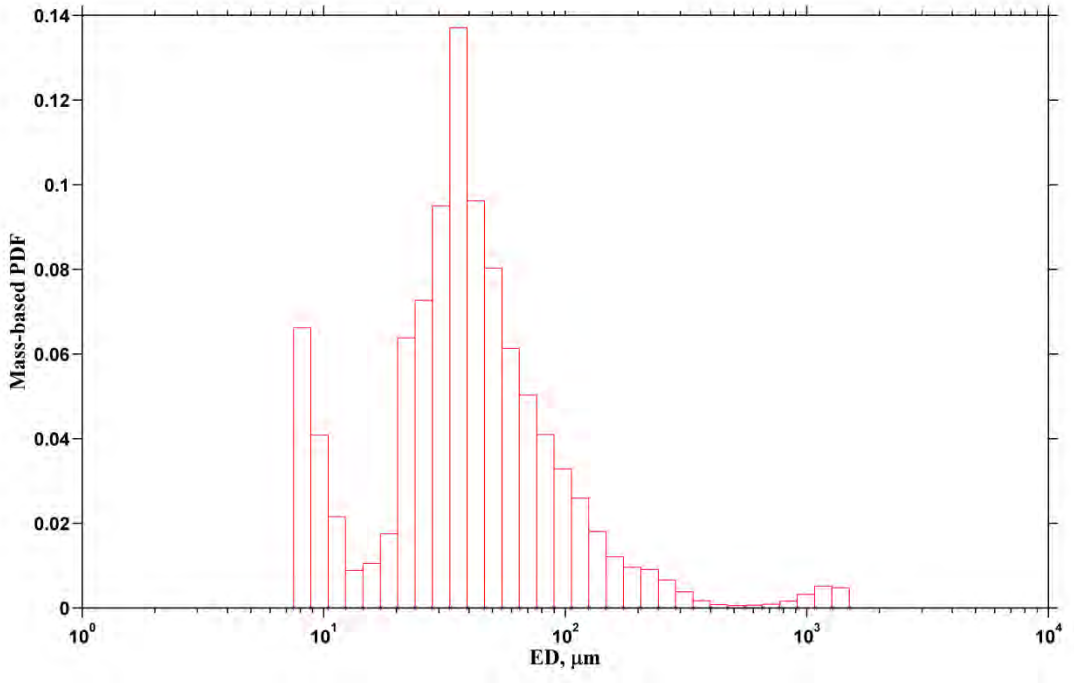

Figure D-317 Mass contribution of each grain-size bin to total calculated mass. Deployment period is November 4, 2013 13:30 to November 5, 2013 09:00 (Pre-Flow).

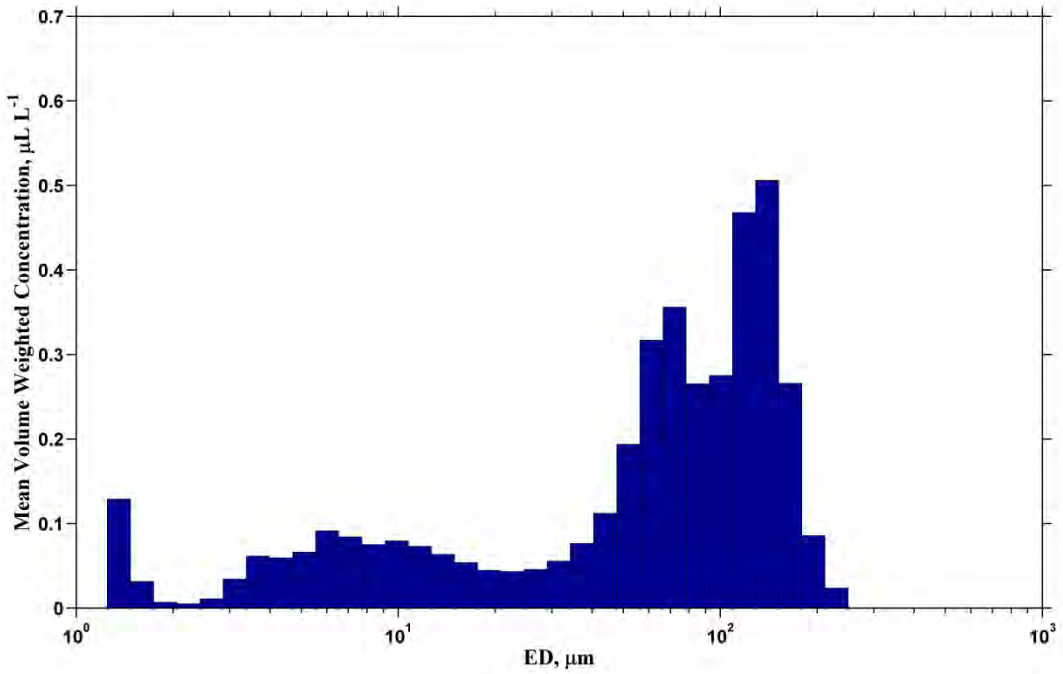

Figure D-318 Mean volume-weighted concentration histogram. Deployment period is November 5, 2013 09:00 to November 6, 2013 13:00 (Transient).

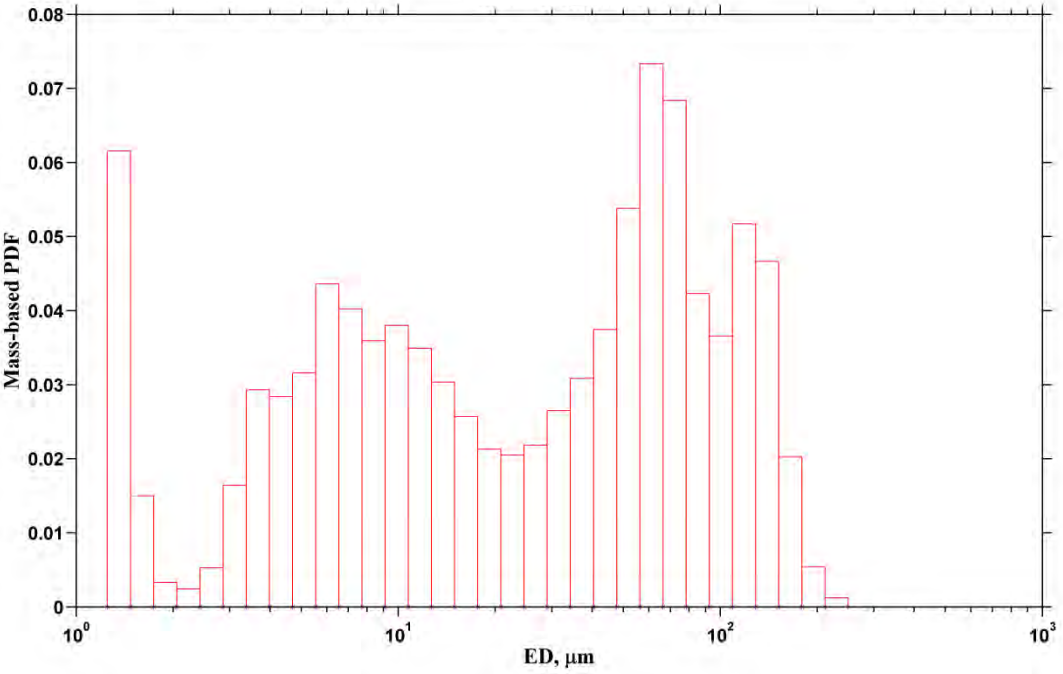

Figure D-319 Mass contribution of each grain-size bin to total calculated mass. Deployment period is November 5, 2013 09:00 to November 6, 2013 13:00 (Transient).

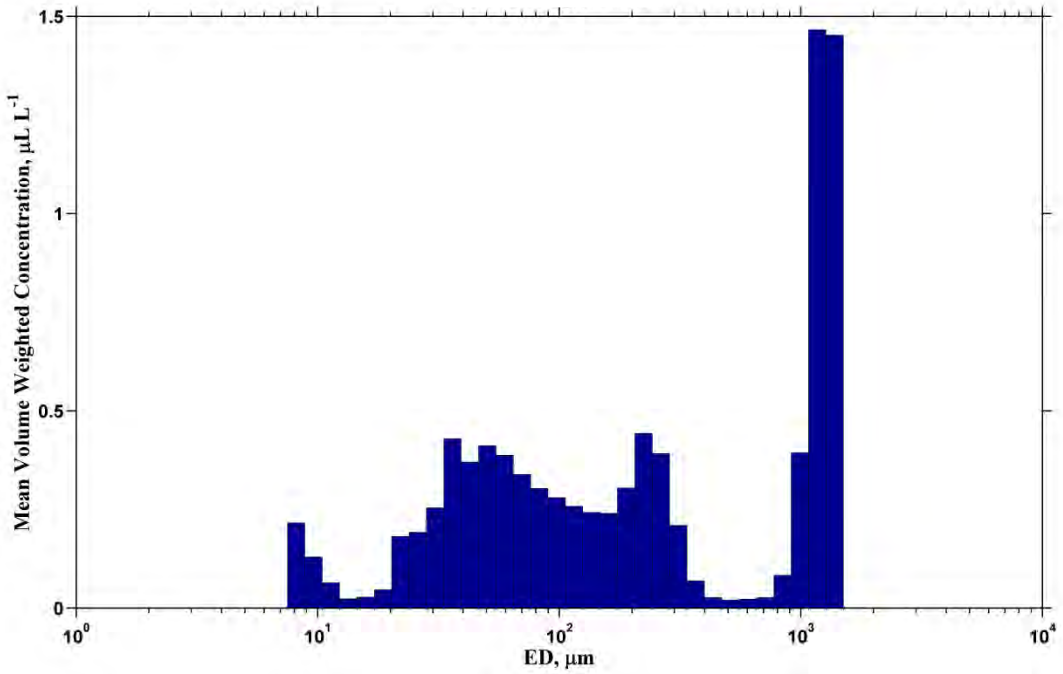

Figure D-320 Mean volume-weighted concentration histogram. Deployment period is November 6, 2013 14:00 to November 7, 2013 10:00 (Transient).

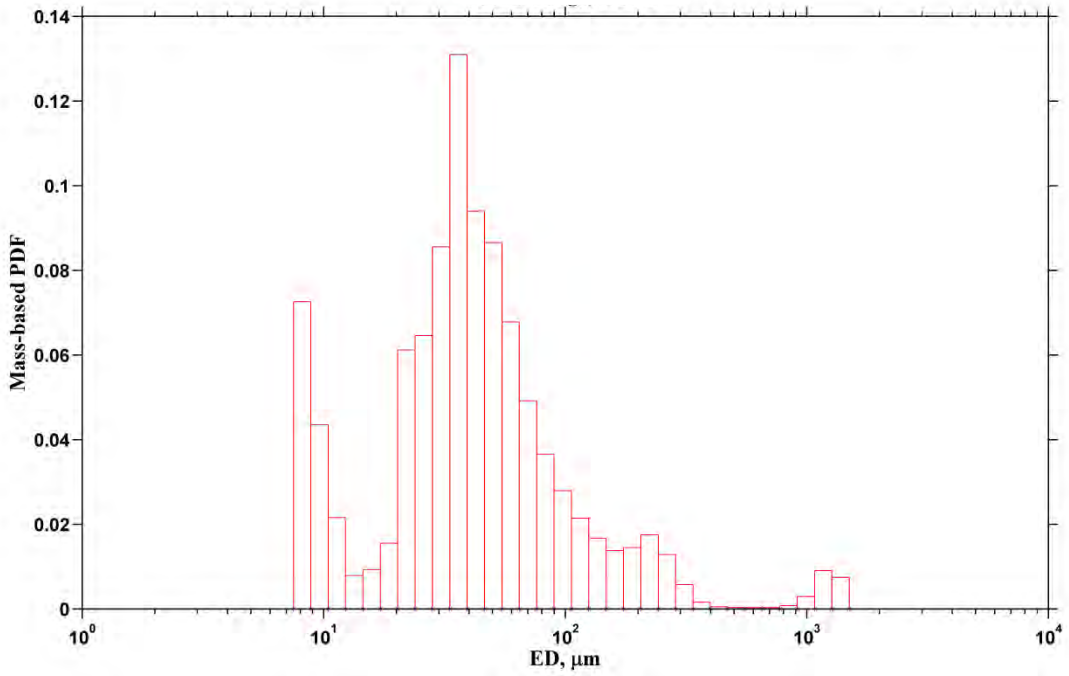

Figure D-321 Mass contribution of each grain-size bin to total calculated mass. Deployment period is November 6, 2013 14:00 to November 7, 2013 10:00 (Transient).

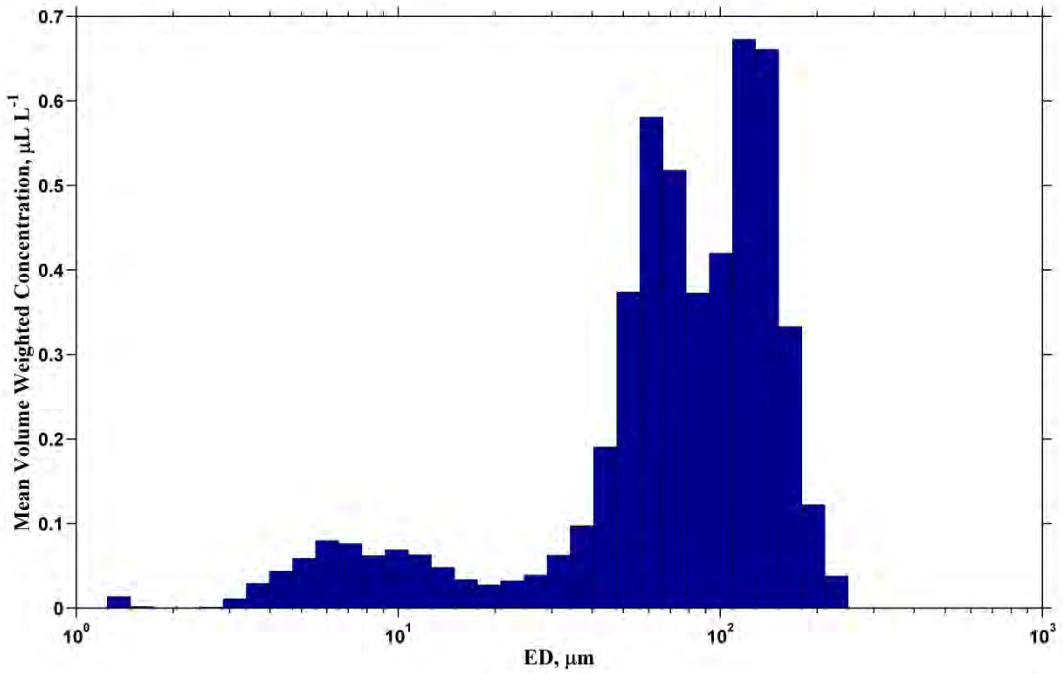

Figure D-322 Mean volume-weighted concentration histogram. Deployment period is November 6, 2013 14:00 to November 7, 2013 10:00 (Transient).

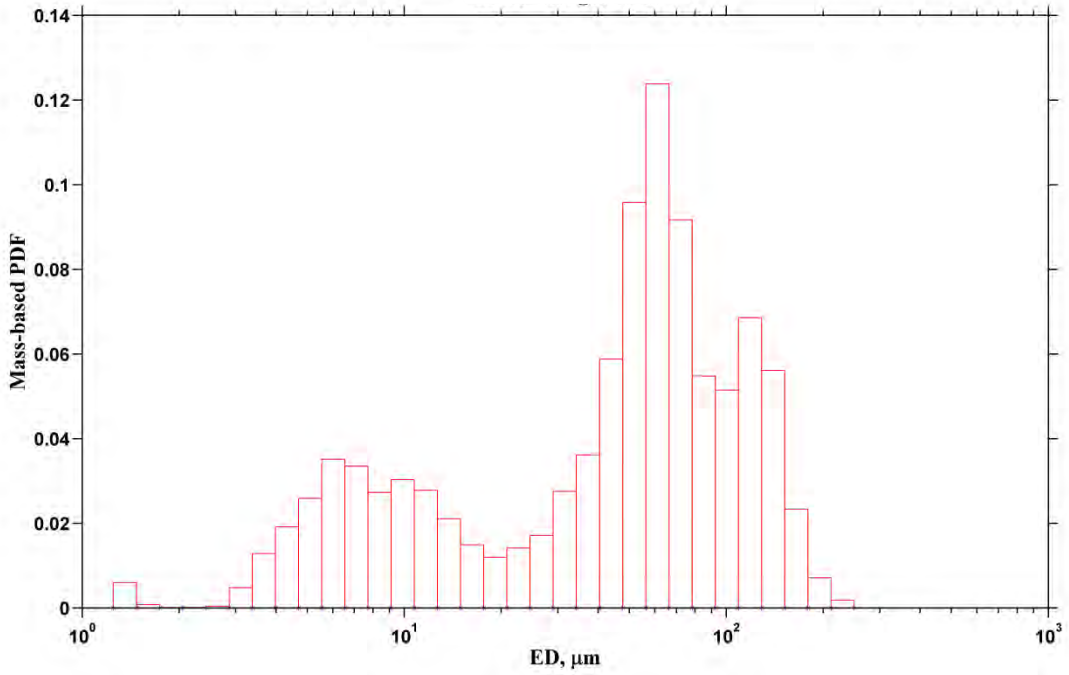

Figure D-323 Mass contribution of each grain-size bin to total calculated mass. Deployment period is November 6, 2013 14:00 to November 7, 2013 10:00 (Transient).

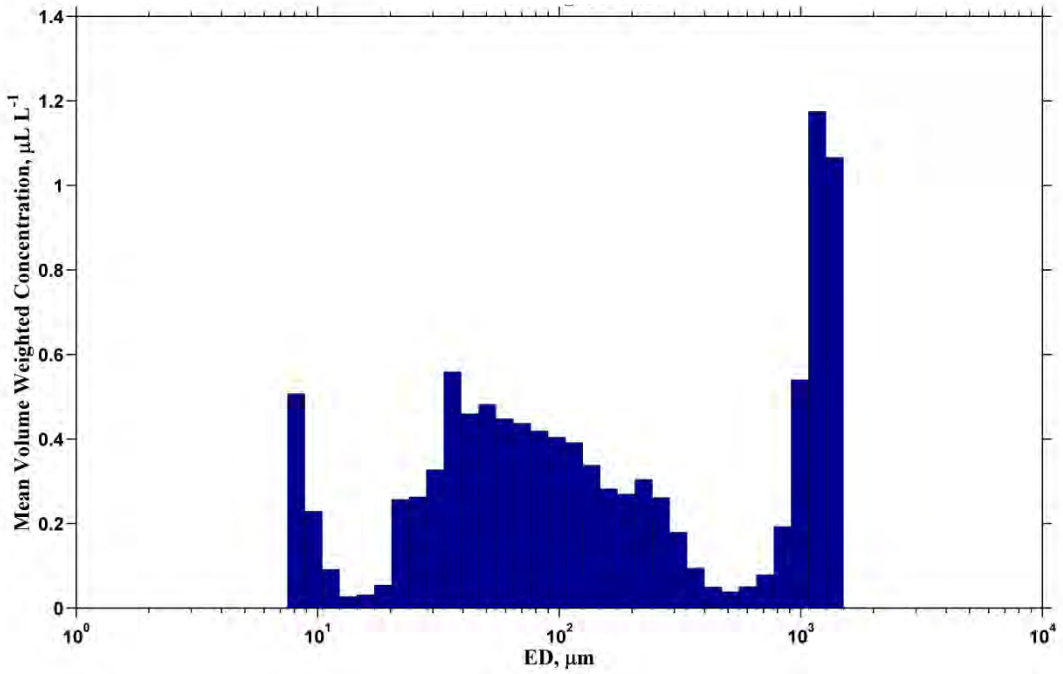

Figure D-324 Mean volume-weighted concentration histogram. Deployment period is November 5, 2013 09:00 to November 6, 2013 13:00 (Transient).

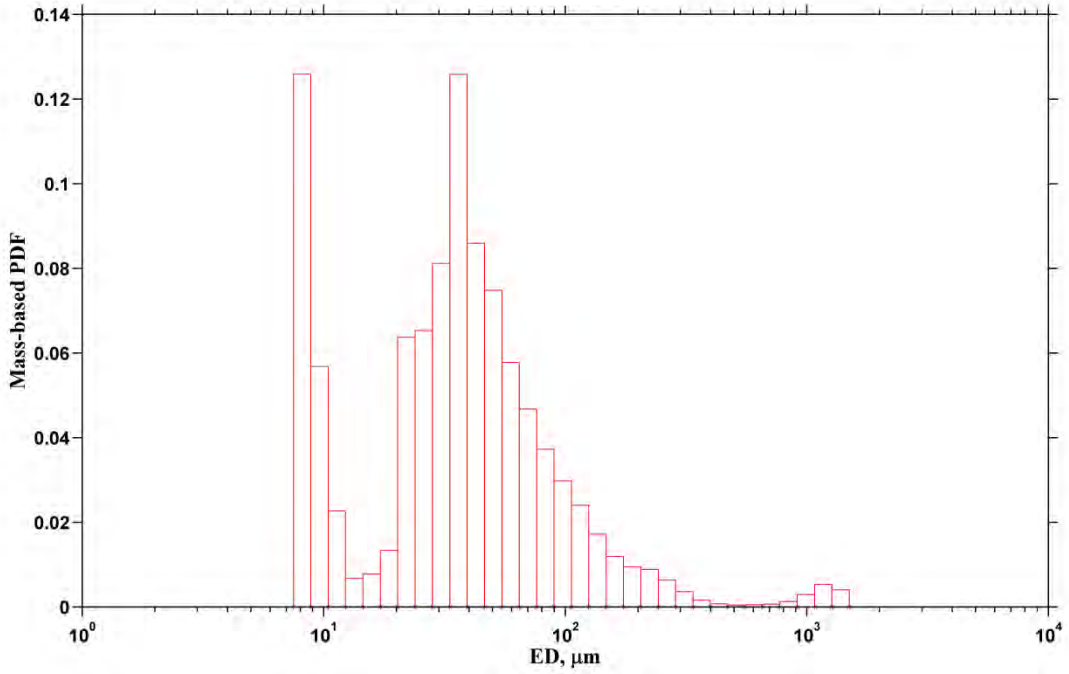

Figure D-325 Mass contribution of each grain-size bin to total calculated mass. Deployment period is November 5, 2013 09:00 to November 6, 2013 13:00 (Transient).

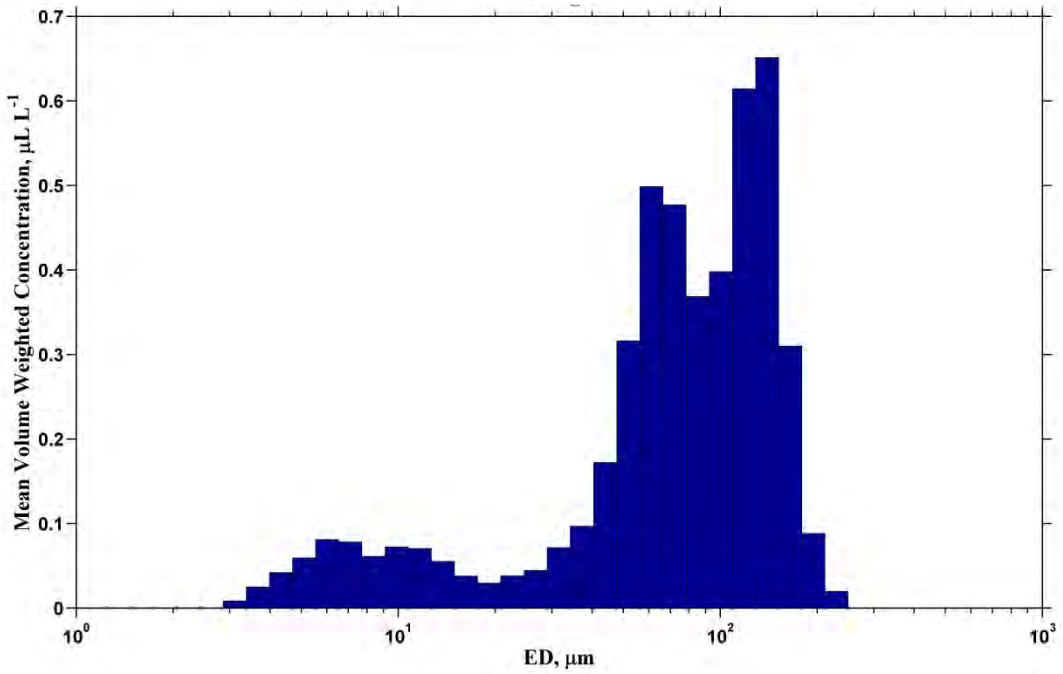

Figure D-326 Mean volume-weighted concentration histogram. Deployment period is November 7, 2013 11:30 to November 9, 2013 08:30 (Steady State).

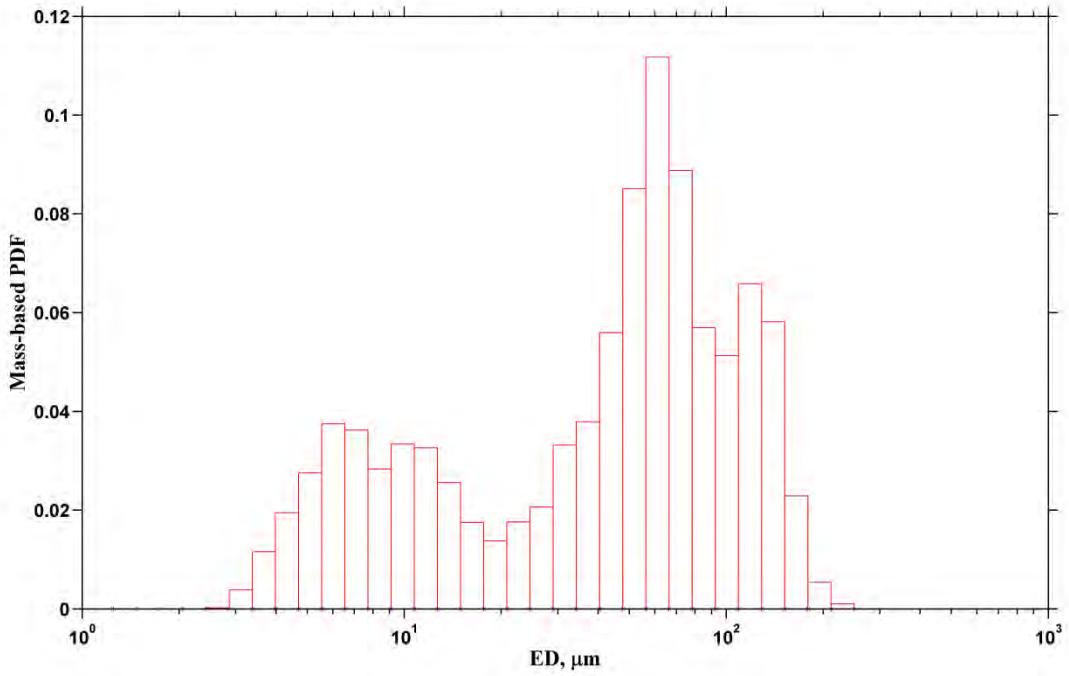

Figure D-327 Mass contribution of each grain-size bin to total calculated mass. Deployment period is November 7, 2013 11:30 to November 9, 2013 08:30 (Steady State).

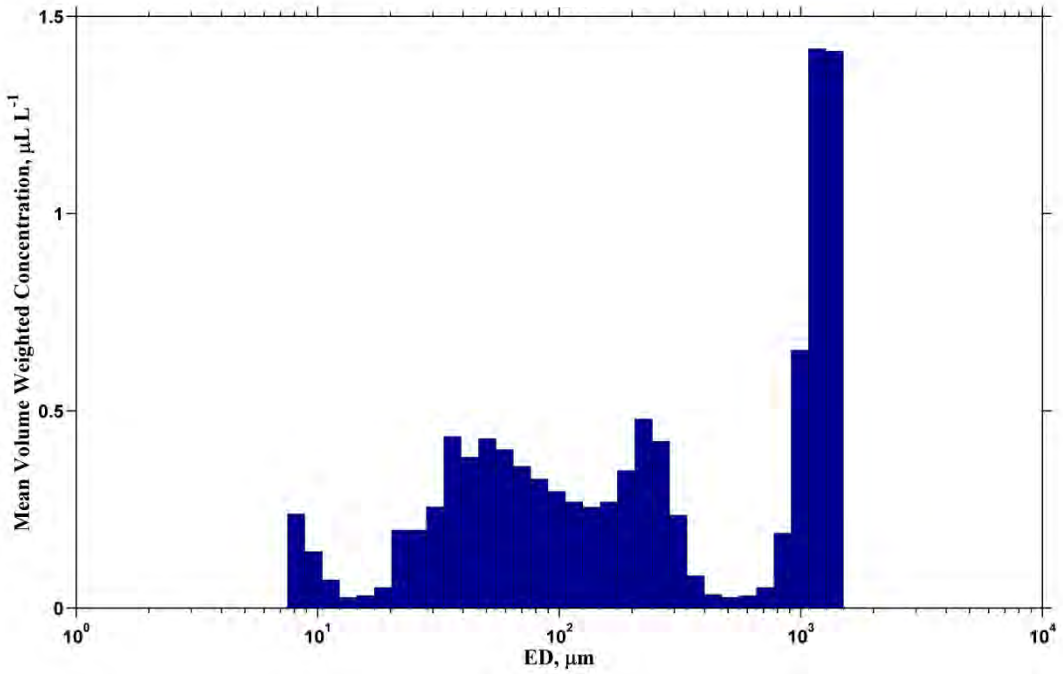

Figure D-328 Mean volume-weighted concentration histogram. Deployment period is November 9, 2013 10:00 to November 10, 2013 08:30 (Steady State).

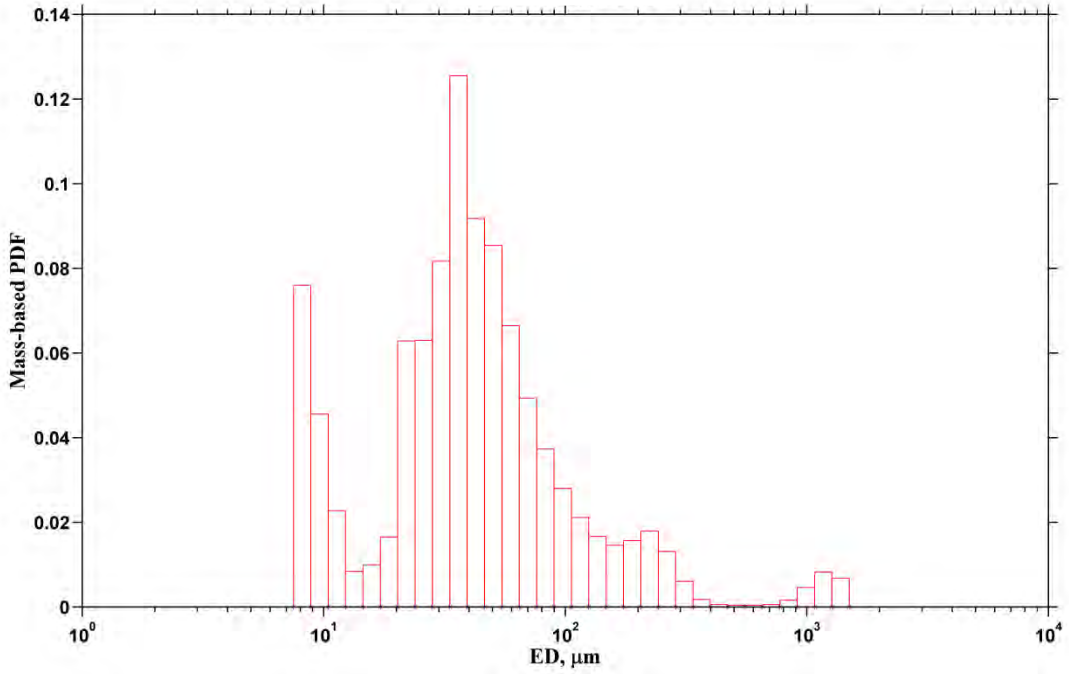

Figure D-329 Mass contribution of each grain-size bin to total calculated mass. Deployment period is November 9, 2013 10:00 to November 10, 2013 08:30 (Steady State).

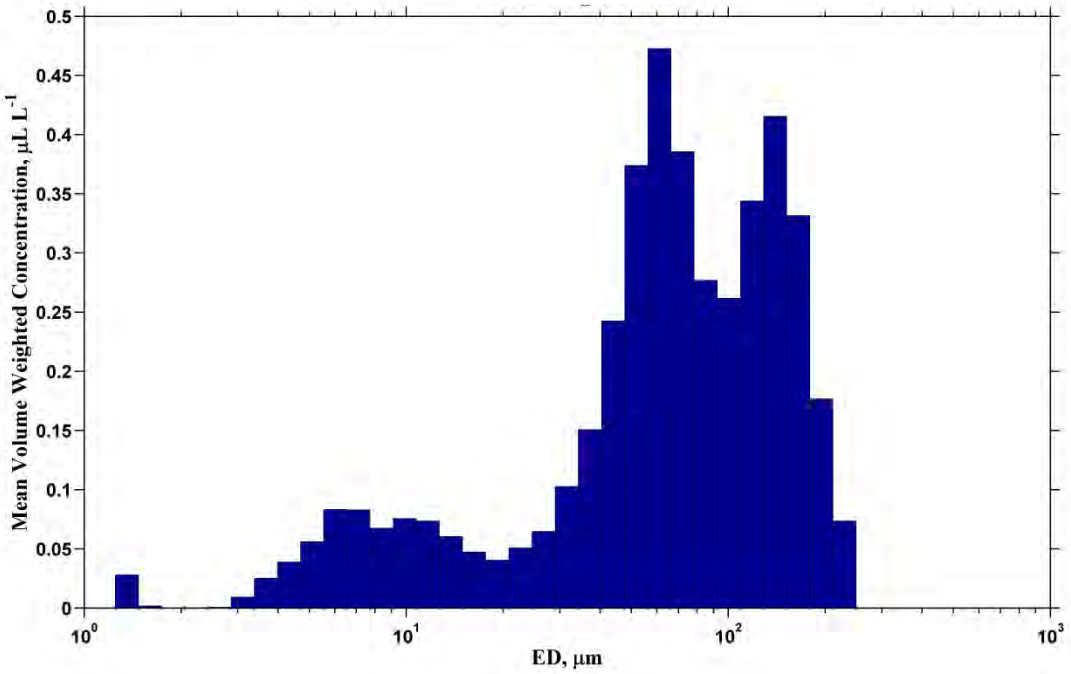

Figure D-330 Mean volume-weighted concentration histogram. Deployment period is November 9, 2013 10:00 to November 10, 2013 08:30 (Steady State).

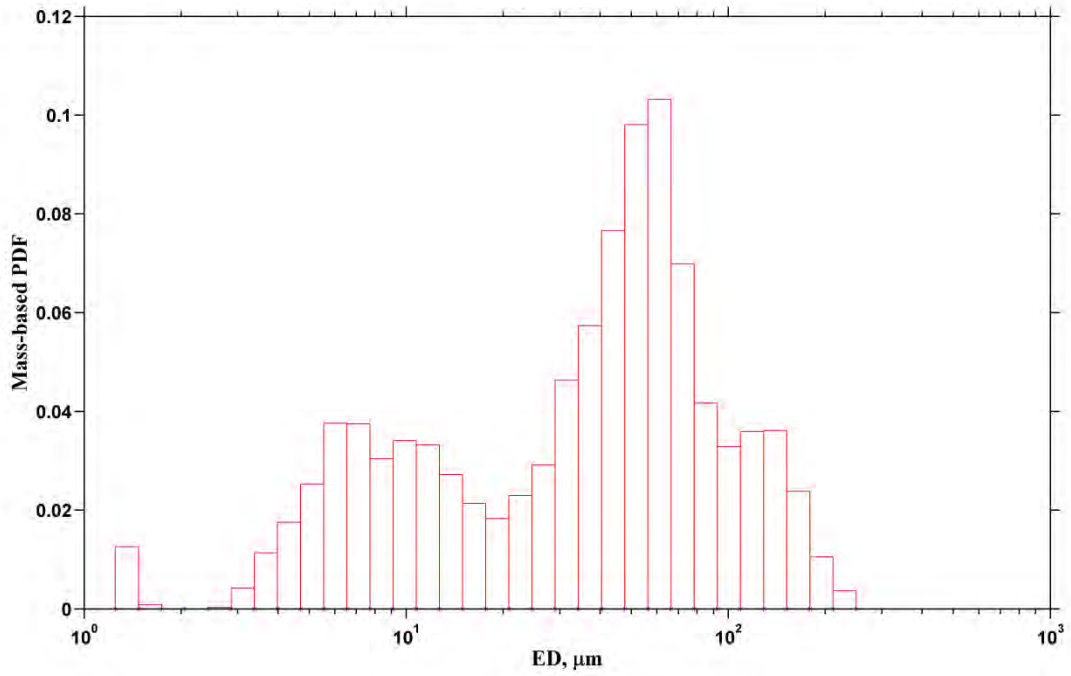

Figure D-331 Mass contribution of each grain-size bin to total calculated mass. Deployment period is November 9, 2013 10:00 to November 10, 2013 08:30 (Steady State).

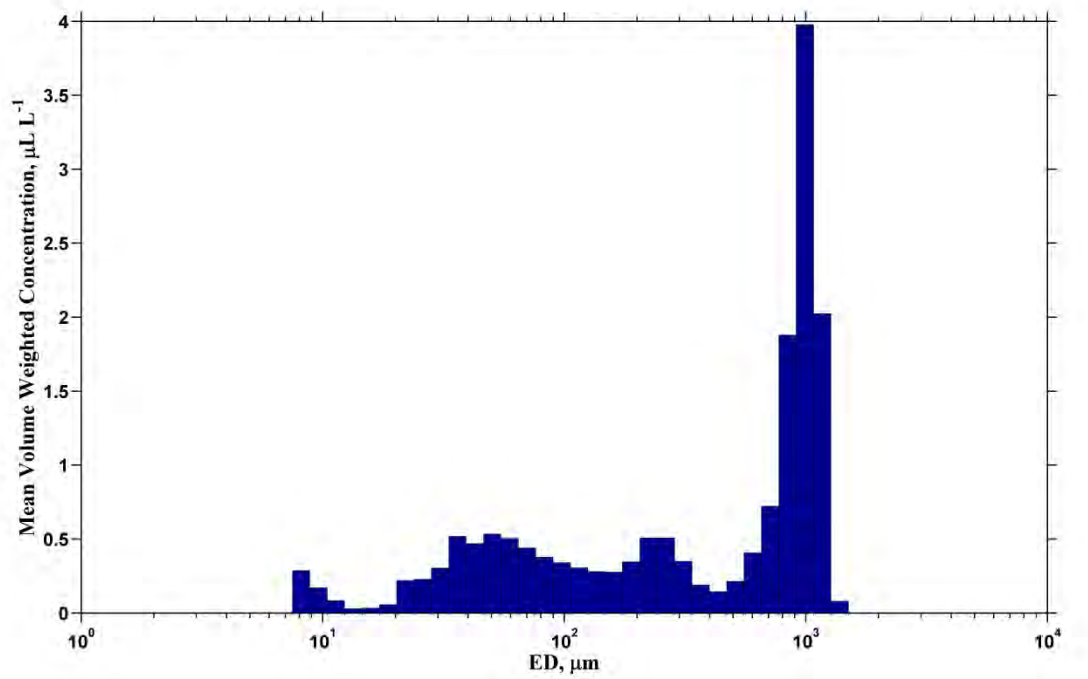

Figure D-332 Mean volume-weighted concentration histogram. Deployment period is November 7, 2013 11:30 to November 9, 2013 08:30 (Steady State).

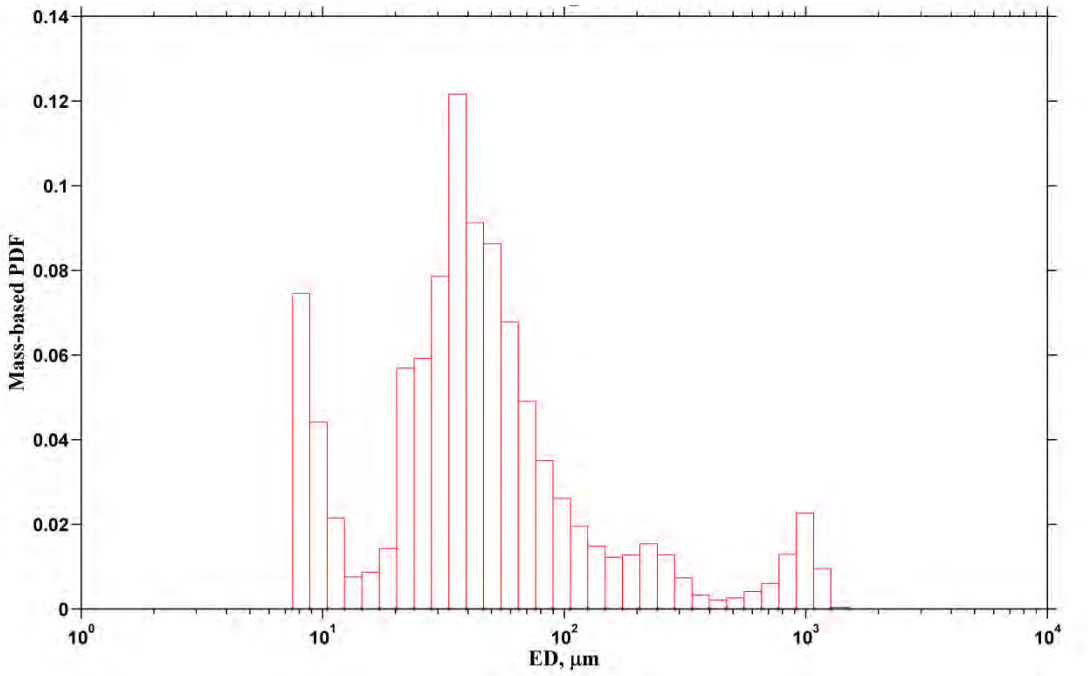

Figure D-333 Mass contribution of each grain-size bin to total calculated mass. Deployment period is November 7, 2013 11:30 to November 9, 2013 08:30 (Steady State).

2014 November

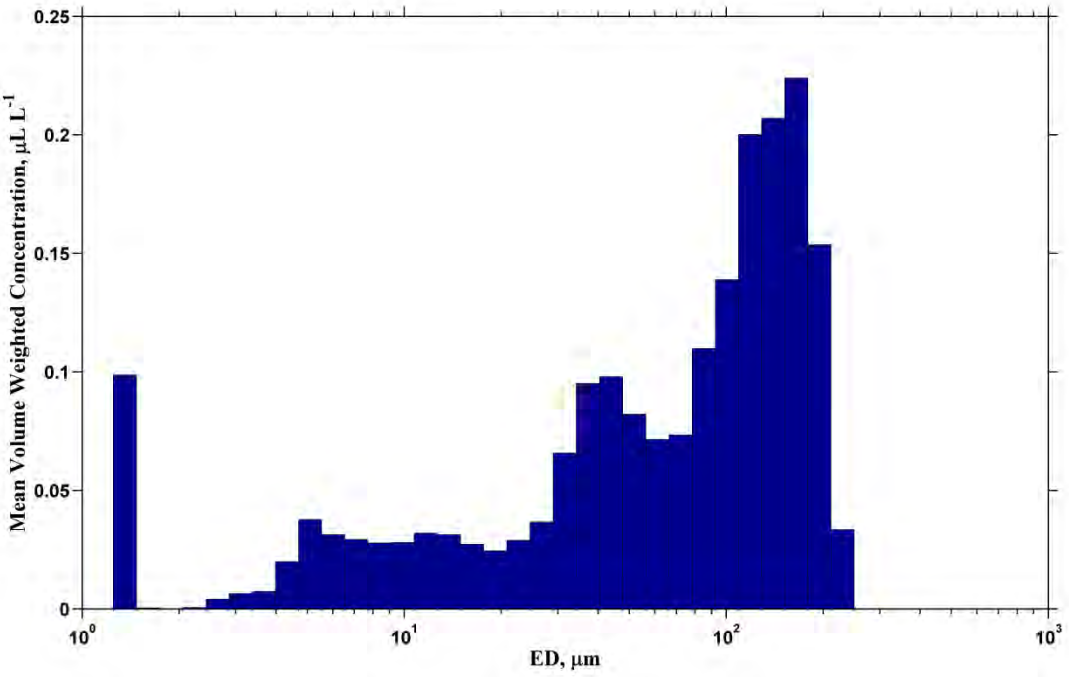

Figure D-334 Mean volume-weighted concentration histogram. Deployment period is November 2, 2014 18:00 to November 3, 2014 08:00 (Pre-flow).

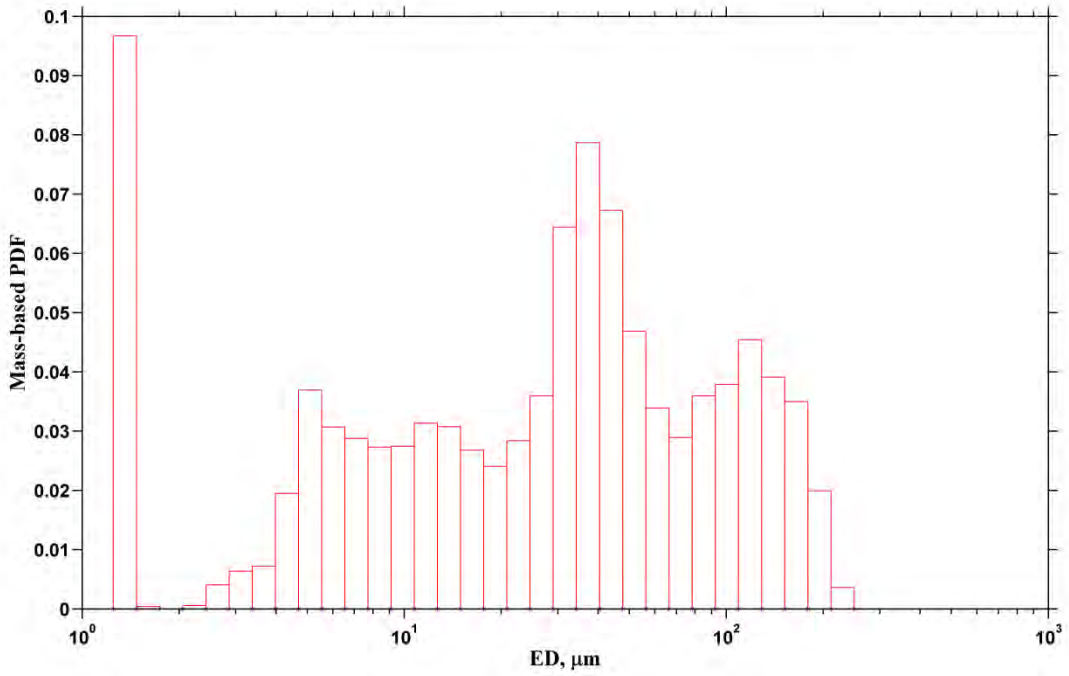

Figure D-335 Mass contribution of each grain-size bin to total calculated mass. Deployment period is November 2, 2014 18:00 to November 3, 2014 08:00 (Pre-flow).

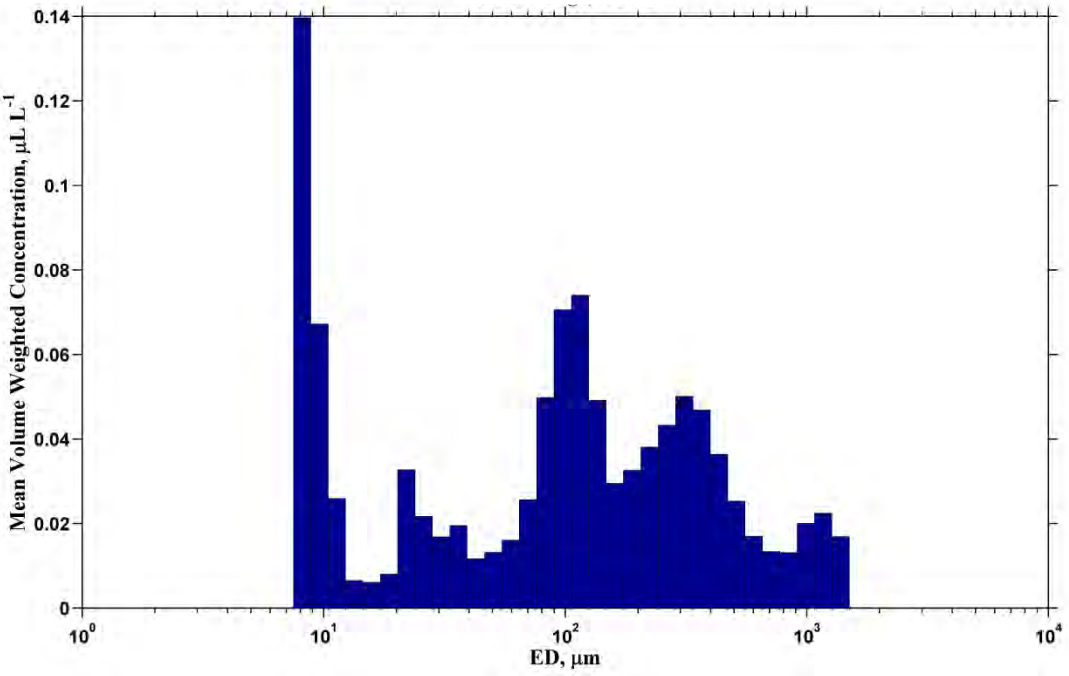

Figure D-336 Mean volume-weighted concentration histogram. Deployment period is November 3, 2014 09:00 to November 4, 2014 09:30 (Pre-flow).

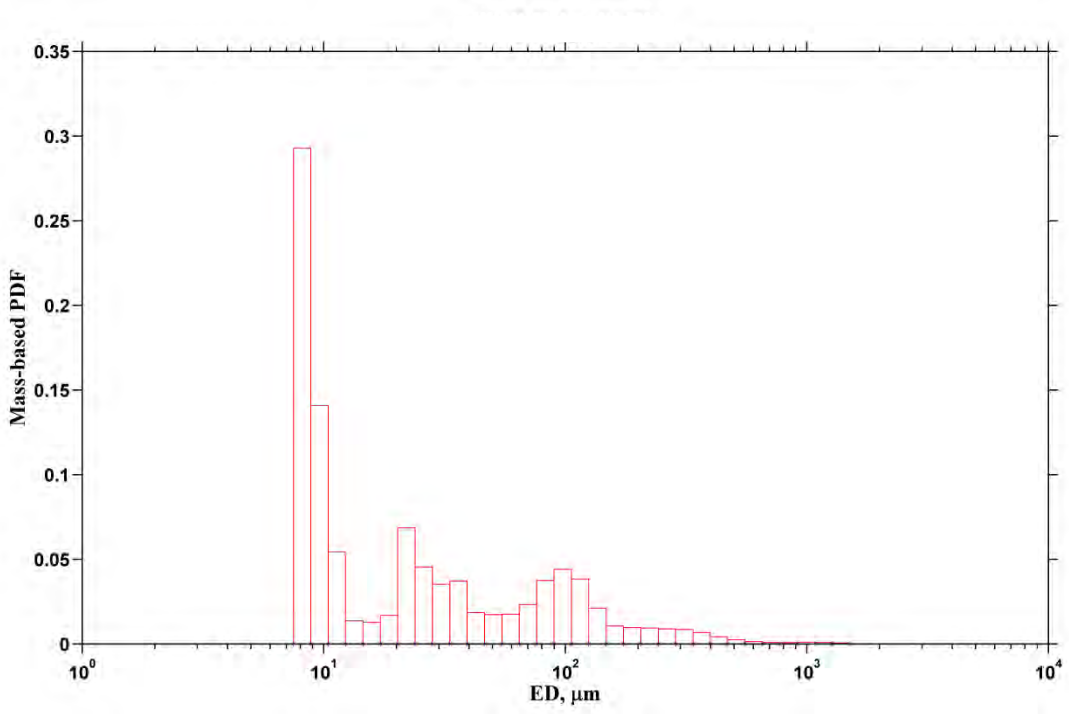

Figure D-337 Mass contribution of each grain-size bin to total calculated mass. Deployment period is November 3, 2014 09:00 to November 4, 2014 09:30 (Pre-flow).

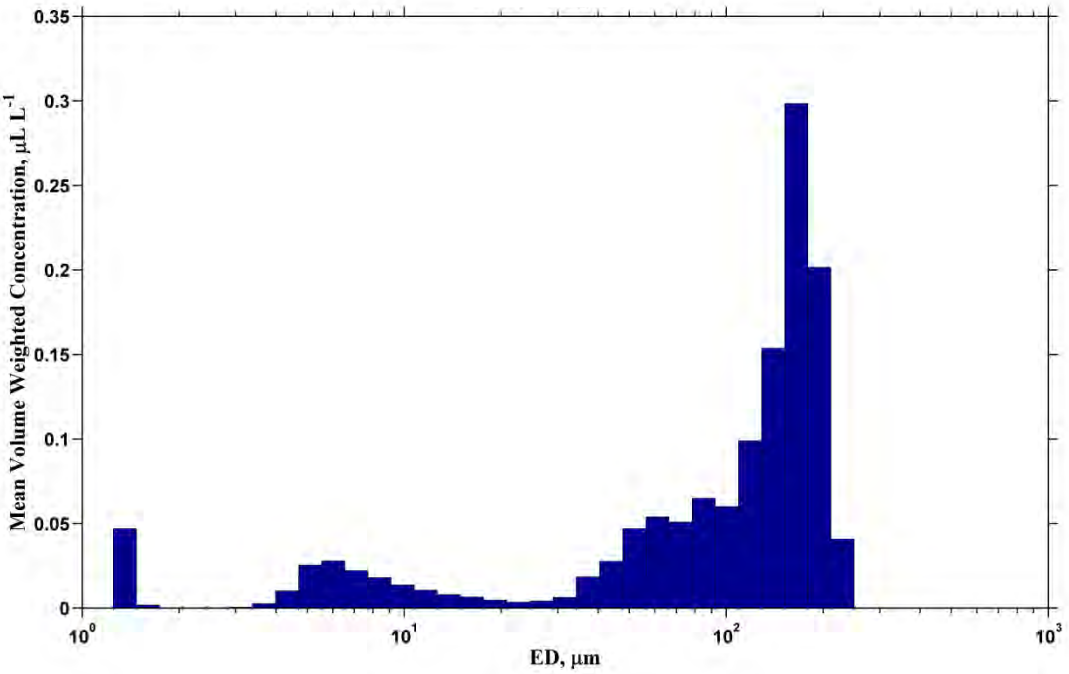

Figure D-338 Mean volume-weighted concentration histogram. Deployment period is November 2, 2014 18:00 to November 3, 2014 08:00 (Pre-flow).

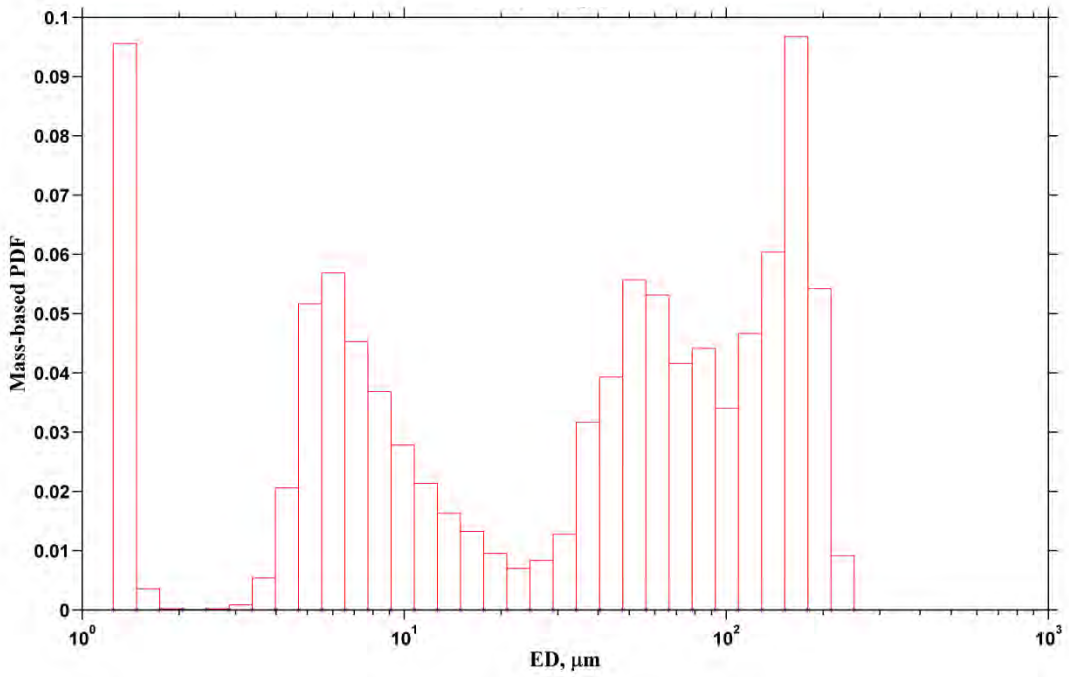

Figure D-339 Mass contribution of each grain-size bin to total calculated mass. Deployment period is November 2, 2014 18:00 to November 3, 2014 08:00 (Pre-flow).

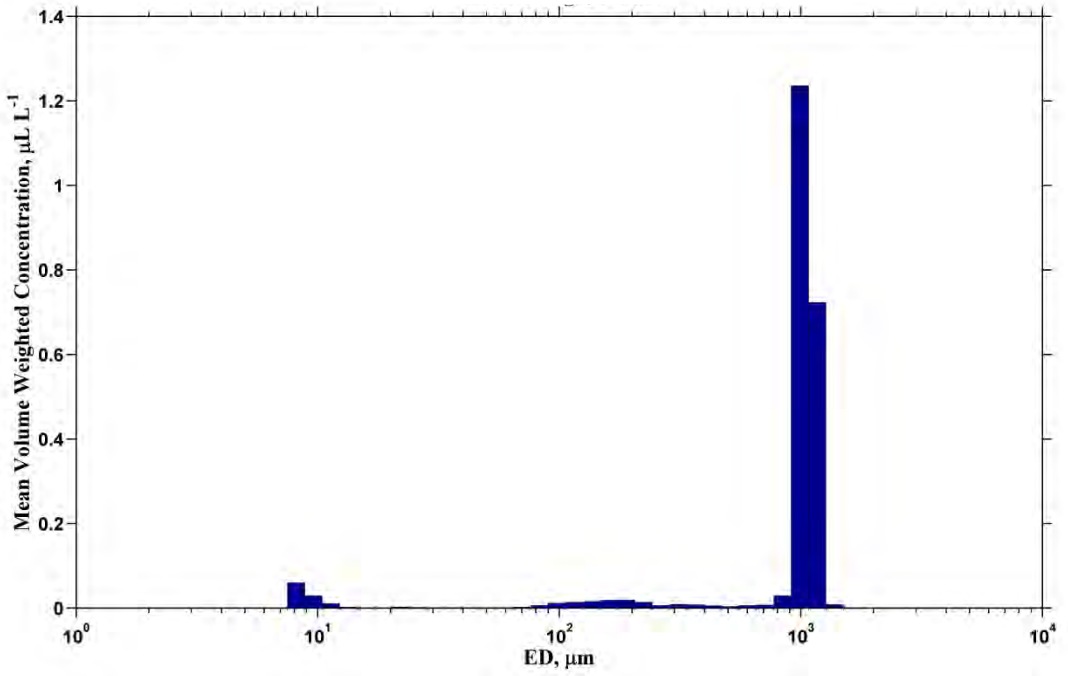

Figure D-340 Mean volume-weighted concentration histogram. Deployment period is November 3, 2014 09:00 to November 4, 2014 09:30 (Pre-flow).

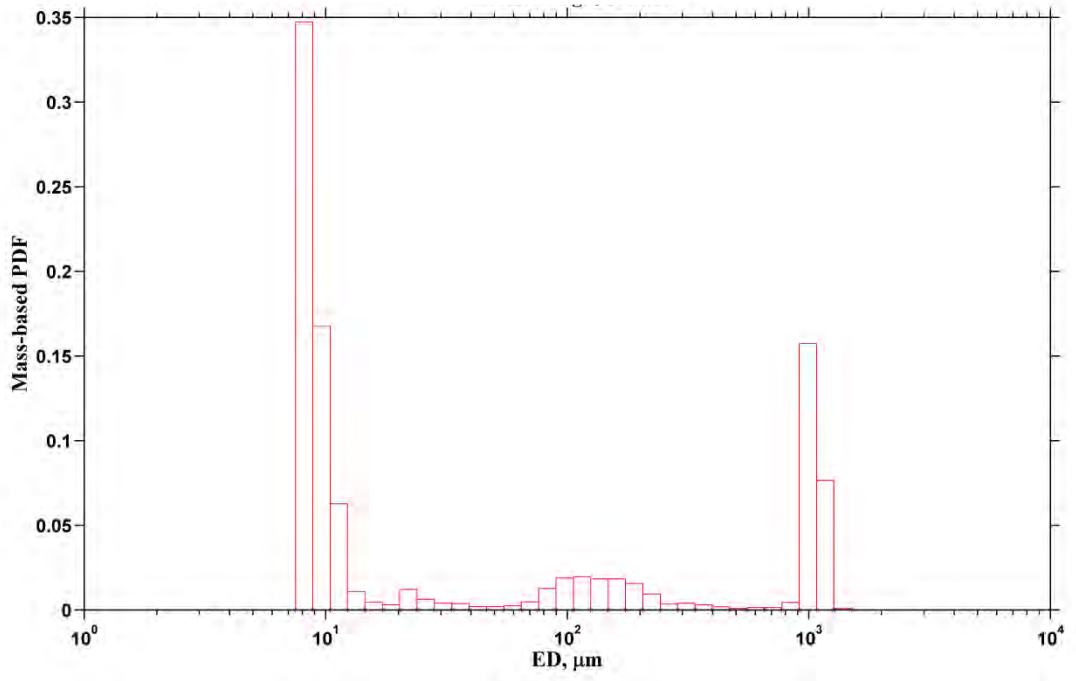

Figure D-341 Mass contribution of each grain-size bin to total calculated mass. Deployment period is November 3, 2014 09:00 to November 4, 2014 09:30 (Pre-flow).

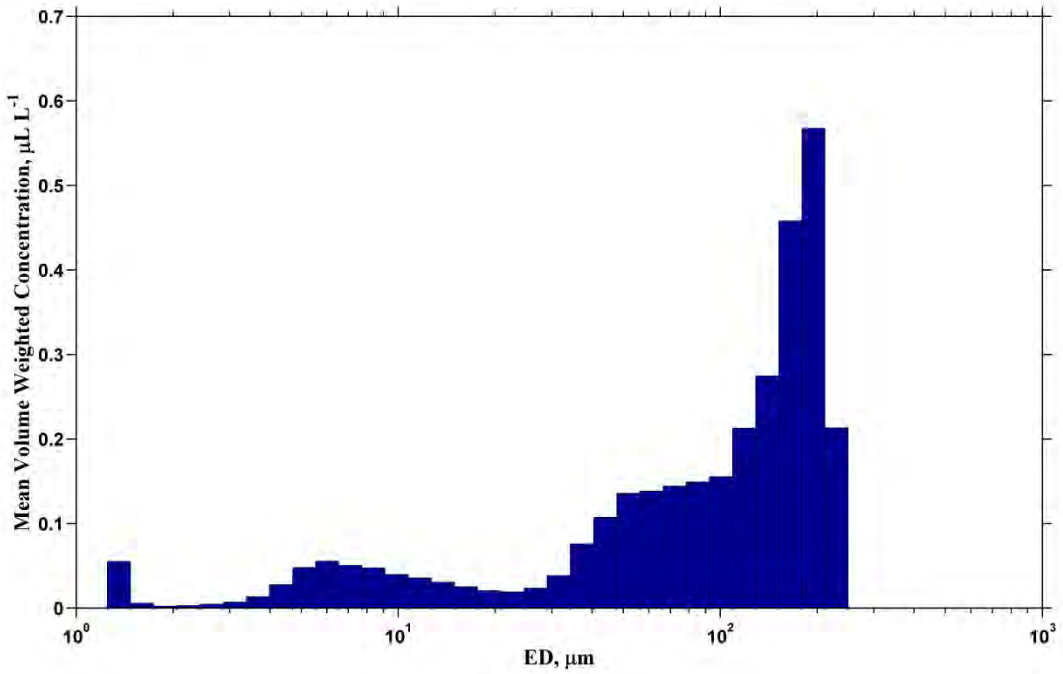

Figure D-342 Mean volume-weighted concentration histogram. Deployment period is November 4, 2014 09:30 to November 5, 2014 10:15 (Transient).

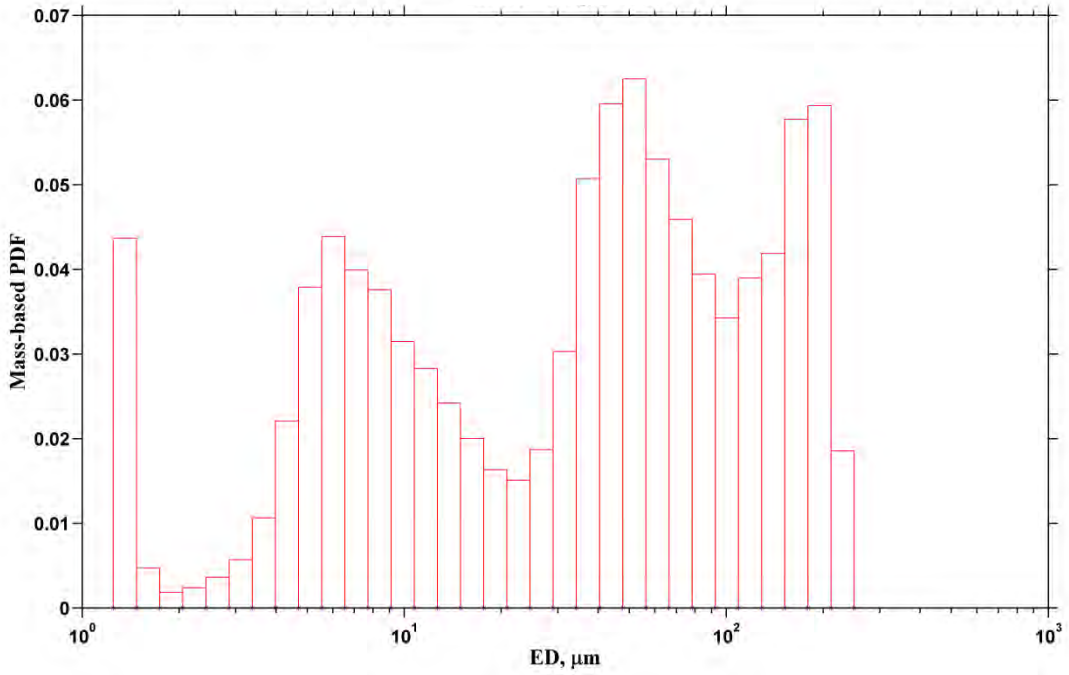

Figure D-343 Mass contribution of each grain-size bin to total calculated mass. Deployment period is November 4, 2014 09:30 to November 5, 2014 10:15 (Transient).

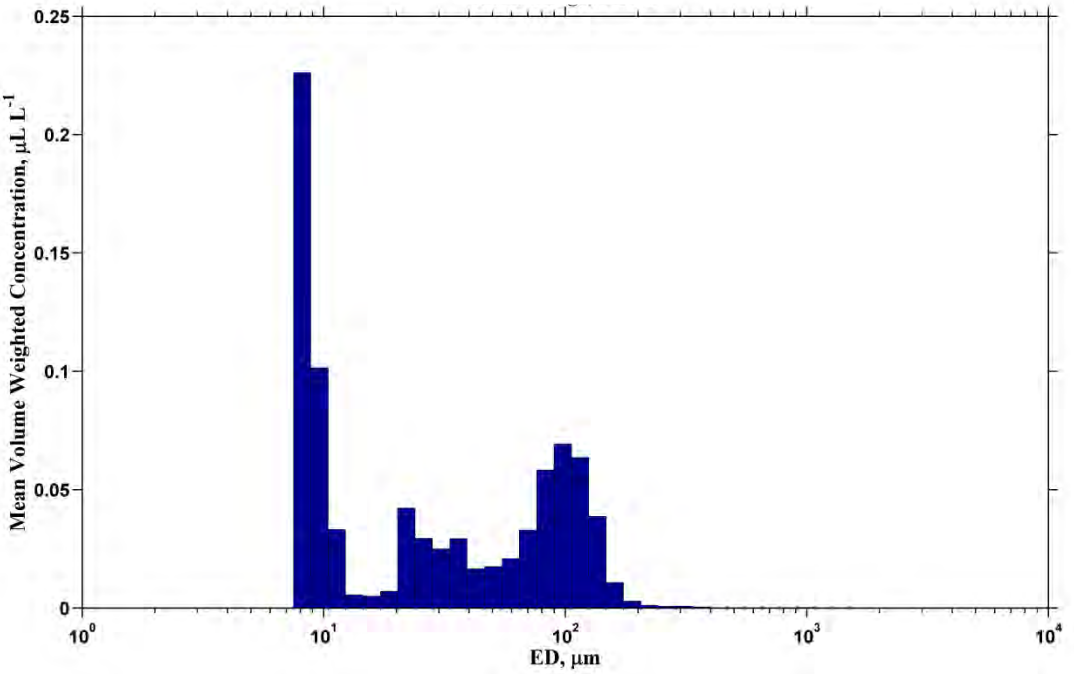

Figure D-344 Mean volume-weighted concentration histogram. Deployment period is November 4, 2014 09:30 to November 5, 2014 10:15 (Transient).

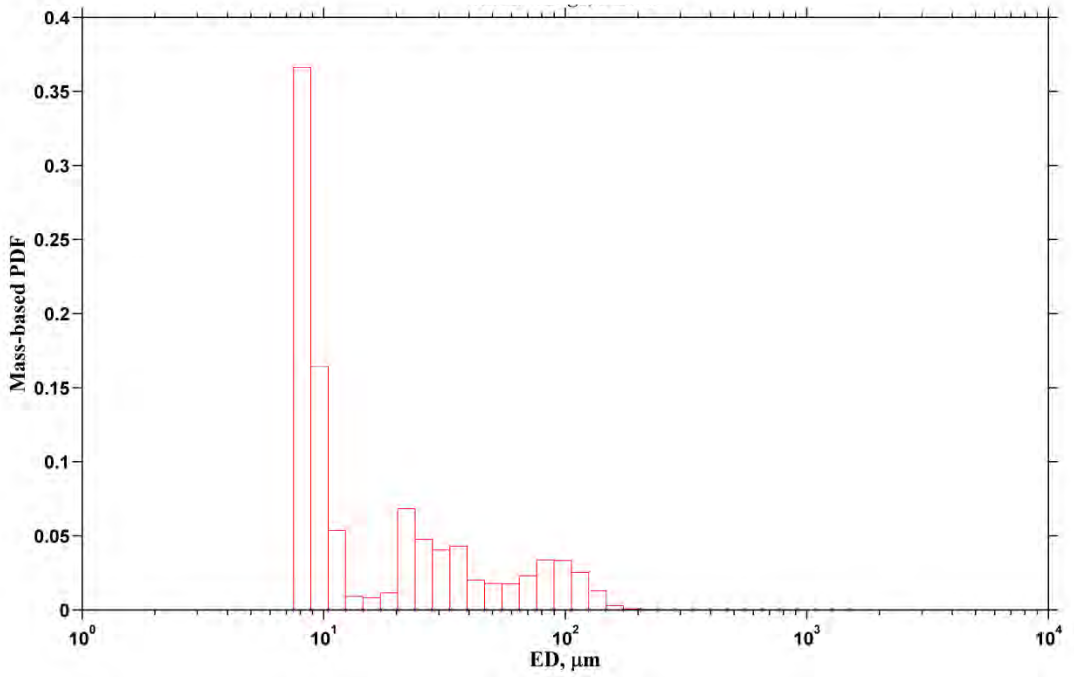

Figure D-345 Mass contribution of each grain-size bin to total calculated mass. Deployment period is November 4, 2014 09:30 to November 5, 2014 10:15 (Transient).

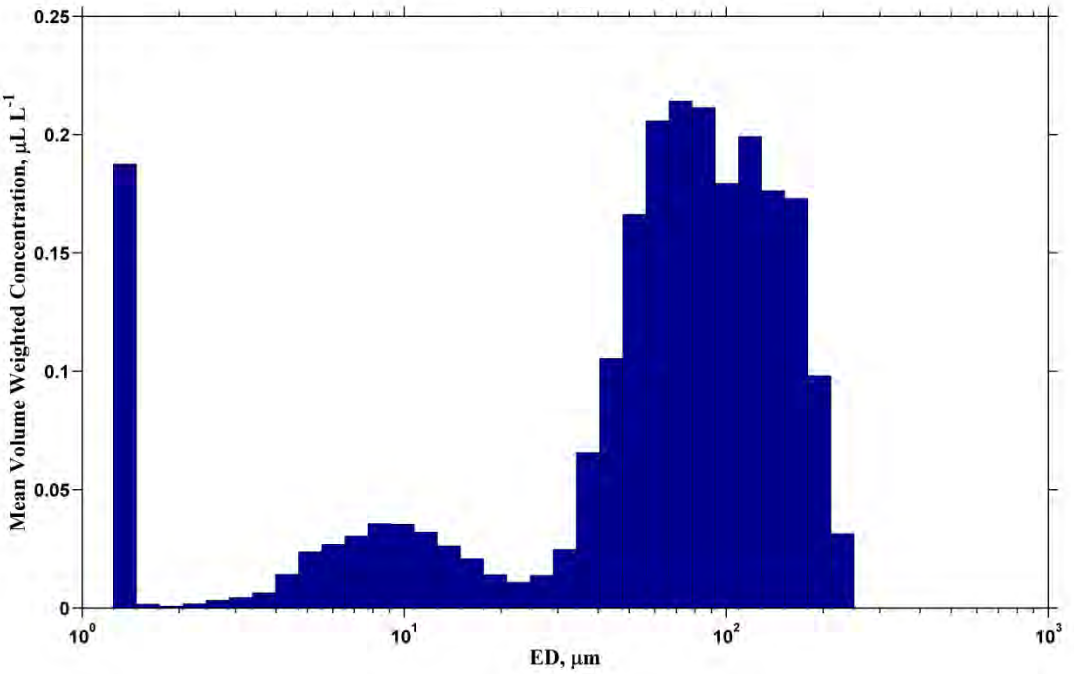

Figure D-346 Mean volume-weighted concentration histogram. Deployment period is November 5, 2014 11:00 to November 6, 2014 10:00 (Steady-state).

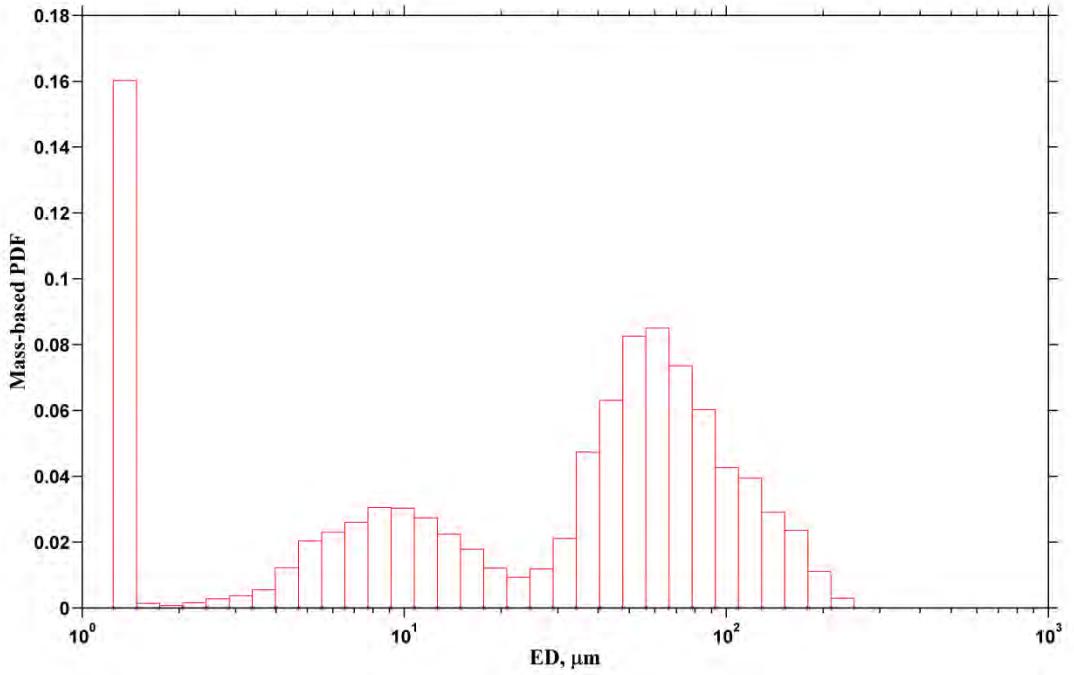

Figure D-347 Mass contribution of each grain-size bin to total calculated mass. Deployment period is November 5, 2014 11:00 to November 6, 2014 10:00 (Steady-state)).

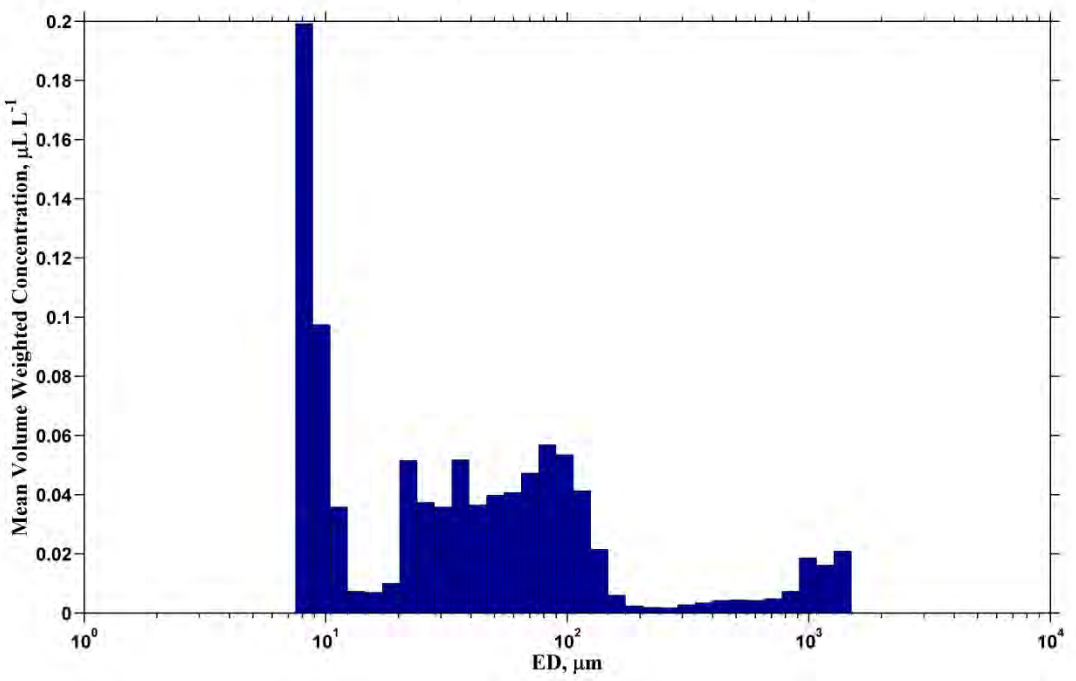

Figure D-348 Mean volume-weighted concentration histogram. Deployment period is November 5, 2014 11:00 to November 6, 2014 08:00 (Steady-state).

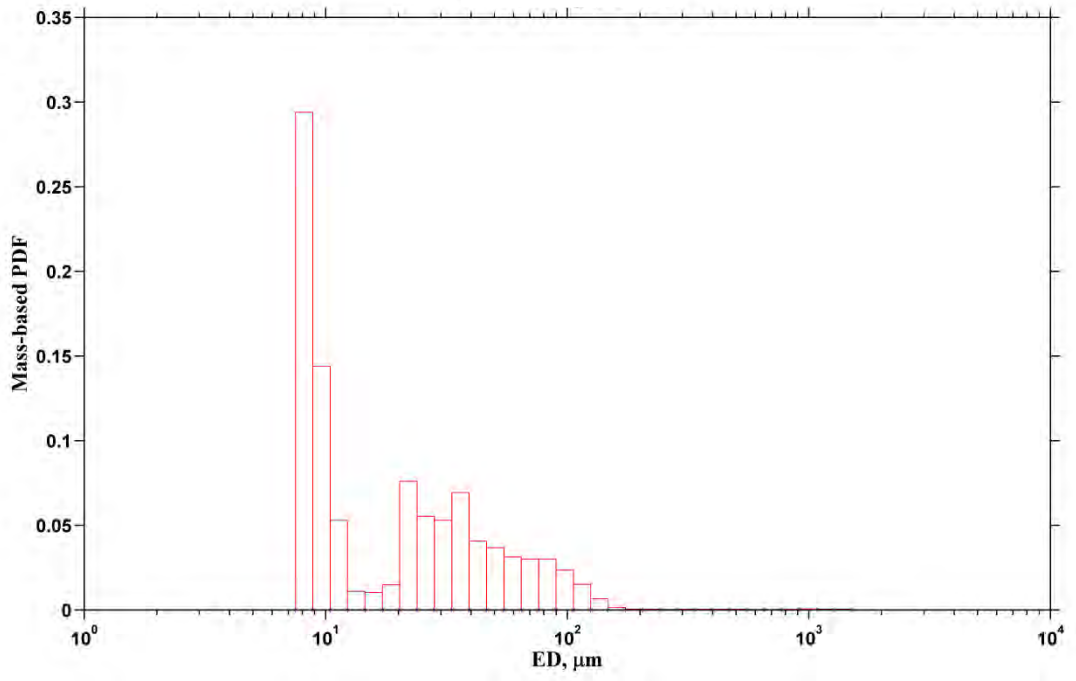

Figure D-349 Mass contribution of each grain-size bin to total calculated mass. Deployment period is November 5, 2014 11:00 to November 6, 2014 08:00 (Steady-state).

2015 Release

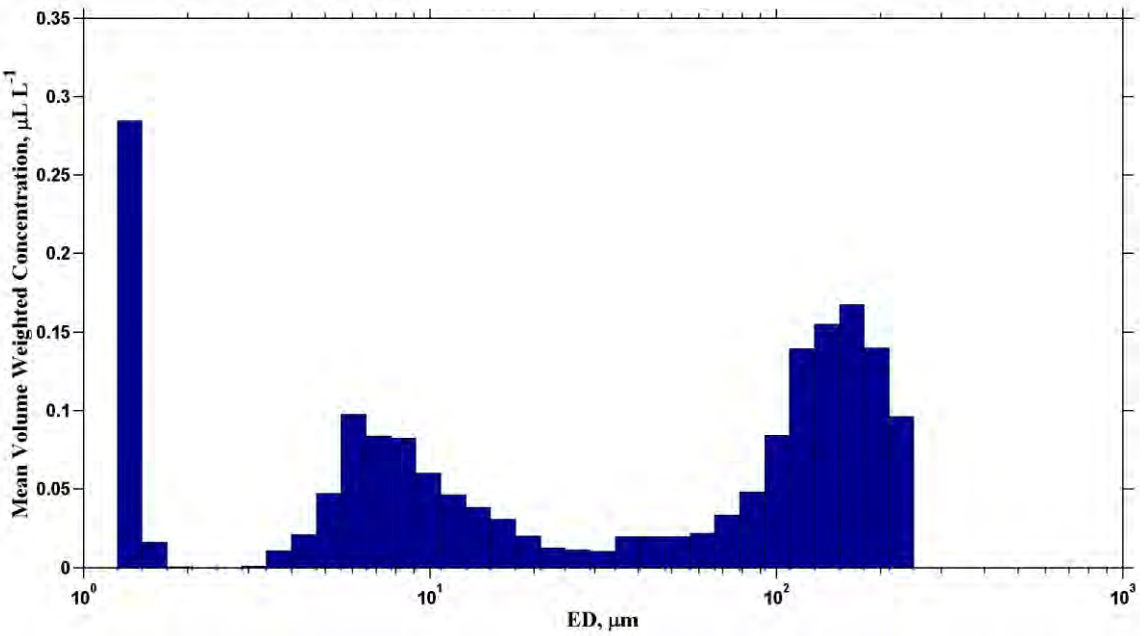

Figure D-350 Mean volume-weighted concentration histogram. Deployed period is November 16, 2015 8:00 to November 16, 2015 09:40 (Pre-Pulse1).

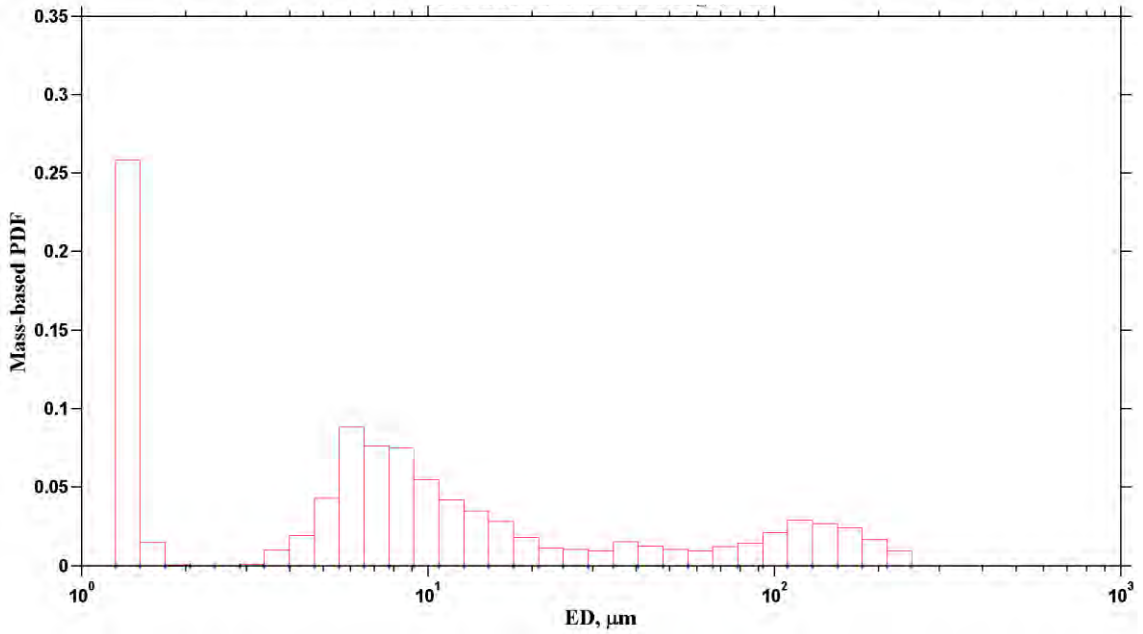

Figure D-351 Mass contribution of each grain-size bin to total calculated mass. Deployed period is November 16, 2015 8:00 to November 16, 2015 09:40 (Pre-Pulse1).

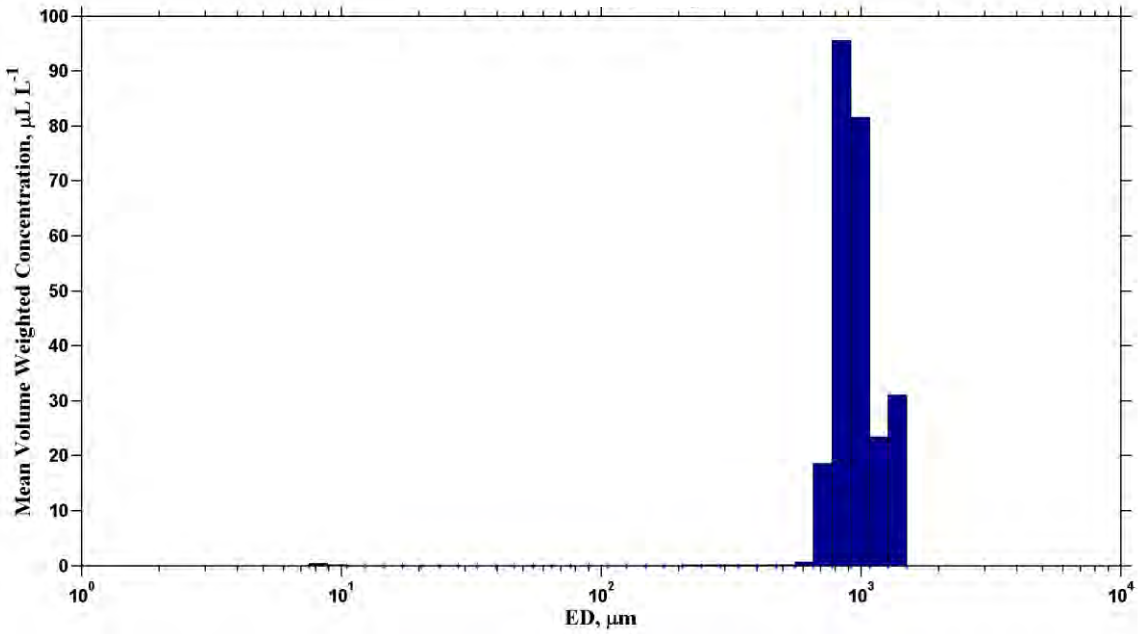

Figure D-352 Mean volume-weighted concentration histogram. Deployed period is November 15, 2015 8:00 to November 16, 2015 09:40 (Pre-Pulse1).

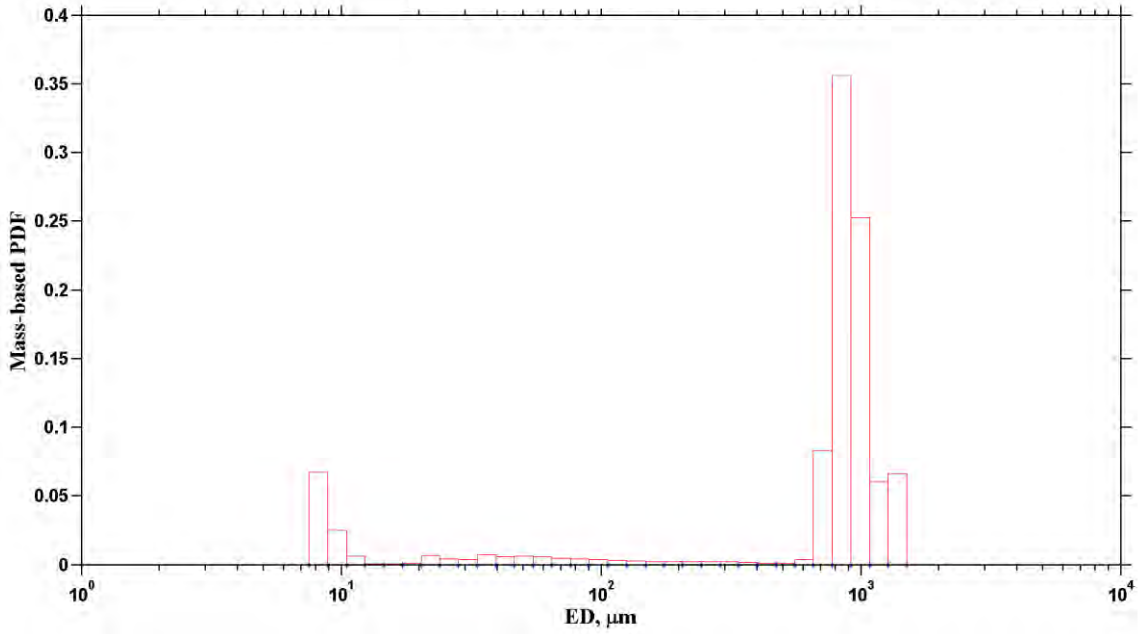

Figure D-353 Mass contribution of each grain-size bin to total calculated mass. Deployed period is November 15, 2015 8:00 to November 16, 2015 09:40 (Pre-Pulse1).

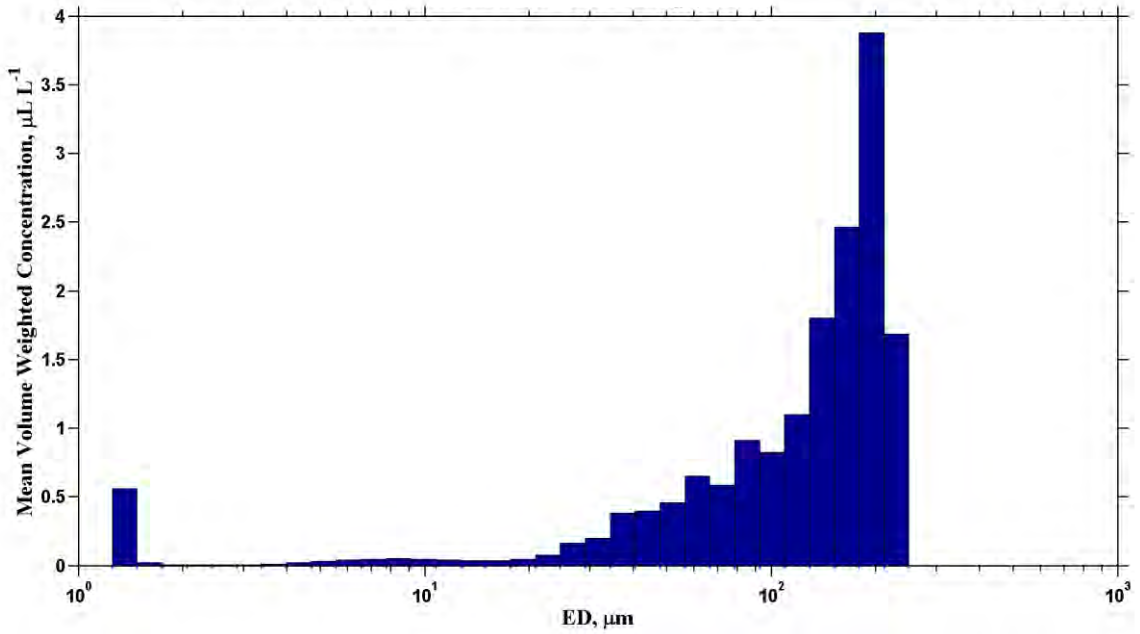

Figure D-354 Mean volume-weighted concentration histogram. Deployed period is November 16, 2015 09:40 to November 17, 2015 15:30 (Pulse 1).

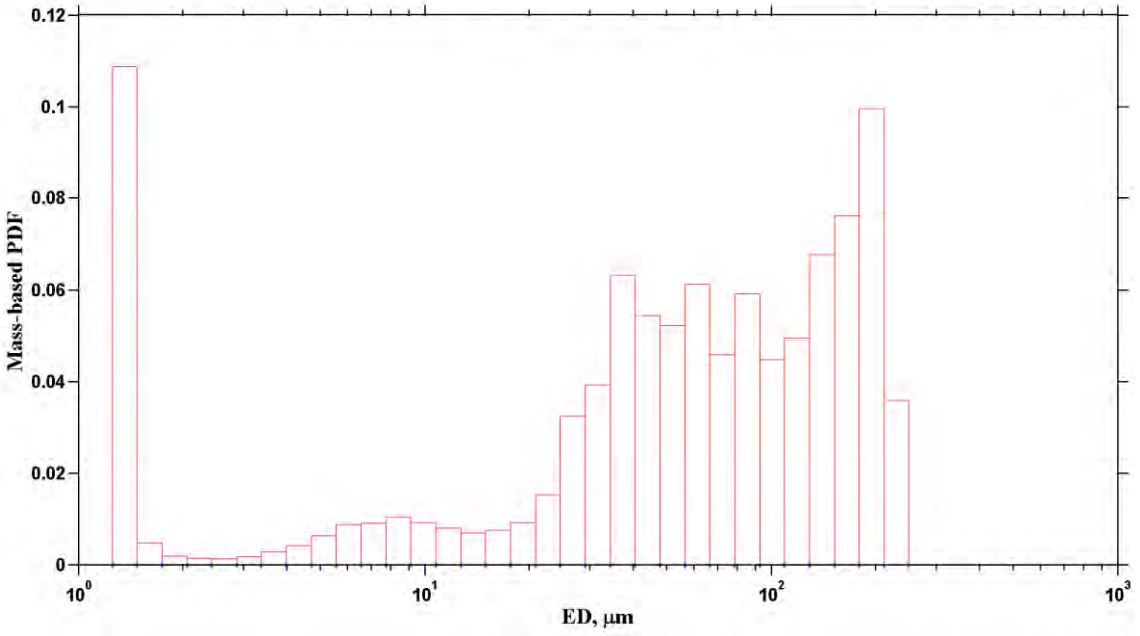

Figure D-355 Mass contribution of each grain-size bin to total calculated mass. Deployed period is November 16, 2015 09:40 to November 17, 2015 15:30 (Pulse 1).

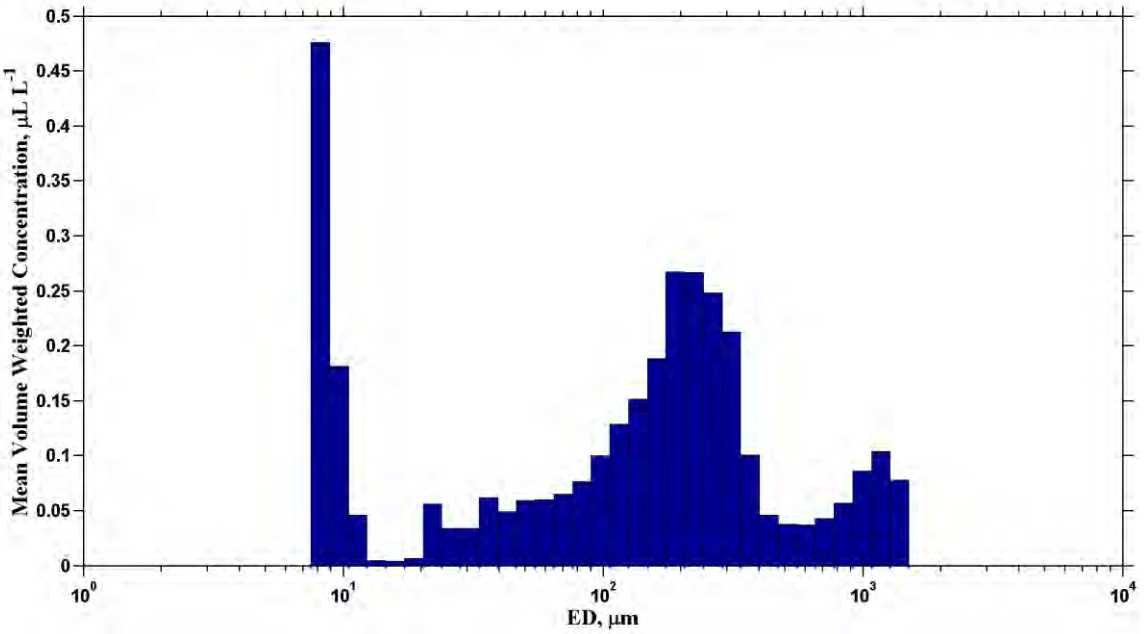

Figure D-356 Mean volume-weighted concentration histogram. Deployed period is November 16, 2015 09:40 to November 17, 2015 15:30 (Pulse 1).

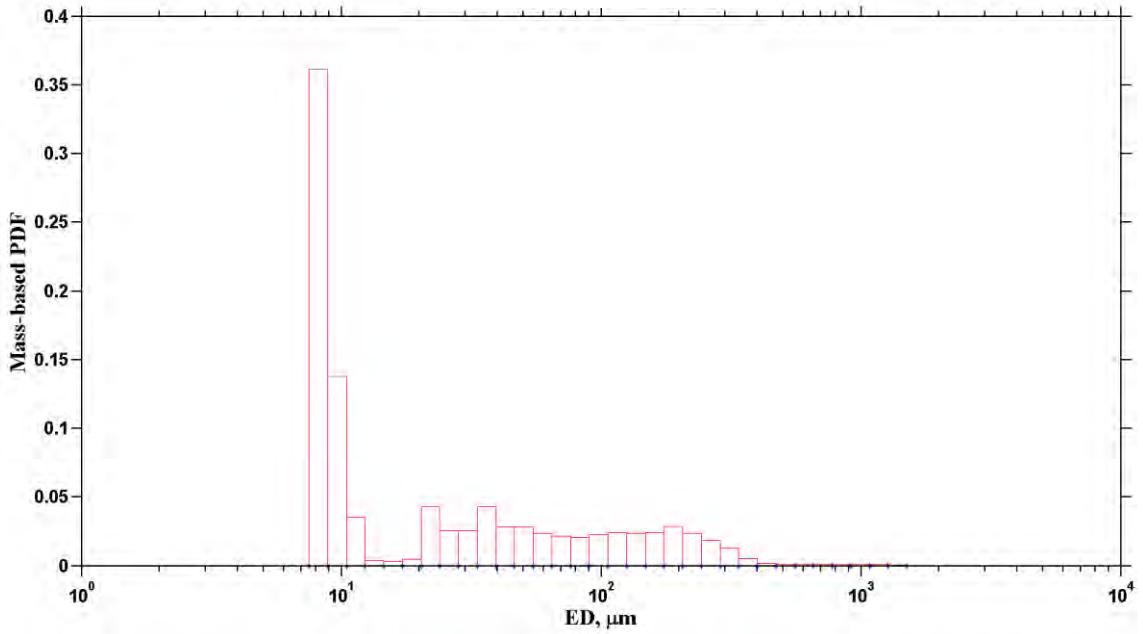

Figure D-357 Mass contribution of each grain-size bin to total calculated mass. Deployed period is November 16, 2015 09:40 to November 17, 2015 15:30 (Pulse 1).

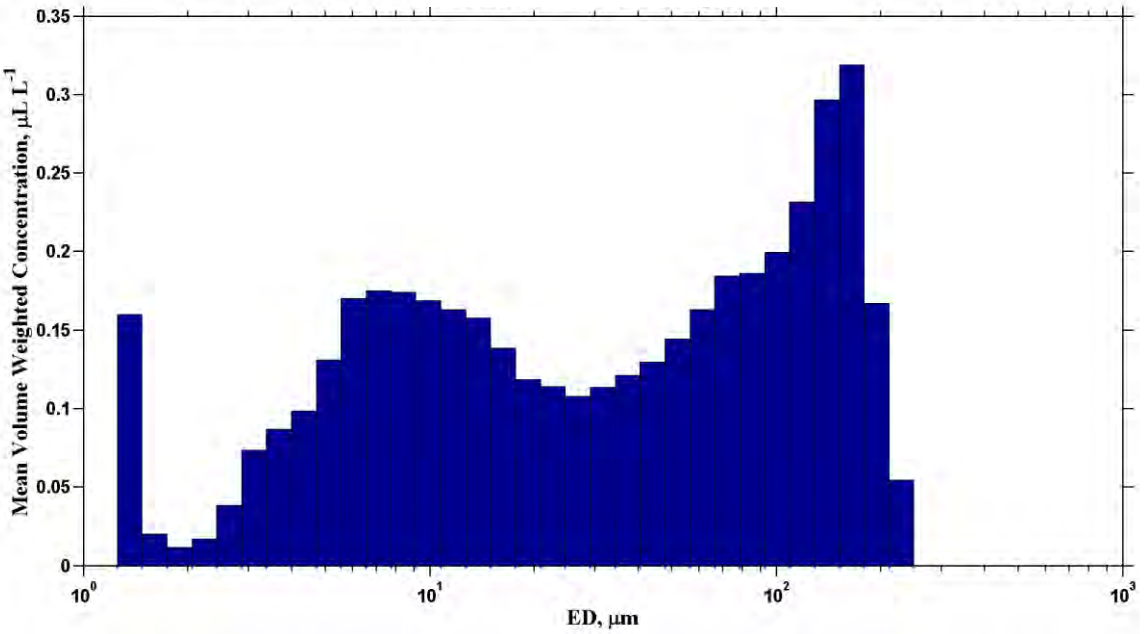

Figure D-358 Mean volume-weighted concentration histogram. Deployed period is November 17, 2015 15:30 to November 19, 2015 9:40 (Pre-Pulse 2).

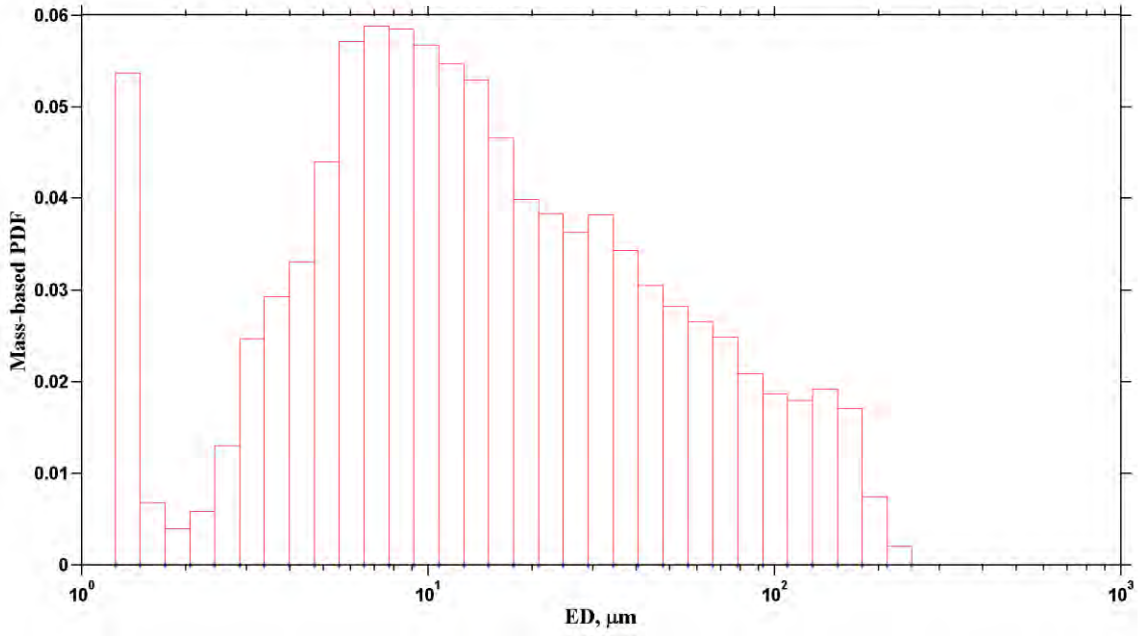

Figure D-359 Mass contribution of each grain-size bin to total calculated mass. Deployed period is November 17, 2015 15:30 to November 19, 2015 9:40 (Pre-Pulse 2).

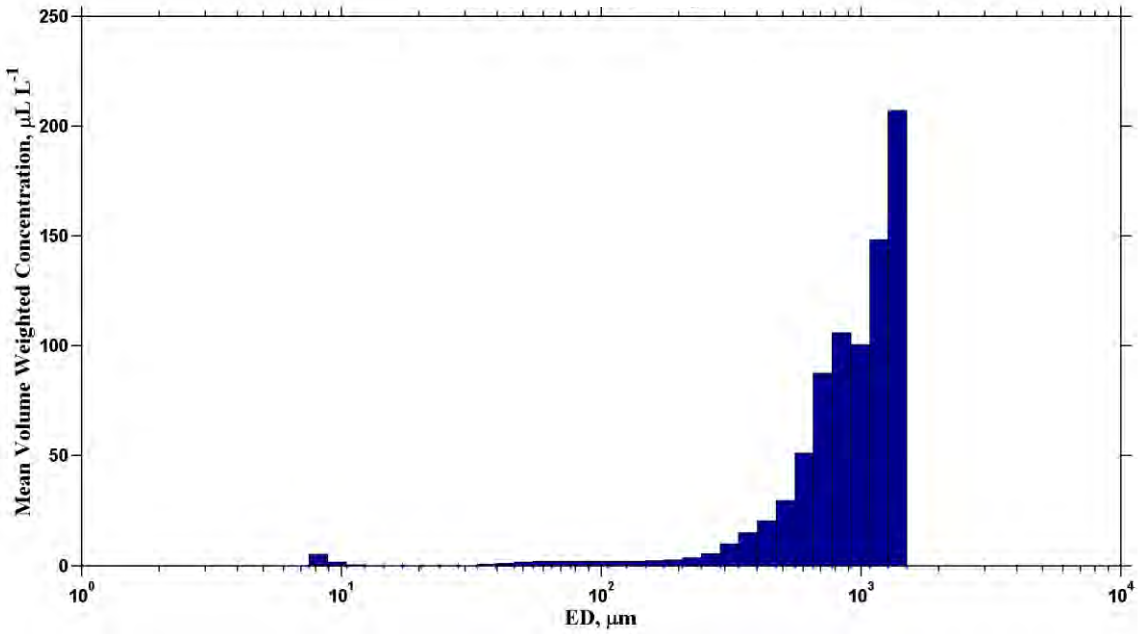

Figure D-360 Mean volume-weighted concentration histogram. Deployed period is November 17, 2015 15:30 to November 19, 2015 9:40 (Pre-Pulse 2).

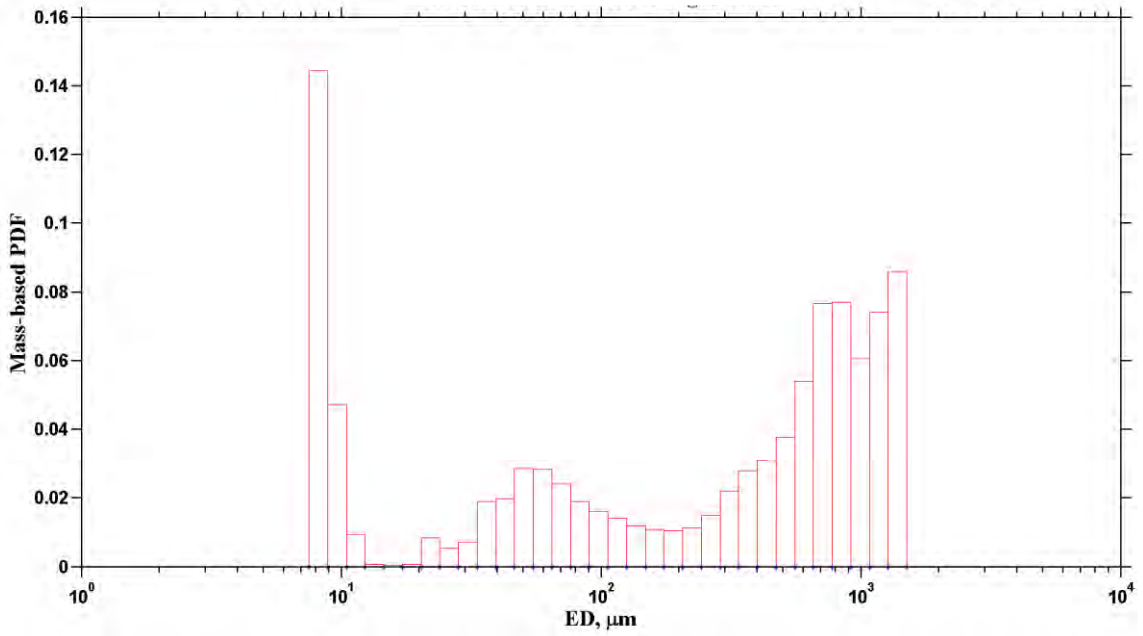

Figure D-361 Mass contribution of each grain-size bin to total calculated mass. Deployed period is November 17, 2015 15:30 to November 19, 2015 9:40 (Pre-Pulse 2).

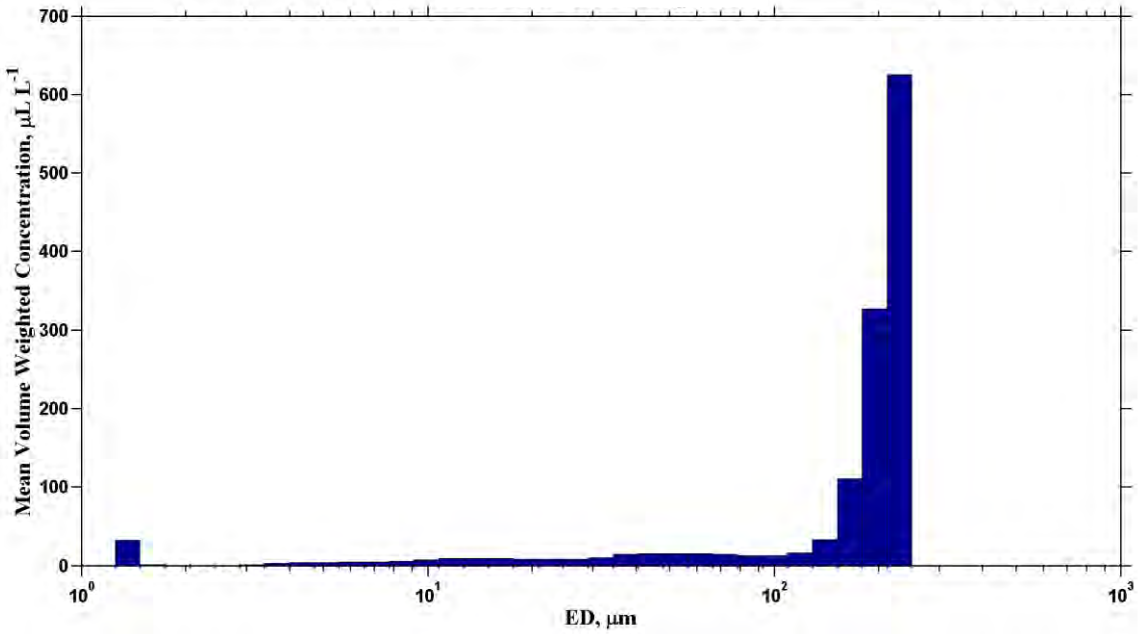

Figure D-362 Mean volume-weighted concentration histogram. Deployed period is November 19, 2015 9:40 to November 20, 2015 16:00 (Pulse 2).

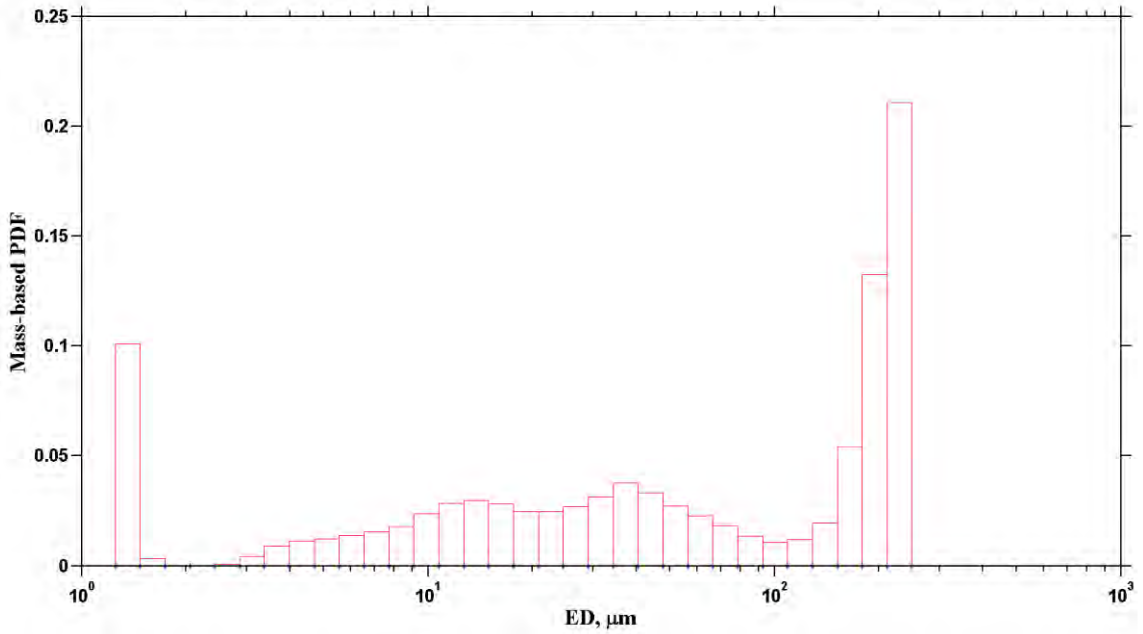

Figure D-363 Mass contribution of each grain-size bin to total calculated mass. Deployed period is November 19, 2015 9:40 to November 20, 2015 16:00 (Pulse 2).

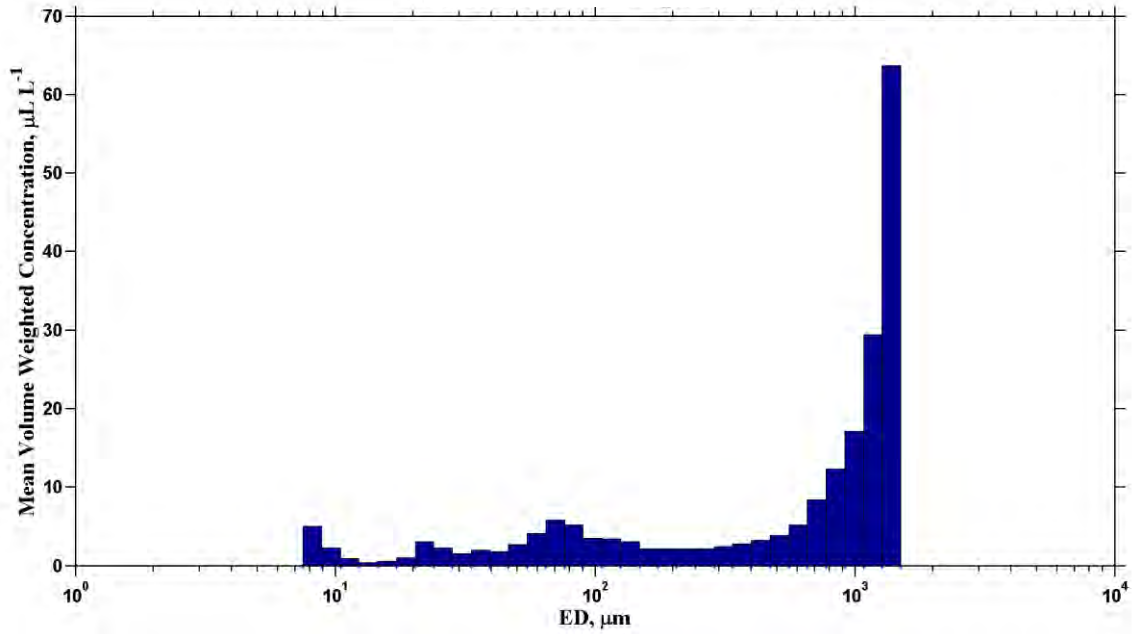

Figure D-364 Mean volume-weighted concentration histogram. Deployed period is November 19, 2015 9:40 to November 20, 2015 16:00 (Pulse 2).

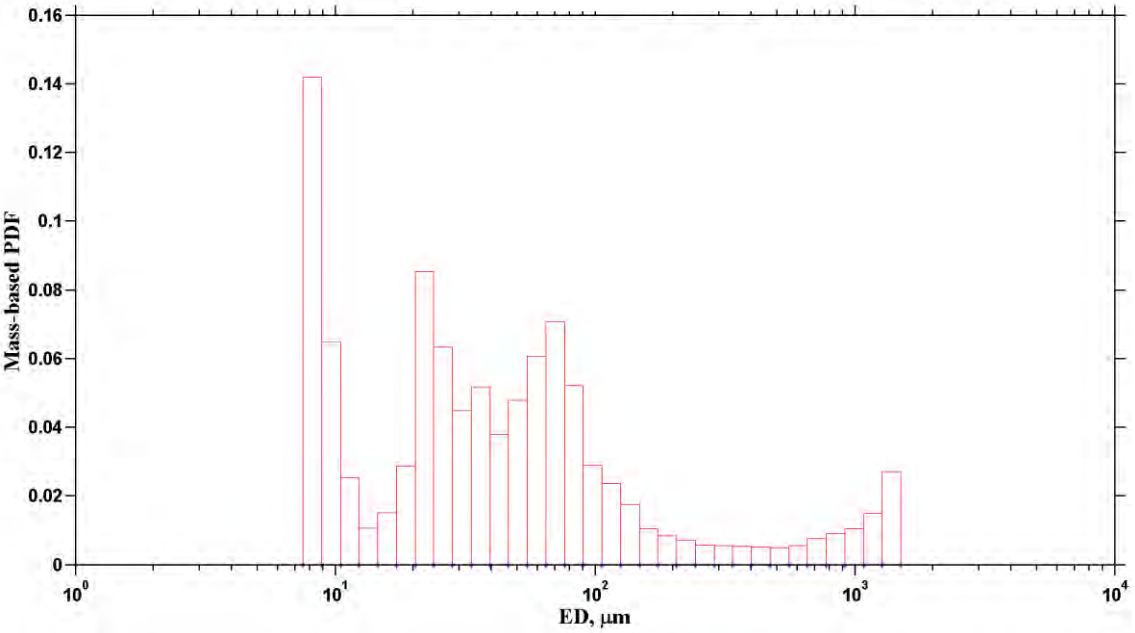

Figure D-365 Mass contribution of each grain-size bin to total calculated mass. Deployed period is November 19, 2015 9:40 to November 20, 2015 16:00 (Pulse 2).

E. Biogeochemical Sampling

Grain-Size Analysis

2013 Flow Release

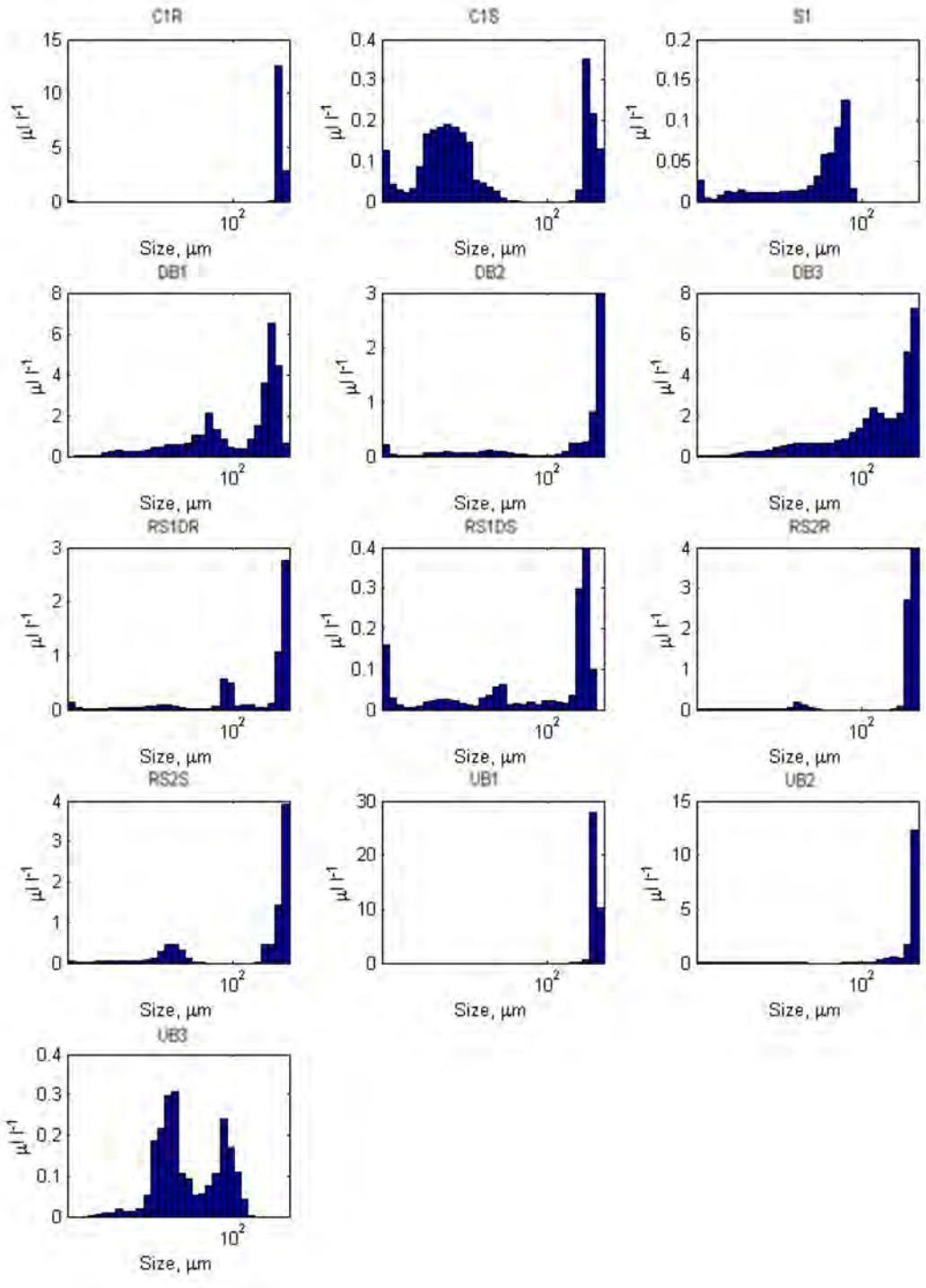

Figure E-1 Volume weighted distributions of suspended particles for water column samples collected November 2-3, 2013.

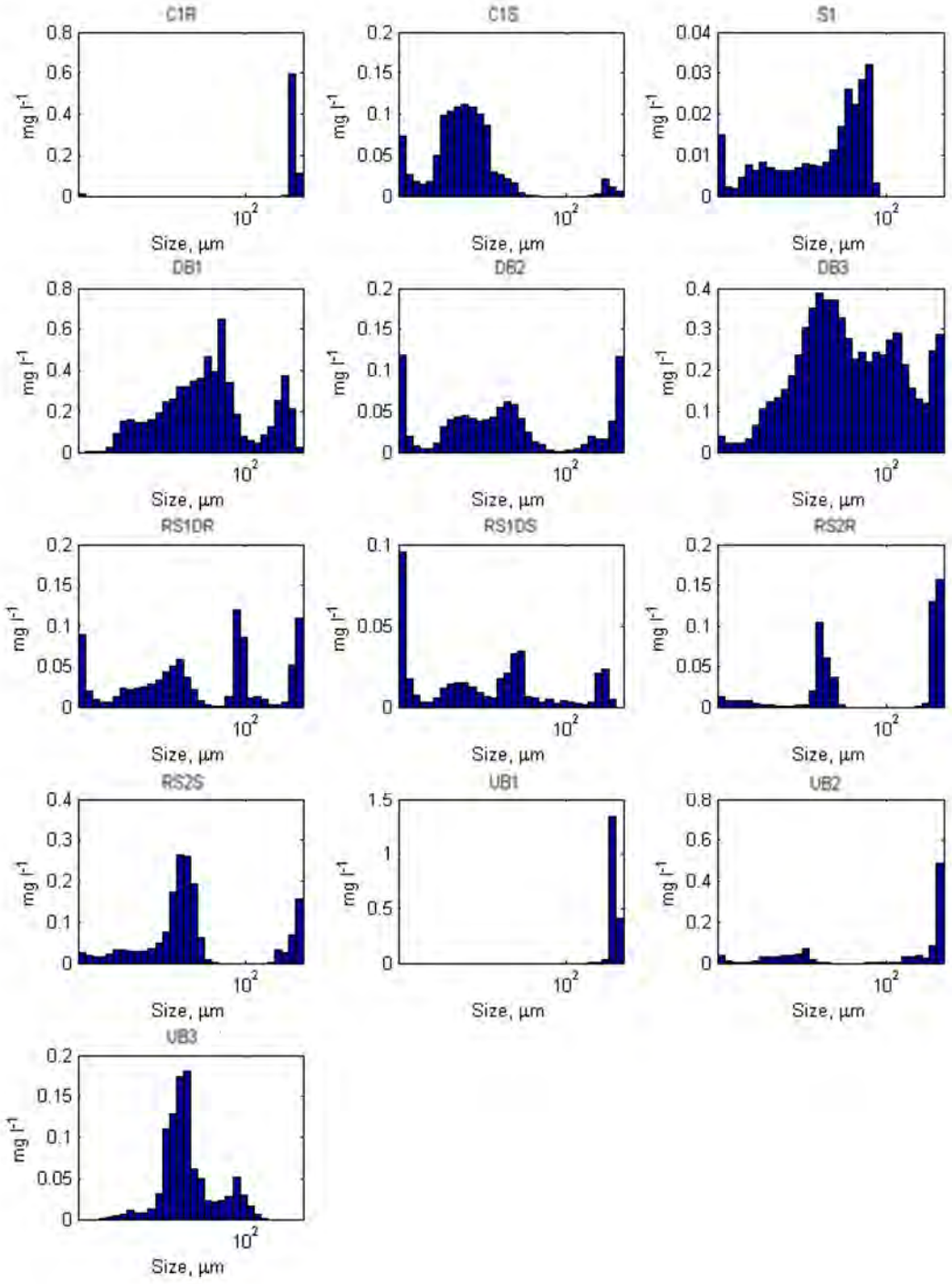

Figure E-2. Mass weighted distributions of suspended particles for water column samples collected November 2-3, 2013.

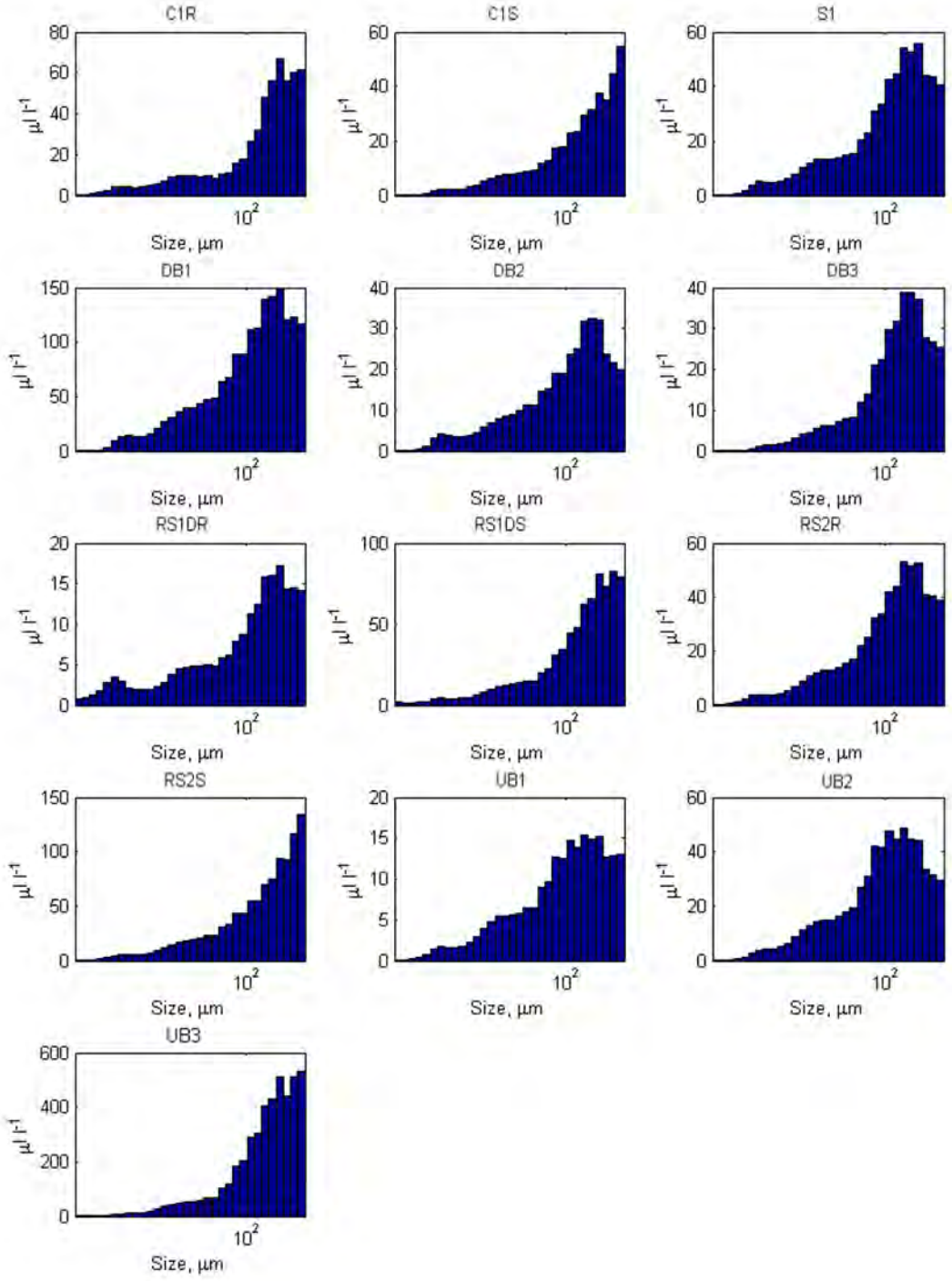

Figure E-3 Volume weighted distributions of suspended particles for epiphyton samples collected November 2-3, 2013.

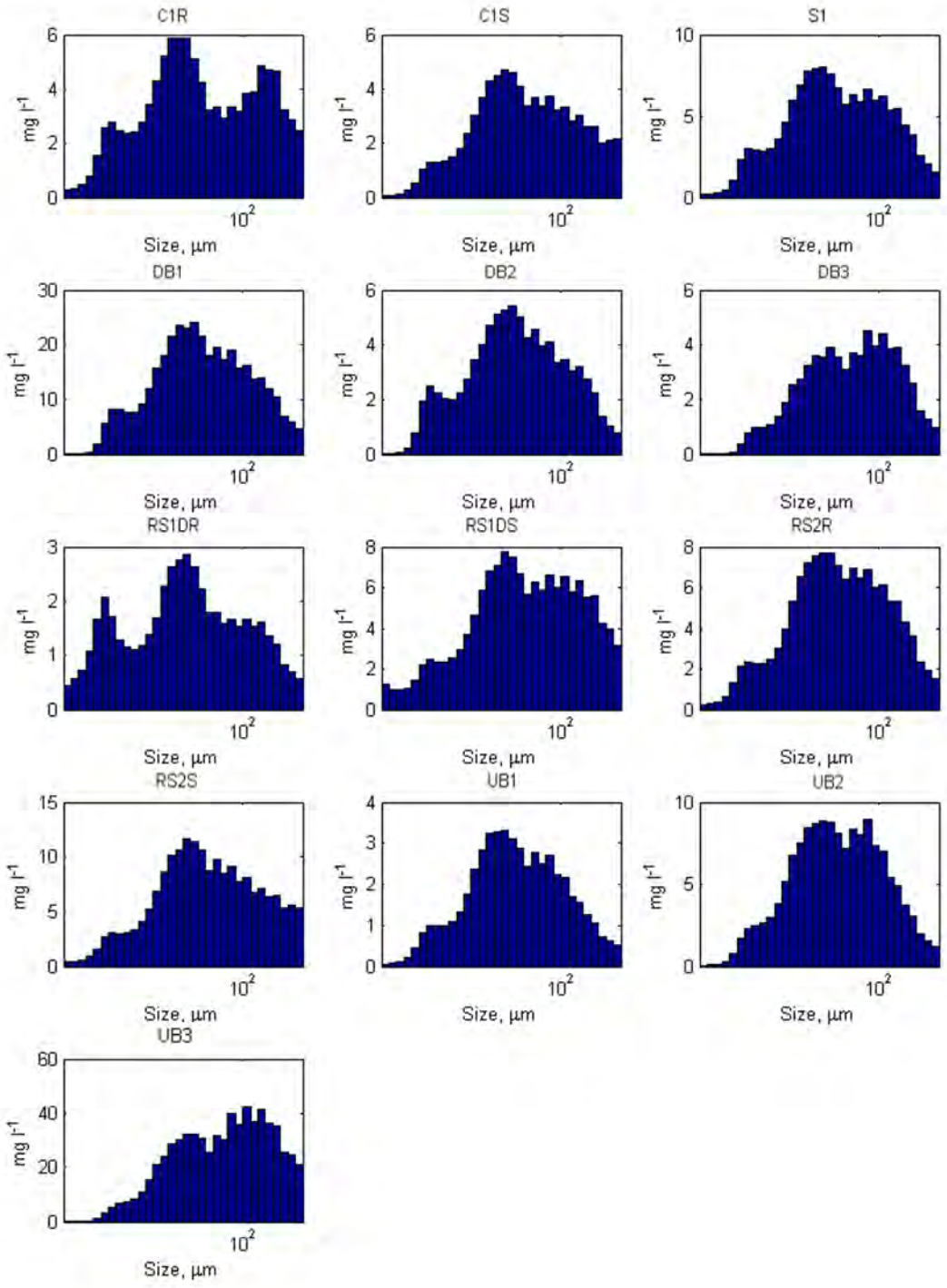

Figure E-4 Mass weighted distributions of suspended particles for epiphyton samples collected November 2-3, 2013.

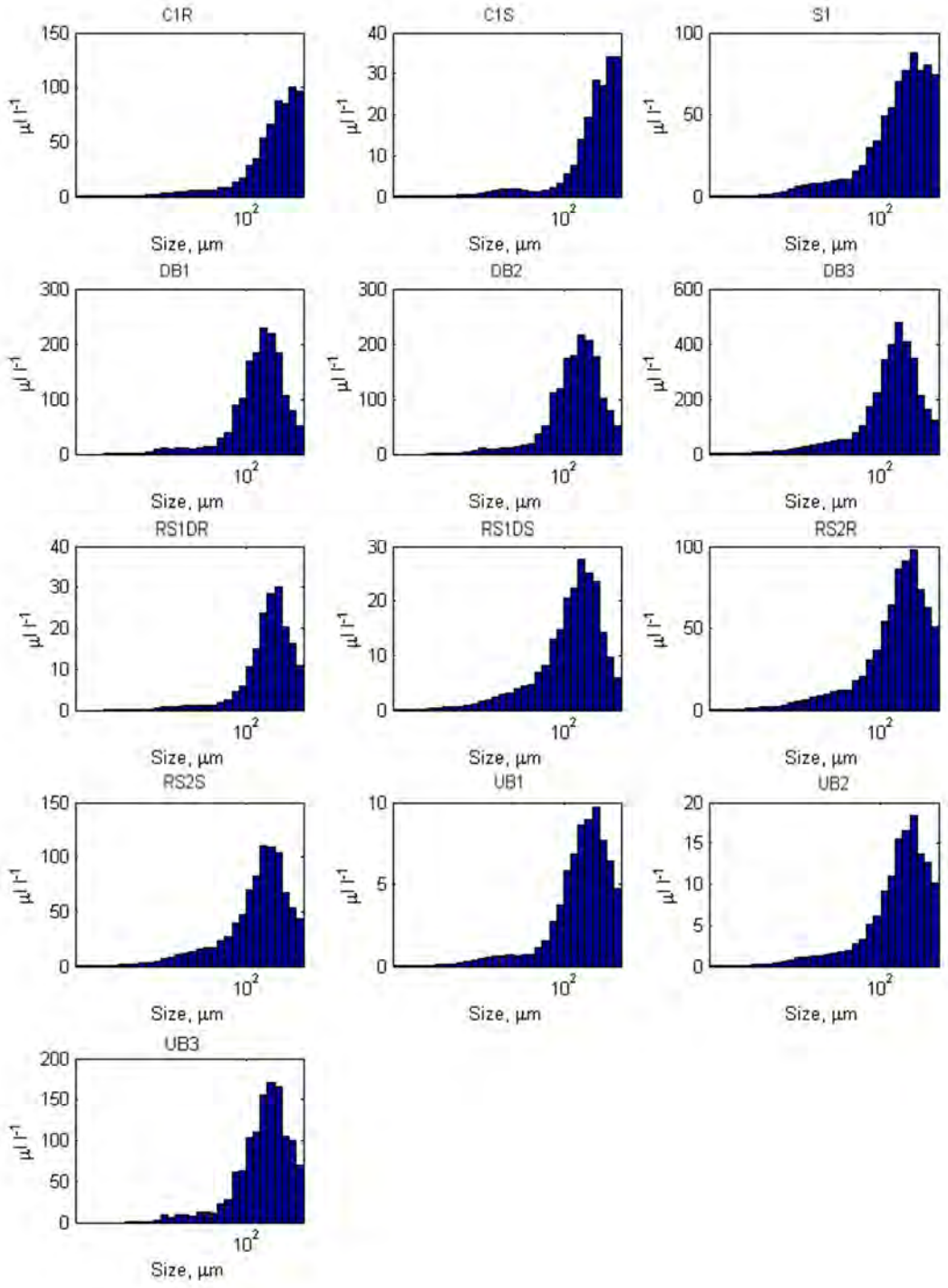

Figure E-5 Volume weighted distributions of suspended particles for floc samples collected November 2-3, 2013.

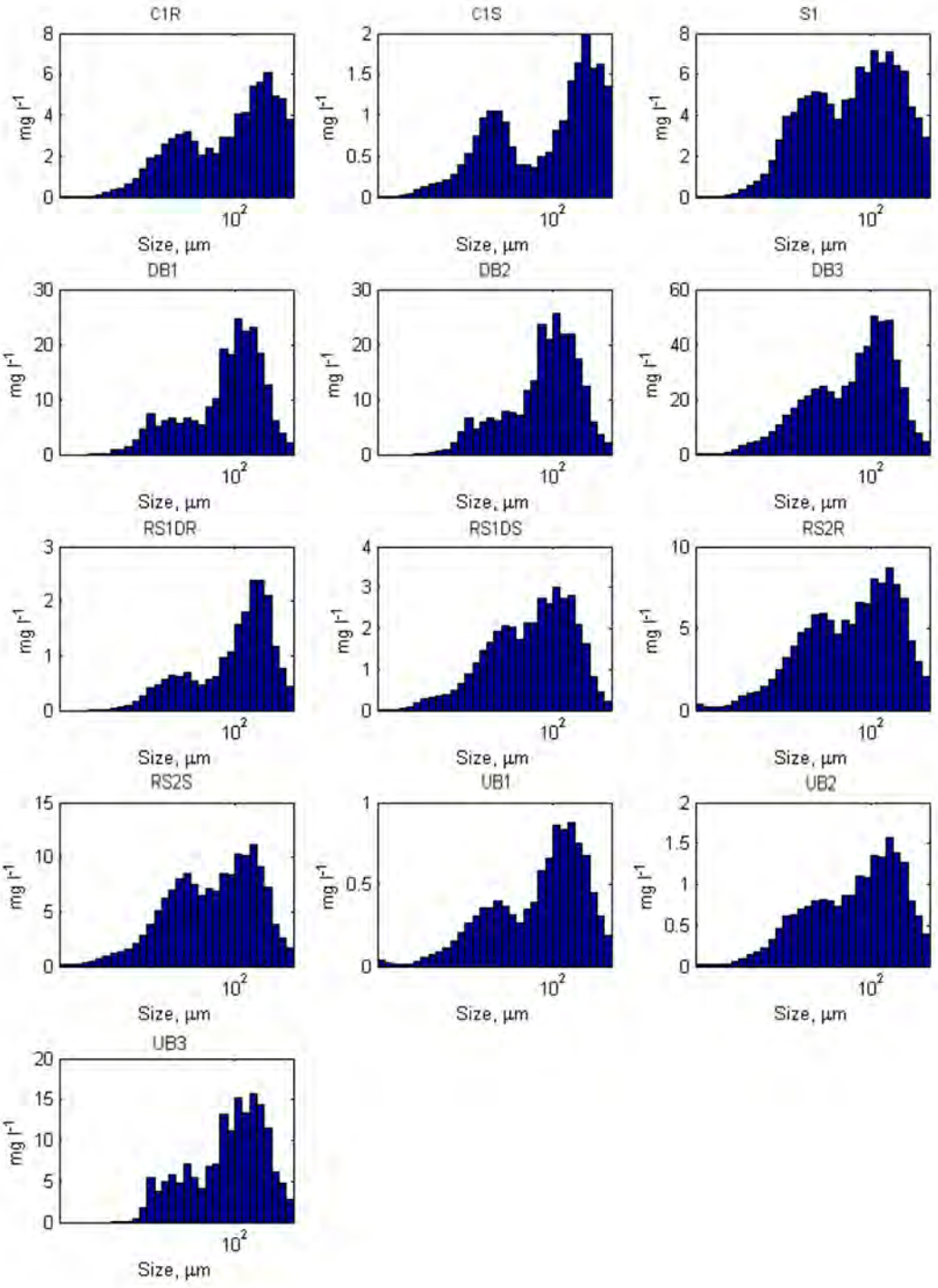

Figure E-6 Mass weighted distributions of suspended particles for floc samples collected November 2-3, 2013.

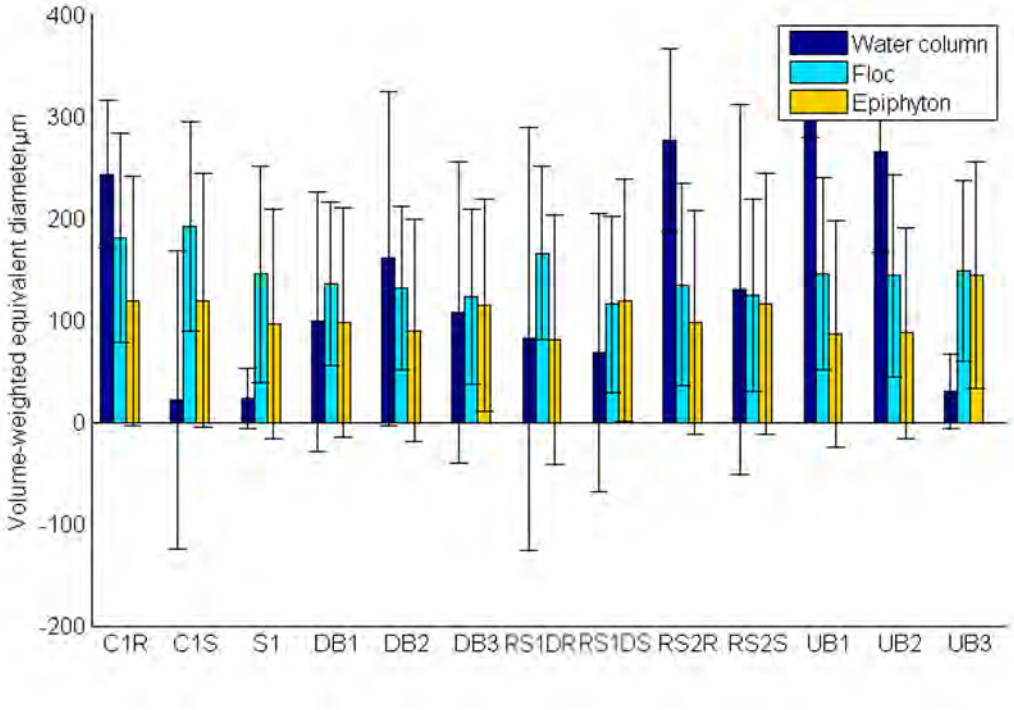

Figure E-7 Comparison of average volume weighted equivalent diameter for each particle type of samples collected November 2-3, 2013.

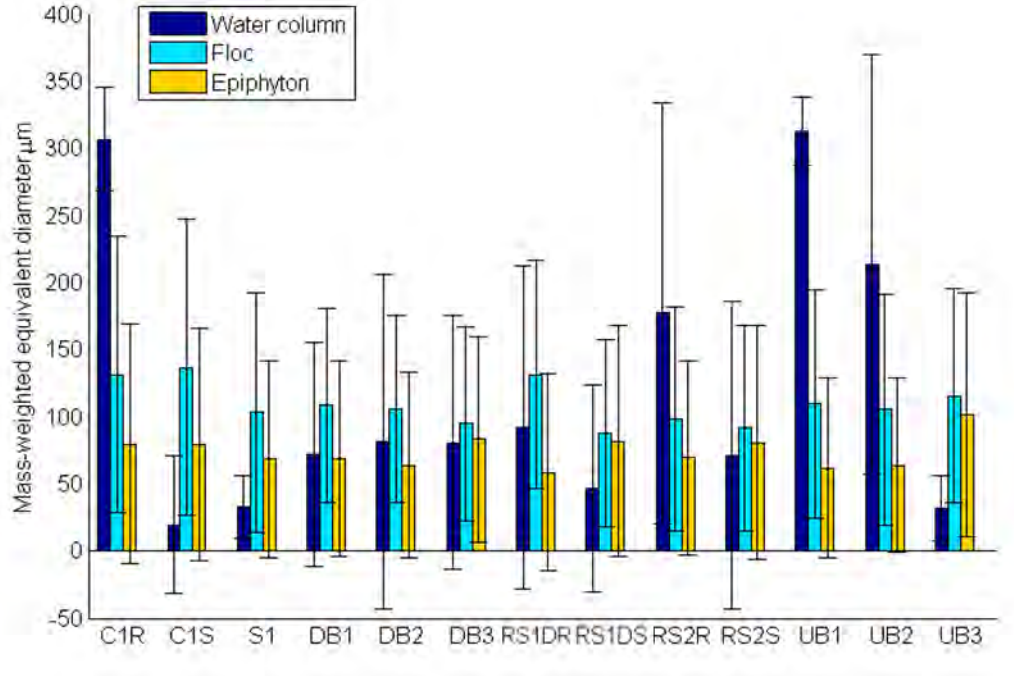

Figure E-8 Comparison of average mass weighted equivalent diameter for each particle type of samples collected November 2-3, 2013.

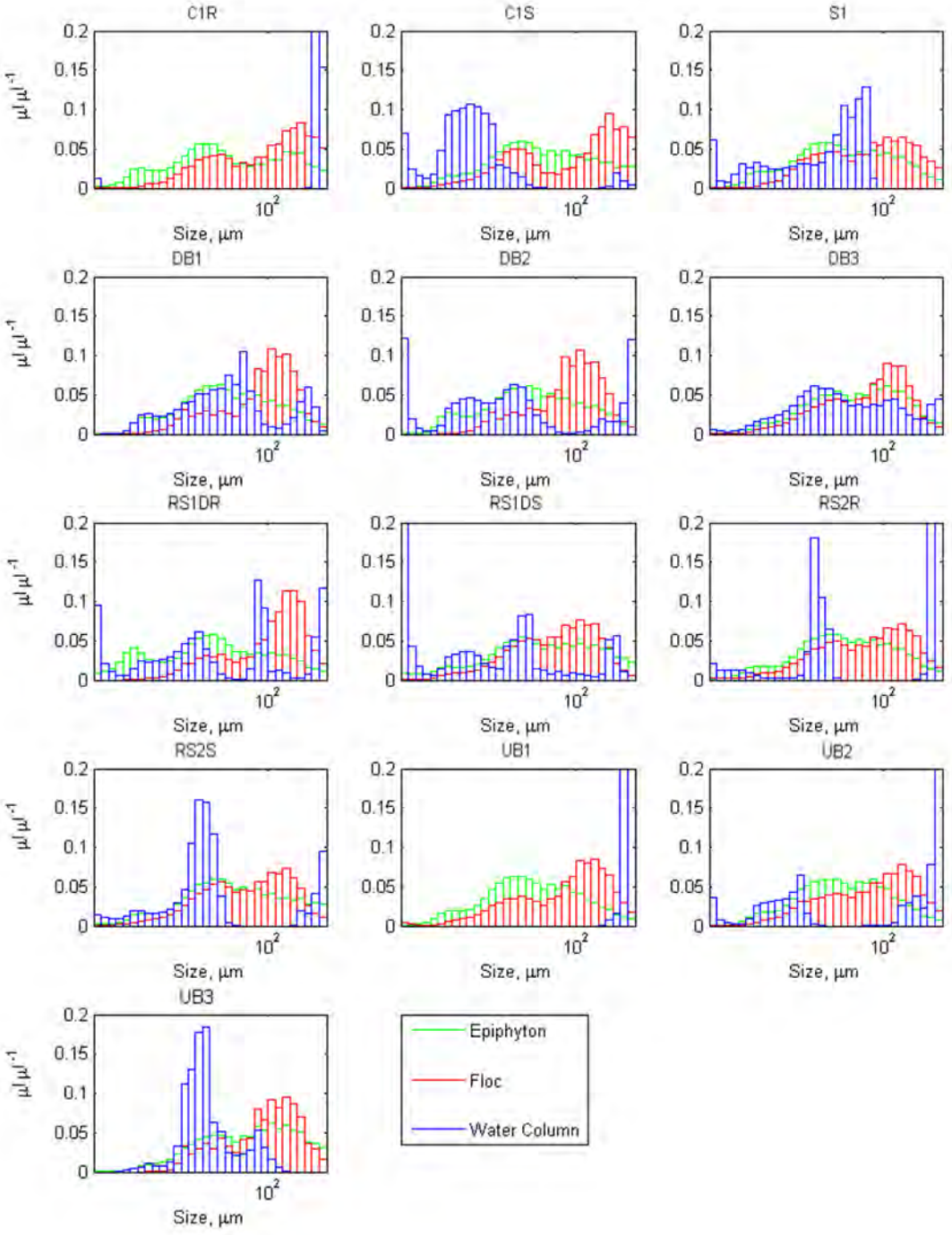

Figure E-9 Comparisons of volumetric fraction distributions of Water Column, Floc and Epiphyton by size for samples collected November 2-3, 2013

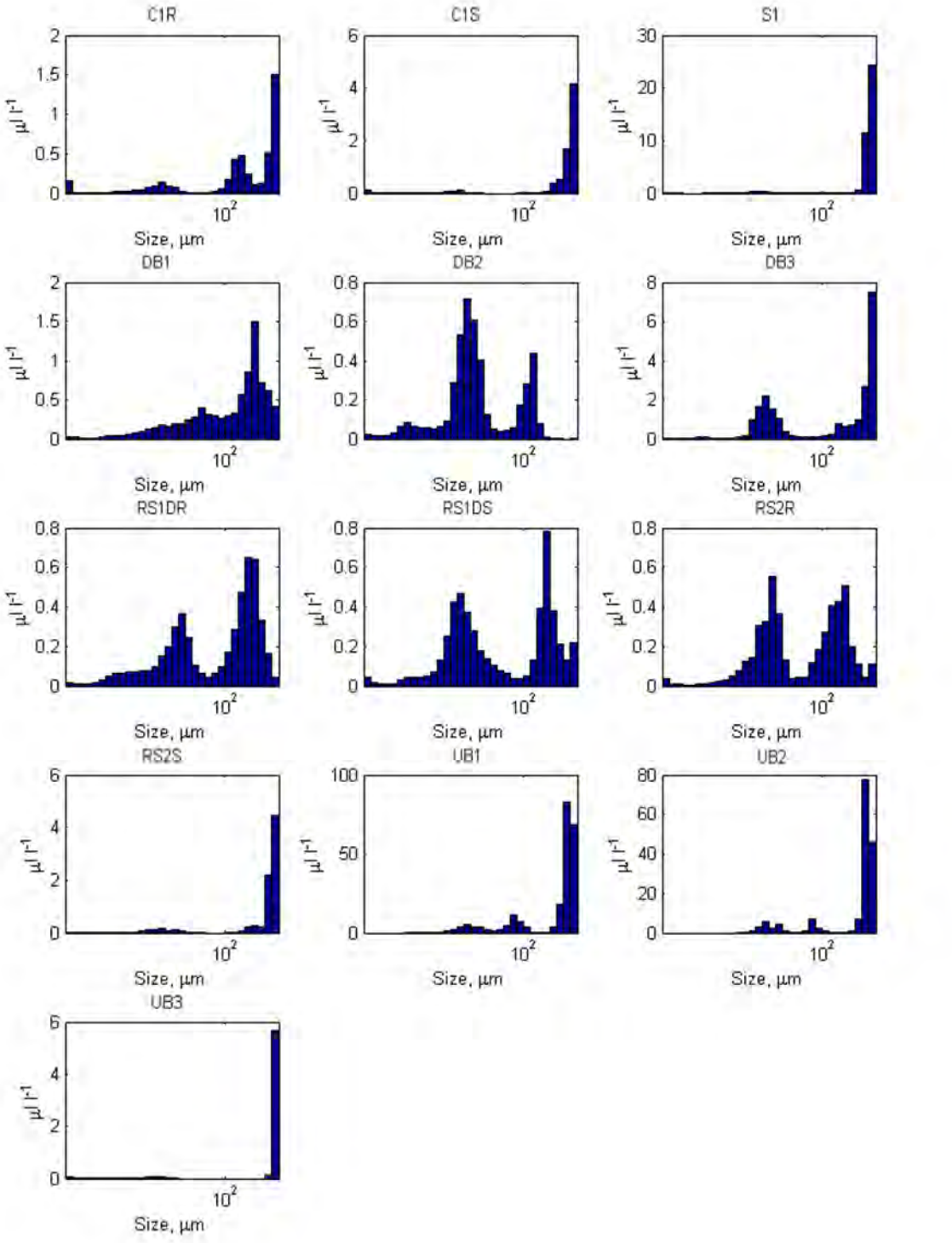

Figure E-10 Volume weighted distributions of suspended particles for water column samples collected November 9-10, 2013.

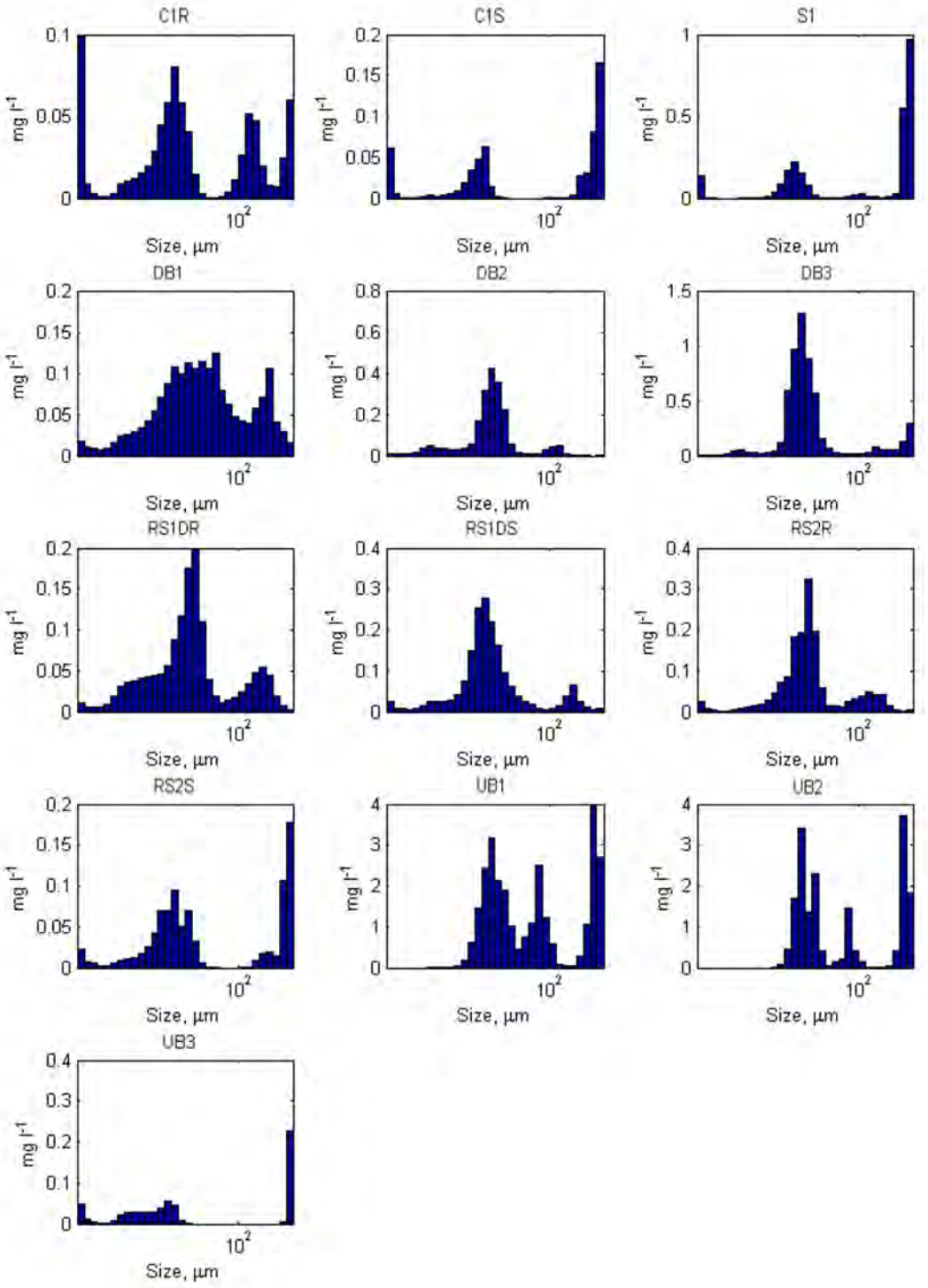

Figure E-11 Mass weighted distributions of suspended particles for water column samples collected November 9-10, 2013.

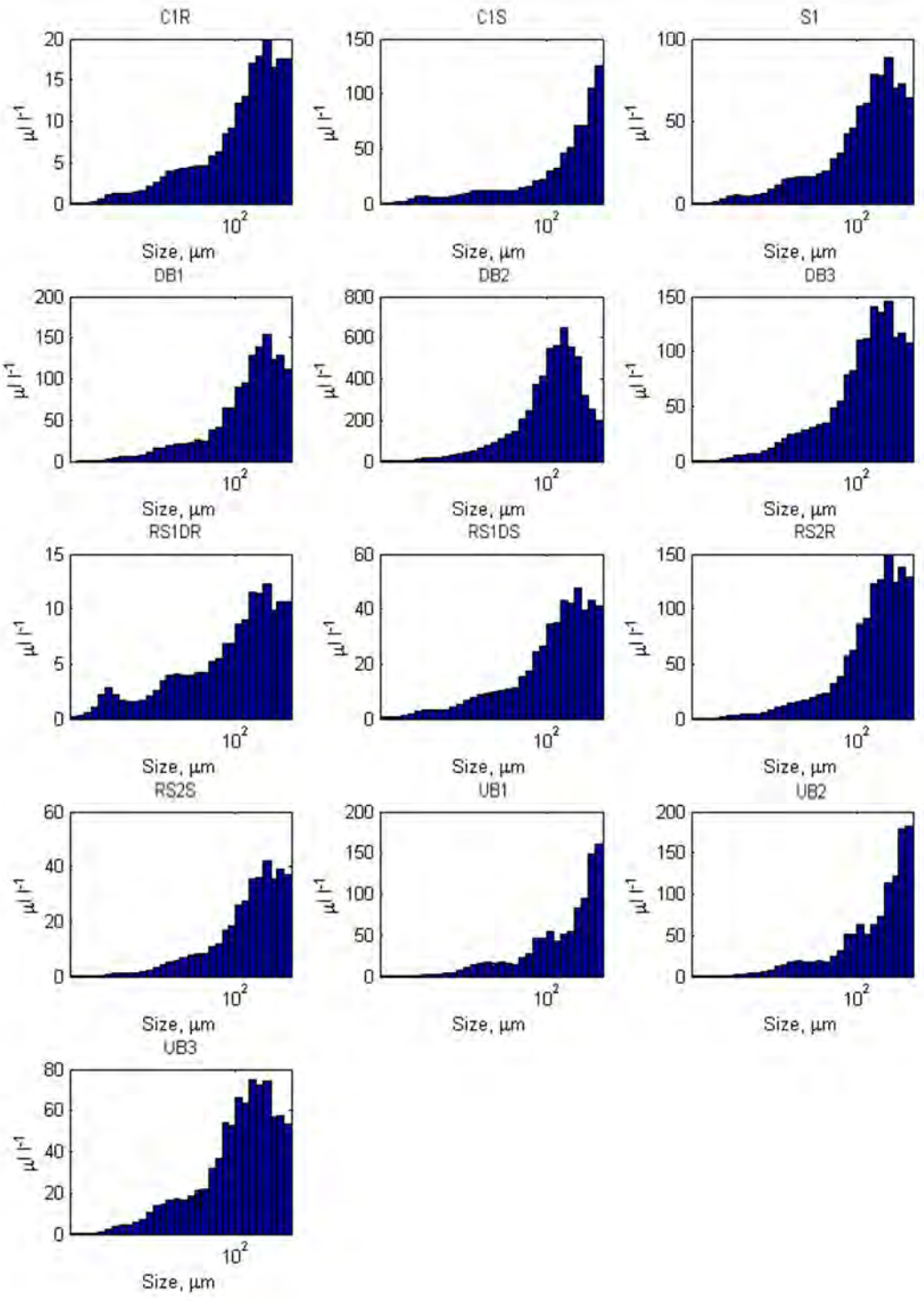

Figure E-12 Volume weighted distributions of suspended particles for epiphyton samples collected November 9-10, 2013.

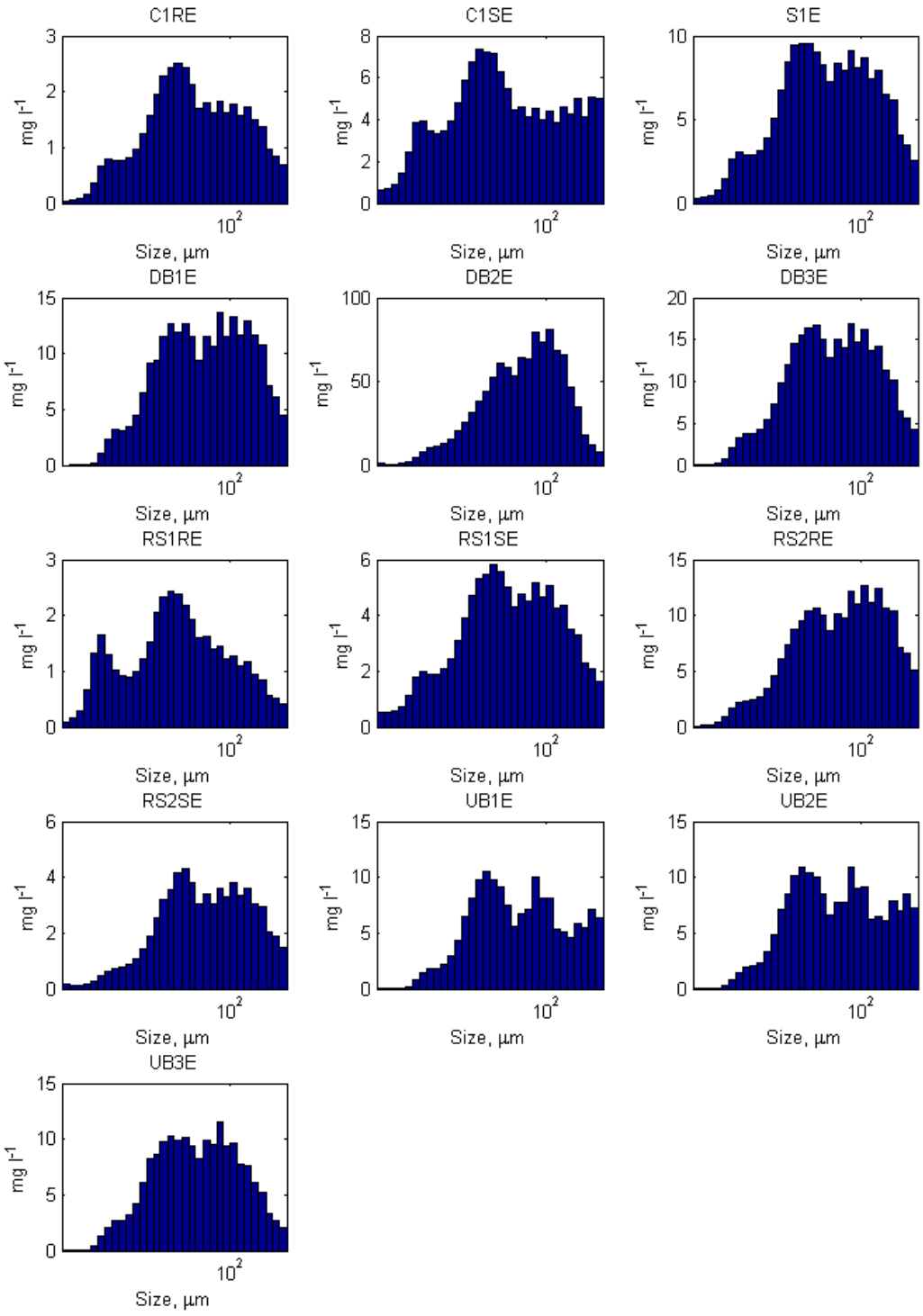

Figure E-13 Mass weighted distributions of suspended particles for epiphyton samples collected November 9-10, 2013.

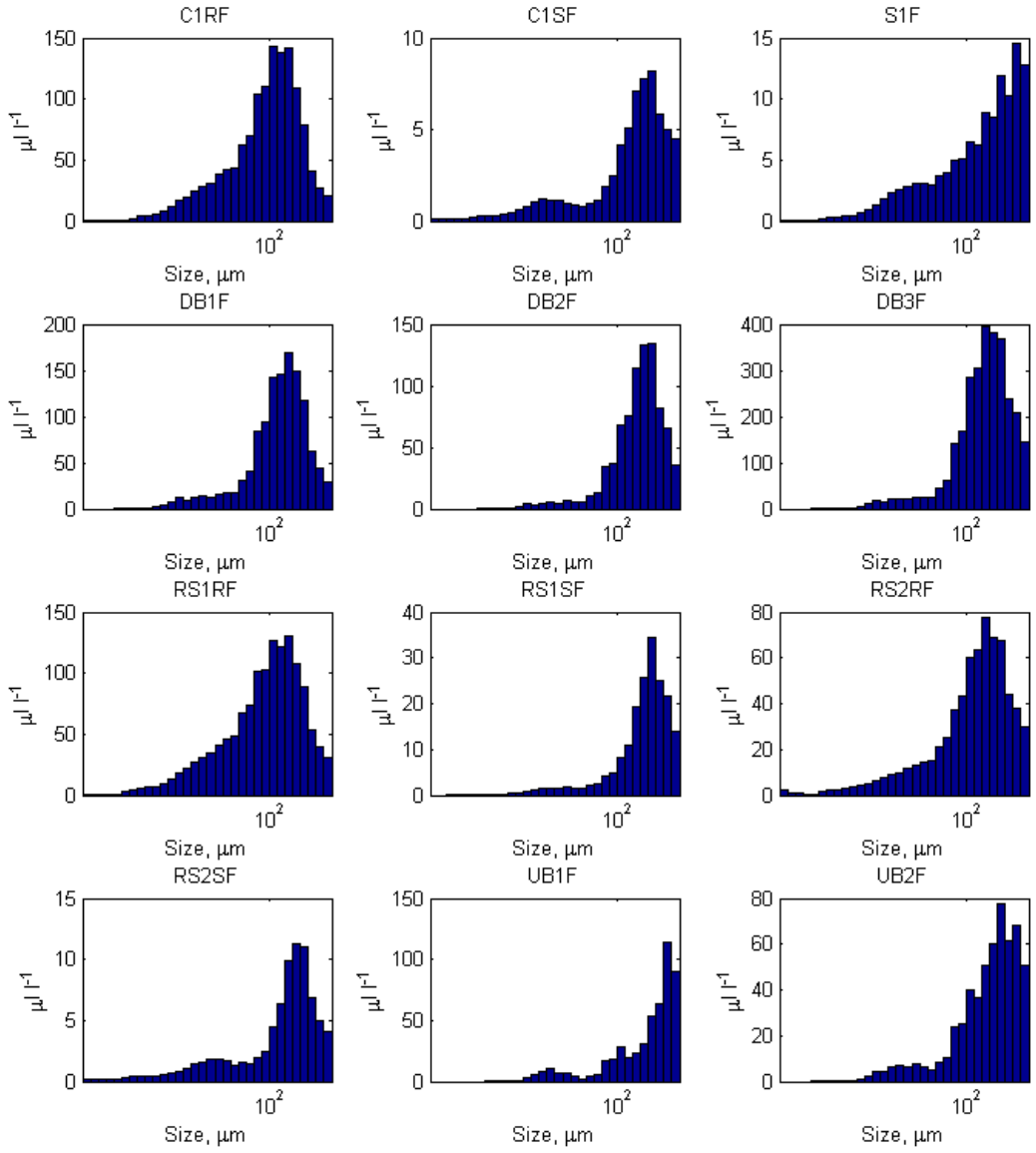

Figure E-14 Volume weighted distributions of suspended particles for floc samples collected November 9-10, 2013.

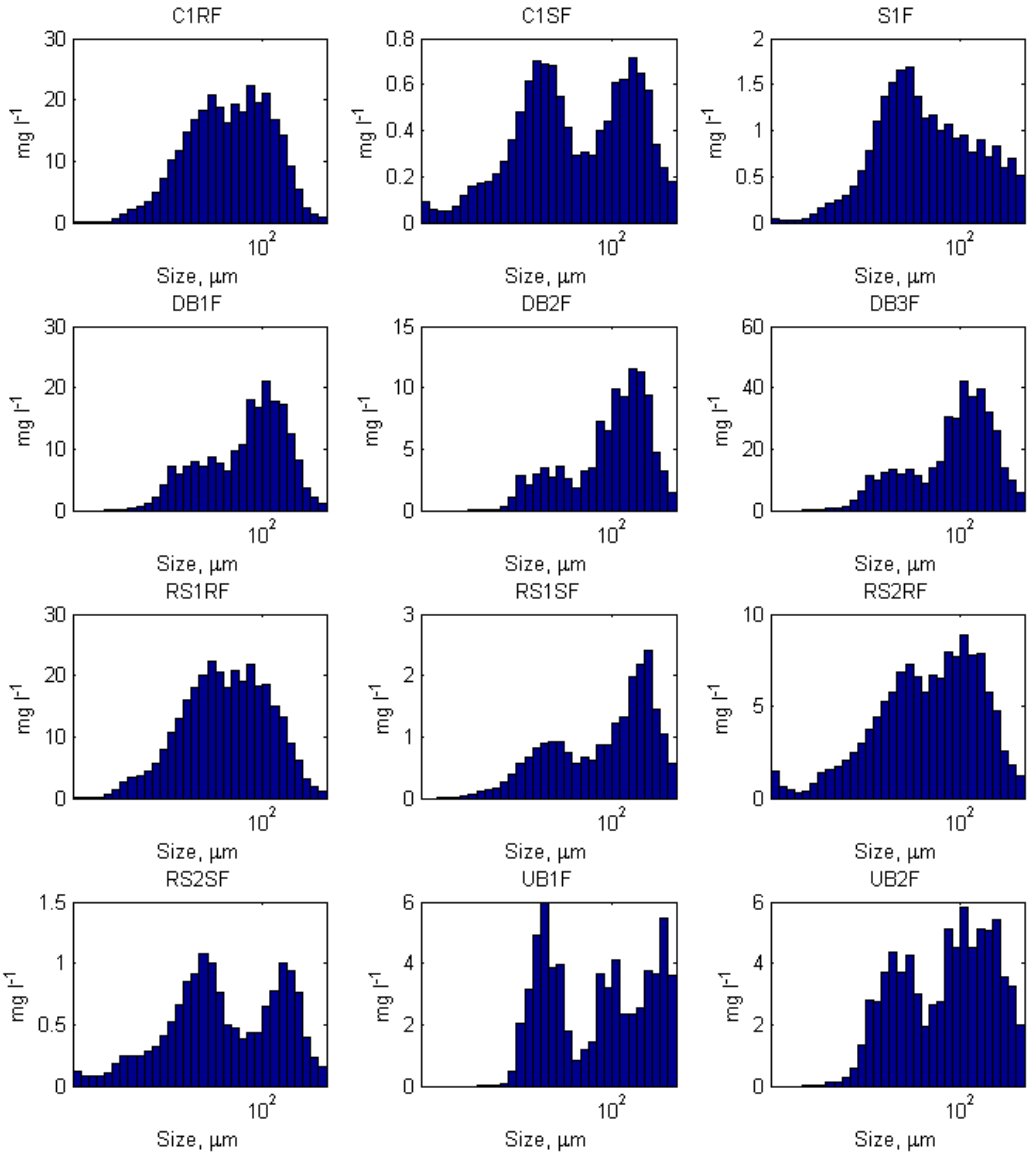

Figure E-15 Mass weighted distributions of suspended particles for floc samples collected November 9-10, 2013.

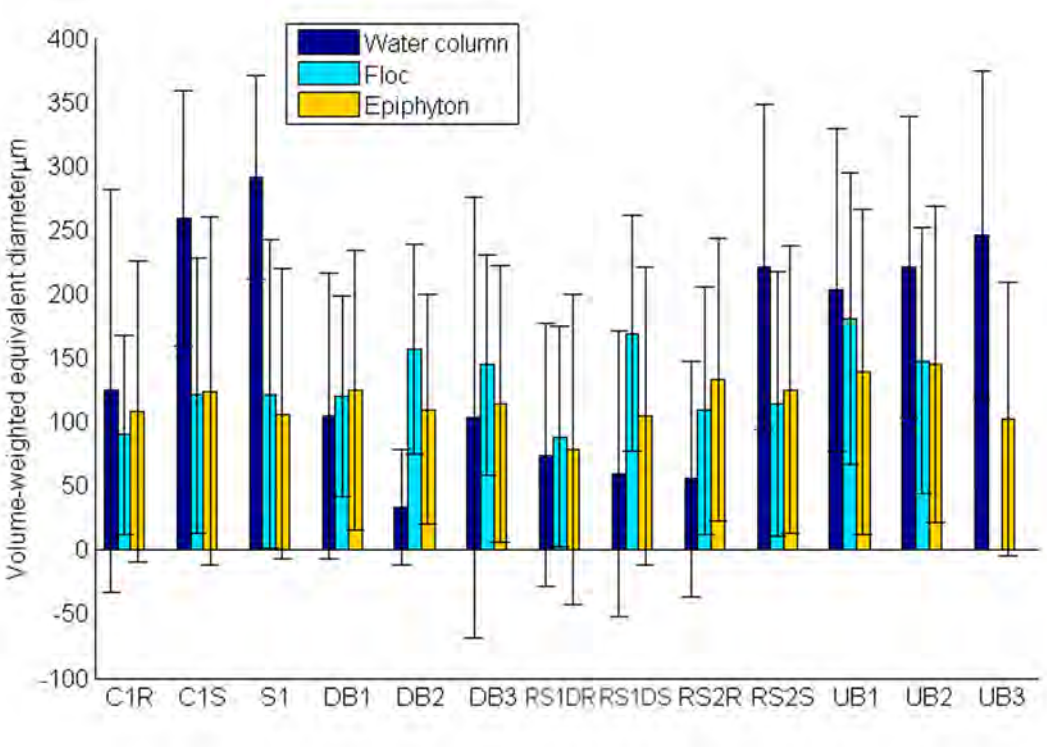

Figure E-16 Comparison of average volume weighted equivalent diameter for each particle type for each DPM site for samples collected November 9-10, 2013.

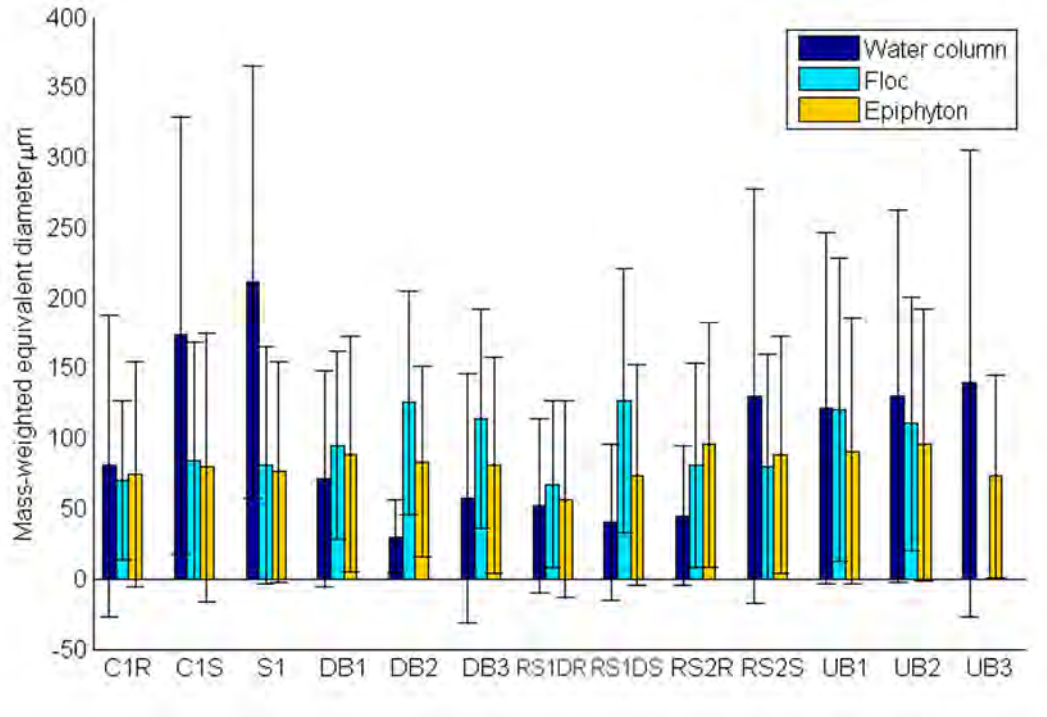

Figure E-17 Comparison of average mass weighted equivalent diameter for each particle type for each DPM site for samples collected November 9-10, 2013.

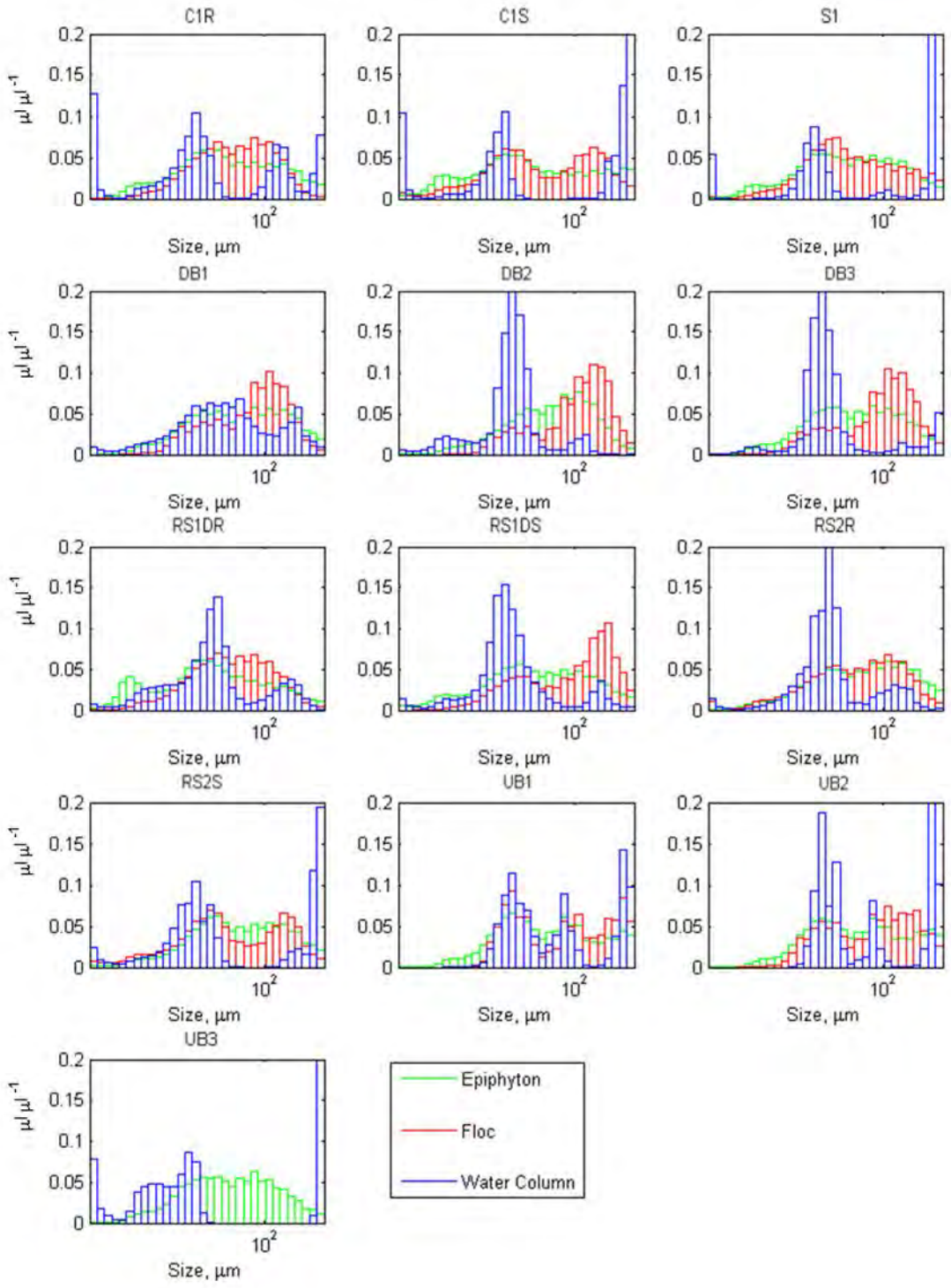

Figure E-18 Comparisons of volumetric fraction distributions of Water Column, Floc and Epiphyton by size for samples collected November 9-10, 2013.

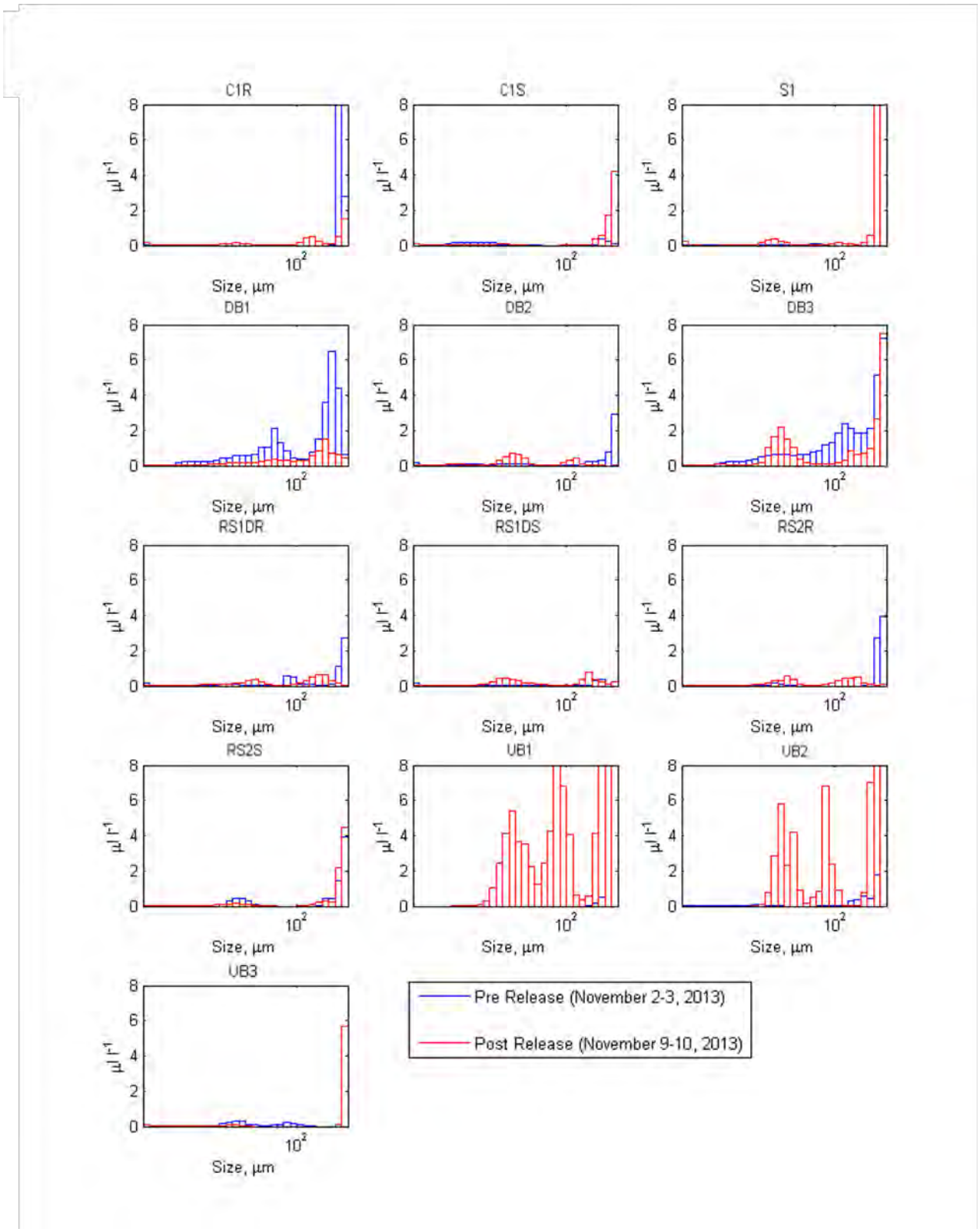

Figure E-19 Pre and post release comparison of volume weighted distributions of water column suspended particles. Samples collected during the 2013 DPM flow release.

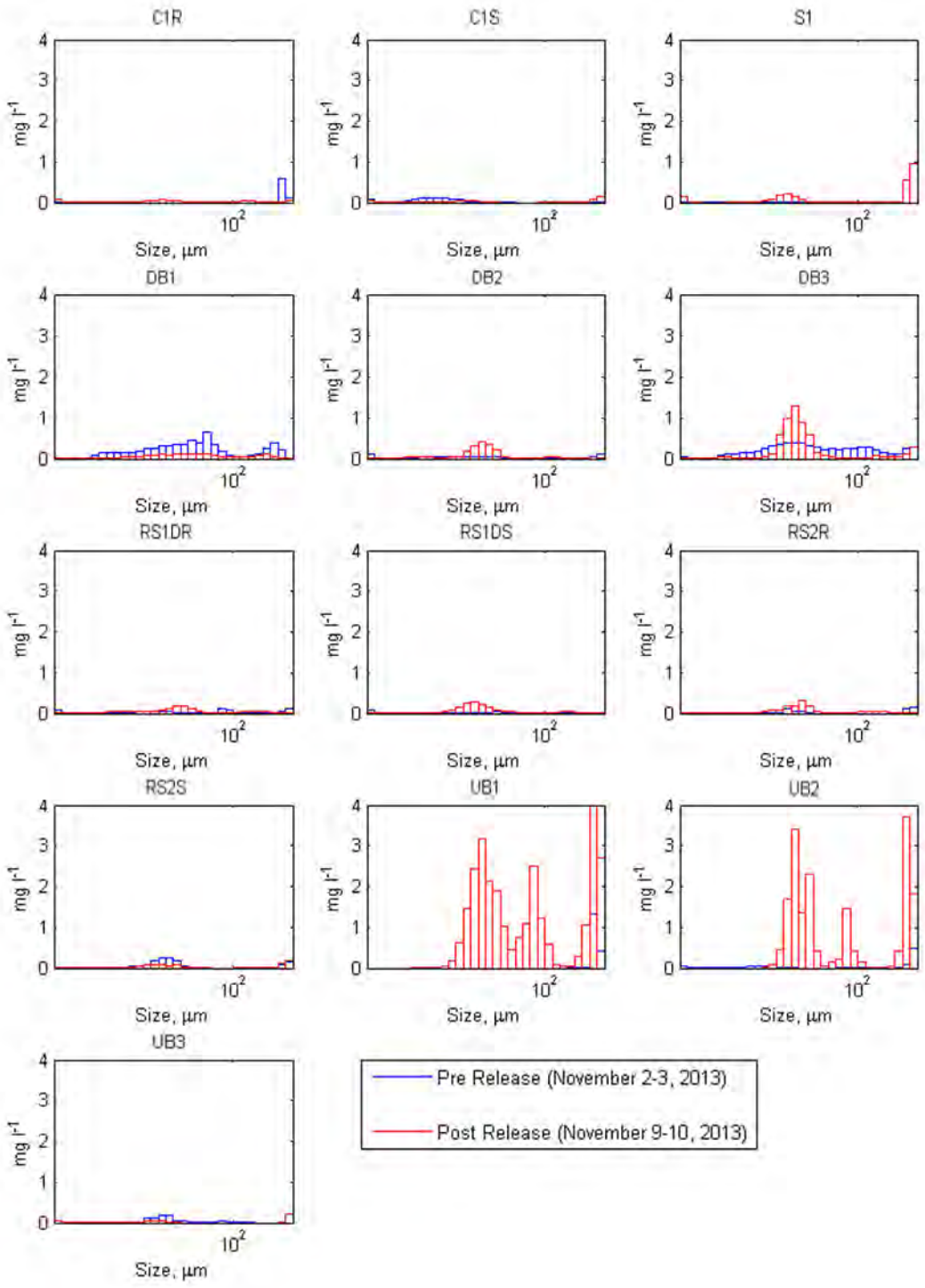

Figure E-20 Pre and post release comparison of mass weighted distributions of water column suspended particles. Samples collected during the 2013 DPM flow release.

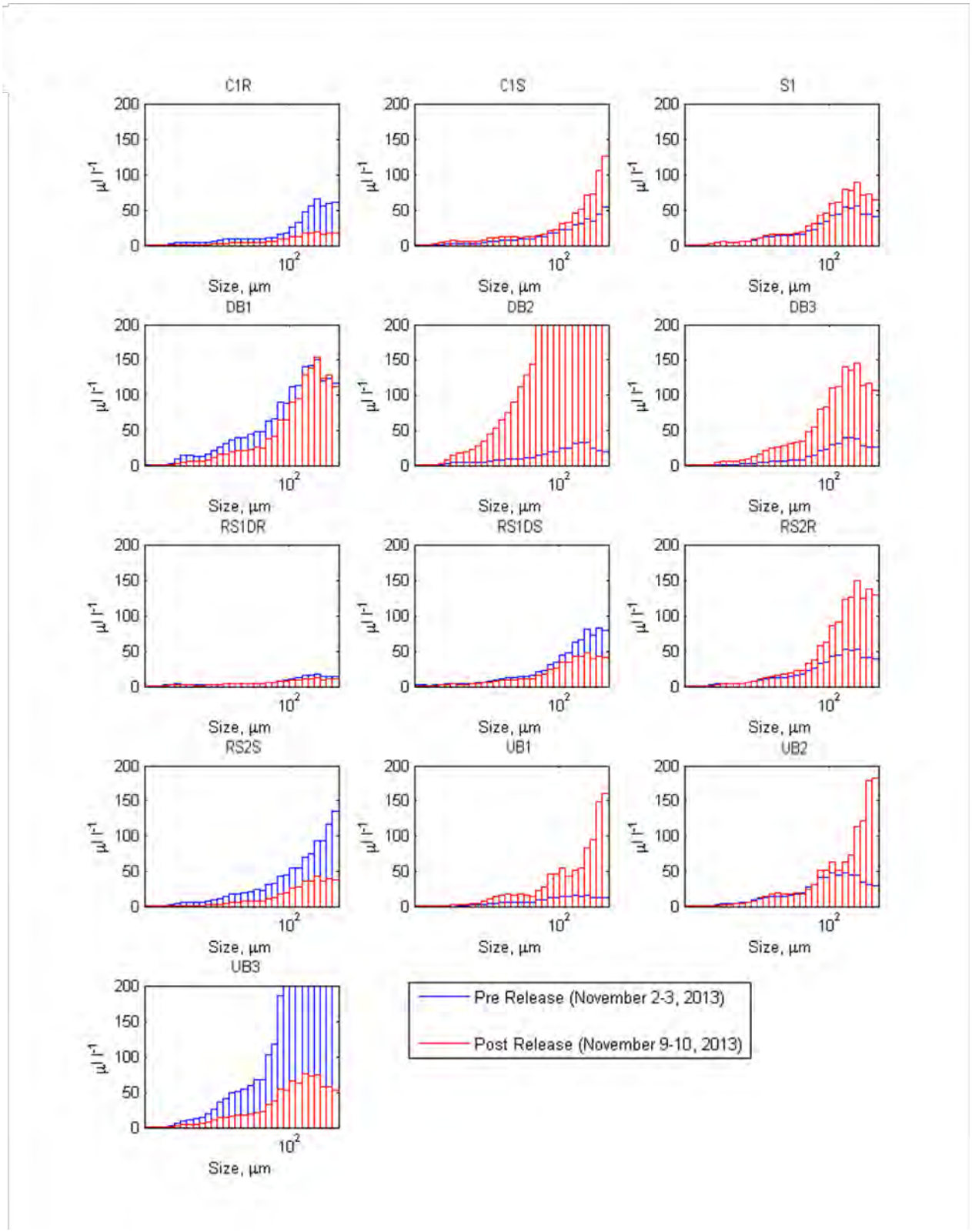

Figure E-21 Pre and post release comparison of volume weighted distributions of epiphyton suspended particles. Samples collected during the 2013 DPM flow release.

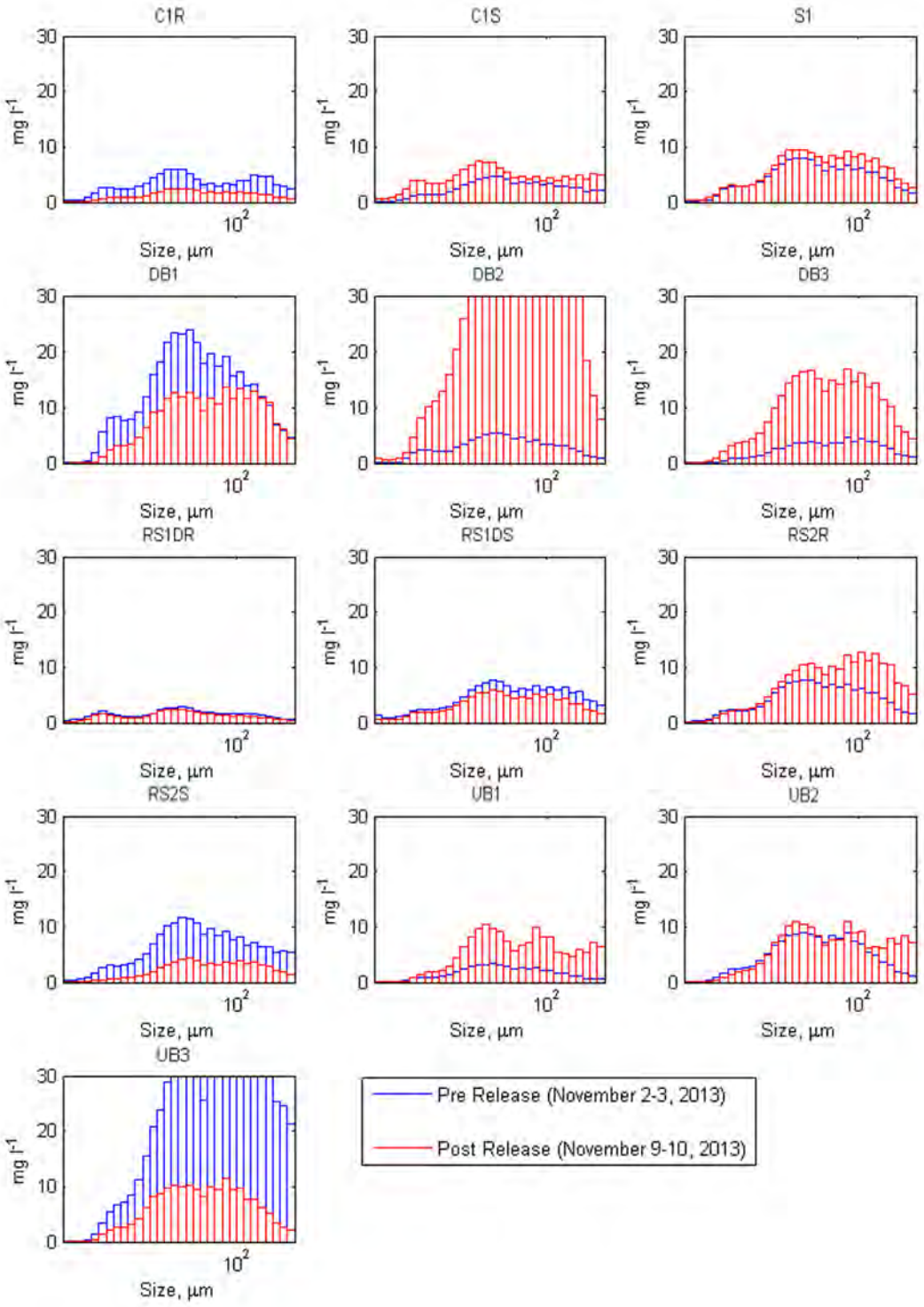

Figure E-22 Pre and post release comparison of mass weighted distributions of epiphyton suspended particles. Samples collected during the 2013 DPM flow release.

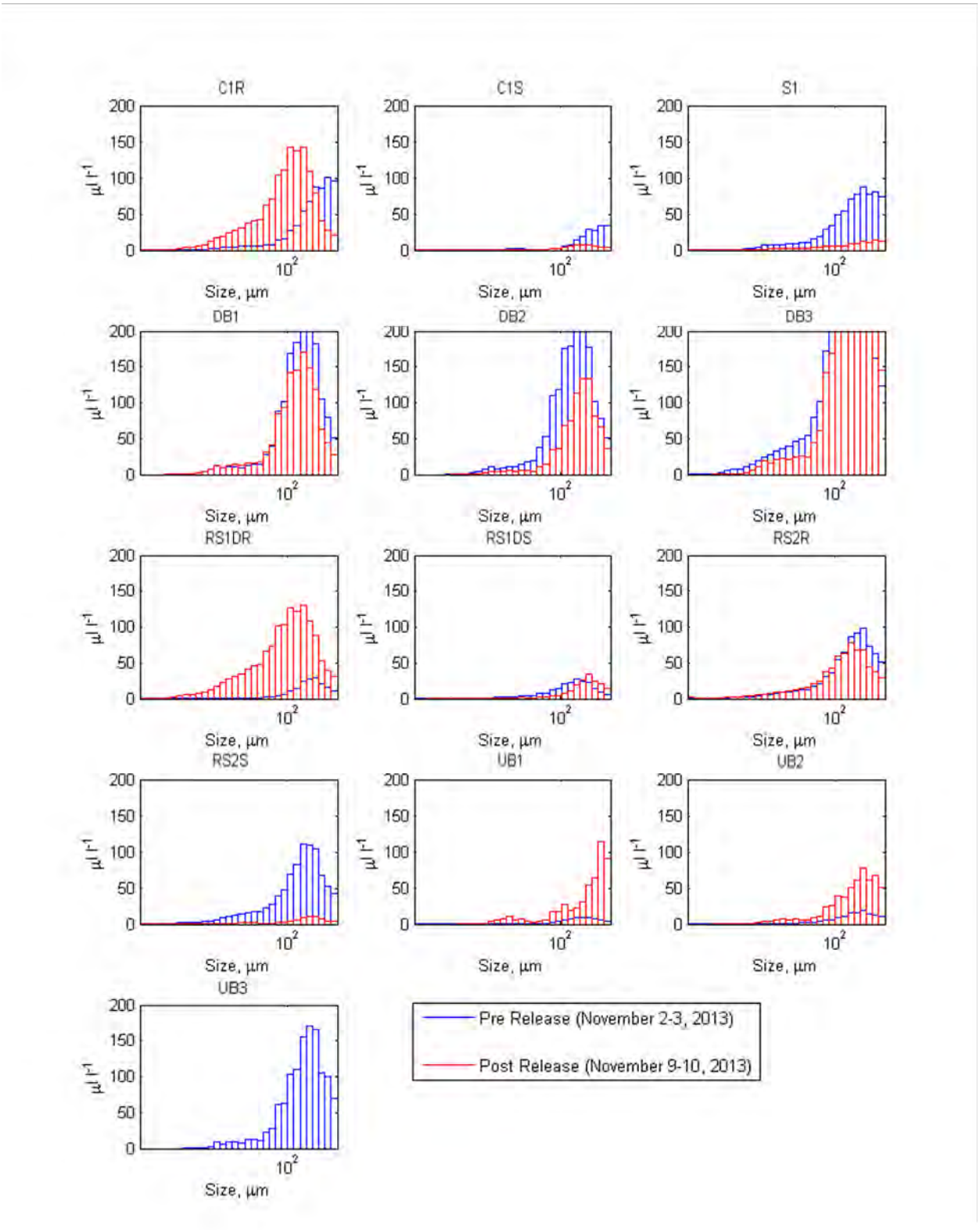

Figure E-23 Pre and post release comparison of volume weighted distributions of floc suspended particles. Samples collected during the 2013 DPM flow release.

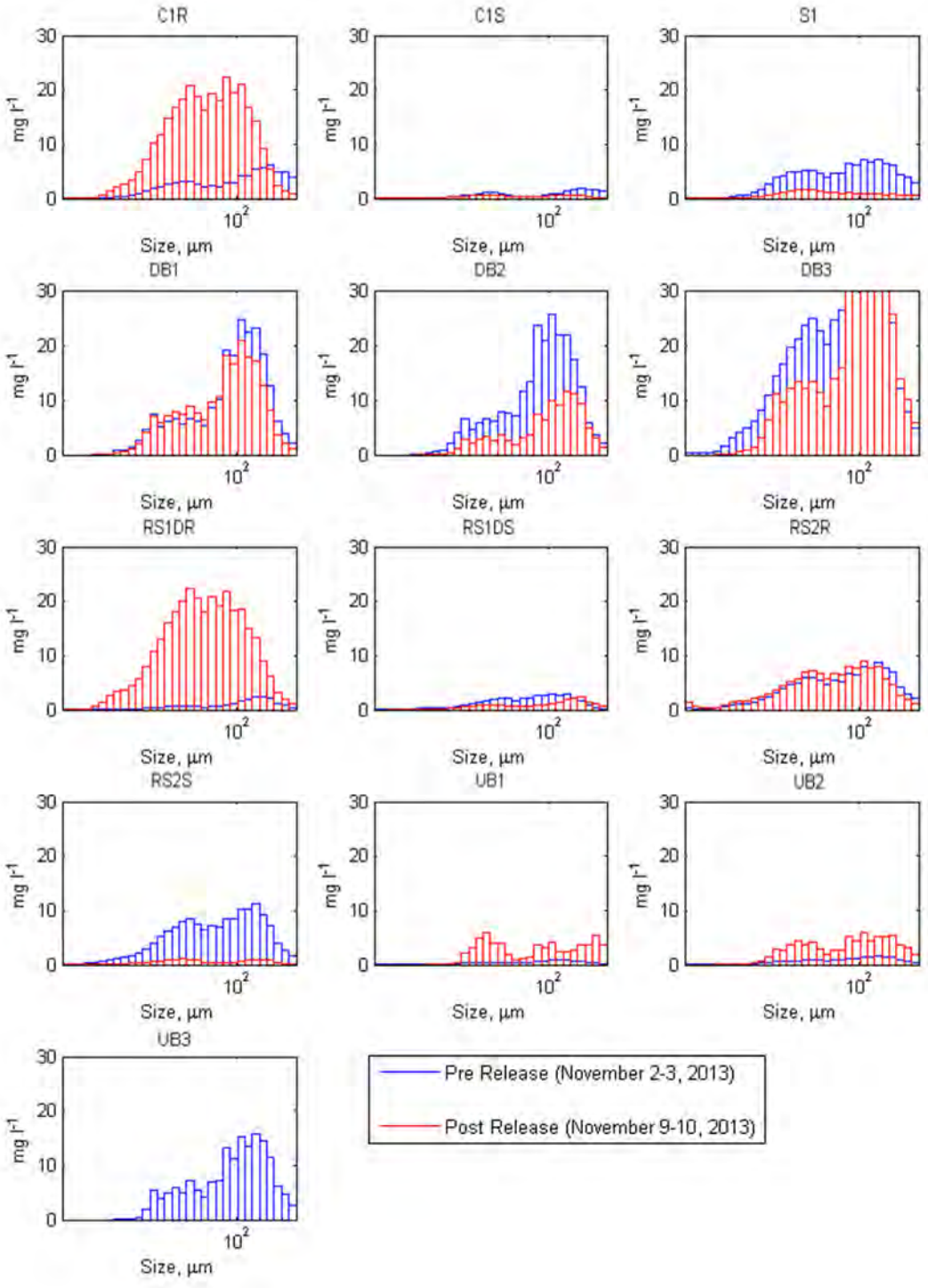

Figure E-24 Pre and post release comparison of mass weighted distributions of floc suspended particles. Samples collected during the 2013 DPM flow release.

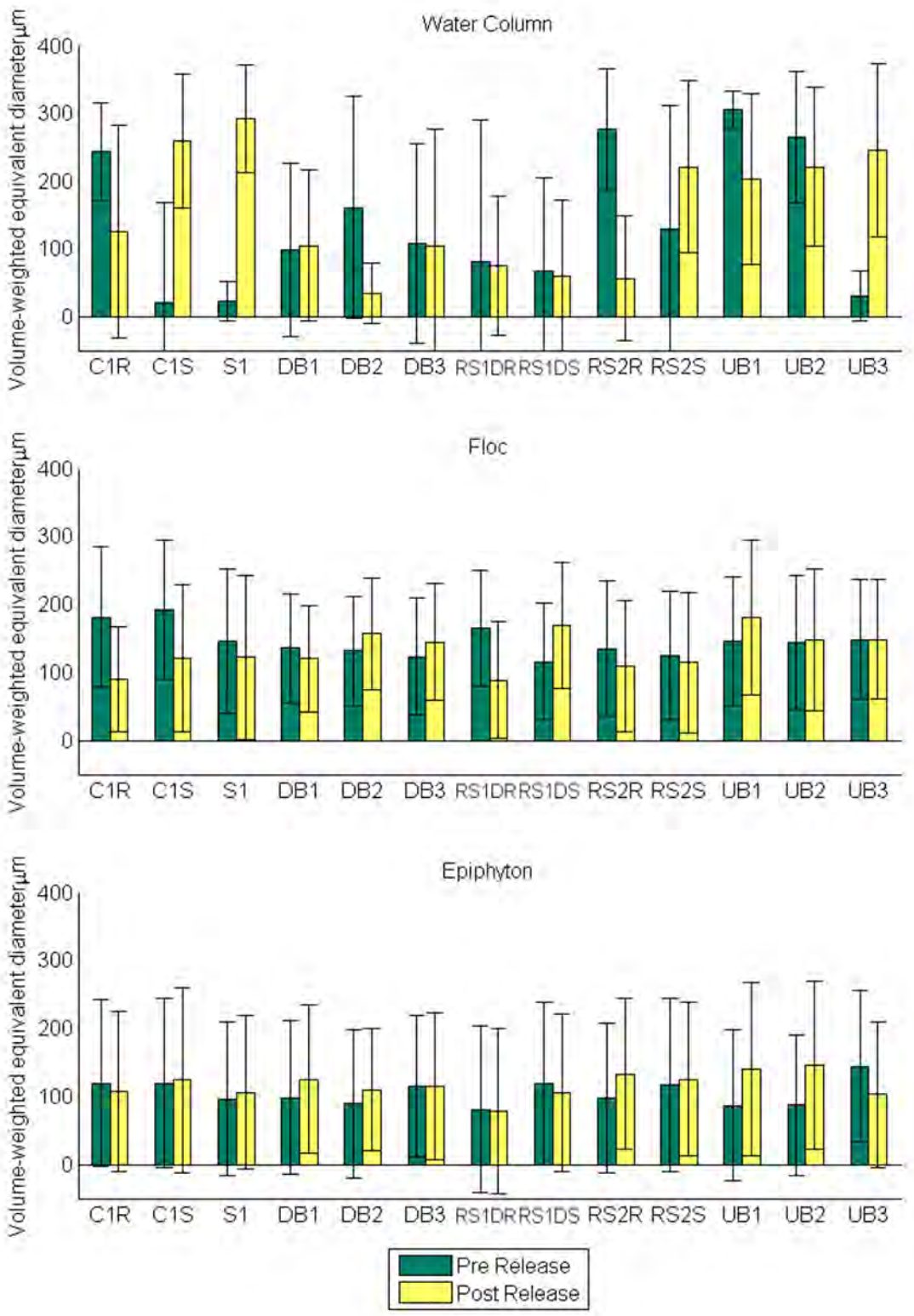

Figure E-25 Pre and post release comparison of average volume weighted equivalent diameter for each particle type for samples collected during the 2013 DPM flow release.

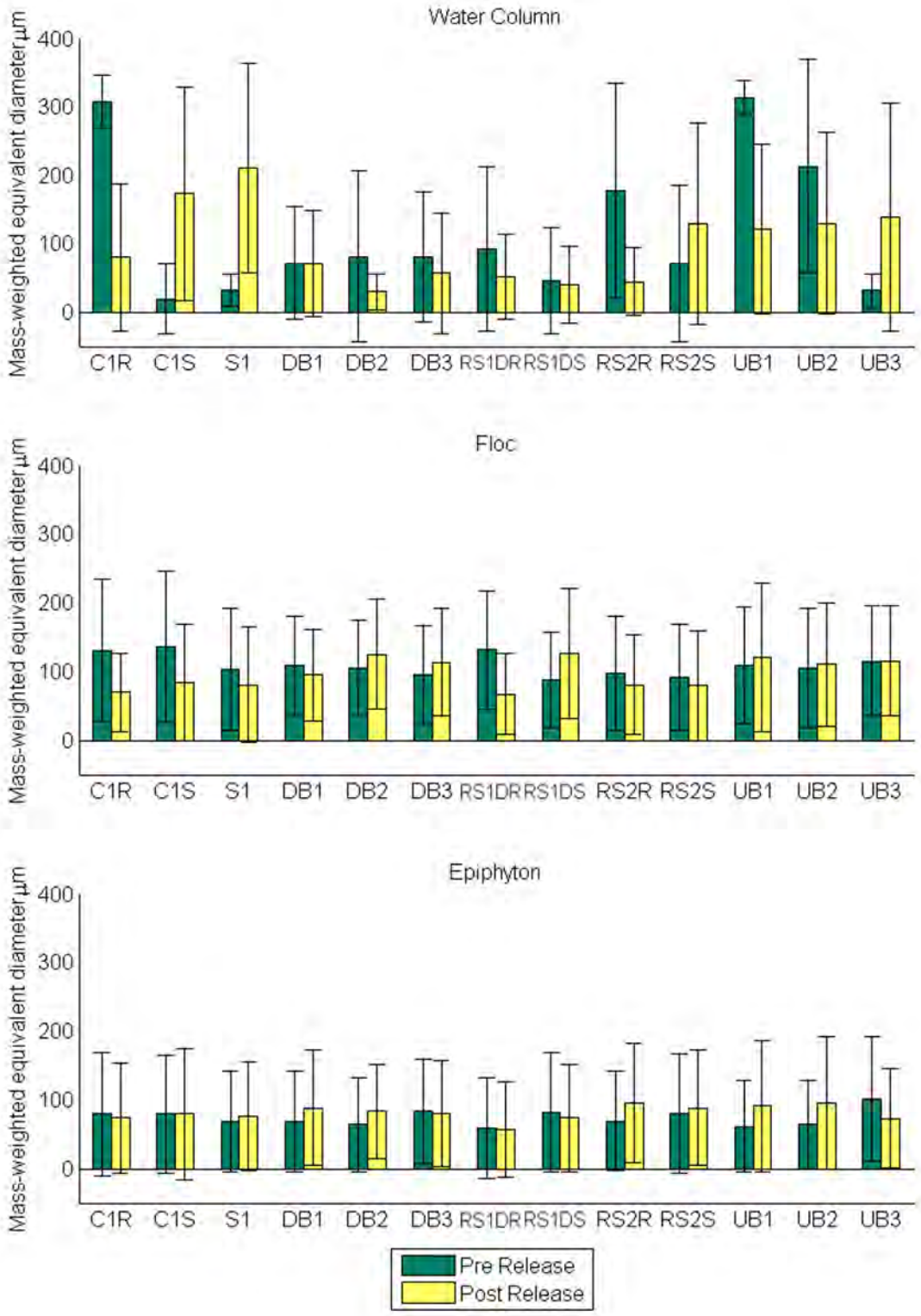

Figure E-26 Pre and post release comparison of average mass weighted equivalent diameter for each particle type for each DPM site for samples collected during the 2013 DPM flow release.

2014 Flow Release

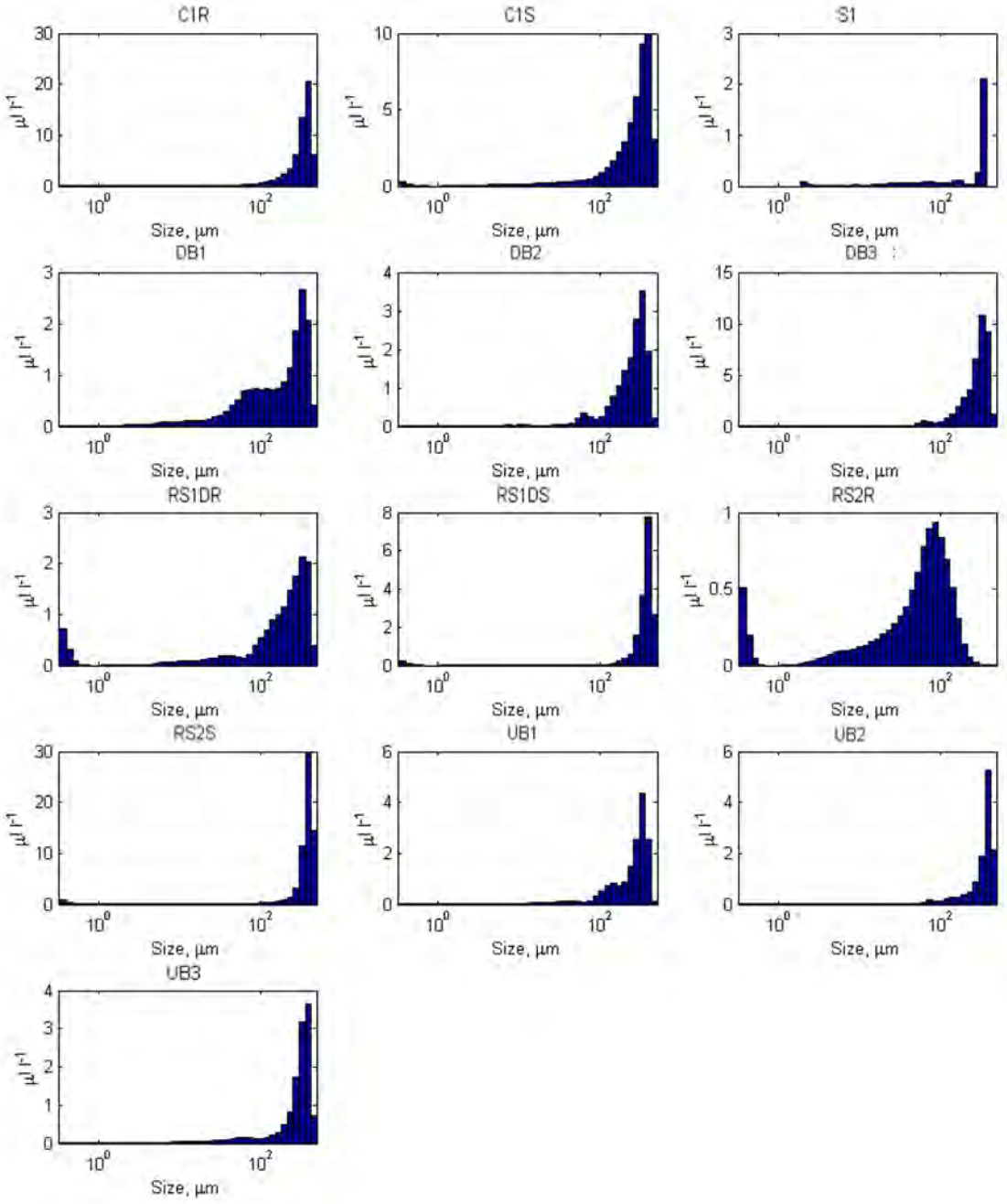

Figure E-27 Volume weighted distributions of suspended particles for water column samples collected November 2-3, 2014.

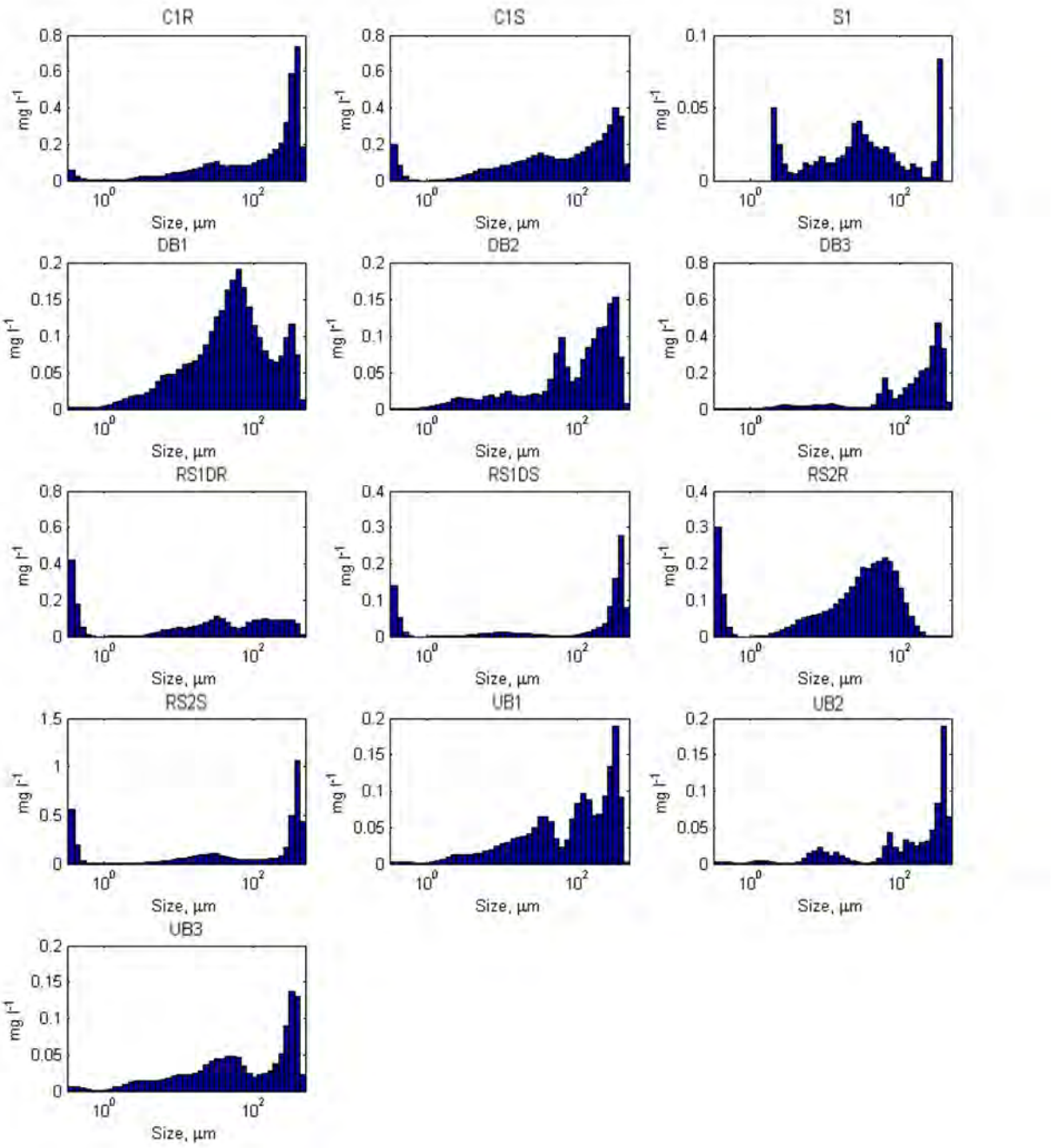

Figure E-28 Mass weighted distributions of suspended particles for water column samples collected November 2-3, 2014.

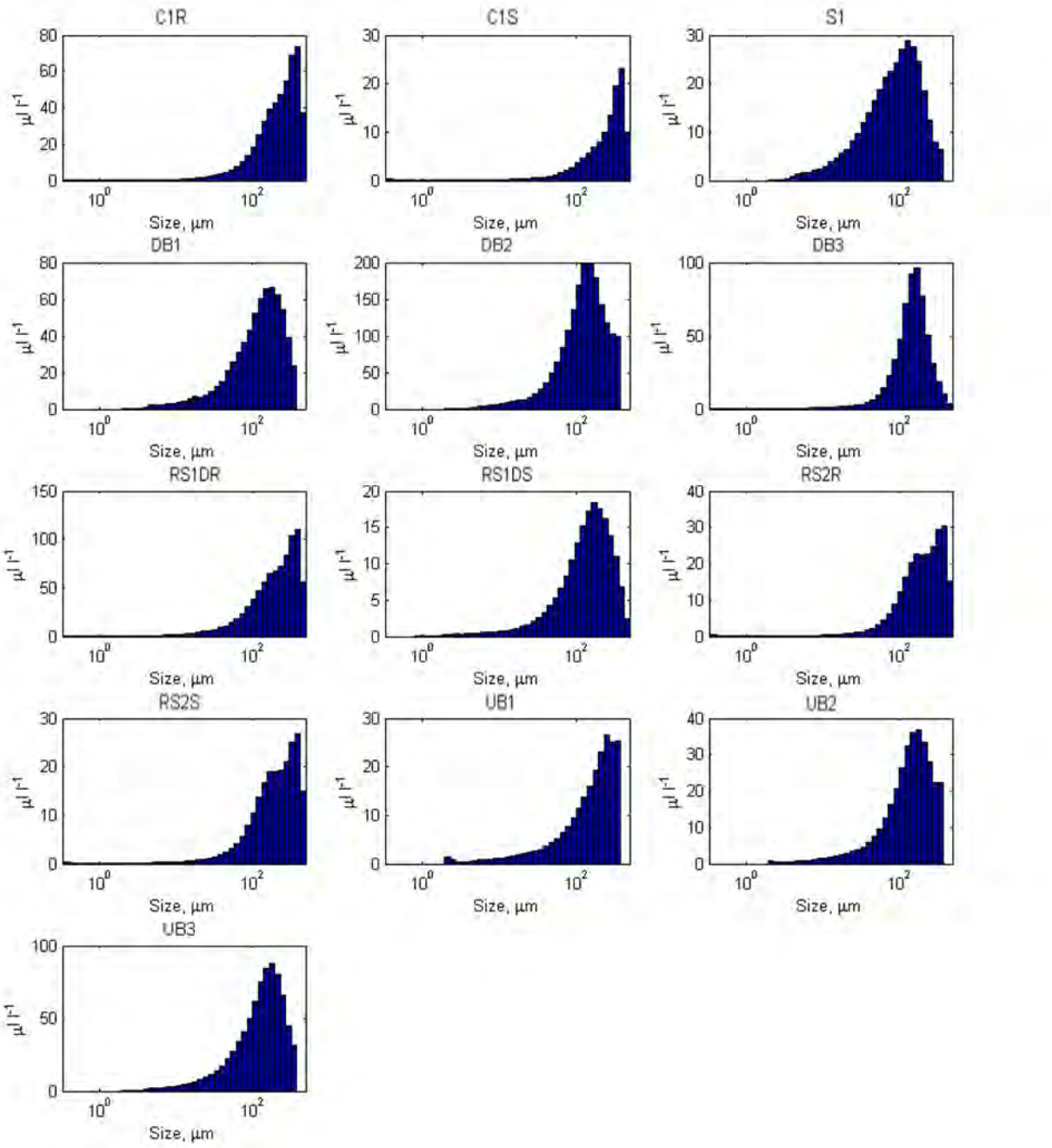

Figure E-29 Volume weighted distributions of suspended particles for floc samples collected November 2-3, 2014.

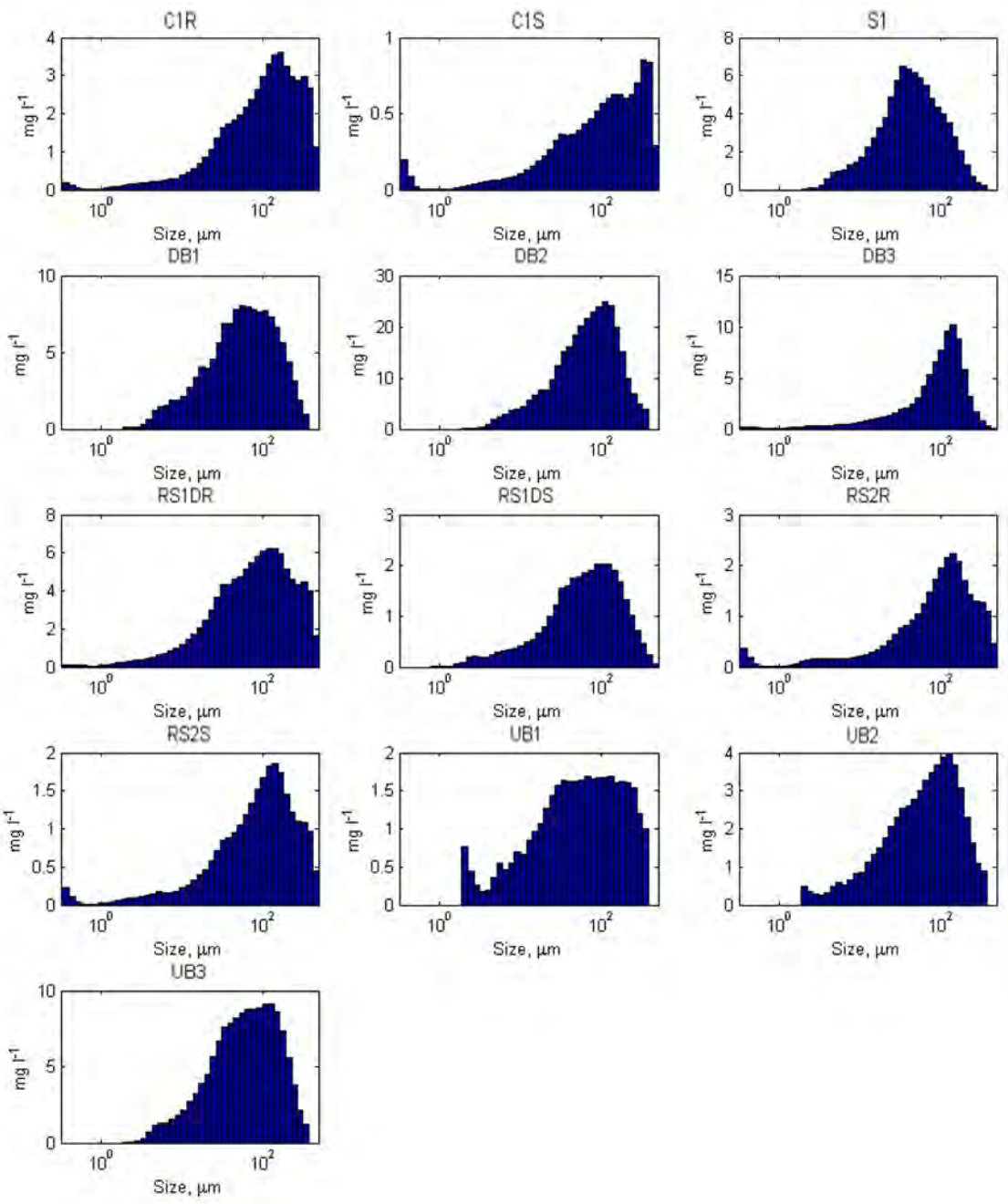

Figure E-30. Mass weighted distributions of suspended particles for floc samples collected November 2-3, 2014.

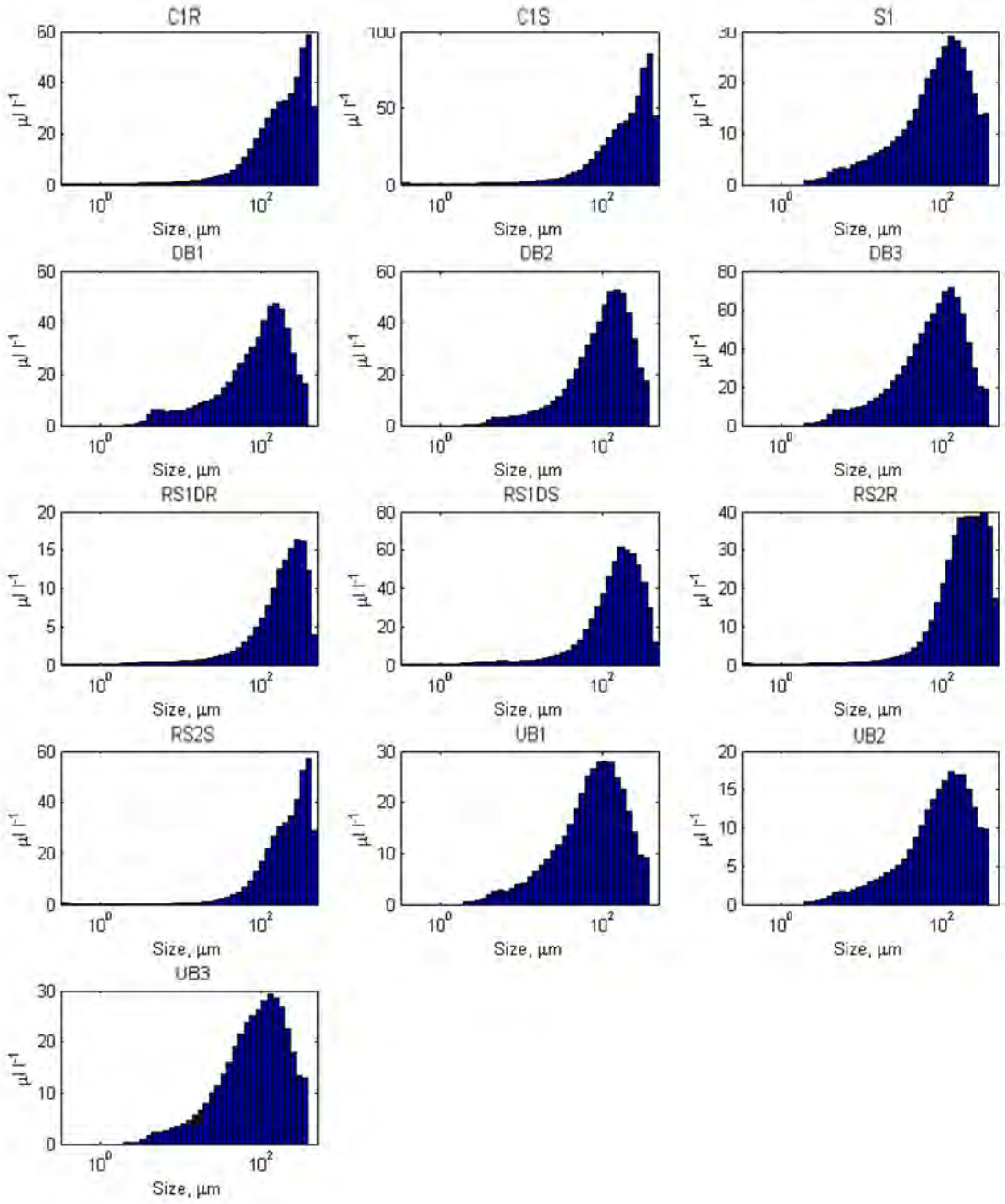

Figure E-31 Volume weighted distributions of suspended particles for epiphyton samples collected November 2-3, 2014.

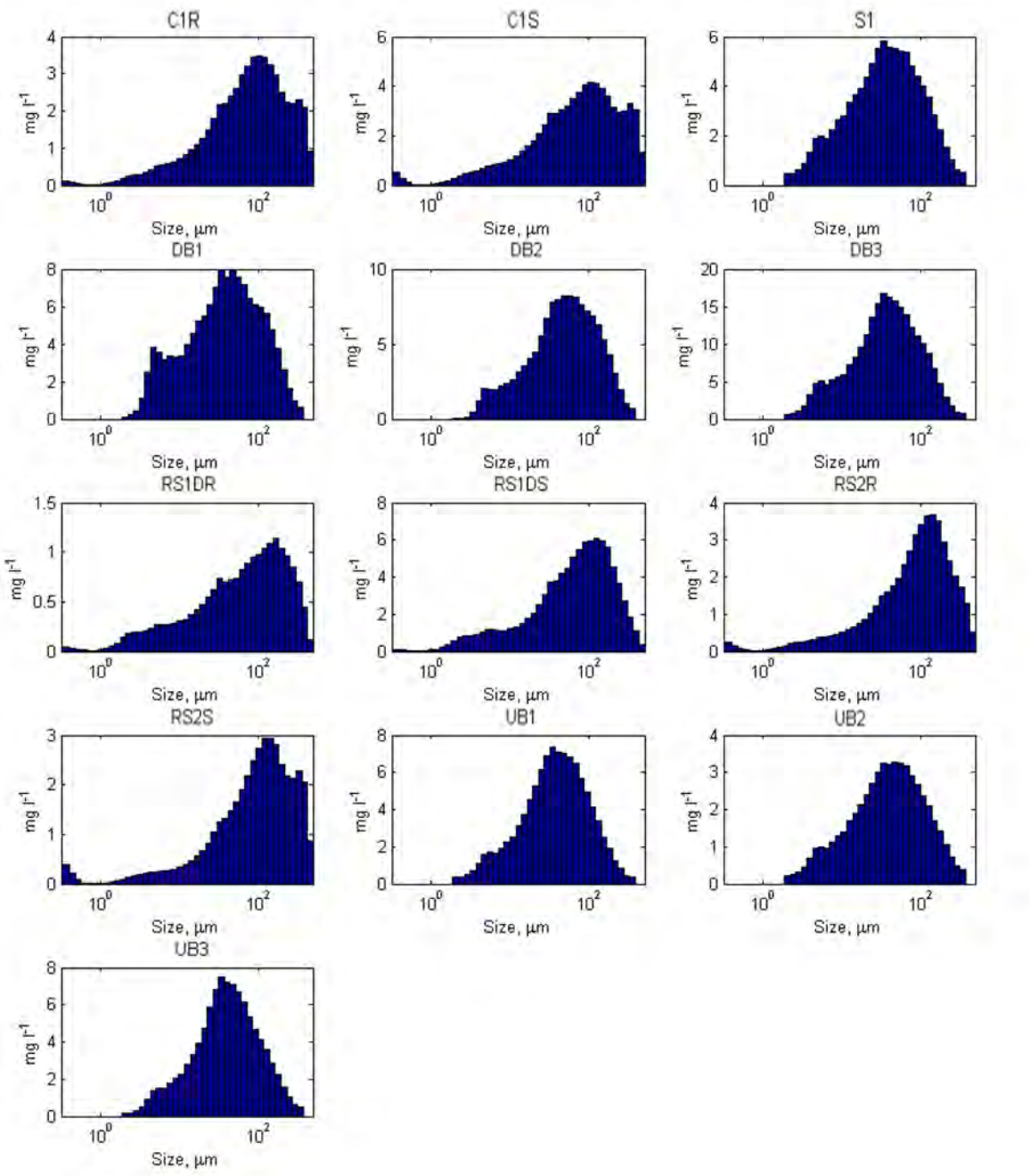

Figure E-32 Mass weighted distributions of suspended particles for epiphyton samples collected November 2-3, 2014.

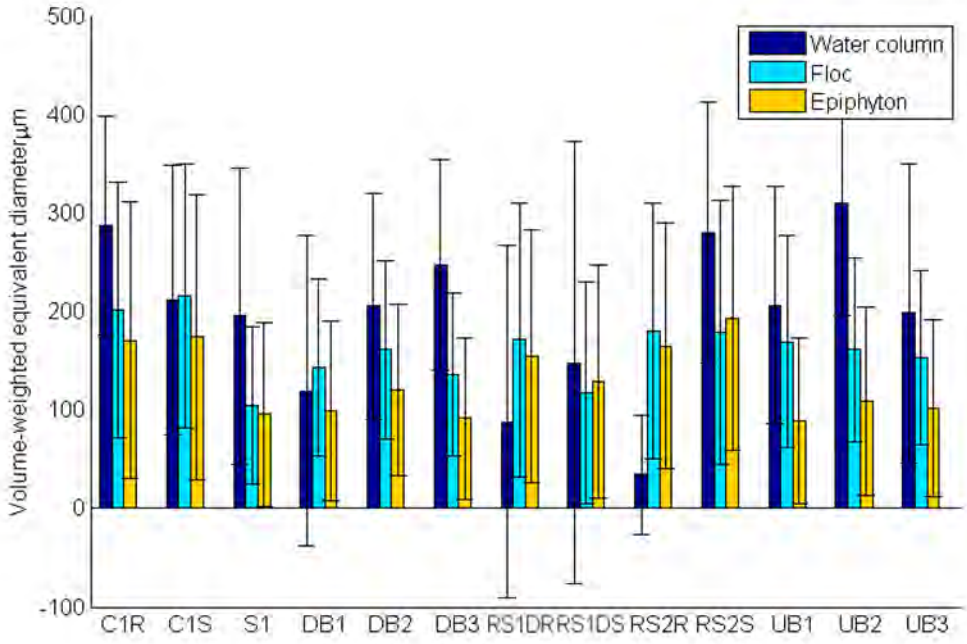

Figure E-33 Comparison of average volume weighted equivalent diameter for each particle type at each DPM site for samples collected November 2-3, 2014.

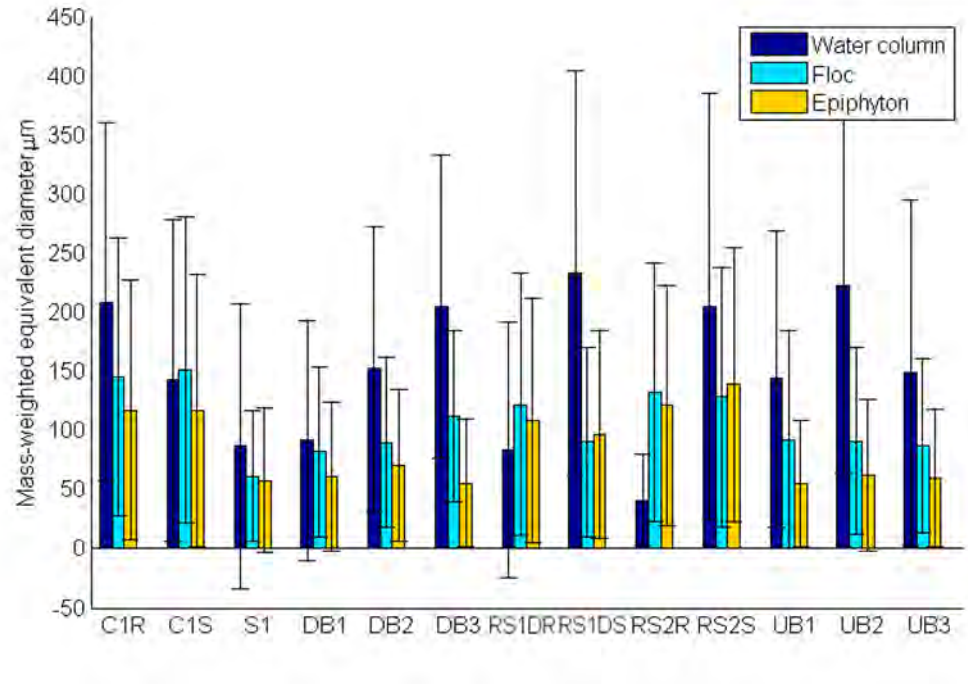

Figure E-34 Comparison of average mass weighted equivalent diameter for each particle type at each DPM site for samples collected November 2-3, 2014.

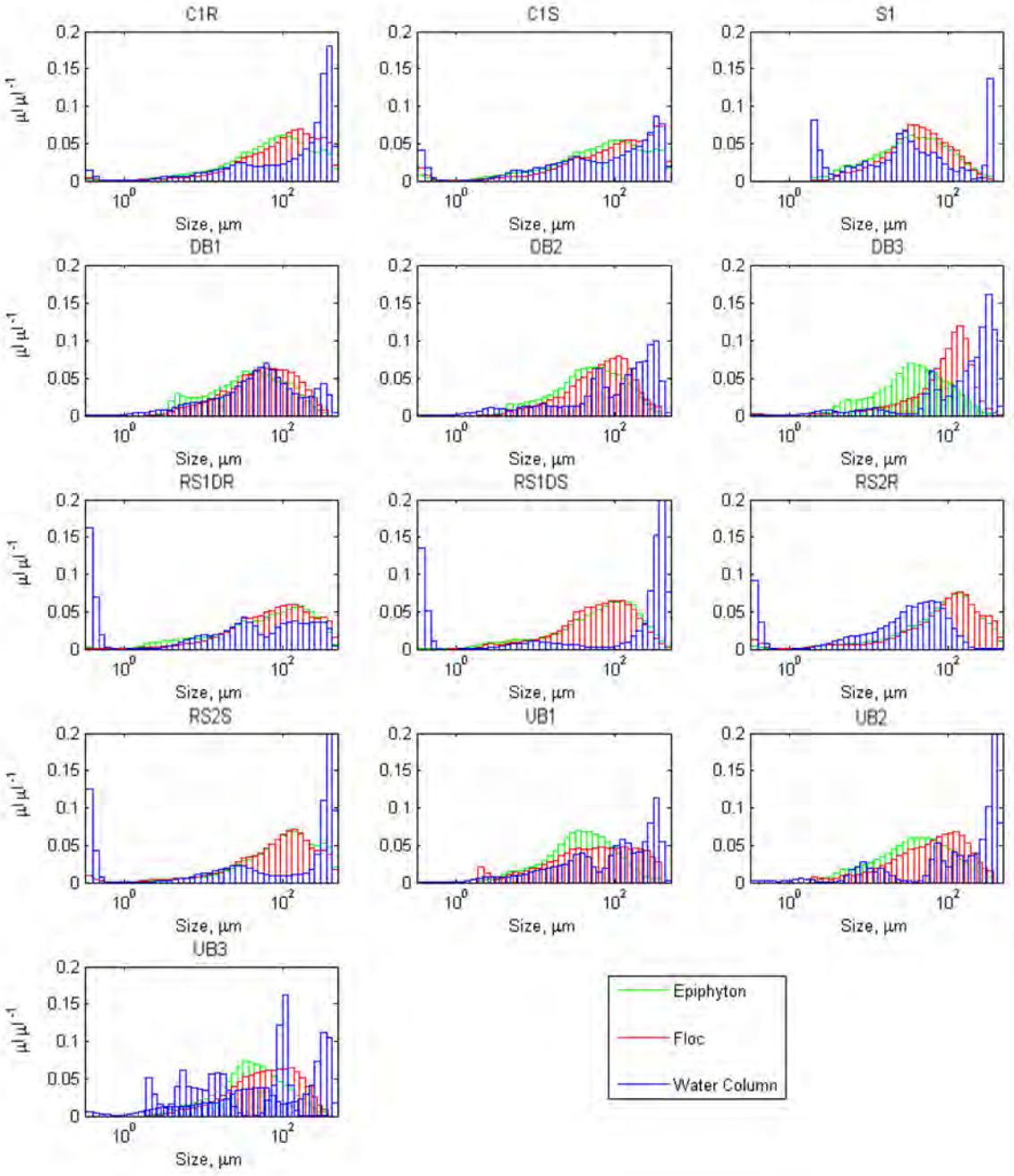

Figure E-35 Comparison of distributions of volumetric fraction Water Column, Floc and Epiphyton by size at each DPM site for samples collected November 2-3, 2014.

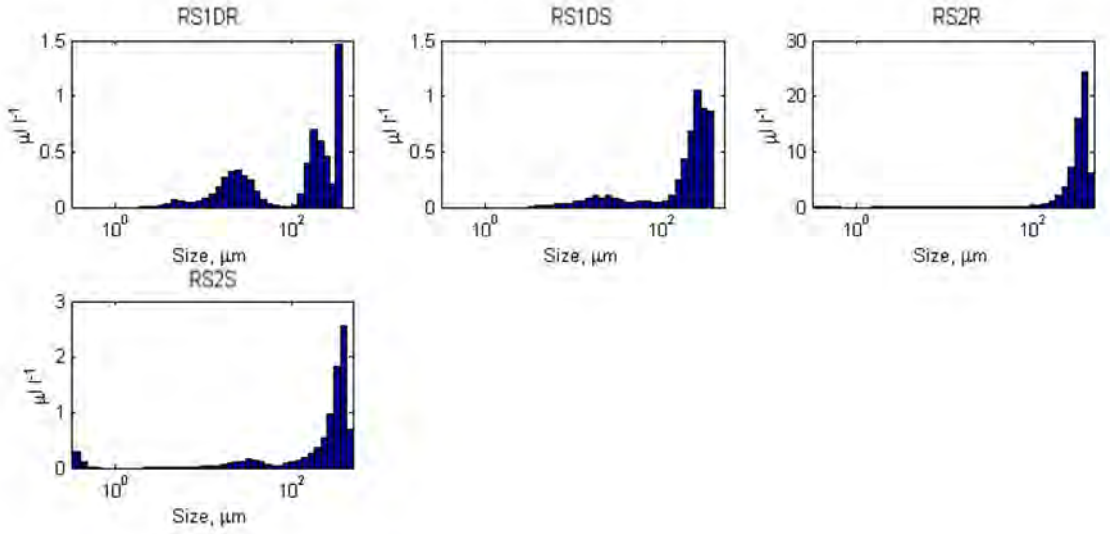

Figure E-36 Volume weighted distributions of suspended particles for water column samples collected November 6, 2014.

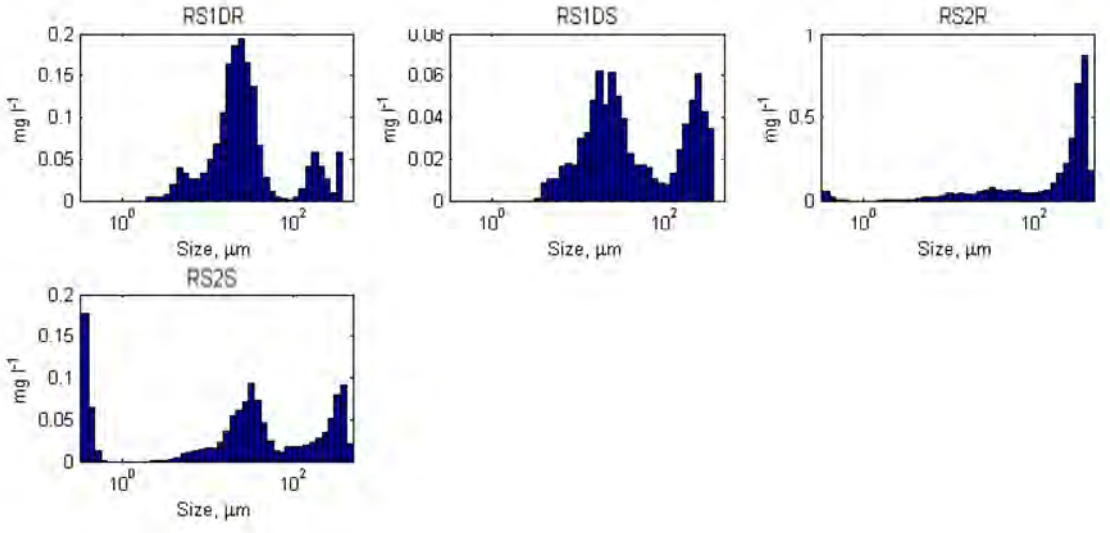

Figure E-37 Mass weighted distributions of suspended particles for water column samples collected November 6, 2014.

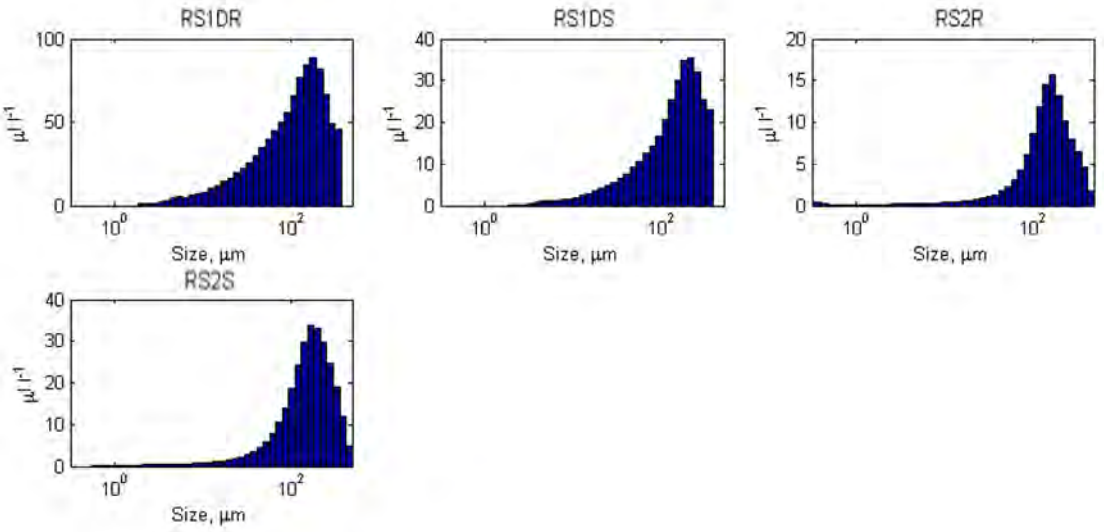

Figure E-38 Volume weighted distributions of suspended particles for floc samples collected November 6, 2014.

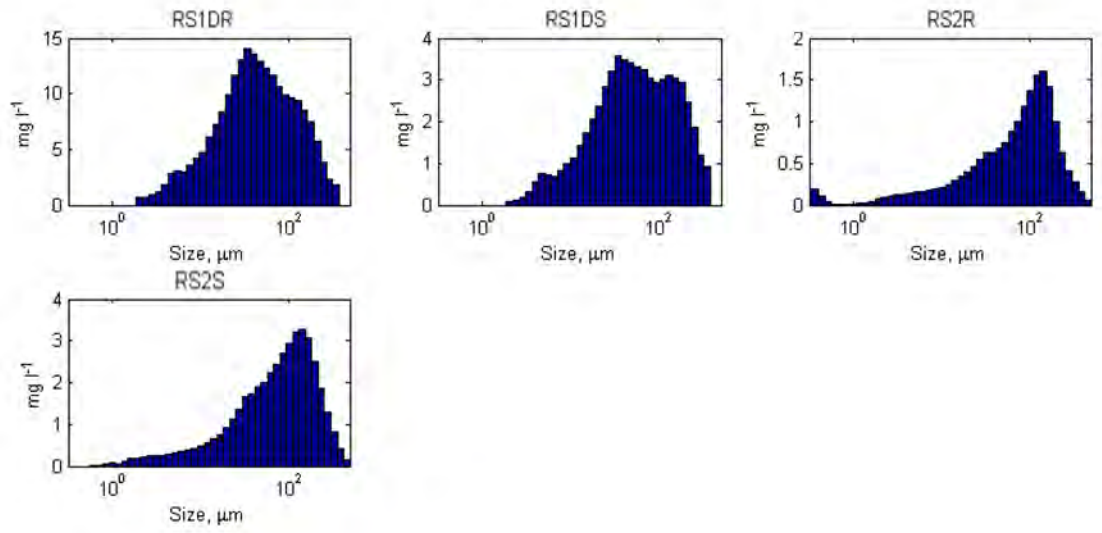

Figure E-39 Mass weighted distributions of suspended particles for floc samples collected November 6, 2014.

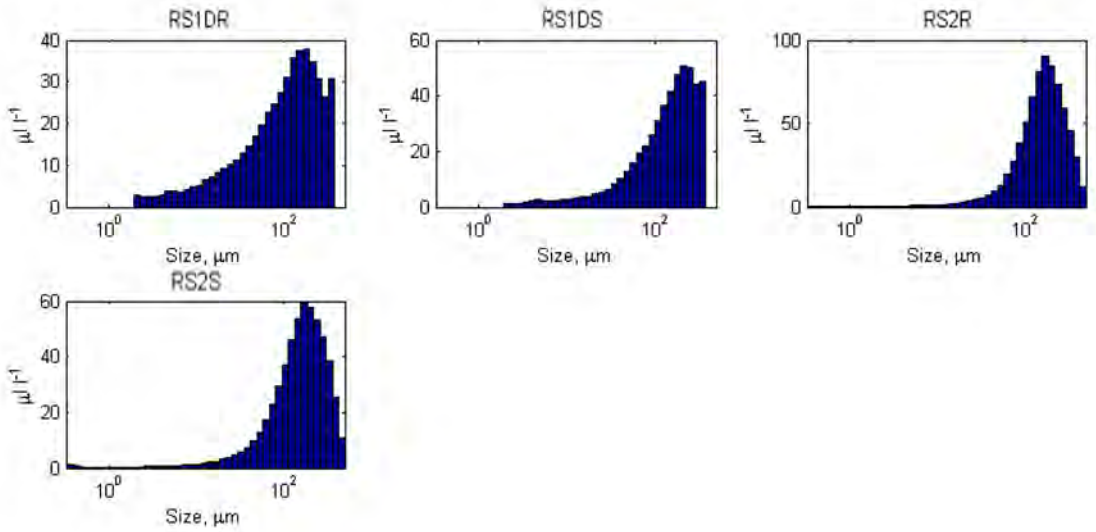

Figure E-40 Volume weighted distributions of suspended particles for epiphyton samples collected November 6, 2014.

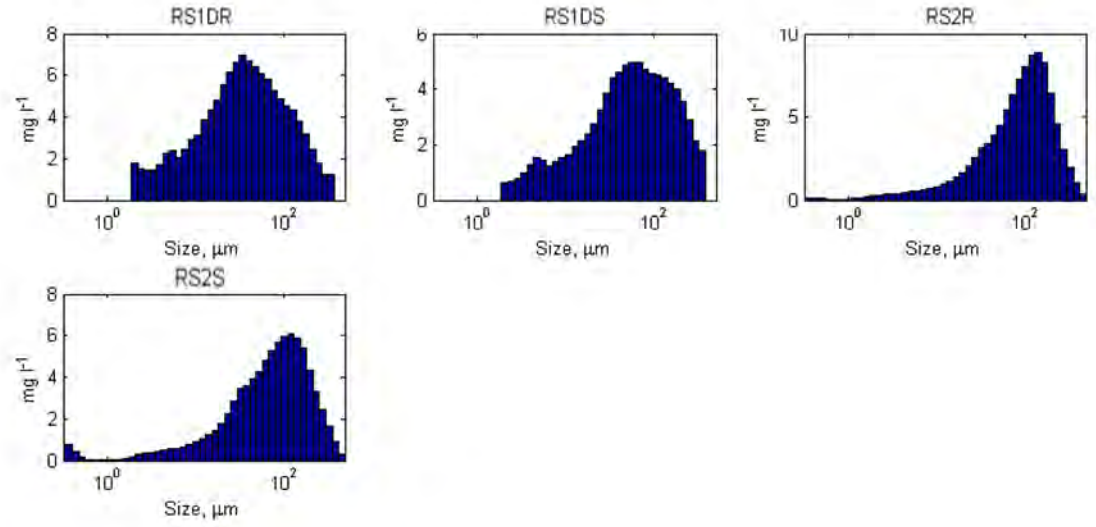

Figure E-41 Mass weighted distributions of suspended particles for epiphyton samples collected November 6, 2014.

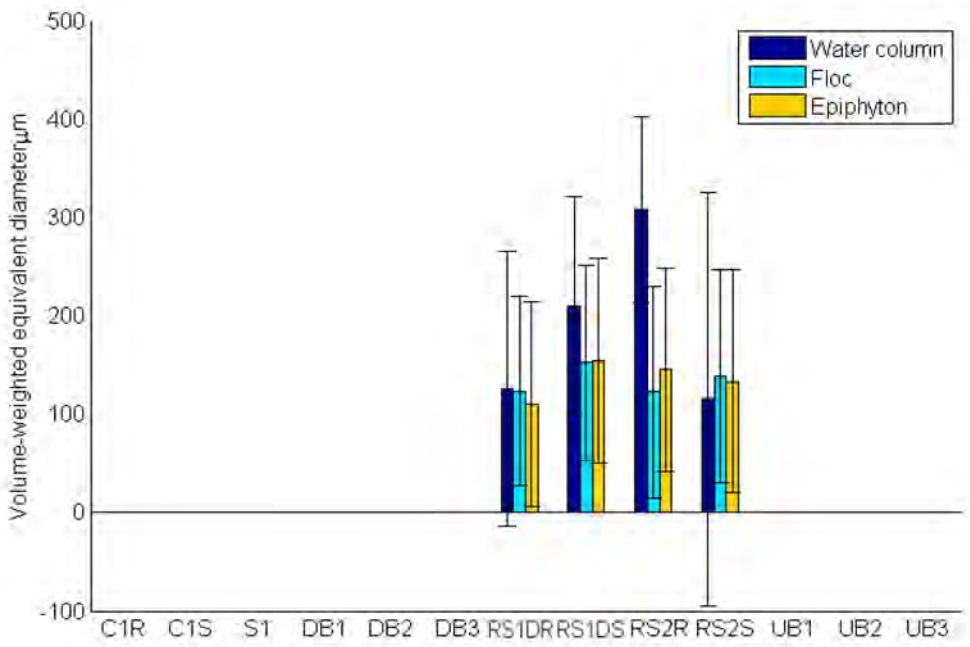

Figure E-42 Comparison of average volume weighted equivalent diameter for each particle type at each DPM site for samples collected November 6, 2014.

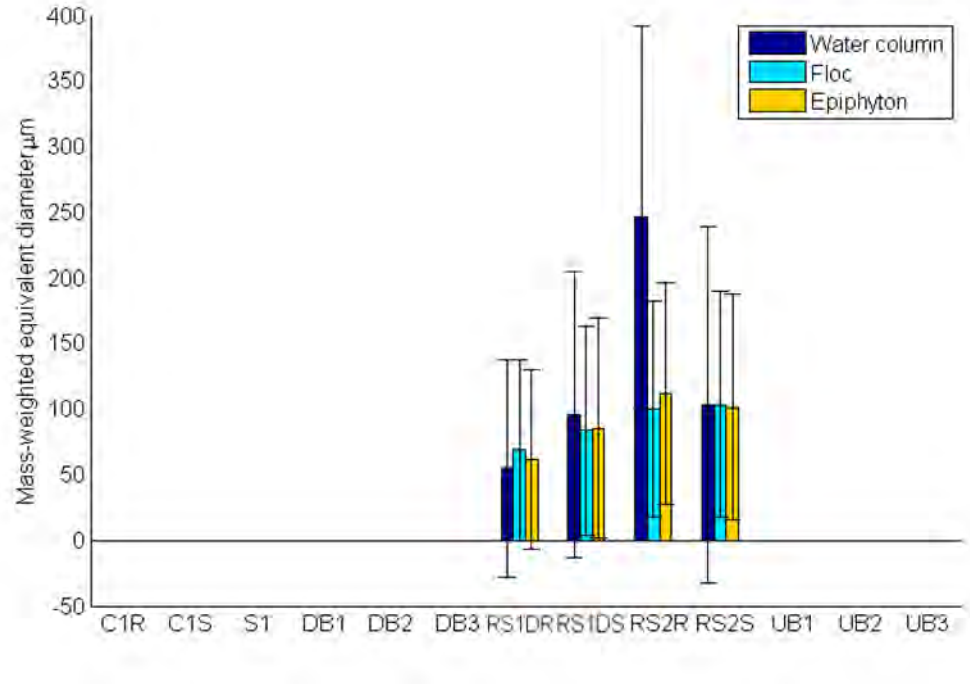

Figure E-43 Comparison of average mass weighted equivalent diameter for each particle type at each DPM site for samples collected November 6, 2014.

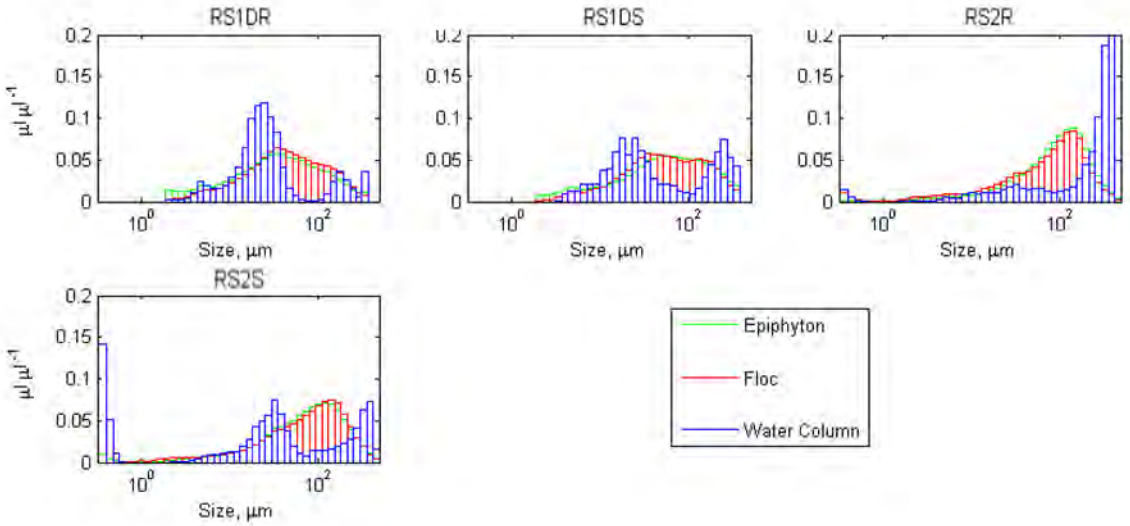

Figure E-44 Comparison of volumetric fraction distributions of Water Column, Floc and Epiphyton by size at each DPM site for samples collected November 6, 2014.

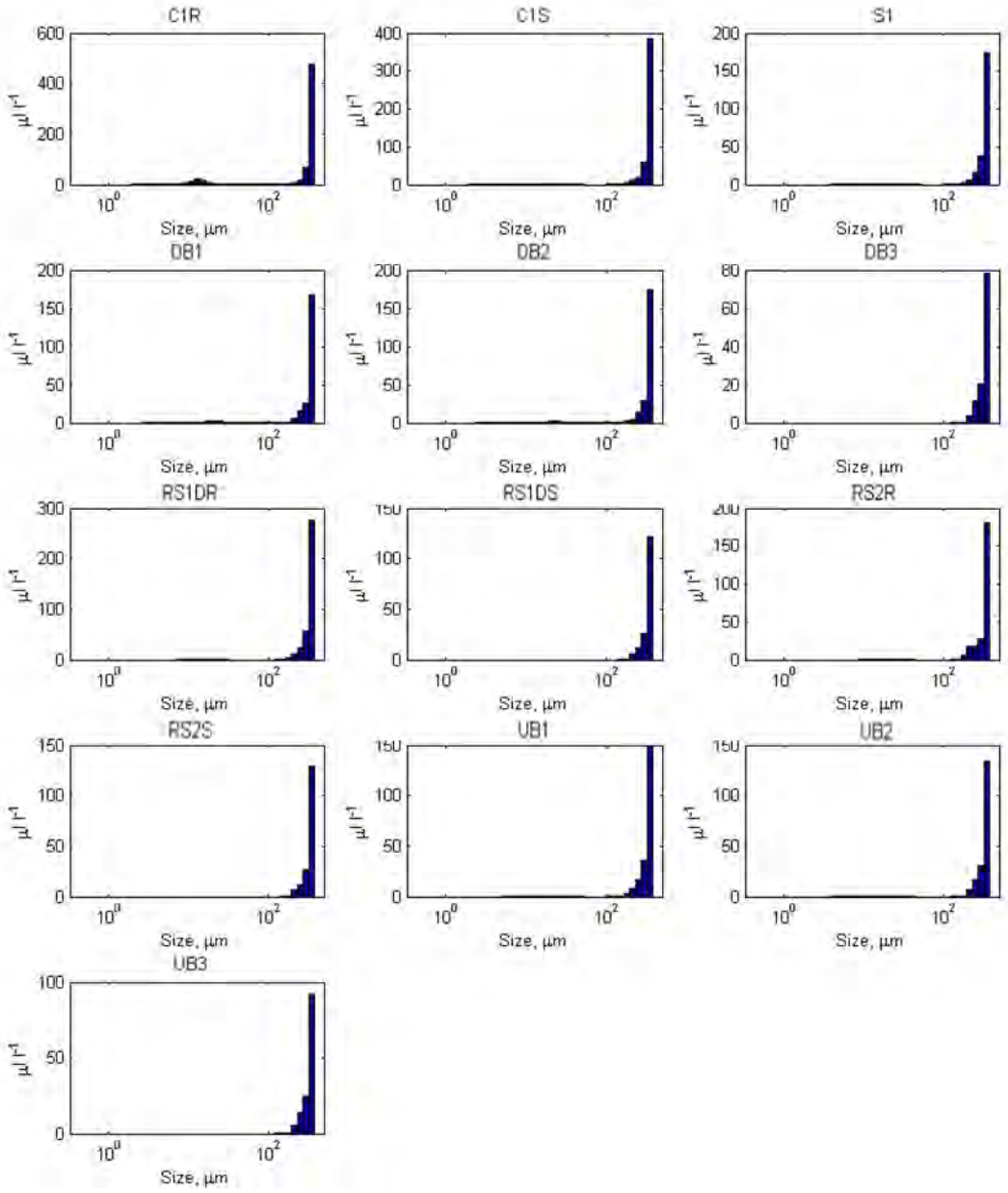

Figure E-45 Volume weighted distributions of suspended particles for water column samples collected January 19-22, 2015.

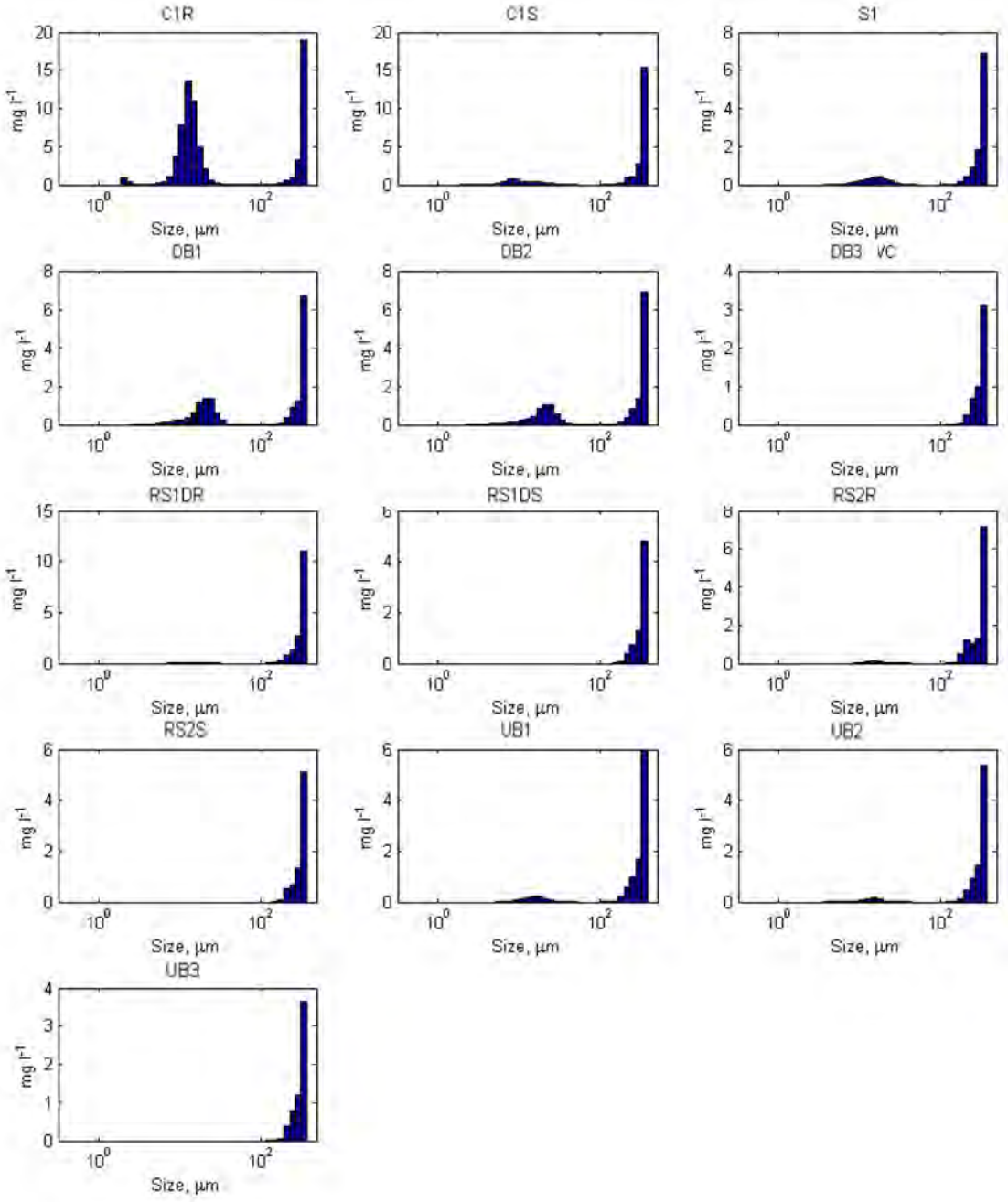

Figure E-46 Mass weighted distributions of suspended particles for water column samples collected January 19-22, 2015.

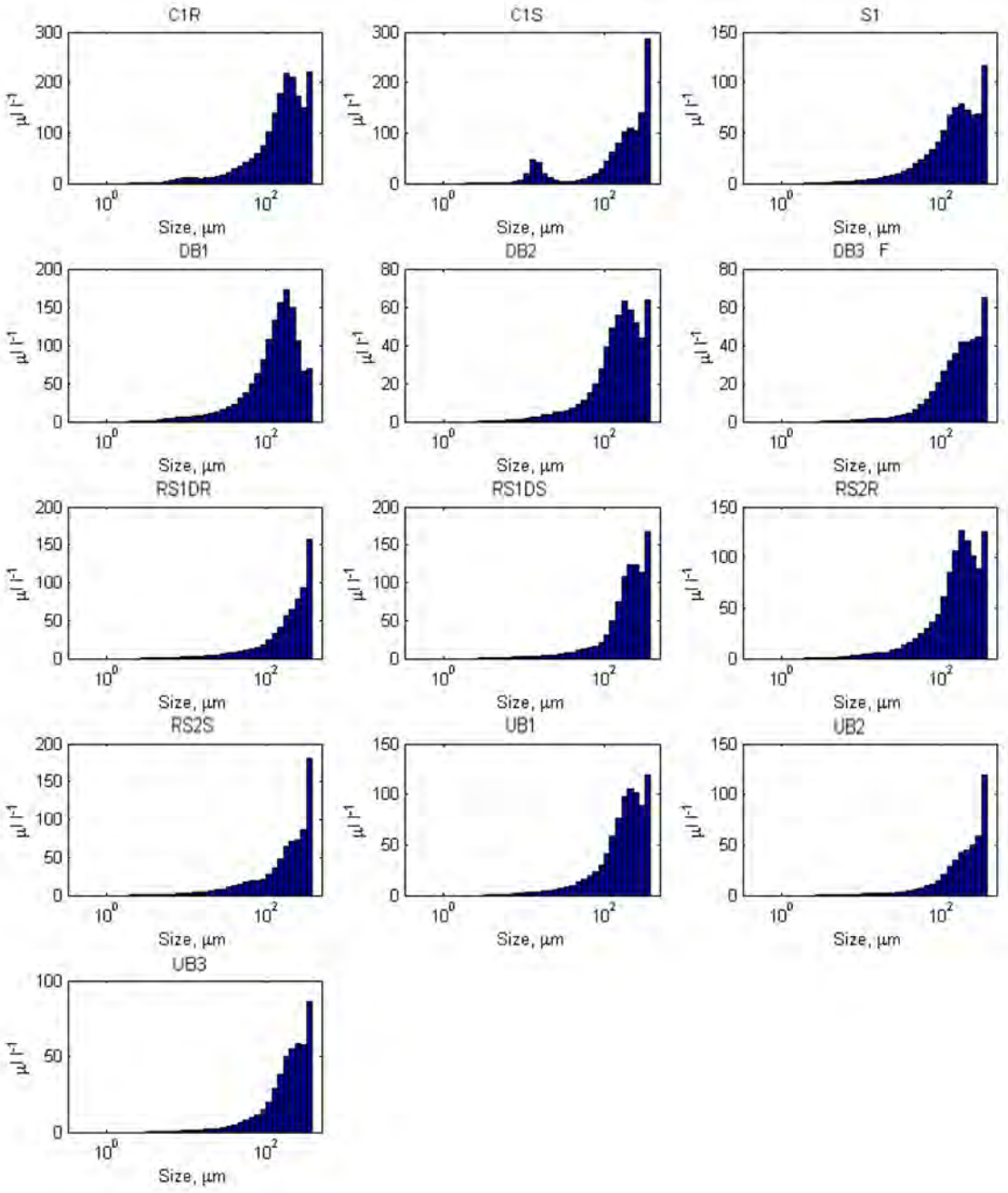

Figure E-47 Volume weighted distributions of suspended particles for floc samples collected January 19-22, 2015.

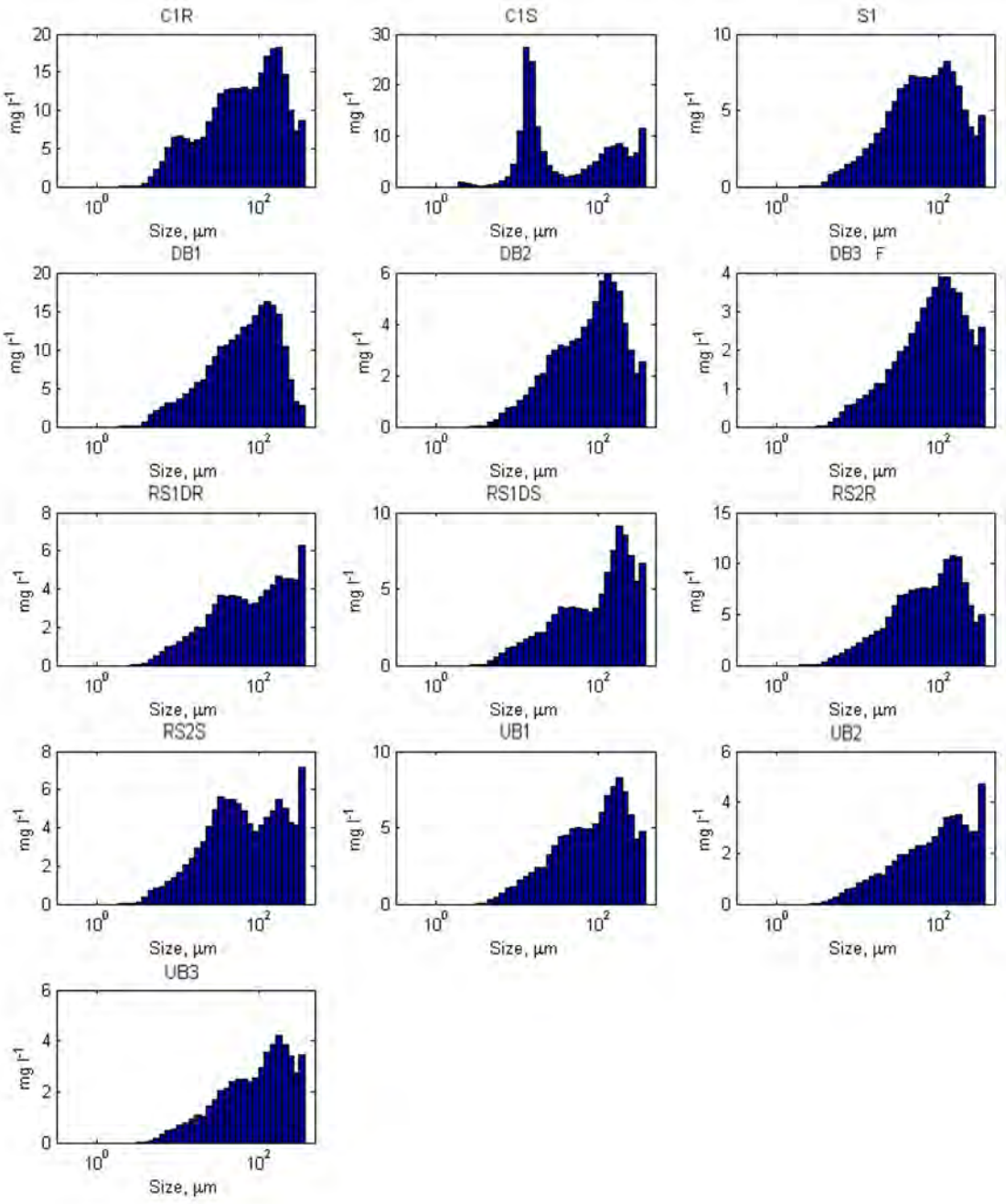

Figure E-48 Mass weighted distributions of suspended particles for floc samples collected January 19-22, 2015.

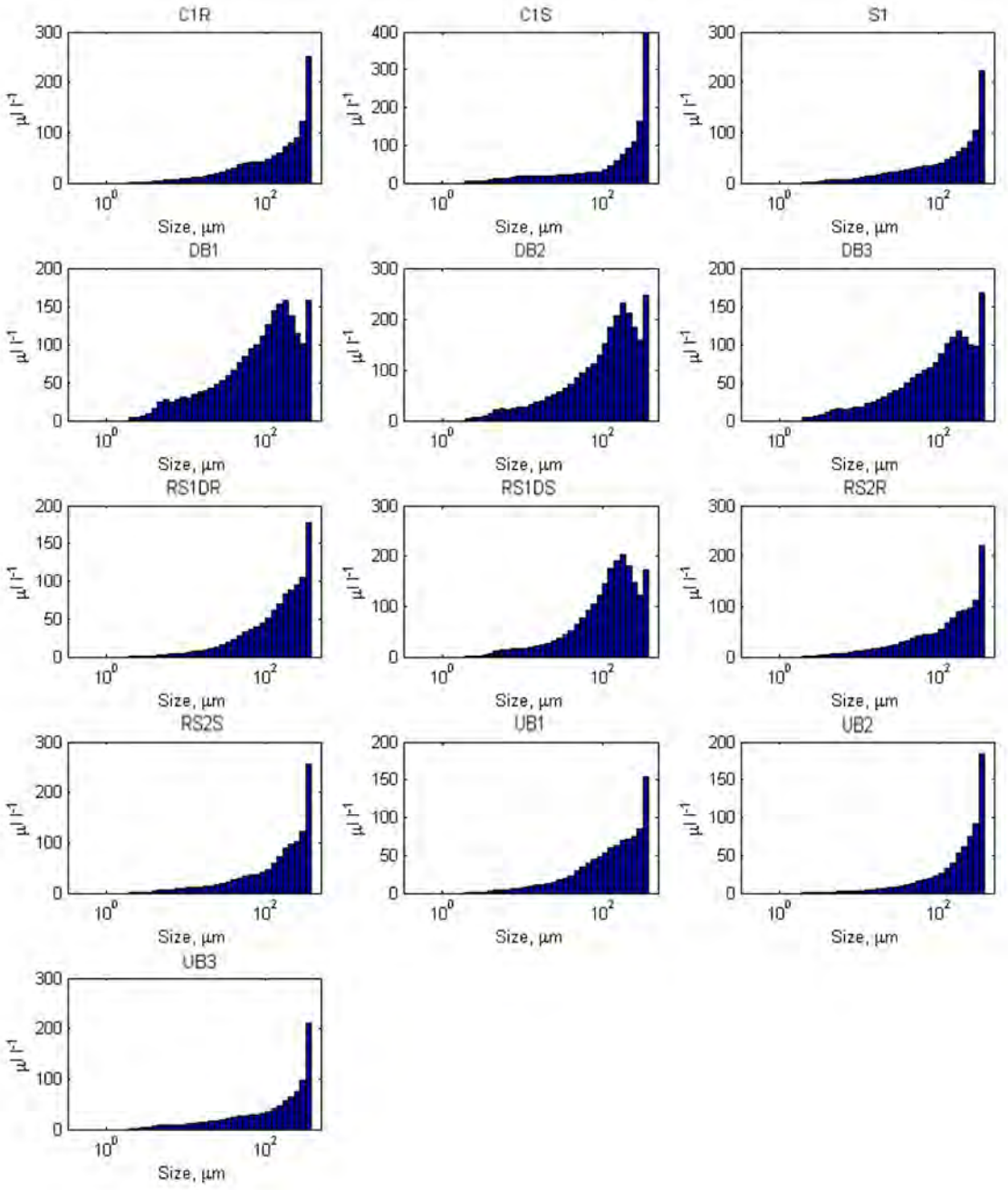

Figure E-49 Volume weighted distributions of suspended particles for epiphyton samples collected January 19-22, 2015.

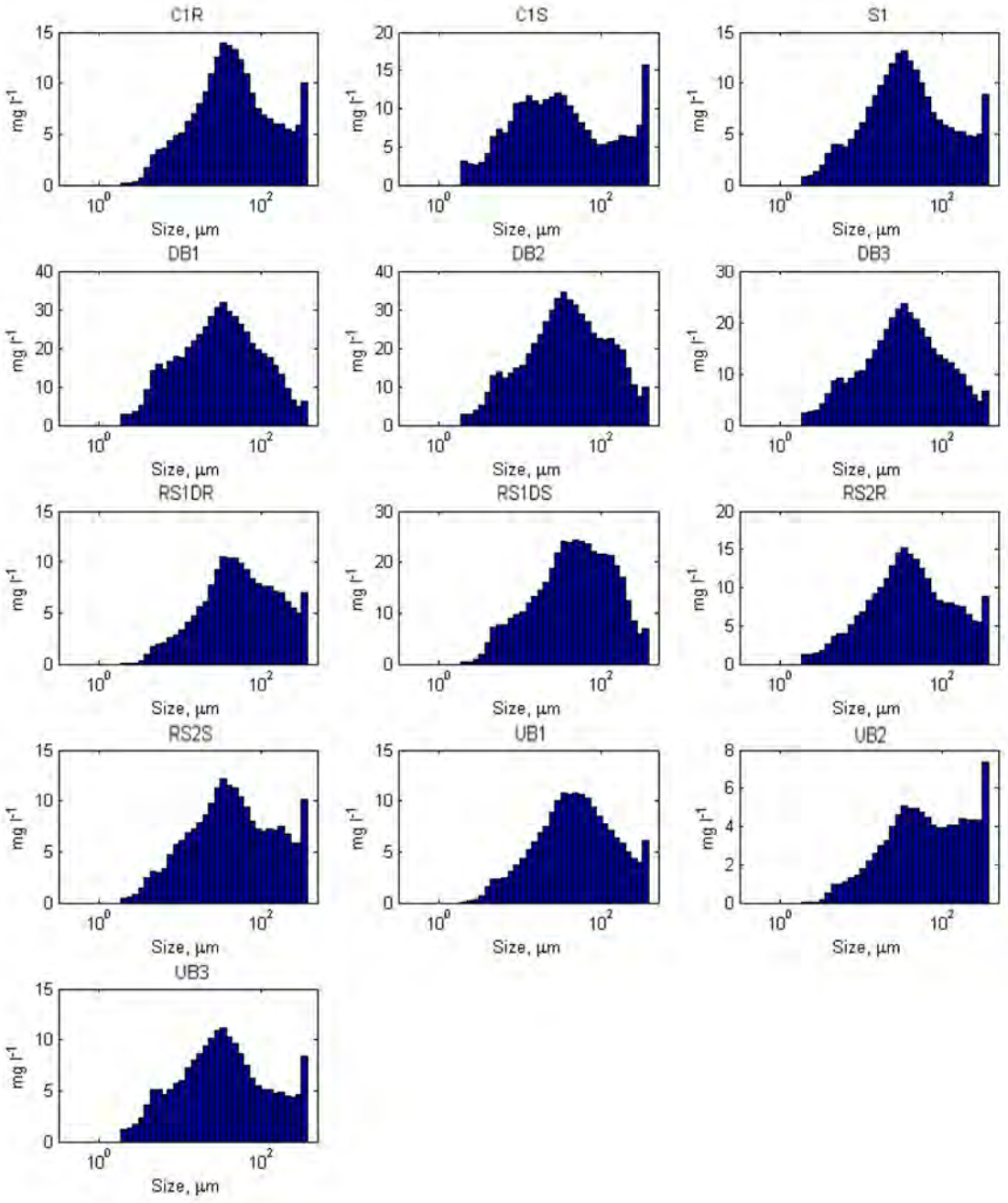

Figure E-50 Mass weighted distributions of suspended particles for epiphyton samples collected January 19-22, 2015.

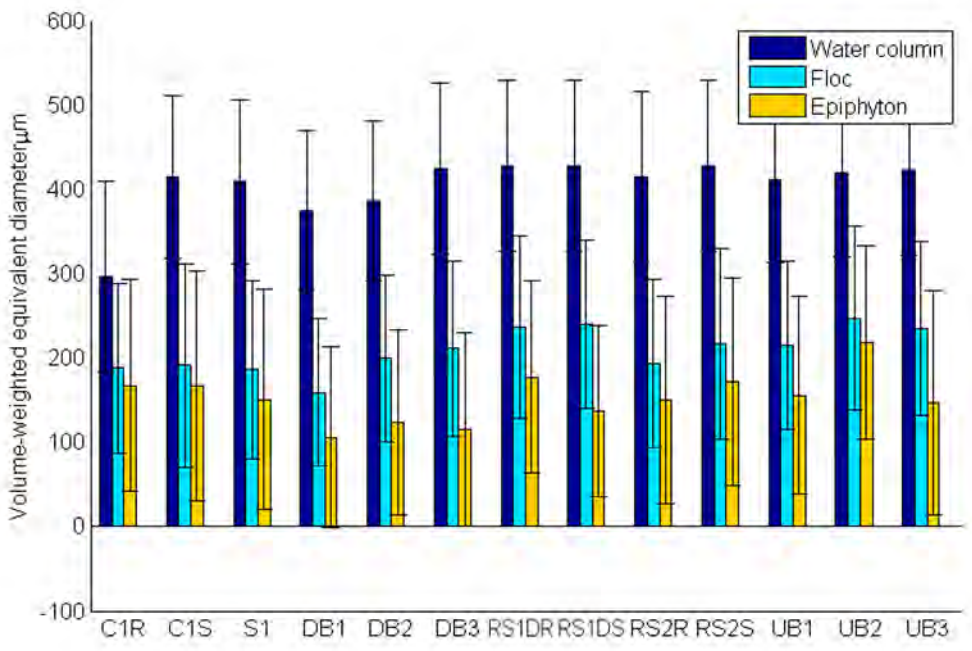

Figure E-51 Comparison of average volume weighted equivalent diameter for each particle type at each DPM site for samples collected January 19-22, 2015.

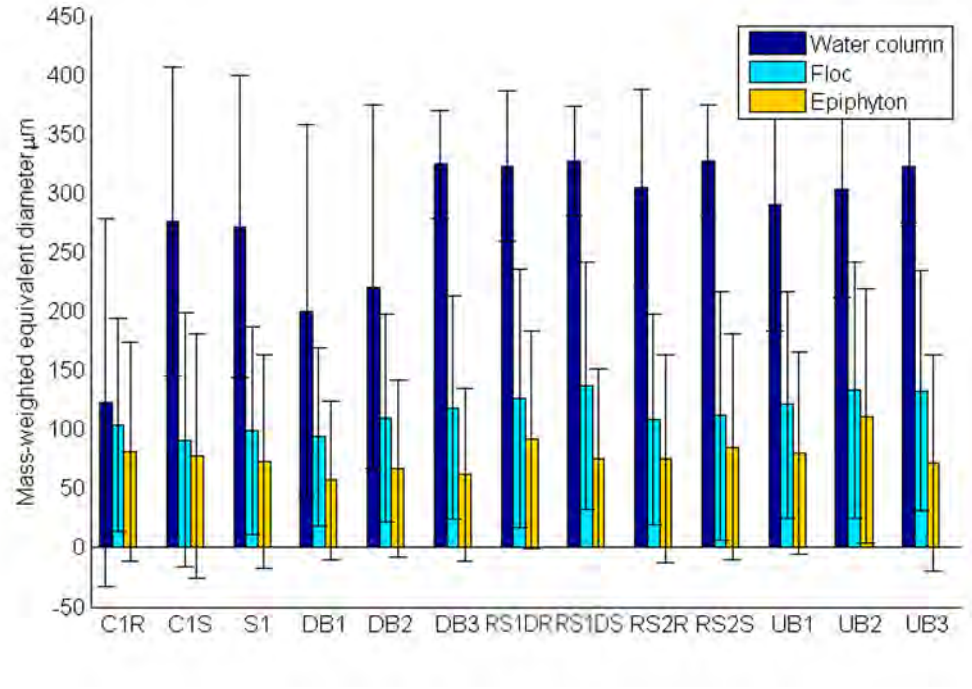

Figure E-52 Comparison of average mass weighted equivalent diameter for each particle type at each DPM site for samples collected January 19-22, 2015.

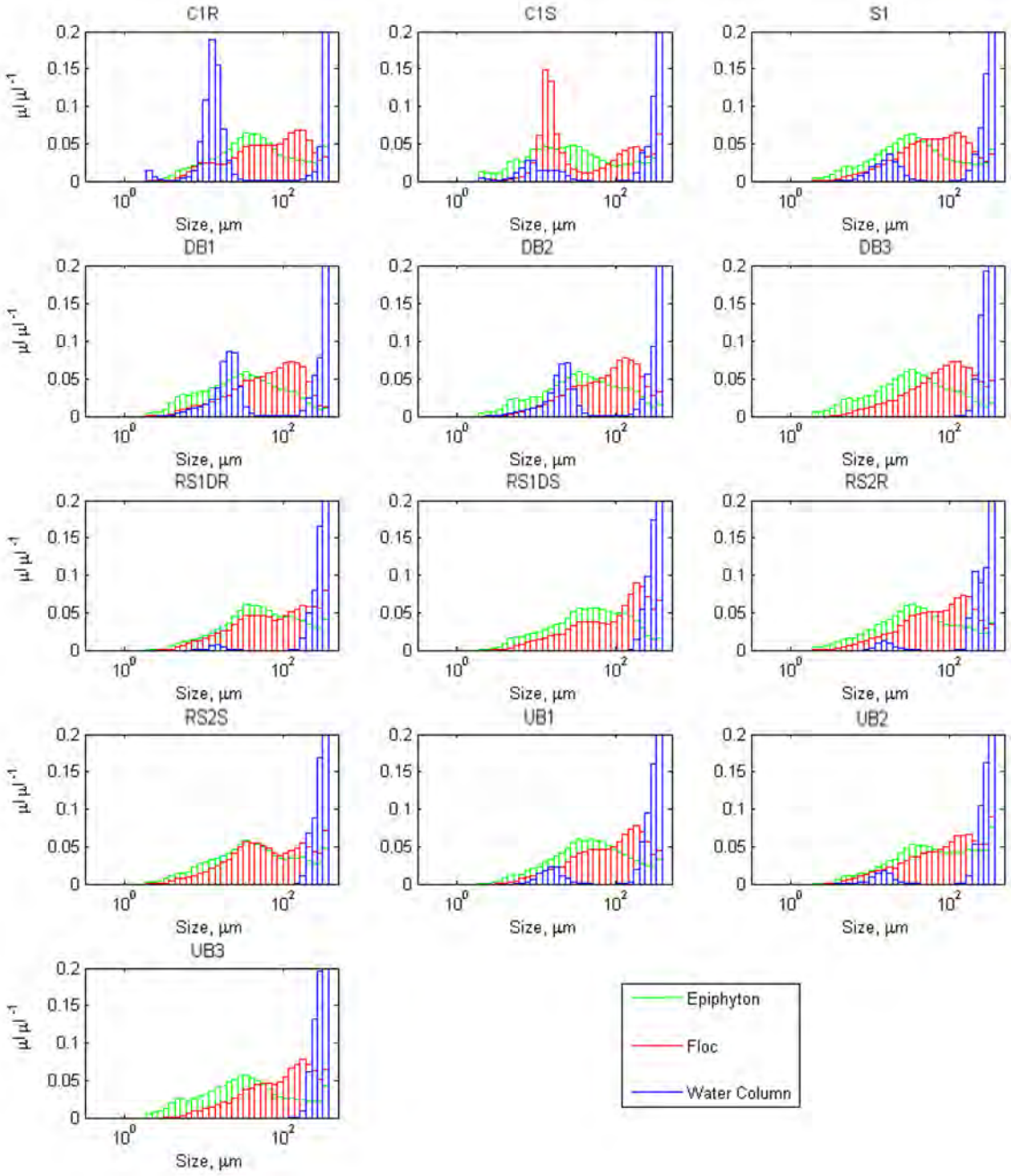

Figure E-53 Comparison of volumetric fraction distributions of Water Column, Floc and Epiphyton by size at each DPM site for samples collected January 19-22, 2015.

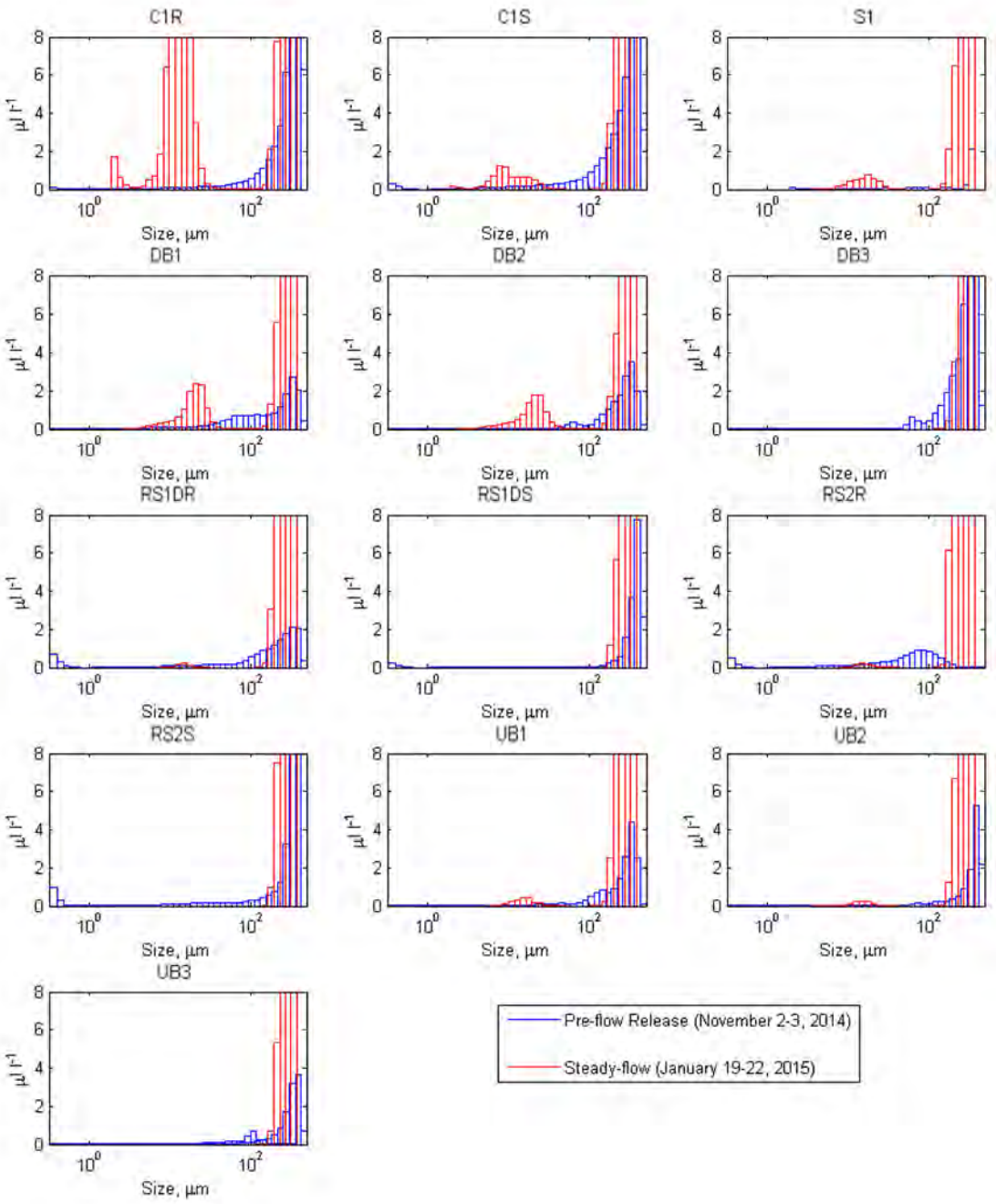

Figure E-54 Pre-flow release and steady-flow comparison of volume weighted distribution of water column suspended particles. Samples collected during the 2014 DPM flow release.

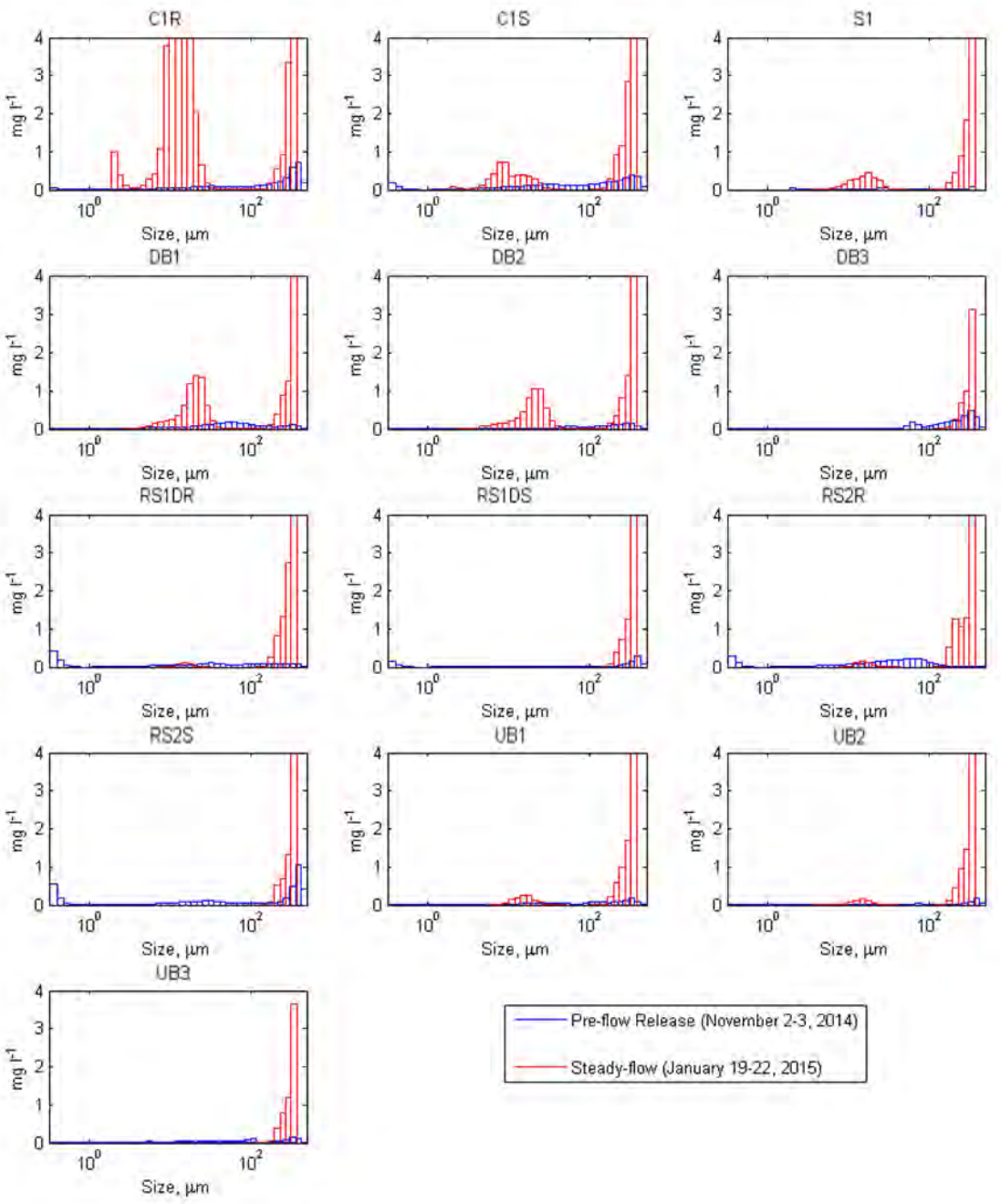

Figure E-55 Pre-flow release and steady-flow comparison of mass weighted distribution of water column suspended particles. Samples collected during the 2014 DPM flow release.

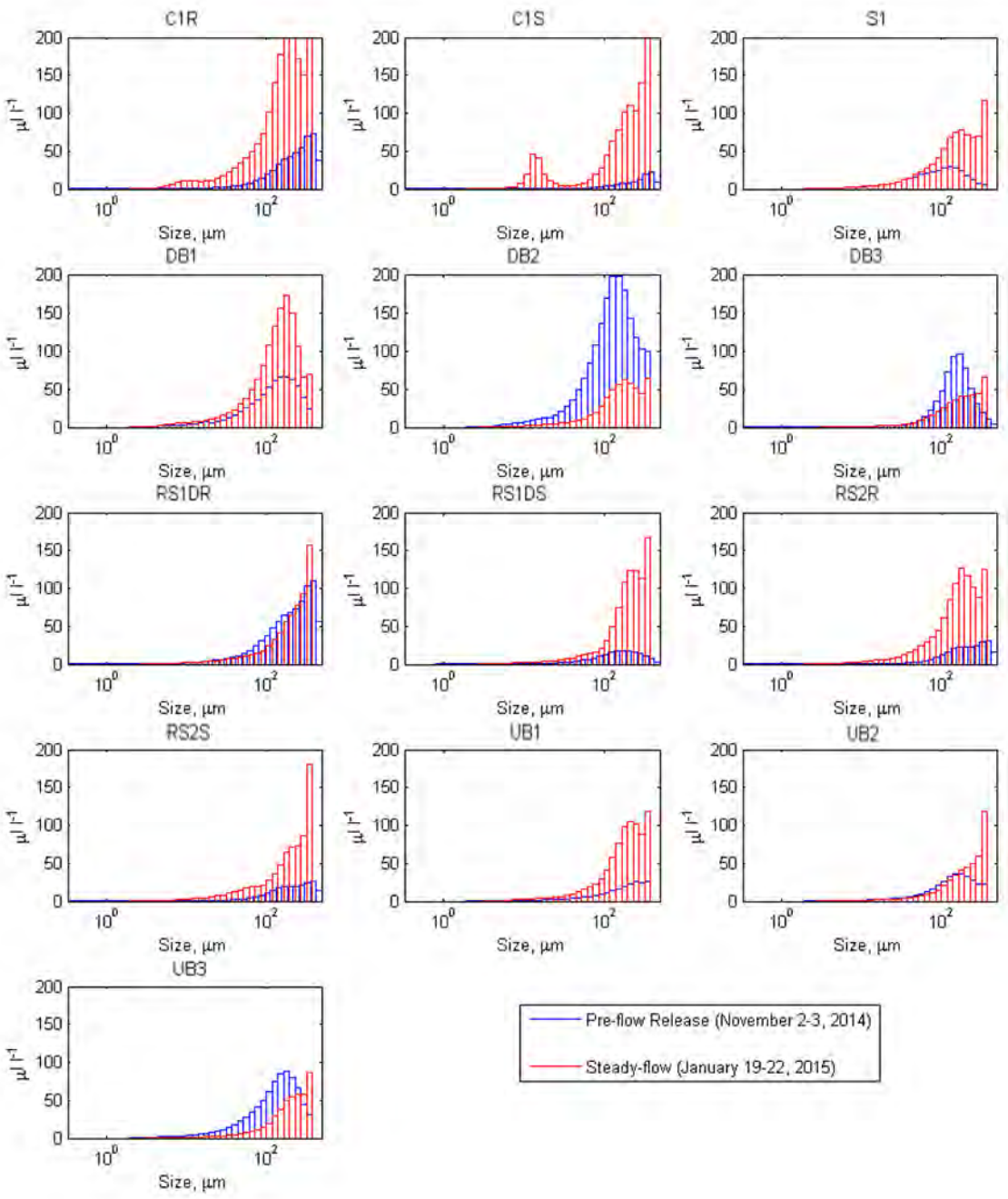

Figure E-56 Pre-flow release and steady-flow comparison of volume weighted distribution of floc suspended particles. Samples collected during the 2014 DPM flow release.

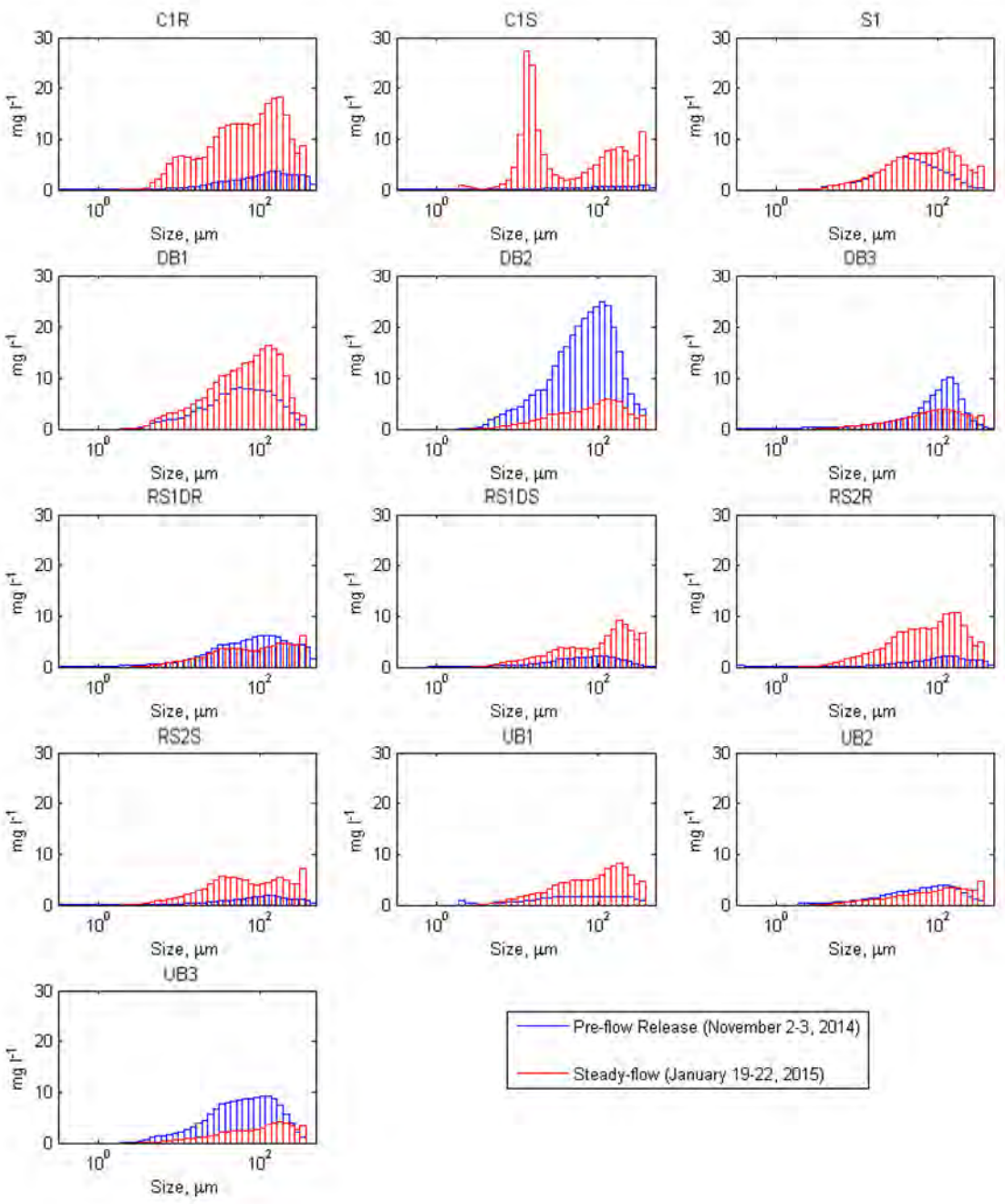

Figure E-57 Pre-flow release and steady-flow comparison of mass weighted size distribution of floc suspended particles. Samples collected during the 2014 DPM flow release.

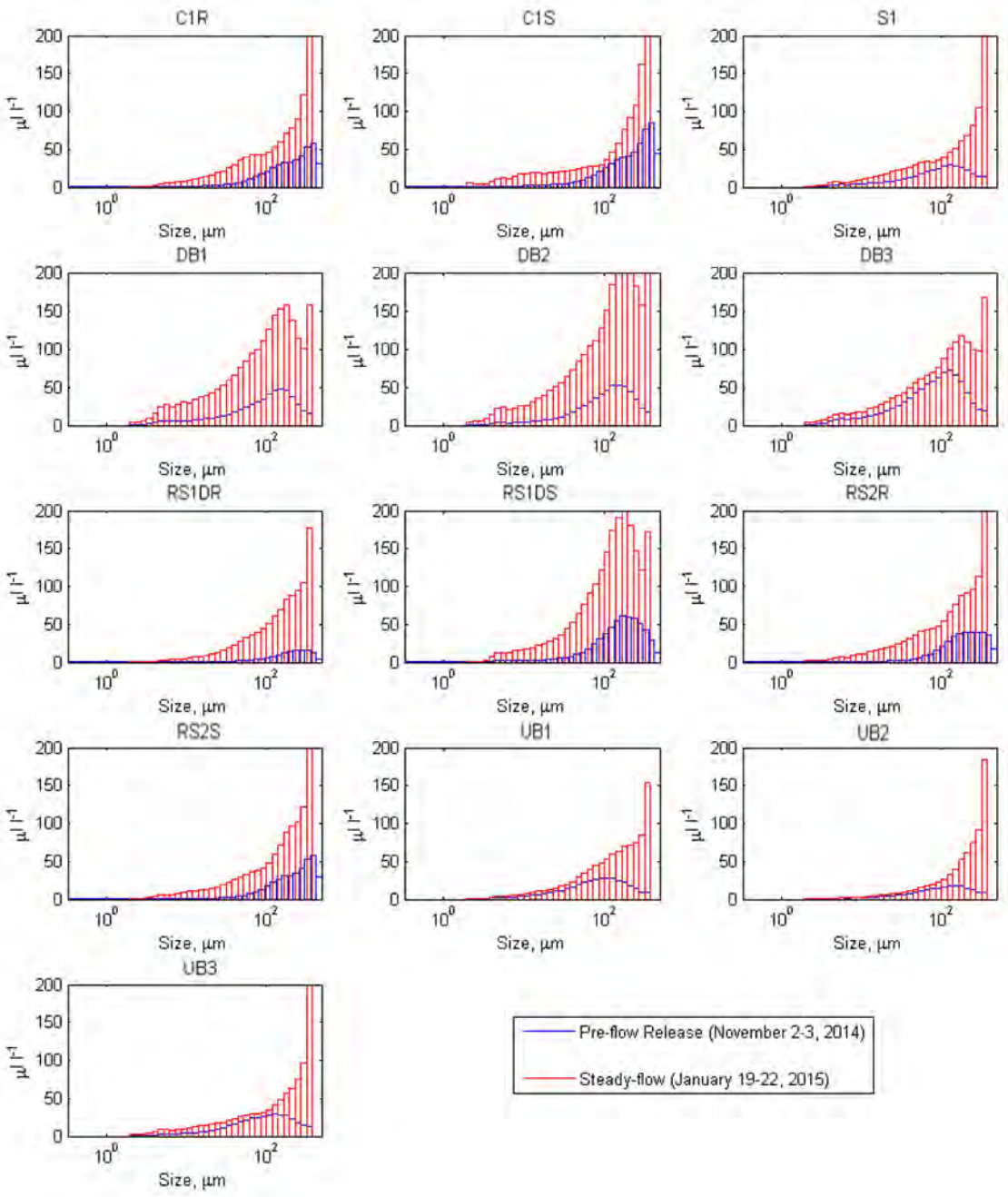

Figure E-58 Pre-flow release and steady-flow comparison of volume weighted distribution of epiphyton suspended particles. Samples collected during the 2014 DPM flow release.

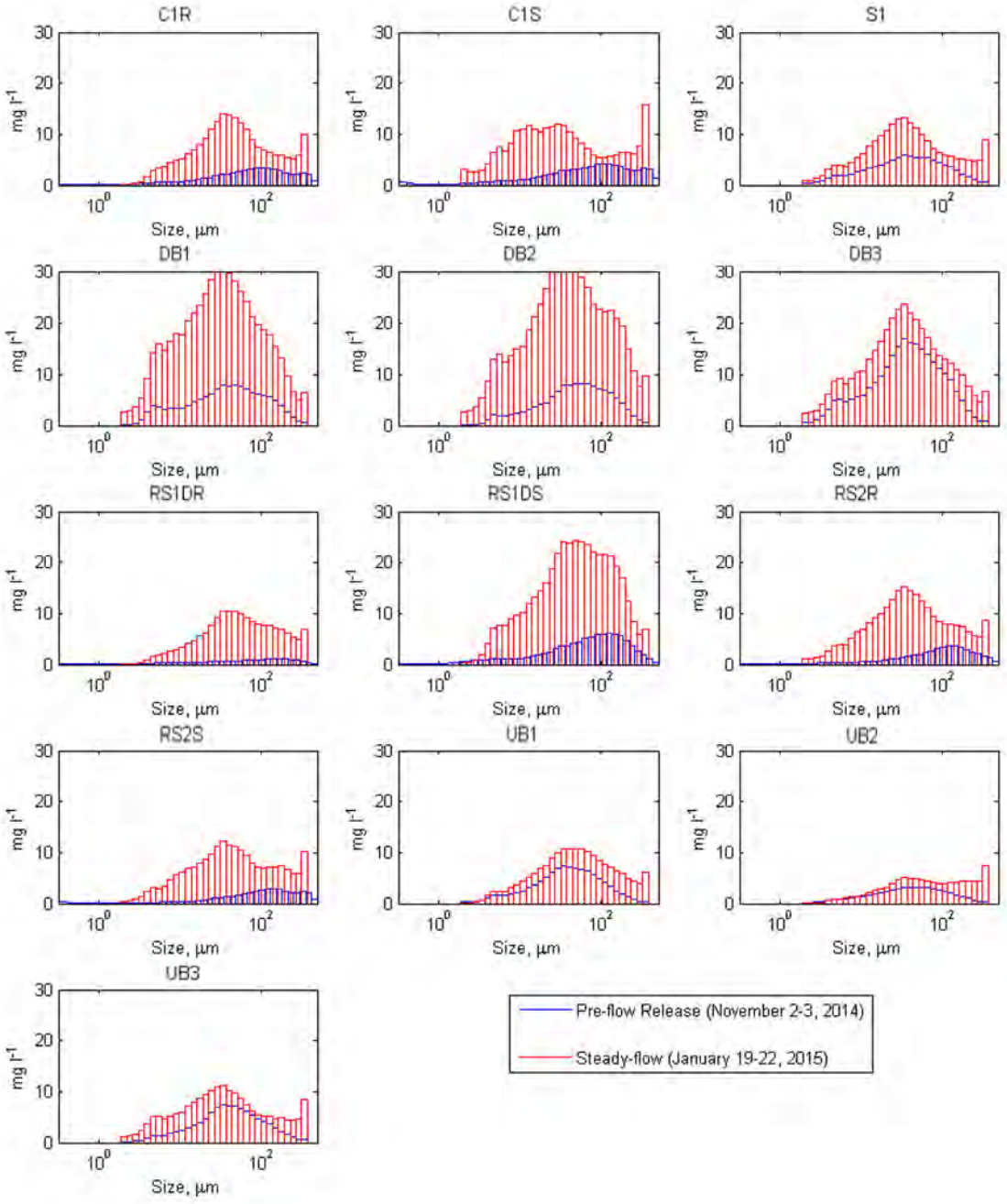

Figure E-59 Pre-flow release and steady-flow comparison of mass weighted distribution of epiphyton suspended particles. Samples collected during the 2014 DPM flow release.

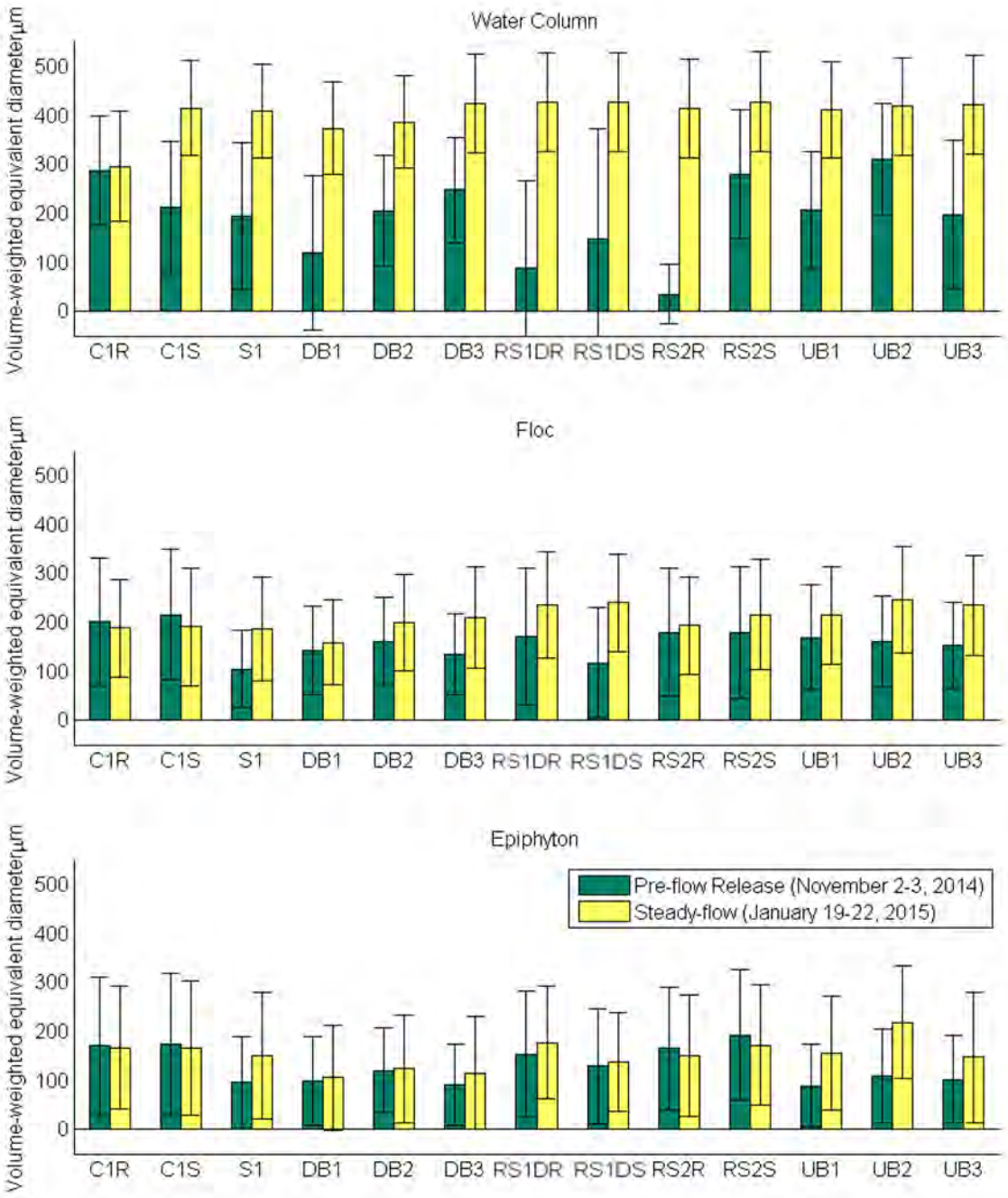

Figure E-60 Pre-flow release and steady-flow comparison of average volume weighted equivalent diameter for each particle type from all DPM sites, samples collected during the 2014 DPM flow release.

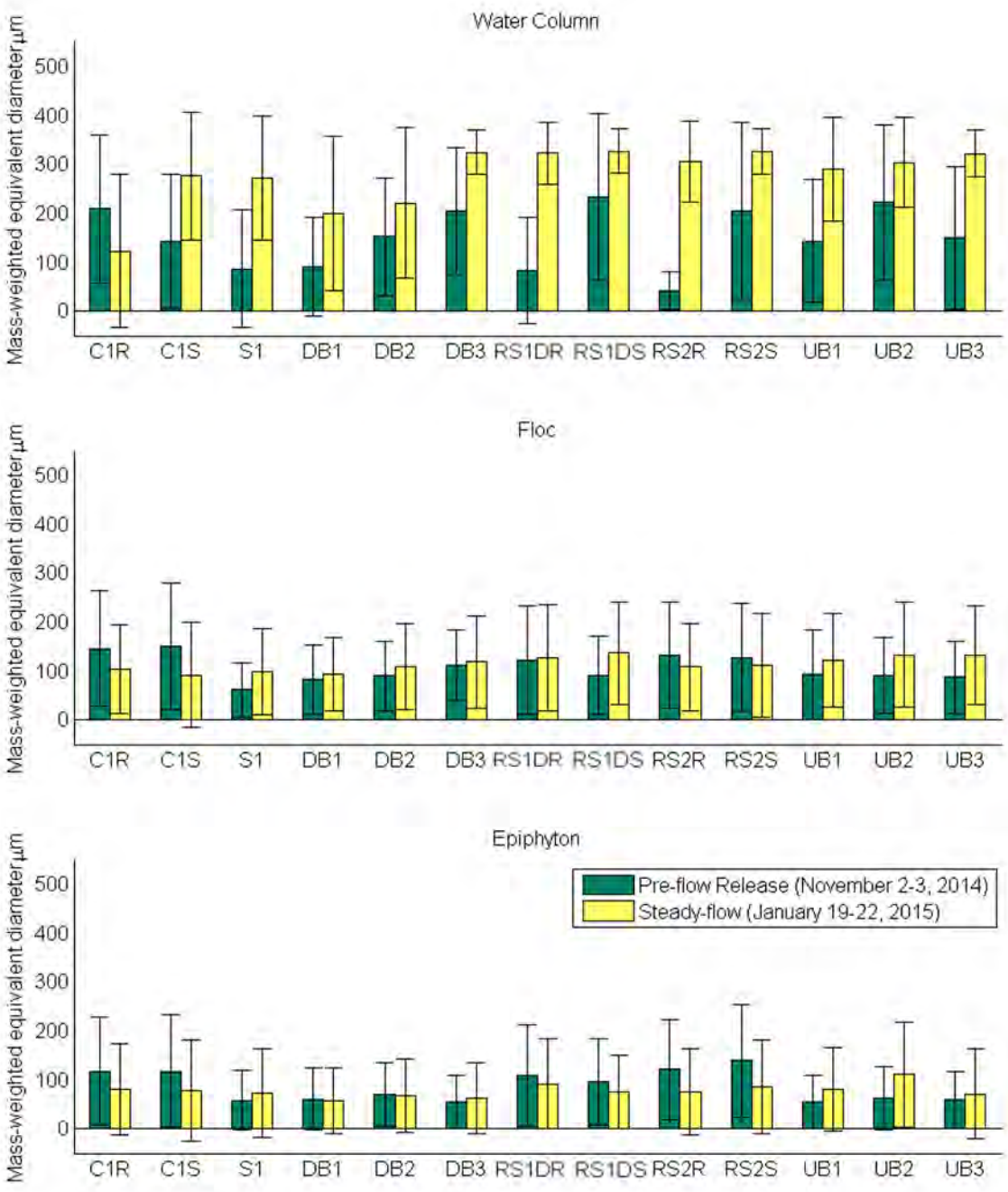

Figure E-61 Pre-flow release and steady-flow release comparison of average mass weighted equivalent diameter for each particle type from all DPM sites, samples collected during the 2014 DPM flow release.

2014 Flow Release

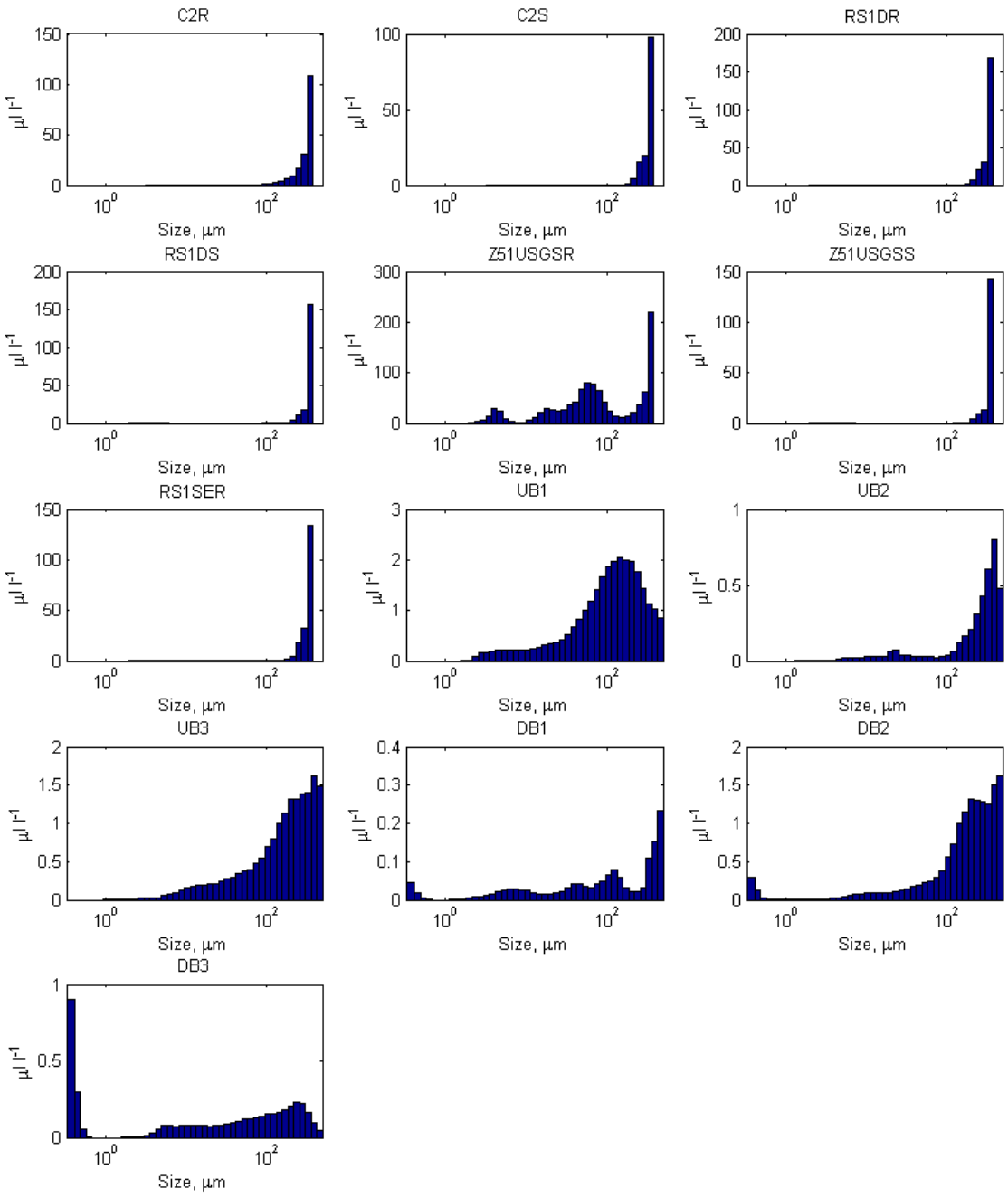

Figure E-62 Volume weighted distributions of suspended particles for water column samples collected November 12-14, 2015.

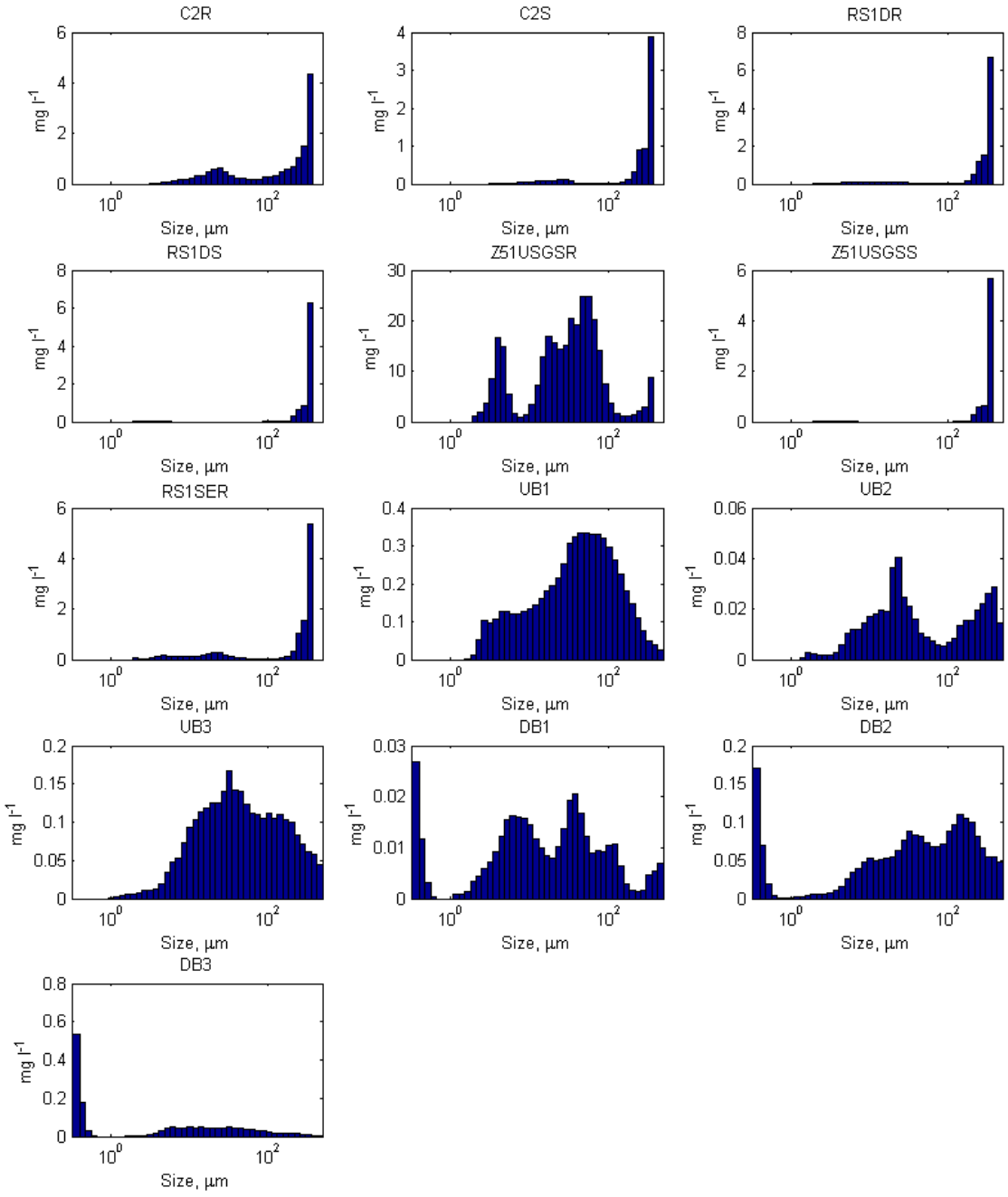

Figure E-63 Mass weighted distributions of suspended particles for water column samples collected November 12-14, 2015.

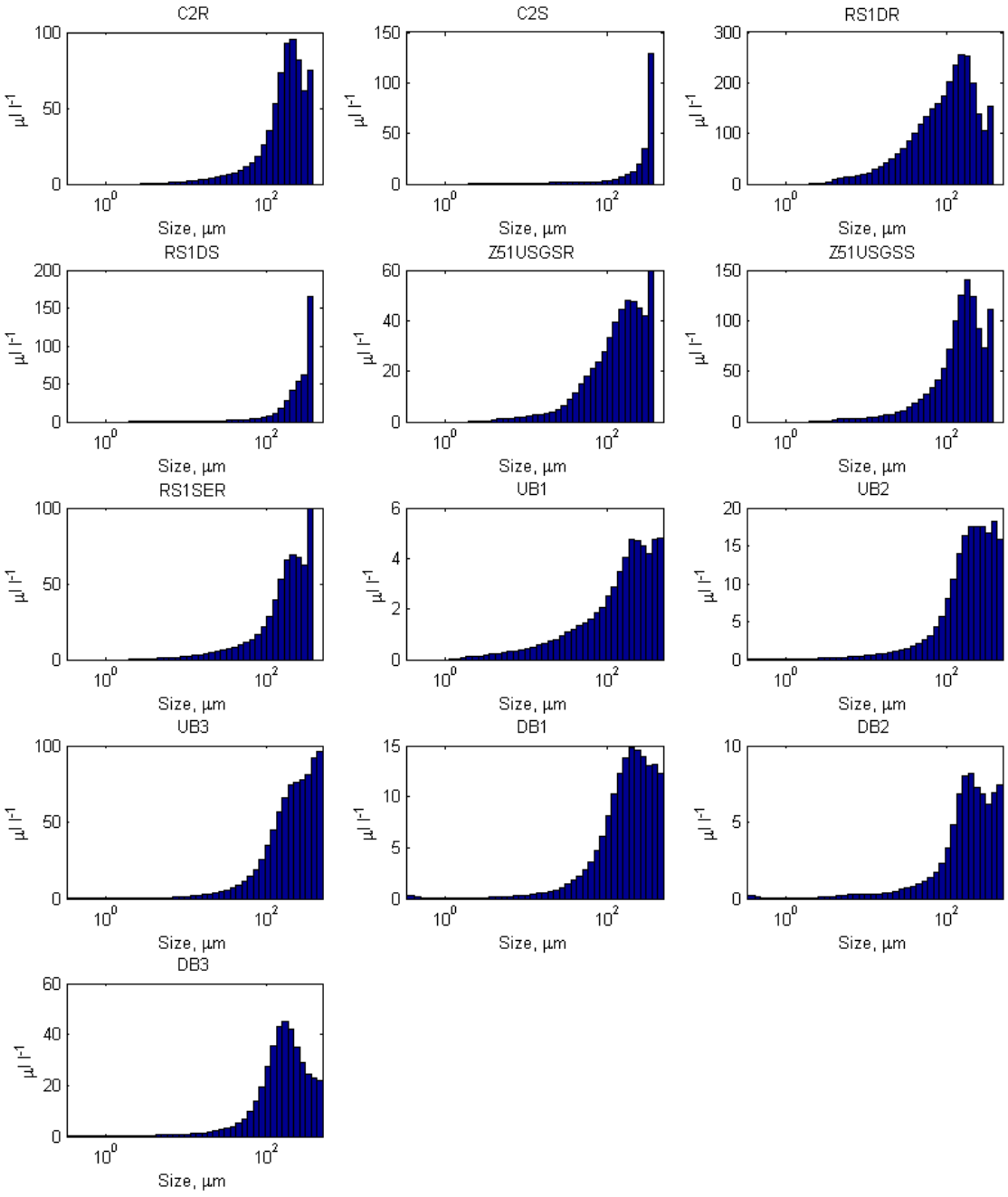

Figure E-64 Volume weighted distributions of suspended particles for floc samples collected November 12-14, 2015.

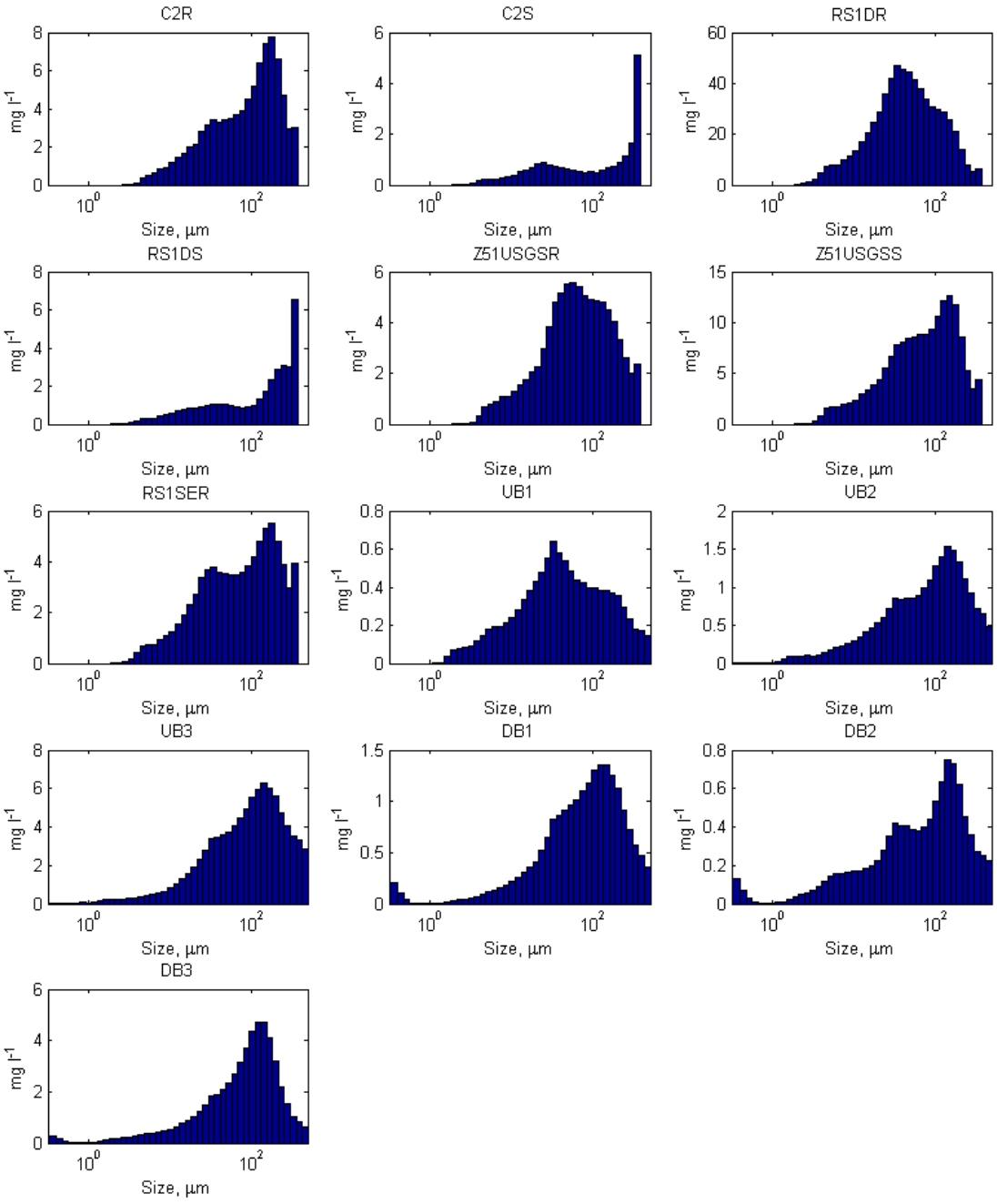

Figure E-65. Mass weighted distributions of suspended particles for floc samples collected November 12-14, 2015.

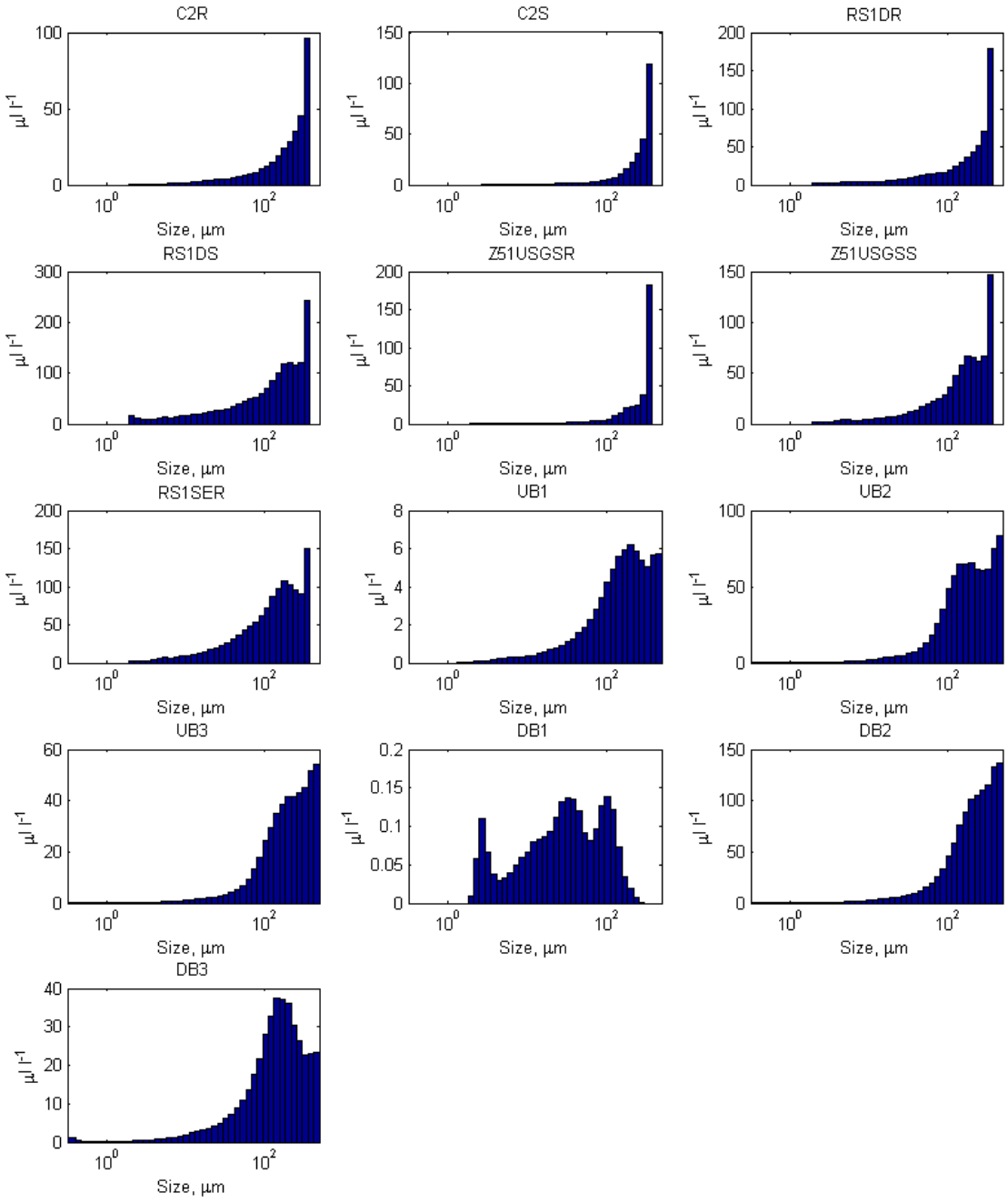

Figure E-66 Volume weighted distributions of suspended particles for epiphyton samples collected November 12-14, 2015.

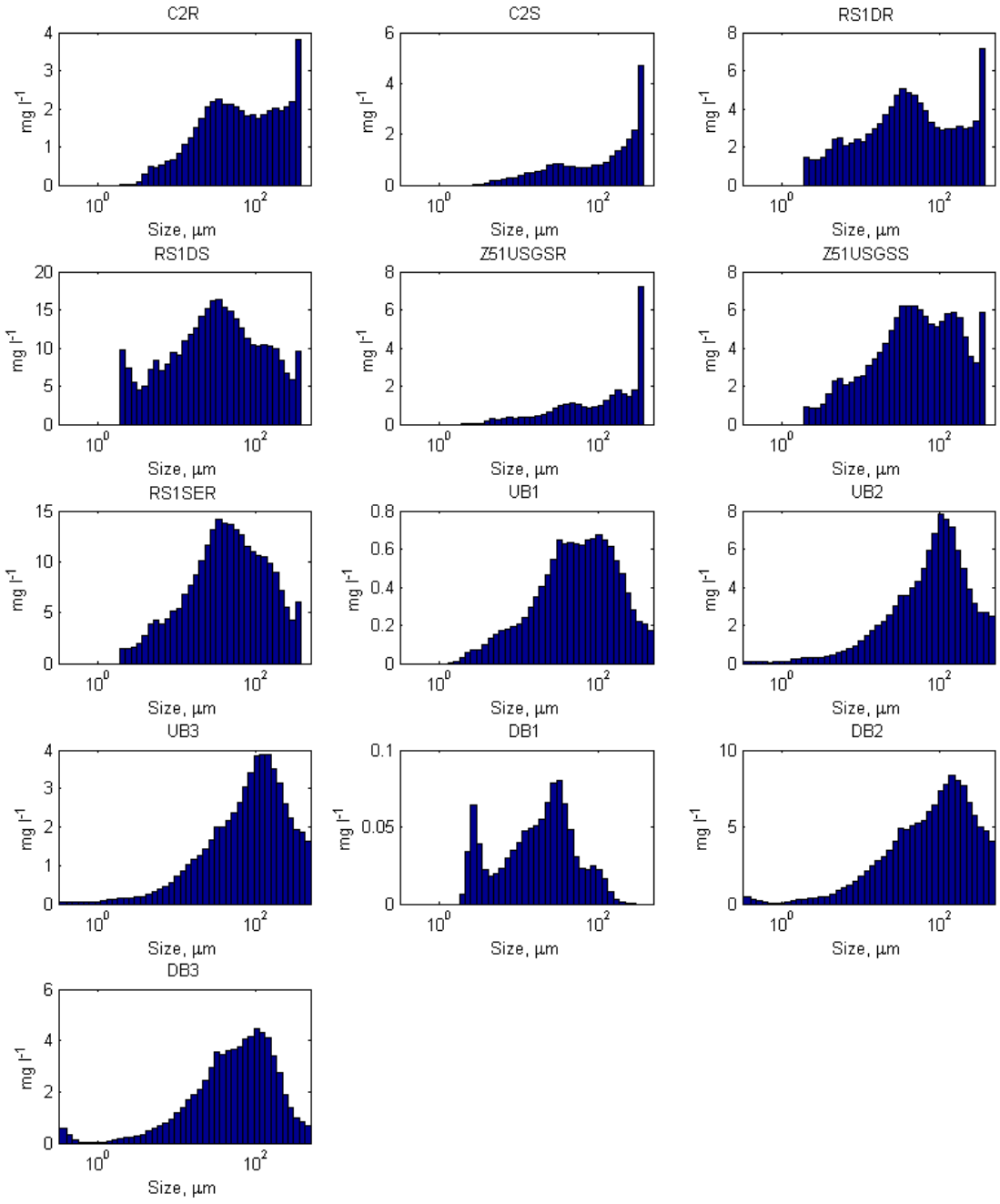

Figure E-67 Mass weighted distributions of suspended particles for epiphyton samples collected November 12-14, 2015.

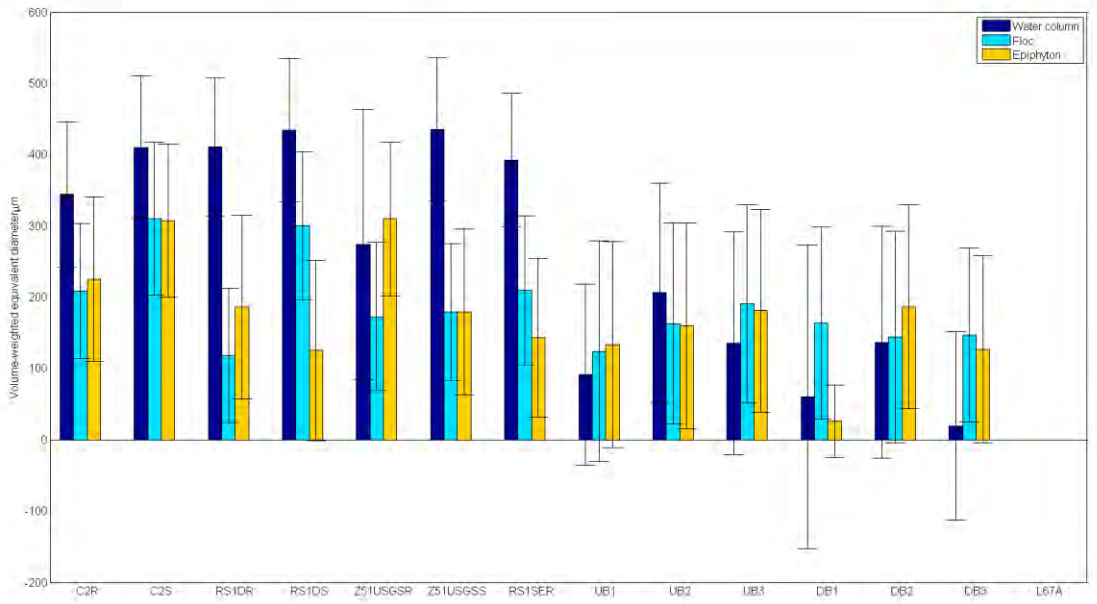

Figure E-68 Comparison of average volume weighted equivalent diameter for each particle type at each DPM site for samples collected November 12-14, 2015.

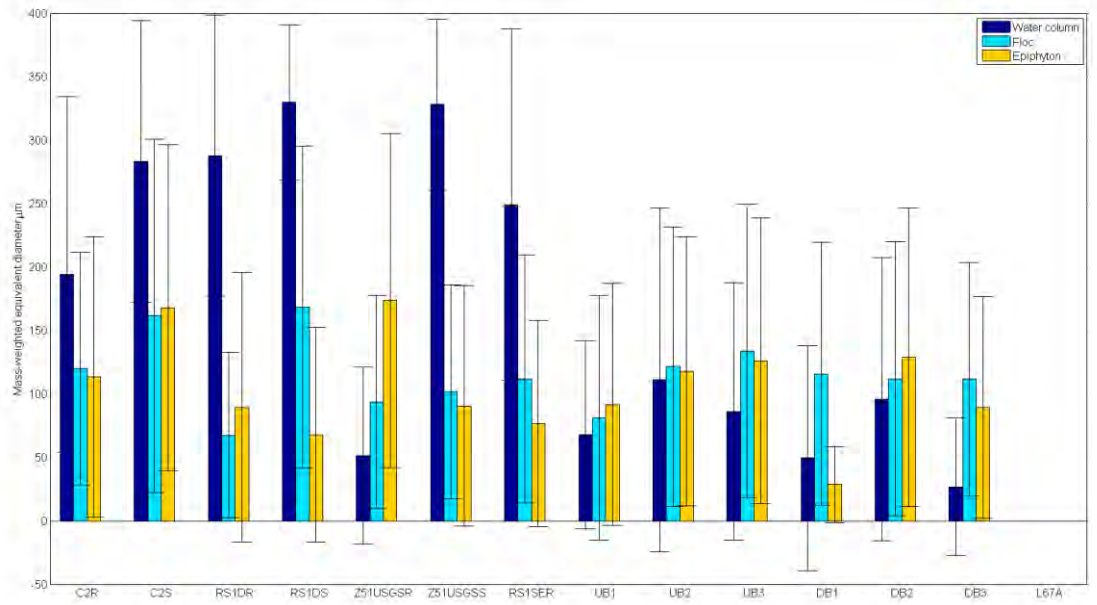

Figure E-69 Comparison of average mass weighted equivalent diameter for each particle type at each DPM site for samples collected November 12-14, 2015.

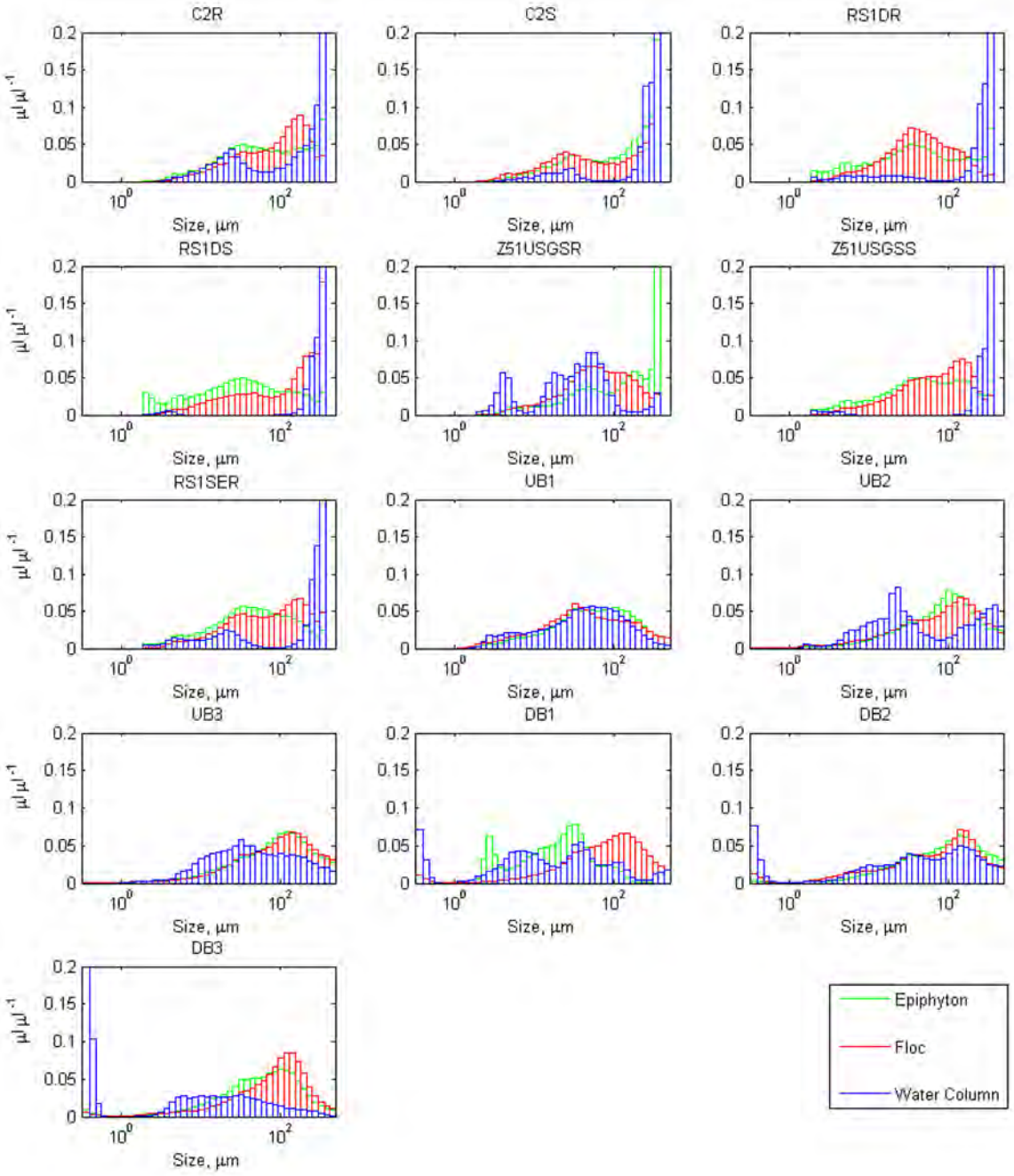

Figure E-70 Comparison of volumetric fraction distributions of Water Column, Floc and Epiphyton by size at each DPM site for samples collected November 12-14, 2015.

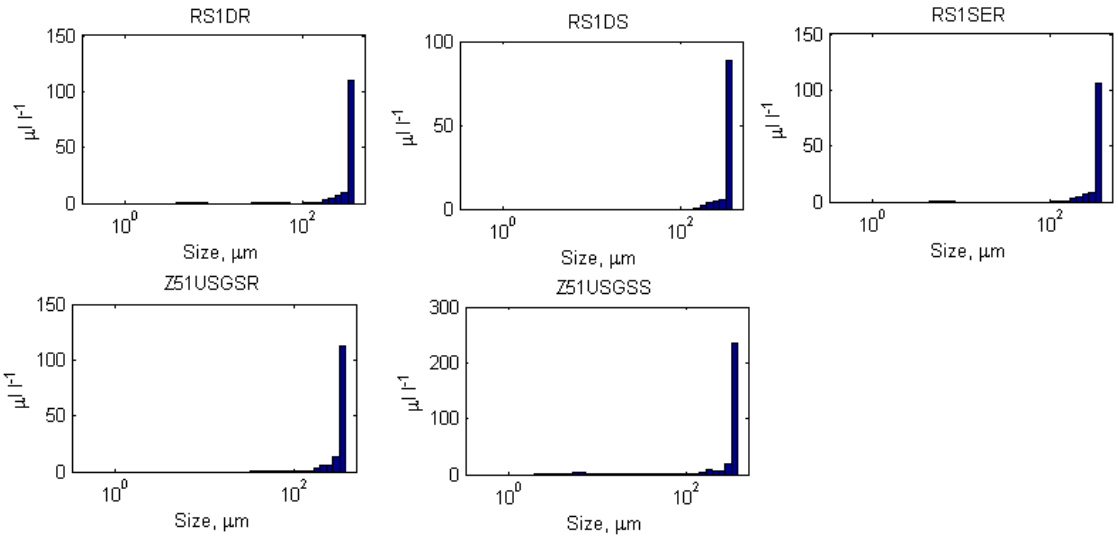

Figure E-71 Volume weighted distributions of suspended particles for water column samples collected November 17, 2015.

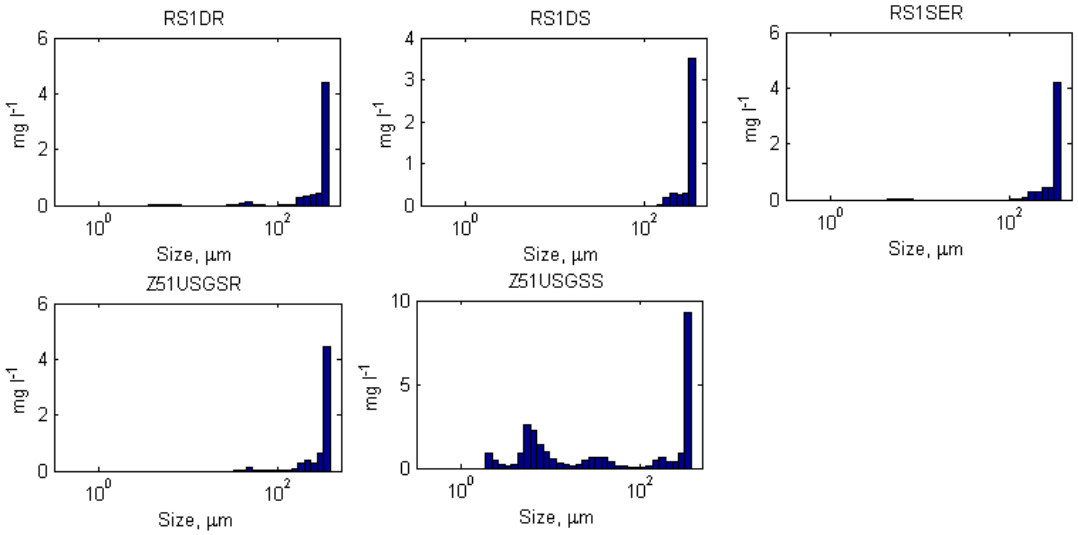

Figure E-72 Mass weighted distributions of suspended particles for water column samples collected November 17, 2015.

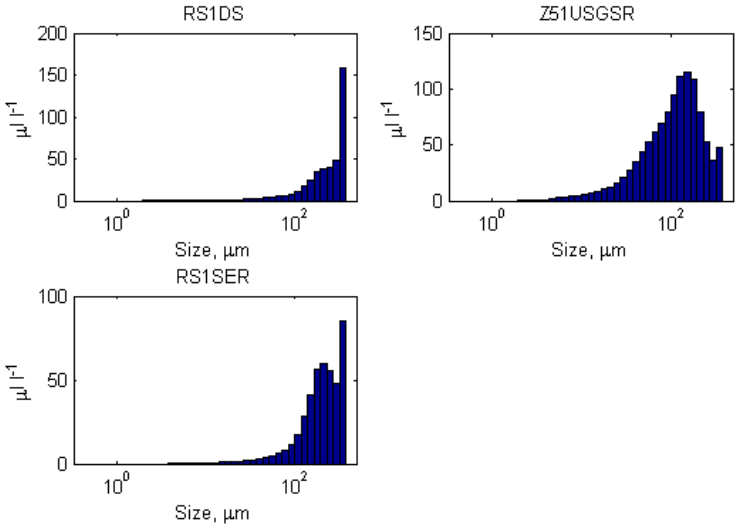

Figure E-73 Volume weighted distributions of suspended particles for floc samples collected November 17, 2015.

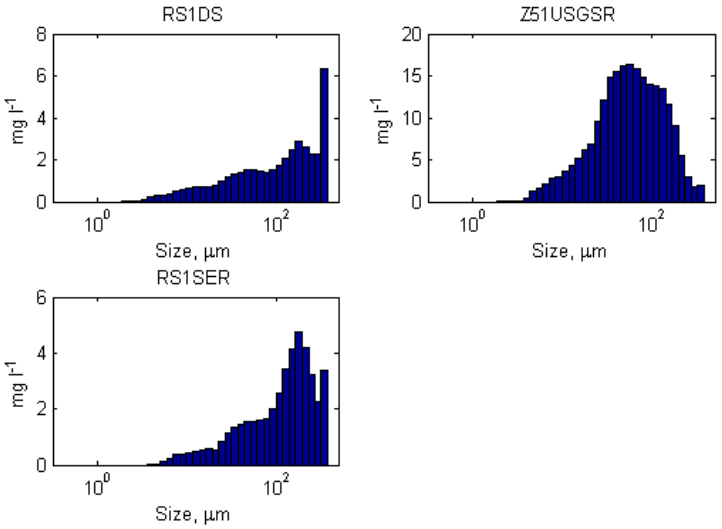

Figure E-74 Mass weighted distributions of suspended particles for floc samples collected November 17, 2015.

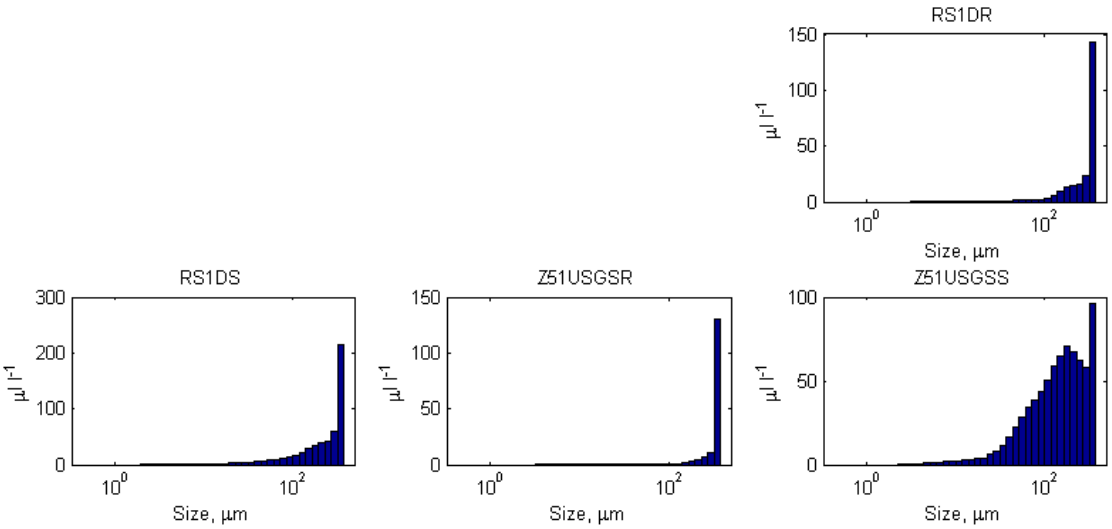

Figure E-75 Volume weighted distributions of suspended particles for epiphyton samples collected November 17, 2015.

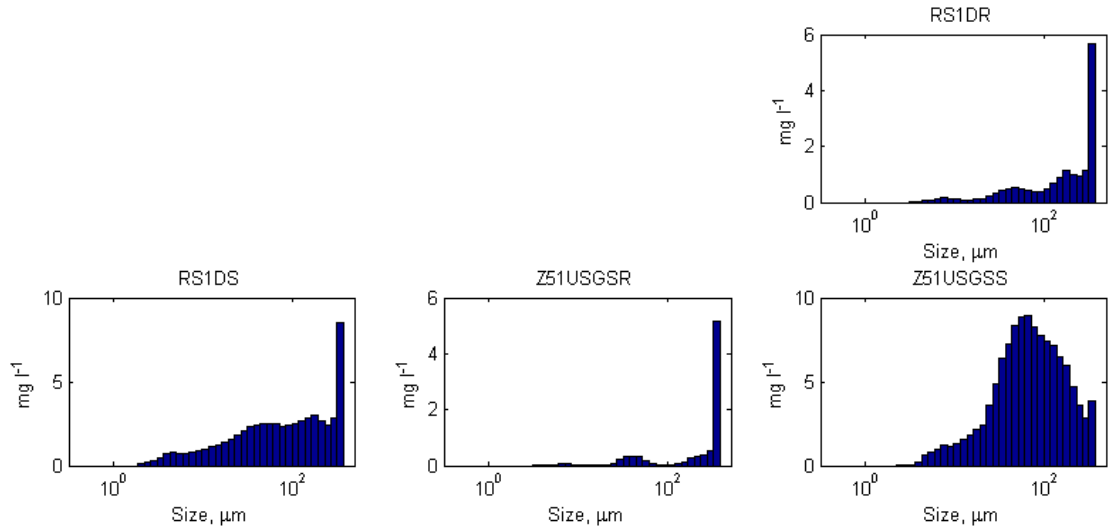

Figure E-76 Mass weighted distributions of suspended particles for epiphyton samples collected November 17, 2015.

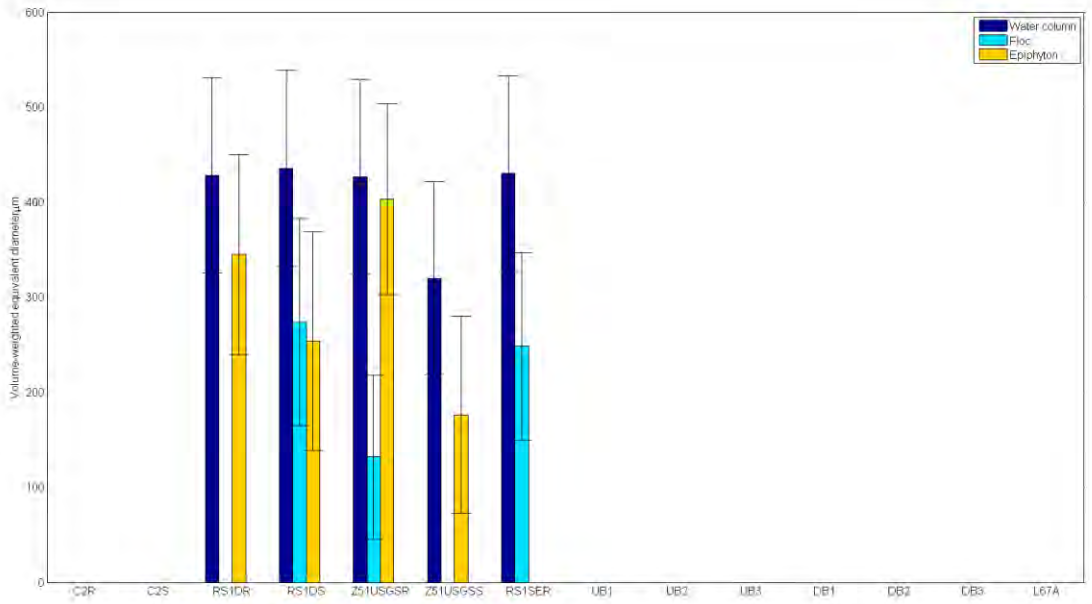

Figure E-77 Comparison of average volume weighted equivalent diameter for each particle type at each DPM site for samples collected November 17, 2015.

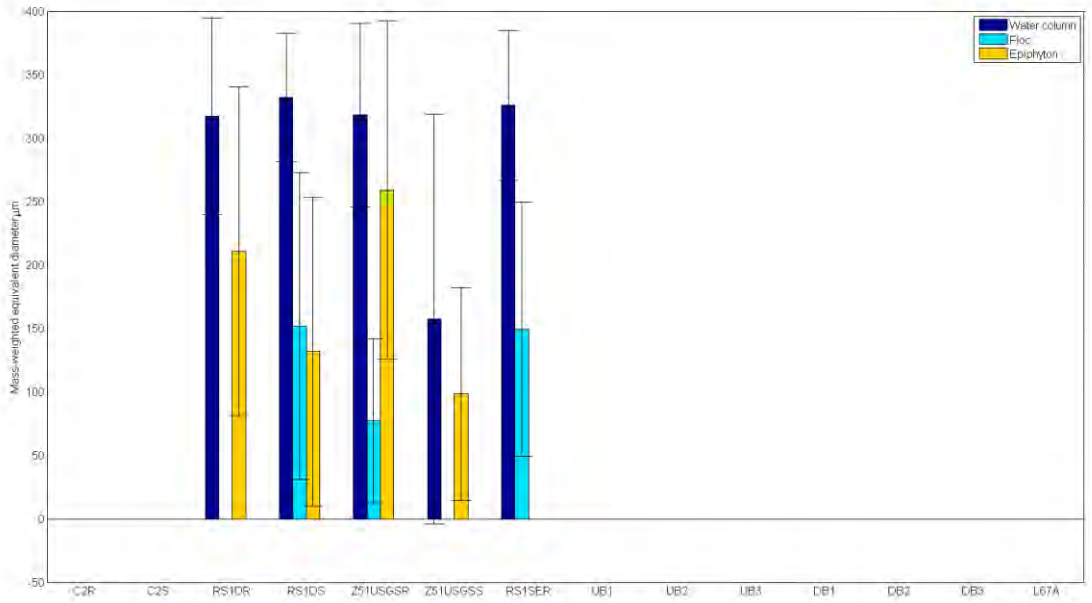

Figure E-78 Comparison of average mass weighted equivalent diameter for each particle type at each DPM site for samples collected November 17, 2015.

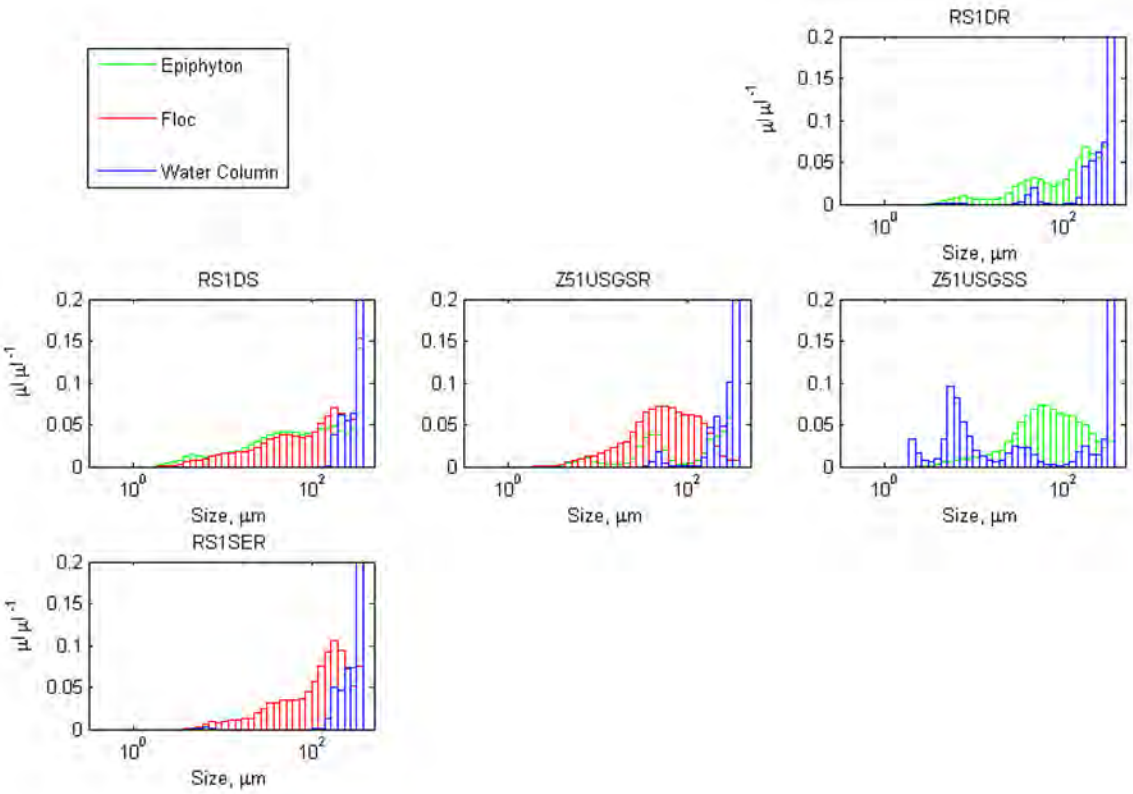

Figure E-79 Comparison of volumetric fraction distributions of Water Column, Floc and Epiphyton by size at each DPM site for samples collected November 17, 2015.

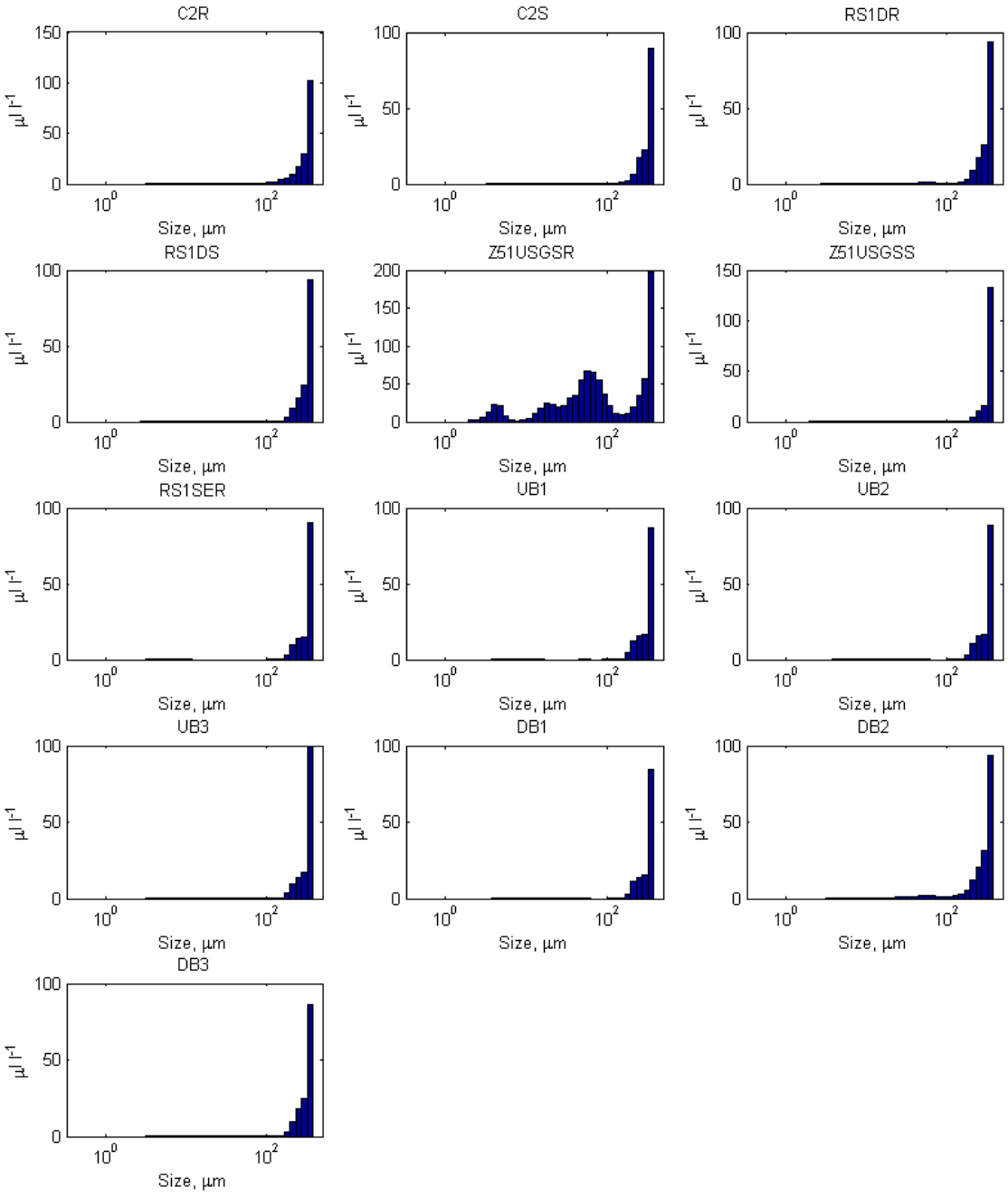

Figure E-80 Volume weighted distributions of suspended particles for water column samples collected December 7-8, 2015.

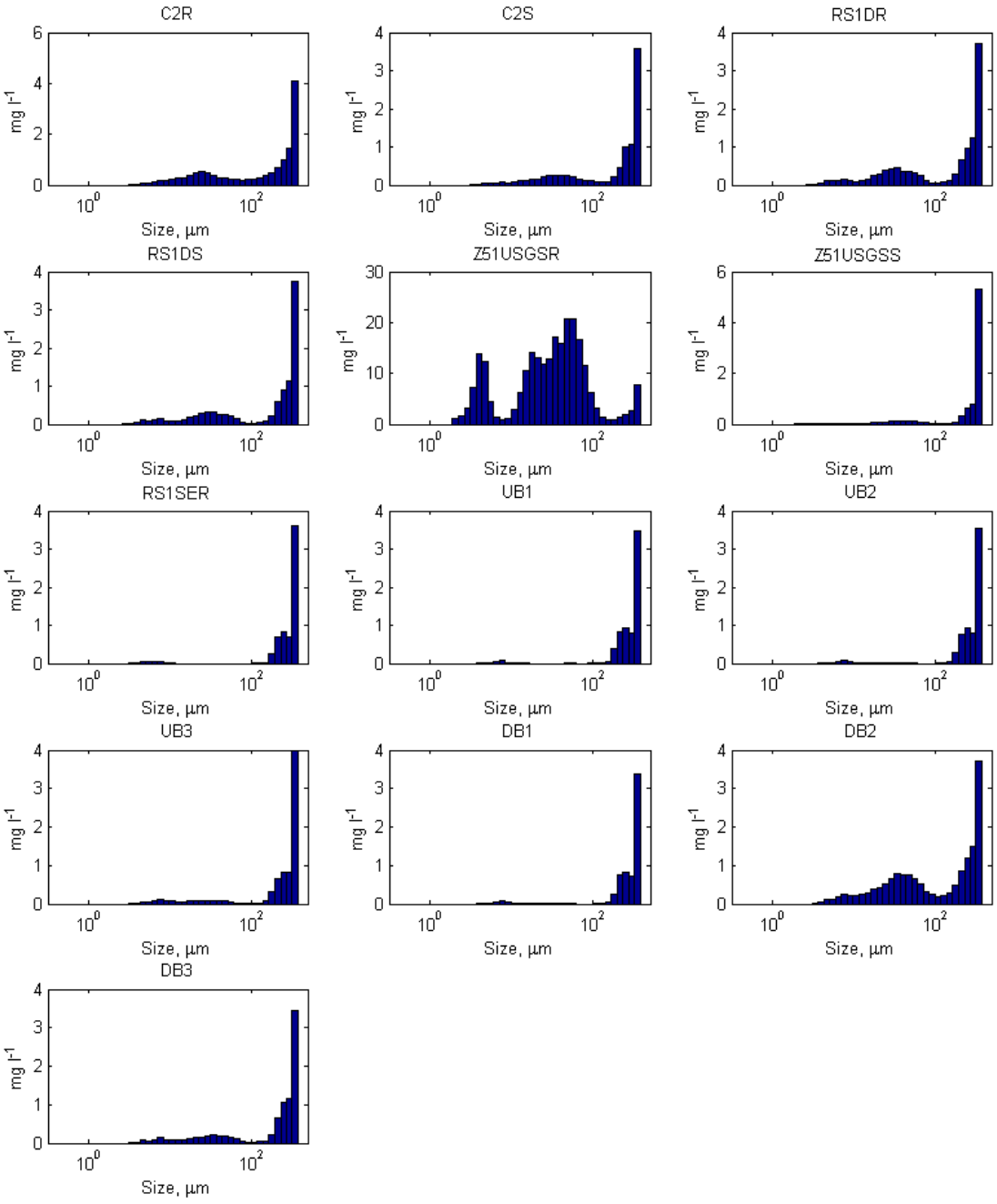

Figure E-81 Mass weighted distributions of suspended particles for water column samples collected December 7-8, 2015.

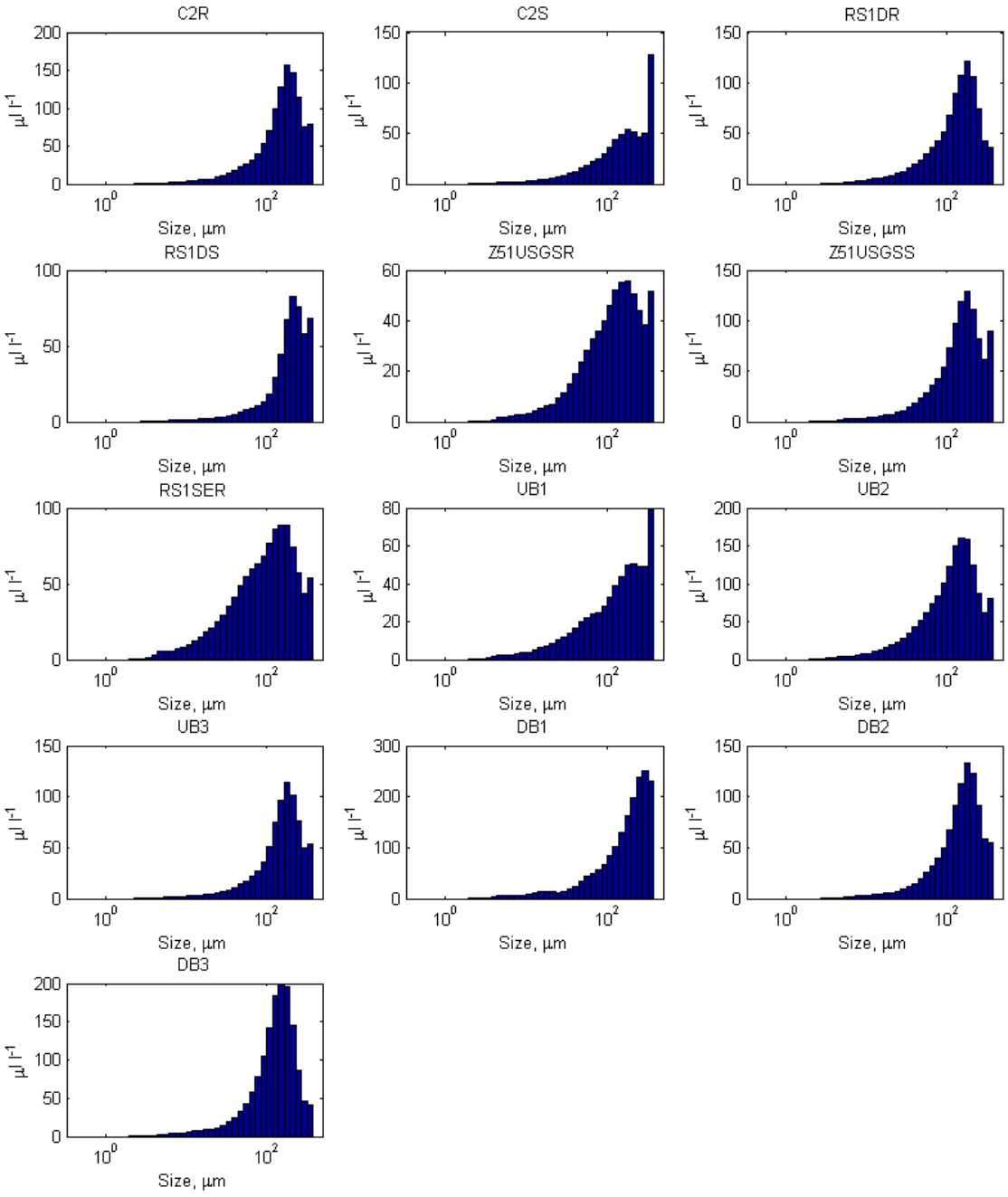

Figure E-82 Volume weighted distributions of suspended particles for floc samples collected December 7-8, 2015.

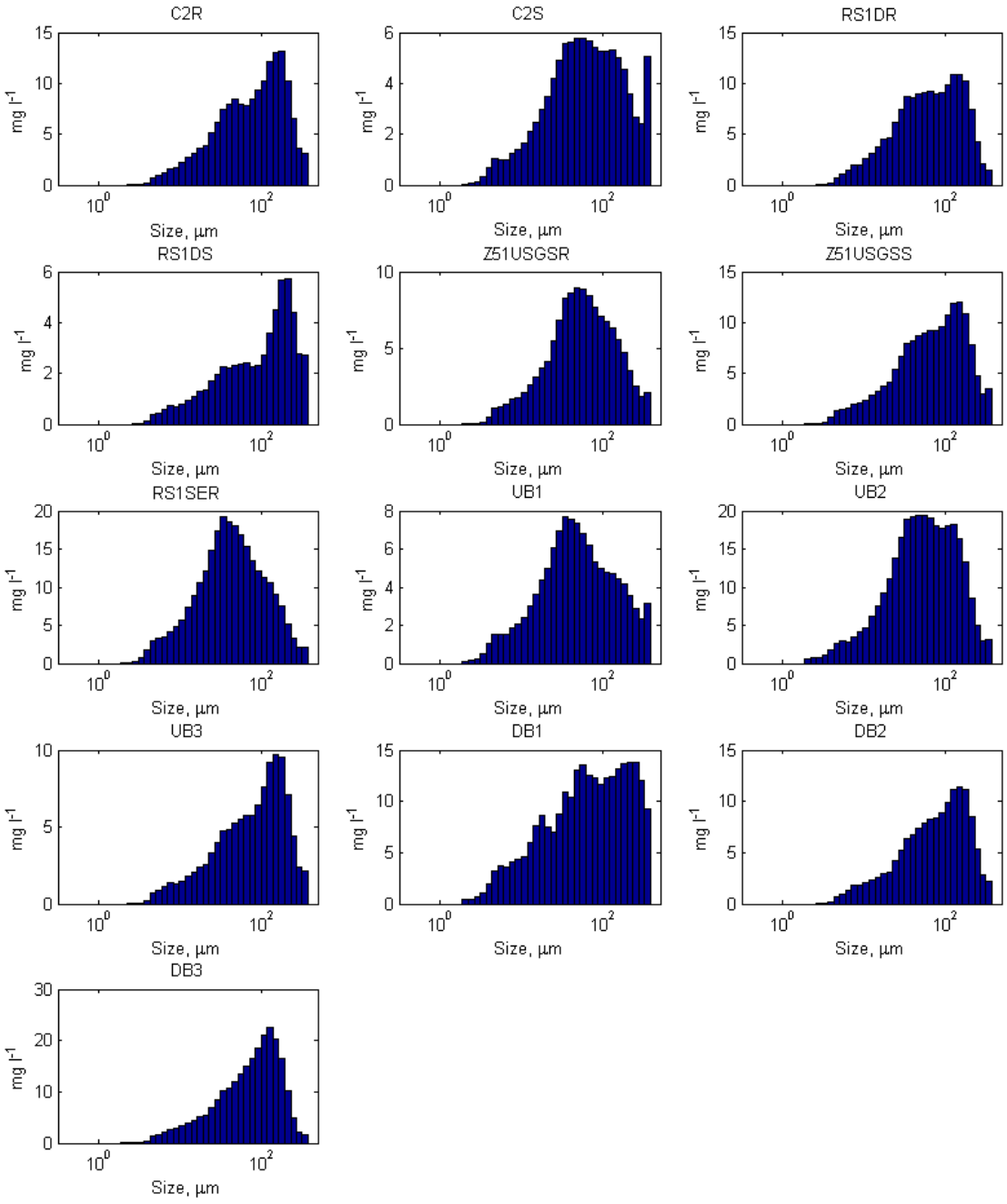

Figure E-83 Mass weighted distributions of suspended particles for floc samples collected December 7-8, 2015.

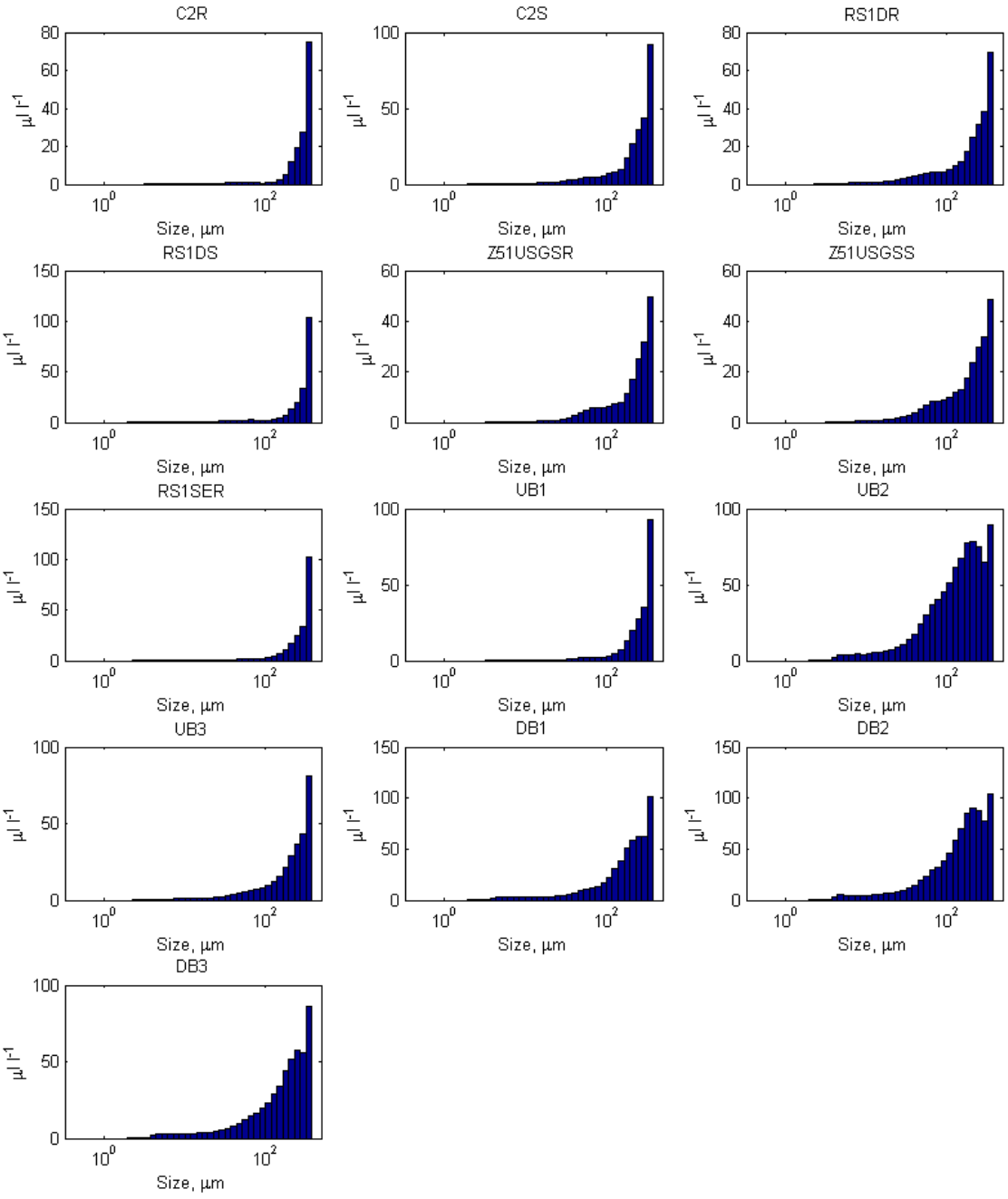

Figure E-84 Volume weighted distributions of suspended particles for epiphyton samples collected December 7-8, 2015.

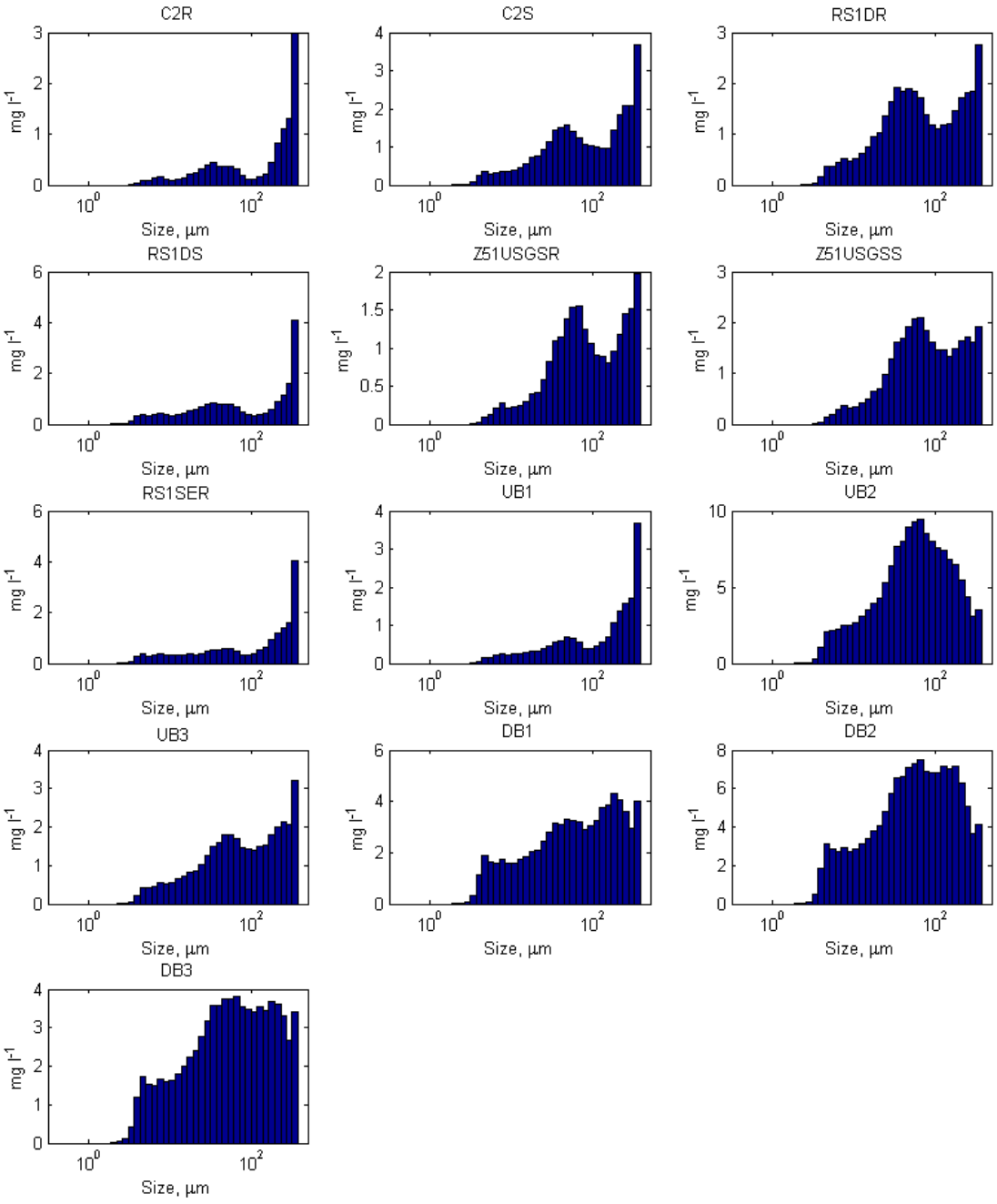

Figure E-85 Mass weighted distributions of suspended particles for epiphyton samples collected December 7-8, 2015

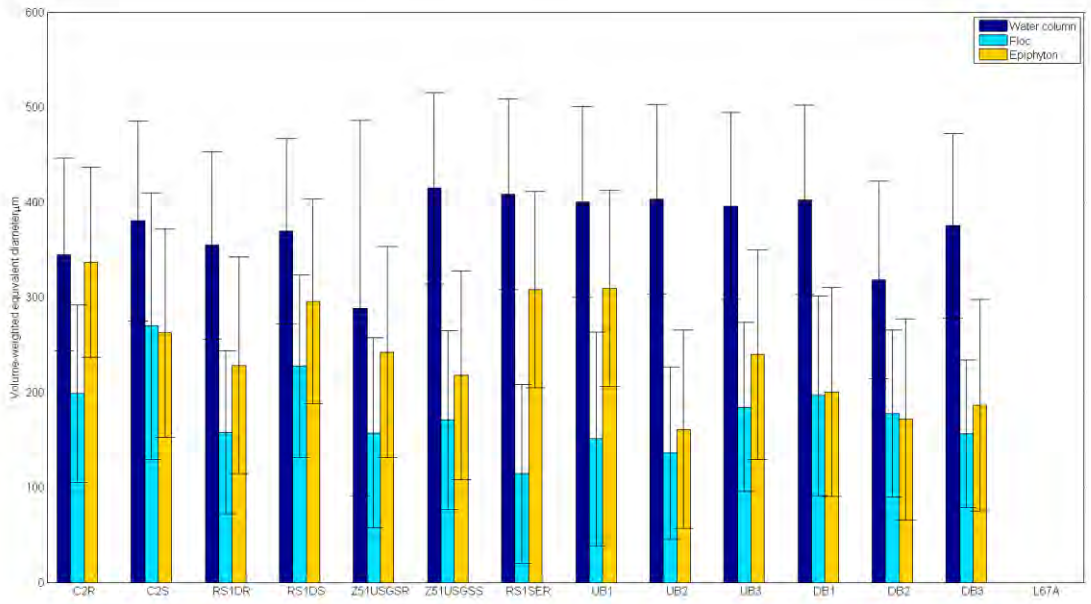

Figure E-86 Comparison of average volume weighted equivalent diameter for each particle type at each DPM site for samples collected December 7-8, 2015.

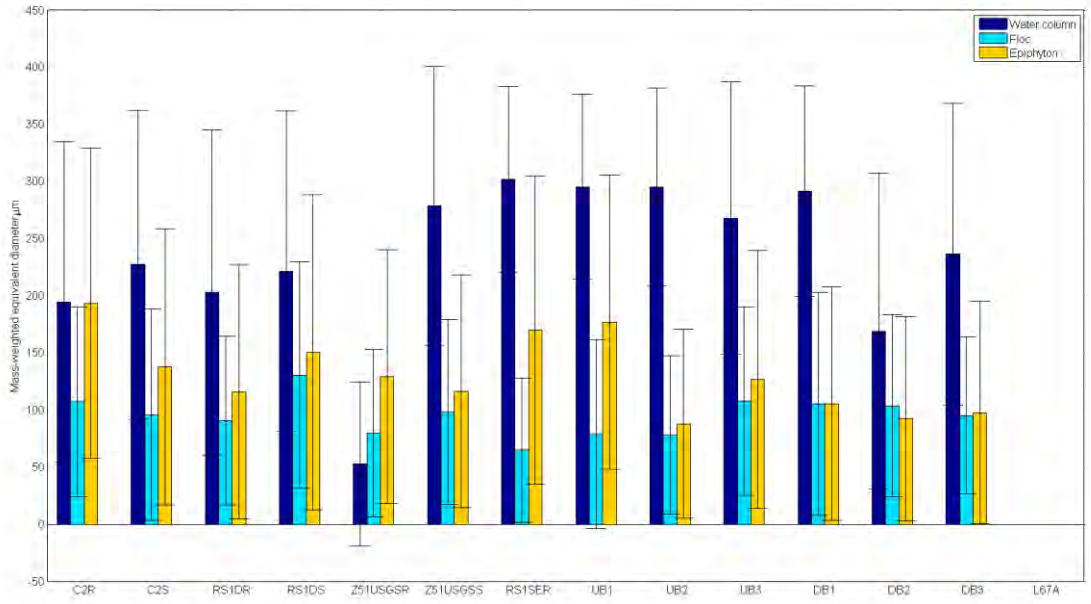

Figure E-87 Comparison of average mass weighted equivalent diameter for each particle type at each DPM site for samples collected December 7-8, 2015.

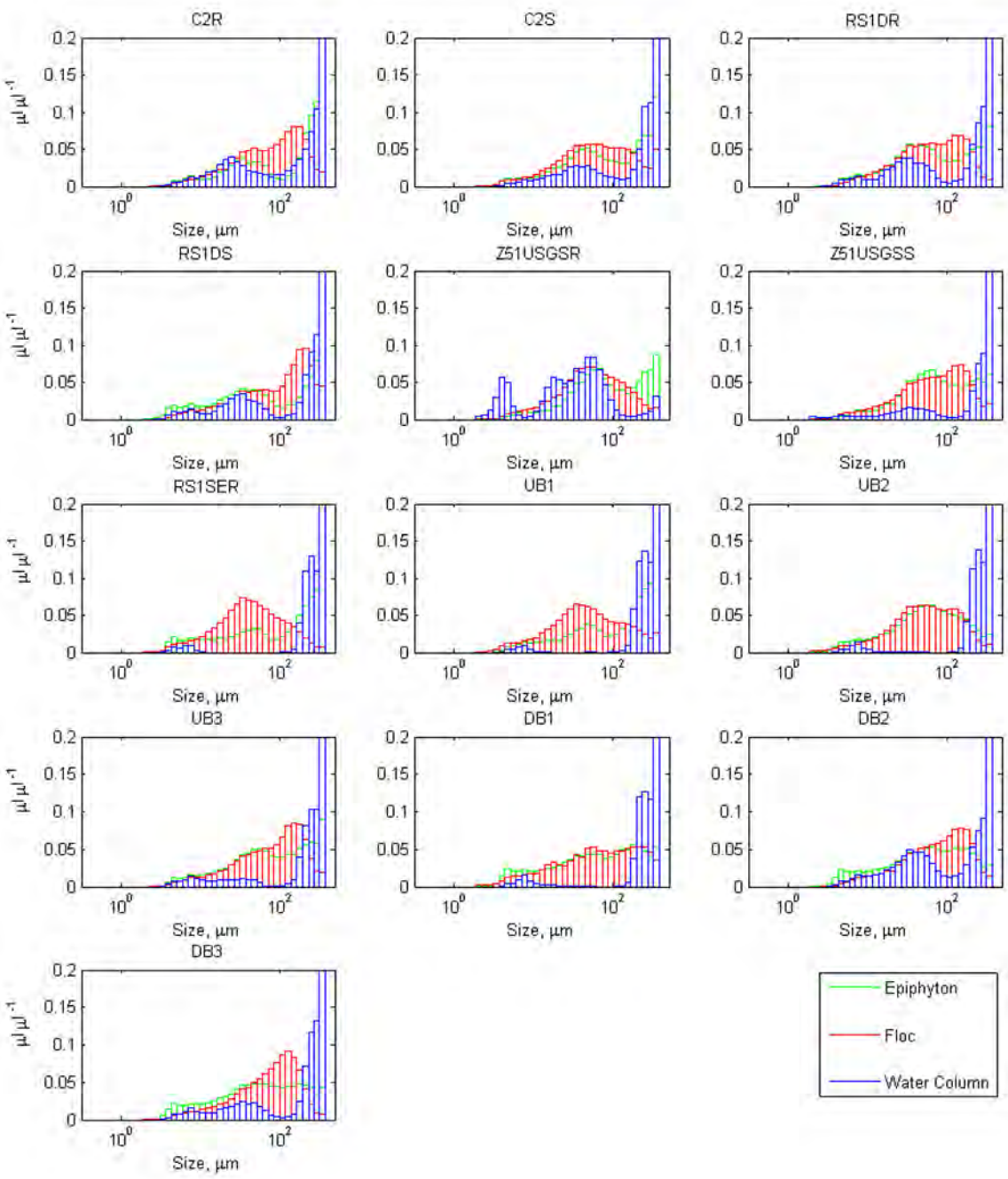

Figure E-88 Comparison of volumetric fraction distributions of Water Column, Floc and Epiphyton by size at each DPM site for samples collected December 7-8, 2015.

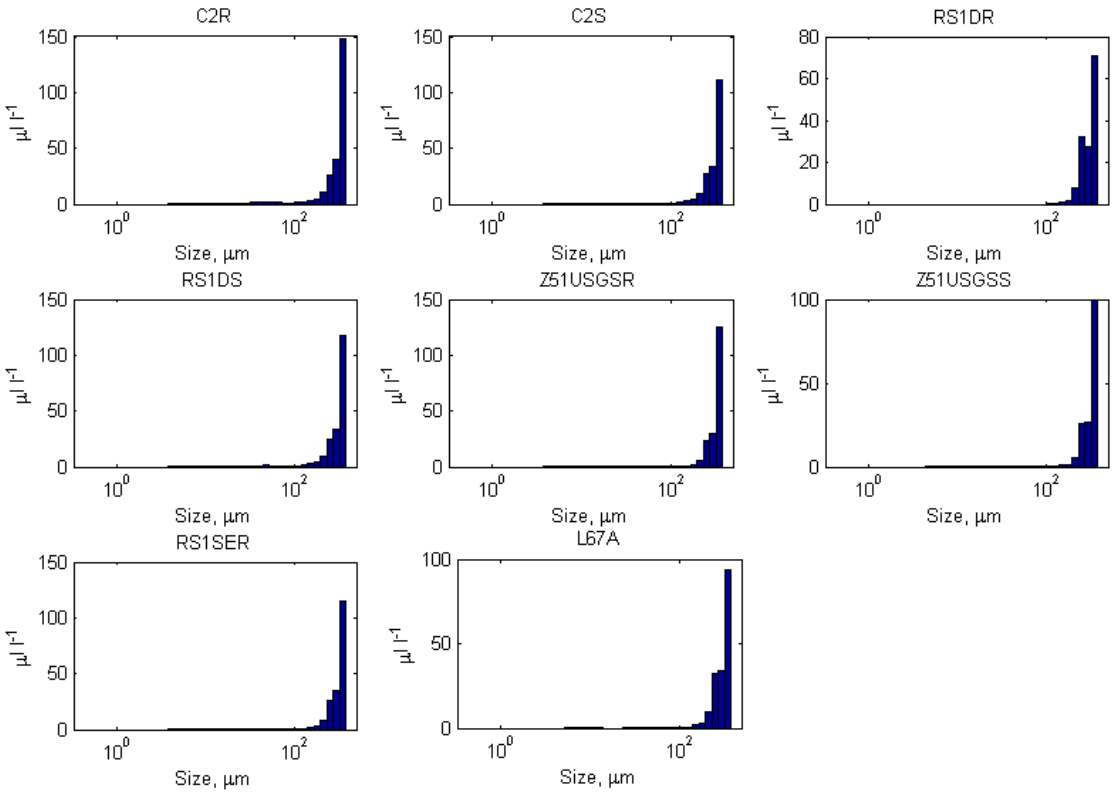

Figure E-89 Volume weighted distributions of suspended particles for water column samples collected January 19-20, 2016.

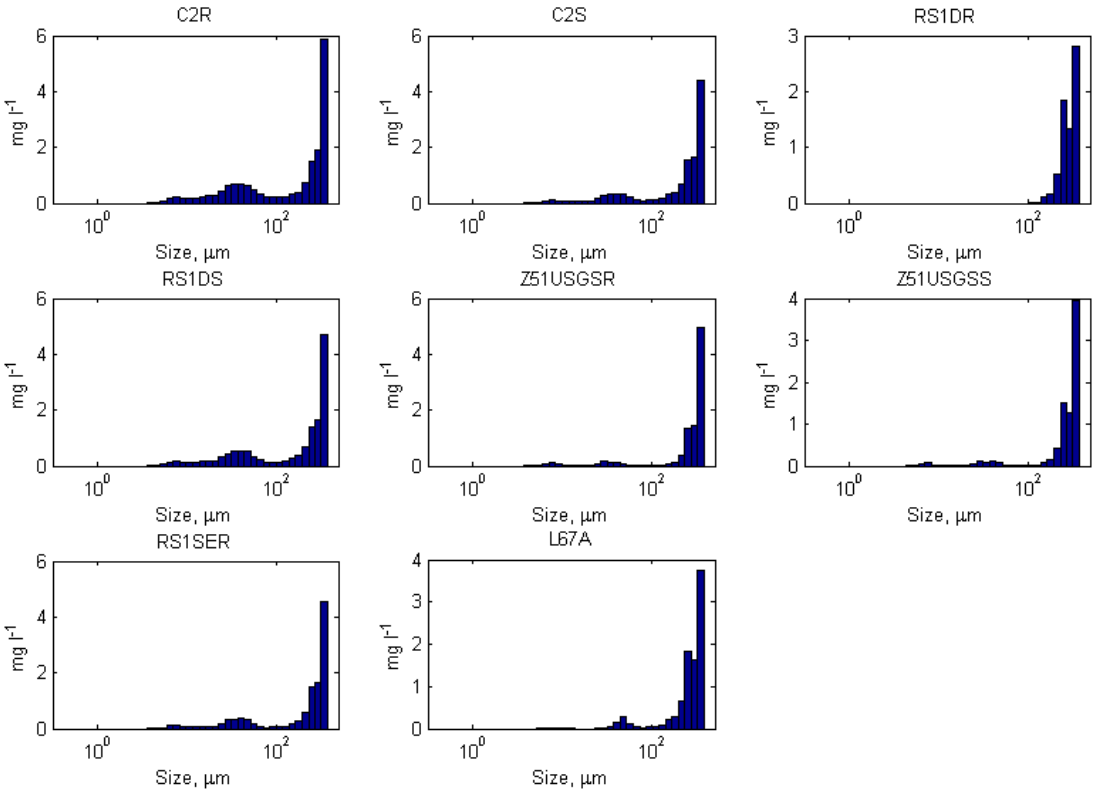

Figure E-90 Mass weighted distributions of suspended particles for water column samples collected January 19-20, 2016.

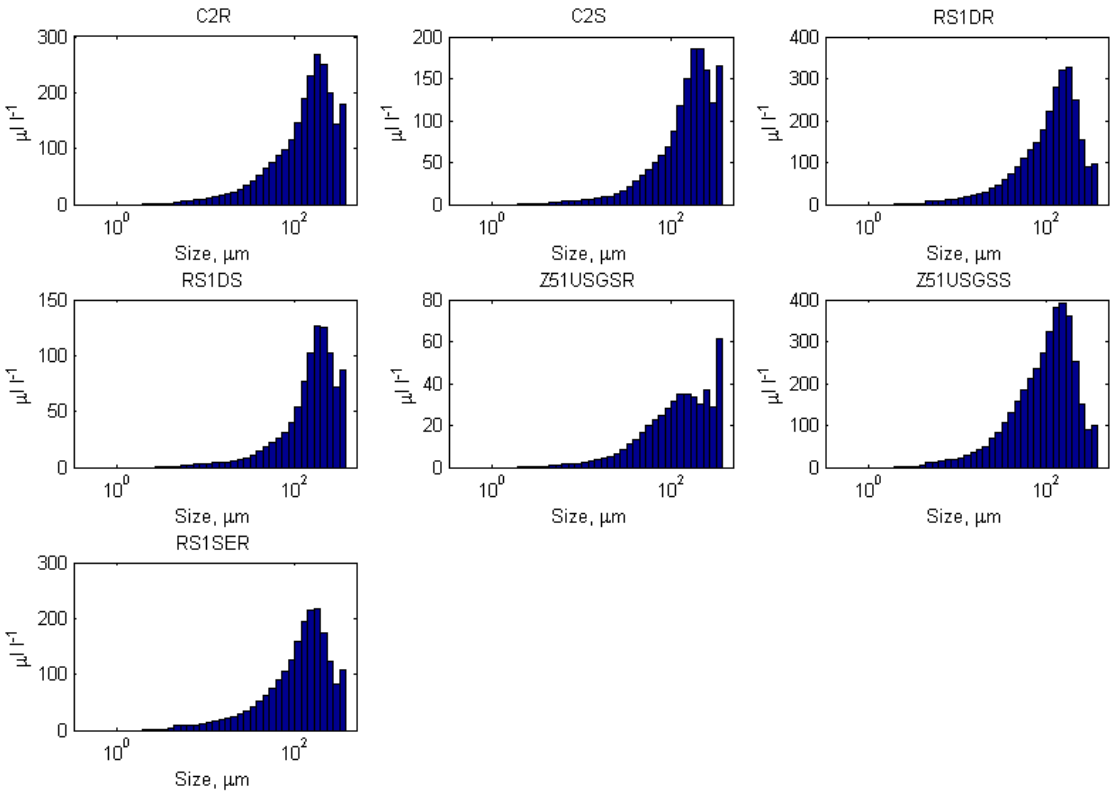

Figure E-91 Volume weighted distributions of suspended particles for floc samples collected January 19-20, 2016.

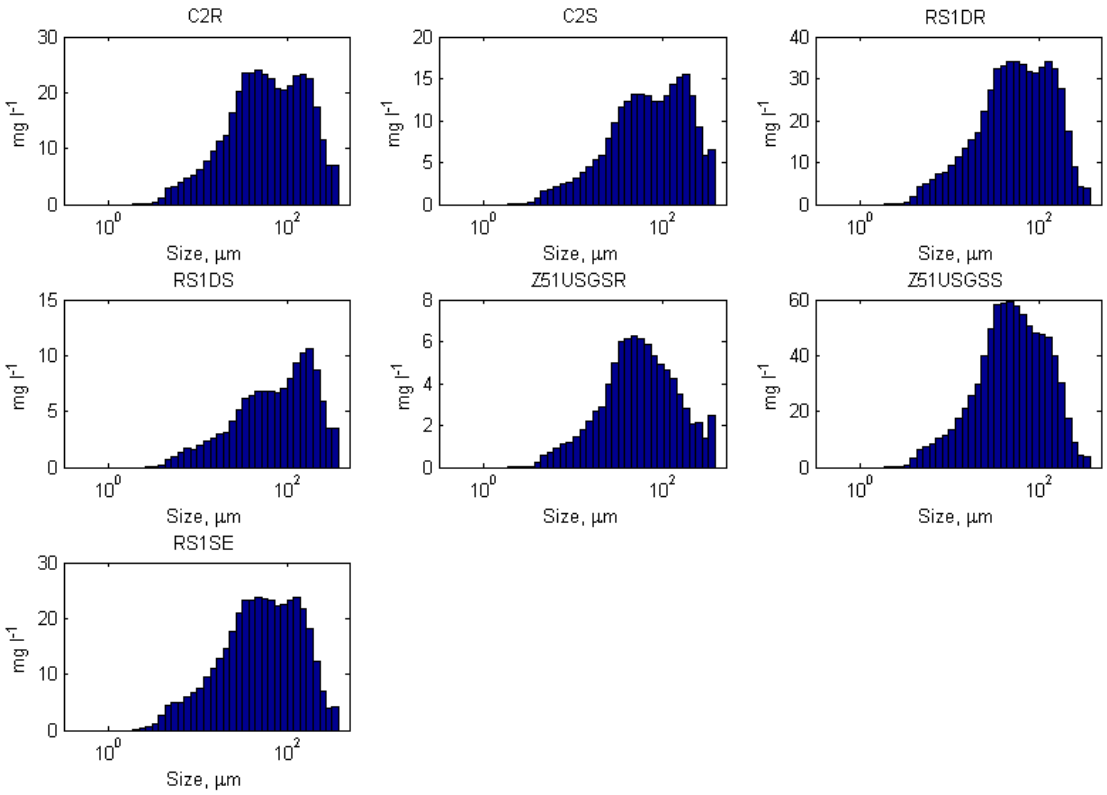

Figure E-92 Mass weighted distributions of suspended particles for floc samples collected January 19-20, 2016.

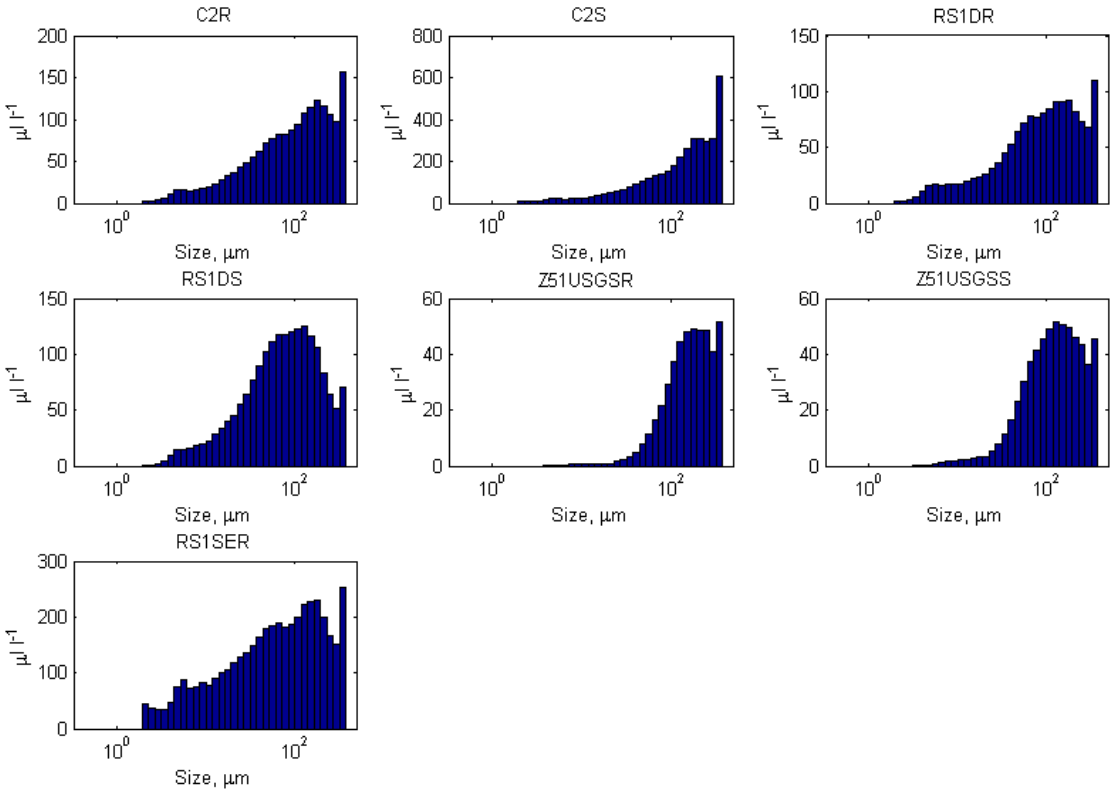

Figure E-93 Volume weighted distributions of suspended particles for epiphyton samples collected January 19-20, 2016.

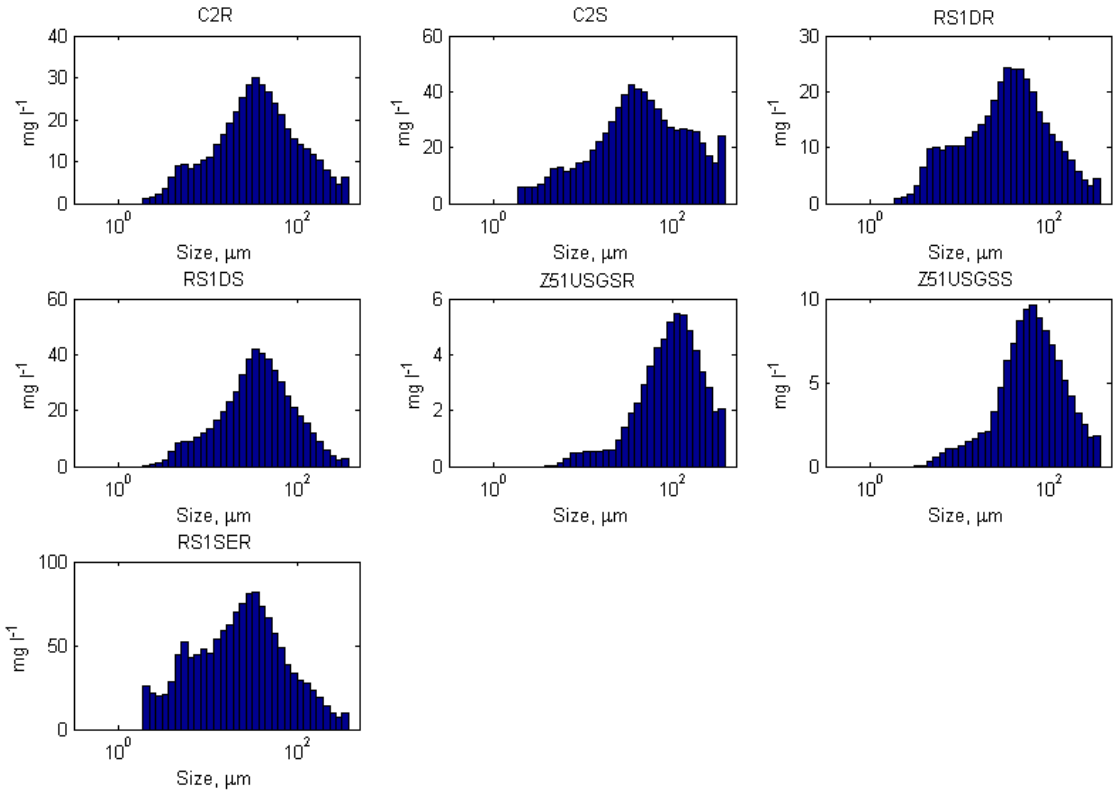

Figure E-94 Mass weighted distributions of suspended particles for epiphyton samples collected January 19-20, 2016.

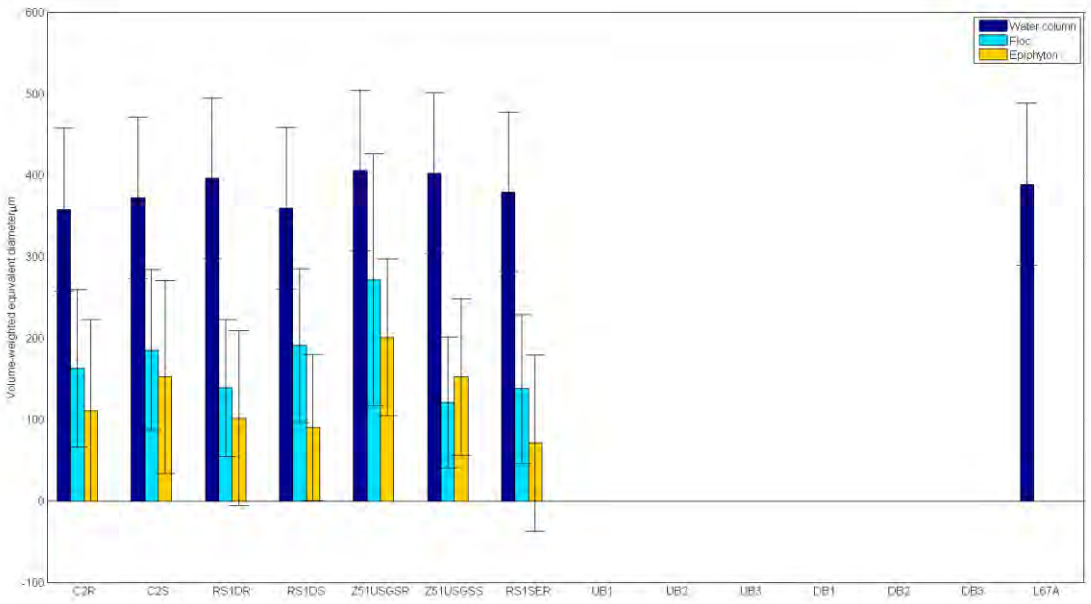

Figure E-95 Comparison of average volume weighted equivalent diameter for each particle type at each DPM site for samples collected January 19-20, 2016.

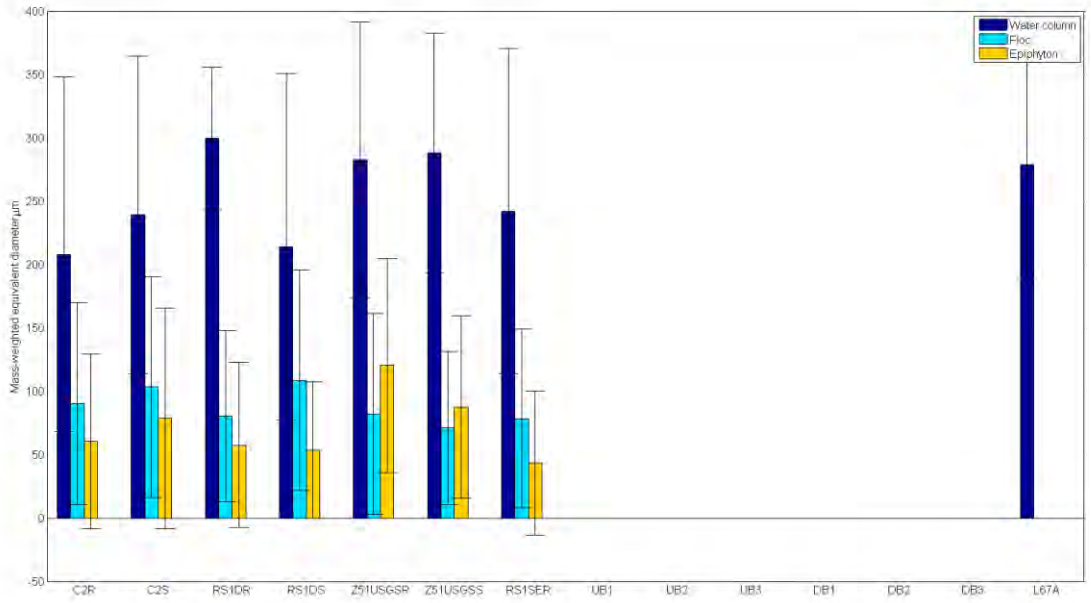

Figure E-96 Comparison of average mass weighted equivalent diameter for each particle type at each DPM site for samples collected January 19-20, 2016.

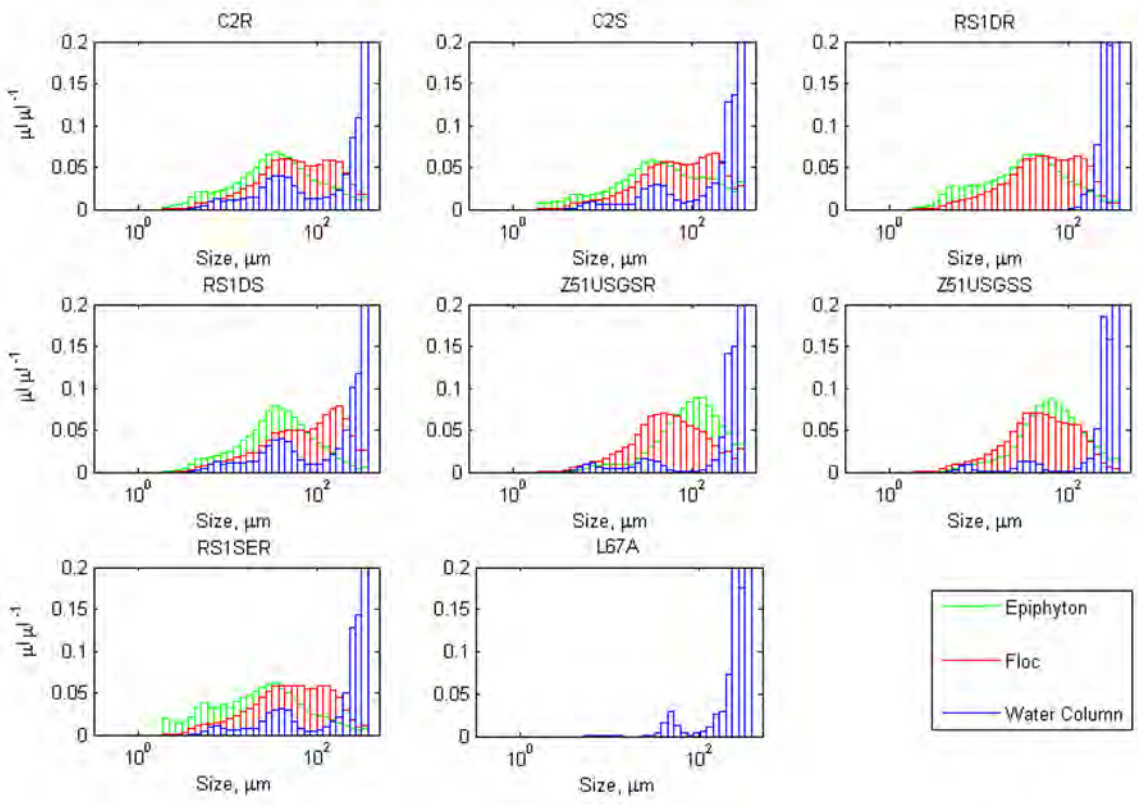

Figure E-97 Comparison of volumetric fraction distributions of Water Column, Floc and Epiphyton by size at each DPM site for samples collected January 19-20, 2016.

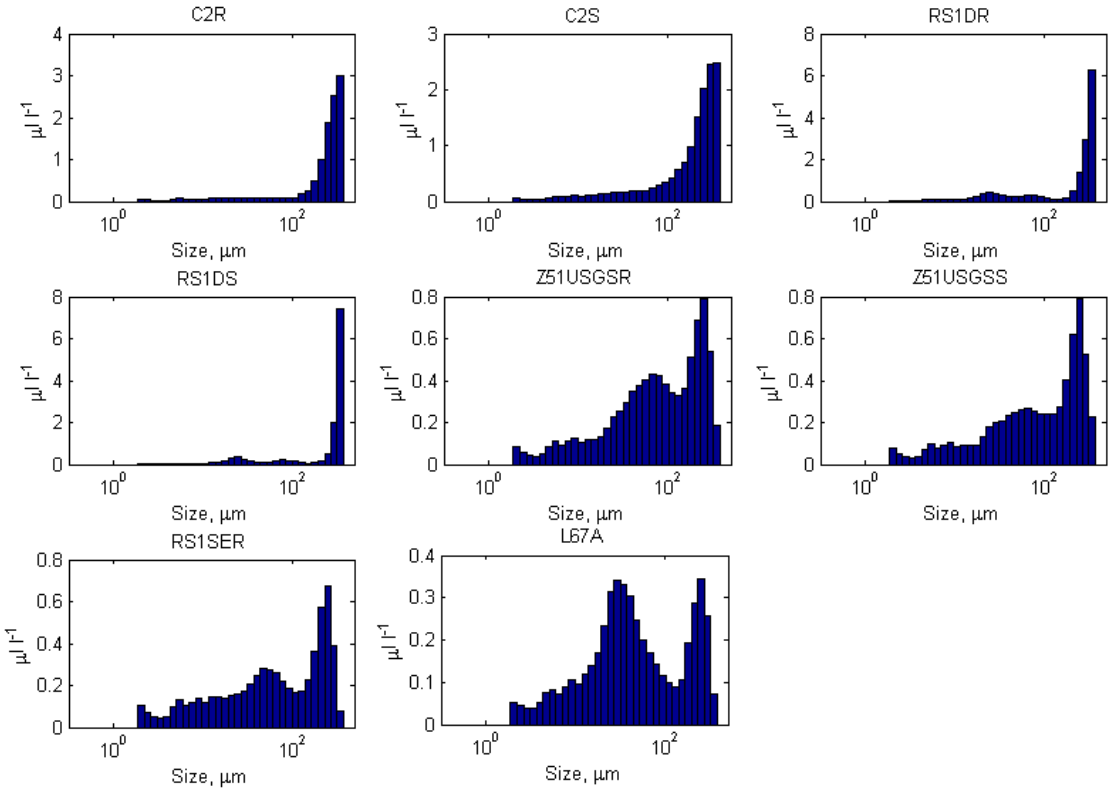

Figure E-98 Volume weighted distributions of suspended particles for water column samples collected February 29, 2016.

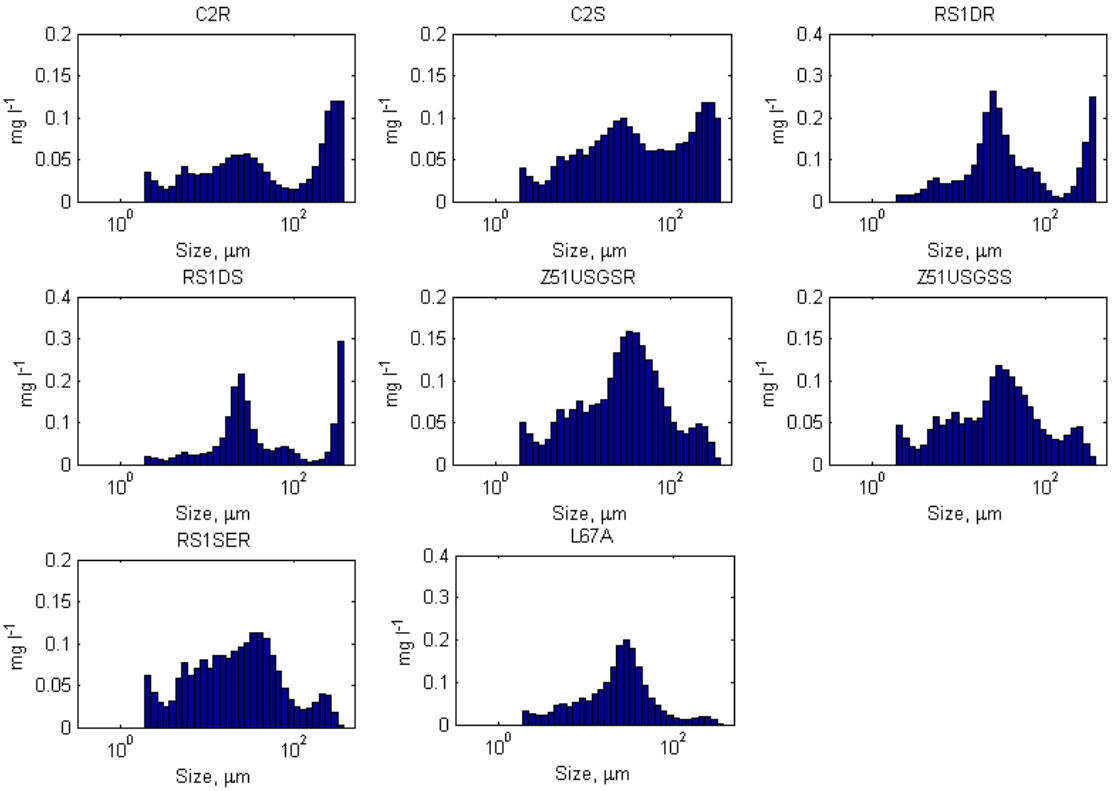

Figure E-99 Mass weighted distributions of suspended particles for water column samples collected February 29, 2016.

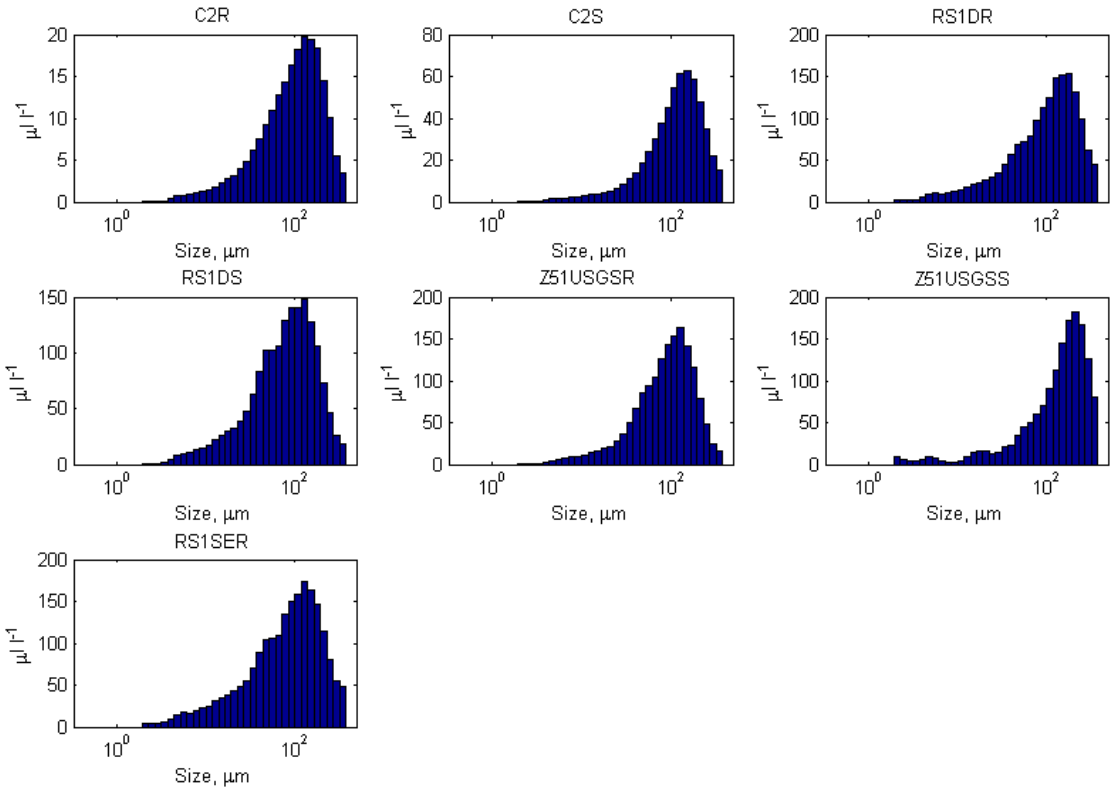

Figure E-100 Volume weighted distributions of suspended particles for floc samples collected February 29, 2016.

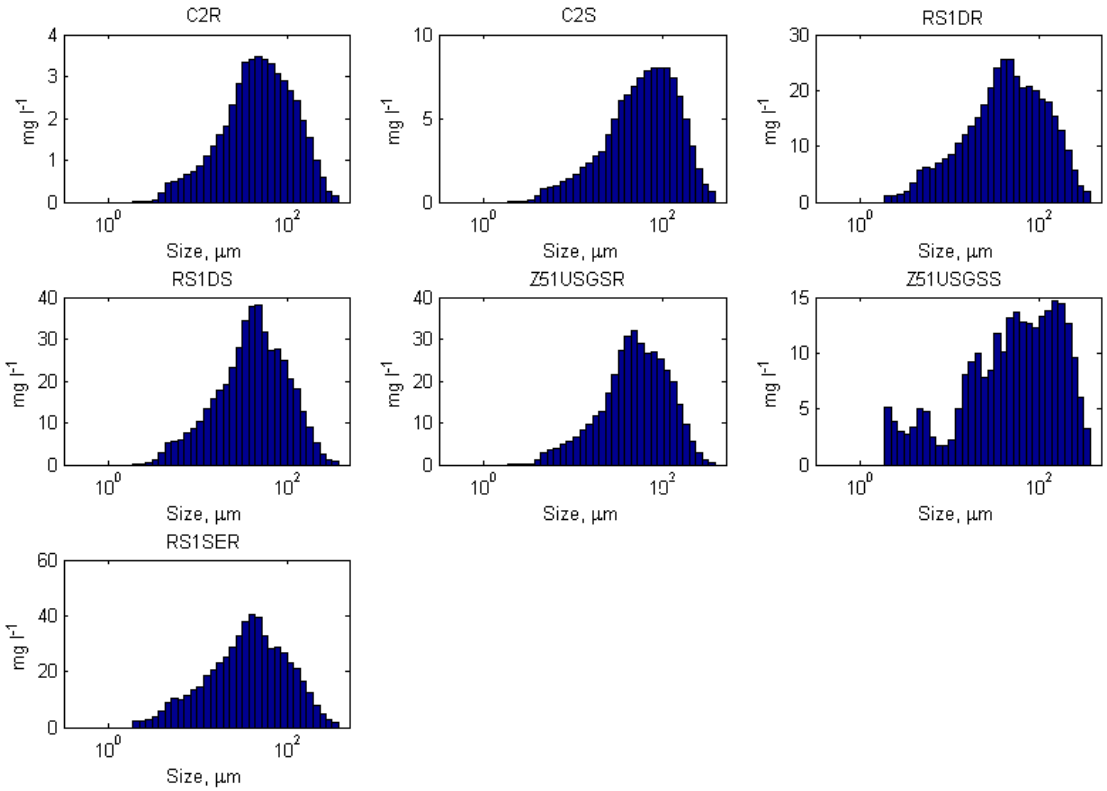

Figure E-101 Mass weighted distributions of suspended particles for floc samples collected February 29, 2016.

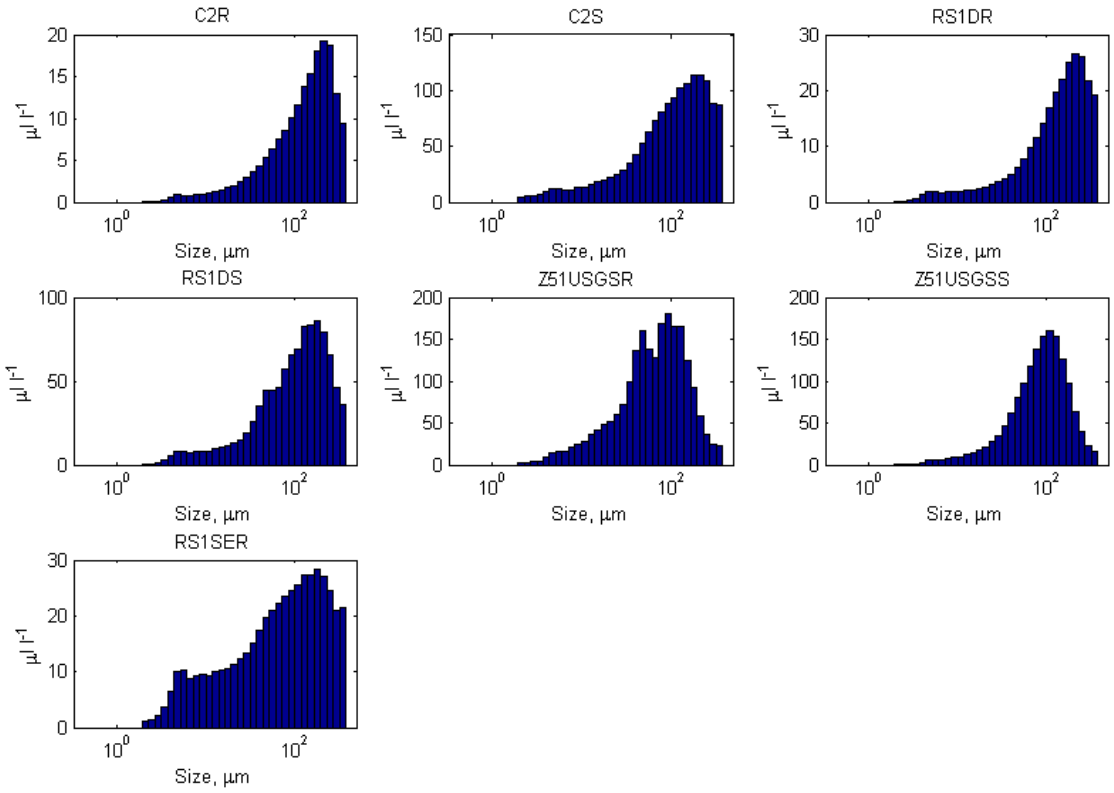

Figure E-102 Volume weighted distributions of suspended particles for epiphyton samples collected February 29, 2016.

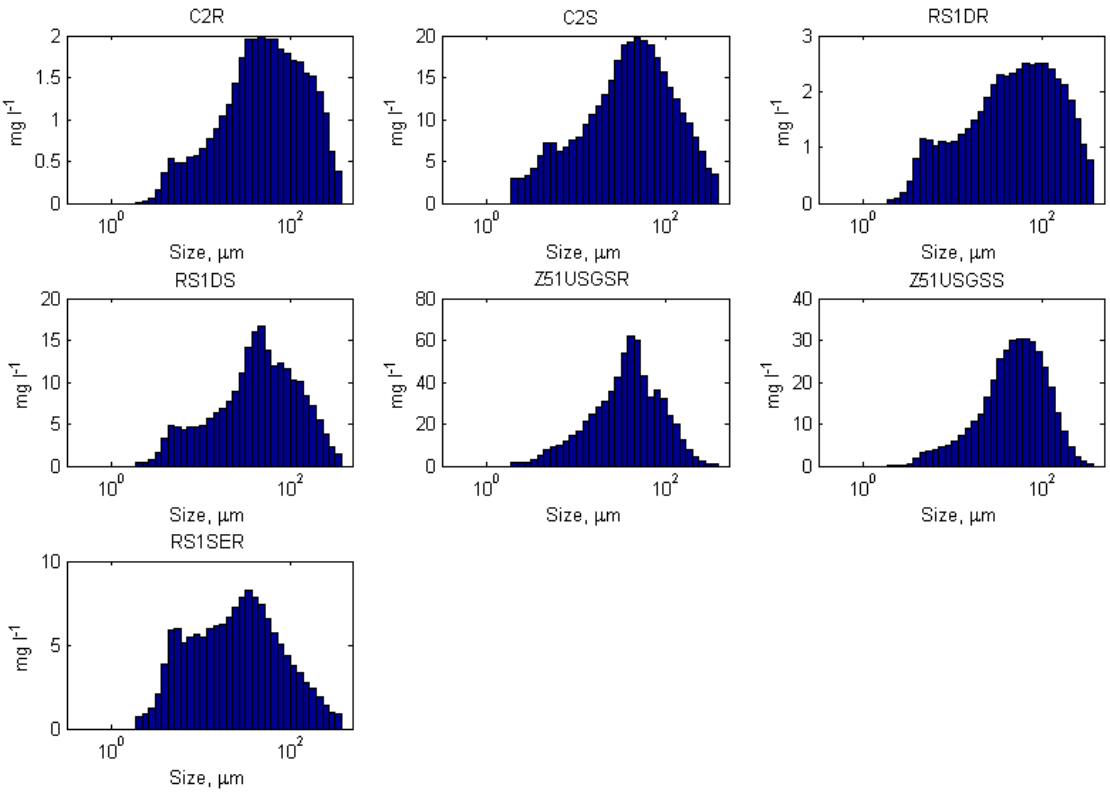

Figure E-103 Mass weighted distributions of suspended particles for epiphyton samples collected February 29, 2016.

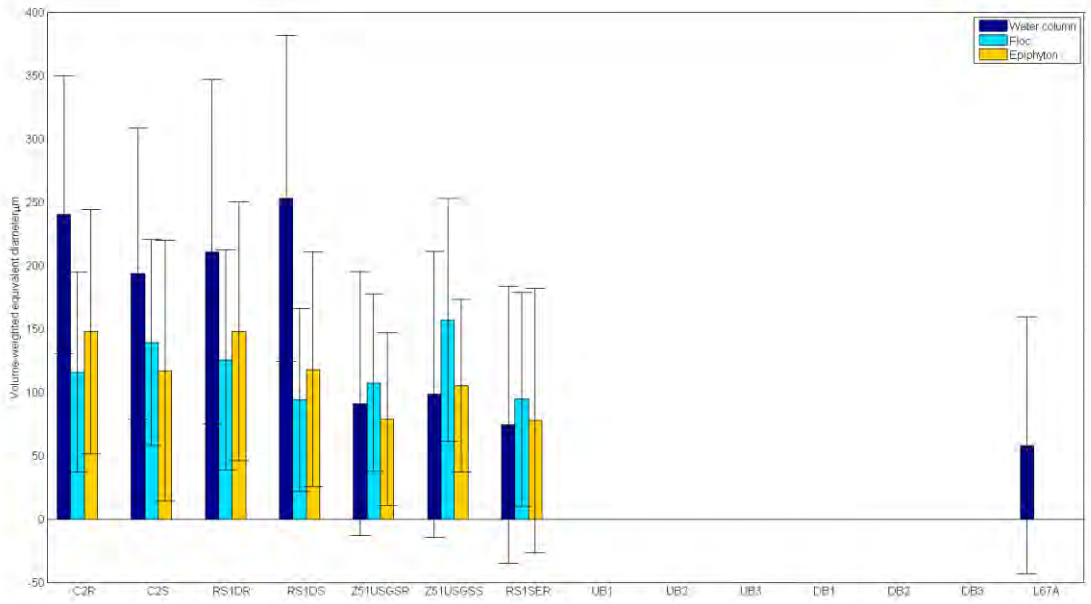

Figure E-104 Comparison of average volume weighted equivalent diameter for each particle type at each DPM site for samples collected February 29, 2016.

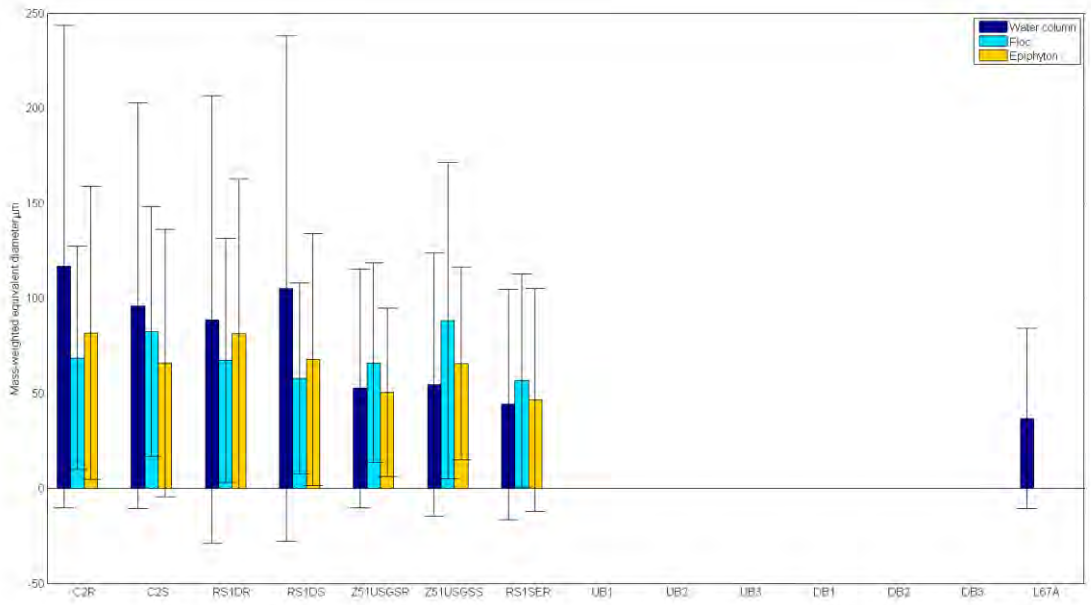

Figure E-105 Comparison of average mass weighted equivalent diameter for each particle type at each DPM site for samples collected February 29, 2016.

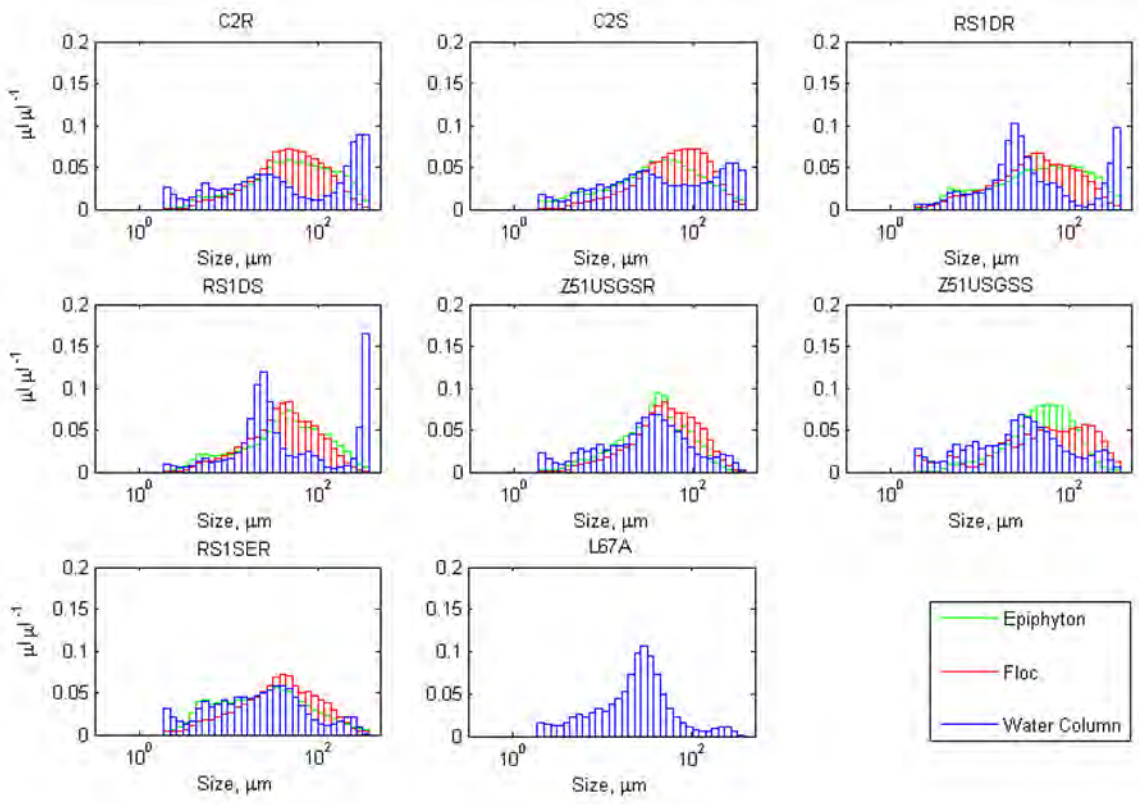

Figure E-106 Comparison of volumetric fraction distributions of Water Column, Floc and Epiphyton by size at each DPM site for samples collected February 29, 2016.

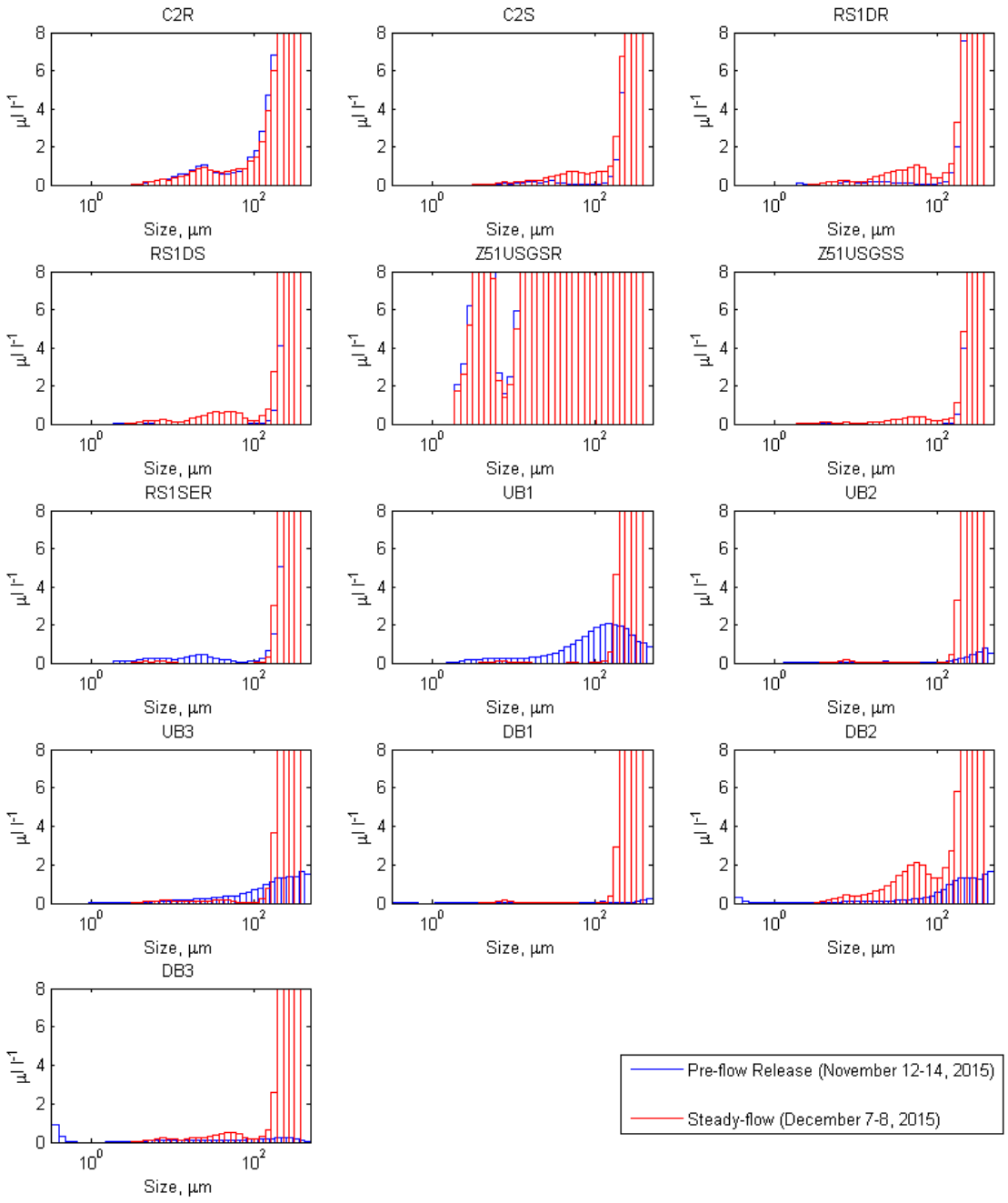

Figure E-107 Pre-flow release and steady-flow comparison of volume weighted distribution of water column suspended particles. Samples collected during the 2015 DPM flow release.

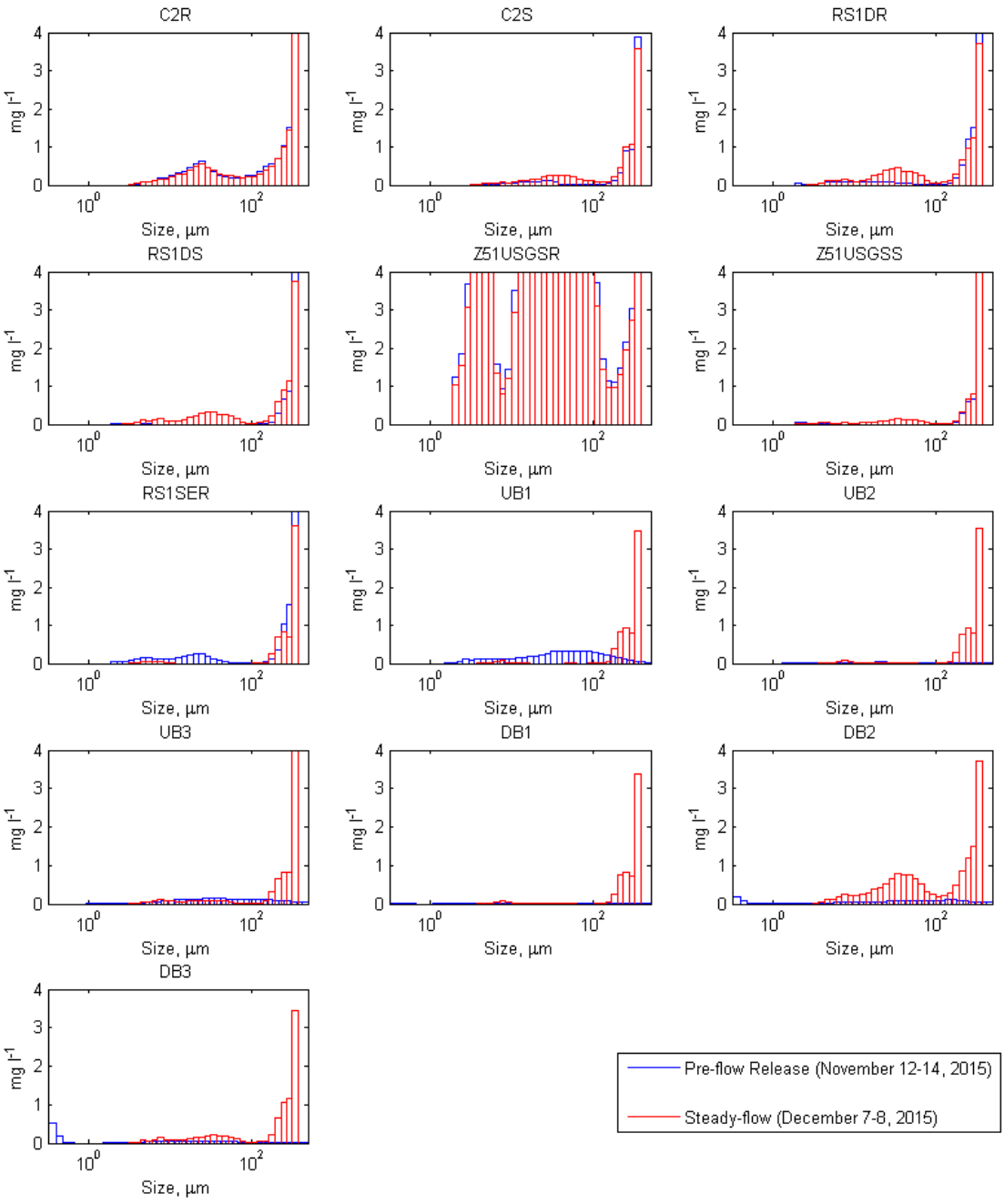

Figure E-108 Pre-flow release and steady-flow comparison of mass weighted distribution of water column suspended particles. Samples collected during the 2015 DPM flow release.

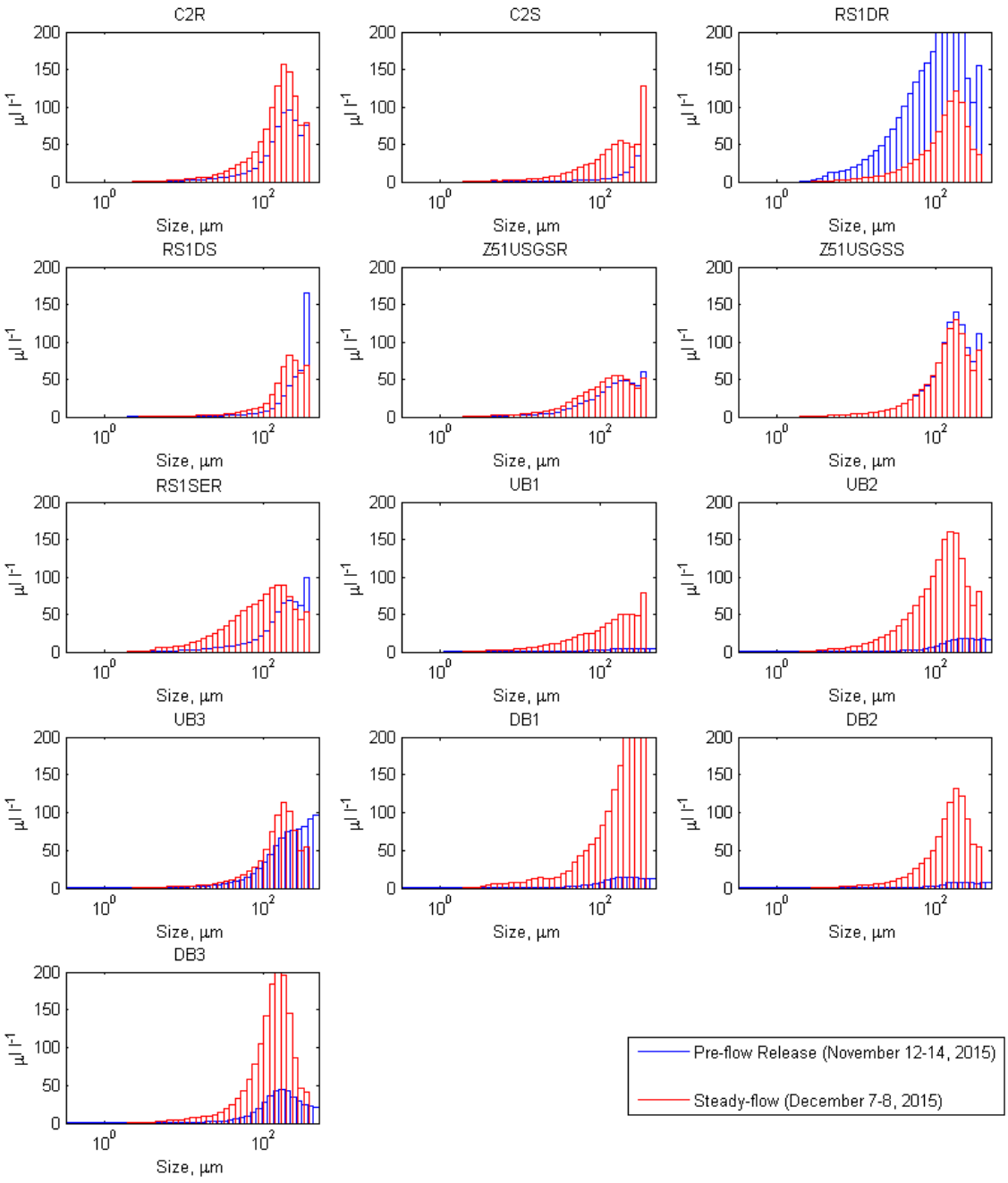

Figure E-109 Pre-flow release and steady-flow comparison of volume weighted distribution of floc suspended particles. Samples collected during the 2015 DPM flow release.

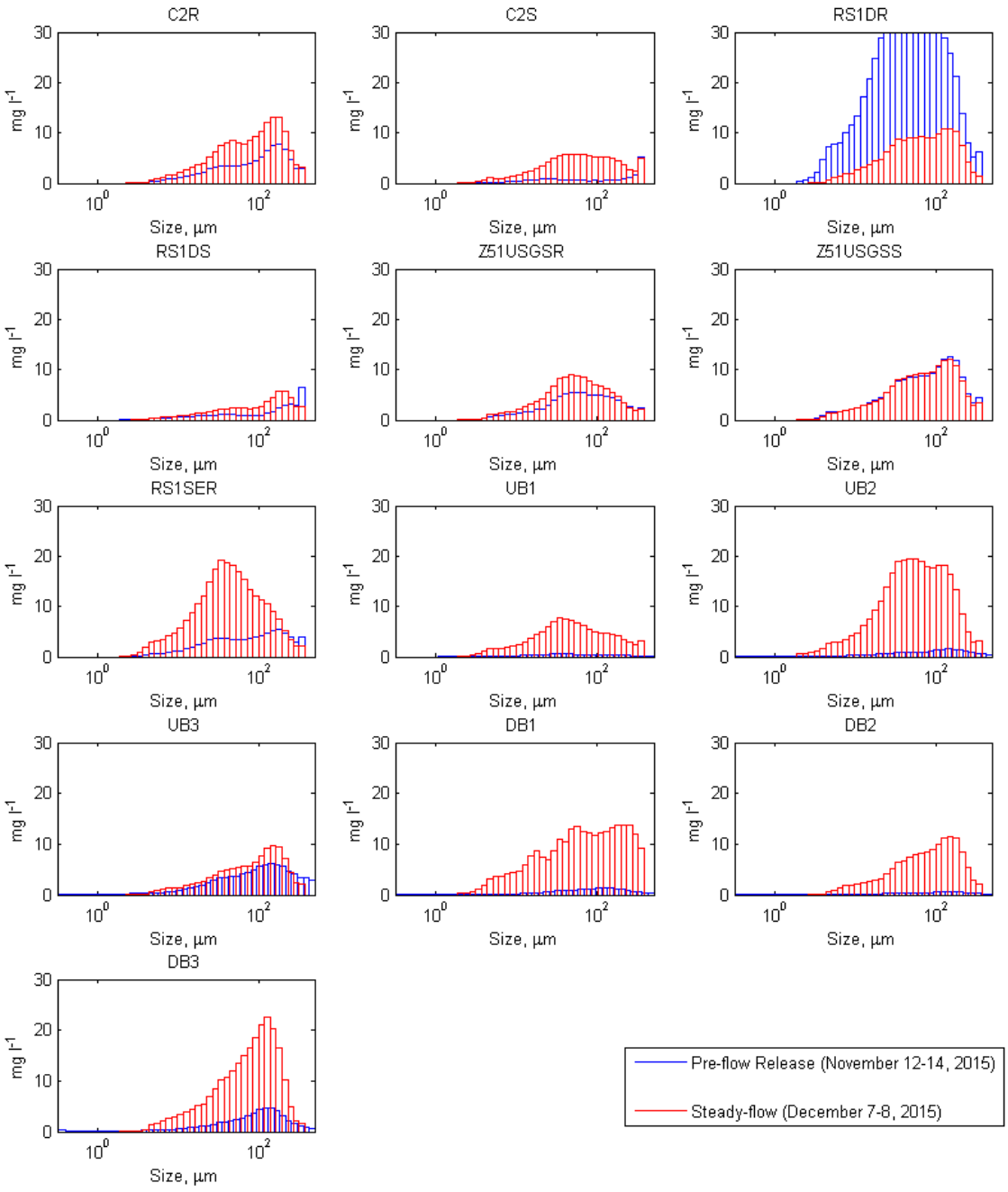

Figure E-110 Pre-flow release and steady-flow comparison of mass weighted size distribution of floc suspended particles. Samples collected during the 2015 DPM flow release.

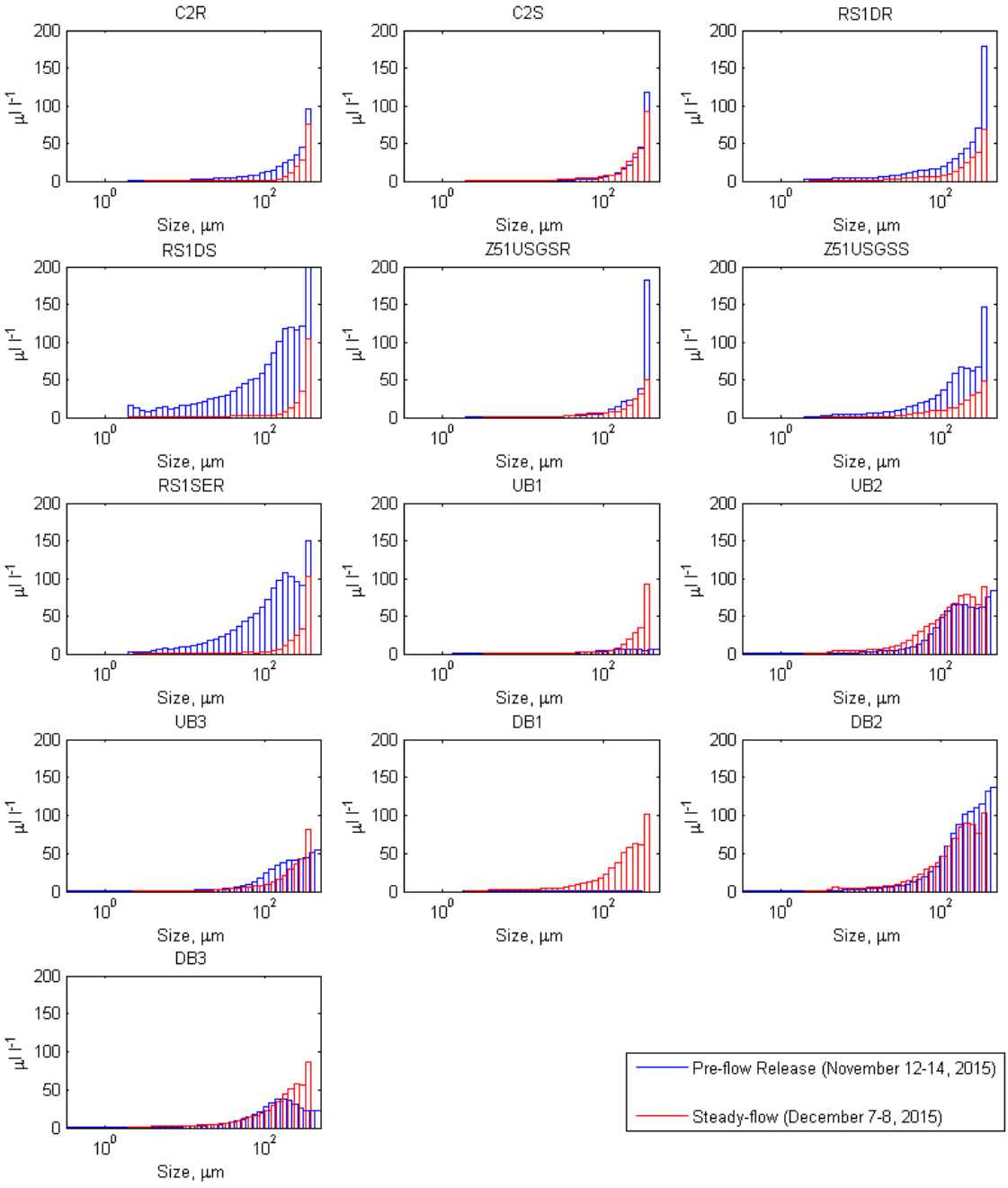

Figure E-111 Pre-flow release and steady-flow comparison of volume weighted distribution of epiphyton suspended particles. Samples collected during the 2015 DPM flow release.

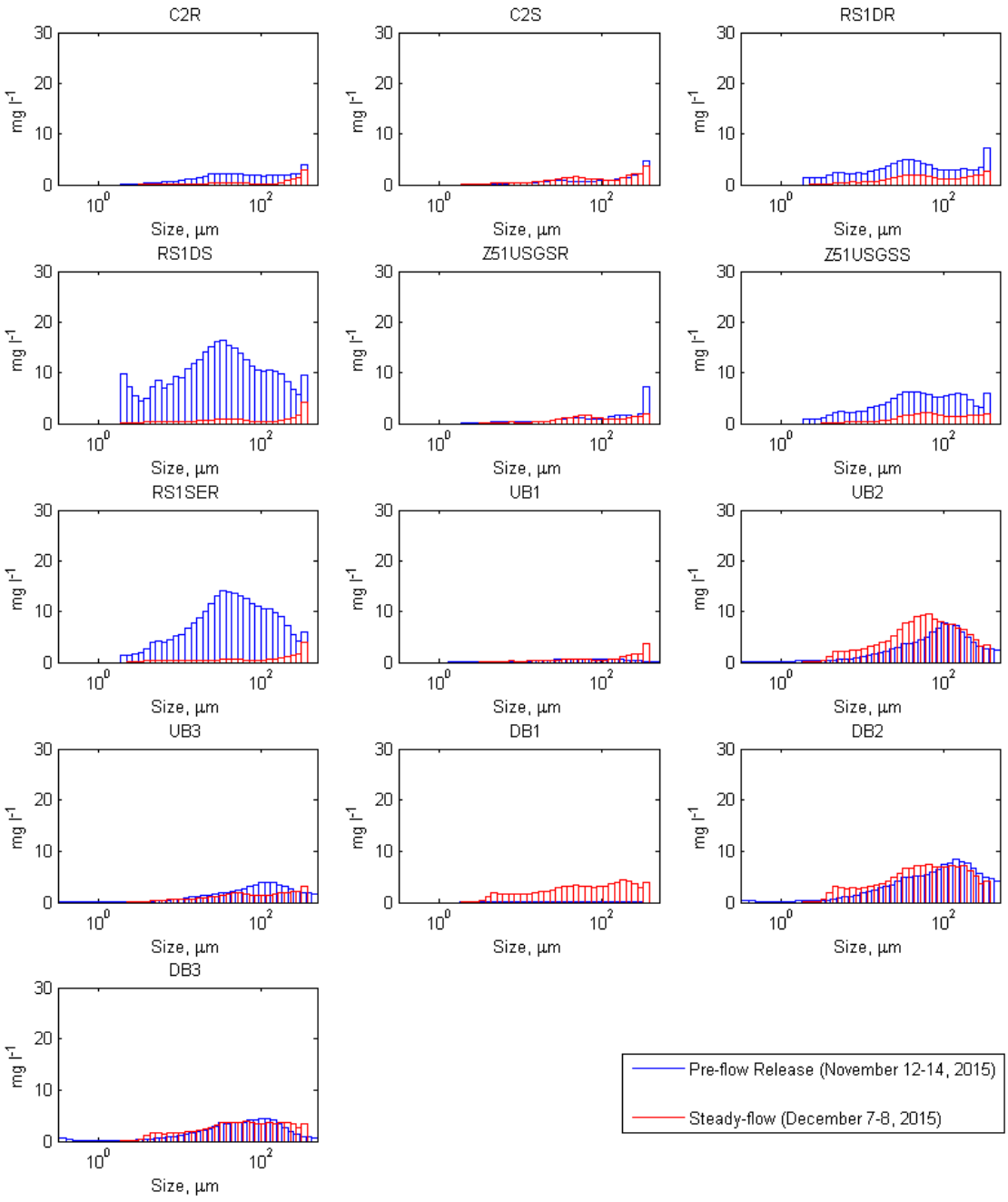

Figure E-112 Pre-flow release and steady-flow comparison of mass weighted distribution of epiphyton suspended particles. Samples collected during the 2015 DPM flow release.

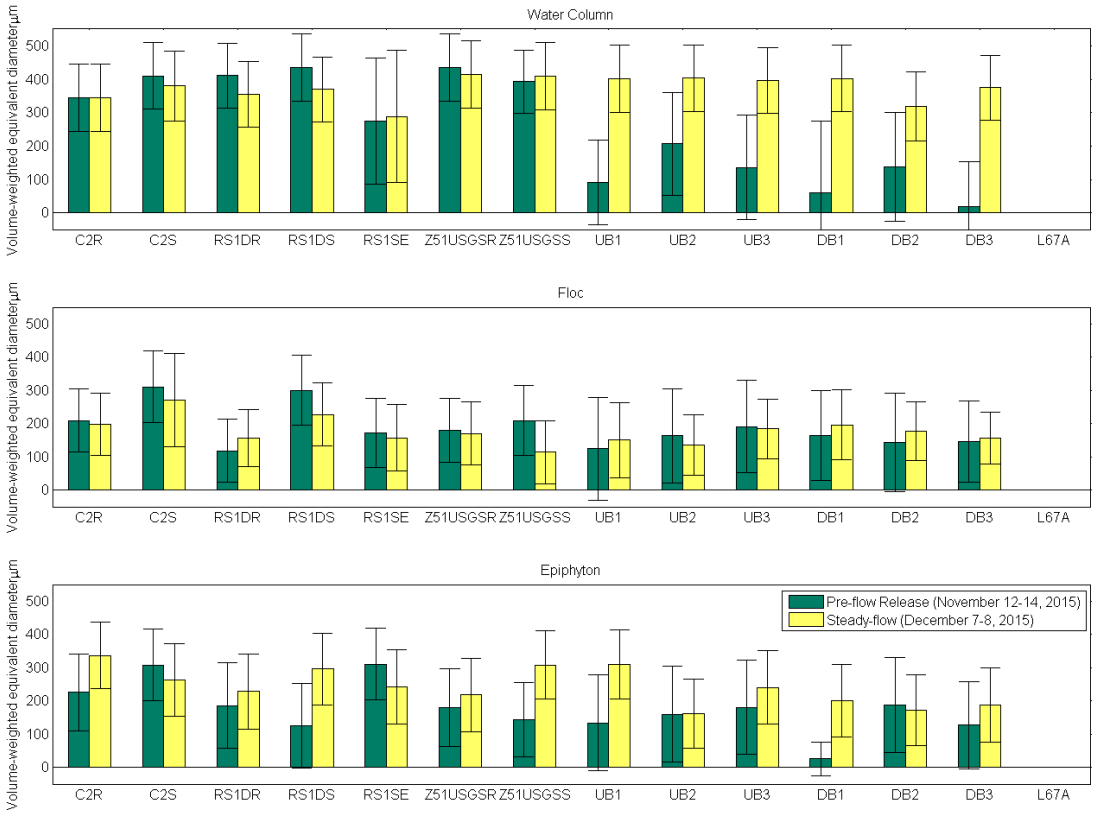

Figure E-113 Pre-flow release and steady-flow comparison of average volume weighted equivalent diameter for each particle type from all DPM sites, samples collected during the 2015 DPM flow release.

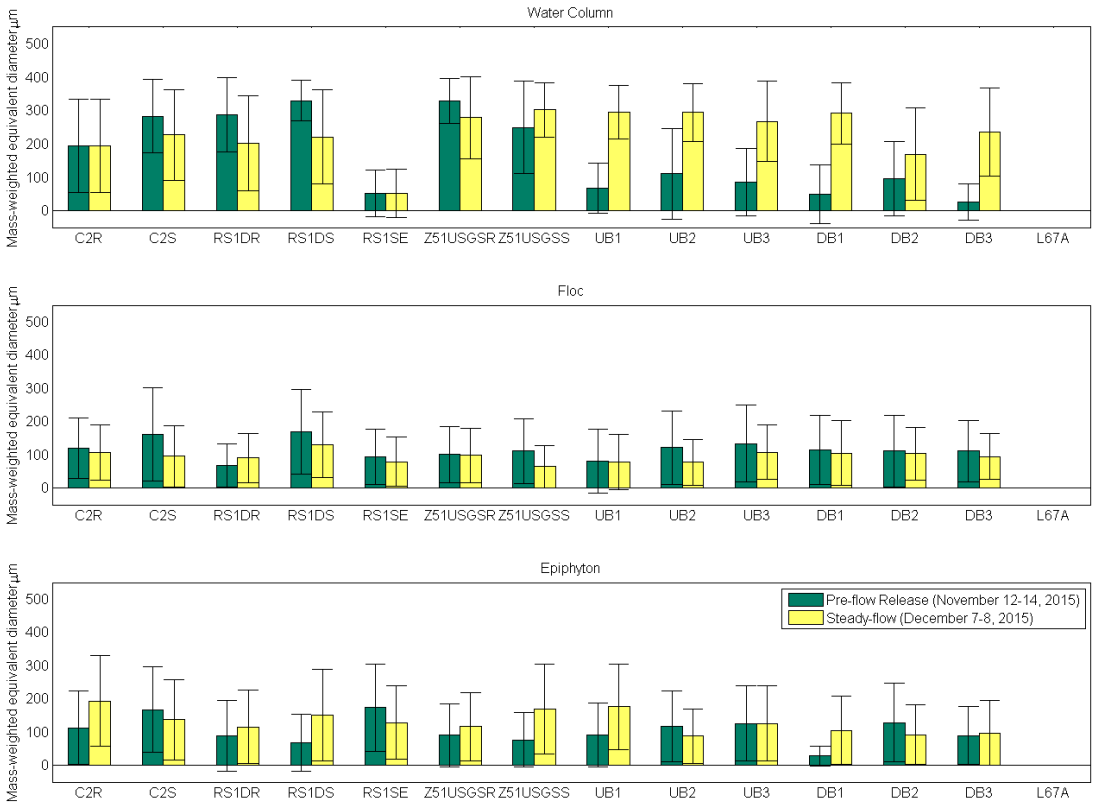

Figure E-114 Pre-flow release and steady-flow release comparison of average mass weighted equivalent diameter for each particle type from all DPM sites, samples collected during the 2015 DPM flow release.

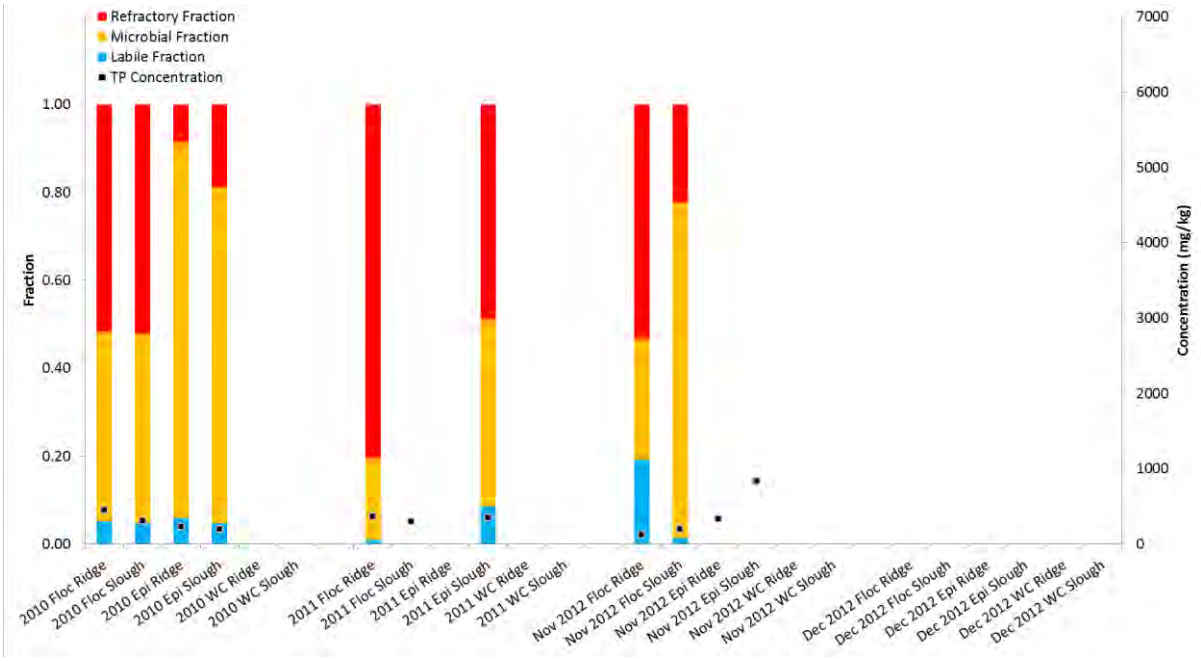

Figure E-115 Labile, microbial and refractory fractionation and total phosphorus concentrations from floc, epiphyton (epi) and water column (WC) samples collected at C1 from 2010 through 2012.

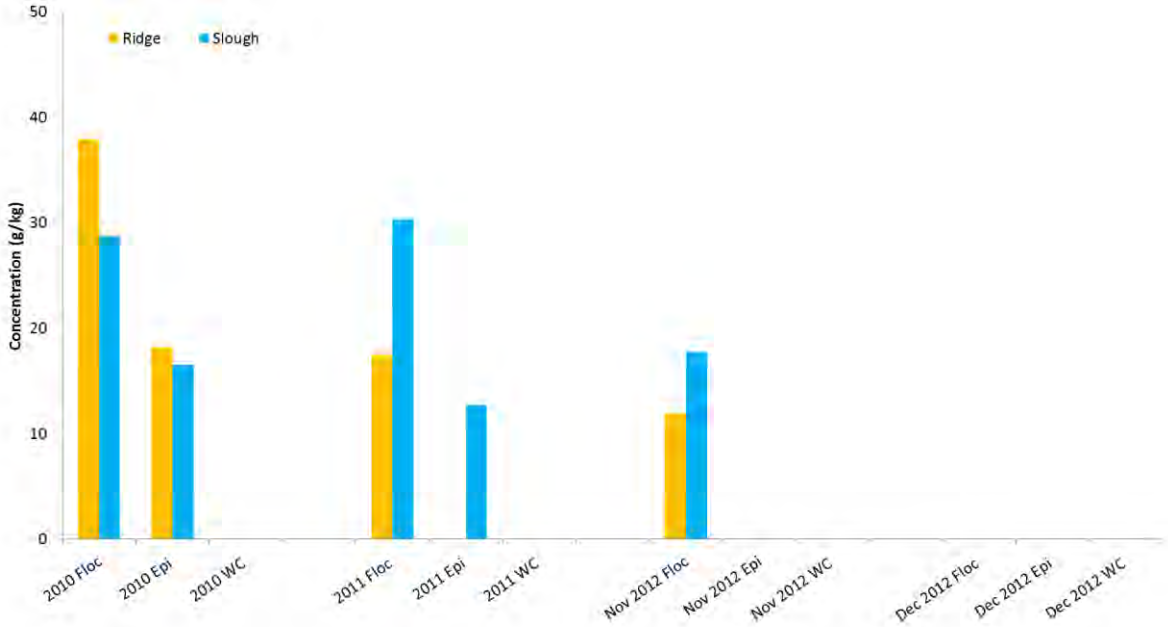

Figure E-117 Total nitrogen concentrations in floc, epiphyton (epi) and water column (WC) samples collected at C1 from 2010 through 2012.

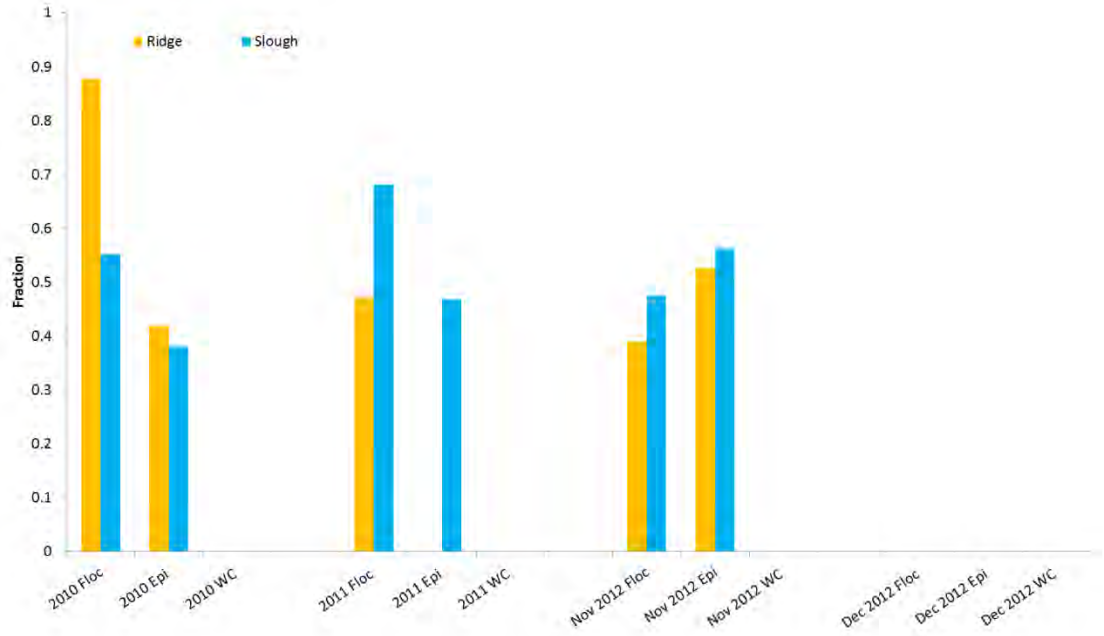

Figure E-116 Ash free dry weight (AFDW) fractions in floc, epiphyton (epi) and water column (WC) samples collected at C1 from 2010 through 2012.

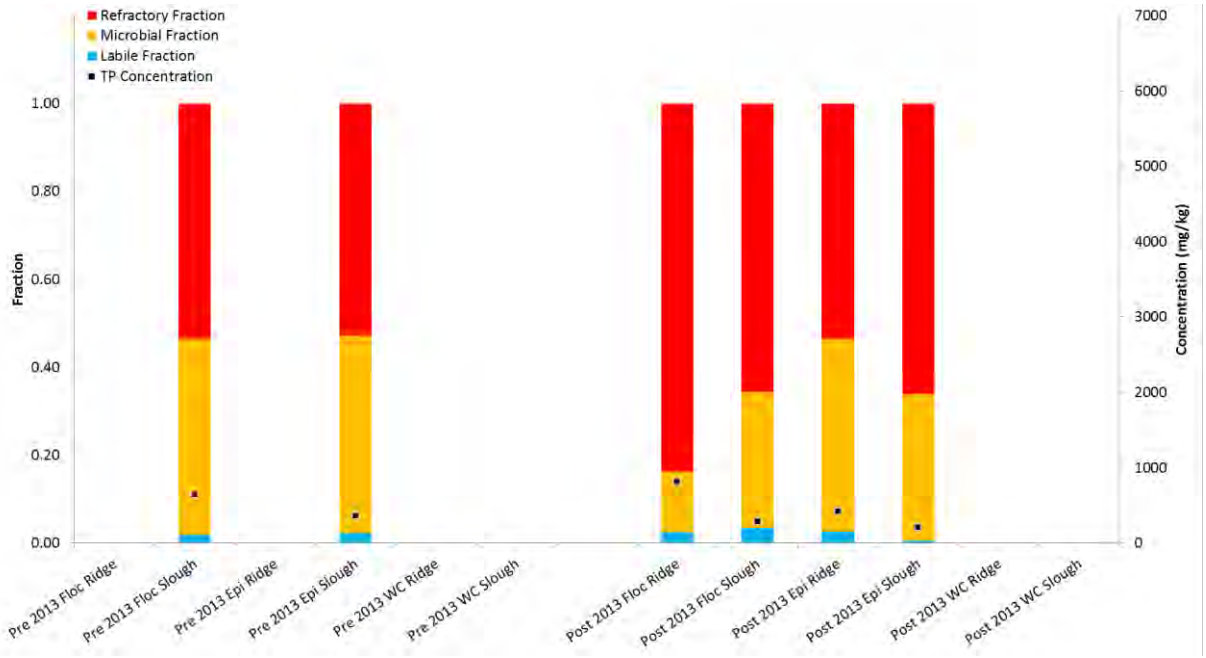

Figure E-118 Labile, microbial and refractory fractionation and total phosphorus concentrations from floc, epiphyton (epi) and water column (WC) samples collected at C1 for flow release 2013.

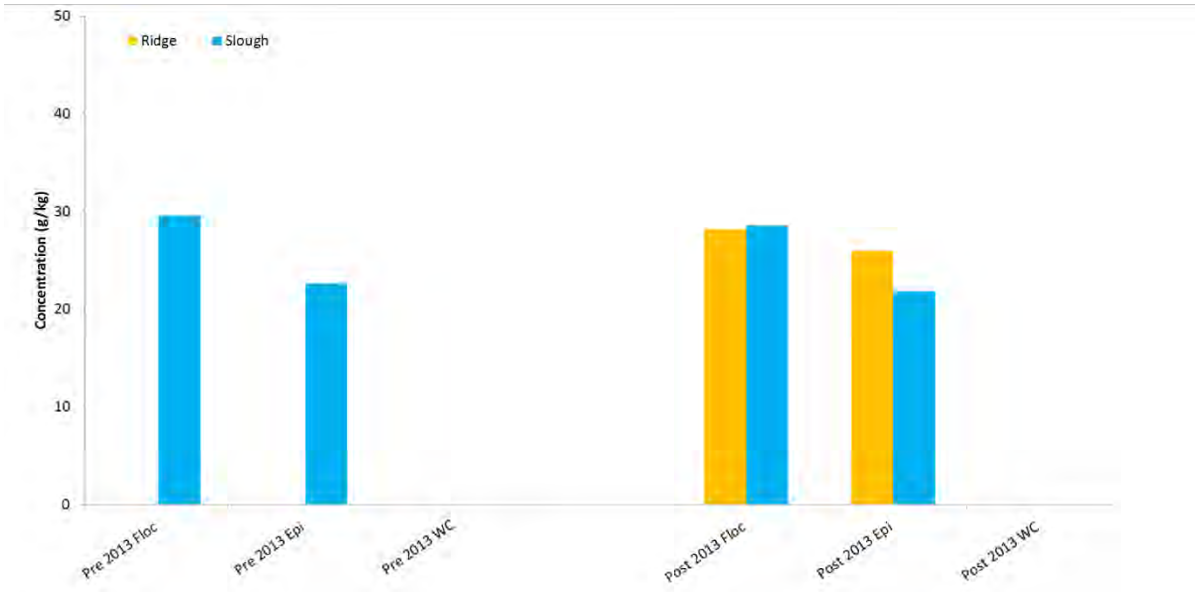

Figure E-119 Total nitrogen concentrations in floc, epiphyton (epi) and water column (WC) samples collected at C1 for flow release 2013.

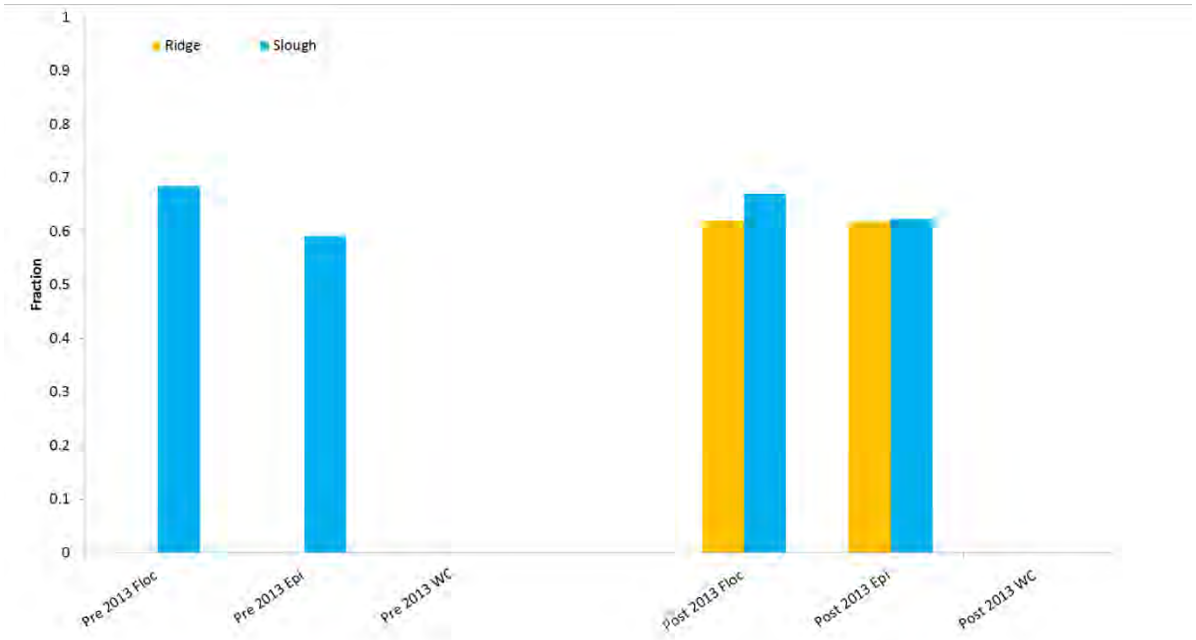

Figure E-120 Ash free dry weight (AFDW) fractions in floc, epiphyton (epi) and water column (WC) samples collected at C1 for flow release 2013.

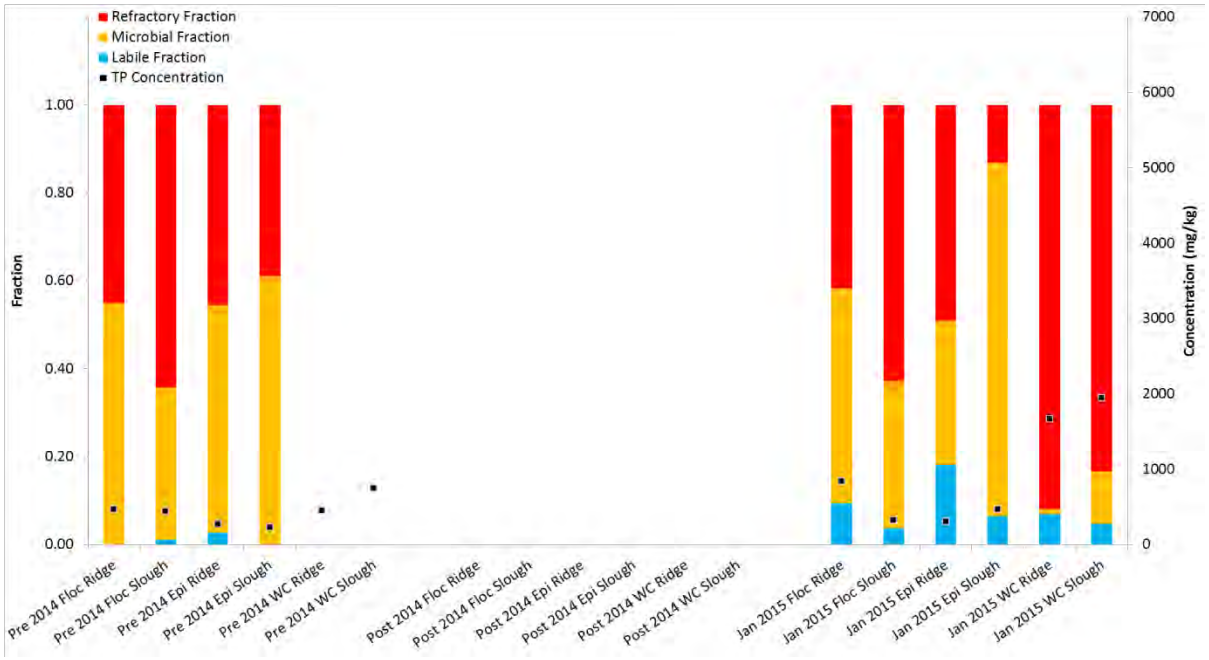

Figure E-121 Labile, microbial and refractory fractionation and total phosphorus concentrations from floc, epiphyton (epi) and water column (WC) samples collected at C1 for flow release 2014.

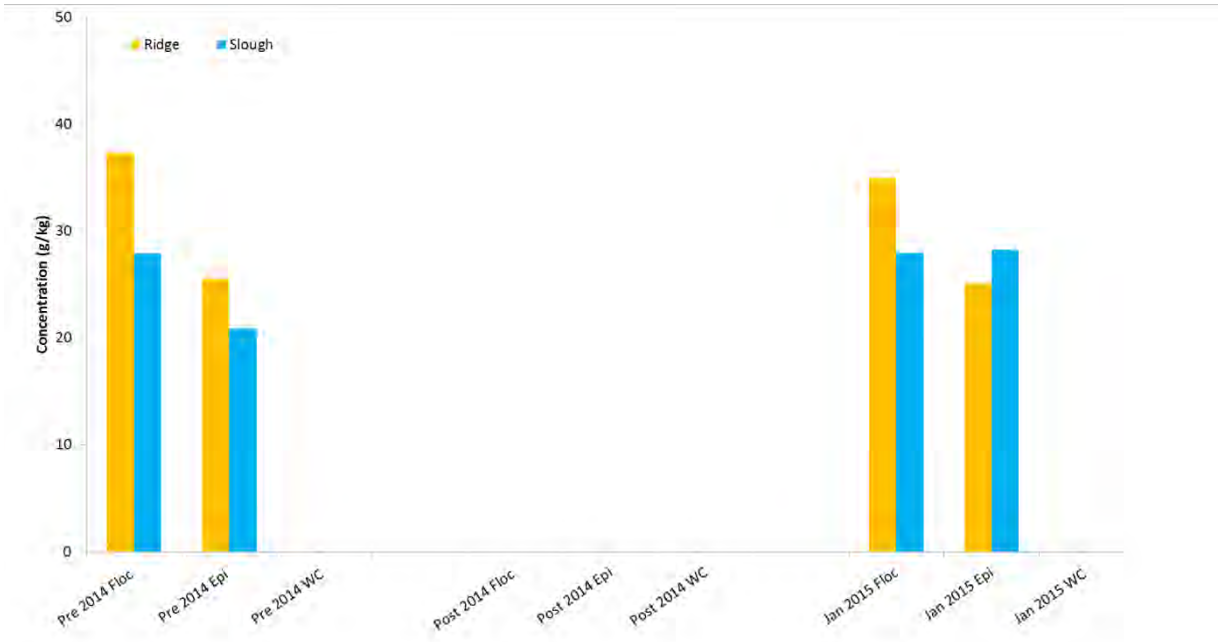

Figure E-122 Total nitrogen concentrations in floc, epiphyton (epi) and water column (WC) samples collected at C1 for flow release 2014.

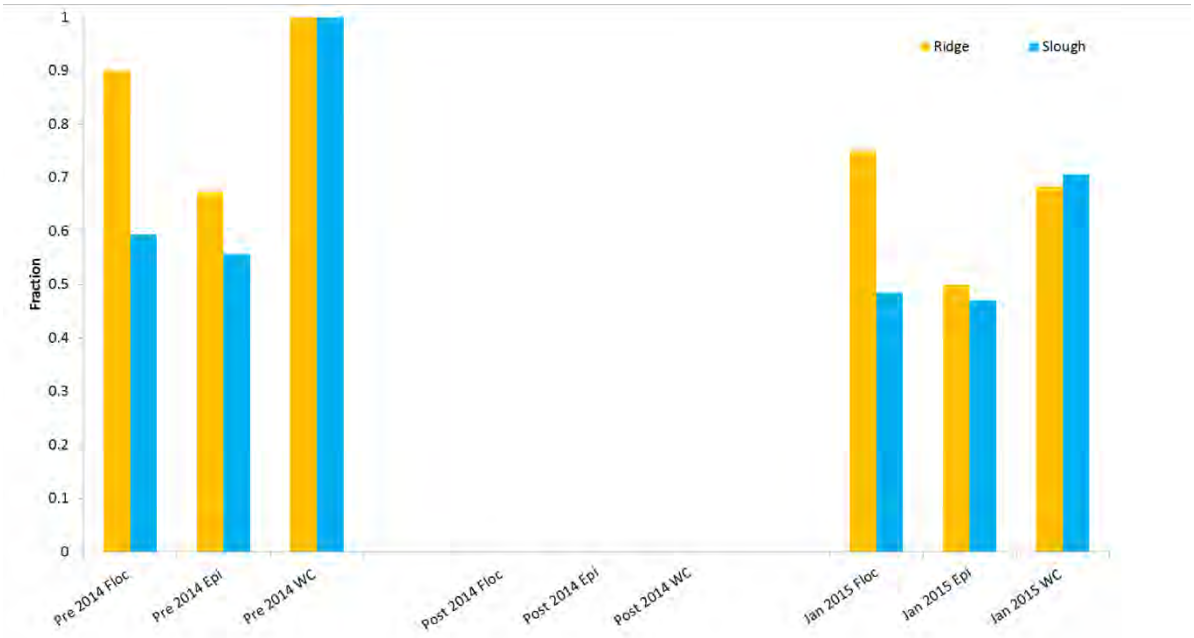

Figure E-123 Ash free dry weight (AFDW) fractions in floc, epiphyton (epi) and water column (WC) samples collected at C1 for flow release 2014.

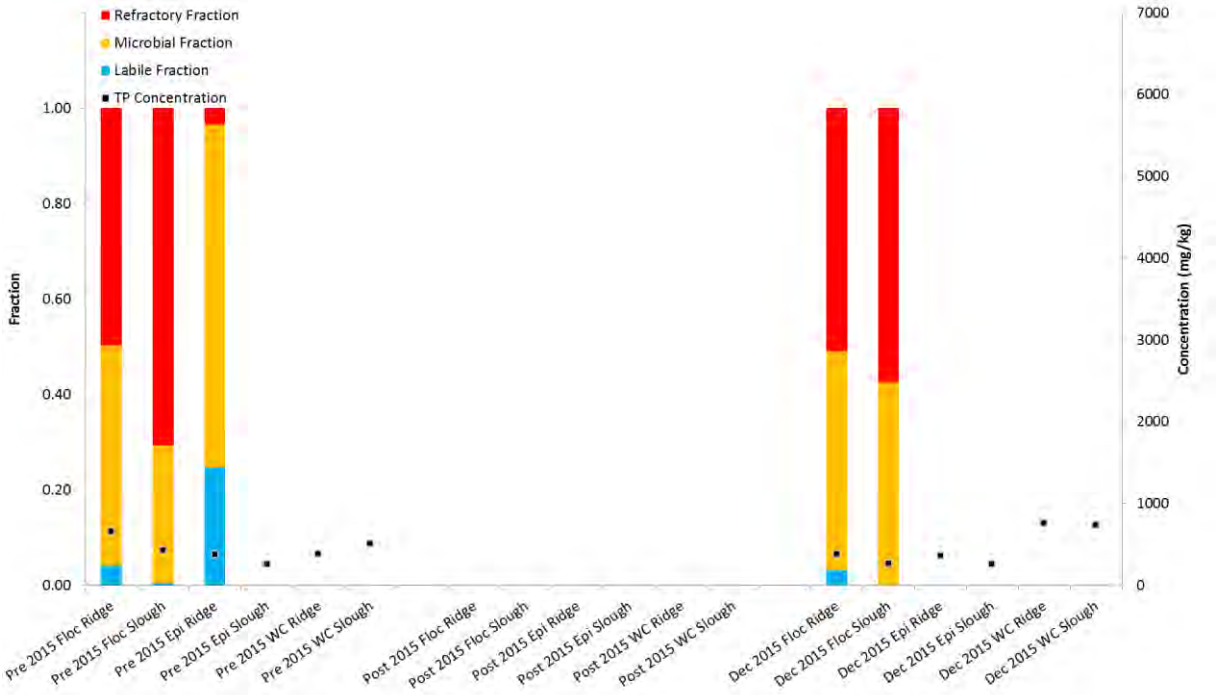

Figure E-124 Labile, microbial and refractory fractionation and total phosphorus concentrations from floc, epiphyton (epi) and water column (WC) samples collected at C2 for flow release 2015.

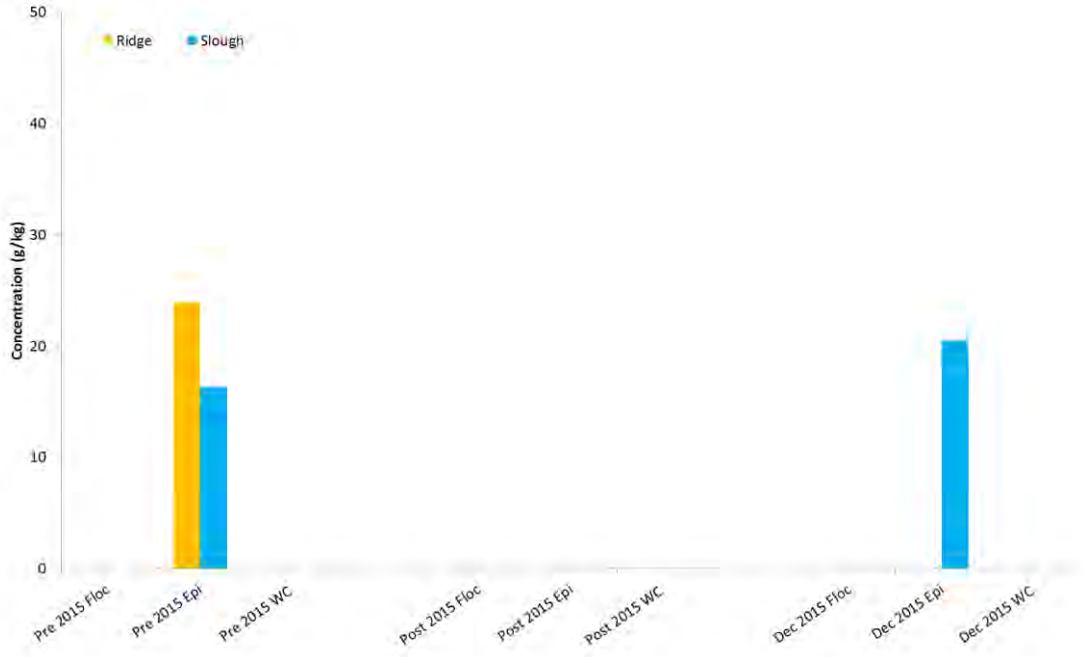

Figure E-125 Total nitrogen concentrations in floc, epiphyton (epi) and water column (WC) samples collected at C2 for flow release 2015.

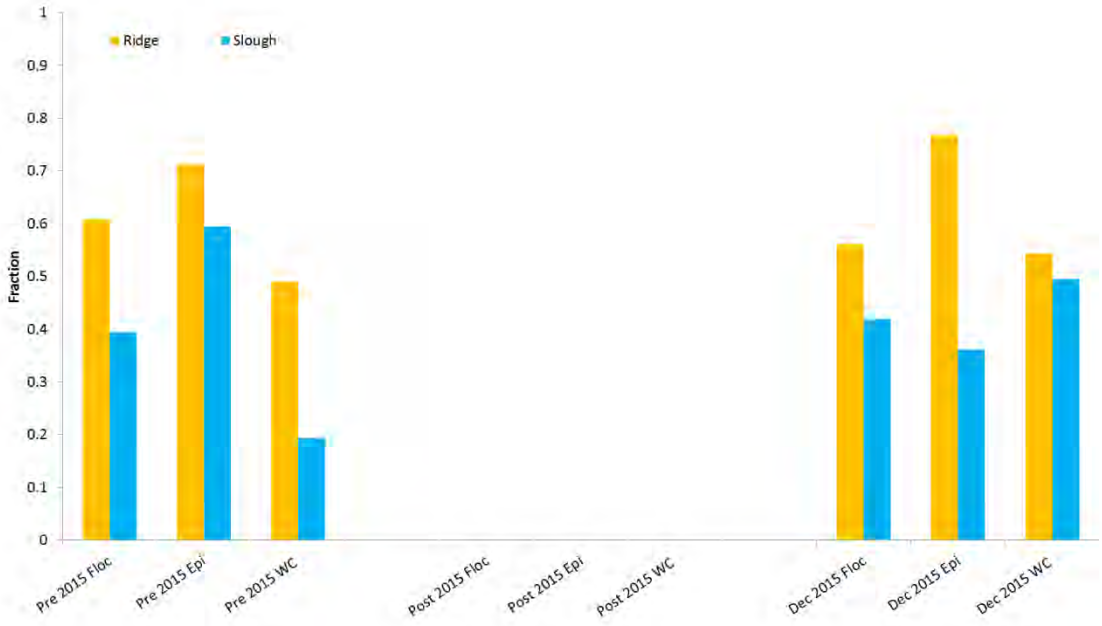

Figure E-126 Ash free dry weight (AFDW) fractions in floc, epiphyton (epi) and water column (WC) samples collected at C2 for flow release 2015.

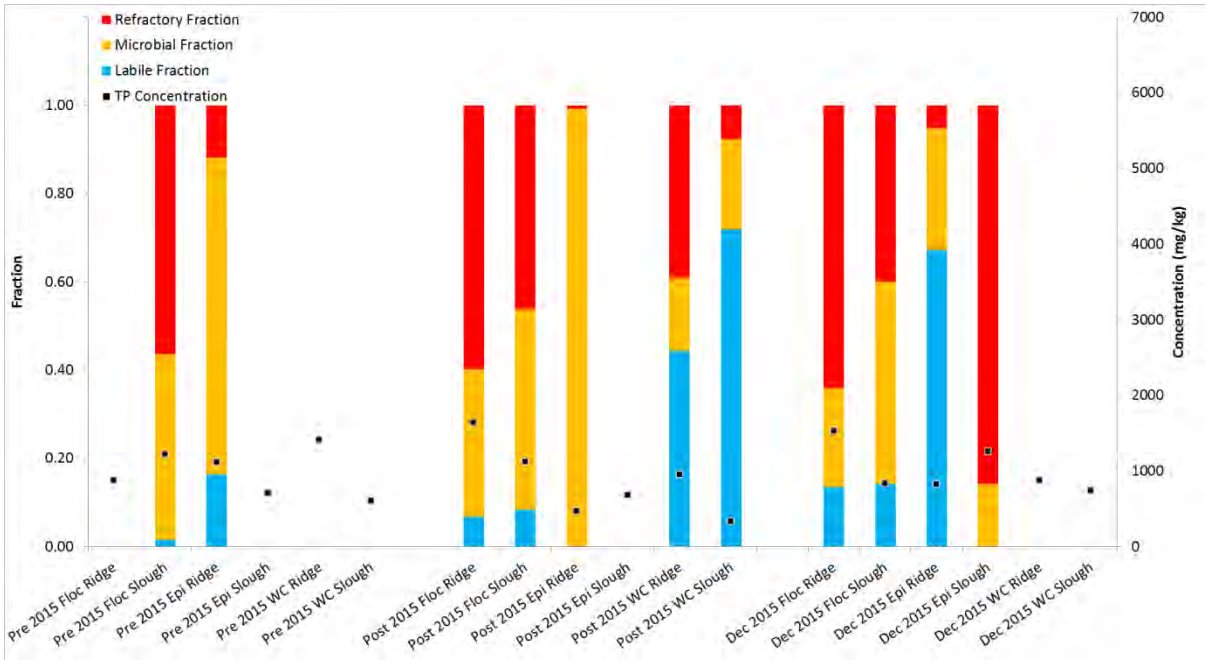

Figure E-127 Labile, microbial and refractory fractionation and total phosphorus concentrations from floc, epiphyton (epi) and water column (WC) samples collected at Z51_USGS for flow release 2015.

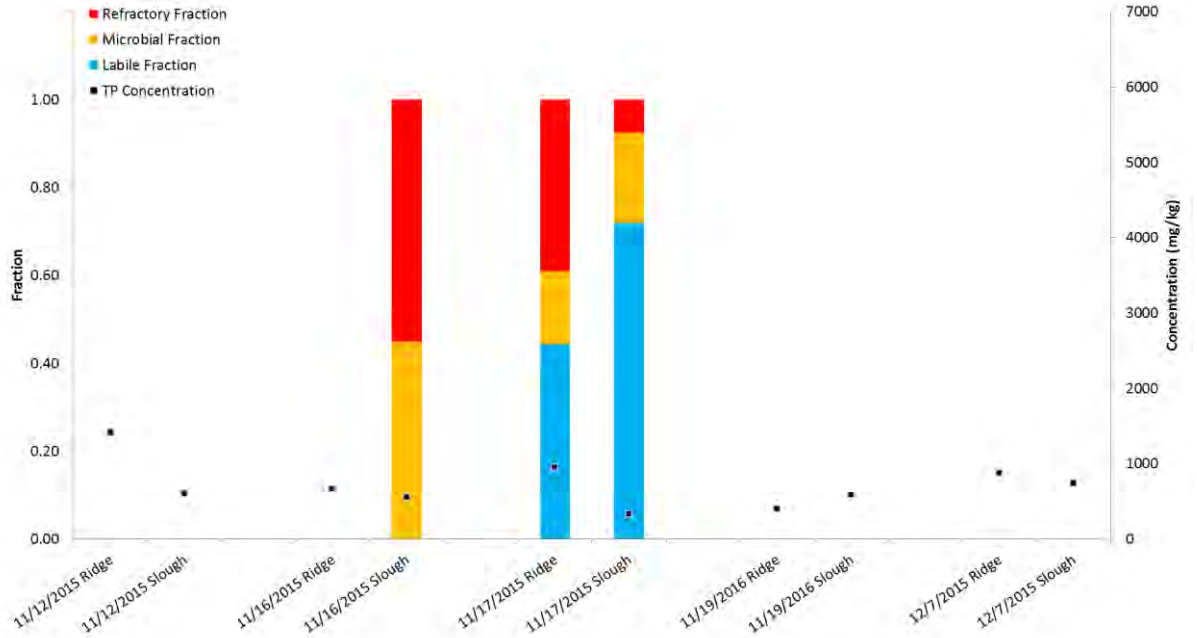

Figure E-128 Labile, microbial and refractory fractionation and total phosphorus concentrations for the complete set of water column (WC) samples collected at Z51_USGS for flow release 2015.

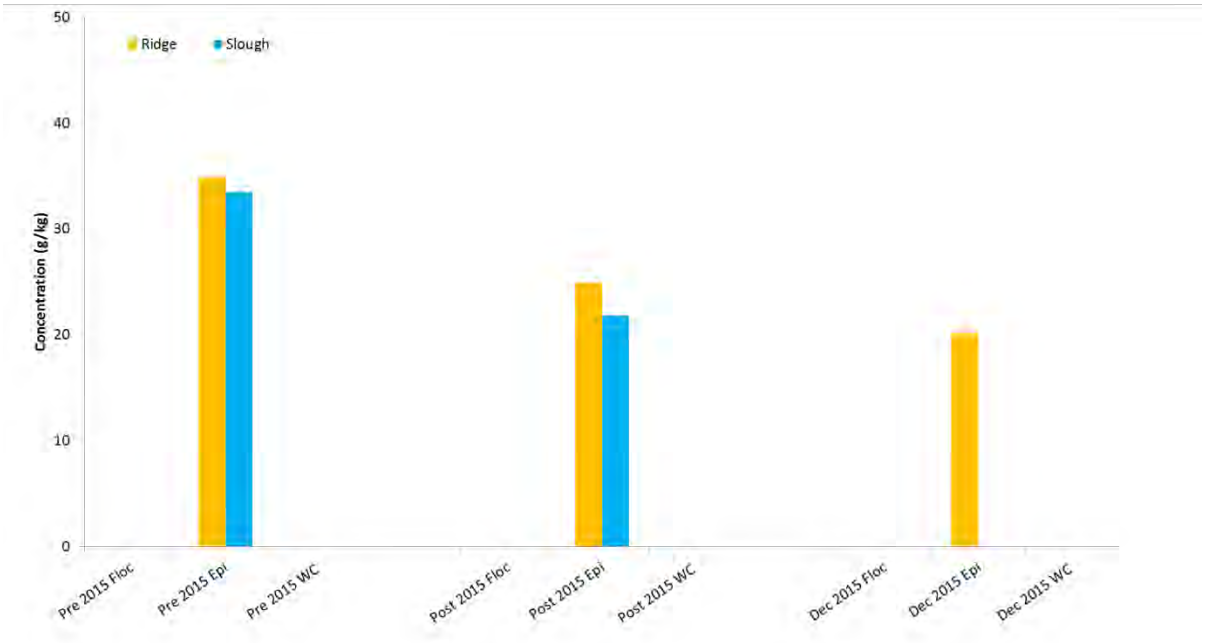

Figure E-129 Total nitrogen concentrations in floc, epiphyton (epi) and water column (WC) samples collected at Z51_USGS for flow release 2015.

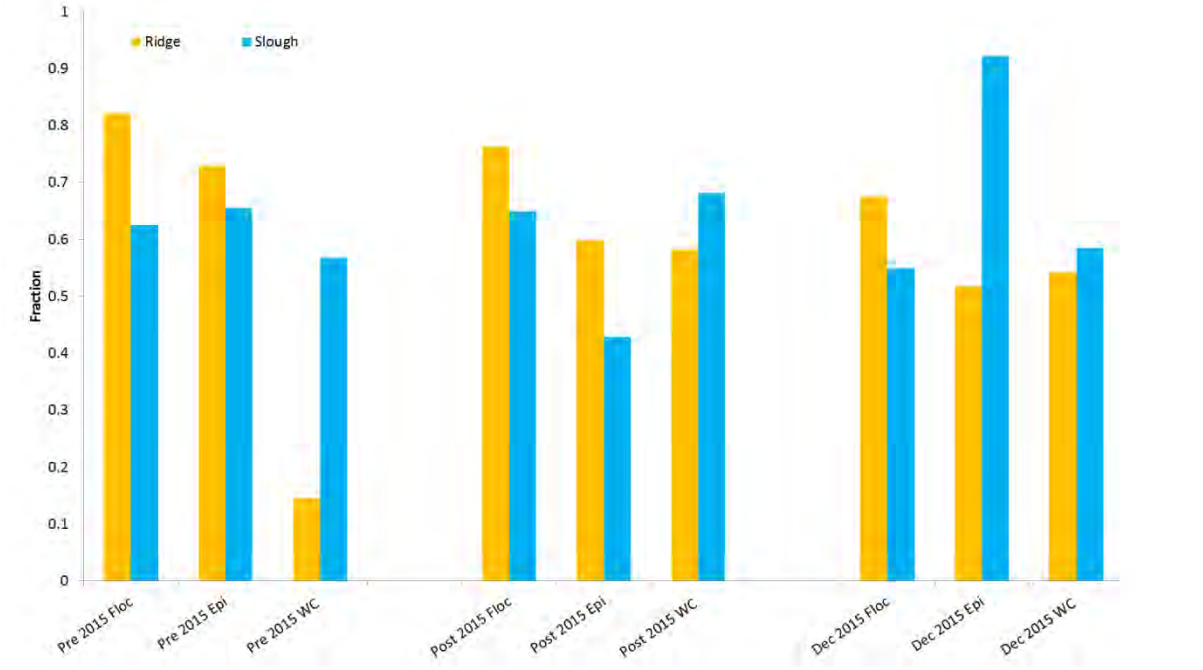

Figure E-130 Ash free dry weight (AFDW) fractions in floc, epiphyton (epi) and water column (WC) samples collected at Z51_USGS for flow release 2015.

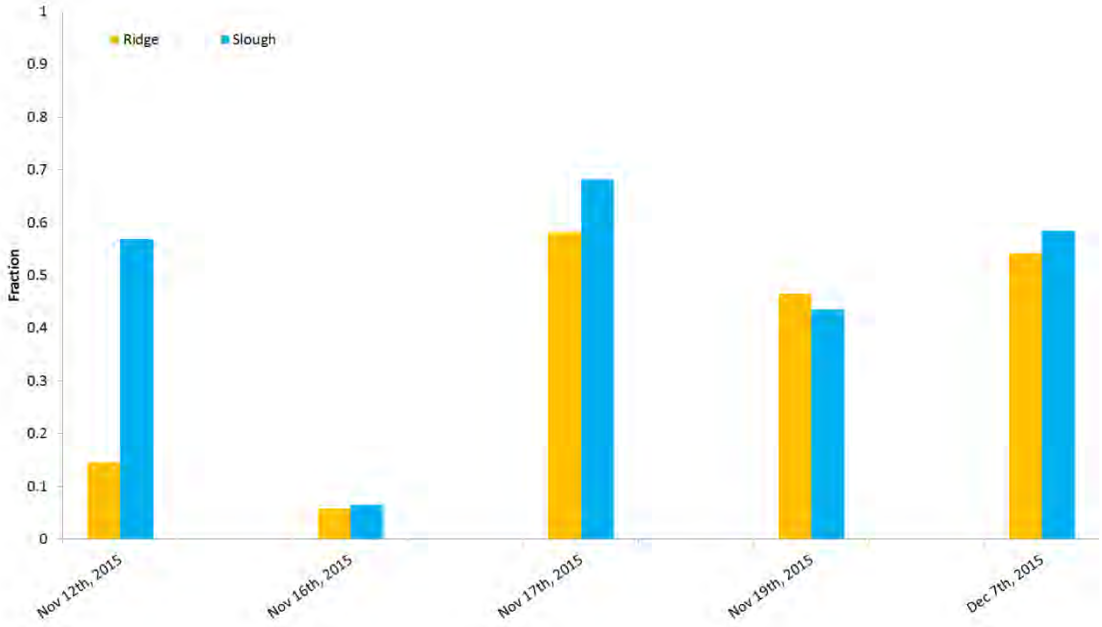

Figure E-131 Ash free dry weight (AFDW) fractions for the complete set of water column (WC) samples collected at Z51_USGS for flow release 2015.

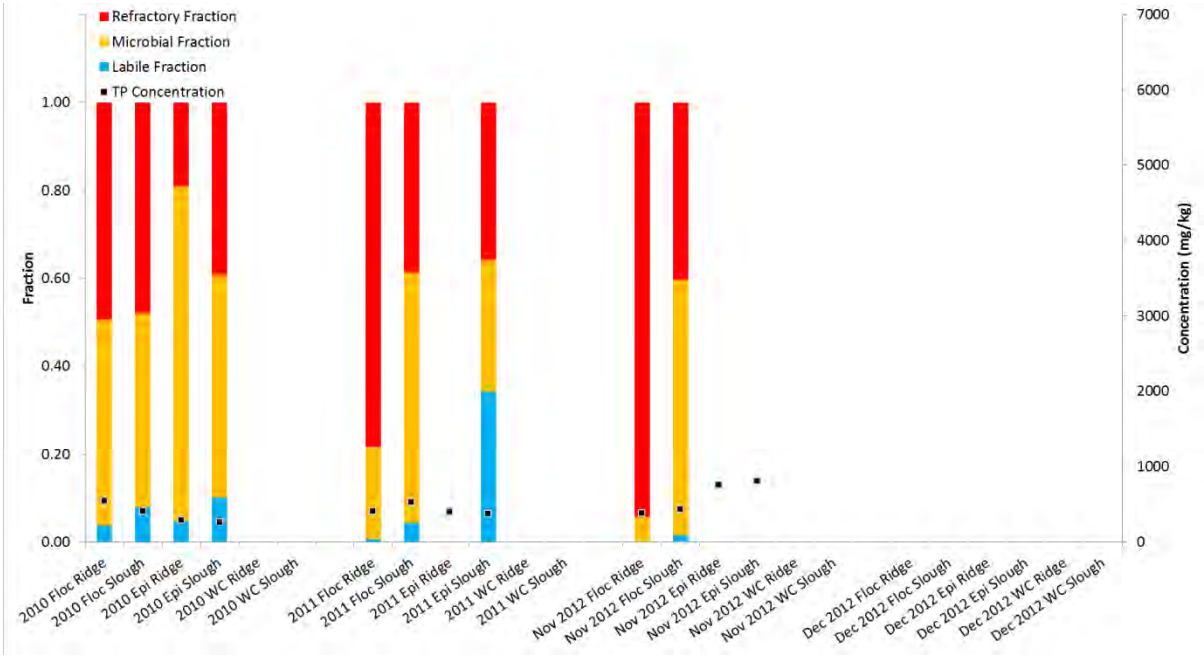

Figure E-132 Labile, microbial and refractory fractionation and total phosphorus concentrations from floc, epiphyton (epi) and water column (WC) samples collected at RS1D from 2010 through 2012.

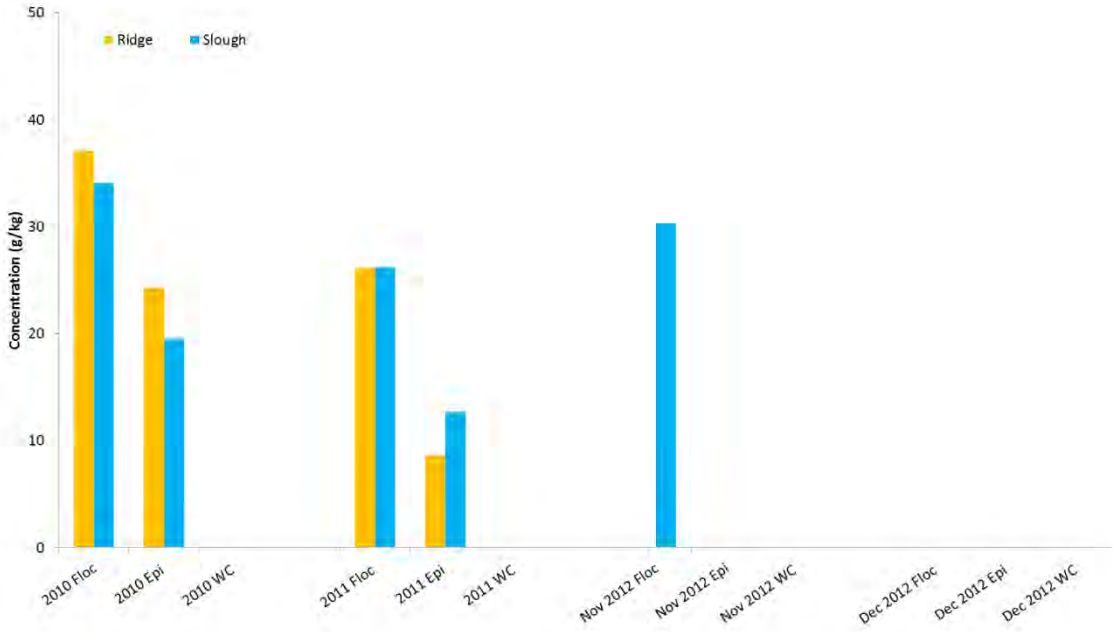

Figure E-133 Total nitrogen concentrations in floc, epiphyton (epi) and water column (WC) samples collected at RS1D from 2010 through 2012.

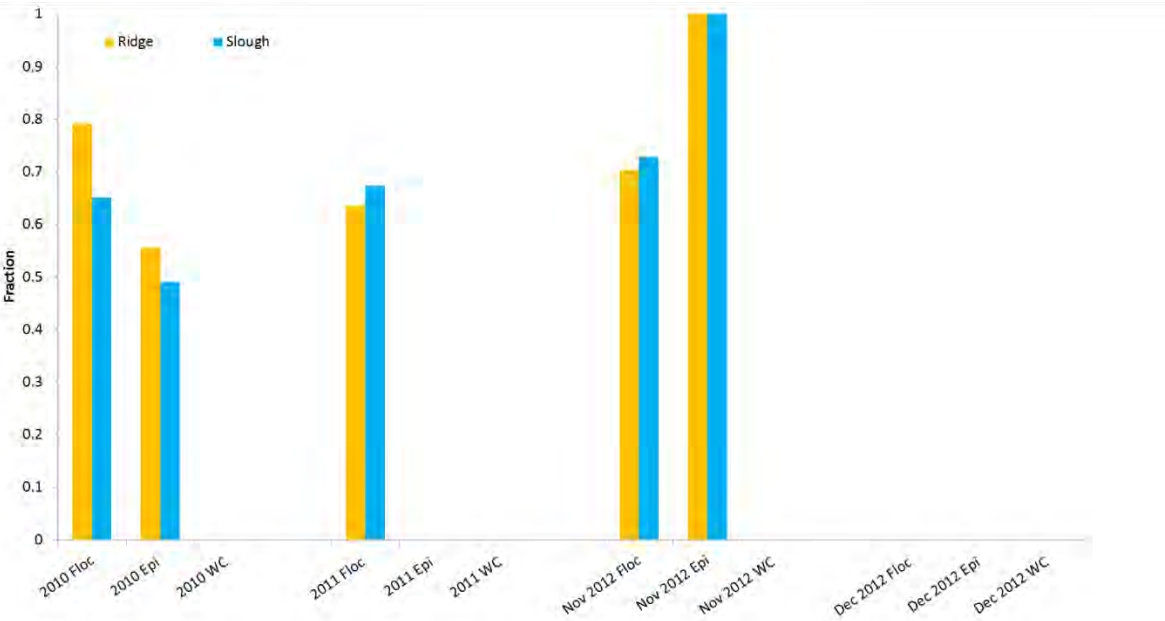

Figure E-134 Ash free dry weight (AFDW) fractions in floc, epiphyton (epi) and water column (WC) samples collected at RS1D from 2010 through 2012.

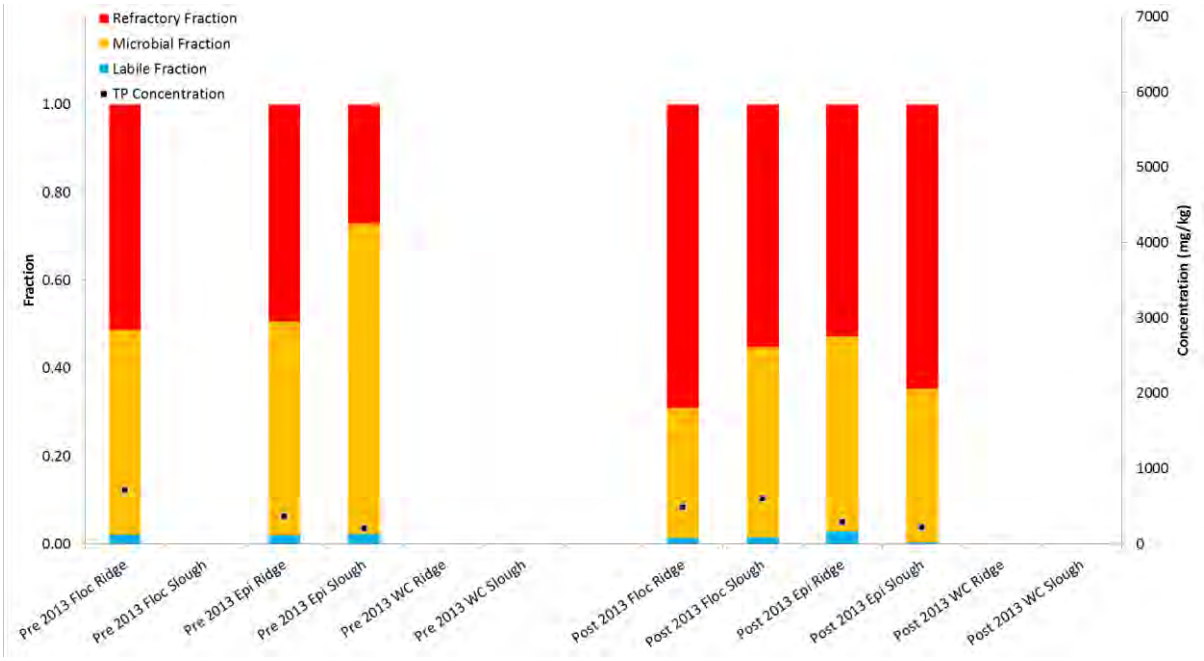

Figure E-135 Labile, microbial and refractory fractionation and total phosphorus concentrations from floc, epiphyton (epi) and water column (WC) samples collected at RS1D for flow release 2013.

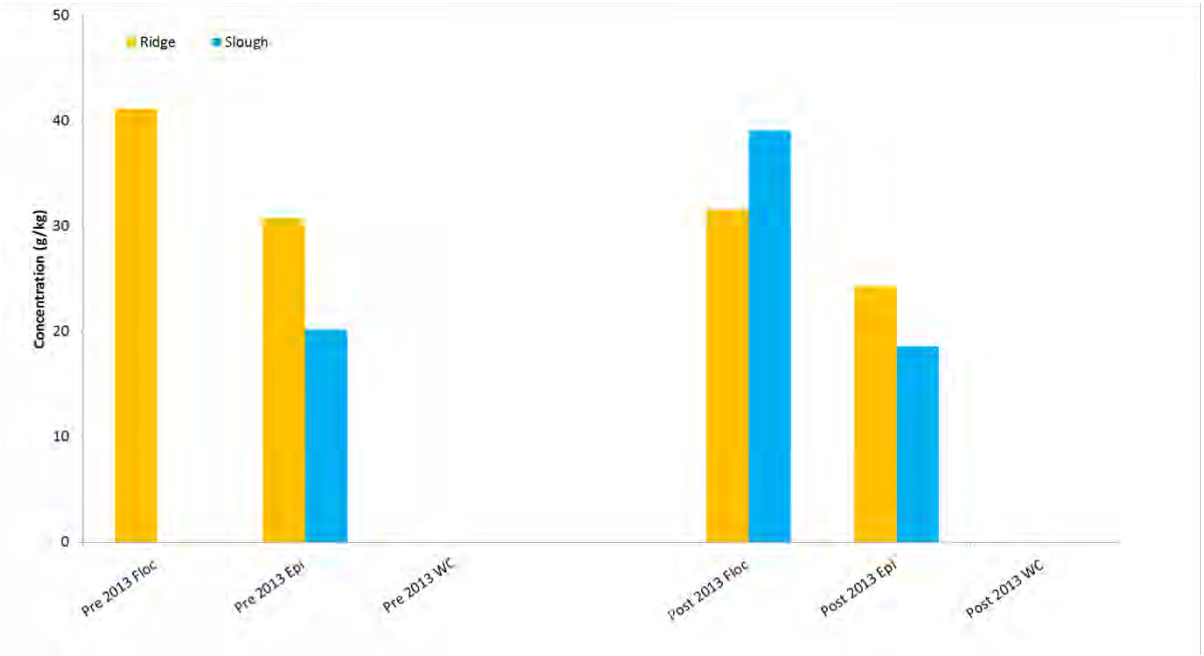

Figure E-136 Total nitrogen concentrations in floc, epiphyton (epi) and water column (WC) samples collected at RS1D for flow release 2013.

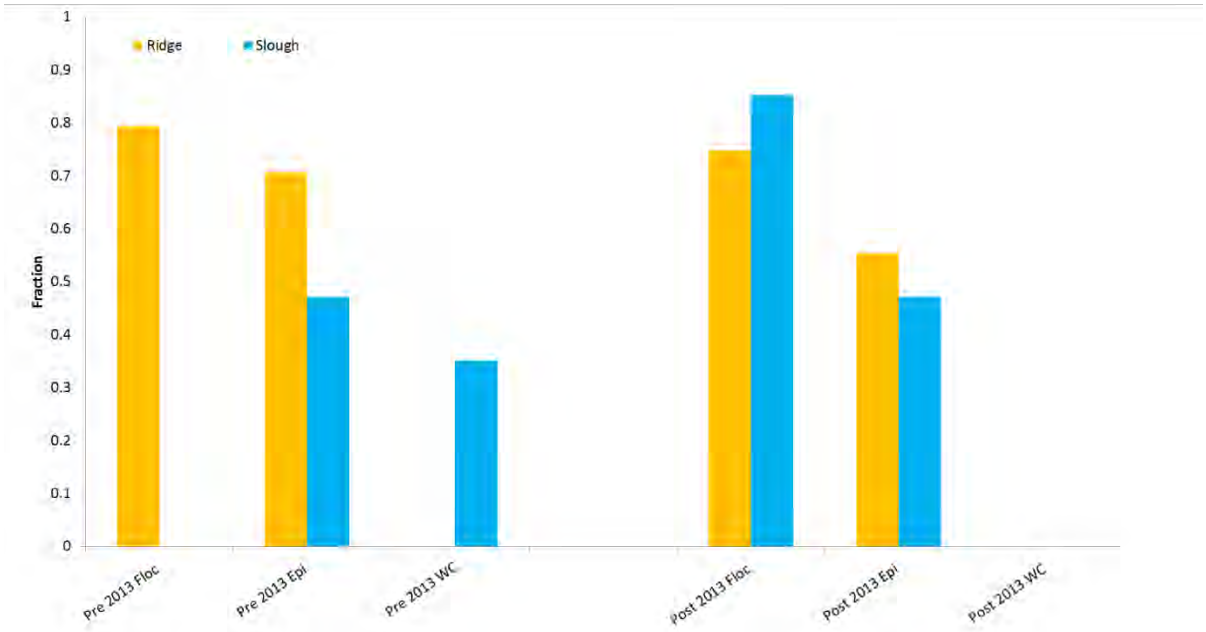

Figure E-137 Ash free dry weight (AFDW) fractions in floc, epiphyton (epi) and water column (WC) samples collected at RS1D for flow release 2013.

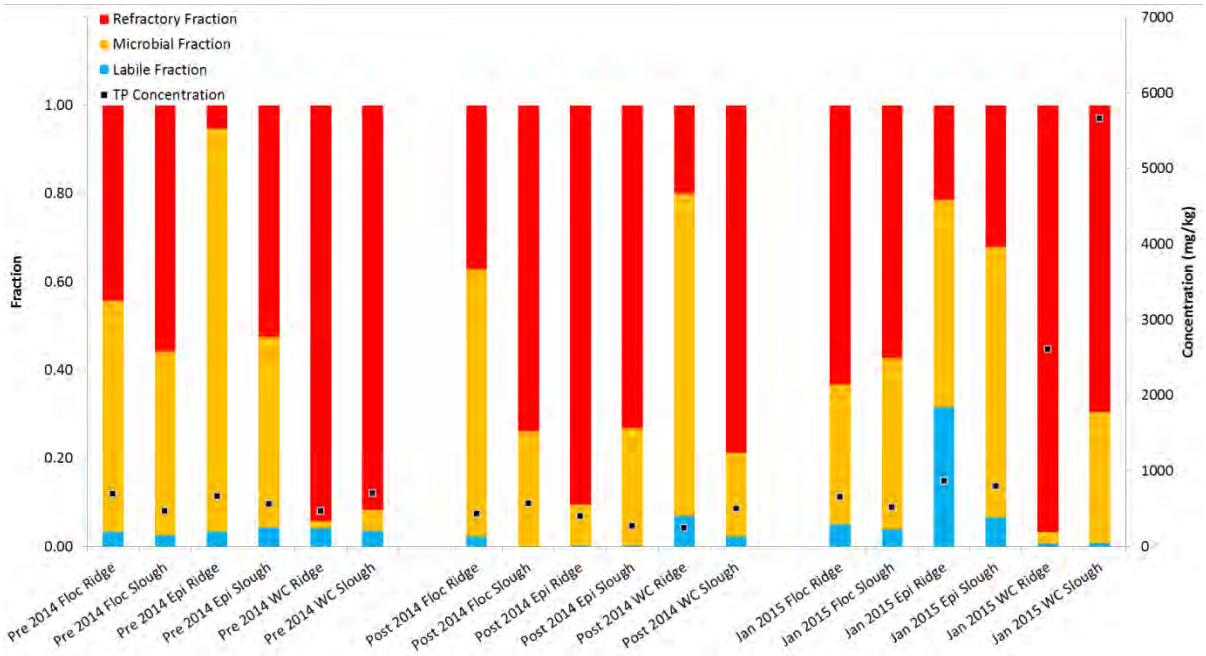

Figure E-138 Labile, microbial and refractory fractionation and total phosphorus concentrations from floc, epiphyton (epi) and water column (WC) samples collected at RS1D for flow release 2014.

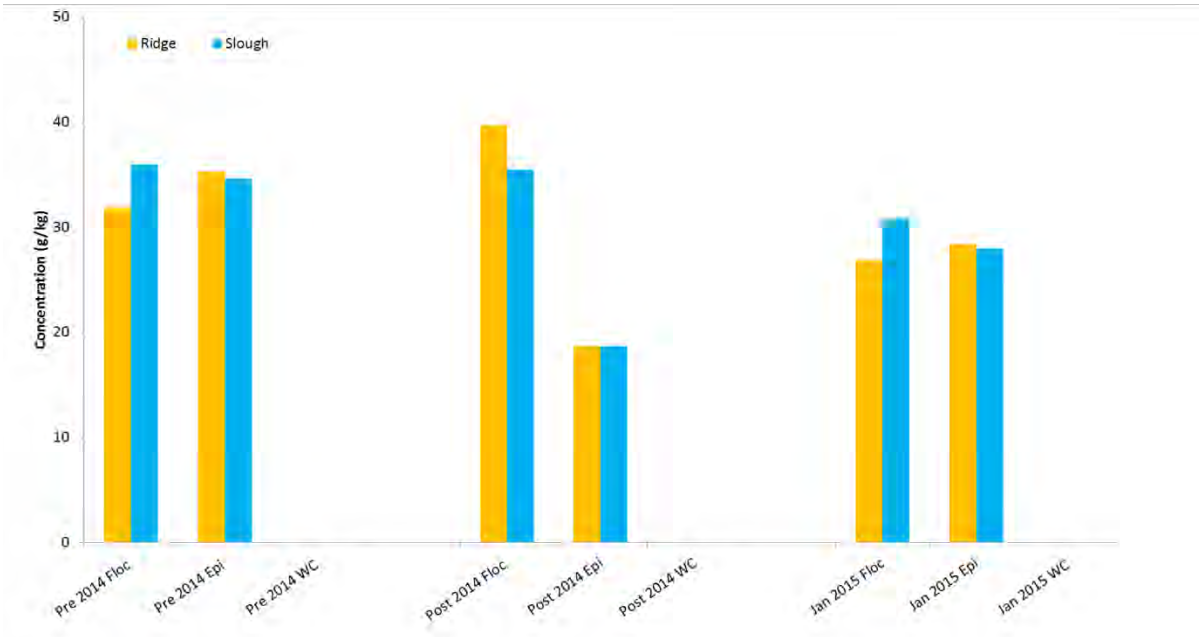

Figure E-139 Total nitrogen concentrations in floc, epiphyton (epi) and water column (WC) samples collected at RS1D for flow release 2014.

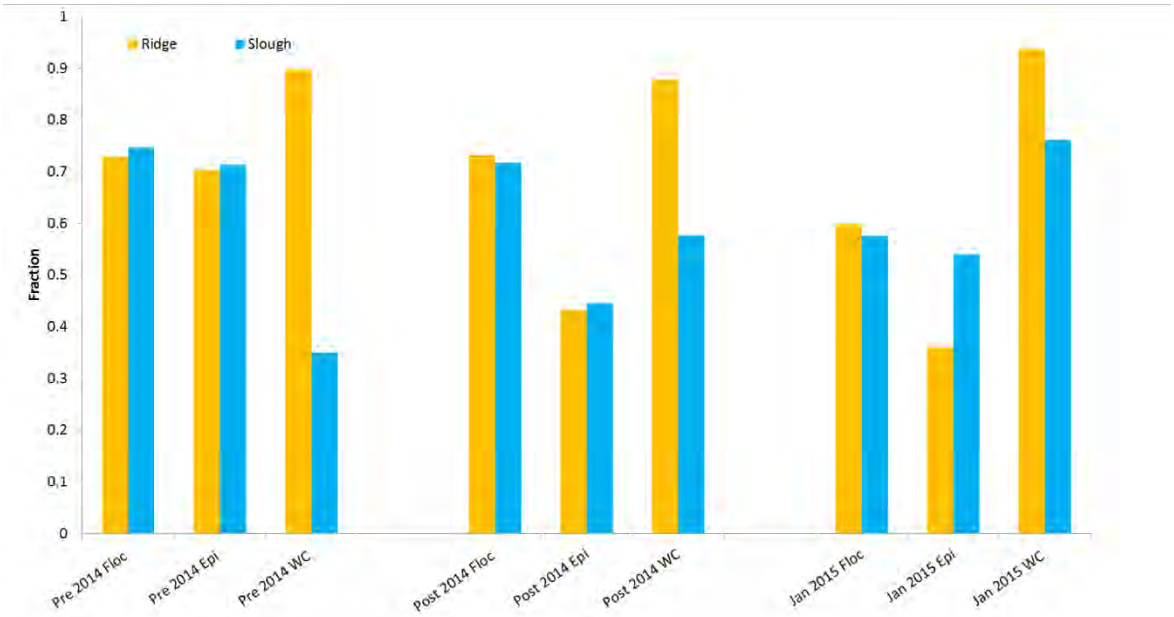

Figure E-140 Ash free dry weight (AFDW) fractions in floc, epiphyton (epi) and water column (WC) samples collected at RS1D for flow release 2014.

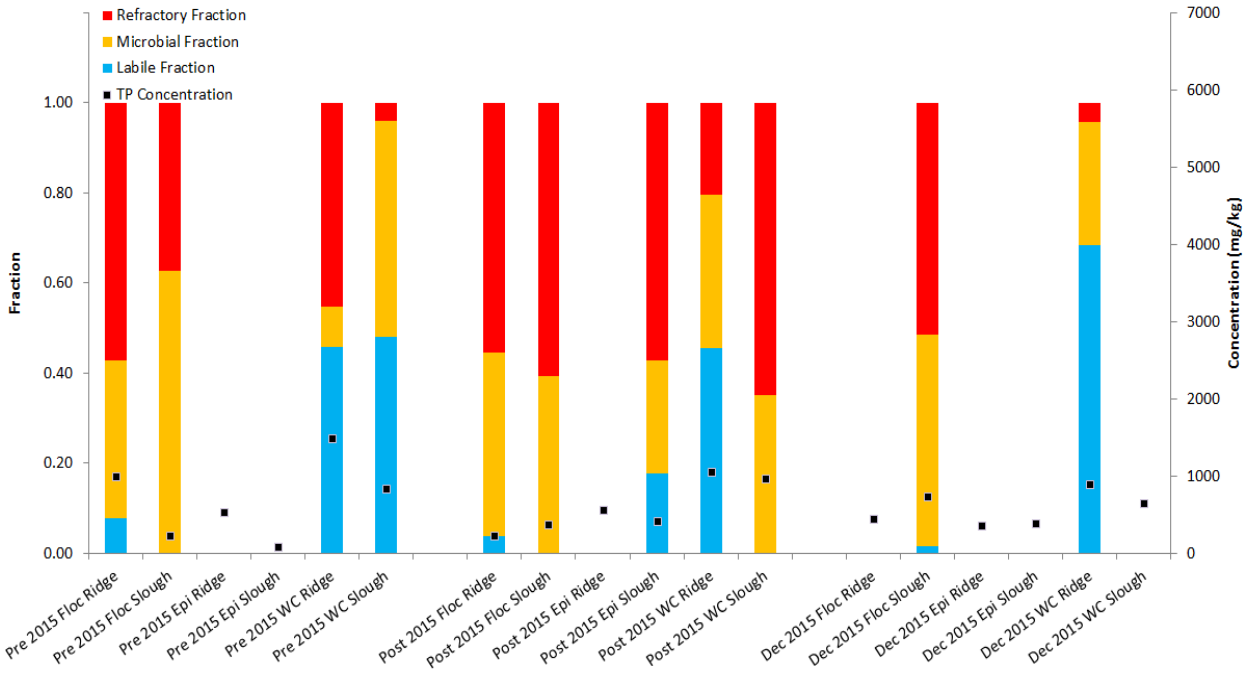

Figure E-141 Labile, microbial and refractory fractionation and total phosphorus concentrations from floc, epiphyton (epi) and water column (WC) samples collected at RS1D for flow release 2015.

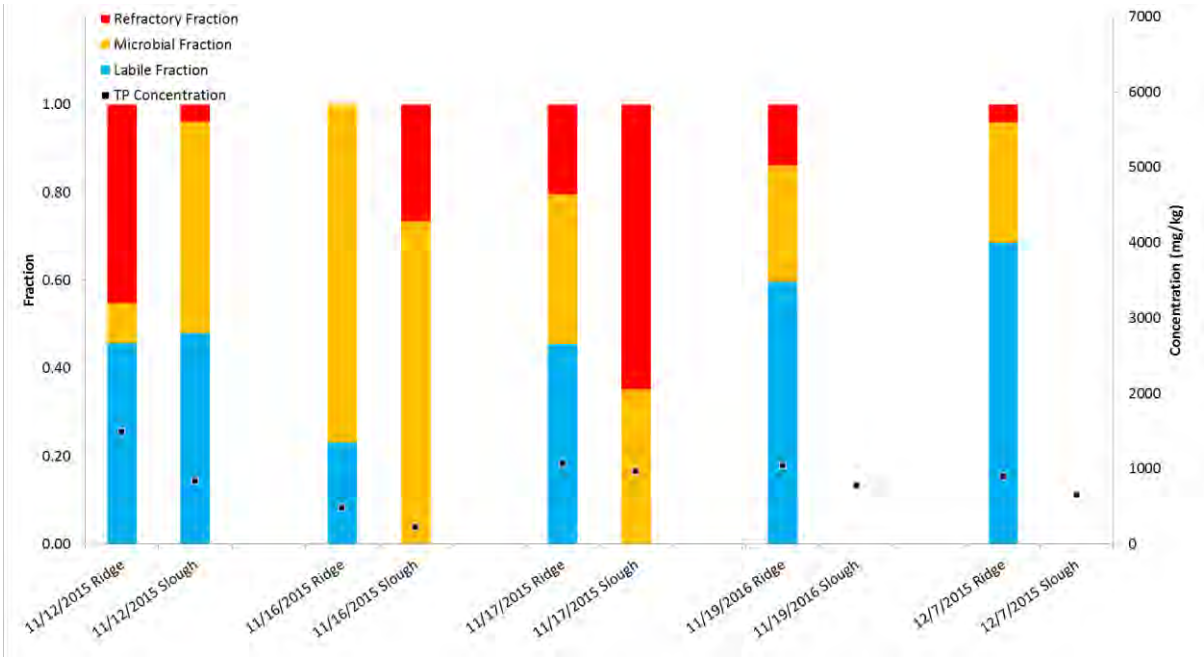

Figure E-142 Labile, microbial and refractory fractionation and total phosphorus concentrations for the complete set of water column (WC) samples collected at RS1D for flow release 2015.

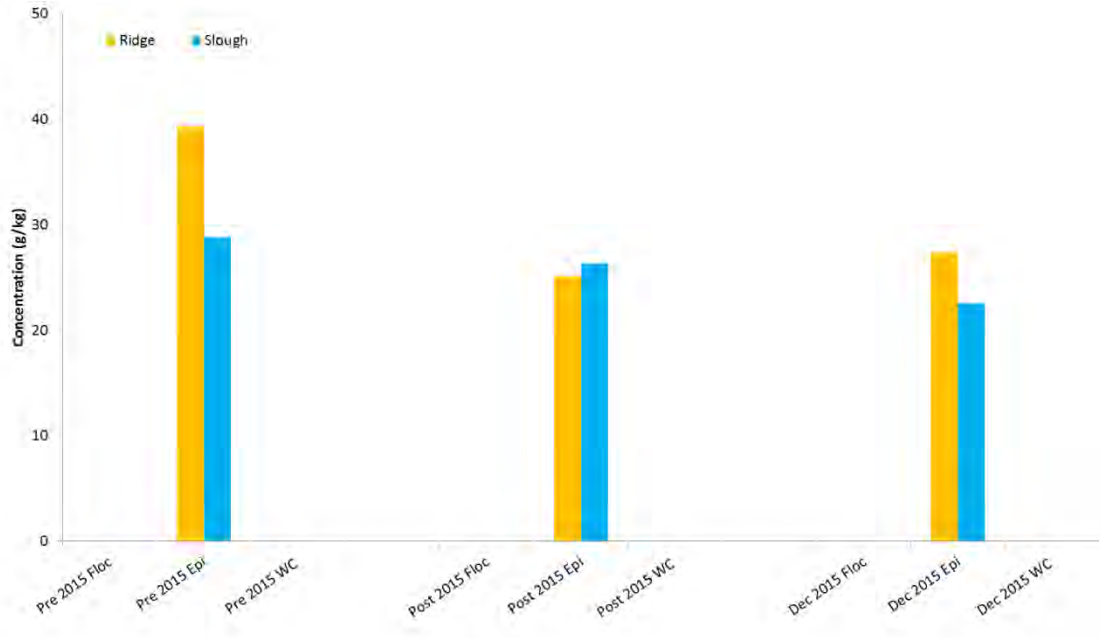

Figure E-143 Total nitrogen concentrations in floc, epiphyton (epi) and water column (WC) samples collected at RS1D for flow release 2015.

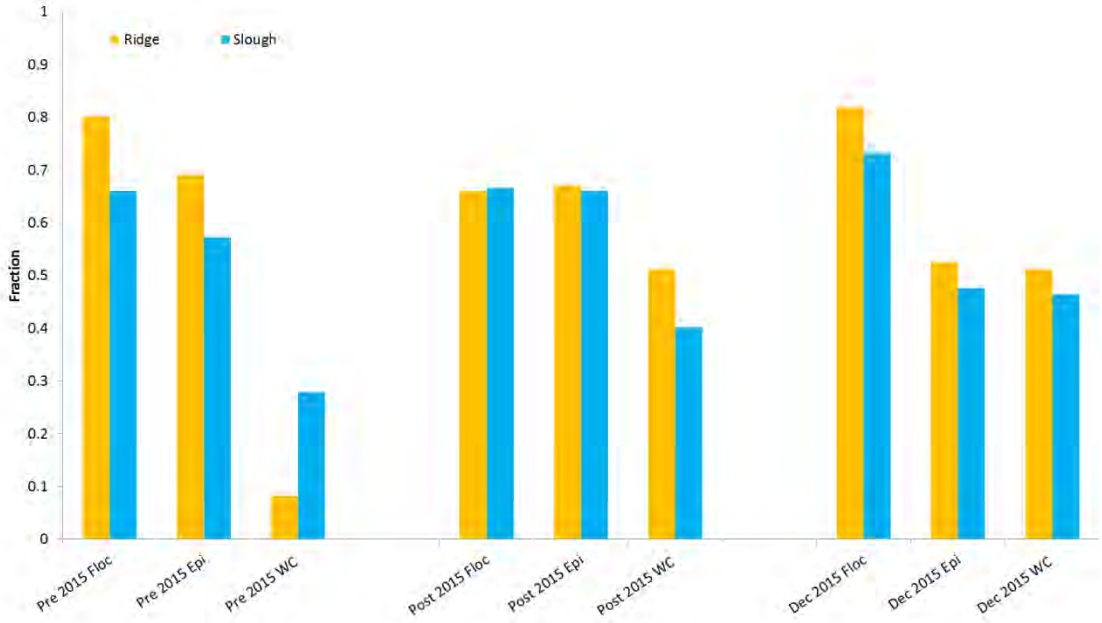

Figure E-144 Ash free dry weight (AFDW) fractions in floc, epiphyton (epi) and water column (WC) samples collected at RS1D for flow release 2015.

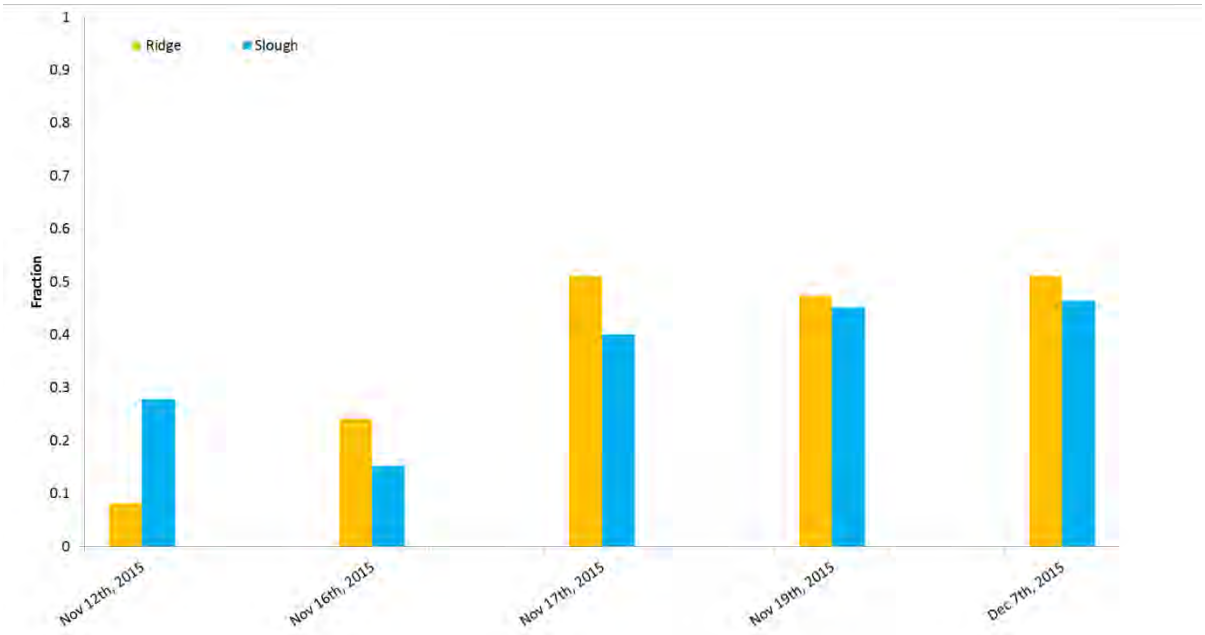

Figure E-145 Ash free dry weight (AFDW) fractions for the complete set of water column (WC) samples collected at RS1D for flow release 2015.

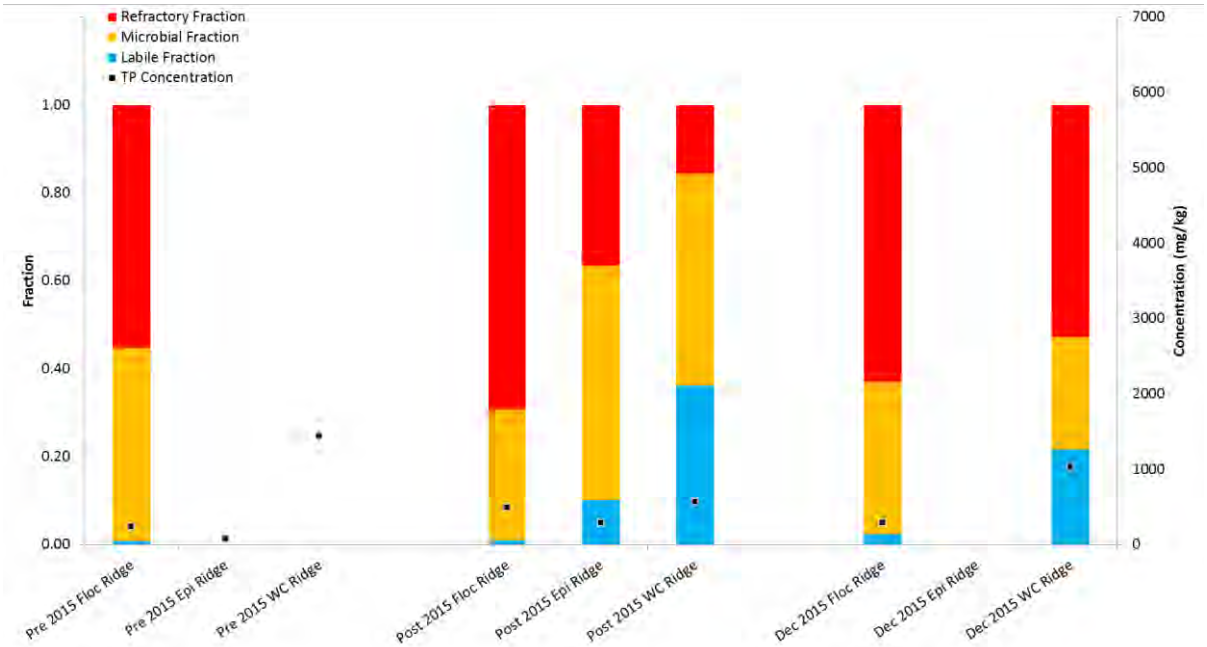

Figure E-146 Labile, microbial and refractory fractionation and total phosphorus concentrations from floc, epiphyton (epi) and water column (WC) samples collected at RS1SE for flow release 2015.

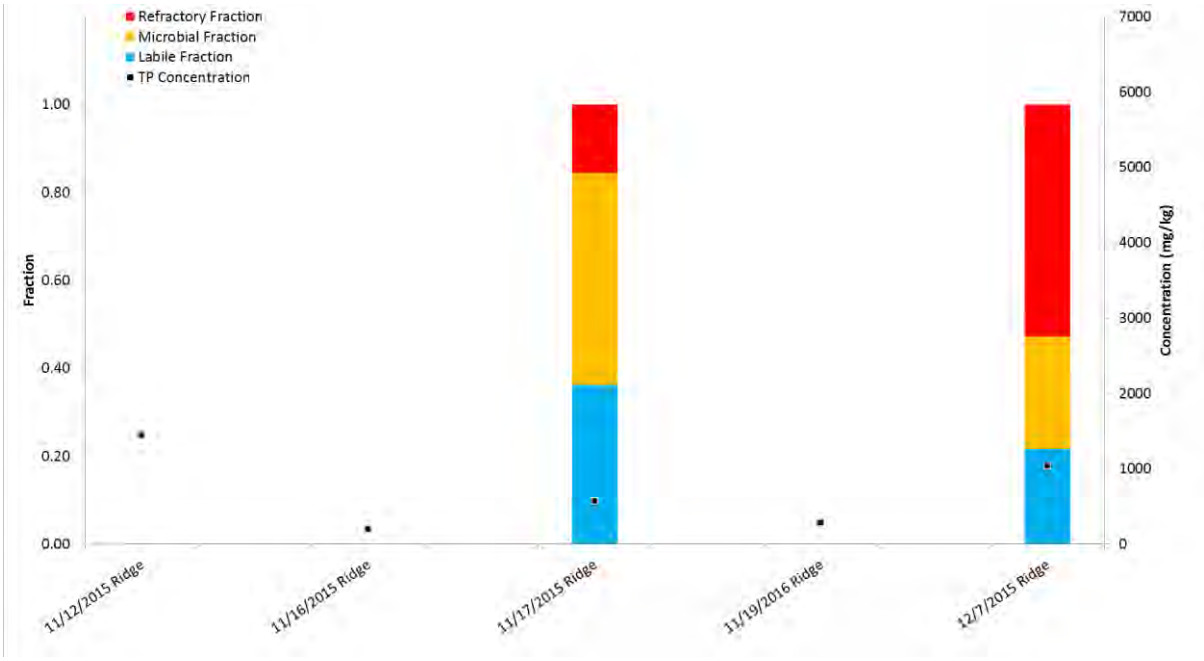

Figure E-147 Labile, microbial and refractory fractionation and total phosphorus concentrations for the complete set of water column (WC) samples collected at RS1SE for flow release 2015.

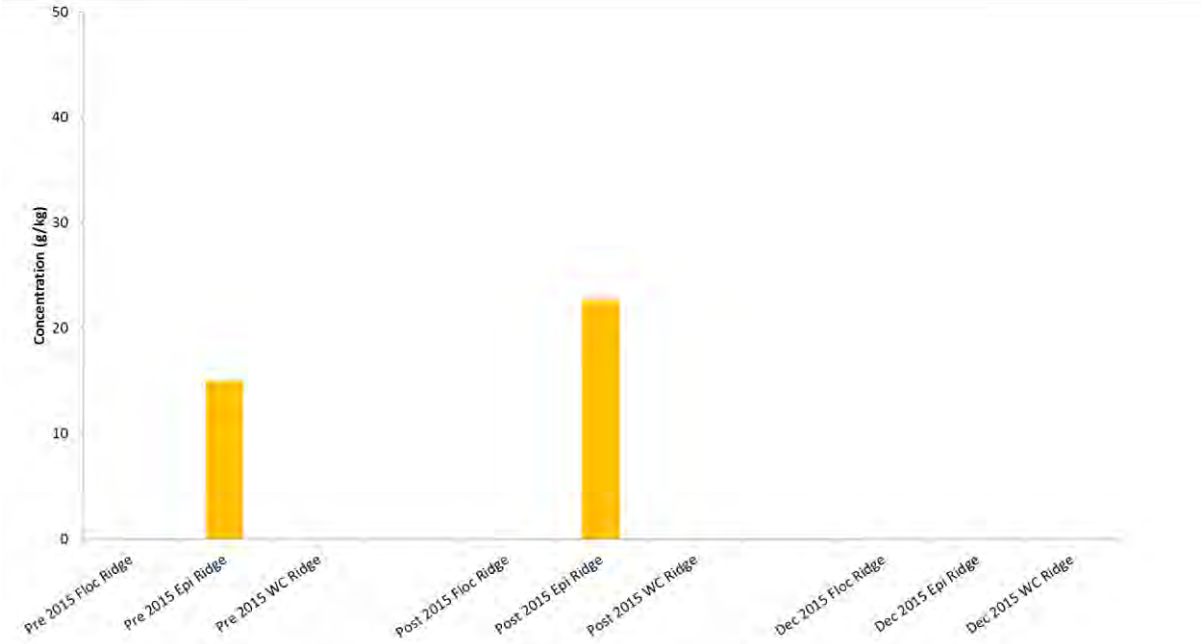

Figure E-148 Total nitrogen concentrations in floc, epiphyton (epi) and water column (WC) samples collected at RS1SE for flow release 2015.

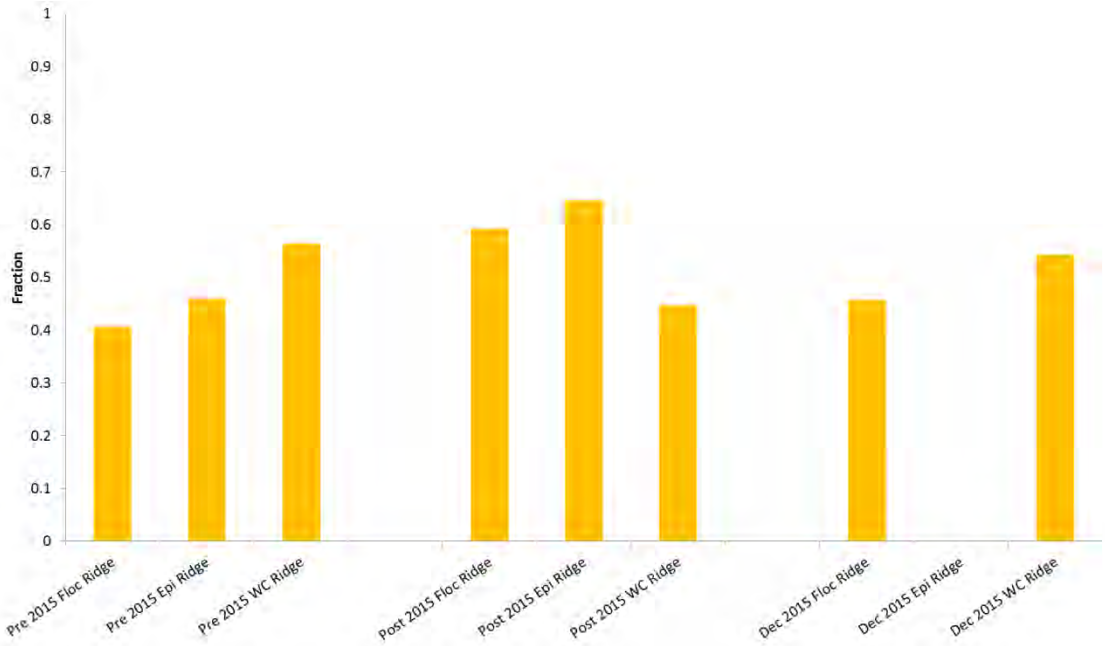

Figure E-149 Ash free dry weight (AFDW) fractions in floc, epiphyton (epi) and water column (WC) samples collected at RS1SE for flow release 2015.

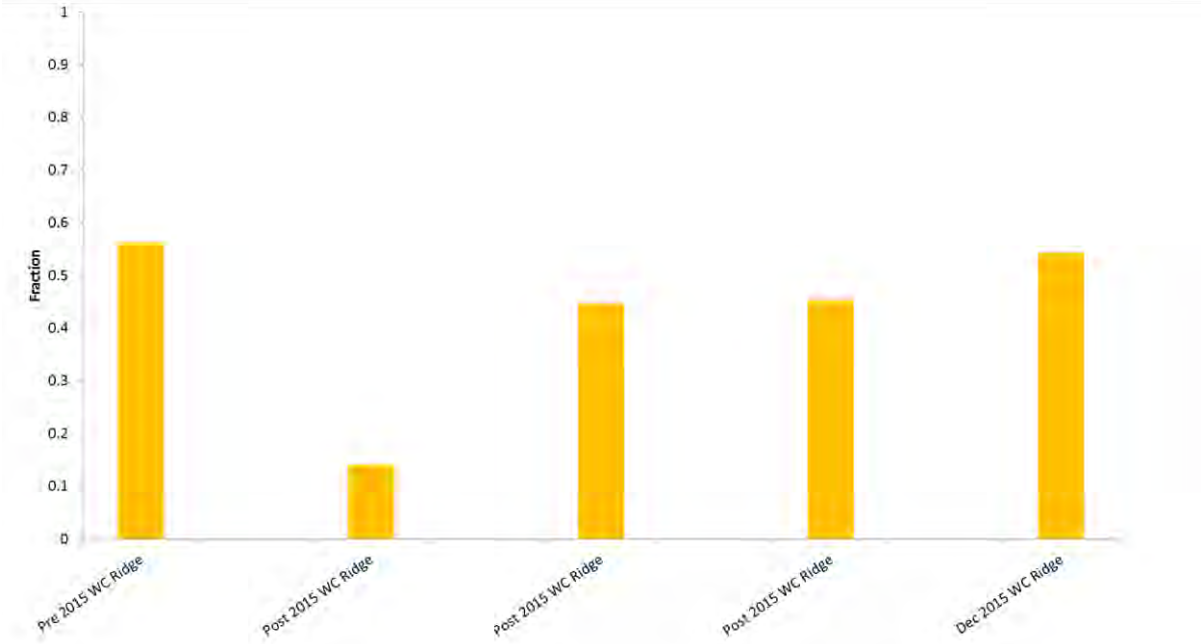

Figure E-150 Ash free dry weight (AFDW) fractions for the complete set of water column (WC) samples collected at RS1SE for flow release 2015.

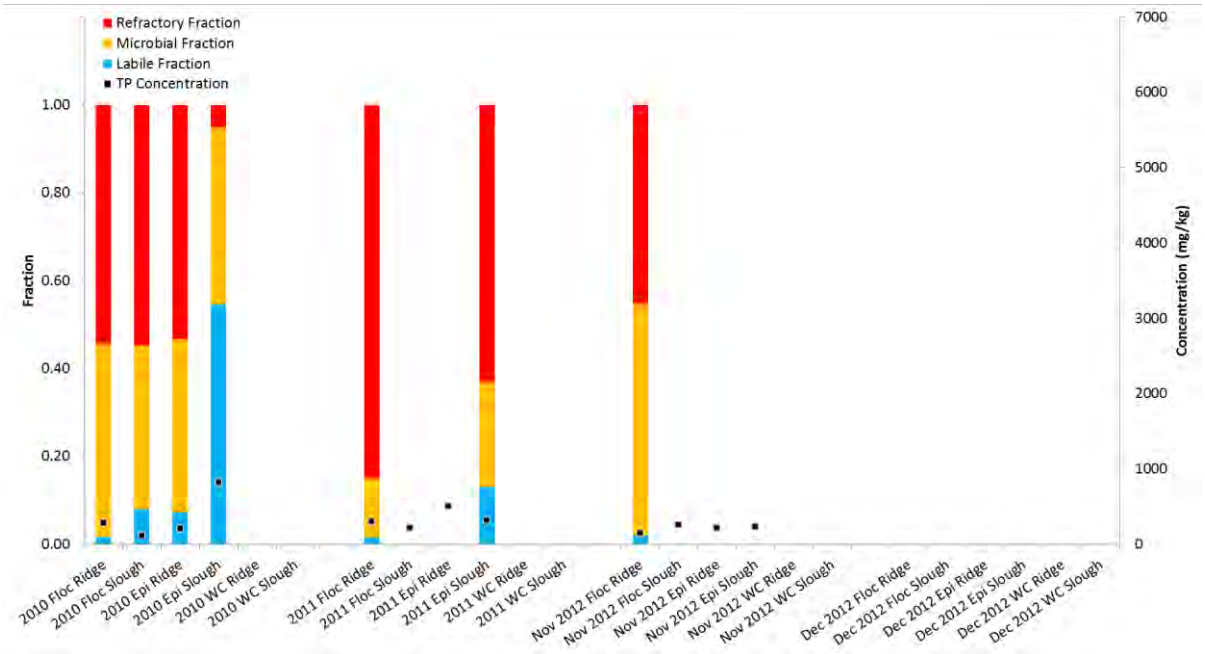

Figure E-151 Labile, microbial and refractory fractionation and total phosphorus concentrations from floc, epiphyton (epi) and water column (WC) samples collected at RS2 from 2010 through 2012.

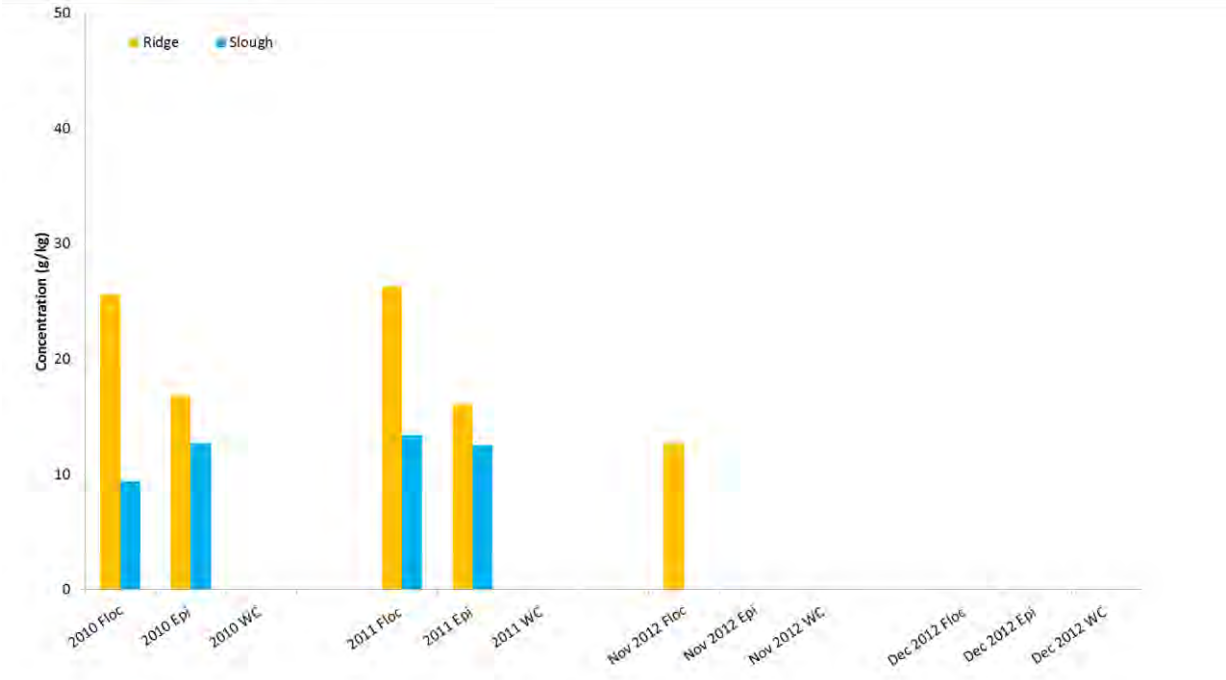

Figure E-152 Total nitrogen concentrations in floc, epiphyton (epi) and water column (WC) samples collected at RS2 from 2010 through 2012.

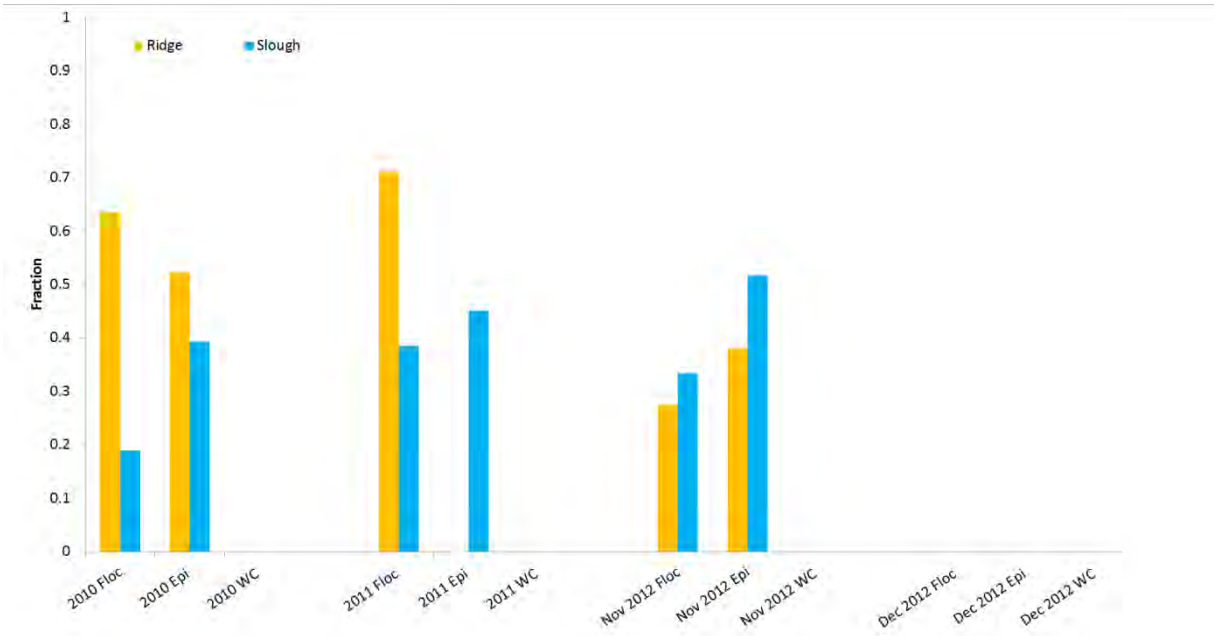

Figure E-153 Ash free dry weight (AFDW) fractions in floc, epiphyton (epi) and water column (WC) samples collected at RS2 from 2010 through 2012.

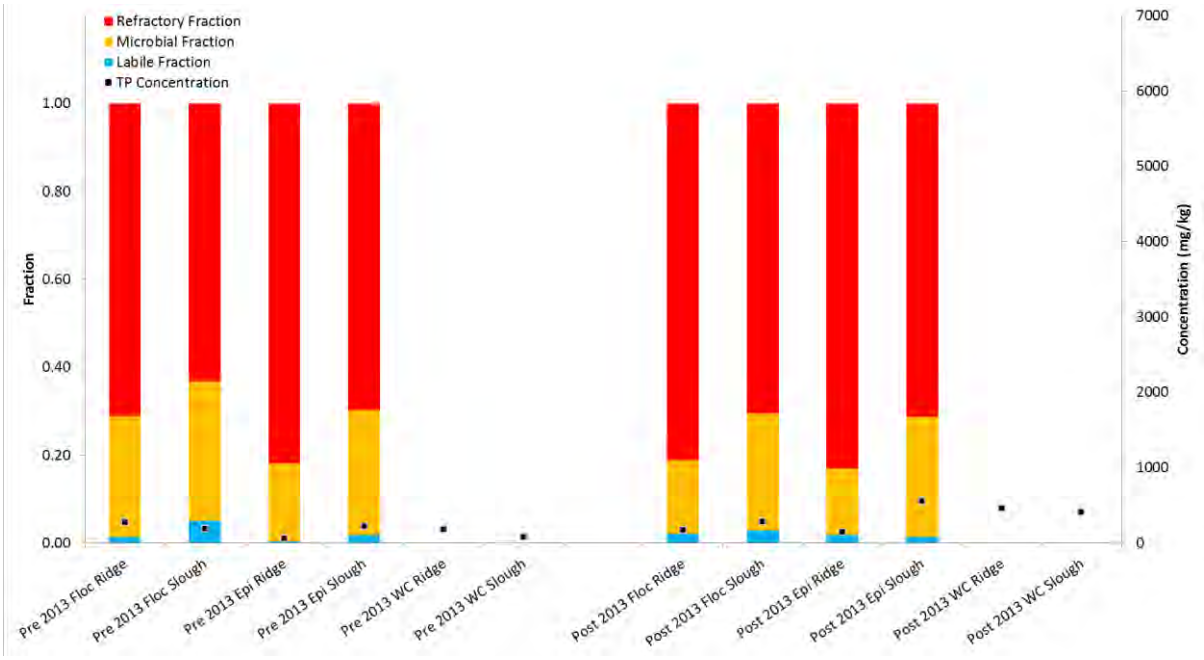

Figure E-154 Labile, microbial and refractory fractionation and total phosphorus concentrations from floc, epiphyton (epi) and water column (WC) samples collected at RS2 for flow release 2013.

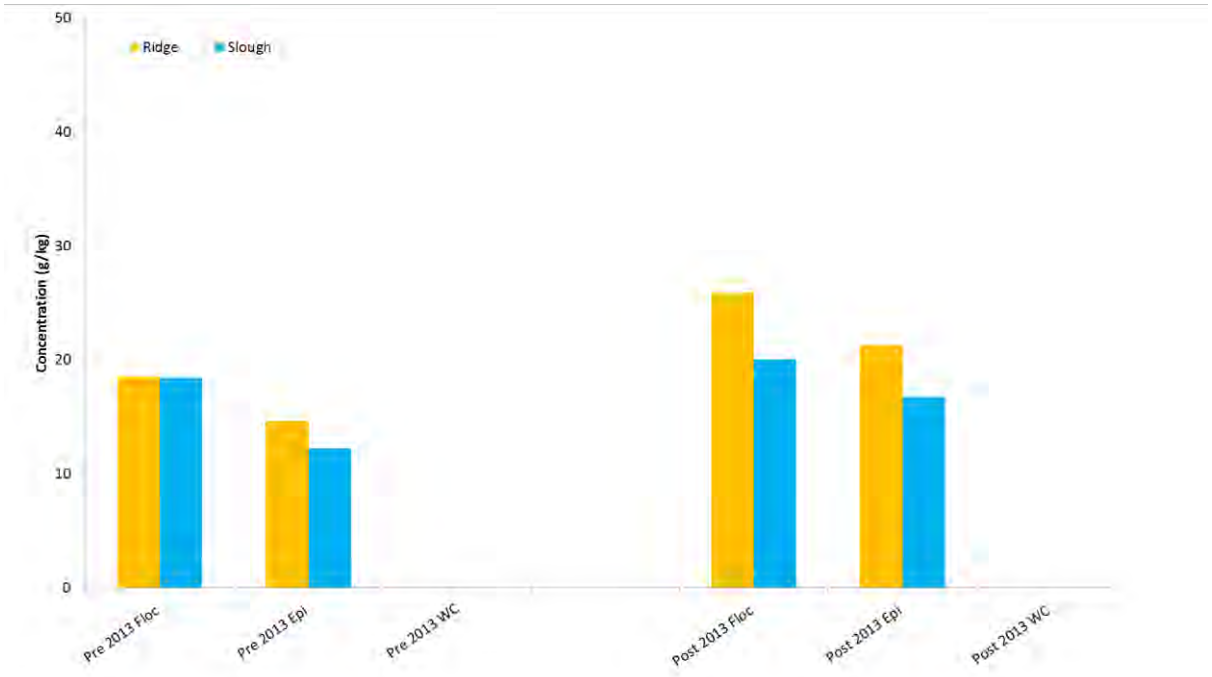

Figure E-155 Total nitrogen concentrations in floc, epiphyton (epi) and water column (WC) samples collected at RS2 for flow release 2013.

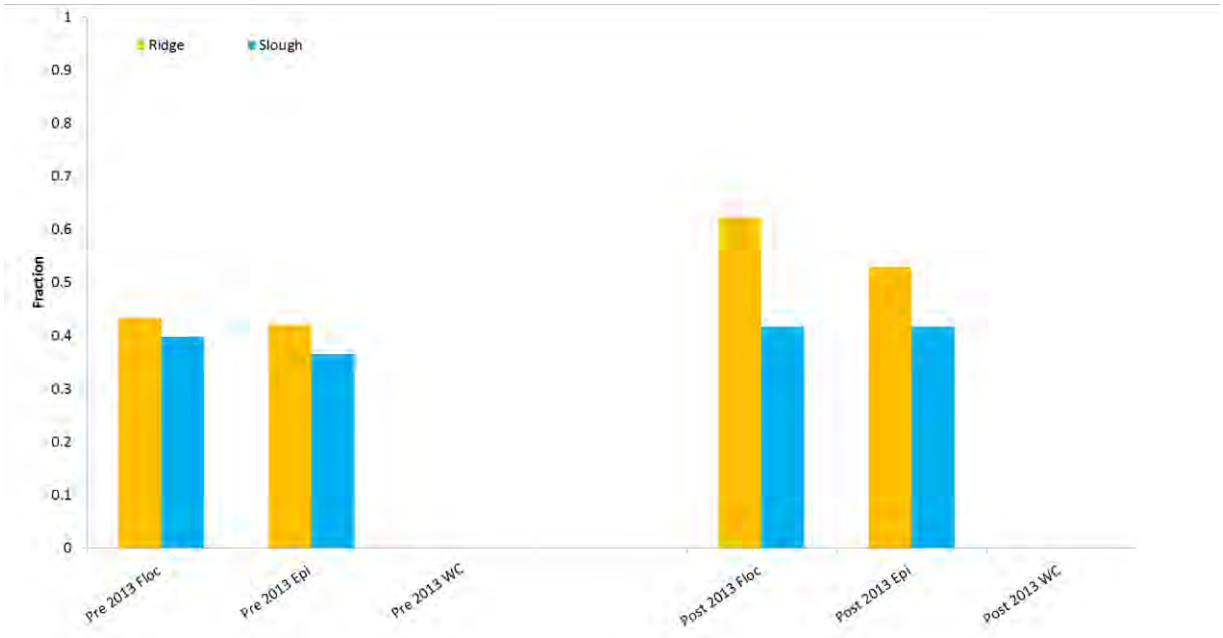

Figure E-156 Ash free dry weight (AFDW) fractions in floc, epiphyton (epi) and water column (WC) samples collected at RS2 for flow release 2013.

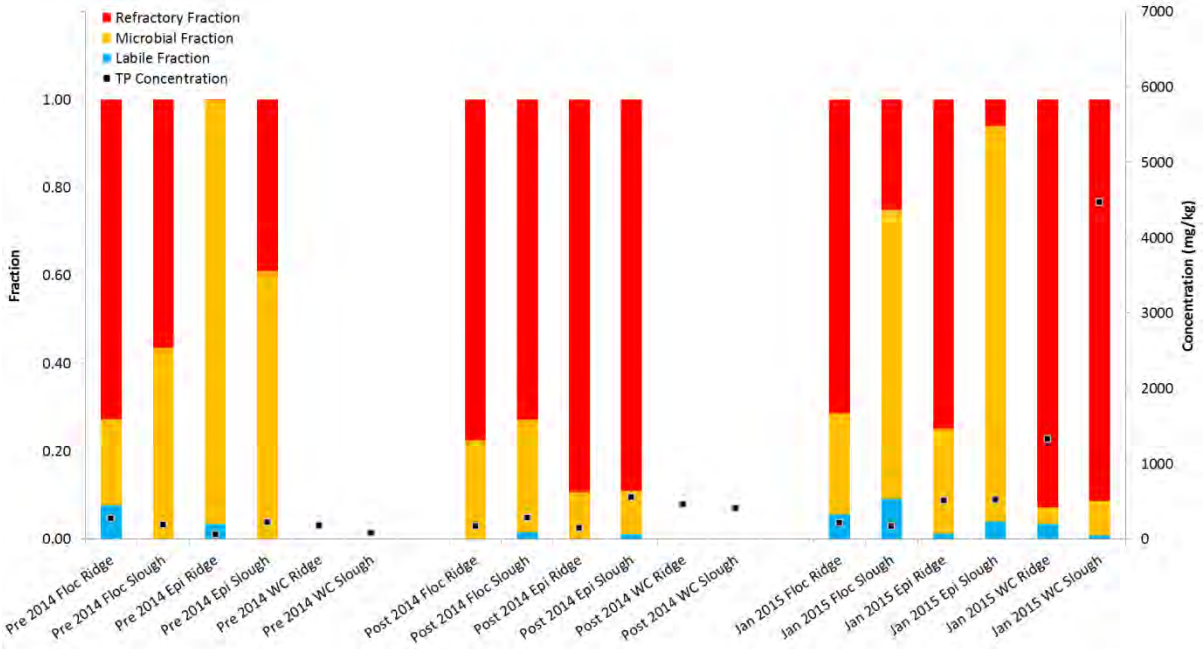

Figure E-157 Labile, microbial and refractory fractionation and total phosphorus concentrations from floc, epiphyton (epi) and water column (WC) samples collected at RS2 for flow release 2014.

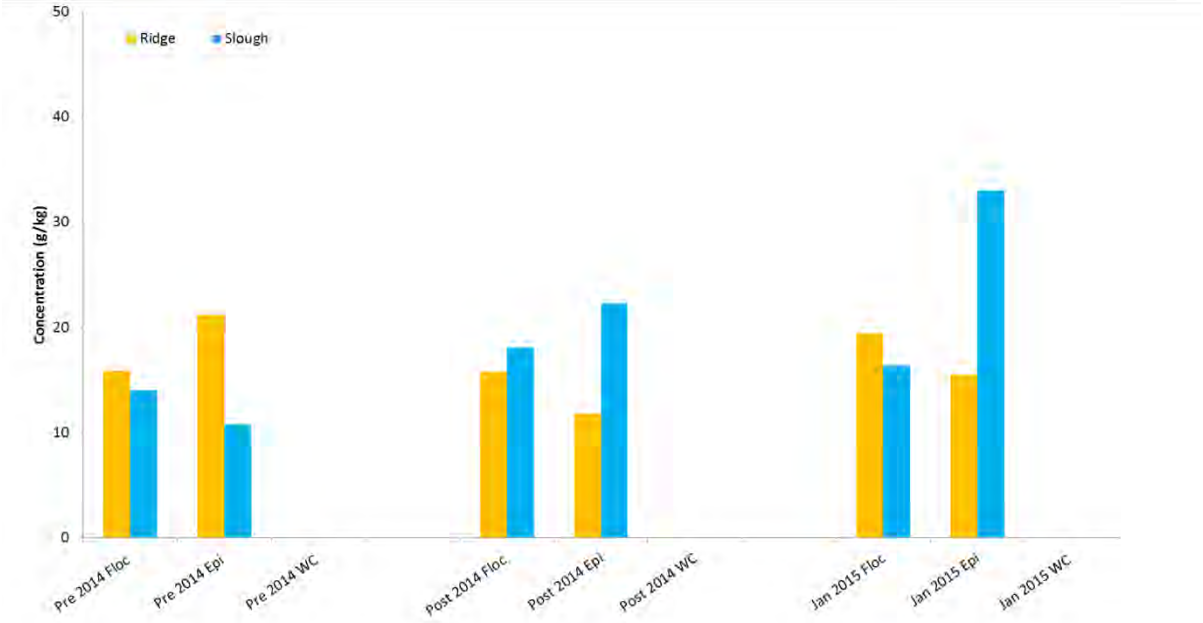

Figure E-158 Total nitrogen concentrations in floc, epiphyton (epi) and water column (WC) samples collected at RS2 for flow release 2014.

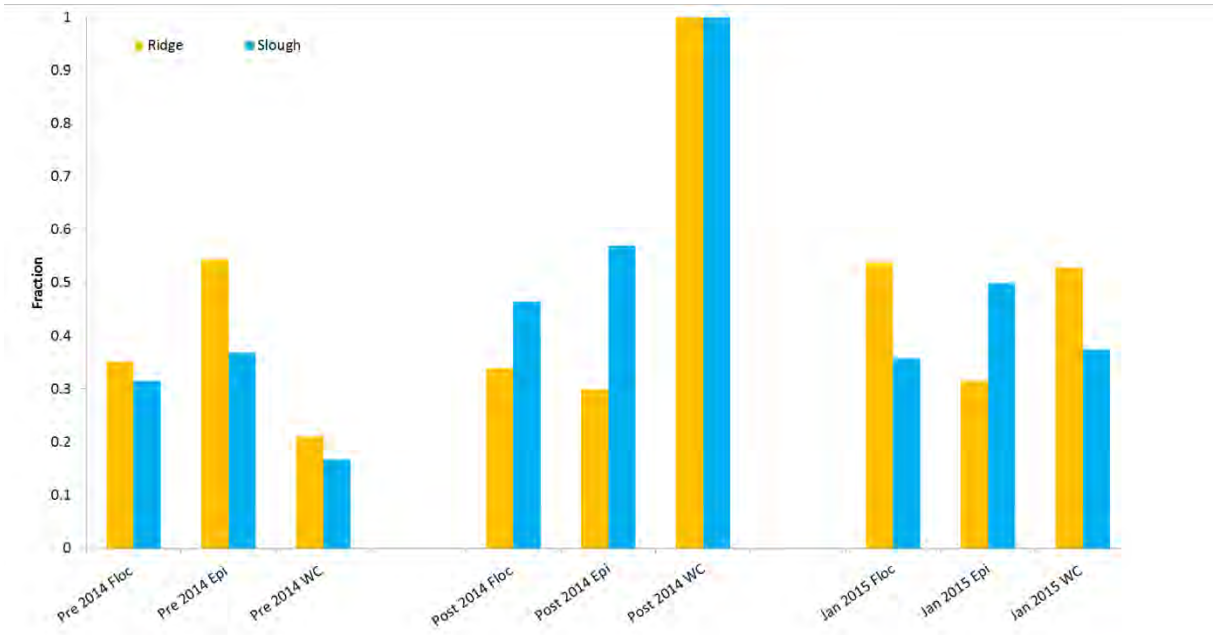

Figure E-159 Ash free dry weight (AFDW) fractions in floc, epiphyton (epi) and water column (WC) samples collected at RS2 for flow release 2014.

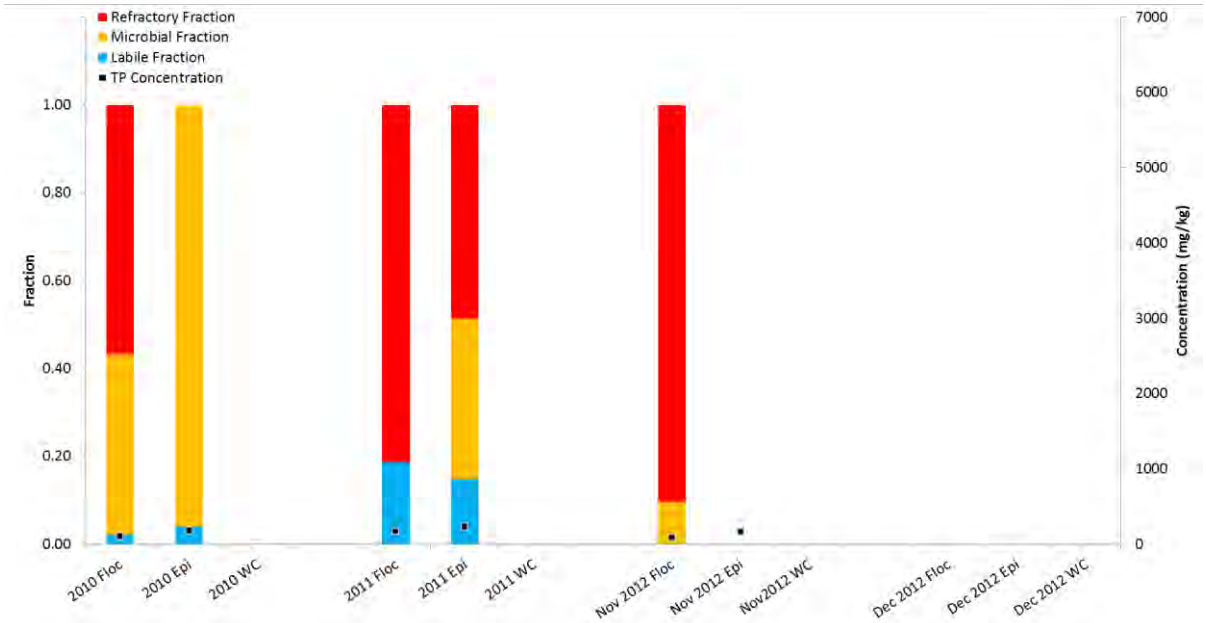

Figure E-160 Labile, microbial and refractory fractionation and total phosphorus concentrations from floc, epiphyton (epi) and water column (WC) samples collected at S1 from 2010 through 2012.

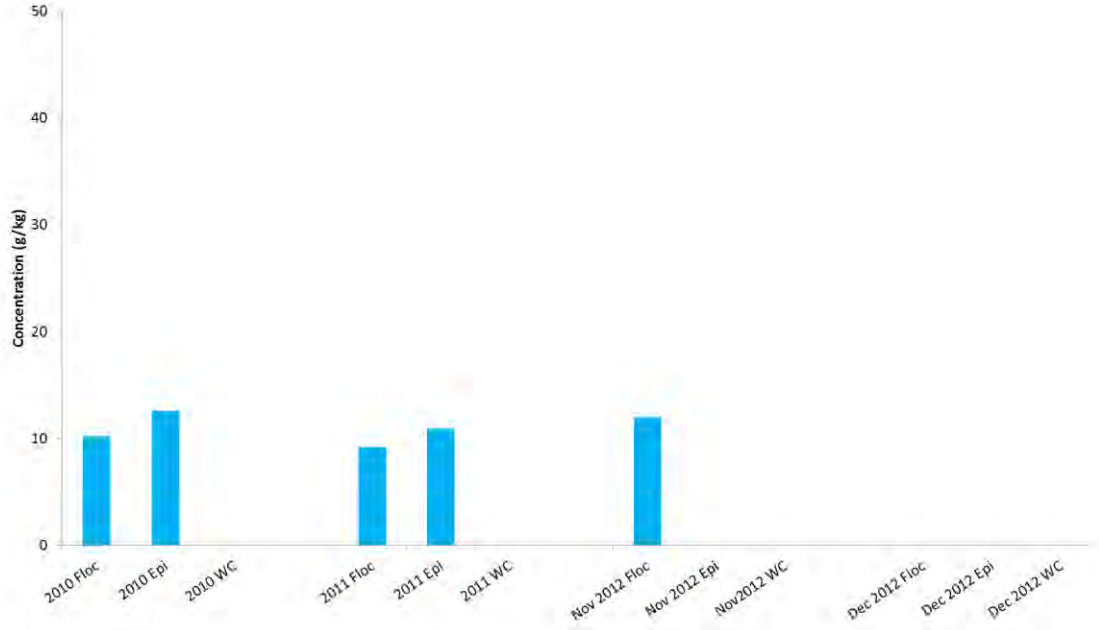

Figure E-161 Total nitrogen concentrations in floc, epiphyton (epi) and water column (WC) samples collected at S1 from 2010 through 2012.

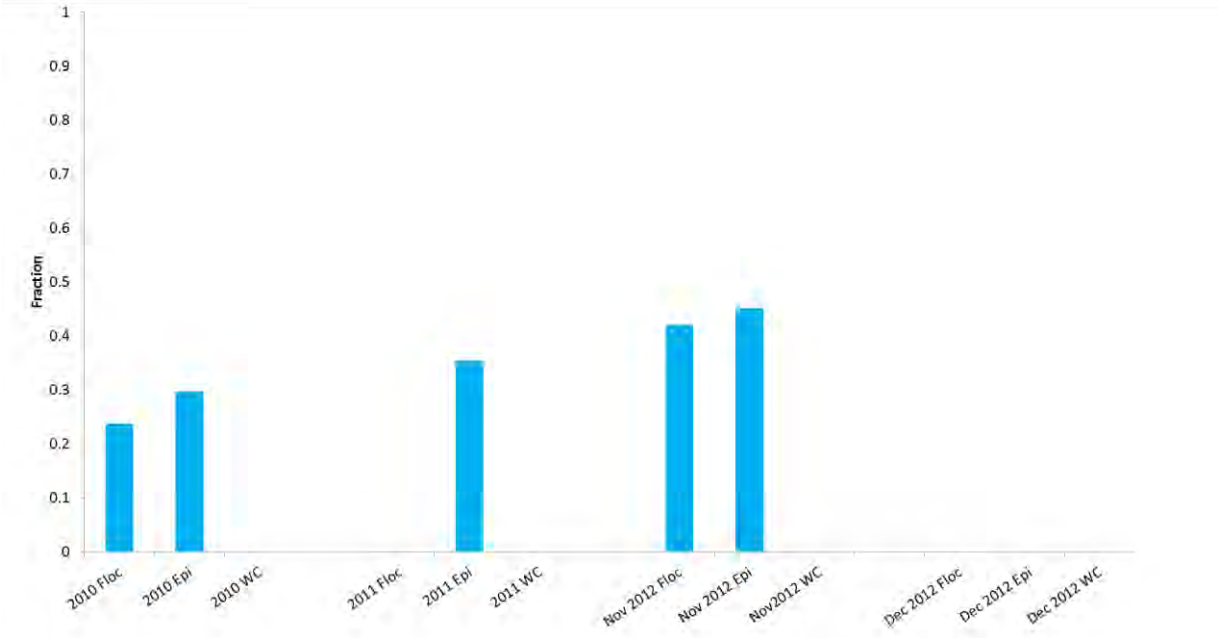

Figure E-162 Ash free dry weight (AFDW) fractions in floc, epiphyton (epi) and water column (WC) samples collected at S1 from 2010 through 2012.

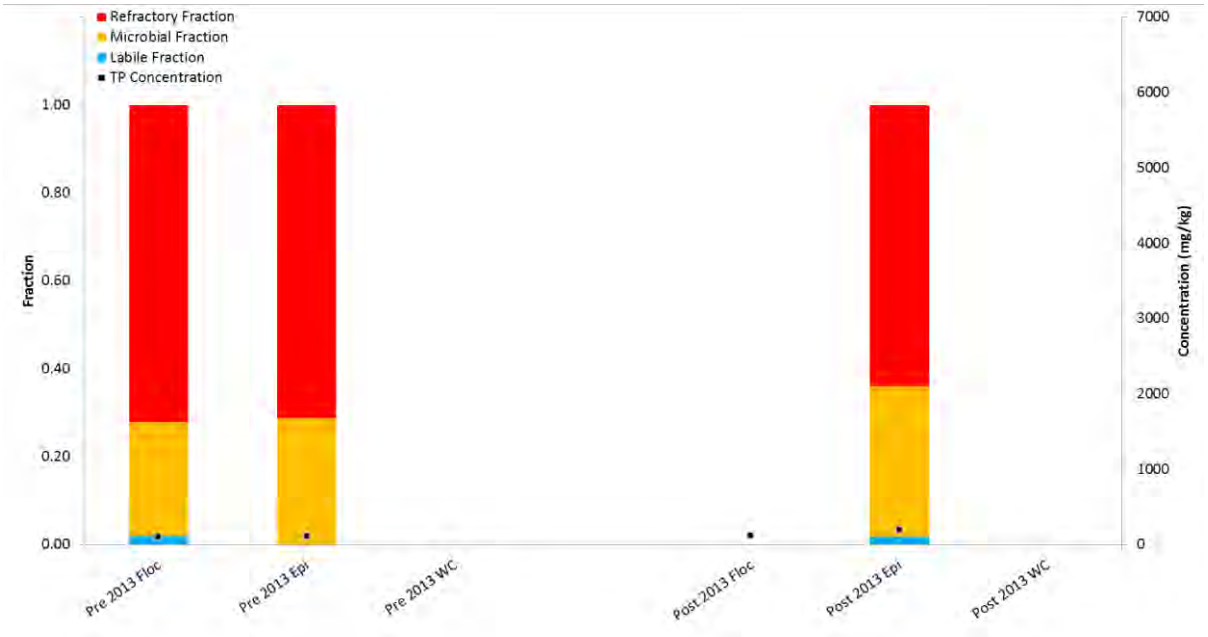

Figure E-163 Labile, microbial and refractory fractionation and total phosphorus concentrations from floc, epiphyton (epi) and water column (WC) samples collected at S1 for flow release 2013.

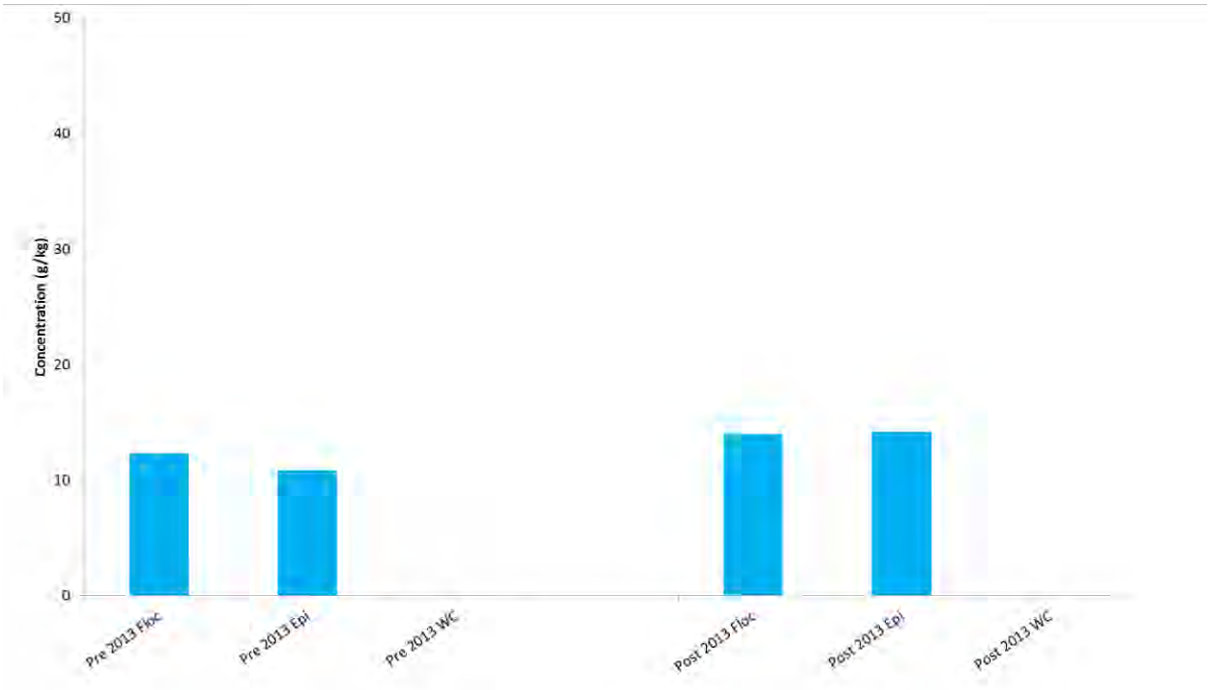

Figure E-164 Total nitrogen concentrations in floc, epiphyton (epi) and water column (WC) samples collected at S1 for flow release 2013.

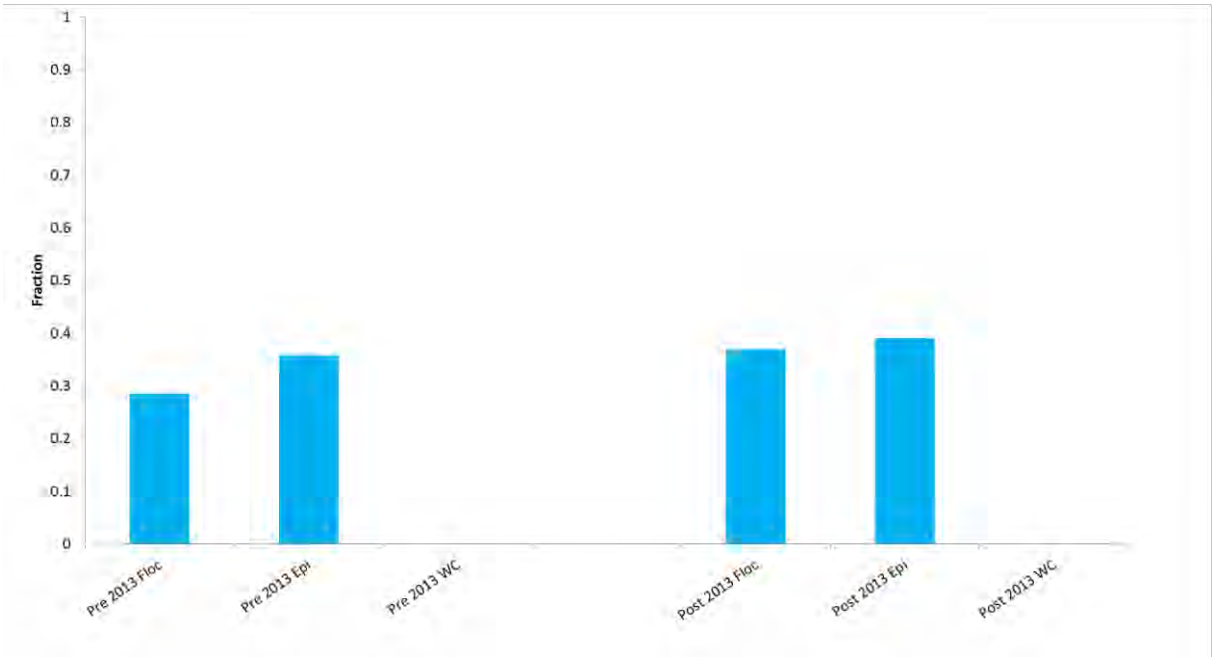

Figure E-165 Ash free dry weight (AFDW) fractions in floc, epiphyton (epi) and water column (WC) samples collected at S1 for flow release 2013.

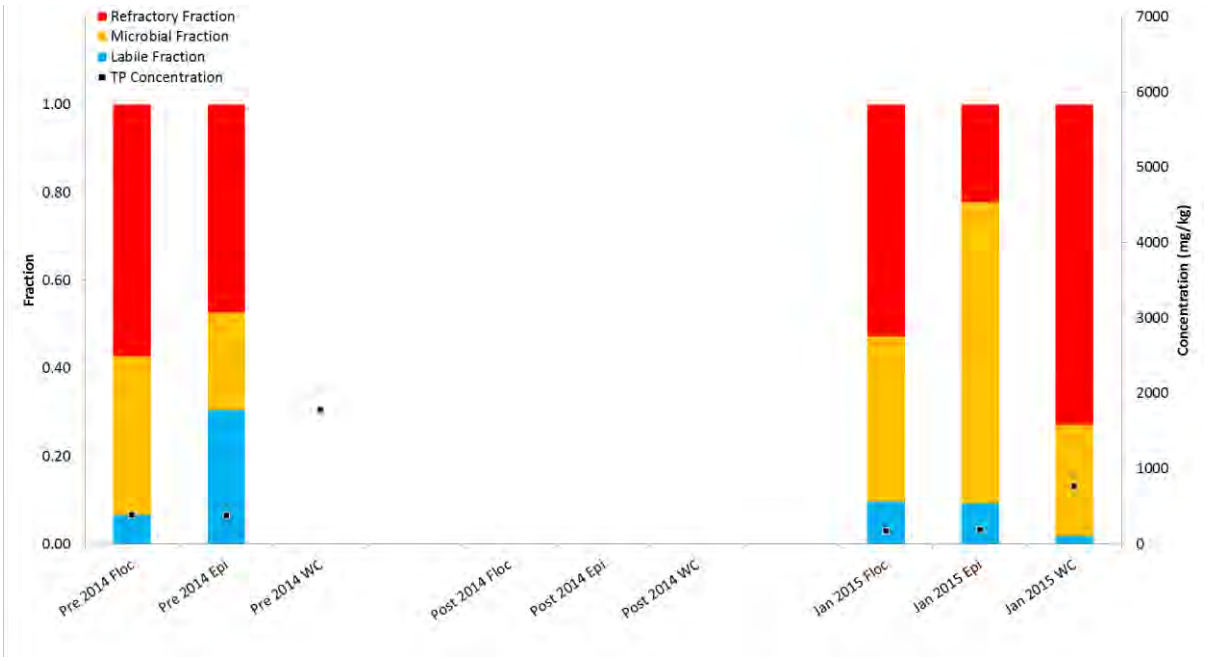

Figure E-166 Labile, microbial and refractory fractionation and total phosphorus concentrations from floc, epiphyton (epi) and water column (WC) samples collected at S1 for flow release 2014.

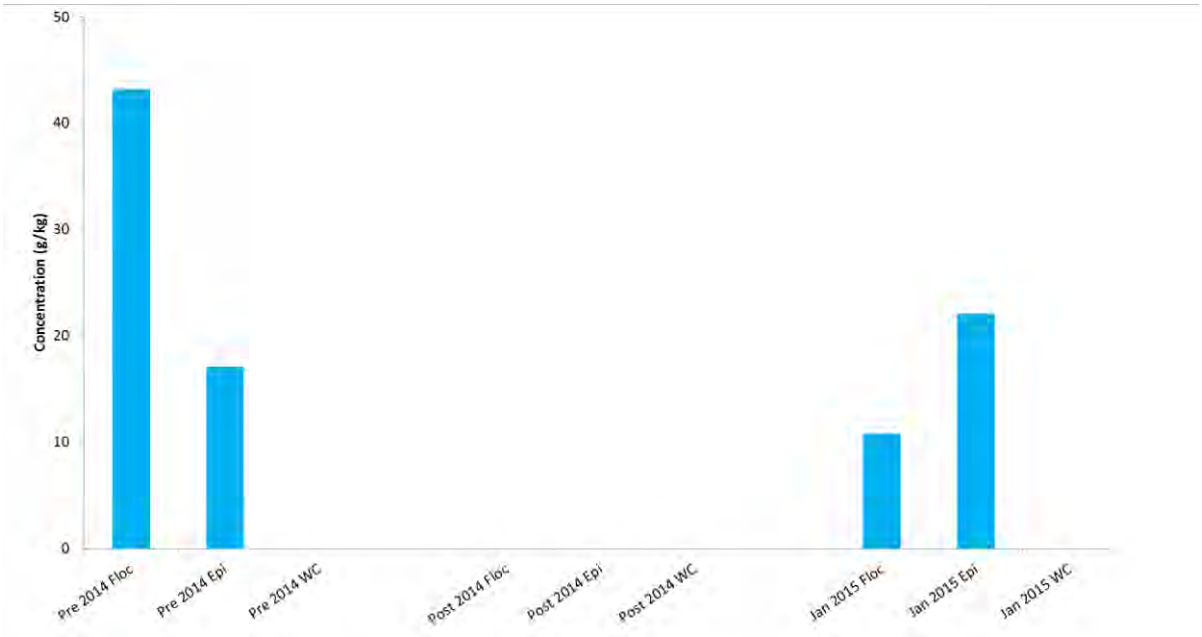

Figure E-167 Total nitrogen concentrations in floc, epiphyton (epi) and water column (WC) samples collected at S1 for flow release 2014.

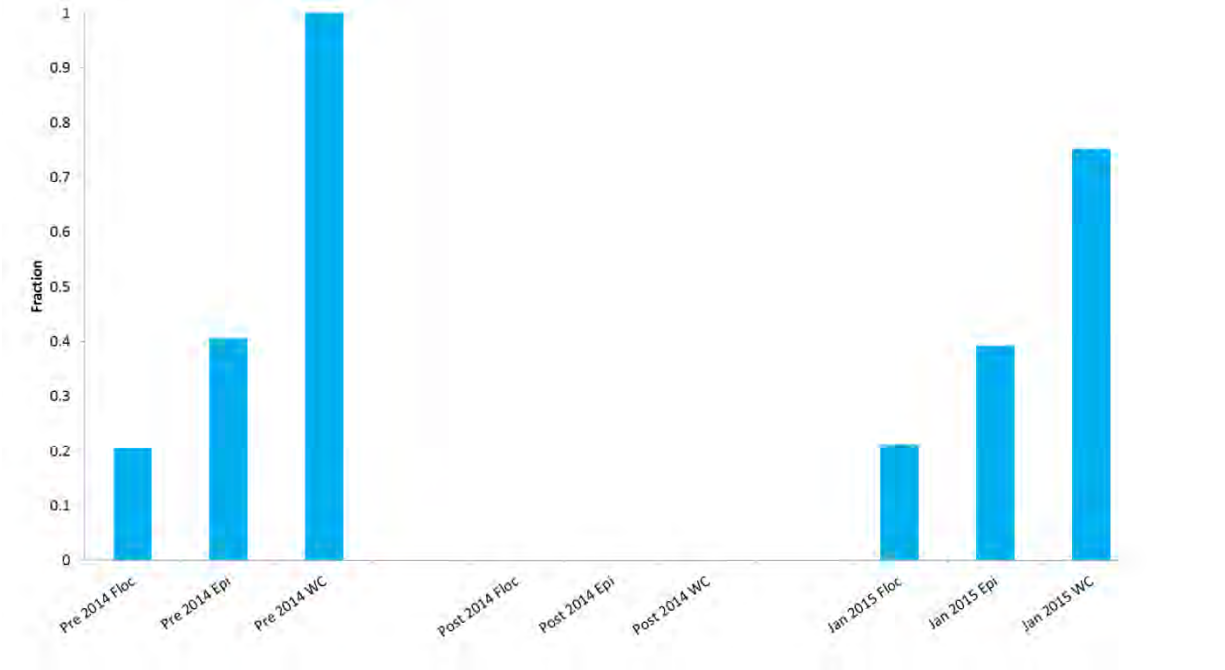

Figure E-168 Ash free dry weight (AFDW) fractions in floc, epiphyton (epi) and water column (WC) samples collected at S1 for flow release 2014.

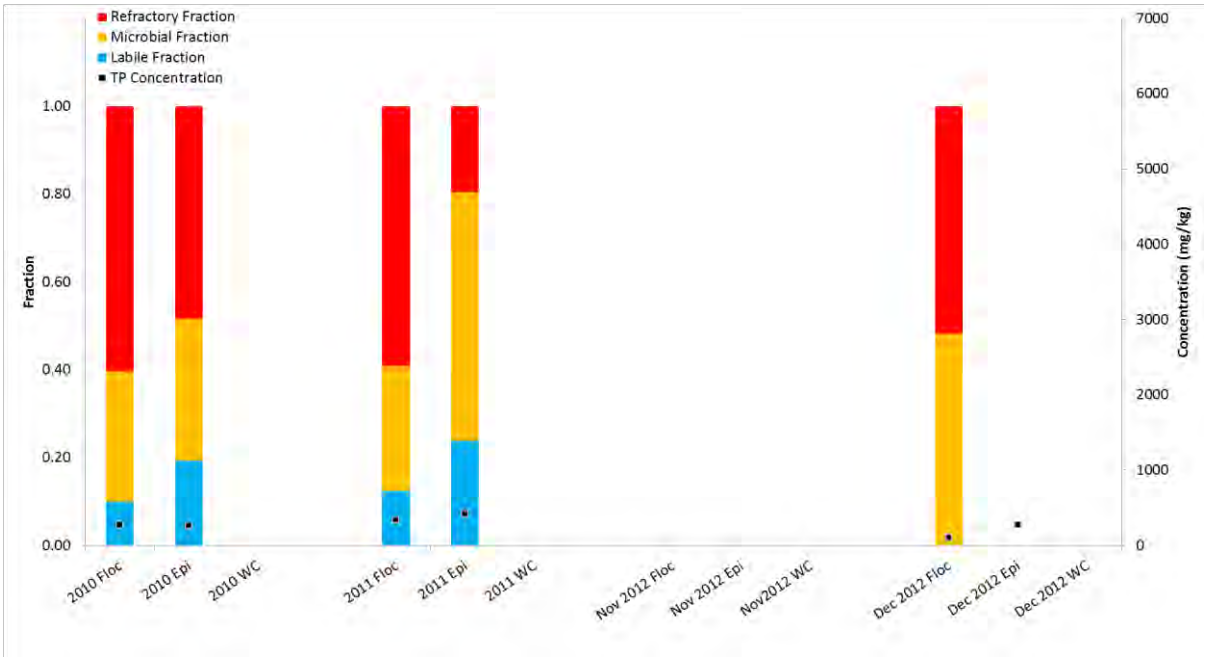

Figure E-169 Labile, microbial and refractory fractionation and total phosphorus concentrations from floc, epiphyton (epi) and water column (WC) samples collected at UB1 from 2010 through 2012.

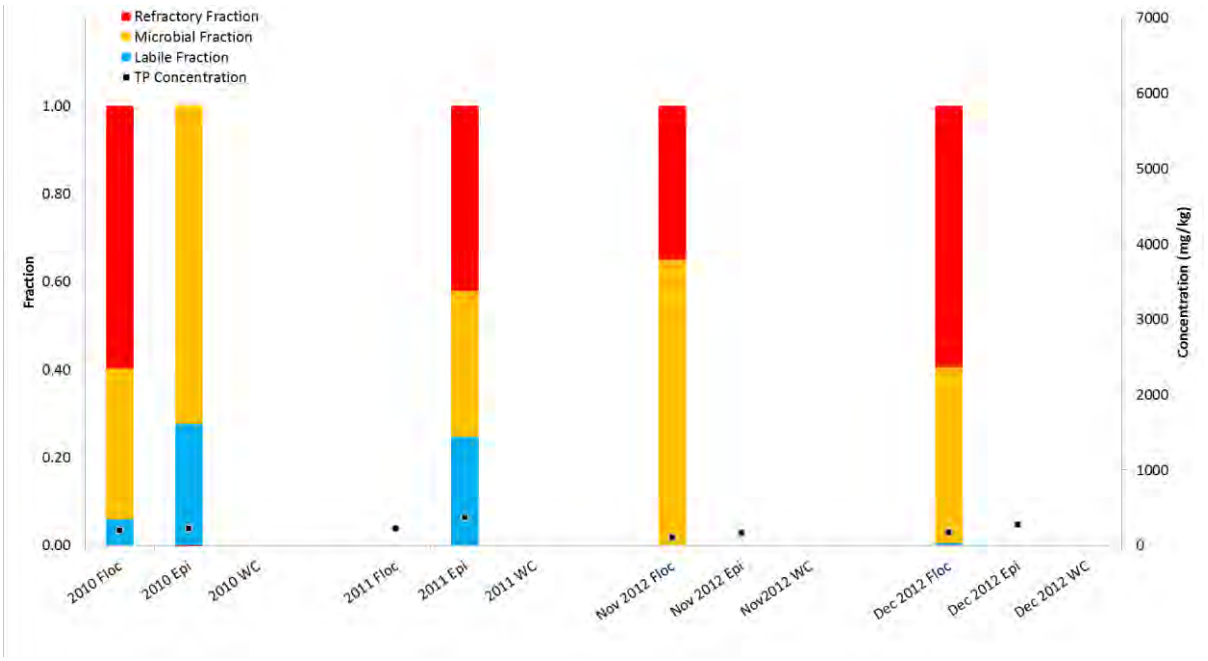

Figure E-170 Labile, microbial and refractory fractionation and total phosphorus concentrations from floc, epiphyton (epi) and water column (WC) samples collected at UB2 from 2010 through 2012.

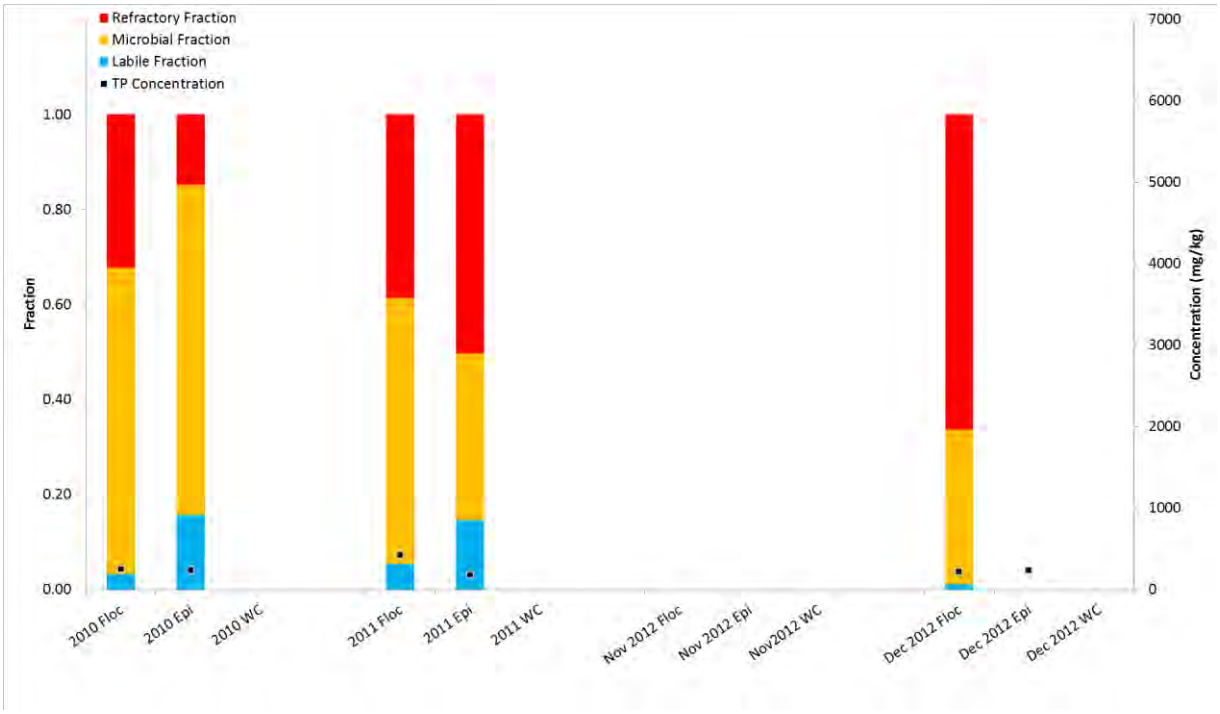

Figure E-171 Labile, microbial and refractory fractionation and total phosphorus concentrations from floc, epiphyton (epi) and water column (WC) samples collected at UB3 from 2010 through 2012.

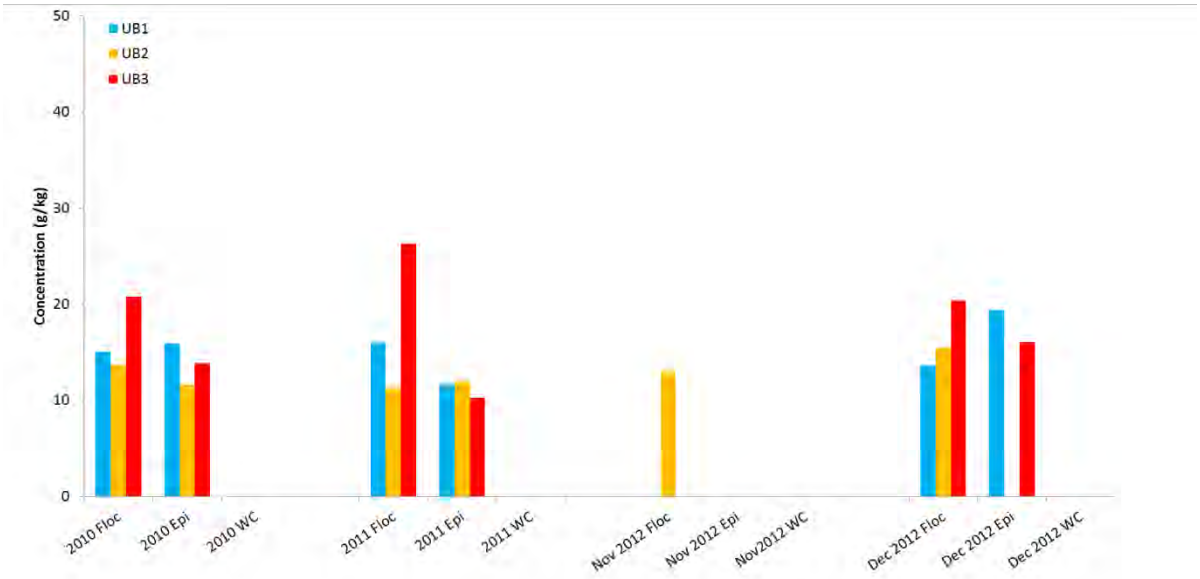

Figure E-172 Total nitrogen concentrations in floc, epiphyton (epi) and water column (WC) samples collected at UB1, UB2 and UB3 for 2010 through 2012.

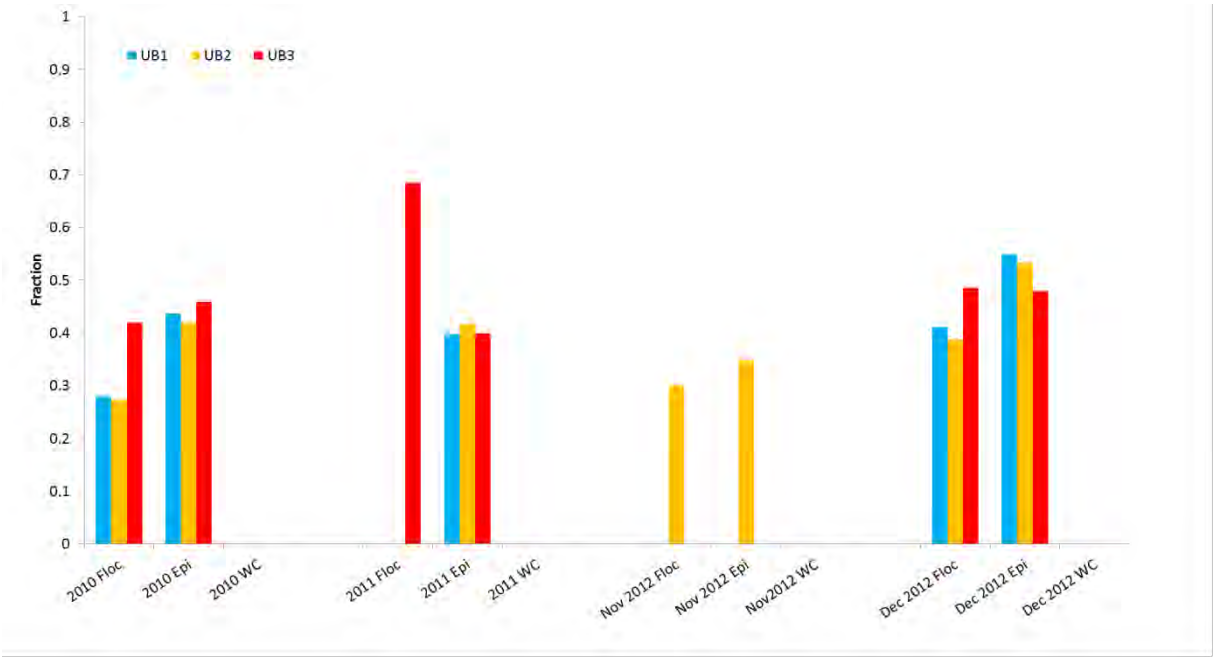

Figure E-173 Ash free dry weight (AFDW) fractions in floc, epiphyton (epi) and water column (WC) samples collected at UB1, UB2 and UB3 for 2010 through 2012.

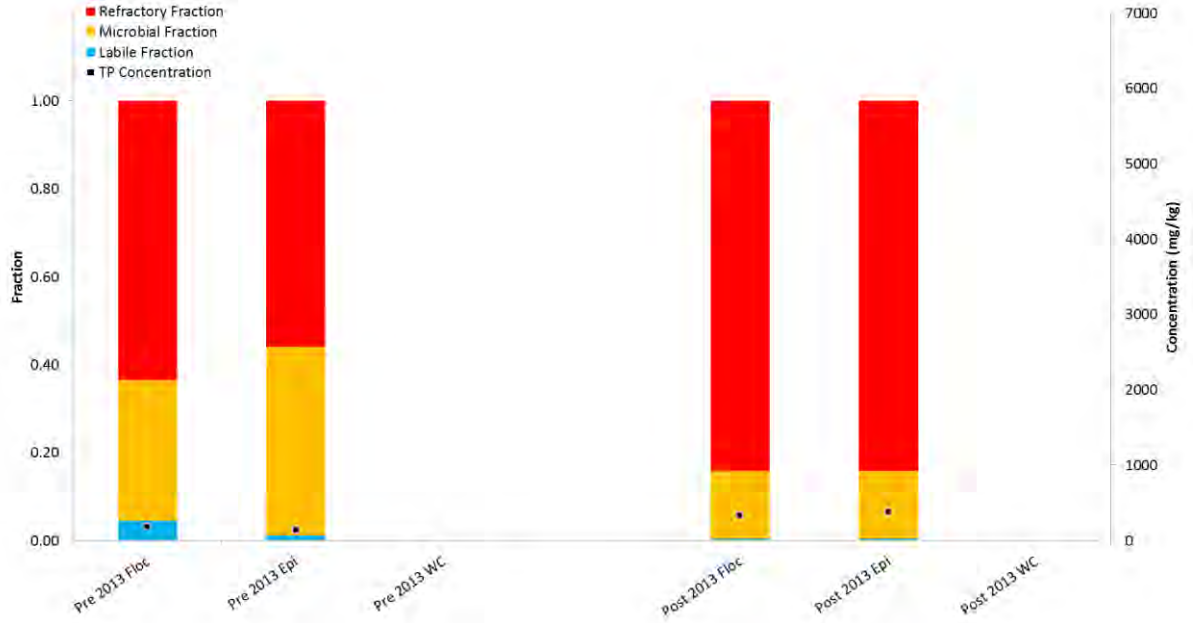

Figure E-174 Labile, microbial and refractory fractionation and total phosphorus concentrations from floc, epiphyton (epi) and water column (WC) samples collected at UB1 for flow release 2013.

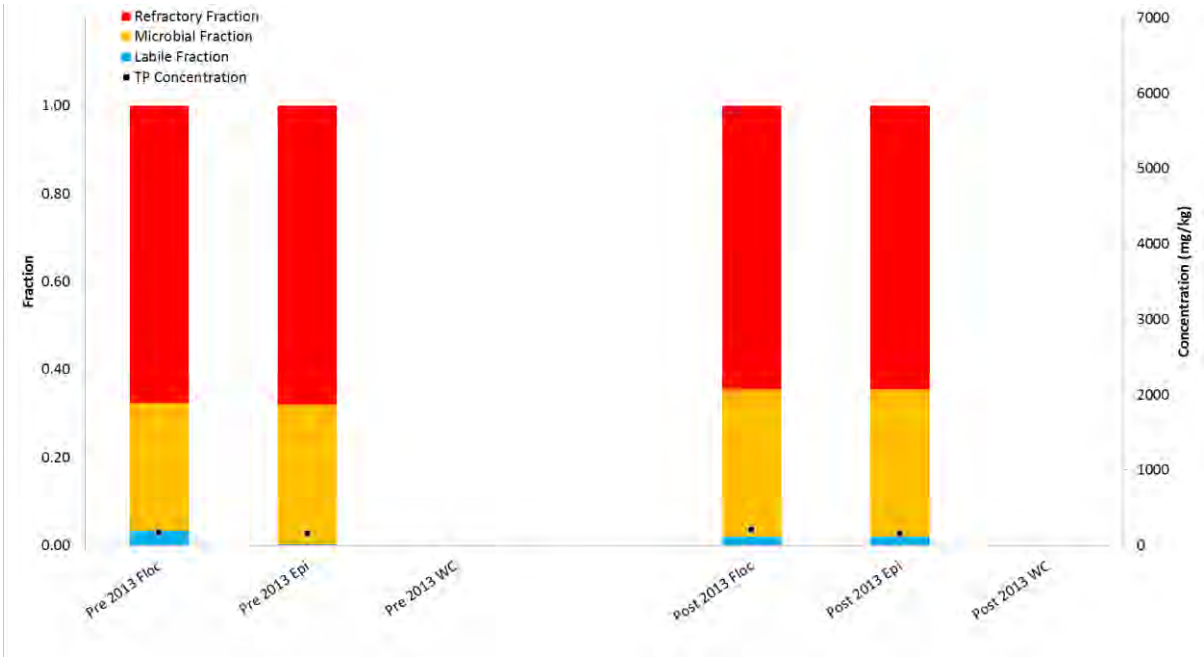

Figure E-175 Labile, microbial and refractory fractionation and total phosphorus concentrations from floc, epiphyton (epi) and water column (WC) samples collected at UB2 for flow release 2013.

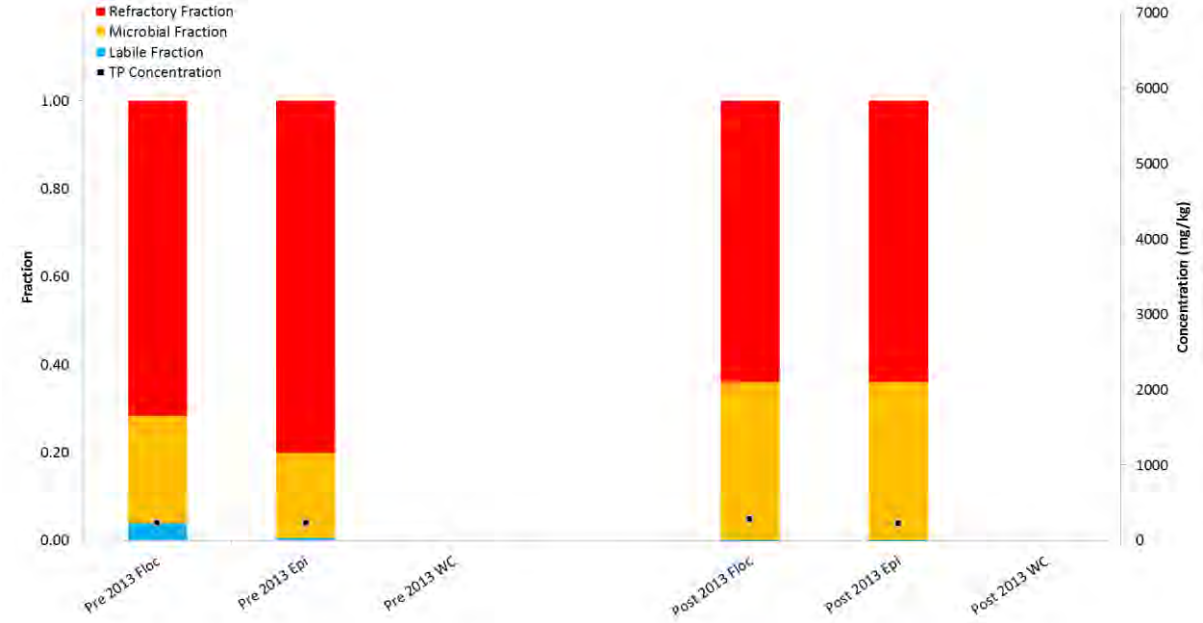

Figure E-176 Labile, microbial and refractory fractionation and total phosphorus concentrations from floc, epiphyton (epi) and water column (WC) samples collected at UB3 for flow release 2013.

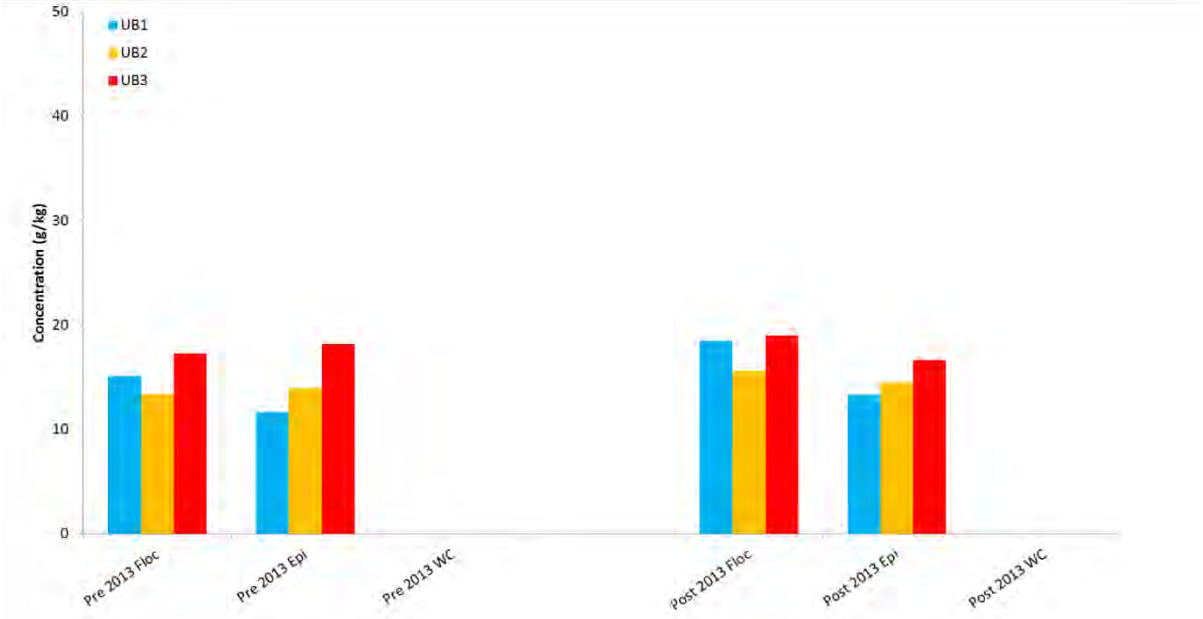

Figure E-177 Total nitrogen concentrations in floc, epiphyton (epi) and water column (WC) samples collected at UB1, UB2 and UB3 for flow release 2013.

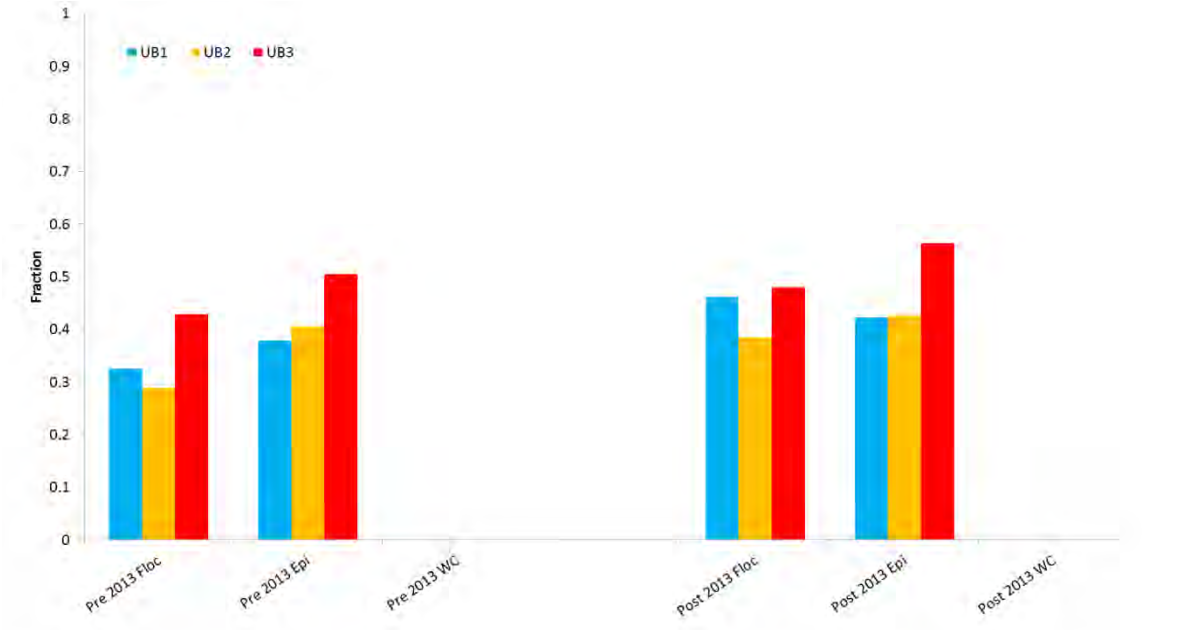

Figure E-178 Ash free dry weight (AFDW) fractions in floc, epiphyton (epi) and water column (WC) samples collected at UB1, UB2 and UB3 for flow release 2013.

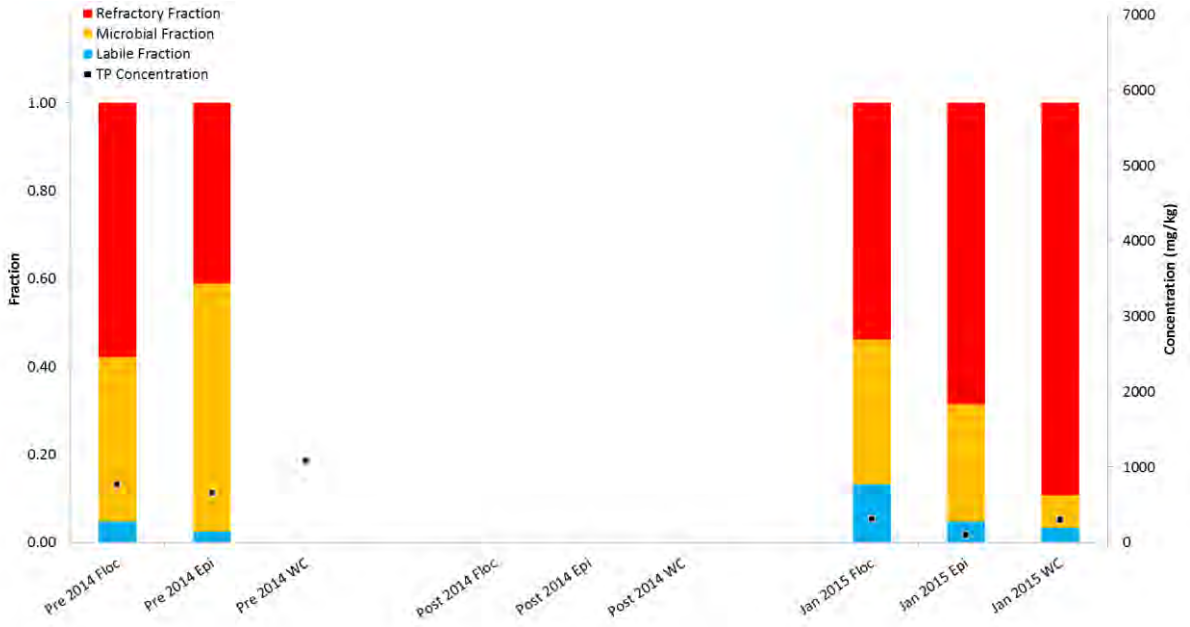

Figure E-179 Labile, microbial and refractory fractionation and total phosphorus concentrations from floc, epiphyton (epi) and water column (WC) samples collected at UB1 for flow release 2014.

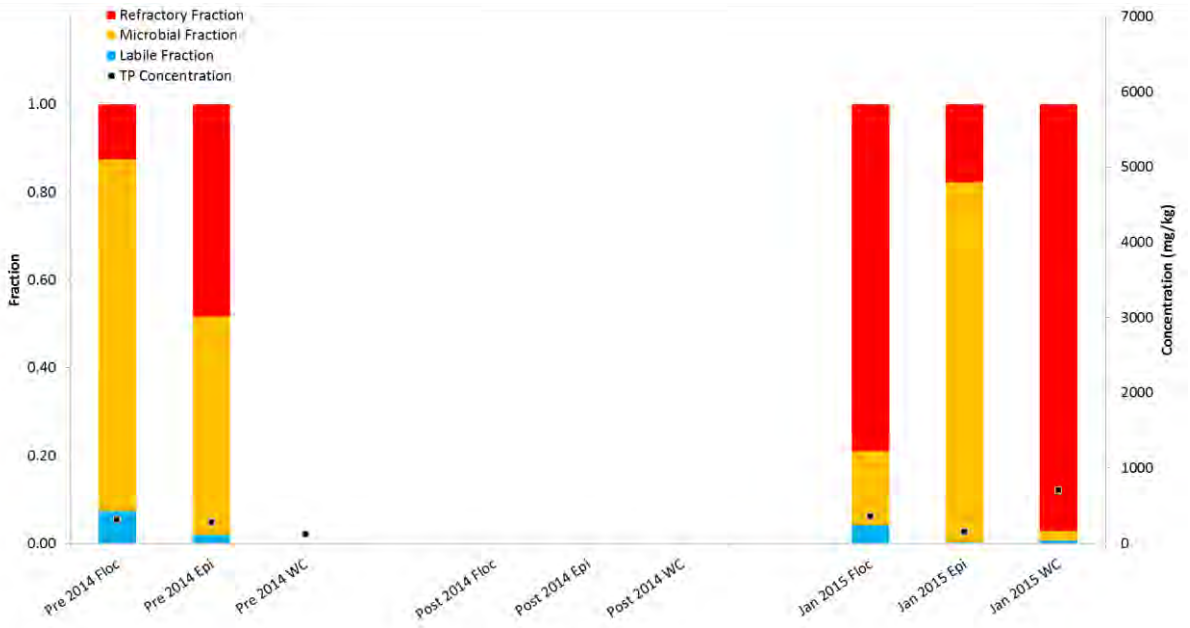

Figure E-180 Labile, microbial and refractory fractionation and total phosphorus concentrations from floc, epiphyton (epi) and water column (WC) samples collected at UB2 for flow release 2014.

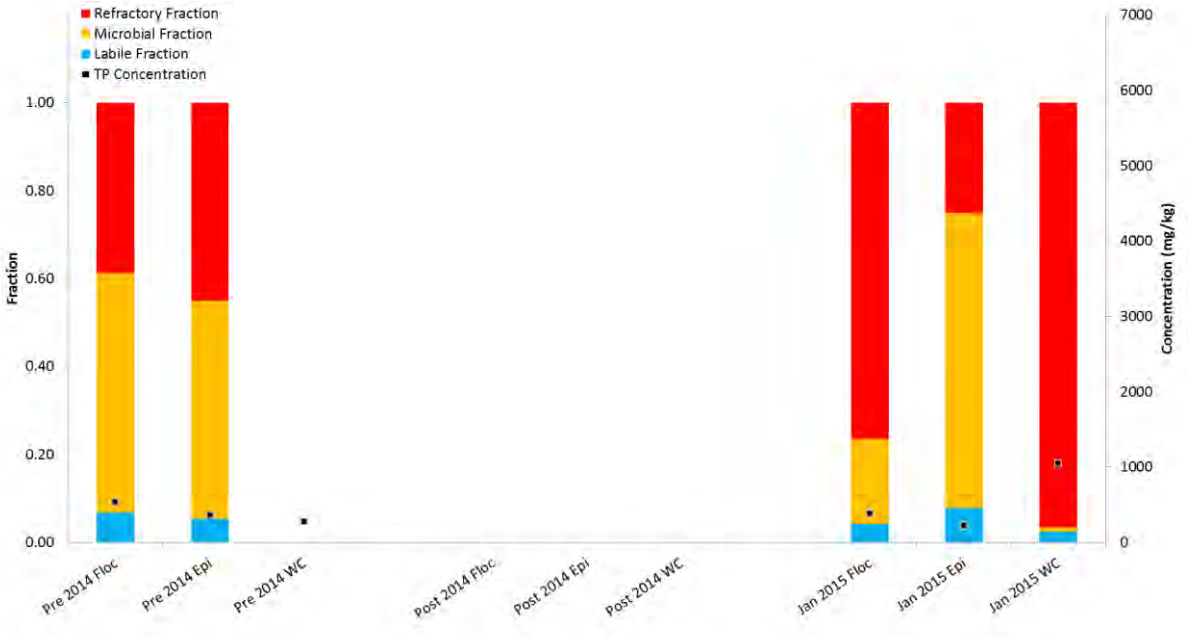

Figure E-181 Labile, microbial and refractory fractionation and total phosphorus concentrations from floc, epiphyton (epi) and water column (WC) samples collected at UB3 for flow release 2014.

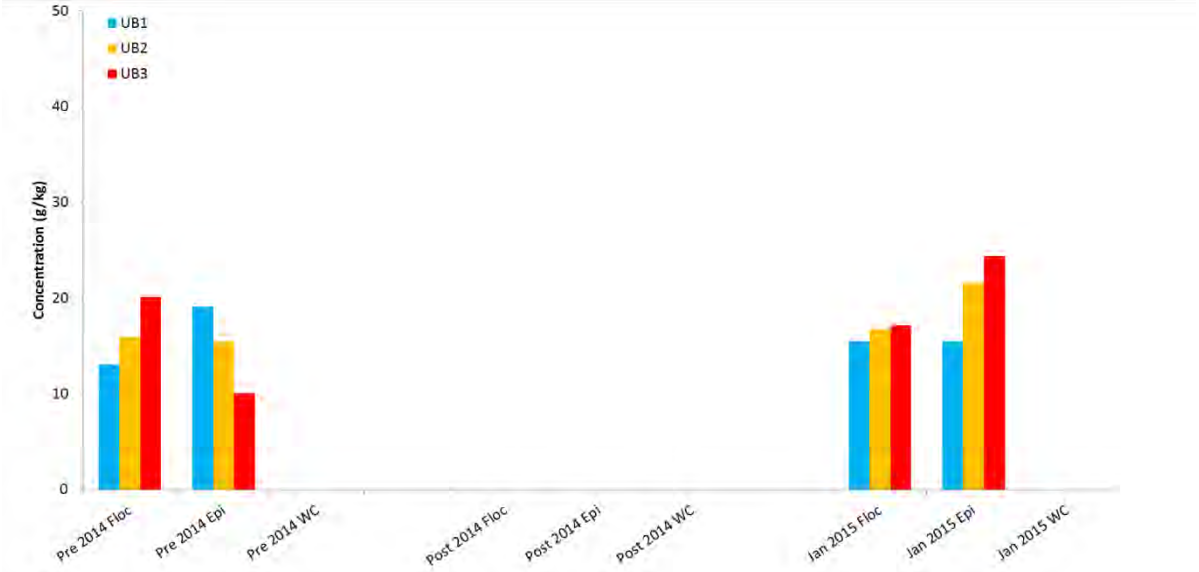

Figure E-182 Total nitrogen concentrations in floc, epiphyton (epi) and water column (WC) samples collected at UB1, UB2 and UB3 for flow release 2014.

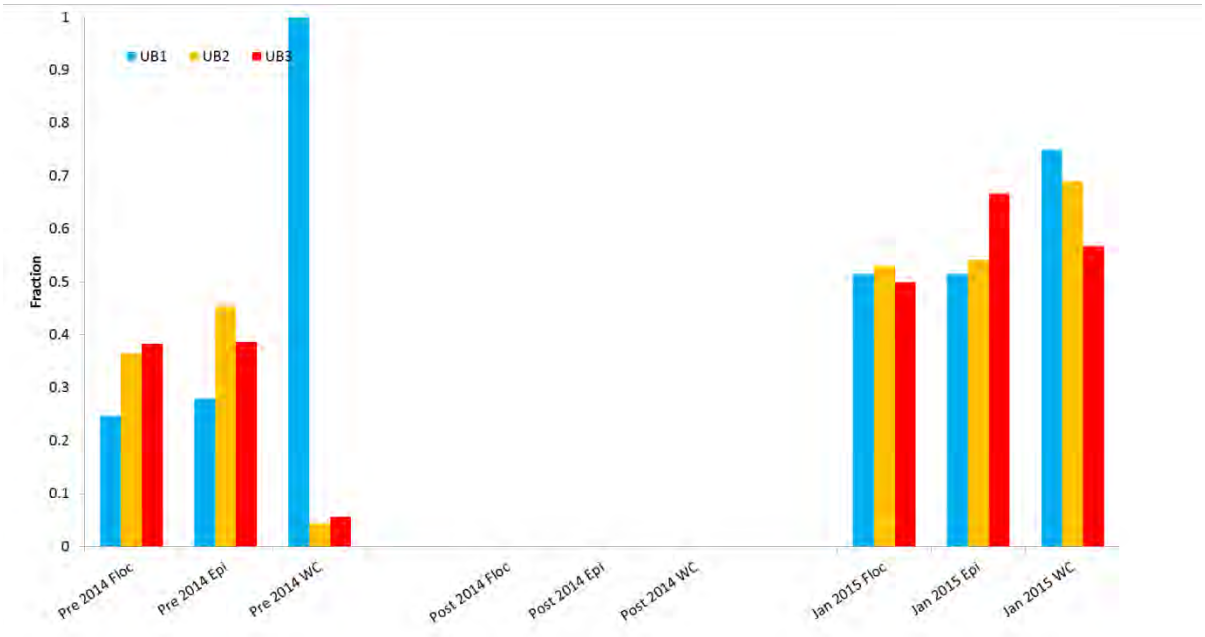

Figure E-183 Ash free dry weight (AFDW) fractions in floc, epiphyton (epi) and water column (WC) samples collected at UB1, UB2 and UB3 for flow release 2014.

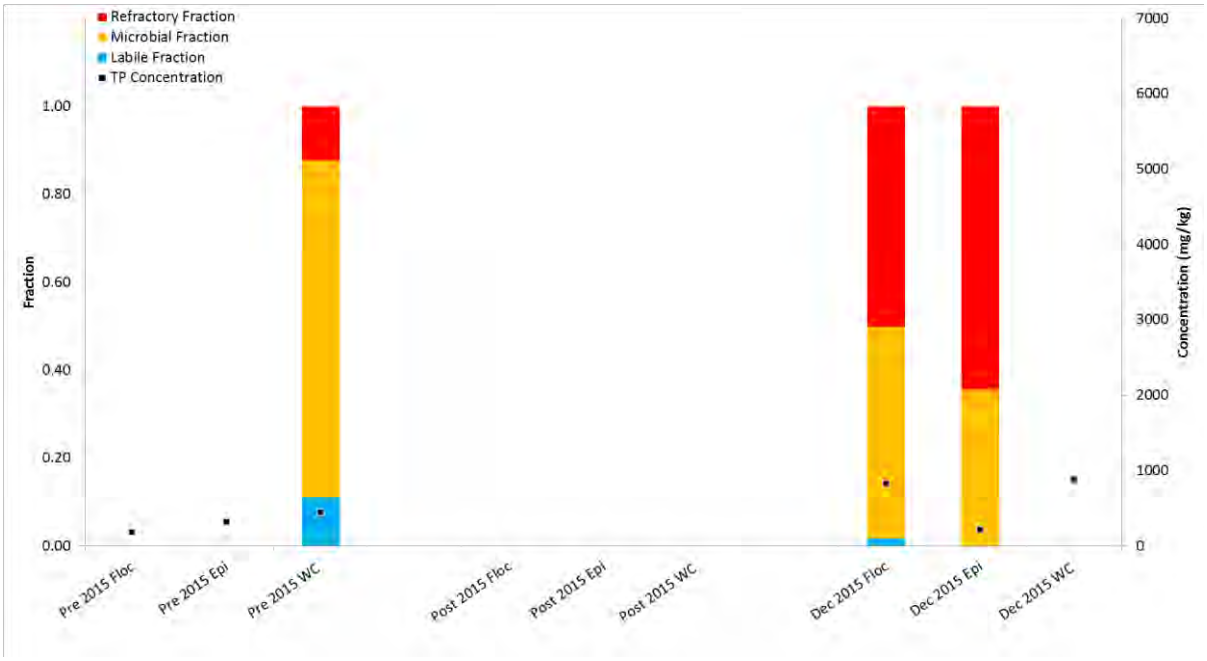

Figure E-184 Labile, microbial and refractory fractionation and total phosphorus concentrations from floc, epiphyton (epi) and water column (WC) samples collected at UB1 for flow release 2015.

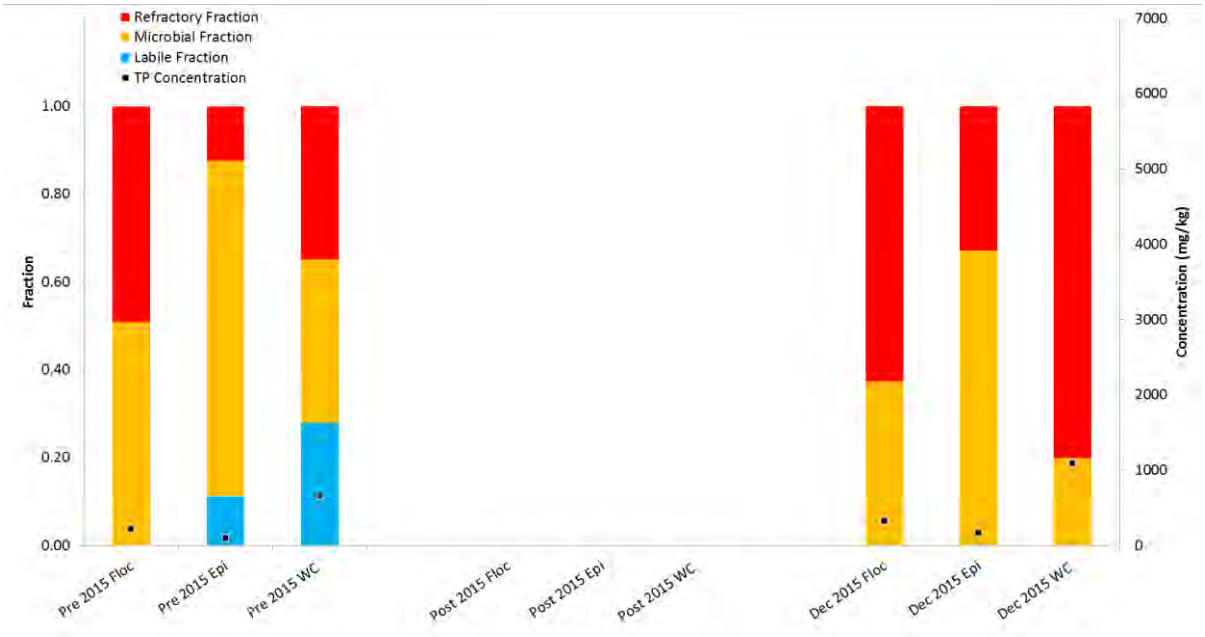

Figure E-185 Labile, microbial and refractory fractionation and total phosphorus concentrations from floc, epiphyton (epi) and water column (WC) samples collected at UB2 for flow release 2015.

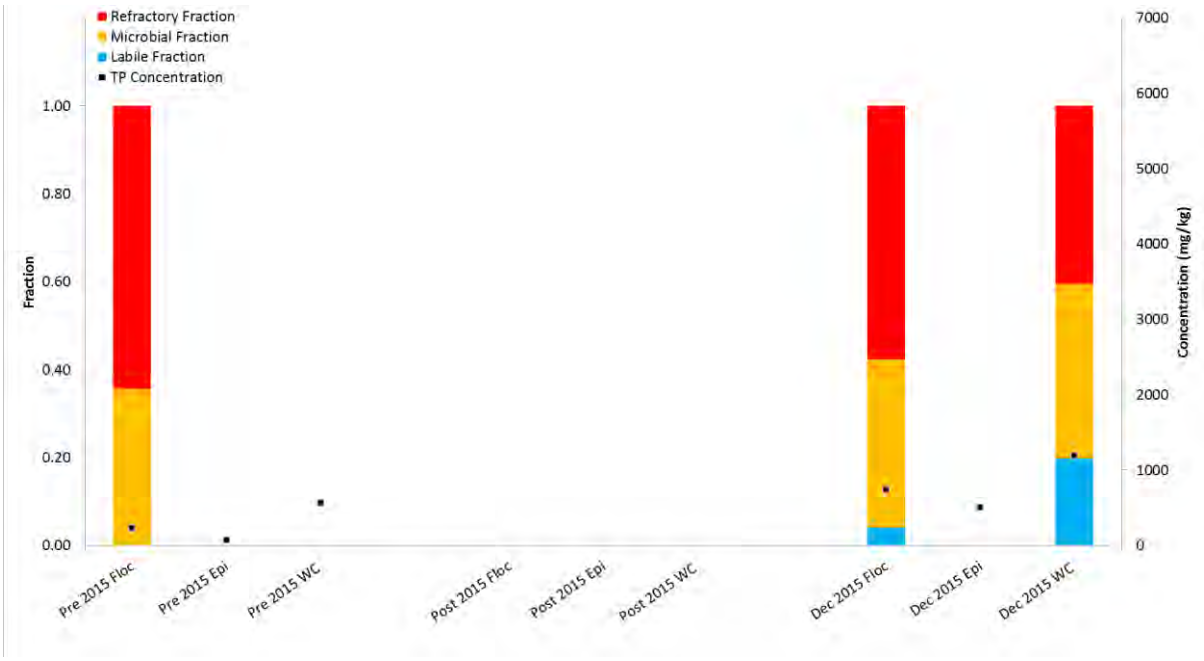

Figure E-186 Labile, microbial and refractory fractionation and total phosphorus concentrations from floc, epiphyton (epi) and water column (WC) samples collected at UB3 for flow release 2015.

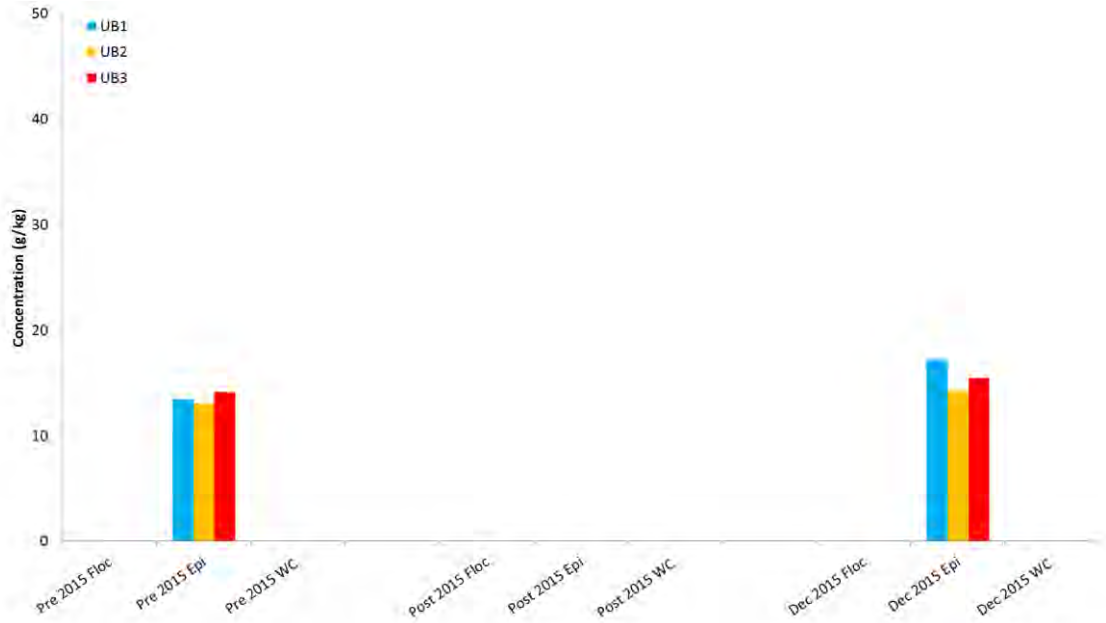

Figure E-187 Total nitrogen concentrations in floc, epiphyton (epi) and water column (WC) samples collected at UB1, UB2 and UB3 for flow release 2015.

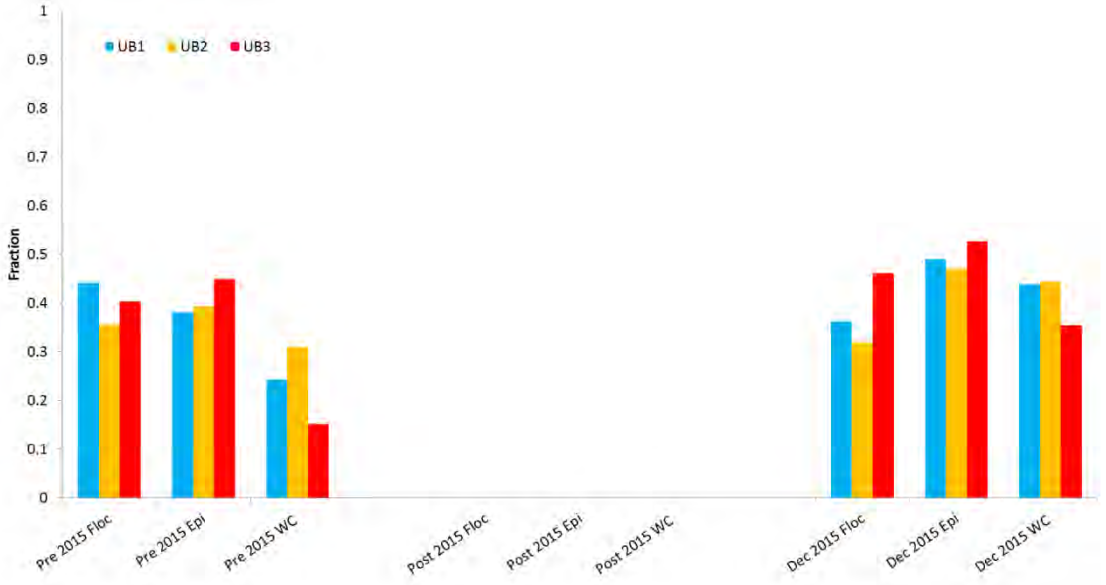

Figure E-188 Ash free dry weight (AFDW) fractions in floc, epiphyton (epi) and water column (WC) samples collected at UB1, UB2 and UB3 for flow release 2015.

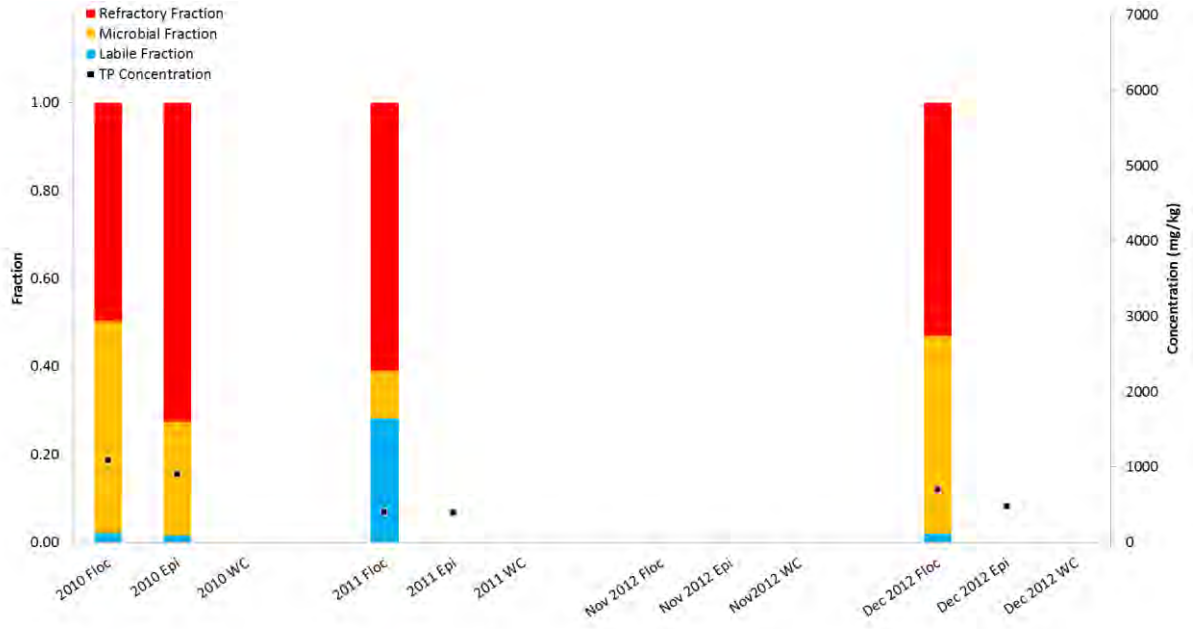

Figure E-189 Labile, microbial and refractory fractionation and total phosphorus concentrations from floc, epiphyton (epi) and water column (WC) samples collected at DB1 from 2010 through 2012.

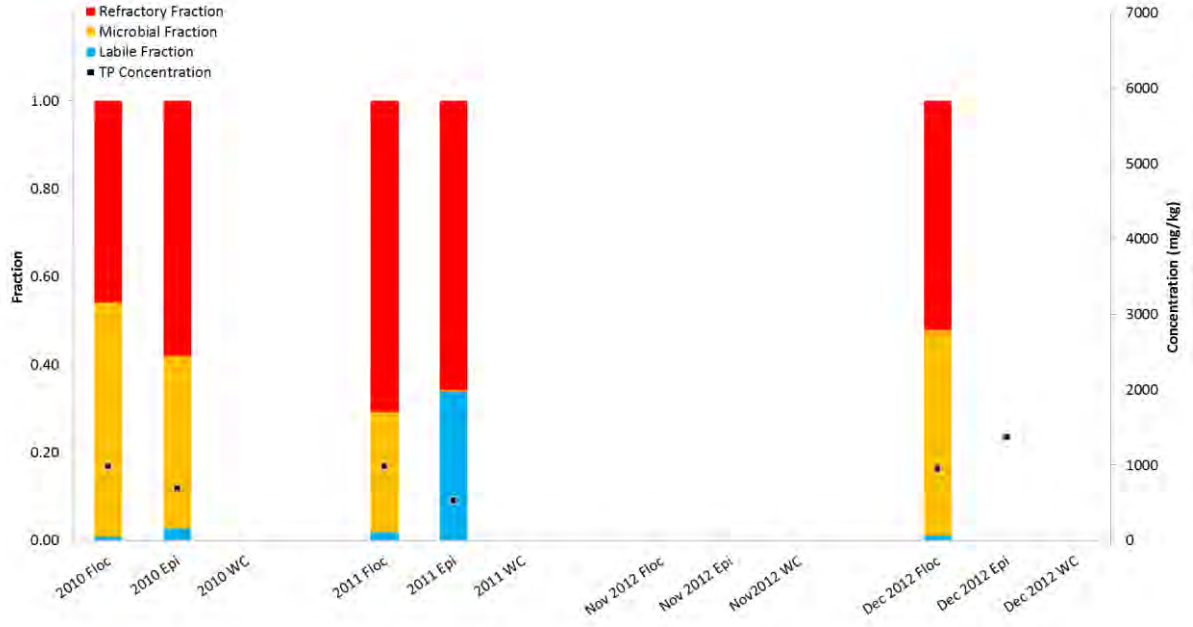

Figure E-190 Labile, microbial and refractory fractionation and total phosphorus concentrations from floc, epiphyton (epi) and water column (WC) samples collected at DB2 from 2010 through 2012.

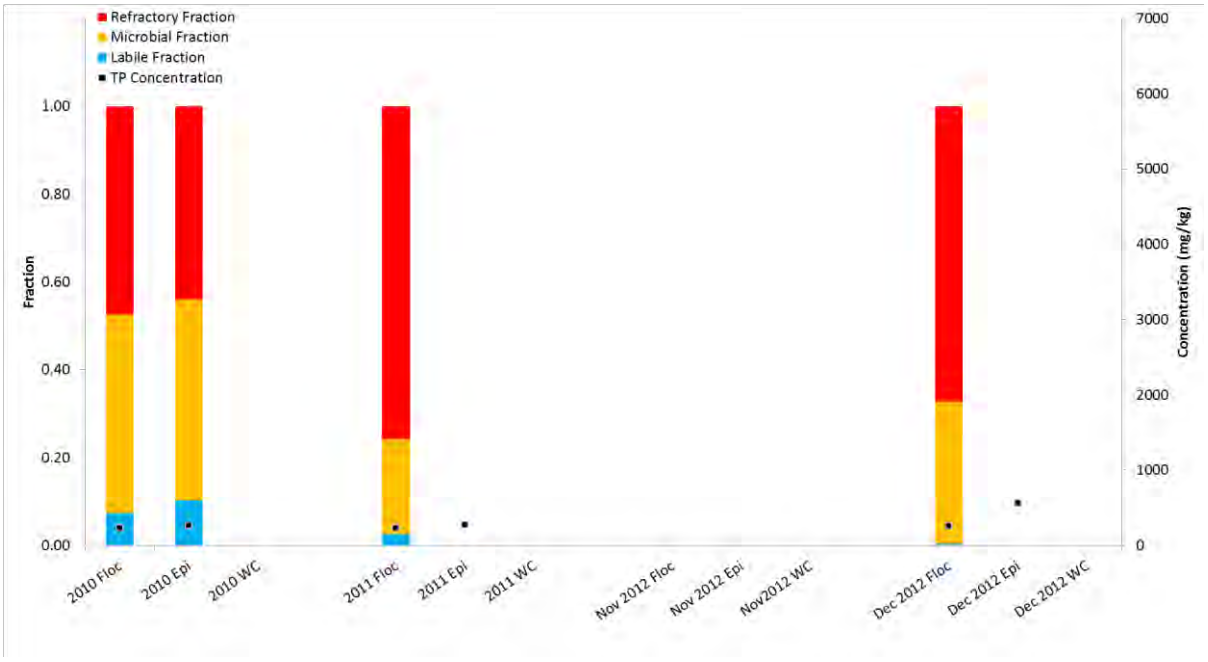

Figure E-191 Labile, microbial and refractory fractionation and total phosphorus concentrations from floc, epiphyton (epi) and water column (WC) samples collected at DB3 from 2010 through 2012.

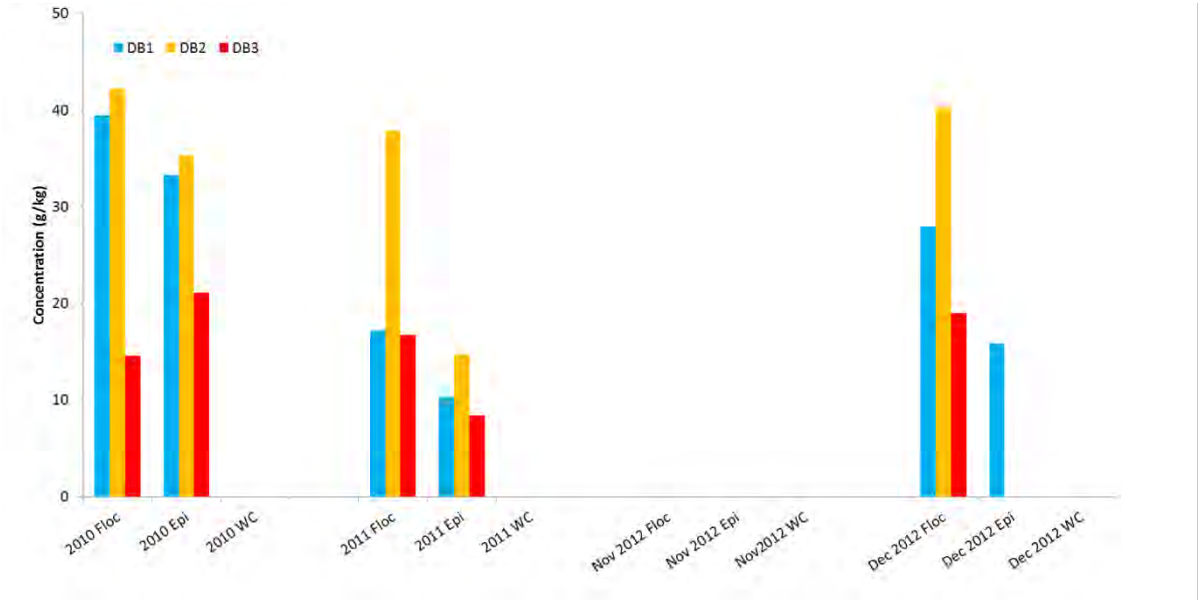

Figure E-192 Total nitrogen concentrations in floc, epiphyton (epi) and water column (WC) samples collected at DB1, DB2 and DB3 for 2010 through 2012.

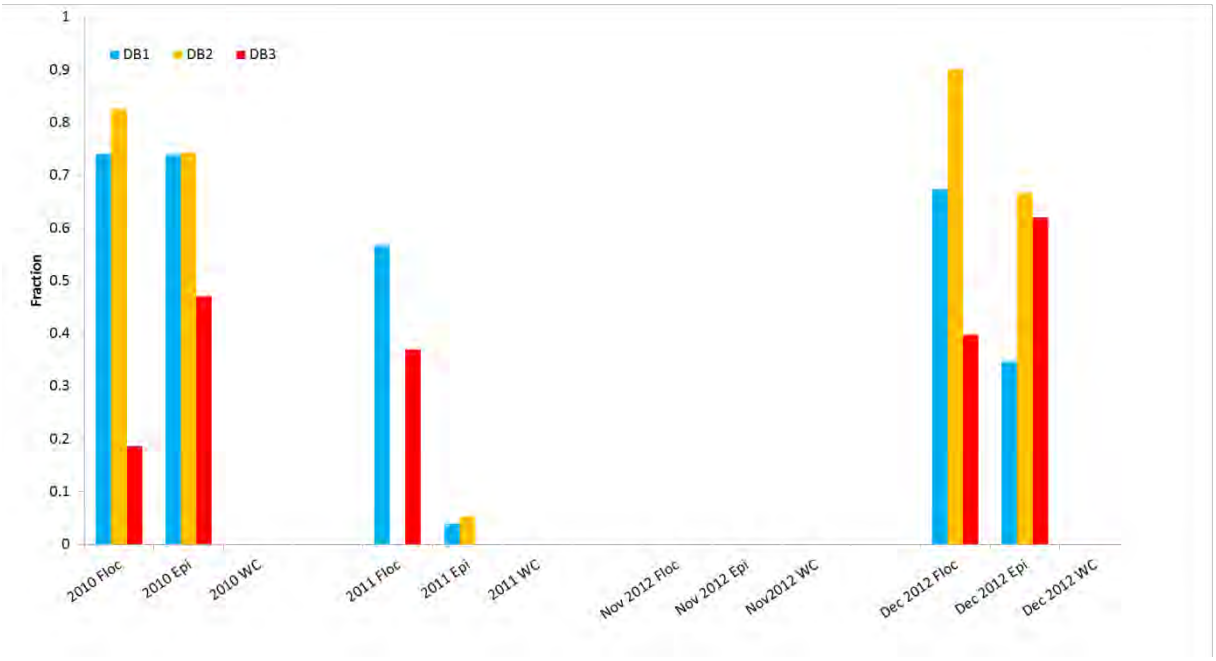

Figure E-193 Ash free dry weight (AFDW) fractions in floc, epiphyton (epi) and water column (WC) samples collected at DB1, DB2 and DB3 for 2010 through 2012.

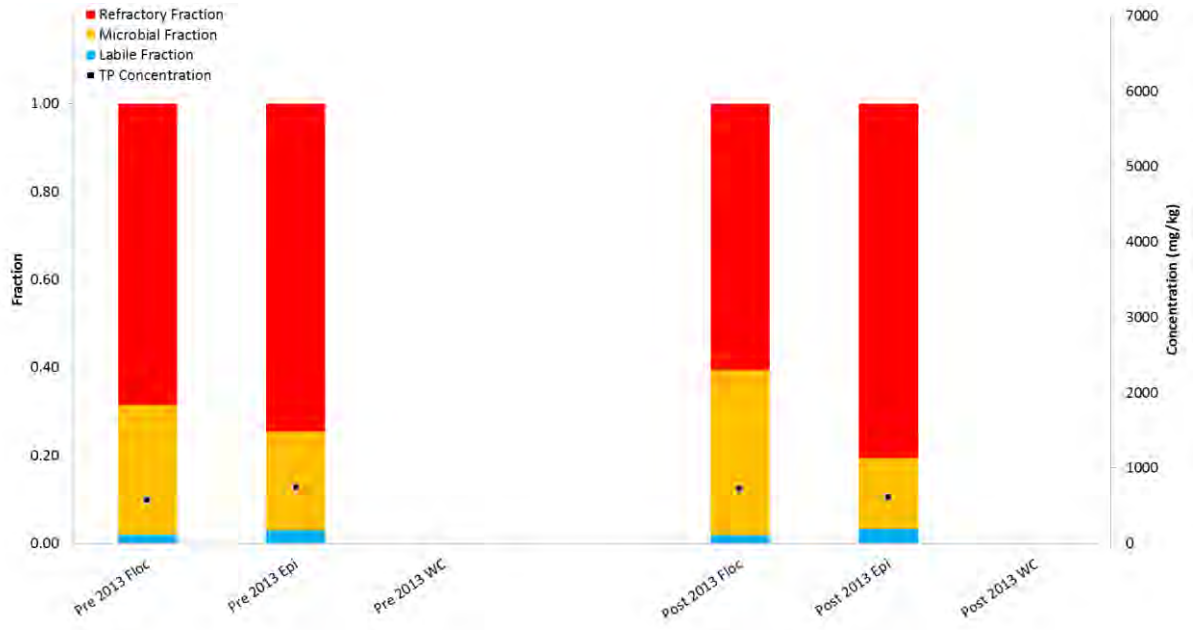

Figure E-194 Labile, microbial and refractory fractionation and total phosphorus concentrations from floc, epiphyton (epi) and water column (WC) samples collected at DB1 for flow release 2013.

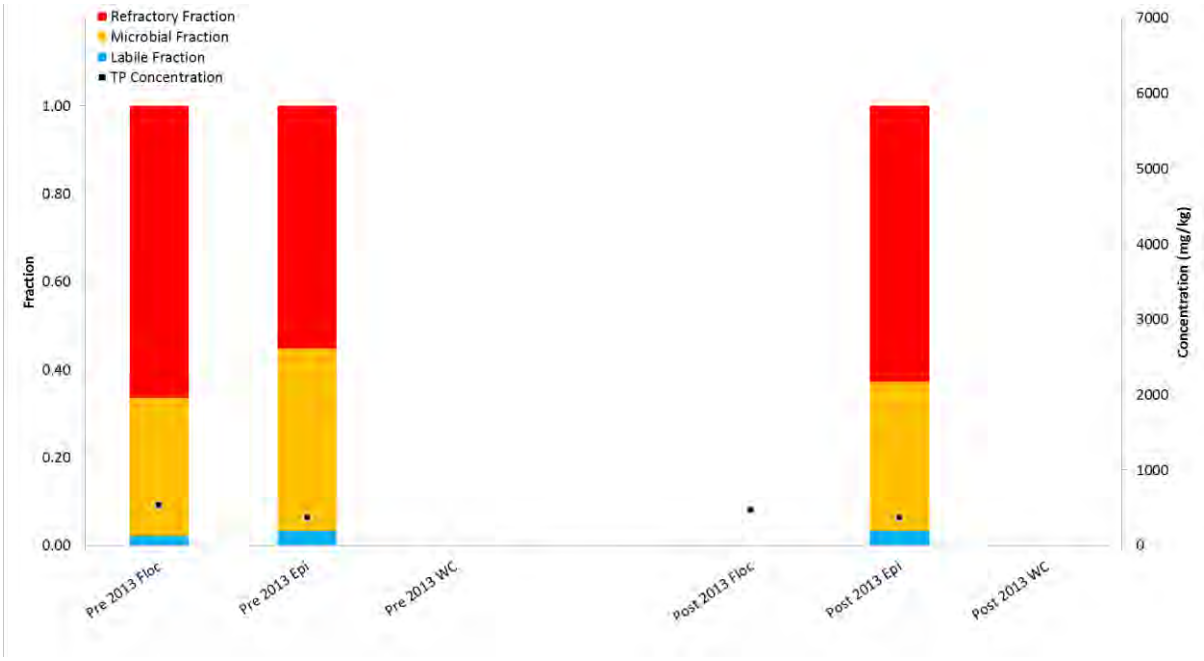

Figure E-195 Labile, microbial and refractory fractionation and total phosphorus concentrations from floc, epiphyton (epi) and water column (WC) samples collected at DB2 for flow release 2013.

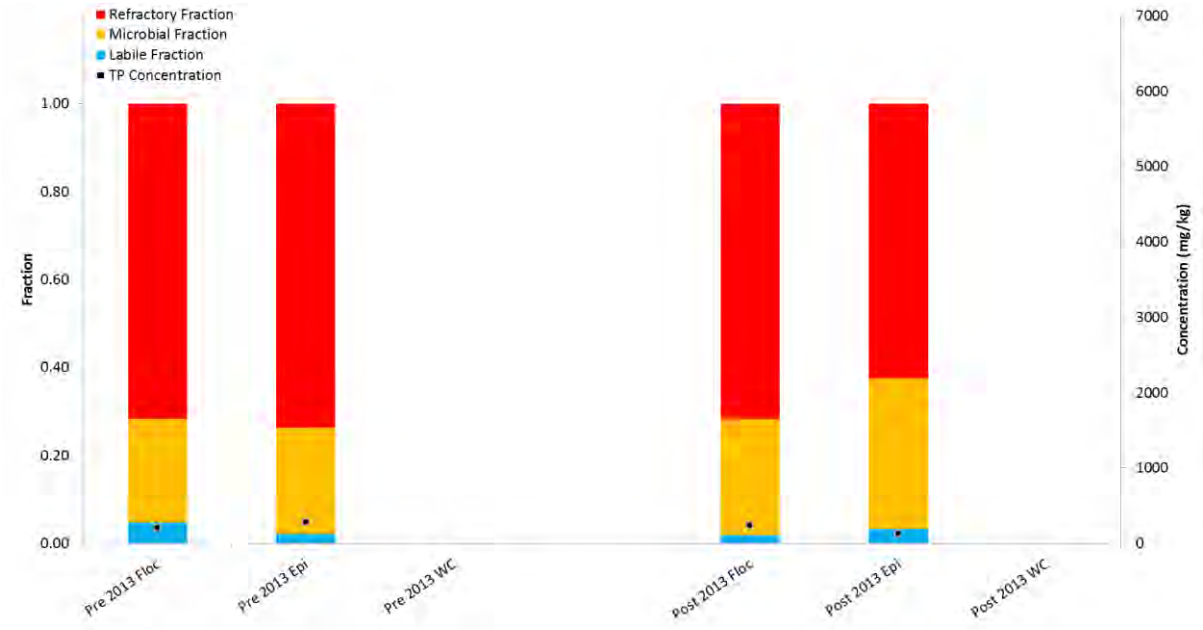

Figure E-196 Labile, microbial and refractory fractionation and total phosphorus concentrations from floc, epiphyton (epi) and water column (WC) samples collected at DB3 for flow release 2013.

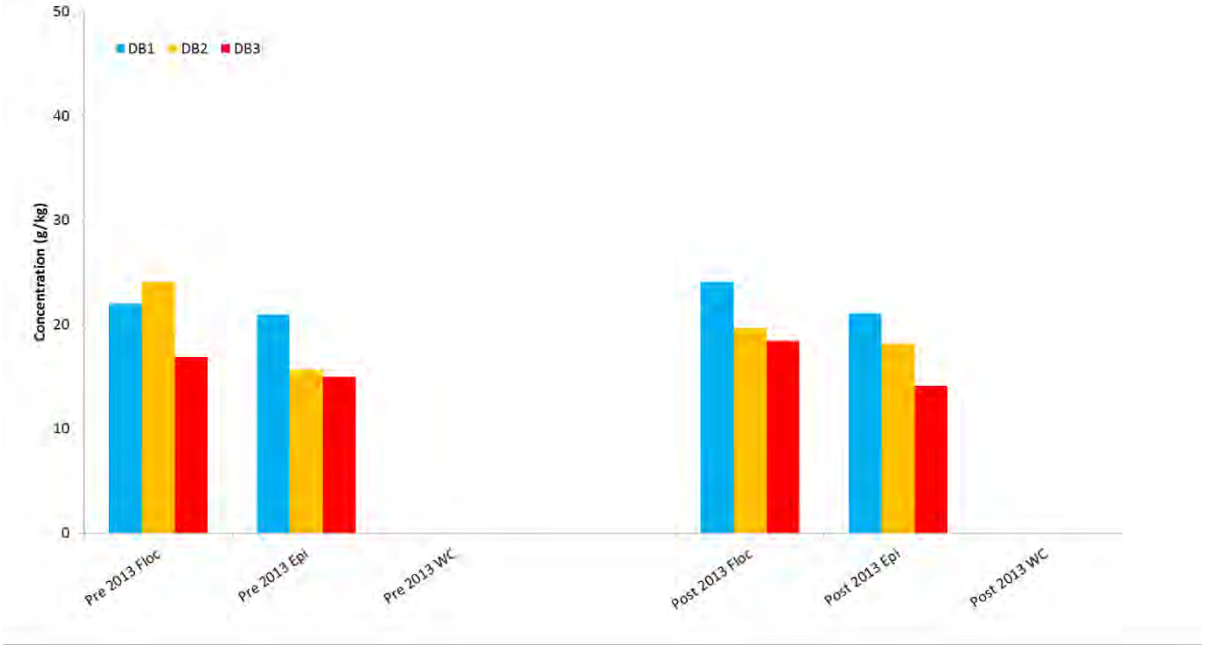

Figure E-197 Total nitrogen concentrations in floc, epiphyton (epi) and water column (WC) samples collected at DB1, DB2 and DB3 for flow release 2013.

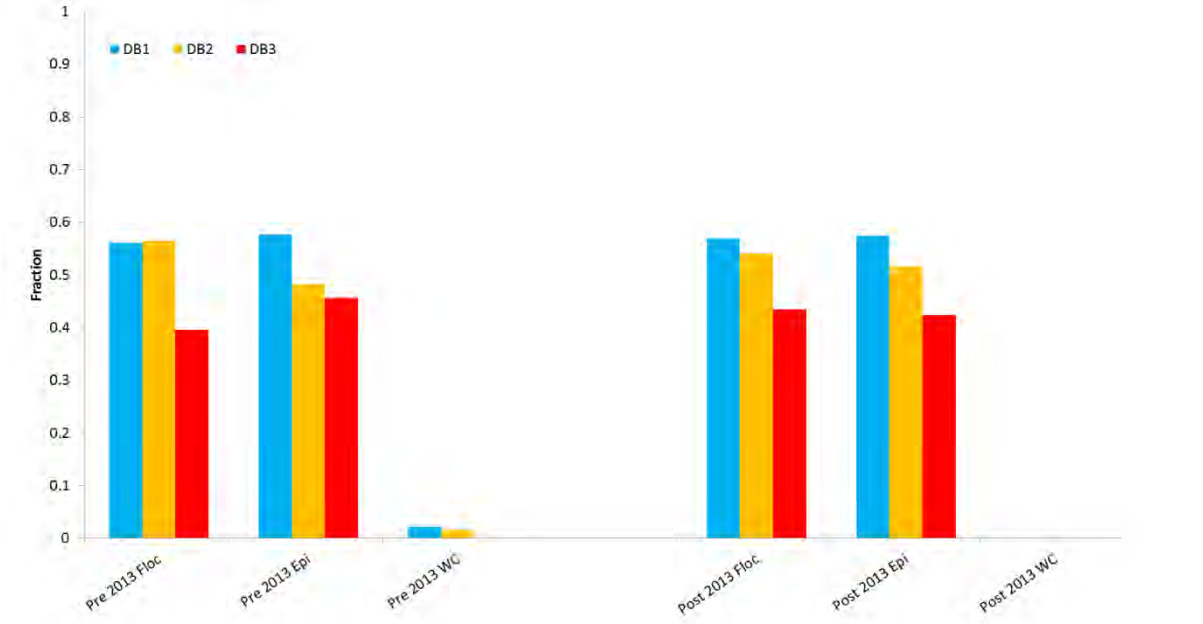

Figure E-198 Ash free dry weight (AFDW) fractions in floc, epiphyton (epi) and water column (WC) samples collected at DB1, DB2 and DB3 for flow release 2013.

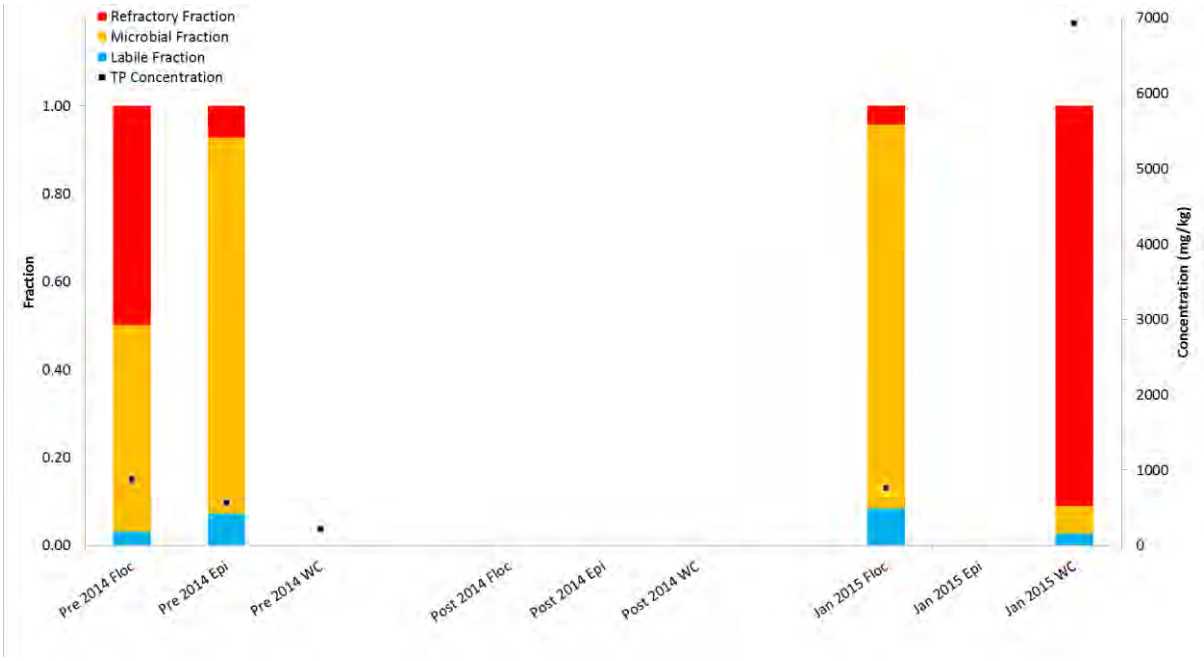

Figure E-199 Labile, microbial and refractory fractionation and total phosphorus concentrations from floc, epiphyton (epi) and water column (WC) samples collected at DB1 for flow release 2014.

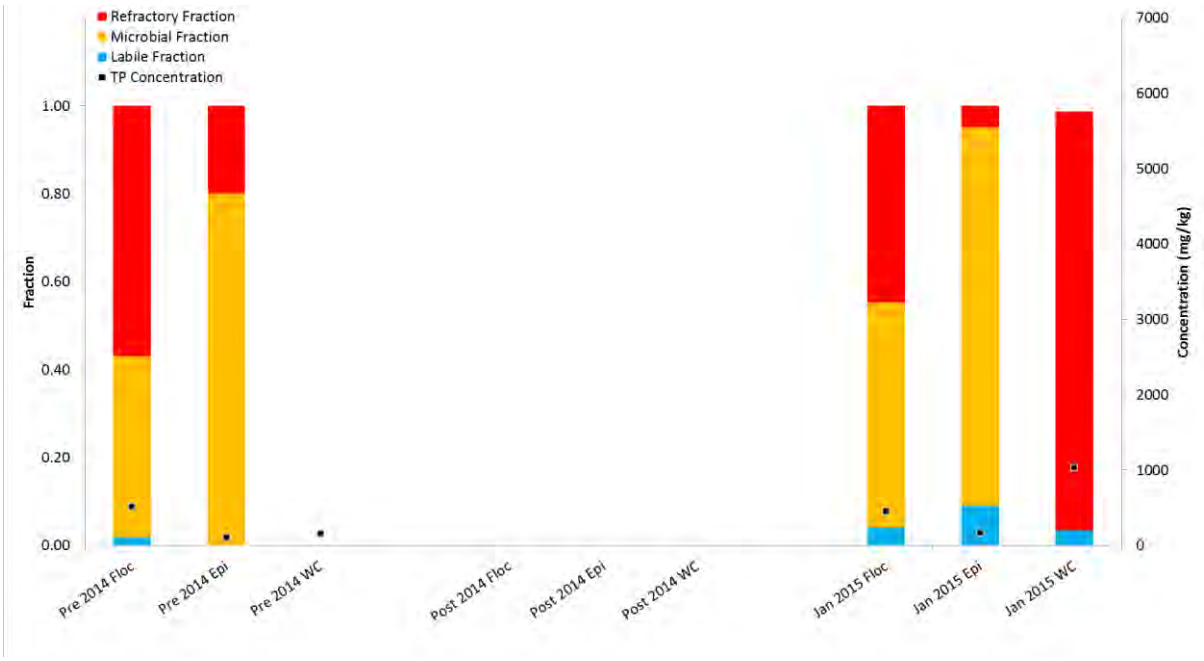

Figure E-200 Labile, microbial and refractory fractionation and total phosphorus concentrations from floc, epiphyton (epi) and water column (WC) samples collected at DB2 for flow release 2014.

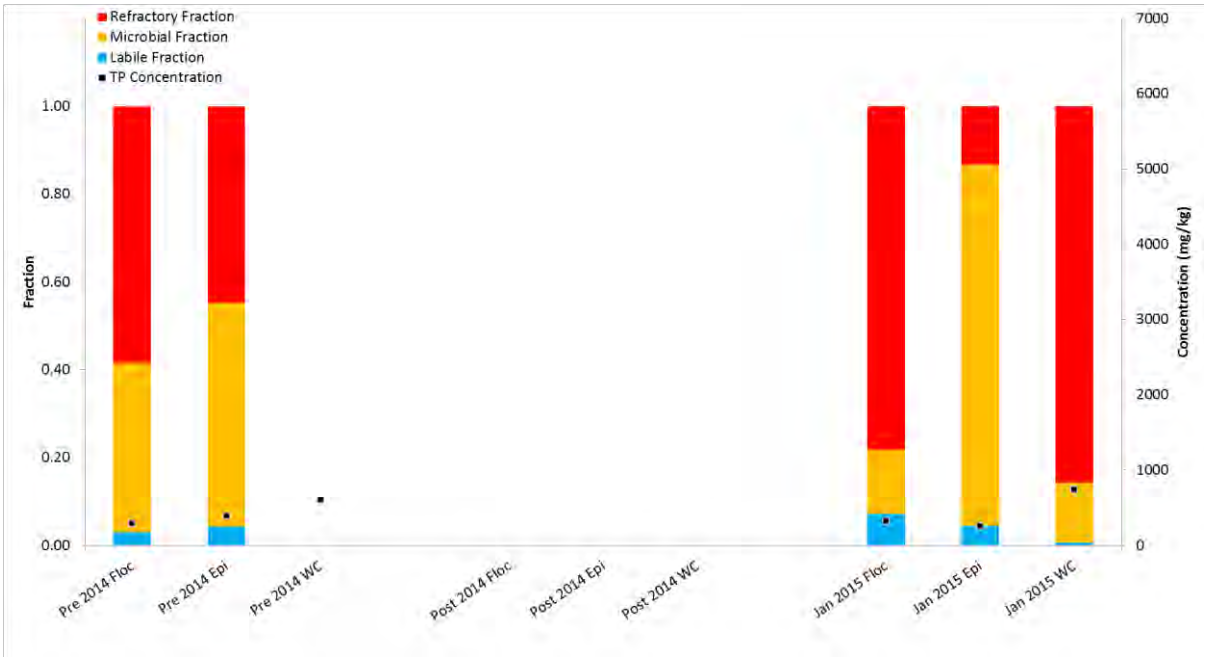

Figure E-201 Labile, microbial and refractory fractionation and total phosphorus concentrations from floc, epiphyton (epi) and water column (WC) samples collected at DB3 for flow release 2014.

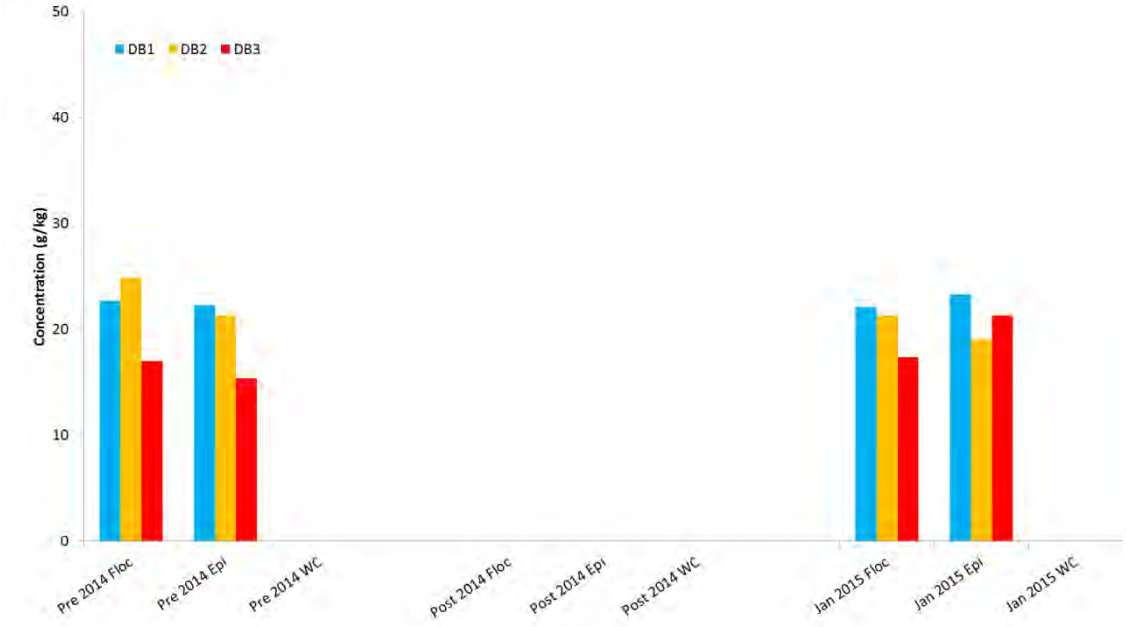

Figure E-202 Total nitrogen concentrations in floc, epiphyton (epi) and water column (WC) samples collected at DB1, DB2 and DB3 for flow release 2014.

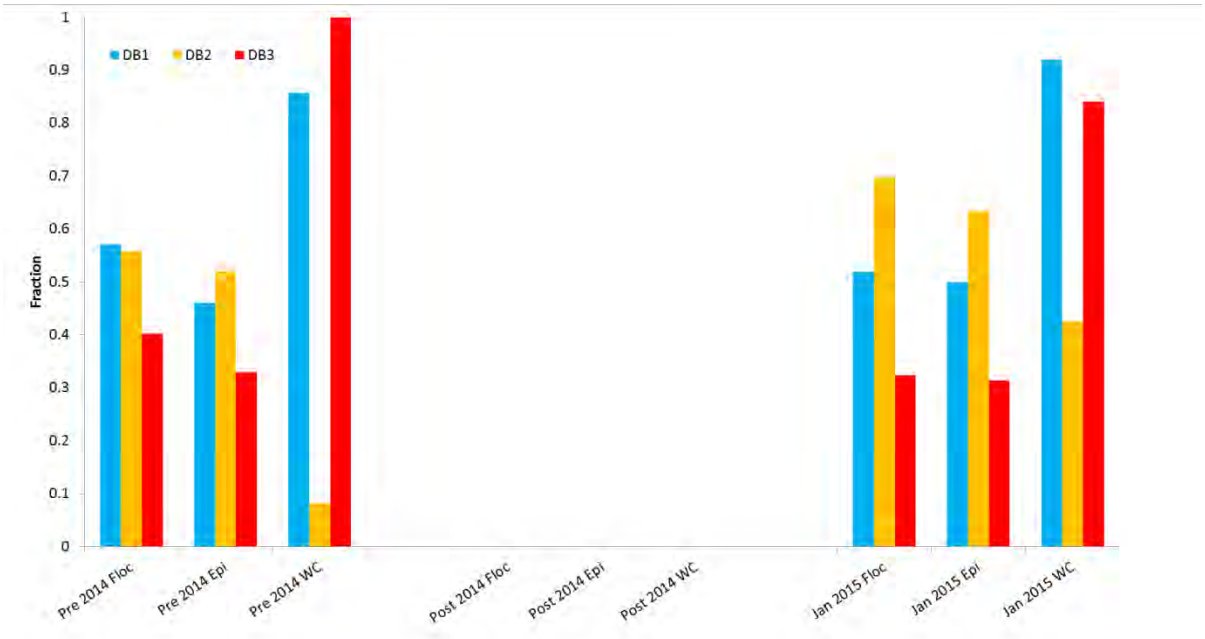

Figure E-203 Ash free dry weight (AFDW) fractions in floc, epiphyton (epi) and water column (WC) samples collected at DB1, DB2 and DB3 for flow release 2014.

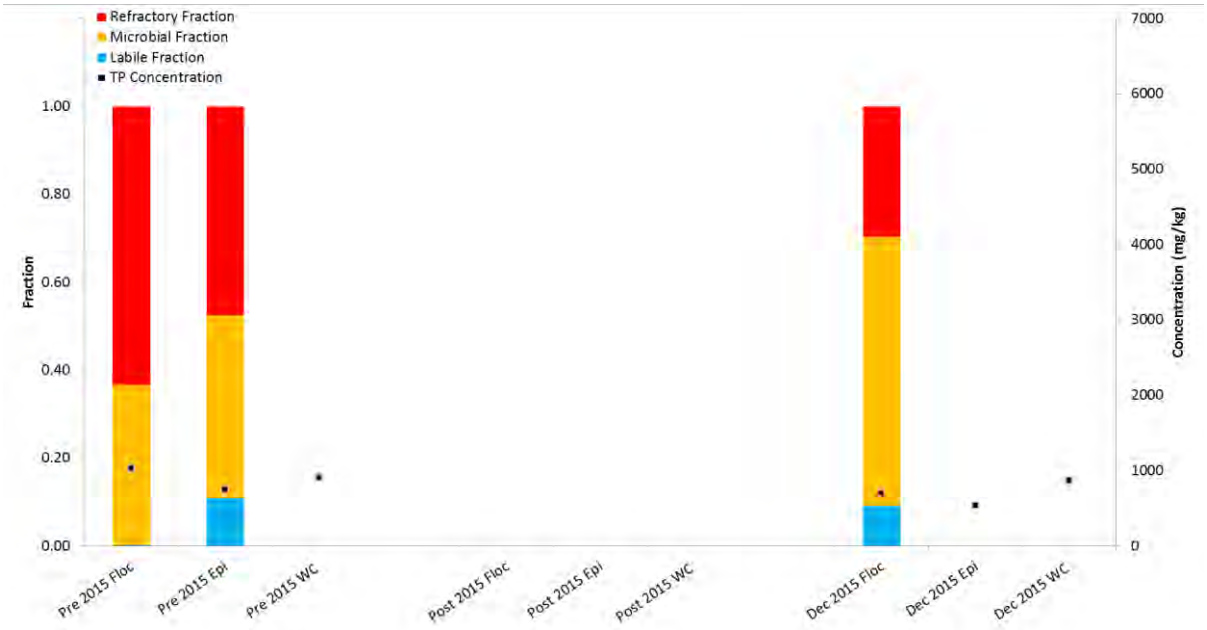

Figure E-204 Labile, microbial and refractory fractionation and total phosphorus concentrations from floc, epiphyton (epi) and water column (WC) samples collected at DB1 for flow release 2015.

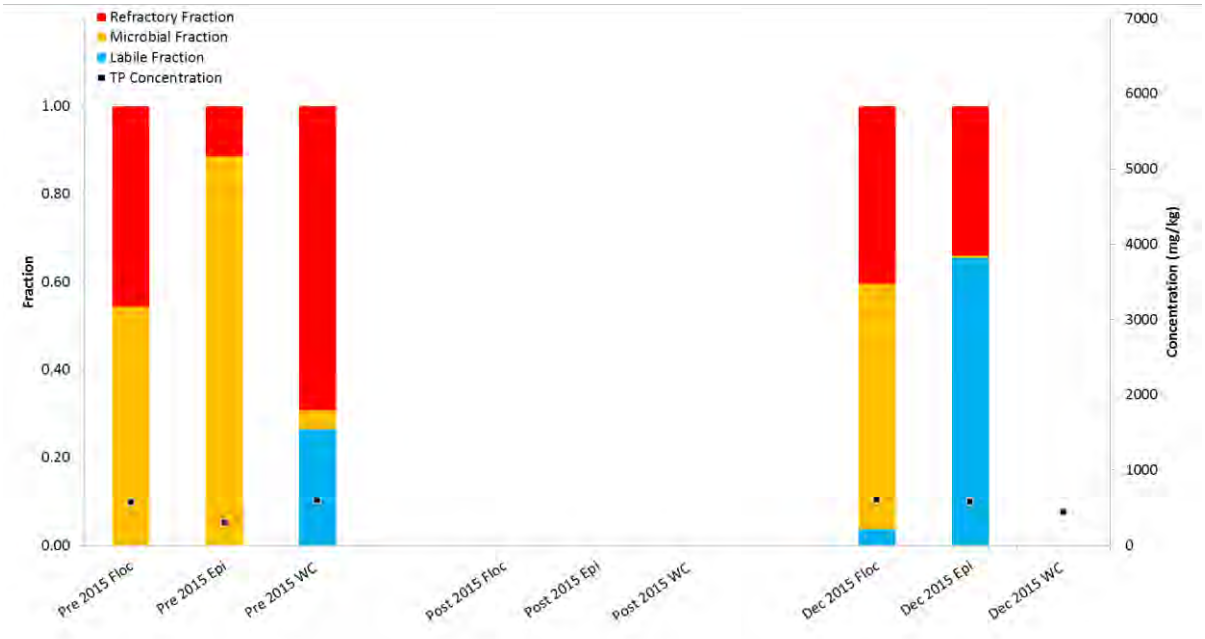

Figure E-205 Labile, microbial and refractory fractionation and total phosphorus concentrations from floc, epiphyton (epi) and water column (WC) samples collected at DB2 for flow release 2015.

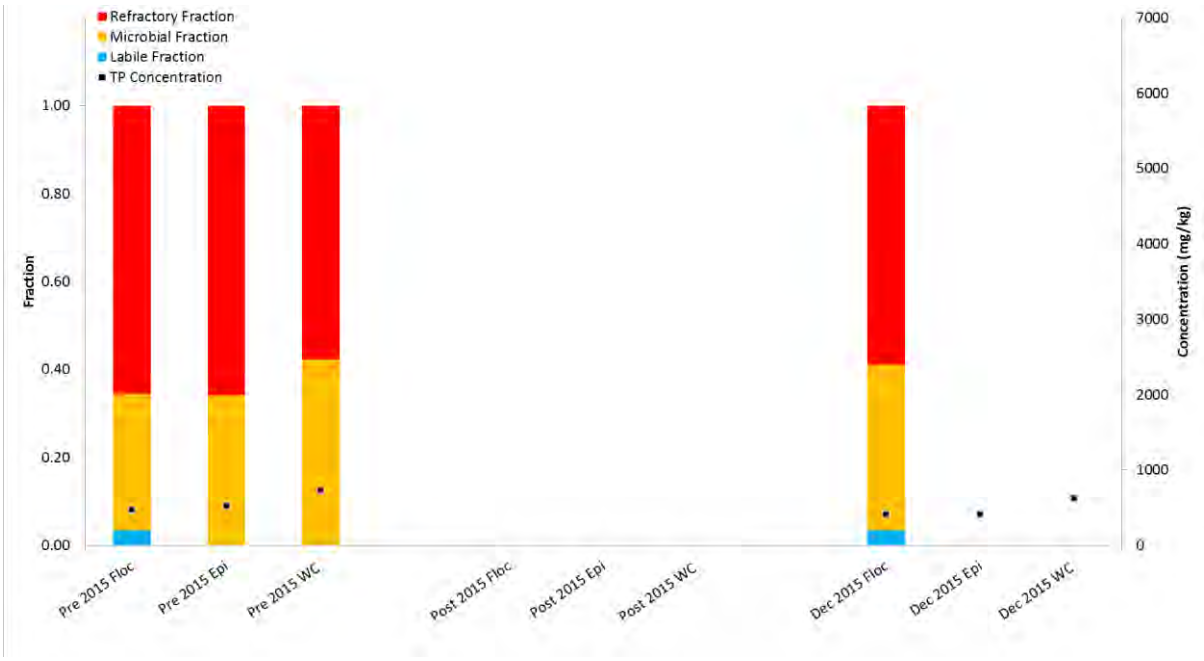

Figure E-206 Labile, microbial and refractory fractionation and total phosphorus concentrations from floc, epiphyton (epi) and water column (WC) samples collected at DB3 for flow release 2015.

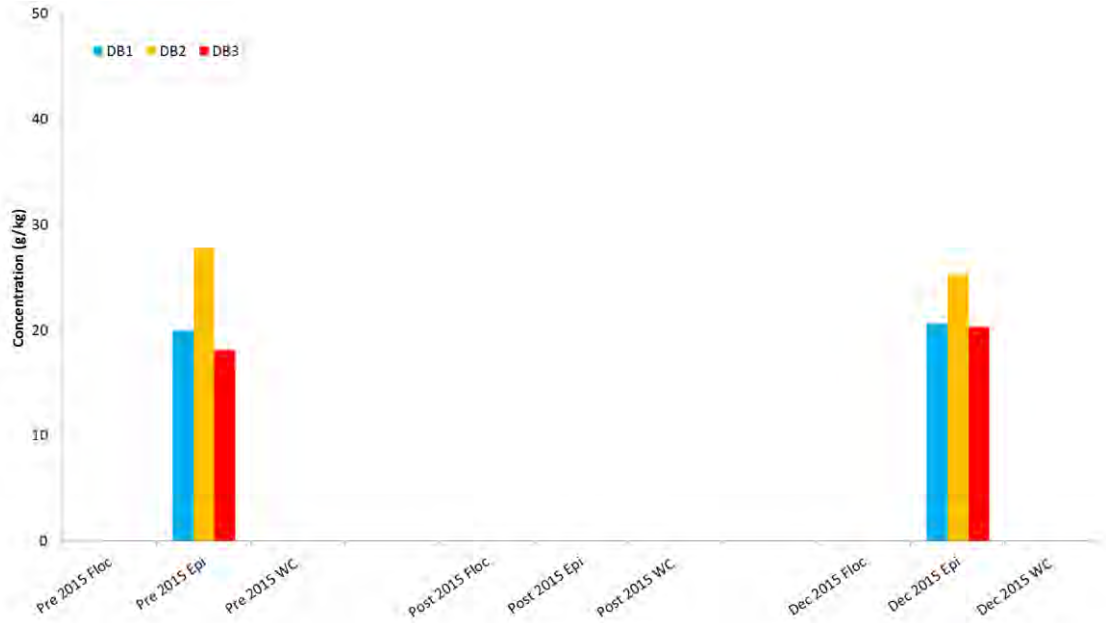

Figure E-207 Total nitrogen concentrations in floc, epiphyton (epi) and water column (WC) samples collected at DB1, DB2 and DB3 for flow release 2015.

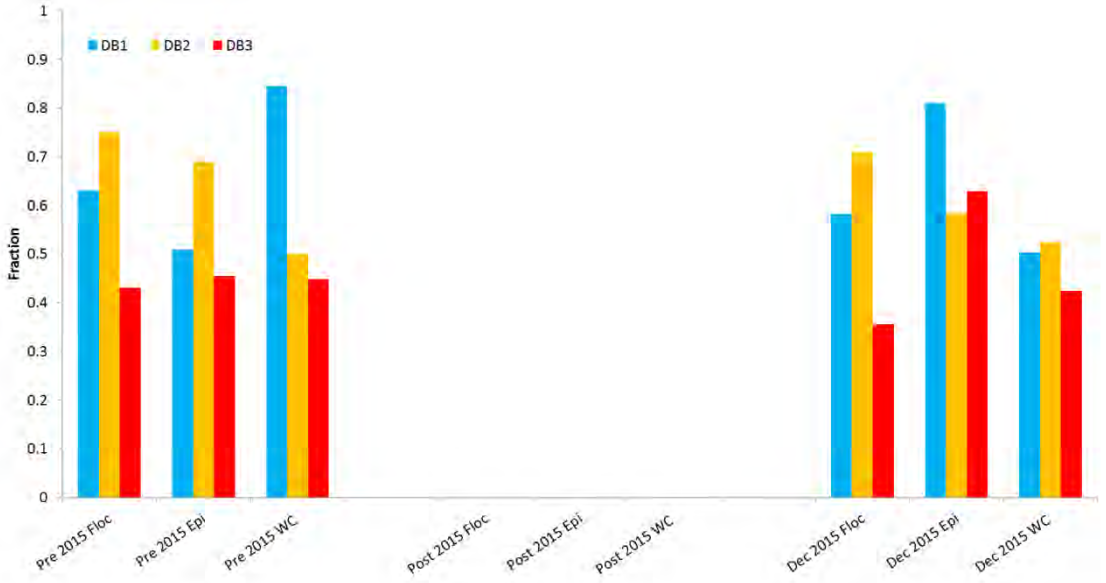

Figure E-208 Ash free dry weight (AFDW) fractions in floc, epiphyton (epi) and water column (WC) samples collected at DB1, DB2 and DB3 for flow release 2015.

F. Vegetation Influence on Flow

Table F-1 The dominant species contributing to each vegetative community. Site codes R, T, and S denote vegetative community: ‘R’ is ridge, ‘T’ is ridge-slough transition, and ‘S’ is slough.

vegetative community	dominant species (in descending order)		
	1	2	3
Ridge (R)	*Cladium jamaciense*	*Typha latifolia*	*Crinum americanum*
Transition (T)	*Cladium jamaciense*	*Eleocharis elongata*	*Eleocharis cellulosa*
Slough (S)	*Eleocharis elongata*	*Eleocharis cellulosa*	*Nymphaea odorata*

Table F-2 Vegetative data refer to stems and leaves greater than 15 cm in length with epiphyton collected in September and November of 2010. Both live and dead materials are included. Measurements are integrated values for depth increments above floc-surface (0 cm) to water-surface. Above-water measurements are recorded at a height equal to 0.5 * average stem length above water-surface. Site codes R, T, and S denote vegetative community: 'R' is ridge, 'T' is ridge-slough transition, and 'S' is slough. Site codes ADV and LAI denote proximity to an autonomous ADV deployment or where PAR measurements were taken to get leaf area index respectively.

Site	Canopy height (cm)	Water surface (cm)	Stem diameter (mm)	Vegetative frontal area (cm^{-1})	Dimensional volume (fraction of bulk volume)	Collection Date	Latitude	Longitude	Datum
L67A R	10	40	9.9E+00	4.9E-02	3.9E-02	11/10/2010	25°52'10.57"N	80°36'52.53"W	WGS 1984
	30		7.4E+00	2.8E-02	1.7E-02				
	96		6.9E+00	3.0E-02	1.6E-02				
C1 R ADV	10	40	1.4E+01	1.5E-01	1.0E-01	11/10/2010	25°52'7.98"N	80°36'39.03"W	WGS 1984
	30		6.3E+00	6.3E-02	1.9E-02				
	82		6.6E+00	3.9E-02	1.3E-02				
C1 R LAI	10	40	1.0E+01	8.0E-02	4.1E-02	11/10/2010	25°52'8.09"N	80°36'39.69"W	WGS 1984
	30		8.0E+00	5.6E-02	2.2E-02				
	72		5.5E+00	2.1E-02	5.7E-03				
C1 S	10	40	2.7E+00	5.7E-03	1.3E-03	11/10/2010	25°52'7.92"N	80°36'37.93"W	WGS 1984
	30		1.7E+00	5.4E-03	1.1E-03				
	56		2.6E+00	1.0E-03	2.5E-04				
RS1D R1	10	37	7.9E+00	8.9E-03	3.3E-03	11/9/2010	25°51'36.25"N	80°37'12.75"W	WGS 1984
	29		6.3E+00	2.5E-02	7.8E-03				
	59		5.3E+00	2.4E-02	6.3E-03				
RS1D R2	10	40	4.4E+00	1.4E-03	2.9E-04	11/9/2010	25°51'36.22"N	80°37'11.97"W	WGS 1984
	30		5.1E+00	1.8E-02	4.5E-03				
	75		5.4E+00	1.4E-02	3.6E-03				
RS1D S	30	40	4.1E+00	1.1E-03	3.6E-04	11/9/2010	25°51'35.80"N	80°37'13.51"W	WGS 1984
C2 R	10	42	1.0E+01	6.7E-02	3.4E-02	11/10/2010	25°49'58.01"N	80°38'7.69"W	WGS 1984
	31		8.4E+00	9.5E-02	4.0E-02				
	76		7.9E+00	5.3E-02	2.0E-02				
C2 S1	8	28	1.4E+00	3.9E-04	4.8E-05	11/10/2010	25°49'58.16"N	80°38'6.86"W	WGS 1984
	22		1.5E+00	8.0E-03	1.0E-03				
C2 S2	5	23	no data	no data	no data	11/10/2010	25°49'56.43"N	80°38'7.10"W	WGS 1984
	17		4.6E+00	1.3E-03	5.1E-04				
C2 S3	8	28	5.4E+00	1.3E-03	5.5E-04	11/10/2010	25°49'55.35"N	80°38'4.82"W	WGS 1984
	22		5.9E+00	7.1E-04	3.3E-04				
RS2 R ADV	10	40	7.0E+00	2.7E-02	9.3E-03	9/28/2010	25°51'4.91"N	80°37'20.44"W	WGS 1984
	30		5.1E+00	1.5E-02	3.8E-03				
	61		5.4E+00	1.5E-02	3.9E-03				
RS2 R LAI	49	22	6.3E+00	3.3E-02	1.0E-02	11/2/2010	25°51'4.89"N	80°37'20.84"W	WGS 1984
	11		7.8E+00	4.8E-02	1.9E-02				
RS2 S ADV	10	45	2.4E+00	3.5E-03	8.1E-04	9/28/2010	25°51'4.97"N	80°37'19.79"W	WGS 1984
	30		2.8E+00	1.4E-03	4.8E-04				
	43		1.7E+00	1.4E-04	2.1E-05				
	57		1.4E+00	3.3E-04	3.6E-05				
S1 R1	10	44	8.7E+00	3.5E-02	1.5E-02	11/5/2010	25°51'4.53"N	80°37'0.77"W	WGS 1984
	32		7.3E+00	2.4E-02	8.6E-03				
	94		6.1E+00	2.2E-02	6.8E-03				
S1 R2	10	42	9.8E+00	5.0E-02	2.4E-02	11/5/2010	25°51'4.63"N	80°37'0.39"W	WGS 1984
	31		6.8E+00	4.6E-02	1.5E-02				
	73		5.8E+00	3.0E-02	8.2E-03				
S1 S	30	62	3.8E+00	1.5E-03	5.2E-04	11/5/2010	25°51'4.40"N	80°37'1.70"W	WGS 1984
	51		2.7E+00	8.5E-04	2.8E-04				
	74		2.6E+00	5.3E-04	1.1E-04				
UB1 R	8	30	8.0E+00	2.0E-02	7.7E-03	11/3/2010	25°50'37.79"N	80°36'57.99"W	WGS 1984
	23		9.7E+00	8.9E-03	4.3E-03				
	51		4.7E+00	4.9E-02	1.1E-02				
UB1 T	10	40	2.6E+00	2.0E-02	4.7E-03	11/3/2010	25°50'37.63"N	80°36'57.93"W	WGS 1984
	30		3.0E+00	2.7E-02	8.2E-03				
	52		2.0E+00	3.8E-03	6.6E-04				
UB1 S	10	65	no data	no data	no data	11/3/2010	25°50'37.87"N	80°36'57.40"W	WGS 1984
	30		1.1E+00	1.5E-02	1.4E-03				
	53		1.3E+00	1.6E-02	1.9E-03				
	77		1.7E+00	6.8E-05	9.0E-06				
UB2 R	10	40	1.2E+01	5.1E-02	3.1E-02	11/8/2010	25°50'26.42"N	80°37'2.57"W	WGS 1984
	30		3.4E+00	1.4E-02	2.2E-03				
	92		6.2E+00	6.8E-02	2.1E-02				
UB2 S	10	55	1.6E+00	4.8E-03	8.6E-04	11/8/2010	25°50'26.32"N	80°37'3.11"W	WGS 1984
	30		1.5E+00	1.1E-02	1.7E-03				
	47		1.5E+00	7.6E-03	1.7E-03				

Table F-3 Vegetative data refer to stems and leaves greater than 15 cm in length after removal of epiphyton collected in September and November of 2010. Both live and dead materials are included. Measurements are integrated values for depth increments above floc-surface (0 cm) to water-surface. Above-water measurements are recorded at a height equal to 0.5 * average stem length above water-surface. Site codes R, T, and S denote vegetative community: 'R' is ridge, 'T' is ridge-slough transition, and 'S' is slough. Site codes ADV and LAI denote proximity to an autonomous ADV deployment or where PAR measurements were taken to get leaf area index respectively.

Site	Canopy height (cm)	Water surface (cm)	Stem diameter (mm)	Vegetative frontal area (cm^{-1})	Dimensional volume (fraction of bulk volume)	Collection Date	Latitude	Longitude	Datum
L67A R	10	40	1.0E+01	4.5E-02	3.7E-02	11/10/2010	25°52'10.57"N	80°36'52.53"W	WGS 1984
	30		7.4E+00	2.8E-02	1.7E-02				
	96		6.9E+00	3.0E-02	1.6E-02				
C1 R ADV	10	40	1.4E+01	1.5E-01	1.0E-01	11/10/2010	25°52'7.98"N	80°36'39.03"W	WGS 1984
	30		6.2E+00	6.1E-02	1.8E-02				
	82		6.6E+00	3.9E-02	1.3E-02				
C1 R LAI	10	40	1.0E+01	8.0E-02	4.1E-02	11/10/2010	25°52'8.09"N	80°36'39.69"W	WGS 1984
	30		7.2E+00	5.0E-02	1.8E-02				
	72		5.5E+00	2.1E-02	5.7E-03				
C1 S	10	40	2.7E+00	5.7E-03	1.3E-03	11/10/2010	25°52'7.92"N	80°36'37.93"W	WGS 1984
	30		1.7E+00	5.4E-03	1.0E-03				
	56		2.6E+00	1.0E-03	2.5E-04				
RS1D R1	10	37	7.9E+00	8.8E-03	3.3E-03	11/9/2010	25°51'36.25"N	80°37'12.75"W	WGS 1984
	29		6.0E+00	2.4E-02	7.2E-03				
	59		5.3E+00	2.4E-02	6.3E-03				
RS1D R2	10	40	4.4E+00	1.4E-03	2.9E-04	11/9/2010	25°51'36.22"N	80°37'11.97"W	WGS 1984
	30		4.6E+00	1.6E-02	3.7E-03				
	75		5.4E+00	1.4E-02	3.6E-03				
RS1D S	30	40	4.1E+00	1.1E-03	3.6E-04	11/9/2010	25°51'35.80"N	80°37'13.51"W	WGS 1984
C2 R	10	42	1.0E+01	6.7E-02	3.3E-02	11/10/2010	25°49'58.01"N	80°38'7.69"W	WGS 1984
	31		7.6E+00	8.5E-02	3.2E-02				
	76		7.9E+00	5.3E-02	2.0E-02				
C2 S1	8	28	1.4E+00	3.9E-04	4.8E-05	11/10/2010	25°49'58.16"N	80°38'6.86"W	WGS 1984
	22		1.4E+00	7.2E-03	8.4E-04				
C2 S2	5	23	no data	no data	no data	11/10/2010	25°49'56.43"N	80°38'7.10"W	WGS 1984
	17		4.6E+00	1.3E-03	5.1E-04				
C2 S3	8	28	5.4E+00	1.3E-03	5.5E-04	11/10/2010	25°49'55.35"N	80°38'4.82"W	WGS 1984
	22		5.9E+00	7.1E-04	3.3E-04				
RS2 R ADV	10	40	6.8E+00	2.6E-02	8.8E-03	9/28/2010	25°51'4.91"N	80°37'20.44"W	WGS 1984
	30		4.8E+00	1.4E-02	3.3E-03				
	61		5.4E+00	1.4E-02	3.8E-03				
RS2 R LAI	49	22	6.3E+00	3.3E-02	1.0E-02	11/2/2010	25°51'4.89"N	80°37'20.84"W	WGS 1984
	11		7.8E+00	4.3E-02	1.7E-02				
RS2 S ADV	10	45	2.4E+00	3.5E-03	8.1E-04	9/28/2010	25°51'4.97"N	80°37'19.79"W	WGS 1984
	30		2.8E+00	1.4E-03	4.8E-04				
	43		1.7E+00	1.4E-04	2.1E-05				
	57		1.4E+00	3.3E-04	3.6E-05				
S1 R1	10	44	8.7E+00	3.4E-02	1.5E-02	11/5/2010	25°51'4.53"N	80°37'0.77"W	WGS 1984
	32		5.9E+00	1.9E-02	5.7E-03				
	94		6.1E+00	2.2E-02	6.8E-03				
S1 R2	10	42	9.8E+00	4.9E-02	2.4E-02	11/5/2010	25°51'4.63"N	80°37'0.39"W	WGS 1984
	31		6.0E+00	4.1E-02	1.2E-02				
	73		5.8E+00	3.0E-02	8.2E-03				
S1 S	30	62	3.8E+00	1.5E-03	5.2E-04	11/5/2010	25°51'4.40"N	80°37'1.70"W	WGS 1984
	51		2.7E+00	8.5E-04	2.8E-04				
	74		2.6E+00	5.3E-04	1.1E-04				
UB1 R	8	30	8.0E+00	2.0E-02	7.7E-03	11/3/2010	25°50'37.79"N	80°36'57.99"W	WGS 1984
	23		9.7E+00	8.9E-03	4.3E-03				
	51		4.7E+00	4.9E-02	1.1E-02				
UB1 T	10	40	2.0E+00	1.6E-02	3.1E-03	11/3/2010	25°50'37.63"N	80°36'57.93"W	WGS 1984
	30		2.9E+00	2.6E-02	7.8E-03				
	52		2.0E+00	3.8E-03	6.6E-04				
UB1 S	10	65	no data	no data	no data	11/3/2010	25°50'37.87"N	80°36'57.40"W	WGS 1984
	30		1.1E+00	1.5E-02	1.4E-03				
	53		1.3E+00	1.6E-02	1.9E-03				
	77		1.7E+00	6.8E-05	9.0E-06				
UB2 R	10	40	1.2E+01	5.1E-02	3.1E-02	11/8/2010	25°50'26.42"N	80°37'2.57"W	WGS 1984
	30		3.4E+00	1.4E-02	2.2E-03				
	92		6.2E+00	6.8E-02	2.1E-02				
UB2 S	10	55	1.6E+00	4.8E-03	8.6E-04	11/8/2010	25°50'26.32"N	80°37'3.11"W	WGS 1984
	30		1.5E+00	1.1E-02	1.7E-03				
	47		1.5E+00	7.6E-03	1.7E-03				

Table F-4. Vegetative data refer to only stems and leaves greater than 15 cm in length collected in November 2011. Both live and dead materials are included. Measurements are integrated values for depth increments above floc-surface (0 cm) to water-surface. Above-water measurements are recorded at a height equal to 0.5 * average stem length above water-surface. Site codes R, T, and S denote vegetative community: 'R' is ridge, 'T' is ridge-slough transition, and 'S' is slough.

Site	Canopy height (cm)	Water surface (cm)	Stem diameter (mm)	Vegetative frontal area (cm^{-1})	Dimensional volume (fraction of bulk volume)	Collection Date	Latitude	Longitude	Datum
C1 R	10	53	5.9E+00	3.3E-03	9.6E-04	11/1/2011	25°52'7.97"N	80°36'39.17"W	WGS 1984
	30		5.4E+00	2.6E-03	6.8E-04				
	47		4.7E+00	2.1E-03	4.8E-04				
	71		2.6E+00	6.1E-04	7.8E-05				
C1 S	10	73	1.6E+00	3.0E-03	3.7E-04	11/1/2011	25°52'7.86"N	80°36'37.82"W	WGS 1984
	30		1.4E+00	1.0E-03	1.3E-04				
	50		2.4E+00	5.8E-04	1.1E-04				
	66		2.0E+00	4.7E-04	7.3E-05				
	79		2.1E+00	5.9E-04	9.8E-05				
RS1D R	10	40	4.0E+00	3.2E-03	6.4E-04	11/1/2011	25°51'36.20"N	80°37'12.59"W	WGS 1984
	30		3.6E+00	2.6E-03	4.6E-04				
	59		2.8E+00	1.0E-03	1.3E-04				
RS1D S	10	60	3.1E+00	1.7E-03	4.2E-04	11/1/2011	25°51'35.82"N	80°37'13.63"W	WGS 1984
	30		2.5E+00	1.2E-03	2.5E-04				
	50		5.3E+00	2.1E-04	8.2E-05				
	64		1.6E+00	1.3E-04	1.6E-05				
RS2 R	10	49	7.9E+00	3.1E-03	1.2E-03	11/2/2011	25°51'4.89"N	80°37'20.52"W	WGS 1984
	30		6.8E+00	2.2E-03	7.4E-04				
	45		3.7E+00	1.0E-03	1.9E-04				
	60		1.9E+00	2.2E-04	2.0E-05				
RS2 S	10	40	1.1E+00	7.7E-04	6.7E-05	11/2/2011	25°51'5.00"N	80°37'19.74"W	WGS 1984
	30		1.9E+00	9.0E-04	1.8E-04				
UB2 R	10	60	7.3E+00	4.4E-03	1.6E-03	11/2/2011	25°50'26.46"N	80°37'2.49"W	WGS 1984
	30		6.5E+00	3.1E-03	1.0E-03				
	50		5.7E+00	2.8E-03	7.9E-04				
	79		2.5E+00	8.1E-04	1.0E-04				
UB2 S	10	77	2.8E+00	1.9E-03	4.1E-04	11/2/2011	25°50'26.31"N	80°37'3.24"W	WGS 1984
	30		2.5E+00	7.1E-04	1.4E-04				
	50		2.1E+00	3.4E-04	5.5E-05				
	69		1.7E+00	2.1E-04	2.8E-05				

Table F-5 Vegetative data refer to only stems and leaves greater than 15 cm in length collected in November 2012. Both live and dead materials are included. Measurements are integrated values for depth increments above floc-surface (0 cm) to water-surface and above the water-surface to the top of the canopy. Measurements both below and above the water-surface are recorded at a height equal to 0.5 * average stem length above the previous increment. Site codes R, T, and S denote vegetative community: 'R' is ridge, 'T' is ridge-slough transition, and 'S' is slough.

Site	Canopy height (cm)	Water surface (cm)	Stem diameter (mm)	Vegetative frontal area (cm^{-1})	Dimensional volume (fraction of bulk volume)	Collection Date	Latitude	Longitude	Datum
C1 R	25	50	4.0E+00	8.9E-03	1.8E-03	11/6/2012	25°52'7.92"N	80°36'39.24"W	WGS 1984
C1 R	79	50	3.5E+00	4.4E-03	7.7E-04	11/6/2012	25°52'7.92"N	80°36'39.24"W	WGS 1984
C1 S	23	45	1.5E+00	2.1E-03	2.5E-04	11/6/2012	25°52'7.97"N	80°36'37.77"W	WGS 1984
C1 S	53	45	1.9E+00	8.4E-04	1.3E-04	11/6/2012	25°52'7.97"N	80°36'37.77"W	WGS 1984
RS1D R	32	65	8.1E+00	1.9E-02	7.6E-03	11/6/2012	25°51'36.14"N	80°37'12.65"W	WGS 1984
RS1D R	110	65	4.3E+00	7.3E-03	1.6E-03	11/6/2012	25°51'36.14"N	80°37'12.65"W	WGS 1984
RS1D S	29	58	3.5E+00	2.0E-03	5.4E-04	11/6/2012	25°51'35.81"N	80°37'13.52"W	WGS 1984
RS1D S	72	58	2.7E+00	5.5E-04	1.2E-04	11/6/2012	25°51'35.81"N	80°37'13.52"W	WGS 1984
S1 S	29	58	2.8E+00	7.4E-03	1.6E-03	11/6/2012	25°51'4.44"N	80°37'1.62"W	WGS 1984
S1 S	70	58	2.0E+00	2.9E-03	4.5E-04	11/6/2012	25°51'4.44"N	80°37'1.62"W	WGS 1984
UB2 S	22	45	1.2E+00	8.4E-04	7.6E-05	11/6/2012	25°50'26.22"N	80°37'3.23"W	WGS 1984
UB2 S	55	45	1.1E+00	6.7E-04	3.8E-05	11/6/2012	25°50'26.22"N	80°37'3.23"W	WGS 1984

Table F-6 Vegetative data refer to only stems and leaves greater than 15 cm in length collected in August 2013. Both live and dead materials are included. Measurements are integrated values for depth increments above floc-surface (0 cm) to water-surface and above the water-surface to the top of the canopy. Measurements both below and above the water-surface are recorded at a height equal to 0.5 * average stem length above the previous increment. Site codes R, T, and S denote vegetative community: 'R' is ridge, 'T' is ridge-slough transition, and 'S' is slough.

Site	Canopy height (cm)	Water surface (cm)	Stem diameter (mm)	Vegetative frontal area (cm^{-1})	Dimensional volume (fraction of bulk volume)	Collection Date	Latitude	Longitude	Datum
C1 R	82	42	3.7E+00	4.7E-03	8.4E-04	8/15/2013	25°52'7.97"N	80°36'39.17"W	WGS 1984
C1 R	21	42	5.0E+00	8.4E-03	2.1E-03	8/15/2013	25°52'7.97"N	80°36'39.17"W	WGS 1984
C2 R	87	42	4.3E+00	5.3E-03	1.1E-03	8/15/2013	25°49'58.01"N	80°38'7.69"W	WGS 1984
C2 R	21	42	7.0E+00	1.0E-02	3.6E-03	8/15/2013	25°49'58.01"N	80°38'7.69"W	WGS 1984
C2 S	78	64	1.9E+00	7.4E-05	1.1E-05	8/15/2013	25°51'36.14"N	80°37'12.65"W	WGS 1984
C2 S	32	64	2.7E+00	7.4E-04	1.6E-04	8/15/2013	25°51'36.14"N	80°37'12.65"W	WGS 1984
RS1D R	74	35	4.5E+00	8.5E-03	1.9E-03	8/15/2013	25°51'36.20"N	80°37'12.59"W	WGS 1984
RS1D R	18	35	6.7E+00	1.0E-02	3.5E-03	8/15/2013	25°51'36.20"N	80°37'12.59"W	WGS 1984
RS1D S	81	68	2.4E+00	2.8E-04	5.3E-05	8/15/2013	25°51'35.82"N	80°37'13.63"W	WGS 1984
RS1D S	34	68	3.7E+00	2.4E-03	8.1E-04	8/15/2013	25°51'35.82"N	80°37'13.63"W	WGS 1984
RS2 R	85	45	5.7E+00	6.6E-03	1.9E-03	8/15/2013	25°51'4.89"N	80°37'20.52"W	WGS 1984
RS2 R	22	45	8.7E+00	7.7E-03	3.4E-03	8/15/2013	25°51'4.89"N	80°37'20.52"W	WGS 1984
RS2 S	74	61	2.1E+00	2.6E-04	4.5E-05	8/15/2013	25°51'5.00"N	80°37'19.74"W	WGS 1984
RS2 S	31	61	3.2E+00	3.0E-03	9.9E-04	8/15/2013	25°51'5.00"N	80°37'19.74"W	WGS 1984
S1 S	27	54	1.7E+00	8.4E-03	1.2E-03	8/15/2013	25°51'4.40"N	80°37'1.70"W	WGS 1984
UB1 S	34	67	1.9E+00	5.7E-03	8.7E-04	8/15/2013	25°50'37.87"N	80°36'57.40"W	WGS 1984
UB2 S	31	63	1.8E+00	1.6E-03	2.7E-04	8/15/2013	25°50'26.31"N	80°37'3.24"W	WGS 1984
UB2 S	89	63	2.5E+00	9.0E-03	3.1E-03	8/15/2013	25°50'26.31"N	80°37'3.24"W	WGS 1984
UB3 S	31	62	2.5E+00	8.8E-04	1.7E-04	8/15/2013	25°50'15.63"N	80°37'11.69"W	WGS 1984
UB3 S	99	62	2.2E+00	4.0E-03	7.6E-04	8/15/2013	25°50'15.63"N	80°37'11.69"W	WGS 1984

Table F-7 Vegetative data refer to only stems and leaves greater than 15 cm in length collected in August 2014. Both live and dead materials are included. Measurements are integrated values for depth increments above floc-surface (0 cm) to water-surface and above the water-surface to the top of the canopy. Measurements both below and above the water-surface are recorded at a height equal to 0.5 * average stem length above the previous increment. Site codes R, T, and S denote vegetative community: 'R' is ridge, 'T' is ridge-slough transition, and 'S' is slough.

Site	Canopy height (cm)	Water surface (cm)	Stem diameter (mm)	Vegetative fron (cm^{-1})	Dimensional volume (fraction of bulk volume)	Collection Date	Latitude	Longitude	Datum
DB2	26	37	2.0E+00	2.9E-03	5.1E-04	8/15/2014	25°50'20.86"N	80°36'56.51"W	WGS 1984
DB2	51	37	2.1E+00	3.2E-03	5.2E-04	8/15/2014	25°50'20.86"N	80°36'56.51"W	WGS 1984
UB2	13	50	1.3E+00	3.5E-03	4.8E-04	8/15/2014	25°50'26.31"N	80°37'3.24"W	WGS 1984
UB2	38	50	1.1E+00	2.1E-03	1.7E-04	8/15/2014	25°50'26.31"N	80°37'3.24"W	WGS 1984
UB2	56	50	1.1E+00	4.4E-05	3.8E-06	8/15/2014	25°50'26.31"N	80°37'3.24"W	WGS 1984
RS1D-R	8	30	8.4E+00	8.0E-03	3.3E-03	8/15/2014	25°51'36.20"N	80°37'12.59"W	WGS 1984
RS1D-R	23	30	9.5E+00	1.7E-02	7.6E-03	8/15/2014	25°51'36.20"N	80°37'12.59"W	WGS 1984
RS1D-R	64	30	4.7E+00	3.5E-03	8.1E-04	8/15/2014	25°51'36.20"N	80°37'12.59"W	WGS 1984
RS1D-S	11	44	3.3E+00	4.0E-04	1.2E-04	8/15/2014	25°51'35.82"N	80°37'13.63"W	WGS 1984
RS1D-S	33	44	2.5E+00	2.0E-04	3.8E-05	8/15/2014	25°51'35.82"N	80°37'13.63"W	WGS 1984
RS1D-S	50	44	2.3E+00	1.9E-04	3.4E-05	8/15/2014	25°51'35.82"N	80°37'13.63"W	WGS 1984
RS2-R	7	29	8.9E+00	1.8E-03	7.9E-04	8/15/2014	25°51'4.89"N	80°37'20.52"W	WGS 1984
RS2-R	22	29	7.2E+00	3.7E-03	1.3E-03	8/15/2014	25°51'4.89"N	80°37'20.52"W	WGS 1984
RS2-R	73	29	4.9E+00	2.1E-03	5.0E-04	8/15/2014	25°51'4.89"N	80°37'20.52"W	WGS 1984
RS2-S	12	46	2.5E+00	9.9E-04	2.7E-04	8/15/2014	25°51'5.00"N	80°37'19.74"W	WGS 1984
RS2-S	35	46	1.4E+00	1.8E-03	2.1E-04	8/15/2014	25°51'5.00"N	80°37'19.74"W	WGS 1984
RS2-S	57	46	1.6E+00	1.9E-04	2.3E-05	8/15/2014	25°51'5.00"N	80°37'19.74"W	WGS 1984

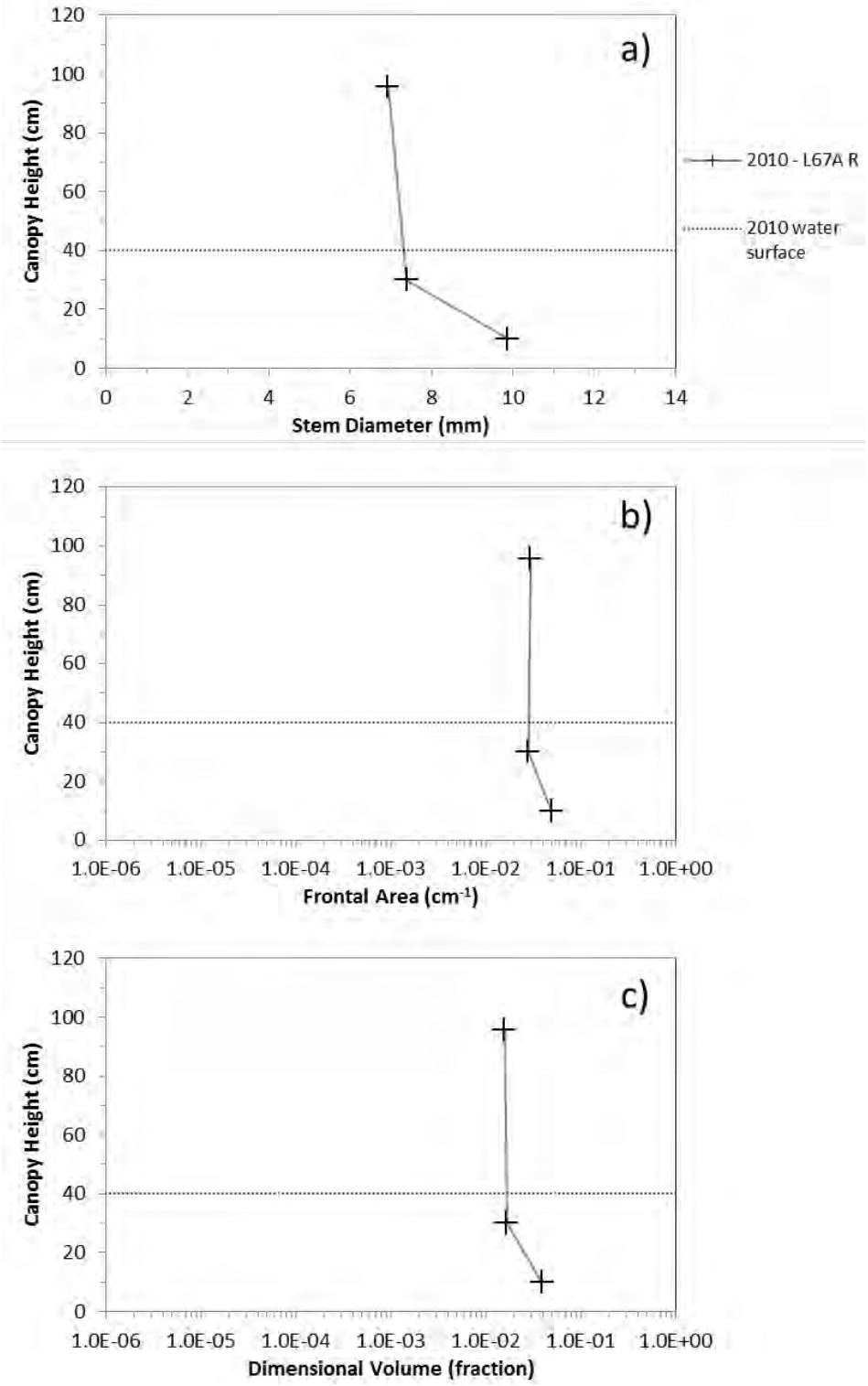

Figure F-1 Average vegetation stem diameter (a), frontal area (b), and dimensional volume (fraction of bulk volume) (c) at site L67A Ridge. Samples collected on 11/10/2010.

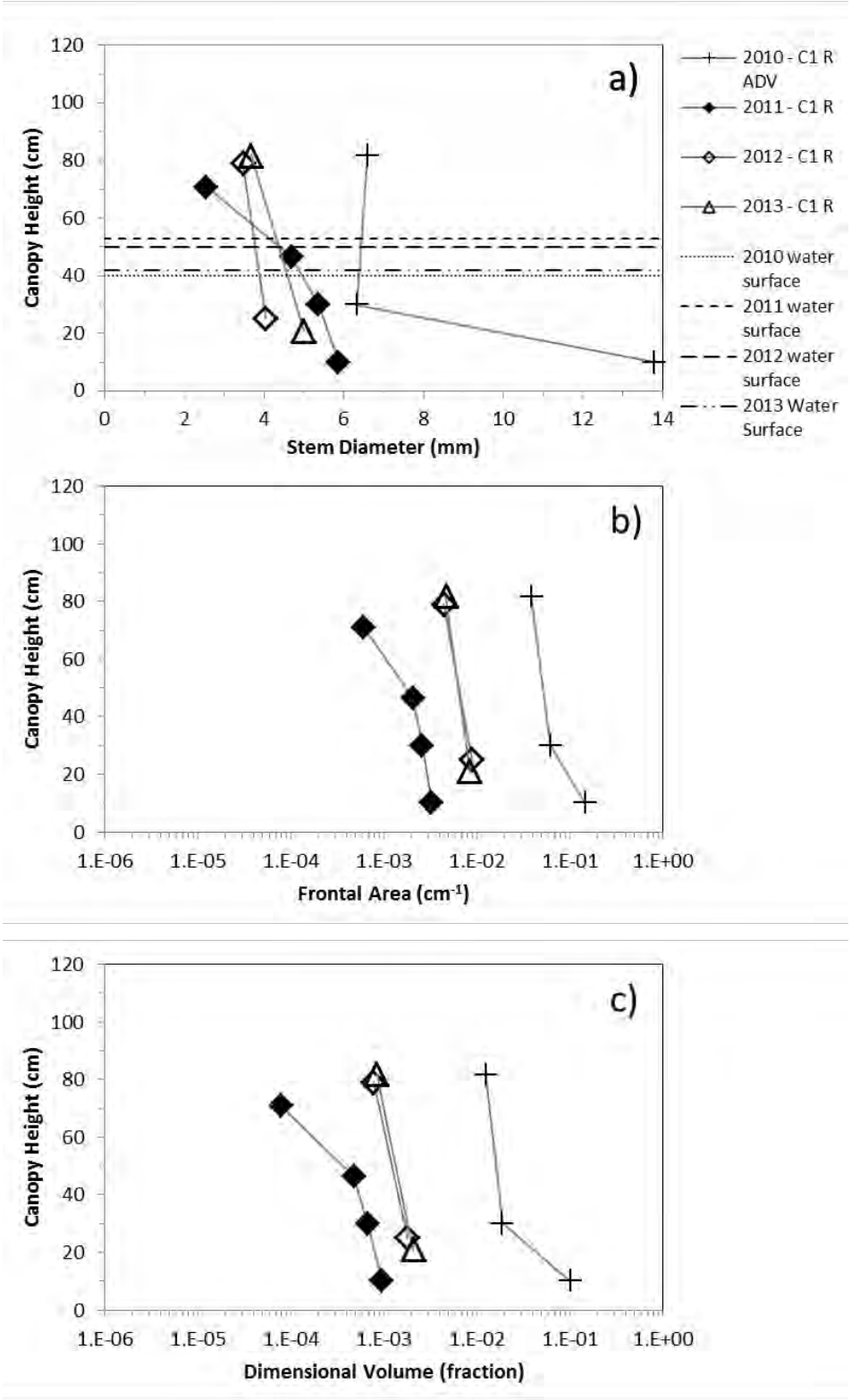

Figure F-2 Average vegetation stem diameter (a), frontal area (b), and dimensional volume (fraction of bulk volume) (c) at site C1 Ridge. Samples collected on 11/10/2010, 11/1/2011, 11/6/2012, and 8/15/2013.

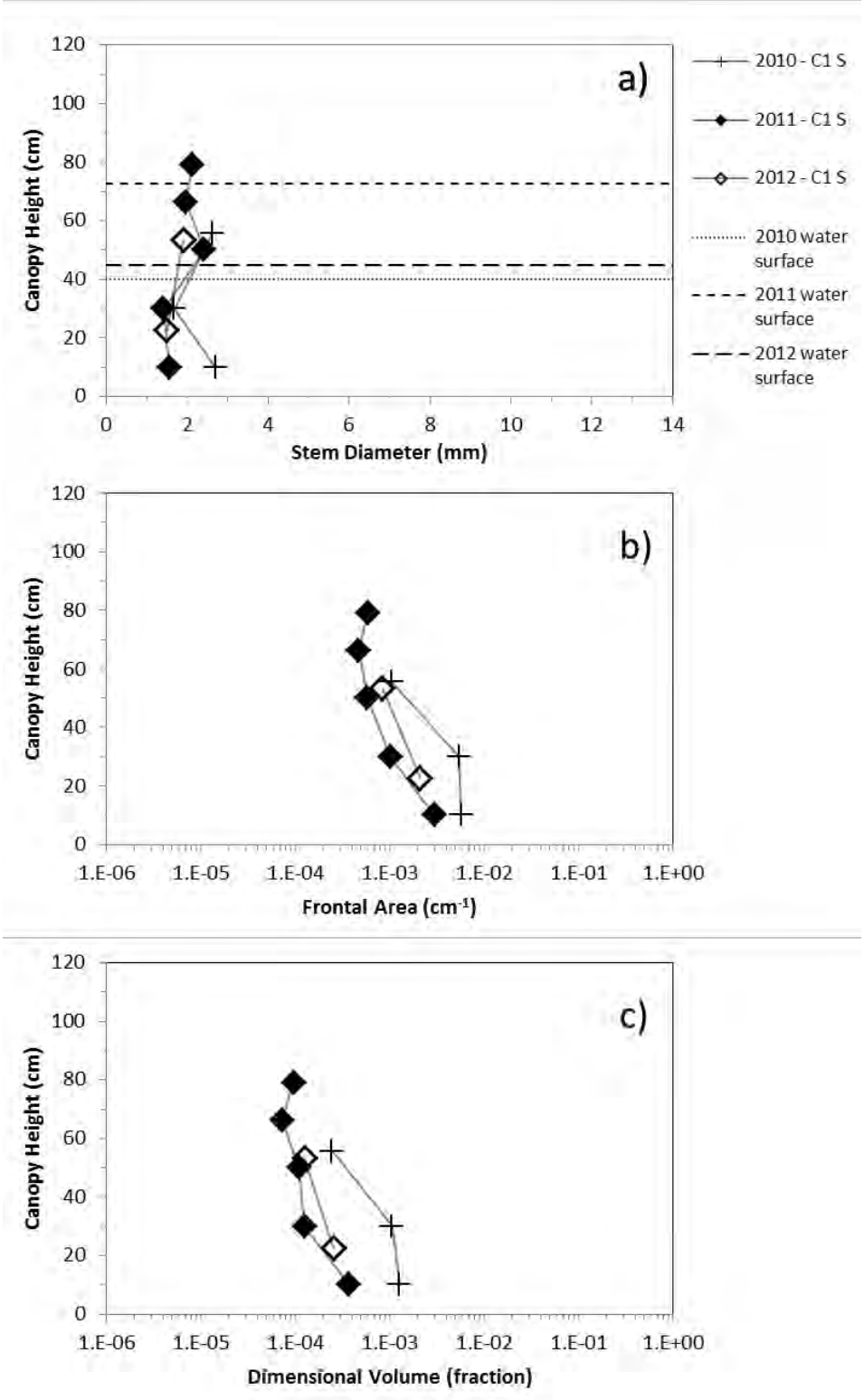

Figure F-3 Average vegetation stem diameter (a), frontal area (b), and dimensional volume (fraction of bulk volume) (c) at site RS1D Ridge. Samples collected on 11/09/2010, 11/1/2011, and 11/6/2012.

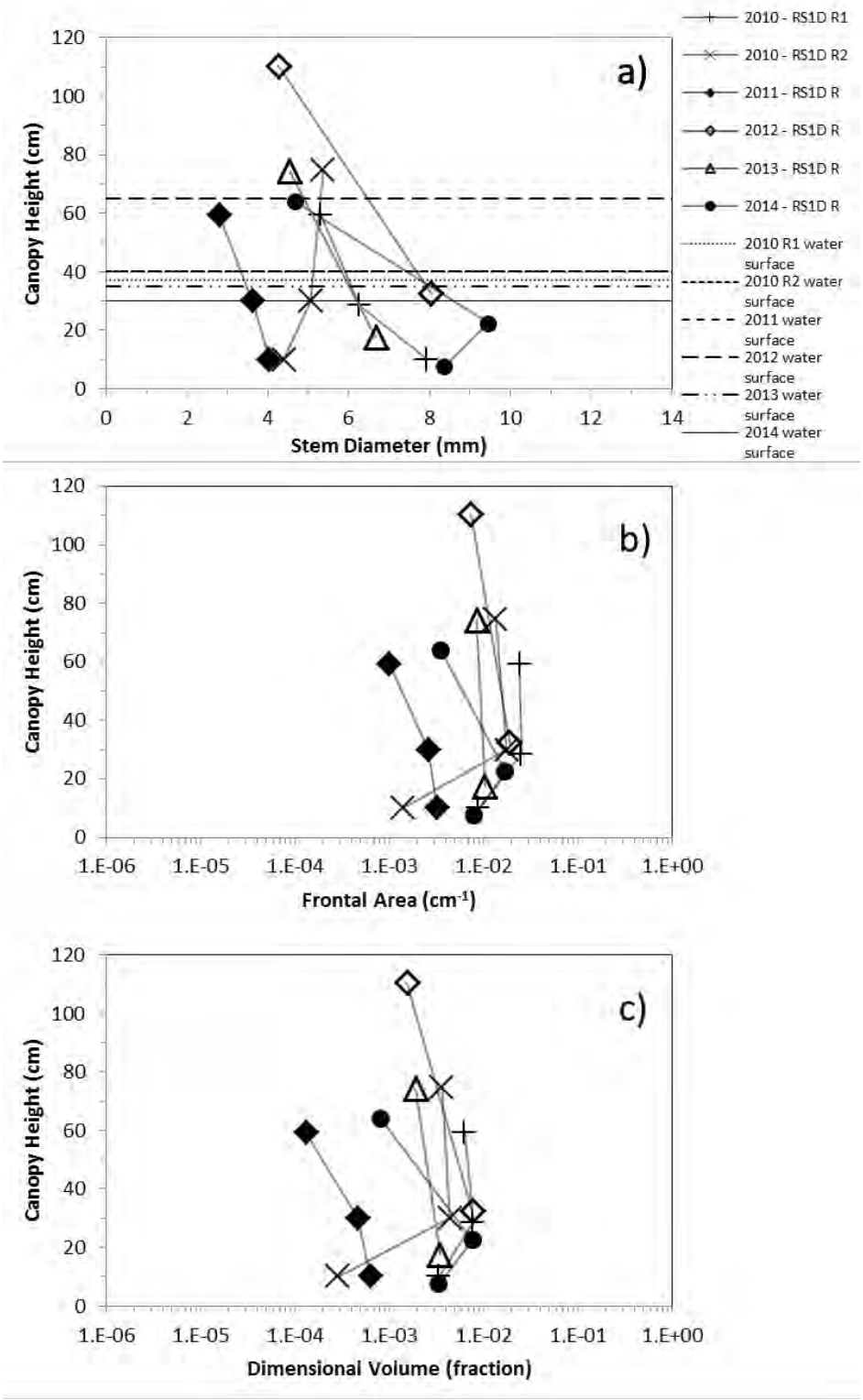

Figure F-4 Average vegetation stem diameter (a), frontal area (b), and dimensional volume (fraction of bulk volume) (c) at site RS1D Slough. Samples collected on 11/09/2010, 11/1/2011, 11/6/2012, 8/15/2013, and 8/15/2014.

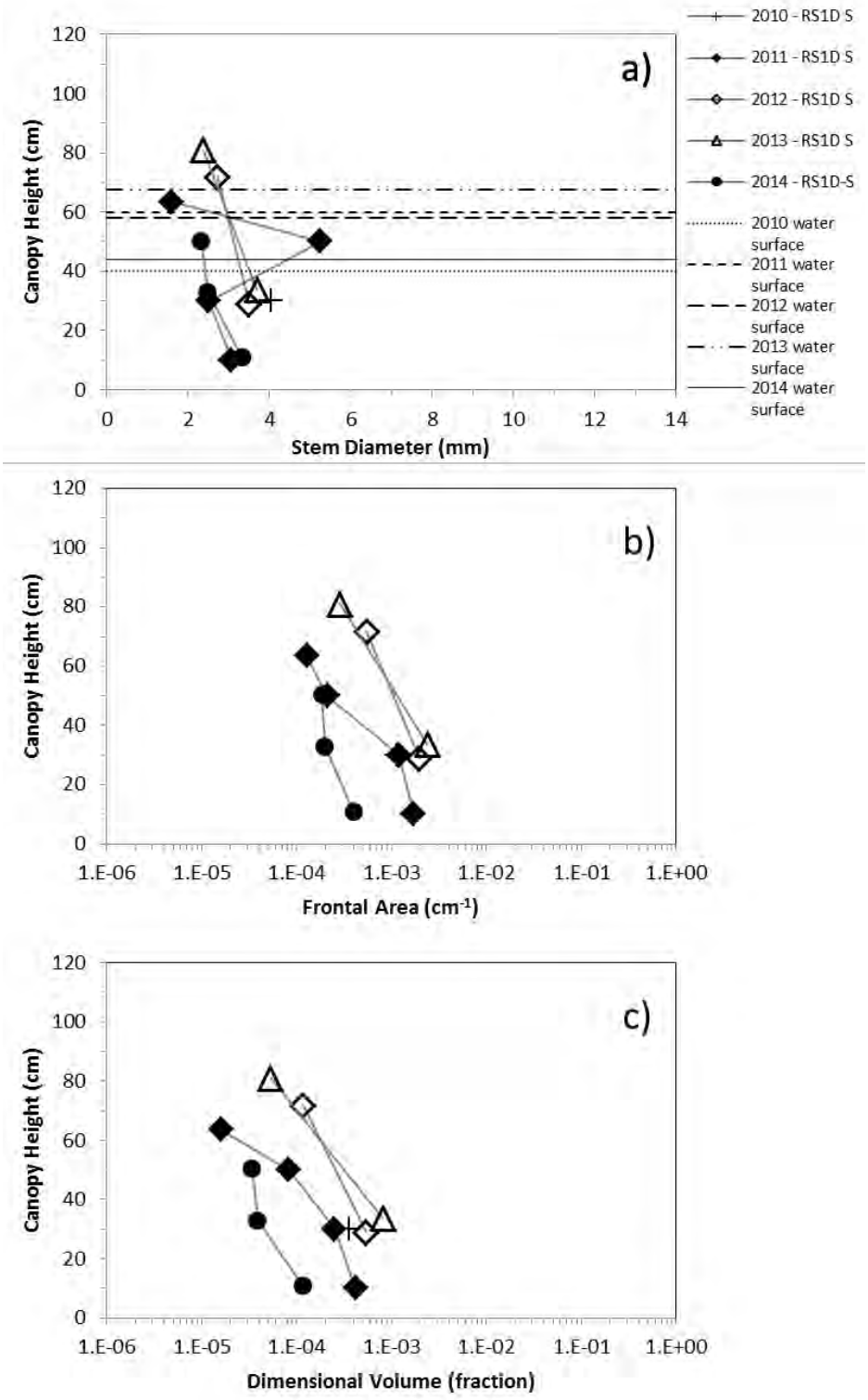

Figure F-5 Average vegetation stem diameter (a), frontal area (b), and dimensional volume (fraction of bulk volume) (c) at site RS1D Slough. Samples collected on 11/09/2010, 11/1/2011, 11/6/2012, 8/15/2013, and 8/15/2014.

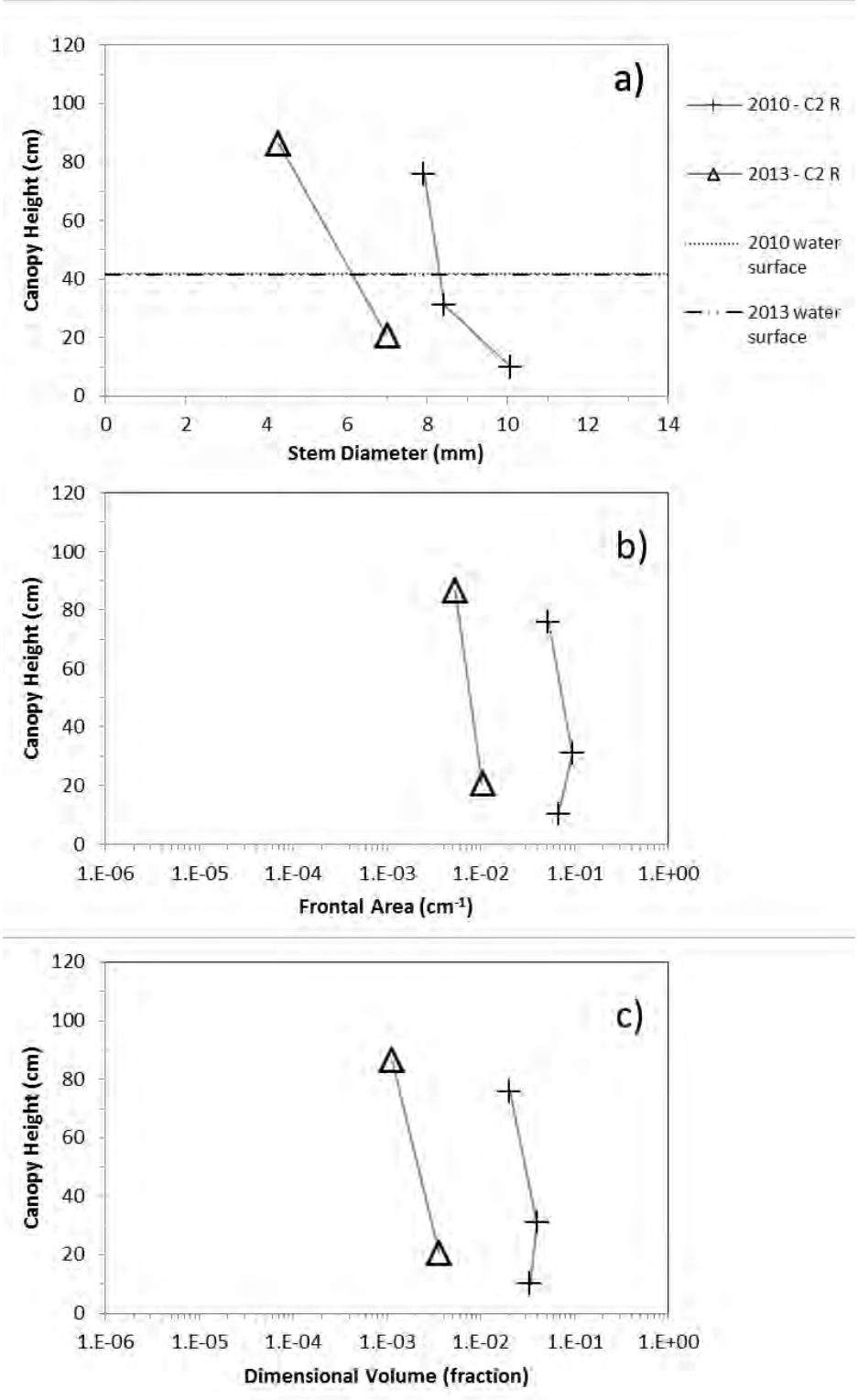

Figure F-6 Average vegetation stem diameter (a), frontal area (b), and dimensional volume (fraction of bulk volume) (c) at site C2 Ridge. Samples collected on 11/10/2010 and 8/15/2013.

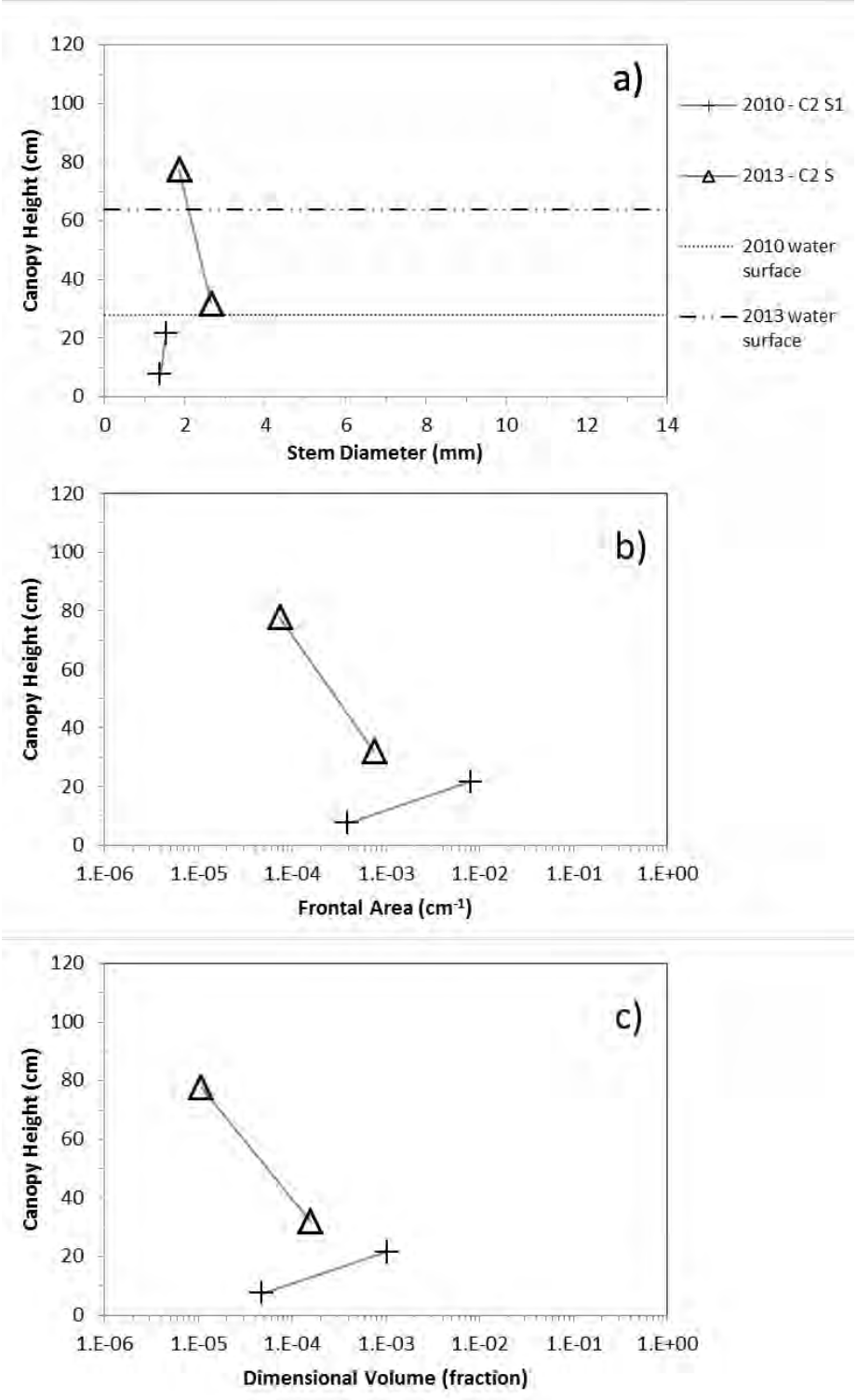

Figure F-7 Average vegetation stem diameter (a), frontal area (b), and dimensional volume (fraction of bulk volume) (c) at site C2 Slough 1. Samples collected on 11/10/2010 and 8/15/2013.

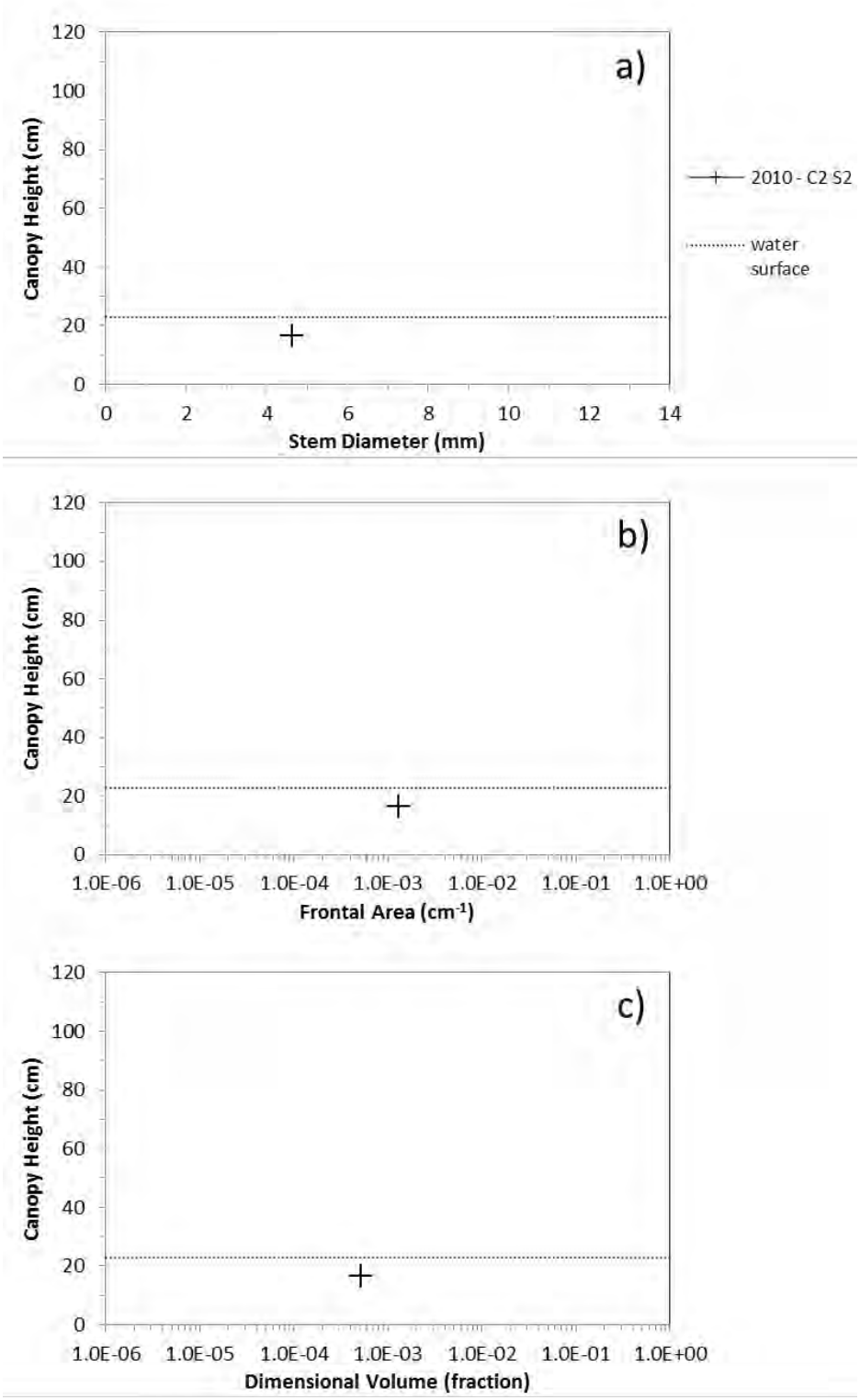

Figure F-8 Average vegetation stem diameter (a), frontal area (b), and dimensional volume (fraction of bulk volume) (c) at site C2 Slough 2. Samples collected on 11/10/2010.

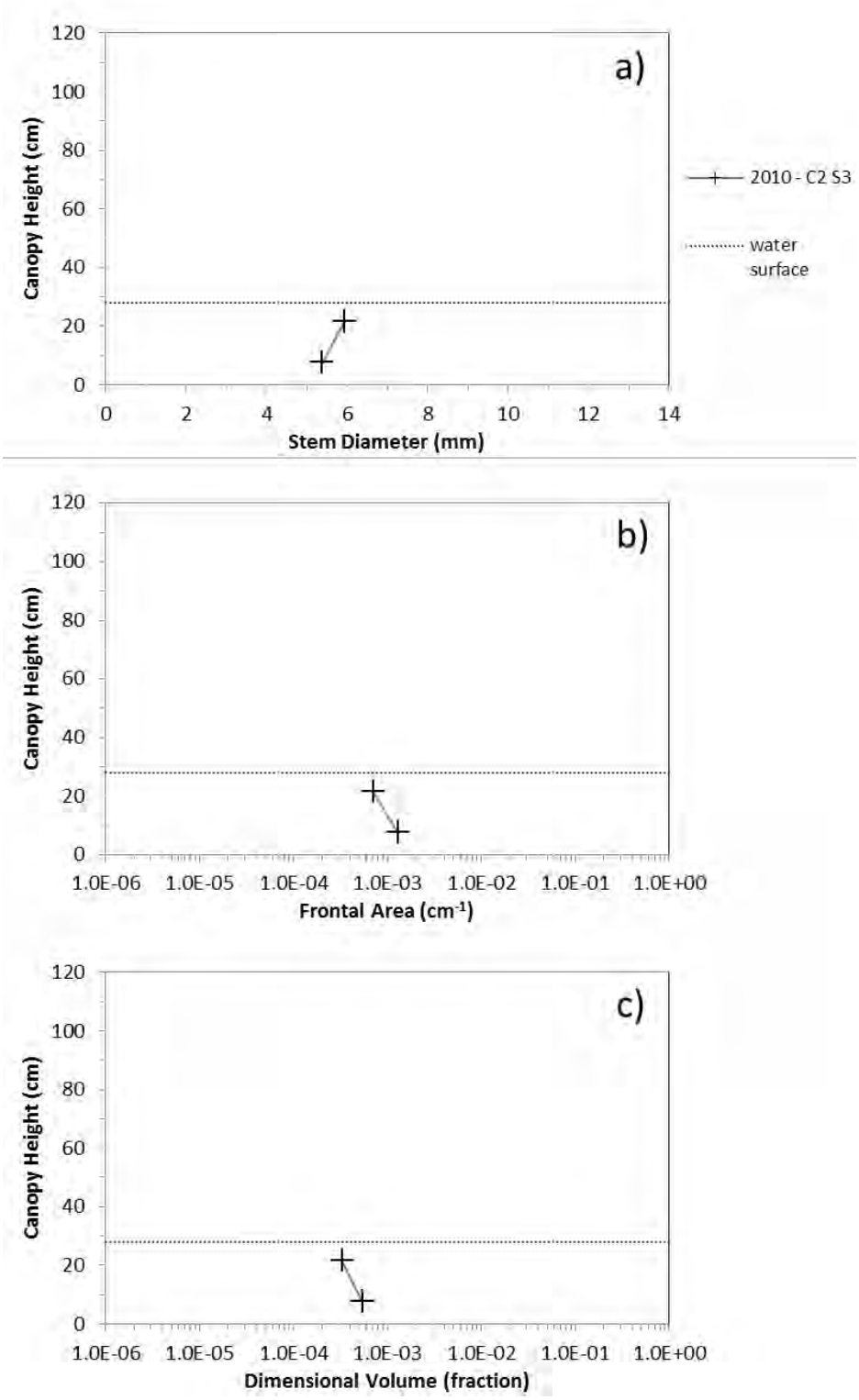

Figure F-9 Average vegetation stem diameter (a), frontal area (b), and dimensional volume (fraction of bulk volume) (c) at site C2 Slough 3. Samples collected on 11/10/2010.

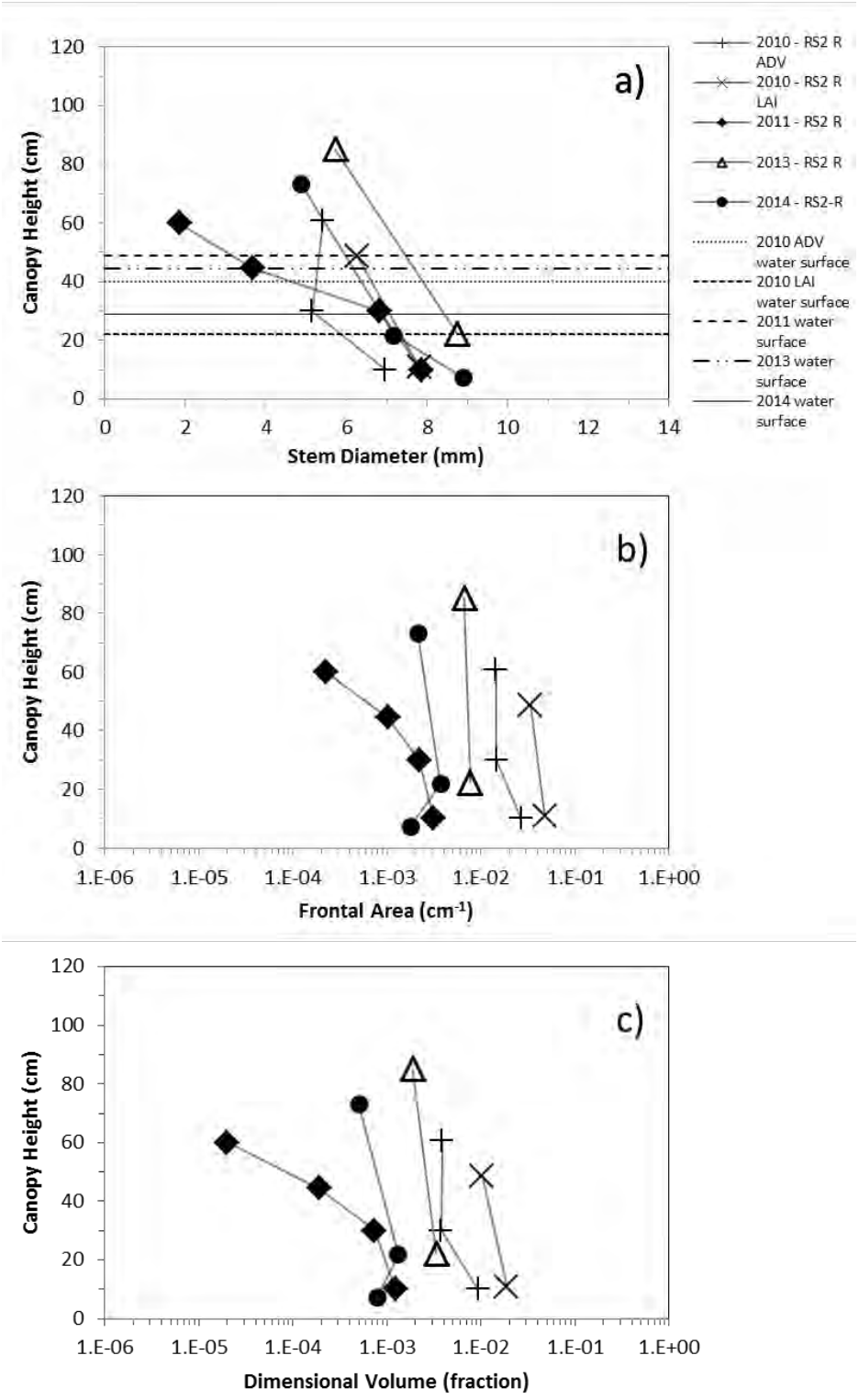

Figure F-10 Average vegetation stem diameter (a), frontal area (b), and dimensional volume (fraction of bulk volume) (c) at site RS2 Ridge. Samples collected on 9/28/2010(ADV), 11022010(LAI), 11/2/2011, 8/15/2013, 8/15/2014.

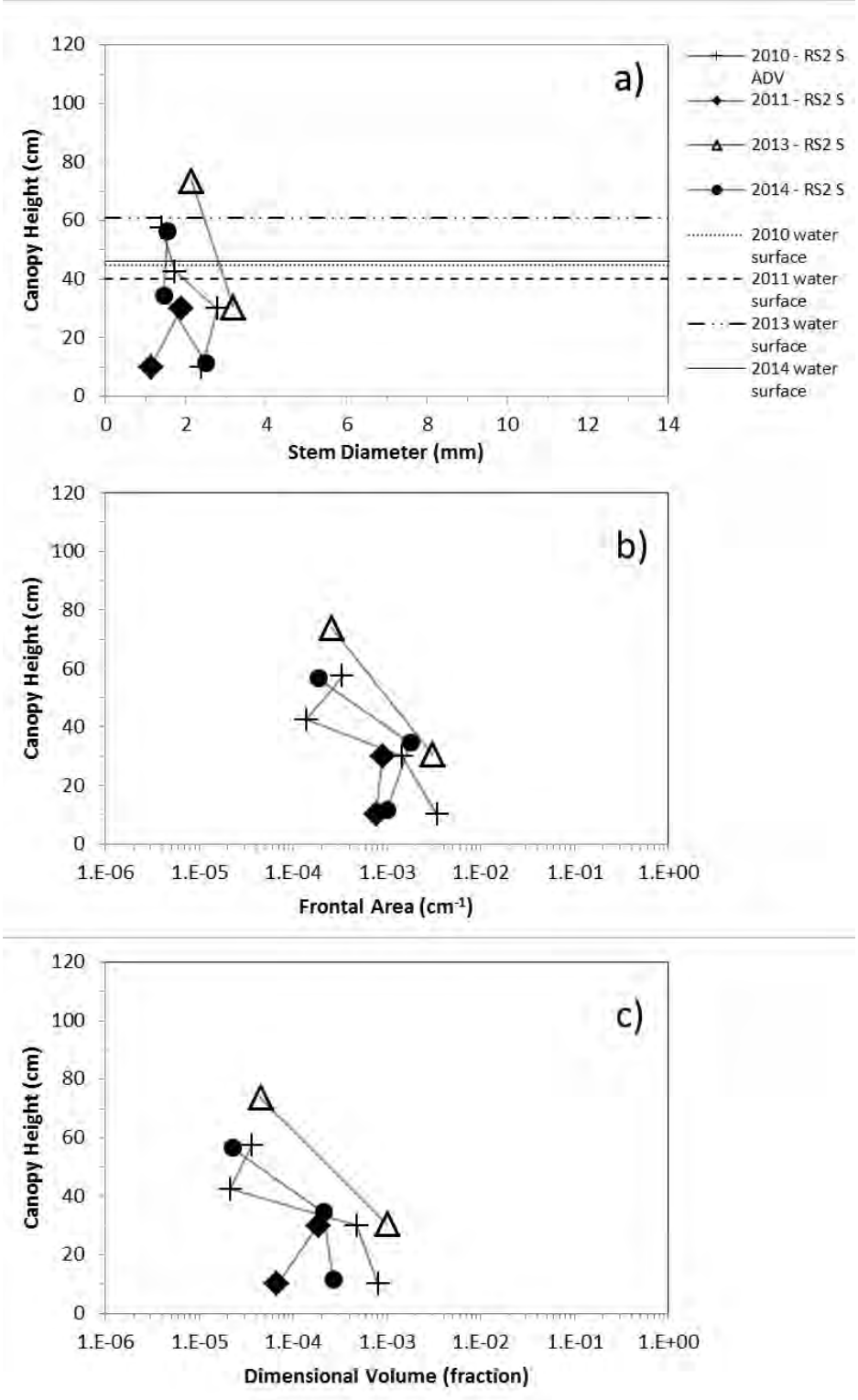

Figure F-11 Average vegetation stem diameter (a), frontal area (b), and dimensional volume (fraction of bulk volume) (c) at site RS2 Slough. Samples collected on 9/28/2010, 11/2/2011, 8/15/2013, 8/15/2014.

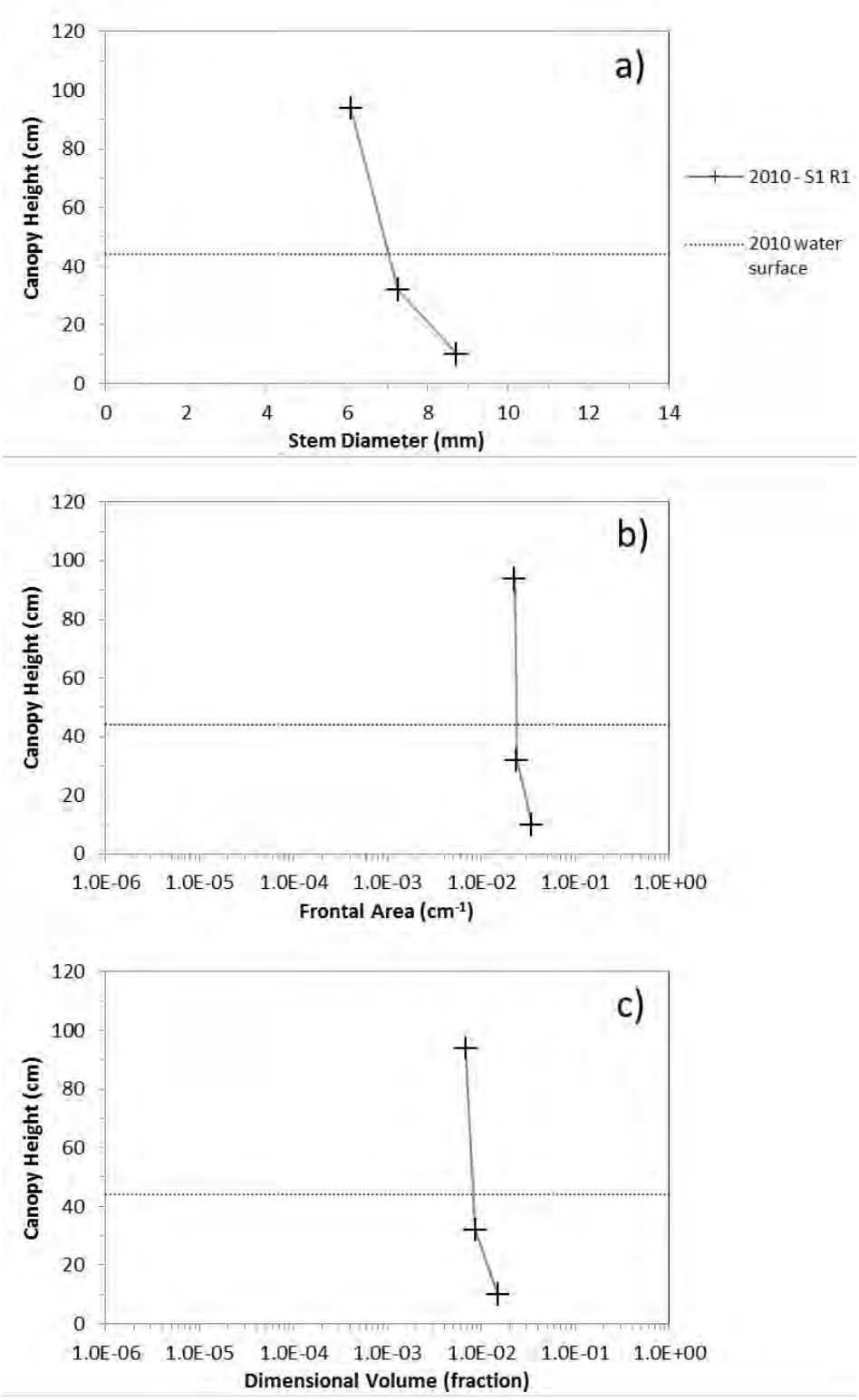

Figure F-12 Average vegetation stem diameter (a), frontal area (b), and dimensional volume (fraction of bulk volume) (c) at site S1 Ridge 1. Samples collected on 11/5/2010.

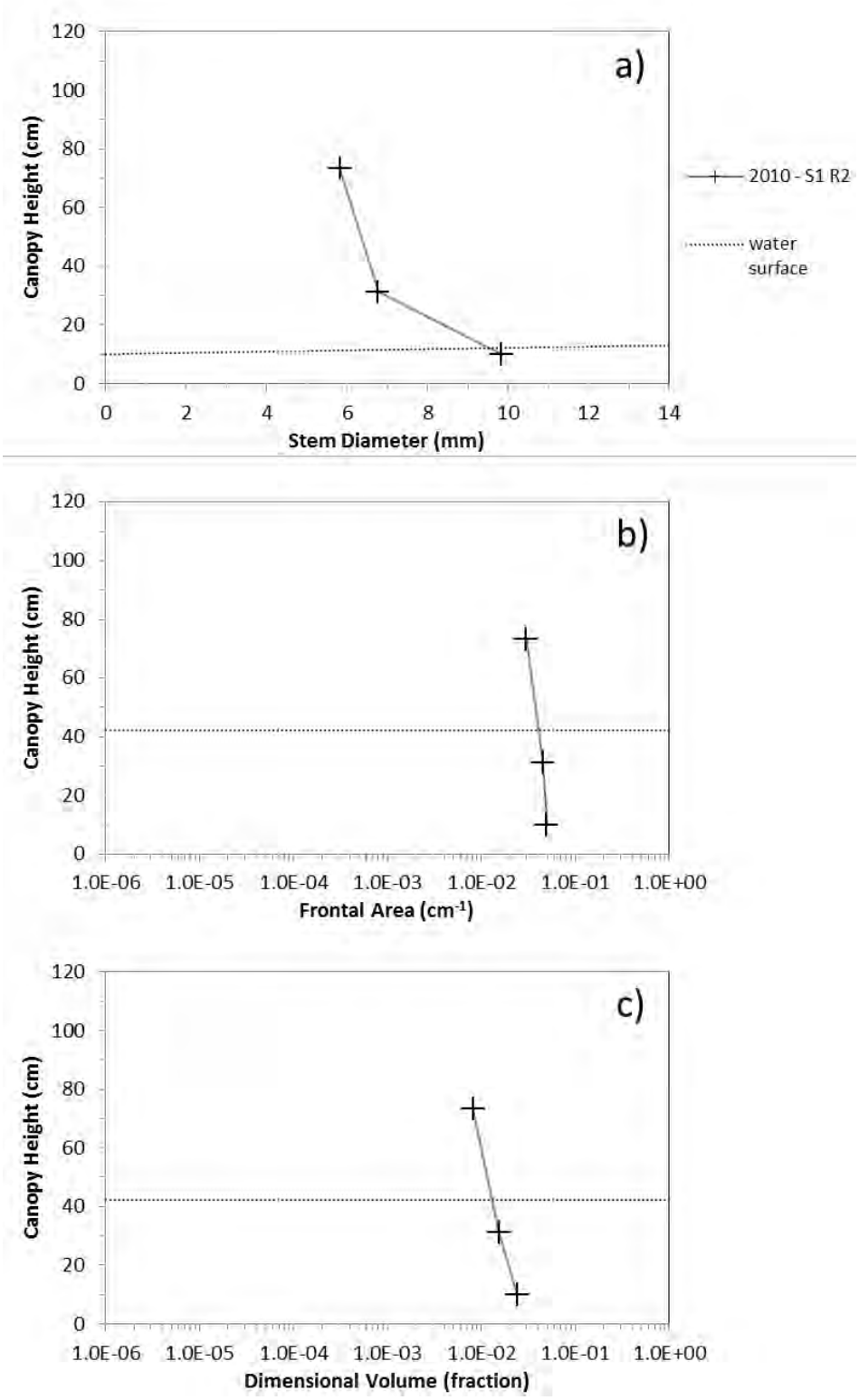

Figure F-13 Average vegetation stem diameter (a), frontal area (b), and dimensional volume (fraction of bulk volume) (c) at site S1 Ridge 2. Samples collected on 11/5/2010.

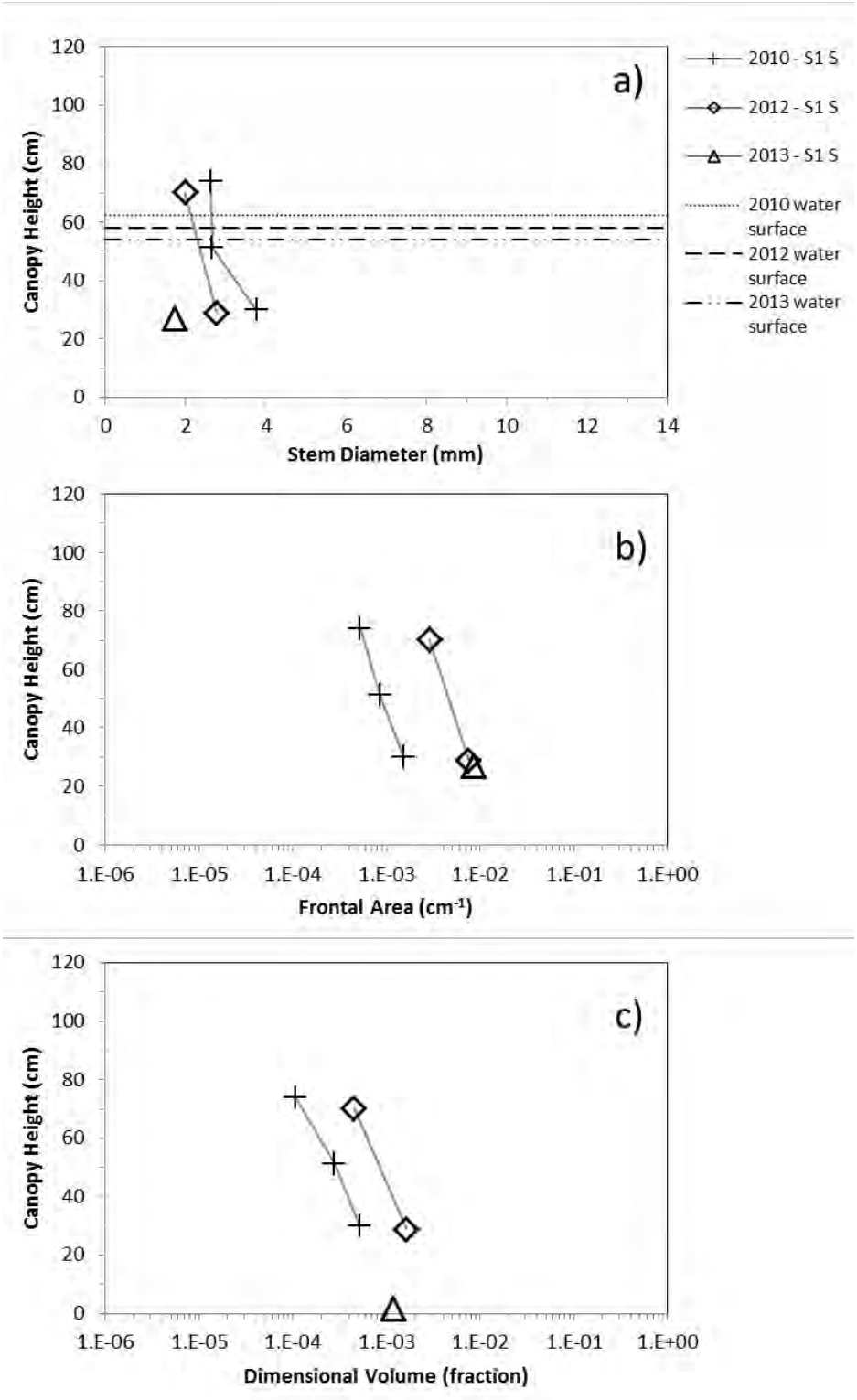

Figure F-14 Average vegetation stem diameter (a), frontal area (b), and dimensional volume (fraction of bulk volume) (c) at site S1 Slough. Samples collected on 11/5/2010, 11/6/2011, and 8/15/2013.

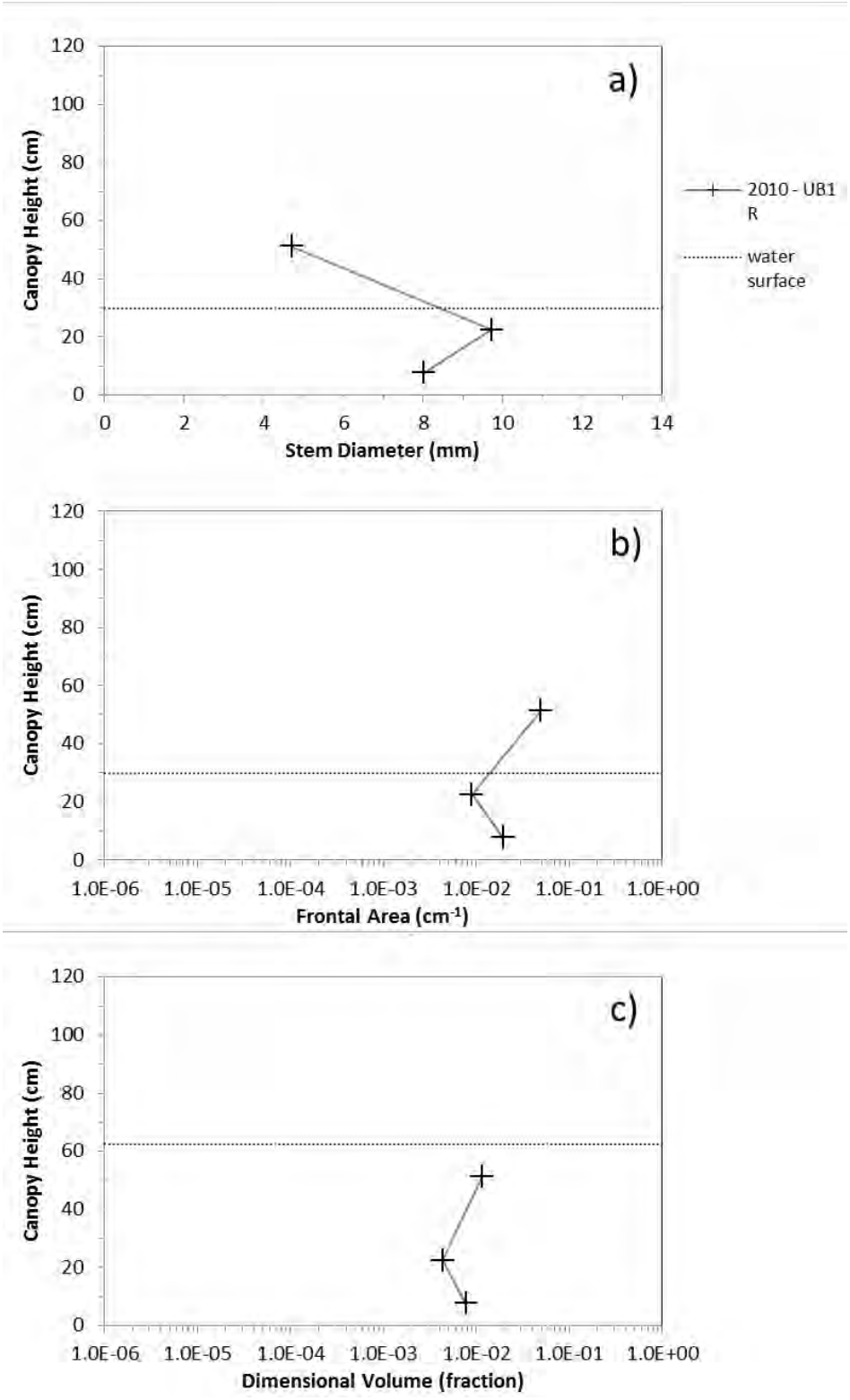

Figure F-15 Average vegetation stem diameter (a), frontal area (b), and dimensional volume (fraction of bulk volume) (c) at site UB1 Ridge. Samples collected on 11/3/2010.

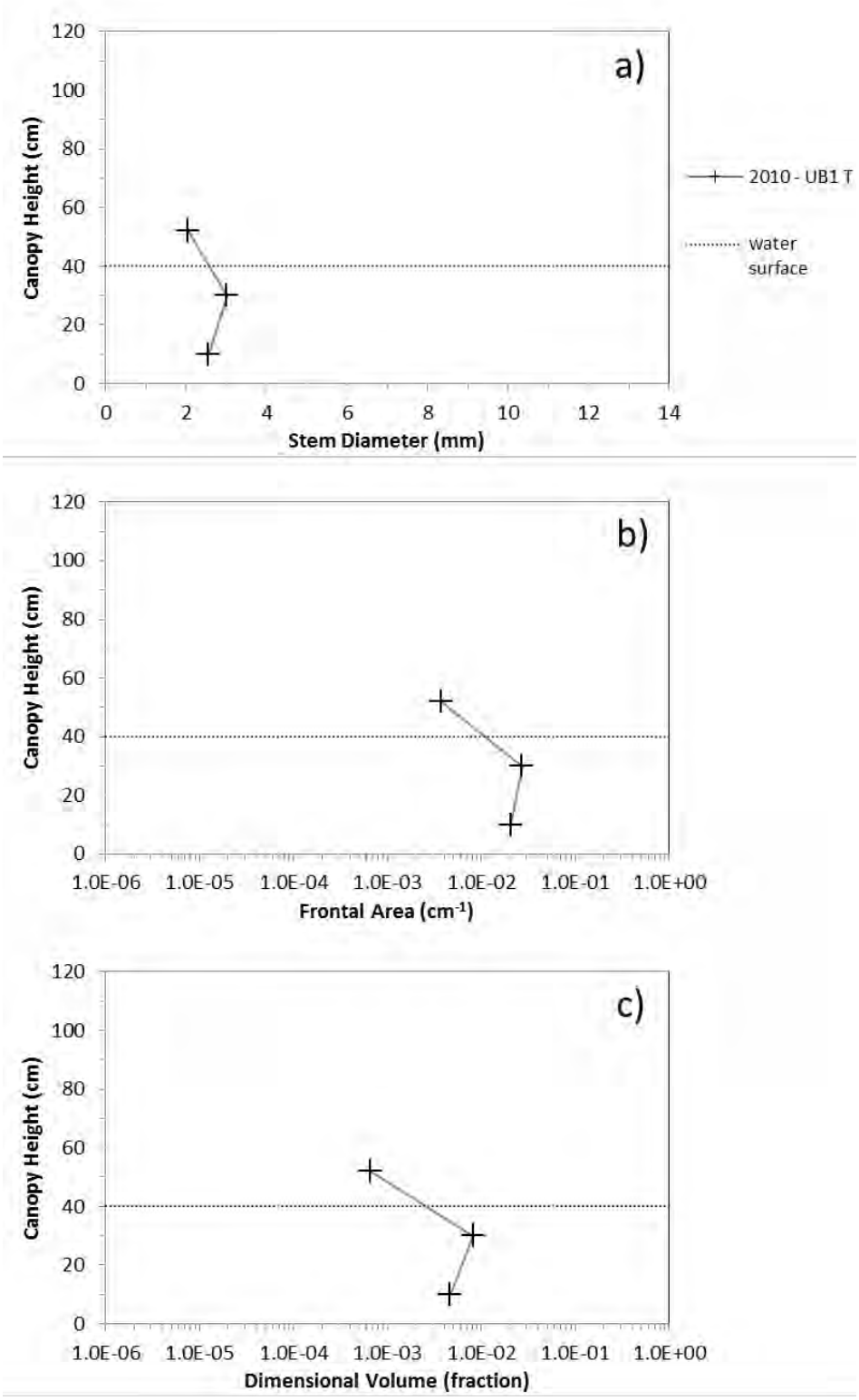

Figure F-16 Average vegetation stem diameter (a), frontal area (b), and dimensional volume (fraction of bulk volume) (c) at site UB1 Transition. Samples collected on 11/3/2010.

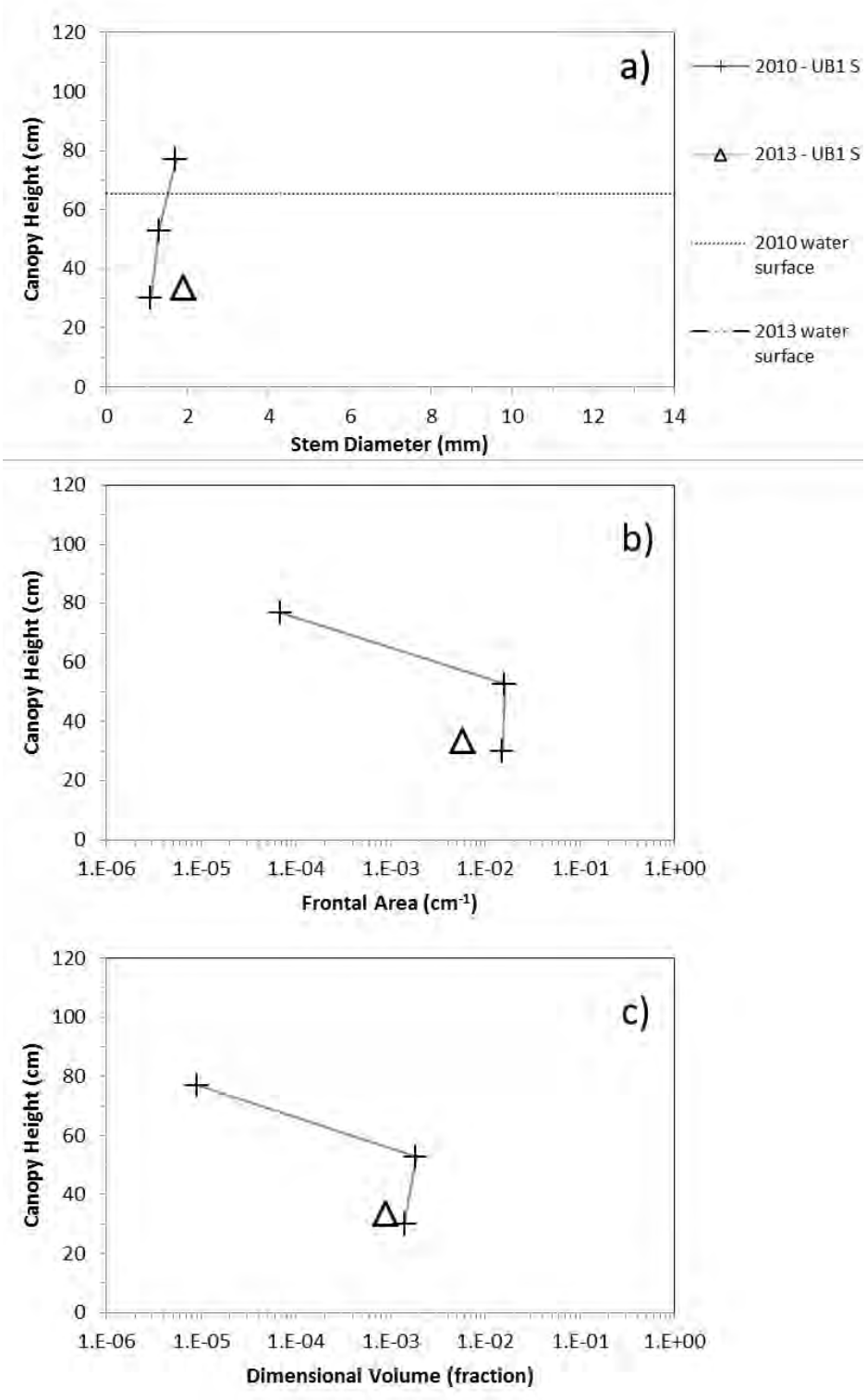

Figure F-17 Average vegetation stem diameter (a), frontal area (b), and dimensional volume (fraction of bulk volume) (c) at site UB1 Slough. Samples collected on 11/3/2010 and 8/15/2013.

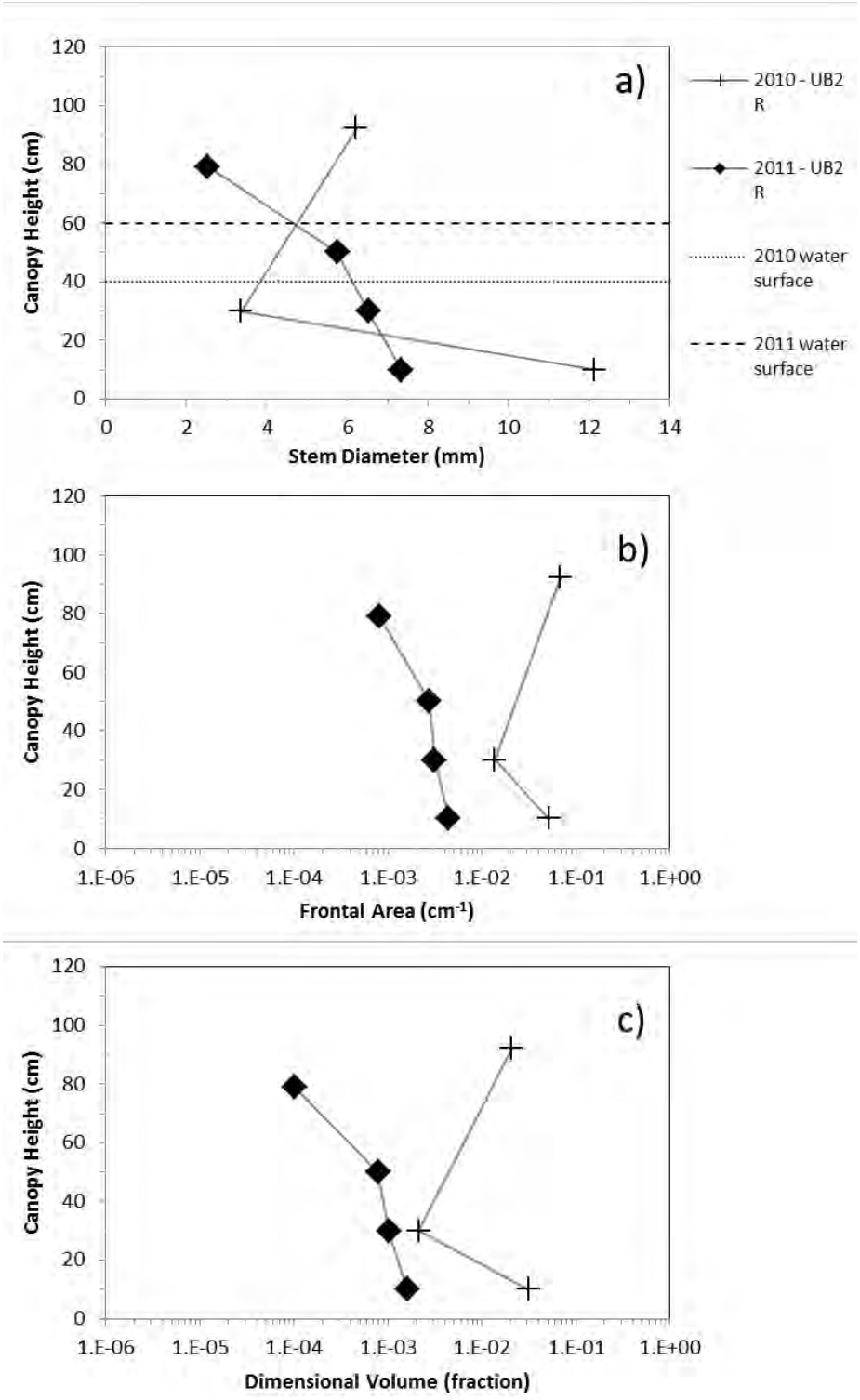

Figure F-18 Average vegetation stem diameter (a), frontal area (b), and dimensional volume (fraction of bulk volume) (c) at site UB2 Ridge. Samples collected on 11/8/2010 and 11/2/2011.

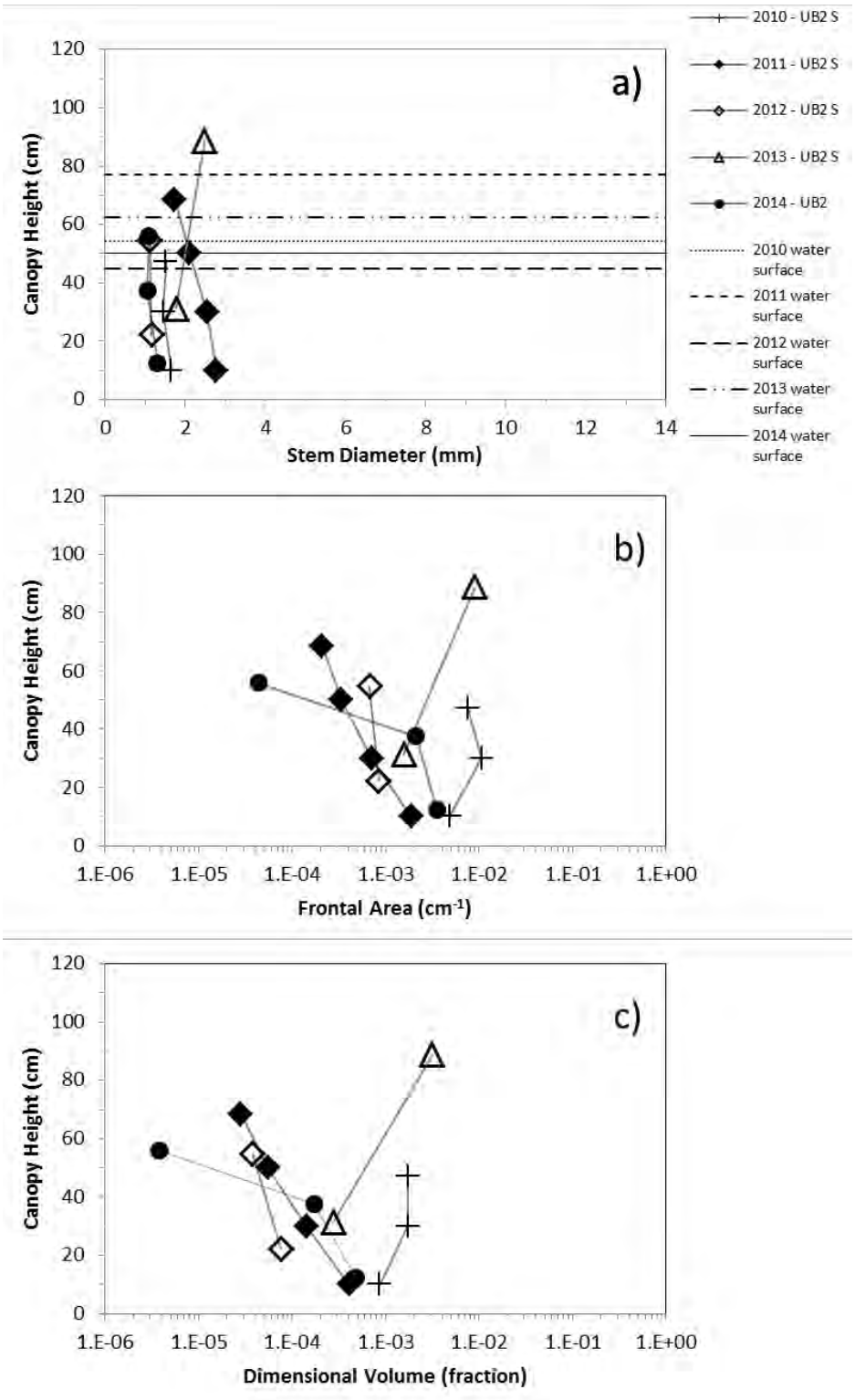

Figure F-19 Average vegetation stem diameter (a), frontal area (b), and dimensional volume (fraction of bulk volume) (c) at site UB2 Slough. Samples collected on 11/8/2010, 11/2/2011, 11/6/2012 8/15/2013, and 8/15/2014.

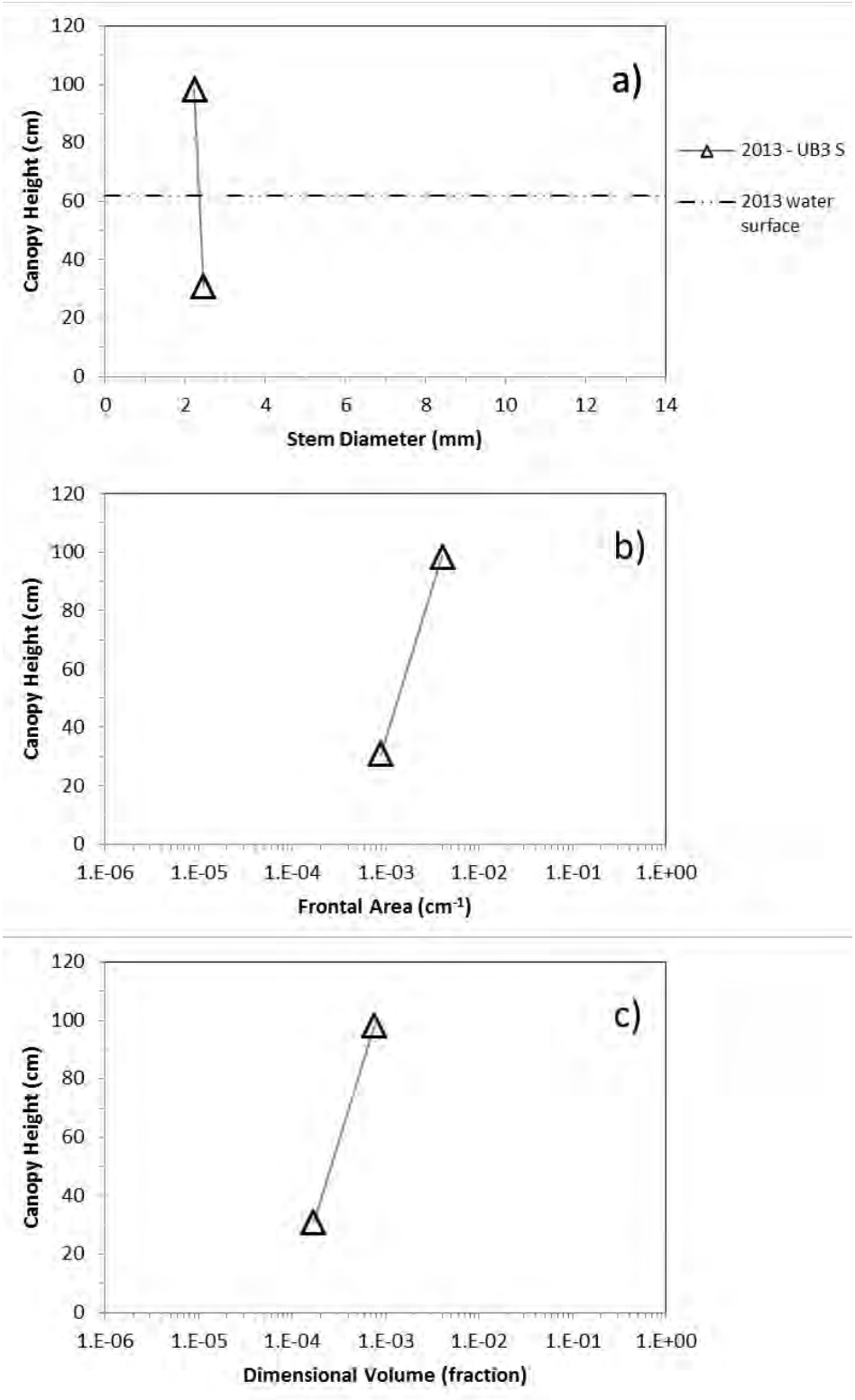

Figure F-20 Average vegetation stem diameter (a), frontal area (b), and dimensional volume (fraction of bulk volume) (c) at site UB3 Slough. Samples collected on 8/15/2013.

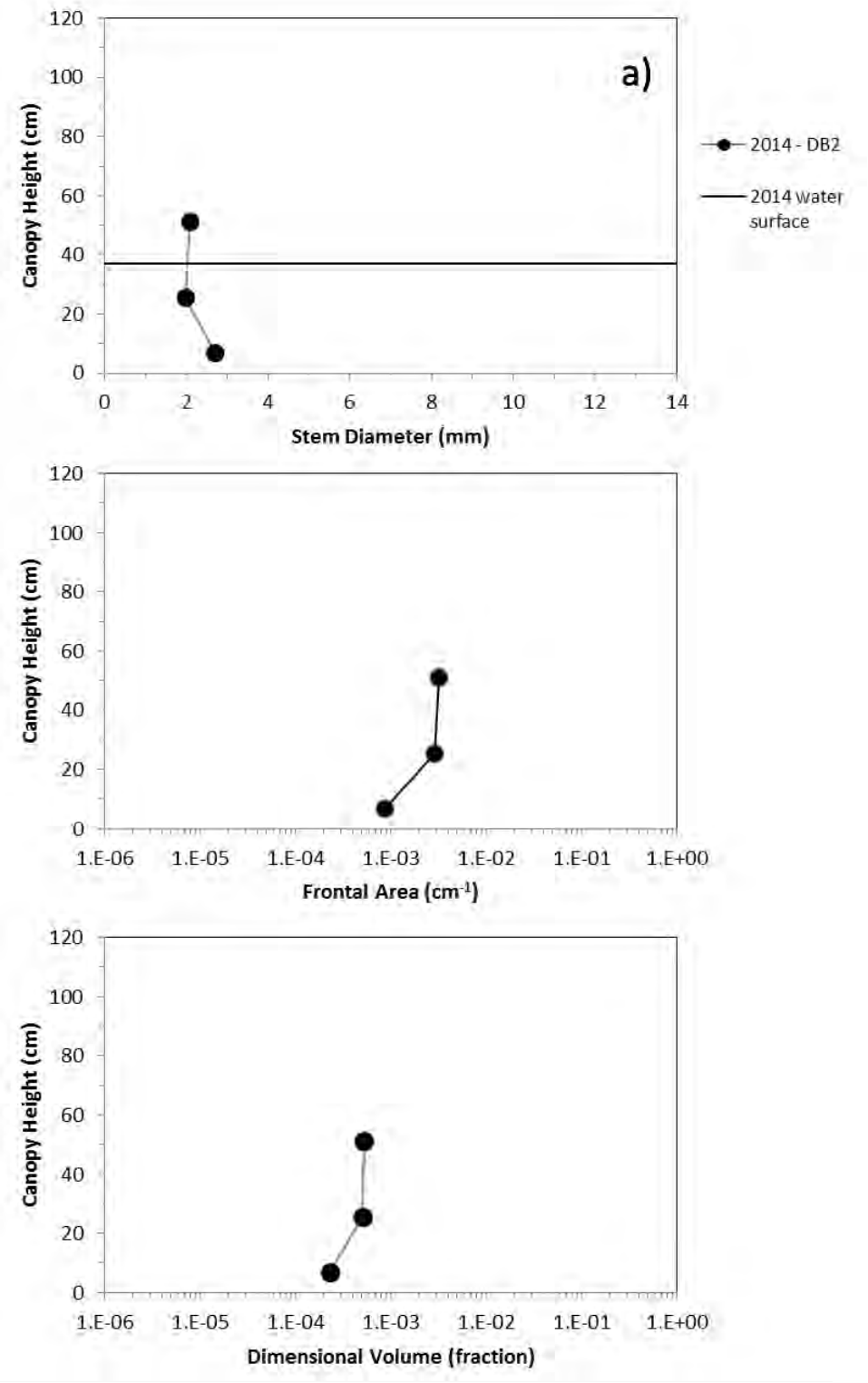

Figure F-21 Average vegetation stem diameter (a), frontal area (b), and dimensional volume (fraction of bulk volume) (c) at site DB2 Slough. Samples collected on 8/15/2014.

G. Water Quality Monitoring

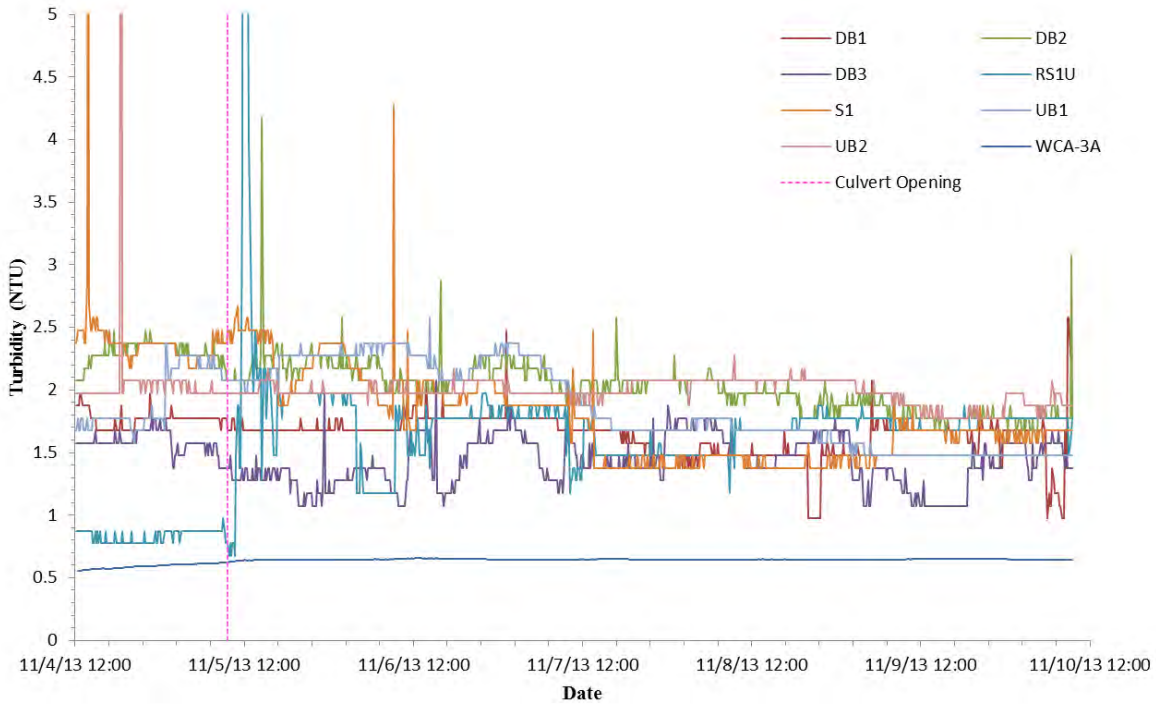

Figure G-1 Time Series of turbidity for all sites during the flow release, November 4-10, 2013.

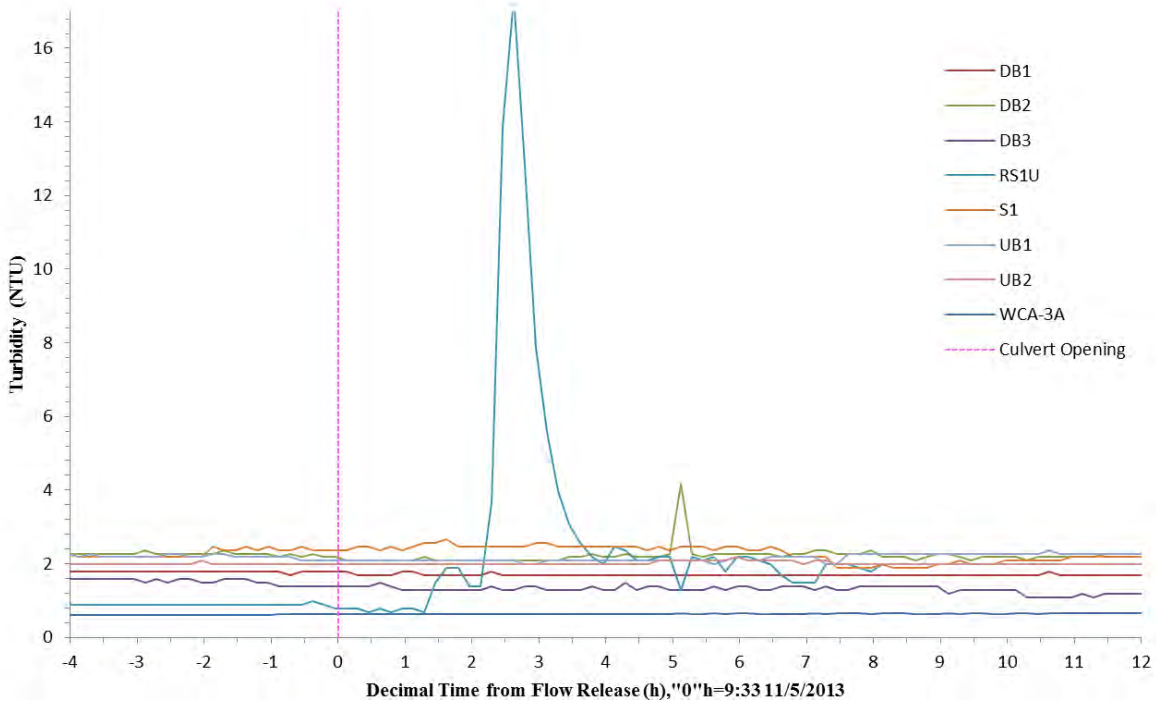

Figure G-2 Time Series of turbidity for all sites during the flow release day, November 5, 2013.

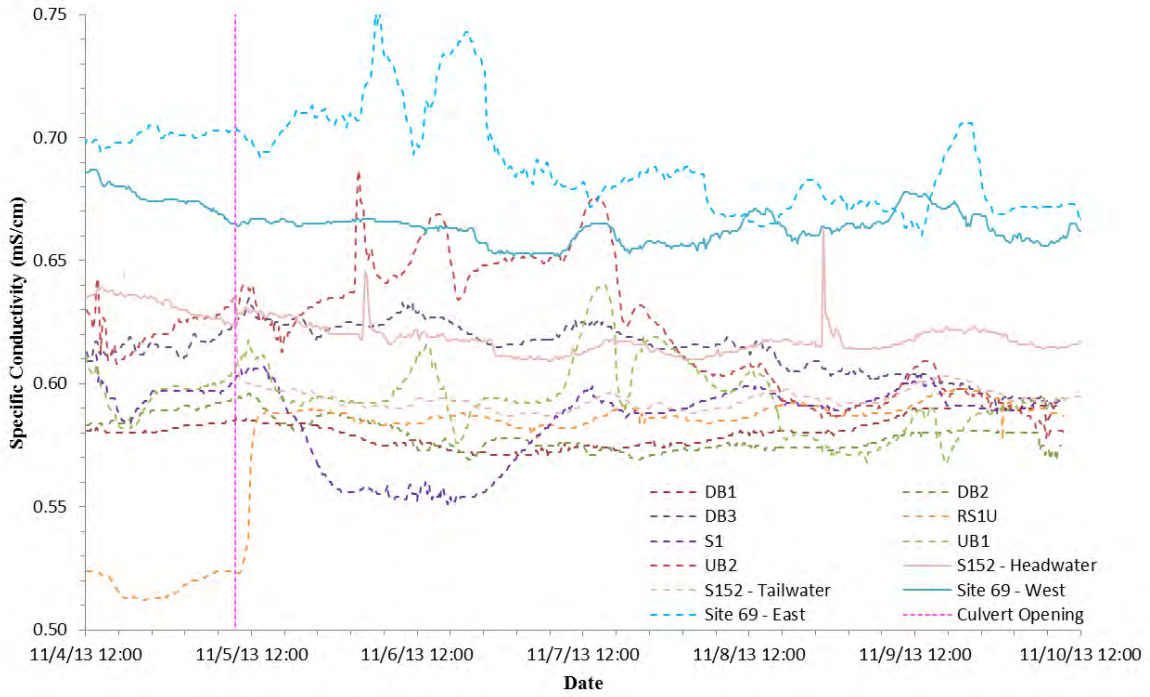

Figure G-3 Time Series of drift-corrected specific conductivity for all sites during the flow release, November 4-10, 2013.

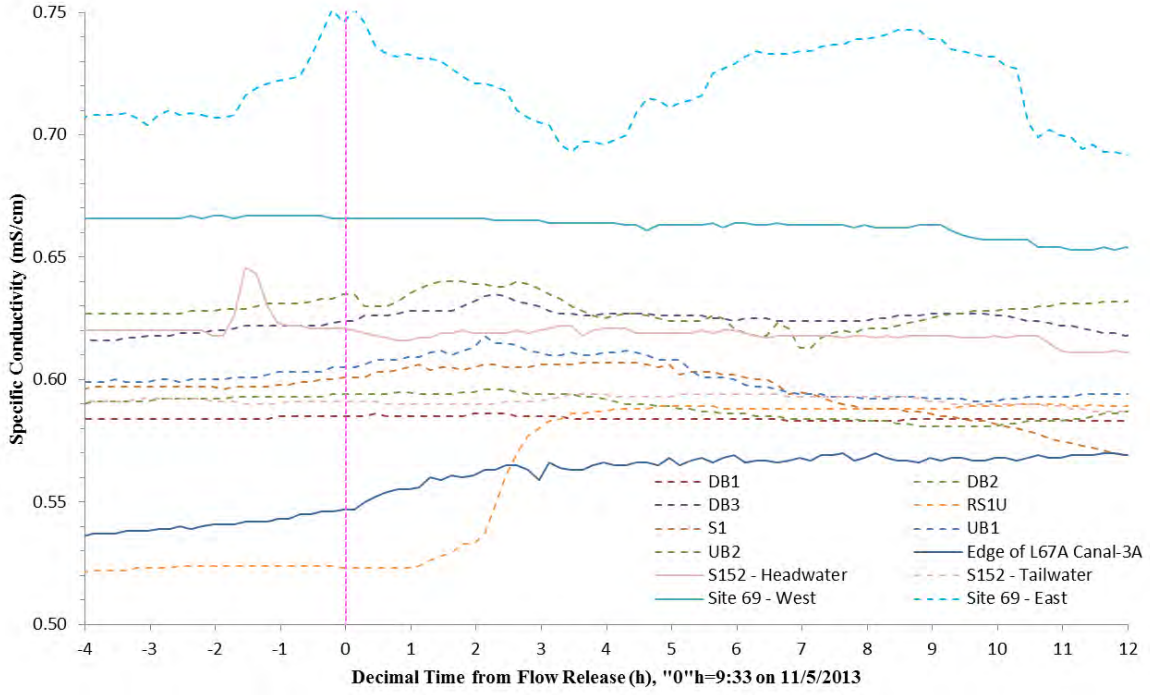

Figure G-4 Time Series of drift-corrected specific conductivity for all sites during the flow release day, November 5, 2013.

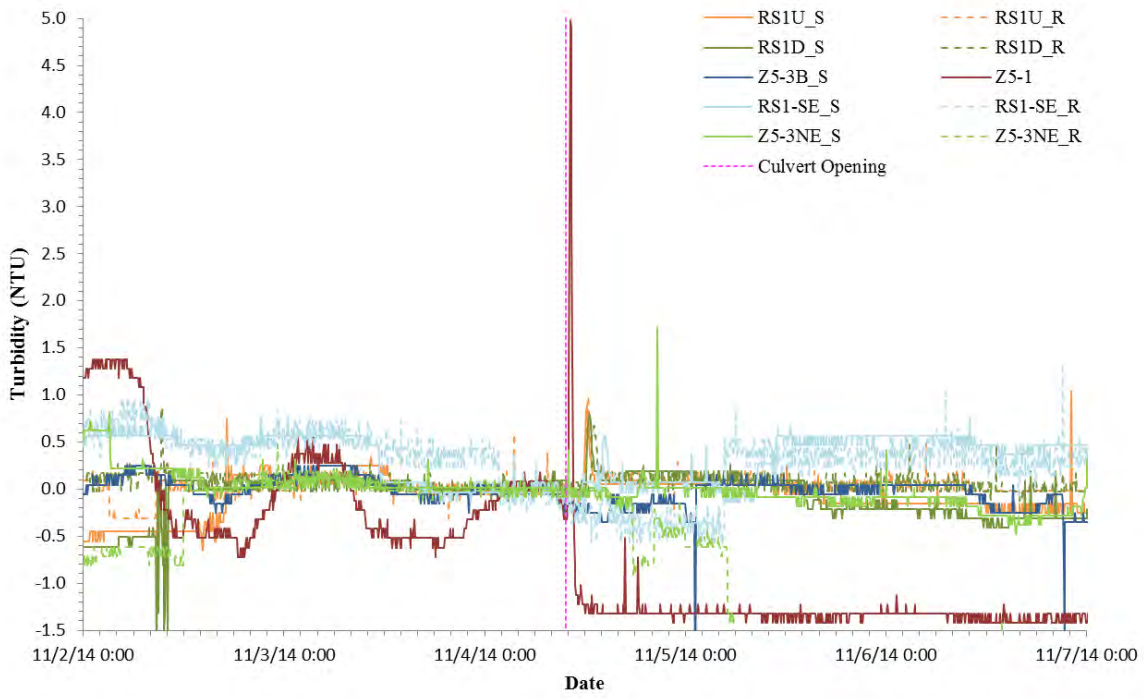

Figure G-5 Time Series of turbidity for all sites during the flow release, November 2-7, 2014.

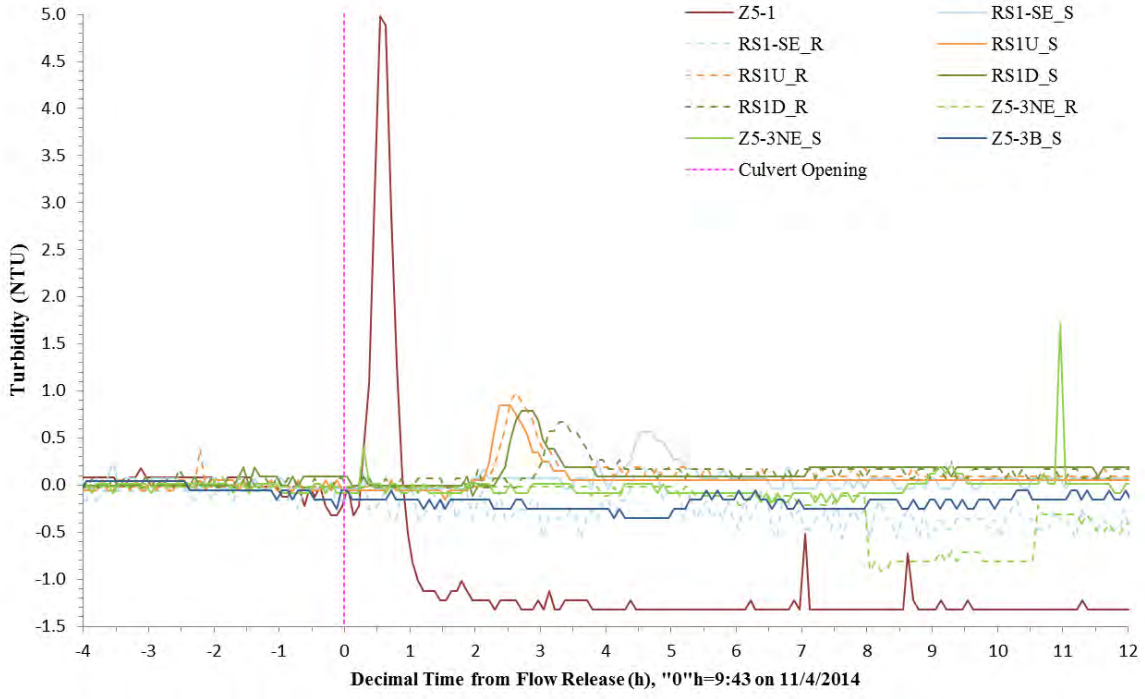

Figure G-6 Time Series of turbidity for all sites during the flow release day, November 4, 2014.

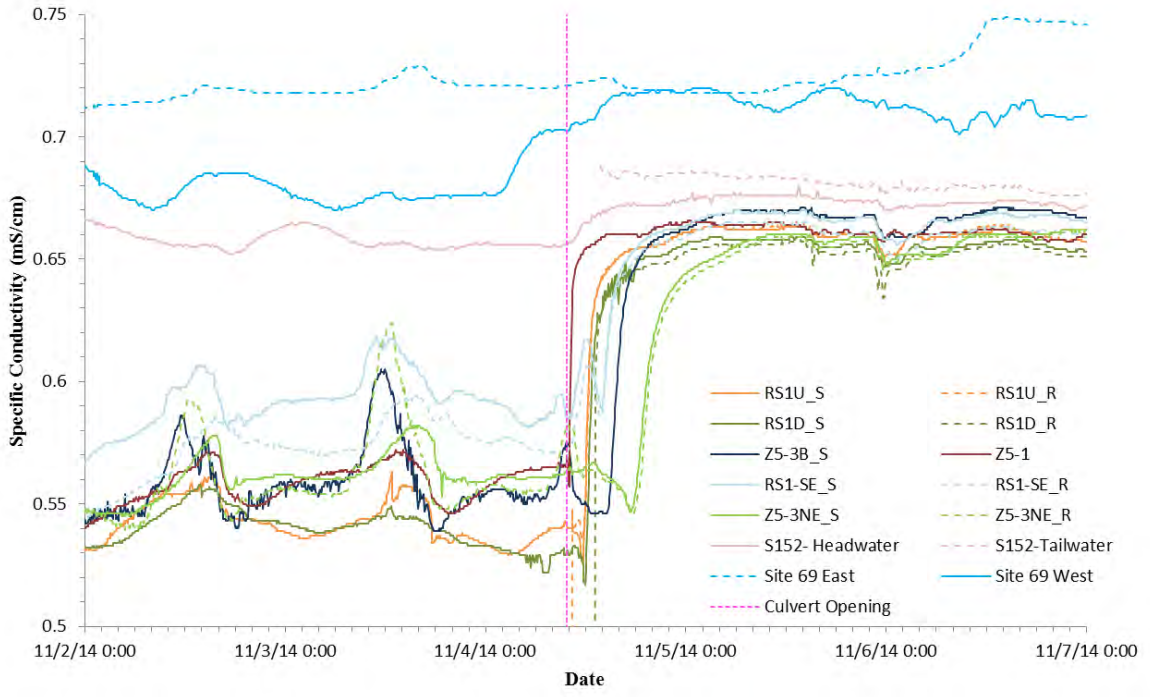

Figure G-7 Time Series of drift-corrected specific conductivity for all sites during the flow release, November 2-7, 2014.

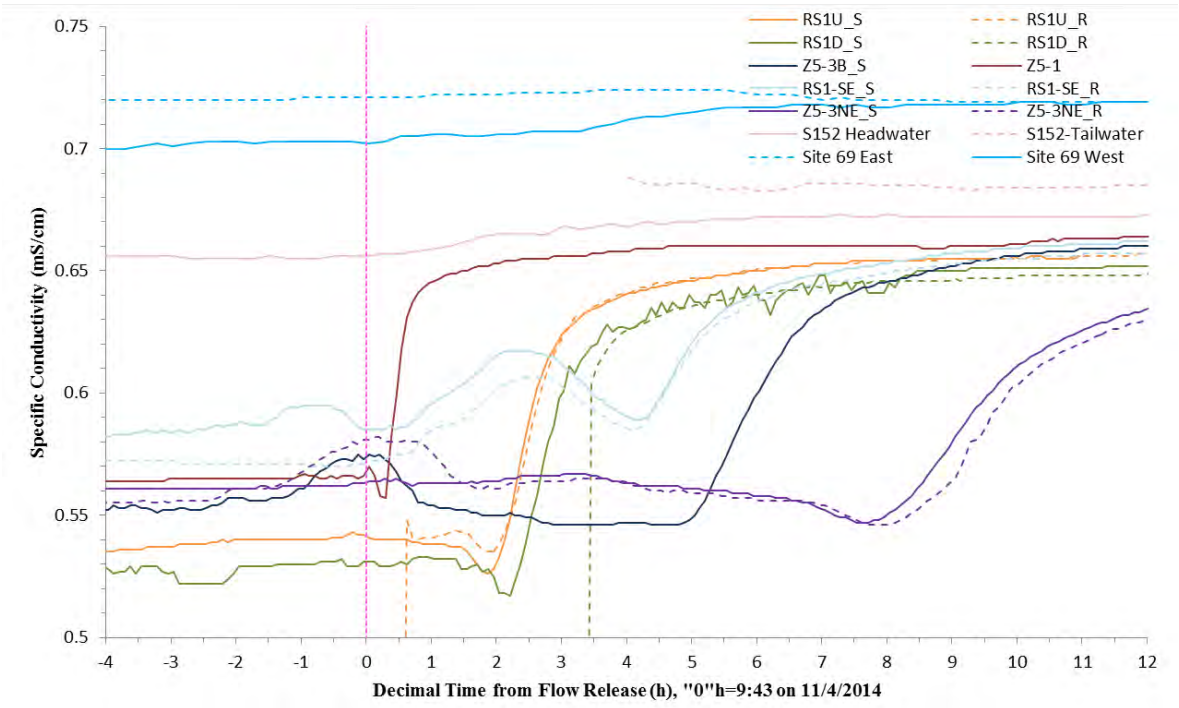

Figure G-8 Time Series of drift-corrected specific conductivity for all sites during the flow release day, November 4, 2014.

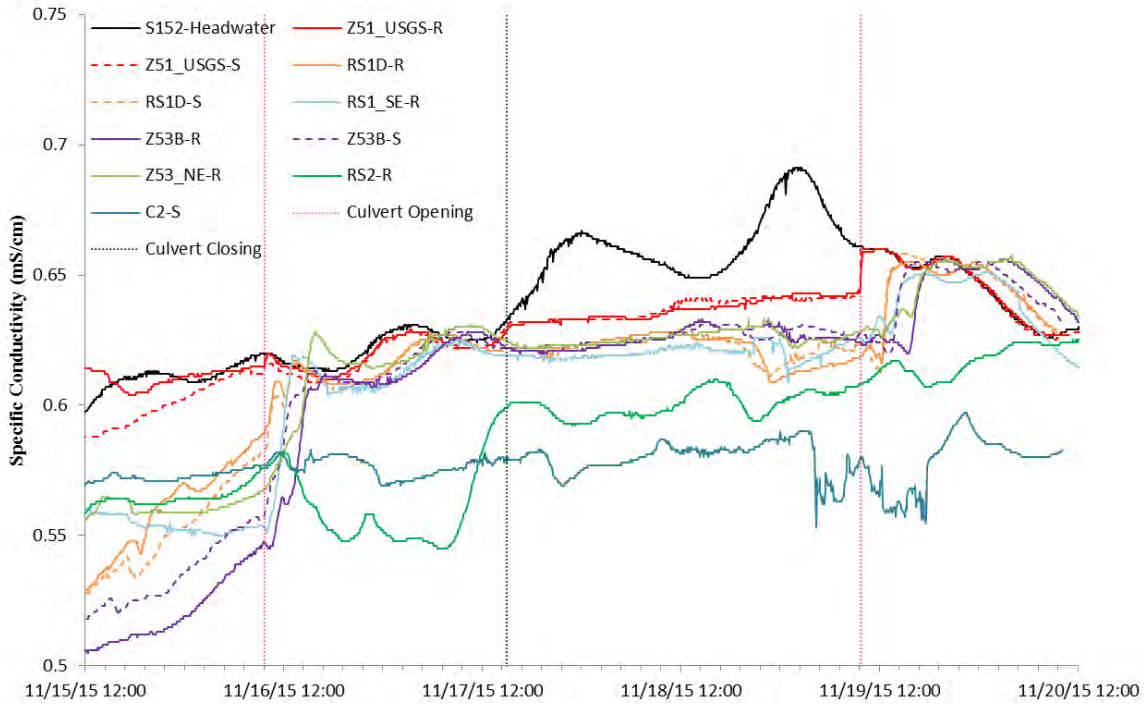

Figure G-9 Time Series of drift-corrected specific conductivity for all sites during the flow release, November 15-20, 2015.

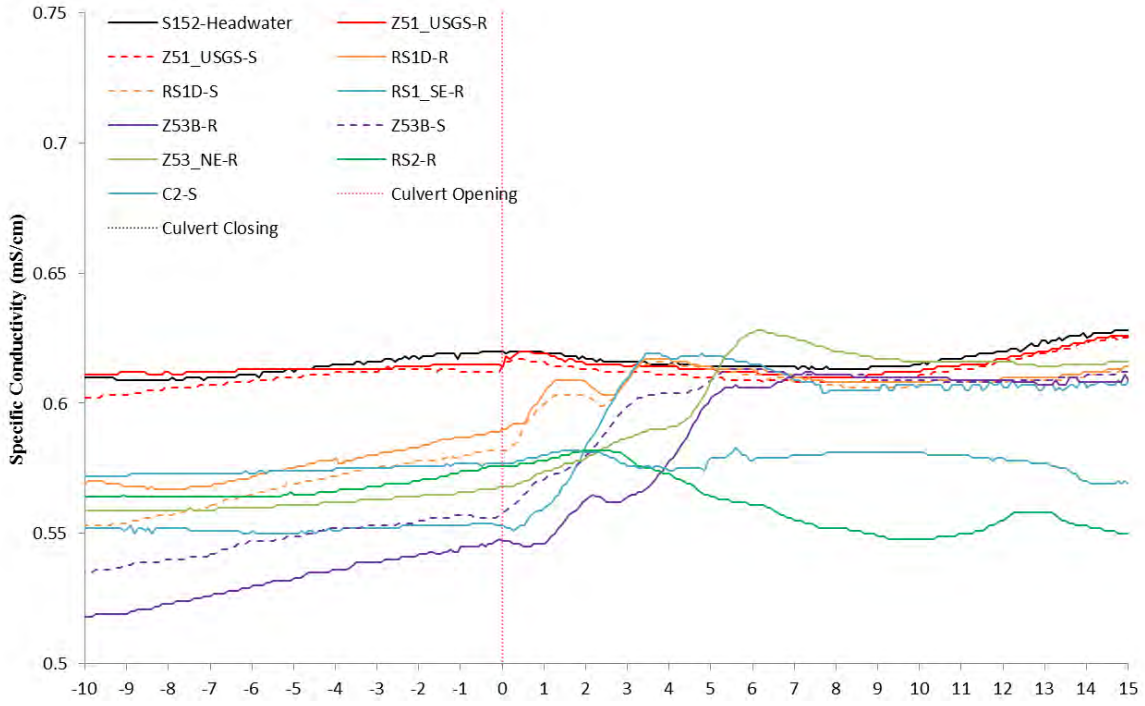

Figure G-10 Time Series of drift-corrected specific conductivity for all sites during the flow release day, November 16, 2015.

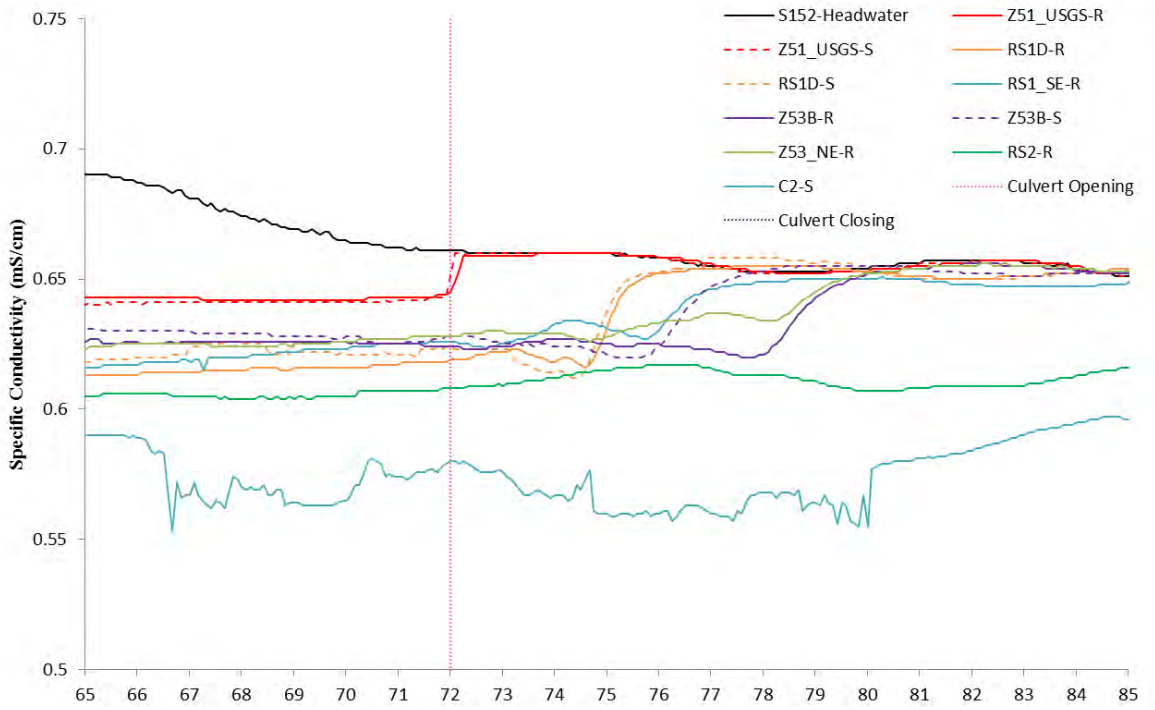

Figure G-11 Time Series of drift-corrected specific conductivity for all sites during the flow release day, November 19, 2015.

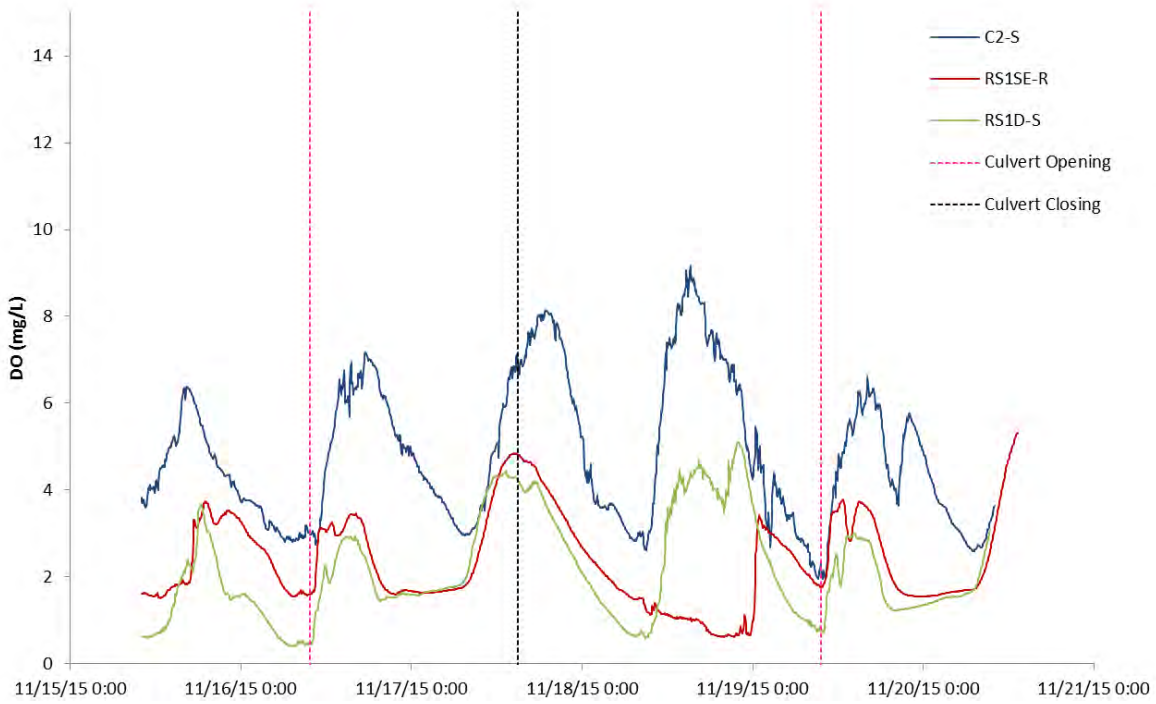

Figure G-12 Time series of dissolved oxygen for sites C2 Slough, RS1SE Ridge and RS1D Slough during the first period of DO data collection (11/15/2015 to 11/20/2015).

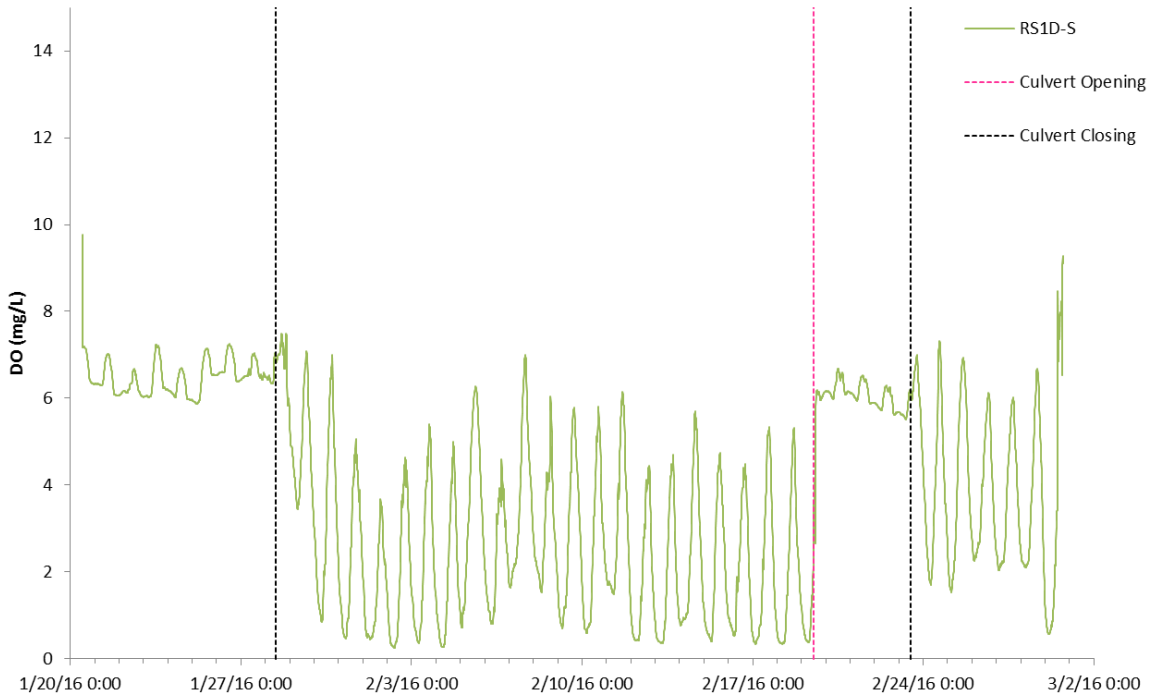

Figure G-13 Time series of dissolved oxygen for RS1D Slough during the second period of DO data collection (1/20/2016 to 2/29/2016).

H. Groundwater – Surface Water Interactions Detected using Heat as a Tracer

Temperature Data

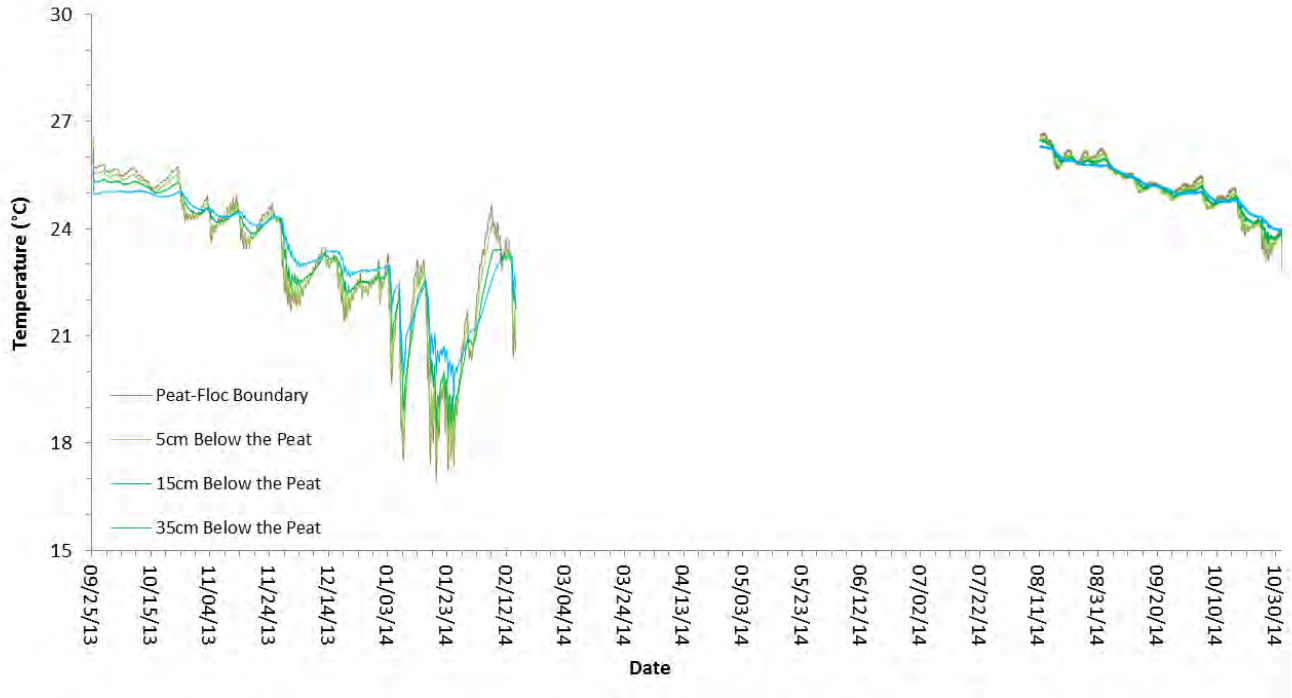

Figure H-1 Temperature data from RS1D collected between September, 2013 and November, 2014 at various depths at and below the peat-floc boundary (0cm).

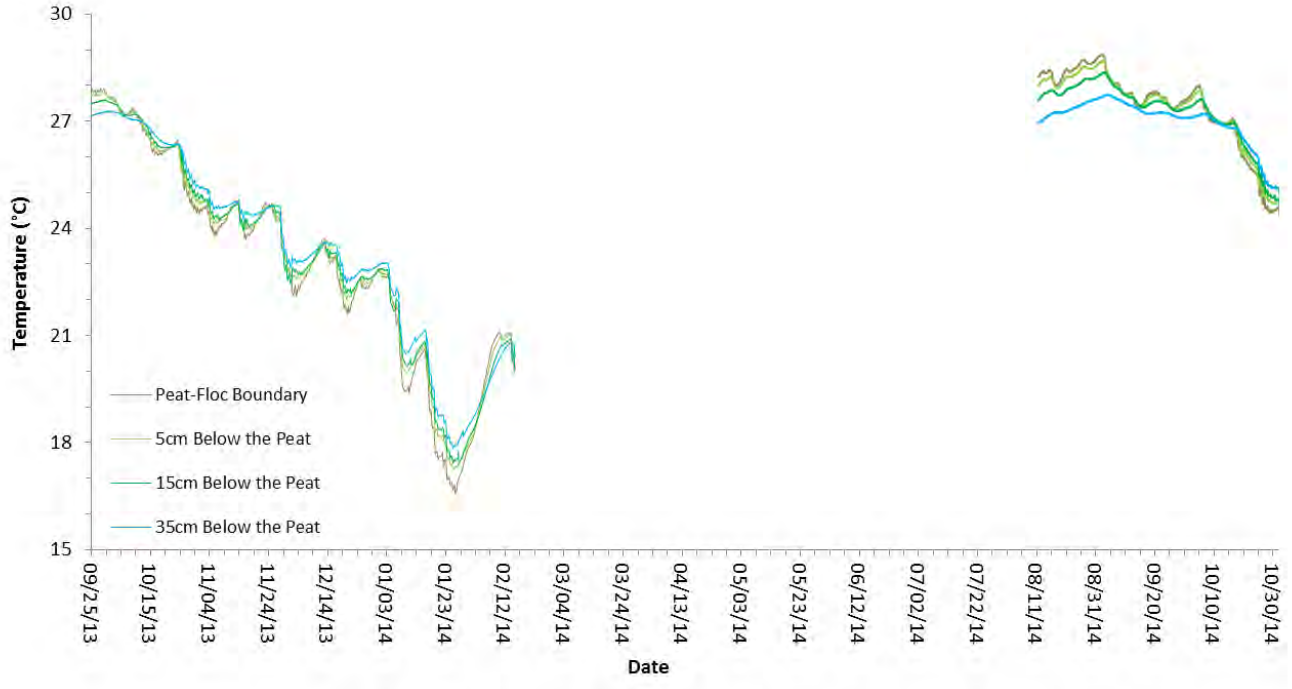

Figure H-2 Temperature data from UB2 collected between September, 2013 and November, 2014 at various depths at and below the peat-floc boundary (0cm).

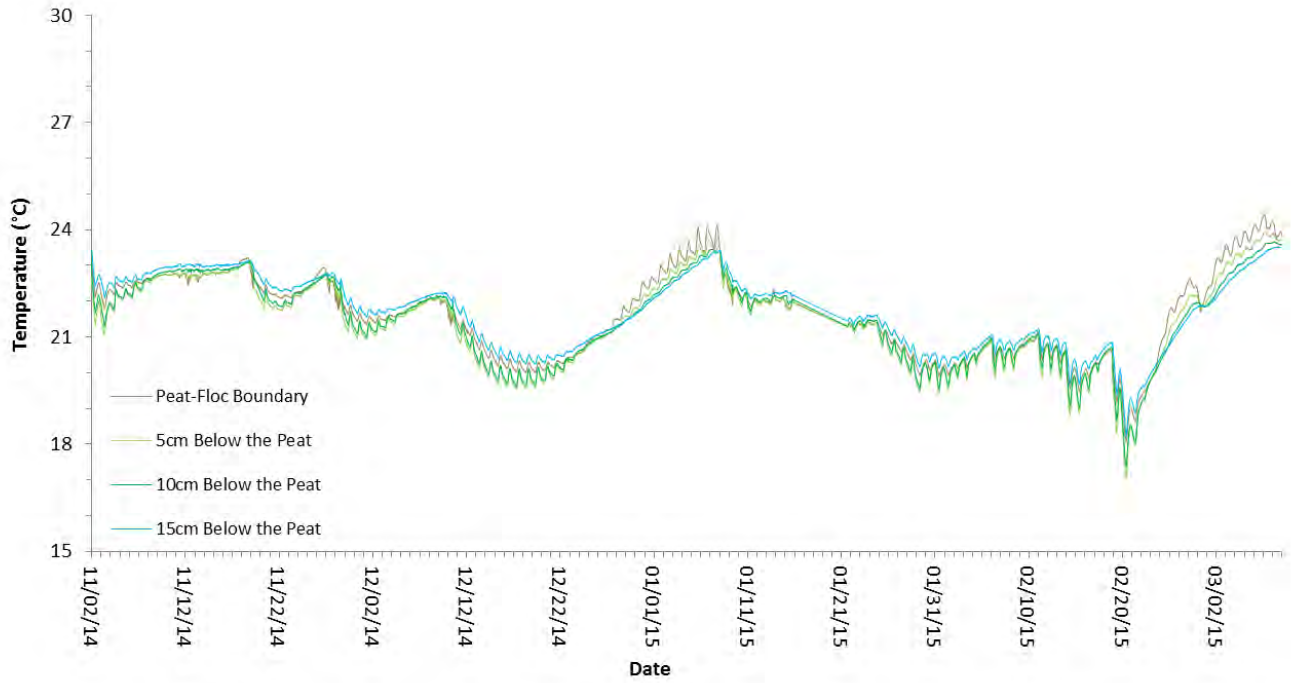

Figure H-3 Temperature data from RS1D collected between November, 2014 and March, 2015 at various depths at and below the peat-floc boundary (0cm).

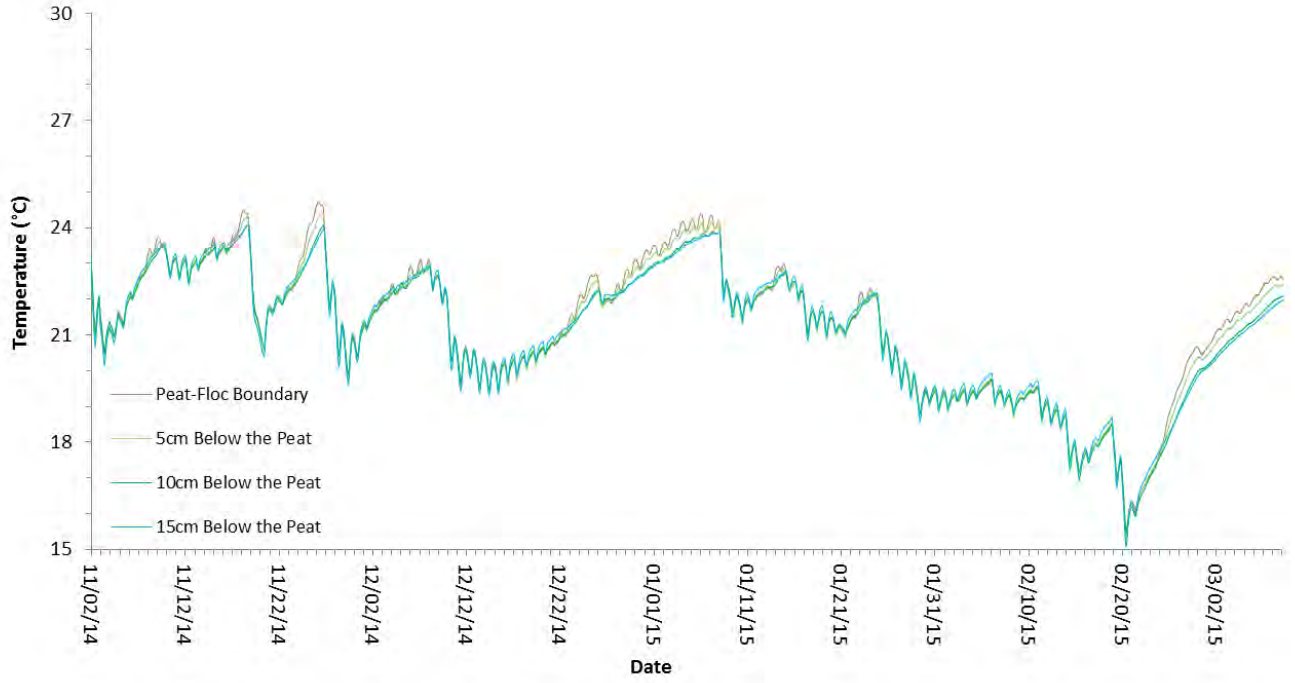

Figure H-4 Temperature data from S1 collected between November, 2014 and March, 2015 at various depths at and below the peat-floc boundary (0cm).

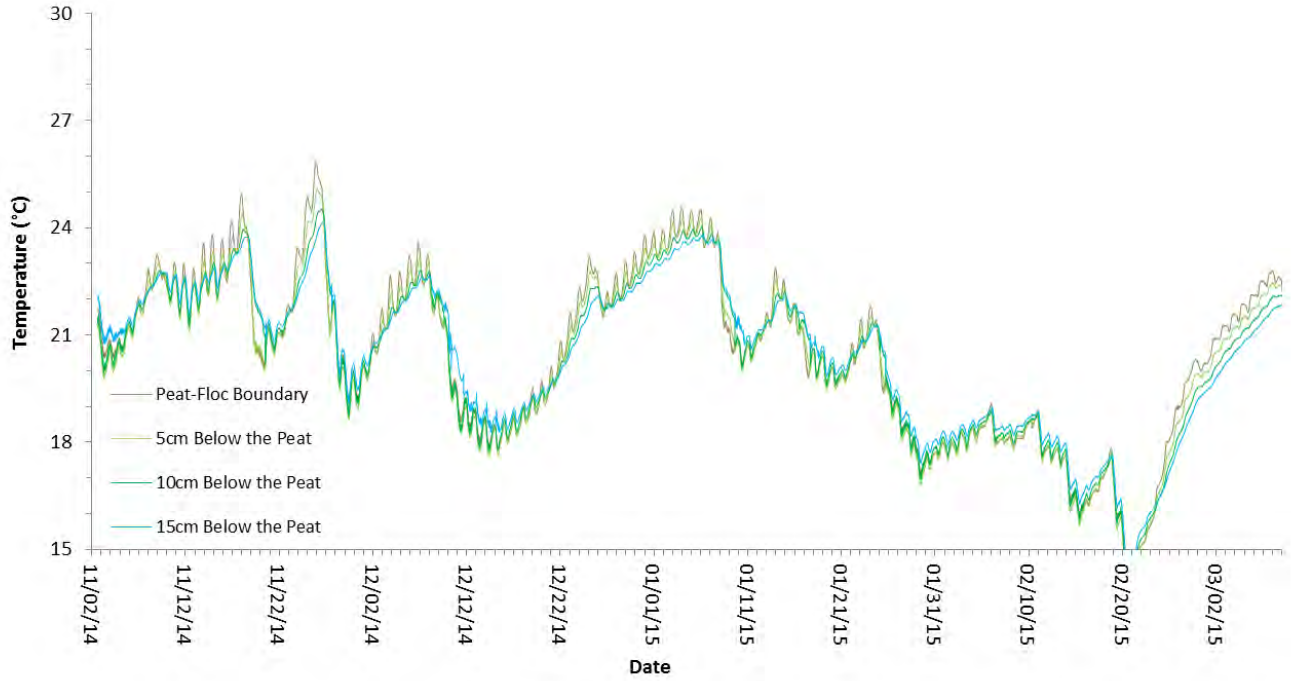

Figure H-5 Temperature data from UB2 collected between November, 2014 and March, 2015 at various depths at and below the peat-floc boundary (0cm).

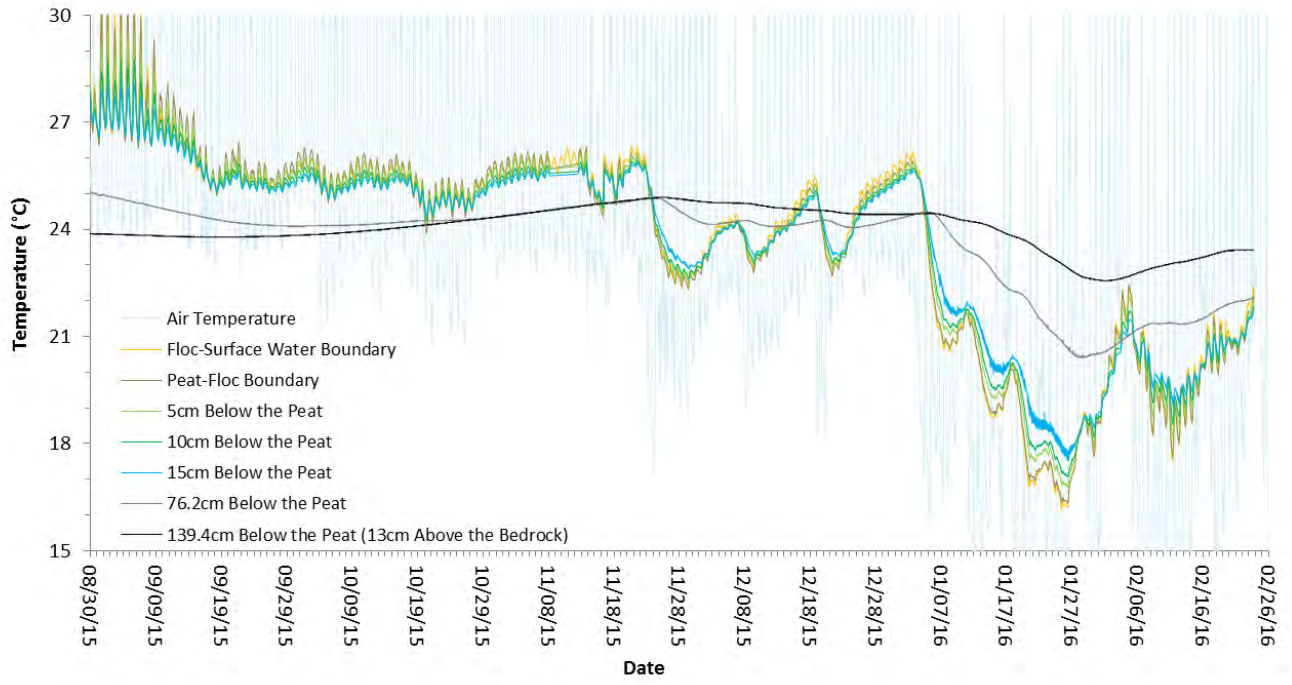

Figure H-6 Temperature data from Z51_USGS collected between August, 2014 and February, 2016. Data were collected at the floc-surface water boundary, peat-floc boundary (0cm), and various depths below the peat-floc boundary. Air temperature data were collected at Z51_USGS.

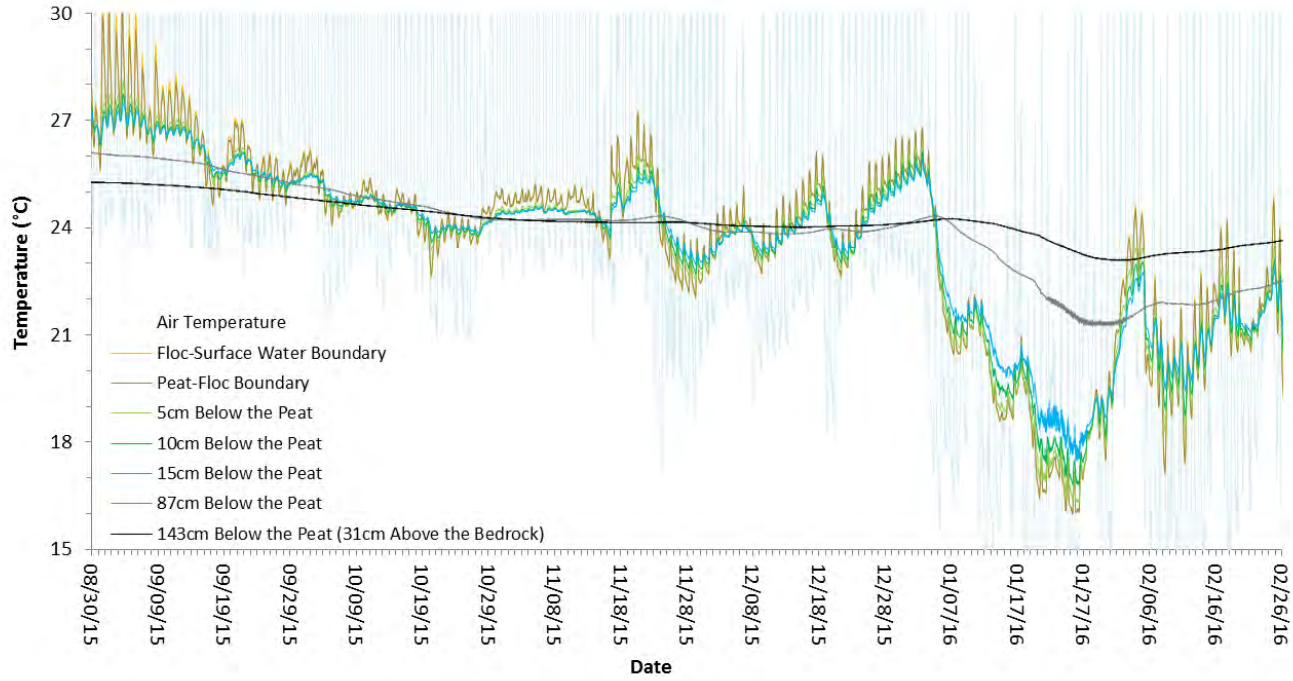

Figure H-7 Temperature data from RS1D collected between August, 2014 and February, 2016. Data were collected at the floc-surface water boundary, peat-floc boundary (0cm), and various depths below the peat-floc boundary. Air temperature data were collected at Z51_USGS.

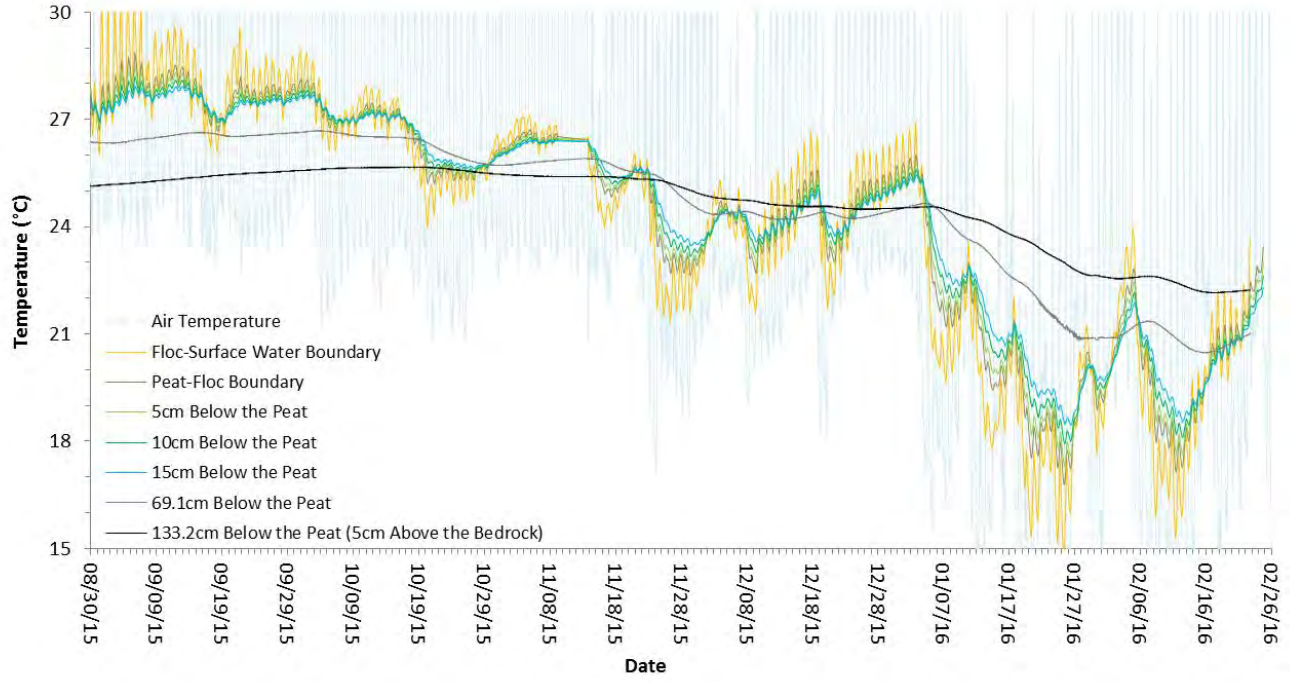

Figure H-8 Temperature data from UB2 collected between August, 2014 and February, 2016. Data were collected at the floc-surface water boundary, peat-floc boundary (0cm), and various depths below the peat-floc boundary. Air temperature data were collected at Z51_USGS.